GROUP B

FOIA/PA NO: 2015-0068

RECORDS BEING RELEASED IN THEIR ENTIRETY

3.2 CLASSIFICATION OF STRUCTURES, SYSTEMS, AND COMPONENTS

This section provides a guide to the classification of the DCPP structures, systems, and components (SSCs).

Criterion 1 of the July 1967 GDC requires that systems and components essential to the prevention of accidents be designed, fabricated, erected, and tested to quality standards commensurate with the importance of the safety functions to be performed. This section describes how Criterion 1 has been implemented by relating the classifications of SSCs to the various criteria, codes, regulations, and standards that dictate specific quality requirements.

In this regard, it is recognized that during the design and construction of DCPP Units 1 and 2, significant industry and regulatory changes were made in establishing common methods of classification, e.g., ANSI N18.2[(1)], SG 26[(2)], SG 29[(3)], and NRC Regulatory Guide (RG) 1.143[(6)]. These methods all differ slightly in detail from those used for the DCPP, but the form and intent of all are equivalent, as will be shown in the following discussion of: (a) the seismic classification of SSCs, and (b) the system quality group classification of pressure-containing components of fluid systems.

Classifications of instruments and controls and requirements for them are discussed in Section 7.1.

3.2.1 SEISMIC CLASSIFICATION

Criterion 2 of the July 1967 GDC, and Appendix A to 10 CFR 100, Seismic and Geologic Siting Criteria for Nuclear Power Plants, require that nuclear power plant SSCs important to safety be designed to withstand the effects of earthquakes. Specifically, Appendix A to 10 CFR 100 requires that all nuclear power plants be designed so that, if the safe shutdown earthquake (SSE) occurs, all structures and components important to safety remain functional. Plant features important to safety are those necessary to ensure (a) the integrity of the reactor coolant pressure boundary, (b) the capability to shut down the reactor and maintain it in a safe shutdown condition, or (c) the capability to prevent or mitigate the consequences of accidents that could result in potential offsite exposures comparable to the guideline exposures of 10 CFR 100.

The SSE of Appendix A to 10 CFR 100 is equivalent to the DCPP double design earthquake (DDE) (see References 9 and 10 for final resolution of issues raised in Supplemental Safety Evaluation Reports 7, 8, and 31 relative to the SSE). Similarly, the operating basis earthquake (OBE) of Appendix A to 10 CFR 100 is equivalent to the DCPP DE.

DCPP's capability to withstand a postulated Richter magnitude 7.5 earthquake centered along an offshore zone of geologic faulting known as the "Hosgri Fault" has been reviewed. Guidance for determining the SSCs designed to remain functional in the

event of an SSE is provided in SG 29. These plant features, including their foundations and supports, are designated as Seismic Category I in SG 29. DCPP SSCs, and their seismic design classifications comply with the intent of SG 29. However, since DCPP design and construction had progressed substantially prior to the issuance of SG 29, different terminology is often used.

Plant features that correspond to Seismic Category I, as identified in SG 29, are designed to remain functional during the design basis earthquakes that they are required to withstand: the DE (equivalent to the OBE of SG 29), the DDE (equivalent to the SSE of SG 29), and/or the postulated Hosgri earthquake (HE). Design Class I plant features are designed to maintain their structural integrity in the event of both the DE/DDE and HE. They may or may not be designed to remain operable for the DE/DDE or HE; the design basis function of the equipment determines whether it is qualified for active or passive function for a DE/DDE and/or an HE.

All plant features designated as Design Class I are also Seismic Category I. SSCs not identified as Seismic Category I in SG 29, are referred to by the guide as Nonseismic Category I features. Under the DCPP classification system, Design Class II features may or may not be Seismic Category I.

SSCs important to reactor operation but not essential to safe shutdown and isolation of the reactor, and failure of which would not result in the release of substantial amounts of radioactivity, are classified as Design Class II.

SSCs not related to reactor operation or safety are classified as Design Class III.

Power and auxiliary service piping systems (as defined in ANSI B31.1, Paragraph 100.1), which might otherwise be considered as Design Class III, are classified as Design Class II (i.e., Design Class III is not used for power and auxiliary service piping systems).

In addition, Appendix B to 10 CFR 50, Quality Assurance Criteria for Nuclear Power Plants and Fuel Reprocessing Plants, requires that SSCs important to safety be designed and constructed in accordance with the quality assurance requirements described in Appendix B. Therefore, as described in Chapter 17, the requirements of the DCPP Quality Assurance Program apply to all SSCs classified as Design Class I. This ensures that plant features important to safety have met the requirements of Appendix B. Specific quality assurance requirements may also be applied to selected Design Class II features.

The general applicability and requirements of the design class, quality/code class classification, and seismic category are provided in Tables 3.2-1 and 3.2-2.

The classifications of specific SSCs are provided in the DCPP Q-List (see Reference 8). The DCPP Q-List is controlled by a written PG&E procedure. The procedure requires that all non-editorial changes to the contents of the Q-List be reviewed pursuant to the

requirements of 10 CFR 50.59. Access to the Q-List is available through hard copy or electronically at PG&E. The piping schematic drawings are illustrated in Figures 3.2-1 through 3.2-27.

The piping symbol system that appears on all piping schematics and drawings to indicate piping fabrication, erection, and test criteria can be correlated to the design and quality code classes as follows:

Piping Schematic Correlation

Piping Symbol	Design Class	Quality Code Class
A	I	I
B	I	II
@[(a)]	I/II	II/None
C	I	III
D	I	III
E	II	None
F	II	None
G	II	None
G1	II	None
H	II	None
J	I	III
-[(b)]	I	Not Applicable
-[(b)]	II or III	None

Those SSCs, including their foundations and supports, that have been classified as Design Class I and designed to remain functional in the event a DDE or HE occurs, and to which the requirements of the Quality Assurance Program apply, are:

(1) The reactor coolant pressure boundary

(2) The reactor core and reactor vessel internals

(3) Systems [see Note (i)](c) or portions of systems that are required for emergency core cooling, postaccident containment heat removal, or postaccident containment atmosphere cleanup [see Note (v)]

(a) The symbol '@' is referred to in the FSAR Update and the Q-List. However, this symbol is not used on the piping schematics for Code Class designation; the line is bubbled (i.e., -0-0-) and the notes describe the applicable code(s).

(b) For HVAC system ductwork symbols, see Figures 3.2-1A and 3.2-2A.

(c) See Notes at the end of this subsection.

(a) The 1971 edition of the ASME Boiler and Pressure Vessel Code, Section III, Nuclear Power Plant Components, uses the term Class I in lieu of Class A.

(4) Systems or portions of systems that are required for reactor shutdown and residual heat removal

(5) Those portions of the main steam, feedwater, and steam generator blowdown systems extending from and including the secondary side of the steam generators up to and including the outermost containment isolation valves, and connected piping up to and including the first valve (including a safety or relief valve) that is either normally closed or capable of automatic closure during all modes of normal reactor operation [see Note (v)]

(6) Auxiliary saltwater, component cooling water, and auxiliary feedwater systems or portions of these systems that are required for emergency core cooling, postaccident containment heat removal, postaccident containment atmosphere cleanup, and residual heat removal

(7) Component cooling water system and seal water systems, or portions of these systems that are required for functioning of other systems or components important to safety

(8) Those portions of systems (other than the radioactive waste management systems) that contain or may contain radioactive material and whose postulated failure could result in conservatively calculated potential offsite exposures in excess of 0.5 rem whole body (or its equivalent to parts of the body) at the site boundary or beyond

(9) Systems or portions of systems that are required to supply fuel for emergency equipment

(10) Systems or portions of systems that are required for (a) post accident monitoring of RG 1.97 Category 1 variables and (b) actuation of systems important to safety

(11) The protection system [see Note (ii)]

(12) The spent fuel storage pool structure, including the spent fuel racks.

(13) The reactivity control systems, i.e., control rods, control rod drives, and boron injection system, that are required to achieve safe shutdown of the plant

(14) The control room, including its associated vital equipment and life support systems, and any structures or equipment inside or outside of the control room whose failure could result in incapacitating injury to the operators

(15) Reactor containment structure, including penetrations [see Note (iv)]

(16) Systems or portions of systems that are required to provide heating, ventilating, and/or air conditioning for safety-related equipment/areas

(17) Portions of the onsite electric power system, including the onsite electric power sources, that provide the emergency electric power needed for functioning of plant features included in Items (1) through (16) above

(18) Portions of the spent fuel pool cooling system used to remove spent fuel decay heat from the spent fuel pool, and portions of the refueling water purification system used to recirculate and cleanup the contents of the refueling water storage tank

Notes:

(i) A system boundary includes those portions of the system required to accomplish the specified safety function and connected piping up to and including the first valve (including a safety or relief valve) that is either normally closed or capable of automatic closure when the safety function is required.

(ii) For purposes of these criteria, the protection system encompasses all electrical and mechanical devices and circuitry (from sensors to actuation devices input terminals) involved in generating those signals associated with the protective function. These signals include those that actuate reactor trip and, in the event of a serious reactor accident, that actuate ESFs such as containment isolation, safety injection, pressure reduction, and air cleaning.

(iii) SSCs that form interfaces between Design Class I and Design Class II or III features are designed to Design Class I requirements.

(iv) Certain valves in these systems that are used for accident mitigation only, and do not support safe shutdown following an HE, were qualified for active function for an HE to provide increased conservatism in accordance with Reference 7.

3.2.2 SYSTEM QUALITY GROUP CLASSIFICATIONS

GDC 1 requires that systems and components essential to the prevention of accidents be designed, fabricated, erected, and tested to quality standards commensurate with the importance of the safety functions to be performed. This section describes the quality classification system that has been used to implement quality standards that satisfy Criterion 1 for DCPP fluid systems and fluid system components. The discussion also shows the relationship of this classification system to fluid system and fluid system components classification systems in ANSI N18.2, Nuclear Safety Criteria for the Design of Stationary Pressurized Water Reactor Plants[1], and SG 26.

DCPP SSCs are classified as Design Class I, II, or III. Design Class I is Seismic Category I and is further categorized as PG&E Quality/Code Class I, II, or III.

Design Classes II or III are usually Nonseismic Category I and have no PG&E quality/code class designation. Specific requirements as dictated by the quality standards applicable to the respective commercial (ASME, ANSI, or ASA) code classes are also applicable. However, some Design Class II components have been seismically designed, e.g., items in the Seismically Induced Systems Interaction Program, specific components required for post-HE shutdown, CCW header C components, and items that were designed for the DE pursuant to RG 1.143. For this reason, there is not a direct correlation between design class and seismic category (except that all Design Class I features are Seismic Category I). In addition, the classification of Seismic Category I does not indicate which of the three design basis earthquakes a feature has been qualified for, nor whether that qualification is for passive or active function (except that all electrical Class 1E and Instrument Class IA components are qualified to remain operable for all three design basis earthquakes). The design basis function of the equipment determines the type of seismic qualification required. These classifications and their relationships are illustrated in Table 3.2-2 and discussed below.

3.2.2.1 Design Class I, Quality/Code Class I Fluid Systems and Fluid System Components

10 CFR 50.55a requires that certain components of the reactor coolant pressure boundary be designed, fabricated, erected, and tested in accordance with the requirements for Class A[a] components of Section III of the ASME Boiler and Pressure Vessel Code, or the most recently available industry codes and standards. Code Class I has been applied to those components of the reactor coolant pressure boundary and implements the quality standards that satisfy the requirements of Section 50.55a, 10 CFR 50. DCPP Code Class I components of the reactor coolant pressure boundary are listed in the DCPP Q-List[8], along with the industry codes and standards used for their design, fabrication, erection, and test. The Code Class I classification includes the components of the reactor coolant pressure boundary identified as Safety Class I in ANSI N18.2 and Quality Group A in SG 26.

3.2.2.2 Design Class I, Quality/Code Class II Fluid Systems and Fluid System Components

Generally, Code Class II has been applied to include fluid systems and fluid system components that are either:

(1) Part of the reactor coolant boundary, but excluded from Code Class I requirements by Section 50.55a of 10 CFR 50

(2) Not part of the reactor coolant pressure boundary, but part of:

(a) Systems or portions of systems[b] that are required for emergency core cooling, postaccident containment heat removal, or postaccident containment atmosphere cleanup

(b) Systems or portions of systems that are required for reactor shutdown and residual heat removal

(c) Those portions of the main steam, feedwater, and steam generator blowdown systems extending from and including the secondary side of steam generators up to and including the outermost containment isolation valves, and connected piping up to and including the first valve (including a safety or relief valve) that are either normally closed or capable of automatic closure during all modes of normal reactor operation

(d) Systems or portions of systems that are connected to the reactor coolant pressure boundary and are not capable of being isolated from the boundary during all modes of normal reactor operation by two valves, each of which is either normally closed or capable of automatic closure

Code Class II fluid systems and fluid system components are listed in the DCPP Q-List (see Reference 8), along with the industry codes and standards used for their design, fabrication, erection, and testing.

3.2.2.3 Design Class I, Quality/Code Class III Fluid Systems and Fluid System Components

Generally, Code Class III has been applied to include fluid systems and fluid system components not part of the reactor coolant pressure boundary, nor included in Code Class II, but part of:

(1) Auxiliary saltwater, component cooling water, and auxiliary feedwater systems, or portions of these systems that are required for (a) emergency core cooling, (b) postaccident containment heat removal, (c) postaccident containment atmosphere cleanup, and (d) residual heat removal from the reactor

(2) Systems or portions of systems that are connected to the reactor coolant pressure boundary and are capable of being isolated from the boundary during all modes of normal reactor operation by two valves, each of which is either normally closed or capable of automatic closure

---

[b] The system boundary includes those portions of the system required to accomplish the specified safety function and connected piping up to and including the first valve (including a safety or relief valve) that is either normally closed or capable of automatic closure when the safety function is required.

(3) Those portions of systems other than radioactive waste management systems that contain or may contain radioactive material, and whose postulated failure could result in conservatively calculated potential offsite exposures in excess of 0.5 rem whole body (or its equivalent to parts of the body) at the site boundary or beyond

(4) Component cooling water system and seal water systems, or portions of these systems, that are required for functioning of other systems or components important to safety

(5) Portions of the spent fuel pool cooling system required for spent fuel cooling, and the refueling water purification system whose postulated failure could result in a loss of refueling water storage tank inventory

Code Class III fluid systems and fluid system components are listed in the DCPP Q-List (see Reference 8), along with the industry codes and standards used for their design, fabrication, erection, and testing.

3.2.2.4 Other Fluid Systems and Fluid System Components

Fluid systems and fluid system components that are not part of the reactor coolant pressure boundary, not essential to shut down the reactor and maintain it in a safe condition, and not essential to prevent or mitigate the consequences of accidents that could result in potential offsite exposures comparable to the guideline exposures of 10 CFR 100, are not included in the Design Class I classification.

These other systems and components are classified as Design Class II or III and are listed in the DCPP Q-List (see Reference 8), along with the industry codes and standards used for their design, fabrication, erection, and testing. They comprise a design class, but have not been assigned a code class. Design Class II includes the fluid systems and fluid system components identified as Quality Group D in SG 26 and as radioactive waste management system in RG 1.143, i.e., those fluid systems and fluid system components that contain or may contain radioactive material, but whose failure would not result in calculated potential exposures in excess of 0.5 rem whole body (or its equivalent to parts of the body) at the site boundary. These fluid systems and fluid system components are in conformance with the accepted industry codes and standards in effect during the design and construction of DCPP. If they were designed and constructed to codes and standards outside of the requirements of SG 26 or RG 1.143, additional quality standards have normally been applied so that the intent has been met.

3.2.2.5 Summary of System Quality Group Classifications

Table 3.2-2 summarizes the design and quality group classifications applied to the DCPP SSCs and their relationships to the other methods of classification.

Generally, codes and standards were applied prior to issuance of the latest codes and standards, such as the 1971 edition of the ASME Boiler and Pressure Vessel Code, Section III, Nuclear Power Plant Components. In some cases, fluid systems and components were designed and built to codes and standards outside the requirements of SG 26, ANSI N18.2, and RG 1.143 definitions. The classification for those fluid systems and fluid system components that do not fall within the strict definition of SG 26, ANSI N18.2, and RG 1.143 were established prior to ANSI N18.2, SG 26, RG 1.143, and the issuance of revised industry codes and standards. For these fluid systems and fluid system components, the design specifications specified the accepted industry codes and standards in effect during the design and construction of DCPP.

While some portions of the fire protection system components are designated Design Class I, the system is not required to ensure the integrity of the reactor coolant pressure boundary or to shut down the reactor and maintain it in a safe shutdown condition. Fire protection features meet the requirements defined in BTP APCSB 9.5-1 (Reference 5) after 1979 and, where designated Design Class I, are designed to withstand the effects of an HE.

3.2.3 REFERENCES

1. Nuclear Safety Criteria for the Design of Stationary Pressurized Water Reactor Plants. N18.2 American Nuclear Society, August 1970 Draft.

2. Quality Group Classifications and Standards for Water, Steam, and Radioactive Waste Containing Components of Nuclear Power Plants, SG 26, Atomic Energy Commission.

3. Seismic Design Classification, SG 29, US Atomic Energy Commission.

4. Spent Fuel Storage Facility Design Basis, RG 1.13, Nuclear Regulatory Commission.

5. Guidelines for Fire Protection for Nuclear Power Plants, BTP APCSP 9.5-1, Nuclear Regulatory Commission.

6. Design Guidance for Radioactive Waste Management Systems, Structures, and Components Installed in Light-Water-Cooled Nuclear Power Plants, RG 1.143, Nuclear Regulatory Commission.

7. PG&E Letter to the NRC, DCL-92-198 (LER 1-92-015).

8. Classification of Structures, Systems, and Components for Diablo Canyon Power Plant Units 1 and 2 (Q-List), PG&E.

9. Letter from NRC (L. F. Miller) to PG&E (G. M. Rueger), dated December 13, 1993, Subject: NRC Inspection of Diablo Canyon Units 1 and 2 (Report No. 50-275, 50-323/93-31) [pages 1 and 2].

10. Letter from NRC (A. W. Beach) to PG&E (G. M. Rueger), dated August 15, 1994, Subject: NRC Inspection Report 50-275/94-18; 50-323/94-18 (Notice of Violation) [pages 14 and 15].

3.2.4 REFERENCE DRAWINGS

Figures representing controlled engineering drawings are incorporated by reference and are identified in Table 1.6-1. The contents of the drawings are controlled by DCPP procedures.

TABLE 3.2-1

DESIGN CLASSIFICATION OF STRUCTURES, SYSTEMS, AND COMPONENTS

Design Class I	Design Class II	Design Class III
Applicability		
Plant features important to safety, including plant features required to assure (1) the integrity of the reactor coolant pressure boundary, (2) the capability to shut down the reactor and maintain it in a safe shutdown condition, or (3) the capability to prevent or mitigate the consequences of accidents which could result in potential offsite exposures comparable to the guideline exposures of 10 CFR 100.	Plant features important to reactor operation, but not essential to safety, including plant features not required to be Design Class I.	Plant features not related to reactor operation or safety.

Design Class I	Design Class II	Design Class III
Requirements		
1. Quality Standards - Plant features required to meet AEC GDC-1.	1. Quality Standards - Plant features not required to meet AEC GDC-1.	1. Quality Standards - Plant features not required to meet AEC GDC-1.
2. Quality Assurance - Plant features required to meet Appendix B to 10 CFR 50.	2. Quality Assurance - Plant features not required to meet Appendix B to 10 CFR 50. Specific QA requirements may be applied to selected features.	2. Quality Assurance – Plant features not required to meet Appendix B to 10 CFR 50.
3. Seismic Design – Plant features required to meet GDC-2 and Appendix A to 10 CFR 100. Plant features designed to withstand effects of double design earthquake (DDE). Features are also designed to maintain their structural integrity (and in some cases their operability) during a Hosgri earthquake.	3. Seismic Design - Plant features not required to meet GDC-2 and Appendix A to 10 CFR 100. Plant features not designed to withstand effects of design earthquakes except for items as required by RG. 1.143, and for selected features where specifically designated.	3. Seismic Design – Plant features not required to meet GDC-2 and Appendix A to 10 CFR 100. Plant features not designed to withstand effects of design Earthquakes, except where specifically designated.

TABLE 3.2-2

DESIGN AND QUALITY GROUP CLASSIFICATIONS

PG&E Engineering			Seismic Design Classification[a]	Quality Group Classification[f]		Remarks
Design Class	Quality/Code Class	Piping Symbol	NRC Reg. Guide 1.29	ANSI N18.2 Safety Group	NRC Reg. Guide 1.26 Quality Group	Other Codes and Standards
I	I	NONE[b]	Category I	1	A	ASA B31.1-1955; ASME B&PV Code, Section III-1971
I	I	A[h]	Category I	1	A	ANSI B31.1-1967; B31.7-1969 with 1970 Addenda, Class I
I	II	B	Category I	2	B	ANSI B31.7-1969 with 1970 Addenda, Class II
I	II	@[g]	Category I	2	B	ANSI B31.1-1967; ASME B&PV Code Section I-1968; Section III-1968
I	III	C	Category I	3	C	ANSI B31.7-1969 With 1970 Addenda, Class III
I	III	D[i]	Category I	3	C	ANSI B31.1-1967; ANSI B31.7-1969 with 1970 Addenda, Class III
II[d]	-	G	Category I[j]			ANSI B31.1-1967 and NFPA Standards
I	III	J[k]	Category I	-	-	ANSI B31.1-1967
II	-	E	Non-Category I	NNS	-	ANSI B31.1, 1967
II	-	F	Non-Category I[e]	NNS	D[c]	ANSI B31.1 1967; RG Guide 1.143

TABLE 3.2-2

PG&E Engineering			Seismic Design Classification[a]	Quality Group Classification[f]		Remarks
Design Class	Quality/Code Class	Piping Symbol	NRC Reg. Guide 1.29	ANSI N18.2 Safety Group	NRC Reg. Guide 1.26 Quality Group	Other Codes and Standards
II[d]	-	G1	Non-Category I	-	-	NFPA Standards
II	-	H	Non-Category I	NNS	D [c]	ANSI B31.1-1967; RG Guide 1.143
II	-	-	Non-Category I	-	-	Applicable industry codes and standards
III	-	-	Non-Category I	-	-	Applicable industry codes and standards
II	-	@[m]	Non-Category I	NNS	-	ASME B&PV Code, Section I-1980

Notes:

(a) General Design Criterion 2 (1967), Appendix A to 10 CFR 50, and Appendix A to 10 CFR 100.

(b) Reactor coolant loop and pressurizer surge line piping. Design to ASA B31.1-1955 using Nuclear (N) Code Cases N-7, N-9, and N-10. Fabrication, erection, and inspection to ASME B&PV Code Section III-1971.

(c) Radioactive system (PG&E QA Class R). Future activities such as repair, replacement, maintenance, or testing shall be performed per RG. 1.143 for those portions of the systems designated as F or H in Figures 3.2-1 through 3.2-27.

(d) The fire protection system may not have been designed or constructed under a quality assurance program meeting all requirements of 10 CFR 50, Appendix B. However, activities such as repair, replacement, maintenance, or testing shall be performed in accordance with the QA recommendations described in Appendix A to NRC Branch Technical Position 9.5.1 and PD OM8 (PG&E QA Class G). Quality requirements administered shall be commensurate with the safety function of the SSC.

(e) Seismic qualification requires Design Earthquake analysis.

(f) Regulatory Guide 1.26 (formerly AEC Safety Guide 26) establishes quality group classifications for reactor coolant pressure boundary and remaining safety-related components containing radioactive material, water, or steam. Other systems not covered by this guide include instrument and service air, diesel engine and its generators and auxiliary support systems, diesel fuel, emergency and normal ventilation, fuel handling, and radioactive waste management systems.

The Code Class I classification generally includes the fluid systems and components identified as Safety Class I in ANSI N18.2 and Quality Group A in AEC Safety Guide 26. However, the classification and quality standards for Diablo Canyon fluid systems and components were established prior to the existence of these documents and, therefore, do not always fall within their strict definitions. All Code Class I fluid systems and components are in accordance with the accepted industry codes and standards that were in effect during the design and construction of Diablo Canyon. If fluid systems and components were designed and constructed to codes and standards outside of the requirements of the above-mentioned documents, additional quality standards have normally been applied, so that their intent has been met.

The Code Class II classification generally includes the fluid systems and components identified as Safety Class 2a in ANSI N18.2 and Quality Group B in AEC Safety Guide 26. However, the classification and quality standards for Diablo Canyon fluid systems and components were established prior to the existence of these documents and, therefore, do not always fall within their strict definitions. All Code Class II fluid systems and components are in accordance with the accepted industry codes and standards that were in effect during the design and construction of Diablo Canyon. If fluid systems and components were designed and constructed to codes and standards outside of the requirements of the above-mentioned documents, additional quality standards have normally been applied, so that their intent has been met.

The Code Class III classification generally includes the fluid systems and components identified as Safety Classes 2b and 3 in ANSI N18.2 and Quality Group C in AEC Safety Guide 26. However, the classification and quality standards for Diablo Canyon fluid systems and components were established prior to the existence of these documents and, therefore, do not always fall within their strict definitions. All Code Class III fluid systems and components are in accordance with the accepted industry codes and standards that were in effect during the design and construction of Diablo Canyon. If fluid systems and components were designed and constructed to codes and standards outside of the requirements of the above- mentioned documents, additional quality standards have normally been applied, so that their intent has been met.

An exception exists to the above for Quality Code Class III piping Code Class D piping. These are systems or portions of systems which were originally constructed as Design Class II and were subsequently upgraded to Design Class I because of later requirement. For such piping, the design analysis is in accordance with Design Class I criteria. All construction, repair, or replacement performed after the upgrade is in accordance with Design Class I requirements.

(g) Feedwater piping from the (final) main feedwater check valve to the steam generator; auxiliary feedwater from the main feedwater line back to the second check valve; main steam piping from the steam generator to the main steam isolation valve; steam generator blowdown piping from the steam generator to the first valve outside containment; design to ANSI B31.1-1967; fabrication, erection, and inspection to ASME B&PV Code Section I-1968. Requirements for the main steam safety valves are in accordance with ASME B&PV Code Section III-1968.

(h) Design to ANSI B31.1-1967. Fabrication, erection, and inspection to ANSI B31.7-1969 with 1970 Addenda, Class I.

(i) This piping code class applies to: (1) the spent fuel pool cooling loop; (2) the auxiliary feedwater pump suction piping from the fire water storage tank; and (3) the refueling water purification loop from and to the refueling water storage tank. This piping was upgraded from Design Class II Code Class E. B31.1 applies for work performed prior to the upgrade. B31.7 applies to work performed after the upgrade.

(j) Piping is seismically qualified for the Hosgri earthquake.

(k) Piping originally installed as Design Class II and has been qualified seismically for the Hosgri earthquake, but is Design Class I for repair, replacement, and new construction.

(l) Certain Design Class II and III SSCs have seismic qualification requirements and may be designated as Seismic Category I; these SSCs are designated as QA Class S.

(m) Auxiliary Boiler 0-2 and its external piping conforms to ASME B&PV Code Section I-1980 through summer 1980 Addenda.

3.8 DESIGN OF DESIGN CLASS I STRUCTURES

Figure 1.2-2 shows the location of all structures for DCPP Units 1 and 2. The design classification of plant structures is given in the DCPP Q-List (see Reference 8 of Section 3.2). In the Q-List, the following Design Class I structures are shown:

(1) Containment structure

(2) Auxiliary building

See Section 3.1 for discussion of the design of DCPP structures in conjunction with AEC General Design Criteria. The design of the containment structure is discussed in Section 3.8.1; the auxiliary building design is discussed in Section 3.8.2; and the Class I outdoor storage tanks, including the condensate storage, refueling water storage, and fire water tanks, are discussed in Section 3.8.3. The foundations and concrete supports of Class I structures are discussed in Section 3.8.4. Section 3.8.5 discusses the Design Class II turbine building and intake structure, both of which contain Design Class I equipment and components.

Note that the analytical results summarized in the following sections for the major plant structures are representative of the evaluations performed for the operating license review (Reference 31), but may not reflect minor changes associated with subsequent plant modifications.

3.8.1 CONTAINMENT STRUCTURE

3.8.1.1 Description of the Containment

The reactor containment for each unit is a steel-lined, reinforced concrete building of cylindrical shape with a dome roof that completely encloses the reactor and RCS. It ensures that essentially no leakage of radioactive materials to the environment would result even if gross failure of the RCS were to occur simultaneously with an earthquake of intensity twice the maximum postulated.

The containment structures for Units 1 and 2 are essentially identical, as mirror images. The following discussion applies to either unit:

The concrete outline and equipment locations are shown in Chapter 1. The exterior shell consists of a 142-foot-high cylinder, topped with a hemispherical dome. The minimum thickness of the concrete walls is 3.6 feet, and the minimum thickness of the concrete roof is 2.5 feet. Both have a nominal inside diameter of 140 feet and a nominal inside height of 212 feet. The concrete floor pad is 153 feet in diameter with a minimum thickness of 14.5 feet, with the reactor cavity near the center. The inside of the dome, cylinder, and base slab is lined with welded steel plate, which forms a leaktight membrane. The nominal thickness of the steel liner is 3/8-inch on the wall and dome and the nominal thickness of the steel liner on the base slab is 1/4-inch.

B/2

The containment is designed and will be maintained for a maximum internal pressure of 47 psig and a temperature of 271°F, coincident with a Double Design Earthquake.

The internal concrete structure approximates a 106-foot-diameter, 51-foot-high cylinder, with a slab on top. However, there are multiple openings and walls, such as the reactor support and the stainless steel lined refueling canal, which complicate the shape. The walls and top slab are generally 3 feet thick. This structure provides support for the reactor and components of the RCS, provides radiation shielding, and provides protection for the liner from postulated missiles originating from the RCS.

A polar crane is mounted on top of the internal concrete cylinder wall. The support of the polar crane, its connection to the concrete, and provisions to resist seismic forces are shown in Figure 3.8-23 and described in Section 9.1.4. Seismic analysis for the polar crane is discussed in Section 3.7.

The piping and electrical connections between equipment inside the containment structure and other parts of the plant are made through specially designed, leaktight penetrations. In addition to the piping and electrical penetrations, other penetrations are the 18-foot 6-inch diameter equipment hatch, the 9-foot 7-inch diameter personnel hatch, the 5-foot 6-inch diameter personnel emergency hatch, and the fuel transfer tube.

The 6-foot 7-inch by 13-foot ventilation duct is attached to the outside of the structure, extending from an elevation 25 feet above the base slab to the top of the dome. The duct is fabricated from steel plate with stiffeners.

A system of lightning rods is installed on the dome to protect against lightning damage.

The following paragraphs describe the various parts of the structure:

3.8.1.1.1 Exterior Shell

(1) *Reinforcing Steel*

The reinforcing steel arrangement is designed to provide continuous reinforcement for tensile and shear membrane forces in the cylinder and dome. The reinforcing in the cylinder wall consists of horizontal hoop bars, and inclined bars, oriented 60° from the horizontal. In Figure 3.8-1, layers (4) and (6) are the Number 18 hoop bars, spaced at 8-1/2 inches center-to-center vertically, and layers (3) and (5) are the inclined Number 18 bars spaced at 8-1/2 inches center-to-center, all spacing measured normal to the bars.

The dome reinforcing is accomplished by extending the inclined bars past the springline and over the dome. After crossing the dome, the same bar once again becomes an inclined bar in the cylinder. A layer (3) bar becomes a layer (5) bar after crossing the dome, as shown in

Figure 3.8-2. No inclined bars are terminated at the springline or in the dome.

The dome steel layout is based on the division of a sphere into 20 equilateral spherical triangles, as shown in Figure 3.8-3. At the springline, two sides of the triangles make an angle of 30° with the vertical. Thus, an inclined cylinder bar is parallel to the sides of the triangles at the springline. The inclined cylinder bars are extended into the dome so that they are always parallel to one side of a spherical triangle.

Figure 3.8-4 shows the five types of bars in the dome. When these five types are superimposed, there are three layers of reinforcing steel at every point above the pentagon ABCDE in Figure 3.8-3. Below pentagon ABCDE, the inclined bars make up two layers at every point, and bars similar to the cylinder hoop bars are used to provide reinforcing in the third direction.

Layers (1) and (2) (Figure 3.8-1) are inclined at 30° to the vertical and extend from the base slab to elevation 172 feet. These bars, spaced at 17 inches center-to-center, provide additional capacity to resist earthquake forces. Above elevation 170 feet, Number 4 bars are spaced at 12 inches center-to-center horizontally and vertically.

(2) *Splices*

All Number 18 bars are spliced by Cadwelding using "T-Series" sleeves, designed to develop the full tensile strength of the bar. As a general rule, splices are staggered a minimum of 3 feet.

For all penetrations except the equipment and personnel hatches, the Number 18 reinforcing bars are bent around openings. For the equipment and personnel hatch openings, a 2.5-inch-thick hexagonal collar, widened to 4 inches thick at the edges, is provided to transfer the reinforcing bar forces around the opening as shown in Figures 3.8-12 and 3.8-13. The reinforcing bars are Cadwelded to special studs threaded into the 4-inch edge of the hexagonal collar.

3.8.1.1.2 Liner

All liner seams are full penetration butt-welded, and are covered with steel channels welded to the inside of the structure. These "leak chase" channels provide a sensitive and accurate means of detecting leakage. They are arranged in zones so that one zone at a time may be pressurized to test the integrity of the liner plate welds.

The liner in the dome and cylinder wall is anchored by welded studs that extend into the concrete wall past the innermost layers of reinforcing steel. Three types of studs are used: a 3/8-inch diameter with an 8-1/2-inch shaft and a plain 4-inch "L" shaped arm, a

3/8-inch diameter with an 8-1/2-inch shaft and a threaded end, and a 1/2-inch diameter with an 11-inch shaft and a threaded end. All threaded studs are provided with an anchorage at the threaded end, and provide resistance to pullout that is equal to or greater than the 3/8-inch stud with a 4-inch arm. The studs are spaced a maximum of 19.6 inches on center (plus a placement tolerance of 1/2 inch) in a pattern that is compatible with the reinforcing steel, as shown in Figure 3.8-5.

For all penetrations in the exterior shell, a thickened plate is welded into the liner.

3.8.1.1.3 Penetrations

In general, a penetration consists of a sleeve embedded in the concrete wall and welded to the containment structure liner. The pipe, electrical conductor cartridge, duct, or access hatch passes through the embedded sleeve and one or both ends of the resulting annulus are closed off by welded end plates, bolted flanges, or flued heads. Typical electrical and piping penetrations are shown in Figures 3.8-6 through 3.8-10, and the fuel transfer tube penetration is shown in Figure 3.8-11. The penetrations are designed to maintain the same high degree of leaktight integrity afforded by the containment structure itself.

3.8.1.1.3.1 Electrical Penetrations

Electrical penetrations are either canister types or feed-through modules that allow electrical conductors to pass through the containment boundary. Penetrations are qualified for a single seal pressure boundary. The canister and feed-through modules are connected to the header plate, which is welded to the containment penetration sleeve. All penetrations are provided with a connection to allow periodic leak testing. The weld connecting the sleeve to the liner plate is provided with a leak chase channel for leak testing.

3.8.1.1.3.2 Piping Penetrations

Piping penetrations are provided for all piping passing through the containment boundary. Typical piping penetrations are shown in Figures 3.8-6 and 3.8-7. Several small pipes may pass through a single embedded sleeve to minimize the number of penetrations required. Welded end plates or flued heads are used to provide end closure. The welded joints are covered with a leak chase channel to allow periodic testing. The weld connecting the sleeve to the liner plate also has a leak chase channel.

Pipes carrying hot fluids through penetrations are designed to maintain the temperature of the concrete adjacent to the sleeve below 200°F under normal operating conditions.

Pipes and penetrations are anchored, as required, to resist the forces and movements incident at the penetration under normal and accident conditions, and to limit the loads imposed on the containment structure liner. Piping loads are transferred to the

penetration sleeve and thence to anchors in the concrete wall rather than to the containment structure liner.

3.8.1.1.3.3 Equipment and Personnel Access Hatches

The equipment hatch is furnished with a double-gasketed flange and bolted dished door. Equipment up to a diameter of approximately 18 feet can be transferred into and out of the containment structure through this hatch. The hatch barrel is embedded in the containment structure wall and welded to the liner. Provision is made for pressurizing the space between the double gaskets of the door flanges and the weld seam leak chase channels at the sleeve-to-liner joint.

The two personnel hatches are double door, mechanically-latched, welded steel assemblies.

A quick-acting type equalizing valve connects each personnel hatch with the interior of the containment vessel for the purpose of equalizing pressure in the two systems when entering or leaving. The personnel hatch doors are interlocked to prevent simultaneous opening. Remote indicating lights and annunciators situated in the control room indicate the door operational status. Provision is made to permit bypassing the door interlocking system to allow doors to be left open during a plant cold shutdown. Each door hinge is capable of independent three-dimensional adjustment to assist proper seating. A lighting and communication system operating from an external supply is provided in the lock interior. Emergency access, to either the inner door from the containment interior, or to the outer door from outside, is possible by the use of special door unlatching tools. All doors on the personnel hatches are double gasketed and provided with fittings to allow pressurization of the space between the double gaskets.

3.8.1.1.3.4 Special Penetrations

(1) *Fuel Transfer Tube Penetration*

A fuel transfer tube penetration is provided for fuel movement between the refueling canal in the containment structure and the spent fuel pool. The penetration consists of a 20-inch-diameter stainless steel pipe installed inside a 24-inch-diameter pipe sleeve as shown in Figure 3.8-11. The inner pipe acts as the transfer tube and is fitted with a quick-opening hatch in the refueling canal and a standard gate valve in the spent fuel pool. This arrangement prevents leakage through the transfer tube in the event of an accident. The outer pipe is welded to the containment liner and provision is made, by use of a special seal ring to permit pressure testing all welds essential to the integrity of the penetration. Bellows expansion joints are provided on the pipes to compensate for any differential movement between the two pipes or other structures.

(2) *Containment Supply and Exhaust Purge Ducts*

The ventilation system purge duct is equipped with two quick-acting tight-sealing valves (one inside and one outside the containment) to be used for isolation purposes. These valves are normally closed during reactor operation. They are manually opened for containment purging but are automatically closed upon a signal of high containment pressure or high containment radiation level. The space between the valves can be pressurized to check the integrity of the penetration. In addition, the shaft seals of the purge valves are equipped with double seals with provision for testing the space between.

(3) *Spare Penetrations*

Capped spare penetrations are provided. The welds between the sleeve and the liner and between the sleeve and the cap are covered with leak chase channels.

All spaces that are equipped for pressurization of penetrations and penetration sleeves are included in the same system of pressurization zones as the liner seam leak chase channels.

Several spare penetrations are also provided with capped, blind flanged or valved and capped end connections. These are 10 CFR 50 Appendix J Type B penetrations and are leak rate tested in accordance with Appendix J, Option B, as modified by approved exemptions.

(4) *Mini-Equipment Hatches (Penetrations 58 and 60)*

The mini-equipment hatch penetrations are provided to facilitate the passage of electrical cables and compressed air/water hoses into containment during refueling outages to support maintenance activities. Each of the two penetrations are comprised of flange connections on both sides of containment. The in-containment flanges are equipped with double O-Rings, which form a double containment isolation boundary. The in-containment blind flanges are provided with pressure test connections to permit pressure testing between the O-Rings. During plant outages, a temporary configuration is used to provide a containment pressure seal while the penetration blind flange is removed from service. Both the O-Rings and temporary blind flange assemblies prevent leakage through the penetrations in the event of an accident.

3.8.1.1.4 Base Slab and Shell-Base Slab Connection

The seams on the base slab and reactor cavity liner are full penetration butt-welded and are covered with leak chase channels. The leak chase channels are arranged in zones in the same manner as those on the exterior shell liner.

There are two penetrations through the base slab for recirculation lines. These are similar to penetrations used in the exterior shell. Weld seams between the liner and the penetration sleeve and between the penetration sleeve and internal, are covered with leak chase channels. The volume in the end of the penetration internal has a fitting for pressurization. These leak chase channels and the volume in the end of the penetration internal are connected in the zones of pressurization used for liner leak chase channels.

The detail of the shell-base slab connection is shown in Figure 3.8-14. The vertical wide flange steel beams provide a gradual transition of load carrying elements between the base slab and the cylinder, and resist the radial bending moments and shears. The beams are keyed and grouted in a groove at the base slab and extend approximately 20 feet up the wall. They do not participate in resisting either uplift due to pressure, or shear and tension forces due to earthquake.

The 3-foot 8-inch thick cylinder wall is designed to offer minimum bending resistance at the junction with the base slab. To achieve this the wall is divided into three layers, with the contact surface between the layers designed as a slip surface. The 12-inch inner layer, next to the liner plate, provides stiffness to the liner plate. The L-shaped stud anchors, welded to the liner plate, and layers (1) and (2) of the wall reinforcing bars are in this layer. The middle layer is the wide flange steel beams. The voids between the beam webs are filled with concrete. The outer layer is 20 inches thick. Layers (3) through (6) of the wall reinforcing bars are in this layer. The slip surface between layers is provided by covering both flanges of the steel beams with two sheets of Johns-Manville #60 asbestos sheet packing. This packing is graphite coated on one side, and the two sheets are placed with the graphite-coated sides in contact. PG&E has successfully used this means of providing sliding supports on penstock piers for several years. The inert nature of the material, and the fact that it is completely isolated from the atmosphere by a minimum of 20 inches of concrete, combine to ensure that it will be fully effective throughout the lifetime of the plant.

The detail at the bottom of each of these three layers is shown in Figure 3.8-14. The innermost and outermost layers have a 1-inch neoprene pad to allow slight rotation without crushing of the concrete. The center layers, consisting of the beams, have a 5-inch-deep pocket in which the beams are placed and grouted.

The diagonal wall reinforcing extends to the bottom of the base slab for anchorage, as shown in Figure 3.8-15. The base slab bars are bent up at 45° and passed through the diagonal bars. The ends of the base slab bars are provided with a mechanical anchorage consisting of a Cadweld sleeve and a steel plate.

The shell liner is anchored to the base slab by Number 14 rebar welded to the bottom course liner plate, which is 3/4-inch-thick. These rebars are embedded 8-1/2 feet in the base slab concrete.

3.8.1.1.5 Internal Structure

The internal structure that is shown in Figures 3.8-16 through 3.8-22 consists of the following parts:

(1) The lower operating floor at elevation 91 feet is a 2-foot-thick concrete slab placed over the containment structure base slab liner.

(2) The circular crane wall is a 3-foot-thick, 106-foot-OD reinforced concrete wall, concentric with the exterior shell, and extending vertically from the containment structure base slab liner at elevation 89 feet to the main operating floor at elevation 140 feet. The runway for the 200-ton polar gantry crane is located on top of the circular crane wall. This wall is anchored to the containment structure base slab by Number 18 reinforcing bars. This anchorage is developed through the containment structure base slab liner by means of Cadweld sleeves welded to each side of the liner at the same locations. The polar crane is shown in Figure 3.8-23.

(3) The reactor shield wall is a 34-foot-OD, 17-foot-ID reinforced concrete wall. This wall is anchored to the containment structure base slab in the same manner as the circular crane wall.

(4) The fuel transfer canal is a stainless steel lined cavity that can be filled with water during refueling. The vertical walls of the fuel transfer canal are 4 feet thick.

(5) The main operating floor at elevation 140 feet is a 3-foot-thick concrete slab supported by the circular crane wall and the fuel transfer canal walls. This slab is thickened locally up to 7 feet near openings.

(6) Main steam line restraint towers are reinforced concrete buttresses extending from the main operating floor at elevations 140 to 184 feet.

(7) Annulus platforms are structural steel platforms at elevations 117 and 140 feet, located between the circular crane wall and the exterior shell. Steel framing is also provided at elevations 106 feet 8 inches and 101 feet 5 inches for support of piping. Figures 3.8-21 and 3.8-22 provide the structural steel framing details for these platforms.

3.8.1.1.6 Polar Crane

The polar crane structural steel frame consists of:

(1) Two main box girders 120 feet long, 10 feet deep and 4 feet wide, spaced 24 feet apart

(2) Four gantry legs, 52 feet long and made of tapered box sections supporting the girders

(3) Two sill beams, 28 feet long with box sections to connect the gantry legs

(4) Four tie beams connecting main girders and gantry legs

The arrangement as described above is shown in Figure 3.8-23.

The sill beams are supported by two wheel assemblies each and are restrained by guide struts. These struts allow the wheels to uplift during a seismic event but guide the wheels back on to the rail.

3.8.1.2 Applicable Codes, Standards, and Specifications

3.8.1.2.1 Codes and Standards

The following codes and standards were used, insofar as they are applicable, in the design and/or construction of the containment structure:

(1) ACI Standard Building Code Requirements for Reinforced Concrete (ACI 318-63)

(2) Manual of Standard Practice for Detailing Reinforced Concrete Structures (ACI 315-65)

(3) Recommended Practice for Evaluation of Compression Test Results of Field Concrete (ACI 214-65)

(4) Inspection of the Cadweld Rebar Splice (Erico Products, Inc., RB-5M 768)

(5) Recommended Practices for Welding Reinforcing Steel, Metal Inserts, and Connections in Reinforced Concrete Construction, American Welding Society, AWS D 12.1-61

(6) AISC Specification for the Design, Fabrication, and Erection of Structural Steel for Buildings, February 12, 1969

(7) Construction of the containment structure liner conforms to the applicable parts of Part UW, "Requirements for Unfired Pressure Vessels Fabricated by Welding," Section VIII, ASME Boiler and Pressure Vessel Code, 1968 Edition, including Addenda through Summer 1968

(8) Those parts of penetration insert plates, penetration sleeves, airlocks, and access hatches, which form part of the pressure boundary, conform to Class B requirements of Section III, ASME Boiler and Pressure Vessel Code, 1968 Edition, including Addenda through Summer 1968

(9) Code for Welding in Building Construction, AWS D 1.0-69. Work performed prior to December 12, 1969 is in accordance with the earlier edition, AWS D 1.0-66. For inspection of non-ASME structural welds or new non-ASME work performed after January 1, 1988, the guidelines of Nuclear Construction Issues Group (Visual Weld Acceptance Criteria, Vol. 1-3, EPRI Report No. NP-5380, September 1987) (Reference 27) may be used except for those cases where:

   (a) Fatigue is a governing design condition

   (b) The weld allowables are permitted to be higher than those allowed by AWS D1.1 (such as the full penetration welds evaluation for the HE)

   (c) The weld is part of work performed in the ASME Section XI Inservice Inspection Program.

(10) Stud welding is in accordance with the Supplement to American Welding Society Specifications AWS D 1.0-66 and AWS D 2.0-66 on Requirements for Stud Welding

(11) Materials, and the quality control tests for materials conform to ASTM standards

(12) Pressure tests of the containment structure, leak chase channels, double penetration volumes, volumes between double seals, and volumes between double isolation valves are in accordance with the requirements of ANSI N45.4-1972, Leakage Rate Testing of Containment Structures for Nuclear Reactors, dated March 16, 1972

(13) SG 12, Instrumentation for Earthquake, dated March 10, 1971

(14) SG 18, Structural Acceptance Test for Concrete Primary Reactor containments, dated October 27, 1971

(15) ASME Section III, Division 2, 1980

(16) ASME Section III, Division 1, Subsection NE, 1974

(17) American Petroleum Institute (API) Code 650, Welded Steel Tanks for Oil Storage

(18) United States of America Standards Institute (USASI) - N6.2 Safety Standard for the Design, Fabrication and Maintenance of Steel Containment Structures, for Stationary Nuclear Power Reactors

3.8.1.2.2 Regulatory Guides

The following guidance documents were issued after construction at the DCPP was partially completed:

(1) SG 10, Mechanical (Cadweld) Splices in Reinforcing Bars of Concrete Containments, dated March 10, 1971

(2) RG 1.15, Testing of Reinforcing Bars for Category I Concrete Structures, dated December 28, 1972

(3) SG 19, Nondestructive Examination of Primary Containment Liner Welds, dated August 11, 1972

(4) RG 1.55, Concrete Placement in Category I Structures, dated June 1973

Because the corresponding programs for the DCPP were conservatively formulated, the inspection provided essentially equals, and in many cases exceeds, that provided by the regulatory position in the guides. Detailed comparisons of the program used for the DCPP with the regulatory position of RG 1.15, SG 10, and SG 19 are presented in Tables 3.8-1 through 3.8-3, respectively. The quality assurance program for the DCPP meets the requirements of RG 1.55. In regard to RG 1.55, the references used for guidance are those listed in Appendix A of the RG, as they existed at the time of the Preliminary Safety Analysis Report (PSAR).

3.8.1.2.3 ACI-ASME for Containments

The technical requirements of the code (Reference 3) were derived from the Building Code Requirements for Reinforced Concrete (ACI 318-71), from Section III, Division 1, of the ASME Boiler and Pressure Vessel Code, and from other codes and standards commonly applied to containment structure design, fabrication, and examination. The requirements for the DCPP containment structures are based on those same codes and standards, except that in many cases an earlier edition was applied to DCPP.

Tables 3.8-1, 3.8-2, and 3.8-3 compare the DCPP programs for reinforcing steel, Cadweld splices, and nondestructive examination of the liner with the regulatory position in RG 1.15, SG 10, and SG 19, respectively.

The general requirements of the code require third party inspection for all containment structure fabrication and construction. For DCPP, third party inspection was provided for fabrication and installation of all containment structure penetrations in accordance with the Class B requirements of Section III, ASME Boiler and Pressure Vessel Code.

3.8.1.3 Loads and Loading Combinations

3.8.1.3.1 Design Loads

The following loads were considered in the design of the containment structure:

3.8.1.3.1.1 Dead Loads

Dead loads consist of the weight of concrete, reinforcing steel, steel liner, structural steel, and permanent equipment loads. Equipment loads are supplied by the manufacturers.

3.8.1.3.1.2 Live Loads

Live loads consist of temporary equipment loads and a uniform load to account for the miscellaneous temporary loadings that may be placed on the structure.

3.8.1.3.1.3 Internal Pressure Due to Loss-of-Coolant Accident

The design peak internal pressure used for design purposes is 47 psig, which is greater than any of the peak pressures calculated in the detailed analysis reported in Chapter 6.

For design purposes, a maximum pressure differential of 15 psi due to the hypothetical LOCA was assumed to exist between the volume within the circular crane wall and the surrounding containment structure volume. The pressurizer enclosure maximum pressure differential was assumed to be 4 psi due to the vent openings provided. These values are greater than the values calculated in the detailed analysis reported in Chapter 6.

3.8.1.3.1.4 Loads Due to Thermal Expansion

These are loads resulting from the internal temperatures associated with normal operation and the hypothetical LOCA. The maximum internal atmospheric temperature during normal operation is 120°F. The temperature transients associated with the LOCA pressure and temperature are shown in Appendix 6.2C of this FSAR Update. The analyses of Appendix 6.2C correspond to a design load factor of 1.0. To determine the temperature transients for load factors equal to 1.25 and 1.5, steam tables are used.

3.8.1.3.1.5 Loads Due to Postulated Pipe Ruptures and Missile Impact

Design of the internal structure includes calculation of the effects of forces from postulated pipe ruptures transmitted through pipe restraints and equipment supports, jet forces for postulated pipe ruptures, and forces resulting from postulated missile impact. The forces from postulated pipe ruptures are calculated as described in Section 3.6. The forces from postulated missile impact are calculated as described in Section 3.5.

3.8.1.3.1.6 Earthquake Loads

Earthquake loads are based on a time-history modal superposition analysis of the containment structure and surrounding rock mass, as appropriate, as described in Section 3.7.2.

3.8.1.3.1.7 Wind Loads

Wind loads are determined in accordance with the criteria presented in Section 3.3.

3.8.1.3.1.8 Test Pressure

Internal pressure is applied to test the structural integrity of the containment vessel up to 115 percent of the design pressure. For this structure, the test pressure is 54 psig.

3.8.1.3.1.9 Negative Pressure

Negative pressure consists of loading from an internal negative pressure of 3.5 psig. This negative pressure has taken into account the Technical Specification limit on lower bound containment pressure and on inadvertent containment spray actuations, which would result in a 70°F temperature decrease.

3.8.1.3.1.10 Crane Operating Loads

Crane-operating loads include:

(1) Live load impact = (LI) = 0.2L

(2) Lateral operating load = (LAT) = 0.1 (L+TD)

(3) Longitudinal operating load = (LONG) = 0.1 (L+TD)

where:

L = Crane rated live load
TD = Trolley dead weight

3.8.1.3.2 Loading Combinations

The following loading combinations are used in design of the containment structure elements.

3.8.1.3.2.1 Operating Conditions

(1) Exterior Structure and Base Slab

Dead load, thermal load, DE, and negative pressure are considered as follows:

$$C = D + T_O + DE + NP \qquad (3.8\text{-}1)$$

where:

C	=	required capacity of section based on the methods described in Section 3.8.1.5.1
D	=	dead load of structure and equipment loads
T_O	=	thermal loads during normal operating conditions
DE	=	loads resulting from the DE
NP	=	load due to negative pressure

(2) Internal Structure

For concrete structures, dead load, live load, thermal load, and DE load are considered as follows:

$$C = D + L + T_O + DE \qquad (3.8\text{-}2)$$

For annulus steel structures, the load combinations are:

$$C = D + T_O + TH + FL \qquad (3.8\text{-}3)$$

$$C = D + T_O + TH + FV + RVOT + DE \qquad (3.8\text{-}4)$$

where:

FL	=	friction loads applied in the direction of thermal movements
FV	=	fast valve closure load
L	=	live load
RVOT	=	relief valve opening thrust load
TH	=	restrained thermal loads of the supported piping

(3) Polar Crane

C = D + TD + L + LI

C = D + TD + L + LAT

C = D + TD + L + LONG

C = D + TD + DE

3.8.1.3.2.2 Accident Conditions

(1) Exterior Shell and Base Slab

$U = 1.0D \pm 0.05D + 1.5P_A + 1.0T''$ (3.8-5)

$U = 1.0D \pm 0.05D + 1.25P_A + 1.0T' + 1.25DE$ (3.8-6)

$U = 1.0D \pm 0.05D + 1.0P_A + 1.0T + 1.0DDE$ (3.8-7)

$U = 1.0D \pm 0.05D + 1.0P_A + 1.0T + 1.0HE$ (3.8-8)

where:

U	=	required load capacity of section based on the methods described in Section 3.8.1.5.2
P_A	=	load due to accident pressure
T	=	load due to maximum temperature associated with $1.0P_A$
T'	=	load due to maximum temperature associated with $1.25P_A$
T"	=	load due to maximum temperature associated with $1.5P_A$
DDE	=	loads resulting from the DDE
HE	=	loads resulting from the HE

(2) Internal Structure

For concrete structures, dead load, live load, earthquake load, compartment pressurization, pipe reactions associated with a postulated pipe rupture, jet forces, and missile loads are considered wherever occurring as follows:

U = D + L + DDE + CP + R + J + M (3.8-9)

U = D + L + HE + CP + R + J + M (3.8-10)

For annulus steel structures, the load combinations are:

U = D + DDE + THA + FV + RVOT (3.8-11)

U = D + HE (3.8-12)

where:

CP	=	compartment pressurization associated with a pipe break
R	=	pipe reactions associated with a postulated pipe rupture
J	=	jet impingement load
M	=	missile impact load
THA	=	restrained thermal expansion loads of the supported piping

(3) Polar Crane

U = D + TD + DDE + T_O

U = D + TD + L + HE

where:

T_O	=	thermal load induced by the temperature differential between the crane structure and supporting concrete structure, during operating condition
U	=	capacity of the section as determined from an increase of allowable stresses by a factor of 1.7

3.8.1.4 Design and Analysis Procedures

3.8.1.4.1 Analysis of Containment Cylinder and Dome

For the loading conditions described in Section 3.8.1.3.2, the exterior wall is subjected to membrane forces and moments. These forces and moments are shown in Figures 3.8-27 through 3.8-34, and have been calculated based on the overall elastic behavior of containment exterior wall and dome in accordance with the conventional close form solution. An exception is that at the juncture of cylinder wall and base slab, the meridional moment and shear forces are computed as described in Section 3.8.1.3.1.4.

The stresses in the reinforcing steel and concrete subject to the above membrane forces and moments are computed by assuming that the concrete cracks under tension. This involved resolving compatibility and equilibrium equations by an iterative method. The stress analysis is performed with two sets of assumptions: (a) the effect of the liner plate is neglected, and (b) the liner plate is included as a stress-carrying element. Since

the thicknesses of the cylinder and dome are small in comparison with the radii of curvature, they are analyzed as a thin walled shell structure.

(1) *Internal pressure and dead load*

The calculated membrane forces due to axisymmetric loads, such as internal pressure and dead load, are shown in Figure 3.8-27.

(2) *Earthquake*

Membrane forces are from the finite element, time-history modal superposition analysis described in Section 3.7.2. The plots of these membrane forces in the cylinder and dome due to the DE, DDE, and HE are shown in Figures 3.8-28 and 3.8-29, respectively. Shear forces in the dome due to the vertical input were calculated. Vertical input produces only radial shear, but no membrane shear. Radial shears were negligible when compared to membrane shears.

(3) *Wind*

Membrane forces from wind are shown in Figure 3.8-34. These are less than the membrane forces due to an earthquake.

(4) *Temperature*

Temperature loads are considered thermal gradients in the reinforced section, including the liner plate. The analysis procedure for thermal load is described in Section 3.8.1.4.4.

The combined membrane forces for the four accident loading conditions are shown in Figures 3.8-30, 3.8-31, 3.8-32, and 3.8-33.

3.8.1.4.2 Liner Anchors

The liner anchors are designed so that they have sufficient strength and flexibility to withstand any combination of liner stress and deformation that can be reasonably assumed to occur under accident loading conditions. The liner plate system is evaluated by developing allowable loads for attached threaded studs to support the mechanical or piping system. The load transfer mechanism from the external mechanical loads through the liner plate to the concrete stud system is developed to ensure the transfer of all loads into the concrete shell with all elements remaining elastic, while maintaining the leaktight boundary.

The concrete anchors are capable of accommodating the displacement of the liner plate under the operating and accident loading conditions.

3.8.1.4.3 Equipment and Personnel Hatch Openings

Membrane forces are transferred around the equipment hatch and personnel hatch openings by means of hexagonal-shaped steel collars to which the reinforcing steel is attached.

The analysis of the equipment hatch and personnel hatch openings takes into account the following:

(1) Direct membrane forces in the shell

(2) Force concentrations in the shell

(3) Bending effect in the shell

The area of the containment shell adjacent to the opening is extended beyond the opening far enough to make the effects of the opening negligible. This area is represented by a finite element mesh consisting of three parallel layers of plate elements which are interconnected by transverse beam elements representing the transverse normal and shear stiffness of concrete wall. The outer surface represents the hexagonal plate and outside reinforcement, the inner surface represents the sleeve, the liner plate and the inner reinforcement, and the intermediate layer represents the additional reinforcement around the opening. The hexagonal plate, sleeve, and liner plate are modeled by isotropic plate elements, and the reinforcement by orthotropic elements, in which the principal directions coincide with the directions of the reinforcement. The stiffness of concrete in the membrane directions is not included, because under tension the concrete is assumed to be cracked. The finite element model is shown in Figure 3.8-35. The analysis is performed by using BSAP/CE 800 computer program.

For axisymmetric loading, the vertical boundaries are restrained in the hoop direction. For the application of tangential shear force, the lower horizontal boundaries are restrained in the vertical and tangential directions. The vertical movement of the lower horizontal boundary is always restrained.

The internal pressure is applied to a large area of the shell wall adjacent to the opening and on the hatch. Since the hatch is not a part of the model, this pressure is transferred to the nodal point around the opening as nodal loads. The pressure on the containment shell and the nodal loads around the opening are applied in the radial direction. By examining the equilibrium of the sector of the wall isolated for modeling, having boundary conditions as described above, hoop membrane forces are induced to the model at the boundary conditions in which the following equation of equilibrium is met:

$$N\Theta = pR \qquad (3.8\text{-}13)$$

where:

$N\Theta$	=	hoop force
p	=	internal pressure
R	=	radius of cylinder

The isostress plots are shown in Figures 3.8-40 through 3.8-42. These stresses are the results of the load combination shown by Equation 3.8-5, which controls the stress evaluation.

3.8.1.4.4 Juncture of Cylinder and Base Slab

At the base of the cylinder, radial expansion from internal pressure is considered compatible with the stiffness of the base slab. In this region, the cylinder undergoes a transition from a very small radial displacement at the base slab to full membrane displacement a short distance up from the base slab. This displacement results in longitudinal curvature in the cylinder.

A system consisting of structural steel wide flange beams, embedded in the bottom 20 feet of the concrete cylinder wall and keyed into the base slab, as shown in Figure 3.8-14, provides radial shear strength. These structural steel beams are located continuously around the circumference of the cylinder and provide bending and shear strength adequate to ensure the integrity of the wall in the transition region.

3.8.1.4.5 Base Slab

The containment base slab is evaluated by performing static analysis of the model shown in Figure 3.8-43. The model is divided into discrete segments represented by beam elements in the two horizontal directions, which simulate the two way action of the base slab. The interconnecting nodal points are supported by horizontal and vertical springs which represent the properties of the underlying foundation rock. The horizontal and vertical stiffness of the containment shell, crane wall, and the reactor cavity are also represented by beams in the respective directions. The base slab model is analyzed for load combinations pertaining to the containment exterior structure as described in Sections 3.8.1.3.2.1 and 3.8.1.3.2.2.

The seismic loads resulting from the containment and the interior structures are applied at the appropriate nodal points. When these loads cause tension at the supports, the springs are released and an iterative analysis is performed until equilibrium is achieved. The results of the analyses are shown in Table 3.8-4, along with the corresponding allowable values.

3.8.1.4.6 Internal Structure

3.8.1.4.6.1 Concrete Structure

The principal structural features and design methods of the containment internal concrete structure are as follows:

The operating deck at elevation 140 feet is supported by the 3-foot-thick, 106-foot-OD circular crane wall, 4-foot-thick fuel transfer canal walls, and structural steel columns placed on the periphery next to the containment wall. The slab within the circular crane wall is, in general, 3 feet thick. Because of irregular shape, it is represented by approximate models with negative moments based on clamped edges and positive moments based on hinged edges. Because of large openings, it was necessary to thicken parts of the slab to 7 feet, and these parts are treated as beams spanning between the circular crane wall and fuel transfer canal walls. Outside the circular crane wall the operating deck consists of a 1-foot 6-inch-thick concrete slab supported on the circular crane wall and on steel beams on the periphery; steel grating is placed over steel beams. Lateral forces are transmitted to the circular crane wall through diaphragm action of concrete slabs. The circular crane wall provides support for the operating floor at elevation 140 feet and also acts as a primary system transmitting lateral loads into the base.

3.8.1.4.6.2 Annulus Structure

The principal structural features and design methods of the annulus structure are:

The structure consists of four main framing levels at elevations 140, 117, 106, and 101 feet. This framing system is located between the circular crane wall and the containment exterior shell. The operating deck at elevation 140 feet consists mainly of a 1-foot 6-inch-thick concrete slab supported on the circular crane wall and on steel beams by columns on the periphery near the exterior containment shell. Portions of the floor consist of steel grating supported on steel beams.

The framing system is anchored to the crane wall which provides all lateral support; lateral forces are transmitted to the circular crane wall through diaphragm action of the concrete slab at elevation 140 feet, and by structural framing system at other floor elevations. Vertical support is provided by the crane wall around the inner perimeter and by the concrete base slab at elevation 90.5 feet around the outer perimeter of the annulus. The annulus framing system is not attached to the exterior shell of the containment.

The annulus structure is modeled into a three-dimensional computer model and is analyzed by the BSAP computer program for Unit 1 and the GT STRUDL and SAP2000 computer programs for Unit 2, using a method of equivalent static loads to represent seismic forces. Stresses in internal structure of containment building, including selected structural steel elements in the annulus framing system, are listed in Table 3.8-5.

3.8.1.4.7 Polar Crane

The polar crane is analyzed using a conventional frame analysis technique. The seismic analysis is described under Section 3.7.

3.8.1.4.8 Computer Programs

The main computer programs used for static and dynamic analyses of containment structure are listed in Table 3.8-6. The table also describes the general function of the programs and their respective verification measures.

3.8.1.5 Structural Acceptance Criteria

The structural acceptance criteria for the containment structure exterior shell and internal structure are as follows:

3.8.1.5.1 Operating Conditions

For operating conditions, the containment structure is designed for the allowable stresses of the applicable code such as ACI 318-63, AISC Specification for the Design, Fabrication, and Erection of Structural Steel for Buildings, and ASME Boiler and Pressure Vessel Code, except that the increase in allowable stress or decrease in load factor usually allowed for load combinations involving earthquake or wind forces is not used.

3.8.1.5.2 Accident Conditions

For accident conditions, the containment structure is designed for overall elastic behavior under all load combinations, except at the juncture of containment exterior wall and base slab where inelastic analysis was performed by taking into consideration cracking of concrete under tension.

For structural elements designed by strength method, the yield stress of the material is reduced by ϕ factors, which are determined as follows:

Exterior shell reinforcing, structural steel embedded in exterior shell, and liner plate	$\phi = 0.95$
Other structural steel	$\phi = 0.90$[(a)]
Reinforced concrete in base slab and internal structure	ϕ factor in accordance with ACI 318-63

(a) See footnote in discussion of loading combinations in Section 3.8.2.

The yield strength values of material under a non-Hosgri event are governed by the following codes:

Reinforced concrete	ACI 318-63
Structural steel	AISC
Hexagonal collars of equipment and personnel hatches	ASME Sect. III, Div. 2, and ASME Sect. III, Div. 1
Penetration sleeves	ASME Sect. III, Div. 1
Liner plate	Table CC-3720-1[(b)] ASME Sect. III, Div. 2

The yield strength of steel and the ultimate strength of concrete for the HE are taken as the average values of properly substantiated test results. However, in no case are the yield values used in strength computations of structural steel greater than 70 percent of the corresponding average ultimate strength values determined by the tests. The ϕ factors described above are still applicable in the HE. The average strength values for concrete are shown in Table 3.8-6A. The minimum and average yield and ultimate strength values for reinforcing and structural steel are shown in Table 3.8-6B.

For structural steel and concrete elements designed by normal working strength method, the allowable stresses determined by AISC and ACI 318-63 codes, respectively, are increased by 1.6 for the DDE and 1.7 for the HE, except for shear in structural steel which is determined by the Von Mises criterion as outlined in the commentary of AISC.

3.8.1.5.3 Factors of Safety

The factors of safety for the exterior shell and internal structure of the containment structure are at least as great as indicated by the load factors given in Section 3.8.1.3.2. The calculated stresses for the exterior shell are given in Figures 3.8-37 through 3.8-39, and the calculated stresses for the internal structure are given in Table 3.8-5.

Separations between the containment structure and the auxiliary building are adequate to ensure these structures will not impact each other when subject to design load combinations. Calculated displacements, separations, and factors of safety against impact are shown in Table 3.8-5B.

The relative seismic displacements between the containment structure exterior shell and the internal structure have been calculated as the sum of the maximum seismic displacement of each structure. Except for a few localized areas, the minimum cold gap

(b) Table CC-3720-1 is referred to establish acceptable design strain levels for the liner plate. The construction of the liner plate is pursuant to the specifications of Section 3.8.1.2.1(7).

between the internal structure and the exterior shell is 2 inches. The factors of safety against contact for all areas, including the localized areas, are greater than 2.33 for the governing seismic event, the DDE, after thermal effects on the gap are considered. The calculated factors of safety for the HE are greater than those for the DDE.

3.8.1.6 Materials, Quality Control, and Special Construction Techniques

During the first 16 months of construction, a PG&E civil engineer was assigned to the construction site on a full-time basis. This engineer was familiar with, and had participated in, the design of the containment structure. For the period he was on site, he was part of the Quality Assurance Department (described in Chapter 17) and his responsibilities included performing audits on the various construction quality assurance programs. This engineer was qualified as ANSI Level II for radiographic, magnetic particle, ultrasonic, and dye penetrant methods of nondestructive testing. In addition, other engineers from PG&E who were involved in the design of the containment structure maintained daily contact with the site by telephone calls, and made periodic visits to the site during construction.

Inspectors from PG&E's engineering staff performed regularly scheduled shop inspections on materials and components for the containment structure.

PG&E's construction staff provided a complete staff of resident engineers, field engineers, quality control engineers, and inspectors for supervision and inspection of construction operations at the site. Their responsibilities for quality control of the containment structure were as follows:

(1) To inspect materials delivered to the jobsite and examine supplier's certified test reports of physical and chemical properties

(2) To inspect handling and placing of concrete, reinforcing bars, embedded items, and forms

(3) To maintain an adequate force of qualified supervisory personnel at all times

(4) To maintain qualified personnel, as a part of its field engineering force, to perform a thorough inspection of each significant construction operation

(5) To supervise and be fully responsible for the quality of work performed by contractors

(6) To maintain records of inspections that were performed

Many of PG&E's construction personnel at the site attended a formal course of instruction in radiographic, magnetic particle, ultrasonic, and dye penetrant methods of

nondestructive testing. PG&E technicians staffed the onsite materials laboratory where tests on cement, aggregate, concrete, and reinforcing steel were performed.

3.8.1.6.1 Concrete

Concrete is a dense, durable mixture of sound aggregate, cement, water, and such admixtures as may be found advantageous. The concrete design strengths used in the containment structure are:

exemption 4

Exterior Shell	3,000 psi
Base Slab	5,000 psi
Internal Structures	5,000 psi

The concrete compressive strength and the modulus of elasticity values used in the analysis for load combinations, including the HE, are given in Table 3.8-6A.

Concrete construction meets, as a minimum, the requirements of ACI 318-63, Building Code Requirements for Reinforced Concrete.

(1) *Cement*

Cement is clean, fresh, Type II, low alkali, moderate heat, Portland cement conforming to the specifications of ASTM C 150, except that the PG&E specification is more stringent in requiring that the compressive strengths for any mill-run or bin be not less than 1,700 psi at 3 days, 2,700 psi at 7 days, and 4,000 psi at 28 days, and that the loss on ignition be less than 2 percent. In addition, the following Optional Chemical Requirements of ASTM C 150 are required by PG&E specification:

(a) Total alkalis of the cement, calculated as the percent of Na_2O + 0.658 times the percent of K_2O, is limited to 0.60 percent.

(b) The sum of tricalcium silicate and tricalcium aluminate is limited to 58 percent. During manufacture, samples of cement were taken once each shift, or at the rate of one sample for every 2,000 barrels. After the quality history was established, in accordance with Section 5 of the Federal Test Method Standard Number 158a, testing was performed at the reduced testing rate specified in that standard. A report of the tests made on each sample was sent to PG&E engineering research staff. In addition, each shipment of cement was accompanied by a mill certificate, and a report of the average of all the individual tests was sent with the initial delivery from each new lot or grind.

Cement shipped to the batch plant was not placed in a plant bin unless it had been accepted by PG&E. In addition to the tests the cement

manufacturer performed, PG&E made the following tests on each new lot to ensure conformance with ASTM C 150:

- ASTM C 109:	Compressive Strength of Hydraulic Cement Mortars (using 2-inch cube specimens)
- ASTM C 114:	Chemical Analysis of Hydraulic Cement
- ASTM C 151:	Autoclave Expansion of Portland Cement
- ASTM C 191:	Time of Setting of Hydraulic Cement by Vicat Needle
- ASTM C 204:	Fineness of Portland Cement by Air Permeability Apparatus

The tests prescribed in ASTM C 114 were also performed periodically during storage to check for any effect on cement characteristics. These tests supplemented visual inspection during storage.

(2) *Aggregates*

Aggregates consist of inert materials that are clean, hard, durable, free from organic matter, not coated with clay or dirt, and conforming to ASTM Designation C 33, Standard Specification for Concrete Aggregates. In addition to the requirements of ASTM C 33, the PG&E specification requires that:

(a) Sodium Sulfate Test for Soundness (ASTM C 88). For fine aggregate, the portion retained on a Number 50 screen, be limited to a weighted average loss of no more than 8 percent after 5 cycles. For coarse aggregate, the weighted average loss after 5 cycles be no more than 10 percent

(b) Sand Equivalent Test (California Division of Highways Test Method Number California 217). Sand equivalent value be at least 75

(c) The fineness modulus be within the limits of 2.6 to 2.9

(d) Los Angeles Rattler Test (ASTM C 131) for coarse aggregate. Loss by weight using Grading A, be a maximum of 10 percent by weight at 100 revolutions and 40 percent by weight at 500 revolutions

(e) Cleanness Value (California Division of Highways Test Method Number California 227-B) for coarse aggregate. Cleanness value be at least 75

(f) Specific Gravity (ASTM C 127) for coarse aggregate. Specific gravity on a saturated surface dry basis be at least 2.60

(g) The chloride content of aggregate be no more than 440 ppm

The following tests were performed by the aggregate supplier at the frequency indicated:

Test	ASTM Destination	Frequency
Screen Analysis and Fineness Modulus	C 136	B
Clay Lumps and Friable Particles	C 142	D
Minus 200 Mesh	C 117	D
Organic Impurities	C 40	D
Soft Particles	C 235	D
Lightweight Particles	C 123	D
Specific Gravity	C 127 & 128	C
Absorption	C 127 & 128	C
Unit Weight	C 29	C
Los Angeles Abrasion (coarse)	C 131	E
Soundness	C 88	E
Effect of Organic Impurities on Fine Aggregate	C 87	F
Petrographic	C 295	F
Sand Equivalent Test	California Test Method 217	A
Cleanness Value	California Test Method 227-B	C

Frequency:

(a) Once each 100 tons, but not more than 10, nor less than one per day of production

(b) Once each 2,000 tons, but not less than one test per week during production

(c) Every 10,000 tons, or once every 10 days of production

(d) Every 20,000 tons, or once every 20 days of production

(e) Once for initial source approval, then once per 30,000 tons

(f) One per deposit

All tests except the Soundness Test (ASTM C 88) and Soft Particles (ASTM C 235) were also performed by PG&E on a periodic basis. Samples were taken at the place where the aggregate entered the batch bin.

(3) *Admixtures*

Admixtures conformed to the following ASTM standards:

(a)	Pozzolan	ASTM C 618	
(b)	Air Entraining Agent	ASTM C 260	
(c)	Water Reducing Agent	ASTM C 494	1.1.1, Type A

A certificate of compliance accompanied each load of admixture delivered to the construction site.

(4) *Water*

Water is clean and free from deleterious amounts of silt, oil, acids, alkali, salts, and organic substances. Chlorides, calculated as Cl, are limited to 1,000 ppm, and sulfates, calculated as SO_4, are limited to 1,000 ppm.

(5) *Concrete Mixing, Placing, and Testing*

The contractor was required to submit concrete mix designs meeting PG&E specification requirements. The mixes were designed in accordance with Method 2, Section 308, of ACI 301. PG&E's material

testing laboratory made sample batches of the proposed mixes and tested them according to:

(a) ASTM C 192, Making and Curing Concrete Test Specimens in the Laboratory

(b) ASTM C 39, Compressive Strength of Molded Concrete Cylinders

(c) ASTM C 143, Slump of Portland Cement Concrete by the Pressure Method

For each design mix, 7-day and 28-day compressive strength tests were made on 6 x 12 inch cylindrical samples in the laboratory.

The contractor was required to submit lift drawings, which showed the location of all construction joints and embedded items, for approval by PG&E. The lift drawings were approved prior to concrete placement. At construction joints in all structural concrete, the surface of the hardened concrete was roughened to expose the coarse aggregate by either bush hammering, wet sandblasting, or cutting with an air-water jet. Prior to placing the next lift of concrete, the surface of the hardened, cleaned concrete was wetted and given a 1/2-inch coat of bonding mortar on all horizontal joints. The bonding mortar had the same sand-cement ratio as the concrete mix, and had a water-cement ratio such as to make a thick slurry but, at most, no greater than that for the concrete. Vertical joints in walls were provided with shear keys. Vertical joints were staggered by at least 6 inches.

The concrete was batched and mixed in an automatic batching and mixing plant located at the construction site. Approved concrete mixes were punched on cards, and the appropriate card was inserted into the control console to initiate batching. The console automatically printed out the quantities of each material in the batch, and the time, date, batch number, and mix identification for each batch. Prior to plant startup, all weighing equipment was certified. This equipment was periodically checked to ensure continuing accuracy.

A full-time PG&E inspector checked the batching and mixing operation. The maximum temperature of concrete at placement was as follows:

(1) 55°F, base slab

(2) 70°F, internal structure and exterior shell

The concrete was placed within 45 minutes after introduction of water to the mix.

Concrete placement was inspected by PG&E inspectors. The concrete was either maintained in a moist condition for 7 days by approved methods, or coated with an approved curing compound.

Concrete was sampled at the frequency required by ACI 301-66. Sampling concrete and making, curing, and testing specimens was in accordance with:

(1)	ACTM C 172	Sampling Fresh Concrete
(2)	ASTM C 31	Making and Curing Concrete Compressive and Flexural Strength Test Specimens in the Field
(3)	ASTM C 39	Compressive Strength of Molded Concrete Cylinders
(4)	ASTM C 143	Slump of Portland Cement Concrete
(5)	ASTM C 231	Air Content of Freshly Mixed Concrete by the Pressure Method

All taking and testing of concrete samples was done by qualified PG&E personnel.

Compressive strength tests were evaluated in accordance with ACI 214. PG&E specifications required that 95 percent of all cylinders tested meet or exceed the specified strength for 5000 psi concrete, and 90 percent meet or exceed the specified strength for 3000 psi concrete. The correlation between field specimens and design strengths was evaluated continuously during construction.

The average strengths and coefficients of variations of concrete tested were:

Mix	Design, psi	Cement[a], sacks/yd	Average Strength, psi	Coefficient of Variation	Number of Tests
Unit 1					
7AP	5000	7.5	6500	4.3%	11
8	5000	7.5	6400	6.5%	134
8A	5000	7.0	6220	8.3%	18
8AP	5000	6.6	6120	6.4%	43
9BP	3000	6.0	3800	7.0%	87
Unit 2					
8A	5000	7.0	6680	6.7%	40
8AP	5000	6.6	6200	7.1%	101

exemption 4

These coefficients of variation represent "excellent control" as defined in Table 2 of ACI 214-65.

Concrete in Unit 1 and 2 containments is Class AP for base slab and interior concrete and Class BP for cylinder and dome. Mixes designated 7AP, 8, 8A, and 8AP are Class AP. Mix 9BP is Class BP.

---

[a] Cement and pozzolan

3.8.1.6.2 Reinforcing Steel

Reinforcing steel is deformed billet-steel bar conforming to ASTM Designation A 615. All reinforcing bars in the containment structure are Grade 60, except for the following, which are Grade 40:

(1) Liner anchorages in the base slab

(2) Anchorages on the structural steel beams embedded at the base of the containment structure wall

Table 3.8-1 compares the program for testing of reinforcing bars at the DCPP to the requirements of RG 1.15, which was issued after construction at DCPP was partially complete. Table 3.8-1 also indicates those areas where the PG&E specification is more stringent than ASTM A 615.

Heat number identification was maintained on reinforcing steel from the start of manufacture through placement in the structure.

Physical and chemical test results were sent to the construction site with the first load of steel from each heat. Test values were checked by PG&E inspectors or quality control engineers.

Detailing was in accordance with ACI Standard 315-65, Manual of Standard Practice for Detailing Reinforced Concrete Structures. Bars to be bent were cold bent around pins of the following minimum diameters:

(1) Stirrups and ties - four times the bar diameter

(2) Number 8 bars or smaller - six times the bar diameter

(3) Numbers 9, 10, and 11 - eight times the bar diameter

(4) Numbers 14 and 18 - ten times the bar diameter

Fabrication tolerances were as follows:

(1) Cut length:

Number 14 and 18 bars	0 inch, -3/8 inch
All other bars	±1 inch

(2) Depth of truss bars:

Number 18 bars	±2 inch
All other bars	0 inch, -1/2 inch

(3) Stirrups, ties, and spirals: ±1/2 inch

(4) All other bends:

Number 14 and 18 bars	±1/2 inch
All other bars	±1 inch

Placement tolerances were as follows:

(1) Concrete cover to formed surfaces:

Number 14 and 18 bars	−1/2 inch, +2 inch
All other bars	±1/2 inch

(2) Longitudinal location of bends:

Number 14 and 18 bars	±2 inch
All other bars	±1 inch

(3) Depth of bars in slabs:

8 inches or less in thickness	±1/4 inch
Over 8 inches in thickness	±1/2 inch

(4) Lateral location in the plane of reinforcing: ±2 inch

Occasionally, reinforcing steel bars had to be moved to avoid interferences. In this situation, a bar could be moved, within the plane of the reinforcing layer or curtain, up to one-half the specified spacing. If this was not sufficient, the resulting arrangement was submitted to PG&E for approval. Also, if the bar had to be moved out of the reinforcing layer or curtain to avoid an interference by more than one bar diameter or the above tolerances, whichever was greater, the resulting arrangement was submitted to PG&E for approval.

Tack welding to reinforcing bars was not permitted.

Reinforcing steel placement was inspected by contractor quality control inspectors and by PG&E inspectors.

The average and minimum properties of the tested Number 18 bars in the containment structure were as follows (these values are also shown in Table 3.8-6B):

(1)	Yield	- minimum	61,750 psi
		- average	66,854 psi

(2)	Tensile	- minimum - average	93,750 psi 105,992 psi
(3)	Elongation	- minimum - average	7.0% 9.4%

3.8.1.6.3 Splices

(1) Cadweld Splices

Cadweld splices were used at all locations for primary reinforcing in the exterior shell and base slab. Cadweld splices were used in a few locations in the internal structure.

Quality control procedures for Cadweld splices are described in Table 3.8-2 that compares the program used at the DCPP to that required by SG 10. SG 10 was issued after construction at DCPP was partially complete.

The average and minimum strengths of tested Cadweld tensile samples were:

(a) Minimum tensile strength 85,000 psi

(b) Average tensile strength 97,725 psi

(c) Number of tests 641

(d) Number of Cadwelds placed 19,068

(2) Butt-welded Splices

Butt-welded splices were used in a few locations where there was insufficient room to properly mount the Cadweld crucible. The quality control measures applied are the same as those described in Section 3.8.2.6.3 for butt-welded splices.

(3) Lap Splices

Lap splices are in accordance with ACI 318-63.

3.8.1.6.4 Liner, Penetration Sleeves, and Penetration Internals

The containment structure liner is carbon steel, conforming to ASTM A 516, Carbon Steel Plates for Pressure Vessels for Moderate and Lower Temperature Service, Grade 70. This steel has a minimum yield strength of 38,000 psi, a minimum tensile

strength of 70,000 psi, and a minimum elongation of 17 percent in an 8-gage length at failure. Charpy V-notch impact tests were performed at +20°F, in accordance with ASTM A 370.

Penetration sleeves conform to one of the following three material specifications:

(1) ASTM A 106, Seamless Carbon Steel Pipe for High Temperature Service, Grade B, with the additional requirement that Charpy V-notch impact tests be performed at 0°F

(2) ASTM A 333, Seamless and Welded Steel Pipe for Low Temperature Service, Grade 1, except that Charpy V-notch impact tests are performed at 0°F

(3) ASTM A 516, Carbon Steel Plates for Pressure Vessels for Moderate and Lower Temperature Service, Grade 70, to ASTM A 300, except that Charpy V-notch impact tests were performed at 0°F

For all three material specifications, the Charpy impact tests were in accordance with the requirements of Paragraph N-330 of ASME Section III, 1968 edition.

Penetration internals conform to the following material specifications:

(1) Equipment and personnel hatches are ASME SA 516, Grade 70, to SA 300 with Charpy impact values at 0°F, in accordance with paragraph N-330 of ASME Section III, 1968 edition

(2) Carbon steel flued heads are ASME SA 105, Grade II, with Charpy impact tests at 0°F, in accordance with paragraph NB-2300 of Section III, ASME B&PV Code, 1971 edition. Ultrasonic and magnetic particle inspections are performed in accordance with Paragraphs NB 2542 and NB 2545, respectively

(3) Stainless steel flued heads are ASME SA 182, Grade F 304. Ultrasonic and liquid penetrant inspections are performed in accordance with Paragraphs NB 2542 and NB 2546, respectively

Welded studs attached to the liner meet the requirements of ASTM A 108, Grade 1015-1018.

The Charpy impact test temperatures stated in the paragraphs above were selected to be at least 30°F below the lowest service temperature in accordance with the ASME B&PV Code, Section III, 1968 Edition for Class B (containment) vessels. For future repair, replacement, or alteration of ferritic containment pressure boundary material, the notch toughness test requirements of Section III, NE-2300 will be used in lieu of the original requirements. Charpy impact tests will be performed at or below the

lowest service temperature and material 5/8 inch or less in thickness will be exempt from notch toughness testing. Further information on notch toughness testing of containment materials appears in Section 3.1.8.14.

Mill test reports certifying the physical and chemical properties of the liner plate delivered to the jobsite were required from the steel supplier. The average and minimum properties of liner plate are as follows:

The Charpy impact test temperature for the hexagonal collars was selected to be at least 30°F below the lowest service temperature in accordance with the ASME B&PV Code, Section III, 1968 Edition for Class B (containment) vessels. For future repair, replacement, or alteration of the hexagonal collars, the notch toughness test requirements of Section III, NE-2300 will be used in lieu of the original requirements. Charpy impact tests will be performed at or below the lowest service temperature and material 5/8 inch or less in thickness will be exempt from notch toughness testing. Further information on notch toughness testing of containment testing materials appears in Section 3.1.8.14.

Reactor Pit and Floor Plates		Unit 1	Unit 2
Yield Strength	- minimum	43,800 psi	39,800 psi
	- average	51,400 psi	55,100 psi
Tensile Strength	- minimum	71,000 psi	74,000 psi
	- average	76,500 psi	78,900 psi
Elongation	- minimum	19%	17%
	- average	25%	24%
Total number of heats		16	11
Total number of slabs		58	62
Total number of tests		58	62

Cylinder and Dome		Unit 1	Unit 2
Yield Strength	- minimum	41,900 psi	38,100 psi
	- average	48,800 psi	46,100 psi
Tensile Strength	- minimum	70,200 psi	70,100 psi
	- average	74,900 psi	73,681 psi
Elongation	- minimum	19%	18%
	- average	26.5%	25.4%

Cylinder and Dome	Unit 1	Unit 2
Total number of heats	23	22
Total number of slabs	251	255
Total number of tests	251	255

Fabrication of the containment structure liner conforms to the applicable parts of Part UW, Requirements for Unfired Pressure Vessels Fabricated by Welding, Section VIII, ASME Boiler and Pressure Vessel Code.

All of the welds were visually examined by contractor quality control inspectors. All field welds were also visually examined by PG&E inspectors.

Table 3.8-3 compares the program for nondestructive testing of containment structure liner welds, including penetration sleeves and inserts, used on the DCPP to that required by SG 19, which was issued after construction at DCPP was partially complete.

Erection tolerances for the liner were as follows:

The liner of the completed structure shall be substantially round. At points not more than 4 inches above the base, the radius of the 3/4-inch liner shall be 69 feet 11-13/16 inches plus or minus 1/2-inch. The maximum diameter of the 3/8-inch liner shall not exceed 140 feet 4 inches and the minimum diameter shall not be less than 139 feet 8 inches.

The liner shall be erected true and plumb. At any point the out-of-plumb shall not exceed 1/240 of the height of the point above the base. For any plate (10 feet ± in height), the out-of-plumpness shall not exceed 1/120.

Flat spots or local out-of-roundness shall not exceed 2 inches in 15 feet of arc.

The base liner shall not deviate from a plane surface between anchorages by more than 1/240.

Stud welding was in accordance with the Supplement to AWS Specification D1.0-66. The tolerance of the location of each stud was ± 1/2-inch. At the beginning of each work day, each welder attached at least two test studs that were then tested by bending the stud approximately 45 percent toward the plate to demonstrate the integrity of the stud-to-plate weld. If failure occurred in the weld, the welding procedure or technique was corrected and two successive studs successfully welded and tested before further studs were attached to the liner plate. These test studs were allowed to remain in place but are not considered as a part of the regular stud pattern required by the design. A 100 percent visual inspection of liner and stud anchors was made prior to pouring concrete.

3.8.1.6.5 Structural Steel

Hexagonal collars at the equipment hatch and personnel hatch meet the requirements of ASTM A 516, Grade 70, and ASTM A 300, except that Charpy V-notch impact tests were performed at 20°F.

The following quality control procedures were followed in the fabrication of the hexagonal steel collars at the equipment hatch and personnel hatch openings:

(1) The 4-inch-thick plate for the edge pieces was ultrasonically examined in accordance with ASTM A 435, except that scanning covered 100 percent of the surface.

(2) Fabrication conformed to the applicable parts of Part UW, Requirements for Unfired Pressure Vessels Fabricated by Welding, of Section VIII of the ASME Boiler and Pressure Vessel Code. All welds are full penetration butt welds and were 100 percent radiographed in accordance with Paragraph UW-51.

(3) The reinforcement plates were heat treated after fabrication in accordance with Paragraph UCS-56, Requirements for Postweld Heat Treatment, of Section VIII of the ASME Boiler and Pressure Vessel Code.

3.8.1.7 Testing and Inservice Surveillance Requirements

After each containment structure was complete, with liner, concrete, and all electrical and piping penetrations, equipment hatch and personnel locks in place, tests were performed as discussed in the following sections.

3.8.1.7.1 Structural Integrity Test

The structural integrity test was performed by pressurizing the containment structure with air up to 115 percent of design pressure, or 54 psig. During this test, structural deflections were measured, crack patterns in the concrete were measured and photographed, and strains in the liner and reinforcing steel measured electrically and recorded. The deflections, crack patterns, and strains were compared to the theoretical predictions to verify the structural integrity of the containment structure. The structural integrity test of each containment structure meets the requirements of RG 1.18, Structural Acceptance Test for Concrete Primary Reactor Containments.

The Unit 1 containment structure is a prototype concrete primary reactor containment, as defined in RG 1.18.

For the structural integrity test, the pressure was increased in increments to the maximum of 54 psig. Measurements were made at 0, 15, 25, 35, 47, and 54 psig during pressurization and again during depressurization. At each pressure level, the

deflection and strain gage readings were made after a 1-hour wait to allow adjustment of strains. The crack patterns were recorded both before and immediately after the test and at the maximum pressure level achieved during the test.

The instrumentation for Unit 1 was as follows:

The radial and vertical growth was measured by means of calibrated targets attached to the exterior shell and sighted by means of high magnification theodolites. Radial deflections were measured at three points on each of six equally spaced meridians: at the springline, at mid-height of the cylinder, and at the top of the base slab. Vertical deflections were measured at the springline and at the top of the dome.

The radial and tangential deflections of the containment structure wall were measured at twelve locations adjacent to the equipment hatch, which is the largest opening.

The pattern of cracks that exceed 0.01-inch in width were mapped or photographed near the base-wall intersection, at mid-height of the wall, at the springline of the dome, and around the equipment hatch. At each location, an area of at least 40 square feet was mapped or photographed.

Strain measurements were made at the following locations, in accordance with the requirements for prototype containment structures:

(1) In the wall at the top of the base mat

(2) In the wall at the equipment hatch, with one gauge located approximately 0.5 times the wall thickness from the edge of the opening

(3) In the wall at the level of the springline

(4) In the wall where pure membrane stress is anticipated, i.e., where there are no discontinuities

Inasmuch as the concrete is assumed cracked, and the strength of the concrete is neglected, strain measurements were made on the reinforcing steel and liner, rather than in the concrete. At the equipment hatch, additional strain measurements were made on the structural steel hexagonal collar. In the wall at the top of the base slab, additional strain measurements were made on the structural steel wide flange beams.

The method used for attaching strain gauges to Number 18 reinforcing bars is shown in Figure 3.8-44.

In evaluating the results of the structural integrity test, the deflection measurements were considered the most reliable result.

Strains, deflections, and crack patterns were compared to the theoretical predictions. The acceptance criterion was that actual readings had to be within 20 percent of the predicted values. This criterion was based on an evaluation of:

(1) Residual stress due to concrete shrinkage

(2) Measurement errors

(3) Temperature variations

(4) As-built deviations of the containment shell from a circular shape

(5) Actual results of other structural integrity tests (primarily at the R. E. Ginna plant)

The deflection measurement and crack mapping program for Unit 2 was identical to that for Unit 1.

3.8.1.7.2 Overall Integrated Leakage Rate Tests

During the depressurization phase of the structural integrity test, the sequence was stopped at 47 psig to conduct an overall integrated leakage rate test at design pressure.

During the overall integrated leakage rate tests, the double penetration and weld seam leak chase channel zones were open to the atmosphere inside the containment structure.

All leakage rate tests are conducted and evaluated in accordance with Appendix J of 10 CFR 50, Option B, as modified by approved exemptions.

3.8.1.7.3 Sensitive Leakage Rate Tests

A sensitive leakage rate test can be performed at some future date with only the volume of the weld seam leak chase channels and double penetrations included in the test. A sensitive leakage rate test would be performed with penetrations and leak chase channels at not less than the peak calculated containment internal pressure (Pa), and with the containment structure at atmospheric pressure.

3.8.1.7.4 Inservice Surveillance Requirements

Periodic leakage rate testing is performed in accordance with the requirements of Appendix J of 10 CFR 50. Inservice surveillance to ensure continued containment integrity is discussed in Section 6.2.1.4. Instrumentation employed to monitor containment status is described in Section 6.2.1.5.

3.8.2 OTHER DESIGN CLASS I STRUCTURES (AUXILIARY BUILDING)

3.8.2.1 Description of the Auxiliary Building

The auxiliary building is located between the Unit 1 and Unit 2 containment structures. It contains the control room that includes consoles and a fuel handling area for each unit. In addition, the auxiliary building contains equipment for the chemical and volume control systems, the safety injection systems, the residual heat removal systems, the component cooling water systems, the liquid radwaste systems, the gaseous radwaste system, and others.

The main floor levels in the auxiliary building are at elevations 85, 100, 115, and 140 feet. Elevations 60 and 73 feet are below ground level, which is at elevation 85 feet, except for the east side of the building where ground level is at elevation 115 feet. Floor plans at elevations 100, 115, and 140 feet are shown in Figures 3.8-60, 61, and 62.

The foundation of the auxiliary building is divided between 3 elevations. The structure is supported at elevations 85 feet (areas GE, GW, and L) 100 feet (area J), and elevation 60 feet (areas H and K).

Figure 1.2-2, Plant Layout, shows relative locations of the plant buildings. The general arrangement of equipment in the auxiliary building, including the fuel handling areas, is shown in Figures 1.2-4 through 1.2-11, Figures 1.2-21 through 1.2-26, and Figures 1.2-29 and 1.2-30. Generally, one-half of the auxiliary building is a mirror image of the other, with each half of the structure containing equipment for one unit. The control room is located at elevation 140 feet. The two fuel handling areas that contain the spent fuel pools, the fuel handling cranes, fuel racks, and related equipment are located on each side of the east end of the auxiliary building with the top of the spent fuel pools at elevation 140 feet.

The auxiliary building is a reinforced concrete shear wall structure, except for the fuel handling area crane support structure which is a structural steel moment resisting and braced frame structure supported on elevation 140 feet and extending up to elevation 188 feet. The shear walls and slabs of the auxiliary building are generally 2 feet thick. The walls of the spent fuel pools are 6 feet thick except for local areas around the fuel transfer tubes. The foundation slabs under the spent fuel pools have a minimum thickness of 5 feet. The spent fuel pool sides and bottoms are lined with stainless steel, 1/4-inch-thick on the bottoms and 1/8-inch nominal thickness on the sides. Representative concrete outlines, reinforcing steel arrangements, and structural steel details for the auxiliary building are shown in Figures 3.8-45 through 3.8-59.

The 125-ton overhead crane in the fuel handling area, shown in Figure 3.8-59, is equipped with restraints that prevent derailing from motions associated with an earthquake.

The only connections between the auxiliary building and other structures are the fuel transfer tube and miscellaneous piping. The fuel transfer tube is fitted with expansion bellows that allow relative movement between the auxiliary building, the containment structure exterior shell, and the internal structure of the containment structure. The design of the expansion bellows considers the maximum axial and lateral relative deflection. Piping systems are analyzed for the maximum relative displacements of the auxiliary building and other structures, and the piping anchor points in the structures are designed to withstand the resulting forces.

3.8.2.2 Applicable Codes, Standards, and Specifications

The following codes and standards are used in the design, construction, inspection, and testing of the auxiliary building:

(1) ACI Standard Building Code Requirements for Reinforced Concrete (ACI 318-63), except that design loading combinations are as described in Section 3.8.2.3.2

(2) Manual of Standard Practice for Detailing Reinforced Concrete Structures (ACI 315-65)

(3) Recommended Practice for Evaluation of Compression Test Results of Field Concrete (ACI 214-65)

(4) Inspection of the Cadweld Rebar Splice (Erico Products, Inc., RB-5M768)

(5) Recommended Practices for Welding Reinforcing Steel, Metal Inserts, and Connections in Reinforced Concrete Construction, American Welding Society AWS D12.1-61

(6) AISC Specification for the Design, Fabrication, and Erection of Structural Steel for Buildings, February 12, 1969

(7) Code for Welding in Building Construction, AWS D1.0-69. Work performed prior to December 12, 1969 is in accordance with the earlier edition, AWS D1.0-66. For inspection of non-ASME structural welds or new non-ASME work performed after January 1, 1988, the guidelines of Nuclear Construction Issues Group (Visual Weld Acceptance Criteria, Vol. 1-3, EPRI Report No. NP-5380, September 1987) may be used except for those cases where:

    (a) Fatigue is a governing design condition.

    (b) The weld allowables are permitted to be higher than those allowed by AWS D1.1 (such as the full penetration welds evaluation for HE).

(c) The weld is part of work performed in the ASME Section XI Inservice Inspection Program.

(8) Stud welding is in accordance with the Supplement to American Welding Society Specifications AWS D1.0-66 and AWS D2.0-66 on Requirements for Stud Welding

(9) Materials and the quality control tests for materials conform to ASTM standards

RG 1.15, Testing of Reinforcing Bars for Category I Concrete Structures (dated December 28, 1972), and RG 1.55, Concrete Placement in Category I Structures (dated June 1973), were issued after construction of the DCPP was nearly complete. A comparison of the program used for the DCPP with the regulatory position of RG 1.15 is presented in Table 3.8-1. The quality assurance program for the DCPP meets the requirements of RG 1.55. In regard to RG 1.55, the references used for guidance are those listed in Appendix A of the RG, as they existed at the time of the PSAR.

3.8.2.3 Loads and Loading Combinations

3.8.2.3.1 Design Loads

The following loads are considered in the design of the auxiliary building.

3.8.2.3.1.1 Dead Loads

Dead loads consist of the weight of the structure, and permanent equipment loads.

3.8.2.3.1.2 Live Loads

Live loads consist of temporary equipment loads and a uniform load to account for the miscellaneous temporary loadings that may be placed on the structure.

3.8.2.3.1.3 Earthquake Loads

Earthquake loads are based on a time-history modal superposition analysis. This analysis is described in Section 3.7.2.

3.8.2.3.1.4 Wind Loads

Wind loads are determined in accordance with the criteria presented in Section 3.3. However, considering the UBC and ASCE Paper 3269 pressures, the forces due to wind are much less than those due to earthquake; consequently, seismic loads, rather than wind, are entered into the load combination equations.

3.8.2.3.1.5 Thermal Loads

Thermal loads are loads induced by local increases in temperature. Thermal loads result from normal operating conditions and from postulated accident conditions.

3.8.2.3.1.6 Pipe Reaction Loads

Pipe reactions that result from hydraulic forces, thermal expansion, and seismic events, are transferred to the structure through pipe supports. Pipe reaction loads result from normal operating conditions and postulated accident conditions.

3.8.2.3.1.7 Jet and Missile Loads

Jet and missile loads are localized forces on structures in the immediate vicinity of a postulated pipe break. Jet forces result from the impingement of high energy fluid on an object. Missile forces result when a part possessing kinetic energy strikes an object.

Missile forces are calculated by the methods described in Section 3.5. Jet forces and pipe reactions from a postulated broken pipe are calculated as described in Section 3.6.

3.8.2.3.1.8 Pressure Loads

Pressure loads are forces generated by a postulated pipe break. Pressures from a postulated broken pipe are calculated as described in Section 3.6.

3.8.2.3.2 Loading Combinations

3.8.2.3.2.1 Normal Conditions

Dead load, live load, loads from the DE, thermal loads, and pipe reactions are considered in all possible combinations. Inasmuch as working stress design is used for normal operating loads, the factored load approach is not used. For each structural member, the combination of these loads that produces the maximum stress is used for design. Stated in equation form:

$$C = D + L + DE + T_o + R_o \qquad (3.8\text{-}14)$$

where:

C	=	required capacity of member based on the methods described in Section 3.8.2.5.1
D	=	dead load of structure and equipment loads
L	=	live load
DE	=	loads resulting from the DE
T_o	=	thermal loads during normal operating conditions
R_o	=	pipe reactions during normal operating conditions

3.8.2.3.2.2 Abnormal Conditions

Dead load, live load, earthquake loads, and loads associated with accidental pipe rupture are considered in the following combinations; for each structural member, the combination that produces the maximum stress is used for design:

Concrete Structural Elements

$$U = D + L + T_A + R_A + 1.5\ P_A \qquad (3.8\text{-}15)$$

$$U = D + L + T_A + R_A + 1.25\ P_A + 1.0\ (Y_j + Y_m + Y_r) + 1.25\ DE \qquad (3.8\text{-}16)$$

$$U = D + L + T_A + R_A + 1.0\ P_A + 1.0\ (Y_j + Y_m + Y_r) + DDE \qquad (3.8\text{-}17)$$

$$U = D + L + T_A + R_A + 1.0\ P_A + 1.0\ (Y_j + Y_m + Y_r) + HE \qquad (3.8\text{-}18)$$

where:

T_A = thermal loads on structure generated by a postulated pipe break, including T_O

R_A = pipe reactions on structure from unbroken pipe generated by postulated pipe break conditions, including R_O

PA = pressure load within or across a compartment and/or building generated by a postulated pipe break, and including an appropriate dynamic factor (DLF) to account for the dynamic nature of the load

Y_j = jet load on structure generated by a postulated pipe break, including an appropriate DLF

Y_m = missile impact load on a structure generated by, or during, a postulated pipe break, such as a whipping pipe, including an appropriate DLF

Y_r = reaction on structure from broken pipe generated by a postulated pipe break, including an appropriate DLF

U = ultimate strength required to resist design loads based on the methods described in ACI 318-63. See Section 3.8.2.5.2 for equation 3.8-16 through 3.8-18

DDE = loads resulting from the DDE

HE = loads resulting from an HE

Steel Structural Elements

Where elastic working stress design methods are used[a][b]:

$$1.6S^{(a)} = D + L + T_A^{(b)} + R_A + P_A \qquad (3.8\text{-}19)$$

$$1.6S^{(a)} = D + L + T_A^{(b)} + R_A + P_A + 1.0(Y_j + Y_m + Y_r) + DE \qquad (3.8\text{-}20)$$

$$1.6S^{(a)} = D + L + T_A^{(b)} + R_A + P_A + 1.0(Y_j + Y_m + Y_r) + DDE \qquad (3.8\text{-}21)$$

$$1.7S = D + L + T_A^{(b)} + R_A + 1.0P_A + 1.0(Y_j + Y_m + Y_r) + HE \qquad (3.8\text{-}22)$$

Where plastic design methods are used:

$$0.90Y^{(a)} = D + L + T_A^{(b)} + R_A + 1.5P_A \qquad (3.8\text{-}23)$$

$$0.90Y^{(a)} = D + L + T_A^{(b)} + R_A + 1.25P_A + 1.0(Y_a + Y_m + Y_r) + 1.25DE \qquad (3.8\text{-}24)$$

$$0.90Y^{(a)} = D + L + T_A^{(b)} + R_A + 1.0P_A + 1.0(Y_j + Y_m + Y_r) + DDE \qquad (3.8\text{-}25)$$

$$1.0Y = D + L + T_A^{(b)} + R_A + 1.0P_A + 1.0(Y_j + Y_m + Y_r) + HE \qquad (3.8\text{-}26)$$

where:

S = required section strength based on elastic design methods and the allowable stresses[c] defined in Part 1 of the AISC "Specifications for the Fabrication and Erection of Structural Steel for Buildings," February 12, 1969

Y = required section strength based on plastic design methods[c] described in Part 2 of AISC Specifications for the Design, Fabrication and Erection of Structural Steel for Buildings, February 12, 1969

(a) For existing structures, the 1.6 factor applied to the required section strength, S, and the 0.90 reduction factor applied to the required section strength, Y, are increased to 1.7 and 1, respectively. In such situations, however, it is verified that deflections will not result in the loss of function of any safety-related system.

(b) Thermal loads are neglected when it can be shown that they are secondary and self-limiting in nature and where the material is ductile.

(c) See Section 3.8.2.5 regarding material properties used in conjunction with load combinations including HE.

For both concrete and steel structural elements, both cases of L having its full value present during the postulated pipe rupture, or being completely absent, are checked.

3.8.2.4 Design and Analysis Procedures

Structural analysis of the auxiliary building is performed by the traditional methods of engineering analysis for structural steel and reinforced concrete structures. These methods are based on the principles of equilibrium, compatibility of deformations, and predictions of material strength by the methods of the AISC Specifications for the Design, Fabrication, and Erection of Structural Steel for Buildings (AISC Code), and the ACI Standard Building Code Requirements for Reinforced Concrete (ACI Code).

The use of these codes is discussed in Section 3.8.2.5. The following sections discuss the specific design methods used for the structural steel and concrete parts of the auxiliary building.

3.8.2.4.1 Structural Steel

The fuel handling area crane support structure is a 370 x 60 x 50-foot high steel framed structure clad with metal siding and covered by metal decking and built-up roofing. The structure is supported on concrete walls at elevation 140 feet on the eastern side of the auxiliary building. Lateral forces are resisted by steel cross-braced frames in the north-south direction, moment resisting frames in the east-west direction, and by the roof, which is a trussed and cross-braced diaphragm covered with metal decking.

Acceleration profiles and forces from the analyses described in Section 3.7.2.1.7.1 are applied to a detailed static model of the entire fuel handling area crane support structure to obtain forces for the stress evaluation of the structural members and connections and to obtain structural displacements. Various crane and lifted load positions are considered. The stress evaluation is carried out for the load combinations described in Section 3.8.2.3. Stresses are evaluated against the criteria in Section 3.8.2.5. The calculated stress ratios for the most critical members are given in Table 3.8-7.

3.8.2.4.2 Concrete

The vertical and the lateral load-resisting system of the auxiliary building consists of reinforced concrete columns and walls tied together with reinforced concrete slabs. The evaluation of these elements is carried out for the loading combinations given in Section 3.8.2.3, according to the criteria in Section 3.8.2.5.

The seismic forces and moments are based on the response of the auxiliary building seismic models described in Section 3.7. A detailed analytical model of the auxiliary building is then developed to distribute forces and moments to the various walls, diaphragms, and columns.

Slabs

Slabs are evaluated separately for out-of-plane loads and in-plane loads.

For out-of-plane loads, shear stresses and moments are calculated assuming one-way or two-way slab action as appropriate. Out-of-plane capacity-to-demand ratios for selected slabs are shown in Tables 3.8-8 through 3.8-10. The slab in-plane capacities are investigated at critical sections. The selection of these sections is based on the location of numerous openings across the entire section of the diaphragm and the magnitudes of shear, moment, and axial forces on the entire section. The in-plane capacity-to-demand ratios for the concrete slabs are shown in Tables 3.8-11 through 3.8-13.

Walls

The critical wall elements are selected based on the magnitude of demand loads and presence of openings. The forces and moments for the governing load combination in those elements are compared to their respective capacities, and the capacity-to-demand ratios are shown in Tables 3.8-14 through 3.8-16.

Concrete Columns

The concrete columns are evaluated for axial and flexural loads. Flexural loads on columns due to the vertical loads are determined by considering frame action with the slabs. Flexural loads include the effect of minimum eccentricity specified by ACI 318-63. Column moments due to interstory drift are found to be negligible. Capacity-to-demand ratios for selected columns are shown in Table 3.8-17.

3.8.2.4.3 Load Dissipation to the Foundation

The adequacy of the structural system, at and below elevation 85 feet, to dissipate lateral loads to the rock foundation is evaluated for the load combinations given in Section 3.8.2.3.2. The results, given in Tables 3.8-18 through 3.8-23, and illustrated for HE loads in Figures 3.8-63 and 3.8-64, indicate the adequacy of the system to dissipate the loads.

3.8.2.4.4 Computer Programs

Computer programs used in the structural analysis, and the verification measures used, are listed in Table 3.8-6.

3.8.2.5 Structural Acceptance Criteria

For DE and DDE load combinations, the nominal design strength for concrete and specified yield strength for reinforcing and structural steel are considered. For load combinations including HE, however, the actual material properties are used. See

Sections 3.8.2.6.1, 3.8.2.6.2, and 3.8.2.6.4 for material properties associated with concrete, reinforcing steel, and structural steel, respectively. See Section 3.8.2.6.5 for allowable stresses for bolted connections. Ductility, when applied for HE load combinations, is in accordance with Table 3.8-24.

3.8.2.5.1 Normal Loads

For normal loads, the auxiliary building is designed for the allowable working stresses of ACI 318-63, as supplemented by Section 3.8.2.5.3, and Part 1 of the AISC Code, except that the increase in allowable stress usually allowed for load combinations involving earthquake forces is not used.

3.8.2.5.2 Abnormal Loads

For abnormal loads, the auxiliary building is designed for overall elastic behavior. For concrete elements, the strength design method of ACI 318-63 applies, as supplemented by Section 3.8.2.5.3. For the evaluation of steel elements using elastic design methods, the allowable stresses are defined in Part 1 of AISC Code. For the evaluation of steel elements using "plastic design," Part 2 of the same AISC specifications applies.

The capacity for the various concrete structural elements is based on the yield strength of the material, reduced by a factor, f, which provides for the possibility that small, adverse variations in material strengths, workmanship, dimensions, and control, while individually within required tolerances and the limits of good practice, occasionally may be additive. The f-factors used are in accordance with ACI 318-63.

For load combinations involving Y_j, Y_m, and Y_r, local stresses due to these concentrated loads may exceed the allowable provided there is no loss of function. See Reference 6, Enclosure Number 3, Document (B), for more detailed information concerning the acceptance criteria for these load combinations.

3.8.2.5.3 In-Plane Loads on Concrete Elements

The design of slab diaphragms and shear walls for in-plane forces is not explicitly covered by ACI 318-63. Section 104 of ACI 318-63 allows criteria based on test data to be used for the design of elements not covered by its provisions. Consequently, the document entitled "Recommended Evaluation Criteria for Diablo Canyon Nuclear Power Plant Auxiliary Building Walls and Diaphragms" (Reference 7) is developed to provide criteria for evaluation of auxiliary building shear walls and floor diaphragms for in-plane seismic forces, including the simultaneous effects of out-of-plane forces.

Accordingly, the structural elements are evaluated as follows:

(1) The columns are evaluated by the provisions of ACI 318-63 for all loading conditions.

(2) The slabs and walls are evaluated for out-of-plane loads according to ACI 318-63, and for in-plane loads according to Reference 7.

3.8.2.5.4 Factors of Safety

The calculated capacity-to-demand ratio for selected structural elements of the auxiliary building are given in Tables 3.8-7 through 3.8-17. In all cases, these ratios are greater than the minimum allowable value of 1. Therefore, all structural elements satisfy the criteria.

The gap between the auxiliary building and the containment structure, as well as the factor of safety against the structure impacting during a seismic event, is discussed in Section 3.8.1.5.3. Separations between the auxiliary building and the turbine building are adequate to ensure these structures will not impact each other when subject to design load combinations. Calculated displacements, separations, and factors of safety against impact are shown in Table 3.8-23A.

3.8.2.6 Materials, Quality Control, and Special Construction Techniques

Sections 3.8.1.6.1 and 3.8.1.6.2 for the containment structure also apply to the auxiliary building, except as superseded by information in the following paragraphs.

3.8.2.6.1 Concrete

Concrete strengths are shown below.

Walls and slabs below elevation 85 feet; slabs 4 feet and thicker at elevation 85 feet; slab at elevation 85 feet bounded by column lines 16.8 - 19.2 - L - H:

Design f'c = 3000 psi (DE and DDE combinations)

All other concrete:

Design f'c = 5000 psi (DE and DDE combinations)

Average 28-day strengths are used with HE load combinations. The average strengths of representative mixes are as follows:

Design Strength	Average 28-day Strength	Number of Tests
3000 psi	3920 psi	167
5000 psi	5650 psi	368

3.8.2.6.2 Reinforcing Steel

Reinforcing steel is ASTM A 615, Grade 40, except in some locations where Grade 60 is used. ASTM minimum values are used with DE and DDE load combinations. Average test values are used with HE load combinations. The average and minimum properties of representative bar sizes, are as follows:

	#8		#11	
	Grade 40	Grade 60	Grade 40	Grade 60
Design Yield Strength, psi	40,000	60,000	40,000	60,000
Average Yield Strength, psi	49,655	66,189	48,302	68,582
Minimum Yield Strength, psi	41,200	60,250	42,950	61,710
Average Tensile Strength, psi	82,236	102,403	81,074	105,822
Minimum Tensile Strength, psi	74,392	96,500	72,940	94,390
Average Elongation, %	18.9	13.94	14.82	14.41
Minimum Elongation, %	13.0	11.0	8.5	9.4
Total Number of Heats	67	18	91	56

3.8.2.6.3 Splices

The majority of splices in the auxiliary building are lap splices, made in accordance with ACI 318-63. Cadweld splices are used in some locations in the auxiliary building. The quality control procedures described for Cadweld splices in the containment structure also apply to Cadweld splices in the auxiliary building.

Butt-welded splices are used where a section of wall has to be temporarily left open for access, and in certain other locations. Butt-welded splices are made in accordance with ACI 318-63, and the American Welding Society's Recommended Practices for Welding Reinforcing Steel, Metal Inserts, and Connections in Reinforced Concrete Construction, using the "short-arc" process or low hydrogen stick electrodes by the shielded arc process. Both processes have minimum preheat and interpass temperatures of 400°F. Completed welds are wrapped with a protective blanket of insulating material to avoid rapid cooling.

Procedure qualification and welder qualification are as follows:

(1) A welding procedure qualification test is made for each position and for each grade and size of bar. The test consists of two tension tests and one nick break test. Bars may not be rolled during welding.

(2) Welder qualification tests are made for each position, type of electrode, grade and size of bar, and joint design. Qualification for one size of bar is considered qualification for all smaller sizes. Each test consists of one tension and one nick break test. Bars may not be rolled during welding.

(3) Tension specimens are tested to failure and must comply with the minimum tensile requirements for the grade of reinforcing steel.

(4) The nick break specimen is broken and visually examined for soundness. The specimen must exhibit the following: the sum of the longest dimension of all inclusions visible in any one joint must not exceed ½-inch; no inclusion may be closer to the weld surface than a distance equal to the largest dimension of the inclusion; there must be no incomplete fusion or lack of penetration or cracks in the weld or base metal.

Testing percentages applicable to butt-welded splices for each welder, position, and grade of bar are as follows:

(1) Two out of the first ten splices

(2) Six out of the next 90 splices

(3) Four out of second and subsequent 100 splice units

Qualification for one size of bar is considered as qualification for all smaller sizes.

3.8.2.6.4 Structural Steel

Structural steel is ASTM A 36 and ASTM A 441; ASTM minimum values are used with DE and DDE load combinations, and average test values are used with HE load combinations. Minimum and average values are as follows:

	ASTM A36	ASTM A441
Design Yield (ksi)	36	42

Testing of structural steel installed through 1977 gave the following:

	ASTM A36	ASTM A441
Average Test Yield (ksi)	43.95	51.62
Average Test Ultimate (ksi)	68.04	75.91

Charpy impact tests were performed on all structural steel at the following temperature:

Framing for pipe rupture restraints	40°F
Structural steel	20°F

3.8.2.6.5 Structural Bolts

Structural bolts are ASTM A307, A325, and A490, allowable stresses per Table 1.5.2.1 of the AISC "Specifications for the Design, Fabrication and Erection of Structural Steel for Buildings," February 12, 1969, are used with the DE, DDE, and HE load

combinations. However, it is acceptable to increase the allowable stresses for the Hosgri load combinations, based on the results of properly substantiated testing (References 34 through 38).

3.8.3 OUTDOOR WATER STORAGE TANKS

3.8.3.1 Description of the Outdoor Water Storage Tanks

The Design Class I outdoor storage tanks, located adjacent to east of auxiliary building, are steel studded tanks with concrete shielding, as shown in Figure 3.8-65, sheets 1 and 2.

There are two refueling water storage tanks and two condensate water storage tanks, one to service each unit of the plant. The firewater and transfer tank, which serves both Units 1 and 2, is made up of two concentric cylindrical steel tanks connected by a common dome roof. The inner cylindrical tank is the firewater tank and the outer tank is the transfer tank. The structural configuration of the condensate tanks is similar to that of the refueling water storage tanks.

The Design Class I tanks are supported on concrete fill down to bed rock and are anchored to bed rock with rock anchors as shown in Figure 3.8-65, Sheet 2.

3.8.3.2 Applicable Codes, Standards, and Specifications

The following codes and standards are used in the design, construction, inspection, and testing of the outdoor water storage tanks.

(1) ACI Standard Building Code Requirements for Reinforced Concrete (ACI 318-63, and ACI 318-71)

(2) Manual of Standard Practice for Detailing Reinforced Concrete Structures (ACI 315-65)

(3) Recommended Practices for Welding Reinforcing Steel, Metal Inserts, and Connections in Reinforced Concrete Construction, American Welding Society AWS D12.1-75

(4) AISC Specification for the Design, Fabrication, and Erection of Structural Steel for Buildings, 6th and 7th Editions

(5) Code for Welding in Building Construction, AWS D1.1-77, Rev. 2. Work performed prior to (December 12, 1969) is in accordance with the earlier edition, AWS D1.0-66. For inspection of non-ASME structural welds or new non-ASME work performed after January 1, 1988, the guidelines of Nuclear Construction Issues Group (Visual Weld Acceptance Criteria,

Vol. 1-3, EPRI Report No. NP-5380, September 1987) may be used except for those cases where:

(a) Fatigue is a governing design condition.

(b) The weld allowables are permitted to be higher than those allowed by AWS D1.1 (such as full penetration weld evaluation for the HE).

(c) The weld is part of work performed in the ASME Section XI Inservice Inspection Program.

(6) Stud loading is in accordance with the Supplement to American Welding Society Specifications AWS D1.0-66 and AWS D2.0-66 on Requirements for Stud Welding

(7) Materials and quality control tests for materials conform to ASTM standards

(8) ASME Section VIII, Division 2, 1974

(9) AWWA D100, American Waterworks Association, Standard to Steel Tanks, Standpipes Reservoirs and Elevated Tanks for Water Storage

3.8.3.3 Loads and Loading Combinations

3.8.3.3.1 Normal Conditions

$$C = D + HS + 1.0\ DE + 1.0\ R_O \qquad (3.8\text{-}27)$$

where:

C	=	required load capacity of section as described in Section 3.8.3.5.1
D	=	dead load of tank
HS	=	hydrostatic load
DE	=	loads resulting from DE
R_O	=	pipe reactions during normal operating conditions, including dead, thermal, and DE loads.

3.8.3.3.2 Abnormal Conditions

$$U = D + HS + 1.0\ DDE + 1.0\ R_A \qquad (3.8\text{-}28)$$

$$U = D + HS + 1.0\ HE + 1.0\ R_A \qquad (3.8\text{-}29)$$

where:

D and HS are defined in Section 3.8.3.3.1, and

U	=	strength required to resist abnormal loads as described in Section 3.8.2.5.2
DDE	=	loads resulting from the DDE
HE	=	loads resulting from the HE
R_A	=	pipe reactions during abnormal conditions, including dead, thermal, and DDE or HE loads

3.8.3.4 Design and Analysis Procedures

Condensate storage tanks, the refueling water storage tanks, the primary water storage tanks, and the fire water and transfer water tanks were originally designed to meet the criteria based on the DE, DDE, and HE. The code used in designing the tanks was AWWA D100, 1967, with stress allowables restricted to those permitted by ASME Section VIII, Division 2. Revised security criteria called for additional resistance to bullet penetration and explosives and required all the above steel tanks, except the primary water storage tanks, to be modified with minimum reinforced concrete protection as determined by Argonne National Laboratory. The Design Class I tanks with concrete protection were reevaluated for DE, DDE, and HE using finite-element computer models as described in Section 3.7.

The stresses in the stiffeners and the steel liner plate around the vault openings were determined by hand calculation and compared with the stress allowables. The forces, moments, and stresses in the refueling water storage tank resulting from dead load, hydrostatic pressure, hydrodynamic loads, and seismic loads are listed in Table 3.8-25. These values are within the allowable limits as described in Section 3.8.3.5.

3.8.3.5 Structural Acceptance Criteria

3.8.3.5.1 Normal Loads

For normal loads, the outdoor water storage tanks are designed for the allowable working stresses of the ACI 318-63 for concrete, Part 1 of the AISC Specification, 6th Edition for structural steel components, and ASME Section VIII, Division 2, 1974, for steel liner plates.

3.8.3.5.2 Abnormal Loads

For abnormal loads, the outdoor water storage tanks are designed for overall elastic behavior. For concrete elements the strength design method of ACI 318-63 applies for DDE loads and of ACI 318-71 for HE loads. For the evaluation of structural steel elements using elastic design methods, for the loading condition including DDE loads, 1.6 times AISC 6th Edition, Part 1 allowables are used; whereas, for the HE load combination, Part 2 of AISC 7th Edition, the Plastic Design method applies.

The steel liner plates are evaluated by using stress intensities as defined in ASME Section VIII, Division 2, 1974, and applying a factor of 0.9 to the minimum specified yield strength for DDE, and 1.0 to the yield strength based on test results for HE load conditions. For local stress intensities around nozzles in the vault opening area for DDE loads, a factor of 1.0 to the minimum specified yield strength applies, whereas for HE loads, a factor of 2.4 to the ASME Section VIII, Division 2, 1974, allowable values applies.

3.8.3.5.3 Factors of Safety

The calculated capacity-to-demand ratios for critical structural elements of the outdoor water storage tanks are greater than the minimum allowable value of 1. Therefore, all structural elements satisfy the criteria.

3.8.3.6 Materials, Quality Control, and Special Construction Techniques

The quality control measures discussed in Sections 3.8.1.6.1 and 3.8.1.6.2 for the containment structure also apply to Design Class I tanks.

3.8.3.6.1 Materials Tank Walls and Roof Dome

Condensate and Inner and Outer Tank Walls of Firewater and Transfer Tank	-	Carbon steel liner plates and stiffeners conform to ASTM A-516 GR 60. The Condensate Storage Tanks are coated with an epoxy coating and the Fire Water and Transfer Tank is coated with Vinyl Paint. Carbon steel studs conform to ASTM A108 GR 1015- 1018.
Refueling Water Tank	-	Stainless steel liner plates and stiffeners conform to ASTM A-240 Type 304L. Stainless steel studs conform to ASTM A276 type 304 annealed.

All Tanks, Except Inner Tank of Firewater and Transfer Tank:

- Concrete strength (minimum specified) f_C = 4 ksi

- Rebar conforms to ASTM A615, GR 60, fy = 60 ksi (minimum specified)

3.8.4 FOUNDATIONS AND CONCRETE SUPPORTS

The foundation structures for the containment and the auxiliary building are included in Sections 3.8.1 and 3.8.2, respectively. The foundations of the Class I outdoor water storage tanks are described in this section.

3.8.4.1 Foundations for Design Class I Tanks

The following Design Class I concrete-protected steel tanks are located adjacent to the east side of the auxiliary building on reinforced concrete foundation slabs:

(1) Condensate water storage tank (one for each unit)

(2) Refueling water storage tank (one for each unit)

(3) Fire water and transfer tank (common to both units)

3.8.4.1.1 Description of the Foundation Slabs

Each of the condensate water storage tanks and refueling water storage tanks has a separate, circular foundation slab. The fire water tank and the transfer tank, which serves both units, are concentric tanks on a common circular foundation slab. Each of the foundation slabs is shown in Figure 3.8-65 and consists of a 1-foot-thick reinforced concrete slab with an integral edge beam tied to a reinforced concrete wall. Each of the tanks, except for the fire water tank, is anchored to its foundation slab with ASTM A 193, Grade B7 anchor bolts. The bolt diameters are 1-1/4 inches for the condensate water storage tanks and the transfer tank, and 1-3/8 inches for the refueling water storage tanks. The wall of the fire water tank is welded to an insert plate in the foundation.

The tank foundation slabs are resting on concrete fill anchored to bedrock with rock anchors. The reinforced concrete protective walls of the steel tanks are anchored to bedrock as shown in Figure 3.8-65, Sheet 2.

3.8.4.1.2 Applicable Codes, Standards, and Specifications

The foundation slabs for the Design Class I outdoor storage tanks listed are designed and constructed in accordance with the ACI 318-63.

3.8.4.1.3 Loads and Loading Combinations

The foundation slabs for the Design Class I outdoor storage tanks are designed for dead loads, hydrostatic load, and seismic load:

$$C = DL + HS + EQ + R \qquad (3.8\text{-}30)$$

where:

C	=	total load on foundation
DL	=	dead load of tank
HS	=	hydrostatic load

EQ	=	maximum seismic loads including inertial, impulsive, and convective loads
R	=	pipe reaction load including dead, thermal, and seismic loads

3.8.4.1.4 Design and Analysis Procedures

The foundation slabs with concrete fill are designed to prevent overturning and sliding of the tank and limit bearing pressure to 80 ksf. The rock anchors attaching the tank to the foundation are designed so that the maximum uplift force is within the allowable capacity provided in Figure 3.8-65, Sheet 2.

3.8.4.1.5 Structural Acceptance Criteria

Stresses in the reinforced concrete foundation slabs are limited to the allowable values in ACI 318-63.

3.8.4.1.6 Materials, Quality Control, and Special Construction Techniques

The quality control measures discussed in Sections 3.8.1.6.1 and 3.8.1.6.2 for the containment structure also apply to the Design Class I tank foundations.

Material strengths for the Design Class I tank foundation slabs are as follows:

(1) Concrete strength of foundation slab and concrete fill is 3000 psi.

(2) Reinforcing steel in foundation slab is ASTM A 615, Grade 40.

(3) Rock anchors conform to VSL 28, strand #ER5-28, with double corrosion protection and are fully grouted with concrete strength of 4000 psi.

3.8.4.2 Concrete and Structural Steel Supports

Concrete and structural steel supports for RCS components are described and evaluated in Section 5.5.14. Loading combinations for these supports are discussed in Section 5.2.

3.8.5 DESIGN CLASS II STRUCTURES CONTAINING DESIGN CLASS I EQUIPMENT

The turbine building and the intake structure are Design Class II structures that contain Design Class I equipment. The turbine building contains the component cooling heat exchangers, emergency diesel generators, 4.16-kV vital switchgear, control room pressurization system, and other Class I systems. The intake structure contains the auxiliary saltwater (ASW) pumps and associated equipment.

To ensure that the Design Class I equipment would not be affected by failure of the Design Class II structures, both the turbine building and the intake structure are evaluated for the HE, using responses from the dynamic analyses discussed in Section 3.7.

The capability of the intake structure to protect the ASW system during design flood events is evaluated to ensure this capability, as described in Sections 2.4 and 3.4.

The OTSC is located in the turbine building buttresses and is designed to meet seismic loading criteria.

3.8.5.1 Turbine Building

3.8.5.1.1 Description

The turbine building was originally designed as a Design Class II structure using static equivalent seismic loads. Subsequently, the building was dynamically analyzed and designed to assure that it would not collapse and impair the function of Class I equipment during a DDE. Later, during the Hosgri evaluation, the building was reevaluated again and upgraded to withstand the Hosgri seismic loads. As a result of the Hosgri evaluation, buttresses and concrete walls were added to the turbine building, and internal modifications, such as reinforcing main columns, strengthening floor diaphragms, and roof and wall bracing, were made.

The turbine pedestal was originally designed as a Design Class II structure, using static equivalent seismic loads. During the Hosgri evaluation, the pedestal was reevaluated and upgraded to withstand the Hosgri seismic loads. As a result of the Hosgri evaluation, six piers were posttensioned and the pedestal-to-building separations were increased along the east and west sides of the pedestal.

The turbine building is located adjacent to the west side of the auxiliary building as shown in Figure 1.2-2, Plant Layout. The general layout of equipment in the turbine building, including the turbine generators, is shown in Figures 1.2-13 through 1.2-20, Figures 1.2-24 through 1.2-27, and Figures 1.2-30 through 1.2-32. Generally, the Unit 1 and Unit 2 portions of the turbine building are opposite hand and similar to the other, with each portion of the structure containing equipment for one unit. Exceptions are the presence of a machine shop and material storage area common to both units in the Unit 1 portion, and the OTSC in the Unit 2 portion of the structure.

Main floor levels in the turbine building are at elevations 85, 104, 119, and 140 feet. The foundation of the building is at elevation 85 feet. Representative plans at the main floor levels roof truss lower chord level, and a typical section are shown in Figures 3.8-66 through 3.8-71.

The turbine building is a reinforced concrete shear wall structure except for the superstructure, which is a structural steel moment resisting and braced frame structure

extending from elevation 140 feet to elevation 217 feet. Shear walls generally range from 16 to 29 inches thick. Floors are 10- to 12-inch-thick reinforced concrete slabs or 1/2-inch-thick steel plate, supported on steel framing and steel columns. The reinforced concrete foundation mat is generally 3 feet thick except under the turbine pedestal, where the thickness is 10 feet. Reinforced concrete turbine pedestals, one for each unit, are located in the building; six piers of each pedestal are posttensioned. The pedestals are structurally isolated from the building floors and extend from the common foundation slab, elevation 85 feet, to elevation 140 feet. Two 135-ton overhead cranes are located in the building.

3.8.5.1.2 Applicable Codes, Standards, and Specifications

The following codes and standards are used in the HE evaluation, and in the design, construction, inspection, and testing of HE modifications to the turbine building:

(1) ACI Standard Building Code Requirements for Reinforced Concrete (ACI 318-71) except that, for the HE evaluation and design, the 1973 Supplement to ACI 318 is used and design load combinations are as described in Section 3.8.5.1.3

(2) Manual of Standard Practice for Detailing Reinforced Concrete Structures (ACI 315-74)

(3) Recommended Practice for Evaluation of Compression Test Results of Field Concrete (ACI 214-65)

(4) Recommended Lateral Force Requirements, 1974 Seismology Committee Structural Engineers Association of California (SEAOC)

(5) Recommended Practices for Welding Reinforcing Steel, Metal Inserts, and Connections in Reinforced Concrete Construction, American Welding Society (AWS D12.1-75)

(6) AISC Specification for the Design, Fabrication, and Erection of Structural Steel for Buildings, February 12, 1969, is generally used for steel structures. AISC Specification, dated November 1, 1978, is also used for evaluating selected connections.

(7) Code for Welding in Building Construction (AWS D1.1 Rev. 2-77). For inspection of non-ASME structural welds or new non-ASME work performed after January 1, 1988, the guidelines of Nuclear Construction Issues Group (Visual Weld Acceptance Criteria, Vol. 1-3, EPRI Report No. NP-5380, September 1987) may be used except for those cases where:

    (a) Fatigue is a governing design condition

(b) The weld allowables are permitted to be higher than those allowed by AWS D1.1 (such as full penetration weld evaluation for the HE)

(c) The weld is part of work performed in the ASME Section XI Inservice Inspection Program

(8) Materials and the quality control tests for materials conform to ASTM standards

3.8.5.1.3 Loads and Loading Combinations

3.8.5.1.3.1 Design Loads

The following loads are considered in the HE evaluation of the turbine building.

3.8.5.1.3.1.1 Dead Loads

Dead loads consist of the weight of the structure, permanent attachments and permanent equipment.

3.8.5.1.3.1.2 Live Loads

Live loads consist of any actual live loads acting on the element considered.

3.8.5.1.3.1.3 Seismic Loads

Seismic loads are based on a response spectrum modal superposition analysis. This analysis is described in Section 3.7.2.

3.8.5.1.3.2 Loading Combination

Concrete Structural Elements

$$U = D + L + HE \qquad (3.8\text{-}31)$$

where:

U	=	Strength determined in accordance with the methods described in ACI 318-71 and 1973 Supplement, except strength of shear walls is based on method described in Section 3(c) of the 1974 SEAOC. (See also Section 3.8.5.1.5.)
D	=	dead load
L	=	live load
HE	=	loads resulting from an HE

Steel Structural Elements

Where plastic design methods are used:

$$Y = D + L + HE \qquad (3.8\text{-}32a)$$

Where elastic working stress design methods are used:

$$1.7S = D + L + HE \qquad (3.8\text{-}32b)$$

where:

S = required section strength based on elastic design methods and the allowable stresses defined in Part 1 of the AISC Specification for the Design, Fabrication, and Erection of Structural Steel for Buildings, February 12, 1969

Y = required section strength based on plastic design methods described in Part 2 of AISC Specification for the Design, Fabrication, and Erection of Structural Steel for Buildings, February 12, 1969 (See also Section 3.8.5.1.5.)

3.8.5.1.4 Design and Analysis Procedures

Structural analysis of the turbine building is based on the traditional methods of engineering analysis for structural steel and reinforced concrete structures. These methods are based on the principles of equilibrium, compatibility of deformations, and predictions of material strength by the methods of the AISC Code and the ACI Code. The use of these codes is discussed in Section 3.8.5.1.5.

The lateral force resisting system of the turbine building above elevation 140 feet consists of moment resisting bents, formed by steel roof trusses and steel plate columns, steel cross-brace frames at exterior walls, and a steel bracing system in the plane of the roof truss lower chords. At and below elevation 140 feet, lateral resistance is provided by concrete and steel plate floors acting as diaphragms; by concrete shear walls; by concrete buttresses along the east and west sides of the building; and by steel cross-braced frames above elevation 104 feet at the north and south ends of the building. Vertical forces are transmitted to the foundation by the steel plate columns, concrete walls, and interior steel columns which support the steel floor framing system.

HE forces on the lateral force resisting system of the turbine building and the turbine pedestal are based on the response of the turbine building and pedestal seismic models described in Section 3.7. In some cases detailed analytical models are developed to calculate building member forces. Structural evaluation of members is performed for the load combinations described in Section 3.8.5.1.3. The evaluation considers bridge crane location and lifted load as described in Section 3.7. Members are evaluated

against the acceptance criteria in Section 3.8.5.1.5. Results of the evaluation are shown in Tables 3.8-26 and 3.8-27.

Computer programs used in the structural analysis and the verification measures are listed in Table 3.8-6.

3.8.5.1.5 Structural Acceptance Criteria

For HE load combinations actual material properties are used. Lateral force resisting elements are allowed inelastic deformation subject to the ductility limits shown in Table 3.8-24. The strength of concrete elements is determined in accordance with the methods of ACI 318-71 and the 1973 Supplement. Strength of concrete shear walls is determined in accordance with Section 3(c) of 1974 SEAOC. Strength of steel elements is determined in accordance with the AISC Code, February 12, 1969.

Calculated forces and capacities for selected structural elements of the turbine building and turbine pedestals are compared in Tables 3.8-26 and 3.8-27. Generally, the predicted forces in combination with earthquake effect do not exceed member strengths. A limited number of members are found to exhibit inelastic behavior which does not exceed the allowable ductility limits of Table 3.8-24. Therefore, all structural elements satisfy the criteria.

Separations between the turbine building's primary structure and the turbine pedestal are adequate to ensure these structures will not impact each other when subject to the HE load combination. The relative displacements between these structures are summarized in Table 3.8-27A.

3.8.5.1.6 Materials, Quality Control, and Special Construction Techniques

The turbine building, including the turbine pedestals, was originally constructed prior to 1978. Following the HE evaluation of the plant, modifications to the turbine building and the turbine pedestals were made during the period 1978 to 1979. Materials installed during these two periods are described in the following paragraphs.

3.8.5.1.6.1 Concrete

Design strengths of concrete are as follows:

	Age, days	Compressive Strength, psi
Original construction:		
East-west walls	28	5000
Elevation 140 feet floor	60	5000
All other concrete	28	3000

Hosgri Modifications:		
Concrete above elevation 85 feet	28	5000
All other concrete	28	3000
Modifications for sixth diesel generator addition, all associated concrete	28	4000

Average strengths are used with the HE load combination. The average strengths are as follows:

	Age, days (except as noted)	Compressive Strength, psi
Original Construction:		
Turbine pedestal	6 years[a]	6000
East-west walls	28	5500
Elevation 140 feet floor	60	6590
All other concrete	28	3870
Hosgri Modifications:		
Concrete above elevation 85 feet	28	5680
All other concrete	28	4260

3.8.5.1.6.2 Reinforcing Steel

Reinforcing steel is ASTM A615, Grade 40, except in some locations where grade 60 is used. Average test values are used with HE load combinations. Properties of the reinforcing steel are as follows:

	Grade 40	Grade 60
Design yield strength, psi	40,000	60,000
Original construction		
Average yield strength, psi	51,400	65,900
Average tensile strength, psi	80,600	101,400
Hosgri Modifications		
Average yield strength, psi	51,900	67,000
Average tensile strength, psi	81,300	106,500

[a] Turbine pedestal concrete strength is based on cylinder tests of 6-year-old stored specimens. The strength is verified by rebound hammer tests and by tests of concrete core samples.

3.8.5.1.6.3 Structural Steel

Structural steel is ASTM A36 except for reinforcing bars installed at flanges of some columns along column lines A and G where ASTM A572 Grade 50, is used. Properties of the structural steel are as follows:

	ASTM A36	ASTM A572, Gr 50
Design yield strength, psi	36,000	50,000
Original construction		
Average yield strength, psi	44,000	
Average tensile strength, psi	68,000	
Hosgri Modifications		
Elevation 140 and 119 feet floor plate		
Average yield strength, psi	40,800	
Average tensile strength, psi	69,300	
Other structural steel		
Average yield strength, psi	44,500	55,200
Average tensile strength, psi	68,200	87,400

3.8.5.2 Intake Structure

3.8.5.2.1 Description of Intake Structure

The seismic Design Class II intake structure is a reinforced concrete building constructed with 3,000 psi minimum-specified-strength concrete. The structure has plan dimensions of approximately 240 x 100 feet. The long dimension corresponds to the north-south direction, and is parallel to the seaward face of the structure. The intake structure is backfilled by rock on three sides, and has water on the fourth (western) side. The top deck of the structure has a maximum elevation of +17.5 feet. A concrete ventilation tower with steel coaxial ventilation pipe extends to an elevation of +49.4 feet. The structure is supported by a concrete mat foundation at elevation -31.5 feet. Figures 3.8-72 through 3.8-74 illustrate plans at elevations +17.5, -2.1, and -31.5 feet; Figures 3.8-75 through 3.8-77 illustrate representative sections through the structure.

The top level of the structure consists of an 18-inch-thick concrete slab, except for the roadway area where it is 24 inches thick. Openings, as shown in Figure 3.8-72, are provided to allow removal of pumps, screens, and gates. The pump deck floor at elevation -2.1 feet supports the four main circulating water pumps and the four seismic Design Class I ASW pumps. Design Class I ASW equipment is located in ventilated watertight compartments. The structure is symmetric about a vertical plane in the east-west direction through its centerline.

3.8.5.2.2 Applicable Codes, Standards, and Specifications

The following codes and standards were used in the Hosgri evaluation and the design, construction, inspection, and testing of the intake structure.

(1) ACI Standard Building Code Requirements for Reinforced Concrete (ACI 318-63, ACI 318-71, ACI 318-77)

(2) Manual of Standard Practice for Detailing Reinforced Concrete Structures (ACI 315-65)

(3) Recommended Practices for Welding Reinforcing Steel, Metal Inserts and Connections in Reinforced Concrete Construction, American Welding Society AWS D12.1-75

(4) AISC Specification for the Design, Fabrication and Erection of Structural Steel for Buildings, February 12, 1969, and November 1, 1978

(5) Code for Welding in Building Construction, AWS D1.1-77, Rev. 2. For inspection of non-ASME structural welds or new non-ASME work performed after January 1, 1988, the guidelines of Nuclear Construction Issues Group (Visual Weld Acceptance Criteria, Vol. 1-3, EPRI Report No. NP-5380, September 1987) may be used except for those cases where:

   (a) Fatigue is a governing design condition

   (b) The weld allowables are permitted to be higher that those allowed by AWS D1.1 (such as the full penetration welds evaluation for the HE)

   (c) The weld is part of work performed in the ASME Section XI Inservice Inspection Program

(6) Recommended Lateral Force Requirements 1974 Seismology Committee, Structural Engineers Association of California (SEAOC)

(7) Materials and quality control tests for materials conform to ASTM standards

3.8.5.2.3 Loads and Loading Combination

Seismic Load Combination

$$U = D + L + HE \qquad (3.8\text{-}33)$$

where:

D	=	dead load of the structure and equipment loads
L	=	live load
HE	=	loads resulting from HE
U	=	strength required to resist design loads as described in Section 3.8.5.2.5

Wave Load Combination

$$U = D + L + W_f \qquad (3.8\text{-}34)$$

where:

U, D, and L are as defined in (1) above

W_f = wave force associated with breakwater degraded to MLLW

3.8.5.2.4 Design and Analysis Procedures

3.8.5.2.4.1 General

Structural analysis of the intake structure is performed by the traditional methods of engineering analysis for structural steel and reinforced concrete structures. These methods are based on the principles of equilibrium, compatibility of deformations, and predictions of material strength by the methods of the AISC Code, and the ACI Code. The use of these codes is discussed in Section 3.8.5.2.5.

3.8.5.2.4.2 Seismic Forces

A time-history dynamic analysis is performed with a computer program to determine the structure response spectra. A response spectrum dynamic modal superposition analysis is performed to determine structure response maxima. The analytical procedure using modal superposition methods is described in Section 3.7.2.

The demands resulting from the combination of north-south, east-west, and vertical components of the HE, in conjunction with dead loads, actual live loads, and soil pressures, are less than the yield capacity of the major portion of the structure, including the area housing the Class I ASW. The only exceptions are some of the flow straighteners (or piers) that exhibit stresses beyond code values. However, these piers demonstrate ductility properties that would preclude structural failure. The ductilities are within allowables as stated in Section 3.8.5.2.5. Table 3.8-28 presents the results of the analysis.

The intake structure is reviewed to verify that there is an adequate factor of safety against sliding and overturning, and the foundation pressure is within the allowable value of 50 ksf as described in Reference 13.

3.8.5.2.4.3 Wave Forces

As shown in Figures 3.8-78 and 3.8-79, a scaled, three-dimensional physical model of the cooling water intake basin, the intake structure, and a hypothetically damaged breakwater was constructed to examine the wave effects on the intake structure as described in References 8 and 9.

Based on the test results, the intake structure was modified to mitigate wave slam (high magnitude, high frequency) pressure behind the curtain wall and to withstand the measured pressures on the bottom of the slab.

The ASW pump compartments were modified to provide the required ventilation on the Design Class I equipment and to prevent flooding due to combined tsunami and storm wave runup conditions as described in Chapter 2. As discussed in Section 3.3.2.3.2.10, the ASW pump compartment modifications were reviewed for a tornado with missiles.

A risk analysis, as described in Reference 14, was performed to determine the frequency of vessel impact with the intake structure which houses the ASW pumps. In the analysis, the breakwater was assumed to be degraded to the MLLW level. The analysis considered only large vessels (greater than 250 tons displacement), since impact on the intake structure by smaller vessels was concluded, on the basis of a deterministic analysis, to be inconsequential to the safety-related function of the ASW pumps.

The results of risk analysis for frequency of impact indicate a frequency of 6.7×10^{-6} breakwater boundary crossings per year for storm-independent analysis and 1.9×10^{-5} breakwater boundary crossings per year for storm-dependent analysis. The probability of large vessels, therefore, crossing the degraded breakwater and impacting the intake structure is quite low.

3.8.5.2.5 Structural Acceptance Criteria

For the load combinations given in Section 3.8.5.2.3, the intake structure is designed so that it does not sustain damage that would adversely affect the function of the Class I ASW system and prevent it receiving an adequate supply of water.

For load combinations with seismic force, strength is based on SEAOC 1974 concrete shear walls; ACI 318-63 and ACI 318-71 for other concrete members; and AISC, Seventh Edition, Part II for steel members. Lateral force resisting elements are allowed inelastic deformation consistent with ductility factors indicated in Table 3.8-24. For these elements, the allowable stress limitations given in the codes above need not apply.

For load combinations with wave forces, strength is based on ACI 318-71 and AISC, Seventh Edition, Part II for all structural members except for ASW pump compartment

modifications. For the latter, strength is based on ACI 318-77 and 1.6 times AISC Eighth Edition, Part I allowable values.

3.8.5.2.6 Materials, Quality Control, and Special Construction Techniques

The intake structure was originally constructed prior to 1981. As a result of January 1981 storm damage to the west-breakwater, hydraulic model studies of wave effects on the intake structure were conducted in 1982 (References 8 through 12), and the intake structure was modified to withstand these wave effects.

The material strengths for these periods are provided below:

Concrete

Prior to 1981	Minimum specified fc'	=	3000 psi @ 28 days
	Average test values fc'	=	3630 psi
1981 modifications	Minimum specified fc'	=	5000 psi @ 28 days

Reinforcing Steel

Prior to 1981	ASTM A615, Grade 40;	Minimum specified fy	= 40 ksi
		Average test values fy	= 49.6 ksi
1981 Modifications	ASTM A615, Grade 60;	Minimum specified fy	= 60 ksi

Structural Steel

Prior to and after1981	ASTM A36;	Minimum specified fy	= 36 ksi

3.8.6 PIPEWAY STRUCTURES

3.8.6.1 Description of Pipeway Structures

The pipeway structure for each unit is a steel frame structure attached to the outside of the containment shell, the auxiliary building, and the turbine building as shown in Figure 3.8-80. The pipeway structure in one unit is essentially a mirror image of the other. The primary function of the pipeway structure is to support main steam and feedwater piping. The pipeway structure has five major platforms located at elevations 109, 114, 118, 127, and 138 feet. Connections between the pipeway structure and the auxiliary and turbine buildings are provided with slotted holes oriented such that horizontal motions cannot be transmitted between the structures.

3.8.6.2 Applicable Codes, Standards, and Specifications

3.8.6.2.1 Codes

The following codes and standards are used, insofar as they are applicable, in the design and/or construction of the pipeway structure.

(1) AISC Specification for Design, Fabrication, and Erection of Structural Steel for Buildings, February 12, 1969

(2) ACI Standard Building Code Requirements for Reinforced Concrete (ACI-318-63)

(3) Standard code for welding in building construction (AWS D1.0-69). For inspection of non-ASME structural welds or new non-ASME work performed after January 1, 1988, the guidelines of Nuclear Construction Issues Group (Visual Weld Acceptance Criteria, Vol. 1-3, EPRI Report No. NP-5380, September 1987) may be used except for those cases where:

   a) Fatigue is a governing design condition.

   b) The weld allowables are permitted to be higher than those allowed by AWS D1.1 (such as the full penetration weld evaluation for the HE).

   c) The weld is part of work performed in the ASME Section XI Inservice Inspection Program.

(4) Materials, and the quality control tests for materials, conform primarily to ASTM and ASME standards. Additional materials and supplemental quality assurance requirements conform to ANSI standards

3.8.6.3 Loads and Loading Combinations

3.8.6.3.1 Design Loads

The following loads are considered in the design of the pipeway structure.

3.8.6.3.1.1 Dead Loads

Dead loads consist of the weight of the structure, piping, pipe rupture restraints, electrical raceways, and equipment.

3.8.6.3.1.2 Live Loads

Live loads are temporary loads that may be placed on the structure. These are considered small in relative magnitude and, therefore, are considered negligible.

3.8.6.3.1.3 Earthquake Loads

Earthquake loads are as described in Section 3.7.2.1.7.1.

3.8.6.3.1.4 Wind Loads

Wind loads are determined in accordance with the criteria presented in Section 3.3. However, the forces due to wind are much less than those due to earthquake; consequently, seismic loads, rather than wind, are entered into the load combination equations.

3.8.6.3.1.5 Thermal Loads

Thermal loads are those induced by the main steam and feedwater pipes through the support system. These loads are considered negligible.

3.8.6.3.2 Loading Combinations

The following loading combinations are used in the design of the pipeway structure.

3.8.6.3.2.1 Normal Conditions

Dead loads and design earthquake (DE) are considered as follows:

$$S = D + DE \qquad (3.8\text{-}35)$$

where:

S	=	required capacity of structural members based on the method described in Section 3.8.6.5.1
D	=	dead load
DE	=	loads resulting from the DE

3.8.6.3.2.2 Abnormal Conditions

Where elastic working stress design methods are used:

$$1.6S = D + DDE \qquad (3.8\text{-}36)$$

$$1.7S = D + DDE + Yr \qquad (3.8\text{-}37)$$

1.7S	=	D + 1.25DE + Yr	(3.8-38)
1.7S	=	D + HE	(3.8-39)

Where plastic design methods are used:

1.0Y	=	D + DDE + Yr	(3.8-40)
1.0Y	=	D + 1.25DE + Yr	(3.8-41)

where:

DDE	=	loads resulting from the DDE
HE	=	loads resulting from the HE
Yr	=	reaction on structure from a broken pipe, generated by a postulated pipe break, including an appropriate dynamic load factor (DLF)
Y	=	required section strength based on plastic design methods described in Part 2 of the AISC specification referenced in Section 3.8.6.2.1

3.8.6.4 Design and Analysis Procedures

3.8.6.4.1 Hosgri Event

Seismic forces from the response spectrum dynamic analysis described in Section 3.7.2.1.7.1 are used in the stress evaluation of the Unit 1 pipeway structure. The Unit 2 pipeway structure is evaluated using a detailed three-dimensional model and the static equivalent method of seismic analysis described in Section 3.7.2.1.7.1. The calculated stress ratios for the most critical members are given in Table 3.8-5A.

3.8.6.4.2 Design Earthquake and Double Design Earthquake

Member forces are calculated using corresponding Hosgri forces adjusted in proportion to ratios of DE or DDE to HE spectral accelerations. These forces are used in the stress evaluation of the Unit 1 and 2 pipeway structures. Stresses obtained by this method are confirmed by time-history dynamic analysis described in Section 3.7.2.1.7.1. Calculated stress ratios for the most critical members are given in Table 3.8-5A.

3.8.6.4.3 Computer Programs

Computer programs used in the structural analysis and the verification measures are listed in Table 3.8-6.

3.8.6.5 Structural Acceptance Criteria

For DE and DDE load combinations in the absence of pipe break loads (Yr), the minimum specified yield strength for structural steel is considered. For load combinations including HE or Yr, the actual material properties are used. In addition, the following conditions apply.

3.8.6.5.1 Normal Conditions

For normal conditions, the pipeway structure is designed to the allowable working stresses in Part 1 of the AISC Code, February 12, 1969; however, the increase in allowable stress usually allowed for load combinations involving earthquake forces is not used.

3.8.6.5.2 Abnormal Conditions

For abnormal conditions, the pipeway structure, in general, is designed for overall elastic behavior. For load combinations (3.8-37), (3.8-38), (3.8-40), and (3.8-41) of Section 3.8.6.3.2.2, the acceptance criteria described therein should be satisfied first without considering the effect of Yr. When considering the effect of Yr, local section strength capacities may be exceeded provided there is no loss of function of any safety-related system.

3.8.6.5.3 Factors of Safety

The calculated capacity-to-demand ratio for the most critical members of the pipeway structure are given in Table 3.8-5A. In all cases these ratios are greater than the minimum allowable value of 1.0. Therefore, all structural elements satisfy the criteria.

3.8.6.6 Materials, Quality Control, and Construction Techniques

Structural steel is ASTM A441 and ASTM A516 Grade 70. ASTM minimum specified values are used with DE and DDE load combinations in the absence of Yr. Average test values are used with load combinations that include HE or Yr. Minimum and average values are as follows:

	ASTM A441	ASTM A516
Minimum yield strength, psi	45,000	38,000
Average yield strength, psi	51,600	51,040

High strength bolts, nuts, and washers used for connections are predominantly ASTM A490. Some ASTM A325 bolts are also used when found acceptable. Impact tests for structural steel and high strength bolts were performed in accordance with ASTM Standard Method A370 at 0°F.

Welding electrodes conform to ASTM A233, E70 series low hydrogen.

Where indicated on drawings, nondestructive testing was performed as required utilizing ultrasonic or magnetic particle techniques.

Approved substitute for ASTM A441 structural steel is ASTM A572 Grade 42. For any new construction after May 2004, the structural steel used may be A572 Grade 42. The impact test is required for this new steel.

3.8.7 SAFETY-RELATED MASONRY WALLS

In accordance with Reference 28, safety-related masonry walls (see Section 3.8.7.1) have been reevaluated and modified as necessary using conservative design and analysis procedures, and structural acceptance criteria as specified in Section 3.8.7.5. Design and analysis methods and structural acceptance criteria are in accordance with Reference 29. NRC Staff acceptance of the wall reevaluation design and analysis methods is documented in Reference 30.

3.8.7.1 Description of Safety-Related Masonry Walls

Safety-related masonry walls are those walls which support safety-related piping or equipment, or whose failure could prevent a safety-related system from performing its intended safety function. Safety-related walls are located in the auxiliary and turbine buildings at locations identified in Figures 3.8-83, -84, and -85, and are evaluated in accordance with Reference 29. These walls are fire walls or nonbearing partitions serving various functions and are not required to resist tornado or missile loads and are not part of the buildings lateral force resisting system. Some of the walls support small piping, conduits, or instrumentation tubing. A few walls support concrete or metal deck ceilings.

All walls are single width, 8 or 12 inches thick, fully grouted, and reinforced in the horizontal and vertical directions with steel reinforcing bars. The bottoms of all walls are tied to the building structure.

In general, walls extend to the underside of the floor structure, where lateral support is provided by a structural supporting system. A separation joint filled with compressible material is provided at the top and side boundaries of all walls where they abut the building structure floors or columns. Walls are braced with steel members. The bottoms of some walls are connected to the floor with bolted steel angles. Some walls are strengthened by steel plates bolted to each face of the wall.

3.8.7.2 Applicable Codes, Standards, and Specifications

The following codes and standards are used in the design, construction, inspection, and testing of safety-related masonry walls:

(1) Building Code Requirements for Concrete Masonry Structures (ACI 531-79) and Commentary (ACI 531R-79)

(2) AISC Specification for the Design, Fabrication, and Erection of Structural Steel for Buildings, February 12, 1969

(3) Materials and quality control tests for materials conform to the applicable ASTM standards

3.8.7.3 Loads and Loading Combinations

3.8.7.3.1 Design Loads

The following loads are considered in the evaluation of safety-related masonry walls:

3.8.7.3.1.1 Dead Loads

Dead loads consist of the weight of the wall and supported items.

3.8.7.3.1.2 Live Loads

Live loads consist of occupancy loads, if any, acting on the wall.

3.8.7.3.1.3 Earthquake Loads

Earthquake loads are those resulting from the HE. The loads are based on the response spectrum, single-degree-of-freedom method described in Section 3.7.2.1. The percentage of critical damping used is 7 percent.

3.8.7.3.1.4 Thermal Loads

Thermal loads are loads induced by local increases in temperature resulting from normal operating and from postulated accident conditions.

3.8.7.3.1.5 Pipe Reaction Loads

Pipe reactions result from hydraulic forces, thermal expansion, and seismic events. These loads are transferred to the structure through pipe supports and result from normal operating conditions and postulated accident conditions.

3.8.7.3.1.6 Pressure Loads

Pressure loads are forces generated by a postulated pipe break. Pressures from a postulated broken pipe are calculated as described in Section 3.6.

3.8.7.3.1.7 Loads and Loading Combinations

The following load combinations are used in evaluation of safety-related masonry walls:

U = D + L + To + Ro + HE

U = D + L + Ta + Ra + 1.5Pa

U = D + L + Ta + Ra + 1.0Pa + HE

where:

U	=	strength determined using acceptance criteria described in Section 3.8.7.5
D	=	dead load
L	=	live load
To	=	thermal loads during normal operating conditions
Ro	=	pipe reactions during normal operating conditions
HE	=	loads resulting from an HE
Ta	=	thermal loads generated by a postulated pipe break, including To
Pa	=	pressure load generated by a postulated pipe break
Ra	=	pipe reactions from unbroken pipes generated by postulated pipe break conditions, including Ro

3.8.7.4 Design and Analysis Procedures

Evaluation of safety-related masonry walls is performed using traditional methods of engineering analysis. Proper consideration is given to boundary conditions, cracking of sections, and the dynamic behavior of the walls. Both in-plane and out-of-plane loads and interstory drift effects are considered.

HE forces on the walls are based on applicable building floor response spectra generated by the analysis described in Section 3.7.2.1. In some cases, detailed models of the walls and supporting steel members are used to calculate forces and stresses in the walls.

HE forces on the walls including wall reactions are calculated by linear elastic analysis. Applied forces on the walls include the combined effects of vertical loads and horizontal out-of-plane wall deflections (P-Δ effect). Masonry wall stiffnesses are based on best estimate (median) properties, which are:

E_m = 750 f'm
F'_m = 1950 psi
f_r = $4(f'_m)^{0.5}$

The stiffness and strength of walls strengthened with steel plates at each face are based on wall panel tests. Drypack grout at the top of the walls is treated as unreinforced and is not relied upon to withstand earthquake loads. An additional evaluation of the walls is performed to address the variability of material properties, workmanship, and construction tolerances.

Computer programs used in the structural analysis and the verification measures are listed in Table 3.8-6.

3.8.7.5 Structural Acceptance Criteria

In the evaluation of safety related masonry walls for load combinations, including HE or pipe break loads, actual material properties may be used.

The moment capacity of a masonry wall is not less than the moment produced by the applied loads. Moment capacity of the masonry wall is determined using the strength design method, with a strength reduction factor, ϕ, equal to 1.0. Allowable masonry shear stress is $1.3 \times 1.1\ (f'_m)^{0.5}$, where f'_m is as defined in Section 3.8.7.4. Allowable masonry bearing stress is $2.5 \times 0.25\ (f'_m)$. Analysis of the behavior of masonry walls strengthened with steel plates is substantiated by tests. Allowable forces on steel members are based on 1.6 times allowable stresses defined in the AISC Code, Part 1, or 0.9 times member strengths defined in the AISC Code, Part 2.

3.8.7.6 Materials, Quality Control, and Special Construction Techniques

3.8.7.6.1 Masonry Units

Masonry units are hollow, load-bearing, open-ended lightweight units of ASTM Designation C90, Grade A. The average compressive test strength of masonry units is 3400 psi on the net area.

3.8.7.6.2 Reinforcing Steel

In general reinforcing steel is ASTM A615, Grade 40. The average yield strength by test is 51,400 psi.

In limited areas, reinforcing steel is ASTM A615, Grade 60. The average yield strength by test is 64,200 psi.

3.8.7.6.3 Core Fill

Grout having a minimum specified compressive strength of 2000 psi is placed in all masonry unit cells. The average tested compressive strength is 3285 psi.

3.8.7.6.4 Mortar

Mortar is ASTM Designation C270, Type S.

3.8.7.6.5 Construction Inspection

Inspection procedures meet the intent of Section 4.5 of Building Code Requirements for Concrete Masonry Structures (ACI 531-79).

3.8.8 PERMANENT SPENT FUEL STORAGE RACKS

3.8.8.1 Description of the Spent Fuel Pool and Racks

The description of the SFP is provided in Sections 3.8.2.1 and 9.1.2.2. Each fuel pool has 16 high density fuel rack modules as shown in Figure 9.1-2. They are free-standing and consist of individual cells with an 8.85 by 8.85-inch square cross-section, each of which stores a single Westinghouse PWR fuel assembly. The number of cells varies from 34 to 110 per module. The cells are fabricated by welding two formed stainless steel channels, which are welded together by stainless steel gap channels to provide the required predetermined distance between the cells. Typically, each module is provided with four support legs, three of which are adjustable and one fixed. The adjustable support legs are used to achieve a leveled free-standing position on the pool floor. For ease of installation and to reduce potential interferences with liner seam welds, each rack support leg is supported on a bridge plate. Typically, each rack module is equipped with girdle bars located near the top, which are designed to accommodate seismically induced impact loads.

3.8.8.2 Applicable Codes, Standards, and Specifications

The following codes and standards are used in the design and construction of the racks.

(1) AISC Specification for the Design, Fabrication, and Erection of Structural Steel for Buildings, 1969 Edition

(2) ASME Boiler and Pressure Vessel Code, Section III and Subsection NF, 1983 Edition

(3) AEC "Spent Fuel Storage Facility Design Basis," SG 13, March 1971

(4) Westinghouse Fuel Assembly, Storage and Refueling Equipment Design Interface Specification No. F-8, Rev. 8

(5) NRC "OT Position for Review and Acceptance of Spent Fuel Storage and Handling Applications," April 14, 1978, and "Modifications to the OT Position," January 18, 1979, letters from B. K. Grimes to All Power Reactor Licensees

(6) Appendix D to Standard Review Plan, Section 3.8.4, "Technical Position on Spent Fuel Pool Racks," Revision 0, July 1981, NRC

3.8.8.3 Loads and Loading Combinations

The loads and loading combinations and the corresponding acceptance criteria are as follows (Reference 20):

Loading Combination		Stress Limit
(a)	D D + T_o D + T_o + E	Level A service limits
(b)	D + T_a + E D + T_o + P_f	Level B service limits
(c)	D + T_f + E' D + F_d	Level D service limits (The functional capability of the fuel racks should be demonstrated)

where:

D	=	Dead weight-induced stresses (including fuel assembly weight)
F_d	=	Force caused by the accidental drop of the heaviest load from the maximum possible height
P_f	=	Upward force on the racks caused by postulated stuck fuel assembly
E	=	DE
E'	=	HE
T_o	=	Differential temperature induced loads (normal or upset condition)
T_a	=	Differential temperature induced loads (abnormal design conditions)

3.8.8.4 Design and Analysis of Racks

3.8.8.4.1 Design Basis Rack Model

The racks are analyzed using a nonlinear dynamic model as shown in Figure 3.8-81. The model simulates the rack as a single stick supported on a rigid base with supports. Impact springs are provided at the girdle bar and the baseplate locations to account for rack-to-rack and/or rack-to-wall impact. The legs are represented by 4 impact springs to account for the impact as well as frictional sliding. The rattling of the fuel assemblies in cells is considered by the use of additional impact springs. The model includes 2 mass points comprising 8 degrees of freedom. Mass 1 is located in the rack module and has 6 degrees of freedom, (i.e., 3-dimensional space with 3 linear translations and 3 rotations). Mass 2 is located at the top of the fuel and moves with 2 translational degrees of freedom. The lower mass point of the fuel assembly is lumped with the rack module mass (Reference 20).

3.8.8.4.2 Design Basis Rack Analysis and Results

Due to the complexity of the nonlinear time-history analysis, the racks, in general, are analyzed using a single rack model (Figure 3.8-81) that uses conservative model parameters. The seismic input motions are provided in the form of three orthogonal time histories at the fuel pool liner location. A minimum value of 0.2 and a maximum value of 0.8 are used for the range of friction coefficients between the rack supports and the pool liner (Reference 23). The effects of fluid are considered in accordance with the method advanced by Fritz (Reference 24). The impact springs are set at values to produce conservative impact forces. Parametric studies have been performed to evaluate the effects of various design variables such as friction coefficients, size of rack, fuel loading (partially loaded, fully loaded, or empty) on rack, spacing between racks (corner rack vs. non-corner rack), fabrication tolerance, etc. The bounding loads are obtained from those parametric analyses, which are then used for the design of rack components.

The racks have been analyzed to store LOPAR, VANTAGE 5, and ZIRLO fuel assemblies. The impact loads between the cell wall and the fuel assemblies are less than those provided by Westinghouse.

3.8.8.4.3 Multi-Rack Confirmatory Model

The design basis analysis includes several conservative assumptions applied to a single rack model to obtain conservative impact loads. To confirm the adequacy of this methodology, additional multi-rack analyses have been performed (References 21 and 22).

Figure 3.8-82 shows the two-dimensional dynamic model used in this analysis. Each rack is represented by four degrees of freedom simulating fuel rattling, translation, and rocking of the racks. The parameters for the model are developed in a manner similar to those used for the design basis model, except more realistic assumptions are made to compute the fluid coupling coefficients and spring constants.

3.8.8.4.4 Multi-Rack Confirmatory Analysis and Results

The analyses are performed using the nonlinear time history method. The governing horizontal (east-west) and vertical ground motions are applied simultaneously to the model. Parametric studies have been performed to evaluate the effects of various friction coefficients, fuel loading on racks, sizes of racks, lateral gaps, and fabrication tolerances. The results of the analysis demonstrate that the use of conservative model parameters in the design basis analysis (Reference 20) yields conservative rack and fuel assembly impact loads.

3.8.8.5 Materials, Quality Control, and Special Construction Techniques

The materials for both Region 1 and Region 2 rack modules are:

Stainless steel sheet and plate	ASTM A-240-304L
Weld filler material	ASME SFA-5-9 Type 308L and 308LSI
Top part of support	ASTM 479-S21800
Bottom part of support	ASTM SA564-630

3.8.8.6 Design and Analysis of Pool Structure

The existing pool structure was evaluated for postulated interactions of the rack modules with the structure as a result of the seismic event. The effect of the change in fuel rack mass on global dynamic response of the pool structure was considered. The change in global mass was determined to be on the order of 1 percent to 2 percent, therefore, the change in dynamic response is insignificant.

The pool walls were evaluated for the out-of-plane effects due to hydrostatic, hydrodynamic, thermal, and seismic loads. They adequately meet the loading combinations and acceptance criteria in Sections 3.8.2.3.2 and 3.8.2.5, respectively. The walls were also checked for additional impact loads that may result from the rack-to-wall impact and they meet the acceptance criteria of Section 3.8.2.5.

The liner was evaluated for the maximum vertical impact load and maximum horizontal sliding load and was determined to be adequate for leak tightness. The concrete slab that supports the liner was evaluated for the floor impact load using the allowable values specified in ACI 349-80 (Reference 25). The liner in-plane loadings that result from the sliding of the rack and thermal effects were evaluated in accordance with the allowable strains and anchor displacements as specified in ASME Section III, Division II, 1983 (Reference 26).

3.8.9 REFERENCES

1. Timoshenko and Woinowsky-Krieger, Theory of Plates and Shells, McGraw-Hill, Inc., New York, 1959, Second Edition.

2. Deleted.

3. Code for Concrete Reactor Vessels and Containments, ACI Standard 359-75.

4. PG&E's response to Governor George Deukmejian's and Joint Intervenors' first set of interrogatories (Docket Nos. 50-275 and 50-323): Interrogatory Number 2 – Unit 1; Interrogatory Number 3 - Unit 2.

5. PG&E's first supplemental response to Governor Deukmejian's and Joint Intervenors' first set of interrogatories. (Docket Nos. 50-275 and 50-323.)

6. Letter dated August 13, 1973, with enclosures, (Docket Nos. 50-275 and 50-323) from A. Giambusso of the AEC to F. T. Searls of PG&E.

7. Recommended Evaluation Criteria for Diablo Canyon Nuclear Power Plant Auxiliary Building Walls and Diaphragms, by Jack R. Benjamin and Associates, Inc., dated February 11, 1983, prepared for Bechtel Power Corporation, San Francisco, California.

8. The Height Limiting Effects of Sea Floor Terrain Features and of Hypothetically Extensively Reduced Breakwaters on Wave Action at Diablo Canyon Sea Water Intake, by Omar J. Lillevang, Fredric Raichlen, Jack C. Cox, March 15, 1982.

9. The Investigation of Wave-Structure Interactions for the Cooling Water Intake Structure of the Diablo Canyon Nuclear Power Plant, by Fredric Raichlen, December 1982.

10. Criteria for Selection of Critical Wave Directions, Omar J. Lillevang, November 2, 1982.

11. Wave Effects on Intake Structure at Diablo Canyon Units 1 and 2, E. N. Matsuda, January 1983.

12. Investigation of Seawater Injection into the Auxiliary Saltwater Pump Room Due to the Splash Runup During the Design Flood Events at Diablo Canyon, P. J. Ryan, January 1983.

13. Geotechnical Studies on Intake Structure, Water Storage Tanks, Diesel Fuel Oil Storage Tanks, for Diablo Canyon Power Plant, San Luis Obispo County, California, by Harding-Lawson Associates, April 12, 1978.

14. Frequency of Vessel Impact with the Diablo Canyon Intake Structure, by Jack R. Benjamin and Associates, December 10, 1982.

15. Deleted in Revision 10.

16. Deleted in Revision 10.

17. Deleted in Revision 10.

18. Deleted in Revision 10.

19. Deleted in Revision 4.

20. Seismic Analysis Report, Seismic Analysis of High Density Fuel Racks for PG&E for Diablo Canyon Nuclear Power Station, Rev. 3, September 3, 1986, A. Soler, TM #779.

21. "Additional Information on Rack to Rack Interaction," Enclosure 1 to PG&E Letter No. DCL-87-070, dated April 7, 1987.

22. "Three-Dimensional Studies (ACORN 10 and ACORN 12)," Enclosure to PG&E Letter No. DCL-87-082, dated April 23, 1987.

23. Rabinowicz, E., Friction Coefficient Value for a High Density Fuel Storage System, Report to General Electric Nuclear Energy Program Division, November 23, 1977.

24. Fritz, R.J., The Effect of Liquids on the Dynamic Motions of Immersed Solids, Journal of Engineering for Industry, pp. 167-173, February 1972.

25. ACI Standard 349-80, Code Requirements for Nuclear Safety Related Concrete Structures, American Concrete Institute, Detroit, Michigan.

26. ASME Boiler and Pressure Vessel Code, American Society of Mechanical Engineers, Section III, Division II, 1983.

27. EPRI NP-5380 Final Report, Visual Weld Acceptance Criteria, Volumes 1-3 (Nuclear Construction Issues Group (NCIG) NCIG-01, Revision 2, NCIG-02 Revision 2, and NCIG-03 Revision 1), September 1987.

28. PG&E Letter DCL-90-289, with enclosure, from J.D. Shiffer to NRC, December 14, 1990.

29. PG&E Letter DCL-91-026, with enclosure, from J.D. Shiffer to NRC, February 12, 1991.

30. Letter dated September 18, 1991, with enclosure, (Docket Nos. 50-275 and 50-323) from R.P. Zimmerman of NRC to J.D. Shiffer of PG&E.

31. Letter from PG&E (J. O. Schuyler) to the NRC (D. G. Eisenhut), Design Verification Program Phase I Final Report, Diablo Canyon Unit 1, October 14, 1983.

32. Deleted in Revision 20.

33. Deleted in Revision 20.

34. Enova Engineering Services, "Position Paper on Shear Strength of A325 Bolts as Specified by the 7th Edition of AISC," dated July 3, 2008.

35. J. W. Fisher and Associates, "Review Comments on Position Paper on Shear Strength of A325 Bolts as Specified by the 7th Edition of the AISC Manual," dated July 10, 2008.

36. NRC (D.P. Allison) Letter to PG&E, "Summary of Meeting Held on February 4, 1977 to Discuss the Diablo Canyon Seismic Design Reevaluation," with enclosures (Docket Nos. 50-275 and 50-323), dated May 18, 1977.

37. NRC, Safety Evaluation Report Related to the Operation of of the Diablo Canyon Nuclear Power Station, Units 1 and 2, NUREG-0675, Supplement No. 7, dated May 1978.

38. Robert P. Kennedy Structural Mechanics Consulting, "Comments on Position Paper on Shear Strength of A325 Bolts as Specified by the 7th Edition of AISC," Report No. RPK-80704, dated July 4, 2008.

39. PG&E Calculation 52.15.9.11, Revision 2, "Evaluation of Fuel Handling Building Crane and Fuel Handling Building Steel Superstructure of Added Loads Due to Attachment of Redundant Tension Links for Spent Fuel Transfer Cask Handling", Page 133.

40. PG&E Calculation No. 2252 C-1 (SAP Calc. No. 9000041231), "Polar Crane ANSR Model Reconstruction and Benchmarking."

3.8.10 REFERENCE DRAWINGS

Figures representing controlled engineering drawings are incorporated by reference and are identified in Table 1.6-1. The contents of the drawings are controlled by DCPP procedures.

TABLE 3.8-1

TESTING OF REINFORCING BARS FOR DESIGN CLASS I CONCRETE STRUCTURES
COMPARISON OF PROGRAM USED ON DIABLO CANYON POWER PLANT WITH REGULATORY GUIDE 1.15

Diablo Canyon Power Plan	Regulatory Guide 1.15
The number of test specimens required for acceptance is in accordance with ASTM A 615, Deformed Billet-Steel Bars for Concrete-Reinforcement, American Society for Testing and Materials. Additional samples were tested as part of the splice testing program. The requirements for acceptance testing are more stringent than ASTM A 615 in that all tests must be conducted using the full section of the bar.	At least one full-diameter specimen from each bar size should be tested for each 50 tons or fraction thereof of reinforcing bars that are produced from each heat and used in Category I structures.
Test procedures are in accordance with ASTM A 615-68.	The test procedures should be in accordance with ASTM A 370-68, Standard Methods and Definitions for Mechanical Testing of Steel Products, American Society for Testing and Materials.
Acceptance standards are in accordance with ASTM A 615-68 using full sections of the bars as rolled. Bend test requirements described in Item 3, Sheet 2 of 2, are more stringent than those in Supplemental Requirements (S-1) of ASTM A 615-72.	The acceptance standards should be in accordance with ASTM A 615-72, Standard Specification for Deformed Billet-Steel Bars for Concrete Reinforcement, American Society for Testing and Materials, including Supplemental Requirement (S-1)[a] using full sections of the bars as rolled.

TABLE 3.8-1

Diablo Canyon Power Plan	Regulatory Guide 1.15
In addition to the requirements of ASTM A 615, the Company specification requires the following: 1. Grade 60 bars be limited in carbon and manganese content to a maximum of 0.45% and 1.3% respectively. 2. Performance of a check analysis, which is listed as an option in ASTM A 615. 3. No. 14 and No. 18 bars be subjected to a 90° bend test using a pin having a diameter eight times the diameter of the bar.	Where any material property such as yield strength to tensile strength ratio, ductility, weldability or other similar property is relied upon by the designer or constructor, then the reinforcing bar chemistry should be controlled to the extent required to achieve the desired material property, and confirmatory testing should be performed.
Deformations were inspected during production to ensure conformance with ASTM A 615.	Deformations of the reinforcing bars should be inspected to assure their compliance with ASTM A 615-72 and with the licensee's specifications pertinent to bonding and other purposes which are dependent on the deformation characteristics.
Adequacy of deformations for splicing was demonstrated by the tensile tests of the Cadweld splices. See Table 3.8-2.	Adequacy of deformations for splicing will be demonstrated by the tensile tests of the splices. mechanical splice. See Safety Guide 10, "Mechanical (Cadweld) Splices in Reinforcing Bars of Category I Concrete Structures."

(a) Supplemental Requirement (S-1) is for a 90° bend test, using a pin diameter 10 times the bar diameter, on No. 14 and No. 18 bars.

TABLE 3.8-2

MECHANICAL (CADWELD) SPLICES IN REINFORCING BARS OF CONCRETE CONTAINMENTS
COMPARISON OF PROGRAM USED ON DIABLO CANYON POWER PLANT WITH SAFETY GUIDE 10

Diablo Canyon Power Plant	Safety Guide 10
Prior to production splicing, each operator was instructed by a representative of the manufacturer. Each operator (a crew consisted of an operator and a helper) prepared one qualification splice for each of the splice positions for which he was qualified. The qualification splice was made using the same materials as those used in the structures. The completed qualification splices had to pass visual inspection and develop the minimum tensile strength of the reinforcing steel. A manufacturer's representative was present for at least the first 20 production splices for each crew to verify that proper procedures were being used and quality splices obtained.	1. <u>Crew Qualification</u> - Each member of splicing crew (or each crew if the members work as a crew) should prepare two qualification splices for each of the splice positions (e.g., horizontal, vertical, diagonal) to be used. The qualification splices should be made using the same materials (e.g., bar, sleeve, powder) as those to be used in the structure. The completed qualification splices should meet the requirements specified by the designer of the containment structure and approved by the licensee, pass visual inspection as provided by Paragraph 2 below, and meet the tensile tests as provided by Paragraph 3 below.
All completed splices were visually inspected in accordance with the recommendations of the Erico Co. inspection manual RB-5M 768, Inspection of the Cadweld Rebar Splice. This visual inspection included both ends of the sleeve, the tap hole, and measurement of void area. In addition, at least twice daily for each Cadweld crew, an inspector observed the entire splicing operation including cleaning of rebar ends, spacing of rebar, centering of rebar ends, loading the crucible,	2. <u>Visual Inspection</u> - All completed mechanical splices should be inspected at both ends of the splice sleeve and at the tap hole in the center of the splice sleeve in accordance with the requirements specified by the designer of the containment structure and approved by the licensee. Among the items should be included in these specifications are longitudinal centering of sleeve on the spliced ends, allowable voids in filler metal, extent of leaking of filler metal,

TABLE 3.8-2

Diablo Canyon Power Plant	Safety Guide 10
and firing the charge. The Cadweld procedure specified for the DCPP includes placing a mark 12 inches ± 1/4-inch back from the end of the bar. This line was used as a reference to determine if the bar ends are centered in the sleeve.	permissible gap between rebar ends, cartridge size, gas blowout, amount of packing and slag at the tap hole. Splices that fail to pass visual inspection should be discarded and replaced, and should not be used as tensile test samples.
Acceptance criteria for splice tensile tests is as follows:	3. <u>Tensile Testing</u> - Splice samples may be production splices (i.e., those cut directly from in place reinforcing) or sister splices (i.e., those removable splices made in-place next to production splices and under the same conditions).
No splice in the test series may have a tensile value below 125% of the specified yield point stress, and no more than 5 % of the splices tested may have an ultimate tensile strength less than 85% of that specified. The average tensile strength of all splices in the test series must equal or exceed the ASTM specified minimum ultimate strength.	Splice samples should be subjected to tensile tests in accordance with the sampling frequency specified in Paragraph 4a or Paragraph 4b below, to determine conformance with the following acceptance standards: a. The tensile strength of each sample tested should be equal or exceed 125 percent of the minimum yield strength specified in the ASTM standard appropriate for the grade of reinforcing bar using loading rates set forth in ASTM Specification A 370 dated August 15, 1968. b. The average tensile strength of each group of 15 consecutive samples should equal or exceed the guaranteed ultimate tensile strength specified for the reinforcing bar.

Diablo Canyon Power Plant	Safety Guide 10
	If any sample tested fails to meet the provisions of Paragraph 3a above, the procedure of Paragraph 5a below should be followed. If the average tensile strength of the 15 samples tested fails to meet the provisions of Paragraph 3b above, the procedure of Paragraph 5b below should be followed.
Testing frequency for each crew, position, and grade of bar was as follows: One out of the first 10 splices. This splice must be a production splice for No. 18, Grade 60 bars and a sister splice for other sizes and grades of bar. Three out of the next 90 splices for No. 18, Grade 60 bars and one out of the next 90 splices for all other sizes and grades of bar. Three out of second and subsequent 100 splice units for No. 18, Grade 60 bars and one out of second and subsequent 100 splice units for all other sizes and grades of bar. At least 25% of the total number of No. 18, Grade 60 test splices must be made by cutting out	4. <u>Tensile Test Frequency</u> - Separate test cycles should be established for mechanical splices in horizontal, vertical, and diagonal bars, for each bar size, and for each splicing crew as follows: a. Test Frequency for Production Splice Test Samples. If only production splices are tested, the sample frequency should be: 1 of the first 10 splices 1 of the next 90 splices 2 of the next and subsequent units of 100 splices b. Test Frequency for Combinations of Production and Sister Splices. If production and sister splices are tested, the sample frequency should be:

TABLE 3.8-2

Diablo Canyon Power Plant	Safety Guide 10
production splices on a random basis. The remaining test splices may be made by having test bars tie wired alongside the production bars and spliced in sequence with those bars. The minimum length of the spliced bars is 3 feet.	1 production splice of the first 10 production splices 1 production and 3 sister splices, for the next 90 production splices 3 splices, either production or sister splices, for the next and subsequent units of 100 splices. At least 1/4 of the total number of splices tested should be production splices.
In the event a splice should fail the tensile test criteria, the specimen was to be examined by a testing laboratory. Based on the results of this investigation, additional splices by the crew responsible, as directed by the Engineer, were to be taken from the structure to ensure that there are no other defective splices. The procedures of the crew responsible for making the failed splice were to be reviewed, and if necessary, the crew retrained and requalified.	5. <u>Procedure for Substandard Tensile Test Results</u> a. If any production or sister splice tested fails to meet the tensile test specification of Paragraph 3a and the observed rate of splices that fail the tensile test at that time does not exceed 1 for each 15 consecutive test samples, the sampling procedure should be started anew. If any production or sister splice used for testing fails to meet the tensile test specification in Paragraph 3a, and the observed rate of splices that fail the tensile test exceeds 1 for each 15 consecutive test samples, mechanical splicing should be stopped. In addition, the adjacent production splices on each side of the last failed splice and 4 other splices distributed uniformly throughout the balance of the 100 production splices under investigation should be tested,

TABLE 3.8-2

Diablo Canyon Power Plant	Safety Guide 10
	and an independent laboratory analysis should be made to identify the cause of all failures. The results of these tests should be evaluated by the designer of the containment structure and the licensee to determine the required corrective action. The designer and the licensee should specify the extent of repairs necessary and the actions required to prevent further failures from the identified causes. b. If two or more splices from any of these 6 additional splice samples fail to meet the tensile test specification of Paragraph 3a, the balance of the 100 production splices under investigation should be rejected and replaced. When mechanical splicing is resumed, the sampling procedure should be started anew. If the average tensile strength of the 15 consecutive samples fails to meet the provisions of paragraph 3b above, the designer of the containment structure and the licensee should evaluate and assess the acceptability of the reduced average tensile strength with respect to the required strength at the location from which the samples were taken.

TABLE 3.8-3

NONDESTRUCTIVE EXAMINATION OF PRIMARY CONTAINMENT LINER WELDS
COMPARISON OF PROGRAM USED ON DIABLO CANYON POWER PLANT WITH SAFETY GUIDE 19

Diablo Canyon Power Plant	Safety Guide 19
	1. Nondestructive Examination of Liner Seam Welds
For each welder and welding position, the first 10 feet of weld was examined radiographically. Thereafter, a minimum of 10% of the welding (to at least include all intersections of joints) was progressively examined radiographically as welding was performed. This was done on a random basis with the location specified in such a manner that an approximately equal number of radiographs were taken from the work of each welder. The techniques of radiographic examination of welds were in accordance with Paragraph UW-51 of Section VIII, ASME Boiler and Pressure Vessel Code (ASME B&PV Code). See Notes 1 and 2.	a. For each welder and welding position (flat, horizontal, and overhead), the first 10 feet of weld, and one spot (not less than 12 inches in length) in each additional 50 foot increment of weld (weld test unit) or fraction thereof should be examined radiographically in accordance with the techniques prescribed in Section V, "Nondestructive Examination," of the ASME Boiler and Pressure Vessel Code (ASME B&PV Code). In any case, a minimum of 2 percent of all liner seam welds should be examined by radiography.
Where radiographic examination of liner seal welds was not feasible, a minimum 10% of the welding (to at least include all locations where there are welded backing strip splices and intersections) was examined by magnetic particle or liquid penetrant testing. Magnetic particle testing was in accordance with Appendix VI of Section VIII, ASME B&PV Code. Liquid penetrant testing was in accordance with Appendix VIII of Section VIII, ASME B&PV Code. See Notes 1 and 2.	b. Where radiographic examination of liner seam welds is not feasible or where the weld is located in areas which will not be accessible after construction, the entire length of weld should be examined by the magnetic particle method or by the ultrasonic method in accordance with the techniques prescribed in Section V of the ASME BP&V Code for such examination methods.

Diablo Canyon Power Plant	Safety Guide 19
All liner seam welds were tested for leaktightness in accordance with the following method:	c. All liner seam welds should be tested for leaktightness in accordance with the following method (or other methods of equivalent sensitivity):
Immediately preceding the test, a soap solution is applied to the weld. The application of the soap solution must not precede the vacuum box by more than 3 minutes. The vacuum box, which contains a viewing window, is placed over the area to be tested and evacuated to a 5 psi differential with the atmospheric pressure.	Immediately preceding the test, a soap solution (or other appropriate solution) should be applied to the weld. A vacuum box containing a viewing window should be placed over the area to be tested and evacuated to produce at least 5 psi differential with the atmospheric pressure. Leaks in welds, if present, should be detected by formation of bubbles. The solution used for the test should have bubble formation properties adequate for identification of leaks. The test solution should be checked every hour, with a suitable test leak to verify the bubble formation property of the solution used.
Leak chase channels are installed over the liner welds. Upon completion of one zone of leak chase channels, the zone was tested at the containment structure design pressure of 47 psi. The acceptance criteria is that there be no loss of pressure within 2 hours as indicated by a pressure gauge.	d. Where leak chase system channels are installed over liner welds, channel-to-liner plate welds should be tested for leak- tightness by pressurizing the channels to containment design pressure. If any indicated loss of channel test pressure occurs within 2 hours, as evidenced by a test gauge, the channel-to-liner welds should be soap bubble tested in accordance with the above procedure.

Diablo Canyon Power Plant	Safety Guide 19
	2. Nondestructive Examination of Penetration, Airlock, and Access Opening Welds
All welds in penetration, airlocks, and access openings that are not backed by concrete were fully examined in accordance with Class B requirements of Section III, ASME B&PV Code. See Notes 1, 2, 3, and 4. All welds between flued heads and pipelines were fully examined in accordance with the Class II requirements of ANSI B 31.7, Nuclear Power Piping.	a. All welds in penetration, airlocks, and access openings that are not backed by concrete, such as welds between penetrations and flued fittings and pipelines, should be fully examined in accordance with examination methods of NE-5120 of Section III of the ASME B&PV Code employing the techniques prescribed in Section V of that code.
Welds backed by concrete in the vicinity of penetrations were examined as follows: 1. Welds between the penetration sleeve and insert plate were fully examined in accordance with the Class B requirements of Section III, ASME B&PV Code. See Notes 1, 2, and 4. 2. Welds between the insert plate and the liner were examined under the same criteria as liner seam welds. All welds backed by concrete in the containment structure are carbon steel.	b. All welds in the vicinity of penetrations and access openings that are backed by concrete, such as welds between penetration and reinforcing plate,[a] penetration and liner, reinforcing plate and liner, liner insert and liner, reinforcing plate and frames for airlocks and access openings, and liners and frames for airlocks and access openings, should be fully examined (1) in accordance with Paragraph 2a above or (2) by magnetic particle, or liquid penetrant when a nonmagnetic weld is used, in accordance with the techniques prescribed in Section V of the ASME B&PV Code.

(a) Thickened liner insert which provides local reinforcement.

Diablo Canyon Power Plant	Safety Guide 19
Examination of welds in penetrant assemblies and in the vicinity of penetrations is described in the preceding paragraphs.	c. All welds in bellow type expansion joints provided in penetration assemblies or appurtenances to the containment vessel should be magnetic-particle or liquid-penetrant tested when a nonmagnetic weld is used, in accordance with the techniques prescribed in Section V of ASME B&PV Code for such examination methods.
	3. Qualification of Welders and Welding Procedures
The qualification of welders, welding machine operators, and welding procedures was in accordance with Section IX, "Welding Qualifications," of the ASME B&PV Code. See Note 2.	The qualification of welders, welding machine operators, and welding procedures should be in accordance with Section IX, "Welding Qualifications," of the ASME B&PV Code.
	4. Qualification of Nondestructive Examination Personnel
Nondestructive examinations were performed by personnel qualified in accordance with the appropriate parts of the ASME B&PV Code. See Notes 1 and 2.	Nondestructive examination should be performed by personnel designated by the licensee or his agent and qualified in accordance with the provisions of Section V of the ASME B&PV Code.
	5. Selection of Spots for Radiographic Examination
The spots of liner seam welds to be radiographically examined were selected on a random basis with the locations selected such that all intersections	The spots of liner seam welds to be radiographically examined should be randomly selected, but no two spots in adjacent weld test units

Diablo Canyon Power Plant	Safety Guide 19
of joints were examined, and an approximately equal number of radiographs were taken from the work of each welder. The location covered by each radiograph was recorded.	should be closer than 10 feet and their locations should be recorded.
	6. Time of Examination
Nondestructive examinations were done progressively as welding was performed.	All examinations should be performed as soon as practicable after the linear increment of weld to be examined is completed.
	7. Acceptance Standards
	a. Containment Liner Seam Welds Examined by Radiography
Where a spot in the seam weld is judged acceptable in accordance with Paragraph UW-51 of Section VIII, ASME B&PV Code, the entire weld test unit represented by this spot radiograph is considered acceptable. See Notes 2 and 3.	Where a spot in the seam weld is judged acceptable in accordance with the referenced standards of NE-5120 of Section III of the ASME B&PV Code, the entire weld test unit represented by this spot radiograph is considered acceptable.
	b. Containment Liner Seam Welds Examined by Ultrasonic or Magnetic Particle
Where a spot in the seam weld examined by magnetic particle or liquid penetrant method is judged	Seam welds examined by ultrasonic or magnetic particle methods are considered acceptable

Diablo Canyon Power Plant	Safety Guide 19
acceptable, in accordance with the acceptance criteria referenced in Section VIII, ASME B&PV Code, the entire weld seam represented by the examination is considered acceptable. See Notes 2 and 3.	provided the examinations meet the acceptance standards referenced for such examination methods in NE-5120 of Section III of the ASME B&PV Code.
	c. <u>Soap Bubble Leak Tests of Containment Liner Welds</u>
The acceptance criterion for the vacuum box test is that no leaks be detected.	Liner welds are considered acceptable provided no leakage is detected by soap bubble tests (or by other methods of equivalent sensitivity).
	d. <u>Penetration, Airlock, and Access Opening Welds</u>
Penetration, airlock, and access opening welds that are not backed by concrete are considered acceptable provided the examinations meet the acceptance standards referenced for Class B vessels in Section III, ASME B&PV Code. See Notes 2, 3, and 4. Welds between flued heads and pipelines are considered acceptable provided the examinations meet the acceptance standards referenced for Class II piping in ANSI B31.7, Nuclear Power Piping.	Penetration, airlock, and access opening welds are considered acceptable provided the examinations meet the acceptance standards referenced in NE-5120 of Section III of the ASME B&PV Code. Welds in bellows type expansion joints are considered acceptable if the examinations meet the acceptance standards referenced in magnetic particle and liquid penetrant methods in NE-5120 of Section III.

Diablo Canyon Power Plant	Safety Guide 19
Welds between the penetration sleeve and insert plate are considered acceptable provided the examinations meet the acceptance standards referenced for Class B vessels in Section III, ASME B&PV Code. See Note 2.	
	8. Repair and Reexamination a. Containment Liner Seam Welds Examined by Radiography
If a radiographed spot failed to meet the specified acceptance standards, two additional spots of the same length were radiographically examined in the same weld seam at locations away from the original spot, but in welds performed by the same welder or welder operator. The locations of these additional spots were determined as provided for the original spot examination.	When a radiographed spot fails to meet the specified acceptance standards, two additional spots should be radiographically examined in the same weld test unit at locations at least one foot removed (on each side) from the original spot. The locations of these additional spots should be determined by the examiner using the same procedure followed in the selection of the original spot for examination and the examination results should determine the following corrective actions:
If the two additional spots examined showed welding that meets the specified acceptance standards, the entire weld represented by the three radiographs is judged acceptable. The defective welding disclosed by the first of the three radiographs was removed and repaired.	(1) If the two additional spots examined meet the specified acceptance standards, the entire weld unit represented by the three spot radiographs is considered acceptable. However, the defective welding disclosed by the first of the three radiographs should be repaired by welding.

Diablo Canyon Power Plant	Safety Guide 19
If either of the two additional spots examined showed welding that does not comply with the specified acceptance standards, the entire portion of the seam represented was considered unacceptable or, optionally, the entire weld represented was completely radiographed and defective welding corrected to meet the specific acceptance standards.	(2)If either of the two additional spots examined fails to meet the specified acceptance standards, the entire weld test unit is considered unacceptable. The entire weld should be removed and the joint should be rewelded or, optionally, the entire weld unit may be completely radiographed and defective welding only need be repaired.
Repair welding was performed using a qualified procedure. The rewelded joints or weld repaired areas were completely reradiographed and meet the specified acceptance standards.	(3)Repair welding should be performed using a procedure as specified under regulatory position 3. above. The weld repaired areas in each weld test unit should be spot radiographed at one selected location to meet the acceptance criteria specified in regulatory position 7.a. or 8.a. (1). above.
	b.<u>Containment Liner Seam Welds Examined by Ultrasonic or Magnetic Particle</u>
If a weld that had been examined did not comply with the specified acceptance standards, additional examination was performed to the same extent as required for radiography. The weld was repaired and reexamined in accordance with the provisions of Section VIII of the ASME B&PV Code. See Notes 2 and 3.	When a weld which has been examined does not comply with the specified acceptance standards, the weld should be repaired and reexamined in accordance with the provisions of Section III of the ASME B&PV Code.

Diablo Canyon Power Plant	Safety Guide 19
	c. Soap Bubble Tests of Containment Liner Welds
If a weld was judged unacceptable because leakage is repaired. Repair welding was performed using a procedure qualified as specified for production welds. The weld repaired areas were reexamined by soap bubble leakage retesting.	Welds judged unacceptable because leakage is detected by the soap bubble test (see regulatory position 7.c. above) should be repaired. Repair welding should be performed using a qualified procedure as specified under regulatory position 3. above. The weld repaired areas should be reexamined by soap bubble leakage retesting.
	d. Penetration, Airlock and Access Opening Welds
If a weld was judged unacceptable on a penetration sleeve airlock, or access opening, the weld was repaired and reexamined in accordance with the provisions for Class B vessels of Section III of the ASME B&PV Code. See Notes 2 and 3.	Welds judged acceptable in accordance with regulatory position 7.d. should be repaired and reexamined in accordance with the provisions of Section III of the ASME B&PV Code.
	9. Records
Retention of records is discussed in Chapter 17.	Records of radiographs and other nondestructive examinations including those for repaired defective welds should be retained by the licensee in compliance with the provisions of Section XVII, "Quality Assurance Records," of Appendix B to 10 CFR Part 50, "Quality Assurance Criteria for Nuclear Power Plants and Fuel Reprocessing Plants."

Notes:

1. Section V, ASME B&PV Code, which provides techniques for nondestructive examination applicable to all sections of the ASME B&PV Code, was first published in July 1971. Although it may eventually replace the corresponding parts of other sections of the ASME B&PV Code, the individual sections still contain techniques for nondestructive examinations.

2. References in the table to ASME B&PV Code for the Diablo Canyon plant refer to 1968 Edition, including addenda through Summer 1968.

3. NE-5120, Section III, ASME B&PV Code, requires examination technique and acceptance criteria in accordance with Section VIII, ASME B&PV Code (Paragraph UW-51 for radiography).

4. Class B requirements of Section III, ASME B&PV Code, specify radiographic examination and acceptance criteria in accordance with Paragraph UW-51, Section VIII, ASME B&PV Code.

TABLE 3.8-4

CONTAINMENT BUILDING
BASE SLAB STRESS RATIOS[(a)]

	Operating		Accident		Accident With Hosgri		
Beam No.[(b)]	Moment Demand (ft-k)	Moment Capacity (ft-k)	Moment Demand (ft-k)	Moment Capacity (ft-k)	Moment Demand (ft-k)	Moment Capacity (ft-k)	Stress Ratio
62	15,293 --	37,640 -50,600	12,827 -37,772	36,925 -156,900	20,134 -44,967	41,250 -175,875	2.05
225	59,630 --	88,835 -18,275	75,492 --	279,275 -54,375	109,844 --	314,000 -61,083	1.49
43	12,126 --	51,880 -18,275	56,623 --	167,925 -54,375	69,444 --	188,124 -61,083	2.71
24	14,483 --	25,940 -9,138	64,157 --	83,963 -27,188	68,263 --	94,062 -30,541	1.31
129	23,425 --	88,835 -18,275	76,480 --	279,275 -54,375	93,238 --	314,000 -61,083	3.65
216	23,013 --	37,640 -50,600	19,780 -21,785	36,925 -156,900	26,007 -67,471	41,250 -175,875	1.59
171	1,898 -6,884	6,675 -30,360	-- -37,497	22,155 -94,140	5,831 -55,206	24,750 -105,525	1.91

(a) Stress Ratio = $\frac{\text{Capacity}}{\text{Demand}}$

(b) See Figure 3.8-38: + = Tension on bottom - = Tension on top

TABLE 3.8-5

CONTAINMENT BUILDING INTERNAL STRUCTURE
STRESS RATIOS IN SELECTED ELEMENTS

Description of Member	Location of Member	Load Combination[(a)]	Demand	Capacity	Stress Ratio[(b)]
Rebar in 3-ft concrete wall	Crane wall:				
	1. Vertical bar	D + L + DDE + CP	58 ksi	60 ksi	1.03
	2. Hoop bar	+ R + J + M	54 ksi	60 ksi	1.11
4-ft concrete wall	Fuel transfer canal:				
	1. Wall @ N & S from el 113 ft-1 1/2 in. to el 140 ft	D + L + DDE + CP + R + J + M	343 k-ft	381 k-ft	1.11
	2. Wall @ W from el 113 ft-1 1/2 in. to el 140 ft	D + L + DDE + CP + R + J + M	162 k-ft	216 k-ft	1.33
Rebar in 2-ft concrete wall	Fuel transfer canal wall @ W from el 88 ft to el 113 ft-1 1/2 in.	D + L + DDE + CP + R + J + M	22 ksi	60 ksi	2.72
3-ft concrete slab	Fuel transfer canal floor @ el 113 ft-1 1/2 in.	D + L + DDE + CP + R + J + M	258 k-ft	269 k-ft	1.04
4-ft Concrete Slab	Fuel transfer canal floor @ el 104 ft	D + L + DDE + CP + R + J + M	306 k-ft	381 k-ft	1.24
Rebar in 6-ft concrete wall	Reactor cavity wall:				
	1. Vertical bar	D+L+DDE+CP+R+J+M	15 ksi	60 ksi	4.0
	2. Hoop bar	D + L + DDE + CP + R + J + M	26 ksi	60 ksi	2.3
3-ft concrete slab	Floor @ el 140 ft	D + L + DE + T	46 k-ft	93 k-ft	2.02

(a) Load combinations with Hosgri do not govern.
(b) Stress Ratio $= \frac{\text{Capacity}}{\text{Demand}}$

Description of Member	Location of Member	Load Combination[a]	Demand	Capacity	Stress Ratio[b]
4 ft 6 in. concrete slab	Floor @ el 140 ft	D + L + DE + T	156 k-ft	229 k-ft	1.46
5 ft concrete slab	Floor @ el 140 ft	D + L + DDE + CP + R + J + M	328 k-ft	500 k-ft	1.52
10 in. concrete slab	Annulus platform @ el 130 ft	D + L + DE + T	10 k-ft	39 k-ft	3.90
1 ft 6 in. concrete slab	Annulus platform @ el 140 ft	D + L + DE + T	35 k-ft	57 k-ft	1.62
W21x73	Annulus platform @ el 130 ft	D + L + DE + T + TH + FV + RVOT	22 ksi	24 ksi	1.09
W21x62	"	"	8 ksi	22 ksi	2.75
W12x40	"	"	9 ksi	22 ksi	2.44
W12x65	Annulus platform column	"	124 k (Unit 1)	268 ksi	2.16
W12x65	"	"	205 k (Unit 2)	268 ksi	1.31
W12x99	"	"	212 k (Unit 1)	366 k	1.73
W21x55	Annulus platform @ el 140 ft	"	24 ksi (Unit 1)	27 ksi	1.12
W21x82	"	"	11 ksi (Unit 1)	22 ksi	2.00
W21x68	"	"	17 ksi (Unit 1)	22 ksi	1.29
W21x96	"	"	23 ksi (Unit 1)	27 ksi	1.17

TABLE 3.8-5

Description of Member	Location of Member	Load Combination[a]	Demand	Capacity	Stress Ratio[b]
W24x100	Annulus platform @ el 140 ft	D + DDE + THA + FV + RVOT	28 (Unit 2)	37.4	1.34
W21x96	"	"	18 (Unit 2)	37.4	2.08
W21x68	"	"	21 (Unit 2)	37.4	1.78
W21x55	"	"	16 (Unit 2)	37.4	2.33
W24x100	"	D + HE	21 (Unit 2)	44.8	2.13
W21x96	"	"	20 (Unit 2)	44.8	2.21
W21x68	"	"	17 (Unit 2)	44.8	2.64
W21x55	"	"	13 (Unit 2)	44.8	3.45
W12x65	Annulus platform column	D + DDE + THA + FV + RVOT	260 (Unit 2)	45.6	1.75
W12x99	"	"	270 (Unit 2)	45.6	1.69
W12x65	"	D + HE	357 (Unit 2)	55.7	1.56
W12x99	"	D + HE	365 (Unit 2)	55.7	1.53

TABLE 3.8-5A

CONTAINMENT BUILDING PIPEWAY STRUCTURE STRESS RATIOS IN SELECTED MEMBERS

Description of Member	Location of Member Unit	Elevation	Load Combination	Stress Ratio[(a)]
W8 x 40	1	114	D + DE	1.10
W8 x 40	1	114	D + DE	1.07
W8 x 40	1	114	D + DE	1.07
W14 x 111	2	109	D + DE	1.72
W14 x 111	2	109	D + DE	1.79
W14 x 111	2	109	D + DE	1.59
W8 x 40	1	114	D + DDE	1.11
W8 x 40	1	114	D + DDE	1.20
W8 x 40	1	114	D + DDE	1.20
W14 x 111	2	109	D + DDE	2.78
W14 x 111	2	109	D + DDE	1.89
W14 x 111	2	109	D + DDE	1.92
W8 x 40	1	114	D + DDE + Yr	1.06
W14 x 111	1	119	D + DDE + Yr	1.27
W14 x 202	1	119	D + DDE + Yr	1.32
W14 x 202	2	114	D + DDE + Yr	1.52
W8 X 17	2	109	D + DDE + Yr	1.11
W14 x 111	2	109	D + DDE + Yr	1.25
W8 x 40	1	114	D + HE	1.05
W8 x 40	1	114	D + HE	1.09
W8 x 40	1	114	D + HE	1.05
W14 x 111	2	109	D + HE	1.03
W10 x 31	2	109	D + HE	1.06
W12 x 106	2	138	D + HE	1.11

(a) Stress ratio = $\frac{\text{Capacity}}{\text{Demand}}$

TABLE 3.8-5B

CONTAINMENT AND AUXILIARY BUILDINGS COMPARISON OF DISPLACEMENTS AND SEPARATIONS

	Maximum Relative Seismic Displacement[a]			
Elevation (ft)	DDE	HE	Minimum Separation (in.)[c]	Minimum Factor of Safety Against Contact[e]
188	6.76	9.59	22	2.06
140	0.44	0.37	8	5.29
115	0.27	0.23	2[d]	3.05
100	0.17	0.11	1.25[d]	4.12

(a) Maximum relative seismic displacements are calculated as sum of maximum containment and auxiliary building displacements.

(b) Not Used.

(c) Minimum separation is measured at normal ambient temperature and pressure.

(d) *Except for a few localized areas, the minimum separation is 4 inches at elevations 100 ft and 115 ft.*

(e) The factor of safety is determined from the relative seismic displacements after the thermal and pressure effects are conservatively accounted for.

TABLE 3.8-6

VERIFICATION OF COMPUTER PROGRAMS

Program Name	General Function	Verification Measure
AISCBM/CE401	Analysis, design, and investigation of structural steel framing system in accordance with AISC specification	Bechtel Verification Manual
ANSR	Linear/nonlinear static and dynamic analysis finite-element program	URS/Blume QA Manual
AXIDYN	Static and dynamic analysis of axisymmetric structures	URS/Blume QA Manual
BLUME SAP IV	General-purpose linear elastic finite-element static and dynamic analysis	URS/Blume QA Manual
BSAP/CE800	General-purpose linear elastic finite-element static and dynamic analysis	Bechtel Verification Manual
BSAP-POST/ CE201&CE217	Postprocessing for BSAP computer program	Bechtel Verification Manual
CECAP/CE987	Computes stress in rebars and liner plate by considering cracking in concrete	Bechtel Verification Manual
Drain-2D	Nonlinear 2-D static and dynamic analysis	URS/Blume QA Manual
FINEL/CE801	Performs finite element static analysis by considering cracking and yielding	Bechtel Verification Manual
LOCAL STRESS/ME210	Calculates local stress in cylindrical shells due to external loading	Bechtel Verification Manual
SMIS	Matrix manipulation program	URS/Blume QA Manual
SPECTRA/CE802	Computes response spectra from acceleration time-histories	Bechtel Verification Manual
STAND/ME425	Design and evaluation of pipe support base plate with concrete anchor bolt assemblies	Bechtel Verification Manual

TABLE 3.8-6

Program Name	General Function	Verification Measure
THERMAL STRESS/ ME643	Performs thermal and stress analysis for 2-D plane or axisymmetric structures	Bechtel Verification Manual
BECHTEL ANSYS/ CE798	Large general-purpose linear/nonlinear static and dynamic analysis	Bechtel Verification Manual
BECHTEL STRUDL/ CE901	Finite element static/dynamic analysis, and design of structures	Bechtel Verification Manual
EASE2/E2SPEC	Linear elastic finite-element static and dynamic analysis computer program	Verification by Control Data Corporation
PG&E STRUDL	General purpose static and dynamic structural analysis	Partial verification of program as originally received. Complete verification performed on a case-by-case basis for each application.
GTSTRUDL/CE701	General-purpose static and dynamic finite element code	Verification by Control Data Corporation
PIPERUP	Performs nonlinear elastic/plastic analysis of 3-D piping system subject to static/dynamic time-history forcing functions	Nuclear Services Corporation Verification Manual
STARDYNE/CE991	General-purpose finite-element static and dynamic analysis	Bechtel Verification Verification
RAP	Pipe whip restraint design program	Nuclear Services Corporation Verification Manual
WECAN	Modal superposition time history analysis and static analysis of structure	Westinghouse Verification Manual
ADDA	Postprocessor to sum the time history responses for two different sets of modes	Westinghouse Verification Manual

TABLE 3.8-6

Program Name	General Function	Verification Measure
TAPES	To reformat the time history response tapes from ADDA for input to GENSPC	Westinghouse Verification Manual
GENSPC2	To calculate the modal response spectra	Westinghouse Verification Manual
COMBSPC	To combine the response spectra by SRSS	Westinghouse Verification Manual
SPREAD	To transform the scale of the spectra from frequency to period and plot the combined response spectra	Westinghouse Verification Manual
MARG3	Qualification analysis of structure	Westinghouse Verification Manual
SAP90	General-purpose linear elastic finite-element static and dynamic analysis	Computers and Structures, Inc. Verification Manual
SAP2000	General-purpose linear and non-linear finite-element program for static and dynamic analysis	Computers and Structures, Inc. Verification Manual
PC-SPECTRA	Pre- and post-processor for response spectra data	PG&E Nuclear Computer Program Acceptance Report
PC-ANSR	Linear/Nonlinear static and dynamic analysis finite-element program	PG&E Calculation No. 2252C-1 (Reference 40)

TABLE 3.8-6A

AVERAGE CONCRETE STRENGTH

CONTAINMENT AND INTERIOR STRUCTURE

Component	Average f'_c (test value) (psi)	E_c[(a)] (psi)
Base slab to elevation 87 ft	6330	4.53×10^6
Skin pour at elevation 89 ft	6330	4.53×10^6
Interior	6330	4.53×10^6
Skin pour	3850	3.54×10^6
Soldier beams	3850	3.54×10^6
Exterior walls	3850	3.54×10^6
Dome	3850	3.54×10^6

(a) $E_c = 57,000 (f'_c)^{1/2}$ per AC1 318-71, in psi

Exemption 4

TABLE 3.8-6B

STEEL STRENGTH DATA

CONTAINMENT AND INTERIOR STRUCTURE

Structure	Designation of Steel	Yield (psi) Minimum	Yield (psi) Average	Ultimate (psi) Minimum	Ultimate (psi) Average
		Reinforcing Steel			
Containment (1 and 2) Exterior #18s	ASTM 615, Grade 60	61,750	66,854	93,750	105,992
Containment (1 and 2) Interior #11s	Grade 60	62,820	68,079	96,795	105,556
		Structural Steel			
ASTM	A36	36,100	43,950	58,200	68,040
ASTM	A441	42,100	51,620	67,200	75,910
ASTM	A516	45,800	51,040	72,200	79,170

TABLE 3.8-7

AUXILIARY BUILDING
FUEL HANDLING CRANE SUPPORT STRUCTURE
STRUCTURAL MEMBERS AND ANCHORAGES STRESS RATIOS

	Description Of Members And Their Functions	Stress Ratios[(a) (b)] Hosgri	DDE	DE
BRACES	Top Chord Roof	1.7	1.5	1.9
	Bottom Chord Roof	1.1	1.2	1.3
	East-West Elevation Diagonals	1.1	1.1	1.4
	N-S Truss Diagonals, West and East Exterior/Interior	1.9	≥ 1.6	≥ 2.0
	East-West Truss Diagonals	1.1	≥ 1.3	≥ 1.1
	East-West Truss Knee	1.1	≥ 1.3	≥ 1.5
CHORDS	North South Trusses, Top	3.4	4.0	4.2
	North South Trusses, Bottom	3.2	4.0	4.3
	East-West Trusses, Top	1.1	1.6	1.9
	East-West Trusses, Bottom	1.1	1.4	1.8
LATERAL & VERTICAL	Frame Horizontals, West and East Sides	4.5	4.8	5.9
	Vertical Columns	1.0	1.1	1.0
	East-West Truss Struts	1.2	1.4	1.6
BASE ANCHORAGE	Axial Tensions	1.0	1.1	1.6
	Axial Compressions	1.3	1.4	1.7
	Lateral Shears	1.9	2.2	2.3

(a) Stress Ratio = $\frac{\text{Capacity}}{\text{Demand}}$

(b) Refer to Calculation 52.15.7.1.1.15 for stress ratios.

TABLE 3.8-8

AUXILIARY BUILDING SLABS STRESS RATIOS[(a)(b)]
OUT-OF-PLANE LOADS (DE)

Slab Location	Member	Shear, psi Demand	Shear, psi Capacity	Moment, kips-ft Demand	Moment, kips-ft Capacity	Stress Ratio
El 73 ft						
Area bounded by column[(c)] lines H, U, 15.7, 16.8	Slab	49	60	24	30	1.2
	Beam	48	60	100	140	1.2
El 85 ft						
Area bounded by column lines H, U, 16.8, 19.2	Slab	64	78	82	120	1.2
El 100 ft & 115 ft						
Area bounded by column[(c)] lines H, T, 10.7, 15.7	Slab	48	78	75	88	1.2
	Beam	70	120	340	470	1.4
El 115 ft						
Area bounded by column lines U, V, 15.7, 20.3	Slab	45.0	78.0	27.0	32.00	1.2
El 115 ft						
Area bounded by column lines H, L.5, 15.7, 20.3	Slab	59	78	56	67	1.2
	Beam	170	210	2,000	2,400	1.2
El 140 ft						
Area bounded by column[(c)] lines H, T, 10.7, 15.7	Slab	120	130	2,050	2,390	1.1
	Beam	130	140	1450	1640	1.1
El 140 ft						
Area bounded by column[(c)] lines R, V, 15.7, 17.4	Slab	55	78	59	77	1.3
	Beam	89	97	2,010	2,240	1.1
El 140 ft						
Area bounded by column lines H, L, 15.7, 20.3	Slab	57.0	78.0	382.0	455.00	1.2
El 154-1/2 ft						
Area bounded by column lines L, R, 15.7, 17.4	Slab	30	78	14	17	1.2
	Beam	60	78	76	100	1.3
El 163-1/3 ft						
Area bounded by column lines H, L, 15.7, 20.3	Composite[(d)] Beam	9,300	14,000	2,260	2,300	1.02

(a) Stress ratio $= \frac{\text{Capacity}}{\text{Demand}}$ for shear or moment, whichever is smaller.

(b) This does not include the effects of pipe break loads which are evaluated locally in accordance with provisions of Reference 6.

(c) Counterpart in Unit 2 is similar.

(d) These values are for structural steel beams embedded in the slab.

TABLE 3.8-9

AUXILIARY BUILDING SLABS STRESS RATIOS[(a)(b)]
OUT-OF-PLANE LOADS (DDE)

Slab Location	Member	Shear, psi Demand	Shear, psi Capacity	Moment, kips-ft Demand	Moment, kips-ft Capacity	Stress Ratio
El 73 ft						
Area bounded by column[(c)]	Slab	53	91	27	56	1.7
lines H, U, 15.7, 16.8	Beam	53	93	110	260	1.8
El 85 ft						
Area bounded by column lines H, U, 16.7, 19.2	Slab	72	120	93	220	1.7
El 100 ft & 115 ft						
Area bounded by column[(c)]	Slab	51	120	81	167	2.1
lines H, T, 10.7, 15.7	Beam	130	200	360	900	1.5
El 115 ft						
Area bounded by column lines U, V, 15.7, 20.3	Slab	49	120	30	62	2.1
El 115 ft						
Area bounded by column	Slab	66	120	63	130	1.8
lines H, L.5, 15.7, 20.3	Beam	190	330	2,200	4,600	1.7
El 140 ft						
Area bounded by column[(c)]	Slab	120	190	2,110	4,310	1.6
lines H, T, 10.7, 15.7	Beam	130	200	1,500	3,140	1.5
El 140 ft						
Area bounded by column[(c)]	Slab	56	120	60	150	2.1
lines R, V, 15.7, 17.4	Beam	93	150	2,110	4,030	1.9
El 140 ft						
Area bounded by column lines H, L, 15.7, 20.3	Slab	61	120	411	858	2.0
El 154-1/2 ft						
Area bounded by column	Slab	32	120	15	33	2.2
lines L, R, 15.7, 17.4	Beam	64	120	81	190	1.9
El 163-1/3 ft						
Area bounded by column lines H, L, 15.7, 20.3	Composite[(d)] Beam	11,000	20,000	2,200	3,100	1.4

(a) Stress ratio = $\frac{\text{Capacity}}{\text{Demand}}$ for shear or moment, whichever is smaller.

(b) This does not include the effects of pipe break loads which are evaluated locally in accordance with provisions of Reference 6.

(c) Counterpart in Unit 2 is similar.

(d) These values are for structural steel beams embedded in the slab.

TABLE 3.8-10

AUXILIARY BUILDING SLABS STRESS RATIOS[a][b]
OUT-OF-PLANE LOADS (HE)

Slab Location	Member	Shear, psi Demand	Shear, psi Capacity	Moment, kips-ft Demand	Moment, kips-ft Capacity	Stress Ratio
El 73 ft						
Area bounded by column[c] lines H, U, 15.7, 16.8	Slab	65	110	32	56	1.7
	Beam	63	110	130	260	1.7
El 85 ft						
Area bounded by column lines H, U, 16.8, 19.2	Slab	91	130	120	270	1.4
El 100 ft & 115 ft						
Area bounded by column[c] lines H, T, 10.7, 15.7	Slab	68	130	110	200	1.8
	Beam	170	220	480	1,100	1.3
El 115 ft						
Area bounded by column lines U, V, 15.7, 20.3	Slab	60.0	130.00	36.0	74.00	2.0
El 115 ft						
Area bounded by column lines H, L.5, 15.7, 20.3	Slab	100	130	120	150	1.2
	Beam	300	360	4,300	5,500	1.2
El 140 ft						
Area bounded by column[c] lines H, T, 10.7, 15.7	Slab	160	200	2,720	5,220	1.3
	Beam	170	200	2,140	3,770	1.2
El 140 ft						
Area bounded by column[c] lines R, V, 15.7, 17.4	Slab	72	130	79	180	1.8
	Beam	145	160	3,280	4,870	1.1
El 140 ft						
Area bounded by column lines H, L, 15.7, 20.3	Slab	105.0	130.00	710.0	1,062.00	1.2
El 154-1/2 ft						
Area bounded by column[c] lines L, R, 15.7, 17.4	Slab	65	130	29	41	1.4
	Beam	92	130	150	230	1.4
El 163-1/3 ft						
Area bounded by column lines H, L, 15.7, 20.3	Composite[d] Beam	16,000	24,000	3,900	4,200	1.1

(a) Stress ratio = $\frac{\text{Capacity}}{\text{Demand}}$ for shear or moment, whichever is smaller.

(b) This does not include the effects of pipe break loads which are evaluated locally in accordance with provisions of Reference 6.

(c) Counterpart in Unit 2 is similar.

(d) These values are for structural steel beams embedded in the slab.

TABLE 3.8-11

AUXILIARY BUILDING SLABS STRESS RATIOS(f)
IN-PLANE LOADS (DE)

Elevation, ft	Section(e)(g) Number	Shear(c), kip		Moment(d), k-ft		Stress Ratio
		Demand	Capacity(a)	Demand	Capacity(b)	
100	1-a	60	2,200	2,650	25,300	9.5
100	1-b	170	2,300	5,700	21,600	3.8
100	2-a	320	2,880	9,500	91,900	9.0
100	2-b	110	1,060	700	6,350	9.1
100	2-c	10	220	50	600	>10.0
115	1	300	2,240	7,350	23,200	3.2
115	2-a	240	4,350	200	50,900	>10.0
115	2-b	120	490	2,100	4,100	2.0
115	3-a	260	1,260	2,650	7,700	2.9
115	3-b	280	1,280	2,150	18,100	4.6
115	4	1,460	8,100	29,700	289,000	5.5
140	1	380	2,240	2,500	4,800	1.9
140	2-a	320	4,130	5,100	64,000	>10.0
140	2-b	270	2,100	3,050	13,800	4.5
140	3-a	160	430	1,950	4,950	2.5
140	3-b	390	1,530	5,900	16,300	2.8
140	4	1,840	8,580	39,500	443,000	4.7

(a) Shear capacity is calculated for the section subjected to demand moment and axial force.
(b) *Moment capacity is calculated for the section subjected to demand axial force.*
(c) Shear capacities and demands are rounded to the nearest 10 kips or 3 significant digits.
(d) Moment capacities and demands are rounded to the nearest 50 ft-kips or 3 significant digits.
(e) Section location is shown on Figures 3.8-60 through 3.8-62.
(f) Stress ratio = $\frac{\text{Capacity}}{\text{Demand}}$ for shear or moment, whichever is smaller
(g) Component in Unit 2 is similar.

TABLE 3.8-12

AUXILIARY BUILDING SLABS STRESS RATIOS[f]
IN-PLANE LOADS (DDE)

Elevation, ft	Section[e][g] Number	Shear[c], Kip		Moment[d], k-ft		Stress Ratio
		Demand	Capacity[a]	Demand	Capacity[b]	
100	1-a	110	3,710	3,400	73,300	>10.0
100	1-b	310	3,770	9,850	63,100	6.4
100	2-a	610	4,800	14,900	303,000	7.9
100	2-b	200	1,770	1,250	17,000	8.9
100	2-c	10	370	50	1,100	>10.0
115	1	500	3,730	15,400	88,700	5.8
115	2-a	430	7,240	3,550	167,000	>10.0
115	2-b	240	1,130	4,500	16,500	3.7
115	3-a	330	2,090	2,900	12,000	4.1
115	3-b	450	2,140	2,350	42,600	4.8
115	4	2,920	13,500	60,000	1,000,000	4.6
140	1	750	3,730	4,250	43,300	5.0
140	2-a	840	6,890	6,150	200,000	8.2
140	2-b	510	3,500	5,550	36,200	6.5
140	3-a	240	720	2,550	10,300	3.0
140	3-b	590	2,550	8,900	46,400	4.3
140	4	3,700	14,300	79,000	1,110,000	3.9

(a) Shear capacity is calculated for the section subjected to demand moment and axial force.
(b) Moment capacity is calculated for the section subjected to demand axial force.
(c) Shear capacities and demands are rounded to the nearest 10 kips or 3 significant digits.
(d) Moment capacities and demands are rounded to the nearest 50 ft-kips or 3 significant digits.
(e) Section location is shown on Figures 3.8-60 through 3.8-62.
(f) Stress ratio = $\frac{\text{Capacity}}{\text{Demand}}$ for shear or moment, whichever is smaller
(g) Component in Unit 2 is similar.

TABLE 3.8-13

AUXILIARY BUILDING SLABS STRESS RATIOS[f]
IN-PLANE LOADS (HE)

Elevation, ft	Section[e][g] Number	Shear[c], Kip		Moment[d], k-ft		Stress Ratio
		Demand	Capacity[a]	Demand	Capacity[b]	
100	1-a	170	4,350	3,650	86,100	>10.0
100	1-b	510	4,500	13,000	65,000	5.0
100	2-a	930	5,580	18,500	180,000	6.0
100	2-b	290	1,830	1,500	13,300	6.3
100	2-c	20	360	100	1,250	>10.0
115	1	770	3,730	25,000	88,500	3.5
115	2-a	710	7,700	11,300	231,000	>10.0
115	2-b	400	1,120	8,050	16,400	2.0
115	3-a	480	2,330	3,100	14,500	4.7
115	3-b	820	2,500	3,200	48,900	3.0
115	4	3,940	15,500	117,000	1,170,000	3.9
140	1	1,120	3,870	9,200	38,000	3.5
140	2-a	1,170	8,010	7,300	240,000	6.8
140	2-b	900	4,150	7,750	43,100	4.6
140	3-a	450	830	3,250	13,800	1.8
140	3-b	970	3,010	11,300	50,700	3.1
140	4	5,210	14,500	157,000	1,160,000	2.8

(a) Shear capacity is calculated for the section subjected to demand moment and axial force
(b) Moment capacity is calculated for the section subjected to demand axial force
(c) Shear capacities and demands are rounded to the nearest 10 kips or 3 significant digits
(d) Moment capacities and demands are rounded to the nearest 50 ft-kips or 3 significant digits
(e) Section location is shown on Figures 3.8-60 through 3.8-62
(f) Stress ratio = $\frac{\text{Capacity}}{\text{Demand}}$ for shear or moment, whichever is smaller
(g) Component in Unit 2 is similar

TABLE 3.8-14

AUXILIARY BUILDING CONCRETE WALLS
STRESS RATIOS (DE)[a]

		Shear, psi		Moment 10^3, k-ft		
Wall Location	Elev., ft	Demand	Capacity[b]	Demand	Capacity[b]	Stress Ratio
On line H (15.7-20.3)	100	120	230	57	188	1.9
	85	160	330	9	173	1.9
On line J (11.7-15.7)[c]	100	130	270	35	126	2.0
	85	150	280	47	126	1.8
On line T(6.4-15.7)[c]	100	75	200	141	343	2.4
	85	85	220	164	664	2.6
On line T (16.8-19.2)	100[d]	55	210	15	65	3.8
On line U.5 (10.3-12.9)[c]	100[d]	45	155	20	113	3.4
On line V (15.7-20.3)	100	50	100	32	250	2.0
	85	50	90	67	245	1.8
On line V (6.4-15.7)[c]	100[d]	70	360	82	200	2.4
On line 6.4 (V-S)[c]	100	80	250	85	158	1.9
	85	100	340	20	31	1.6
On line 10.3 (T-V)[c]	100[d]	80	250	54	146	2.7
On line 12.9 (T-V)[c]	100[d]	80	240	54	145	2.7
On line 15.7 (H-T.6)[c]	100	110	250	382	782	2.1
	85	110	220	481	818	1.7
On line 15.7 (H-T.6)[c]	100	110	260	7	19	2.3
	85	60	170	12	19	1.6

(a) Stress ratio = $\frac{\text{Capacity}}{\text{Demand}}$ for shear or moment, whichever is smaller
(b) Axial demand effect is included in the capacities
(c) Counterpart in Unit 2 is similar
(d) Wall does not extend below elevation 100 ft

TABLE 3.8-15

AUXILIARY BUILDING CONCRETE WALLS
STRESS RATIOS (DDE)[a]

		Shear, psi		Moment 10^3, k-ft		
Wall Location	Elev., ft	Demand	Capacity[b]	Demand	Capacity[b]	Stress Ratio
On line H (15.7-20.3)	100	240	390	114	407	1.6
	85	310	550	178	556	1.8
On line J (11.7-15.7)[c]	100	250	450	62	253	1.8
	85	290	460	90	253	1.6
On line T (6.4-15.7) [c]	100	140	340	273	987	2.4
	85	170	370	316	1086	2.2
On line T (16.8-19.2)	100[d]	110	350	31	147	3.2
On line U.5(10.3-12.9) [c]	100[d]	85	260	40	244	3.0
On line V (15.7-20.3)	100	90	170	63	394	1.9
	85	100	150	133	327	1.5
On line V (6.4-15.7) [c]	100[d]	140	600	133	400	3.0
On line 6.4 (V-S) [c]	100	160	420	141	333	2.4
	85	190	570	34	92	2.7
On line 10.3 (T-V) [c]	100[d]	160	420	105	280	2.6
On line 12.9 (T-V) [c]	100[d]	160	410	106	268	2.5
On line 15.7 (H-T.6) [c]	100	220	420	553	1205	1.9
	85	220	370	740	1155	1.6
On line 15.7 (U-V) [c]	100	220	430	13	32	1.9
	85	115	290	23	30	1.3

(a) Stress ratio = $\frac{\text{Capacity}}{\text{Demand}}$ for shear or moment, whichever is smaller
(b) Axial demand effect is included in the capacities
(c) Counterpart in Unit 2 is similar
(d) Wall does not extend below elevation 100 ft

TABLE 3.8-16

AUXILIARY BUILDING CONCRETE WALLS
STRESS RATIOS (HE)[a]

		Shear, psi		Moment 10^3, k-ft		
Wall Location	Elev., ft	Demand	Capacity[b]	Demand	Capacity[b]	Stress Ratio
On line H (15.7-20.3)	100	400	480	176	504	1.2
	85	510	630	270	682	1.2
On line J (11.7-15.7)[c]	100	390	500	107	313	1.3
	85	440	580	145	313	1.3
On line T (6.4-15.7)[c]	100	190	310	438	860	1.6
	85	230	320	493	979	1.4
On line T (16.8-19.2)	100[d]	150	350	42	168	2.3
On line U.5 (10.3-12.9)[c]	100[d]	130	190	60	197	1.5
On line V (15.7-20.3)	100	140	200	90	489	1.4
	85	150	170	182	405	1.15
On line V (6.4-15.7)[c]	100[d]	220	640	291	500	1.7
On line 6.4 (V-S)[c]	100	380	460	301	434	1.2
	85	390	450	63	84	1.15
On line 10.3 (T-V)[c]	100[d]	330	480	220	339	1.4
On line 12.9 (T-V)[c]	100[d]	270	460	199	324	1.6
On line 15.7 (H-T.6)[c]	100	330	520	666	1494	1.6
	85	320	450	859	1425	1.4
On line 15.7 (U-V)[c]	100	340	480	19	36	1.4
	85	160	300	30.5	32.6	1.07

(a) Stress ratio = $\frac{\text{Capacity}}{\text{Demand}}$ for shear or moment, whichever is smaller
(b) Axial demand effect is included in the capacities
(c) Counterpart in Unit 2 is similar
(d) Wall does not extend below elevation 100 ft

TABLE 3.8-17

AUXILIARY BUILDING COLUMNS STRESS RATIOS[a]

Column Location[b]	Stress Ratio		
	DE	DDE	HE
14 - J.7	2.9	3.7	2.6
15 – N	5.3	7.7	4.8
15 - R.8	3.6	3.3	2.5
15 - J.7	1.04	1.8	1.3
15 – S	1.9	2.9	2.3

(a) Stress ratio = $\frac{\text{Capacity}}{\text{Demand}}$

(b) Counterpart in Unit 2 is similar

TABLE 3.8-18

AUXILIARY BUILDING SHEAR DISSIPATION TO FOUNDATION (DE NORTH-SOUTH)

	Shear Demand at Elevation 85 ft.					
	Shear from Upper Level					
Building Portion Location[a]	Direct Shear, kips	Torsional Shear, kips[b]	Torsional + Direct Shear, kips	Inertial Load at El 85 ft, kips	Total, kips	Remarks
Central Portion	23,600	1,800	25,400	4,400	29,800	Capacity is 57,900 kips
North Wing	2,300 900 200 4,700 600	500 100	2,800 1,000 200 4,700 600	600 600 400	10,900	Load is directly dissipated to the foundation
South Wing	2,300 900 200 4,700 600	500 100	2,800 1,000 200 4,700 600	600 600 400	10,900	Load is directly dissipated to the foundation

<u>Shear Capacity at Elevation 85 ft (Central Portion)</u>

Capacity of diaphragm to dissipate shear force to the foundation at elevation 85 ft (kips)	by bearing by rebar tension	4,700 + 18,000 = 22,700 1,100 + 1,100 = 2,200
Shear capacity of walls below elevation 85 ft (kips)		33,000
Total shear capacity at and below elevation 85 ft (kips)		57,900

(a) For building portion location only, see Figures 3.8-63 and 3.8-64
(b) Torsional shears on only one side of the center of rigidity are considered

TABLE 3.8-19

AUXILIARY BUILDING SHEAR DISSIPATION TO FOUNDATION (DE EAST-WEST)

Building Portion Location[a]	Shear Demand at Elevation 85 ft. — Shear from Upper Level — Direct Shear, kips	Torsional Shear, kips	Torsional + Direct Shear, kips	Inertial Load at El 85 ft, kips	Total, kips	Remarks
Central Portion	35,500	-0-	35,500	4,400	39,900	Capacity is 76,200 kips
North Wing	900 1,100 400 400	-0-	900 1,100 400 400	600 600 400	4,400	Load is directly dissipated to the foundation
South Wing	900 1,100 400 400	-0-	900 1,100 400 400	600 600 400	4,400	Load is directly dissipated to the foundation

<u>Shear Capacity at Elevation 85 ft (Central Portion)</u>

Capacity of diaphragm to dissipate shear force to the foundation at elevation 85 ft (kips)	4,100 4,100
Shear capacity of walls below elevation 85 ft (kips)	68,000
Total shear capacity at and below elevation 85 ft (kips)	76,200

(a) For building portion location only, see Figures 3.8-63 and 3.8-64

TABLE 3.8-20

AUXILIARY BUILDING SHEAR DISSIPATION TO FOUNDATION (DDE NORTH-SOUTH)

	Shear Demand at Elevation 85 ft.					
	Shear from Upper Level					
Building Portion Location[(a)]	*Direct* Shear, kips	*Torsional* Shear, kips[(b)]	*Torsional +* Direct Shear, kips	Inertial *Load at* El 85 ft, kips	Total, kips	Remarks
Central Portion	46,500	3,700	50,200	9,200	59,400	Capacity is 115,700 kips
North Wing	4,300 1,600 400 9,100 1,200	1,000 300 100	5,300 1,900 500 9,100 1,200	1,100 1,100 800	21,000	Load is directly dissipated to the foundation
South Wing	4,300 1,600 400 9,100 1,200	1,000 300 100	5,300 1,900 500 9,100 1,200	1,100 1,100 800	21,000	Load is directly dissipated to the foundation

<u>Shear Capacity at Elevation 85 ft (Central Portion)</u>

Capacity of diaphragm to dissipate shear force to the foundation at elevation 85 ft (kips)	by bearing by rebar tension	11,000 + 42,000 = 53,000 1,000 + 1,900 = 3,800
Shear capacity of walls below elevation 85 ft (kips)		58,000
Total shear capacity at and below elevation 85 ft (kips)		115,700

(a) For building portion location only see Figures 3.8-63 and 3.8-64
(b) Torsional shears on only one side of the center of rigidity are considered

TABLE 3.8-21

AUXILIARY BUILDING SHEAR DISSIPATION TO FOUNDATION (DDE EAST-WEST)

Building Portion Location[(a)]	Shear Demand at Elevation 85 ft. — Shear from Upper Level: Direct Shear, kips	Shear Demand at Elevation 85 ft. — Shear from Upper Level: Torsional Shear, kips	Shear Demand at Elevation 85 ft. — Shear from Upper Level: Torsional + Direct Shear, kips	Shear Demand at Elevation 85 ft. — Inertial Load at El 85 ft, kips	Total, kips	Remarks
Central Portion	68,700	-0-	68,700	9,200	77,900	Capacity is 128,000 kips
North Wing	1,600 2,100 900 700	-0-	1,600 2,100 900 700	1,100 1,100 800	8,300	Load is directly dissipated to the foundation
South Wing	1,600 2,100 900 700	-0-	1,600 2,100 900 700	1,100 1,100 800	8,300	Load is directly dissipated to the foundation

Shear Capacity at Elevation 85 ft (Central Portion)

Capacity of diaphragm to dissipate shear force to the foundation at elevation 85 ft (kips)	7,000 7,000
Shear capacity of walls below elevation 85 ft (kips)	114,000
Total shear capacity at and below elevation 85 ft (kips)	128,000

(a) For building portion location only see Figures 3.8-63 and 3.8-64

TABLE 3.8-22

AUXILIARY BUILDING SHEAR DISSIPATION TO FOUNDATION (HE NORTH-SOUTH)[(a)]

Building Portion Location[(a)]	Shear Demand at Elevation 85 ft. Shear from Upper Level: Direct Shear, kips	Torsional Shear, kips[(b)]	Torsional + Direct Shear, kips	Inertial Load at El 85 ft, kips	Total, kips	Remarks
Central Portion	63,000	9,000	72,000	12,500	84,500	Capacity is 136,800 kips
North Wing	5,700 2,100 500 12,200 1,700	2,300 500 300	8,000 2,600 800 12,200 1,700	1,600 1,600 1,000	29,500	Load is directly dissipated to the foundation
South Wing	5,700 2,100 500 12,200 1,700	2,300 500 300	8,000 3,600 800 12,200 1,700	1,600 1,600 1,000	29,500	Load is directly dissipated to the foundation

Shear Capacity at Elevation 85 ft (Central Portion)

Capacity of diaphragm to dissipate shear force to the foundation at elevation 85 ft (kips)	by bearing by rebar tension	14,600 + 48,400 = 63,000 2,940 + 2,400 = 4,800
Shear capacity of walls below elevation 85 ft (kips)		69,000
Total shear capacity at and below elevation 85 ft (kips)		136,800

(a) For illustration, see Figures 3.8-63 and 3.8-64.
(b) Torsional shears on only one side of the center of rigidity are considered.

TABLE 3.8-23

AUXILIARY BUILDING SHEAR DISSIPATION TO FOUNDATION (HE EAST-WEST)[(a)]

Building Portion Location[(a)]	Shear Demand at Elevation 85 ft. Shear from Upper Level: Direct Shear, kips	Shear from Upper Level: Torsional Shear, kips[(b)]	Shear from Upper Level: Torsional + Direct Shear, kips	Inertial Load at El 85 ft, kips	Total, kips	Remarks
Central Portion	84,700	5,300	90,000	12,500	102,500	Capacity is 154,200 kips
North Wing	2,000 2,500 1,100 900	1,600 1,900 600 100	3,600 4,400 1,700 1,000	1,600 1,600 1,000	14,900	Load is directly dissipated to the foundation
South Wing	2,000 2,500 1,100 900		2,000 2,500 1,100 900	1,600 1,600 1,000	10,700	Load is directly dissipated to the foundation

Shear Capacity at Elevation 85 ft (Central Portion)

Capacity of Diaphragm to Dissipate Shear Force to the Foundation at Elevation 85 ft (kips)	8,600 8,600
Shear Capacity of Walls Below Elevation 85 ft (kips)	137,000
Total Shear Capacity at and Below Elevation 85 ft (kips)	154,200

(a) For illustration, see Figures 3.8-63 and 3.8-64.
(b) Torsional shears on only one side of the center of rigidity are considered.

TABLE 3.8-23A

AUXILIARY BUILDING AND TURBINE BUILDING
COMPARISON OF DISPLACEMENTS AND SEPARATIONS

Elevation (ft)	Maximum Total Displacement (in.)[a] DDE	HE	Separation (in.)	Minimum Factor of Safety Against Contact
163	2.7	4.5	8.0	1.78
140	0.9	0.9	8.0	8.89
115	0.7	1.1	8.0	7.27
100	0.5	0.7	3.0	4.29

(a) Displacements are calculated as sum of maximum auxiliary and turbine building displacements.

TABLE 3.8-24

DUCTILITY[(a)]

Structure	Blume Ductility	Newmark Ductility	
Containment	1.3[(b)]	1.0[(b)]	
Auxiliary Building	1.3[(b)]	1.0[(b)]	
		Class I	Class II
Turbine Building	[(c)]	1.0[(b)]	[(c)]
Intake	[(c)]	1.0[(b)]	[(c, d)]

(a) Ductilities are on story basis; however, floor response spectra were, in general, computed on an elastic analysis basis.

(b) Under normal conditions Newmark ductility is 1.0 maximum; higher ductility may be considered for special cases where supporting evidence justifies its use. Blume ductility for Class I structures is 1.3, and may be used only in specific situations.

(c) Concrete 1.3; steel 3, with up to 6 locally.

(d) Or as may be required to demonstrate that function of Design Class I equipment will not be adversely affected.

TABLE 3.8-25

REFUELING WATER STORAGE TANK
STRESS RATIO[(a)]

		DL + HS + DE + R_A			DL + HS + DDE + R_A			DL + HS + HE + R_A		
Force Component	Material	Demand	Capacity	Stress Ratio	Demand	Capacity	Stress Ratio	Demand	Capacity	Stress Ratio
Longitudinal force, Kips/ft	Concrete	63.5	96.0	1.51	121.2	216.0	1.78	133.3	216.0	1.62
Circumferential force, kips/ft	Concrete	54.4	96.0	1.76	71.5	216.0	3.02	79.6	216.0	2.71
In plane shear force, kips/ft	Concrete	26.1	45.5	1.74	52.1	77.4	1.49	58.9	77.4	1.31
Longitudinal moment, Kips-ft/ft	Concrete	40.4	78.2	1.94	56.3	179.7	3.19	58.6	179.7	3.07
Stress intensity outside vault opening area, Kips/in^2	Steel	6.4	16.7	2.61	11.2	22.5	2.01	15.4	40.6	2.64
Stress intensity within vault opening area, Kips/in^2	Steel	12.1	16.7	1.38	20.5	22.5	1.10	34.0	40.6	1.19

(a) Stress Ratio = $\frac{\text{Capacity}}{\text{Demand}}$

TABLE 3.8-26

TURBINE BUILDING
STRUCTURAL STEEL MEMBERS
STRESS RATIOS (HE)

Member Description	Stress Ratios[a]
Exterior columns, lines A and G	[b]
East-west roof trusses – chords	1.2[c]
East-west roof trusses – diagonals	1.0[c]
North-south walls diagonal tension bracing	1.1[c]
North-south walls diagonal compression bracing	1.0[c]
Crane runway girder	[b]
Floor beams	[b]

(a) Stress Ratio = $\frac{\text{Capacity}}{\text{Demand}}$

(b) Inelastic deformation occurs, ductility meets limits of Table 3.8-24.

(c) Effects of force redistribution are included.

TABLE 3.8-27

TURBINE BUILDING
CONCRETE MEMBERS
STRESS RATIOS (HE)[a]

Member	Location	Stress Ratios[b]
Wall, line A	Elev. 85 ft (20-30.3)	1.9
Wall, line G	Elev. 85 ft (20-30.3)	1.3
Wall, line 19	Elev. 123 ft (A-G)	1.1
Buttress, line 27	Elev. 85 ft	1.5
Floor slab	Elev. 140 ft line 21 (A-C), line C (19-21)	1.2 1.5[c]
Turbine Pedestal	Frame 6 (See Figure 3.7-15G)	1.0[d]

(a) Stress Ratio = $\frac{\text{Capacity}}{\text{Demand}}$ for shear or moment, whichever is smaller.

(b) Axial demand effect is included in the capacity.

(c) Effects of concrete cracking are considered.

(d) Effects of force distribution are included.

TABLE 3.8-27A

TURBINE BUILDING AND TURBINE PEDESTAL (UNITS 1 & 2)[a]
COMPARISON OF DISPLACEMENTS AND SEPARATIONS AT EL 140 FT
HE ANALYSIS

Side of Pedestal Location	Maximum Calculated Displacement, in.[b]			Minimum Separation, in.[c]	Factor of Safety Against Contact
	Building	Pedestal	Total		
East	0.53	1.67	2.20	2.88	1.31
West	0.58	1.67	2.25	3.00	1.33
North	0.20	0.73	0.93	1.25	1.34
South	0.21	0.76	0.97	1.31	1.35

(a) Values shown are for Unit 1 or Unit 2, whichever has the lowest factor of safety.

(b) Displacements are an envelope of maximum displacements calculated using Newmark-Hosgri design response spectra.

(c) Separations are an envelope of minimum as-built separations.

TABLE 3.8-28

INTAKE STRUCTURE
CAPACITIES AND DUCTILITIES OF FLOW STRAIGHTENERS (OR PIERS)[1]

Pier	P (Tension)	M	M_{allow}	U (Ductility)
1	129.0	10,600	15,600	N/A
2	81.5	14,300	15,900	N/A
3	44.6	15,700	16,100	N/A
4	24.1	16,400	16,200	1.24
5	39.1	17,300	16,100	1.33
6	141.0	17,700	15,500	1.44
7	146.0	16,300	15,400	1.32

Notes:

(1) These values are due to the Newmark earthquake, which governs for all piers:

P = Axial tension, kips

M = Moment, in.-kips (value of M based on linear analysis)

M_{allow} = Factored (0=0.90) ultimate moment capacity including tension effects

u = Ductility of tensile steel (ratio between calculated strain to yield strain)

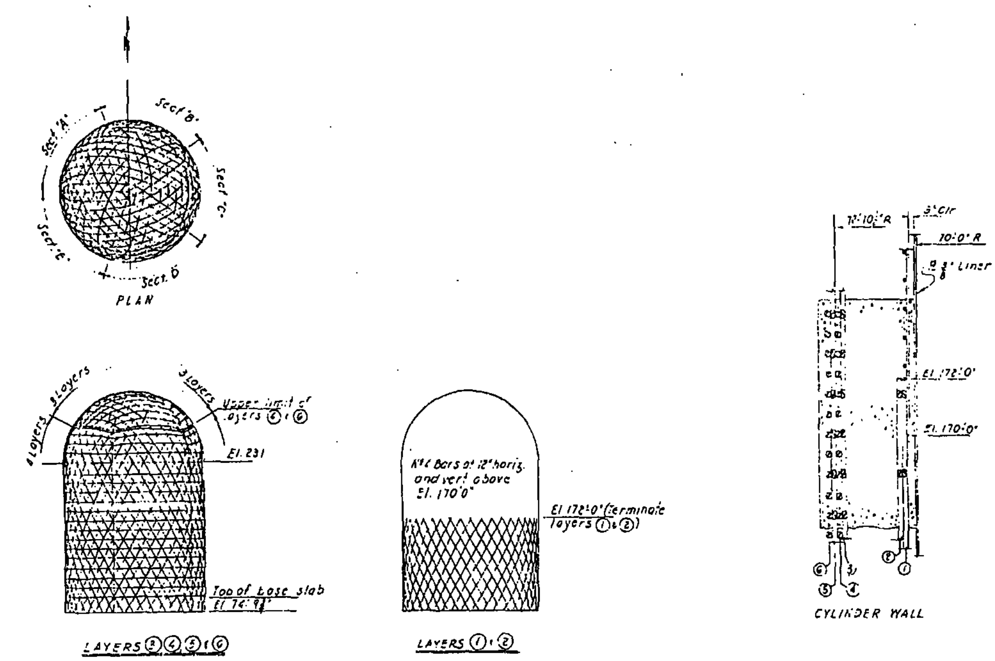

FSAR UPDATE

UNITS 1 AND 2
DIABLO CANYON SITE

FIGURE 3.8-1

CONTAINMENT STRUCTURE
REINFORCING STEEL ARRANGEMENT

Revision 11 November 1996

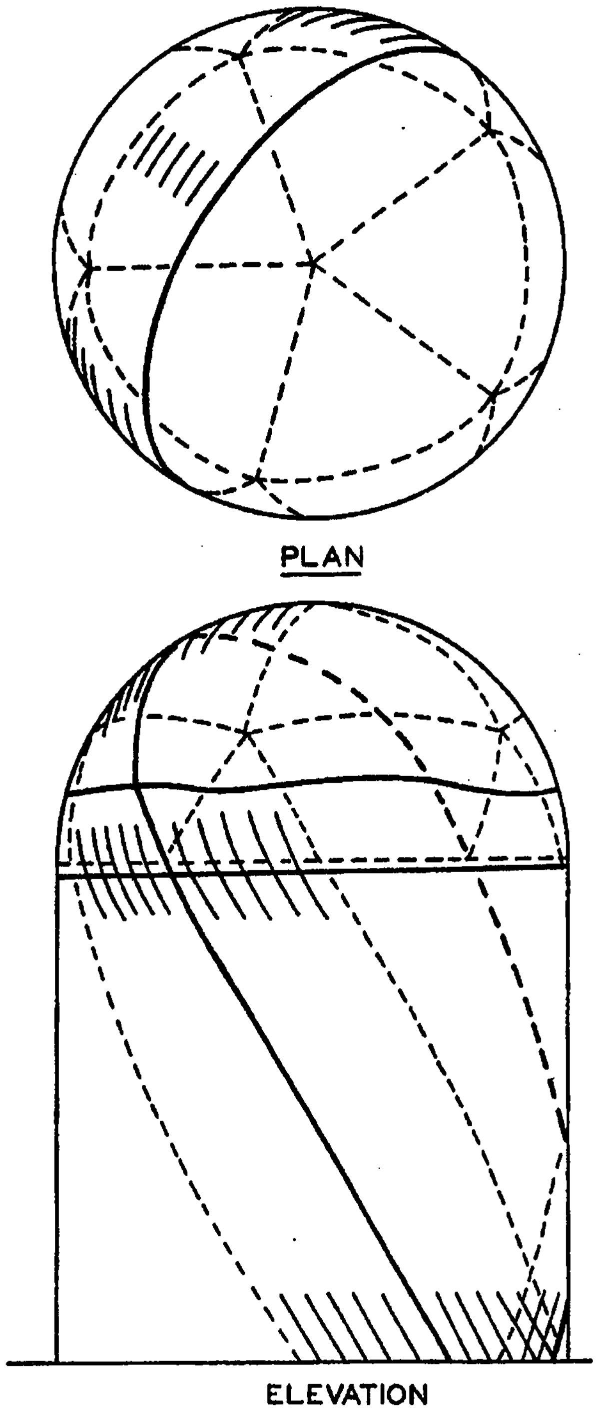

FSAR UPDATE

UNITS 1 AND 2
DIABLO CANYON SITE

FIGURE 3.8-2

CONTAINMENT STRUCTURE

TYPICAL REINFORCING LOOP

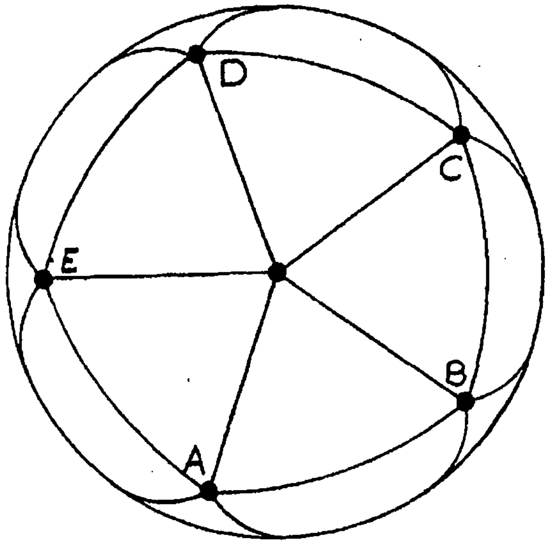

SKETCH 1

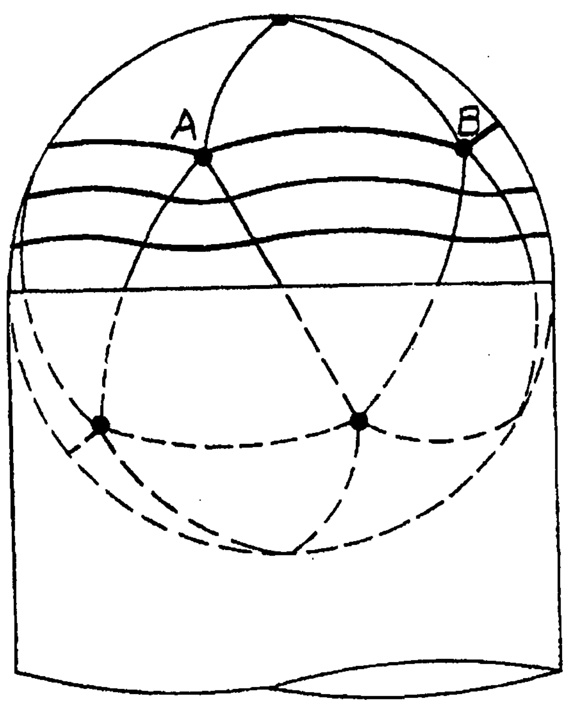

SKETCH 2

FSAR UPDATE

UNITS 1 AND 2
DIABLO CANYON SITE

FIGURE 3.8-3

CONTAINMENT STRUCTURE

DOME SPHERICAL TRIANGLES

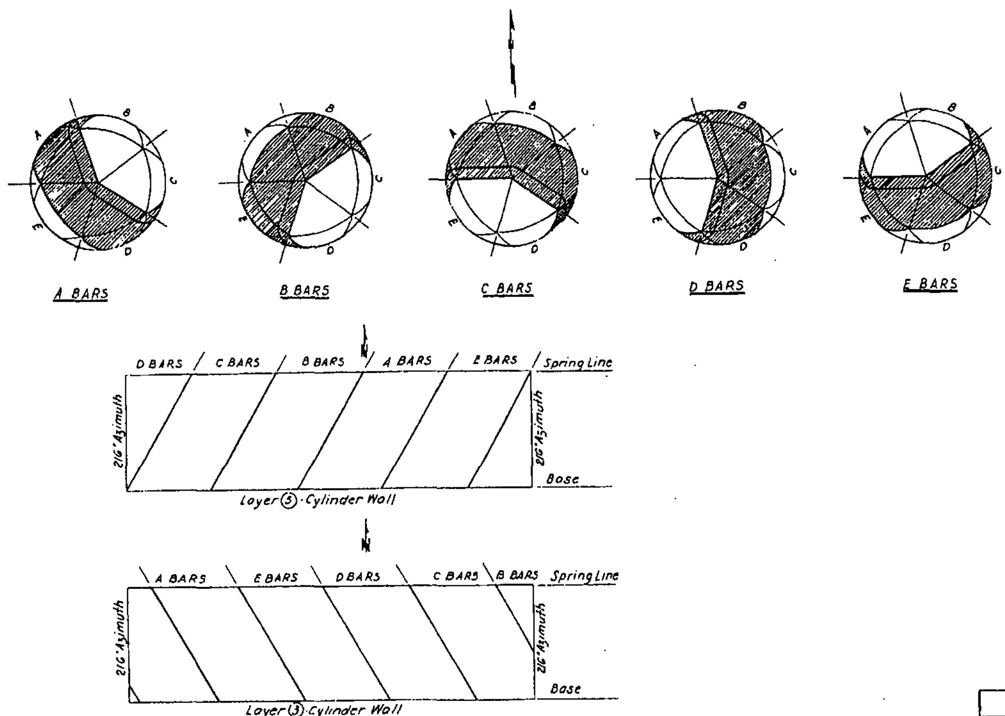

FSAR UPDATE

UNITS 1 AND 2
DIABLO CANYON SITE

FIGURE 3.8-4
CONTAINMENT STRUCTURE
DOME AND CYLINDER BARS

Revision 11 November 1996

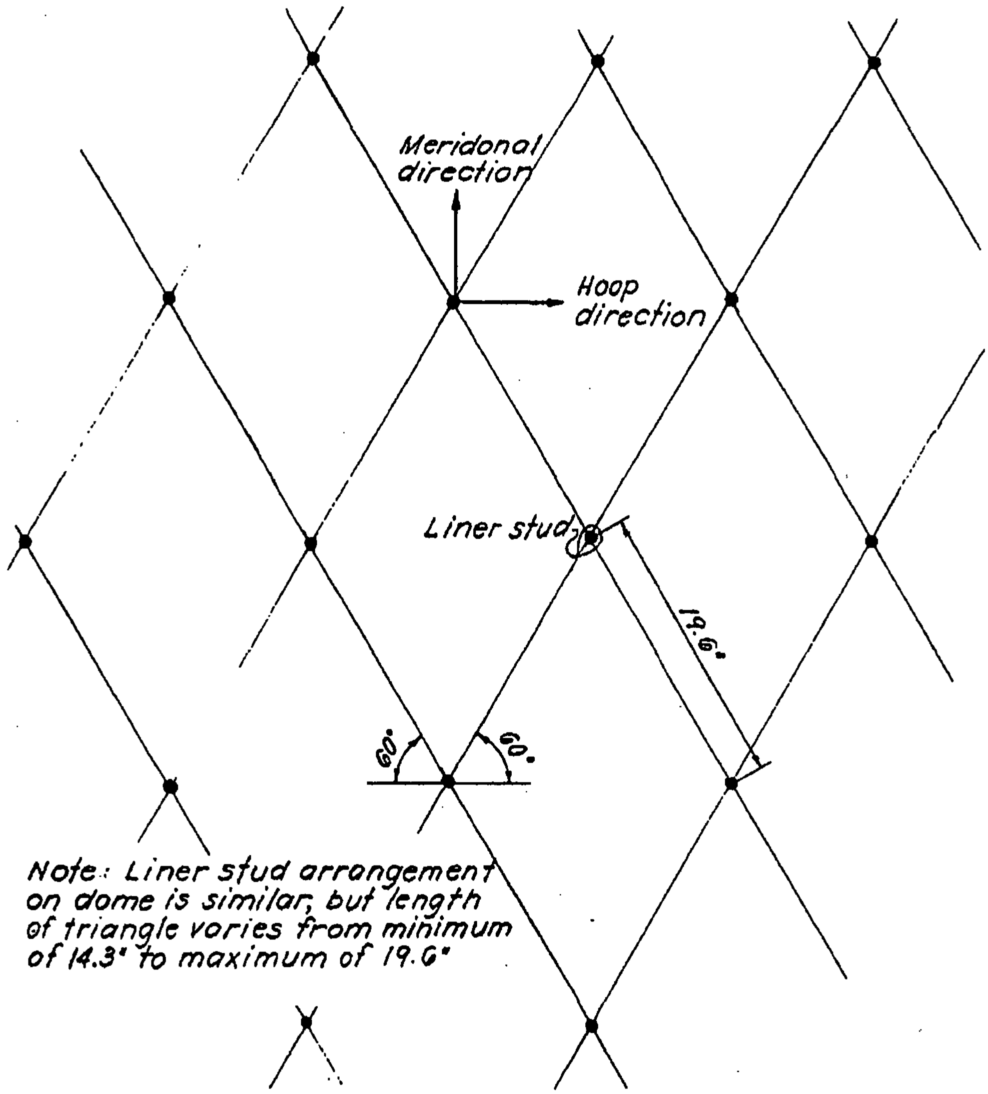

FSAR UPDATE

UNITS 1 AND 2
DIABLO CANYON SITE

FIGURE 3.8-5

CONTAINMENT STRUCTURE

LINER STUD ARRANGEMENT

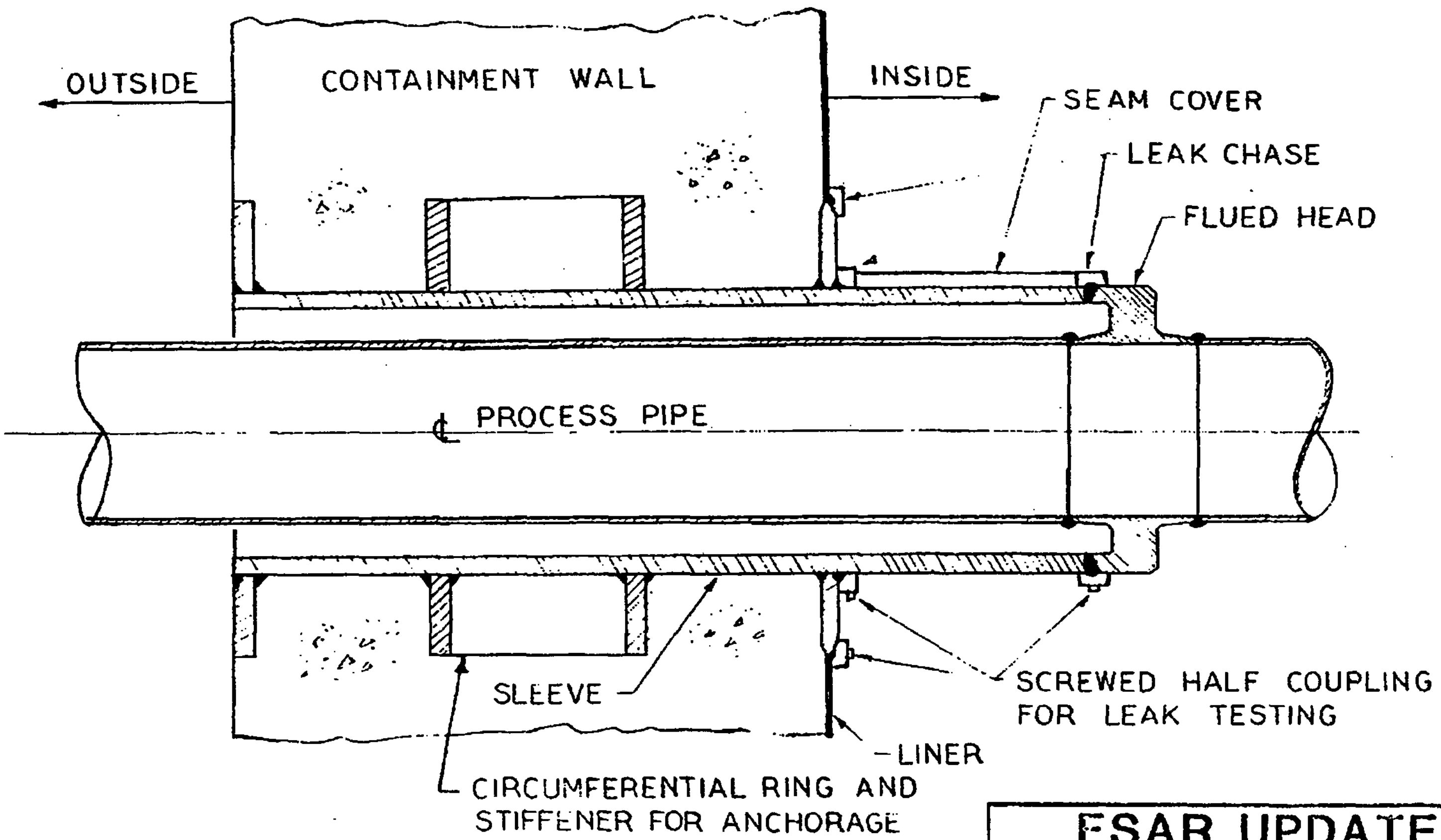

FSAR UPDATE

UNITS 1 AND 2
DIABLO CANYON SITE

FIGURE 3.8-6

CONTAINMENT STRUCTURE

TYPICAL PIPING PENETRATION

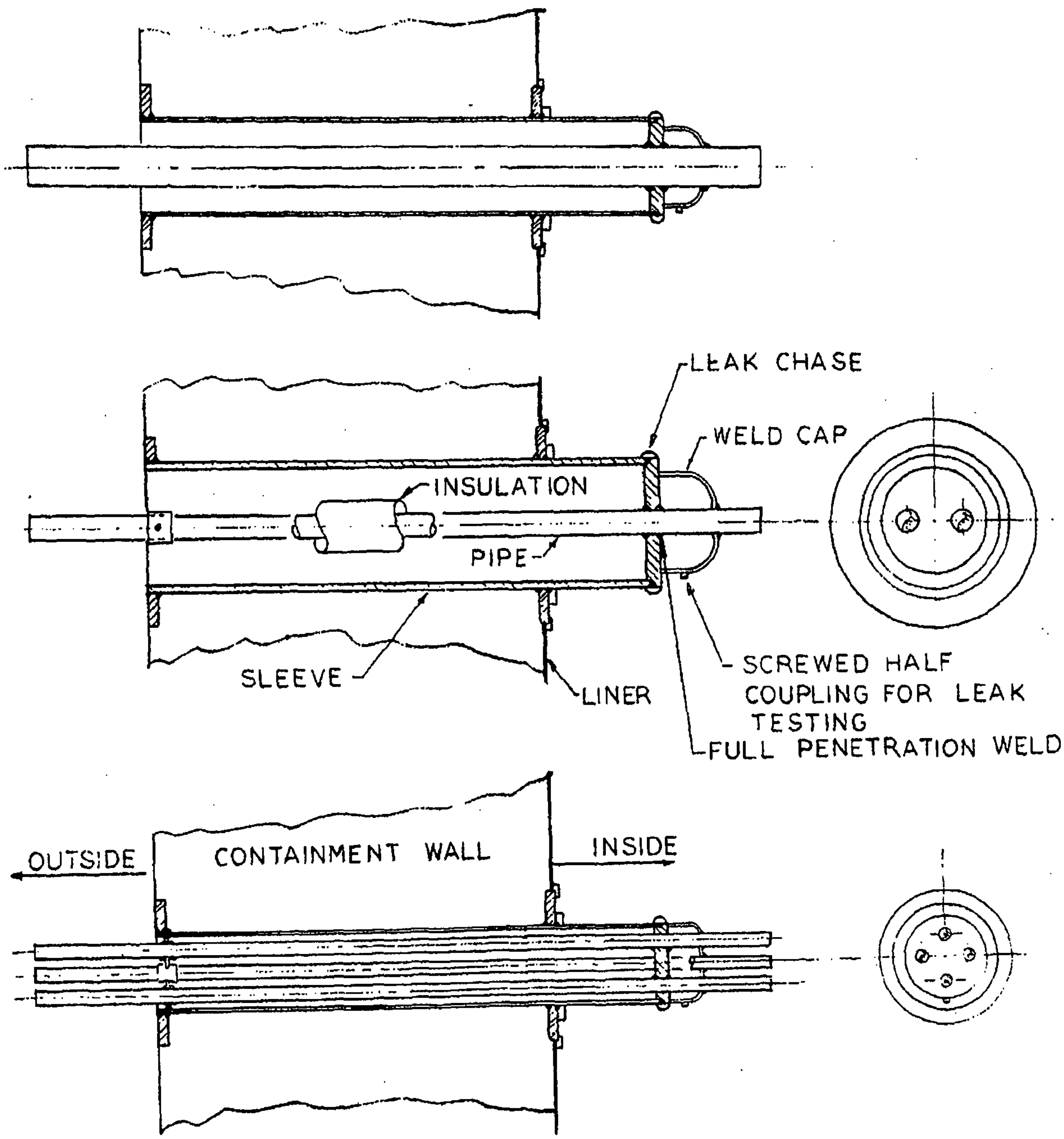

FSAR UPDATE

UNITS 1 AND 2
DIABLO CANYON SITE

FIGURE 3.8-7

CONTAINMENT STRUCTURE

TYPICAL PIPING PENETRATION

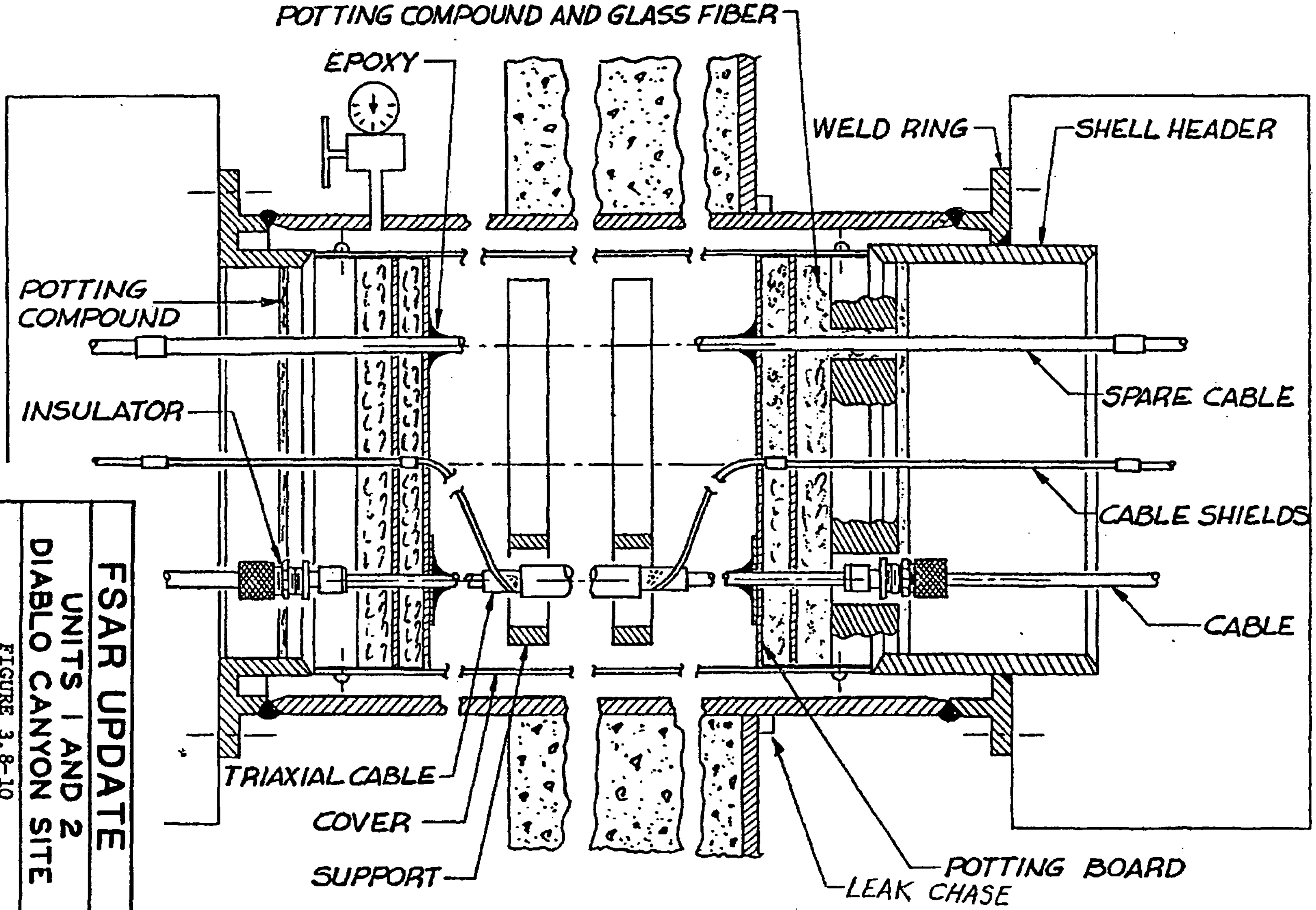

FSAR UPDATE

UNITS 1 AND 2

DIABLO CANYON SITE

FIGURE 3.8-10

CONTAINMENT STRUCTURE

TYPICAL INSTRUMENTATION PENETRATION

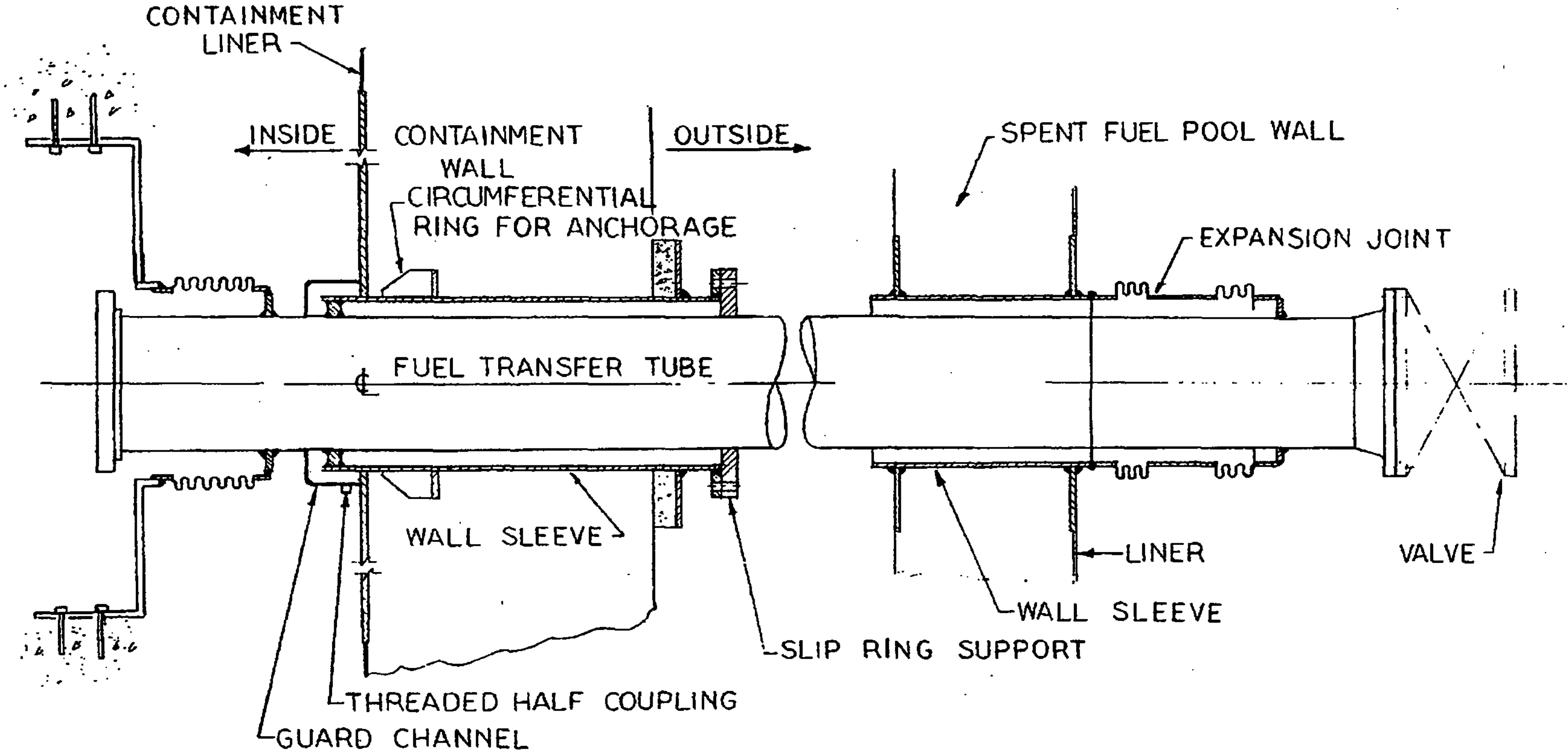

FSAR UPDATE

UNITS 1 AND 2
DIABLO CANYON SITE

FIGURE 3.8-11

CONTAINMENT STRUCTURE

FUEL TRANSFER TUBE PENETRATION

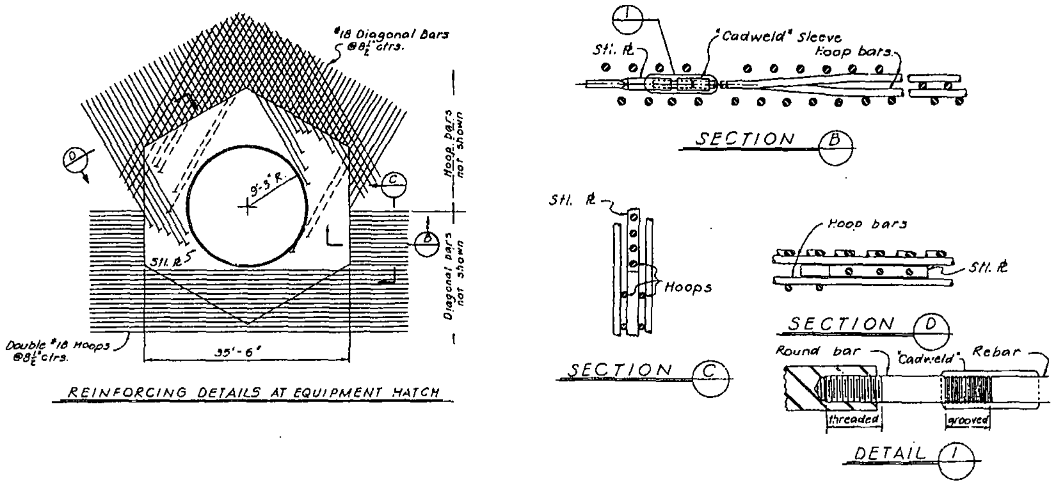

FSAR UPDATE

UNITS 1 AND 2
DIABLO CANYON SITE

FIGURE 3.8-12

CONTAINMENT STRUCTURE

HEXAGONAL COLLARS

Revision 11 November 1996

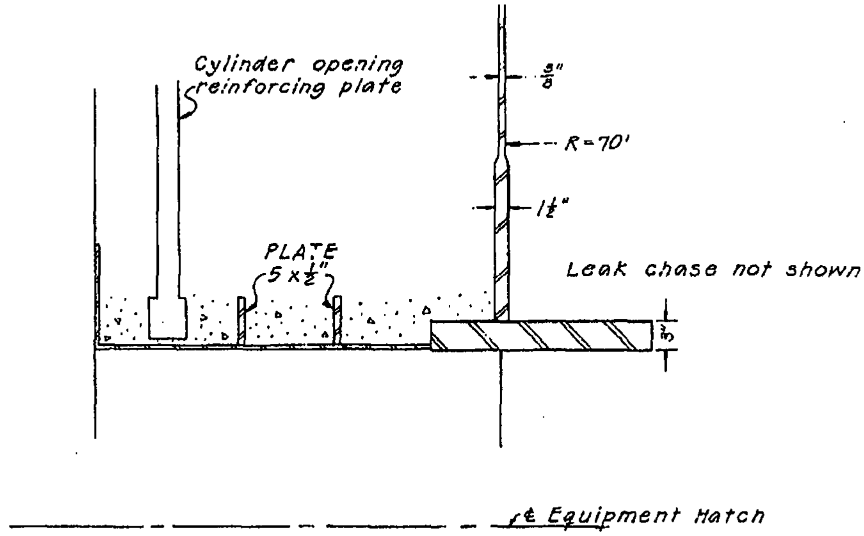

EQUIPMENT HATCH

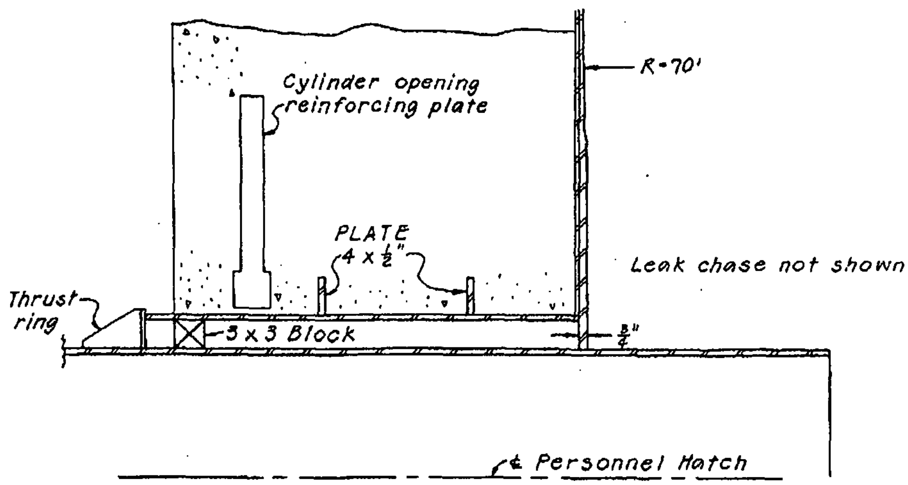

Unit 1 PERSONNEL HATCH

FSAR UPDATE

UNITS 1 AND 2
DIABLO CANYON SITE

FIGURE 3.8-13

CONTAINMENT STRUCTURE
ACCESS HATCH SLEEVES

Revision 11 November 1996

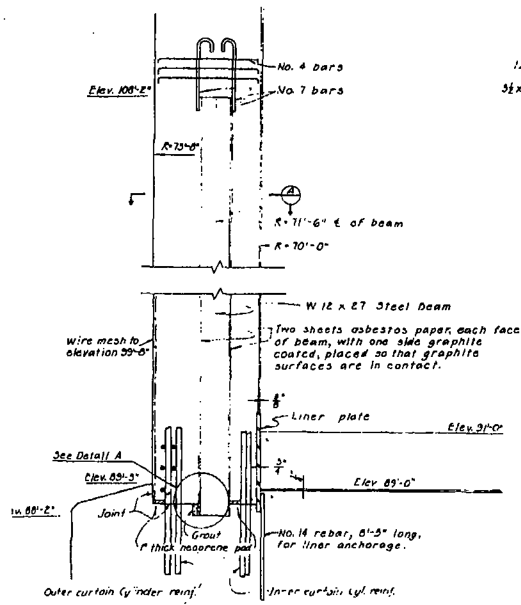

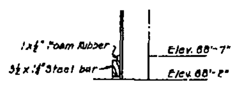

DETAIL A

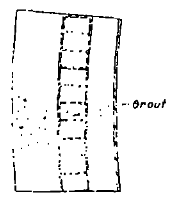

SECTION (A)

NOTES :

SEE FIGURE 3.8-15 FOR REINFORCING STEEL IN THIS REGION.

FSAR UPDATE

UNITS 1 AND 2
DIABLO CANYON SITE

FIGURE 3.8-14
CONTAINMENT STRUCTURE
EMBEDDED BEAMS
CYLINDER-BASE SLAB JUNCTURE

Revision 11 November 1996

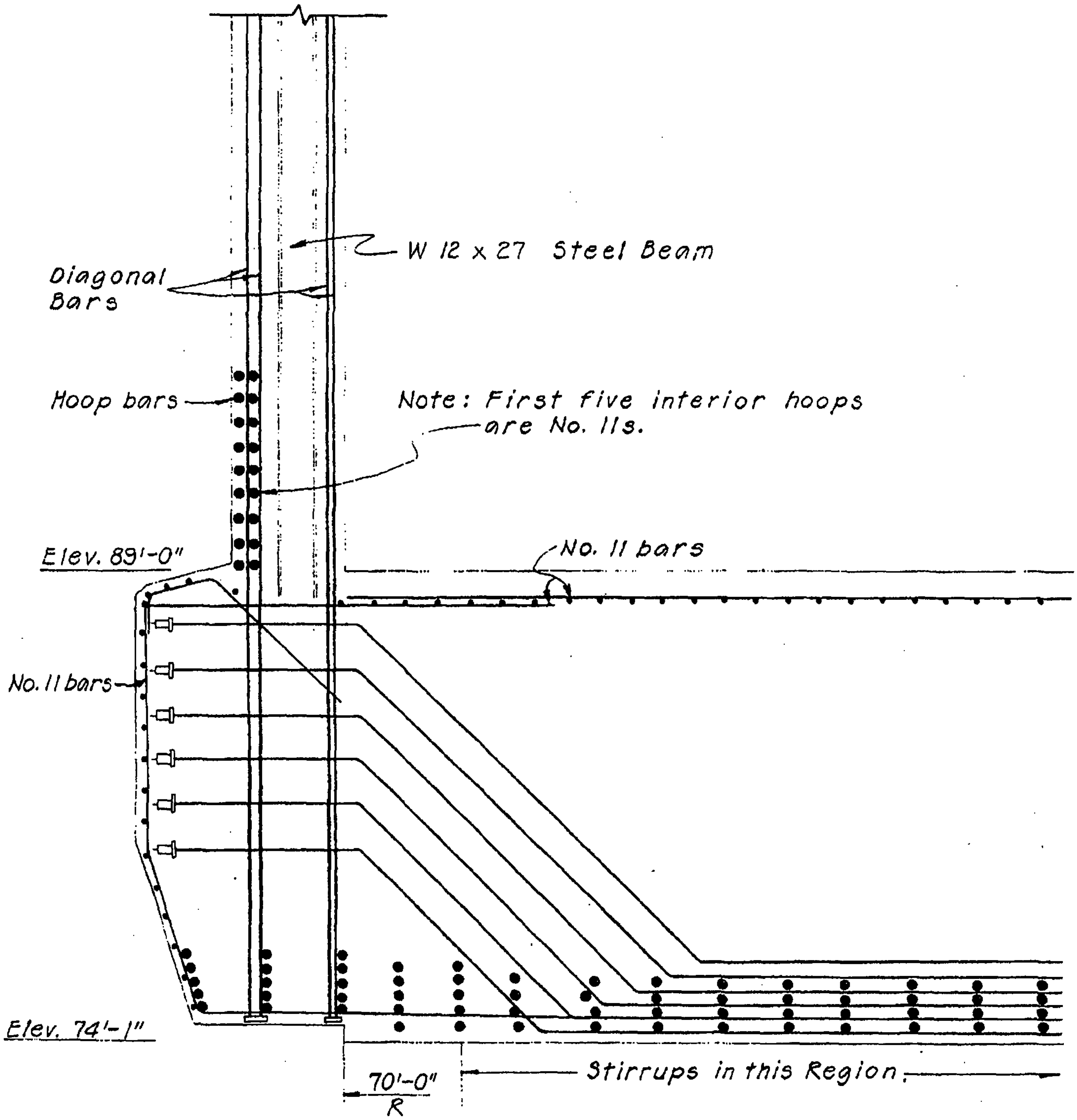

Bars are No. 18 unless noted.

FSAR UPDATE

UNITS 1 AND 2
DIABLO CANYON SITE

FIGURE 3.8-15
CONTAINMENT STRUCTURE
REINFORCING STEEL
BASE SLAB AND WALL

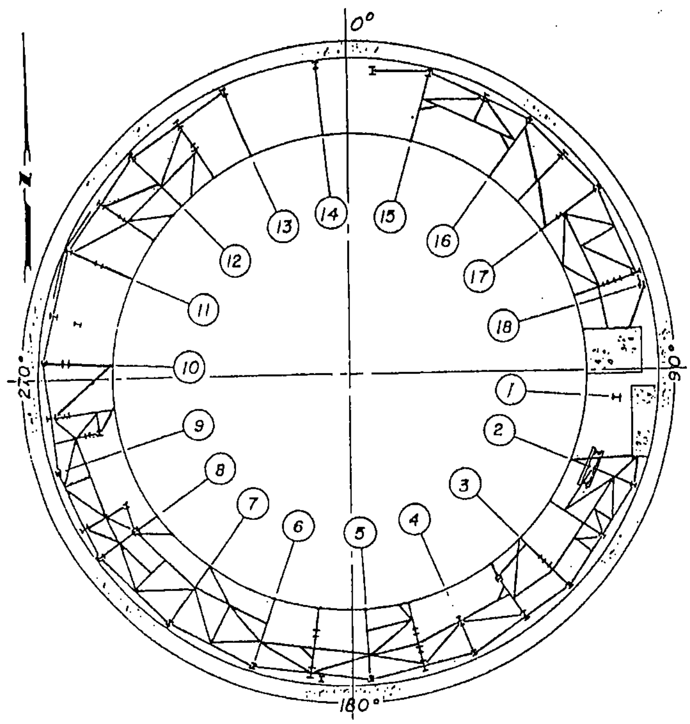

FRAMING PLAN T.O.S. EL 101'-4 1/2"

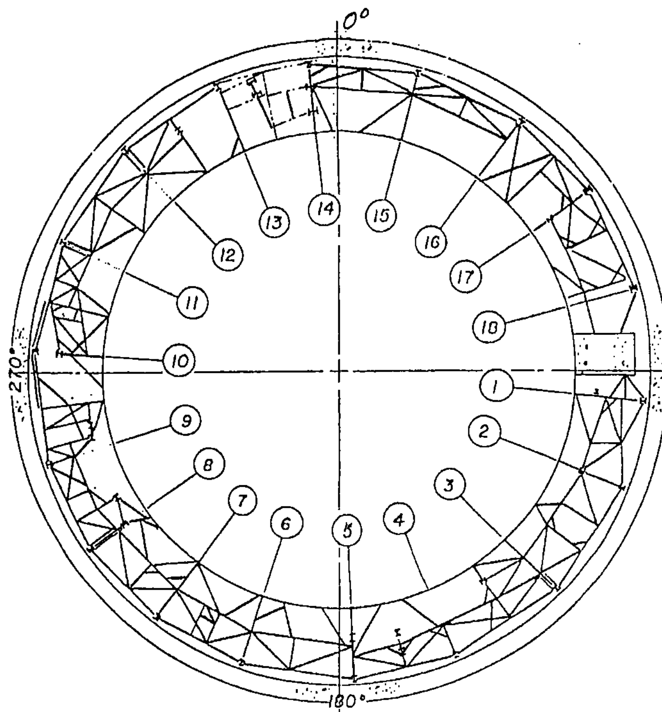

FRAMING PLAN T.O.S. EL 106'-8"

FSAR UPDATE
UNIT 1
DIABLO CANYON SITE
FIGURE 3.8-21, (Sheet 1 of 2) INTERNAL STRUCTURE ANNULUS PLATFORM ELEVATIONS 101 AND 106'

Revision 11 November 1996

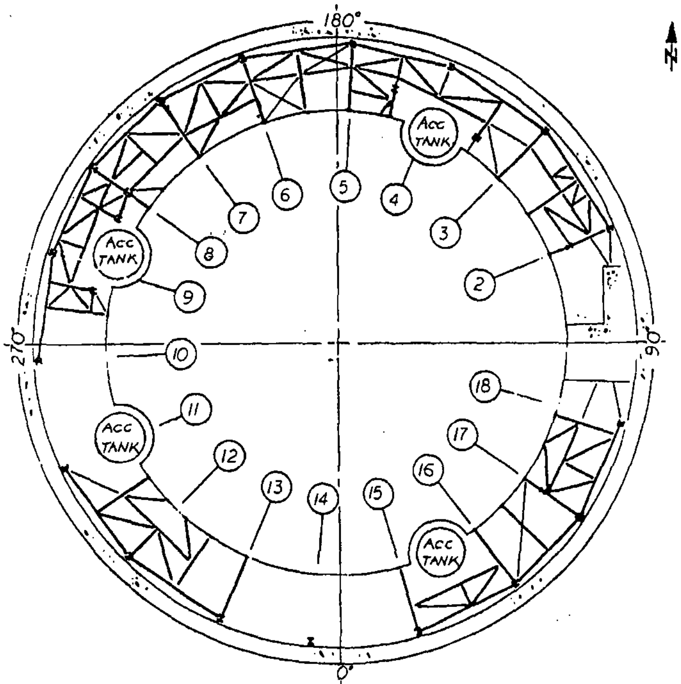

FRAMING PLAN T.O.S. EL. 101'-4½"

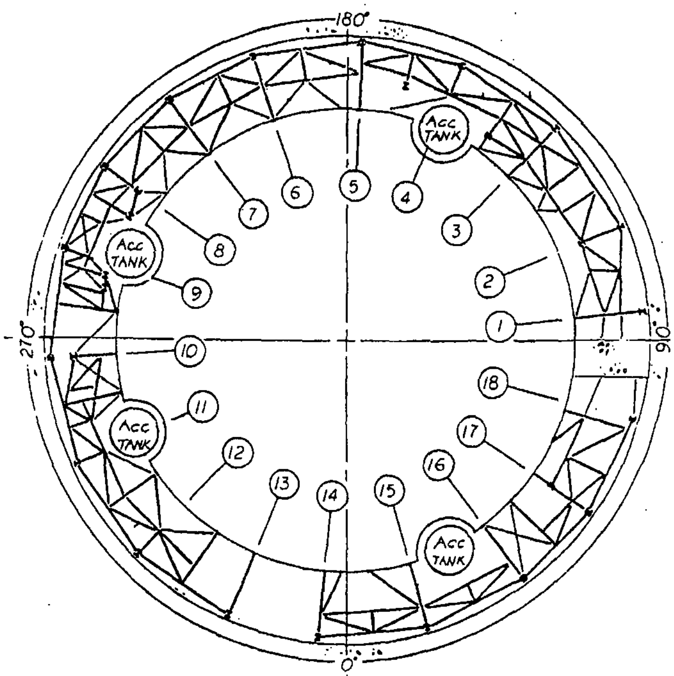

FRAMING PLAN T.O.S. EL. 106'-8"

FSAR UPDATE
UNIT 2
DIABLO CANYON SITE
FIGURE 3.8-21, (Sheet 2 of 2) INTERNAL STRUCTURE ANNULUS PLATFORM ELEVATIONS 101 AND 106'

Revision 11 November 1996

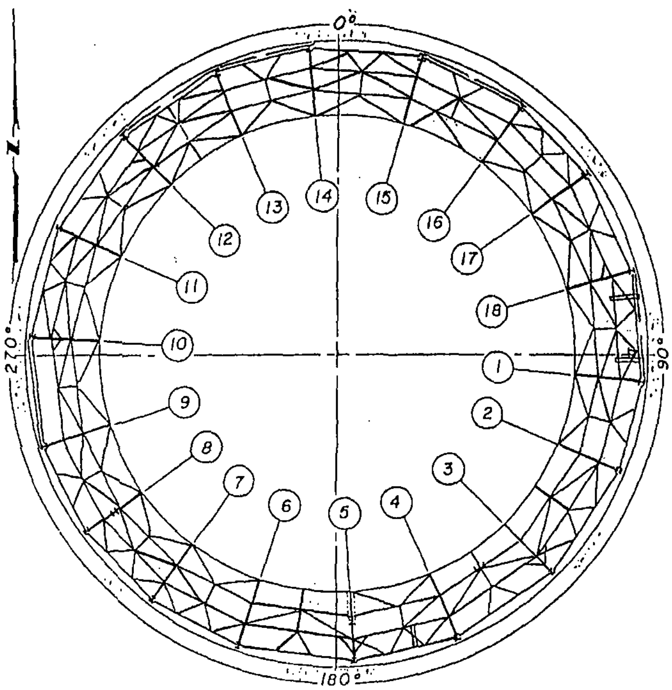

FRAMING PLAN T.O.S. EL 116'-10 3/4"

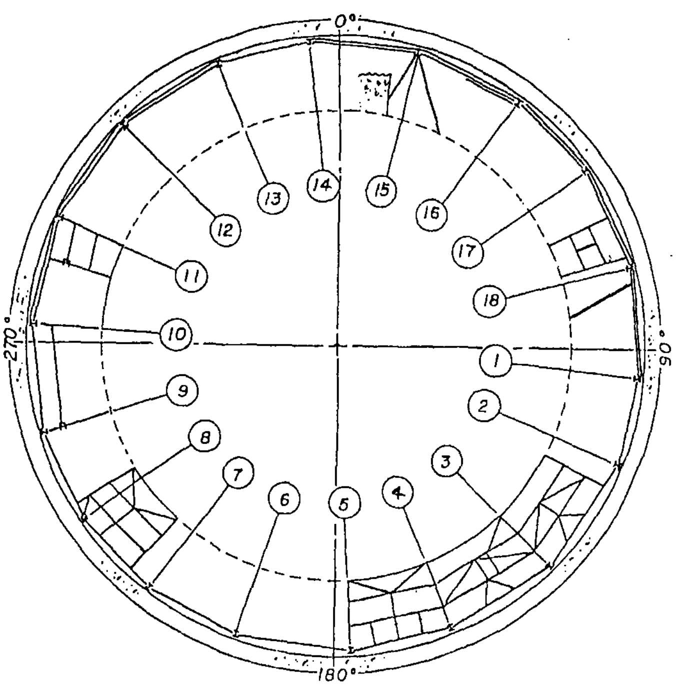

FRAMING PLAN T.O.S. EL 139'-10 3/4"

FSAR UPDATE
UNIT 1 **DIABLO CANYON SITE**
FIGURE 3.8-22 (Sheet 1 of 2) INTERNAL STRUCTURE ANNULUS PLATFORM ELEVATIONS 117 AND 140'

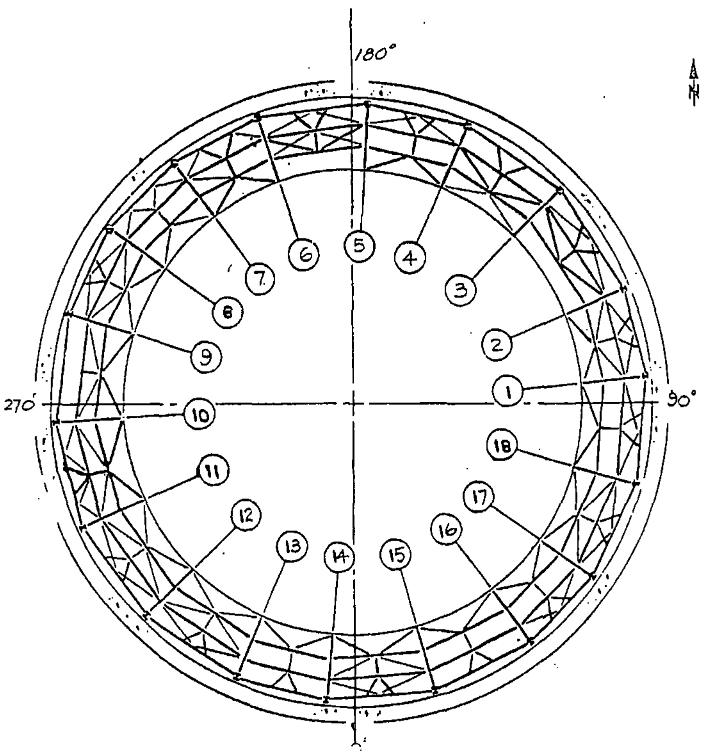

FRAMING PLAN T.O.S. EL. 116'-10¾"

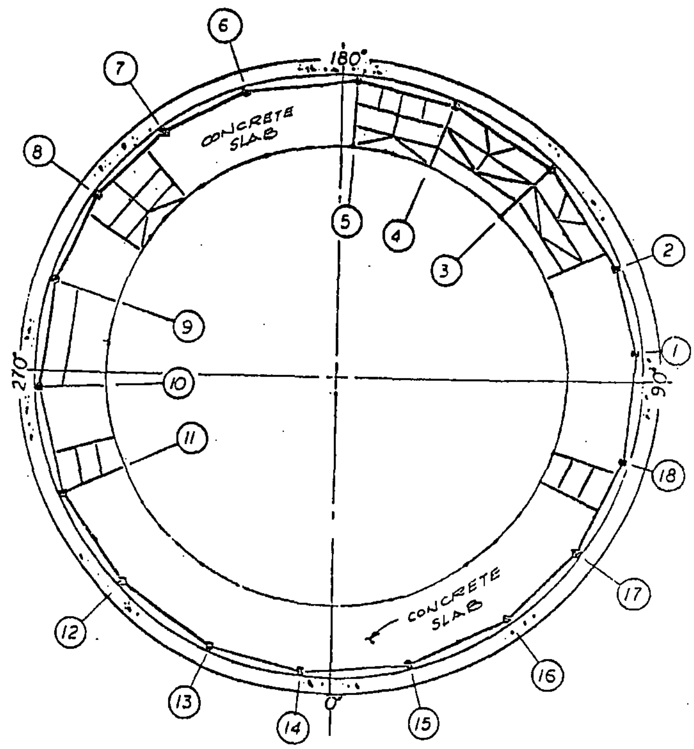

FRAMING PLAN AT EL. 140'-0"

FSAR UPDATE

UNIT 2
DIABLO CANYON SITE

FIGURE 3.8-22 (Sheet 2 of 2)
INTERNAL STRUCTURE
ANNULUS PLATFORM
ELEVATIONS 117 AND 140'

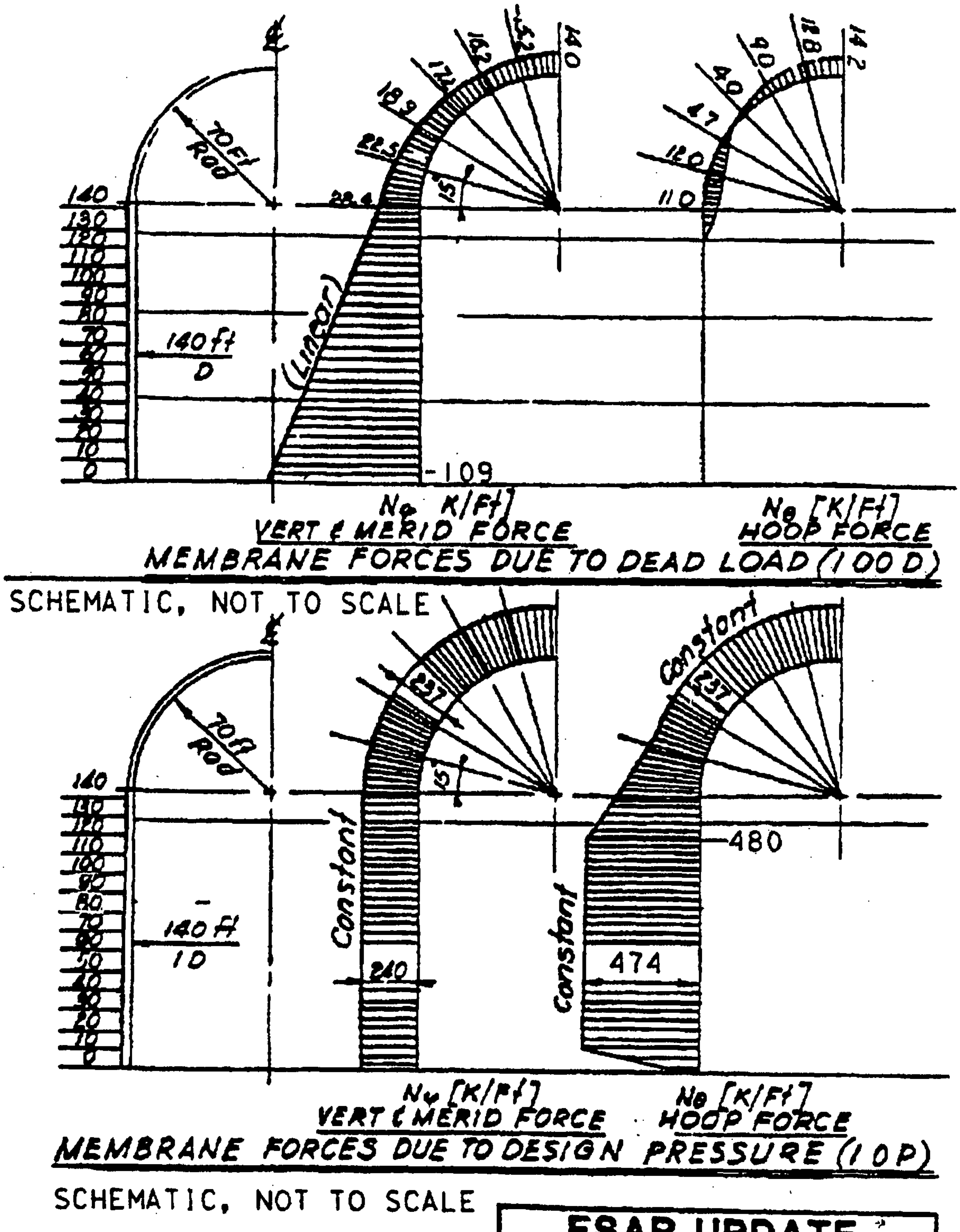

FSAR UPDATE

UNITS 1 AND 2
DIABLO CANYON SITE

FIGURE 3.8-27
CONTAINMENT STRUCTURE
MEMBRANE FORCES
DEAD LOAD AND PRESSURE

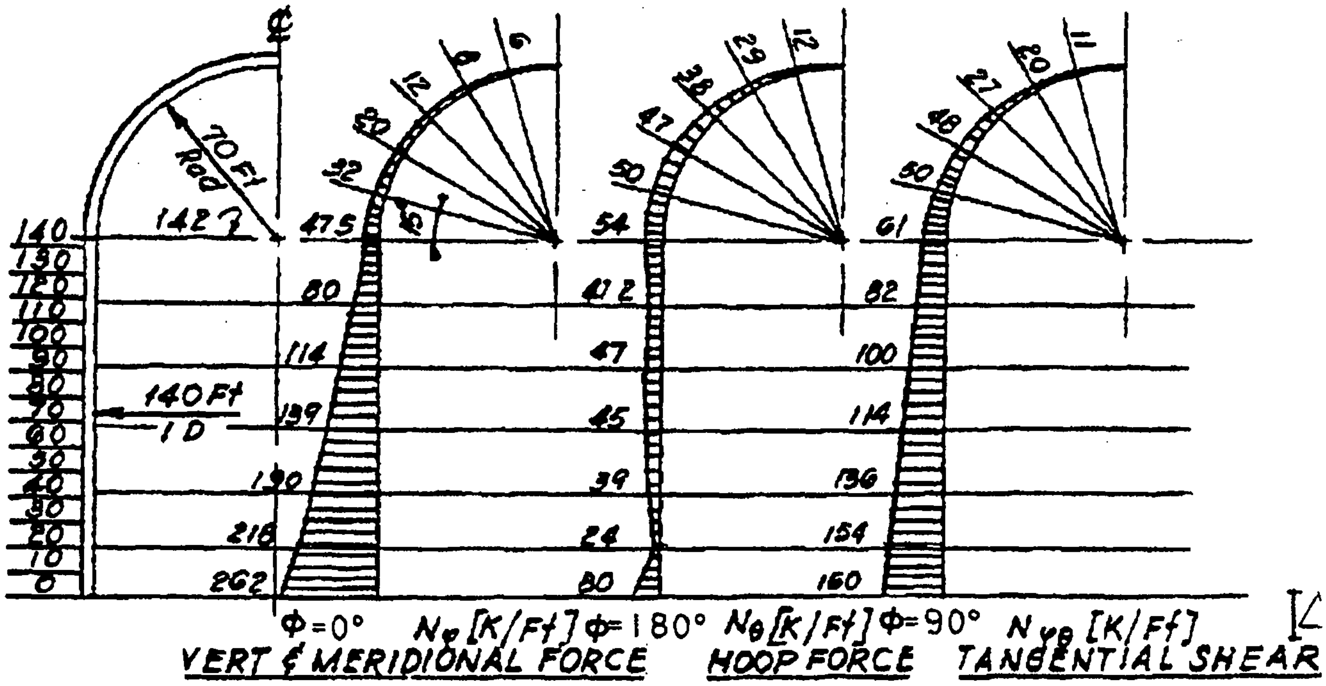

MEMBRANE FORCES DUE TO 1.25x DESIGN EARTHQUAKE (1.25DE)

SCHEMATIC, NOT TO SCALE

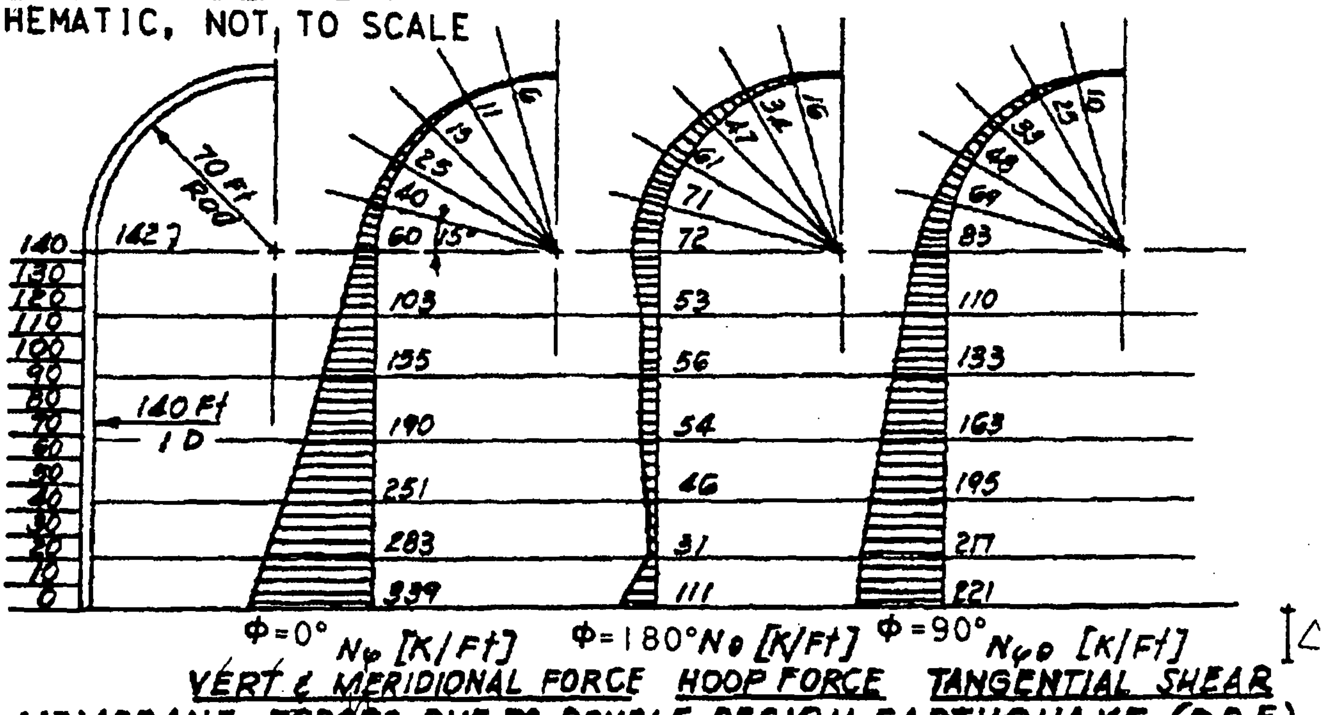

MEMBRANE FORCES DUE TO DOUBLE DESIGN EARTHQUAKE (DDE)

SCHEMATIC, NOT TO SCALE

FSAR UPDATE
UNITS 1 AND 2 DIABLO CANYON SITE
FIGURE 3.8-28 CONTAINMENT STRUCTURE MEMBRANE FORCES DE and DDE EARTHQUAKES

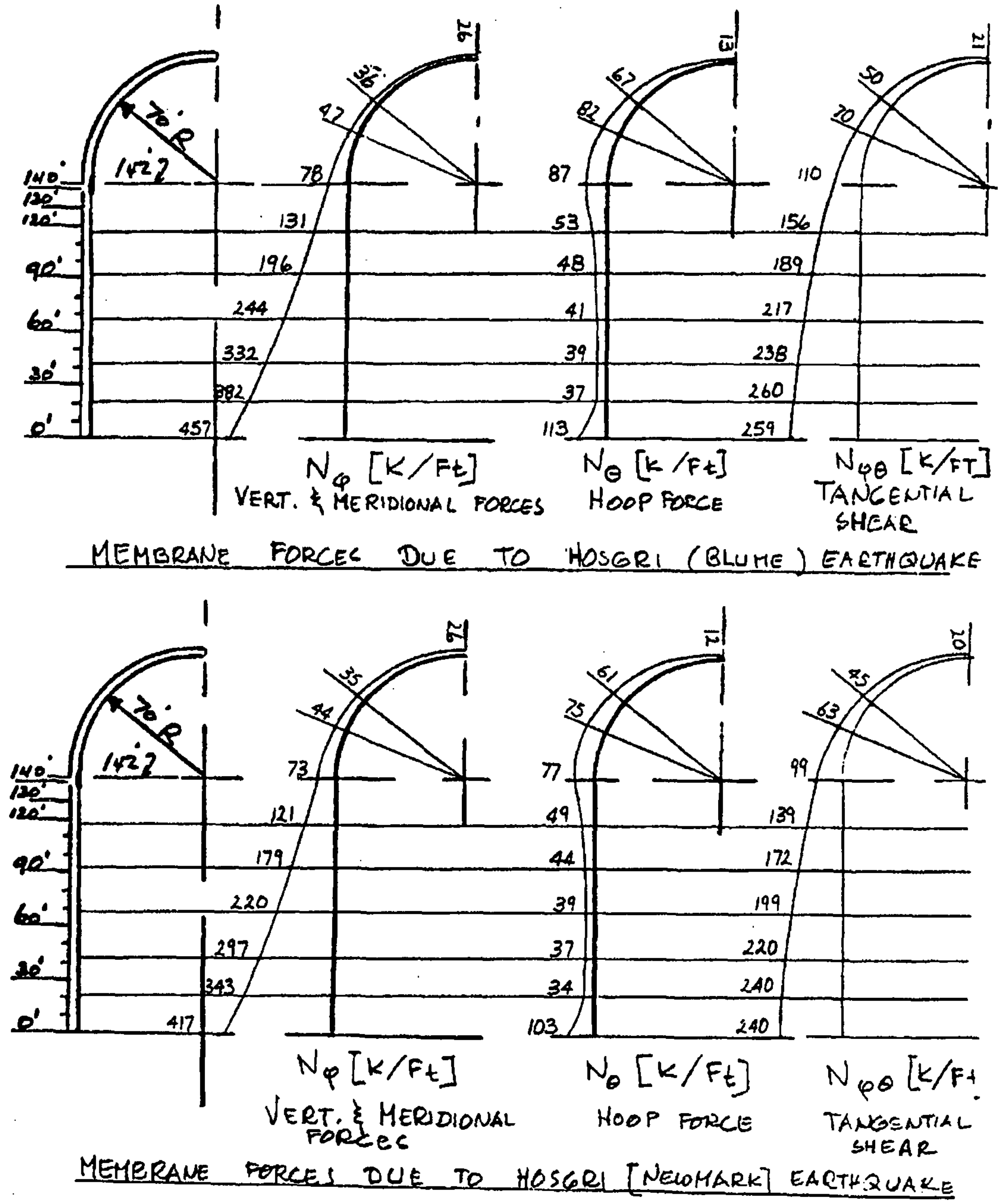

FSAR UPDATE

UNITS 1 AND 2
DIABLO CANYON SITE

FIGURE 3.8-29
CONTAINMENT STRUCTURE
MEMBRANE FORCES
HOSGRI EARTHQUAKE

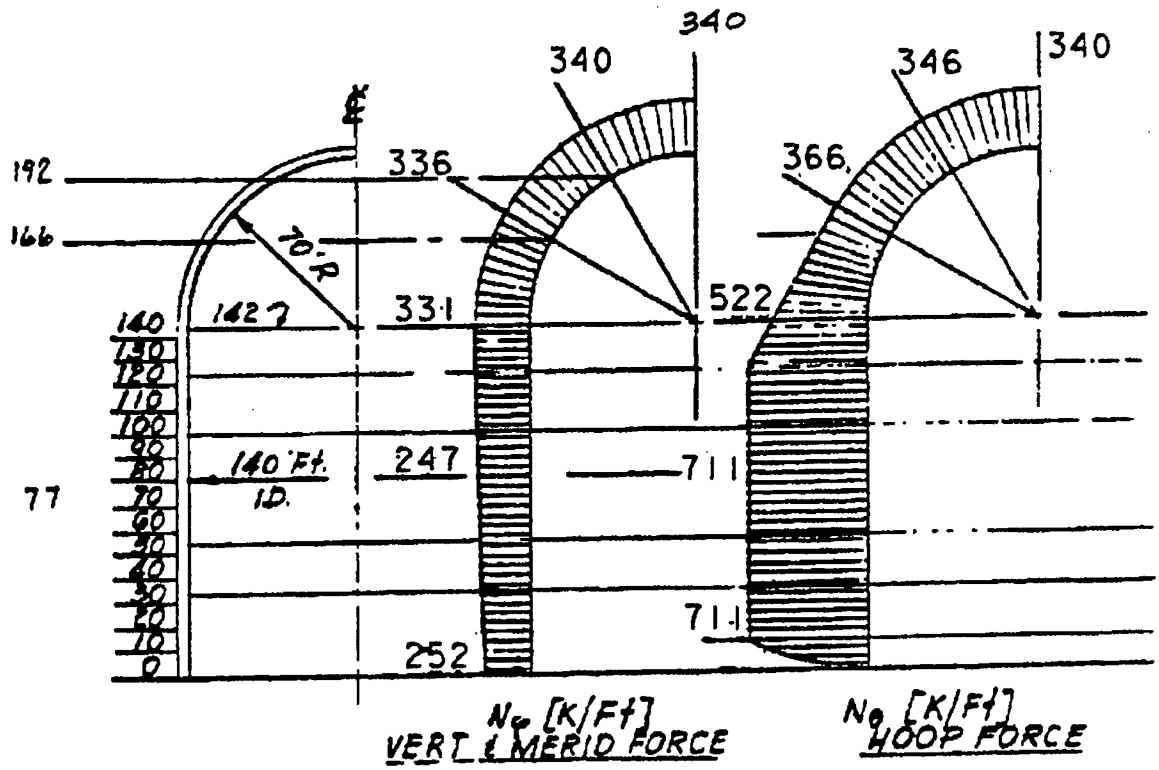

MAMBRANE FORCES

DUE TO LOAD CONDITION (I) U = 1.0D ± .05D + 1.5P +1.0T"

SCHEMATIC NOT TO SCALE

FSAR UPDATE

UNITS 1 AND 2
DIABLO CANYON SITE

FIGURE 3.8-30
CONTAINMENT STRUCTURE
MEMBRANE FORCES
ACCIDENT CONDITION 1

Revision 11 November 1996

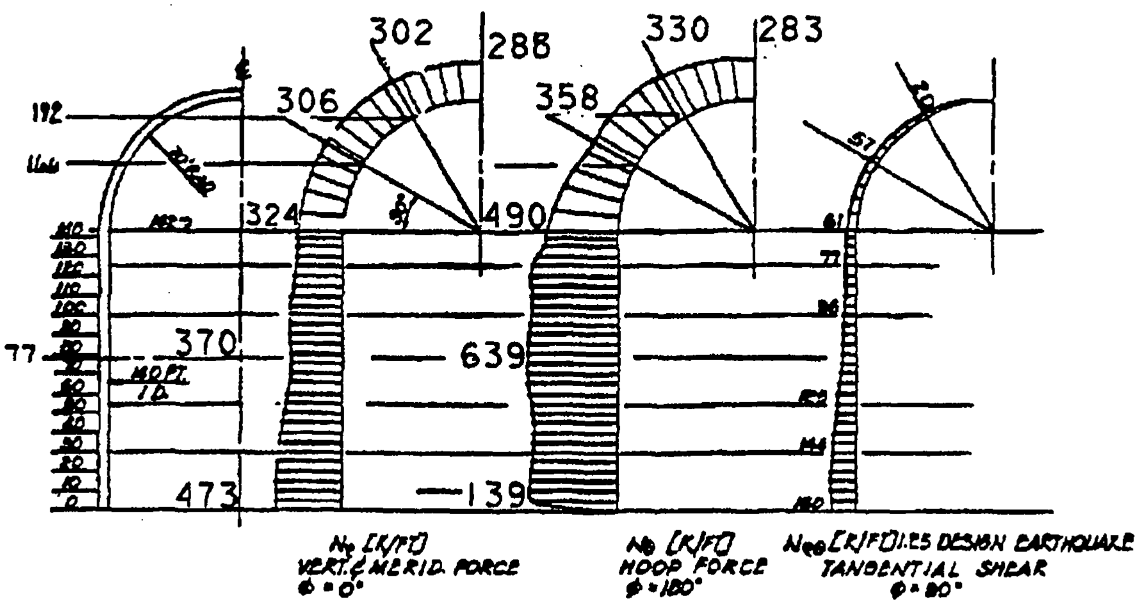

MAMBRANE FORCES

DUE TO LOAD CONDITION (2) U = 1.0D ± .05D + 1.25P + 1.25DE

SCHEMATIC NOT TO SCALE

FSAR UPDATE
UNITS 1 AND 2 DIABLO CANYON SITE
FIGURE 3.8-31 CONTAINMENT STRUCTURE MEMBRANE FORCES ACCIDENT CONDITION 2

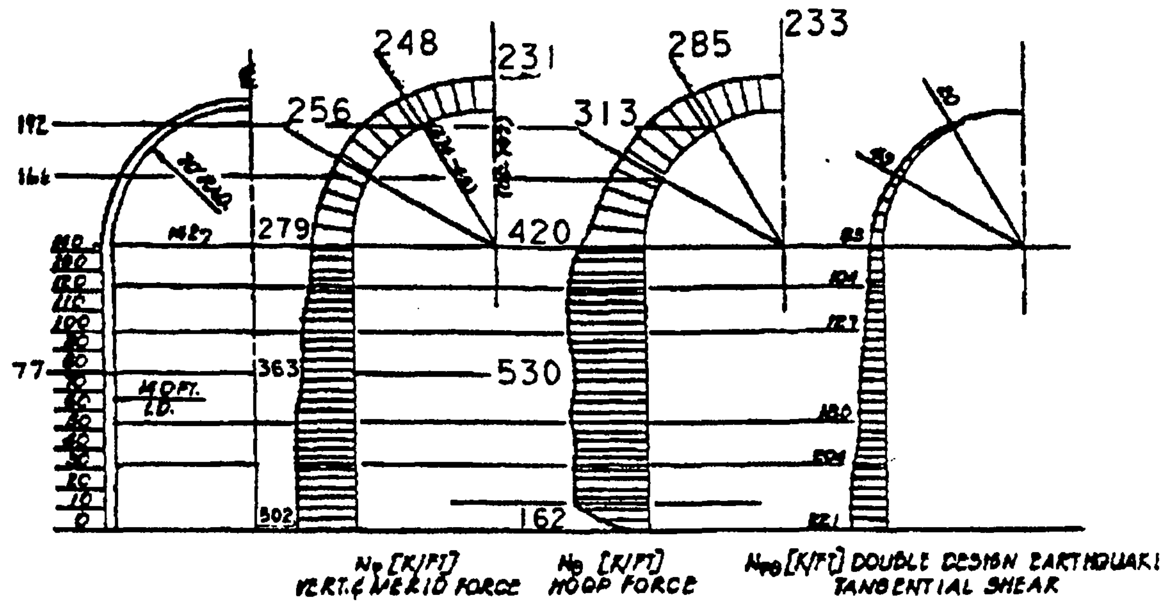

MAMBRANE FORCES

NOTE VALUES ARE FORCES IN REBAR

FORCES DUE TO LOAD CONDITION (3) U = 1.0D ± .05D + 1.0P + 1.0T + 1.0DDE

SCHEMATIC NOT TO SCALE

FSAR UPDATE

UNITS 1 AND 2
DIABLO CANYON SITE

FIGURE 3.8-32
CONTAINMENT STRUCTURE
MEMBRANE FORCES
ACCIDENT CONDITION 3

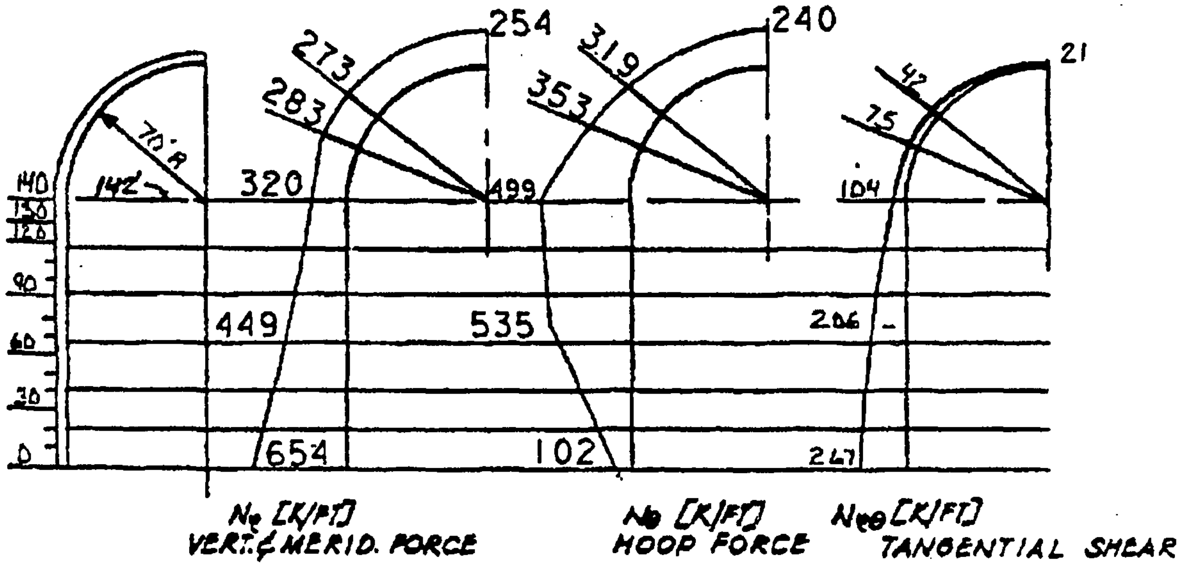

MEMBRANE FORCES

FORCES DUE TO LOAD CONDITION (4): $U = (1 \pm .05)\,D + P_A + T + HE$

SCHEMATIC NOT TO SCALE

FSAR UPDATE
UNITS 1 AND 2 DIABLO CANYON SITE
FIGURE 3.8-33 CONTAINMENT STRUCTURE MEMBRANE FORCES ACCIDENT CONDITION 4

Revision 11 November 1996

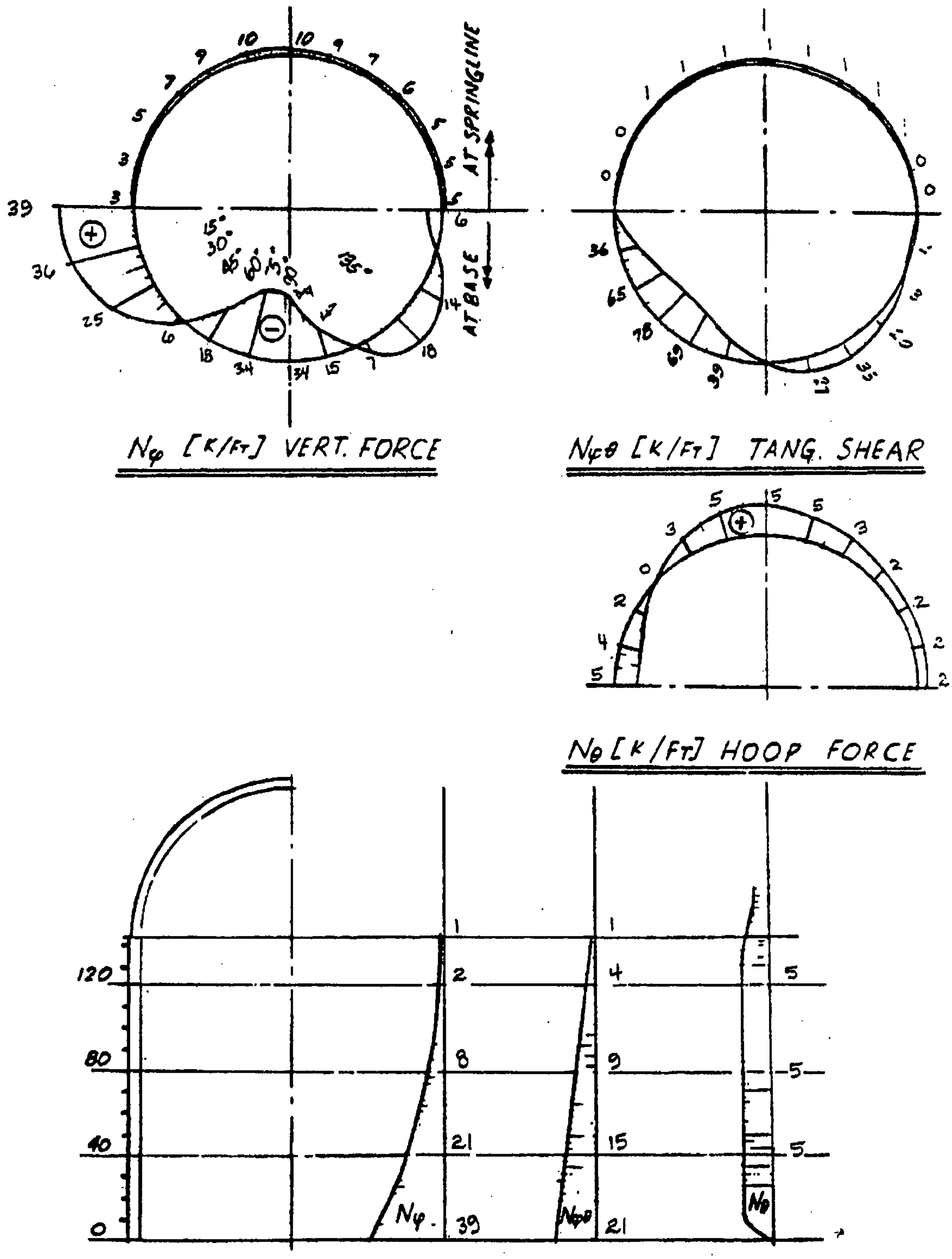

MEMBRANE FORCES DUE TO 80 MPH WIND

FSAR UPDATE

UNITS 1 AND 2
DIABLO CANYON SITE

FIGURE 3.8-34
CONTAINMENT STRUCTURE
MEMBRANE FORCES
WIND LOAD

Revision 11 November 1996

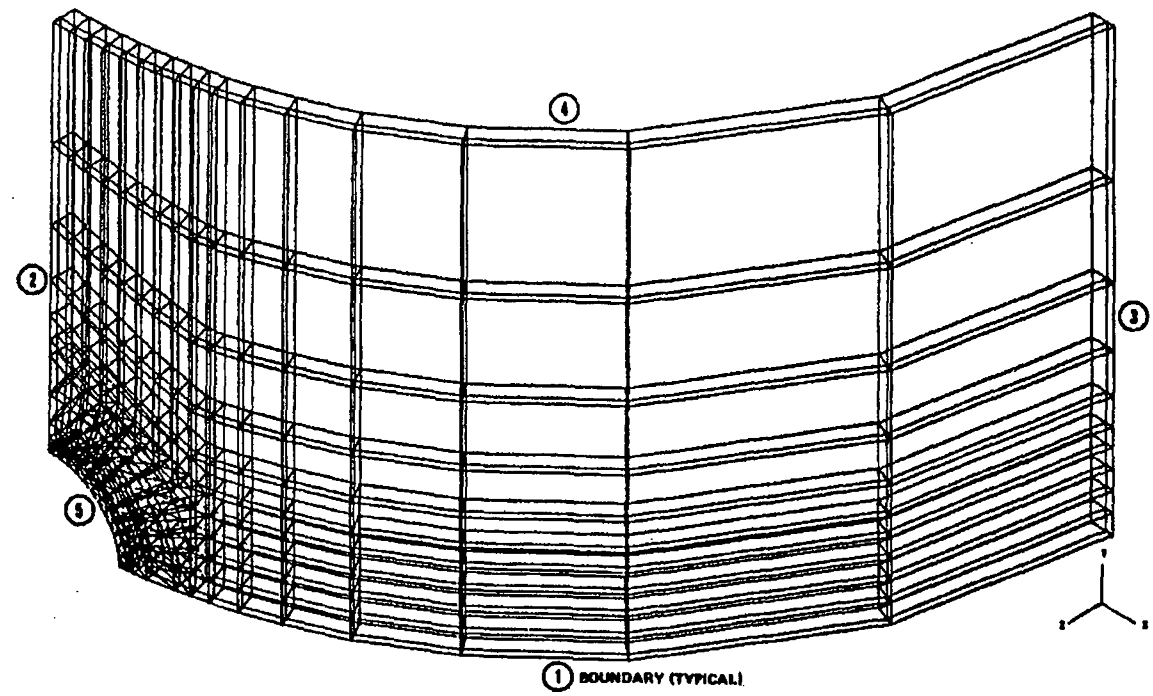

FSAR UPDATE

UNITS 1 AND 2
DIABLO CANYON SITE

FIGURE 3.8-35
CONTAINMENT STRUCTURE
EQUIPMENT HATCH ANALYTICAL MODEL
ISOMETRIC VIEW

Revision 11 November 1996

CRACKED SECTION

CONDITION (a) C = 1.0D + 0.05D + 1.5P + 1.0 T "

ALLOWABLE STRESS ELEVATION (ABOVE BASE SLAB)	LINER NOT CONSIDERED REBAR STRESSES 1	2	3	LINER CONSIDERED REBAR STRESSES 1	2	3	LINER STRESS σ_{MAX}	σ_{MIN}
	57.0	57.0	57.0	57.0	57.0	57.0		
DOME 212				42.8	42.8	42.8	-5.1	-5.1
185				42.8	44.5	42.8	-3.4	-5.2
169				42.3	41.0	42.3	-5.6	-7.0
CYLINDER 142	38.7	52.6	38.7	42.2	50.3	42.2	2.1	-6.5
83	34.3	54.4	34.3	39.7	51.9	39.7	2.7	-10.2
0	19.0	0	19.0	31.6	0	31.6	-23.8 (*)	-52.7 (*)

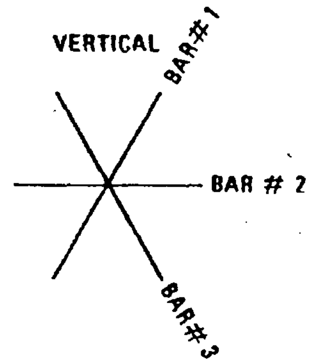

ALL STRESSES IN HIPS/SQUARE INCH

MINUS SIGN INDICATES COMPRESSION

(*) Maximum strain levels for the liner plate are within acceptable limits.

FSAR UPDATE

UNITS 1 AND 2 DIABLO CANYON SITE

FIGURE 3.8-37
CONTAINMENT STRUCTURE
EXTERIOR SHELL STRESSES
ACCIDENT CONDITION 1

CRACKED SECTION – LINER CONSIDERED

	CONDITION	$U = 1.0D \pm 0.05D + 1.25P + 1.0T' + 1.25DE$					$U = 1.0D \pm 0.05D + 1.0P + 1.0T' + 1.0DDE$				
		REBAR STRESSES			LINER STRESS		REBAR STRESSES			LINER STRESS	
	ELEVATION (ABOVE BASE SLAB)	1	2	3	σ_{MAX}	σ_{MIN}	1	2	3	σ_{MAX}	σ_{MIN}
	ALLOWABLE STRESS	57.0	57.0	57.0			57.0	57.0	57.0		
DOME	212	38.7	38.3	37.7	-8.4	-8.5	32.1	31.6	30.9	-8.6	-8.6
DOME	185	41.7	40.7	35.5	-5.9	-8.1	36.0	34.1	27.9	-6.0	-8.2
DOME	169	42.7	37.6	34.2	-9.0	-8.0	37.6	31.7	26.2	-8.1	-8.3
	142	45.2	44.9	32.9	-1.6	-7.8	41.0	37.5	24.2	-2.4	-7.4
CYLINDER	83	50.1	45.1	31.0	-.9	-5.7	48.9	36.7	22.7	-2.0	-2.9
CYLINDER	0	43.8	0	29.3	-10.4 (*)	-47.2 (*)	46.6	0	22.9	-4.8 (*)	-39.1 (*)

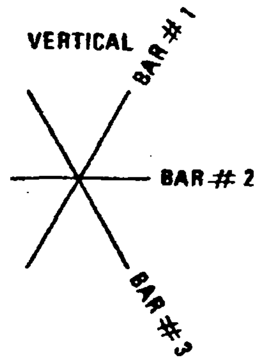

ALL STRESSES IN KIPS/SQUARE INCH

MINUS SIGN INDICATES COMPRESSION

NOTE:
REBAR STRESSES FOR REBAR IN OUTER LAYER ONLY.

(*) Maximum strain levels for the liner plate are within acceptable limits.

FSAR UPDATE

UNITS 1 AND 2 DIABLO CANYON SITE

FIGURE 3.8-38

CONTAINMENT STRUCTURE EXTERIOR SHELL STRESSES ACCIDENT CONDITIONS 2 AND 3

CRACKED SECTION

CONDITION (c) C = 1.00 ± 0.05D + 1.0P + 1.0T + 1.0 HE

ELEVATION (FT) (ABOVE BASE SLAB)		REBAR STRESSES * 1	REBAR STRESSES * 2	REBAR STRESSES * 3		LINER PLATE * STRESS MAX	LINER PLATE * STRESS MIN	
ALLOWABLE STRESS		63.5	63.5	63.5				
DOME	213	33.6	31.4	32.2		-6.4	-8.6	WITH LINER PLATE
DOME	185	37.7	34.7	28.4		-4.9	-6.7	WITH LINER PLATE
DOME	169	39.6	31.9	26.1		-6.7	-7.7	WITH LINER PLATE
CYLINDER	142	44.2	36.8	23.0		-2.6	-6.0	WITH LINER PLATE
CYLINDER	83	53.4	37.5	18.4		-1.2	-2.8	WITH LINER PLATE
CYLINDER	83	61.2	38.1	11.0				WITHOUT LINER PLATE
CYLINDER	0	49.5	0	24.8		-1.0 (*)	-38.1 (*)	WITH LINER PLATE

(*) Maximum strain levels for the liner plate are within acceptable limits.

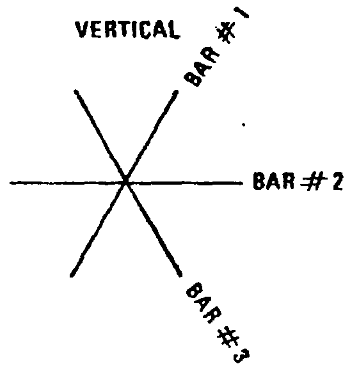

ALL STRESSES IN KIPS/SQUARE INCH

MINUS SIGN INDICATES COMPRESSION

* STRESSES ARE MAXIMUM OR MINIMUM AT ANY SECTION:

FSAR UPDATE

UNITS 1 AND 2 DIABLO CANYON SITE

FIGURE 3.8-39

CONTAINMENT STRUCTURE, EXTERIOR SHELL STRESSES – ACCIDENT CONDITION 4

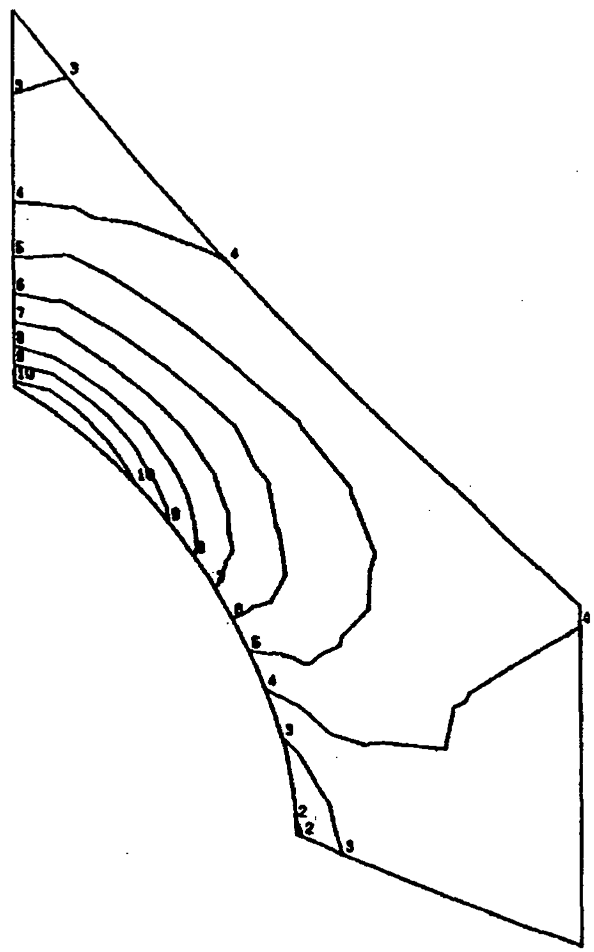

CONTOURING INFORMATION

LEVEL	VALUE
1	.13600+05
2	.17000+05
3	.20400+05
4	.23800+05
5	.27200+05
6	.30600+05
7	.34000+05
8	.37400+05
9	.40800+05
10	.44200+05

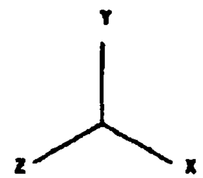

FSAR UPDATE

UNITS 1 AND 2
DIABLO CANYON SITE

FIGURE 3.8-40
EQUIPMENT HATCH HEXAGONAL
PLATE MAXIMUM STRESSES
(1.05D + 1.5P + T")

Revision 11 November 1996

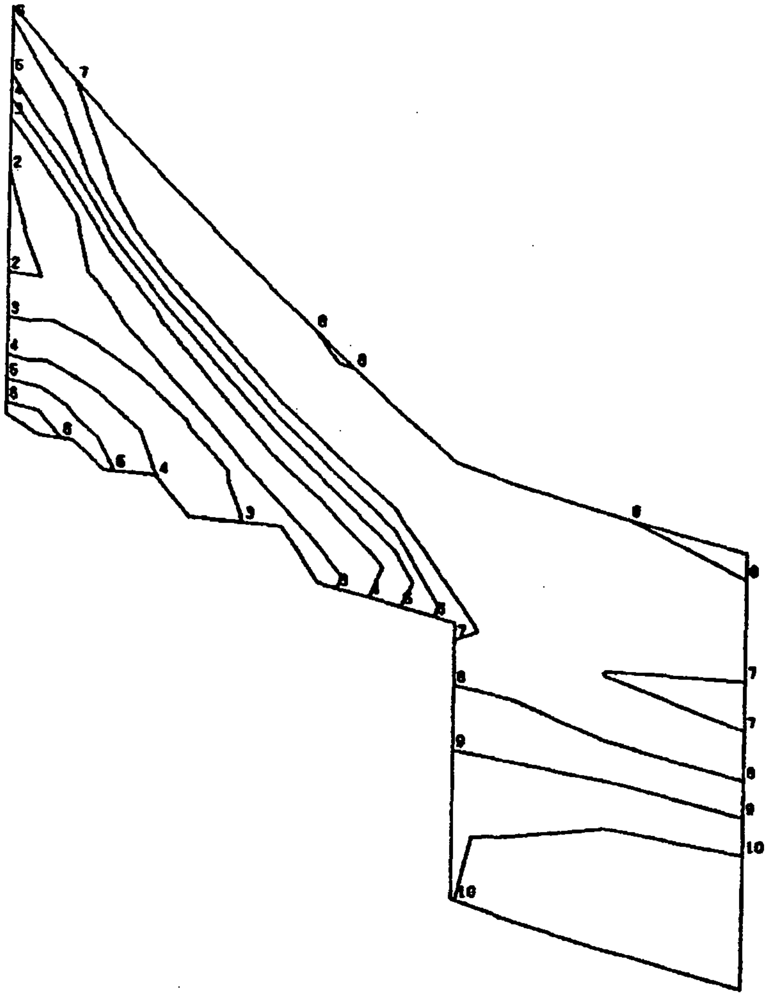

CONTOURING INFORMATION

LEVEL	VALUE
1	.15200+05
2	.19000+05
3	.22800+05
4	.26600+05
5	.30400+05
6	.34200+05
7	.38000+05
8	.41800+05
9	.45600+05
10	.49400+05

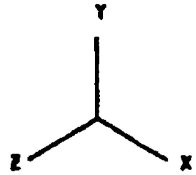

FSAR UPDATE

UNITS 1 AND 2
DIABLO CANYON SITE

FIGURE 3.8-41

EQUIPMENT HATCH HOOP
REINFORCEMENT STRESSES
(1.05D + 1.5P + T'')

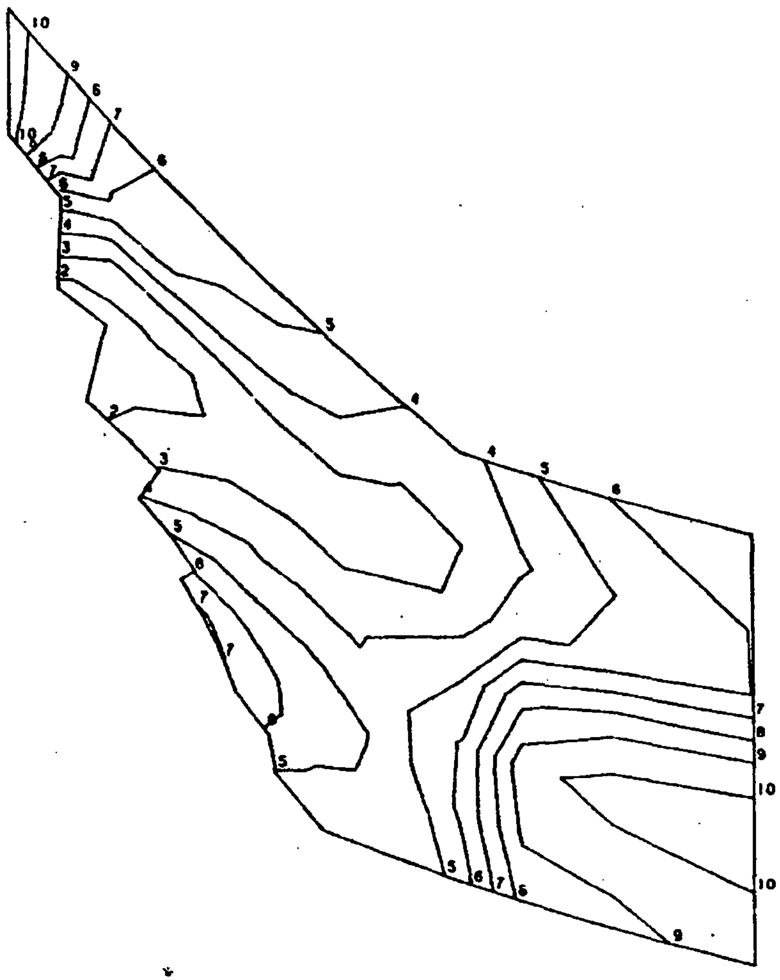

CONTOURING INFORMATION

LEVEL	VALUE
1	.96000+04
2	.12000+05
3	.14400+05
4	.16800+05
5	.19200+05
6	.21600+05
7	.24000+05
8	.26400+05
9	.28800+05
10	.31200+05

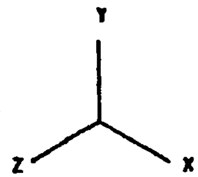

FSAR UPDATE

UNITS 1 AND 2 DIABLO CANYON SITE

FIGURE 3.8-42
EQUIPMENT HATCH DIAGONAL REINFORCEMENT STRESSES
(1.05D + 1.5P + T")

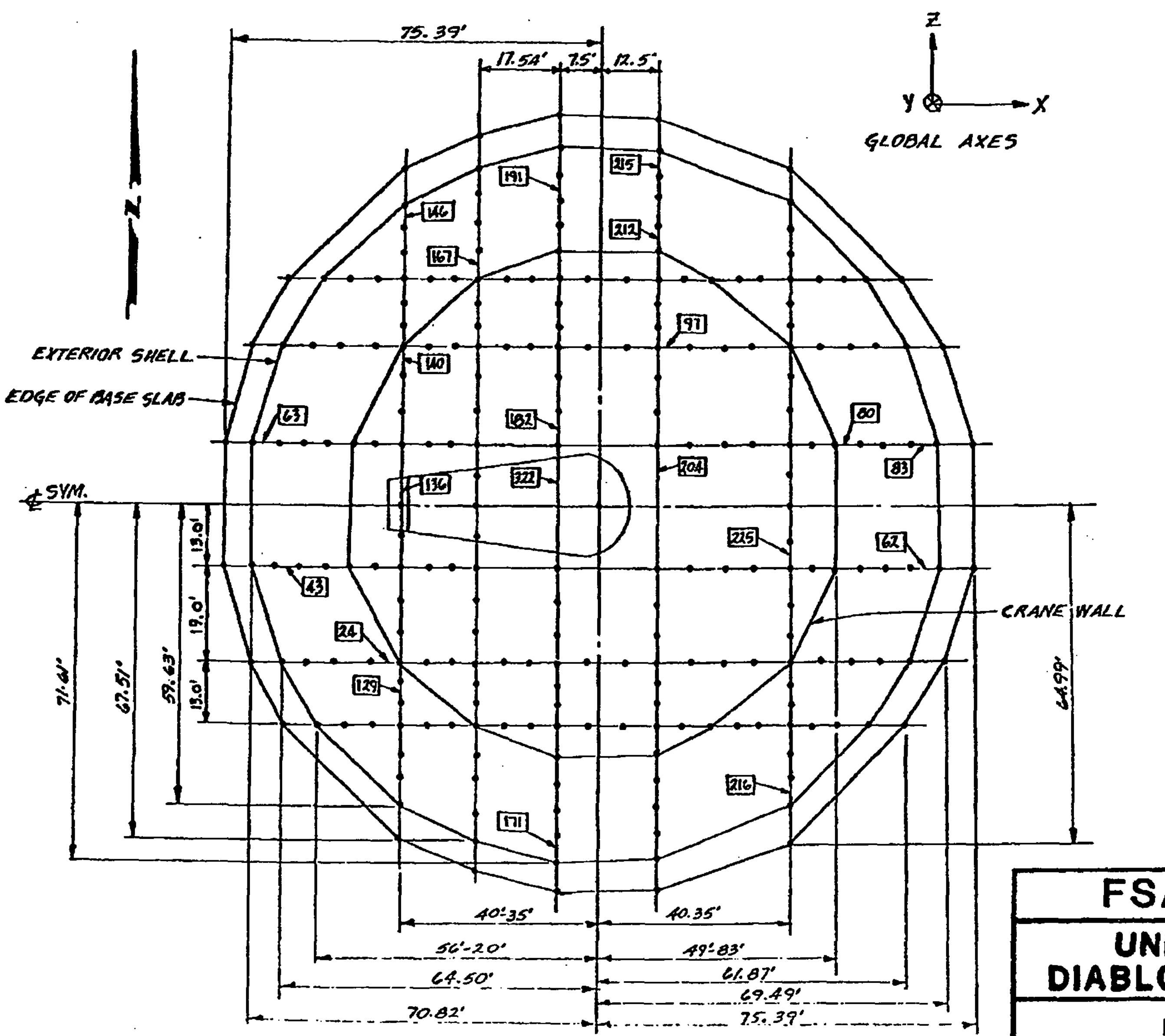

FSAR UPDATE

UNITS 1 AND 2
DIABLO CANYON SITE

FIGURE 3.8-43

CONTAINMENT
BASE SLAB MODEL

NOTES FOR FIELD INSTALLATION

1. REMOVE MILL SCALE AND POLISH REBAR SURFACE INSIDE OF DIAMOND AREA
2. BOND SHIM ASSEMBLY TO POLISHED REBAR
3. PLACE SEALANT AND PROTECTIVE COVER OVER SHIM ASSEMBLY.

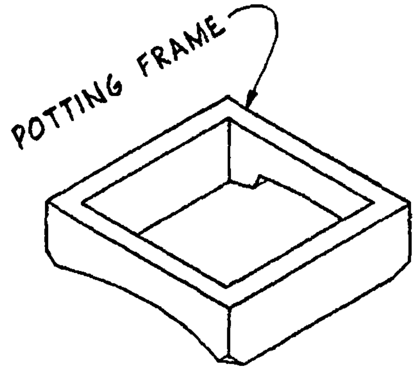

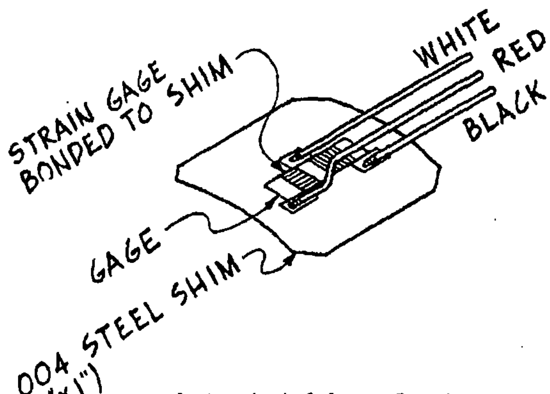

SHIM ASSEMBLY

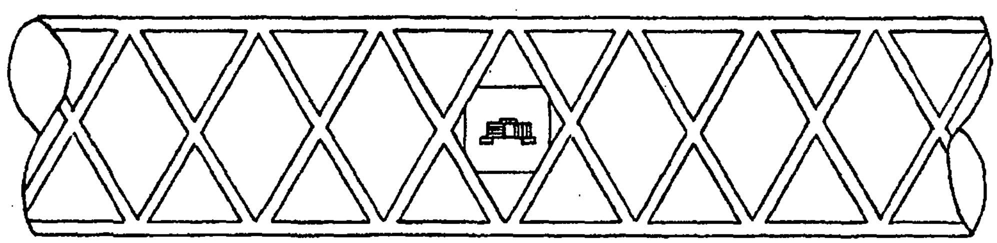

FSAR UPDATE

UNITS 1 AND 2
DIABLO CANYON SITE

FIGURE 3.8-44

CONTAINMENT STRUCTURE
TYPICAL REBAR STRAIN GAUGE

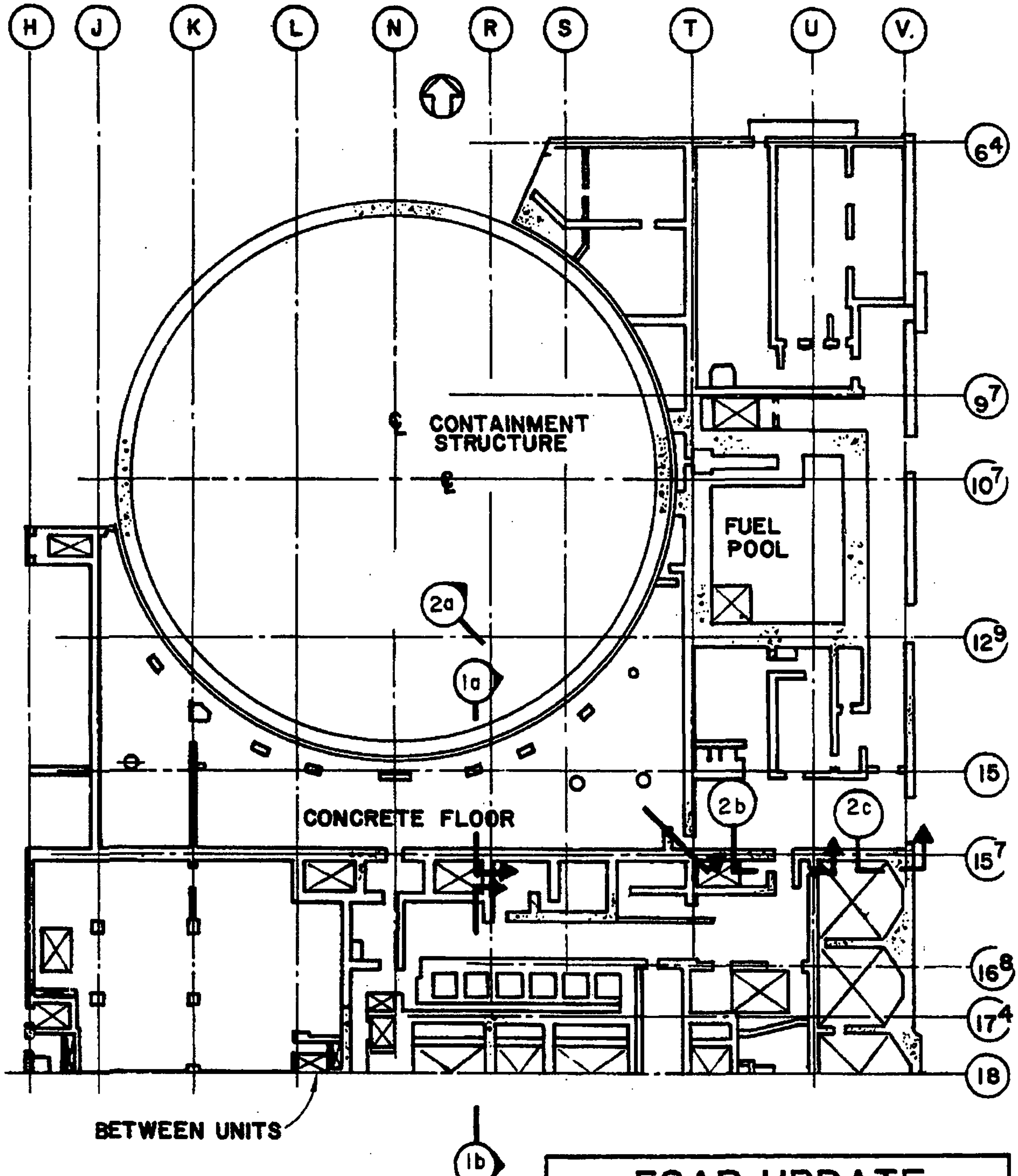

FSAR UPDATE

UNIT 1
DIABLO CANYON SITE

FIGURE 3.8-60

AUXILIARY BUILDING
FLOOR PLAN AT EL 100'-0"

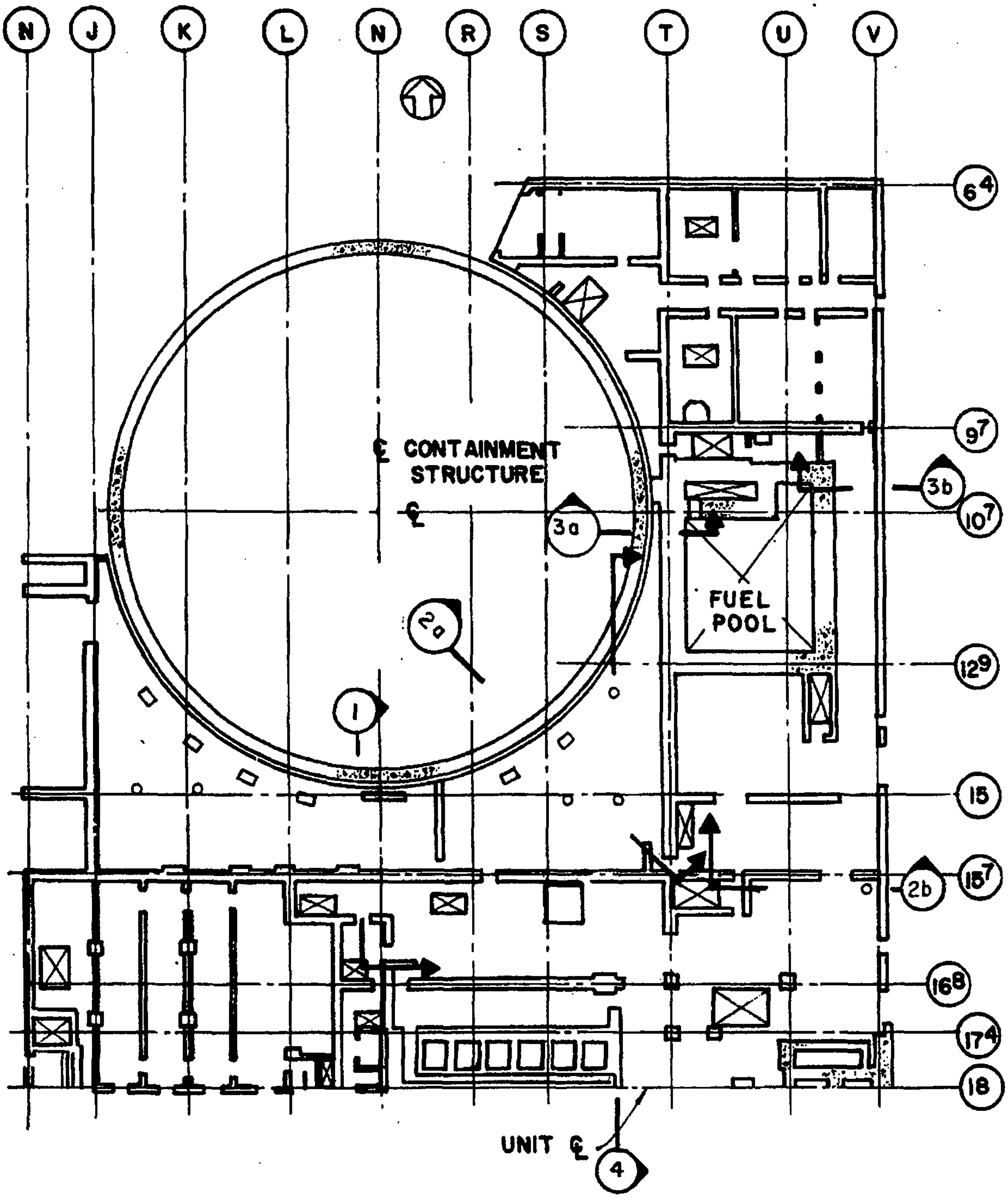

FSAR UPDATE

UNIT 1
DIABLO CANYON SITE

FIGURE 3.8-61

AUXILIARY BUILDING
FLOOR PLAN AT EL 115'-0"

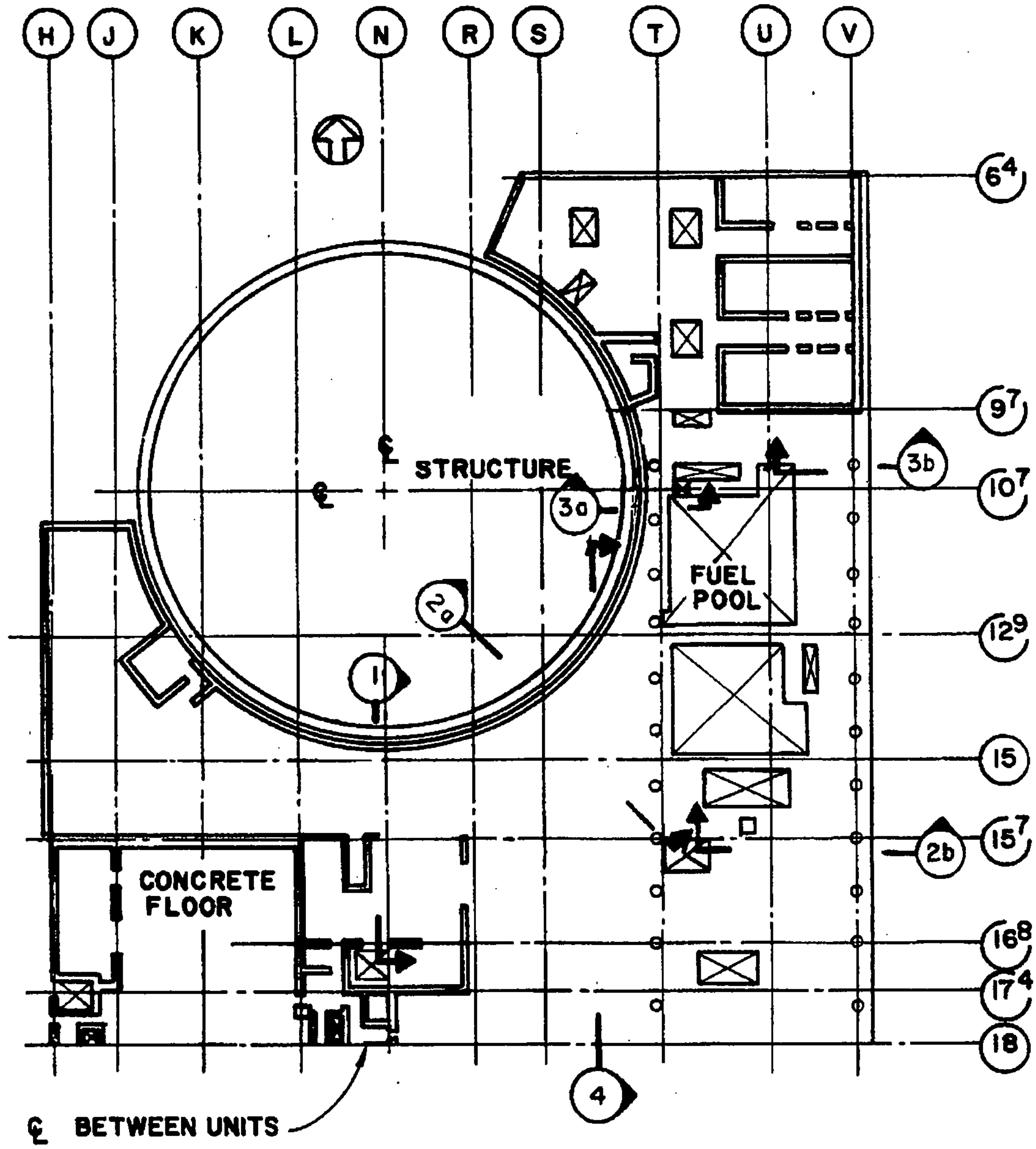

FSAR UPDATE
UNIT 1 **DIABLO CANYON SITE**
FIGURE 3.8-62 AUXILIARY BUILDING FLOOR PLAN AT EL 140'-0"

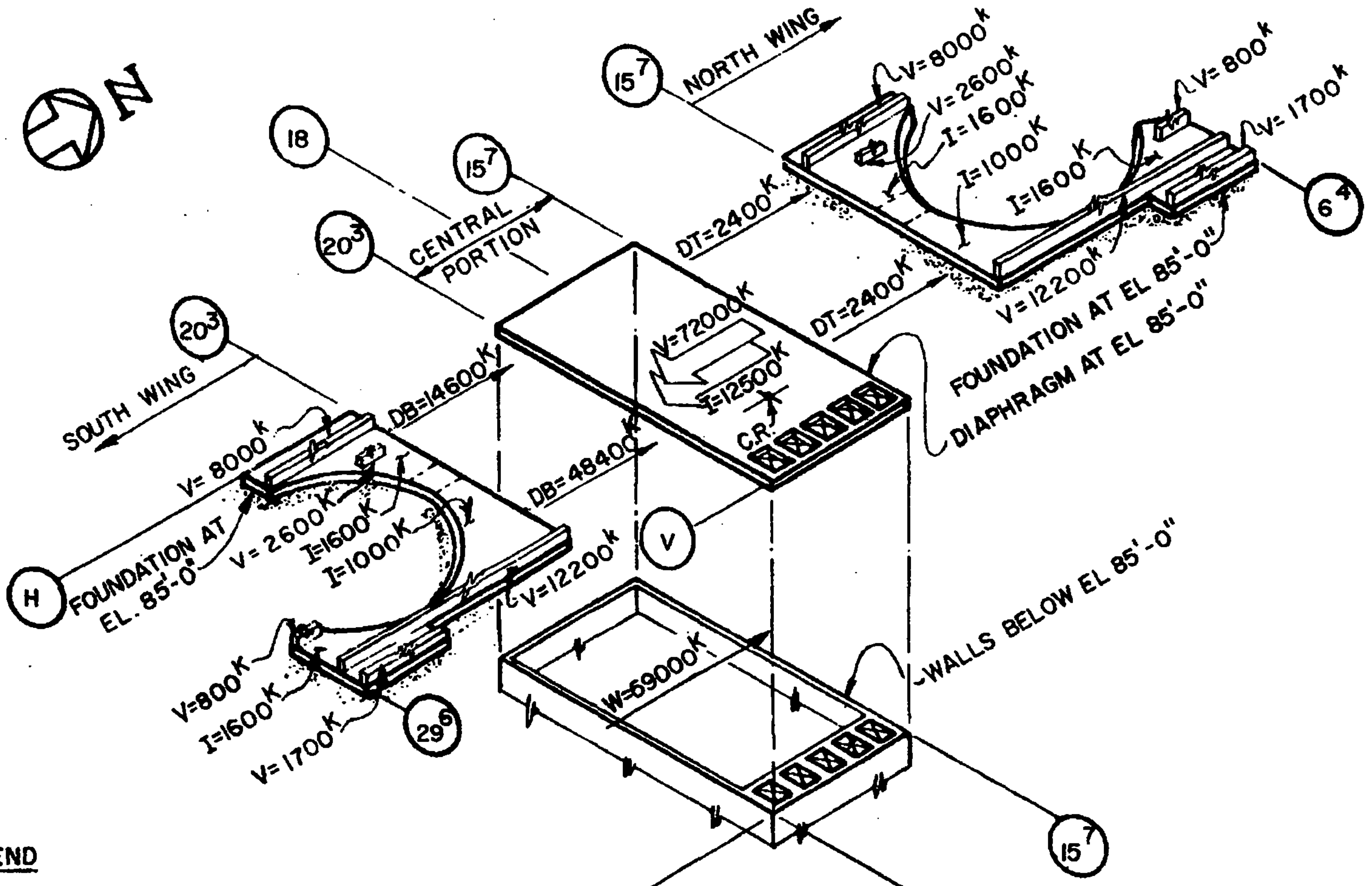

LEGEND

V= DEMAND SHEAR FORCE IN THE WALLS (KIPS)
I= DEMAND INERTIA LOAD AT EL. 85'-0" (KIPS)
W= SHEAR CAPACITY OF WALLS BELOW EL. 85'-0" (KIPS)
DT= CAPACITY THROUGH DIAPHRAGM REBAR TENSION (KIPS)
DB= CAPACITY THROUGH DIAPHRAGM BEARING (KIPS)

NOTE: DEMAND SHEARS IN WALLS WEST OF CENTER OF RIGIDITY CONSIDER DIRECT PLUS POSITIVE TORSIONAL SHEARS. THOSE IN WALLS EAST OF CENTER OF RIGIDITY CONSIDER ONLY DIRECT SHEARS.

FSAR UPDATE

UNITS 1 AND 2
DIABLO CANYON SITE

FIGURE 3.8-63
AUXILIARY BUILDING
LOAD DISSIPATION TO FOUNDATION
HOSGRI N – S

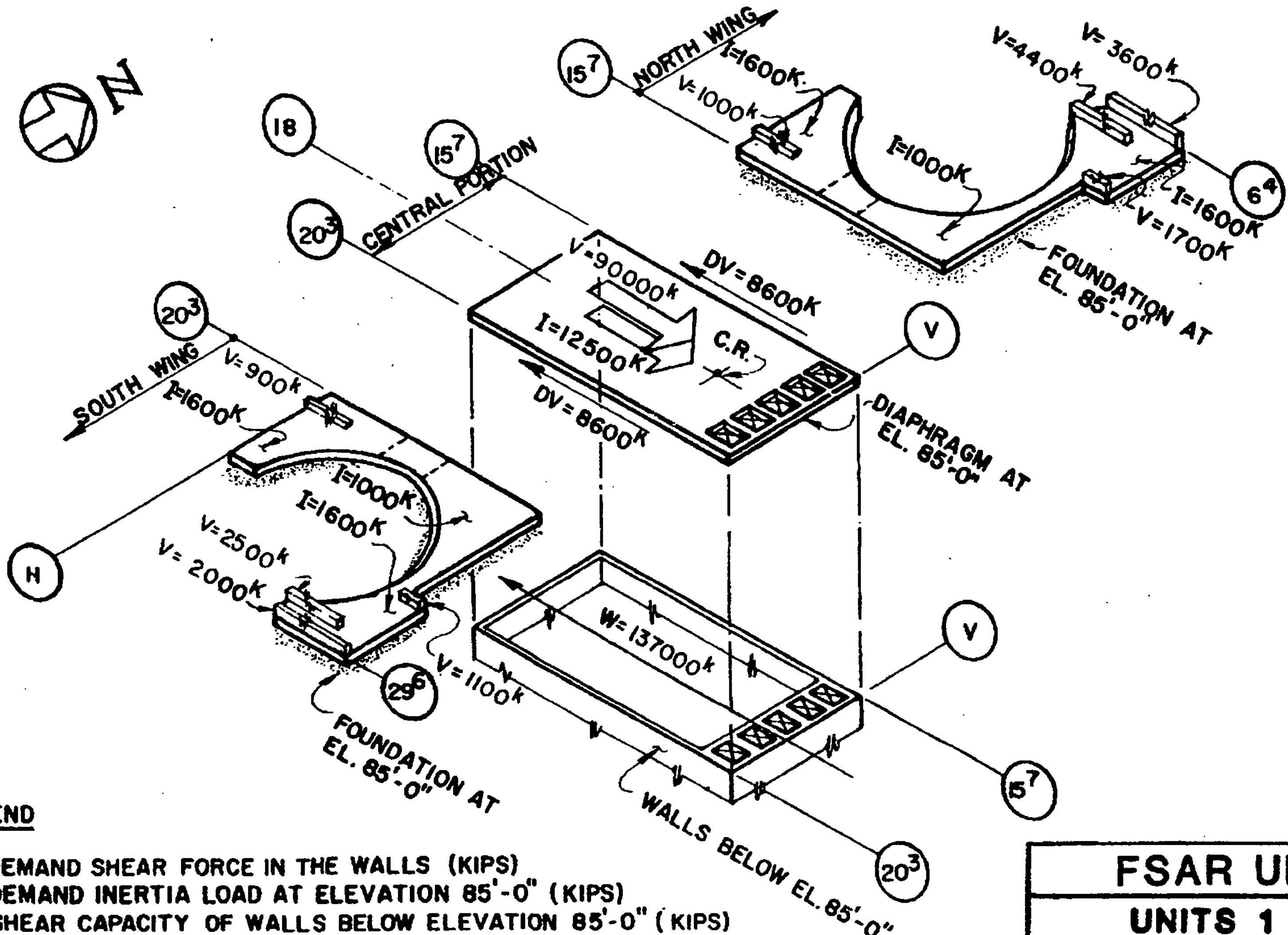

LEGEND

V= DEMAND SHEAR FORCE IN THE WALLS (KIPS)
I = DEMAND INERTIA LOAD AT ELEVATION 85'-0" (KIPS)
W= SHEAR CAPACITY OF WALLS BELOW ELEVATION 85'-0" (KIPS)
DV= SHEAR CAPACITY OF DIAPHRAGM (KIPS)

NOTE: WALLS NORTH OF LINE 18 CONSIDER DIRECT PLUS POSITIVE TORSIONAL EFFECT AND THOSE SOUTH OF LINE 18 CONSIDER ONLY DIRECT SHEARS.

FSAR UPDATE

UNITS 1 AND 2
DIABLO CANYON SITE

FIGURE 3.8-64
AUXILIARY BUILDING
LOAD DISSIPATION TO FOUNDATION
HOSGRI E – W

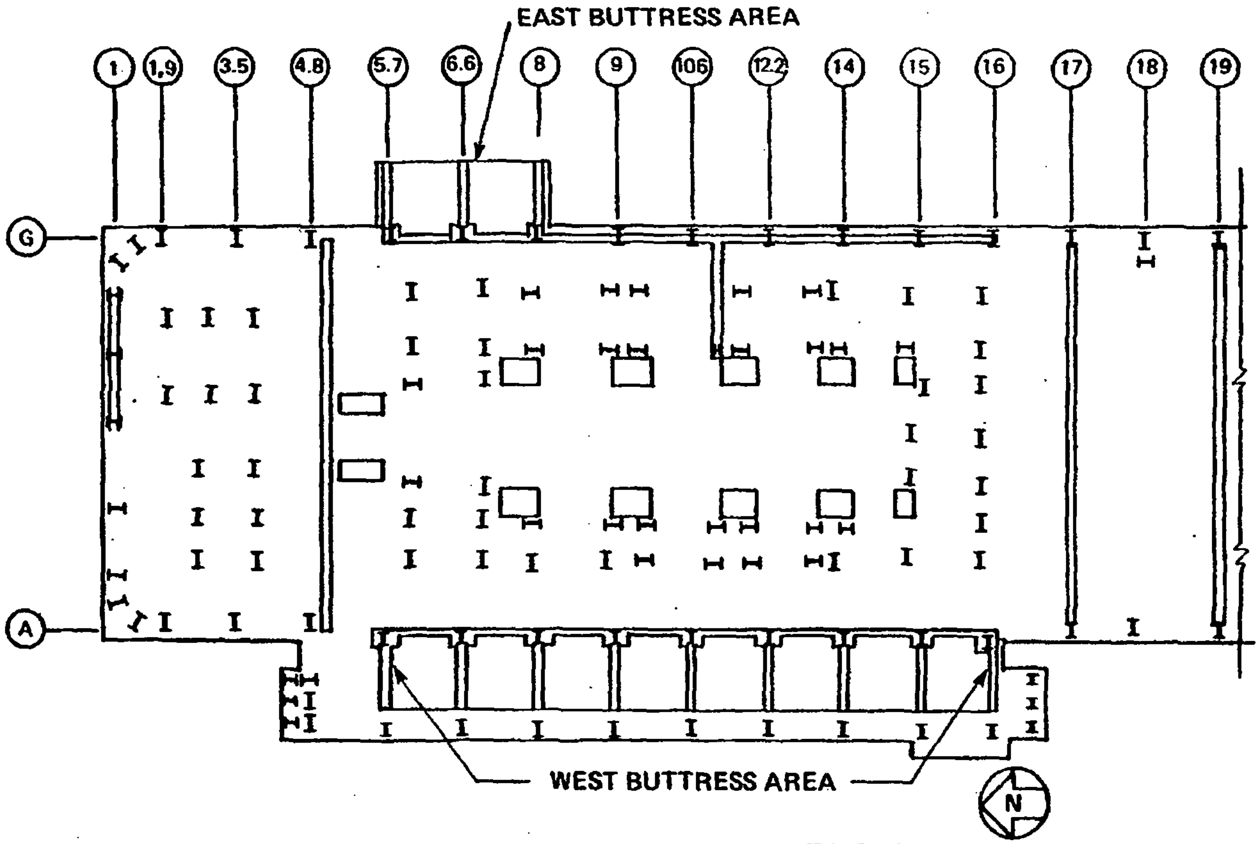

FSAR UPDATE

UNITS 1 AND 2 DIABLO CANYON SITE

FIGURE 3.8–66

TURBINE BUILDING PLAN AT EL. 85'

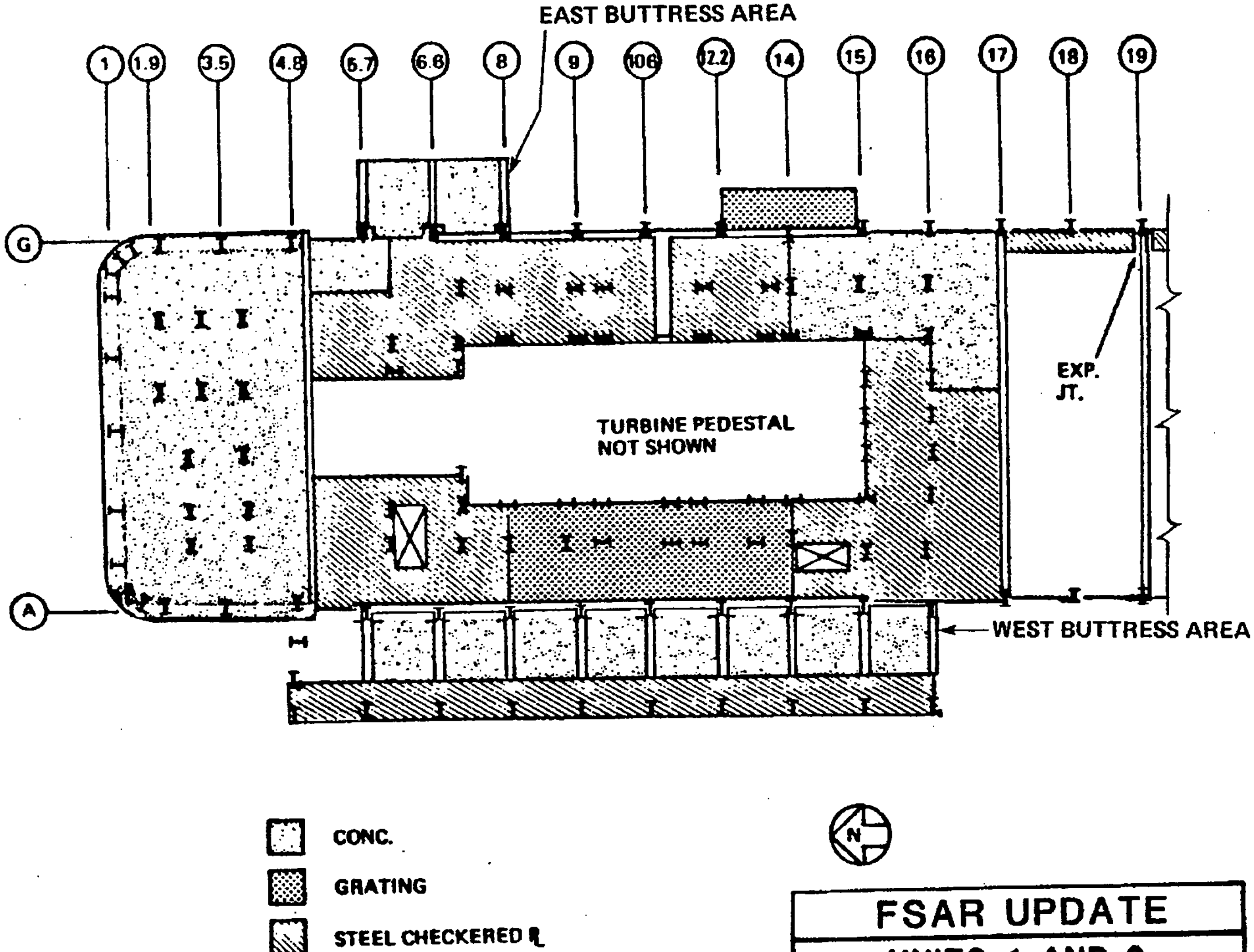

FSAR UPDATE

UNITS 1 AND 2
DIABLO CANYON SITE

FIGURE 3.8-67

TURBINE BUILDING
PLAN AT EL. 104'

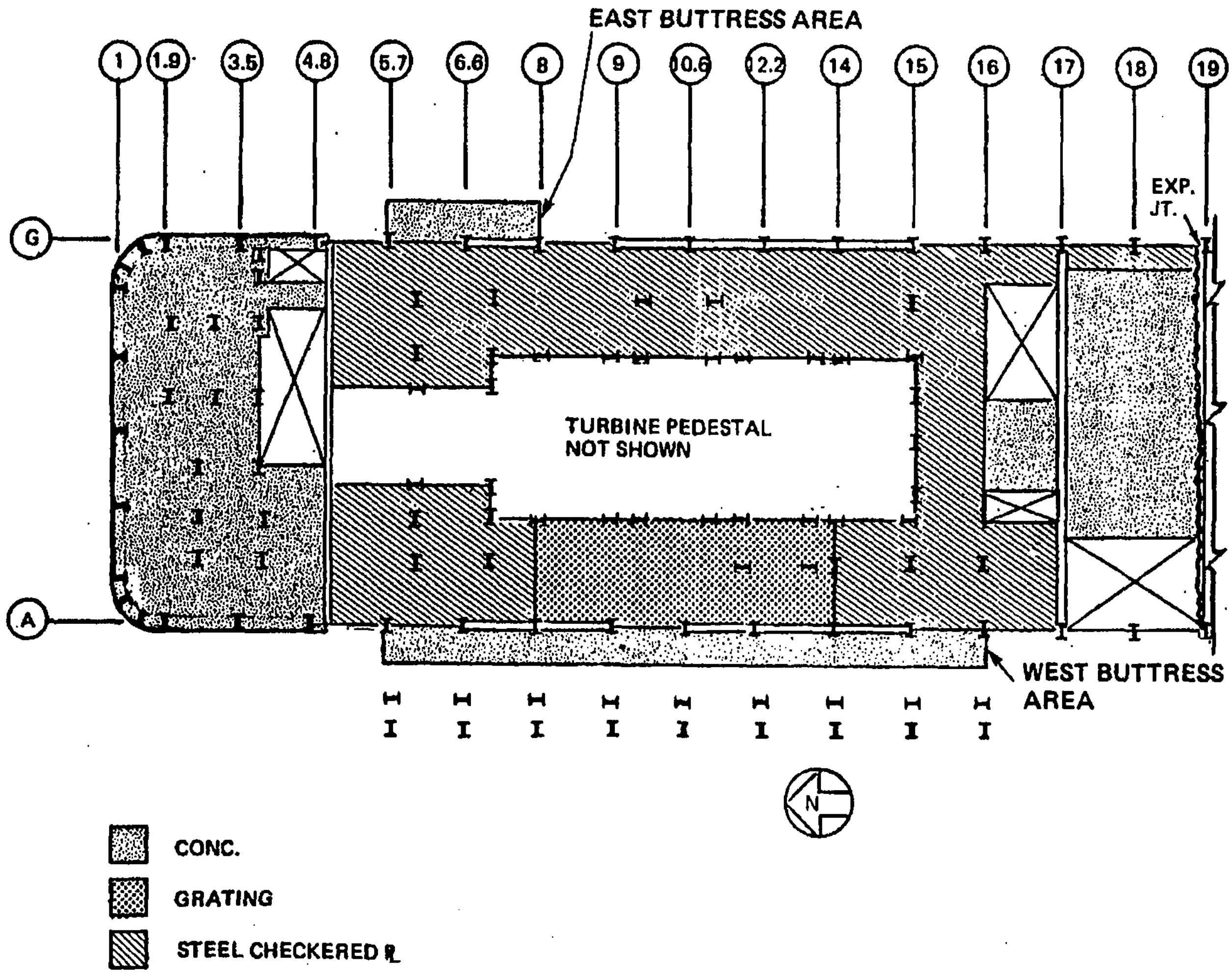

FSAR UPDATE
UNITS 1 AND 2 DIABLO CANYON SITE
FIGURE 3.8-68 TURBINE BUILDING PLAN AT EL. 119'

Revision 11 November 1996

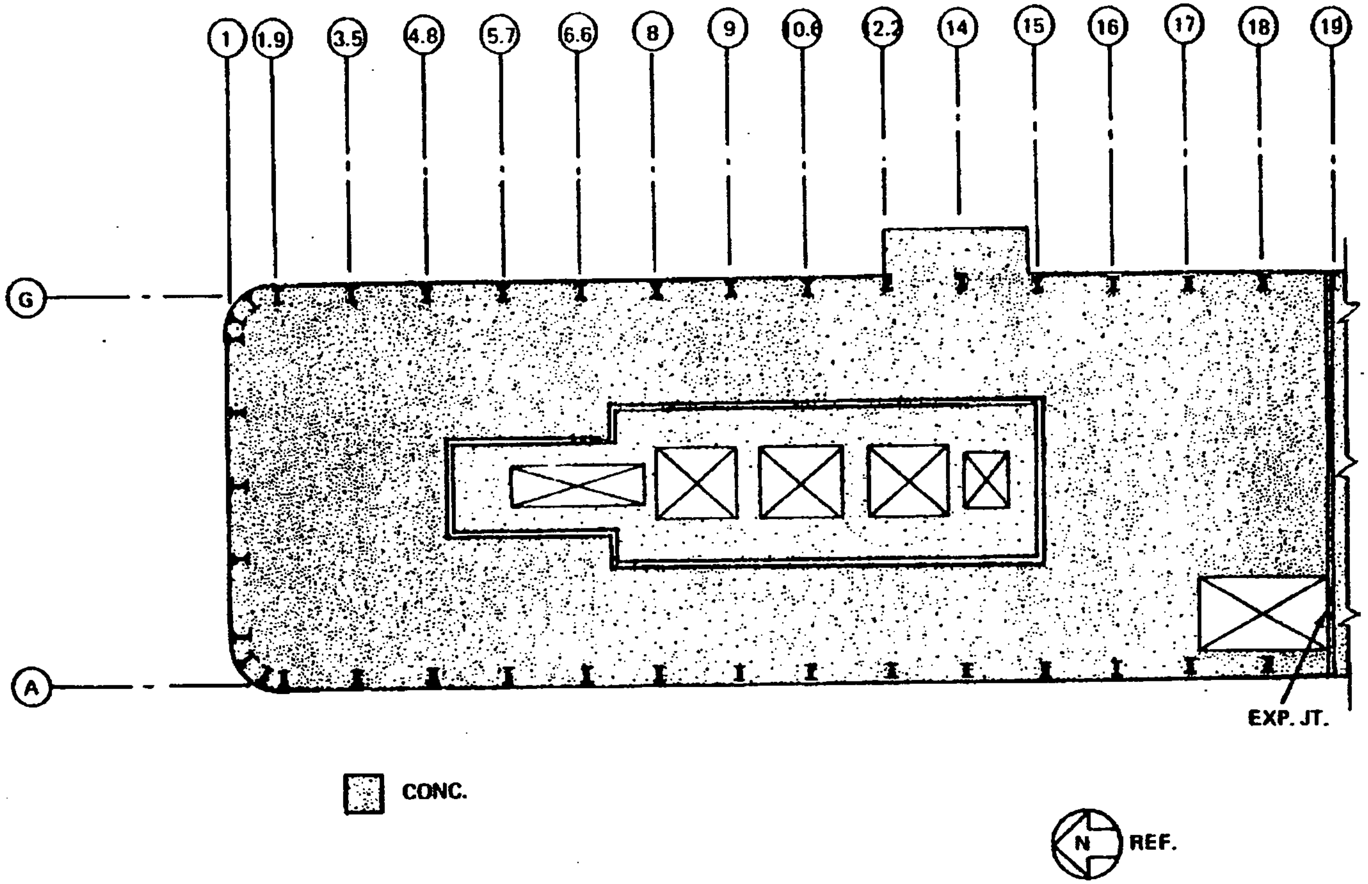

FSAR UPDATE

UNITS 1 AND 2
DIABLO CANYON SITE

FIGURE 3.8–69

TURBINE BUILDING
PLAN AT EL. 140'

Revision 11 November 1996

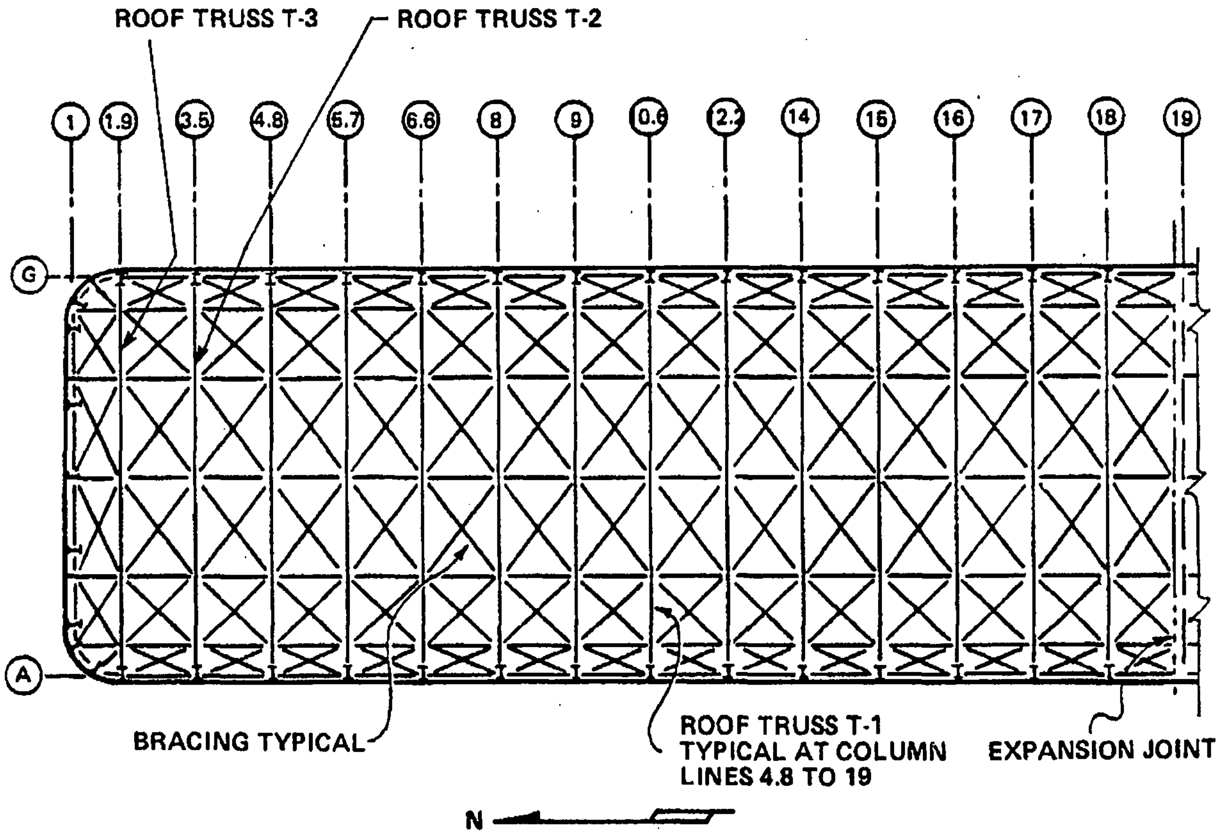

FSAR UPDATE

UNITS 1 AND 2
DIABLO CANYON SITE

FIGURE 3.8-70

TURBINE BUILDING
PLAN AT LOWER CHORD OF
ROOF TRUSS

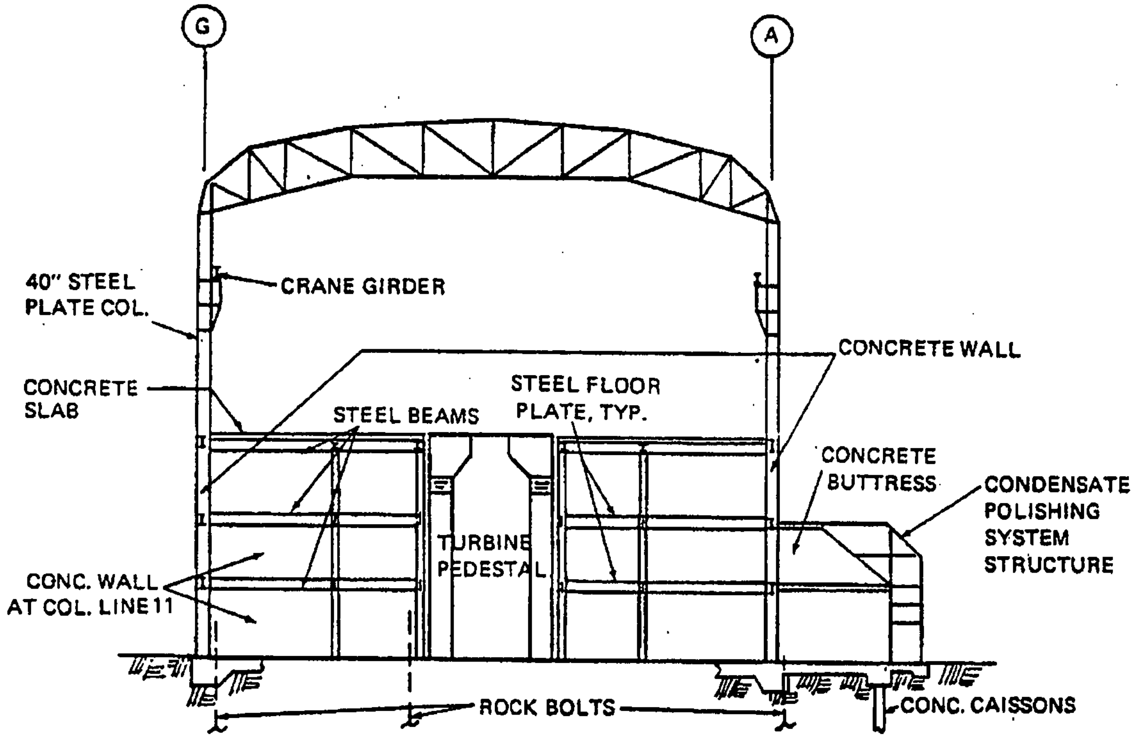

FSAR UPDATE
UNITS 1 AND 2 DIABLO CANYON SITE
FIGURE 3.8–71 TURBINE BUILDING TYPICAL SECTION

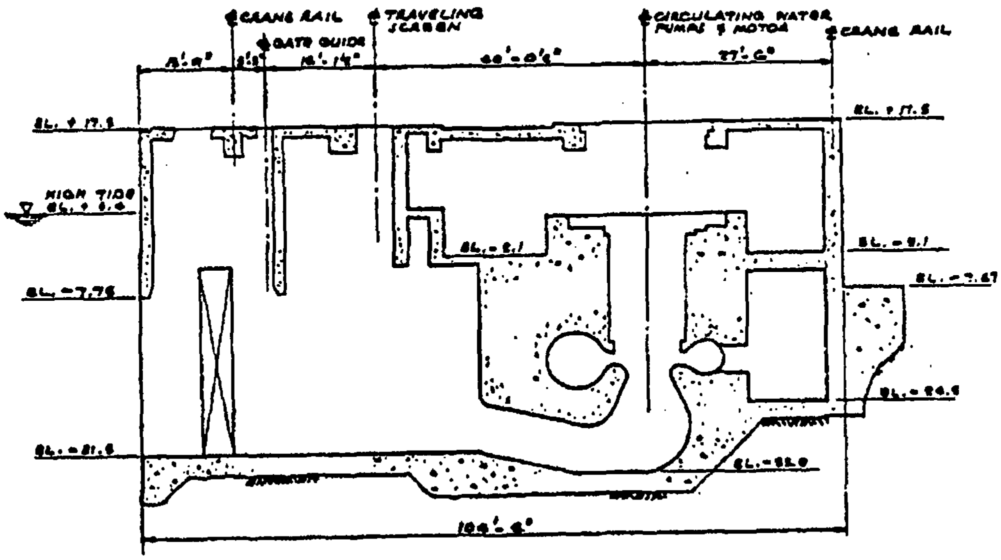

FSAR UPDATE

UNITS 1 AND 2
DIABLO CANYON SITE

FIGURE 3.8–75

INTAKE STRUCTURE
TRANSVERSE SECTION A

Revision 11 November 1996

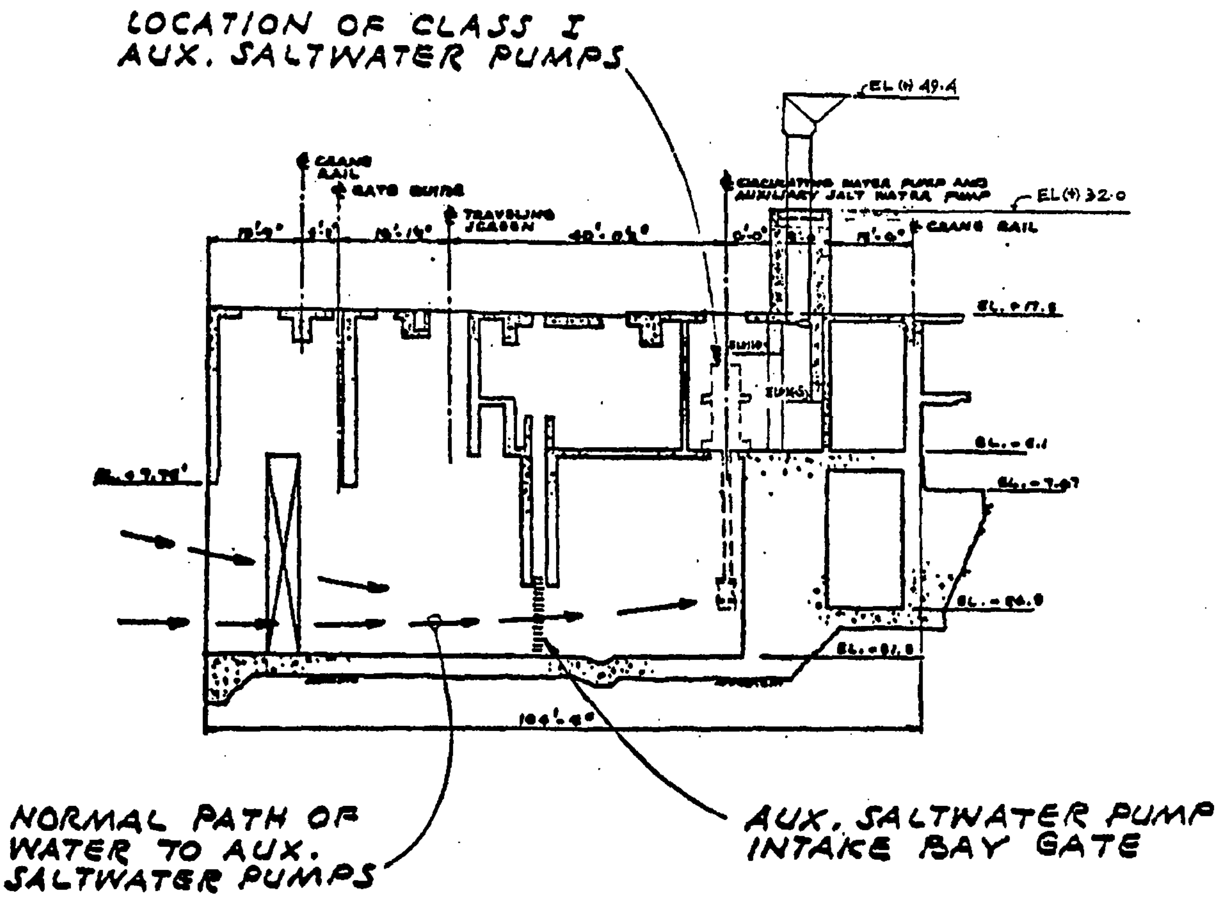

FSAR UPDATE

UNITS 1 AND 2
DIABLO CANYON SITE

FIGURE 3.8–76
INTAKE STRUCTURE
TRANSVERSE SECTION B

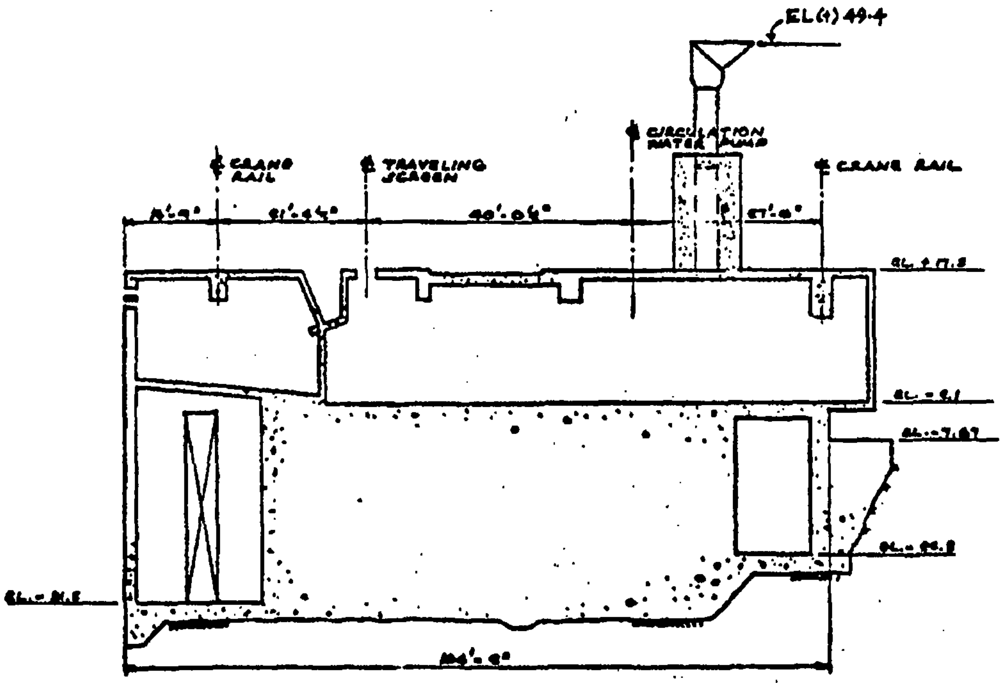

FSAR UPDATE

UNITS 1 AND 2 DIABLO CANYON SITE

FIGURE 3.8–77

INTAKE STRUCTURE TRANSVERSE SECTION C

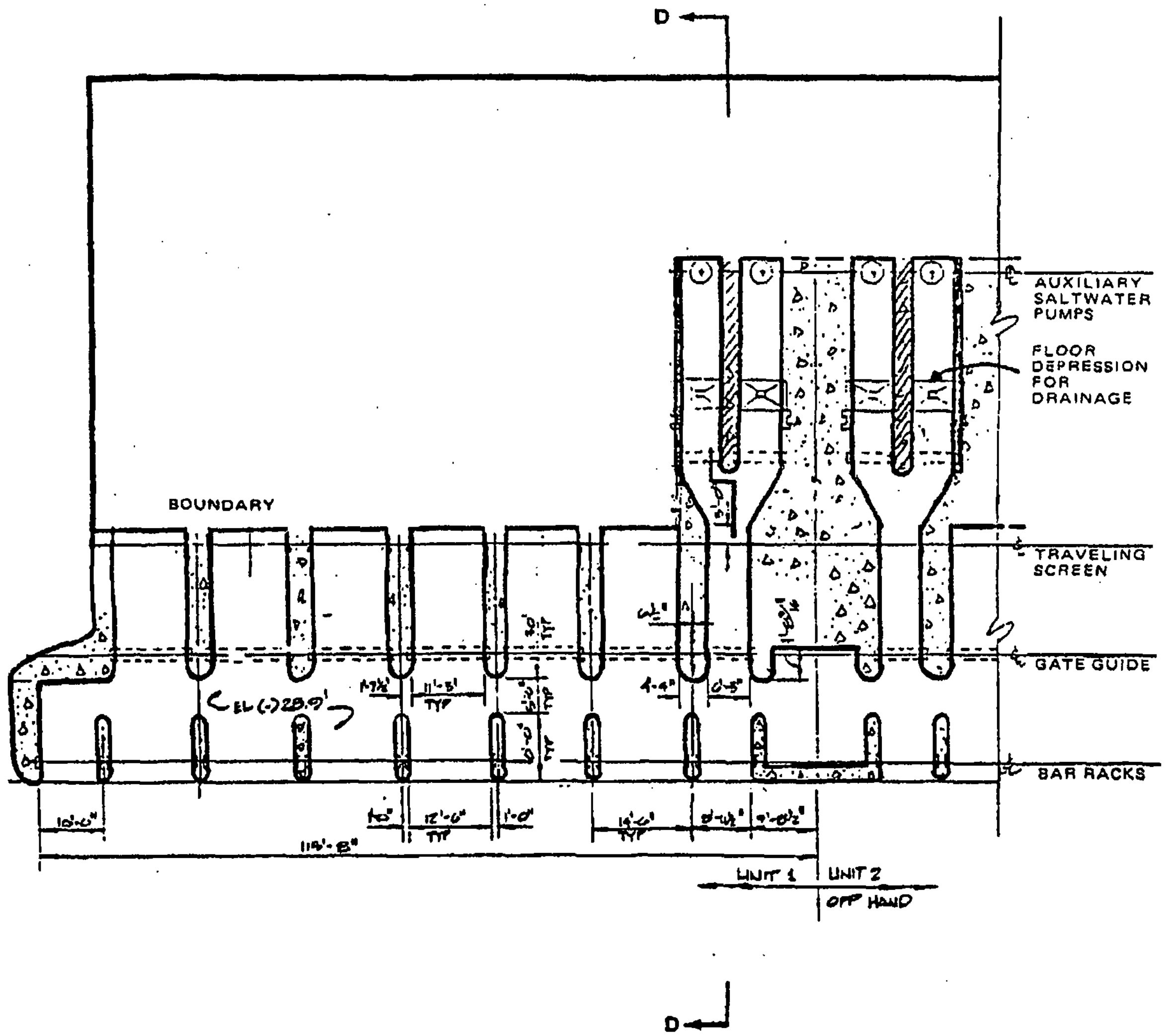

FSAR UPDATE

UNITS 1 AND 2 DIABLO CANYON SITE

FIGURE 3.8-78

INTAKE STRUCTURE WAVE SCALE MODEL PLAN-INVERT (UNIT 1) NTS

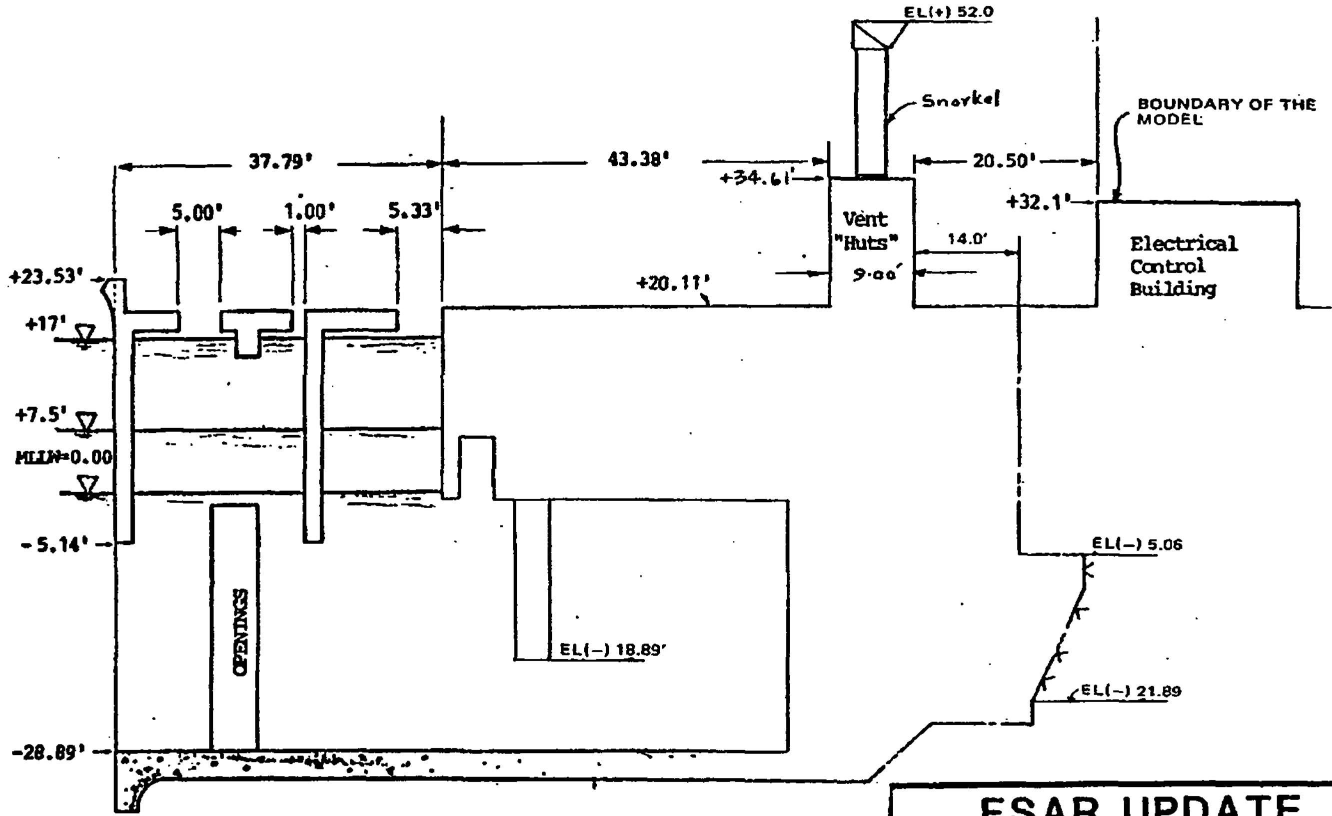

NOTE: (All Elevations Refer to Mean Lower Low Water Datum)

FSAR UPDATE

UNITS 1 AND 2 DIABLO CANYON SITE

FIGURE 3.8-79

INTAKE STRUCTURE WAVE SCALE MODEL TRANSVERSE SECTION D

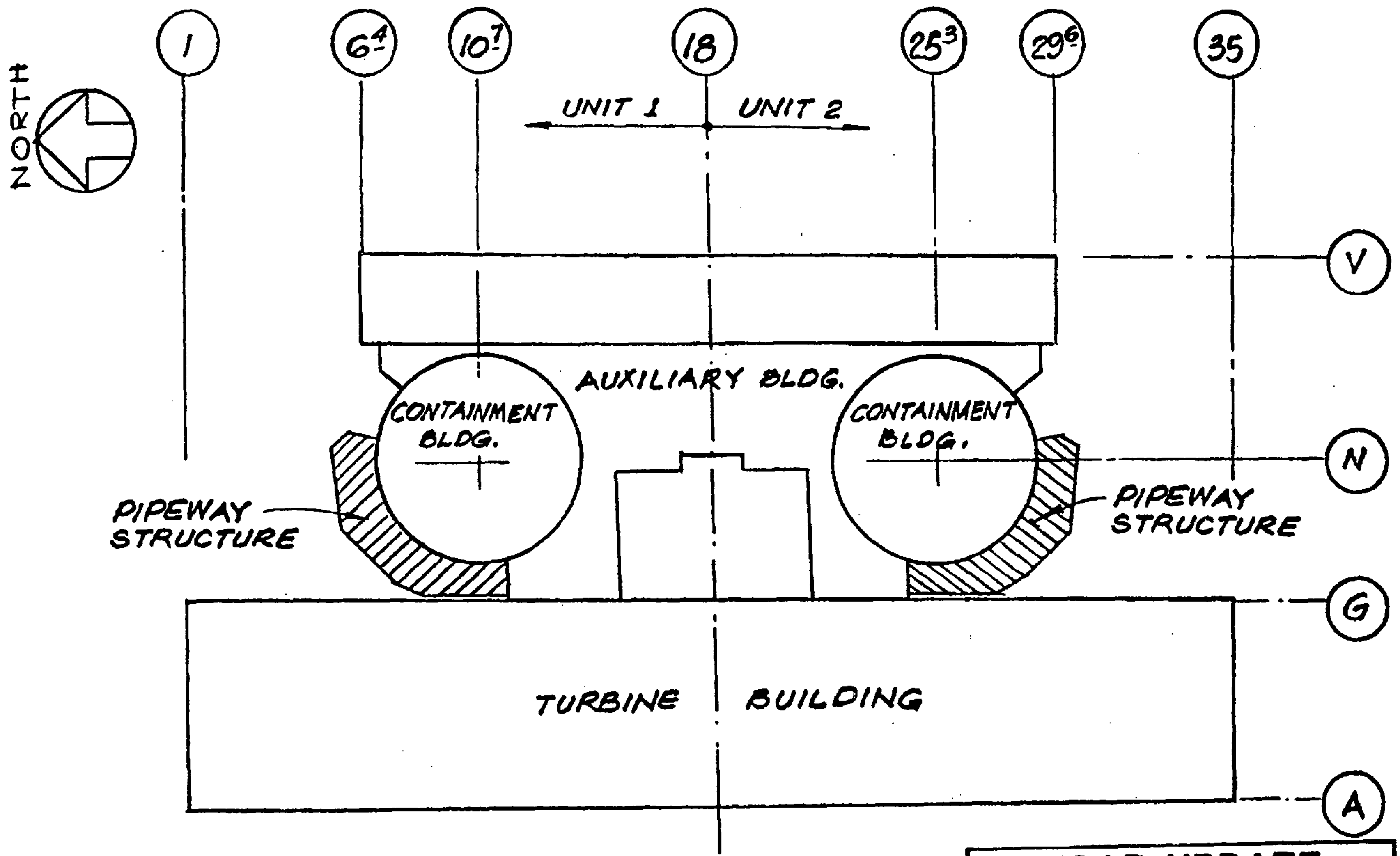

FSAR UPDATE

UNITS 1 AND 2
DIABLO CANYON SITE

FIGURE 3.8–80
PIPEWAY STRUCTURE LAYOUT

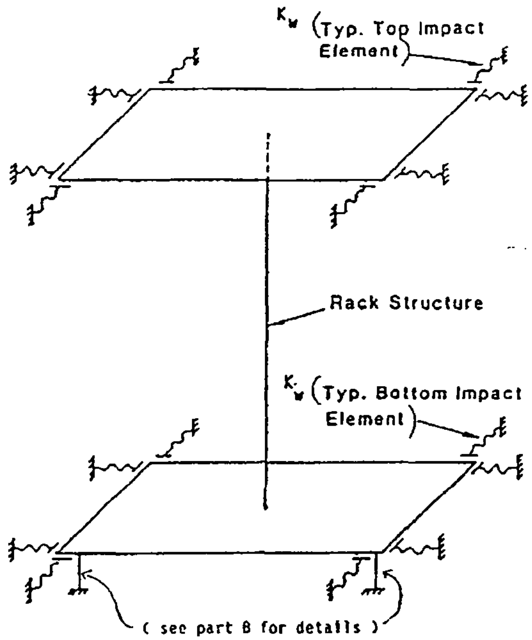

Part A. Three-Dimensional Representation of Rack Dynamic Model

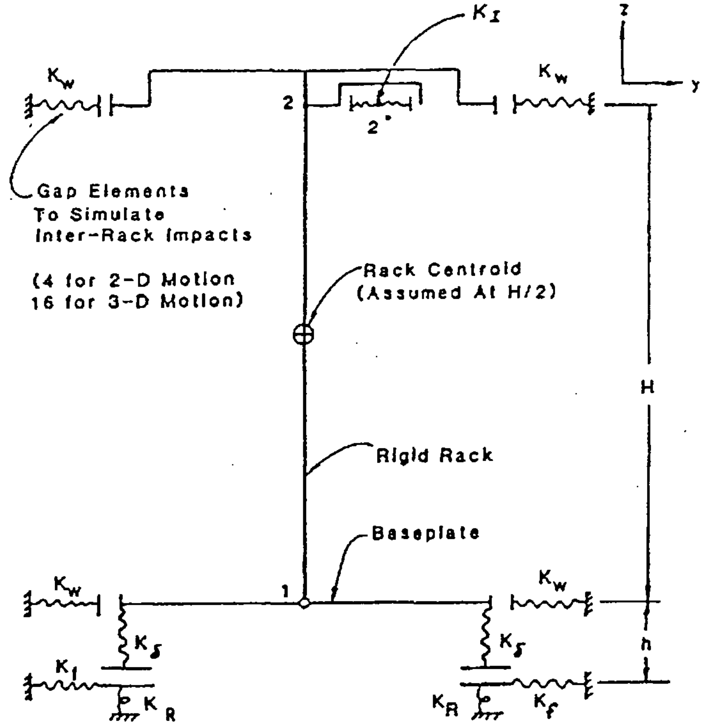

Part B. Two-Dimensional Representation of Rack Dynamic Model

FSAR UPDATE
UNITS 1 AND 2 DIABLO CANYON SITE
Figure 3.8-81. Rack Dynamic Model

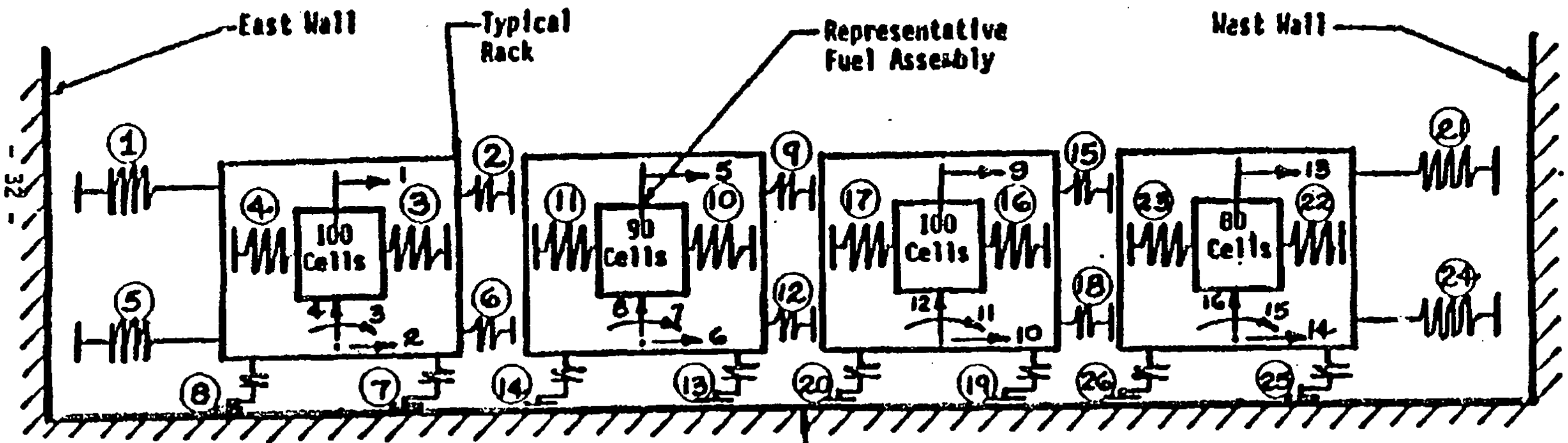

- 32 -

FSAR UPDATE

UNITS 1 AND 2
DIABLO CANYON SITE

Figure 3.8-82.

MULTI-RACK MODEL

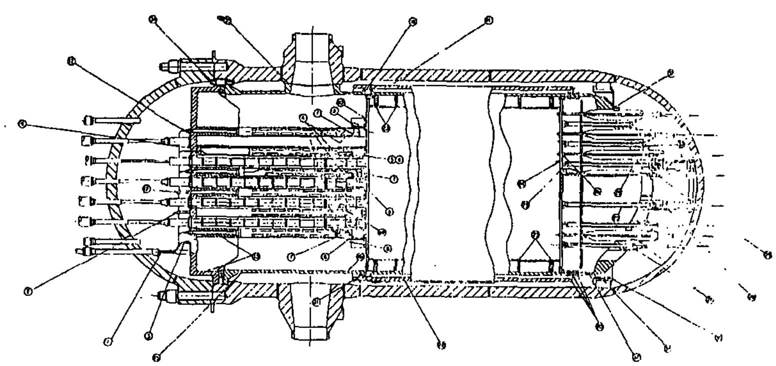

	FEATURES TO BE EXAMINED	COMMENTS AND OBSERVATIONS BEFORE FUNCTIONAL TEST
1	THERMOCOUPLE CONDUIT CLAMPS INSIDE THE THERMOCOUPLE COLUMN	
2	CLAMP ARRANGEMENTS AT THE [illegible] LOCATIONS.	
3	[illegible] SUPPORT COLUMNS ADJACENT TO THE THERMOCOUPLE COLUMNS.	
4	ACCESSIBLE ANGLE CONDUIT CLAMPS INSIDE THE UPPER SUPPORT COLUMNS.	
5	ACCESSIBLE WELD JOINTS AT THE THERMOCOUPLE [illegible] INSTRUMENTATION COLUMNS	
6	[illegible]	
7	[illegible]	
8	[illegible] OF THE ACCESSIBLE [illegible] THERMOCOUPLE TIPS	
9	THERMOCOUPLE COLUMN AND GUIDE TUBE SCREW LOCKING DEVICES	
10	ACCESSIBLE SUPPORT COLUMN [illegible] PLATE, AND CORE PLATE [illegible] SCREW LOCKING DEVICES.	
11	UPPER CORE PLATE INSERTS.	
12	CONDUIT CONNECTION FITTINGS AND [illegible] CLAMP ARRANGEMENTS.	
13	[illegible]	
14	ACCESSIBLE GUIDE TUBE WELDS.	
15	UPPER BARREL TO FLANGE GIRTH WELD	
16	UPPER BARREL TO LOWER BARREL GIRTH WELD	
17	LOWER BARREL TO CORE SUPPORT GIRTH WELD	
18	UPPER CORE PLATE ALIGNING [illegible] SURFACES	
19	OUTLET NOZZLE INTERFACE SURFACE CONDITION	
20	[illegible]	
21	THERMAL SHIELD INTERFACE AT THE [illegible]	
22	IRRADIATION SPECIMEN BASKET WELDS.	
23	[illegible]	
24	CORE SUPPORT COLUMN TO LOWER CORE PLATE SCREW LOCKING DEVICES [illegible]	
25	CORE SUPPORT COLUMN [illegible]	
26	[illegible]	
27	LOCKING DEVICES OF THE [illegible] INSTRUMENTATION GUIDE COLUMNS	
28	LOCKING DEVICES OF THE SECONDARY CORE SUPPORT	
29	ACCESSIBLE LOCKING DEVICES OF THE [illegible] INSTRUMENTATION COLUMN [illegible]	
30	RADIAL SUPPORT [illegible] AND BEARING SURFACES	
31	HEAD AND VESSEL ALIGNING [illegible] SCREW LOCKING DEVICES AND BEARING SURFACES	
32	CONTACT AT INTERFACE OF THE ACCESSIBLE INSTRUMENTATION GUIDE COLUMNS	
33	CONTACT AT INTERFACE OF THE ACCESSIBLE CORE SUPPORT COLUMN [illegible]	
34	VESSEL [illegible] ARRANGEMENTS AND BEARING SURFACES	
35	VESSEL NOZZLE INTERFACE SURFACE CONDITION	

FSAR UPDATE

UNIT 1
DIABLO CANYON SITE

FIGURE 3.9-1
VIBRATION CHECKOUT - FUNCTIONAL
TEST INSPECTION DATA

Revision 11 November 1996

3.9 MECHANICAL SYSTEMS AND COMPONENTS

3.9.1 DYNAMIC SYSTEM ANALYSIS AND TESTING

A mechanical design description of the internals and core components showing the differences and similarities between the two DCPP units is presented in Section 4.2.2. The dynamic analysis techniques and methods used to determine and confirm the dynamic response of the reactor internals are presented in the following section. Detailed information of the dynamic system analysis and testing is presented in the reports listed in Section 3.9.6. Chapter 14 describes the plant initial tests and operation.

A description of the analyses used in the design of safety-related mechanical equipment, such as pumps and heat exchangers, to withstand the DE, DDE, and HE seismic loadings is provided in Section 3.7.

3.9.1.1 Vibration Operational Test Programs

This section describes the nature of flow-induced vibrations in the reactor coolant loops and the analyses performed to ensure such vibrations are at an acceptable level.

3.9.1.1.1 Main Piping System, Flow-Induced Vibration

Pressure pulses, from the reactor coolant pump impeller are prevented from resulting in flow-induced vibrations in the main piping systems of the RCL. The reactor coolant pump perturbing frequency is quite high when compared to the piping natural frequency. Frequency separation, therefore, ensures a very small probability of self-excited or sympathetic vibration.

3.9.1.1.2 Reactor Internals Flow-Induced Vibration

The dynamic behavior of reactor components has been studied using experimental data obtained from operating reactors along with results of model tests and static and dynamic tests. The following procedures have been performed in the study of thermal shield vibration:

(1) During a test program performed with a 1/7th-scale model, the natural frequencies of the thermal shield in water and the maximum vibration amplitude were measured.

(2) Shaker test programs performed on a prototype thermal shield with the actual boundary conditions provided full-scale natural frequencies and mode shapes in air. These modes were established by measuring accelerations at the center, top (support elevation), and bottom of the shield. In Figure 3.9-3, the results obtained are plotted for n = 4 and correspond to a thermal shield with eight supports which are indicated on

8/3

the same figure. The amplitudes of vibration are fitted with a curve y = A sin 4*q*.

(3) Maximum displacements were measured during the preoperational reactor test and were correlated with the information obtained in the 1/7th-scale model and shaker test.

(4) In Figure 3.9-4, the maximum amplitudes of vibration are plotted as measured on a thermal shield with six supports. The experimental points have been least-square fitted with a curve y = A sin 3*q*.

In general, the study follows two parallel procedures. Frequencies and spring constants are derived analytically, and these values are confirmed from the results of the tests. Damping coefficients are established experimentally, and forcing functions are estimated from pressure fluctuations measured during operation and in models. In parallel, the responses of important reactor structures were measured during preoperational reactor tests and the frequencies and mode shapes of the structures obtained. Once all the dynamic parameters were obtained as explained above, the forcing functions could be estimated. Internals behavior during reactor operation is measured using mechanical devices and nuclear noise methods.

Some components, such as control rod guide tubes, fuel rods, and incore instrumentation tubes are subjected to cross flow and parallel flow with respect to the axis of the structure. For both cases, cross and parallel, the response is obtained after the forcing function and the damping of the system are determined.

3.9.1.1.3 Vibration Monitoring

Since internals of four loop reactors are designed and manufactured to essentially the same procedures, processes, and similar drawings, the response of these structures is similar. Performance data from the instrumentation of actual reactors, as well as mechanical and flow scale models, are available (References 2, 4, and 5). The pre- and post-operational flow test examinations of the Indian Point II Plant internals, the four loop prototype plant, have been completed indicating that all the components performed as predicted. No evidence or sign of damage or incipient failure was found.

The testing programs consisted of measurements of the stresses, deflections, and responses of selected key points in the internals structures during hot functional and low power physics tests. The main purpose of this testing program was to ensure that no unexpected large amplitudes of vibration existed in the internals structure during operation. The tests were extended to provide data and results on what were assumed to be indicators of overall core support structure performance and to verify particular stress and deflection quantities.

3.9.1.1.4 Loose-Parts Monitoring

A loose-parts monitoring system is provided for early detection of possible loose parts in the RCS, in order to reduce the probability of loose parts causing damage to RCS components. This system is described in Section 4.4.5.

3.9.1.2 Dynamic Testing Procedure

During startup functional testing, piping, including supports and restraints, of certain systems was observed carefully by experienced startup personnel. At selected points of calculated maximum movement, visual inspection and/or measurements were taken and compared with those calculated to establish that stress limits are not exceeded.

If vibration was noted to cause piping or supports movements beyond those allowed, corrective action in the form of additional or redesigned supports, snubbers, etc. was taken and the system was retested to determine that vibrations have been reduced to an acceptable level. Stress analysis on the system was rerun if deemed necessary by the designer. The systems and transients included in this program are listed below:

(1) Reactor coolant pumps start

(2) Reactor coolant pumps trip

(3) Main steam turbine stop valves trip

(4) Steam dump to condenser valves open

(5) Main steam safety and relief valves lift and blowdown

(6) Pressurizer relief valves lift and blow down (Unit 1 only)

(7) Auxiliary feedwater pump turbine stop valve trip

(8) Charging pumps start and trip

(9) Safety injection pumps start and trip

(10) Residual heat removal (RHR) pumps start and trip

(11) Containment spray pumps start and trip

(12) Accumulators discharge to loops

(13) Pressurizer spray valves open and trip closed

(14) Pressurizer power relief valves open

Locations of observation points for piping movements for preoperational piping vibration tests for the above systems were determined from dynamic analysis performed on the piping systems, with system stiffness and restraint locations taken into account. Observed deflections were compared with code allowable values.

3.9.1.3 Dynamic System Analysis Methods for Reactor Internals

To verify structural adequacy of reactor internal components and the reactor core for Diablo Canyon Units, nonlinear LOCA and seismic dynamic analyses are performed. These dynamic analyses are performed for both LOCA cold and hot leg breaks, as well as for seismic excitations of DDE and Hosgri (HE).

For faulted conditions, the response of reactor internals due to DDE and LOCA conditions are additive by the SRSS (Square Root of the Sum of Squares) method. A HE and LOCA are also considered to occur simultaneously and, therefore, the combined response is considered by SRSS. The methods and techniques for these dynamic analyses are described below.

3.9.1.3.1 LOCA (Loss-Of-Coolant-Accident) Analysis

Details of the RPV system finite element model which is used in these analyses are described. Results of these analyses consist of the nodal time history displacements and the interface impact loads on the reactor vessel, reactor internals and the core. The time history displacements of all major components such as reactor vessel head, vessel bottom and the vessel/barrel nozzles are also generated for their later use in the component stress analyses.

The RPV system finite element model consists of three concentric structural submodels connected by nonlinear impact elements and linear stiffness matrices. The first sub-model represents the reactor vessel shell and its associated components. The reactor vessel is restrained by four reactor vessel supports (situated beneath alternate nozzles) and the attached primary coolant piping.

The second sub-model represents the reactor core barrel, thermal shield, lower support plate, tie plates, and the secondary support components for Unit 1, whereas, for Unit 2 the second sub-model is identical to that of unit 1 except that it has core barrel with neutron pads instead of thermal shield.

These sub-models are physically located inside the first, and are connected to them by stiffness matrices at the internals support ledges. The core barrel to the reactor vessel shell impact is represented by nonlinear elements at the core barrel flange, upper support plate flange, core barrel outlet nozzles, and the lower radial restraints. In addition, vertical impact loads on the fuel assembly top and bottom nozzles.

The third and innermost sub-model represents the upper support plate assembly consisting of guide tubes, upper support columns, upper and lower core plates, and

fuel. The third sub-model is connected to the first and second by stiffness matrices and nonlinear elements. The fluid-solid interactions in the LOCA analysis are accounted for through the hydraulic forcing functions generated by Multiflex Code (Reference 3).

The WECAN computer code, which is used to determine the response of the reactor vessel and its internals, is a general purpose finite element code. In the finite element approach, the structure is divided into a finite number of discrete members or elements. The inertia and stiffness matrices, as well as the force array, are first calculated for each element in the local coordinates. Employing appropriate transformations, the element global matrices and arrays are assembled into global structural matrices and arrays, and used for dynamic solution of the differential equation of motion for the structure.

The WECAN Code solves equations of motion using the nonlinear modal superposition theory. Initial computer runs such as dead weight analysis and the vibration (modal) analyses are made to set the initial vertical interface gaps and to calculate eigen values and eigenvectors. The modal analysis information is stored on magnetic tapes, and is used in a subsequent computer run which solves equations of motion. The first time step performs the static solution of equations to determine steady state solution under normal operating hydraulic forces. After the initial time step, WECAN calculates the dynamic solution of equations of motion, nodal displacements, and impact forces, which are stored on tape for post-processing.

Reactor internals response to both cold and hot leg pipe ruptures was analyzed. The LOCA hydraulic forcing functions used in the RPV system analyses were obtained for hypothetical breaks considered in the main loop line. However, with the acceptance of DCPP Leak-Before-Break (LBB) by USNRC (Reference 14), the dynamic effects of breaks in the main reactor coolant loop no longer have to be considered in the design basis of analyses. Only the next most limiting breaks in auxiliary lines have to be considered.

Note that the preceding paragraphs describe the RPV and internals system dynamic analyses for which the WECAN computer code was used. Current analyses (such as the dynamic analyses performed in support of the replacement reactor vessel head project) utilize the ANSYS computer code. The methodology used to develop the ANSYS system models is consistent with the methodology used to develop historic WECAN models. The direct time integration method is used in ANSYS to solve the dynamic equations of motion for the system; whereas the nonlinear mode superposition method is used in WECAN to solve the dynamic equations of motion for the system.

The breaks considered for the replacement vessel head project included: (1) the accumulator line; (2) the pressurizer surge line; and (3) the residual heat removal line.

3.9.1.3.2 Reactor Internals Components Subjected to Horizontal Excitations

The analysis methodology is summarized below for components that are subject to horizontal excitations during LOCA conditions. The components include the core barrel, guide tubes, and upper support columns. It should be noted that with the acceptance of DCPP Leak-Before-Break (Reference 14), the dynamic effects of the main reactor coolant loop piping no longer have to be considered in the design basis analysis. Only the dynamic effects of the next most limiting breaks of auxiliary lines need to be considered; and consequently the components will experience considerably less load than those from the main loop line breaks.

3.9.1.3.2.1 Core Barrel

For the hydraulic analysis of the pressure transients during hot leg blowdown, the maximum pressure drop across the barrel is a uniform radial compressive impulse. The barrel was analyzed for dynamic buckling using the following conservative assumptions:

(1) The effect of the fluid environment is neglected (water stiffening is not considered).

(2) The shell is treated as simply supported.

During cold leg blowdown, the upper barrel is subjected to a nonaxisymmetric expansion radial impulse that changes as the rarefaction wave propagates both around the barrel and down the outer flow annulus between vessel and barrel. The analysis of transverse barrel response to cold leg blowdown was performed as follows:

(1) The upper core barrel was treated as a simply supported cylindrical shell of constant thickness between the upper flange weldment and the lower core barrel weldment. No credit was taken for the supports at the barrel midspan offered by the outlet nozzles. This assumption leads to conservative deflection estimates of the upper core barrel.

(2) The upper core barrel was analyzed as a shell with four variable sections to model the support flange, upper core barrel, reduced girth weld section, and a portion of the lower core barrel.

(3) The barrel with the core and neutron shield panels[a] was analyzed as a beam elastically supported at the lower radial support, and the dynamic response obtained.

While the above described blowdown analyses were performed in the original analysis, with the acceptance of the DCPP leak-before-break analysis by the NRC (Reference 14), dynamic loads resulting from pipe rupture events in the main reactor coolant loop piping

---

[a] Neutron shield panels on Unit 2 only.

no longer have to be considered in the design basis structural analyses. Only the much smaller loads from RCS branch line breaks have to be considered.

3.9.1.3.2.2 Guide Tubes

The dynamic loads on rod cluster control guide tubes are more severe for a LOCA caused by hot leg rupture than for an accident by cold leg over the rod cluster control guide tubes. Thus, the analysis was performed only for a hot leg blowdown.

The guide tubes in closest proximity to the ruptured outlet nozzle are the most severely loaded. The transverse guide tube forces during the hot leg blowdown decrease with increasing distance from the ruptured nozzle location.
A detailed structural analysis of the rod cluster control guide tubes was performed to establish the equivalent cross section properties and elastic end support conditions. An analytical model was verified both dynamically and statically by subjecting the control rod cluster tube to a concentrated force applied at the transition plate. In addition, the guide tube was loaded experimentally using a load distribution to conservatively approximate the hydraulic loading. The experimental results consist of a load deflection curve for the rod cluster control guide tube, plus verification of the deflection criteria to ensure rod cluster control insertion.

While the above described blowdown analyses were performed in the original analysis, with the acceptance of the DCPP leak-before-break analysis by the NRC (Reference 14), dynamic loads resulting from pipe rupture events in the main reactor coolant loop piping no longer have to be considered in the design basis structural analyses. Only the much smaller loads from RCS branch line breaks have to be considered.

3.9.1.3.2.3 Upper Support Column

Upper support columns located close to the broken nozzle during the hot leg break will be subjected to transverse loads due to cross flow. The loads applied to the columns were computed with a method similar to the one used for the guide tubes, i.e., by taking into consideration the increase in flow across the column during the accident. The columns were studied as beams with variable sections and the resulting stresses were obtained using the reduced section modulus at the slotted portions. The models used for static (or steady-state dynamic) analysis are:

- The upper support, deep beam, and upper core plate were modeled with flat shell elements, the support columns with three-dimensional beam elements, and the fuel assemblies and holddown springs with three-dimensional spring elements. Because of symmetry, a one-eighth slice of the upper package was modeled. The core plate is perforated and was modeled as a geometrically equivalent solid plate that has elastic constants modified according to the theory of perforated plates.

- Columns of two different lengths were modeled: the long columns connecting the plates and the short columns connecting the beam grid with the upper core plate.

- The lower support structure was modeled using a finite-element structural analysis computer program. The lower core plate and upper core support, as well as the lower part of the core barrel, was represented by flat triangular shell elements. Reduced plate strength, due to the perforations, was accounted for by using an equivalent elastic modulus and Poisson ratio in the calculations. This structure was loaded with various vertical forces, due to normal and abnormal operation, and the deflections and stresses are obtained for each case. The experimental values were converted according to basic scaling laws and applied to the prototype structure. The test values are larger, as expected, since they are obtained in the absence of the core plate and support columns structures, making the lower core support more flexible. Using the same model, this code was also used to compute stresses and deformation due to nonuniform temperature distributions. With temperature at the component surfaces and the gradient generated by the γ-heat generation as input for the system code, the deflected shape of the structure was obtained.

Stresses in components, such as the perforated upper and lower core plates, core support plate, and top support plate, were then computed using the stress intensification factor provided by the standard theory of perforated plates.

3.9.1.4 Correlation of Test and Analytical Results

The program used to establish the integrity of reactor internals has involved extensive design analysis, model testing, and post-hot functional inspection. Additionally, a full-size reactor has been instrumented to measure the dynamic behavior of a plant the size and type of DCPP. Measured values have been compared to predicted values.

The Indian Point II reactor has been established as the prototype for the DCPP Unit 1 internals verification program. The Trojan plant (Portland General Electric Company) provides additional internals verification for Unit 2. (Unit 1 has a thermal shield similar to Indian Point II; Unit 2 has neutron panels similar to Trojan.)

The only significant differences between the DCPP units' internals and Indian Point II are the modifications resulting from the use of a 17 x 17 fuel array in place of 15 x 15, and the replacement of the annular thermal shield with neutron shield panels. The change to neutron shield panels applies only to Unit 2. The change to 17 x 17 applies to both Units 1 and 2.

The only structural changes in the internals resulting from the design change from the 15 x 15 to the 17 x 17 fuel assembly are in the support columns and assembly guide tubes. The new 17 x 17 guide tubes are stronger and more rigid, hence they are less susceptible to flow-induced vibration problems. The fuel assembly itself is relatively unchanged in mass and spring rate, and thus no significant deviation is expected from the 15 x 15 fuel assembly vibration characteristics.

The remainder of the core structure design is identical to the prototypes that have been tested and proven to be well within design expectations and limits.

The Trojan plant is the lead plant featuring neutron panels and 17 x 17 fuel assemblies.

The Trojan plant internals were instrumented for strain measurements on the core barrel and on the guide tube subject to highest cross flow. The data obtained provided verification of Westinghouse analysis and scale model predictions of neutron panels and 17 x 17 internals behavior in a full-size plant.
The Four Loop Internals Assurance Program conducted on Indian Point II, supplemented by the Trojan data on neutron shield panels and 17 x 17 fuel assemblies, jointly satisfy the intent of RG 1.20 (Reference 12) with respect to adequate plant testing of internals similar to those employed at DCPP. The core support structures received, in addition, the normal pre- and post-hot functional testing examination for integrity in accordance with Paragraph D, "Regulations for Reactor Internals Similar to the Prototype Design," of RG 1.20. This examination included the points shown in Figure 3.9-1 for Unit 1 and Figure 3.9-2 for Unit 2, and also:

(1) All major load bearing elements of the reactor internals relied on to retain the core structure in place

(2) The lateral, vertical, and torsional restraints provided within the vessel

(3) Those locking and bolting devices whose failure could adversely affect the structural integrity of the internals

(4) Those other locations on the reactor internal components that are similar to those which were examined on the prototype Indian Point II and Trojan designs

The interior of the reactor vessel was also examined for evidence of loose parts or foreign material. Specifically, the inside of the vessel was inspected before and after the hot functional tests, with all the internals removed, to verify that no loose parts or foreign materials were in evidence.

Lower Internals

A particularly close inspection was made on the following items or areas, using a 5x or 10x magnifying glass or penetrant test where applicable. The locations of these areas are shown in Figures 3.9-1 and 3.9-2 for Units 1 and 2, respectively:

(1) Upper barrel flange and girthweld

(2) Upper barrel to lower barrel girthweld

(3) Upper core plate aligning pin (examine for any shadow marks, burnishing, buffing, or scoring; check for the soundness of lockwelds)

(4) Irradiation specimen basket welds

(5) Baffle assembly locking devices (check for lockweld integrity)

(6) Lower barrel to core support girthweld

(7) For Unit 1, the flexible tie connections (flexures) at the lower end of the thermal shield

(8) For Unit 2, the neutron shield panel locking devices and dowel pin cover plate welds (examine the connections for evidence of change in tightness of lockweld integrity)

(9) Radial support key welds to barrel

(10) Insert locking devices (examine soundness of lockwelds)

(11) Core support columns and instrumentation guide tubes (check all the joints for tightness and soundness of the locking devices)

(12) Secondary core support assembly welds

(13) Lower radial support lugs and inserts (Examine for any shadow marks, burnishing, buffing, or scoring. Checking the integrity of the lockwelds: these members supply the radial and torsional constraint of the internals at the bottom relative to the reactor vessel while permitting axial growth between the two. One would expect to see, on the bearing surfaces of the key and keyway, burnishings, buffing, or shadowing marks that would indicate pressure loading and relative motion between the two parts. Some scoring of engaging surfaces is also possible and acceptable.)

(14) For Unit 1, mounting blocks thermal shield to core barrel (examine the connections for evidence of change in tightness or lockweld integrity)

(15) For Units 1 and 2, gaps at baffle joints (check for gaps between baffle and top former and at baffle-to-baffle joints)

Upper Internals

A particularly close inspection was made on the following items or areas, using a magnifying glass of 5x or 10x magnification where necessary:

The locations of these areas are shown in Figures 3.9-1 and 3.9-2 for Units 1 and 2, respectively.

(1) Thermocouple conduits, clamps, and couplings

(2) Guide tube, support column, and thermocouple column assembly locking devices

(3) Support column and conduit assembly clamp welds

(4) Upper core plate alignment inserts (Examine for any shadow marks, burnishing, buffing or scoring. Check for tightness and lock device integrity)

(5) Connections of the support columns, mixing devices, and orifice plates to the upper core plate (check for tightness and lock device integrity)

(6) Thermocouple conduit gusset and clamp welds

(7) Thermocouple end-plugs (check for tightness)

(8) Guide tube closure welds, tube-transition plate welds, and card welds

Acceptance standards are the same as required in the shop by the original design drawings and specifications.

During the hot functional test, the internals were subjected to a total operating time at greater than normal full flow conditions (four pumps operating) of at least 10 days. This provides a cyclic loading of approximately 10^7 cycles on the main structural elements of the internals. In addition, there was some operating time with only one, two, and three pumps operating. No signs of abnormal wear were found, no harmful vibrations were detected, and no apparent structural changes took place; therefore, the four loop core support structures are considered to be structurally adequate and sound for operation.

3.9.1.5 Analysis Methods Under LOCA Loadings

The analysis methods used to confirm the structural design adequacy of the RCS under LOCA loadings are described in Section 5.2.1. With the acceptance of the DCPP leak-before-break analysis by the NRC (Reference 14), dynamic LOCA loads resulting from pipe rupture events in the main reactor coolant loop piping no longer have to be considered in the design basis structural analyses; only the much smaller LOCA loads from RCS branch line breaks have to be considered (see Section 3.6.2.1.1.1). Since the breaks postulated for the original analyses are more severe than those that are now required to be considered, the original analyses are conservative.

3.9.1.6 Analytical Methods for ASME Code Class I Components

Plastic instability allowable limits given in ASME Section III are not used when dynamic analysis is performed, except as noted in Section 5.2.1.11. The analysis methods have the limits established by the ASME Section III for Normal, Upset, and Emergency conditions. For these cases, the limits are sufficiently low to ensure that the analysis is not invalidated. For ASME Code Class I components, the stress limits for faulted loading conditions are specified in Section 5.2. For ASME components other than Class I and components not covered by the ASME Code, the stress limits for faulted loading conditions are specified in Sections 3.9.2 and 3.9.3, respectively. These faulted condition limits are established in such a manner that there is an equivalence with the adopted elastic limits and consequently will not invalidate the elastic system analysis.

3.9.1.7 Design and Analysis Details for the Pressurizer Safety and Relief System

The method of analysis for safety valves and relief valves suitably accounts for the time-history of loads acting during and subsequent to valve opening (i.e., less than one second). The fluid-induced forcing functions are calculated for pertinent safety valve and relief valve discharge cases using one-dimensional equations for the conservation of mass, momentum, and energy.

The calculated forcing functions are applied at locations along the associated piping. Application of these forcing functions to the associated piping model constitutes the dynamic time-history analysis.

The dynamic response of the piping system is determined for the input forcing functions. Therefore, a dynamic amplification factor is inherently accounted for in the analyses.

Snubbers or strut-type restraints are used as required. The stresses resulting from the loads produced by the sudden opening of a relief or safety valve are combined with stresses due to other pertinent loads and are shown to be allowable limits of the ANSI B31.1/B31.7 Codes. Also, the analyses show that the loads applied to the nozzles of the safety and relief valves do not exceed the maximum loads specified by the manufacturer.

The pressurizer safety and relief valve discharge piping systems provide overpressure protection for the RCS. The three spring-loaded safety valves, located on top of the pressurizer, are designed to prevent system pressure from exceeding design pressure by more than 10 percent. The three power-operated relief valves, also located on top of the pressurizer, are designed to prevent system pressure from exceeding the normal operating pressure by more than 100 psi. The valve outlet side is sloped to prevent the formation of water pockets. The safety valves have been converted from water-seated to steam-seated, and the water loop seal was eliminated by providing a continuous drain.

The pressurizer safety valves, manufactured by Crosby, are self-actuated, spring-loaded valves with backpressure compensation. The power-operated relief valves, manufactured by Masoneilan, are air-operated globe valves, capable of automatic operation via high pressure signal or remote manual operation. The safety valves and relief valves are located in the pressurizer cubicle and are supported by the attached piping which, in turn, is supported by a system of beams, struts, and snubbers. If the pressure exceeds the setpoints, the valves open. With a pressurizer safety valve water loop seal (now eliminated), the water slug from the loop seal discharges and the water slug, driven by high system pressure, generates transient thrust forces at each location where a change in flow direction occurs. The valve discharge conditions are considered in the analysis of the PSARV piping systems as follows: (a) the three safety valves remain closed, and (b) the three relief valves open simultaneously while the safety valves are closed. In addition to these two cases, which consider water seal discharge (water slug followed by steam), solid water from the pressurizer (cold overpressure) is also investigated. Even though the water loop seal has been eliminated, the analysis has not been revised to reflect any added margins because the valve discharge conditions without the water slug are less severe than those originally considered with the water slug.

For each pressurizer safety and relief piping system, an analytical hydraulic model is developed. The piping from the pressurizer nozzle to the relief tank nozzle is modeled as a series of single pipes. The pressurizer is modeled as a reservoir which contains stream at constant pressure (approximately 2500 psia for safety system and approximately 2350 psia for relief system) and at constant temperature of approximately 680°F. The pressurizer relief tank is modeled as a sink which contains steam and water mixture.

Fluid acceleration inside the pipe generates reaction forces on all segments of the line which are bounded at either end by an elbow or bend. Reaction forces resulting from fluid pressure and momentum variations are calculated. These forces are defined in terms of the fluid properties for the transient hydraulic analysis. Unbalanced forces are calculated for each straight segment of pipe from the pressurizer to the relief tank. The time histories of these forces are used for the subsequent structural analysis of the pressurizer safety and relief lines.

The structural model used in the seismic analysis of the safety and relief lines is modified for the valves thrust analysis to represent the safety and relief valve discharge. The time-history hydraulic forces are applied to the piping system lump mass points. The dynamic solution for the valve thrust is obtained by using a modified predictor-corrector-integration technique and normal mode theory.

The time-history solution is performed in subprogram FIXFM3. The input to this subprogram consists of the natural frequencies and normal modes, applied forces, and nonlinear elements. The natural frequencies and normal modes for the modified pressurizer safety and relief line dynamic model are determined with the WESTDYN program. The support loads are computed by multiplying the support stiffness matrix and the displacement vector at each support point. The time-history displacements of the FIXFM3 subprogram are used as input to the WESDYN2 subprogram to determine the internal forces, deflections, and stresses at each end of the piping elements.

The loading combinations considered in the analysis of the pressurizer safety and relief valve (PSARV) piping are given in Table 3.9-1. These load combinations are consistent with the final recommendations of the piping subcommittee of the EPRI PWR PSARV performance test program.

3.9.2 ASME CODE CLASS II AND III COMPONENTS

This section discusses the design criteria for DCPP Code Class II and III components. The design of these components is based on the requirements of various codes and standards that were in effect when the items were purchased. These codes and standards have been widely used by the nuclear industry and were, to a large extent, incorporated or referenced in the 1971 edition of the ASME Boiler and Pressure Vessel Code, Section III. If the 1971 edition of the ASME Boiler and Pressure Vessel Code, Section III, had been available during the design of DCPP, all these Code Class II and III components would have been in accordance with the requirements for ASME Code Class II and III components.

The DCPP Q-List (see Reference 8 of Section 3.2) lists the codes and standards to which Code Class II and III components were designed. The quality group classifications for DCPP fluid systems and fluid systems components are described in Section 3.2.2.

3.9.2.1 Plant Conditions and Design Loading Combinations

Design pressure, temperature, and other loading conditions that provide the bases for design of fluid systems or components are presented in the corresponding sections that describe the components and systems; see Chapters 6, 7, 9, and 11. Design codes, standards, and their applicability to systems and components are presented in Section 3.2.2.

3.9.2.2 Design Loading Combinations

Design Criteria for Westinghouse Code Class II and III components, are provided in Tables 3.9-2 through 3.9-7. Table 3.9-8 provides design information for selected tanks.

3.9.2.3 Design Stress Limits

Stress limits for Westinghouse ASME Code Class II and III components are provided in Table 3.9-2 through 3.9-7. Stress limits were selected to comply with the intent of ASME Code Section III and are sufficiently low to provide assurance that no gross deformation will occur in active components and that the active components[(a)] will operate as required following the event. The limits established for passive (inactive) components[(b)] are intended to ensure that violation of the pressure retaining boundary will not occur.

The designs of the condensate storage tanks, refueling water storage tanks, and the fire water and transfer tank are based on the AWWA D100, 1967 Code, with stress allowables restricted to those permitted by ASME Code Section VIII, Division 1. The design basis of these tanks is discussed in Section 3.8.3. Piping stresses resulting from the seismic analyses are combined with deadload stresses, pressure stresses, and other stresses caused by other sustained loads, as suggested in ANSI B31.1 by the following equations:

$$\frac{PDo}{4t_n} + \frac{0.75iM_A}{Z} \leq 1.0S_h \qquad (3.9\text{-}1)$$

$$\frac{PDo}{4t_n} + \frac{0.75iM_A}{Z} + \frac{0.75iM_B}{Z} \leq 1.2S_h \qquad (3.9\text{-}2)$$

$$\frac{PDo}{4t_n} + \frac{0.75iM_A}{Z} + \frac{0.75iM_B'}{Z} \leq 1.8S_h \qquad (3.9\text{-}3)$$

$$\frac{PDo}{4t_n} + \frac{0.75iM_A}{Z} + \frac{0.75iM_B''}{Z} \leq 2.4S_h \qquad (3.9\text{-}4)$$

$$\frac{iMc}{Z} \leq S_A \qquad (3.9\text{-}5)$$

where:

S_h = basic material allowable stress at operating temperature, psi

---

(a) Active components are those whose operability is relied upon to perform a safety function such as safe shutdown of the reactor or mitigation of the consequences of a postulated pipe break in the reactor coolant pressure boundary.

(b) Passive components are those whose operability (e.g., valve opening or closing, pump operation, or trip) are not relied upon to perform a safety function.

P	=	internal pressure, psig
Do	=	outside diameter of pipe, in
t_n	=	nominal wall thickness of pipe, in
Z	=	section modulus, in^3
i	=	stress intensification factor. The product of 0.75 x i shall never be taken as less than 1
M_A	=	resultant moment loading on cross section due to deadload and other sustained loads, in-lb
M_B	=	one-half of the resultant moment due to DE loads plus one-half of the full range of the resultant moment due to DE seismic anchor movements (SAM) if not included in Equations 3.9-5 or 3.9-6
M_B'	=	same as M_B except that moments from DDE are used instead of DE and anchor movements due to DDE are excluded
M_B''	=	same as M except the moments from HE are used instead of DE and anchor movements due to HE are excluded
M_C	=	the larger of (a) the full range of resultant moment due to seismic anchor movements (SAM), or (b) the range of resultant moment due to normal thermal expansion and anchor movements plus one-half of the full range of resultant moment due to SAM, in-lb
S_A	=	f (1.25 S_c + 0.25 S_h)
S_c	=	basic allowable stress at cold (ambient) temperature, psi
f	=	stress range reduction factor for cyclic loading = 1 (There are no events causing more than 7000 loading cycles for DCPP)

If Equation 3.9-5 is not satisfied, then the following equation must be satisfied:

$$\frac{PDo}{4t_n} + \frac{0.75iM_A}{Z} + \frac{iM_C}{Z} \leq (S_h + S_A) \qquad (3.9\text{-}6)$$

For hydrodynamic loadings the following stress equations must be satisfied:

$$\frac{PDo}{4t_n} + \frac{0.75iM_A}{Z} + \frac{0.75iM_D}{Z} \leq 1.2S_h \qquad (3.9\text{-}7)$$

$$\frac{PDo}{4t_n} + \frac{0.75iM_A}{Z} + \frac{0.75i}{Z}(M_B{}^2 + M_D{}^2)^{1/2} \leq 1.8S_h \qquad (3.9\text{-}8)$$

where:

M_D = one half of the resultant moment due to hydrodynamic loads

All Design Class I pipe stresses were found to be within allowable limits specified in Equations 3.9-1 to 3.9-8.

3.9.2.4 Analytical and Empirical Methods for the Design of Pumps and Valves

The Quality Code Class II and III pumps and valves were designed and constructed to Design Class I standards and manufactured under approved quality assurance programs. PG&E inspectors routinely performed audits, inspections, and witnessed testing of Quality Code Class II and III components as they were manufactured.

Quality Code Class II and III pumps and valves were designed in accordance with the codes and standards listed in the DCPP Q-List (see Reference 8 of Section 3.2) and Table 3.2-2. These were the codes and standards that were in effect when the items were purchased. The stress limits selected are sufficiently low to provide assurance that no gross deformations will occur in active components; therefore, the active components will perform as required.

The pumps purchased by Westinghouse were analyzed for the forces resulting from seismic accelerations in the horizontal and vertical directions applied simultaneously. The pumps were designed to have a natural frequency in excess of 30 cps to eliminate any amplification of the seismic floor accelerations in the pump support structures.

The Westinghouse pumps were subjected to a series of tests prior to installation in the plant. The in-shop tests included (a) hydrostatic tests to 150 percent of the design pressure, (b) seal leakage tests, (c) net positive suction head (NPSH) tests to develop the minimum suction head necessary to allow operation, and (d) functional performance tests.

The pumps purchased by PG&E were designed in accordance with ASME standards or PG&E power plant pump standards. The design standards required were determined for each pump by reviewing the pump service conditions. Seismic calculations provided by the manufacturers were reviewed by PG&E to ensure that the loads developed from the combination of the design seismic horizontal and vertical acceleration did not exceed those allowed by applicable codes or standard engineering practices. Seismic calculations were not requested when the seismic adequacy could be ensured by testing or a comparative review of pump design. Hydrostatic tests to 150 percent of design pressure were performed on the pumps purchased by PG&E. The pumps also were subjected to performance tests consistent with the requirements of the Hydraulic Institute Standards or PG&E's power plant pump standards.

In addition to the above described tests, which were performed prior to installation in the plant, numerous tests were performed on the pumps during the preoperational test period. Cold hydrostatic pressure tests, hot functional qualification tests, periodic inservice inspections, and periodic inservice operational tests are performed on Quality Code Class II and III pumps after installation in the plant. These tests verify the functional ability of the pumps and ensure the operability of active safety-related pumps for the design life of the plant.

The supports of all Quality Code Class II and III pumps were designed to withstand the effects of the DE and reviewed for the DDE and HE. These considerations prevent supports of active safety-related pumps from deflecting and impairing the operability of the pump.

The Quality Code Class II and III valves purchased by Westinghouse were designed to the pressure and temperature requirements of the American Standard Association (ASA) B16.5 or the Manufacturers Standardization Society Standard Practice No. 66 (MSS SP66). The valves were tested to the requirements of MSS SP61. These tests included hydrostatic shell and seat leakage tests.

The Quality Code Class II and III valves purchased by the Company were designed, manufactured, and tested in accordance with the Draft ASME Code for Pumps and Valves for Nuclear Power, November 1968 or later editions, the ASME Code, Section III, 1974 edition, ANSI B16.5, and/or the MSS SP66.

In situ seismic testing of five representative valves was performed at the DCPP site. The purpose of this testing was to demonstrate that valves would indeed function when subjected to simulated seismic loads. Each valve was subjected to a static load applied at the center of gravity of the extended structure. The load was applied in the direction that would yield the largest deflection for the given load. While the valve was held in the deflected position, the valve was stroked. Any differences in deflected valve stroking time, line voltage, and motor current (as compared to the undeflected readings) would indicate the effect of a seismic event on valve operability. The valve was again stroked open and closed after removal of the static load to demonstrate that the valve had returned to its initial condition.

The five selected valves tested by this method performed satisfactorily while subjected to the simulated load. The operability indicators of motor current, voltage, and valve stroke time were essentially the same for both the deflected and undeflected tests. During the preoperational piping dynamics effects test program described in Section 3.9.1.2, any excessive piping deflections and vibrations were noted and corrected. Since all valves are supported as part of adjoining piping, this program ensures that the deflections by the pipe (and valve) supports will not impair the operability of active safety-related valves. The attention given to the design, manufacture, and testing of the Quality Code Class II and III pumps and valves ensures that the components will operate as required during or following any expected plant transient.

An evaluation and tabulation of all active valves is presented in Tables 3.9-9 and 6.2-39. An active valve is a valve that must perform a mechanical motion in order to shut down the plant or mitigate the consequences of a postulated event. Check valves with flow through the valves secured are considered passive devices. Check valves designed to close without operator action following an accident are considered active devices. The position each valve assumes on power failure is listed in these tables.

The design approach and criteria used to ensure the protection of all critical systems and containment from the effects of pipe whip, are presented in Section 3.6. Section 3.6 also presents the criteria for postulated pipe breaks. Section 3.6 also discusses that with the acceptance of the DCPP leak-before-break analyses by the NRC (Reference 14), the dynamic effects of breaks in the main reactor coolant loop piping no longer have to be considered in the design basis analyses (see Section 3.6.2.1.1.1). Only the dynamic effects of postulated breaks in the RCS branch lines and other high energy lines have to be considered.

3.9.2.5 Design and Installation Criteria, Pressure-Relieving Devices

The main steam safety valves are located outside the primary containment directly on main steam leads 1 and 2, and on external headers on main steam leads 3 and 4. Five safety valves are provided for each steam generator, for a total of 20 safety valves. The safety valve headers and main steam lead connections were designed to ANSI B31.1-1967. Fabrication and erection were in accordance with the ASME Boiler and Pressure Vessel Code, Section I, 1968.

The safety valves are of the single discharge type and were built in accordance with ASME Boiler and Pressure Vessel Code, Section III. The valve discharge consists of an elbow attached to the safety valve outlet. The elbow discharges into a stack that is structurally independent of the valve and is oriented at approximately 36° to the vertical centerline of the safety valve. The stacks are supported to restrain the discharge reactions. Provisions are made to ensure that the safety valve discharge elbow and stack have adequate clearances during all phases of operation.

With the above safety valve discharge arrangement, the sustained blow force developed during valve operation intersects the vertical centerline of the safety valve header nozzle and the base of the header nozzle extrusion. The safety valve nozzles on the headers and on the main steam leads have been analyzed to ensure that the sustained forces developed during valve operation will not develop stresses in excess of those allowed by ANSI B31.1.

The main steam leads are anchored by the main steam flued heads which are structurally located in the reactor containment wall and are supported for the deadweight, thermal, seismic, and safety valve forces that may develop within the Design Class I portion. The two external safety valve headers on main steam leads 3 and 4 are independently supported in a similar fashion.

3.9.2.6 Stress Levels for Design Class I Components and Supports

The loading combinations and acceptance criteria used for piping (except for PSARV piping) primary equipment, and primary equipment supports in the Westinghouse scope of analysis are provided in Table 5.2-5, 5.2-6, 5.2-7, and 5.2-8, and also in Table 3.9-2 through 3.9-7. The load combinations and acceptance criteria used by Westinghouse for the PSARV analysis are provided in Table 3.9-1 and are consistent with the final

recommendations of the piping subcommittee of the EPRI PWR PSARV performance test program.

Maximum allowable stresses for various loading combinations on hangers within B31.1 Code jurisdiction are as follows:

	DE	DDE	HE
Tension	0.417 Fy	0.9 Fy	Least of 1.2 Fy or 0.7 Fu
Shear	0.694 Fv	1.44 Fv	1.44 Fv
Compression	0.694 Fa	1.33 Fa	1.33 Fa
Bending	0.694 Fb	1.5 Fb	1.88 Fb
Bearing	0.625 Fy	Not Applicable	Not Applicable

where Fy, Fu, Fv, Fa, and Fb are from Part 5 of the AISC Steel Construction Manual, 7th Edition.

Supporting structures (supplemental steel) are in accordance with the 7th Edition of the AISC Steel Construction Manual. The stress limits and load combinations used by PG&E for equipment and equipment supports for their scope of analysis are:

DE Seismic Event

Component	Stress Limits[(a)(b)(c)(d)]
(Except cast iron) (active or inactive)	$Q_m \leq 1.1\ S$ $(Q_m \text{ or } Q_L) + Q_b \leq 1.65\ S$
Inactive cast iron, pressure-retaining components	$Q_p \leq 0.1\ S_u$ $(Q_m \text{ or } Q_L) + Q_b \leq 1.5 \times 0.1\ S_u$
Inactive cast iron, nonpressure-retaining components	$(Q_m \text{ or } Q_L) + Q_b \leq 1.0 \times 0.2\ S_u$

(a) Q_m = general membrane stress, ksi. This stress is equal to the average stress across the solid section under consideration. It excludes discontinuities and concentrations and is produced only by pressure and other mechanical loads.

(b) Q_L = local membrane stress, ksi. This stress is the same as Q_m except that it includes the effect of discontinuities.

(c) Q_b = bending stress, ksi. This stress is equal to the linear varying portion of the stress across the solid section under consideration, excludes discontinuities and concentration, and is produced only by mechanical loads.

(d) S = material allowable stress listed in either 1971 or 1974 ASME Code, Section III, or the code the component was purchased and manufactured under, allowable stress values. The allowable stress shall correspond to the highest metal temperature at the section under consideration during the condition under consideration.

Support Element	
Plate and shell[(e)]	$Q_m \leq 1.0\ S$ $Q_m + Q_b \leq 1.5\ S$
Linear[(f)]	1974 ASME Code, Section III, Appendix XVII and Subsection NF
Bolts	1974 ASME Code, Section III, Appendix XVII and/or Code Case 1644, and/or AISC Manual, 7th Edition

DDE/HE Seismic Event

Component	Stress Limits (see notes a, b, c)
Inactive (Except cast iron)	$Q_m \leq 2.0\ S$ $(Q_m \text{ or } Q_L) + Q_b \leq 2.4\ S$
Active (Except cast iron)	$Q_m \leq 1.2\ S$ $(Q_m \text{ or } Q_L) + Q_b \leq 1.8\ S$
Inactive cast iron, pressure-retaining components	$Q_p \leq 0.1\ S_u$ $(Q_m \text{ or } Q_L) + Q_b \leq 2.4 \times 0.1\ S_u$
Inactive cast iron, nonpressure-retaining components	$(Q_m \text{ or } Q_L) + Q_b \leq 2.0 \times 0.2\ S_u$
Support Elements	
Plate and shell (see note e) (active components)	$Q_m \leq 1.2\ S$ $(Q_m + Q_b) \leq 1.8\ S$

(e) Plate and shell type supports: Plate and shell type component supports are supports such as vessel skirts and saddles that are fabricated from plate and shell elements and are normally subjected to a biaxial stress field.

(f) S = material allowable stress listed in either 1971 or 1974 ASME Code, Section III, or the code the component was purchased and manufactured under, allowable stress values. The allowable stress shall correspond to the highest metal temperature at the section under consideration during the condition under consideration.

Plate and shell (inactive components)	$Q_m \leq 2.0$ S $(Q_m + Q_b) \leq 2.4$ S Linear 1974 ASME Code, Section III, Appendix XVII, (see note f) Subsection NF and Appendix F (stresses not to exceed S_y[(g)] for active components)
Bolts	1974 ASME Code, Section III, Appendix XVII and/or Code Case 1644 plus Appendix F and/or ASIC Manual, 7th Edition

Load Combinations

(3.1.1)	DE + P_n + T_n + D + N + O
(3.1.2)	DDE + P_a + T_a + D + N + O
(3.1.3)	HE + P_n + D + N + O

where the following loads apply, as applicable:

HE	=	loads from Hosgri earthquake
P_n	=	Pressure, normal
P_a	=	Pressure, accident
T_n	=	Temperature, normal
T_a	=	Temperature, accident
DE	=	DE
DDE	=	DDE
D	=	Deadweight
N	=	Nozzle
O	=	Operating

Table 3.9-12 lists PG&E Class I equipment that has been seismically qualified.

3.9.2.7 Field Run Piping Systems

All Category I piping and pipe supports designed in the field are either analyzed or designed to a conservative standard, provided by PG&E engineering staff, for seismic and thermal loads.

(g) S_y = material allowable stress listed in either 1971 or 1974 ASME Code, Section III, or the code the component was purchased and manufactured under, minimum yield stress. The yield stress shall correspond to the highest metal temperature at the section under consideration during the condition under consideration.

3.9.3 CORE AND REACTOR INTERNALS

3.9.3.1 Core and Internals Integrity Analysis (Mechanical Analysis)

Stainless steel clad silver-indium-cadmium alloy absorber rods are resistant to radiation and thermal damage, thereby ensuring their effectiveness under all operating conditions. Rods of similar design have been successfully used in the original and reload cores of San Onofre, Connecticut Yankee, and others.

Two burnable poison rods (Reference 6) of smaller length but similar in design to those used in DCPP were exposed to in-pile test conditions in the Saxton Test Reactor in October 1967. A visual examination of the rods was made in early June 1968 and a visual and profilometer examination was made on July 30, 1968, after an exposure of 1900 effective full power hours (approximately 25 percent B^{10} depletion). The rods were found to be in excellent condition and profilometry results showed no dimensional variation from the initial condition.

An experimental verification of the reactivity worth calculations for borosilicate glass tubing has been accomplished. Similar rods have been successfully operated in the Ginna Reactor (Reference 7) with no evidence of deficiency.

Manufacturing defects did not appear during the hot functional tests because any manufacturing defects were detected in the shop or during the assembly period. The basic program that is currently being used to ensure adequacy of manufacturing practices consists of:

(1) Extremely thorough nil ductility temperature and quality assurance programs at the internals vendors

(2) Extensive visual examination at the plant site prior to hot functional testing of the primary system

(3) Running the hot functional test with full flow for 240 hours that accumulates approximately 10^7 cycles on the majority of the core structure components

(4) Reexamining all areas of the internals after the 240-hour hot functional test

The response of the reactor core and vessel internals under excitation produced by a simultaneous complete severance of a reactor coolant pipe and seismic excitation for a typical Westinghouse pressurized water reactor plant internals was determined. The following mechanical functional performance requirements applied:

(1) Following the DBA, the basic operational or functional requirement to be met for the reactor internals is that the plant shall be shut down and cooled in an orderly fashion so that fuel cladding temperature is kept within

specified limits. This implies that the deformation of certain critical reactor internals must be kept sufficiently small to allow core cooling.

(2) For large breaks, the reduction in water density greatly reduces the reactivity of the core, thereby shutting down the core whether the rods are tripped or not. The subsequent reflooding of the core by the ECCS with borated water maintains the core in a subcritical state. Therefore, the main requirement is to ensure effectiveness of the ECCS. Insertion of the control rods, although not needed, gives further assurance of the ability to shut the plant down and keep it in a safe shutdown condition.

(3) The functional requirements for the core structures during the DBA are shown in Table 3.9-10. The inward upper barrel deflections are controlled to ensure no contacting of the nearest rod cluster control guide tube. The outward upper barrel deflections are controlled in order to maintain an adequate annulus for the coolant between the vessel inner diameter and core barrel outer diameter.

(4) The rod cluster control guide tube deflections are limited to ensure operability of the control rods.

(5) To ensure no column loading of rod cluster control guide tubes, the upper core plate deflection is limited to the value shown in Table 3.9-10.

(6) The reactor has mechanical provisions that are sufficient to maintain the design core and internals and to ensure that the core is intact with acceptable heat transfer geometry following transients arising from the DBA operating conditions (References 2, 8, and 13).

(7) The core internals are designed to withstand mechanical loads arising from DE, DDE, and pipe ruptures (References 2, 4, 8, and 13).

While these performance requirements originally had to be met for load combinations that included the contribution from a main RCS loop line break, with the acceptance of the DCPP leak-before-break analysis by the NRC (Reference 14), dynamic loads resulting from pipe rupture events in the main reactor coolant loop piping no longer have to be considered in the design basis structural analyses and included in the loading combinations; only the much smaller loads from RCS branch line breaks have to be considered (see Section 3.6.2.1.1.1).

3.9.3.2 Faulted Conditions

The following events were considered in the faulted conditions category:

(1) Loads produced by a double-ended pipe rupture of the main coolant loop DBA for both the cold and hot leg breaks. The methods of analysis adopted were related to the type of accident assumed (cold leg break or hot leg break).

(2) Response due to a DDE or HE, as described previously in the seismic analysis

(3) Most unfavorable combination of DDE and DBA. Maximum stresses obtained in each case were added in the most conservative manner.

Maximum stress intensities are compared with allowables for each condition. When fatigue is of concern, the applicable stress concentrations factors are utilized and peak stresses are used to establish the usage factor. Elastic analysis is used to obtain the response of the structure and the stress analysis for each component is performed on an elastic basis. For faulted conditions, stresses are above yield in a few locations. For these cases only, when deformation requirements exist, a plastic analysis is independently performed to ensure that functional requirements are maintained (guide tubes deflections and core barrel expansions). The elastic limit allowable stresses are used to compare with the results of the analysis. No inelastic stress limits are used.

These analyses showed that the stresses and deflections that would result following a faulted condition are less than those that would adversely affect the integrity of the structures. Also, the natural and applied frequencies were such that resonance problems should not occur.

While these events and event combinations were considered in the original analysis for faulted conditions, with the acceptance of the DCPP leak-before-break analysis by the NRC (Reference 14), dynamic loads resulting from pipe rupture events in the main reactor coolant loop piping no longer have to be considered in the design basis structural analyses and included in the loading combinations; only the much smaller loads from RCS branch line breaks have to be considered (see Section 3.6.2.1.1.1).

3.9.3.3 Reactor Internals Response Under LOCA and Seismic Excitations

The reactor vessel/internals/fuel system dynamic analyses for Diablo Canyon Units 1 & 2 were performed in the 1987-1988 timeframe to verify structural adequacy of the core during transition from 17x17 standard fuel to 17x17 VANTAGE 5 fuel. These dynamic analyses were performed for the LOCA and seismic design conditions of DE, DDE, and Hosgri; and details of these analyses are given in Reference 15.

The system mathematical models for Diablo Canyon Units 1 & 2 used in the LOCA and seismic analyses are three-dimensional nonlinear finite element models, which are described in detail in Reference 15. The major difference between the LOCA and seismic models is that the seismic model includes the hydrodynamic mass matrices in the vessel/barrel downcomer annulus to account for the fluid-solid interactions. The fluid-solid interactions in the LOCA analysis are accounted through the hydraulic forcing functions generated by Multiflex Code (Reference 3). Another difference between the LOCA and seismic models is the difference in loop stiffness matrices. The seismic model uses the unbroken loop stiffness matrix, whereas the LOCA model uses the broken loop stiffness matrix. Except for these two differences, the RPV system seismic model is identical to that of the LOCA model.

It is important to note that the LOCA analyses described below are the analyses originally performed for the RCS faulted conditions. With the acceptance of the DCPP Leak-Before-Break (LBB) by the USNRC (Reference 14), the dynamic LOCA loads resulting from the pipe rupture events in the main reactor coolant loop piping no longer have to be considered in the design basis structural analyses and including the loading combinations. With LBB acceptance, the next most limiting breaks which need to be considered are the auxiliary line breaks consisting of accumulator line, pressurizer surge line and RHR line. The LOCA loads imposed on the RPV system from these auxiliary line breaks are generally significantly lower than those obtained from the main loop line breaks discussed below. This reduction in LOCA loads for the auxiliary line breaks is due to the fact that the auxiliary lines have a smaller break size, location of the breaks are farther away from the vessel nozzles, and the absence of cavity pressurization loads.

It should also be noted that, in general, for faulted conditions the imposed loading on the reactor vessel and its internals due to seismic (DDE) and LOCA conditions are additive by the square root of the sum of squares (SRSS) method. A Hosgri Earthquake (HE) and LOCA are also considered to occur simultaneously and, therefore, the combined loading is considered by SRSS. Therefore, with LBB invoked, the combination of LOCA and seismic loads on the RPV system will be considerably lower than those obtained from main loop piping breaks.

3.9.3.3.1 Reactor Internals Response Under Seismic Excitations.

The seismic analysis included the effects of simultaneous application of time history accelerations in three orthogonal directions. The Westinghouse generated synthesized time history accelerations for DE, DDE, and Hosgri response spectra were used in a 1987-1988 analyses. The references of these Westinghouse generated synthesized time histories are also given in Reference 15.

As mentioned earlier, fluid-structure or hydroelastic interaction is included in the reactor pressure vessel model for seismic evaluations. The horizontal hydroelastic interaction is significant in the cylindrical fluid flow region between the core barrel and the reactor vessel annulus. Mass matrices with off-diagonal terms (horizontal degrees-of-freedom

only) attach between nodes on the core barrel, thermal shield and the reactor vessel shell (see, e.g., Figure 2-5 of Reference 15, assembled finite element model for Unit 1). The mass matrices for the hydro-elastic interactions of two concentric cylinders are developed using the work of Reference 17. For the case of an incompressible, frictionless fluid displaced in the annulus due to motion of the cylinders, the expression for the hydrodynamic mass matrix connecting the inner and outer cylinders is derived. The diagonal terms of the mass matrix are similar to the lumping of water mass to the vessel shell, thermal shield, and core barrel. The off-diagonal terms reflect the fact that all the water mass does not participate when there is no relative motion of the vessel and core barrel. It should be pointed out that the hydrodynamic mass matrix has no artificial virtual mass effect and is derived in a straight-forward, quantitative manner.

The matrices are a function of the properties of two cylinders with the fluid in the cylindrical annulus, specifically, inside and outside radius of the annulus, density of the fluid and length of the cylinders. Vertical segmentation of the reactor vessel and the core barrel allows inclusion of radii variations along their heights and approximates the effects of beam mode deformation. These mass matrices were inserted between the selected nodes on the core barrel, thermal shield, and the reactor vessel (see Figure 2-5 of Reference 15).

The WECAN computer code, which is used to determine the response of the reactor vessel and its internals, is a general purpose finite element code. In the finite element approach, the structure is divided into a finite number of discrete members or elements. The inertia and stiffness matrices, as well as the force array, are first calculated for each element in the local coordinates. Employing appropriate transformations, the element global matrices and arrays are assembled into global structural matrices and arrays, and used for dynamic solution of the differential equation of motion for the structure.

Note that the preceding paragraphs describe the RPV and internals system dynamic analyses for which the WECAN computer code was used. Current analyses (such as the dynamic analyses performed in support of the replacement vessel head project) utilize the ANSYS computer code. The methodology used to develop the ANSYS system models is consistent with the methodology used to develop historic WECAN models. The direct time integration method is used in ANSYS to solve the dynamic equations of motion for the system; whereas the nonlinear mode superposition method is used in WECAN to solve the dynamic equations of motion for the system.

3.9.3.3.2 Reactor Internals Response During Loss-Of-Coolant-Accident (LOCA) Conditions

The mechanical response of the reactor coolant system subjected to a LOCA transient is performed in three steps. First, the reactor coolant system is analyzed for the effects of loads induced by normal operation which include thermal, pressure and dead weight effects. From this analysis, the loop mechanical forces acting on the RPV that would result from the release of equilibrium forces at the break locations are obtained. In the second step, the loop mechanical loads, reactor internal hydraulic forces, jet

impingement forces, and reactor cavity pressurization forces are simultaneously applied; and the RPV displacements due to the LOCA are calculated. Finally, the structural integrity of the reactor coolant loop and component supports to deal with the LOCA are evaluated by applying the reactor vessel displacements to a mathematical model of the reactor coolant loop.

In 1987-1988, the RPV system LOCA analyses for the Diablo Canyon units were performed for the most limiting breaks consisting of: (a) RPV inlet nozzle break, (b) RPV outlet nozzle break, and (c) RCP outlet nozzle break. These break locations have been determined by detailed stress and fatigue analyses of the reactor coolant loop piping system (Reference 18). As mentioned earlier, the RPV system finite element model for LOCA analysis is identical to that of the seismic model except that it does not have hydrodynamic mass matrices in the downcomer region.

In 2005, the RPV system LOCA analysis was performed for the Unit 2 barrel/baffle region conversion from downflow to the upflow configuration. For DCPP Unit 2, considering LBB acceptance, the next most limiting auxiliary line breaks are the pressurizer surge line break (98.31 in^2) on the hot leg and the accumulator line break (60.13 in^2) on the cold leg. Postulated residual heat removal (RHR) auxiliary line breaks are bounded by the pressurizer surge line break for Unit 2.

In order to study LOCA hydraulic forces for the DCPP Unit 2 Upflow Conversion Program, the following vessel/internal break cases were analyzed:

1. Pressurizer Surge Line Break
2. Accumulator Line Break

A 1 millisecond break-opening-time (BOT) was employed in the vessel forces analyses for DCPP Unit 2, consistent with the MULTIFLEX licensing requirements. All break cases used flexible beam modeling for the core barrel. The analysis conservatively assumed a limiting full power RCS cold leg temperature of 526°F (including uncertainty) which bounds the minimum cold leg temperature of 531.9°F (excluding uncertainty) for DCPP Unit 2. These conditions bound the most severe operating conditions, which encompasses Tavg coastdown conditions. Thus, the effects of a Tavg coastdown are accounted for in the vessel forces analysis. In addition, the Delta-54 replacement steam generator (RSG) was accounted for in the analyses. Previous studies have shown that the steam generator design has a relatively insignificant effect on the vessel forces analyses, so operation of Unit 2 with either the original Model 51 steam generators or the Delta-54 stream generators is acceptable with respect to the vessel forces analyses.

Following a postulated LOCA pipe rupture, forces are imposed on the reactor vessel and its internals. These forces result from the release of the pressurized primary system coolant, and for guillotine pipe breaks from the disturbance of the mechanical equilibrium in the piping system prior to the rupture. The release of pressurized coolant results in traveling depressurization waves in the primary system. These

depressurization waves are characterized by a wave-front with low pressure on one side and high pressure on the other. The wave-front translates and reflects throughout the primary system until the system is completely depressurized. The rapid depressurization results in transient hydraulic loads on the mechanical equipment of the system. The release of coolant resulting from a postulated RPV nozzle break also results in a pressure increase in the region surrounding the postulated break. Pressurization occurs rapidly in the cavity around the reactor vessel, which can exert an asymmetric force on the outside of the vessel.

The loads on the RPV and internals that result from the depressurization of the system and from the pressurization of the area around the break may be categorized as: (a) reactor internal hydraulic loads (vertical and horizontal), (b) reactor coolant loop mechanical loads, (c) reactor cavity pressurization loads (only for breaks at the RPV safe end locations), and (d) jet impingement loads. Description of such loads acting for a typical reactor vessel inlet or outlet nozzle is given below (for more details, see Reference 6), and these loads are combined into a single time history forcing function which are then applied to the RPV system finite element model.

3.9.3.3.2.1 Reactor Pressure Vessel Internal Hydraulic Loads

Depressurization waves propagate from the postulated break location into the reactor vessel through either a hot leg or a cold leg nozzle. After a postulated cold leg break, the depressurization path for waves entering the reactor vessel is through the nozzle that contains the broken pipe and into the region between the core barrel and the reactor vessel (that is, the downcomer region). The initial wave propagates up, around, and down the downcomer annulus, then up through the region circumferentially enclosed by the core barrel, that is, the fuel region. In the case of a cold leg break, the region of the downcomer annulus close to the break depressurizes rapidly but, because of the restricted flow areas and finite wave speed (approximately 3000 feet per second), the opposite side of the core barrel remains at a high pressure. This results in a net horizontal force on the core barrel and the reactor vessel. As the depressurization wave propagates around the downcomer annulus and up through the core, the core barrel differential pressure reduces and, similarly, the resulting hydraulic forces drop.

In the case of a postulated break in the hot leg, the wave follows a similar depressurization path, passing through the outlet nozzle and directly into the upper internals region depressurizing the core and entering the downcomer annulus from the bottom exit of the core barrel. Thus, after a hot leg break, the downcomer annulus would be depressurized with very little difference in pressure forces across the outside diameter of the core barrel. A hot leg break produces less horizontal force because the depressurization wave travels directly to the inside of the core barrel (so that the downcomer annulus is not directly involved), and internal differential pressures are not as large as for a cold leg break of the same size. Since the differential pressure is less for a hot leg break, the horizontal force applied to the core barrel is less for hot leg break than for a cold leg break. For breaks in both the hot leg and cold leg, the

depressurization waves continue to propagate by reflection and translation through the reactor vessel and loops.

The MULTIFLEX computer code (Reference 3) calculates the hydraulic transients within the entire primary coolant system. It considers subcooled, transition, and two-phase (saturated) blowdown regimes. The MULTIFLEX code employs the method of characteristics to solve the conservation laws, and assumes one-dimensionality of flow and homogeneity of the liquid-vapor mixture. The MULTIFLEX code considers a coupled fluid-structure interaction by accounting for the deflection of constraining boundaries, which are represented by separate spring-mass oscillator system. A beam model of the core support barrel has been developed from the structural properties of the core barrel; in this model, the pressure as well as the wall motions are projected onto the plane parallel to the broken nozzle. The spatial pressure variation at each time step is transformed into ten horizontal forces, which act on the ten mass points of the beam model. Each flexible wall is bounded on either side by a hydraulic flow path. The motion of the flexible wall is determined by solving the global equations of motions for the masses representing the forced vibration of an undamped beam.

The reanalysis performed in support of the conversion of the barrel/baffle region for Unit 2 has made use of the MULTIFLEX 3.0 (Reference 9) computer code. The MULTIFLEX versions are an extension of the BLODWN-2 computer code and includes mechanical structure models and their interactions with the thermal-hydraulic system. Both versions of the MULTIFLEX code share a common hydraulic modeling scheme, with differences being confined to a more realistic downcomer hydraulic network and a more realistic core barrel structural model that accounts for non-linear boundary conditions and vessel motion. Generally, this improved modeling results in lower, more realistic, but still conservative hydraulic forces on the core barrel. The NRC staff has accepted (Reference 10) the use of MULTIFLEX 3.0 for calculating the hydraulic forces on reactor vessel internals (Reference 11).

3.9.3.3.2.2 Reactor Coolant Loop Mechanical Loads

The loop mechanical loads result from the release of normal operating forces present in the pipe prior to the separation as well as transient hydraulic forces in the reactor coolant system. The magnitudes of the loop release forces are determined by performing a reactor coolant loop analysis for normal operating loads (that is, pressure, thermal, and deadweight). The loads existing in the pipe at the postulated break location are calculated and are "released" at the initiation of the LOCA transient by application of the loads to the broken piping ends. These forces are applied with a ramp time of one millisecond because of the assumed instantaneous break opening time.

3.9.3.3.2.3 Reactor Cavity Pressurization Loads

Reactor cavity forces arise from the steam and water that are released into the reactor cavity through the annulus around the broken pipe. These forces occur only for

postulated breaks at the RPV nozzle safe end locations. The reactor cavity is pressurized asymmetrically, with high pressures on the side adjacent to the break. The horizontal differences in pressure across the reactor cavity result in horizontal forces on the reactor vessel. Vertical forces on the reactor vessel arise from similar variations in pressures on the upper and lower head and the tapered parts of the vessel.

3.9.3.3.2.4 Jet Impingement Loads

The jet impingement load is an axial force along the broken pipe centerline that is caused by the pressure of the escaping jet of coolant acting on the exposed pipe cross section at the break location. The jet force is calculated by multiplying the saturation pressure corresponding to the temperature of the coolant at break location times the cross-sectional area of the pipe. This force is applied with a ramp time of one millisecond.

3.9.3.4 Acceptance Criteria

3.9.3.4.1 Structural Adequacy of Reactor Internal Components

The reactor internal components of Diablo Canyon Units 1 and 2 are not ASME Code components because Sub-section NG of the ASME Boiler and Pressure Code edition applicable to DCPP Units reactor internals did not include design criteria for the reactor internals. However, these components were originally designed to meet the intent of the 1971 Edition of Section III of the ASME Boiler and Pressure Vessel Code with addenda through the Winter 1971. The allowable stress limits for the design basis accident (DBA) for core support structures are based on limits specified in Section 5.2.1.

3.9.3.4.2 Allowable Deflection and Stability Criteria.

The criterion for acceptability in regard to mechanical integrity analyses is that adequate core cooling and core shutdown must be ensured. This implies that the deformation of reactor internals must be sufficiently small so that the geometry remains substantially intact. Consequently, the limitations established on the reactor internals are concerned principally with the maximum allowable deflections and stability of the components.

For faulted conditions, deflections of critical internal structures are limited to values given in Table 3.9-10. In a hypothesized vertical displacement of internals, energy absorbing devices limit the displacement to 1.25 inches by contacting the vessel bottom head.

Upper Core Barrel

The upper core barrel has the following deformation limits:

(1) To ensure shutdown and cooldown of the core during cold leg blowdown, the basic requirement is a limitation on the outward deflection of the barrel at the locations of the inlet nozzles connected to unbroken lines. A large outward deflection of the upper barrel in front of the inlet nozzles, accompanied with permanent strains, could close the inlet area and restrict the cooling water coming from the accumulators. Consequently, a permanent barrel deflection in front of the unbroken inlet nozzles larger than a certain limit, called "no loss of function" limit, could impair the efficiency of the ECCS.

(2) During the hot leg break, the rarefaction wave enters through the outlet nozzle into the upper internals region and thus depressurizes the core and then enters the downcomer annulus from the bottom exit of the core barrel. This depressurization of the annulus region subjects the core barrel to external pressures and this condition requires a stability check of the core barrel during hot leg break. Therefore, to ensure rod insertion and to avoid disturbing the control rod cluster guide structure, the barrel should not interfere with the guide tubes.

Control Rod Cluster Guide Tubes

The deflection limits of the guide tubes were established from test data (see Table 3.9-10).

Upper Package

The local vertical deformation of the upper core plate, where a guide tube is located, shall be less than 0.100 inch. This deformation will cause the plate to contact the guide tube, since the clearance between the plate and the guide tube is 0.100 inch. This limit will prevent the guide tubes from undergoing compression. For a plate local deformation of 0.150 inch, the guide tube will be compressed and deformed transversely to the upper limit previously established. Consequently, the value of 0.150 inch is adopted as the no loss function local deformation with an allowable limit of 0.100 inch. These limits are given in Table 3.9-10.

3.9.3.5 Methods of Analysis

Faulted condition LOCA analyses were originally performed for limiting breaks of the reactor vessel inlet nozzle and reactor vessel outlet nozzle with a limited displacement allowing a break area of 115 in^2. Subsequent calculations of the loop displacements found the maximum displacement at the reactor vessel inlet and outlet nozzles was 81in^2, confirming the 115 in^2 break area was a conservative assumption. These original 115 in^2 break area forces were later confirmed to be bounding relative to LOCA forces generated for 81 in^2 limited displacement breaks calculated at reduced operating temperatures consistent with temperature coastdown. Although the leak-before-break analysis (Reference 14) now allows for exclusion of main loop piping breaks from the design basis,

no credit has yet been taken for the smaller branch line areas (60 in^2 for the largest cold leg branch line - the accumulator line) in the current reactor vessel LOCA forces analyses for Unit 1. When credit for this break area reduction is taken, it is expected to provide substantial margin relative to the existing design basis accident loads.

For the Unit 2 conversion to the upflow configuration, as previously mentioned, the pressurizer surge line break (98.31 in^2) on the hot leg and the accumulator line break (60.13 in^2) on the cold leg were analyzed with the MULTIFLEX 3.0 code. The analysis used a 1 millisecond BOT, consistent with the MULTIFLEX licensing requirements. All break cases used flexible beam modeling for the core barrel. The analysis conservatively assumed limiting full power RCS temperatures for DCPP Unit 2. These conditions bound the most severe operating conditions, which encompasses Tavg coastdown conditions. The effects of a Tavg coastdown are thus accounted for in the vessel forces analyses. Additionally, the Delta-54 RSG was included in the analyses. Previous studies have shown that the steam generator design has a relatively insignificant effect on the vessel forces analyses, so operation of either Unit 1 or Unit 2 with either the original Model 51 steam generator or the Delta-54 steam generator configuration is acceptable with respect to the vessel forces analyses.

3.9.3.5.1 Blowdown Forces Due to Cold and Hot Leg Break

A USNRC approved FORTRAN-IV computer program called MULTIFLEX (Reference 3) is used to calculate the local fluid pressure, flow, and density transients that occur during a LOCA. MULTIFLEX is an extension of the BLODOWN-2 computer code and includes mechanical structure models and their interaction with the thermal-hydraulic system.

The analysis is performed for the subcooled decompression period of the transient, where the hydraulic loads are the greatest. These loads are used for the structural evaluation of the reactor pressure vessel support system, in conjunction with other loads associated with a LOCA and with a safe shutdown earthquake (SSE).

3.9.3.5.2 FORCE2 and LATFORC Models for Blowdown

The MULTIFLEX code evaluates the pressure and velocity transients throughout the RCS. These pressure and velocity transients are made available to the programs FORCE2 and LATFORC, which utilize detailed geometric descriptions in evaluating the loadings on the reactor internals.

LATFORC (Reference 3) is used to calculate the horizontal force components on the vessel, core barrel, and thermal shield as a function of elevation and time using the MULTIFLEX hydraulic data. The force components significant to the horizontal forces are primarily a function of the pressure times area.

FORCE2 (Reference 3) is used to calculate the vertical force components acting on the reactor vessel and internals. Each reactor component for which FORCE2 calculations are

required is designated as an element and assigned an element number. Forces acting on each of the elements are calculated summing the effects of:

(1) The pressure differential across the element.

(2) Flow stagnation on, and unrecovered orifice losses across, the element.

(3) Friction losses along the element.

The most significant assumption made for the analysis is that the thermal-hydraulic analysis has been performed to include mechanical structural models of the core barrel, which allows for fluid structure interaction in the downcomer region of the vessel to decrease the peak pressures calculated on the core barrel and vessel. No other fluid structure interaction has been modeled in the vessel LOCA forces calculation.

3.9.3.5.3 Reactor Vessel/Internals/Fuel Analysis Under LOCA Conditions

The three dimensional LOCA analysis of the RPV system (i.e., reactor vessel/internals/fuel) is discussed in Section 3.9.1.3.1, and Section 3.9.1.3.2 provides insight into the description of major core support components during LOCA transients.

3.9.3.5.4 Reactor Vessel/Internals/Fuel Analysis Under Seismic Conditions

The three dimensional Seismic analysis of the RPV system (i.e., reactor vessel/internals/fuel) is discussed in Section 3.7.2, and the methods of analyses for seismic loads of major subsystems are discussed in Section 3.7.3.

3.9.3.5.5 Methods and Results (Mechanical)

To verify structural adequacy of the reactor internal components and the core under LOCA and seismic loading, nonlinear time history dynamic analyses of the RPV system were performed to generate component interface loads as well as the time history displacements of the lower core plate, upper core plate, and the core barrel. These time history displacements of the core plates and the barrel were then used by Nuclear Fuel Division (NFD) to determine the fuel grid impact loads and the structural adequacy of the core components.

Reference 15 documents in detail the results of RPV system LOCA and seismic analyses. From these analyses it is seen that the reactor internals component interface loads for the Diablo Canyon units during LOCA, seismic and combined (SRSS LOCA + seismic) are bounded by those of the Generic 4-Loop Stress Report (Reference 19). In the generic stress report, the four-loop reactor internals components are analyzed to meet the ASME Code stress requirements.

The results also indicate that the maximum deflections in the critical structures are below the established allowable limits (see e.g., Table 3.9-10). During the hot leg

break, the core barrel does not buckle, and during the cold leg break has stresses that are within allowable limits. The design evaluation of the internals structure is presented in Section 4.2.2.

It should be reiterated that LOCA analyses described above are for the main loops line breaks; and with the LBB acceptance, the next most limiting breaks which need to be considered are the auxiliary line breaks consisting of the accumulator line, the pressurizer surge line, and the RHR line. The LOCA loads imposed on the RPV system from these auxiliary line breaks are generally significantly lower than those obtained from the main loop line breaks. Therefore, with LBB the combination of LOCA and seismic loads on the RPV system will yield higher margins of safety.

For DCPP Unit 2, an upflow conversion in conjunction with the upper head temperature reduction program has been implemented. The impacts due to these modifications were evaluated and documented in Reference 20.

3.9.3.6 Control Rod Drive Mechanisms

The control rod drive mechanisms are Class A components designed to meet the stresses of the ASME Boiler and Pressure Vessel Code and therefore are presented in Section 4.2.

3.9.4 NON-DESIGN CLASS I COMPONENTS

Several non-Design Class I components were also seismically qualified to preclude seismic interaction with Design Class I equipment and/or to ensure structural integrity of the component cooling water system.

3.9.5 MISCELLANEOUS PRESSURIZED GAS CONTAINERS

Table 3.9-11 provides a summary of all storage tanks containing significant quantities (over 100 lbs) of gas under pressure in excess of 100 psig. These tanks are of both Design Class I and II.

3.9.6 REFERENCES

1. Deleted.

2. Bohm, Indian Point Unit No. 2 Internals Mechanical Analysis for Blowdown Excitation, WCAP-7822, December 1971.

3. Takeuchi, K. et al., MULTIFLEX, A FORTRAN IV Computer Program for Analyzing Thermal-Hydraulic Structure System Dynamics," WCAP-8708-P-A (Westinghouse Proprietary Class 2), WCAP-8709-A, NES Class 3 (Non-Proprietary), September 1977.

4. Moore, Westinghouse PWR Core Behavior Following a Loss-of-Coolant Accident, WCAP-7422, September 1971.

5. Bohm, and J. P. Lafaille, Reactor Internals Response under a Blowdown Accident, First Intl. Conf. on Structural Mech. in Reactor Tech., Berlin, September 20-24, 1971.

6. Wood et al., Use of Burnable Poison Rods in Westinghouse Pressurized Water Reactors, WCAP-7113, October 1967.

7. Barry et al., Topical Report - Power Distribution Monitoring in the R.E. Ginna PWR, WCAP-7756, September 1971.

8. Gesinski, Fuel Assembly Safety Analysis for Combined Seismic and Loss-of-Coolant Accident, WCAP-7950, July 1972.

9. Takeuchi, K. et al., MULTIFLEX 3.0, A FORTRAN IV Computer Program for Analyzing Thermal-Hydraulic-Structural System Dynamics Advanced Beam Model," WCAP-9735, Revision 2, Westinghouse Proprietary Class 2/WCAP-9736, Revision 1, Non-Proprietary, February 1998.

10. Letter, T. H. Essig (USNRC) to Lou Liberatori (WOG), Safety Evaluation of Topical Report WCAP-15029, "Westinghouse Methodology for Evaluating the Acceptability of Baffle-Former-Barrel Bolting Distributions Under Faulted Load Conditions", (TAC No. MA1152)," November 10, 1998 (Enclosure 1 – Safety Evaluation Report.

11. Schwirian, R. E., et al., Westinghouse Methodology for Evaluating the Acceptability of Baffle-Former-Barrel Bolting Distributions Under Faulted Load Conditions, WCAP-15029-P-A, Westinghouse Proprietary Class 2 / WCAP-15030-NP-A, Revision 0, Non-Proprietary, January 1999.

12. Comprehensive Vibration Assessment Program for Reactor Internals During Preoperational and Initial Startup Testing, NRC, RG 1.20.

13. PG&E Letter DCL-88-288, LAR 88-08, Request to Use VANTAGE 5 Fuel Assemblies, November 29, 1989.

14. Letter dated March 2, 1993, Leak-Before-Break Evaluation of Reactor Coolant System Piping for DCPP Units 1 and 2, (Docket Nos. 50-275 and 50-323), from Sheri R. Peterson of the NRC to Gregory M. Rueger of PG&E.

15. Bhandari, D. R. ,et. Al, System Dynamic Seismic and LOCA Analyses of Reactor Pressure Vessel System for the Pacific Gas and Electric Company Diablo Canyon Power Plants (DCPP) Units 1 & 2, WCAP-14693, Revision 1, February 11, 1997 (Westinghouse Proprietary Class 2).

16. Deleted in Revision 21

17. Fritz, R. J., The Effects of Liquids on the Dynamic Motions of Immersed Solids, Trans. ASME, Journal of Engineering for Industry, 1972, pp. 167-173.

18. WCAP-8172-A, Pipe Breaks for the LOCA Analysis of the Westinghouse Primary Coolant Loop, January 1975.

19. WNEP-7904, 4 Loop Standard Generic Stress Report - Structural and Fatigue Analyses.

20. WCAP-16487-P, Revision 1, Diablo Canyon Nuclear Power Plant Unit 2 Upflow Conversion and Upper Head Temperature Reduction Engineering Report, March 2006.

TABLE 3.9-1

LOAD COMBINATIONS AND ACCEPTANCE CRITERIA FOR
PRESSURIZER SAFETY AND RELIEF VALVE PIPING

Combination	Plant/System Operation Condition	Load Combination	Piping Allowable Stress Intensity
Upstream of Valves			
1	Normal	N	1.0 S_h
2	Upset	N + DE + SOT_U	1.2 S_h
3	Emergency	N + SOT_E	1.8 S_h
4	Faulted	N + MAX(DDE, HOSGRI) + SOT_F	2.4 S_h
5	Faulted(Note 5)	N + LOCA + MAX(DDE, HOSGRI) + SOT_F	2.4 S_h
Downstream of Valves			
1	Normal	N	1.0 S_h
2	Upset	N + SOT_U	1.2 S_h
3	Upset	N + DE + SOT_U	1.8 S_h
4	Emergency	N + SOTE	1.8 S_h
5	Faulted	N + MAX(DDE, HOSGRI) + SOT_F	2.4 S_h
6	Faulted(Note 5)	N + LOCA + MAX(DDE, HOSGRI) + SOT_F	2.4 S_h

NOTES:

(1) This table is applicable to the seismically designed portion of downstream non-Category I piping necessary to isolate the response, and to assure acceptable valve loading on the discharge nozzle.

(2) See SOT definitions and other load abbreviations.

(3) The bounding number of valves (and discharge sequence if setpoints are significantly different) for the applicable system operating transient defined on this page should be used.

(4) Use SRSS for combining dynamic load responses.

(5) The LOCA loads used in this load combination in the original analyses were the loads resulting from breaks in the main reactor coolant loop. With the acceptance of the DCPP leak-before-break analyses by the NRC, LOCA loads resulting from breaks in the main RCS loop piping no longer have to be considered in the design basis structural analyses and included in the load combinations. Only the LOCA loads from RCS branch line breaks have to be considered.

Abbreviations

N	=	Sustained loads during normal plant operation
SOT	=	System Operating Transient
SOT_U	=	Relief Valve Discharge Transient
SOT_E	=	Safety Valve Discharge Transient
SOT_F	=	Max (SOT_U; SOT_E)
DE	=	Design Earthquake
DDE	=	Double Design Earthquake
HOSGRI	=	Hosgri earthquake
LOCA	=	Loss-of-coolant accident
S_h	=	Basic material allowable stress at maximum (hot) temperature

TABLE 3.9-2

HOSGRI AND DDE SEISMIC LOADING COMBINATIONS AND STRUCTURAL CRITERIA MECHANICAL EQUIPMENT[1]

COMPONENT (2, 3)	LOADING COMBINATIONS (4)	CRITERIA (7, 8, 9, 10, 11, 12, 13, 14)	
Tanks, Heat Exchangers, Filters, Demineralizers	Deadweight + Pressure + HOSGRI/DDE + Nozzle/Piping Loads	σ_m $(\sigma_m$ or $\sigma_L) + \sigma_b$	$\leq 2.0S$ $\leq 2.4S$
Active Pumps	Deadweight + Pressure + HOSGRI/DDE + Nozzle/Piping Loads + Operating Loads	σ_m $(\sigma_m$ or $\sigma_L) + \sigma_b$	$\leq 1.2S$ $\leq 1.8S$
Inactive Pumps	Deadweight + Pressure + HOSGRI/DDE + Nozzle/Piping Loads + Operating Loads	σ_m $(\sigma_m$ or $\sigma_L) + \sigma_m$	$\leq 2.0S$ $\leq 2.4S$
Active Valves	Deadweight + Pressure + HOSGRI/DDE + Nozzle/Piping Loads + Operating Loads[12]	Extended Structure: Pressure Boundary: Valve Nozzles: Bolting:	$\sigma_m \leq 1.2S$ $(\sigma_m$ or $\sigma_L)$ $+ \sigma_b \leq 1.8S$ or S_y (higher of) ANSI B16.5 or MSS-SP-66 (5) $\sigma_m \leq 2.0S$
Inactive Valves	Deadweight + Pressure + HOSGRI/DDE + Nozzle/Piping Loads + Operating Loads[12]	Extended Structure: Pressure Boundary: Valve Nozzles: Bolting:	$\sigma_m \leq 2.0S$ $(\sigma_m$ or $\sigma_L)$ $+ \sigma_b \leq 2.4S$ ANSI B16.5 or MSS-SP-66 (6) $\sigma_m \leq 2.0S$

TABLE 3.9-2

COMPONENT (2, 3)	LOADING COMBINATIONS (4)	CRITERIA (7, 8, 9, 10, 11, 12, 13, 14)	
Inactive Cast Iron Pressure Retaining Components	Deadweight + Pressure + HOSGRI/DDE + Nozzle/Piping Loads + Operating Loads(12)	σ_p $(\sigma_m$ or $\sigma_L) + \sigma_b$	0.1 S_u $\leq 2.4 \times 0.1\ S_u$
Inactive Cast Iron Non-pressure Retaining Components	Deadweight + Pressure + HOSGRI/DDE + Nozzle/Piping Loads + Operating Loads(12)	$(\sigma_m$ or $\sigma_L) + \sigma_b$	$\leq 2.0 \times 0.2\ S_u$

Notes:

(1) See Chapter 5 Table 5.2-8 for structural components.

(2) Active: Mechanical equipment which is needed to go from normal full power operation to safe shutdown following the earthquake and which must perform mechanical motions during the course of accomplishing its design function.

(3) Inactive: Mechanical Equipment which is not required to perform mechanical motions in taking the plant from normal full power operation to safe shutdown following the earthquake.

(4) Nozzle loads shall include piping loads transmitted to the component during the HOSGRI/DDE earthquake.

(5) Piping loads at piping/active-valve interfaces shall be limited such that maximum fiber stresses in the piping at the interface are less than the piping yield strength at temperature (S_y).

(6) Valves, being stronger than the attached piping and having a proven history without any gross failures of pressure boundaries, can safely transmit piping loads without compromising their pressure retaining integrity. Therefore piping integrity assures valve integrity.

(7) σ_m = General membrane stress. This stress is equal to the average stress across the solid section under consideration, excludes discontinuities and concentrations and is produced only by mechanical loads.

Notes: (Cont'd)

(8) σ_L = Local membrane stress. This stress is equal to the same as σ_m except that it includes the effect of discontinuities.

(9) σ_b = Bending stress. This stress is equal to the linear varying portion of the stress across the solid section under consideration, excludes discontinuities and concentrations, and is produced only by mechanical loads.

(10) S = 1971 or 1974 ASME Code allowable stress. The allowable stress shall correspond to the highest metal temperature at the section under consideration during the condition consideration.

(11) S_y = 1971 or 1974 ASME Code minimum yield stress. The yield stress shall correspond to the highest metal temperature at the section under consideration during the condition consideration.

(12) Except racked-out valves.

(13) σ_p = Local membrane stress. This stress is equal to the average stress across the solid section under consideration. It excludes discontinuities and concentrations and is produced only by pressure.

(14) S_u = Material minimum tensile strength listed in either the code the component was purchased and manufactured under, or ASME Code Section III.

TABLE 3.9-3

HOSGRI AND DDE SEISMIC LOADING COMBINATIONS AND STRUCTURAL CRITERIA MECHANICAL EQUIPMENT SUPPORTS AND STRUCTURAL COMPONENT[1]

ELEMENT	LOADING COMBINATIONS (4, 5)	CRITERIA (6, 7, 8, 9, 10, 11, 12, 13)	
Linear[3]	Deadweight + HOSGRI/DDE + Nozzle/Piping Loads	1974 ASME Code Appendix XVII, Subsection NF, and Appendix F or AISC Manual, 7th Edition[11] (Stresses not to exceed S_y for active components supports)	
Plate and shell[2] (active components)	Deadweight + HOSGRI/DDE + Nozzle/Piping Loads	σ_m $(\sigma_m + \sigma_b)$	$\leq 1.2S$ $\leq 1.8S$ or S_y
Plate and shell (inactive components)	Deadweight + HOSGRI/DDE + Nozzle/Piping Loads	σ_m $(\sigma_m + \sigma_b)$	$\leq 2.0S$ $\leq 2.4S$
Bolts	Deadweight + HOSGRI/DDE + Nozzle/Piping Loads	1974 ASME Code Section III, Appendix XVII, Code Case 1644-6 and Appendix F, or AISC Manual, 7th Edition	

Notes:

(1) Includes reactor cavity manipulator crane, spent fuel pit bridge crane, flux mapping transfer devices and rcs seal table and parts. qualification of reactor cavity manipulator crane, spent fuel pit bridge crane, and flux mapping transfer device, not required for DDE (required for HOSGRI only in order to insure structural integrity and preclude seismic interaction).

(2) Plate and shell type supports: Plate and shell type components supports are supports such as vessel skirts and saddles which are fabricated from plate and shell elements and are normally subjected to a biaxial stress field.

Notes (Continued):

(3) Linear type support: A linear type component support is defined as acting under essentially as single components of direct stress. Such elements may also be subjected to shear stresses. Examples of such structural elements are: tension and compression struts, beams and columns subjected to bending, trusses, frames, rings, arches, and cables.

(4) Nozzle loads shall be those nozzle loads acting on the supported components during the HOSGRI/DDE earthquake.

(5) Plus operating loads, as applicable.

(6) σ_m = General membrane stress. This stress is equal to the average stress across the solid section under consideration, excludes discontinuities and concentrations and is produced only by mechanical loads.

(7) σ_b = Bending stress. This stress is equal to the linear varying portion of the stress across the solid section under consideration, excludes discontinuities and concentrations, and is produced only by mechanical loads.

(8) S = 1971 or 1974 ASME Code allowable stress value. The allowable stress shall correspond to the highest metal temperature at the section under consideration during the condition under consideration.

(9) S_y = 1971 or 1974 ASME Code minimum yield stress. The yield stress shall correspond to the highest metal temperature at the section under consideration during the condition under consideration.

(10) For the reactor cavity manipulator crane, the spent fuel pit bridge crane, and the flux mapping transfer device, the stress limits for the above loading combinations are obtained by increasing the normal condition allowable stresses by a factor of 1.7.

(11) The reference, "AISC Manual, 7th Edition," where used in this section, refers to the AISC Code, Part 5, "Specification for the Design, Fabrication and Erection of Structural Steel for Buildings," 1969 version.

(12) σ_p = Local membrane stress. This is equal to the average stress across the solid section under consideration. It excludes discontinuities and concentrations and is produced only by pressure.

(13) S_u = Material minimum tensile strength listed in either the code the component was purchased and manufactured under, or ASME Code Section III.

TABLE 3.9-4

DE SEISMIC LOADING COMBINATIONS AND STRUCTURAL CRITERIA MECHANICAL EQUIPMENT[1]

COMPONENT (2, 3)	LOADING COMBINATIONS (4)	CRITERIA (7, 8, 9, 10, 11, 12, 13, 14)	
Tanks, heat-exchangers filters, demineralizers	Deadweight + Pressure + DE + Nozzle/Piping Loads.	σ_m $(\sigma_m \text{ or } \sigma_L) + \sigma_b$	$\leq 1.0S$[13] $\leq 1.65S$
Active pumps	Deadweight + Pressure + DE + Nozzle/Piping Loads + Operating Loads.	σ_m $(\sigma_m \text{ or } \sigma_L) + \sigma_b$	$\leq 1.1S$ $\leq 1.65S$
Inactive pumps	Deadweight + Pressure + DE + Nozzle/Piping Loads + Operating Loads.	σ_m $(\sigma_m \text{ or } \sigma_m) + \sigma_b$	$\leq 1.1S$ $\leq 1.65S$
Active valves	Deadweight + Pressure + DE + Nozzle/Piping Loads + Operating Loads.[12]	Extended structure:	$\sigma_m \leq 1.1S$ $(\sigma_m \text{ or } \sigma_L)$ $+ \sigma_b \leq 1.0S_y$
		Pressure boundary: valve nozzles: bolting:	ANSI B16.5 or MSS-SP-66 (6) $\sigma_b \leq 2.0S$
Inactive valves	Deadweight + Pressure + DE + Nozzle/Piping Loads + Operating Loads.[12]	Extended structure:	$\sigma_b \leq 1.1S$ $(\sigma_m \text{ or } \sigma_L)$ $+ \sigma_b \leq 1.0S_y$
		Pressure boundary: valve nozzles: bolting:	ANSI B16.5 or MSS-SP-66 (6) $\sigma_m \leq 2.0S$

COMPONENT (2, 3)	LOADING COMBINATIONS (4)	CRITERIA (7, 8, 9, 10, 11, 12, 13, 14)	
Inactive cast iron, pressure retaining components	Deadweight + Pressure + DE + Nozzle/Piping Loads + Operating Loads(12)	σ_p (σ_m or σ_L) + σ_b	$\leq 0.1\ S_u$ $\leq 1.5 \times 0.1\ S_u$
Inactive cast iron non-pressure retaining Components	Deadweight + Pressure + DE + Nozzle/Piping Loads + Operating Loads(12)	(σ_m or σ_L) + σ_b	$\leq 1.0 \times 0.2\ S_u$

Notes:

(1) See Chapter 5, Table 5.2.8 for sructural components.

(2) Active: Mechanical equipment which is needed to go from normal full power operation to safe shutdown following the earthquake and which must perform mechanical motions during the course of accomplishing its design function.

(3) Inactive: Mechanical equipment which is not required to perform mechanical motions in taking the plant from normal full power operations to safe shutdown following the earthquake.

(4) Nozzle loads shall include piping loads transmitted to the component during the DE earthquake.

(5) Deleted.

(6) Valves, being stronger than the attached piping and having a proven history without any gross failures of pressure boundaries, can safely transmit piping loads without compromising their pressure retaining integrity. Therefore, piping integrity assures valve integrity.

(7) σ_m = General membrane stress. This stress is equal to the average stress across the solid section under consideration, excludes discontinuities and concentrations and is produced only by mechanical loads.

(8) σ_L = Local membrane stress. This stress is the same as σ_m except that it includes the effect of discontinuities.

TABLE 3.9-4

Notes (Continued):

(9) σ_b = Bending stress. The stress is equal to the linear varying portion of the stress across the solid section under consideration, excludes discontinuities and concentrations, and is produced only by mechanical loads.

(10) S_y = 1971 or 1974 ASME code allowable stress value. The allowable stress shall correspond to the highest metal temperature at the section under consideration during the condition under consideration.

(11) Except racked-out valves.

(12) The primary membrane stress limit for pressure vessels under DE loading is conservatively selected to be lower than the level permitted by the present ASME Code, in order to insure that it is also conservative with respect to earlier editions of the code of which these components were designed.

(13) σ_p = Local membrane stress. This is equal to the average stress across the solid section under consideration. It excludes discontinuities and concentrations and is produced only by pressure.

(14) S_u = Material minimum tensile strength listed in either the code the component was purchased and manufactured under, or ASME Code Section III.

TABLE 3.9-5

DE SEISMIC LOADING COMBINATION
STRUCTURAL CRITERIA MECHANICAL EQUIPMENT SUPPORTS
AND STRUCTURAL COMPONENTS(1)

ELEMENT (2, 3)	LOADING COMBINATIONS (4,5)	CRITERIA (6,7, 8)	
Linear(3)	Deadweight + DE + Pressure + Nozzle/Piping Loads	1974 ASME Code Section III Appendix XVII, Subsection NF or AISC Manual, 7th Edition.	
Plate and shell(2) (active components)	Deadweight + DE + Pressure + Nozzle/Piping Loads	σ_m $(\sigma_m + \sigma_b)$	$\leq 1.0S$ $\leq 1.5S$
Plate and shell (inactive components)	Deadweight + DE + Pressure + Nozzle/Piping Loads	σ_m $(\sigma_m + \sigma_b)$	$\leq 1.0S$ $\leq 1.5S$
Bolts	Deadweight + DE + Pressure + Nozzle/Piping Loads	1974 ASME Code Section III Appendix XVII, Code Case 1644-6 or AISC Manual, 7th Edition.	

TABLE 3.9-5

Notes:

(1) Includes RCS seal table and parts. Qualification of reactor cavity manipulator crane and spent fuel pit bridge crane and flux mapping transfer device not required for DE. Structural integrity insured by HOSGRI qualification.

(2) Plate and shell type supports: Plate and shell type component supports are supports such as vessel skirts and saddles which are fabricated from plate and shell elements and are normally subjected to a biaxial stress field.

(3) Linear type support: A linear type component support is defined as acting under essentially a single component of direct stress. Such elements may also be subjected to shear stresses. Examples of such structural elements are: tension and compression struts, beams and columns subjected to bending, trusses, frames, rings, arches, and cables.

(4) Nozzle loads shall be those nozzle loads acting on the supported component during the DE earthquake.

(5) Plus Operating Loads, as applicable.

(6) σ_m = General membrane stress. This stress is equal to the average stress across the solid section under consideration, excludes discontinuities and concentrations and is produced only by mechanical loads.

(7) σ_b = Bending stress. This stress is equal to the linear varying portion of the stress across the solid section under consideration, excludes discontinuities and concentrations, and is produced only by mechanical loads.

(8) S_y = 1971 or 1974 code allowable stress value. The allowable stress shall correspond to the highest metal temperature at the section under consideration during the condition under consideration.

TABLE 3.9-6

NORMAL CONDITIONS LOADING COMBINATIONS AND STRUCTURAL CRITERIA MECHANICAL EQUIPMENT[1]

COMPONENT (2, 3)	LOADING COMBINATIONS (4)	CRITERIA (7, 8, 9, 10, 11, 12, 13)	
Tanks, heat-exchangers filters, demineralizers	Deadweight + Pressure + Nozzle/ Piping Loads.	σ_m $(\sigma_m$ or $\sigma_L) + \sigma_b$	$\leq 1.0S$ $\leq 1.5S$
Active pumps	Deadweight + Pressure + Nozzle/ Piping Loads + Operating Loads.	σ_m $(\sigma_m$ or $\sigma_L) + \sigma_b$	$\leq 1.0S$ $\leq 1.5S$
Inactive pumps	Deadweight + Pressure + Nozzle/ Piping Loads + Operating Loads.	σ_m $(\sigma_m$ or $\sigma_L) + \sigma_b$	$\leq 1.0S$ $\leq 1.5S$
Active valves	Deadweight + Pressure + Nozzle/ Piping Loads + Operating Loads.	Extended Structure:	$\sigma_m \leq 1.0S$ $(\sigma_m$ or $\sigma_L) +$ $\sigma_b \leq 1.5S$
		Pressure Boundary: Valve Nozzles: Bolting:	ANSI B16.5 or MSS-SP-66 (6) $\sigma_m \leq 2.0S$
Inactive valves	Deadweight + Pressure + Nozzle/ Piping Loads + Operating Loads.	Extended Structure:	$\sigma_m \leq 1.1S$ $(\sigma_m$ or $\sigma_L)$ $+ \sigma_b \leq 1.5S$
		Pressure Boundary: Valve Nozzles: Bolting:	ANSI B16.5 or MSS-SP-66 (6) $\sigma_m \leq 2.0S$

TABLE 3.9-6

COMPONENT (2, 3)	LOADING COMBINATIONS (4)	CRITERIA (7, 8, 9, 10, 11, 12, 13)	
Inactive cast iron, pressure retaining Components	Deadweight + Pressure + Nozzle/Piping Loads + Operating Loads(12)	σ_p $(\sigma_m$ or $\sigma_L) + \sigma_b$	$\leq 0.1\ S_u$ $\leq 1.5 \times 0.1\ S_u$
Inactive cost iron non-pressure retaining Components	Deadweight + Pressure + Nozzle/Piping Loads + Operating Loads(12)	$(\sigma_m$ or $\sigma_L) + \sigma_b$	$\leq 1.0 \times 0.2\ S_u$

Notes:

(1) See Chapter 5, Table 5.2.8 for structural components.

(2) Active: Mechanical equipment which is needed to go from normal full power operation to safe shutdown following the earthquake and which must perform mechanical motions during the course of accomplishing its design function.

(3) Inactive: Mechanical equipment which is not required to perform mechanical motions in taking the plant from normal full power operations to safe shutdown following the earthquake.

(4) Nozzle loads shall include piping loads transmitted to the component during the normal conditions.

(5) Deleted.

(6) Valves, being stronger than the attached piping and having a proven history without any gross failures of pressure boundaries, can safely transmit piping loads without compromising their pressure retaining integrity. Therefore, piping integrity assures valve integrity.

TABLE 3.9-6

Notes (Continued):

(7) σ_m = General membrane stress. This stress is equal to the average stress across the solid section under consideration, excludes discontinuities and concentrations and is produced only by mechanical loads.

(8) σ_L = Local membrane stress. This stress is the same as σ_m except that it includes the effect of discontinuities.

(9) σ_b = Bending stress. The stress is equal to the linear varying portion of the stress across the solid section under consideration, excludes discontinuities and concentrations, and is produced only by mechanical loads.

(10) S = 1971 or 1974 ASME code allowable stress value. The allowable stress shall correspond to the highest metal temperature at the section under consideration during the condition under consideration.

(11) S_y = 1971 or 1974 ASME code yield stress value. The yield stress shall correspond to the highest metal temperature at the section under consideration during the condition under consideration.

(12) S_p = Local membrane stress. This is equal to the average stress across the solid section under consideration. It excludes discontinuities and concentrations and is produced only by pressure.

(13) S_u = Material minimum tensile strength listed in either the code the component was purchased and manufactured under, or ASME Code Section III.

TABLE 3.9-7

NORMAL CONDITIONS LOADING COMBINATIONS AND STRUCTURAL CRITERIA MECHANICAL EQUIPMENT SUPPORTS AND STRUCTURAL COMPONENTS[1]

ELEMENT	LOADING COMBINATIONS (4, 5)	CRITERIA (6, 7, 8)	
Linear[3]	Deadweight + Nozzle/Piping Loads	1974 ASME Code Appendix XVII, Subsection NF or AISC Manual, 7th Edition	
Plate and shell[2] (active components)	Deadweight + Nozzle/Piping Loads	σ_m $(\sigma_m + \sigma_b)$	≤ 1.0S (and/or 1974 ASME Code, ≤ 1.5S Subsection NF)
Plate and shell (inactive components)	Deadweight + Nozzle/Piping Loads	σ_m $(\sigma_m + \sigma_b)$	≤ 1.0S (and/or 1974 ASME Codes, ≤ 1.5S Subsection NF)
Bolts	Deadweight + Nozzle/Piping Loads	1974 ASME Code Appendix XVII, Code Case 1644-6 or AISC Manual, 7th Edition	

TABLE 3.9-7

Notes:

(1) Includes RCS seal table and parts. Qualification of reactor cavity manipulator crane and spent fuel pit bridge crane and flux mapping transfer device not required for DE. Structural integrity insured by HOSGRI qualification.

(2) Plate and shell type supports: Plate and shell type component supports are supports such as vessel skirts and saddles which are fabricated from plate and shell elements and are normally subjected to a biaxial stress field.

(3) Linear type support: A linear type component support is defined as acting under essentially a single component of direct stress. Such elements may also be subjected to shear stresses. Examples of such structural elements are: tension and compression struts, beams and columns subjected to bending, trusses, frames, rings, arches, and cables.

(4) Nozzle loads shall be those nozzle loads acting on the supported component during the normal conditions.

(5) Plus Operating Loads, as applicable.

(6) σ_m = General membrane stress. This stress is equal to the average stress across the solid section under consideration, excludes discontinuities and concentrations and is produced only by mechanical loads.

(7) σ_b = B ending stress. This stress is equal to the linear varying portion of the stress across the solid section under consideration, excludes discontinuities and concentrations, and is produced only by mechanical loads.

(8) S = 1971 or 1974 code allowable stress value. The allowable stress shall correspond to the highest metal temperature at the section under consideration during the condition under consideration.

TABLE 3.9-8

TANK DESIGN

Storage Function	Design Code	Tank Plate Material	ASME Code Allowable Design Stress, (psi)	Code
Boric acid	ASME Sec. VIII, Div. 1 *(no code stamp)*	ASTM A240 T304	16,000	ASME Sec. VIII, Div. 1
Liquid holdup	ASME Sec. III, Class C	ASTM A240 T304	16,000	ASME Sec. VIII, Div. 1
Component cooling water surge	ASME Sec. VIII,	ASTM A285 Gr. C	13,750	ASME Sec. VIII, Div. 1
Waste gas decay	ASME Sec. III, Class C	ASTM A285 Gr. C	13,750	ASME Sec. VIII, Div. 1
Diesel fuel oil storage (underground)	UL 58	ASTM A36	12,650	ASME Sec. VIII, Div. 1
Volume control	ASME Sec. III, Class C	ASTM A240 T304	16,000	ASME Sec. VIII, Div. 1

TABLE 3.9-8

Storage Function	Design Code	Tank Plate Material	ASME Code Allowable Design Stress, (psi)	Code
Accumulator	ASME Sec. III, Class C	ASTM A516 Gr. 70 W/ A240 T304 Cladding	17,500	ASME Sec. VIII, Div. 1
Boron injection	ASME Sec. III, Class C	ASTM A516 Gr. 70 W/ A240 T304L Cladding	17,500	ASME Sec. VIII, Div. 1
Spray additive	ASME Sec. VIII, Div. 1 (no code stamp)	ASTM A240 T304	16,000	ASME Sec. VIII, Div. 1
Transfer storage & firewater	AWWA D100	ASTM A516 Gr. 60	19,500	ASME Sec. VIII, Div. 2
Reactor coolant drain tank	ASME Sec. III, Class C	ASTM A240 T304	16,000	ASME Sec. VIII, Div. 1
Waste concentrates holding	ASME Sec. III, Class C	ASTM A240 T304	16,000	ASME Sec. VIII, Div. 1

TABLE 3.9-8

Storage Function	Design Code	Tank Plate Material	ASME Code Allowable Design Stress, (psi)	Code
Spent Resin Storage	ASME Sec. III, Class C	ASTM A240 T304	16,000	ASME Sec. VIII, Div. 1
Equipment Drain Receiver	ASME Sec. VIII, Div. 1 (no code stamp)	ASTM A240 T304	16,000	ASME Sec. VIII, Div. 1

1. ASME Section III - American Society of Mechanical Engineers, Boiler and Pressure Vessel, Section III (1968, 1971).
2. ASME Section VIII - American Society of Mechanical Engineers, Boiler and Pressure Vessel Code, Section VIII (1968, 1971) Div. 1.
3. UL-58 - Underwriters Standards, Steel Underground Tanks for Flammable and Combustible Liquids.
4. AWWAD100 - American Waterworks Association, Standard for Steel Tanks, Standpipes Reservoirs and Elevated Tanks for Water Storage.

LIST OF ACTIVE VALVES

System or Service Description	Valve Identification	FSAR Fig. No.	Body Type	Size in.	Actuator Type	Valve Position On Failure	Position for Safe Shutdown[a]	Failure Analysis Comments
AUX FW PUMP 1 TURBINE GOV	FCV-15	3.2-4	Globe	-	Speed Governor	NA	Open	11
MSIV BYPASS – LEAD 4	FCV-22	3.2-4	Globe	3	Air	Closed	Closed	
MSIV BYPASS – LEAD 3	FCV-23	3.2-4	Globe	3	Air	Closed	Closed	
MSIV BYPASS – LEAD 2	FCV-24	3.2-4	Globe	3	Air	Closed	Closed	
MSIV BYPASS – LEAD 1	FCV-25	3.2-4	Globe	3	Air	Closed	Closed	
MAIN STM LEAD 2 TO AUX FW PUMP 1 TURBINE	FCV-37	3.2-4	Gate	4	Motor	FA	Operable	10, 25
MAIN STM LEAD 3 TO AUX FW PUMP 1 TURBINE	FCV-38	3.2-4	Gate	4	Motor	FA	Operable	10, 25
MAIN STEAM ISOL LEAD 1	FCV-41	3.2-4	Swing Check	28	Air	See Note 7	Closed	7
MAIN STEAM ISOL LEAD 2	FCV-42	3.2-4	Swing Check	28	Air	See Note 7	Closed	7
MAIN STEAM ISOL LEAD 3	FCV-43	3.2-4	Swing Check	28	Air	See Note 7	Closed	7

System or Service Description	Valve Identification	FSAR Fig. No.	Body Type	Size in.	Actuator Type	Valve Position On Failure	Position for Safe Shutdown[(a)]	Failure Analysis Comments
MAIN STEAM ISOL LEAD 4	FCV-44	3.2-4	Swing Check	28	Air	See Note 7	Closed	7
MN STM TO AUX FW PUMP 1 TURBINE	FCV-95	3.2-4	Gate	4	Motor	FA	Open	11
BORIC ACID BLENDER INLET	FCV-110A	3.2-8	Globe	2	Air	Open	Open	23
STEAM GEN NO. 1 TO BLOWDN TANK	FCV-151	3.2-8	Globe	3	Air	Closed	Closed	
AUX FP TURB 1 STM INLET	FCV-152	3.2-4	Globe	4	Manual	NA	Open	11
STEAM GEN NO. 2 TO BLOWDN TANK	FCV-154	3.2-4	Globe	3	Air	Closed	Closed	
STEAM GEN NO. 3 TO BLOWDN TANK	FCV-157	3.2-4	Globe	3	Air	Closed	Closed	
STEAM GEN NO. 4 TO BLOWDN TANK	FCV-160	3.2-4	Globe	3	Air	Closed	Closed	
CTMT H_2 SAMPLE SUPPLY IN CTMT	FCV-235	3.2-23	Globe	3/8	Solenoid	Closed	Operable	
CTMT H_2 SAMPLE SUPPLY OUT CTMT	FCV-236	3.2-23	Globe	3/8	Solenoid	Closed	Operable	

System or Service Description	Valve Identification	FSAR Fig. No.	Body Type	Size in.	Actuator Type	Valve Position On Failure	Position for Safe Shutdown[a]	Failure Analysis Comments
CTMT H_2 SAMPLE RETURN OUT CTMT	FCV-237	3.2-23	Globe	3/8	Solenoid	Closed	Operable	
CTMT H_2 SAMPLE SUPPLY IN CTMT	FCV-238	3.2-23	Globe	3/8	Solenoid	Closed	Operable	
CTMT H_2 SAMPLE SUPPLY OUT CTMT	FCV-239	3.2-23	Globe	3/8	Solenoid	Closed	Operable	
CTMT H_2 SAMPLE RETURN OUT CTMT	FCV-240	3.2-23	Globe	3/8	Solenoid	Closed	Operable	
STM GEN 4 BD SAMPLE OS CNTMT	FCV-244	3.2-4	Globe	¾	Air	Closed	Closed	
STM GEN 3 BD SAMPLE OS CNTMT	FCV-246	3.2-4	Globe	¾	Air	Closed	Closed	
STM GEN 2 BD SAMPLE OS CNTMT	FCV-248	3.2-4	Globe	¾	Air	Closed	Closed	
STM GEN 1 BD SAMPLE OS CNTMT	FCV-250	3.2-4	Globe	¾	Air	Closed	Closed	
RC DRN PPS DISCH IN CNTMT	FCV-253	3.2-19	Ball	2-1/2	Air	Closed	Closed	
RC DRN PPS DISCH OUT CNTMT	FCV-254	3.2-19	Ball	2-1/2	Air	Closed	Closed	

System or Service Description	Valve Identification	FSAR Fig. No.	Body Type	Size in.	Actuator Type	Valve Position On Failure	Position for Safe Shutdown[(a)]	Failure Analysis Comments
RC DRN TANK VENT HEADER IN CONTAINMENT	FCV-255	3.2-19	Ball	3/4	Air	Closed	Closed	
RC DRN TANK VENT HEADER OUT CONTAINMENT	FCV-256	3.2-19	Ball	3/4	Air	Closed	Closed	
RC DRN TANK GAS ANALYZER OUT CONTAINMENT	FCV-257	3.2-19	Ball	1/2	Air	Closed	Closed	
RC DRN TANK GAS ANALYZER IN CONTAINMENT	FCV-258	3.2-19	Ball	1/2	Air	Closed	Closed	
RC DRN TANK N2 SUPPLY OUT CONTAINMENT	FCV-260	3.2-19	Ball	3/4	Air	Closed	Closed	
CCW SUPPLY HEADER C	FCV-355	3.2-14	B'fly	20	Motor	FAI	Closed	
CCW TO RC PUMPS	FCV-356	3.2-14	B'fly	10	Motor	FAI	Closed	
RCP THERMAL BARRIER CCW RETURN	FCV-357	3.2-14	Globe	6	Motor	FAI	Closed	
EXCESS LETDOWN HT EXCH CCW RETURN	FCV-361	3.2-14	B'fly	4	Air	Closed	Closed	
RCP OIL COOLER CCW RETURN	FCV-363	3.2-14	B'fly	6	Motor	FAI	Closed	
RHR HT EXCHANGER 2 CCW RETURN	FCV-364	3.2-14	B'fly	12	Air	21	Functional	10

System or Service Description	Valve Identification	FSAR Fig. No.	Body Type	Size in.	Actuator Type	Valve Position On Failure	Position for Safe Shutdown[a]	Failure Analysis Comments
RHR HT EXCHANGER 3 CCW RETURN	FCV-365	3.2-14	B'fly	12	Air	21	Functional	10
CCW SUPPLY HEADER A	FCV-430	3.2-14	B'fly	30	Motor	FAI	Open	
CCW SUPPLY HEADER B	FCV-431	3.2-14	B'fly	30	Motor	FAI	Open	
RAW WATER STG RES AUX FEED PUMP 1	FCV-436	3.2-3	B'fly	8	Manual	FAI	Open	
RAW WATER STG RES AUX FEED PUMPS 2 & 3	FCV-437	3.2-3	B'fly	8	Manual	FAI	Open	
MAIN FEEDWATER ISOLATION LEAD 1	FCV-438	3.2-3	Gate	16	Motor	FAI	Closed	5
MAIN FEEDWATER ISOLATION LEAD 2	FCV-439	3.2-3	Gate	16	Motor	FAI	Closed	5
MAIN FEEDWATER ISOLATION LEAD 3	FCV-440	3.2-3	Gate	16	Motor	FAI	Closed	5
MAIN FEEDWATER ISOLATION LEAD 4	FCV-441	3.2-3	Gate	16	Motor	FAI	Closed	5
AUX SALTWATER PUMPS CROSS	FCV-495	3.2-17	B'fly	24	Motor	FAI	Operable	
AUX. SALTWATER PUMPS CROSS	FCV-496	3.2-17	B'fly	24	Motor	FAI	Operable	

TABLE 3.9-9

System or Service Description	Valve Identification	FSAR Fig. No.	Body Type	Size in.	Actuator Type	Valve Position On Failure	Position for Safe Shutdown[a]	Failure Analysis Comments
CNT BLDG SUMP PP DISCHARGE IN CNTMT	FCV-500	3.2-19	Ball	2	Air	Closed	Closed	
CNT BLDG SUMP PP DISCHARGE OUT CNTMT	FCV-501	3.2-19	Ball	2	Air	Closed	Closed	
STEAM GEN 1 MAIN FW SUPPLY	FCV-510	3.2-3	Globe	16	Air	Closed	Closed	
STEAM GEN 2 MAIN FW SUPPLY	FCV-520	3.2-3	Globe	16	Air	Closed	Closed	
STEAM GEN 3 MAIN FW SUPPLY	FCV-530	3.2-3	Globe	16	Air	Closed	Closed	
STEAM GEN 4 MAIN FW SUPPLY	FCV-540	3.2-3	Globe	16	Air	Closed	Closed	
CNT WEST INSTRUMENT AIR	FCV-584	3.2-25	Ball	2	Air	Closed	Closed	
AUX SW TO CCW HT EXCH NO. 1	FCV-602	3.2-17	B'fly	24	Air	Open	21, 22	
AUX SW TO CCW HT EXCH NO. 2	FCV-603	3.2-17	B'fly	24	Air	Open	21, 22	
CNTMT FIRE WATER ISOLATION	FCV-633	3.2-18	Globe	3	Air	Closed	21, 22	

System or Service Description	Valve Identification	FSAR Fig. No.	Body Type	Size in.	Actuator Type	Valve Position On Failure	Position for Safe Shutdown[(a)]	Failure Analysis Comments
RHR PUMP 1 RECIRC	FCV-641A	3.2-10	Globe	2	Motor	FAI	Functional	
RHR PUMP 2 RECIRC	FCV-641B	3.2-10	Globe	2	Motor	FAI	Functional	
CNTMT ISO CHPS EXHAUST	FCV-658	3.2-23	Gate	4	Motor	FAI	Functional	
CNTMT ISO CHPS EXHAUST	FCV-659	3.2-23	Gate	4	Motor	FAI	Functional	
CONT PURGE SUPPLY IC	FCV-660	3.2-23	B'fly	48	Air	Closed	Closed	
CONT PURGE SUPPLY OC	FCV-661	3.2-23	B'fly	48	Air	Closed	Closed	
CONT VAC/PRESS RELIEF 1C	FCV-662	3.2-23	B'fly	12	Air	Closed	Closed	
CONT PRESSURE RELIEF OC	FCV-663	3.2-23	B'fly	12	Air	Closed	Closed	
CONT VACUUM RELIEF OC	FCV-664	3.2-23	B'fly	12	Air	Closed	Closed	
CNTMT ISO CHPS EXHAUST	FCV-668	3.2-23	Gate	4	Motor	FAI	Functional	
CNTMT ISO CHPS EXHAUST	FCV-669	3.2-23	Gate	4	Motor	FAI	Functional	
CNT AIR SAMPLE (INSIDE CNT)	FCV-678	3.2-23	Ball	1	Air	Closed	Closed	5
CNT AIR SAMPLE (OUTSIDE CNT)	FCV-679	3.2-23	Ball	1	Air	Closed	Closed	5

System or Service Description	Valve Identification	FSAR Fig. No.	Body Type	Size in.	Actuator Type	Valve Position On Failure	Position for Safe Shutdown[a]	Failure Analysis Comments
CNT AIR SAMPLE (OUTSIDE CNT)	FCV-681	3.2-23	Ball	1	Air	Closed	Closed	5
POST-LOCA SAMPLING SYST	FCV-696	3.2-19	Globe	3/8	Solenoid	Closed	Closed	5
POST-LOCA SAMPLING SYST	FCV-697	3.2-19	Globe	3/8	Solenoid	Closed	Closed	5
POST-LOCA SAMPLING SYST	FCV-698	3.2-23	Globe	3/8	Solenoid	Closed	Closed	5
POST-LOCA SAMPLING SYST	FCV-699	3.2-23	Globe	3/8	Solenoid	Closed	Closed	5
POST-LOCA SAMPLING SYST	FCV-700	3.2-23	Globe	3/8	Solenoid	Closed	Closed	5
RCP OIL COOLER CCW RETURN	FCV-749	3.2-14	B'fly	6	Motor	FAI	Closed	
RCP THERMAL BARRIER CCW RETURN	FCV-750	3.2-14	Globe	6	Motor	FAI	Closed	
STEAM GEN NO. 1 BLOWDOWN AND SAMPLE	FCV-760	3.2-4	Globe	3	Air	Closed	Closed	
STEAM GEN NO. 2 BLOWDOWN AND SAMPLE	FCV-761	3.2-4	Globe	3	Air	Closed	Closed	
STEAM GEN NO. 3 BLOWDOWN AND SAMPLE	FCV-762	3.2-4	Globe	3	Air	Closed	Closed	

System or Service Description	Valve Identification	FSAR Fig. No.	Body Type	Size in.	Actuator Type	Valve Position On Failure	Position for Safe Shutdown[(a)]	Failure Analysis Comments
STEAM GEN NO. 4 BLOWDOWN AND SAMPLE	FCV-763	3.2-4	Globe	3	Air	Closed	Closed	
STEAM GEN NO. 1 MAIN FW SUPPLY BY-PASS	FCV-1510	3.2-3	Globe	6	Air	Closed	Closed	
STEAM GEN NO. 2 MAIN FW SUPPLY BY-PASS	FCV-1520	3.2-3	Globe	6	Air	Closed	Closed	
STEAM GEN NO. 3 MAIN FW SUPPLY BY-PASS	FCV-1530	3.2-3	Globe	6	Air	Closed	Closed	
STEAM GEN NO. 4 MAIN FW SUPPLY BY-PASS	FCV-1540	3.2-3	Globe	6	Air	Closed	Closed	
CHG PUMPS DISCH TO REGEN HT EXCH	HCV-142	3.2-4	Globe	3	Air	Closed	21	23
RHR TO COLD LEGS 3 & 4	HCV-637	3.2-10	Ball	8	Air	Open	Open	
RHR TO COLD LEGS 1 & 2	HCV-638	3.2-10	Ball	8	Air	Open	Open	
DSL FO DAY TK 1-2 HEADER B	LCV-85	3.2-21	Ball	1-1/2	Air	Closed	Functional	
DSL FO DAY TK 2-1 HEADER B	LCV-86	3.2-21	Ball	1-1/2	Air	Closed	Functional	
DSL FO DAY TK 1-3 HEADER B	LCV-87	3.2-21	Ball	1-1/2	Air	Closed	Functional	
DSL FO DAY TK 1-2 HEADER A	LCV-88	3.2-21	Ball	1-1/2	Air	Closed	Functional	

System or Service Description	Valve Identification	FSAR Fig. No.	Body Type	Size in.	Actuator Type	Valve Position On Failure	Position for Safe Shutdown[a]	Failure Analysis Comments
DSL FO DAY TK 2-1 HEADER A	LCV-89	3.2-21	Ball	1-1/2	Air	Closed	Functional	
DSL FO DAY TK 1-3 HEADER A	LCV-90	3.2-21	Ball	1-1/2	Air	Closed	Functional	
AUX FEEDWATER FROM TURB AFW PP TO SG 1	LCV-106	3.2-3	Globe	2	Motor	FAI	Operable	4
AUX FEEDWATER FROM TURB AFW PP TO SG 2	LCV-107	3.2-3	Globe	2	Motor	FAI	Operable	4
AUX FEEDWATER FROM TURB AFW PP TO SG 3	LCV-108	3.2-3	Globe	2	Motor	FAI	Operable	4
AUX FEEDWATER FROM TURB AFW PP TO SG 4	LCV-109	3.2-3	Globe	2	Motor	FAI	Operable	4
AUX FEEDWATER FROM MOTOR AFW PP TO SG 1	LCV-110	3.2-3	Globe	2	Electro Hydraulic	Open	Operable	4
AUX FEEDWATER FROM MOTOR AFW PP TO SG 2	LCV-111	3.2-3	Globe	2	Electro Hydraulic	Open	Operable	4
VOLUME CONTROL TANK TO CHARG PUMPS	LCV-112B	3.2-8	Gate	4	Motor	FAI	Closed	5
VOLUME CONTROL TANK TO CHARG PUMPS	LCV-112C	3.2-8	Gate	4	Motor	FAI	Closed	5
AUX FEEDWATER FROM MOTOR AFW PP TO SG 4	LCV-113	3.2-3	Globe	2	Electro Hydraulic	Open	Operable	4

System or Service Description	Valve Identification	FSAR Fig. No.	Body Type	Size in.	Actuator Type	Valve Position On Failure	Position for Safe Shutdown[a]	Failure Analysis Comments
AUX FEEDWATER FROM MOTOR AFW PP TO SG 3	LCV-115	3.2-3	Globe	2	Electro Hydraulic	Open	Operable	4
STEAM GEN 1 10% ATM STM DUMP	PCV-19	3.2-4	Globe	8	Air	Closed	Functional 21	
STEAM GEN 2 10% ATM STM DUMP	PCV-20	3.2-4	Globe	8	Air	Closed	Functional 21	
STEAM GEN 3 10% ATM STM DUMP	PCV-21	3.2-4	Globe	8	Air	Closed	Functional 21	
STEAM GEN 4 10% ATM STM DUMP	PCV-22	3.2-4	Globe	8	Air	Closed	Functional 21	
PRESSURIZER POWER-OPERATED RELIEF	PCV-455C	3.2-7	Globe	3	Air	Closed	Functional 21	8,12
PRESSURIZER POWER-OPERATED RELIEF	PCV-456	3.2-7	Globe	3	Air	Closed	Functional 21	8,12
CONT PURGE EXHAUST 1C	RCV-11	3.2-23	B'fly	48	Air	Closed	Closed	
CONT PURGE EXHAUST OC	RCV-12	3.2-23	B'fly	48	Air	Closed	Closed	
MAIN STM SAFETY LEAD 1	RV-3	3.2-4	Relief	6	Spring	NA	Operable	9
MAIN STM SAFETY LEAD 1	RV-4	3.2-4	Relief	6	Spring	NA	Operable	9

System or Service Description	Valve Identification	FSAR Fig. No.	Body Type	Size in.	Actuator Type	Valve Position On Failure	Position for Safe Shutdown[a]	Failure Analysis Comments
MAIN STM SAFETY LEAD 1	RV-5	3.2-4	Relief	6	Spring	NA	Operable	9
MAIN STM SAFETY LEAD 1	RV-6	3.2-4	Relief	6	Spring	NA	Operable	9
MAIN STM SAFETY LEAD 2	RV-7	3.2-4	Relief	6	Spring	NA	Operable	9
MAIN STM SAFETY LEAD 2	RV-8	3.2-4	Relief	6	Spring	NA	Operable	9
MAIN STM SAFETY LEAD 2	RV-9	3.2-4	Relief	6	Spring	NA	Operable	9
MAIN STM SAFETY LEAD 2	RV-10	3.2-4	Relief	6	Spring	NA	Operable	9
MAIN STM SAFETY LEAD 3	RV-11	3.2-4	Relief	6	Spring	NA	Operable	9
MAIN STM SAFETY LEAD 3	RV-12	3.2-4	Relief	6	Spring	NA	Operable	9
MAIN STM SAFETY LEAD 3	RV-13	3.2-4	Relief	6	Spring	NA	Operable	9
MAIN STM SAFETY LEAD 3	RV-14	3.2-4	Relief	6	Spring	NA	Operable	9
CCW SURGE TK RV	RV-45	3.2-14	Relief	3	Spring	NA	Operable	
MAIN STM SAFETY LEAD 4	RV-58	3.2-4	Relief	6	Spring	NA	Operable	9
MAIN STM SAFETY LEAD 4	RV-59	3.2-4	Relief	6	Spring	NA	Operable	9
MAIN STM SAFETY LEAD 4	RV-60	3.2-4	Relief	6	Spring	NA	Operable	9

System or Service Description	Valve Identification	FSAR Fig. No.	Body Type	Size in.	Actuator Type	Valve Position On Failure	Position for Safe Shutdown[a]	Failure Analysis Comments
MAIN STM SAFETY LEAD 4	RV-61	3.2-4	Relief	6	Spring	NA	Operable	9
MAIN STM SAFETY LEAD 1	RV-222	3.2-4	Relief	6	Spring	NA	Operable	9
MAIN STM SAFETY LEAD 2	RV-223	3.2-4	Relief	6	Spring	NA	Operable	9
MAIN STM SAFETY LEAD 3	RV-224	3.2-4	Relief	6	Spring	NA	Operable	9
MAIN STM SAFETY LEAD 4	RV-225	3.2-4	Relief	6	Spring	NA	Operable	9
FIRE WATER TANK CROSSTIE	8X42B (FP-0-306)	3.2-18	Gate	8	Manual	NA	Open	
FIRE WATER TANK CROSSTIE BYPASS	8X42B (FP-0-307)	3.2-18	Gate	8	Manual	NA	Open	
PRESSURIZER POWER RELIEF ISO	8000A	3.2-7	Gate	3	Motor	FAI	Operable	
PRESSURIZER POWER RELIEF ISO	8000B	3.2-7	Gate	3	Motor	FAI	Operable	
PRESSURIZER POWER RELIEF ISO	8000C	3.2-7	Gate	3	Motor	FAI	Operable	
PRESSURIZER SAFETY	8010A	3.2-7	R.V.	6	Spring	NA	Functional	9
PRESSURIZER SAFETY	8010B	3.2-7	R.V.	6	Spring	NA	Functional	9

System or Service Description	Valve Identification	FSAR Fig. No.	Body Type	Size in.	Actuator Type	Valve Position On Failure	Position for Safe Shutdown[a]	Failure Analysis Comments
PRESSURIZER SAFETY	8010C	3.2-7	R.V.	6	Spring	NA	Functional	9
PRESSURIZER RELIEF TK PRIMARY WTR	8029	3.2-7	Ball	3	Air	Closed	Closed	
PRESSURIZER RELIEF TK GAS ANALYZER IC	8034A	3.2-7	Globe	3/8	Air	Closed	Closed	
PRESSURIZER RELIEF TK GAS ANALYZER OC	8034B	3.2-7	Globe	3/8	Air	Closed	Closed	
PRESSURIZER RELIEF TK N2 SUPPLY	8045	3.2-7	Dia-phragm	3/4	Air	Closed	Closed	
REACTOR VESSEL HEAD VENT SYS	8078A	3.2-7	Globe	1	Solenoid	Closed	Operable	
REACTOR VESSEL HEAD VENT SYS	8078B	3.2-7	Globe	1	Solenoid	Closed	Operable	
REACTOR VESSEL HEAD VENT SYS	8078C	3.2-7	Globe	1	Solenoid	Closed	Operable	
REACTOR VESSEL HEAD VENT SYS	8078D	3.2-7	Globe	1	Solenoid	Closed	Operable	
REACTOR COOL PPS SEAL WTR RET	8100	3.2-7	Gate	4	Motor	FAI	Closed	

System or Service Description	Valve Identification	FSAR Fig. No.	Body Type	Size in.	Actuator Type	Valve Position On Failure	Position for Safe Shutdown[a]	Failure Analysis Comments
BORIC ACID TO CHARGING PPS	8104	3.2-8	Globe	2	Motor	FAI	Operable	
CENTRIFUGAL I CHG PPS RECRC	8105	3.2-8	Globe	2	Motor	FAI	Functional	5
CENTRIFUGAL CHG PPS RECRC	8106	3.2-8	Globe	2	Motor	FAI	Functional	5
CHG PPS DISCH TO LETDOWN HX	8107	3.2-8	Gate	3	Motor	FAI	Functional	
CHG PPS DISCH TO LETDOWN HX	8108	3.2-8	Gate	3	Motor	FAI	Functional	
REACT COOL PPS SEAL WTR RET	8112	3.2-8	Gate	4	Motor	FAI	Closed	
LETDOWN LINE RV	8117	3.2-8	Relief	2	Spring	Open	Closed	
RCP SEAL WTR RTN RV	8121	3.2-8	Relief	2	Spring	Open	Closed	
SEAL WTR HX INLET RV	8123	3.2-8	Relief	2	Spring	Open	Closed	
CHARGING PUMP SUCTION HEADER	8125	3.2-8	Relief	3/4	Spring	Open	Closed	
PRESSURIZER AUX SPRAY	8145	3.2-8	Globe	2	Air	Closed	Operable 21	

System or Service Description	Valve Identification	FSAR Fig. No.	Body Type	Size in.	Actuator Type	Valve Position On Failure	Position for Safe Shutdown[(a)]	Failure Analysis Comments
CHG PUMP TO LOOP 4 COLD LEG	8146	3.2-8	Globe	3	Air	Open	Operable 21	
CHG PUMP TO LOOP 3 COLD LEG	8147	3.2-8	Globe	3	Air	Open	Operable 21	
RCS PRESSURIZER AUX SPRAY	8148	3.2-8	Globe	2	Air	Closed	Operable 21	
LETDOWN LINE ISOL	8149A	3.2-8	Globe	2	Air	Closed	Closed	
LETDOWN LINE ISOL	8149B	3.2-8	Globe	2	Air	Closed	Closed	
LETDOWN LINE ISOL	8149C	3.2-8	Globe	2	Air	Closed	Closed	
LETDOWN LINE ISOL	8152	3.2-8	Globe	2	Air	Closed	Closed	
CCP 1 FCV-128 MANUAL BYPASS	8387B	3.2-8	Globe	3	Manual	NA	Functional	23
CCP 2 FCV-128 MANUAL BYPASS	8387C	3.2-8	Globe	3	Manual	NA	Functional	23
HCV-142 MANUAL BYPASS	8403	3.2-8	Globe	3	Manual	NA	Functional	23
MANUAL EMERGENCY BORATE VALVE	8471	3.2-08	Diaphragm	2	Manual	NA	Functional	23

System or Service Description	Valve Identification	FSAR Fig. No.	Body Type	Size in.	Actuator Type	Valve Position On Failure	Position for Safe Shutdown[(a)]	Failure Analysis Comments
BA TRANSFER PUMP SUCTION CROSSTIE	8476	3.2-8	Diaphragm	2	Manual	NA	Open	23
RHR PP 1 SUCT	8700A	3.2-10	Gate	14	Motor	FAI	Operable	
RHR PP 2 SUCT	8700B	3.2-10	Gate	14	Motor	FAI	Operable	
RHR SUCTION FROM LOOP 4 HOT LEG	8701	3.2-10	Gate	14	Motor	FAI	Operable	
RHR SUCTION FROM LOOP 4 HOT LEG	8702	3.2-10	Gate	14	Motor	FAI	Operable	
RHR DISCHARGE TO HOT LEGS 1 & 2	8703	3.2-10	Gate	12	Motor	FAI	Functional	10, 19
RHR SUCTION PIPING RV	8707	3.2-10	Relief	3	Spring	Open	Closed	
RHR COOLDOWN LINE RV	8708	3.2-10	Relief	3/4	Spring	Open	Closed	
RHR HT EXCH 1 TO RCS HOT LEGS 1 & 2	8716A	3.2-10	Gate	8	Motor	FAI	Operable	
RHR HT EXCH 2 TO RCS HOT LEGS 1 & 2	8716B	3.2-10	Gate	8	Motor	FAI	Operable	
CHARGING INJECT LINE DISCHARGE	8801A	3.2-9	Gate	4	Motor	FAI	Open	

System or Service Description	Valve Identification	FSAR Fig. No.	Body Type	Size in.	Actuator Type	Valve Position On Failure	Position for Safe Shutdown[(a)]	Failure Analysis Comments
CHARGING INJECT LINE DISCHARGE	8801B	3.2-9	Gate	4	Motor	FAI	Open	
SAFETY INJECT PUMP 1 DISCH TO HOT LEGS 1 & 2	8802A	3.2-9	Gate	4	Motor	FAI	Operable	19
SAFETY INJECT PUMP 2 DISCH TO HOT LEGS 3 & 4	8802B	3.2-9	Gate	4	Motor	FAI	Operable	19
CHARG PUMPS TO CHARGING INJECT LINE	8803A	3.2-9	Gate	4	Motor	FAI	Open	10
CHARG PUMPS TO CHARGING INJECT LINE	8803B	3.2-9	Gate	4	Motor	FAI	Open	10
RHR HT EXCH 1 TO CHG PPS SUCT	8804A	3.2-9	Gate	8	Motor	FAI	Functional	13
RHR HT EXCH 2 TO CHG PPS SUCT	8804B	3.2-9	Gate	8	Motor	FAI	Functional	13
RWST TO CHARG PUMP SUCT	8805A	3.2-9	Gate	8	Motor	FAI	Open	10
RWST TO CHARG PUMP SUCT	8805B	3.2-9	Gate	8	Motor	FAI	Open	10
CHARGING PPS SIS PPS SUC CROSSTIE	8807A	3.2-9	Gate	4	Motor	FAI	Functional	10, 13

System or Service Description	Valve Identification	FSAR Fig. No.	Body Type	Size in.	Actuator Type	Valve Position On Failure	Position for Safe Shutdown[(a)]	Failure Analysis Comments
CHARGING PPS SIS PPS SUC CROSSTIE	8807B	3.2-9	Gate	4	Motor	FAI	Functional	10, 13
RHR HT EXCH 1 TO COLD LEGS 1 & 2	8809A	3.2-9	Gate	8	Motor	FAI	Functional	20
RHR HT EXCH 2 TO COLD LEGS 3 & 4	8809B	3.2-9	Gate	8	Motor	FAI	Functional	20
SIS PUMP 1 DISCH TO COLD LEGS	8821A	3.2-9	Gate	4	Motor	FAI	Functional	
SIS PUMP 2 DISCH TO COLD LEGS	8821B	3.2-9	Gate	4	Motor	FAI	Functional	
SIS PUMP DISCH TO COLD LEGS	8835	3.2-9	Gate	4	Motor	FAI	Open	14
SI PUMP DISCHARGE RV	8851	3.2-9	Relief	¾	Spring	Open	Closed	
SI PUMP DISCHARGE RV	8853A	3.2-9	Relief	¾	Spring	Open	Closed	
SI PUMP DISCHARGE RV	8853B	3.2-9	Relief	¾	Spring	Open	Closed	
ACCUM RV	8855A	3.2-9	Relief	1	Spring	Open	Closed	
ACCUM RV	8855B	3.2-9	Relief	1	Spring	Open	Closed	
ACCUM RV	8855C	3.2-9	Relief	1	Spring	Open	Closed	

System or Service Description	Valve Identification	FSAR Fig. No.	Body Type	Size in.	Actuator Type	Valve Position On Failure	Position for Safe Shutdown[(a)]	Failure Analysis Comments
ACCUM RV	8855D	3.2-9	Relief	1	Spring	Open	Closed	
RHR HT EXCH OUTLET RELIEF RV	8856A	3.2-10	Relief	2	Spring	Open	Closed	
RHR HT EXCH OUTLET RELIEF	8856B	3.2-10	Relief	2	Spring	Open	Closed	
SI PUMP SUCT HEADER RV	8858	3.2-9	Relief	3/4	Spring	Open	Closed	
ACCUM TEST IN CTMT	8871	3.2-9	Globe	3/4	Air	Closed	Closed	
ACCUM N2 SUPPLY HEADER	8880	3.2-9	Globe	1	Air	Closed	Closed	
SAFETY INJECTION TEST LINE	8883	3.2-9	Globe	3/4	Air	Closed	Closed	5
SAFETY INJECT PUMP NO. 1 SUCT	8923A	3.2-9	Gate	6	Motor	FAI	Operable	
SAFETY INJECT PUMP NO. 2 SUCT	8923B	3.2-9	Gate	6	Motor	FAI	Operable	
ACCUM TEST OUTSIDE CONTAINMENT	8961	3.2-9	Globe	3/4	Air	Closed	Closed	
SAFETY INJECT PUMP MIN. RECIRC. VALVES	8974A	3.2-9	Globe	2	Motor	FAI	Operable	
SAFETY INJECT PUMP MIN. RECIRC. VALVES	8974B	3.2-9	Globe	2	Motor	FAI	Operable	

System or Service Description	Valve Identification	FSAR Fig. No.	Body Type	Size in.	Actuator Type	Valve Position On Failure	Position for Safe Shutdown[a]	Failure Analysis Comments
RWST TO SAFETY INJECTION PUMP SUCT	8976	3.2-9	Gate	8	Motor	FAI	Open	14
RWST TO RHR PUMP SUCTION	8980	3.2-9	Gate	12	Motor	FAI	Operable	14
CNTMT SUMP TO RHR PP1 SUCT	8982A	3.2-10	Gate	14	Motor	FAI	Operable	
CNTMT SUMP TO RHR PP2 SUCT	8982B	3.2-10	Gate	14	Motor	FAI	Operable	
SPRAY ADDITIVE SYSTEM	8987	3.2-12	Relief	3/4	Spring	Open	Close	
SPRAY ADD TK OUT ISOL	8994A	3.2-12	Gate	3	Motor	FAI	Open	10
SPRAY ADD TK OUT ISOL	8994B	3.2-12	Gate	3	Motor	FAI	Open	10
CNTMT SPRAY PP 1 DISCHG	9001A	3.2-12	Gate	8	Motor	FAI	Open	10
CNTMT SPRAY PP 2 DISCHG	9001B	3.2-12	Gate	8	Motor	FAI	Open	10
RHR HT EXCH 1 TO CONT SPRAY	9003A	3.2-12	Gate	8	Motor	FAI	Open	10
RHR HT EXCH 2 TO CONT SPRAY	9003B	3.2-12	Gate	8	Motor	FAI	Open	10

System or Service Description	Valve Identification	FSAR Fig. No.	Body Type	Size in.	Actuator Type	Valve Position On Failure	Position for Safe Shutdown[a]	Failure Analysis Comments
RCS SAMPLE	9351A	3.2-11	Globe	3/8	N_2	Closed	Operable (21)	23
RCS SAMPLE	9351B	3.2-11	Globe	3/8	N_2	Closed	Operable (21)	23
PRESS STEAM SPACE IN CONTMT	9354A	3.2-7	Globe	3/8	Air	Closed	Closed	
PRESS STEAM SPACE OUT CONTMT	9354B	3.2-7	Globe	3/8	Air	Closed	Closed	
PRESS LIQUID SPACE IN CONTMT	9355A	3.2-7	Globe	3/8	Air	Closed	Closed	
PRESS LIQUID SPACE OUT CONTMT	9355B	3.2-7	Globe	3/8	Air	Closed	Closed	
HOT LEGS 1 & 4 IN CONTMT SAMPLE	9356A	3.2-7	Globe	3/8	N_2	Closed	Operable 21	
HOT LEGS 1 & 4 IN CONTMT SAMPLE	9356B	3.2-7	Globe	3/8	N_2	Closed	Operable 21	
ACCUM SAMPLE HDR IN CONTAINMENT	9357A	3.2-9	Globe	3/8	Air	Closed	Closed	
ACCUM SAMPLE HDR OUT CONTAINMENT	9357B	3.2-9	Globe	3/8	Air	Closed	Closed	

System or Service Description	Valve Identification	FSAR Fig. No.	Body Type	Size in.	Actuator Type	Valve Position On Failure	Position for Safe Shutdown[a]	Failure Analysis Comments
CCW PUMP SUCT CROSSTIE VALVE (2 VALVES ON LINES 97 & 2285)	CCW-4 & -5	3.2-14	B'fly	20	Manual	NA	Closed	
CCW PUMP 1-2 DISCH ISOLATION (TO HDR B)	CCW-16	3.2-14	B'fly	20	Manual	NA	Closed	
CCW PUMP 1-3 DISCH ISOLATION (TO HDR B)	CCW-17	3.2-14	B'fly	20	Manual	NA	Closed	
CCW PUMP 1-1 DISCH ISOLATION (TO HDR A)	CCW-18	3.2-14	B'fly	20	Manual	NA	Closed	
CCW PUMP 1-2 DISCH ISOLATION (TO HDR A)	CCW-19	3.2-14	B'fly	20	Manual	NA	Closed	
CCW HDR C SUPPLY FROM HDR A	CCW-23	3.2-14	B'fly	24	Manual	NA	Closed	
CCW HDR C SUPPLY FROM HDR B	CCW-24	3.2-14	B'fly	24	Manual	NA	Closed	
MAIN STEAM LEAD ONE 10% STEAM DUMP ISOLATION	MS-1015	3.2-4	Gate	8	Manual	NA	Closed Note 24	
MAIN STEAM LEAD TWO 10% STEAM DUMP ISOLATION	MS-2015	3.2-4	Gate	8	Manual	NA	Closed Note 24	
MAIN STEAM LEAD THREE 10% STEAM DUMP ISOLATION	MS-3015	3.2-4	Gate	8	Manual	NA	Closed Note 24	

System or Service Description	Valve Identification	FSAR Fig. No.	Body Type	Size in.	Actuator Type	Valve Position On Failure	Position for Safe Shutdown[(a)]	Failure Analysis Comments
MAIN STEAM LEAD FOUR 10% STEAM DUMP ISOLATION	MS-4015	3.2-4	Gate	8	Manual	NA	Closed Note 24	

(a) The valves whose positions are listed in this column are those valves whose operability is relied on to perform an active function such as safe shutdown of the reactor or mitigation of the consequences of a Design Basis Accident coincidental with loss of offsite power. An entry of "functional" or equivalently "operable" means that the valve must be capable of being opened and/or closed to perform its active function. For DCPP, safe shutdown is defined as Mode 3 following an accident (SSER 7 and SSER 22), Mode 5 following a Hosgri earthquake (Section 3.7.6.2), and Mode 3, followed by Mode 5 within 72 hours, following an Appendix R fire (10 CFR 50, Appendix R).

Failure Analysis Comment Notes:

1. Deleted in Revision 9.
2. Deleted in Revision 9.
3. Deleted in Revision 9.
4. Valve is provided for control. Failure, open or close, is remedied by redundant train and EOP RNO actions.
5. Valve provides isolation. Failure to close is remedied by valve in series.
6. Deleted in Revision 9.
7. Locally mounted air accumulators protected against compressed air system failure by check valves can hold open the main steam isolation valves for a short duration of time after the compressed air system is lost. In the event of loss of all air to the main steam isolation valves, the valves will fail closed.
8. These valves are provided for controlled steam release. Failure to open is remedied by redundant valves. Failure to close is remedied by closure of series valve or system shutdown.
9. These valves provide vessel protection. Failure to open is remedied by redundant valves in parallel. Valve size limits flow on failure to close.
10. Valve provides isolation. Failure to close (or stay closed) is remedied by a redundant valve in series. Failure to open (or stay open) is remedied by a redundant line (or system).
11. Valve opens to start device. Failure to open is remedied by use of redundant system.
12. Air-operated valve operation is not required for safe shutdown.
13. Used during recirculation mode.

Failure Analysis Comment Notes (continued)

14. Valve provides isolation. Failure to stay open could defeat system function. "Hot" short could close valve, but is not considered credible.
15. Deleted in Revision 9.
16. Deleted in Revision 9.
17. Deleted in Revision 9.
18. Deleted in Revision 9.
19. Valves operated (opened) during changeover from cold leg recirculation to hot leg injection. Failure to stay closed during cold leg injection or cold leg recirculation could defeat system function. "Hot" short could open valve but is not considered credible.
20. Valve 8809A operated (closed) during the changeover from cold leg injection to cold leg recirculation. Valve 8809B operated (closed) during the changeover from cold leg recirculation to hot leg recirculation. Failure of one valve to stay open during cold leg injection remedied by redundant system.
21. Air operated valves required to operate or maintain position after a loss of the compressed air system are supplied with compressed gas from the backup air/nitrogen supply system. See Section 9.3.1.6 for details.
22. If one of the CCW heat exchangers is valved out-of-service, then backup air is supplied to the respective CCW heat exchanger saltwater inlet valve to maintain the valve closed. This ensures all ASW flow is directed to in-service CCW heat exchangers.
23. Valve does not have an active safety function to support accident mitigation or Mode 3 safe shutdown. Valve is active to support achieving post-Hosgri cold shutdown in the manner defined in the Hosgri Report. Valve needs to be seismically qualified for active function for Hosgri only.
24. Valve has an active safety function to support accident mitigation or Mode 3 safe shutdown. Valve is passive to support achieving post-Hosgri cold shutdown in the manner defined in the Hosgri Report.
25. Normal position for Safe Shutdown is Open. For Containment Isolation and the condition described in section 6.5.3.4, valve must be Operable.

Abbreviations:

FCV	=	Flow control valve	RCP	=	Reactor coolant pump	B'fly	=	Butterfly
LCV	=	Level control valve	FAI	=	Fail as is	RC	=	Reactor coolant
PCV	=	Pressure control valve	PP & PPS	=	Pump(s)	CCW	=	Component cooling water
HCV	=	Hand control valve	CNT	=	Containment	RHR	=	Residual heat removal
RV	=	Relief valve	CHG	=	Charging	AWF	=	Auxiliary feedwater
TCV	=	Temperature control valve	DSL FO	=	Diesel fuel oil	NA	=	Not applicable

TABLE 3.9-10

MAXIMUM DEFLECTIONS ALLOWED FOR REACTOR INTERNAL SUPPORT STRUCTURES FOR FAULTED CONDITIONS

Component	Allowable Deflection, Inches	No Loss of Function Deflection, Inches
Upper Barrel		
Radial inward	4.1	8.2
Radial outward	1.0	1.0
Upper Core Plate	0.100[a]	0.150
Rod Cluster Control Guide Tubes	1.0	1.75

(a) Only to ensure that the plate will not touch a guide tube.

TABLE 3.9-11

PRESSURIZED GAS CONTAINERS (Above 100 psig)

Vessel	Design Class	Design Code	Design Pressure	Vessel Operating Pressure	Vessel Volume[c]	Type Relief Device[a]	Relief Set-point	Stored Energy ft-lb(ea)	Attached Piping: Vessel Location	Attached Piping: Design Class	Attached Piping: Largest Size	Deviations from OSHA 29 CFR Section 1910
CO_2 storage tanks (Cardox)	I	ASME B&PV Code Sec. VIII	363 psig	300 psig	7.5 ton	Relief valve Pop safety	341 psig 357 psig	N.A.[b]	Turbine building	II	6 in.	None
Diesel generator starting air receivers	I	ASME B&PV Code Sec. VIII	342 psig	250 psig	53 cu ft	Relief valve	260 psig	3×10^6	Turbine building	I	2 in.	None
Diesel generator turbocharger booster air receivers	I	ASME B&PV Code Sec. VIII	342 psig	250 psig	106 cu ft	Relief valve	260 psig	5.9×10^6	Turbine building	I	2 in.	None
Air plant receiver	II	ASME B&PV Code Sec. VIII-Div. I	120 psig	110 psig	650 cu ft	Relief valve	115 psig	12.6×10^6	Turbine building	III	4 in.	None
N_2 storage vessels	II	ASME B&PV Code Sec. VIII Case 1205	2450 psig	2200 psig	51 cu ft per vessel	Relief valve rupture disk	2450 psig 3500 psig ± 5%	34.5×10^6	Yard vault	III	3/4 in.	None
Instrument air receivers	II	ASME B&PV Code Sec. VIII	120 psig	105 psig per receiver 2 receivers	152 cu ft	Relief valve	110 psig	3×10^6	Auxiliary building & intake Structure	III	2 in.	None
H_2 storage vessels	II	ASME B&PV Code Sec VIII Case1205	2450 psig	2200 psig	51 cu. ft. per vessel 6 vessels	Relief Valve Rupture Disc	2450 psig 3500 psig ± 5%	34.5×10^6	Yard Vault	III	3/4 in.	None

TABLE 3.9-11

Vessel	Design Class	Design Code	Design Pressure	Vessel Operating Pressure	Vessel Volume(c)	Type Relief Device[(a)]	Relief Set-point	Stored Energy ft-lb(ea)	Attached Piping: Vessel Location	Attached Piping: Design Class	Attached Piping: Largest Size	Deviations from OSHA 29 CFR Section 1910
H_2 bottles standard commercial bottles (rental)	II	ICC Std. 3A	3225 psig	2000 psig	6.7 cu. ft. bottle 4 bottles	Relief Valve	3200 psig	6,000	Turbine Building	II	3/4 in.	None
CO_2 bottles standard commer-cial bottles (rental)	II	ICC Std. 3A	3225 psig	2000 psig	75 lb CO_2 per vessel 11 vessels	Relief Valve	3200 psig	2.245×10^6 (Calc. M-634)	Intake Structure	III	1/2 in.	None
Compressed breath air storage vessels	II	ASME B&PV Code Sec. VIII	3873 psig	3500 psig	21 cu. ft. per vessel 9 vessels	Relief Valve	3870 psig	23.4×10^6	Unit 2 Turbine Building	III	3/4 in.	None
Carbon dioxide Storage bottles	II	ICC Std. 3AA-2265	2265 psig	2000 psig	1.5 cu. ft. per bottle 16 bottles	Relief Valve	2200 psig		Turbine Building Elev. 85'	II	2 in.	None
N_2 storage bottles	II	ICC Std. 3AA-3500	3500 psig	2800 psig	1.5 cu. ft. per bottle 4 bottles	Relief Valve	3000 psig		Aux Bldg	II	1 in.	None
Argon storage bottles	II	ICC Std. 3AA-2015	2015 psig	2000 psig	1.5 cu. ft. per bottle 5 bottles	Relief Valve	2015 psig		Penetration Area	II	1 in.	None

(a) Relief setpoint and capacity based on the applicable design code.

(b) Filled with liquid, which requires heat input to flash.

(c) Table lists significant gas quantities greater than 100 lbs net weight

TABLE 3.9-12

MECHANICAL EQUIPMENT SEISMIC
QUALIFICATION RESULTS
UNIT 1

Equipment	Location Building/ Elevation, ft	Qualification Method	Qualifying Spectra HE, DDE, DE	Damping Value Used
Feedwater System				
AFW Pump (Motor Driven)	Aux/100	A	DE DDE HE	R R R
AFW Pump Motor	Aux/100	A	DE DDE HE	R R R
AFW Pump (Turbine-driven)	Aux/100	A	DE DDE HE	R R R
AFW Pump Turbine	Aux/100	A	DE DDE HE	R R R
CVC System				
Boric Acid Tank and Heater	Aux/115	A	DE DDE HE	2 2 4
Safety Injection System				
SI Pump Lube Oil Filter Stand	Aux/85	A	DE DDE HE	R R R

Equipment	Location Building/ Elevation, ft	Qualification Method	Qualifying Spectra HE, DDE, DE	Damping Value Used
Component Cooling System				
CCW Pump	Aux/73	A	DE DDE HE	R R R
CCW Pump Motor	Aux/73	A	DE DDE HE	R R R
CCW Heat Exchanger	Turb/85	A	DE DDE HE	2 2 4
CCW Surge Tank	Aux/163	A	DE DDE HE	R R R
CCW Pump Lube Oil Cooler	Aux/73	A	DE DDE HE	R R R
Makeup Water System				
Makeup Water Transfer Pump and Motor	Aux/100	A	DE DDE HE	R R R

TABLE 3.9-12

Equipment	Location Building/ Elevation, ft	Qualification Method	Qualifying Spectra HE, DDE, DE	Damping Value Used
Saltwater System				
ASW Pump and Motor	Intake/-2	A	DE	R
			DDE	R
			HE	4
Fire Protection System				
Fire Pump	Aux/115	A	DE	R
			DDE	R
			HE	R
Fire Pump Motor	Aux/115	A	DE	R
			DDE	R
			HE	R
Portable Fire Pump (diesel)	MSS/85	T	DE	R
			DDE	R
			HE	R
Diesel Generator System				
Diesel Generator	Turb/85	A, T	DE	2
			DDE	2
			HE	4

Equipment	Location Building/ Elevation, ft	Qualification Method	Qualifying Spectra HE, DDE, DE	Damping Value Used
Diesel Transfer Pump	MSS/77	A	DE	R
			DDE	R
			HE	R
Diesel Transfer Pump Motor	MSS/77	A	DE	R
			DDE	R
			HE	R
Diesel Transfer Filter	MSS/77	A	DE	R
			DDE	R
			HE	R
Diesel Transfer Strainer	MSS/77	A	DE	R
			DDE	R
			HE	R
Priming Tank	Turb/85	A	DE	R
			DDE	R
			HE	R
Starting Air Receiver	Turb/85	A	DE	2
			DDE	2
			HE	4
Turbocharger Air Receiver	Turb/85	A	DE	R
			DDE	R
			HE	R

TABLE 3.9-12

Equipment	Location Building/ Elevation, ft	Qualification Method	Qualifying Spectra HE, DDE, DE	Damping Value Used
Ventilation System				
Containment H_2 Purge Supply Filters	Aux/100	A	DE DDE HE	R R R
Containment H_2 Purge Exhaust Filters	Aux/115	A	DE DDE HE	R R R
Containment Fan Cooler Box	Cont/140	A	DE DDE HE	R R R
Gaseous Radwaste System				
Waste Gas Compressor	Aux/60	A	DE[(a)]	R
Waste Gas Moisture Separator	Aux/60	A	DE[(a)]	R
Waste Gas Decay Tank	Aux/60	A	DE[(a)]	R

(a) Qualified for DE only per Regulatory Guide 1.143.

(b) Legend:

A = Qualification by analysis (Qualification Method Column)
T = Qualification by testing
R = Rigid

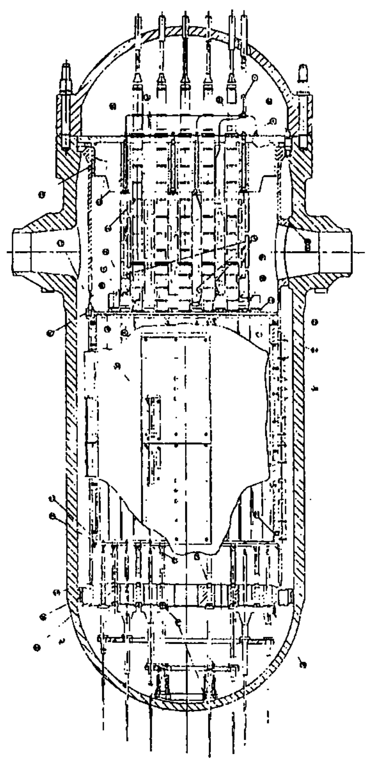

	FEATURES TO BE EXAMINED	COMMENTS AND OBSERVATIONS BEFORE FUNCTIONAL TEST	COMMENTS AND OBSERVATIONS AFTER FUNCTIONAL TEST
[illegible]	[illegible]		
[illegible]	[illegible]		
[illegible]	[illegible]		
[illegible]	[illegible]		
[illegible]	[illegible]		
[illegible]	[illegible]		
[illegible]	[illegible]		
[illegible]	[illegible]		
[illegible]	[illegible]		
[illegible]	[illegible]		
[illegible]	[illegible]		
[illegible]	[illegible]		
[illegible]	[illegible]		
[illegible]	[illegible]		
[illegible]	[illegible]		
[illegible]	[illegible]		
[illegible]	[illegible]		
[illegible]	[illegible]		
[illegible]	[illegible]		
[illegible]	[illegible]		
[illegible]	[illegible]		
[illegible]	[illegible]		
[illegible]	[illegible]		
[illegible]	[illegible]		
[illegible]	[illegible]		
[illegible]	[illegible]		
[illegible]	[illegible]		
[illegible]	[illegible]		
[illegible]	[illegible]		
[illegible]	[illegible]		
[illegible]	[illegible]		
[illegible]	[illegible]		
[illegible]	[illegible]		
[illegible]	[illegible]		
[illegible]	[illegible]		

FSAR UPDATE

UNIT 2

DIABLO CANYON SITE

FIGURE 3.9-2
VIBRATION CHECKOUT - FUNCTIONAL
TEST INSPECTION DATA

SHOP TEST ACCELEROMETER DATA

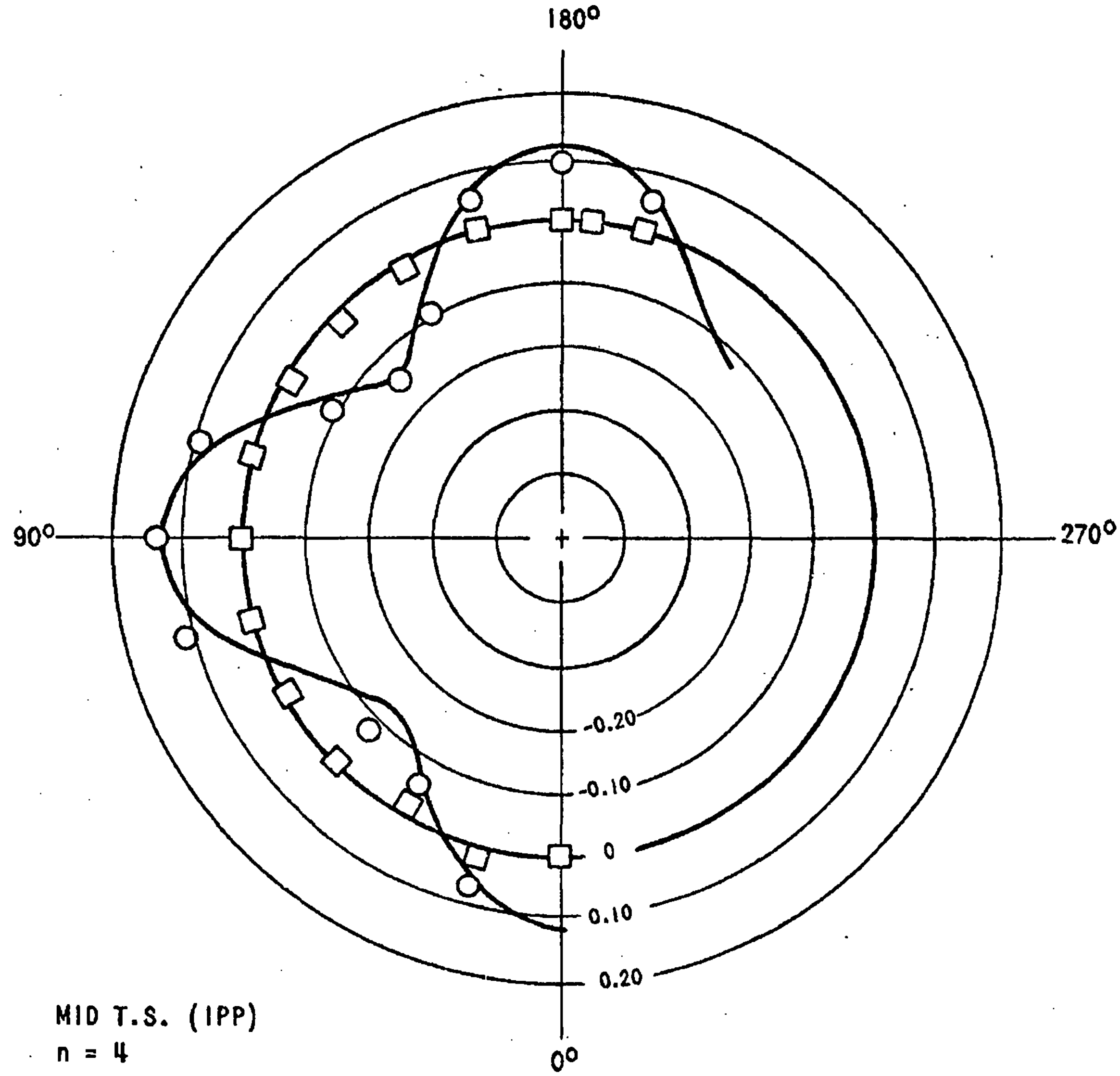

MID T.S. (IPP)
n = 4
f = 72 H_z FORCE = 6 LB
CURVE = 0.12 COS 4θ (LEAST SQUARE)
○ MIDDLE □ BOTTOM

FSAR UPDATE

UNIT 1
DIABLO CANYON SITE

FIGURE 3.9-3
THERMAL SHIELD, MODEL SHAPE n=4
OBTAINED FROM SHAKER TEST

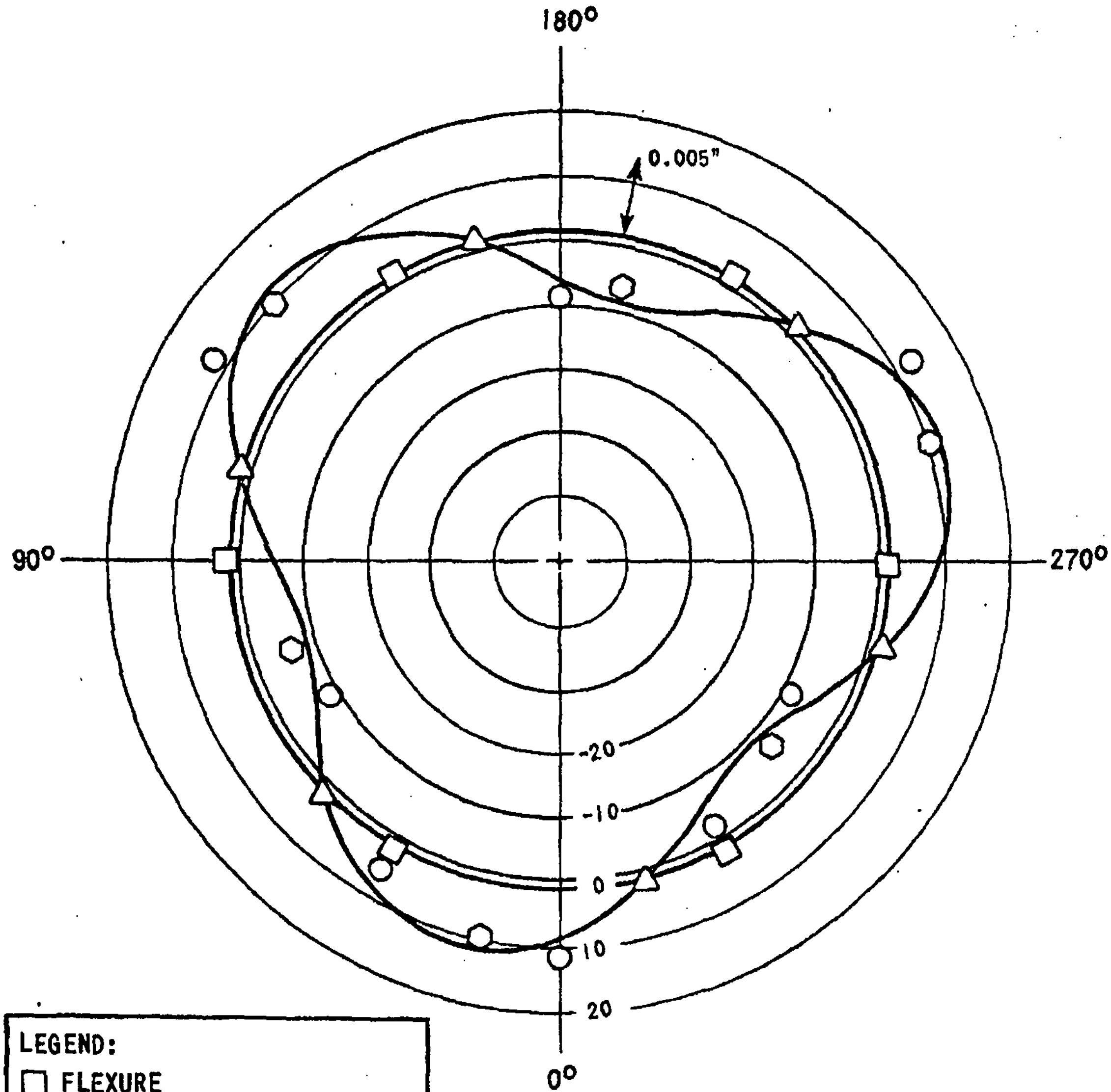

LEGEND:
- □ FLEXURE
- △ TOP SUPPORT
- ⬡ TOP INDICATOR READING
- ○ BOTTOM INDICATOR READING

FSAR UPDATE

UNIT 1
DIABLO CANYON SITE

FIGURE 3.9-4
THERMAL SHIELD, MAXIMUM AMPLITUDE OF VIBRATION DURING PREOPERATIONAL TEST

2.5 GEOLOGY AND SEISMOLOGY

This section presents the findings of the regional and site-specific geologic and seismologic investigations of the Diablo Canyon Power Plant (DCPP) site. Information presented is in compliance with the criteria in Appendix A of 10 CFR 100 and meets the format and content recommendations of Regulatory Guide 1.70, Revision 1[(39)].

Location of earthquake epicenters within 200 miles of the plant site, and faults and earthquake epicenters within 75 miles of the plant site for either magnitudes or intensities, respectively, are shown in Figures 2.5-2, 2.5-3, and 2.5-4. A geologic and tectonic map of the region surrounding the site is given in two sheets of Figure 2.5-5, and detailed information about site geology is presented in Figures 2.5-8 through 2.5-16. Geology and seismology are discussed in detail in Sections 2.5.1 through 2.5.4. Additional information on site geology is contained in References 1 and 2.

On November 2, 1984, the NRC issued the Diablo Canyon Unit 1 Facility Operating License DPR-80. In DPR-80, License Condition Item 2.C.(7), the NRC stated, in part:

> "PG&E shall develop and implement a program to reevaluate the seismic design bases used for the Diablo Canyon Power Plant."

PG&E's reevaluation effort in response to the license condition was titled the "Long Term Seismic Program" (LTSP). PG&E prepared and submitted to the NRC the "Final Report of the Diablo Canyon Long Term Seismic Program" in July 1988[(40)]. Between 1988 and 1991, the NRC performed an extensive review of the Final Report, and PG&E prepared and submitted written responses to formal NRC questions. In February 1991, PG&E issued the "Addendum to the 1988 Final Report of the Diablo Canyon Long Term Seismic Program"[(41)]. In June 1991, the NRC issued Supplement Number 34 to the Diablo Canyon Safety Evaluation Report (SSER)[(42)]. in which the NRC concluded that PG&E had satisfied License Condition 2.C.(7) of Facility Operating License DPR-80. In the SSER the NRC requested certain confirmatory analyses from PG&E, and PG&E subsequently submitted the requested analyses. The NRC's final acceptance of the LTSP is documented in a letter to PG&E dated April 17, 1992[(43)].

The LTSP contains extensive data bases and analyses that update the basic geologic and seismic information in this section of the FSAR Update. However, the LTSP material does not address or alter the current design licensing basis for the plant, and thus is not included in the FSAR Update. A complete listing of bibliographic references to the LTSP reports and other documents may be found in References 40, 41 and 42.

Detailed supporting data pertaining to this section are presented in Appendices 2.5A, 2.5B, 2.5C, and 2.5D of Reference 27 in Section 2.3. Geologic and seismic information from investigations that responded to Nuclear Regulatory Commission (NRC) licensing review questions are presented Appendices 2.5E and 2.5F of the same reference. A brief synopsis of the information presented in Reference 27 (Section 2.3) is given below.

The DCPP site is located in San Luis Obispo County approximately 190 miles south of San Francisco and 150 miles northwest of Los Angeles, California. It is adjacent to the Pacific Ocean, 12 miles west-southwest of the city of San Luis Obispo, the county seat. The plant site location and topography are shown in Figure 2.5-1.

The site is located near the mouth of Diablo Creek which flows out of the San Luis Range, the dominant feature to the northeast. The Pacific Ocean is southwest of the site. Facilities for the power plant are located on a marine terrace that is situated between the mountain range and the ocean.

The terrace is bedrock overlain by surficial deposits of marine and nonmarine origin. Seismic Category I structures at the site are situated on bedrock that is predominantly stratified marine sedimentary rocks and volcanics, all of Miocene age. A more extensive discussion of the regional geology is presented in Section 2.5.1.1 and site geology in Section 2.5.1.2.

Several investigations were performed at the site and in the vicinity of the site to determine: potential vibratory ground motion characteristics, existence of surface faulting, and stability of subsurface materials and cut slopes adjacent to Seismic Category I structures. Details of these investigations are presented in Sections 2.5.2 through 2.5.5. Consultants retained to perform these studies included: Earth Science Associates (geology and seismicity), John A. Blume and Associates (seismic design and foundation materials dynamic response), Harding-Lawson and Associates (stability of cut slope), Woodward-Clyde-Sherard and Associates (soil testing), and Geo-Recon, Incorporated (rock seismic velocity determinations). The findings of these consultants are summarized in this section and the detailed reports are included in Appendices 2.5A, 2.5B, 2.5C, 2.5D, 2.5E, and 2.5F of Reference 27 in Section 2.3.

Geologic investigation of the Diablo Canyon coastal area, including detailed mapping of all natural exposures and exploratory trenches, yielded the following basic conclusions:

(1) The area is underlain by sedimentary and volcanic bedrock units of Miocene age. Within this area, the power plant site is underlain almost wholly by sedimentary strata of the Monterey Formation, which dip northward at moderate to very steep angles. More specifically, the reactor site is underlain by thick-bedded to almost massive Monterey sandstone that is well indurated and firm. Where exposed on the nearby hillslope, this rock is markedly resistant to erosion.

(2) The bedrock beneath the main terrace area, within which the power plant site has been located, is covered by 3 to 35 feet of surficial deposits. These include marine sediments of Pleistocene age and nonmarine sediments of Pleistocene and Holocene age. In general, they are thickest in the vicinity of the reactor site.

(3) The interface between the unconsolidated terrace deposits and the underlying bedrock comprises flat to moderately irregular surfaces of Pleistocene marine planation and intervening steeper slopes that also represent erosion in Pleistocene time.

(4) The bedrock beneath the power plant site occupies the southerly flank of a major syncline that trends west to northwest. No evidence of a major fault has been recognized within or near the coastal area, and bedrock relationships in the exploratory trenches positively indicate that no such fault is present within the area of the power plant site.

(5) Minor surfaces of disturbance, some of which plainly are faults, are present within the bedrock that underlies the power plant site. None of these breaks offsets the interface between bedrock and the cover of terrace deposits, and none of them extends upward into the surficial cover. Thus, the latest movements along these small faults must have antedated erosion of the bedrock section in Pleistocene time.

(6) No landslide masses or other gross expressions of ground instability are present within the power plant site or on the main hillslope east of the site. Some landslides have been identified in adjacent ground, but these are minor features confined to the naturally oversteepened walls of Diablo Canyon.

(7) No water of subsurface origin was encountered in the exploratory trenches, and the level of permanent groundwater beneath the main terrace area probably is little different from that of the adjacent lower reaches of the deeply incised Diablo Creek.

2.5.1 BASIC GEOLOGIC AND SEISMIC INFORMATION

This section presents the basic geologic and seismic information for DCPP site and surrounding region. Information contained herein has been obtained from literature studies, field investigations, and laboratory testing and is to be used as a basis for evaluations required to provide a safe design for the facility. The basic data contained in this section and in Reference 27 of Section 2.3 are referenced in several other sections of this FSAR Update.

2.5.1.1 Regional Geology

2.5.1.1.1 Regional Physiography

Diablo Canyon is in the southern Coast Range which is a part of the California Coast Ranges section of the Pacific Border physiographic province (see Figure 2.5-1). The region surrounding the power plant site consists of mountains, foothills, marine terraces, and valleys. The dominant features are the San Luis Range adjacent to the site to the

northeast, the Santa Lucia Range farther inland, the lowlands of the Los Osos and San Luis Obispo Valleys separating the San Luis and Santa Lucia Ranges, and the marine terrace along the coastal margin of the San Luis Range.

Landforms of the San Luis Range and the adjacent marine terrace produce the physiography at the site and in the region surrounding the site. The westerly end of the San Luis Range is a mass of rugged high ground that extends from San Luis Obispo Creek and San Luis Obispo Bay on the east and is bounded by the Pacific Ocean on the south and west. Except for its narrow fringe of coastal terraces, the range is featured by west-northwesterly-trending ridge and canyon topography. Ridge crest altitudes range from about 800 to 1800 feet. Nearly all of the slopes are steep, and they are modified locally by extensive slump and earthflow landslides.

Most of the canyons have narrow-bottomed, V-shaped cross sections. Alluvial fans and talus aprons are prominent features along the bases of many slopes and at localities where ravines debouch onto relatively gentle terrace surfaces. The coastal terrace belt extends between a steep mountain-front backscarp and a near-vertical sea cliff 40 to 200 feet in height. Both the bedrock benches of the terraces and the present offshore wave-cut bench are irregular in detail, with numerous basins and rock projections.

The main terrace along the coastal margin of the San Luis Range is a gently to moderately sloping strip of land as much as 2000 feet in maximum width. The more landward parts of its surface are defined by broad aprons of alluvial deposits. This cover thins progressively in a seaward direction and is absent altogether in a few places along the present sea cliff. The main terrace represents a series of at least three wave-cut rock benches that have approximate shoreline-angle elevations of 70, 100, and 120 feet.

Owing to both the prevailing seaward slopes of the rock surfaces and the variable thickness of overlying marine and nonmarine cover, the present surface of the main terrace ranges from 70 to more than 200 feet in elevation. Remnants of higher terraces exist at scattered locations along upper slopes and ridge crests. The most extensive among these is a series of terrace surfaces at altitudes of 300+, 400+, and 700+ feet at the west end of the ridge between Coon and Islay Creeks, north of Point Buchon. A surface described by Headlee[19] as a marine terrace at an altitude of about 700 feet forms the top of San Luis Hill. Remnants of a lower terrace at an altitude of 30 to 45 feet are preserved at the mouth of Diablo Canyon and at several places farther north.

Owing to contrasting resistance to erosion among the various bedrock units of the San Luis Range, the detailed topography of the wave-cut benches commonly is very irregular. As extreme examples, both modern and fossil sea stacks rise as much as 100 feet above the general levels of adjacent marine-eroded surfaces at several localities.

2.5.1.1.2 Regional Geologic and Tectonic Setting

2.5.1.1.2.1 Geologic Setting

The San Luis Range is underlain by a synclinal section of Tertiary sedimentary and volcanic rocks, which have been downfolded into a basement of Mesozoic rocks now exposed along its southwest and northeast sides. Two zones of faulting have been recognized within the range. The Edna fault zone trends along its northeast side, and the Miguelito fault zone extends into the range from the vicinity of Avila Bay. Minor faults and bedding-plane shears can be seen in the parts of the section that are well exposed along the sea cliff fringing the coastal terrace benches. None of these faults shows evidence of geologically recent activity, and the most recent movements along those in the rocks underlying the youngest coastal terraces can be positively dated as older than 80,000 to 120,000 years. Geologic and tectonic maps of the region surrounding the site are shown in Figures 2.5-5 (2 sheets), 2.5-6, 2.5-8, and 2.5-9.

2.5.1.1.2.2 Tectonic Features of the Central Coastal Region

DCPP site lies within the southern Coast Ranges structural province, and approximately upon the centerline axis of the northwest-trending block of crust that is bounded by the San Andreas fault on the northeast and the continental margin on the southwest. This crustal block is characterized by northwest-trending structural and geomorphic features, in contrast to the west-trending features of the Transverse Ranges to the south. A major geologic boundary within the block is associated with the Sur-Nacimiento and Rinconada faults, which separate terrains of contrasting basement rock types. The ground southwest of the Sur-Nacimiento zone and the southerly half of the Rinconada fault, referred to as the Coastal Block, is underlain by Franciscan basement rocks of dominantly oceanic types, whereas that to the northeast, referred to as the Salinia Block, is underlain by granitic and metamorphic basement rocks of continental types. Page(10) outlined the geology of the Coast Ranges, describing it generally in terms of "core complexes" of basement rocks and surrounding sections of younger sedimentary rocks. The principal Franciscan core complex of the southern Coast Range crops out on the coastal side of the Santa Lucia Range from the vicinity of San Luis Obispo to Point Sur, a distance of 120 miles. Its complex features reflect numerous episodes of deformation that evidently included folding, faulting, and the tectonic emplacement of extensive bodies of ultrabasic rocks. Other core complexes consisting of granitic and metamorphic basement rocks are exposed in the southern Coast Ranges in the ground between the Sur-Nacimiento and Rinconada and in the San Andreas fault zones. The locations of these areas of basement rock exposure are shown in Figure 2.5-6 and in Figure 1 of Appendix 2.5D of Reference 27 in Section 2.3.

Younger structural features include thick folded basins of Tertiary strata and the large faults that form structural boundaries between and within the core complexes and basins.

The structure of the southern Coast Ranges has evolved during a lengthy history of deformation extending from the time when the ancestral Sur-Nacimiento zone was a site for subduction (a Benioff zone) along the then-existing continental margin, through subsequent parts of Cenozoic time when the San Andreas fault system was the principal expression of the regional stress-strain system. The latest episodes of major deformation involved folding and faulting of Pliocene and older sediments during mid-Pliocene time, and renewed movements along preexisting faults during early or mid-Pliocene time. Present tectonic activity within the region is dominated by interaction between the Pacific and American crustal plates on opposite sides of the San Andreas fault and by continuing vertical uplift of the Coast Ranges. In the regional setting of DCPP site, the major structural features are the San Andreas, Rinconada-San Marcos-Jolon, Sur-Nacimiento, and Santa Lucia Bank faults. The San Simeon fault may also be included with this group. These faults are described as follows:

1. San Andreas Fault

The San Andreas fault is recognized as a major transform fault of regional dimensions that forms an active boundary between the Pacific and North American crustal plates. Cumulative slip along the San Andreas fault may have amounted to several hundred miles, and a substantial fraction of the total slip has occurred during late Cenozoic time. The fault has spectacular topographic expression, generally lying within a rift valley or along an escarpment mountain front, and having associated sag ponds, low scarps, right-laterally deflected streams, and related manifestations of recent activity.

The most recent episode of large-scale movement along the reach of the San Andreas fault that is closest to the San Luis Range occurred during the great Fort Tejon earthquake of 1857. Geologic evidence pertinent to the behavior of the fault during this and earlier seismic events was studied in great detail by Wallace[15, 32] who reported in terms of infrequent great earthquakes accompanied by ground rupture of 10 to 30 feet, with intervening periods of near total quiescence. Allen[16] suggested that such behavior has been typical for this reach of the San Andreas fault and has been fundamentally different from the behavior of the fault along the reach farther northwest, where creep and numerous small earthquakes have occurred. He further suggested that release of accumulating strain energy might have been facilitated by the presence of large amounts of serpentine in the fault zone to the northwest, and retarded by the locking effect of the broad bend of the fault zone where it crosses the Transverse Ranges to the southeast.

Movement is currently taking place along large segments of the San Andreas fault. The active reach of the fault between Parkfield and San Francisco is currently undergoing relative movement of at least 3 to 4 cm/yr, as determined geodetically and analyzed by Savage and Burford[33]. When the movement that occurs during the episodes of fault displacement in the western part of the Basin and Ranges Province is added to the minimum of 3 to 4 cm/yr of continuously and intermittently released strain, the total probably amounts to at least 5 to 6 cm/yr. This may account for essentially all of the relative motion between the Pacific and North American plates at present. In the

Transverse Ranges to the south, this strain is distributed between lateral slip along the San Andreas system and east-west striking lateral slip faulting, thrust faulting, and folding. North of the latitude of Monterey Bay and south of the Transverse Ranges, transcurrent movement is again concentrated along the San Andreas system, but in those regions, it is distributed among several major strands of the system.

2. Sur-Nacimiento Fault Zone

The Sur-Nacimiento fault zone has been regarded as the system of faults that extends from the vicinity of Point Sur, near the northwest end of the Santa Lucia Range, to the Big Pine fault in the western Transverse Ranges, and that separates the granitic-metamorphic basement of the Salinian Block from the Franciscan basement of the Coastal Block. The most prominent faults that are included within this zone are, from northwest to southeast, the Sur, Nacimiento, Rinconada, and (south) Nacimiento faults. The Sur fault, which extends as far northward as Point Sur on land, continues to the northwest in the offshore continental margin. At its southerly end, the zone terminates where the (south) Nacimiento fault is cut off by the Big Pine fault. The overall length of the Sur-Nacimiento fault zone between Point Sur and the Transverse Ranges is about 180 miles. The 60 mile long Nacimiento fault, between points of juncture with the Sur and Rinconada faults, forms the longest segment within this zone. Page(11) stated that:

> "It is unlikely that the Nacimiento fault proper has displaced the ground surface in Late Quaternary time, as there are no indicative offsets of streams, ridges, terrace deposits, or other topographic features. The Great Valley-type rocks on the northeast side must have been down-dropped against the older Franciscan rocks on the southwest, yet they commonly stand higher in the topography. This implies relative quiescence of the Late Quaternary time, allowing differential erosion to take place. In a few localities, the northeast side is the low side, and this inconsistency favors the same conclusion. In addition to the foregoing circumstances, the fault is offset by minor cross-faults in a manner suggesting that little, if any, Late Quaternary near-surface movement had occurred along the main fracture."

Hart(14), on the other hand, stated that: ". . . youthful topographic features (offset streams, sag ponds, possible fault scarplets, and apparently oversteepened slopes) suggest movement along both (Sur-Nacimiento and Rinconada) fault zones." The map compiled by Jennings(23), however, shows only the Rinconada with a symbol indicating "Quaternary fault displacement."

The results of photogeologic study of the region traversed by the Sur-Nacimiento fault zone tend to support Page's view. A pronounced zone of fault-controlled topographic lineaments can be traced from the northwest end of the Nacimiento fault southeastward to the Rinconada (south Nacimiento), East Huasna, and West Huasna faults. Only along the Rinconada, however, are there topographic features that seem to have originated through fault disturbances of the ground surface rather than through differential erosion along zones of shearing and juxtaposition of differing rocks.

Richter[13] noted that some historic seismicity, particularly the 1952 Bryson earthquake, appears to have originated along the Nacimiento fault. This view is supported by recent work of S. W. Smith[30] that indicates that the Bryson shock and the epicenters of several smaller, more recent earthquakes were located along or near the trace of the Nacimiento.

3. Rinconada (Nacimiento)-San Marcos-Jolon-San Antonio Fault System

A system of major faults extends northwestward, parallel to the San Andreas fault, from a point of junction with the Big Pine fault in the western Transverse Ranges. This system includes several faults that have been mapped as separate features and assigned individual names. Dibblee[27] however, has suggested that these faults are part of a single system, provisionally termed the Rinconada fault zone after one of its more prominent members. He also proposed abandoning the name Nacimiento for the large fault that constitutes the most southerly part of this system, as it is not continuous with the Nacimiento fault to the north, near the Nacimiento River. The newly defined Rinconada fault system comprises the old (south) Nacimiento, Rinconada, and San Marcos faults. Dibblee proposed that the system also include the Espinosa and Reliz faults, to the north, but detailed work by Durham[28] does not seem to support this interpretation. Instead, the system may extend into Lockwood Valley and die out there along the Jolon and San Antonio faults. All the faults of the Rinconada system have undergone significant movement during middle and late Cenozoic time, though the entire system did not behave as a unit. Dibblee pointed out that: "Relative vertical displacements are controversial, inconsistent, reversed from one segment to another; the major movement may be strike slip, as on the San Andreas fault."

Regarding the structural relationship of the Rinconada fault to nearby faults, Dibblee wrote as follows:

> "Thrust or reverse faults of Quaternary age are associated with the Rinconada fault along much of its course on one or both sides, within 9 miles, especially in areas of intense folding. In the northern part several, including the San Antonio fault, are present along both margins of the range of hills between the Salinas and Lockwood Valleys . . . . along which this range was elevated in part. Near the southern part are the major southwest-dipping South Cuyama and Ozena faults along which the Sierra Madre Range was elevated against Cuyama Valley, with vertical displacements possibly up to 8000 feet. All these thrust or reverse faults dip inward toward the Rinconada fault and presumably either splay from it at depth, or are branches of it. These faults, combined with the intense folding between them, indicated that severe compression accompanied possible transcurrent movement along the Rinconada fault."
>
> "The La Panza fault along which the La Panza Range was elevated .... in Quaternary time, is a reverse fault that dips northeast under the range, and is not directly related to the Rinconada fault.

"The Big Pine fault against which the Rinconada fault abuts . . . is a high angle left-lateral transcurrent fault active in Quaternary time[35]. The Pine Mountain fault south of it . . . . is a northeast-dipping reverse fault along which the Pine Mountain Range was elevated in Quaternary time. This fault may have been reactivated along an earlier fault that may have been continuous with the Rinconada fault, but displaced about 8 miles from it by left slip on the Big Pine fault[12] in Quaternary time."

"The Rinconada and Reliz faults were active after deposition of the Monterey Shale and Pancho Rico Formation, which are severely deformed adjacent and near the faults. The faults were again active after deposition of the Paso Robles Formation but to a lesser degree. These faults do not affect the alluvium or terrace deposits. There are no offset stream channels along these faults. However, in two areas several canyons and streams are deviated, possibly by right-lateral movement on the (Espinosa and San Marcos segments of the) Rinconada fault. There are no indications that these faults are presently active."

4. San Simeon Fault

The fault here referred to as the San Simeon fault trends along the base of the peninsula that lies north of the settlement of San Simeon. This fault is on land for a distance of 12 miles between its only outcrop, north of Ragged Point, and Point San Simeon. It may extend as much as 16 miles farther to the southeast, to the vicinity of Point Estero. This possibility is suggested by the straight reach of coastline between Cambria and Point Estero, which is directly aligned with the onshore trend of the fault; its linear form may well have been controlled by a zone of structural weakness associated with the inferred southerly part of the fault. South of Port Estero, however, there is no evidence of faulting observable in the seismic reflection profiles across Estero Bay, and the trend defined by the Los Osos Valley-Estero Bay series of lower Miocene or Oligocene intrusives extends across the San Simeon trend without deviation.

North of Point Piedras Blancas, Silver[26] reports a fault with about 5 kilometers of vertical separation between the 4-kilometer-thick Tertiary section in the offshore basin and the nearby 1-kilometer-high exposure of Franciscan basement rocks in the coastline mountain front. The existence of a fault in this region is also indicated by the 30- milligal gravity anomaly between the offshore basin and the onshore ranges (Plate II of Appendix 2.5D of Reference 27 in Section 2.3). This postulated fault may well be a northward extension of the San Simeon fault. If this is the case, the San Simeon fault may have a total length of as much as 60 miles.

Between Point San Simeon and Ragged Point, the San Simeon fault lies along the base of a broad peninsula, the surface of which is characterized by elevated marine terraces and younger, steep-walled ravines and canyons. The low, terraced topography of the peninsula contrasts sharply with that of the steep mountain front that rises immediately

behind it. Clearly, the ground west of the main fault represents a part of the sea floor that has been locally arched up.

This has resulted in exposure of the fault, which elsewhere is concealed underwater off the shoreline.

The ground between the San Simeon fault and the southwest coastline of the Piedras Blancas peninsula is underlain by faulted blocks and slivers of Franciscan rocks, serpentinites, Tertiary sedimentary breccia and volcanic rocks, and Miocene shale. The faulted contacts between these rock masses trend somewhat more westerly than the trend of the San Simeon fault. One north-dipping reverse fault, which separates serpentinite from graywacke, has broken marine terrace deposits in at least two places, one of them in the basal part of the lowest and youngest terrace. Movement along this branch fault has therefore occurred less than 130,000 years before the present, although the uppermost, youngest Pleistocene deposits are apparently not broken. Prominent topographic lineations defined by northwest-aligned ravines that incise the upper terrace surface, on the other hand, apparently have originated through headward gully erosion along faults and faulted contacts, rather than through the effects of surface faulting.

The characteristics of the San Simeon fault can be summarized as follows: The fault may be related to a fault along the coast to the north that displays some 5 kilometers of vertical displacement. Near San Simeon, it exhibits probable Pleistocene right-lateral strike-slip movement of as much as 1500 feet near San Simeon, although it apparently does not break dune sand deposits of late Pleistocene or early Holocene age. A branch reverse fault, however, breaks upper Pleistocene marine terrace deposits. The San Simeon fault may extend as far south as Point Estero, but it dies out before crossing the northern part of Estero Bay.

5. Santa Lucia Bank Fault

South of the latitude of Point Piedras Blancas, the western boundary of the main offshore Santa Maria Basin is defined by the east-facing scarp along the east side of the Santa Lucia Bank. This scarp is associated with the Santa Lucia Bank fault, the structure that separates the subsided block under the basin from the structural high of the bank. The escarpment that rises above the west side of the fault trace has a maximum height of about 450 feet, as shown on U.S. Coast and Geodetic Survey (USC&GS) Bathymetric Map 1306N-20.

The Santa Lucia Bank fault can be traced on the sea floor for a distance of about 65 miles. Extensions that are overlapped by upper Tertiary strata continue to the south for at least another 10 miles, as well as to the north. The northern extension may be related to another, largely buried fault that crosses and may intersect the trend of the Santa Lucia Bank fault. This second fault extends to the surface only at points north of the latitude of Point Piedras Blancas.

West of the Santa Lucia Bank fault, between N latitudes 34°30' and 30°, several subparallel faults are characterized by apparent surface scarps. The longest of these faults trends along the upper continental slope for a distance of as much as 45 miles, and generally exhibits a west-facing scarp. Other faults are present in a zone about 30 miles long lying between the 45 mile fault and the Santa Lucia Bank fault. These faults range from 5 to 15 or more miles in length, and have both east-and west-facing scarps.

This zone of faulting corresponds closely in space with the cluster of earthquake epicenters around N latitude 34°45' and 121°30'W longitude, and it probably represents the source structure for those shocks (Figure 2.5-3).

2.5.1.1.2.3 Tectonic Features in the Vicinity of the DCPP Site

Geologic relationships between the major fold and fault structures in the vicinity of Diablo Canyon are shown in Figures 2.5-5, 2.5-6, and 2.5-7, and are described and illustrated in Appendix 2.5D of Reference 27 of Section 2.3. The San Luis Ranges-Estero Bay area is characterized structurally by west-northwest-trending folds and faults. These include the San Luis-Pismo syncline and the bordering Los Osos Valley and Point San Luis antiformal highs, and the West Huasna, Edna, and San Miguelito faults. A few miles offshore, the structural features associated with this trend merge into a north-northwest-trending zone of folds and faults that is referred to herein as the offshore Santa Maria Basin East Boundary zone of folding and faulting. The general pattern of structural highs and lows of the onshore area is warped and stepped downward to the west across this boundary zone, to be replaced by more northerly-trending folds in the lower part of the offshore basin section. The overall relationship between the onshore Coast Ranges and the offshore continental margin is one of differential uplift and subsidence. The East Boundary zone represents the structural expression of the zone of inflection between these regions of contrasting vertical movement.

In terms of regional relationships, structural style, and history of movement, the faults in the San Luis Ranges-Estero Bay vicinity may be characterized as follows:

1. West Huasna Fault

This fault zone separates the large downwarp of the Huasna syncline on the northeast from Franciscan assemblage rocks of the Los Osos Valley antiform and the Tertiary section of the southerly part of the San Luis-Pismo syncline on the southwest. The West Huasna fault is thought to join with the Suey fault to the south. Differences in thicknesses and facies relationships between units of apparently equivalent age on opposite sides of the fault are interpreted as indicating lateral movement along the fault; however, the available evidence regarding the amount and even the relative sense of displacement is not consistent. The West Huasna shows no evidence of late Quaternary activity.

2. Edna Fault Zone

The Edna fault zone lies along a west-northwesterly trend that extends obliquely from the West Huasna fault at its southeast end to the hills of the San Luis Range south of Morro Bay. Several isolated breaks that lie on a line with the trend are present in the Tertiary strata beneath the south part of Estero Bay, east of the Santa Maria Basin East Boundary fault zone across the mouth of the bay.

The Edna fault is typically a zone of two or more anastomosing branches that range in width from 1/2 mile to as much as 1-1/2 miles. Although individual strands are variously oriented and exhibit various senses of amounts of movement, the zone as a whole clearly expresses high-angle dip-slip displacement (down to the southwest). The irregular traces of major strands suggest that little, if any, strike-slip movement has occurred. Preliminary geologic sections shown by Hall and Surdam(21) and Hall(20) imply that the total amount of vertical separation ranges from 1500 to a few thousand feet along the central part of the fault zone. The amount of displacement across the main fault trend evidently decreases to the northwest, where the zone is mostly overlapped by upper Tertiary strata.

It may be, however, that most of the movement in the Baywood Park vicinity has been transferred to the north-trending branch of the Edna, which juxtaposes Pliocene and Franciscan rocks where last exposed. In the northwesterly part of the San Luis Range, the Edna fault forms much of the boundary between the Tertiary and basement rock sections. Most of the measurable displacements along this zone of rupture occurred during or after folding of the Pliocene Pismo Formation but prior to deposition of the lower Pleistocene Paso Robles Formation. Some additional movement has occurred during or since early Pleistocene time, however, because Monterey strata have been faulted against Paso Robles deposits along at least one strand of the Edna near the head of Arroyo Grande valley. This involved steep reverse fault movement, with the southwest side raised, in contrast to the earlier normal displacement down to the southwest.

Search has failed to reveal dislocation of deposits younger than the Paso Robles Formation, disturbance of late Quaternary landforms, or other evidence of Holocene or late Pleistocene activity.

3. San Miguelito Fault Zone

Northwesterly-trending faults have been mapped in the area between Pismo Beach and Arroyo Grande, and from Avila Beach to the vicinity of the west fork of Vineyard Canyon, north of San Luis Hill. Because these faults lie on the same trend, appear to reflect similar senses of movement, and are "separated" only by an area of no exposure along the shoreline between Pismo Beach and Avila Beach, they may well be part of a more or less continuous zone about 10 miles long. As on the Edna fault, movements along the San Miguelito fault appear to have been predominantly dip-slip, but with displacement down on the northeast. Hall's preliminary cross section indicates total

vertical separation of about 1400 feet. The fault is mapped as being overlain by unbroken deposits of the Paso Robles Formation near Arroyo Grande.

Field checking of the ground along the projected trend of the San Miguelito fault zone northwest of Vineyard Canyon in the San Luis Range has substantiated Hall's note that the fault cannot be traced west of that area.

Detailed mapping of the nearly continuous sea cliff exposures extending across this trend northeast of Point Buchon has shown there is no faulting along the San Miguelito trend at the northwesterly end of the range. Like the Edna fault zone, the San Miguelito fault zone evidently represents a zone of high-angle dip-slip rupturing along the flank of the San Luis-Pismo syncline.

4. East Boundary Zone of the Offshore Santa Maria Basin

The boundary between the offshore Santa Maria Basin and the onshore features of the southern Coast Ranges is a 4 to 5 wide zone of generally north-northwest-trending folds, faults, and onlap unconformities referred to as the "Hosgri fault zone" by Wagner[31]. The geology of this boundary zone has been investigated in detail by means of extensive seismic reflection profiling, high resolution surface profiling, and side scan sonar surveying.

More general information about structural relationships along the boundary zone has been obtained from the pattern of Bouguer Gravity anomaly values that exist in its vicinity. These data show the East Boundary zone to consist of a series of generally parallel north-northwest-trending faults and folds, developed chiefly in upper Pliocene strata that flank upwarped lower Pliocene and older rocks. The zone extends from south of the latitude of Point Sal to north of Point Piedras Blancas. Within the zone, individual fault breaks range in length from less than 1000 feet up to a maximum of about 30 miles. The overall length of the zone is approximately 90 miles, with about 60 miles of relatively continuous faulting.

The apparent vertical component of movement is down to the west across some faults and down to the east across others. Along the central reach of the zone, opposite the San Luis Range, a block of ground has been dropped between the two main strands of the fault to form a graben structure. Within the graben, and at other points along the East Boundary zone, bedding in the rock has been folded down toward the upthrown side of the west side down fault. This feature evidently is an expression of "reverse drag" phenomena.

The axes of folds in the ground on either side of the principal fault breaks can be traced for distances of as much as 22 miles. The fold axes typically are nearly horizontal; maximum axial plunges seem to be 5° or less. The structure and onlap relationships of the upper Pliocene, as reflected in the configuration of the unconformity at its base, are such that it consistently rises from the offshore basin and across the boundary zone via a series of upwarps, asymmetric folds, and faults. This configuration seems to

correspond generally to a zone of warping and partial disruption along the boundary between relatively uplifting and subsiding regions.

2.5.1.1.3 Geologic History

The geologic history reflected by the rocks, structural features, and landforms of the San Luis Range is typical of that of the southern Coast Ranges of California in its length and complexity. Six general episodes for which there is direct evidence can be tabulated as follows:

Age	Episode	Evidence
Late Mesozoic	Development of Franciscan and Upper Cretaceous rock assemblages	Franciscan and other Mesozoic rocks
Late Mesozoic - Early Tertiary	Early Coast Ranges deformation	Structural features pre-served in the Mesozoic rocks
Mid-Tertiary	Uplift and erosion	Erosion surface at the base of the Tertiary section
Mid- and late-Tertiary	Accumulation of Miocene and Pliocene sedimentary and volcanic rocks	Vaqueros, Rincon, Obispo, Point Sal, Monterey, and Pismo Formation and associated volcanic intrusive, and brecciated rocks
Pliocene	Folding and faulting associated with the Pliocene Coast Ranges deformation	Folding and faulting of the Tertiary and basement rocks
Pleistocene	Uplift and erosion, development of successive tiers of wave-cut-benches alluvial fan, talus, and landslide deposition.	Pleistocene and Holocene deposits, present land-forms.

The earliest recognizable geologic history of the southern Coast Ranges began in Mesozoic time, during the Jurassic period when eugeosynclinal deposits (graywacke sandstone, shale, chert, and basalt) accumulated in an offshore trench developed in oceanic crust.

Some time after the initiation of Franciscan sedimentation, deposition of a sequence of miogeosynclinal or shelf sandstones and shales, known as the Great Valley Sequence, began on the continental crust, at some distance to the east of the Franciscan trench. Deposition of both sequences continued into Cretaceous time, even while the crustal basement section on which the Great Valley strata were being deposited was undergoing plutonism involving emplacement of granitic rocks. Subsequently, the Franciscan assemblage, the Great Valley Sequence, and the granite-intruded basement rocks were tectonically juxtaposed. The resulting terrane consisted generally of granitic

basement thrust over intensely deformed Franciscan, with Great Valley Sequence strata overlying the basement, but thrust over and faulted into the Franciscan.

The processes that were involved in the tectonic juxtaposition evidently were active during the Mesozoic, and continued into the early Tertiary. Page[25] has shown that they were completed by no later than Oligocene time, so that the dual core complex basement of the southern Coast Ranges was formed by then.

The Miocene and later geologic history of the southern Coast Ranges region began with deposition of the Vaqueros and Rincon Formations on a surface eroded on the Franciscan and Great Valley core complex rocks.

Following deposition and some deformation and erosion of these formations, the stratigraphic unit that includes the Point Sal and Obispo Formations as approximately contemporaneous facies was laid down. The Obispo consists of a section of tuffaceous sandstone and mudstone, with lesser amounts of shale, and lensing layers of vitric and lithic-crystal tuff. Locally, the unit is featured by masses of clastic-textured tuffaceous rock that exhibit cross-cutting intrusive relations with the bedded parts of the formation. The Obispo and Point Sal were folded and locally eroded prior to initiation of the main episode of upper Miocene and Pliocene marine sedimentation.

During late middle Miocene to late Miocene time, deposition of the thick sections of silica-rich shale of the Monterey Formation began. Deposition of this formation and equivalent strata took place throughout much of the coastal region of California, but apparently was centered in a series of offshore basins that all developed at about the same time, some 10 to 12 million years ago. Local volcanism toward the latter part of this time is shown by the presence of diabase dikes and sills in the Monterey. Near the end of the Miocene, the Monterey strata were subjected to compressional deformation resulting in folding, in part with great complexity, and in faulting. Near the old continental margin, represented by the Sur-Nacimiento fault zone, the deformation was most intense, and was accompanied by uplift. This apparently resulted in the first development of many of the large folds of the southern Coast Ranges including the Huasna and San Luis-Pismo synclines, and in the partial erosion of the folded Monterey section in areas of uplift. The pattern of regional uplift of the Coast Ranges and subsidence of the offshore basins, with local upwarping and faulting in a zone of inflection along the boundary between the two regions, apparently became well established during the episode of late Miocene and Mio-Pliocene diastrophism.

Sedimentation resumed in Pliocene time throughout much of the region of the Miocene basins, and several thousand feet of siltstone and sandstone was deposited. This was the last significant episode of marine sedimentation in the region of the present Coast Ranges. Pliocene deposits in the region of uplift were then folded, and there was renewed movement along most of the preexisting larger faults.

Differential movements between the Coast Ranges uplift and the offshore basins were again concentrated along the boundary zone of inflection, resulting in upwarping and

faulting of the basement, Miocene, and Pliocene sections. Relative displacement across parts of this zone evidently was dominantly vertical, because the faulting in the Pliocene has definitely extensional character, and Miocene structures can be traced across the zone without apparent lateral offset. The basement and Tertiary sections step down seaward, away from the uplift, along a system of normal faults having hundreds to nearly a thousand feet of dip-slip offset. A second, more seaward system of normal faults is antithetic to the master set and exhibits only tens to a few hundreds of feet of displacement. Strata between these faults locally exhibit reverse drag downfolding toward the edge of the Pliocene basin, whereas the section is essentially undeformed farther offshore. This style of deformation indicates a passive response, through gravity tectonics, to the onshore uplift.

The Plio-Pleistocene uplift was accompanied by rapid erosion, with consequent nearby deposition of clastic sediments such as the Paso Robles Formation in valleys throughout the southern Coast Ranges. The high-angle reverse and normal faulting observed by Compton(38) in the northern Santa Lucia Range also occurred farther south, probably more or less contemporaneously with accumulation of the continental deposits. Much of the Quaternary faulting other than that related to the San Andreas right lateral stress-strain system may well have occurred at this time.

Tectonic activity during the Quaternary has involved continued general uplift of the southern Coast Ranges, with superimposed local downwarping and continued movement along faults of the San Andreas system. The uplift is shown by the general high elevation and steep youthful topography that characterizes the Coast Ranges and by the widespread uplifted marine and stream terraces. Local downwarping can be seen in valleys, such as the Santa Maria Valley, where thick sections of Plio-Pleistocene and younger deposits have accumulated. Evidence of significant late Quaternary fault movement is seen in the topography along the Rinconada-San Marcos, Espinosa, San Simeon, and Santa Lucia Bank faults, as well as along the San Andreas itself. Only along the San Andreas, however, is there evidence of Holocene or contemporary movement.

The latest stage in the evolution of the San Luis Range has extended from mid-Pleistocene time to the present, and has involved more or less continuous interaction between apparent uplift of the range and alternating periods of erosion or deposition, especially along the coast, during times of relatively rising, falling, or unchanging sea level. The development of wave-cut benches and the accumulation of marine deposits on these benches have provided a reliable guide to the minimum age of latest displacements along breaks in the underlying bedrock. Detailed exploration of the interfaces between wave-cut benches and overlying marine deposits at the site of DCPP has shown that no breaks extend across these interfaces. This demonstrates that the youngest faulting or other bedrock breakage in that area antedated the time of terrace cutting, which is on the order of 80,000 to 120,000 years before the present.

The bedrock section and the surficial deposits that formerly capped this bedrock on which the power plant facilities are located have been studied in detail to determine

whether they express any evidence of deformation or dislocation ascribable to earthquake effects.

The surficial geologic materials at the site consisted of a thin, discontinuous basal section of rubbly marine sand and silty sand, and an overlying section of nonmarine rocky sand and sandy clay alluvial and colluvial deposits. These deposits were extensively exposed by exploratory trenches, and were examined and mapped in detail. No evidence of earthquake-induced effects such as lurching, slumping, fissuring, and liquefaction was detected during this investigation.

The initial movement of some of the landslide masses now present in Diablo Canyon upstream from the switchyard area may have been triggered by earthquake shaking. It is also possible that some local talus deposits may represent earthquake-triggered rock falls from the sea cliff or other steep slopes in the vicinity.

Deformation of the rock substrata in the site area may well have been accompanied by earthquake activity at the time of its occurrence in the geologic past. There is no evidence, however, of post-terrace earthquake effects in the bedrock where the power plant is being constructed.

2.5.1.1.4 Stratigraphy of the San Luis Range and Vicinity

The geologic section exposed in the San Luis Range comprises sedimentary, igneous, and tectonically emplaced ultrabasic rocks of Mesozoic age, sedimentary, pyroclastic, and hypabyssal intrusive rocks of Tertiary age, and a variety of surficial deposits of Quaternary age. The lithology, age, and distribution of these rocks were studied by Headlee and more recently have been mapped in detail by Hall. The geology of the San Luis Range is shown in Figure 2.5-6 with a geologic cross section constructed using exploratory oil wells shown in Figure 2.5-7. The geologic events that resulted in the stratigraphic units described in this section are discussed in Section 2.5.1.1.3, Geologic History.

2.5.1.1.4.1 Basement Rocks

An assemblage of rocks typical of the Coast Ranges basement terrane west of the Nacimiento fault zone is exposed along the south and northeast sides of the San Luis Range. As described by Headlee, this assemblage includes quartzose and greywacke sandstone, shale, radiolarian chert, intrusive serpentine and diabase, and pillow basalt. Some of these rocks have been dated as Upper Cretaceous from contained microfossils, including pollen and spores, and Headlee suggested that they may represent dislocated parts of the Great Valley Sequence. There is contrasting evidence, however, that at least the pillow basalt and associated cherty rocks may be more typically Franciscan. Certainly, such rocks are characteristic of the Franciscan terrane. Further, a potassium-argon age of 156 million years, equivalent to Upper Jurassic, has been determined for a core of similar rocks obtained from the bottom of the Montodoro Well No. 1 near Point Buchon.

2.5.1.1.4.2 Tertiary Rocks

Five formational units are represented in the Tertiary section of the San Luis Range. The lower part of this section comprises rocks of the Vaqueros, Rincon, and Obispo Formations, which range in age from lower Miocene through middle Miocene. These strata crop out in the vicinity of Hazard Canyon, at the northwest end of the range, and in a broad band along the south coastal margin of the range. In both areas the Vaqueros rests directly on Mesozoic basement rocks. The core of the western San Luis Range is underlain by the Upper Miocene Monterey Formation, which constitutes the bulk of the Tertiary section. The Upper Miocene to Lower Pliocene Pismo Formation crops out in a discontinuous band along the southwest flank and across the west end of the range, resting with some discordance on the Monterey section and elsewhere directly on older Tertiary or basement rocks.

The coastal area in the vicinity of Diablo Canyon is underlain by strata that have been variously correlated with the Obispo, Point Sal, and Monterey Formations. Headlee, for example, has shown the Point Sal as overlying the Obispo, whereas Hall has considered these two units as different facies of a single time-stratigraphic unit. Whatever the exact stratigraphic relationships of these rocks might prove to be, it is clear that they lie above the main body of tuffaceous sedimentary rocks of the Obispo Formation and below the main part of the Monterey Formation. The existence of intrusive bodies of both tuff breccia and diabase in this part of the section indicates either that local volcanic activity continued beyond the time of deposition of the Obispo Formation, or that the section represents a predominantly sedimentary facies of the upper part of the Obispo Formation. In either case, the strata underlying the power plant site range downward through the Obispo Formation and presumably include a few hundred feet of the Rincon and Vaqueros Formations resting upon a basement of Mesozoic rocks.

A generalized description of the major units in the Tertiary section follows, and a more detailed description of the rocks exposed at the power plant site is included in a later section.

The Vaqueros Formation has been described by Headlee as consisting of 100 to 400 feet of resistant, massive, coarse-grained, calcareously cemented bioclastic sandstone. The overlying Rincon Formation consists of 200 to 300 feet of dark gray to chocolate brown calcareous shale and mudstone.

The Obispo Formation (or Obispo Tuff) is 800 to 2000 feet thick and comprises alternating massive to thick-bedded, medium to fine grained vitric-lithic tuffs, finely laminated black and brown marine siltstone and shale, and medium grained light tan marine sandstone. Headlee assigned to the Point Sal Formation a section described as consisting chiefly of medium to fine grained silty sandstone, with several thin silty and fossiliferous limestone lenses; it is gradational upward into siliceous shale characteristic of the Monterey Formation. The Monterey Formation itself is composed predominantly of porcelaneous and finely laminated siliceous and cherty shales.

The Pismo Formation consists of massive, medium to fine grained arkosic sandstone, with subordinate amounts of siltstone, sandy shale, mudstone, hard siliceous shale, and chert.

2.5.1.1.4.3 Quaternary Deposits

Deposits of Pleistocene and Holocene age are widespread on the coastal terrace benches along the southwest margin of the San Luis Range, and they exist farther onshore as local alluvial and stream-terrace deposits, landslide debris, and various colluvial accumulations. The coastal terrace deposits include discontinuous thin basal sections of marine silt, sand, gravel, and rubble, some of which are highly fossiliferous, and generally much thicker overlying sections of talus, alluvial-fan debris, and other deposits of landward origin. All of the marine deposits and most of the overlying nonmarine accumulations are of Pleistocene age, but some of the uppermost talus and alluvial deposits are Holocene. Most of the alluvial and colluvial materials consist of silty clayey sand with irregularly distributed fragments and blocks of locally exposed rock types. The landslide deposits include chaotic mixtures of rock fragments and fine-grained matrix debris, as well as some large masses of nearly intact to thoroughly disrupted bedrock.

A more detailed description of surficial deposits that are present in the vicinity of the power plant site is included in a later section.

2.5.1.1.5 Structure of the San Luis Range and Vicinity

2.5.1.1.5.1 General Features

The geologic structure of the San Luis Range-Estero Bay and adjacent offshore area is characterized by a complex set of folds and faults (Figures 2.5-5, 2.5-6, and 2.5-7). Tectonic events that produced these folds and faults are discussed in Section 2.5.1.1.3, Geologic History. The San Luis Range-Estero Bay and adjacent offshore area lies within the zone of transition from the west-trending Transverse Range structural province to the northwest-trending Coast Ranges province. Major structural features are the long narrow downfold of the San Luis-Pismo syncline and the bordering antiformal structural highs of Los Osos Valley on the northeast, and of Point San Luis and the adjacent offshore area on the southwest. This set of folds trends obliquely into a north-northwest aligned zone of basement upwarping, folding, and high-angle normal faulting that lies a few miles off the coast. The main onshore folds can be recognized, by seismic reflection and gravity techniques, in the structure of the buried, downfaulted Miocene section that lies across (west of) this zone.

Lesser, but yet important structural features in this area include smaller zones of faulting and trends of volcanic intrusives. The Edna and San Miguelito fault zones disrupt parts of the northeast and southwest flanks of the San Luis-Pismo syncline. A southward extension of the San Simeon fault, the existence of which is inferred on the basis of the linearity of the coastline between Cambria and Point Estero, and of the gravity gradient

in that area, may extend into, and die out within, the northern part of Estero Bay. An aligned series of plugs and lensoid masses of Tertiary volcanic rocks that intrude the Franciscan Formation along the axis of the Los Osos Valley antiform extends from the outer part of Estero Bay southeastward for 22 miles (Figure 2.5-6).

These features define the major elements of geologic structure in the San Luis Range-Estero Bay area. Other structural elements include the complex fold and fault structures within the Franciscan core complex rocks and the numerous smaller folds within the Tertiary section.

2.5.1.1.5.2 San Luis-Pismo Syncline

The main synclinal fold of the San Luis Range, referred to here as the San Luis-Pismo syncline, trends about N60°W and forms a structural trend more than 15 miles in length. The fold system comprises several parallel anticlines and synclines across its maximum onshore width of about 5 miles. Individual folds of the system typically range in length from hundreds of feet to as much as 10,000 feet. The folds range from zero to more than 30° in plunge, and have flank dips as steep as 90°. Various kinds of smaller folds exist locally, especially flexures and drag folds associated with tuff intrusions and with zones of shear deformation.

Near Estero Bay, the major fold extends to a depth of more than 6000 feet. Farther south, in the central part of the San Luis Range, it is more than 11,000 feet deep. Parts of the northeast flank of the fold are disrupted by faults associated with the Edna fault zone. Local breaks along the central part of the southwest flank have been referred to as the San Miguelito fault zone.

2.5.1.1.5.3 Los Osos Valley Antiform

The body of Franciscan and Great Valley Sequence rocks that crops out between the San Luis-Pismo and Huasna synclines is here referred to as the Los Osos Valley antiform. This composite structure extends southward from the Santa Lucia Range, across the central and northern part of Estero Bay, and thence southeastward to the point where it is faulted out at the juncture of the Edna and the West Huasna fault zones.

Notable structural features within this core complex include northwest- and west-northwest- trending-faults that separate Franciscan melange, graywacke, metavolcanic, and serpentinite units. The serpentinites have been intruded or dragged within faults, apparently over a wide range of scales. One of the more persistent zones of serpentinite bodies occurs along a trend which extends west-northwestward from the West Huasna fault. It has been suggested that movement from this fault may have taken place within this serpentine belt. The range of hills that lies between the coast and Highway 1 between Estero Bay and Cambria is underlain by sandstone and minor shale of the Great Valley Sequence, referred to as the Cambria slab, which has been underthrust by Franciscan rocks. The thrust contact extends southeastward under

Estero Bay near Cayucos. This contact is probably related to the fault contact between Great Valley and Franciscan rocks located just north of San Luis Obispo, which Page has shown to be overlain by unbroken lower Miocene strata.

A prominent feature of the Los Osos Valley antiform is the line of plugs and lensoid masses of intrusive Tertiary volcanic rocks. These distinctive bodies are present at isolated points along the approximate axis of the antiform over a distance of 22 miles, extending from the center of outer Estero Bay to the upper part of Los Osos Valley (Figure 2.5-6). The consistent trend of the intrusives provides a useful reference for assessing the possibility of northwest-trending lateral slip faulting within Estero Bay. It shows that such faulting has not extended across the trend from either the inferred San Simeon fault offshore south extension, or from faults in the ground east of the San Simeon trend.

2.5.1.1.5.4 Edna and San Miguelito Fault Zones

These fault zones are described in Section 2.5.1.1.2.3.

2.5.1.1.5.5 Adjacent Offshore Area and East Boundary of the Offshore Santa Maria Basin

The stratigraphy and west-northwest-trending structure that characterize the onshore region from Point Sal to north of Point Estero have been shown by extensive marine geophysical surveying to extend into the adjacent offshore area as far as the north-northwest trending structural zone that forms a boundary with the main offshore Santa Maria Basin. Owing to the irregular outline of the coast, the width of the offshore shelf east of this boundary zone ranges from 2-1/2 to as much as 12 miles. The shelf area is narrowest opposite the reach of coast between Point San Luis and Point Buchon, and widest in Estero Bay and south of San Luis Bay.

The major geologic features that underlie the near-shore shelf include, from south to north, the Casmalia Hills anticline, the broad Santa Maria Valley downwarp, the anticlinal structural high off Point San Luis, the San Luis-Pismo syncline, and the Los Osos Valley antiform.

The form of these features is defined by the outcrop pattern and structure of the older Pliocene, Miocene, and basement core complex rocks. The younger Pliocene strata that constitute the upper 1000 to 2000 feet of section in the adjacent offshore Santa Maria Basin are partly buttressed and partly faulted against the rocks that underlie the near-shore shelf, and they unconformably overlap the boundary zone and parts of the shelf in several areas.

The boundaries between the San Luis-Pismo syncline and the adjacent Los Osos Valley and Point San Luis antiforms can be seen in the offshore area to be expressed chiefly as zones of inflection between synclinal and anticlinal folds, rather than as zones of fault rupture such as occurs farther south along the Edna and San Miguelito faults.

Isolated west-northwest- trending faults of no more than a few hundred feet displacement are located along the northeast flank of the syncline in Estero Bay. These faults evidently are the northwesternmost expressions of breakage along the Edna fault trend.

The main San Luis-Pismo synclinal structure opens to the northwest, attaining a maximum width of 8 or 9 miles in the southerly part of Estero Bay. The Point San Luis high, on the other hand, is a domal structure, the exposed basement rock core of which is about 10 miles long and 5 miles wide.

The general characteristics of the Santa Maria Basin East Boundary zone have been described in Section 2.5.1.1.2.3. As was noted there, the zone is essentially an expression of the boundary between the synclinorial downwarp of the offshore basin and the regional uplift of the southern Coast Ranges. In the vicinity of the San Luis Range, the zone is characterized by pronounced upwarping and normal faulting of the basement and overlying Tertiary rock sections. Both modes of deformation have contributed to the structural relief of about 500 feet in the Pliocene section, and of 1500 feet or more in the basement rocks, across this boundary. Successively younger strata are banked unconformably against the slopes that have formed from time to time in response to the relative uplifting of the ground east of the boundary zone.

A series of near-surface structural troughs forms prominent features within the segment of the boundary zone structure that extends between the approximate latitudes of Arroyo Grande and Estero Bay. This trough structure apparently has formed through the extension and subsidence of a block of ground in the zone where the downwarp of the offshore basin has pulled away from the Santa Lucia uplift. Continued subsidence of this block has resulted in deformation and partial disruption of the buttress unconformity between the offshore Pliocene section and the near-shore Miocene and older rocks. This deformation is expressed by normal faulting and reverse drag type downfolding of the Pliocene strata adjacent to the contact, along the east side of the trough.

On the opposite, seaward side of the trough, a series of antithetic down-to-the-east normal faults of small displacement has formed in the Pliocene strata west of the contact zone. These faults exhibit only a few tens of feet displacement, and they seem to exhibit constant or even decreasing displacement downward.

The structural evolution of the offshore area near Estero Bay and the San Luis Range involved episodes of compressional deformation that affected the upper Tertiary section similarly on opposite sides of the boundary zone. The section on either side exhibits about the same intensity and style of folding. Major folds, such as the San Luis-Pismo syncline and the Piedras Blancas anticline, can be traced into the ground across the boundary zone.

The internal structure of the zone, including the presence of several on-lap unconformities in the adjacent Pliocene section, shows that, at least during Pliocene

and early Pleistocene time, the boundary zone has been the inflection line between the Coast Ranges uplift and the offshore Santa Maria Basin downwarp.

Evidence that uplift has continued through late Pleistocene time, at least in the vicinity of the San Luis Range, is given by the presence of successive tiers of marine terraces along the seaward flank of the range. The wave-cut benches and back scarps of these terraces now exist at elevations ranging from about -300 feet (below sea level) to more than 300 feet above sea level.

The ground within which the East Boundary zone lies has been beveled by the post-Wisconsin marine transgression, and so the zone generally is not expressed topographically. Small topographic features, such as a seaward topographic step-up of the sea floor surface across the east-down fault at the BBN[37] (offshore) survey line 27 crossing, in Estero Bay, and several possible fault-line notch back scarps, however, may represent minor topographic expressions of deformation within the zone.

2.5.1.1.6 Structural Stability

The potential for surface or subsurface subsidence, uplift, or collapse at the site or in the region surrounding the site, is discussed in Section 2.5.4, Stability of Subsurface Materials.

2.5.1.1.7 Regional Groundwater

Groundwater in the region surrounding the site is used as a backup source due to its poor quality and the lack of a significant groundwater reservoir. Section 2.4.13 states that most of the groundwater at the site or in the area around the site is either in the alluvial deposits of Diablo Creek or seeps from springs encountered in excavations at the site.

2.5.1.2 Site Geology

2.5.1.2.1 Site Physiography

The site consists of approximately 750 acres near the mouth of Diablo Creek and is located on a sloping coastal terrace, ranging from 60 to 150 feet above sea level. The terrace terminates at the Pacific Ocean on the southwest and extends toward the San Luis Mountains on the northeast. The terrace consists of bedrock overlain by surficial deposits of marine and nonmarine origin.

The remainder of this section presents a detailed description of site geology.

2.5.1.2.2 General Features

The area of the DCPP site is a coastal tract in San Luis Obispo County approximately 6.5 miles northwest of Point San Luis. It lies immediately southeast of the mouth of

Diablo Canyon, a major westward-draining feature of the San Luis Range, and about a mile southeast of Lion Rock, a prominent offshore element of the highly irregular coastline.

The ground being developed as a power plant site occupies an extensive topographic terrace about 1000 feet in average width. In its pregrading, natural state, the gently undulating surface of this terrace sloped gradually southwestward to an abrupt termination along a cliff fronting the ocean; in a landward, or northeasterly, direction, it rose with progressively increasing slope to merge with the much steeper front of a foothill ridge of the San Luis Range. The surface ranged in altitude from 65 to 80 feet along the coastline to a maximum of nearly 300 feet along the base of the hillslope to the northeast, but nowhere was its local relief greater than 10 feet. Its only major interruption was the steep-walled canyon of lower Diablo Creek, a gash about 75 feet in average depth.

The entire subject area is underlain by a complex sequence of stratified marine sedimentary rocks and tuffaceous volcanic rocks, all of Tertiary (Miocene) age. Diabasic intrusive rocks are locally exposed high on the walls of Diablo Canyon at the edge of the area. Both the sedimentary and volcanic rocks have been folded and otherwise disturbed over a considerable range of scales.

Surficial deposits of Quaternary age are widespread. In a few places, they are as thick as 50 feet, but their average thickness probably is on the order of 20 feet over the terrace areas and 10 feet or less over the entire mapped ground. The most extensive deposits underlie the main topographic terrace.

Like many other parts of the California coast, the Diablo Canyon area is characterized by several wave-cut benches of Pleistocene age. These surfaces of irregular but generally low relief were developed across bedrock by marine erosion, and they are ancient analogues of the benches now being cut approximately at sea level along the present coast. They were formed during periods when the sea level was higher, relative to the adjacent land, than it is now. Each is thinly and discontinuously mantled with marine sand, gravel, and rubble similar to the beach and offshore deposits that are accumulating along the present coastline. Along its landward margin each bears thicker and more localized coarse deposits similar to the modern talus along the base of the present sea cliff.

Both the ancient wave-cut benches and their overlying marine and shoreline deposits have been buried beneath silty to gravelly detritus derived from landward sources after the benches were, in effect, abandoned by the ocean. This nonmarine cover is essentially an apron of coalescing fan deposits and other alluvial debris that is thickest adjacent to the mouths of major canyons.

Where they have been deeply trenched by subsequent erosion, as along Diablo Canyon in the map areas, these deposits can be seen to have buried some of the benches so deeply that their individual identities are not reflected by the present (pregrading) rather

smooth terrace topography. Thus, the surface of the main terrace is defined mainly by nonmarine deposits that conceal both the older benches of marine erosion and some of the abruptly rising ground that separates them (see Figures 2.5-8 and 2.5-10).

The observed and inferred relationships among the terrace surfaces and the wave-cut benches buried beneath them can be summarized as follows:

Wave-cut Bench		Terrace Surface	
Altitude, feet	Location	Altitude, feet	Location
170-175	Small remnants on side of Diablo Canyon	Mainly 170-190	Sides of Diablo Canyon upper parts of main terrace; in places separated from lower
145-155	Very small remnants on sides of Diablo Canyon	Mainly 150-170	parts of terrace by scarps
120-130 90-100	Subparallel benches elongate in a northwest-southeast direction but with considerable aggregate width wholly beneath main terrace surface	Mainly 70-160	Most of main terrace, a widespread surface on a composite section of nonmarine deposits; no well-defined scarps
30-45	Small remnants above modern sea cliff		No depositional terrace
Approx. 0	Small to moderately large area along present coastline		

Within the subject area the wave-cut benches increase progressively in age with increasing elevation above present sea level; hence, their order in the above list is one of decreasing age. By far, the most extensive of these benches slopes gently seaward from a shoreline angle that lies at an elevation of 100 feet above present sea level.

The geology of the power plant site is shown in the site geologic maps, Figures 2.5-8 and 2.5-9, and geologic section, Figure 2.5-10.

2.5.1.2.3 Stratigraphy

2.5.1.2.3.1 Obispo Tuff

The Obispo Tuff, which has been classified either as a separate formation or as a member of the Miocene Monterey Formation, is the oldest bedrock unit exposed in the site area. Its constituent rocks generally are well exposed, appear extensively in the coastward parts of the area, and form nearly all of the offshore prominences and shoals. They are dense to highly porous, and thinly layered to almost massive. Their color

ranges from white to buff in fresh exposures, and from yellowish to reddish brown on weathered surfaces, many of which are variegated in shades of brown. Outcrop surfaces have a characteristic "punky" to crusty appearance, but the rocks in general are tough, cohesive, and relatively resistant to erosion.

Several pyroclastic rock types constitute the Obispo Tuff ("To" on map, Figure 2.5-8) in and near the subject area. By far, the most widespread is fine-grained vitric tuff with rare to moderately abundant tabular crystals of sodic plagioclase. The constituent glass commonly appears as fresh shards, but in many places it has been partly or completely devitrified. Crystal tuffs are locally prominent, and some of these are so crowded with 1/8 to 3/8 inch crystals of plagioclase that they superficially resemble granitoid plutonic rocks. Other observed rock types include pumiceous tuffs, pumice-pellet tuff breccias, perlitic vitreous tuffs, tuffaceous siltstones and mudstones, and fine-grained tuff breccias with fragments of glass and various Monterey rocks. No massive flow rocks were recognized anywhere in the exposed volcanic section.

In terms of bulk composition, the pyroclastic rocks appear to be chiefly soda rhyolites and soda quartz latites. Their plagioclase, which ranges from calcic albite to sodic oligoclase, commonly is accompanied by lesser amounts of quartz as small rounded crystals and irregular crystal fragments. Biotite, zircon, and apatite also are present in many of the specimens that were examined under the microscope. Most of the tuffaceous rocks, and especially the more vitreous ones, have been locally to pervasively altered. Products of silicification, zeolitization, and pyritization are readily recognizable in many exposures, where the rocks generally are traversed by numerous thin, irregular veinlets and layers of cherty to opaline material. Veinlets and thin, pod-like concentrations of gypsum also are widespread. Where pyrite is present, the rocks weather yellowish to brownish and are marked by gossan-like crusts.

The various contrasting rock types are simply interlayered in only a few places; much more typical are abutting, intertonguing, and irregularly interpenetrating relationships over a wide range of scales. Septa and inclusions of Monterey rocks are abundant, and a few of them are large enough to be shown separately on the accompanying geologic map (Figure 2.5-8). Highly irregular inclusions, a few inches to several feet in maximum dimension, are so densely packed together in some places that they form breccias with volcanic matrices.

The Obispo Tuff is underlain by mudstones of early Miocene (pre-Monterey) age, on which it rests with a highly irregular contact that appears to be in part intrusive. This contact lies offshore in the vicinity of the power plant site, but it is exposed along the seacoast to the southeast.

In a gross way, the Obispo underlies the basal part of the Monterey formation, but many of its contacts with these sedimentary strata are plainly intrusive. Moreover, individual sills and dikes of slightly to thoroughly altered tuffaceous rocks appear here and there in the Monterey section, not uncommonly at stratigraphic levels well above its base (see Figures 2.5-8 and 2.5-13). The observed physical relationships, together with the local

occurrence of diatoms and foraminifera within the principal masses of volcanic rocks, indicate that much of the Obispo Tuff in this area probably was emplaced at shallow depths beneath the Miocene sea floor during accumulation of the Monterey strata. The tuff unit does not appear to represent a single, well-defined eruptive event, nor is it likely to have been derived from a single source conduit.

2.5.1.2.3.2 Monterey Formation

Stratified marine rocks variously correlated with the Monterey Formation, Point Sal Formation, and Obispo Tuff underlie most of the subject area, including all of that portion intended for power plant location. They are almost continuously exposed along the crescentic sea cliff that borders Diablo Cove, and elsewhere they appear in much more localized outcrops. For convenience, they are here assigned to the Monterey Formation ("Tm" on map, Figure 2.5-8) in order to delineate them from the adjacent more tuffaceous rocks so typical of the Obispo Tuff.

The observed rock types, listed in general order of decreasing abundance, are silty and tuffaceous sandstone, siliceous shale, shaly siltstone and mudstone, diatomaceous shale, sandy to highly tuffaceous shale, calcareous shale and impure limestone, bituminous shale, fine- to coarse-grained sandstone, impure vitric tuff, silicified limestone and shale, and tuff-pellet sandstone. Dark colored and relatively fine-grained strata are most abundant in the lowest part of the section, as exposed along the east side of Diablo Cove, whereas lighter colored sandstones and siliceous shales are dominant at stratigraphically higher levels farther north. In detail, however, the different rock types are interbedded in various combinations, and intervals of uniform lithology rarely are thicker than 30 feet. Indeed, the closely-spaced alternations of contrasting strata yield a prominent rib-like pattern of outcrop along much of the sea cliff and shoreline bench forming the margin of Diablo Cove.

The sandstones are mainly fine- to medium-grained, and most are distinctly tuffaceous. Shards of volcanic glass generally are recognizable under the microscope, and the very fine-grained siliceous matrix may well have been derived largely through alteration of original glassy material. Some of the sandstone contains small but megascopically visible fragments of pumice, perlitic glass, and tuff, and a few beds grade along strike into submarine tuff breccia. The sandstones are thinly to very thickly layered; individual beds 6 inches to 4 feet thick are fairly common, and a few appear to be as thick as 15 feet. Some of them are hard and very resistant to erosion, and they typically form subdued but nearly continuous elongated projections on major hillslopes (Figure 2.5-8).

The siliceous shales are buff to light gray platy rocks that are moderately hard to extremely hard according to their silica content, but they tend to break readily along bedding and fracture surfaces. The bituminous rocks and the siltstones and mudstones are darker colored, softer, and grossly more compact. Some of them are very thinly bedded or laminated, others appear almost massive or form matrices for irregularly ellipsoidal masses of somewhat sandier material. The diatomaceous, tuffaceous, and sandy rocks are lighter colored. The more tuffaceous types are softer, and the

diatomaceous ones are soft to the degree of punkiness; both kinds of rocks are easily eroded, but are markedly cohesive and tend to retain their gross positions on even the steepest of slopes.

The siliceous shale and most of the hardest, highly silicified rocks weather to very light gray, and the dark colored, fine-grained rocks tend to bleach when weathered. The other types, including the sandstones, weather to various shades of buff and light brown. Stains of iron oxides are widespread on exposures of nearly all the Monterey rocks, and are especially well developed on some of the finest-grained shales that contain disseminated pyrite. All but the hardest and most thick-bedded rocks are considerably broken to depths of as much as 6 feet in the zone of weathering on slopes other than the present sea cliff, and the broken fragments have been separated and displaced by surface creep to somewhat lesser depths.

2.5.1.2.3.3 Diabasic Intrusive Rocks

Small, irregular bodies of diabasic rocks are poorly exposed high on the walls of Diablo Canyon at and beyond the northeasterly edge of the map area. Contact relationships are readily determined at only a few places where these rocks evidently are intrusive into the Monterey Formation. They are considerably weathered, but an ophitic texture is recognizable. They consist chiefly of calcic plagioclase and augite, with some olivine, opaque minerals, and zeolitic alteration products.

2.5.1.2.3.4 Masses of Brecciated Rocks

Highly irregular masses of coarsely brecciated rocks, a few feet to many tens of feet in maximum dimension, are present in some of the relatively siliceous parts of the Monterey section that adjoin the principal bodies of Obispo Tuff. The fracturing and dislocation is not genetically related to any recognizable faults, but instead seems to have been associated with emplacement of the volcanic rocks; it evidently was accompanied by, or soon followed by, extensive silicification. Many adjacent fragments in the breccias are closely juxtaposed and have matching opposed surfaces, so that they plainly represent no more than coarse crackling of the brittle rocks. Other fragments, though angular or subangular, are not readily matched with adjacent fragments and hence may represent significant translation within the entire rock masses.

The ratio of matrix materials to coarse fragments is very low in most of the breccias and nowhere was it observed to exceed about 1:3. The matrices generally comprise smaller angular fragments of the same Monterey rocks that are elsewhere dominant in the breccias, and they characteristically are set in a siliceous cement. Tuffaceous matrices, with or without Monterey fragments, also are widespread and commonly show the effects of pervasive silicification. All the exposed breccias are firmly cemented, and they rank among the hardest and most resistant units in the entire bedrock section.

A few 3 to 18 inch beds of sandstone have been pulled apart to form separate tabular masses along specific stratigraphic horizons in higher parts of the Monterey sequence. Such individual tablets, which are boudins rather than ordinary breccia fragments, are especially well exposed in the sea cliff at the northern corner of Diablo Cove. They are flanked by much finer-grained strata that converge around their ends and continue essentially unbroken beyond them. This boudinage or separation and stringing out of sandstone beds that lie within intervals of much softer and more shaly rocks has resulted from compression during folding of the Monterey section. Its distribution is stratigraphically controlled and is not systematically related to recognizable faults in the area.

2.5.1.2.3.5 Surficial Deposits

1. Coastal Terrace Deposits

The coastal wave-cut benches of Pleistocene age, as described in a foregoing section, are almost continuously blanketed by terrace deposits (Qter in Figure 2.5-8) of several contrasting types and modes of origin. The oldest of these deposits are relatively thin and patchy in their occurrence, and were laid down along and adjacent to ancient beaches during Pleistocene time. They are covered by considerably thicker and more extensive nonmarine accumulations of detrital materials derived from various landward sources.

The marine deposits consist of silt, sand, gravel, and cobbly to bouldery rubble. They are approximately 2 feet in average thickness over the entire terrace area and reach a maximum observed thickness of about 8 feet. They rest directly upon bedrock, some of which is marked by numerous holes attributable to the action of boring marine mollusks, and they commonly contain large rounded cobbles and boulders of Monterey and Obispo rocks that have been similarly bored. Lenses and pockets of highly fossiliferous sand and gravel are present locally.

The marine sediments are poorly to very well sorted and loose to moderately well consolidated. All of them have been naturally compacted; the degree of compaction varies according to the material, but it is consistently greater than that observed in any of the associated surficial deposits of other types. Near the inner margins of individual wave-cut benches the marine deposits merge landward into coarser and less well-sorted debris that evidently accumulated along the bases of ancient sea cliffs or other shoreline slopes. This debris is locally as much as 12 feet thick; it forms broad but very short aprons, now buried beneath younger deposits, that are ancient analogues of the talus accumulations along the inner margin of the present beach in Diablo Cove. One of these occurrences, identified as "fossil Qtb" in the geologic map of Figure 2.5-8, is well exposed high on the northerly wall of Diablo Canyon.

A younger, thicker, and much more continuous nonmarine cover is present over most of the coastal terrace area. It consistently overlies the marine deposits noted above, and, where these are absent, it rests directly upon bedrock. It is composed in part of alluvial

detritus contributed during Pleistocene time from Diablo Canyon and several smaller drainage courses, and it thickens markedly as traced sourceward toward these canyons. The detritus represents a series of alluvial fans, some of which appear to have partly coalesced with adjacent ones. It is chiefly fine- to moderately-coarse-grained gravel and rubble characterized by tabular fragments of Monterey rocks in a rather abundant silty to clayey matrix. Most of it is thinly and regularly stratified, but the distinctness of this layering varies greatly from place to place.

Slump, creep, and slope-wash deposits, derived from adjacent hillsides by relatively slow downhill movement over long periods of time, also form major parts of the nonmarine terrace cover. All are loose and uncompacted. They comprise fragments of Monterey rocks in dark colored clayey matrices, and their internal structure is essentially chaotic. In some places they are crudely interlayered with the alluvial fan deposits, and elsewhere they overlie these bedded sediments. On parts of the main terrace area not reached by any of the alluvial fans, a cover of slump, creep, and slope-wash deposits, a few inches to nearly 10 feet thick, rests directly upon either marine terrace deposits or bedrock.

Thus, the entire section of terrace deposits that caps the coastal benches of Pleistocene marine erosion is heterogeneous and internally complex; it includes contributions of detritus from contrasting sources, from different directions at different times, and via several basically different modes of transport and deposition.

2. Stream-terrace Deposits

Several narrow, irregular benches along the walls of Diablo Canyon are veneered by a few inches to 6 feet of silty gravels that are somewhat coarser but otherwise similar to the alluvial fan deposits described above. These stream-terrace deposits (Qst) originally occupied the bottom of the canyon at a time when the lower course of Diablo Creek had been cut downward through the alluvial fan sediments of the main terrace and well into the underlying bedrock. Subsequent deepening of the canyon left remnants of the deposits as cappings on scattered small terraces.

3. Landslide Deposits

The walls of Diablo Canyon also are marked by tongue- and bench-like accumulations of loose, rubbly landslide debris (Qls), consisting mainly of highly broken and jumbled masses of Monterey rocks with abundant silty and soily matrix materials. These landslide bodies represent localized failure on naturally oversteepened slopes, generally confined to fractured bedrock in and immediately beneath the zone of weathering. Individual bodies within the mapped area are small, with probable maximum thicknesses no greater than 20 feet. All of them lie outside the area intended for power plant construction.

Landslide deposits along the sea cliff have been recognized at only one locality, on the north side of Diablo Cove about 400 feet northwest of the mouth of Diablo Canyon.

Here slippage has occurred along bedding and fracture surfaces in siliceous Monterey rocks, and it has been confined essentially to the axial region of a well-defined syncline (see Figure 2.5-8). Several episodes of sliding are attested by thin, elongate masses of highly broken ground separated from one another by well-defined zones of dislocation. Some of these masses are still capped by terrace deposits. The entire composite accumulation of debris is not more than 35 feet in maximum thickness, and ground failure at this locality does not appear to have resulted in major recession of the cliff. Elsewhere within the mapped area, landsliding along the sea cliff evidently has not been a significant process.

Large landslides, some of them involving substantial thickness of bedrock, are present on both sides of Diablo Canyon not far northeast of the power plant area. These occurrences need not be considered in connection with the plant site, but they have been regarded as significant factors in establishing a satisfactory grading design for the switchyard and other up-canyon installations. They are not dealt with in this section.

4. Slump, Creep, and Slope-wash Deposits

As noted earlier, slump, creep, and slope-wash deposits (Qsw) form parts of the nonmarine sedimentary blanket on the main terrace. These materials are shown separately on the geologic map only in those limited areas where they have been considerably concentrated along well-defined swales and are readily distinguished from other surficial deposits. Their actual distribution is much wider, and they undoubtedly are present over a large fraction of the areas designated as Qter; their average thickness in such areas, however, is probably less than 5 feet.

Angular fragments of Monterey rocks are sparsely to very abundantly scattered through the slump, creep, and slope-wash deposits, whose most characteristic feature is a fine-grained matrix that is dark colored, moderately rich in clay minerals, and extremely soft when wet. Internal layering is rarely observable and nowhere is sharply expressed. The debris seems to have been rather thoroughly intermixed during its slow migration down hillslopes in response to gravity. That it was derived mainly from broken materials in the zone of weathering is shown by several exposures in which it grades downward through soily debris into highly disturbed and partly weathered bedrock, and thence into progressively fresher and less broken bedrock.

5. Talus and Beach Deposits

Much of the present coastline in the subject area is marked by bare rock, but Diablo Cove and a few other large indentations are fringed by narrow, discontinuous beaches and irregular concentrations of sea cliff talus. These deposits (Qtb) are very coarse grained. Their total volume is small, and they are of interest mainly as modern analogues of much older deposits at higher levels beneath the main terrace surface.

The beach deposits consist chiefly of well-rounded cobbles. They form thin veneers over bedrock, and in Diablo Cove they grade seaward into patches of coarse pebbly

sand. The floors of both Diablo Cove and South Cove probably are irregular in detail and are featured by rather hard, fresh bedrock that is discontinuously overlain by irregular thin bodies of sand and gravel. The distribution and abundance of kelp suggest that bedrock crops out over large parts of these cove areas where the sea bottom cannot be observed from onshore points.

6. Stream-laid Alluvium

Stream-laid alluvium (Qal) occurs as a strip along the present narrow floor of Diablo Canyon, where it is only a few feet in average thickness. It is composed of irregularly intertongued silt, sand, gravel, and rubble. It is crudely to sharply stratified, poorly to well sorted, and, in general, somewhat compacted. Most of it is at least moderately porous.

7. Other Deposits

Earlier inhabitation of the area by Indians is indicated by several midden deposits that are rich in charcoal and fragments of shells and bones. The most extensive of these occurrences marks the site of a long-abandoned village along the edge of the main terrace immediately northwest of Diablo Canyon. Others have been noted on the main terrace just east of the mouth of Diablo Canyon, on the shoreward end of South Point, and at several places in and near the plant site.

2.5.1.2.4 Structure

2.5.1.2.4.1 Tectonic Structures Underlying the Region Surrounding the Site

The dominant tectonic structure in the region of the power plant site is the San Luis-Pismo downwarp system of west-northwest-trending folds. This structure is bounded on the northeast by the antiformal basement rock structure of the Los Osos and San Luis Valley trend. The west-northwest-trending Edna fault zone lies along the northeast flank of the range, and the parallel Miguelito fault extends into the southeasterly end of the range. A north-northwest- trending structural discontinuity that may be a fault has been inferred or interpolated from widely spaced traverses in the offshore, extending within about 5 miles of the site at its point of closest approach. To the west of this discontinuity, the structure is dominated by north to north-northwest-trending folds in Tertiary rocks. These features are illustrated in Figure 2.5-3 and described in this section.

Tectonic structures underlying the site and region surrounding the site are identified in the above and following sections, and they are shown in Figures 2.5-3, 2.5-5, 2.5-8, 2.5-10, 2.5-15, and 2.5-16. They are listed as follows:

2.5.1.2.4.2 Tectonic Structures Underlying the Site

The rocks underlying the DCPP site have been subjected to intrusive volcanic activity and to later compressional deformation that has given rise to folding, jointing and fracturing, minor faulting, and local brecciation. The site is situated in a section of moderately to steeply north-dipping strata, about 300 feet south of an east-west-trending synclinal fold axis (Figures 2.5-8 and 2.5-10). The rocks are jointed throughout, and they contain local zones of closely spaced high-angle fractures (Figure 2.5-16).

A minor fault zone extends into the site from the west, but dies out in the vicinity of the Unit 1 turbine building. Two other minor faults were mapped for distances of 35 to more than 200 feet in the bedrock section exposed in the excavation for the Unit 1 containment structure. In addition to these features, cross-cutting bodies of tuff and tuff brecia, and cemented "crackle breccia" could be considered as tectonic structures.

Exact ages of the various tectonic structures at the site are not known. It has been clearly demonstrated, however, that all of them are truncated by, and therefore antedate, the principal marine erosion surface that underlies the coastal terrace bench. This terrace can be correlated with coastal terraces to the north and south that have been dated as 80,000 to 120,000 years old. The tectonic structures probably are related to the Pliocene-lower Pleistocene episode of Coast Ranges deformation, which occurred more than 1 million years ago.

The bedrock units within the entire subject area form part of the southerly flank of a very large syncline that is a major feature of the San Luis Range. The northerly-dipping sequence of strata is marked by several smaller folds with subparallel trends and flank-to-flank dimensions measured in hundreds of feet. One of these, a syncline with gentle to moderate westerly plunge, is the largest flexure recognized in the vicinity of the power plant site. Its axis lies a short distance north of the site and about 450 feet northeast of the mouth of Diablo Canyon (Figures 2.5-8 and 2.5-10). East of the canyon this fold appears to be rather open and simple in form, but farther west it probably is complicated by several large wrinkles and may well lose its identity as a single feature. Some of this complexity is clearly revealed along the northerly margin of Diablo Cove, where the beds exposed in the sea cliff have been closely folded along east to northeast trends. Here a tight syncline (shown in Figure 2.5-8) and several smaller folds can be recognized, and steep to near-vertical dips are dominant in several parts of the section.

The southerly flank of the main syncline within the map area steepens markedly as traced southward away from the fold axis. Most of this steepening is concentrated within an across-strike distance of about 300 feet as revealed by the strata exposed in the sea cliff southeastward from the mouth of Diablo Canyon; farther southward the beds of sandstone and finer-grained rocks dip rather uniformly at angles of 70° or more. A slight overturning through the vertical characterizes the several hundred feet of section exposed immediately north of the Obispo Tuff that underlies South Point and the north shore of South Cove (see Figure 2.5-8). Thus the main syncline, though simple in gross form, is distinctly asymmetric. The steepness of its southerly flank may well have

resulted from buttressing, during the folding, by the relatively massive and competent unit of tuffaceous rocks that adjoins the Monterey strata at this general level of exposure.
Smaller folds, corrugations, and highly irregular convolutions are widespread among the Monterey rocks, especially the finest-grained and most shaley types. Some of these flexures trend east to southeast and appear to be drag features systematically related to the larger-scale folding in the area. Most, however, reflect no consistent form or trend, range in scale from inches to only a few feet, and evidently are confined to relatively soft rocks that are flanked by intervals of harder and more massive strata. They constitute crudely tabular zones of contortion within which individual rock layers can be traced for short distances but rarely are continuous throughout the deformed ground.

Some of this contortion appears to have derived from slumping and sliding of unconsolidated sediments on the Miocene sea floor during accumulation of the Monterey section. Most of it, in contrast, plainly occurred at much later times, presumably after conversion of the sediments to sedimentary rocks, and it can be most readily attributed to highly localized deformation during the ancient folding of a section that comprises rocks with contrasting degrees of structural competence.

2.5.1.2.4.3 Faults

Numerous faults with total displacements ranging from a few inches to several feet cut the exposed Monterey rocks. Most of these occur within, or along the margins of, the zones of contortion noted above. They are sharp, tight breaks with highly diverse attitudes, and they typically are marked by 1/16-inch or less of gouge or microbreccia. Nearly all of them are curving or otherwise somewhat irregular surfaces, and many can be seen to terminate abruptly or to die out gradually within masses of tightly folded rocks. These small faults appear to have been developed as end products of localized intense deformation caused by folding of the bedrock section. Their unsystematic attitudes, small displacements, and limited effects upon the host rocks identify them as second-order features, i.e., as results rather than causes of the localized folding and convolution with which they are associated.

Three distinctly larger and more continuous faults also were recognized within the mapped area. They are well exposed on the sea cliff that fringes Diablo Cove (see Figure 2.5-8), and each lies within a zone of moderately to severely contorted fine-grained Monterey strata. Each is actually a zone, 6 inches to several feet wide, within which two or more subparallel tight breaks are marked by slickensides, 1/4-inch or less of gouge, and local stringers of gypsum. None of these breaks appears to be systematically related to individual folds within the adjoining rocks. None of them extends upward into the overlying blanket of Quaternary terrace deposits.

One of these faults, exposed on the north side of the cove, trends north-northwest essentially parallel to the flanking Monterey beds, but it dips more steeply than these beds. Another, exposed on the east side of the cove, trends east-southeast and is essentially vertical; thus, it is essentially parallel to the structure of the host Monterey

section. Neither of these faults projects toward the ground intended for power plant construction. The third fault, which appears on the sea cliff at the mouth of Diablo Canyon, trends northeast and projects toward the ground in the northernmost part of the power plant site. It dips northward somewhat more steeply than the adjacent strata.

Total displacement is not known for any of these three faults on the basis of natural exposures, but it could amount to as much as tens of feet. That these breaks are not major features, however, is strongly suggested by their sharpness, by the thinness of gouge along individual surfaces of slippage, and by the essential lack of correlation between the highly irregular geometry of deformation in the enclosing strata and any directions of movement along the slip surfaces.

The possibility that these surfaces are late-stage expressions of much larger-scale faulting at this general locality was tested by careful examination of the deformed rocks that they transect. On megascopic scales, the rocks appear to have been deformed much more by flexing than by rupture and slippage, as evidenced by local continuity of numerous thin beds that denies the existence of pervasive faulting within much of the ground in question. That the finer-grained rocks are not themselves fault gouged was confirmed by examination of 34 samples under the microscope.

Sedimentary layering, recognized in 27 of these samples, was observed to be grossly continuous even though dislocated here and there by tiny fractures. Moreover, nearly all the samples were found to contain shards of volcanic glass and/or the tests of foraminifera; some of these delicate components showed effects of microfracturing and a few had been offset a millimeter or less along tiny shear surfaces, but none appeared to have been smeared out or partially obliterated by intense shearing or grinding. Thus, the three larger faults in the area evidently were superimposed upon ground that already had been deformed primarily by small-scale and locally very intense folding rather than by pervasive grinding and milling.

It is not known whether these faults were late-stage results of major folding in the region or were products of independent tectonic activity. In either case, they are relatively ancient features, as they are capped without break by the Quaternary terrace deposits exposed along the upper part of the sea cliff. They probably are not large-scale elements of regional structure, as examination of the nearest areas of exposed bedrock along their respective landward projections revealed no evidence of substantial offsets among recognizable stratigraphic units.

Seaward projection of one or more of these faults might be taken to explain a possible large offset of the Obispo Tuff units exposed on North Point and South Point. The notion of such an offset, however, would rest upon the assumption that these two units are displaced parts of an originally continuous body, for which there is no real evidence. Indeed, the two tuff units are bounded on their northerly sides by lithologically different parts of the Monterey Formation; hence, they were clearly originally emplaced at different stratigraphic levels and are not directly correlative.

2.5.1.2.5 Geological Relationships at the Units 1 and 2 Power Plant Site

2.5.1.2.5.1 Geologic Investigations at the Site

The geologic relationships at DCPP site have been studied in terms of both local and regional stratigraphy and structure, with an emphasis on relationships that could aid in dating the youngest tectonic activity in the area. Geologic conditions that could affect the design, construction, and performance of various components of the plant installation also were identified and evaluated. The investigations were carried out in three main phases, which spanned the time between initial site selection and completion of foundation construction.

2.5.1.2.5.2 Feasibility Investigation Phase

Work directed toward determining the pertinent general geologic conditions at the plant site comprised detailed mapping of available exposures, limited hand trenching in areas with critical relationships, and petrographic study of the principal rock types. The results of this feasibility program were presented in a report that also included recommendations for determining suitability of the site in terms of geologic conditions. Information from this early phase of studies is included in the preceding four sections and illustrated in Figures 2.5-8, 2.5-9, and 2.5-10.

2.5.1.2.5.3 Suitability Investigation Phase

The record phase of investigations was directed toward testing and confirming the favorable judgments concerning site feasibility. Inasmuch as the principal remaining uncertainties involved structural features in the local bedrock, additional effort was made to expose and map these features and their relationships. This was accomplished through excavation of large trenches on a grid pattern that extended throughout the plant area, followed by photographing the trench walls and logging the exposed geologic features. Large-scale photographs were used as a mapping base, and the recorded data were then transferred to controlled vertical sections at a scale of 1 inch = 20 feet. The results of this work were reported in three supplements to the original geologic report[1]. Supplementary Reports I and III presented data and interpretation based on trench exposures in the areas of the Unit 1 and Unit 2 installations, respectively. Supplementary Report II described the relationships of small bedrock faults exposed in the exploratory trenches and in the nearby sea cliff.
During these suitability investigations, special attention was given to the contact between bedrock and overlying terrace deposits in the plant site area. It was determined that none of the discontinuities present in the bedrock section displaces either the erosional surface developed across the bedrock or the terrace deposits that rest upon this surface. The pertinent data are presented farther on in this section and illustrated in Figures 2.5-11, 2.5-12, 2.5-13, and 2.5-14.

2.5.1.2.5.4 Construction Geology Investigation Phase

Geologic work done during the course of construction at the plant site spanned an interval of 5 years, which encompassed the period of large-scale excavation. It included detailed mapping of all significant excavations, as well as special studies in some areas of rock bolting and other work involving rock reinforcement and temporary instrumentation. The mapping covered essentially all parts of the area to be occupied by structures for Units 1 and 2, including the excavations for the circulating water intake and outlet, the turbine-generator building, the auxiliary building, and the containment structures. The results of this mapping are described farther on and illustrated in Figures 2.5-15 and 2.5-16.

2.5.1.2.5.5 Exploratory Trenching Program, Unit 1 Site

Four exploratory trenches were cut beneath the main terrace surface at the power plant site, as shown in Figures 2.5-8, 2.5-11, 2.5-12, and 2.5-13. Trench AF (Trench A), about 1080 feet long, extended in a north-northwesterly direction and thus was roughly parallel to the nearby margin of Diablo Cove. Trench BE (Trench B), 380 feet long, was parallel to Trench A and lay about 150 feet east of the northerly one-third of the longer trench. Trenches C and D, 450 and 490 feet long, respectively were nearly parallel to each other, 130 to 150 feet apart, and lay essentially normal to Trenches A and B. The two pairs of trenches crossed each other to form a "#" pattern that would have been symmetrical were it not for the long southerly extension of Trench A. They covered the area intended for Unit 1 power plant construction, and the intersection of Trenches B and C coincided in position with the center of the Unit 1 nuclear reactor structure.

All four trenches, throughout their aggregate length of approximately 2400 feet, revealed a section of surficial deposits and underlying bedrock that corresponds to the two-ply sequence of surficial deposits and Monterey strata exposed along the sea cliff in nearby Diablo Cove. The trenches ranged in depth from 10 feet to nearly 40 feet, and all had sloping sides that gave way downward to essentially vertical walls in the bedrock encountered 3 to 8 feet above their floors.

To facilitate detailed geologic mapping, the easterly walls of Trenches A and B and the southerly walls of Trenches C and D were trimmed to near-vertical slopes extending upward from the trench floors to levels well above the top of bedrock. These walls subsequently were scaled back by means of hand tools in order to provide fresh, clean exposures prior to mapping of the contact between bedrock and overlying unconsolidated materials.

1. Bedrock

The bedrock that was continuously exposed in the lowest parts of all the exploratory trenches lies within a portion of the Montery Formation characterized by a preponderance of sandstone. It corresponds to the part of the section that crops out in lower Diablo Canyon and along the sea cliff souteastward from the canyon mouth. The

sandstone ranges from light gray through buff to light reddish brown, from silty to markedly tuffaceous, and from thin-bedded and platy to massive. The distribution and thickness of beds can be readily appraised from sections along Trenches A and B (Figure 2.5-12) that show nearly all individual bedding surfaces that could be recognized on the ground.

The sandstone ranges from very hard to moderately soft, and some of it feels slightly punky when struck with a pick. All of it is, however, firm and very compact. In general, the most platy parts of the sequence are also the hardest, but the soundest rock in the area is almost massive sandstone of the kind that underlies the site of the intended reactor structure. This rock is well exposed on the nearby hillslope adjoining the main terrace area, where it has been markedly resistant to erosion and stands out as distinct low ridges.

Tuff, consisting chiefly of altered volcanic glass, forms irregular sills and dikes in several parts of the bedrock section. This material, generally light gray to buff, is compact but distinctly softer than the enclosing sandstone. Individual bodies are 1/2 inch to 4 feet thick. They are locally abundant in Trench C west of Trench A, and in Trench A southward beyond the end of the section in Figure 2.5-12. They are very rare or absent in Trenches B and D, and in the easterly parts of Trench C and the northerly parts of Trench A. These volcanic rocks probably are related to the Obispo Tuff as described earlier, but all known masses of typical Obispo rocks in this area lie at considerable distances west and south of the ground occupied by the trenches.

2. Bedrock Structure

The stratification of the Monterey rocks dips northward wherever it was observable in the trenches, in general, at angles of 35 to 55°. Thus, the bedrock beneath the power plant site evidently lies on the southerly flank of the major syncline noted and described earlier. Zones of convolution and other expressions of locally intense folding were not recognized, and probably are much less common in this general part of the section than in other, previously described parts that include intervals of softer and more shaley rocks.

Much of the sandstone is traversed by fractures. Planar, curving, and irregular surfaces are well represented, and, in places, they are abundant and closely spaced. All prominent fractures and many of the minor and discontinuous ones are shown in the sections of Figure 2.5-12. Also shown in these sections are all recognized slip joints, shear surfaces, and faults, i.e., all surfaces along which the bedrock has been displaced. Such features are most abundant in Trenches A and C near their intersection, in Trench D west of the intersection with Trench A, and near the northerly end of Trench B.

Most of the surfaces of movement are hairline features with or without thin films of clay and/or gypsum. Displacements range from a small fraction of an inch to several inches. The other surfaces are more prominent, with well-defined zones of gouge and fine-

grained breccia ordinarily 1/8 inch or less in thickness. Such zones were observed to reach a maximum thickness of nearly 1/2 inch along two small faults, but only as local lenses or pockets. Exposures were not sufficiently extensive in three dimensions for definitely determining the magnitude of slip along the more prominent faults, but all of these breaks appeared to be minor features. Indeed, no expressions of major faulting were recognized in any of the trenches despite careful search, and the continuous bedrock exposures precluded the possibility that such features could have been readily overlooked.

A northeast-trending fault that appears on the sea cliff at the mouth of Diablo Canyon projects toward the ground in the northernmost part of the power plant site, as noted in a foregoing section. No zone of breaks as prominent as this one was identified in the trench exposures, and any distinct northeastward continuation of the fault would necessarily lie north of the trenched ground. Alternatively, this fault might well separate northeastward into several smaller faults; some or all of these could correspond to some or all of the breaks mapped in the northerly parts of Trenches A and B.

3. Terrace Deposits

Marine terrace deposits of Pleistocene age form a cover, generally 2 to 5 feet thick, over the bedrock that lies beneath the power plant site. This cover was observed to be continuous in Trench C and the northerly part of Trench A, and to be nearly continuous in the other two trenches. Its lithology is highly variable, and includes bouldery rubble, loose beach sand, pebbly silt, silty to clayey sand with abundant shell fragments, and soft clay derived from underlying tuffaceous rocks. Nearly all of these deposits are at least sparsely fossiliferous, and, in a few places, they consist mainly of shells and shell fragments. Vertebrate fossils, chiefly vertebral and rib materials representing large marine mammals, are present locally; recognized occurrences are designated by the symbol X in the sections of Figure 2.5-12.

At the easterly ends of Trenches C and D, the marine deposits intergrade and intertongue in a landward direction with thicker and coarser accumulations of poorly sorted debris. This material evidently is talus that was formed along the base of an ancient sea cliff or other shoreline slope. In some places, the marine deposits are overlain by nonmarine terrace sediments with a sharp break, but elsewhere the contact between these two kinds of deposits is a dark colored zone, a few inches to as much as 2 feet thick, that appears to represent a soil developed on the marine section. Fragments of these soily materials appear here and there in the basal parts of the nonmarine section.

The nonmarine sediments that were exposed in Trenches B, C, and D and in the northerly part of Trench A are mainly alluvial deposits derived in ancient times from Diablo Canyon. They consist of numerous tabular fragments of Monterey rocks in a relatively dark colored silty to clayey matrix, and, in general, they are distinctly bedded and moderately to highly compact. As indicated in the sections of Figure 2.5-12, they

thicken progressively in a north-northeastward direction, i.e., toward their principal source, the ancient mouth of Diablo Canyon.

Slump, creep, and slope-wash deposits, which constitute the youngest major element of the terrace section, overlie the alluvial fan gravels and locally are interlayered with them. Where the gravels are absent, as in the southerly part of Trench A, this younger cover rests directly upon bedrock. It is loose and uncompacted, internally chaotic, and is composed of fragments of Monterey rocks in an abundant dark colored clayey matrix.

All the terrace deposits are soft and unconsolidated, and hence are much less resistant to erosion than is the underlying bedrock. Those appearing along the walls of exploratory trenches were exposed to heavy rainfall during two storms, and showed some tendency to wash and locally to rill. Little slumping and no gross failure were noted in the trenches, however, and it was not anticipated that these materials would cause special problems during construction of a power plant.

4. Interface Between Bedrock and Surficial Deposits

As once exposed continuously in the exploratory trenches, the contact between bedrock and overlying terrace deposits represents a broad wave-cut platform of Pleistocene age. This buried surface of ancient marine erosion ranges in altitude between extremes of 82 and 100 feet, and more than three-fourths of it lies within the more limited range of 90 to 100 feet. It terminates eastward against a moderately steep shoreline slope, the lowest parts of which were encountered at the extreme easterly ends of Trenches C and D, and beyond this slope is an older buried bench at an altitude of 120 to 130 feet.

Available exposures indicate that the configuration of the erosional platform is markedly similar, over a wide range of scales, to that of the platform now being cut approximately at sea level along the present coast. Grossly viewed, it slopes very gently in a seaward (westerly) direction and is marked by broad, shallow channels and by upward projections that must have appeared as low spines and reefs when the bench was being formed (Figures 2.5-12 and 2.5-13). The most prominent reef, formerly exposed in Trenches B and D at and near their intersection, is a wide, westerly-trending projection that rises 5 to 15 feet above neighboring parts of the bench surface. It is composed of massive sandstone that was relatively resistant to the ancient wave erosion.

As shown in the sections and sketches of Figure 2.5-12, the surface of the platform is nearly planar in some places but elsewhere is highly irregular in detail. The small-scale irregularities, generally 3 feet or less in vertical extent, including knob, spine, and rib like projections and various wave-scoured pits, crevices, notches, and channels. The upward projections clearly correspond to relatively hard, resistant beds or parts of beds in the sandstone section. The depressions consistently mark the positions of relatively soft silty or shaley sandstone, of very soft tuffaceous rocks, or of extensively jointed rocks. The surface traces of most faults and some of the most prominent joints are in sharp depressions, some of them with overhanging walls. All these irregularities of

detail have modern analogues that can be recognized on the bedrock bench now being cut along the margins of Diablo Cove.

The interface between bedrock and overlying surficial deposits is of particular interest in the trenched area because it provides information concerning the age of youngest fault movements within the bedrock section. This interface is nowhere offset by faults revealed in the trenches, but instead has been developed irregularly across these faults after their latest movements. The consistency of this general relationship was established by highly detailed tracing and inspection of the contact as freshly exhumed by scaling of the trench walls. Gaps in exposure of the interface necessarily were developed at the four intersections of trenches; at these localities, the bedrock was carefully laid bare so that all joints and faults could be recognized and traced along the trench floors to points where their relationships with the exposed interface could be determined.

Corroborative evidence concerning the age of the most recent fault displacements stems from the marine deposits that overlie the bedrock bench and form the basal part of the terrace section. That these deposits rest without break across the traces of faults in the underlying bedrock was shown by the continuity of individual sedimentary beds and lenses that could be clearly recognized and traced.

Further, some of the faults are directly capped by individual boulders, cobbles, pebbles, shells, and fossil bones, none of which have been affected by fault movements. Thus, the most recent fault displacements in the plant site area occurred prior to marine planation of the bedrock and deposition of the overlying terrace sediments. As pointed out earlier, the age of the most recent faulting in this area is therefore at least 80,000 years and more probably at least 120,000 years. It might be millions of years.

2.5.1.2.5.6 Exploratory Trenching Program, Unit 2 Site

Eight additional trenches were cut beneath the main terrace surface south of Diablo Canyon (Figure 2.5-13) in order to extend the scope of subsurface exploration to include all ground in the Unit 2 plant site. As in the area of the Unit 1 plant site, the trenches formed two groups; those in each group were parallel with one another and were oriented nearly normal to those of the other group. The excavations pertinent to the Unit 2 plant site can be briefly identified as follows:

1. *North-northwest Alignment*

    a. Trench EJ, 240 feet long, was a southerly extension of older Trench BE (originally designated as Trench B).

    b. Trench WU, 1300 feet long, extended southward from Trench DG (originally designated as Trench D), and its northerly part lay about 65 feet east of Trench EJ. The northernmost 485 feet of this trench was mapped in connection with the Unit 2 trenching program.

c. Trench MV, 700 feet long, lay about 190 feet east of Trench WU. The northernmost 250 feet of this trench was mapped in connection with the Unit 2 trenching program.

d. Trench AF (originally designated as Trench A) was mapped earlier in connection with the detailed study of the Unit 1 plant site. A section for this trench, which lay about 140 feet west of Trench EJ, was included with others in the report on the Unit 1 trenching program.

2. East-northeast Alignment

a. Trench KL, about 750 feet long, lay 180 feet south of Trench DG (originally designated as Trench D) and crossed Trenches AF, EJ, and WU.

b. Trench NO, about 730 feet long, lay 250 feet south of Trench KL and crossed Trenches AF, WU, and MV.

These trenches, or parts thereof, covered the area intended for the Unit 2 power plant construction, and the intersection of Trenches WU and KL coincided in position with the center of the Unit 2 nuclear reactor structure.

All five additional trenches, throughout their aggregate length of nearly half a mile, revealed a section of surficial deposits and underlying Monterey bedrock that corresponded to the two-ply sequence of surficial deposits and Monterey strata exposed in the older trenches and along the sea cliff in nearby Diablo Cove. The trenches ranged in depth from 10 feet (or less along their approach ramps) to nearly 35 feet, and all had sloping sides that gave way downward to essentially vertical walls in the bedrock encountered 3 to 22 feet above their floors. To facilitate detailed geologic mapping, the easterly walls of Trenches EJ, WU, and MV and the southerly walls of Trenches KL and NO were trimmed to near-vertical slopes extending upward from the trench floors to levels well above the top of bedrock. These walls subsequently were scaled back by means of hand tools in order to provide fresh, clean exposures prior to mapping of the contact between bedrock and overlying unconsolidated materials.

The geologic sections shown in Figures 2.5-12 and 2.5-13 correspond in position to the vertical portions of the mapped trench walls. Relationships exposed at higher levels on sloping portions of the trench walls have been projected to the vertical planes of the sections. Centerlines of intersecting trenches are shown for convenience, but the planes of the geologic sections do not contain the centerlines of the respective trenches.

3. Bedrock

The bedrock that was continuously exposed in the lowest parts of all the exploratory trenches lies within a part of the Monterey Formation characterized by a preponderance

of sandstone. It corresponds to the portion of the section that crops out along the sea cliff southward from the mouth of Diablo Canyon. The sandstone is light to medium gray where fresh, and light gray to buff and reddish brown where weathered. It ranges from silty to markedly tuffaceous, with tuffaceous units tending to dominate southward and southwestward from the central parts of the trenched area (see geologic section in Figure 2.5-13). Much of the sandstone is thin-bedded and platy, but the most siliceous parts of the section are characterized by a strata a foot or more in thickness. Individual beds commonly are well defined by adjacent thin layers of more silty material.

Bedding is less distinct in the more tuffaceous parts of the section, some of which seem to be almost massive. These rocks typically are broken by numerous tight fractures disposed at high angles to one another so that, where weathered, their appearance is coarsely blocky rather than layered.

As broadly indicated in the geologic sections, the sandstone ranges from very hard to moderately soft, and some of it feels slightly punky when struck with a pick. All of it, however, is firm and very compact. In general, the most platy parts of the sequence are relatively hard, but the hardest and soundest rock in the area is thick-bedded to almost massive sandstone of the kind at and immediately north of the site for the intended reactor structure. This resistant rock is well exposed as distinct low ridges on the nearby hillslope adjoining the main terrace area.

Tuff, consisting chiefly of altered volcanic glass, is abundant within the bedrock section. Also widely scattered, but much less abundant, is tuff breccia, consisting typically of small fragments of older tuff, pumice, or Monterey rocks in a matrix of fresh to altered volcanic glass. These materials, which form sills, dikes, and highly irregular intrusive masses, are generally light gray to buff, gritty, and compact but distinctly softer than much of the enclosing sandstone. Individual bodies range from stringers less than a quarter of an inch thick to bulbous or mushroom-shaped masses with maximum exposed dimensions measured in tens of feet. As shown on the geologic sections, they are abundant in all the trenches.

These volcanic rocks probably are related to the Obispo Tuff, large masses of which are well exposed west and south of the trenched ground. The bodies exposed in the trenches doubtless represent a rather lengthy period of Miocene volcanism, during which the Monterey strata were repeatedly invaded by both tuff and tuff breccia. Indeed, several of the mapped tuff units were themselves intruded by dikes of younger tuff, as shown, for example, in Sections KL and NO.

4. Bedrock Structure

The stratification of the Monterey rocks dips northward wherever it was observable in the trenches, in general, at angles of 45 to 85°. The steepness of dip increases progressively from north to south in the trenched ground, a relationship also noted along the sea cliff southward from the mouth of Diablo Canyon. Thus, the bedrock beneath the power plant site evidently lies on the southerly flank of the major syncline that was

described previously. Zones of convolution and other expressions of locally intense folding were not recognized, and they probably are much less common in this general part of the section than in other (previously described) parts that include intervals of softer and more shaley rocks.

Much of the sandstone is traversed by fractures. Planar, curving, and irregular surfaces are well represented, and in places they are abundant and closely spaced. All prominent fractures and nearly all of the minor and discontinuous ones are shown on the geologic sections (Figure 2.5-13). Also shown in these sections are all recognized shear surfaces, faults, and other discontinuities along which the bedrock has been displaced. Such features are nowhere abundant in the trench exposures.

Most of the surfaces of movement are hairline breaks with or without thin films of clay, calcite, and/or gypsum. Displacements range from a small fraction of an inch to several inches. A few other surfaces are more prominent, with well-defined zones of fine-grained breccia and/or infilling mineral material ordinarily 1/8 inch or less in thickness. Such zones were observed to reach maximum thicknesses of 3/8 to 1/2 inch along three small faults, but only as local lenses or pockets.

Exposures are not sufficiently extensive in three dimensions for definitely determining the magnitude of slip along all the faults, but for most of them it is plainly a few inches or less. None of them appears to be more than a minor break in a bedrock section that has been folded on a large scale. Indeed, no expressions of major faulting were recognized in any of the trenches despite careful search, and the continuous bedrock exposures preclude the possibility that such features could be readily overlooked.

Most surfaces of past movement probably were active during times when the Monterey rocks were being deformed by folding, when rupture and some differential movements would be expected in a section comprising such markedly differing rock types. Some of the fault displacements may well have been older, as attested in two places by relationships involving small faults, the Monterey rocks, and tuff.

In Trench WU south of Trench KL, for example, sandstone beds were seen to have been offset about a foot along a small fault. A thin sill of tuff occupies the same stratigraphic horizon on opposite sides of this fault, but the sill has not been displaced by the fault. Instead, the tuff occupies a short segment of the fault to effect the slight jog between its positions in the strata on either side. Intrusion of the tuff plainly postdated all movements along this fault.

5. Terrace Deposits

Marine terrace deposits of Pleistocene age form covers, generally 2 to 5 feet thick, but locally as much as 12 feet thick, over the bedrock that lies beneath the Unit 2 plant site. These covers were observed to be continuous in some parts of all the trenches, and thin and discontinuous in a few other parts. Elsewhere, the marine sediments were

absent altogether, as in the lower and more southerly parts of Trenches EJ and WU and in the lower and more westerly parts of Trenches KL and NO.

The range in lithology of these deposits is considerable, and includes bouldery rubble, gravel composed of well-rounded fragments of shells and/or Monterey rocks, beach sand, loose accumulations of shells, pebbly silt, silty to clayey sand with abundant shell fragments, and soft clay derived from underlying tuffaceous rocks. Nearly all of the deposits are at least sparsely fossiliferous, and many of them contain little other than shell material. Vertebrate fossils, chiefly vertebral and rib materials representing large marine mammals, are present locally.

The trenches in and near the site of the reactor structure exposed a buried narrow ridge of hard bedrock that once projected westward as a bold promontory along an ancient sea coast, probably at a time when sea level corresponded approximately to the present 100 foot contour (see Figure 2.5-11). Along the flanks of this promontory and the face of an adjoining buried sea cliff that extends southeastward through the area in which Trenches MV and NO intersected, the marine deposits intergrade and intertongue with thicker and coarser accumulations of poorly sorted debris. This rubbly material evidently is talus that was formed and deposited along the margins of the ancient shoreline cliff.

Similar gradations of older marine deposits into older talus deposits were observable at higher levels in the easternmost parts of Trenches KL and NO, where the rubbly materials doubtless lie against a more ancient sea cliff that was formed when sea level corresponded to the present 140 foot contour. The cliff itself was not exposed, however, as it lies slightly beyond the limits of trenching.

In many places, the marine covers are overlain by younger nonmarine terrace sediments with a sharp break, but elsewhere the contact between these two kinds of deposits is a zone of dark colored material, a few inches to as much as 6 feet thick, that represents weathering and development of soils on the marine sections. Fragments of these soily materials are present here and there in the basal parts of the nonmarine section. Over large areas, the porous marine deposits have been discolored through infiltration by fine-grained materials derived from the overlying ancient soils.

The nonmarine accumulations, which form the predominant fraction of the entire terrace cover, consist mainly of slump, creep, and slope-wash debris that is characteristically loose, uncompacted, and internally chaotic. These relatively dark colored deposits are fine grained and clayey, but they contain sparse to very abundant fragments of Monterey rocks generally ranging from less than an inch to about 2 feet in maximum dimension. Toward Diablo Canyon they overlie and, in places, intertongue with silty to clayey gravels that are ancient contributions from Diablo Creek when it flowed at levels much higher than its present one. These "dirty" alluvial deposits appeared only in the most northerly parts of the more recently trenched terrace area, and they are not distinguished from other parts of the nonmarine cover on the geologic sections (Figure 2.5-13).

All the terrace deposits are soft and unconsolidated, and hence are much less resistant to erosion than is the underlying bedrock. Those appearing along the walls of the exploratory trenches showed some tendency to wash and locally to rill when exposed to heavy rainfall, but little slumping and no gross failure were noted in the trenches.

6. Interface Between Bedrock and Surficial Deposits

As exposed continuously in the exploratory trenches, the contact between bedrock and overlying terrace deposits represents two wave-cut platforms and intervening slopes, all of Pleistocene age. The broadest surface of ancient marine erosion ranges in altitude from 80 to 105 feet, and its shoreward margin, at the base of an ancient sea cliff, lies uniformly within 5 feet of the 100 foot contour. A higher, older, and less extensive marine platform ranges in altitude from 130 to 145 feet, and most of it lies within the ranges of 135 to 140 feet. As noted previously, these are two of several wave-cut benches in this coastal area, each of which terminates eastward against a cliff or steep shoreline slope and westward at the upper rim of a similar but younger slope.

Available exposures indicate that the configurations of the erosional platforms are markedly similar, over a wide range of scales, to that of the platform now being cut approximately at sea level along the present coast. Grossly viewed, they slope very gently in a seaward (westerly) direction and are marked by broad, shallow channels and by upward projections that must have appeared as low spines and reefs when the benches were being formed. The most prominent reefs, which rise from a few inches to about 5 feet above neighboring parts of the bench surfaces, are composed of hard, thick-bedded sandstone that was relatively resistant to ancient wave erosion.
As shown in the geologic sections (Figure 2.5-13), the surfaces of the platforms are nearly planar in some places but elsewhere are highly irregular in detail. The small scale irregularities, generally 3 feet or less in vertical extent, include knob-, spine-, and rib-like projections and various wave-scoured pits, notches, crevices, and channels. Most of the upward projections closely correspond to relatively hard, resistant beds or parts of beds in the sandstone section. The depressions consistently mark the positions of relatively soft silty or shaley sandstone, of very soft tuffaceous rocks, or of extensively jointed rocks. The surface traces of most faults and some of the most prominent joints are in sharp depressions, some of them with overhanging walls. All these irregularities of detail have modern analogues that can be recognized on the bedrock bench now being cut along the margins of Diablo Cove.

The interface between bedrock and overlying surficial deposits provides information concerning the age of youngest fault movements within the bedrock section. This interface is nowhere offset by faults that were exposed in the trenches, but instead has been developed irregularly across the faults after their latest movements. The consistency of this general relationship was established by highly detailed tracing and inspection of the contact as freshly exhumed by scaling of the trench walls. Gaps in exposure of the interface necessarily were developed at the intersections of trenches as in the exploration at the Unit 1 site. At such localities, the bedrock was carefully laid

bare so that all joints and faults could be recognized and traced along the trench floors to points where their relationships with the exposed interface could be determined.

Corroborative evidence concerning the age of the most recent fault displacements stems from the marine deposits that overlie the bedrock bench and form a basal part of the terrace section. That these deposits rest without break across the traces of faults in the underlying bedrock was shown by the continuity of individual sedimentary beds and lenses that could be clearly recognized and traced. As in other parts of the site area, some of the faults are directly capped by individual boulders, cobbles, pebbles, shells, and fossil bones, none of which have been affected by fault movements. Thus, the most recent fault displacements in the plant site area occurred before marine planation of the bedrock and deposition of the overlying terrace sediments.

The age of the most recent faulting in this area is therefore at least 80,000 years. More probably, it is at least 120,000 years, the age most generally assigned to these terrace deposits along other parts of the California coastline. Evidence from the higher bench in the plant site area indicates a much older age, as the unfaulted marine deposits there are considerably older than those that occupy the lower bench corresponding to the 100 foot terrace. Moreover, it can be noted that ages thus determined for most recent fault displacements are minimal rather than absolute, as the latest faulting actually could have occurred millions of years ago.

During the Unit 2 exploratory trenching program, special attention was directed to those exposed parts of the wave-cut benches where no marine deposits are present, and hence where there are no overlying reference materials nearly as old as the benches themselves. At such places, the bedrock beneath each bench has been weathered to depths ranging from less than 1 inch to at least 10 feet, a feature that evidently corresponds to a lengthy period of surface exposure from the time when the bench was abandoned by the sea to the time when it was covered beneath encroaching nonmarine deposits derived from hillslopes to the east.

Stratification and other structural features are clearly recognizable in the weathered bedrock, and they obviously have exercised some degree of control over localization of the weathering. Moreover, in places where upward projections of bedrock have been gradually bent or rotationally draped in response to weathering and creep, their contained fractures and surfaces of movement have been correspondingly bent. Nowhere in such a section that has been disturbed by weathering have the materials been cut by younger fractures that would represent straight upward projections of breaks in the underlying fresh rocks. Nor have such fractures been observed in any of the overlying nonmarine terrace cover.

Thus, the minimum age of any fault movement in the plant site area is based on compatible evidence from undisplaced reference features of four kinds: (a) Pleistocene wave-cut benches developed on bedrock, (b) immediately overlying marine deposits that are very slightly younger, (c) zones of weathering that represent a considerable span of subsequent time, and (d) younger terrace deposits of nonmarine origin.

2.5.1.2.5.7 Bedrock Geology of the Plant Foundation Excavations

Bedrock was continuously exposed in the foundation excavations for major structural components of Units 1 and 2. Outlines and invert elevations of these large openings, which ranged in depth from about 5 to nearly 90 feet below the original ground surface, are shown in Figures 2.5-15 and 2.5-16. The complex pattern of straight and curved walls with various positions and orientations provided an excellent three-dimensional representation of bedrock structure. These walls were photographed at large scales as construction progressed, and the photographs were used directly as a geologic mapping base. The largest excavations also were mapped in detail on a surveyed planimetric base.

Geologic mapping of the plant excavations confirmed the conclusions based on earlier investigations at the site. The exposed section of Monterey strata was found to correspond in lithology and structure to what had been predicted from exposures at the mouth of Diablo Canyon, along the sea cliffs in nearby Diablo Cove, and in the test trenches. Thus, the plant foundation is underlain by a moderately to steeply north-dipping sequence of thin to thick bedded sandy mudstone and fine-grained sandstone. The rocks at these levels are generally fresh and competent, as they lie below the zone of intense near-surface weathering.

Several thin interbeds of claystone were exposed in the southwestern part of the plant site in the excavations for the Unit 2 turbine-generator building, intake conduits, and outlet structure. These beds, which generally are less than 6 inches thick, are distinctly softer than the flanking sandstone. Some of them show evidence of internal shearing.

Layers of tuffaceous sandstone and sills, dikes, and irregular masses of tuff and tuff breccia are present in most parts of the foundation area. They tend to increase in abundance and thickness toward the south, where they are relatively near the large masses of Obispo Tuff exposed along the coast south of the plant site.

Some of the tuff bodies are conformable with the enclosing sandstone, but others are markedly discordant. Most are clearly intrusive. Individual masses, as exposed in the excavations, range in thickness from less than 1 inch to about 40 feet. The tuff breccia, which is less abundant than the tuff, consists typically of small fragments of older tuff, pumice, or Monterey rocks in a matrix of fresh to highly altered volcanic glass. At the levels of exposure in the excavations, both the tuff and tuff breccia are somewhat softer than the enclosing sandstone.

The stratification of the Monterey rocks dips generally northward throughout the plant foundation area. Steepness of dips increases progressively and, in places, sharply from north to south, ranging from 10 to 15° on the north side of Unit 1 to 75 to 80° in the area of Unit 2. A local reversal in direction of dip reflects a small open fold or warp in the Unit 1 area. The axis of this fold is parallel to the overall strike of the bedding, and strata on the north limb dip southward at angles of 10 to 15°. The more general

steepening of dips from north to south may reflect buttressing by the large masses of Obispo Tuff south of the plant site.

The bedrock of the plant area is traversed throughout by fractures, including various planar, broadly curving, and irregular breaks. A dominant set of steeply dipping to vertical joints trends northerly, nearly normal to the strike of bedding. Other joints are diversely oriented with strikes in various directions and dips ranging from 10° to vertical. Many fractures curve abruptly, terminate against other breaks, or die out within single beds or groups of beds.

Most of the joints are widely spaced, ranging from about 1 to 10 feet apart, but within several northerly trending zones, ranging in width from 10 to 20 feet, closely spaced near vertical fractures give the rocks a blocky or platy appearance. The fracture and joint surfaces are predominantly clean and tight, although some irregular ones are thinly coated with clay or gypsum. Others could be traced into thin zones of breccia with calcite cement.

Several small faults were mapped in the foundation excavations for Unit 1 and the outlet structure. A detailed discussion of these breaks and their relationship to faults that were mapped earlier along the sea cliff and in the exploratory trenches is included in the following section.

2.5.1.2.5.8 Relationships of Faults and Shear Surfaces

Several subparallel breaks are recognizable on the sea cliff immediately south of Diablo Canyon, where they transect moderately thick-bedded sandstone of the kind exposed in the exploratory trenches to the east. These breaks are nearly concordant with the bedrock stratification but, in general, they dip more steeply (see detailed structure section, Figure 2.5-14) and trend more northerly than the stratification. Their trend differs significantly from much of their mapped trace, as the trace of each inclined surface is markedly affected by the local steep topography. The indicated trend, which projects eastward toward ground north of the Unit 1 reactor site, has been summed from numerous individual measurements of strike on the sea cliff exposures, and it also corresponds to the trace of the main break as observed in nearly horizontal outcrop within the tidal zone west of the cliff.

The structure section shows all recognizable surfaces of faulting and shearing in the sea cliff that are continuous for distances of 10 feet or more. Taken together, they represent a zone of dislocation along which rocks on the north have moved upward with respect to those on the south as indicated by the attitude and roughness sense of slickensides. The total amount of movement cannot be determined by any direct means, but it probably is not more than a few tens of feet and could well be less than 10 feet. This is suggested by the following observed features:

(1) All individual breaks are sharp and narrow, and the strata between them are essentially undeformed except for their gross inclination.

(2) Some breaks plainly die out as traced upward along the cliff surface, and others merge with adjoining breaks. At least one well-defined break butts downward against a cross-break, which in turn butts upward against a break that branches and dies out approximately 20 feet away (see structure section, Figure 2.5-14, for details).

(3) Nearly all the breaks curve moderately to abruptly in the general direction of movement along them.

(4) Most of the breaks are little more than knife-edge features along which rock is in direct contact with rock, and others are marked by thin films of gouge. Maximum thickness of gouge anywhere observed is about 1/2 inch, and such exceptional occurrences are confined to short curving segments of the main break at the southerly margin of the zone.

(5) No fault breccia is present; instead, the zone represents transection of otherwise undeformed rocks by sharply-defined breaks. No bedrock unit is cut off and juxtaposed against a unit of different lithology along any of the breaks.

(6) Local prominence of the exposed breaks, and especially the main one, is due to slickensides, surface coatings of gypsum, and iron-oxide stains rather than to any features reflecting large-scale movements.

This zone of faulting cannot be regarded as a major tectonic element, nor is it the kind of feature normally associated with the generation of earthquakes. It appears instead to reflect second-order rupturing related to a marked change in dip of strata to the south, and its general sense of movement is what one would expect if the breaks were developed during folding of the Monterey section against what amounts to a broad buttress of Obispo Tuff farther south (see geologic map, Figure 2.5-8). That the fault and shear movements were ancient is positively indicated by upward truncation of the zone at the bench of marine erosion along the base of the overlying terrace deposits.

As indicated earlier, bedrock was continuously exposed along several exploratory trenches. This bedrock is traversed by numerous fractures, most of which represent no more than rupture and very small amounts of simple separation. The others additionally represent displacement of the bedrock, and the map in Figure 2.5-14 shows every exposed break in the initial set of trenches along which any amount of displacement could be recognized or inferred.

That the surfaces of movement constitute no more than minor elements of the bedrock structure was verified by detailed mapping of the large excavations for the plant structures. Detailed examination of the excavation walls indicated that the faults exposed in the sea cliff south of Diablo Canyon continue through the rock under the Unit 1 turbine-generator building, where they are expressed as three subparallel breaks with easterly trend and moderately steep northerly dips (Figure 2.5-15).

Stratigraphic separation along these breaks ranges from a few inches to nearly 5 feet, and, in general, decreases eastward on each of them. They evidently die out in the ground immediately west of the containment excavation, and their eastward projections are represented by several joints along which no offsets have occurred. Such joints, with eastward trend and northward dip, also are abundant in some of the ground adjacent to the faults on the south (Figure 2.5-15).

The easterly reach of the Diablo Canyon sea cliff faults apparently corresponds to the two most northerly of the north-dipping faults mapped in Trench A (Figure 2.5-14). Dying out of these breaks, as established from subsequent large excavations in the ground east of where Trench A was located, explains and verifies the absence of faults in the exposed rocks of Trenches B and C. Other minor faults and shear surfaces mapped in the trench exposures could not be identified in the more extensive exposures of fresher rocks in the Unit 1 containment and turbine-generator building excavations. The few other minor faults that were mapped in these large excavations evidently are not sufficiently continuous to have been present in the exploratory trenches.

2.5.1.2.6 Site Engineering Properties

2.5.1.2.6.1 Field and Laboratory Investigations

In order to determine anticipated ground accelerations at the site, it was necessary to conduct field surveys and laboratory testing to evaluate the engineering properties of the materials underlying the site.

Bore holes were drilled into the rock upon which Category I structures are founded. The borings were located at or near the intersection of the then existing Unit 1 exploration trenches. (See Figures 2.5-11, 2.5-12, and 2.5-13 for exploratory trenching programs and boring locations.) These holes were cored continuously and representative samples were taken from the cores and submitted for laboratory testing.

The field work also included a reconnaissance to evaluate physical condition of the rocks that were exposed in trenches, and samples were collected from the ground surface in the trenches for laboratory testing. These investigations included seismic refraction measurements across the ground surface and uphole seismic measurements in the various drill holes to determine shear and compressional velocities of vertically propagated waves.

Laboratory testing, performed by Woodward-Clyde-Sherard & Associates, included unconfined compression tests, dynamic elastic moduli tests under controlled stress conditions, density and water content determinations, and Poisson's ratio tests. Tests were also carried out by Geo-Recon, Incorporated, to determine seismic velocities on selected rock samples in the laboratory. The results of seismic measurements in the field were used to construct a three-dimensional model of the subsurface materials beneath the plant site showing variations of shear wave velocity and compressional wave velocity both laterally and vertically. The seismic velocity data and elastic moduli

determined from laboratory testing were correlated to determine representative values of elastic moduli necessary for use in dynamic analyses of structures.

Details of field investigations and results of laboratory testing and correlation of data are contained in Appendices 2.5A and 2.5B of Reference 27 in Section 2.3.

2.5.1.2.6.2 Summary and Correlation of Data

The foundation material at the site can be categorized as a stratified sequence of fine to very fine grained sandstone deeply weathered to an average elevation of 75 to 80 feet, mean sea level (MSL). The rock is closely fractured, with tightly closed or healed fractures generally present below elevation 75 feet. Compressional and shear wave velocity interfaces generally are at an average elevation of 75 feet, correlating with fracture conditions.

Time-distance plots and seismic velocity profiles presenting results of each seismic refraction line and time depth plots with results for each uphole seismic survey are included in Appendices 2.5A and 2.5B of Reference 27 in Section 2.3. Compressional wave velocities range from 2350 to 5700 feet per second and shear wave velocities from 1400 to 3600 feet per second as determined by the refraction survey. These same parameters range from 2450 to 9800 and 1060 to 6050 feet per second as determined by the uphole survey. An isometric diagram summarizing results of the refraction survey for Unit 1 is also included in Appendix 2.5A of Reference 27 in Section 2.3.

Table 1 of Appendix 2.5A of Reference 27 of Section 2.3 shows calculations of Poisson's ratio and Young's Modulus based on representative compressional and shear wave velocities from the field geophysical investigations and laboratory measurements of compressional wave velocities. Table 2 of Appendix 2.5A of the same reference presents laboratory test results including density, unconfined compressive strength, Poisson's ratio and calculated values for compressional and shear wave velocities, shear modulus, and constrained modulus. Secant modulus values in Table 2 were determined from cyclic stress-controlled laboratory tests.

Compressional wave velocity measurements were made in the laboratory of four selected core samples and three hand specimens from exposures in the trench excavations. Measured values ranged from 5700 to 9500 feet per second. A complete tabulation of these results can be found in Appendix 2.5A of Reference 27 of Section 2.3.

2.5.1.2.6.3 Dynamic Elastic Moduli and Poisson's Ratio

Laboratory test results are considered to be indicative of intact specimens of foundation materials. Field test results are considered to be indicative of the gross assemblage of foundation materials, including fractures and other defects. Load stress conditions are obtained by evaluating cyclic load tests. In-place load stress conditions and confinement of the material at depth are also influential in determining elastic behavior.

Because of these considerations, originally recommended representative values for Young's Modulus of Elasticity and Poisson's ratio for the site were:

Depth Below Bottom of Trench	E	δ
0 to approximately 15 feet	44×10^6 lb/ft^2	0.20
Below 15 feet	148×10^6 lb/ft^2	0.18

A single value was selected for Young's Modulus below 15 feet because the initial analyses of the seismic response of the structures utilized a single value that was considered representative of the foundation earth materials as a whole.

More detailed seismic analyses were performed subsequent to the initial analyses. These analyses, discussed in Section 3.7.2, incorporated the finite element method and made it possible to model the rock beneath the plant site in a more refined manner by accounting for changes in properties with increasing depth. To determine the refined properties of the founding materials for these analyses, the test data were reviewed and consideration was given to: (a) strain range of the materials at the site, (b) overburden pressure and confinement, (c) load imposed by the structure, (d) observation of fracture condition and geometry of the founding rock in the open excavation, (e) decreases in Poisson's ratio with depth, and (f) significant advances in state-of-the-art techniques of testing and analysis in rock mechanics that had been made and which resulted in considerably more being known about the behavior of rock under seismic strains in 1970 than in 1968 or 1969.

For the purposes of developing the mathematical models that represented the rock mass, the foundation was divided into horizontal layers based on: (a) the estimated depth of disturbance of the foundation rock below the base of the excavation, (b) changes in rock type and physical condition as determined from bore hole logs, (c) velocity interfaces as determined by refraction geophysical surveys, and (d) estimated depth limit of fractures across which movement cannot take place because of confinement and combined overburden and structural load. Based on these considerations, the founding material properties as shown in Figure 2.5-19 were selected as being representative of the physical conditions in the founding rock.

2.5.1.2.6.4 Engineered Backfill

Backfill operations were carefully controlled to ensure stability and safety. All engineered backfill was placed in lifts not exceeding 8 inches in loose depth. Yard areas and roads were compacted to 95 percent relative compaction as determined by the method specified in ASTM D1557. Rock larger than 8 inches in its largest dimension that would not break down under the compactors was not permitted. Figures 2.5-17 and 2.5-18 show the plan and profile view of excavation and backfill for major plant structures.

2.5.1.2.6.5 Foundation Bearing Pressures

Seismic Category I structures were analyzed to determine the foundation pressures resulting from the combination of dead load, live load, and the double design earthquake (DDE). The maximum pressure was found to be 158 ksf and occurs under the containment structure foundation slab. This analysis assumed that the lateral seismic shear force will be transferred to the rock at the base of the slab which is embedded 11 feet into rock. This computed bearing pressure is considered conservative in that no passive lateral pressure was assumed to act on the sides of the slab. Based on the results of the laboratory tests of unconfined compressive strength of representative samples of rock at the site, which ranged from 800 to 1300 ksf, the calculated foundation pressure is well below the ultimate in situ rock bearing capacity.

Adverse hydrologic effects on the foundations of Seismic Category I structures (there are no Seismic Category I embankments) can be safely neglected at this site, since Seismic Category I structures are founded on a substantial layer of bedrock, and the groundwater level lies well below grade, at a level corresponding to that of Diablo Creek. Additionally, the computed factors of safety (minimum of 5 under DDE) of foundation pressures versus unconfined compressive strength of rock are sufficiently high to ensure foundation integrity in the unlikely event groundwater levels temporarily rose to foundation grade.

Soil properties such as grain size, Atterberg limits, and water content need not be considered since Seismic Category I structures and non-Seismic Category I structures housing Design Class I equipment are founded on rock.

2.5.2 VIBRATORY GROUND MOTION

2.5.2.1 Geologic Conditions of the Site and Vicinity

DCPP is situated at the coastline on the southwest flank of the San Luis Range, in the southern Coast Ranges of California. The San Luis Range branches from the main coastal mountain chain, the Santa Lucia Range, in the area north of the Santa Maria Valley and southeast of the plant site, and thence follows an alignment that curves toward the west. Owing to this divergence in structural grain, the range juts out from the regional coastline as a broad peninsula and is separated from the Santa Lucia Range by an elongated lowland that extends southeasterly from Morro Bay and includes Los Osos and San Luis Obispo Valleys. It is characterized by rugged west-northwesterly trending ridges and canyons, and by a narrow fringe of coastal terraces along its southwesterly flank.

Diablo Canyon follows a generally west-southwesterly course from the central part of the range to the north-central part of the terraced coastal strip. Detailed discussions of the lithology, stratigraphy, structure, and geologic history of the plant site and surrounding region are presented in Section 2.5.1.

2.5.2.2 Underlying Tectonic Structures

Evidence pertaining to tectonic and seismic conditions in the region of the DCPP site is summarized later in the section, and is illustrated in Figures 2.5-2, 2.5-3, 2.5-4, and 2.5-5. Table 2.5-1 includes a summary listing of the nature and effects of all significant historic earthquakes within 75 miles of the site that have been reported. Table 2.5-2 shows locations of 19 selected earthquakes that have been investigated by S. W. Smith. Table 2.5-3 lists the principal faults in the region and indicates major elements of their histories of displacement, in geological time units.

Benioff and Smith[5] have assessed the maximum earthquakes to be expected at the site, and John A. Blume and Associates[6,7] have derived the site vibratory motions that could result from these maximum earthquakes. An extensive discussion of the geology of the southern Coast Ranges, the western Transverse Ranges, and the adjoining offshore region is presented in Appendix 2.5D of Reference 27 of Section 2.3. Tectonic features of the central coastal region are discussed in Section 2.5.1.1.2, Regional Geologic and Tectonic Setting.

2.5.2.3 Behavior During Prior Earthquakes

Physical evidence that indicates the behavior of subsurface materials, strata, and structure during prior earthquakes is presented in Section 2.5.1.2.5. The section presents the findings of the exploratory trenching programs conducted at the site.

2.5.2.4 Engineering Properties of Materials Underlying the Site

A description of the static and dynamic engineering properties of the materials underlying the site is presented in Section 2.5.1.2.6, Site Engineering Properties.

2.5.2.5 Earthquake History

The seismicity of the southern Coast Ranges region is known from scattered records extending back to the beginning of the 19th century, and from instrumental records dating from about 1900. Detailed records of earthquake locations and magnitudes became available following installation of the California Institute of Technology and University of California (Berkeley) seismograph arrays in 1932.

A plot of the epicenters for all large historical earthquakes and for all instrumentally recorded earthquakes of Magnitude 4 or larger that have occurred within 200 miles of DCPP site is given in Figure 2.5-2. Plots of all historically and instrumentally recorded epicenters and all mapped faults within about 75 miles of the site are shown in Figures 2.5-3 and 2.5-4.

A tabulated list of seismic events, representing the computer printout from the Berkeley Seismograph Station records, supplemented with records of individual shocks of greater than Magnitude 4 that appear only in the Caltech records, is included as Table 2.5-1.

Table 2.5-2 gives a summary of revised epicenters of a representative sample of earthquakes off the coast of California near San Luis Obispo, as determined by S. W. Smith.

2.5.2.6 Correlation of Epicenters With Geologic Structures

Studies of particular aspects of the seismicity of the southern Coast Ranges region have been made by Benioff and Smith, Richter, and Allen. From results of these studies, together with data pertaining to the broader aspects of the geology and seismicity of central and eastern California, it can be concluded that, although the southern Coast Ranges region may be subjected to vibratory ground motion from earthquakes originating along faults as distant as 200 miles or more, the region itself is traversed by faults capable of producing large earthquakes, and that the strongest shaking possible for sites within the region probably would be caused by earthquakes no more than a few tens of miles away. Therefore, only the seismicity of the southern Coast Ranges, the adjacent offshore area, and the western Transverse Ranges is reviewed in detail.

Figure 2.5-3 shows three principal concentrations of earthquake epicenters, three smaller or more diffuse areas of activity, and a scattering of other epicenters. The most active areas, in terms of numbers of shocks, are the reach of the San Andreas fault north of about 35°7' latitude, the offshore area near Santa Barbara, and the offshore Santa Lucia Bank area. Notable concentrations of epicenters also are located as occurring in Salinas Valley, at Point San Simeon, and near Point Conception. The scattered epicenters are most numerous in the general vicinities of the most active areas, but they also occur at isolated points throughout the region.

The reliability of the position of instrumentally located epicenters of small shocks in the central California region has been relatively poor in the past, owing to its position between the areas covered by the Berkeley and Caltech seismograph networks. A recent study by Smith, however, resulted in relocation of nineteen epicenters in the coastal and offshore region between the latitudes of Point Arguello and Point Sur. Studies by Gawthrop[29] and reported in Wagner have led to results that seem to accord generally with those achieved by Smith.

The epicenters relocated by Smith and those recorded by Gawthrop are plotted in Figure 2.5-3. This plot shows that most of the epicenters recorded in the offshore region seem to be spatially associated with faults in the Santa Lucia Bank region, the East Boundary zone, and the San Simeon fault. Other epicenters, including ones for the 1952 Bryson shock, and several smaller shocks originally located in the offshore area, were determined to be centered on or near the Sur-Nacimiento fault north of the latitude of San Simeon.

2.5.2.7 Identification of Active Faults

Faults that have evidence of recent activity and have portions passing within 200 miles of the site are identified in Section 2.5.1.1.2.

2.5.2.8 Description of Active Faults

Active faults that have any part passing within 200 miles of the site are described in Section 2.5.1.1.2.

2.5.2.9 Maximum Earthquake

Benioff and Smith, in reviewing the seismicity of the region around DCPP site, determined the maximum earthquakes that could reasonably be expected to affect the site. Their conclusions regarding the maximum size earthquakes that can be expected to occur during the life of the reactor are listed below:

(1) Earthquake A: A great earthquake may occur on the San Andreas fault at a distance from the site of more than 48 miles. It would be likely to produce surface rupture along the San Andreas fault over a distance of 200 miles with a horizontal slip of about 20 feet and a vertical slip of 3 feet. The duration of strong shaking from such an event would be about 40 seconds, and the equivalent magnitude would be 8.5.

(2) Earthquake B: A large earthquake on the Nacimiento (Rinconada) fault at a distance from the site of more than 20 miles would be likely to produce a 60 mile surface rupture along the Nacimiento fault, a slip of 6 feet in the horizontal direction, and have a duration of 10 seconds. The equivalent magnitude would be 7.5.

(3) Earthquake C: Possible large earthquakes occurring on offshore fault systems that may need to be considered for the generation of seismic sea waves are listed below:

Location	Length of Fault Break	Slip, feet	Magnitude	Distance to Site
Santa Ynez Extension	80 miles	10 horizontal	7.5	50 miles
Cape Mendocino, NW Extension of San Andreas fault	100 miles	10 horizontal	7.5	420 miles
Gorda Escarpment	40 miles	5 vertical or 7 horizontal		420 miles

(4) Earthquake D: Should a great earthquake occur on the San Andreas fault, as described in "A" above, large aftershocks may occur out to distances of about 50 miles from the San Andreas fault, but those aftershocks which are not located on existing faults would not be expected to produce new surface faulting, and would be restricted to depths of about 6 miles or more and magnitudes of about 6.75 or less. The distance from the site to such aftershocks would thus be more than 6 miles.

A further assessment of the seismic potential of faults mapped in the region of DCPP site has been made following the extensive additional studies of on- and offshore geology of the last few years that are reported in Appendix 2.5D of Reference 27 of Section 2.3. This was done in terms of observed Holocene activity, to achieve assessment of what seismic activity is reasonably probable, in terms of observed late Pleistocene activity, fault dimensions, and style of deformation.

PG&E was requested by the NRC to evaluate the plant's capability to withstand a postulated Richter Magnitude 7.5 earthquake centered along an offshore zone of geologic faulting, generally referred to as the "Hosgri fault." The detailed methods, results, and plant modifications performed based on this evaluation are dealt with in Section 3.7.

The available information suggests that the faults in this region can be associated with contrasting general levels of seismic potential. These are as follows:

(1) Level I: Potential for great earthquakes involving surface faulting over distances on the order of 100 miles: seismic activity at this level should occur only on the reach of the San Andreas fault that extends between the locales of Cajon Pass and Parkfield. This was the source of the 1857 Fort Tejon earthquake, estimated to have been of Magnitude 8.

(2) Level II: Potential for large earthquakes involving faulting over distances on the order of tens of miles: seismic activity at this level can occur along offshore faults in the Santa Lucia Bank region (the likely source of the Magnitude 7.3 earthquake of 1927), and possibly along the Big Pine and Santa Ynez faults in the Transverse Ranges.

    Although the Rinconada-San Marcos-Jolon, Espinosa, Sur-Nacimiento, and San Simeon faults do not exhibit historical or even Holocene activity indicating this level of seismic potential, the fault dimensions, together with evidence of late Pleistocene movements along these faults, suggest that they may be regarded as capable of generating similarly large earthquakes.

(3) Level III: Potential for earthquakes resulting chiefly from movement at depth with no surface faulting, but at least with some possibility of surface faulting of as much as a few miles strike length and a few feet of slip:

Seismic activity at this level probably could occur on almost any major fault in the southern Coast Ranges and adjacent regions.

From the observed geologic record of limited fault activity extending into Quaternary time, and from the historical record of apparently associated seismicity, it can be inferred that both the greater frequency of earthquake activity and larger shocks from earthquake source structures having this level of seismic potential probably will be associated with one of the relatively extensive faults. Faults in the vicinity of the San Luis Range that may be considered to have such seismic potential include the West Huasna, Edna, and offshore Santa Maria Basin East Boundary zone.

(4) Level IV: Potential for earthquakes and aftershocks resulting from crustal movements that cannot be associated with any near-surface fault structures: such earthquakes apparently can occur almost anywhere in the region.

2.5.2.10 Ground Accelerations and Response Spectra

The maximum ground acceleration that would occur at DCPP site has been estimated for each of the postulated earthquakes listed in Section 2.5.2.9, using the methods set forth in References 12 and 24. The plant site acceleration is primarily dependent on the following parameters: Gutenberg-Richter magnitude and released energy, distance from the earthquake focus to the plant site, shear and compressional velocities of the rock media, and density of the rock. Rock properties are discussed under Section 2.5.1.2.6, Site Engineering Properties.

The maximum rock accelerations that would occur at the DCPP site are estimated as:

Earthquake A . . . . 0.10 g	Earthquake C . . . . 0.05 g
Earthquake B . . . . 0.12 g	Earthquake D . . . . 0.20 g

In addition to the maximum acceleration, the frequency distribution of earthquake motions is important for comparison of the effects on plant structures and equipment. In general, the parameters affecting the frequency distribution are distance, properties of the transmitting media, length of faulting, focus depth, and total energy release. Earthquakes that might reach the site after traveling over great distances would tend to have their high frequency waves filtered out. Earthquakes that might be centered close to the site would tend to produce wave forms at the site having minor low frequency characteristics.

In order to evaluate the frequency distribution of earthquakes, the concept of the response spectrum is used.

For nearby earthquakes, the resulting response spectra accelerations would peak sharply at short periods and would decay rapidly at longer periods. Earthquake D would

produce such response spectra. The March 1957 San Francisco earthquake as recorded in Golden Gate Park (S80°E component) was the same type. It produced a maximum recorded ground acceleration of 0.13 g (on rock) at a distance of about 8 miles from the epicenter. Since Earthquake D has an assigned hypocentral distance of 12 miles, it would be expected to produce response spectra similar in shape to those of the 1957 event.

Large earthquakes centered at some distance from the plant site would tend to produce response spectra accelerations that peak at longer periods than those for nearby smaller shocks. Such spectra maintain a higher spectral acceleration throughout the period range beyond the peak period. Earthquakes A and C are events that would tend to produce this type of spectra. The intensity of shaking as indicated by the maximum predicted ground acceleration shows that Earthquake C would always have lower spectral accelerations than Earthquake A.

Since the two shocks would have approximately the same shape spectra, Earthquake C would always have lower spectral accelerations than Earthquake A, and it is therefore eliminated from further consideration. The north-south component of the 1940 El Centro earthquake produced response spectra that emphasized the long period characteristics described above. Earthquake A, because of its distance from the plant site, would be expected to produce response spectra similar in shape to those produced by the El Centro event. Smoothed response spectra for Earthquake A were constructed by normalizing the El Centro spectra to 0.10 g. These spectra, however, show smaller accelerations than the corresponding spectra for Earthquake B (discussed in the next paragraph) for all building periods, and thus Earthquake A is also eliminated from further consideration.

Earthquake B would tend to produce response spectra that emphasize the intermediate period range inasmuch as the epicenter is not close enough to the plant site to produce large high frequency (short-period) effects, and it is too close to the site and too small in magnitude to produce large low frequency (long-period) effects. The N69°W component to the 1952 Taft earthquake produced response spectra having such characteristics. That shock was therefore used as a guide in establishing the shape of the response spectra that would be expected for Earthquake B.

Following several meetings with the AEC staff and their consultants, the following two modifications were made in order to make the criteria more conservative:

(1) The Earthquake D time-history was modified in order to obtain better continuity of frequency distribution between Earthquakes D and B.

(2) The accelerations of Earthquake B were increased by 25 percent in order to provide the required margin of safety to compensate for possible uncertainties in the basic earthquake data.

Accordingly, Earthquake D-modified was derived by modifying the S80°E component of the 1957 Golden Gate Park, San Francisco earthquake, and then normalizing to a maximum ground acceleration of 0.20 g. Smoothed response spectra for this earthquake are shown in Figure 2.5-21. Likewise, Earthquake B was derived by normalizing the N69°W component of the 1952 Taft earthquake to a maximum ground acceleration of 0.15 g. Smoothed response spectra for Earthquake B are shown in Figure 2.5-20. The maximum vibratory motion at the plant site would be produced by either Earthquake D-modified or Earthquake B, depending on the natural period of the vibrating body.

As mentioned earlier, based on a review of the studies presented in Appendices 2.5D and 2.5E (of Reference 27 in Section 2.3) by the NRC and the USGS (acting as the NRC's geological consultant), Supplement No. 4 to the NRC Safety Evaluation Report (SER) was issued in May 1976. This supplement included the USGS conclusion that a magnitude 7.5 earthquake could occur on the Hosgri fault at a point nearest to the Diablo Canyon site. The USGS further concluded that such an earthquake should be described in terms of near fault horizontal ground motion using techniques and conditions presented in Geological Survey Circular 672. The USGS also recommended that an effective, rather than instrumental, acceleration be derived for seismic analysis.

The NRC adopted the USGS recommendation of the seismic potential of the Hosgri fault. In addition, based on the recommendation of Dr. N. M. Newmark, the NRC prescribed that an effective horizontal ground acceleration of 0.75g be used for the development of response spectra to be employed in a seismic evaluation of the plant. The NRC outlined procedures considered appropriate for the evaluation including an adjustment of the response spectra to account for the filtering effect of the large building foundations. An appropriate allowance for torsion and tilting was to be included in the analysis. A guideline for the consideration of inelastic behavior, with an associated ductility ratio, was also established.

The NRC issued Supplement No. 5 to the SER in September 1976. This supplement included independently-derived response spectra and the rationale for their development. Parameters to be used in the foundation filtering calculation were delineated for each major structure. The supplement prescribed that either the spectra developed by Blume or Newmark would be acceptable for use in the evaluation with the following conditions:

(1) In the case of the Newmark spectra no reduction for nonlinear effects would be taken except in certain specific areas on an individual case basis.

(2) In the case of the Blume spectra a reduction for nonlinear behavior using a ductility ratio of up to 1.3 may be employed.

(3) The Blume spectra would be adjusted so as not to fall below the Newmark spectra at any frequency.

The development of the Blume ground response spectra, including the effect of foundation filtering, is briefly discussed below. The rationale and derivation of the Newmark ground response spectra is discussed in Appendix C to Supplement No. 5 of the SER.

The time-histories of strong motion for selected earthquakes recorded on rock close to the epicenters were normalized to a 0.75g peak acceleration. Such records provide the best available models for the Diablo Canyon conditions relative to the Hosgri fault zone. The eight earthquake records used are listed in the table below.

Earthquake	M	Depth, km	Recorded at	Epicentral Distance, km	Component	Peak Acceleration g
Helena 1935	6	5	Helena	3 to 8	EW	0.16
Helena 1935	6	5	Helena	3 to 8	NS	0.13
Daly City 1957	5.3	9	Golden Gate Park	8	N80W	0.13
Daly City 1957	5.3	9	Golden Gate Park	8	N10E	0.11
Parkfield 1966	5.6	7	Temblor 2	7	S25W	0.33
Parkfield 1966	5.6	7	Temblor 2	7	N65W	0.28
San Fernando 1971	6.6	13	Pacoima Dam	3	S14W	1.17
San Fernando 1971	6.6	13	Pacoima	3	N76W	1.08

The magnitudes are the greatest recorded thus far (September 1985) close in on rock stations and range from 5.3 to 6.6. Adjustments were made subsequently in the period range of the response spectrum above 0.40 sec for the greater long period energy expected in a 7.5M shock as compared to the model magnitudes.

The procedure followed was to develop 7 percent damped response spectra for each of the eight records normalized to 0.75g and then to treat the results statistically according to period bands to obtain the mean, the median, and the standard deviations of spectral response. At this stage, no adjustments for the size of the foundation or for ductility were made. The 7 percent damped response spectra were used as the basis for calculating spectra at other damping values.

Figures 2.5-29 and 2.5-30 show free-field horizontal ground response spectra as determined by Blume and Newmark, respectively, at damping levels from two to seven percent.

Figures 2.5-31 and 2.5-32 show vertical ground response spectra as determined by Blume and Newmark, respectively, for two to seven percent damping. The ordinates of vertical spectra are taken as two-thirds of the corresponding ordinates of the horizontal spectra.

2.5.3 SURFACE FAULTING

2.5.3.1 Geologic Conditions of the Site

The geologic history and lithologic, stratigraphic, and structural conditions of the site and the surrounding area are described in Section 2.5.1 and are illustrated in the various figures included in Section 2.5.

2.5.3.2 Evidence for Fault Offset

Substantive geologic evidence, described under Section 2.5.1.2, Geology of DCPP Site, indicates that the ground at and near the site has not been displaced by faulting for at least 80,000 to 120,000 years. It can be inferred, on the basis of regional geologic history, that minor faults in the site bedrock date from the mid-Pliocene or, at the latest, from mid-Pleistocene episodes of tectonic activity.

2.5.3.3 Identification of Active Faults

Three zones that include faults greater than 1000 feet in length have been mapped within about 5 miles of the site. Two of these, the Edna and San Miguelito fault zones, were mapped on land in the San Luis Range. The third, consisting of several breaks associated with the offshore Santa Maria Basin East Boundary zone of folding and faulting, is described in Sections 2.5.1.1.2.3 and 2.5.1.1.5.5 under Regional Geologic and Tectonic Setting. The mapped trace of each of these structures is shown in Figures 2.5-3 and 2.5-4.

2.5.3.4 Earthquakes Associated With Active Faults

The Edna fault or fault zone has been active at some time since the deposition of the Plio-Pleistocene Paso Robles Formation, which it displaces. It has no morphologic expression suggestive of late Pleistocene activity, nor is it known to displace late Pleistocene or younger deposits. Four epicenters of small (3.9 to 3M) shocks and 42 other epicenters for shocks of "small" or "unknown" intensity have been reported as occurring in the approximate vicinity of the Edna fault (Figures 2.5-3 and 2.5-4). Owing to the small size of the earthquakes that they represent, however, all of these epicenters are only approximately located. Further, they fall in the energy range of shocks that can be generated by fairly large construction blasts. At present, no conclusive evidence is available to determine whether the Edna fault could be classified as seismically active, or as geologically active in the sense of having undergone multiple movements within the last 500,000 years.

The San Miguelito fault has been mapped as not displacing the Plio-Pleistocene Paso Robles Formation. No instrumental epicenter has been reliably recorded from its vicinity, but the Berkeley Seismological Laboratory indicates Avila Bay as the presumed epicentral location for a moderately damaging (Intensity VII at Avila) earthquake that

occurred on December 1, 1916. It seems likely, however, that this shock occurred along the offshore East Boundary zone rather than on the San Miguelito fault zone.

The East Boundary zone has an overall length of about 70 miles. Individual breaks within the zone are as much as 30 miles long, though the varying amount of displacement that occurs along specific breaks indicates that movement along them is not uniform, and it suggests that breakage may have occurred on separate, limited segments of the faults. The reach of the zone that is opposite DCPP site contains four fault breaks. These breaks range from 1 to 15 miles in length, and they have minimum distances of 2.1 to 4.5 miles from the site. The East Boundary zone is considered to be seismically active, since at least five instrumentally well located epicenters and as many as ten less reliably located other epicenters are centered along or near the zone. One of the breaks (located 3-1/2 miles offshore from the site) exhibits topographic expression that may represent a tectonic offset of the sea floor surface at a point along its trace 6 miles north of the site. Other faults in the East Boundary zone have associated erosion features, a few of which could possibly be partly of faultline origin.

The earthquake of December 1, 1916, though listed as having an epicentral location at Avila Bay, is considered more probably to have originated along either the East Boundary zone or, possibly, the Santa Lucia Bank fault. Effects of this shock at Avila included landsliding in Dairy Canyon, 2 miles north of town, and "...disturbance of waters in the Bay of San Luis Obispo." "...plaster in several cottages...was jarred loose...while some of the smokestacks on the (Union Oil Company) refinery were toppled over." It is apparently on this basis that the Berkeley listing of earthquakes assigns this shock a "large" intensity and places its approximate epicentral location at Port San Luis.

A small (Magnitude 2.9) shock that apparently originated near the East Boundary zone a short distance south of DCPP site was lightly felt at the site on September 24, 1974. This shock, like most of those recorded along the East Boundary zone, was not damaging.

The minor fault zone that was mapped in the sea cliff at the mouth of Diablo Creek and in the excavation for the Unit 1 turbine building has an onshore length of about 550 feet, and it probably continues for some distance offshore. It has been definitely determined to be not active.

2.5.3.5 Correlation of Epicenters With Active Faults

Earthquake epicenters located within 50 miles of DCPP site have been approximately located in the vicinity of each of the faults. The reported earthquakes are listed in Table 2.5-1 and as follows, and their indicated epicentral locations are shown in Figures 2.5-3 and 2.5-4:

Earthquake Epicenters Reported as Being Located Approximately in the Vicinities of San Luis Obispo, Avila, and Arroyo Grande

Date	Geographic N Latitude	Coordinates W Longitude	Magnitude	Intensity	Notes and Greenwich Mean Time (GMT)
7.10.1889	35.17°	120.58°			Arroyo Grande. Shocks for several days.
12.1.1916	35.17°	120.75°		VII	VII at Avila. Considerable glass broken and goods in stores thrown from shelves at San Luis Obispo. Water in bay disturbed, plaster in cottages jarred loose, smoke stacks of Union Oil refinery toppled over at Avila. Severe at Port San Luis. III at Santa Maria: 22:53:00
4.26.1950	35.20°	120.60°	3.5	V	V at Santa Maria. Also felt at Orcutt: 7:23:29
1.26.1971	35.20°	120.70°	3		Near San Luis Obispo: 21:53:53
1830 to 7.21.1931	35.25°	120.67°			42 epicenters

Earthquake Epicenters Reported as Being Located Approximately in the Vicinity of the Offshore Santa Maria Basin East Boundary Zone

Date	Geographic Coordinates N Latitude	W Longitude	Magnitude	Intensity	Notes and Greenwich Mean Time (GMT)
5.27.1935(30-1)	35.62°	121.64°	3	III	Felt at Templeton: 16:08:00
9.7.1939(30-6)	34.46°	121.50°	3		Off San Luis Obispo County; felt at Cambria: 2:50:30
1.27.1945	34.75°	120.67°	3.9		17:50:31
12.31.1948(30-10)	35.60°	121.23°	4.6		Felt along coast from Lompoc to Moss Landing. VI at San Simeon. V at Cayucos, Creston, Moss Landing, Piedras Blancas Light Station: 14:35:46
11.17.1949	34.80°	120.70°	2.8		IV at Santa Maria. Near Priest: 5:06:60
2.5.1955(30-23)	35.86°	121.15°	3.3		West of San Simeon: 7:10:19
6.21.1957(30-25A)	35.23°	120.95°	3.7		Off Coast. Felt in San Luis Obispo, Morro Bay: 20:46:42
8.18.1958	35.60°	121.30	3.4		Near San Simeon: 5:30:42
10.25.1967	35.73°	121.45°	2.6		Near San Simeon: 23:05:39.5

(Figures in parentheses refer to events relocated by S. W. Smith, see Table 2.5-2).

2.5.3.6 Description of Active Faults

Data pertaining to faults with lengths greater than 1000 feet and reaches within 50 miles of the site are included in Section 2.5.1.1.5, Structure of the San Luis Range and Vicinity, and in Figures 2.5-3 and 2.5-4. These data indicate the fault lengths, relationship of the faults to regional tectonic structures, known history of displacements, outer limits, and whether the faults can be considered as active.

2.5.3.7 Results of Faulting Investigation

The site for Units 1 and 2 of DCPP was investigated in detail for faulting and other possibly detrimental geologic conditions. From studies made prior to design of the plant, it was determined that there was need to take into account the possibility of surface faulting in such design. The data on which this determination was based are presented in Section 2.5.1.2, Site Geology.

2.5.4 Stability of Subsurface Materials

The possibility of past or potential surface or subsurface ground subsidence, uplift, or collapse in the vicinity of DCPP was considered during the course of the geologic investigations for Units 1 and 2.

2.5.4.1 Geologic Features

The site is underlain by folded bedrock strata consisting predominantly of sandy mudstone and fine-grained sandstone. The existence of an unbroken and otherwise undeformed section of upper Pleistocene terrace deposits overlying a wave-cut bedrock bench at the site provides positive evidence that all folding and faulting in the bedrock antedated formation of the terrace. Local depressions and other irregularities on the bedrock surface plainly reflect erosion in an ancient surf zone.

The rocks that constitute the bedrock section are not subject to significant solution effects (i.e., development of cavities or channels that could affect the engineering or fluid conducting character of the rock) because the bedrock section does not contain thick or continuous bodies of soluble rock types such as limestone or gypsum. Voids encountered during excavation at the site were limited to thin zones of vuggy breccia and isolated vugs in some beds of calcareous mudstone. Areas where such minor vuggy conditions were present were noted at a few locations in the excavation for the Unit 2 containment and fuel handling structures (at plant grid coordinates N59, N597, E10, E005 and N59, N700, E10, E120).

The maximum size of any individual opening was 3 inches or less, and most were less than 1 inch in maximum dimension. Because of the limited extent and isolated nature of these small voids, they were not considered significant in foundation engineering or slope stability analyses.

It has been determined by field examination that no sea caves exist in the immediate vicinity of the site. The only cave like natural features in the area are shallow pits and hollows in some of the sea cliff outcrops of resistant tuff. These features generally have dimensions of a few inches to about 10 feet. They are superficial, and have originated through differential weathering of variably cemented rock.

Several exploratory wells have been drilled for petroleum within the San Luis Range, but no production was achieved and the wells were abandoned. The area is not now active in terms of either production or exploration. The location of the abandoned wells is shown in Figure 2.5-6, and the geologic relationships in the Range are illustrated in Section A-A' of Figure 2.5-6 and in Figure 2.5-7, Section D-D'. The nearest oil-producing area is the Arroyo Grande field, about 15 miles to the southeast.

The potential for future problems of ground instability at the site, because of nearby petroleum production, can be assessed in terms of the geologic potential for the occurrence of oil within, or offshore from, the San Luis Range. In addition, assessment can be made in terms of the geologic relationships in the site as contrasted with geologic conditions in places where oil field exploitation has resulted in deformation of the ground surface.

As shown in Figures 2.5-6 and 2.5-7, the San Luis Range has the structural form of a broad synclinal fold, which in turn is made up of several tightly compressed anticlines and synclines of lesser order. The configuration is not conducive to entrapment of hydrocarbon fluids, as such fluids tend to migrate upward through bedding and fracture-controlled zones of higher primary and secondary permeability until they reach a local trap or escape into the near surface or surface environment.

Within the San Luis Range, the only recognizable structural traps are in local zones where plunge reversals exist along the crests of the second-order anticlines. Such structures evidently were the actual or hoped-for targets for most of the exploratory wells that have been drilled in the San Luis Range, but none of these wells has produced enough oil or gas to record; thus, the traps have not been effective, or perhaps the strata are essentially lacking in hydrocarbon fluids. Other conditions that indicate poor petroleum prospects for the Range include the general absence of good reservoir rocks within the section and the relatively shallow basement of non petroliferous Franciscan rocks.

In the offshore, adjacent to the southerly flank of the San Luis Range, subsurface conditions are not well known, but are probably generally similar. Scattered data suggest that a structural high, perhaps defined by a west-northwest plunging anticline, may exist a few miles offshore from DCPP site. Such a feature could conceivably serve as a structural trap, if local closure were present along its axis; however, it seems unlikely that it would contain significant amounts of petroleum.

Available data pertaining to exploratory oil wells drilled in the region of the site are given here:

Exploratory Oil Wells in the Vicinity of DCPP Site

Data from exploratory wells drilled outside of oil and gas fields in California to December 31, 1963: Division of Oil and Gas, San Francisco.

Mount Diablo B. & M. T R Sec	Operator	Well No.	Elev, ft	Date Started	Total Depth, ft	Stratigraphy (depth in ft) Age at Bottom of Hole
31S 10E 3	Tidewater Oil Co.	"Montadoro" 1	365	April 1954	6,146	Monterey 0-3800; Obispo Tuff 3800: Franciscan; U. Jurassic
30S 10E 24	Gretna Corp.	"Maino-Gonzales" 1	275	March 1937	1,575	Franciscan; Jurassic
24	Wm. H. Provost	"Spooner" 1	325	July 1952	1,749	Jurassic
24	Shell Oil Co.	"Buchon"	-	-	-	-
34	A. O. Lewis	"Pecho" 1	177	May 1937	2,745	Monterey 0-2612; U. Miocene
30S 11E 9	Van Stone and Dallaston	"Souza" 1	42	Oct 1951	1,233	Franciscan; Jurassic
31S 11E 15	Tidewater Oil Co.	"Honolulu-Tidewater-U.S.L.-Heller Lease " 1	1,614	Jan 1958	10,788	Monterey 0-4363; Pt. Sal 4363; Obispo Tuff 4722; Rincon Shale 5370; 2nd Tuff 5546; 2nd Rincon Shale 6354; 3rd Tuff 10,174; L. Miocene

For the purpose of assessing the potential for the occurrence of adverse oil field related ground deformation effects at DCPP site, in the unlikely event that petroleum should be discovered and produced at a nearby location, it is useful to review the nature and causes of such ground deformation, and the types of geologic conditions at places where it has been observed.

The general subject of surface deformation associated with oil and gas field operations has been reviewed by Yerkes and Castle[22], among others. Such deformation includes differential subsidence, development of horizontally compressive strain effects within the central parts of subsidence bowls and horizontally extensive strain effects around their margins, and development or activation of cracks and faults. Pull-apart cracks and normal faults may develop in the marginal zone of extensive strain, while reverse and thrust faults sometimes occur in the central, compressive part of subsidence bowls. These effects all can develop when extraction of petroleum, water, and sand, plus lowering of fluid pressures, result in compression within and adjacent to producing zones, and attendant subsidence of the overlying ground. Other effects, including rebound of the ground surface, fault activation, and earthquake generation, have resulted from injection of fluid into the ground for purposes of secondary recovery, subsidence control, and disposal of fluid waste.

In virtually all instances of ground-surface deformation associated with petroleum production, the producing field has been centered on an anticlinal structure, in general relatively broad and internally faulted. The strata in the producing and overlying parts of the section typically are poorly consolidated sandstone, siltstone, claystone, and shale of low structural competence. The field generally is one with relatively large production, with significant decline of fluid pressure in the producing zones.

The conditions just cited can be contrasted with those obtained in the vicinity of DCPP site, where the rocks lie along the flank of a major syncline. They consist of tight sandstone, tuffaceous sandstone, mudstone, and shale, together with large resistant masses of tuff and diabase. Bedding dips range from near horizontal to vertical and steeply overturned, as shown in Section D-D' of Figure 2.5-7 and Section A-B of Figure 2.5-10. This structural setting is unlike any reported from areas where oil-field-associated surface deformation has occurred.

The foregoing discussion leads to the following conclusions: (a) future development of a producing oil field in the vicinity of DCPP site is highly unlikely because of unfavorable geologic conditions, and (b) geologic conditions in the site vicinity are not conducive to the occurrence of surface deformation, even if nearby petroleum production could be achieved.

As was noted in Section 2.4, the rocks underlying the site do not constitute a significant groundwater reservoir, so that future development of deep rock water wells in the vicinity is not a reasonable possibility. The considerations pertaining to surface deformation resulting from water extraction are about the same as for petroleum extraction, so there is no likelihood that DCPP site could experience artificially induced and potentially damaging subsidence, uplift, collapse, or changes in subsurface effective stress related to pore pressure phenomena.

There are no mineral deposits of economic significance in the ground underlying the site.

Although some regional warping and uplift may well be taking place in the southern Coast Ranges, such deformation cannot be sufficiently rapid and local to impose significant effects on coastal installations. Apparent elevation of the San Luis Range has increased about 100 feet relative to sea level since the cutting of the main terrace bench at least 80,000 years ago.

Expressions of deformation preserved in the bedrock at the site include minor faults, folds, and zones of blocky fracturing in sandstone and intra-bed shearing in claystone. Zones of cemented breccia also are present, as is widespread evidence of disturbance adjacent to intrusive bodies of tuff. Local weakening of the rocks in some of these zones led to some problems during construction, but these were handled by conventional techniques such as overexcavation and rock bolting. No observed features of deformation are large or continuous enough to impose significant effects on the overall performance of the site foundation.

The foundation excavations for Units 1 and 2 were extended below the zone of intense near surface weathering so that the exposed bedrock was found to be relatively fresh and firm. The principal zones of structural weakness are associated with small bodies of altered tuff and with internally sheared beds of claystone. The claystone intra-bed shear was expressed by the development of numerous slickensided shear surfaces within parts of the beds, especially in places where the claystone had locally been squeezed into pod like masses. The shearing and local squeezing clearly are expressions of the preferential occurrence of differential adjustments in the relatively weaker claystone beds during folding of the section.

The claystone beds are localized in a part of the rock section that underlies the discharge structure and extends across the southerly part of the Unit 2 turbine-generator building, thence continuing easterly, along a strike through the ground south of the Unit 2 containment. The bedding dips 48 to 75° north within this zone. Individual claystone beds range from 1/2 inch to about 6 inches in thickness, and they occur as interbeds in the sandstone-mudstone rock section.

The relationship of the claystone layers to the foundation excavation is such that they crop out in several narrow bands across the floor and walls (see Figures 2.5-15 and 2.5-16). Thus, the claystone bed remains confined within the rock section, except in a narrow strip at the face of the excavation. Because of the small amount of claystone mass and the geometric relationship of the steeply dipping claystone interbeds to the foundation structures, it was determined that the finished structure would not be affected by any tendency of the claystone to undergo further changes in volume.

The only area in which claystone swelling was monitored was along the north wall of the lower part of the large slot cut for the cooling water discharge structure. There are several thin (6 inches or less) claystone interbeds in the sandstone-mudstone section. Because the orientation of the bedding and the plane of the cut face differ by only about 30°, and the bedding dips steeply into the face, opening of the cut served both to remove lateral support from the rock behind the face, and also to expose the clay beds

to rainfall and runoff. This apparently resulted in both load relief and hydration swelling of the newly exposed claystone, which in turn caused some outward movement of the cut face. The movement then continued as gravity creep of the locally destabilized mass of rock between the claystone beds and the free face. The movement was finally controlled by installation of drilled-in lateral tie-backs, prior to placement of the reinforced concrete wall of the discharge structure.

No evidence of unrelieved residual stresses in the bedrock was noted during the excavation or subsequent construction of the plant foundation. Isolated occurrences of temporary slope instability clearly were related to locally weathered and fractured rock, hydration swelling of claystone interbeds, and local saturation by surface runoff. The Units 1 and 2 power plant facilities are founded on physically and chemically stable bedrock.

2.5.4.2 Properties of Underlying Materials

Static and dynamic engineering properties of materials in the subsurface at the site are presented in Section 2.5.1.2.6, Site Engineering Properties.

2.5.4.3 Plot Plan

Plan views of the site indicating exploratory boring and trenching locations are presented in Figures 2.5-8 and 2.5-11 through 2.5-15. Profiles illustrating the subsurface conditions relative to the Seismic Category I structures are furnished in Figures 2.5-12 through 2.5-16. Discussions of engineering properties of materials and groundwater conditions are included in Section 2.5.1.2.6, Site Engineering Properties.

2.5.4.4 Soil and Rock Characteristics

Information on compressional and shear wave velocity surveys performed at the site are included in Appendices 2.5A and 2.5B of Reference 27 of Section 2.3. Values of soil modulus of elasticity and Poisson's ratio calculated from seismic measurements are presented in Table 1 of Appendix 2.5A of Reference 27 of Section 2.3, and in Figure 2.5-19. Boring and trench logs are presented in Figures 2.5-23 through 2.5-28.

2.5.4.5 Excavations and Backfill

Plan and profile drawings of excavations and backfill at the site are presented in Figures 2.5-17 and 2.5-18. The engineered backfill placement operations are discussed in Section 2.5.1.2.6.4, Engineered Backfill.

2.5.4.6 Groundwater Conditions

Groundwater conditions at the site are discussed in Section 2.4.13. The effect on foundations of Seismic Category I structures is discussed in Section 2.5.1.2.6, Site Engineering Properties.

2.5.4.7 Response of Soil and Rock to Dynamic Loading

Details of dynamic testing on site materials are contained in Appendices 2.5A and 2.5B of Reference 27 in Section 2.3.

2.5.4.8 Liquefaction Potential

As stated in Section 2.5.1.2.6.5, adverse hydrologic effects on foundations of Seismic Category I structures can be neglected due to the structures being founded on bedrock and the groundwater level lying well below final grade.

There is a small local zone of medium dense sand located northeast of the intake structure and beneath a portion of buried ASW piping that is not attached to the circulating water tunnels. This zone is susceptible to liquefaction during design basis seismic events (References 45 and 46). The associated liquefaction-induced settlements from seismic events are considered in the design of the buried ASW piping. (References 48 and 49)

2.5.4.9 Earthquake Design Basis

The earthquakes postulated for DCPP site are discussed in Section 2.5.2.9, and a discussion of the design response spectra is in Section 3.7. Response acceleration curves for the site resulting from Earthquake B and Earthquake D-modified are shown in Figures 2.5-20 and 2.5-21, respectively. Response spectrum curves for the 7.5M Hosgri earthquake are shown in Figures 2.5-29 through 2.5-32.

2.5.4.10 Static Analysis

A discussion of the analyses performed on materials at the site is presented in Section 2.5.1.2.6, Site Engineering Properties.

2.5.4.11 Criteria and Design Methods

The criteria and methods used in evaluating subsurface material stability are presented in Section 2.5.1.2.6, Site Engineering Properties.

2.5.4.12 Techniques to Improve Subsurface Conditions

Due to the bearing of in situ rock being well in excess of the foundation pressure, no treatment of the in situ rock is necessary. Compaction specifications for backfill are presented in Section 2.5.1.2.6.4, Engineered Backfill.

2.5.5 SLOPE STABILITY

2.5.5.1 Slope Characteristics

The only slope whose failure during a DDE could adversely affect the nuclear power plant is the slope east of the building complex (see Figures 2.5-17, 2.5-18, and 2.5-22). To evaluate the stability of this slope, the soil and rock conditions were investigated by exploratory borings, test pits, and a thorough geological reconnaissance by the soil consultant, Harding-Lawson Associates, and was in addition to the overall geologic investigation performed by other consultants.

The slope configuration and representative locations of the subsurface conditions determined from the exploration are shown on Plates 2, 3, and 4 of Appendix 2.5C of Reference 27 of Section 2.3. Reference 44 provides further information compiled in 1997 in response to NRC questions on landslide potential.

Bedrock is exposed along the lower portions of the cut slope up to about the lower bench at elevation 115 feet. It consists of tuffaceous siltstone and fine-grained sandstone of the Monterey Formation. Terrace gravel overlies bedrock and extends to an approximate elevation of 145 feet. Stiff clays and silty soils with gravel and rock fragments constitute the upper material on the site. The upper few feet of fine-grained soils are dark brown and expansive.

No free groundwater was observed in any of the borings which were drilled in April 1971, nor was any evidence of groundwater observed in this slope during the previous years of investigation and construction of the project.

2.5.5.2 Design Criteria and Analyses

Undisturbed samples of the materials encountered in pits and borings were examined by the soil consultant in the laboratory and were subsequently tested to determine the shear strength, moisture content, and dry density. Strain controlled, unconsolidated, undrained triaxial tests at field moisture were performed on the clay to evaluate the shear strength of the materials penetrated. (The samples were maintained at field moisture since adverse moisture or seepage conditions were not encountered during this investigation nor previous investigations.) The confining stress was varied in relation to depth at which the undisturbed sample was taken. The test results are presented on the boring logs and are explained by the Key to Test Data, Figure 2.5-28.

The results of strength tests were correlated with the results developed during earlier investigations of DCPP site. Mohr circles of stresses at failure (6 to 7 percent strain) were drawn for each strength test result, and failure lines were developed through points representing one-half the deviator stresses. An average C-θ strength equal to a cohesion (C) value of 1000 psf and an angle of internal friction (θ) of 29° was selected for the slope stability analysis. The analysis was checked by maintaining the angle of

internal friction (θ) constant at 19° and varying the cohesion (C) from 950 psf (weakest layer) to 3400 psf (deepest and strongest layer).

Because of the presence of large gravel sizes, it was not possible to accurately determine the strength of the sand and gravel lense. However, based on tests on sand samples from other parts of the site, an angle of internal friction of 35° was selected as being the minimum available. An assumed rock strength of 5000 psf was used. This value is consistent with strength tests performed on remold rock samples from other areas of the site.

The stability of the slope was analyzed for the forces of gravity using a static method that is, the conventional method of slices. This analysis was checked using Bishop's modified method. The static method of analysis was chosen because, for the soil conditions at the site, it was judged to be more conservative than a dynamic analysis.

Because the overall strength of the rock would preclude a stability failure except along a plane of weakness which was not encountered in the borings or during the many geologic mappings of the slope, only the stability of the soil over the rock was analyzed. The strength parameters were varied as previously discussed to determine the minimum factor of safety under the most critical strength condition. For the static analysis excluding horizontal forces, the factor of safety was computed to be 3. When the additional unbalanced horizontal force of 0.4 times the weight of the soil within the critical surface combined with a vertical force of 0.26 times the weight was included, the minimum computed factor of safety was 1.1.

On the basis of the investigation and analysis, it was concluded that the slope adjacent to DCPP site would not experience instability of sufficient magnitude to damage adjacent safety-related structures.

The above conclusion is substantiated by additional field exploration, laboratory tests, and dynamic analyses using finite element techniques. See Appendix 2.5C of Reference 27 in Section 2.3, Harding-Lawson Associates' report on this work.

In response to an NRC request in early 1997, PG&E conducted further investigations of slope stability at the site[44]. The results of the investigations showed that earthquake loading following periods of prolonged precipitation will not produce any significant slope failure that can impact Design Class I structures and equipment. In addition, potential slope failures under such conditions will not adversely impact other important facilities, including the raw water reservoirs, the 230 kV and 500 kV switchyards, and the intake and discharge structures. Potential landslides may temporarily block the access road at several locations. However, there is considerable room adjacent to and north of the road to reroute emergency traffic.

2.5.5.3 Field Exploration

The investigation of the cut slope included geologic mapping of the soil and rock conditions exposed on the surface of slope and existing benches. Subsurface conditions were investigated by drilling test borings and by excavating test pits in the natural slope above the plant site (see Figure 2.5-22). The test borings were drilled with a truck mounted, 24 inch flight auger drill rig, and the test pits were excavated with a track-mounted backhoe. Boring and Log of Test Pits 1, 2, and 3 were logged by the soil consultant; borings 2 and 3 were logged by PG&E engineering personnel. The logs of all borings were verified by the soil consultant, who examined all samples obtained from each boring. Undisturbed samples were obtained from boring 2 and each of the test pits. Because of the stiffness of the soil, hardness of the rock, and type of drilling equipment used, the undisturbed samples were obtained by pushing an 18-inch steel tube that measured 2.5 inches in outside diameter. A Sprague & Henwood split-barrel sampler containing brass liners was used to obtain undisturbed soil samples from the test pits. The brass liners measured 2.5 inches in outside diameter and 6 inches in height. Logs of the borings and pits are shown in Figures 2.5-23 through 2.5-27. The soils were classified in accordance with the Unified Soil Classification System presented in Figure 2.5-28.

2.5.5.4 Slope Stability for Buried Auxiliary Saltwater System Piping

A portion of the buried ASW piping for Unit 1 ascends an approximate 2:1 (horizontal/vertical) slope to the parking area near the meteorology tower (Plates 1 and 2 of Reference 47). To ensure the stability of this slope in which the ASW piping is buried, a geotechnical evaluation, considering various design basis seismic events, was performed by Harding Lawson Associates. This evaluation is described in Reference 47. Based on this evaluation, it was concluded that this slope will be stable during seismic events and that additional loads resulting from permanent deformation of the slope will not impact the buried ASW piping.

2.5.6 REFERENCES

1. R. H. Jahns, "Geology of the Diablo Canyon Power Plant Site, San Luis Obispo County, California," 1967-Supplementary Reports I and II, 1968-Supplementary Report III, Diablo Canyon PSAR, Docket No. 50-275, (Main Report and Supplementary Report I). Diablo Canyon PSAR, Docket No. 50-323, (All reports, 1966 and 1967).

2. R. H. Jahns, "Guide to the Geology of the Diablo Canyon Nuclear Power Plant Site, San Luis Obispo County, California," Geol. Soc. Amer., Guidebook for 66th Annual Meeting, Cordilleran Section, 1970.

3. Deleted in Revision 1

4. Deleted in Revision 1

5. H. Benioff and S. W. Smith, "Seismic Evaluation of the Diablo Canyon Site," Diablo Canyon Unit 1 PSAR, Docket No. 50-275. Also, Diablo Canyon Unit 2 PSAR Docket No. 50-323, 1967.

6. John A. Blume & Associates, Engineers, "Earthquake Design Criteria for the Nuclear Power Plant - Diablo Canyon Site," Diablo Canyon Unit 1 PSAR, Docket No. 50-275., January 12, 1967. Also, Diablo Canyon Unit 2 PSAR Docket No. 50-323.

7. John A. Blume & Associates, Engineers, "Recommended Earthquake Design Criteria for the Nuclear Power Plant - Unit No. 2, Diablo Canyon Site," Diablo Canyon Unit 2 PSAR, Docket No. 50-323, June 24, 1968.

8. Deleted in Revision 1

9. Deleted in Revision 1

10. B. M. Page, "Geology of the Coast Ranges of California," E. H. Bailey (editor), Geology of Northern California, California Division, Mines and Geology, Bull. 190, 1966, pp 255-276.

11. B. M. Page, "Sur-Nacimiento Fault Zone of California: Continental Margin Tectonics," Geol. Soc. Amer., Bull., Vol. 81, 1970, pp 667-690.

12. J. G. Vedder and R. D. Brown, "Structural and Stratigraphic Relations Along the Nacimiento Fault in the Santa Lucia Range and San Rafael Mountains, California," W. R. Dickinson and Arthur Grantz (editors), Proceedings of Conference on Geologic Problems of the San Andreas Fault System, Stanford University Publs. in the Geol. Sciences, Vol. XI, 1968, pp 242-258.

13. C. F. Richter, "Possible Seismicity of the Nacimiento Fault, California," Geol. Soc. Amer., Bull., Vol. 80, 1969, pp 1363-1366.

14. E. W. Hart, "Possible Active Fault Movement Along the Nacimiento Fault Zone, Southern Coast Ranges, California," (abs.), Geol. Soc. Amer., Abstracts with Programs for 1969, pt. 3, 1969, pp 22-23.

15. R. E. Wallace, "Notes on Stream Channels Offset by the San Andreas Fault, Southern Coast Ranges, California," W. R. Dickinson and Arthur Grantz (editors), Proceedings of Conference on Geologic Problems of the San Andreas Fault System, Stanford University Publs. in the Geol. Sciences, Vol. XI, 1968, pp 242-258.

16. C. R. Allen, "The Tectonic Environments of Seismically Active and Inactive Areas Along the San Andreas Fault System," W. R. Dickinson and Arthur Grantz (editors), Proceedings of Conference on Geologic Problems of the San Andreas Fault System, Stanford University Publs. in the Geol. Sciences, Volume XI, 1968, pp 70-82.

17. Deleted in Revision 1

18. Deleted in Revision 1

19. L. A. Headlee, Geology of the Coastal Portion of the San Luis Range, San Luis Obispo County, California, Unpublished MS thesis, University of Southern California, 1965.

20. C. A. Hall, "Geologic Map of the Morro Bay South and Port San Luis Quadrangles, San Luis County, California," U.S. Geological Survey Miscellaneous Field Studies Map MF-511, 1973.

21. C. A. Hall and R. C. Surdam, "Geology of the San Luis Obispo-Nipomo Area, San Luis Obispo County, California," Geol. Soc. Amer., Guidebook for 63rd Ann. Meeting, Cordilleran Section, 1967.

22. R. F. Yerkes and R. O. Castle, "Surface Deformation Associated with Oil and Gas Field Operations in the United States in Land Subsidence," Proceedings of the Tokyo Symposium, Vol. 1, 1ASH/A1HS Unesco, 1969, pp 55-65.

23. C. W. Jennings, et al., Geologic Map of California, South Half, scale 1:750,000, California Div. Mines and Geology, 1972.

24. John H. Wiggins, Jr., "Effect of Site Conditions on Earthquake Intensity," ASCE Proceedings, Vol. 90, ST2, Part 1, 1964.

25. B. M. Page, "Time of Completion of Underthrusting of Franciscan Beneath Great Valley Rocks West of Salinian Block, California," Geol. Soc. Amer., Bull., Vol. 81, 1970, pp 2825-2834.

26. Eli A. Silver, "Basin Development Along Translational Continental Margins," W. R. Dickinson (editor), Geologic Interpretations from Global Tectonics with Applications for California Geology and Petroleum Exploration, San Joaquin Geological Society, Short Course, 1974.

27. T. W. Dibblee, The Riconada Fault in the Southern Coast Ranges, California, and Its Significance, Unpublished abstract of talk given to the AAPG, Pacific Section, 1972.

28. D. L. Durham, "Geology of the Southern Salinas Valley Area, California," U.S. Geol. Survey Prof. Paper 819, 1974, p 111.

29. William Gawthrop, Preliminary Report on a Short-term Seismic Study of the San Luis Obispo Region, in May 1973 (Unpublished research paper), 1973.

30. S. W. Smith, Analysis of Offshore Seismicity in the Vicinity of the Diablo Canyon Nuclear Power Plant, report to Pacific Gas and Electric Company, 1974.

31. H. C. Wagner, "Marine Geology between Cape San Martin and Pt. Sal, South-Central California Offshore; a Preliminary Report, August 1974," USGS Open File Report 74-252, 1974.

32. R. E. Wallace, "Earthquake Recurrence Intervals on the San Adreas Fault", Geol. Soc. Amer., Bull., Vol. 81, 1970, pp 1875-2890.

33. J. C. Savage and R. O. Burford, "Geodetic Determination of Relative Plate Motion in Central California", Jour. Geophys. Res., Vol. 78, No. 5, 1973, pp 832-845.

34. Deleted in Revision 1

35. Hill, et al., "San Andreas, Garlock, and Big Pine faults, California" - A Study of the character, history, and significance of their displacements, Geol. Soc. Amer., Bull., Vol. 64, No. 4, 1953, pp 443-458.

36. C.A. Hall and C.E. Corbato, "Stratigraphy and Structure of Mesozoic and Cenozoic Rocks, Nipomo Quadrangle, Southern Coast Ranges, California," Geol. Soc. Amer., Bull., Vol. 78, No. 5, 1969, pp 559-582. (Table 2.5-3, Sheet 1 of 2).

37. Bolt, Beranek, and Newman, Inc., Sparker Survey Line, Plates III and IV, 1973/1974. (Appendix 2.5D, to Diablo Canyon Power Plant Final Safety Analysis Report as amended through August 1980). (See also Reference 27 of Section 2.3.)

38. R. R. Compton, "Quatenary of the California Coast Ranges," E. H. Bailey (editor), Geology of Northern California, California Division Mines and Geology, Bull. 190, 1966, pp 277-287.

39. Regulatory Guide 1.70, Revision 1, Standard Format and Content of Safety Analysis Reports for Nuclear Power Plants, USNRC, October 1972.

40. Pacific Gas and Electric Company, Final Report of the Diablo Canyon Long Term Seismic Program, July 1988.

41. Pacific Gas and Electric Company, Addendum to the 1988 Final Report of the Diablo Canyon Long Term Seismic Program, February 1991.

42. NUREG-0675, Supplement No. 34, Safety Evaluation Report Related to the Operation of Diablo Canyon Nuclear Power Plant, Units 1 and 2, USNRC, June 1991.

43. NRC letter to PG&E, Transmittal of Safety Evaluation Closing Out Diablo Canyon Long-Term Seismic Program, (TAC Nos. M80670 and M80671), April 17, 1992.

44. Pacific Gas and Electric Company, Assessment of Slope Stability Near the Diablo Canyon Power Plant, April 1997.

45. Harding Lawson Associates, Liquefaction Evaluation - Proposed ASW Bypass - Diablo Canyon Power Plant, August 23, 1996.

46. Harding Lawson Associates Letter, "Geotechnical Consultation - Liquefaction Evaluation - Proposed ASW Bypass - Diablo Canyon Power Plant," October 1, 1996.

47. Harding Lawson Associates Report, Geotechnical Slope Stability Evaluation - ASW System Bypass, Unit 1 - Diablo Canyon Power Plant, July 3, 1996.

48. License Amendment Request 97-11, Submitted to the NRC by PG&E Letters DCL-97-150, dated August 26, 1997; DCL-97-177, dated October 14, 1997; DCL-97-191, dated November 13, 1997; and DCL-98-013, dated January 29, 1998.

49. NRC Letter to PG&E dated March 26, 1999, granting License Amendment No. 131 to Unit 1 and No. 129 to Unit 2.

TABLE 2.5-1

LISTING OF EARTHQAKES WITHIN 75 MILES OF THE DIABLO CANYON POWER PLANT SITE
SELECTED EARTHQUAKES

MM/DD/YY	HR/MN/SE	NORTH LAT	WEST LONG	QUALITY	MAG.	STA. REC.	FELT	MAXIMUM INTENSITY - COMMENTS
-?/-?/1800	-?--?--?	34.50	119.67	D			F	SANTA BARBARA.
03/25/1806	08--?--?	34.50	119.67	D			F	VIII AT SANTA BARBARA.
12/21/1812	18--?--?	34.50	120.00	D			F	VIII AT SAN FERNANDO.
12/21/1812	19--?--?	34.50	120.00	D			F	IX AT SAN FERNANDO.
01/18/1815	-?--?--?	34.50	119.67	D			F	SANTA BARBARA; 5 SHOCKS.
01/30/1815	-?--?--?	34.50	119.67	D			F	SANTA BARBARA.
07/08/1815	-?--?--?	34.50	119.67	D			F	SANTA BARBARA; 6 SHOCKS ON THE EIGHTH AND NINTH.
-?/-?/1830	-?--?--?	35.25	120.67	D			F	VIII AT SAN LUIS OBISPO.
07/03/1841	-?--?--?	36.30	122.30		6.3			(CALTECH FILE)
06/13/1851	-?--?--?	35.25	120.67	D			F	V AT SAN LUIS OBISPO.
10/26/1852	-?--?--?	35.67	121.17	D			F	X AT SAN SIMEON; 11 SHOCKS.
12/17/1852	-?--?--?	35.25	120.67	D			F	IX AT SAN LUIS OBISPO; 2 SHOCKS.
01/10/1853	-?--?--?	35.25	120.67	D			F	DANA RANCHO.
01/29/1853	-?--?--?	34.50	119.67	D			F	SANTA BARBARA.
02/01/1853	21--?--?	35.67	121.17	D			F	VIII AT SAN SIMEON.
02/14/1853	-?--?--?	35.25	120.67	D			F	SAN LUIS OBISPO.
03/01/1853	-?--?--?	34.50	119.67	D			F	V AT SAN LUIS OBISPO.
04/20/1854	-?--?--?	34.50	119.67	D			F	SANTA BARBARA.
04/29/1854	-?--?--?	34.50	119.67	D			F	III AT SANTA BARBARA.
05/03/1854	13-10--?	34.50	119.67	D			F	SANTA BARBARA; 3 SEVERE SHOCKS.
05/13/1854	-?--?--?	34.50	119.67	D			F	SANTA BARBARA.
05/29/1854	-?--?--?	34.50	119.67	D			F	SANTA BARBARA.
05/31/1854	12-50--?	34.50	119.67	D			F	VI AT SANTA BARBARA; 3 SHOCKS.
01/14/1855	02-30--?	35.75	120.67	D			F	SAN BENITO AND SAN MIGUEL.
06/25/1855	22--?--?	34.50	119.67	D			F	V AT SANTA BARBARA.
01/08/1857	14--?--?	34.50	119.67	D			F	SANTA BARBARA.
01/08/1857	17--?--?	34.50	119.67	D			F	SANTA BARBARA.
01/08/1857	18--?--?	34.50	119.67	D			F	SANTA BARBARA.
01/09/1857	07-20--?	34.50	119.67	D			F	IX AT SANTA BARBARA.
01/21/1857	-?--?--?	36.50	121.08	D			F	III AT A POINT NORTHWEST OF SAN BENITO.
03/14/1857	23--?--?	34.50	119.67	D			F	V AT MONTECITO AND SANTA BARBARA.
09/02/1858	-?--?--?	34.50	119.67	D			F	V AT SANTA BARBARA.
04/03/1860	04--?--?	36.50	121.08	D			F	VI AT SAN JOSE.
04/17/1860	-?--?--?	34.50	119.67	D			F	SANTA BARBARA.
-?/-?/1862	-?--?--?	34.42	119.63	D			F	VIII AT GOLETA.
09/13/1869	-?--?--?	35.25	120.67	D			F	V AT SAN LUIS OBISPO.
09/14/1869	-?--?--?	35.25	120.67	D			F	SAN LUIS OBISPO.
12/15/1869	-?--?--?	35.25	120.67				F	V AT SAN LUIS OBISPO.
02/06/1872	-?--?--?	34.50	119.67	D			F	SANTA BARBARA; FIRST SINCE APRIL 1860.
11/07/1875	-?--?--?	36.50	121.08	D			F	V IN SAN BENITO COUNTY.
12/21/1875	-?--?--?	34.50	119.67	D			F	SANTA BARBARA.
05/10/1876	-?--?--?	34.50	119.67	D			F	SANTA BARBARA.
05/30/1877	-?--?--?	35.67	120.67	D			F	V AT PASO ROBLES.

MM/DD/YY	HR/MN/SE	NORTH LAT	WEST LONG	QUALITY	MAG.	STA. REC.	FELT	MAXIMUM INTENSITY - COMMENTS
06/24/1877	07-30--?	34.50	119.67	D			F	SANTA BARBARA.
01/08/1878	-?--?--?	34.50	119.67	D			F	SANTA BARBARA.
11/13/1880	06-30--?	34.50	119.67	D			F	SANTA BARBARA.
02/02/1881	-?--?--?	36.37	121.67	D			F	III AT SALINAS.
08/31/1881	03--?--?	34.50	119.67	D			F	III AT SANTA BARBARA.
09/13/1883	22-30--?	34.50	119.67	D			F	IV AT SANTA BARBARA.
08/03/1884	-?--?--?	34.50	119.67	D			F	III AT SANTA BARBARA; NIGHT.
08/04/1884	09--?--?	34.50	119.67	D			F	III AT SANTA BARBARA; 3 SHOCKS.
03/31/1885	-?--?--?	36.30	121.00		7.0			(CALTECH FILE)
04/07/1885	10--?--?	34.50	119.67	D			F	SANTA BARBARA AND SAN BUENAVENTURA.
04/09/1885	-?--?--?	35.58	121.08	D			F	CAMBRIA.
04/12/1885	04-05--?	36.25	120.80	D			F	IX IN CENTRAL CALIFORNIA; FELT OVER AN AREA OF 125,000 SQ. MI.- EPICENTER PROBABLY EAST OF KING CITY.
04/12/1885	11--?--?	36.33	119.67	D			F	HANFORD.
07/09/1885	09-15--?	34.50	119.67	D			F	V AT SANTA BARBARA.
07/09/1885	16-15--?	34.50	119.67	D			F	V AT SANTA BARBARA; 5 EARTHQUAKES.
10/03/1888	20-52--?	35.75	120.67	D			F	III AT SAN MIGUEL.
10/03/1888	21-02--?	35.75	120.67	D			F	VI AT SAN MIGUEL.
10/04/1888	-?--?--?	35.67	120.67	D			F	PASO ROBLES.
05/01/1889	19-55--?	34.67	120.42	D			F	SUSANVILLE.
05/26/1889	15-13--?	36.50	121.42	D			F	GONZALES, SAN FRANCISCO, AND SANTA CRUZ; RECORDED AT MT. HAMILTON.
07/10/1889	-?--?--?	35.17	120.58	D			F	ARROYO GRANDE; SHOCKS FOR SEVERAL DAYS.
09/30/1889	20-17--?	36.50	119.58	D			F	KINGSBURG.
01/-?/1890	23-30--?	34.50	119.67	D			F	SANTA BARBARA.
11/13/1892	-?--?--?	36.30	122.00		6.0			(CALTECH FILE)
05/19/1893	-?-35--?	34.17	119.50	D			F	VII FELT FROM SAN DIEGO TO LOMPOC, INLAND TO SAN BERNADINO. MOST SEVERE SE OF VENTURA. POSSIBLY OF SUBMARINE ORIGIN OFF THE COAST OF VENTURA COUNTY
06/01/1893	12--?--?	34.50	119.67	D			F	VII AT NORDHOFF (OJAI), SANTA BARBARA, AND VENTURA.
06/01/1893	12--?--?	34.50	119.67	D			F	NORDHOFF, SANTA BARBARA, AND VENTURA.
06/01/1893	12-10--?	34.50	119.67	D			F	NORDHOFF, SANTA BARBARA, AND VENTURA.
12/06/1893	04-56--?	35.67	121.33	D			F	PIEDRAS BLANCAS LIGHTHOUSE.
07/27/1895	-?-10--?	34.50	119.67	D			F	SANTA BARBARA.
12/24/1895	05-30--?	34.50	119.67	D			F	SANTA BARBARA.
06/24/1897	14-10--?	34.50	119.67	D			F	SANTA BARBARA.
07/18/1897	-?--?--?	34.50	119.67	D			F	CASTLE PINCKNEY.
07/20/1897	07-45--?	34.50	119.67	D			F	SANTA BARBARA.
05/30/1898	03-03--?	34.50	119.67	D			F	SANTA BARBARA.
06/04/1898	06-20--?	34.67	120.08	D			F	LOS OLIVOS; FELT THROUGHOUT THE SANTA YNEZ VALLEY; AT SANTA BARBARA THE HEAVIEST FOR SOME YEARS.
02/08/1899	04-55--?	36.33	121.92	D			F	POINT SUR LIGHT STATION.
06/05/1899	-?--?--?	35.83	120.83	D			F	BRADLEY.
06/25/1899	-?--?--?	35.75	120.67	D			F	SAN MIGUEL.
06/09/1900	-?--?--?	36.00	120.92	D			F	SAN ARDO.
10/18/1900	-?--?--?	35.25	120.67	D			F	SAN LUIS OBISPO.
03/03/1901	-?--?--?	35.25	120.67	D			F	SAN LUIS OBISPO.

MM/DD/YY	HR/MN/SE	NORTH LAT	WEST LONG	QUALITY	MAG.	STA. REC.	FELT	MAXIMUM INTENSITY - COMMENTS
03/03/1901	07-45--?	36.08	120.58	D			F	IX AT STONE CANYON - SURFACE CRACKS IN THE GROUND; ALSO FELT AT ADELAIDA, ESTRELLA, PARKFIELD, PASO ROBLES, PORTERVILLE, SAN JOSE, SAN LUIS OBISPO, AND SAN MIGUEL.
03/05/1901	-?--?--?	35.67	120.67	D			F	PASO ROBLES.
03/06/1901	-?--?--?	36.00	120.92	D			F	SAN ARDO AND SAN LUIS OBISPO.
06/03/1901	-?--?--?	35.25	120.67	D			F	SAN LUIS OBISPO.
07/30/1901	19--?--?	35.25	120.67	D			F	SAN LUIS OBISPO.
08/14/1901	11-11--?	35.42	120.92	D			F	CAYUCOS, HOLLISTER, SALINAS, SAN LUIS OBISPO, AND SANTA CRUZ.
02/07/1902	-?--?--?	34.50	119.67	D			F	SANTA BARBARA.
02/09/1902	15--?--?	34.50	119.67	D			F	PINE CREST, SAN LUIS OBISPO, SANTA BARBARA, AND VENTURA.
04/06/1902	-?--?--?	35.25	120.67	D			F	SAN LUIS OBISPO.
07/21/1902	-?--?--?	34.75	120.00	D			F	PINE CREST.
07/28/1902	06-57--?	34.75	120.25	D			F	IX AT LOMPOC AND LOS ALAMOS; CONFINED TO THE NORTHERN PART OF SANTA BARBARA COUNTY.
07/28/1902	13--8--?	35.25	120.67	D			F	SAN LUIS OBISPO; AFTERSHOCK OF 06-57-?.
07/31/1902	09-20--?	34.75	120.25	D			F	IX AT LOS ALAMOS AND SURROUNDING COUNTRY; FISSURES, CRACKS IN THE GROUND, AND LANDSLIDES.
08/01/1902	-?--?--?	34.75	120.25	D			F	LOS ALAMOS. SEVERAL SHOCKS.
08/01/1902	03-30--?	34.75	120.25	D			F	VIII AT LOS ALAMOS.
08/02/1902	-?--?--?	34.75	120.25	D			F	LOS ALAMOS.
08/03/1902	-?--?--?	34.75	120.25	D			F	LOS ALAMOS.
08/04/1902	10 -5--?	34.75	120.25	D			F	LOS ALAMOS.
08/04/1902	11-18--?	34.75	120.25	D			F	LOS ALAMOS.
08/04/1902	12-15--?	34.75	120.25	D			F	LOS ALAMOS.
08/04/1902	21-29--?	34.75	120.25	D			F	LOS ALAMOS.
08/04/1902	23-40--?	34.75	120.25	D			F	LOS ALAMOS.
08/05/1902	-?-55--?	34.75	120.25	D			F	LOS ALAMOS.
08/10/1902	-?--?--?	34.75	120.25	D			F	LOS ALAMOS; DISTINCT EARTHQUAKE DETONATION AND TREMOR.
08/10/1902	10-40--?	34.75	120.25	D			F	LOS ALAMOS; HEAVY DETONATION FOLLOWED BY TREMBLING.
08/10/1902	22-40--?	34.50	119.67	D			F	SANTA BARBARA.
08/14/1902	10-15--?	34.75	120.25	D			F	LOS ALAMOS.
08/14/1902	11-05--?	34.75	120.25	D			F	LOS ALAMOS.
08/14/1902	11-20--?	34.75	120.25	D			F	LOS ALAMOS; SHOOK GROUND VIOLENTLY.
08/14/1902	21-50--?	34.75	120.25	D			F	LOS ALAMOS.
08/14/1902	23-50--?	34.75	120.25	D			F	LOS ALAMOS.
08/28/1902	-?--?--?	35.25	120.67	D			F	SAN LUIS OBISPO.
08/31/1902	-?--?--?	35.25	120.67	D			F	SAN LUIS OBISPO.
09/11/1902	05-30--?	34.25	120.25	D			F	V AT LOS ALAMOS.
10/21/1902	21-45--?	34.75	120.25	D			F	LOMPOC AND LOS ALAMOS.
10/21/1902	22-15--?	34.75	120.25	D			F	LOMPOC AND LOS ALAMOS.
10/22/1902	10--?--?	34.75	120.25	D			F	LOS ALAMOS.
12/12/1902	-?--?--?	34.75	120.25	D			F	VIII AT LOS ALAMOS -3 SHOCKS IN 5 MINUTES; FELT THROUGHOUT THE NORTHERN PART OF SANTA BARBARA COUNTY, ESPECIALLY AT LOMPOC, LOS ALAMOS, SAN LUIS OBISPO, SANTA BARBARA, AND SANTA MARIA.
01/11/1903	-?--?--?	35.25	120.67	D			F	SAN LUIS OBISPO.

MM/DD/YY	HR/MN/SE	NORTH LAT	WEST LONG	QUALITY	MAG.	STA. REC.	FELT	MAXIMUM INTENSITY - COMMENTS
03/07/1903	-?--?--?	36.50	121.42	D			F	GONZALES.
03/24/1903	-?--?--?	36.50	121.42	D			F	GONZALES AND SANTA MARGARITA.
04/24/1903	-?--?--?	35.42	120.58	D			F	SANTA MARGARITA.
07/29/1903	07-13--?	35.67	121.33	D			F	V AT POINT PIEDRAS BLANCAS LIGHTHOUSE.
07/29/1903	10-30--?	35.67	121.33	D			F	POINT PIEDRAS BLANCAS LIGHTHOUSE.
08/24/1903	-?--?--?	34.67	120.08	D			F	LOS OLIVOS.
01/22/1904	-?--?--?	34.75	120.25	D			F	LOS ALAMOS.
01/23/1904	-?--?--?	34.75	120.25	D			F	LOS ALAMOS.
09/10/1904	-?--?--?	35.25	120.67	D			F	SAN LUIS OBISPO.
05/26/1905	05-49--?	35.25	120.67	D			F	LOS GATOS, SALINAS, SAN FRANCISCO, SAN LUIS OBISPO, SANTA CRUZ AND SOLEDAD.
07/06/1906	-?--?--?	35.25	120.67	D			F	SAN LUIS OBISPO.
07/22/1906	-?--?--?	35.25	120.67	D			F	SAN LUIS OBISPO.
08/01/1906	-?--?--?	35.25	120.67	D			F	SAN LUIS OBISPO.
12/07/1906	06-40--?	35.67	121.33	D			F	VII AT SAN LUIS OBISPO AND SANTA MARIA; DURATION 30 SECONDS, FOLLOWED BY SECOND SHOCK HALF AN HOUR LATER.
+12/08/1906	06-55--?	35.75	120.67	D			F	SAN MIGUEL.
06/19/1907	12--?--?	36.17	120.67	D			F	PRIEST VALLEY.
07/02/1907	18-10--?	35.25	120.67	D			F	SAN LUIS OBISPO.
07/21/1907	-?--?--?	35.25	120.67	D			F	SAN LUIS OBISPO.
07/29/1907	05-10--?	34.75	120.00	D			F	PINE CREST.
08/-?/1907	-?--?--?	34.75	120.00	D			F	PINE CREST AND SANTA BARBARA.
12/27/1907	09-15--?	34.50	119.67	D			F	SANTA BARBARA; ALSO FELT AT VENTURA; REPORTED FROM OJAI AND PINE CREST.
04/27/1908	10-50--?	36.00	121.17	D			F	JOLON, PASO ROBLES, PRIEST VALLEY, SAN LUIS OBISPO, SANTA MARGARETA, AND SAN MIGUEL.
05/19/1908	-?--?--?	35.25	120.67	D			F	SAN LUIS OBISPO.
09/16/1908	-?--?--?	36.17	120.67	D			F	PRIEST VALLEY.
11/-?/1908	19-30--?	36.17	120.67	D			F	PRIEST VALLEY.
01/23/1909	14-58--?	34.50	119.67	D			F	PINE CREST AND SANTA BARBARA.
04/10/1909	-?--?--?	34.50	119.67	D			F	MONO RANCH AND SANTA PAULA CANYON.
06/17/1909	08-20--?	36.42	121.33	D			F	SOLEDAD.
07/03/1909	07--?--?	34.50	119.67	D			F	MONTECITO AND SANTA BARBARA.
07/05/1909	06-10--?	34.50	119.67	D			F	III AT SANTA BARBARA.
07/16/1909	10-28--?	34.50	119.67	D			F	IV AT LOS ANGELES AND SANTA BARBARA.
07/31/1909	19-37--?	34.50	119.67	D			F	IV AT OJAI AND SANTA BARBARA.
08/18/1909	-?--?--?	35.25	120.67	D			F	SAN LUIS OBISPO.
11/24/1909	15--?--?	36.00	121.17	D			F	JOLON.
03/08/1910	09-30--?	36.17	120.67	D			F	PRIEST VALLEY.
04/30/1910	18-25--?	36.17	120.67	D			F	PRIEST VALLEY; 3 SHOCKS, THE SECOND ONE QUITE VIOLENT.
11/-?/1910	-?--?--?	34.50	119.67	D			F	SANTA BARBARA; 2 SLIGHT QUAKES DURING NOVEMBER.
02/02/1911	-?--?--?	34.75	120.25	D			F	LOS ALAMOS.
03/22/1911	10-55--?	35.75	120.67	D			F	SAN MIGUEL; QUITE SEVERE.
06/02/1911	-?--?--?	36.17	120.67	D			F	PRIEST VALLEY.
06/18/1912	22-27--?	36.00	121.17	D			F	JOLON. (RECORDED AT BERKELEY.)
10/20/1913	11-25--?	35.25	120.67	D			F	BETTERAVIA, PASO ROBLES, SAN LUIS OBISPO,AND SANTA MARIA.
11/27/1913	19--?--?	34.50	119.67	D			F	MONO RANCH.

MM/DD/YY	HR/MN/SE	NORTH LAT	WEST LONG	QUALITY	MAG.	STA. REC.	FELT	MAXIMUM INTENSITY - COMMENTS
12/26/1913	12--?--?	36.17	121.00	D			F	SAN LUCAS.
11/24/1914	04-25--?	35.25	120.67	D			F	II AT SAN LUIS OBISPO; ABRUPT TREMBLING, LASTING 20 SECONDS.
01/12/1915	-?--?--?	34.92	120.50	D			F	BETTERAVIA.
01/12/1915	04-31--?	34.75	120.25	B			F	VIII AT LOS ALAMOS - EPICENTER 2 OR 3 MI. EAST OF LOS ALAMOS; FELT FROM SAN JOSE TO LOS ANGELES; SHAKEN AREA IN EXCESS OF 50,000 SQ. MI. - PRACTICALLY EVERY CHIMNEY DAMAGED AT LOS ALAMOS, VII AT LOMPOC, VI-VII AT SANTA MARIA, V AT SAN LUIS OBISPO AND SANTA BARBARA, IV AT PASO ROBLES, AND II AT LOS ANGELES, WEATHER BUREAU REPORTED V-VI AT SANTA BARBARA, V AT OZENA AND SAN LUIS OBISPO, IV AT PASO ROBLES, III AT OJAI, AND II IN PRIEST VALLEY; ALSO II AT BAKERSFIELD.
01/14/1915	-?--?--?	34.92	120.50	D			F	BETTERAVIA.
01/15/1915	-?--?--?	34.75	120.25	D			F	LOS ALAMOS.
01/20/1915	-?--?--?	34.75	120.25	D			F	LOS ALAMOS.
01/26/1915	-?--?--?	34.75	120.25	D			F	LOS ALAMOS.
01/27/1915	-?--?--?	34.75	120.25	D			F	LOS ALAMOS.
04/21/1915	09-58--?	35.25	120.67	D			F	IV AT SAN LUIS OBISPO; ALSO FELT 3 MI. NW OF PRIEST VALLEY.
08/23/1915	23-15--?	34.75	119.75	D			F	HILL CAMP.
08/31/1915	21--?--?	34.75	119.75	D			F	HILL CAMP.
09/08/1915	12-45--?	35.67	120.67	D			F	V IN REGION EAST OF PASO ROBLES; ANTELOPE - 2 SHOCKS, FIRST THE HEAVIER, OIL CAME UP WITH WATER IN WELL AFTER SHOCK. AT SHANDON A SEATED MAN WAS SHAKEN SO HARD HE THOUGHT A PERSON WAS SHAKING HIM. AT CRESTON THE SHOCK WAS SHORT AND SHARP. A SLIGHT LANDSLIDE AT PORT SAN LUIS. WEATHER BUREAU REPORTS -PASO ROBLES V AND SAN LUIS OBISPO III-IV.
09/14/1915	-?--?--?	34.75	119.75	D			F	HILL CAMP; 3 HARD SHOCKS - EARTH TREMBLED FOR 15 MINUTES AFTERWARDS.
02/27/1916	13-26--?	34.75	120.25	D			F	LOS ALAMOS.
03/01/1916	19-15--?	34.75	120.25	D			F	LOS ALAMOS.
05/06/1916	03-45--?	34.75	120.25	D			F	III AT LOS ALAMOS. FELT BY MANY AT EL ROBLAR RANCH, 2 MI. SE OF LOS ALAMOS.
08/06/1916	-?--?--?	36.00	121.00		7.0			(CALTECH FILE)
10/24/1916	13-03--?	35.25	120.67	D			F	II AT SAN LUIS OBISPO; PROBABLY NEXT SHOCK, WITH TIME ERROR.
10/24/1916	13-30--?	36.00	121.17	D			F	V AT JOLON; III AT A POINT 3.5 MI. NW OF PRIEST VALLEY.
12/01/1916	22-53--?	35.17	120.75	D			F	VII AT AVILA - CONSIDERABLE GLASS BROKEN AND GOODS IN STORES THROWN FROM SHELVES. FELT AT SAN LUIS OBISPO; WATER IN BAY DISTURBED, PLASTER IN COTTAGES JARRED LOOSE, SMOKESTACKS OF UNION OIL CO. REFINERY TOPPLED OVER. SEVERE AT PORT SAN LUIS; III AT SANTA MARIA.
02/01/1917	05-18--?	34.92	120.42	D			F	III AT SANTA MARIA.
04/05/1917	19--?--?	34.67	120.33	D			F	IV AT SANTA RITA; ALSO FELT AT LOMPOC.

MM/DD/YY	HR/MN/SE	NORTH LAT	WEST LONG	QUALITY	MAG.	STA. REC.	FELT	MAXIMUM INTENSITY - COMMENTS
04/13/1917	03-59--?	34.25	119.67	D			F	VI AT SANTA BARBARA CHANNEL REGION; FELT OVER AN AREA OF COAST SOUTH AND EAST OF SANTA BARBARA AS FAR AS VENTURA, AND ON SANTA CRUZ ISLAND.
04/21/1917	06-59--?	34.25	119.67	D			F	V AT SANTA BARBARA CHANNEL; PERCEPTIBLE OVER AN AREA OF PERHAPS 4000 SQ. MI.
07/07/1917	20-57--?	35.25	120.50	D			F	LOPEZ CANYON; ALSO AT SAN LUIS OBISPO.
07/07/1917	21-02--?	35.25	120.50	D			F	LOPEZ CANYON.
07/07/1917	21-15--?	35.25	120.50	D			F	LOPEZ CANYON.
07/08/1917	03-20--?	34.92	120.42	D			F	II AT SANTA MARIA.
07/08/1917	11-29--?	35.25	120.50	D			F	IV IN LOPEZ CANYON.
07/09/1917	22-22--?	35.25	120.50	D			F	VII IN LOPEZ CANYON; IV AT SAN LUIS OBISPO.
07/09/1917	22-38--?	35.25	120.50	D			F	LOPEZ CANYON.
07/10/1917	-?-43--?	35.25	120.50	D			F	LOPEZ CANYON.
07/10/1917	-?-45--?	35.25	120.50	D			F	LOPEZ CANYON.
07/26/1917	08-31--?	34.92	120.42	D			F	V AT SANTA MARIA - FURNITURE MOVED. IV AT LOS OLIVOS - AWAKENED SLEEPERS AT SAN LUIS OBISPO
12/05/1918	02-38--?	35.67	120.67	D			F	IV AT PASO ROBLES; II AT SAN LUIS OBISPO.
12/05/1918	04-30--?	35.25	120.67	D			F	SAN LUIS OBISPO.
03/01/1919	04-19--?	36.17	120.67	D			F	IV IN PRIEST VALLEY.
03/15/1919	07-53--?	35.25	120.67	D			F	SAN LUIS OBISPO.
07/31/1919	21-31--?	36.33	120.67	D			F	V IN SAN BENITO COUNTY; FELT AT IDRIA - ORIGIN SOME DISTANCE FROM IDRIA
08/26/1919	12-12--?	34.50	119.67	D			F	V IN SANTA BARBARA COUNTY - FELT AT OJAI, SAN LUIS OBISPO (3 SHOCKS), SANTA BARBARA.
08/26/1919	14.57--?	34.50	119.67	D			F	V IN SANTA BARBARA COUNTY - THIS SHOCK STRONGER AT SANTA BARBARA THAN PREVIOUS SHOCK. BUILDINGS AND WHARVES SWAYED; FELT AT OJAI.
12/18/1919	07-15--?	35.67	120.67	D			F	PASO ROBLES.
01/30/1920	23-30--?	34.50	119.67	D			F	III AT SANTA BARBARA.
01/30/1920	23-33--?	34.50	119.67	D			F	II AT SANTA BARBARA.
01/30/1920	23-35--?	34.50	119.67	D			F	II AT SANTA BARBARA.
01/30/1920	23-38--?	34.50	119.67	D			F	II AT SANTA BARBARA.
01/31/1920	01--?--?	34.50	119.67	D			F	III AT SANTA BARBARA.
01/31/1920	01-03--?	34.50	119.67	D			F	III AT SANTA BARBARA.
01/31/1920	01-07--?	34.50	119.67	D			F	III AT SANTA BARBARA.
03/20/1920	07-04--?	35.25	120.67	D			F	II AT SAN LUIS OBISPO.
05/07/1920	01-59--?	35.25	120.67	D			F	IV AT SAN LUIS OBISPO.
06/28/1920	09-01--?	35.25	120.67	D			F	V AT SAN LUIS OBISPO.
12/01/1920	01-30--?	35.17	119.50	D			F	VI AT TAFT - MANY PEOPLE MADE "SEASICK", DISHES SHAKEN FROM SHELVES, IV AT MARICOPA.
12/05/1920	11-58--?	34.50	119.67	D			F	V IN SANTA BARBARA COUNTY MOUNTAINS, V AT LOMPOC, LOS ALAMOS, MARICOPA, OJAI, AND SANTA BARBARA.
12/06/1920	-?--?--?	35.25	120.67	D			F	SAN LUIS OBISPO.
03/10/1922	11-21-20	35.75	120.25	C	6.5	43	F	IX IN CHOLAME VALLEY REGION OF SAN ANDREAS FAULT. FELT OVER AN AREA OF 100,000 SQ. MI. - CRACKS IN THE GROUND AND NEW SPRINGS. VII-VIII AT PARKFIELD AND SHANDON. VI-VII AT SAN LUIS OBISPO AND SIMMLER, AND V AT LOS ANGELES.

MM/DD/YY	HR/MN/SE	NORTH LAT	WEST LONG	QUALITY	MAG.	STA. REC.	FELT	MAXIMUM INTENSITY - COMMENTS
03/16/1922	23-10--?	35.75	120.33	D			F	VI IN CHOLAME VALLEY - RATHER STRONG AFTERSHOCKS, V AT PASO ROBLES AND SAN LUIS OBISPO, AND IV AT ANTELOPE VALLEY; ALSO IV AT SHANDON.
03/19/1922	11--?--?	35.67	120.67	D			F	III AT PASO ROBLES.
03/23/1922	10--?--?	35.67	120.67	D			F	III AT PASO ROBLES.
03/25/1922	12--?--?	35.67	120.67	D			F	III AT PASO ROBLES.
05/31/1922	01-25--?	35.67	120.67	D			F	III AT PASO ROBLES; 2 SHOCKS.
07/05/1922	19--?--?	34.75	120.25	D			F	LOS ALAMOS.
07/09/1922	12--?--?	34.75	120.25	D			F	LOS ALAMOS.
07/11/1922	03--?--?	34.75	120.25	D			F	LOS ALAMOS.
07/11/1922	15-30--?	34.75	120.25	D			F	LOS ALAMOS.
08/18/1922	05-12--?	35.75	120.33	D			F	VII IN CHOLAME VALLEY; V AT PASO ROBLES AND SAN LUIS OBISPO.
08/20/1922	21-14--?	35.50	120.67	D			F	III AT ATASCADERO.
09/04/1922	10-15--?	35.67	120.67	D			F	IV AT PASO ROBLES.
09/05/1922	09-05--?	35.25	120.67	D			F	V AT SAN LUIS OBISPO; 2 SHOCKS.
12/29/1922	11--?--?	35.67	120.67	D			F	III AT PASO ROBLES.
12/29/1922	12--?--?	35.67	120.67	D			F	III AT PASO ROBLES.
03/12/1923	06--?--?	34.75	120.25	D			F	LOS ALAMOS.
05/04/1923	22-45--?	35.25	120.67	D			F	V AT SAN LUIS OBISPO; 2 SHOCKS, SECOND EQUALED INTENSITY II.
05/08/1923	05-02--?	35.75	120.33	D			F	II AT CHOLAME.
06/16/1923	20-40--?	35.67	120.67	D			F	IV AT PASO ROBLES - DURATION 15-20 SECONDS.
06/25/1923	13-21--?	35.25	120.67	D			F	II AT SAN LUIS OBISPO.
12/19/1923	07-35--?	34.92	120.42	D			F	II AT SANTA MARIA - DURATION 20 SECONDS.
07/02/1924	58-02--?	34.50	119.67	D			F	SANTA BARBARA.
12/30/1924	12-17--?	34.50	119.67	D			F	SANTA BARBARA.
12/30/1924	14-15--?	34.50	119.67	D			F	SANTA BARBARA.
06/29/1925	14-42-16	34.30	119.80	B	6.3	1	F	IX AT SANTA BARBARA; FELT OVER AN AREA OF 100,000 SQ. MI. - RECORDED WORLD-WIDE. RUPTURE AT DEPTH ON THE MESA AND RECORDED WORLD-WIDE. RUPTURE AT DEPTH ON THE MESA AND SANTA YNEZ FAULTS (BAILEY WILLIS); A FEW DEATHS, SEVERAL MILLION DOLLARS DAMAGE; IX AT GOLETA, NAPLES, AND SANTA BARBARA; VIII AT GAVIOTA, MIRAMAR, AND SANTA YNEZ, LOS ALAMOS, LOS OLIVOS; VII AT ARROYO GRANDE, NIPOMO, ORCOTT, ALAMOS, LOS OLIVOS; VII AT ARROYO GRANDE, NIPOMO, ORCOTT, ALAMOS, LOS OLIVOS; VII AT ARROYO GRANDE, NIPOMO, ORCOTT, PISMO BEACH, SANTA MARIA, AND VENTURA, AND VI AT AVILA, LOMPOC, AND PORT SAN LUIS.
06/29/1925	15-20--?	35.25	120.67	D			F	III AT SAN LUIS OBISPO.
06/29/1925	16-35--?	34.50	119.67	D			F	SANTA BARBARA; II AT OXNARD.
06/29/1925	18-54--?	34.50	119.67	D			F	IV AT SANTA BARBARA; II AT OXNARD - STRONGEST AFTERSHOCK OF THE DAY.
06/30/1925	01-37--?	34.50	119.67	D			F	SANTA BARBARA.
06/30/1925	02-47--?	34.50	119.67	D			F	SANTA BARBARA.
06/30/1925	09-19--?	34.50	119.67	D			F	SANTA BARBARA - VIOLENT; FELT AT OJAI AND OXNARD.

MM/DD/YY	HR/MN/SE	NORTH LAT	WEST LONG	QUALITY	MAG.	STA. REC.	FELT	MAXIMUM INTENSITY - COMMENTS
07/03/1925	16-38--?	34.50	119.67	D			F	VII AT SANTA BARBARA; III AT PASADENA AND OJAI - STIFF TREMOR AT VENTURA.
07/03/1925	18-21--?	34.50	119.67	D			F	VII AT SANTA BARBARA - STRONGEST AFTERSHOCK; FELT AT LOS ANGELES, OJAI, AND PASADENA.
07/03/1925	18-46--?	34.50	119.67	D			F	SANTA BARBARA.
07/04/1925	19-18--?	34.50	119.67	D			F	SANTA BARBARA - ANOTHER SHOCK FELT LATER IN DAY.
07/05/1925	12--?--?	34.50	119.67	D			F	SANTA BARBARA; 11 SHOCKS IN THE NEXT 19 HOURS.
07/06/1925	21-45--?	34.50	119.67	D			F	SANTA BARBARA - SEVERAL FAIRLY SEVERE SHOCKS.
07/09/1925	-?--?--?	34.50	119.67	D			F	SANTA BARBARA.
07/20/1925	09-50--?	34.50	119.67	D			F	SANTA BARBARA.
07/29/1925	14--?--?	34.50	119.67	D			F	V AT WASIOJA - CEMENT WALK CRACKED.
07/30/1925	09-50--?	34.50	119.67	D			F	SANTA BARBARA.
07/30/1925	12--?--?	34.50	119.67	D			F	SANTA BARBARA.
08/13/1925	11--?--?	34.50	119.67	D			F	SANTA BARBARA - 5 LIGHT SHOCKS DURING NIGHT; THE STRONGEST TOOK PLACE JUST BEFORE 11--?--?.
10/04/1925	-?-50--?	34.50	119.67	D			F	SANTA BARBARA.
10/08/1925	21-30--?	34.50	119.67	D			F	SANTA BARBARA.
10/30/1925	09-45--?	34.50	119.67	D			F	SANTA BARBARA.
10/30/1925	13-30--?	34.50	119.67	D			F	SANTA BARBARA AND VENTURA.
02/18/1926	18-18--?	34.17	119.50	D			F	VII ORIGIN AT SEA, SW OF VENTURA; FELT ALONG COAST FROM SAN LUIS OBISPO ON NW TO SOUTH OF SANTA ANA, A DISTANCE OF 200 MI. AT SANTA BARBARA WINDOWS OF A SCHOOL WERE BROKEN, WATER PIPE IN ROUNDHOUSE WAS BROKEN. THERE WAS DAMAGE TO TELEPHONE EQUIPMENT AT SIMI. ALSO FELT AT LOS ANGELES, PASADENA, SANTA MONICA, SANTA SUSANA, AND VENTURA.
04/29/1926	12-18--?	34.67	120.17	D			F	IV AT BUELLTON.
06/18/1926	-?--?--?	34.50	119.67	D			F	SANTA BARBARA.
06/24/1926	15-30--?	34.50	119.67	D			F	V AT SANTA BARBARA.
06/29/1926	23-21--?	34.50	119.67	D			F	VII-VIII AT SANTA BARBARA - ONE PERSON KILLED BY FALLING CHIMNEY. VI AT BUELLTON AND VENTURA; ALSO FELT AT CAMARILLO, LOS ANGELES, OJAI, OXNARD, PORT HUENEME, AND SANTA PAULA - POSSIBLY SUBMARINE ORIGIN; FELT OVER AN AREA OF 30,000 SQ. MI.
07/03/1926	23--?--?	34.50	119.67	D			F	II AT SANTA BARBARA.
07/06/1926	17-45--?	34.50	119.67	D			F	V AT SANTA BARBARA.
07/25/1926	-?--?--?	36.30	120.30					(CALTECH FILE)
08/06/1926	17-42--?	34.50	119.67	D			F	IV IN SANTA BARBARA REGION; 2 SHOCKS AT OJAI - LASTED 30 SECONDS AT VENTURA WITH SHARP SHOCK AT SANTA BARBARA.
08/09/1926	04-12--?	34.50	119.67	D			F	V AT SANTA BARBARA; 2 SHOCKS AT VENTURA.
10/22/1926	10-10--?	35.67	120.67	D			F	III AT PASO ROBLES.
10/22/1926	-?--?--?	36.45	122.00					(CALTECH FILE)
12/09/1926	-?-03--?	35.67	120.67	D			F	IV AT PASO ROBLES - PROBABLY MISTIMED REPORT OF SHOCK AT -? 41-?.
12/09/1926	-?-41--?	35.25	120.67	D			F	NE OF SAN LUIS OBISPO; AT SAN LUIS OBISPO DURATION 20 SECONDS; FELT AT COALINGA WITH ORIGIN ABOUT 120 MI. FROM MT HAMILTON.

MM/DD/YY	HR/MN/SE	NORTH LAT	WEST LONG	QUALITY	MAG.	STA. REC.	FELT	MAXIMUM INTENSITY - COMMENTS
12/27/1926	09-19--?	36.17	120.33	D			F	VI NEAR COALINGA; FELT OVER AN AREA OF 25,000 SQ. MI. FELT AT FIREBAUGH, FRESNO, LOS BANOS, MENDOTA, OAKDALE, OILFIELDS, PORTERVILLE, AND SAN LUIS OBISPO.
11/04/1927	11--?--?	34.58	120.67	D			F	LOMPOC, POINT ARGUELLO, AND SAN LUIS OBISPO.
11/04/1927	11-30--?	34.58	120.67	D			F	LOMPOC.
11/04/1927	13-50-53	34.54	121.40	A	7.3	3	F	X AT SEA, WEST OF POINT ARGUELLO. AREA SHAKEN WITH INTENSITY VI OR GREATER WAS 40,000 SQ. MI. A SMALL SEA WAVE WAS PRODUCED, RECORDED ON TIDE GAUGES AT SAN DIEGO AND SAN FRANCISCO, AND OBSERVED AS 6 FEET HIGH AT SURF; IX AT HONDA, ROBERDS RANCH, SURF, AND WHITE HILLS, VIII AT ARLIGHT, ARROYO GRANDE, BERROS, BETTERAVIA, CAMBRIA, CASMALIA, CAYUCOS, GUADOCEANO, PISMO BEACH, POINT CONCEPTION, SAN JULIAN RANCH, SAN LUIS OBISPO, AND SANTA MARIA, VI-VII AT GUADOCEANO, PISMO BEACH, POINT CONCEPTION, SAN JULIAN RANCH, SAN LUIS OBISPO, AND SANTA MARIA, VI-VII AT ALUPE, HALCYON, HARRISTON, HUASNO, LOMPOC, LOS ALAMOS, LOS OLIVOS, MORRO BAY, NIPOMO, ADELAIDA, ATASCADERO, BAKERSFIELD, BICKNELL, BUTTONWILLOW,CARPINTERIA CHOLAME, CRESTON, EDNA GAVIOTA, GOLETA, HARMONY, KING CITY, LAS CRUCES, NAPLES, OXNARD, PASO ROBLES, REWARD, SANTA BARBARA, SANTA MARGARITA, SANTA YNEZ, SOLVANG, TAFT, TEMPLETON, VENTURA, AND WASIOJA, AND IV-V AT ANNETTE, BIG SUR, CASTROVILLE, COALINGA, FELLOWS, GONZALES, GORMAN, HOLLISTER, LOCKWOOD, LUCIA, MCKITTRICK, MONTEREY, PARKFIELD, PATTIWAY, PORT SAN LUIS, POZO, PRIEST, SALINAS, SANGER, SAN LUCAS, SAN SIMEON, SANTA PAULA, SCHEIDECK, SESPE, SIMMLER, SOLEDAD, AND TEHACHAPI. DATA FROM BSSA V. 17, P. 258 AND V. 20, P. 53.
11/04/1927	14-12--?	34.58	120.67	D			F	SANTA MARIA - AFTERSHOCK.
11/04/1927	14-14--?	34.58	120.67	D			F	SANTA MARIA - AFTERSHOCK.
11/04/1927	15--?--?	34.58	120.67	D			F	SAN LUIS OBISPO - AFTERSHOCK.
11/04/1927	15-42--?	34.58	120.67	D			F	SANTA MARIA - AFTERSHOCK.
1/05/1927	08-17--?	34.58	120.67	D			F	POINT ARGUELLO - AFTERSHOCK; MILD AT SURF.
11/05/1927	09--?--?	34.58	120.67	D			F	POINT ARGUELLO - AFTERSHOCK; REPORTED FROM PASO ROBLES TO HADLEY TOWER.
11/05/1927	11-37--?	34.58	120.67	D			F	POINT ARGUELLO - AFTERSHOCK; REPORTED FROM SURF TO HADLEY TOWER, AND SOUTH OF SAN LUIS OBISPO.
11/06/1927	-?-06--?	34.67	120.17	D			F	IV AT BUELLTON.
11/06/1927	02-25--?	34.67	120.17	D			F	POINT ARGUELLO - AFTERSHOCK; STRONGEST IMMEDIATE AFTERSHOCK AT LOMPOC.
11/06/1927	03-10--?	34.67	120.17	D			F	IV AT BUELLTON.
11/06/1927	22-10--?	34.67	120.17	D			F	OFF POINT CONCEPTION.
11/06/1927	22-50--?	34.67	120.17	D			F	IV AT BUELLTON.
11/06/1927	23-10--?	34.67	120.17	D			F	OFF POINT CONCEPTION.
11/08/1927	10-10--?	34.67	120.17	D			F	IV AT BUELLTON - SHARP BUMPING AT 10-02--?, AROUSED NEARLY ALL. AT LOMPOC MANY AWAKENED BY SHOCK AT 10-15--?.

MM/DD/YY	HR/MN/SE	NORTH LAT	WEST LONG	QUALITY	MAG.	STA. REC.	FELT	MAXIMUM INTENSITY - COMMENTS
11/19/1927	03-32--?	34.92	120.42	D			F	VII AT SANTA MARIA - CENTERED TO NW OF ORIGIN OF NOVEMBER 4 QUAKE -WEAKER, YET NEARLY AS STRONG AT SANTA MARIA,AND VI AT BETTERAVIA AND BICKNELL; REPORTED FROM SAN MIGUEL AND PARKFIELD ON THE NORTH TO SANTA BARBARA CHANNEL ON THE SOUTH.
12/05/1927	11-45--?	34.58	120.67	D			F	IV AT POINT ARGUELLO, AND IV AT BUELLTON WITH 2 SHOCKS 15 SECONDS APART; FELT AT GUADALUPE, SANTA MARGARITA, SANTA MARIA AND SURF.
12/31/1927	10-10--?	34.58	120.67	D			F	V AT POINT ARGUELLO.
03/15/1928	12-03--?	34.92	120.42	D			F	SANTA MARIA.
03/15/1928	12-20--?	34.50	119.67	D			F	SANTA BARBARA.
03/16/1928	14-30--?	34.92	120.42	D			F	SANTA MARIA.
03/29/1928	06-25--?	34.92	120.42	D			F	VII AT SANTA MARIA.
06/09/1928	08-22--?	35.17	119.50	D			F	TAFT.
06/09/1928	08-31--?	35.17	119.50	D			F	TAFT.
06/09/1928	12-25--?	35.17	119.50	D			F	TAFT.
09/03/1928	04-01-54	34.50	122.50	D	5.0	1		OFF POINT ARGUELLO - LICK OBSERVATORY S-P= 39 SECONDS.
11/02/1928	05--?--?	34.67	120.42	D			F	LOMPOC.
05/28/1929	07-10--?	36.17	120.33	D			F	COALINGA.
07/03/1929	09-24--?	34.50	119.67	D			F	SANTA BARBARA.
07/12/1929	13-10--?	36.17	120.33	D			F	COALINGA.
08/28/1929	18-10--?	34.50	119.67	D			F	SANTA BARBARA.
09/09/1929	05-15--?	34.50	119.67	D			F	GAVIOTA, NAPLES, AND SANTA BARBARA.
09/16/1929	03-16--?	35.42	120.92	D			F	CAYUCOS.
09/16/1929	06-15--?	35.42	120.92	D			F	CAYUCOS.
10/05/1929	20-03--?	36.17	120.33	D			F	COALINGA AND LIGHTHIPE.
10/06/1929	21-14--?	36.17	120.33	D			F	COALINGA.
10/07/1929	08--?--?	36.17	120.33	D			F	COALINGA.
10/07/1929	11-30--?	34.83	120.42	D			F	ORCUTT.
10/11/1929	17-55--?	36.17	120.33	D			F	COALINGA.
10/15/1929	22-02--?	36.17	120.67	D			F	COALINGA, KETTLEMEN HILLS, OILFIELDS, AND PRIEST VALLEY,.
11/07/1929	06-30--?	36.33	119.67	D			F	HANFORD.
11/09/1929	02-30--?	36.17	120.33	D			F	BITTER WATER, COALINGA, AND MCKITTRICK.
11/20/1929	22-50--?	36.42	121.00	D			F	BITTER WATER.
11/24/1929	09-54--?	36.42	121.00	D			F	LONOAK, BITTER WATER, AND LEWIS CREEK.
11/26/1929	08-05--?	36.42	121.00	D			F	V AT BITTER WATER AND SAN ARDO; FELT FROM HOLLISTER TO SANTA MARGARITA.
11/26/1929	09--?--?	36.42	120.83	D			F	HERNANDEZ.
11/26/1929	18-06--?	36.42	121.00	D			F	BITTER WATER.
12/05/1929	07-40--?	36.33	119.67	D			F	HANFORD.
03/11/1930	23-59--?	36.42	121.25	D			F	PINNACLES.
06/21/1930	05-15--?	34.83	120.50	D			F	CASMALIA.
08/05/1930	11-25--?	34.42	119.50	D			F	NEAR SANTA BARBARA - FELT OVER AN AREA OF 9000 SQ. MI. V-VI AT CARPINTERIA, GOLETA, OJAI, OXNARD, AND SANTA BARBARA,.
08/08/1930	16.46--?	34.42	119.67	D			F	SANTA BARBARA AND GOLETA.
08/18/1930	13-09--?	34.33	120.58	D			F	OFF POINT CONCEPTION; V OVER A LAND AREA OF 500 SQ. MI. NEAR POINT CONCEPTION.

MM/DD/YY	HR/MN/SE	NORTH LAT	WEST LONG	QUALITY	MAG.	STA. REC.	FELT	MAXIMUM INTENSITY - COMMENTS
08/28/1930	05-15--?	36.42	121.33	D			F	SOLEDAD.
09/02/1930	13-35--?	35.00	121.00	D			F	OFF COAST - FELT AT HALCYON AND SAN LUIS OBISPO.
09/09/1930	05-27--?	34.42	119.50	D			F	SANTA BARBARA.
10/02/1930	14-18--?	34.58	120.67	D			F	OFF POINT ARGUELLO - FELT AT HALCYON.
10/28/1930	13-57--?	35.42	120.92	D			F	OFF COAST NEAR CAYUCOS - FELT AT NIPOMO.
12/08/1930	01-23--?	34.50	119.67	D			F	GOLETA AND SANTA BARBARA.
12/08/1930	01-29--?	34.50	119.67	D			F	GOLETA AND SANTA BARBARA.
02/21/1931	08-10--?	35.67	121.33	D			F	NW OF SAN LUIS OBISPO - FELT AT BRYSON AND PIEDRAS BLANCAS.
02/23/1931	10-01--?	35.83	120.50	D			F	OVER AN AREA OF 5000 SQ. MI.; V AT CAYUCOS, PARKFIELD, AND TEMPLETON.
02/23/1931	10-33--?	35.83	120.50	D			F	SAME AS ABOVE.
04/05/1931	03--?--?	36.17	121.00	D			F	SE OF KING CITY.
07/15/1931	18-40--?	35.00	120.58	D			F	GUADALUPE, NIPOMO, AND SANTA MARGARITA.
07/21/1931	03-25--?	35.25	120.67	D			F	SAN LUIS OBISPO.
07/21/1931	12-08--?	35.25	120.67	D			F	IV AT HALCYON, LOS ALAMOS, NIPOMO, OCEANO, AND TEMPLETON:ALSO FELT AT CAMBRIA, GAVIOTA, PIEDRAS BLANCAS, PORT SAN LUIS, SAN LUIS OBISPO, SANTA MARGARITA, AND SANTA MARIA
09/03/1931	13-50--?	34.50	119.67	D			F	SANTA BARBARA.
09/10/1931	14-35--?	35.50	120.67	D			F	ATASCADERO.
09/30/1931	14-35--?	35.50	120.67	D			F	ATASCADERO.
10/13/1931	12-25--?	36.33	121.67	D			F	JAMESBURG.
10/18/1931	19-58--?	36.33	121.67	D			F	IV AT HOLLISTER, JAMESBURG, AND SPRECKLES; ALSO FELT AT APTOS, CARMEL, CHUALAR, MOSS LANDING, MONTEREY, PARAISO, SALINAS, AND SANTA CRUZ.
12/04/1931	-?-53--?	36.50	121.67	D			F	10 MI. S OF SPRECKELS. FELT AT HOLLISTER, METZ, PIGEON POINT, SPRECKELS, AND SANTA CRUZ.
02/04/1932	16-02-58	34.55	119.73	C	3.0	1	F	SANTA BARBARA AND VENTURA.
02/05/1932	04-14-45	35.83	121.47	C	3.5	1	F	COAST OF MONTEREY COUNTY; FELT AT PIEDRAS BLANCAS LIGHT AND SALMON CREEK.
02/05/1932	06-46-54	35.83	121.47	C	3.5	1	F	COAST OF MONTEREY COUNTY; FELT AT PIEDRAS BLANCAS LIGHT AND SALMON CREEK.
02/05/1932	07-10--?	35.83	121.47	C			F	AFTERSHOCK OF PRECEDING.
02/26/1932	16-58--?	36.00	121.00		5.0		F	IV AT APTOS, ASILOMAR, CARMEL, DEL MONTE, GONZALES, METZ, MONTEREY, PACIFIC GROVE, AND PEBBLE BEACH.
03/13/1932	23-09-24	34.44	120.17	B	3.5	1	F	OFF POINT CONCEPTION; FELT AT BUELLTON.
04/21/1932	03-36-20	35.50	120.67	D	3.0		F	ATASCADERO.
05/06/1932	03-37-08	36.00	120.50	C	3.0	1	F	PARKFIELD.
06/27/1932	05-17-25	36.00	122.00	D	4.0			COAST OF MONTEREY COUNTY.
10/24/1932	04-45--?	35.75	120.75	D			F	PASO ROBLES.
01/30/1933	17--?--?	34.67	120.42	D			F	LOMPOC.
02/26/1933	09-34-32	36.40	121.30	D			F	III AT HOLLISTER, SALINAS, AND SPRECKLES.
04/12/1933	10-03--?	36.33	121.75	D			F	IV AT PORTERVILLE AND VISALIA.
06/26/1933	06-26--?	34.42	120.50	D			F	V AT BUELLTON AND POINT CONCEPTION.
06/26/1933	06-29--?	34.42	120.50	D			F	V AT BUELLTON AND POINT CONCEPTION.
01/09/1934	12-48--?	35.13	120.08	C	3.0			

MM/DD/YY	HR/MN/SE	NORTH LAT	WEST LONG	QUALITY	MAG.	STA. REC.	FELT	MAXIMUM INTENSITY - COMMENTS
01/12/1934	12-50--?	34.45	120.15	D			F	IV AT LOS ALAMOS.
02/01/1934	16-09--?	34.55	119.53	B	3.5		F	II AT SANTA BARBARA.
02/11/1934	15-16--?	34.55	119.53	C	2.0			
03/20/1934	11-48--?	36.00	120.00	D	3.0			
05/06/1934	20-14--?	35.83	120.75	B	3.5			
05/10/1934	11-28--?	34.50	119.58	C	3.0			
05/19/1934	06-37--?	34.58	120.75	D	3.0			
05/24/1934	06-52--?	34.42	119.75	C	2.5			
05/24/1934	09-04--?	34.42	119.75	C	2.5			
05/24/1934	11-18--?	34.42	119.75	C	2.0			
06/05/1934	09-51--?	35.80	120.33	D			F	COALINGA AND KETTLEMAN HILLS; ALSO FELT AT MONTEREY AND SANTA CRUZ.
06/05/1934	11-30--?	35.80	120.33	D			F	SAN MIGUEL AND SHANDON.
06/05/1934	11-47--?	35.80	120.33	B	3.0			
06/05/1934	13-46--?	35.80	120.33	C	3.0			
06/05/1934	21-30--?	35.80	120.33	D			F	SAN MIGUEL.
06/05/1934	21-48--?	35.80	120.33	B	5.0		F	V AT ADELAIDA, PARKFIELD, AND PRIEST, IV AT ATASCADERO, AVENAL, BIG SUR, BRYSON, CARMEL, HANFORD, KING CITY, LEMOORE, LONOAK, PARAISO, SAN MIGUEL, SANTA CRUZ, SHANDON, AND TEMPLETON, III AT APTOS, BOULDER CREEK, CAMBRIA, CHUALAR, COALINGA, GONZALES, HOLLISTER, MONTEREY, MORRO BAY, PASO ROBLES, SALINAS, SAN FRANCISCO, SAN JOAQUIN VALLEY, SAN LUIS OBISPO, SOLEDAD, SPRECKLES, ETC.; NOT FELT AT ANTIOCH, ETC., BAKERSFIELD, FRESNO, GILROY, LIVERMORE, LOS GATOS, MARICOPA, MERCED, MODESTO, MORGAN HILL, REDWOOD CITY, SAN JOSE, SANTA MARIA, TULARE, OR WATSONVILLE.
06/05/1934	22-52--?	35.80	120.33	C	4.0		F	VI AT ADELAIDA; IV AT ATASCADERO.
06/05/1934	23-30--?	35.80	120.33	D			F	V AT LEMOORE; ALSO FELT AT CASTROVILLE.
06/06/1934	-?-55--?	35.80	120.33	C	3.0			
06/06/1934	16-40--?	35.80	120.33	C	3.5			
06/06/1934	22-40--?	35.80	120.33	C	3.5		F	ADELAIDA, GRAEAGLE, AND PAYNES CREEK.
06/07/1934	22-30--?	35.80	120.33	D			F	STONE CANYON.
06/08/1934	04-15--?	35.80	120.33	D			F	IV AT GONZALES AND MCKITTRICK.
06/08/1934	04-30--?	35.80	120.33	B	5.0		F	VI TO VII AT CHOLOME RANCH, PARKFIELD, AND STONE CANYON DURATION 30 SECONDS, DAMAGE SLIGHT, V AT ATASCADERO, AT ANTELOPE, BIG SUR, CAMBRIA, CASTROVILLE, DELANO, MONTEREY, PASO ROBLES, SAN LUIS OBISPO, SANTA BARBARASANTA MARGARITA, SANTA MARIA, SOLEDAD, TAFT, VENTURA, VISALIA, ETC., AND III OR LESS AT ARVIN, BAKERSFIELD, FRESNO, KERNVILLE, LOMPOC, LOS ANGELES, MENDOTA, PORTERVILLE, SALINAS, SAN BENITO, SANTA ANA, SANTA BARBARA, TULARE, WATSONVILLE, ETC.; NOT FELT AT BIG BASIN, CAJON, COYOTE, GILROY, HUNTINGTON BEACH, INDEPENDENCE, INYOKERN, LANCASTER, MERCED, POMONA, OR SAN JOSE.
06/08/1934	04-37--?	35.60	121.30	D			F	IV AT PIEDRAS BLANCAS, SAN LUIS OBISPO, AND SANTA CRUZ; ALSO FELT AT BRYSON AND LOS ALAMOS.

MM/DD/YY	HR/MN/SE	NORTH LAT	WEST LONG	QUALITY	MAG.	STA. REC.	FELT	MAXIMUM INTENSITY - COMMENTS
06/08/1934	04-45--?	35.80	120.33	D			F	ATASCADERO, COALINGA, LOCKWOOD, PASO ROBLES, PORT SAN LUIS, PRIEST, SAN MIGUEL, AND WESTHAVEN.
06/08/1934	04-47--?	35.80	120.33	B	6.0		F	WITHIN A RADIUS OF 250 KM FROM THE EPICENTER NEAR THE SOUTHEASTERN ANGLE OF MONTEREY COUNTY; VII TO VIII AT PARKFIELD, VI AT COALINGA, KETTLEMAN CITY, LEMOORE, AND STONE CANYON, V AT ATASCADERO, DUDLEY, HOLLISTER, KING CITY, OILFIELDS, SAN MIGUEL, SEASIDE, SHALE PUMP STATION, AND SHANDON, IV AT ANTELOPE, AVILA, CANOGA PARK, HANFORD, LOS ALAMOS, MARICOPA, MORRO BAY, NIPOMO, PASO ROBLES, PRIEST, SAN LUIS OBISPO, SANTA CRUZ, SANTA MARIA, SOLEDAD, VISALIA ETC., AND III OR LESS AT APTOS, FRESNO, KERNVILLE, LONE PINE, LOS BANOS, MENDOTA, MONTEREY, OAKLAND HARBOR, SALINAS, SAN BENITO, SANTA ANA, TEHACHAPI, TULARE, ETC.
06/08/1934	05--?--?	35.60	121.30	D			F	PIEDRAS BLANCAS LIGHT; ALSO BRYSON, KERNVILLE, LA PANZA, LEMOORE, PARKFIELD, SANDBERG, AND SAN FERNANDO.
06/08/1934	05-20--?	35.80	120.33	D			F	III AT ATASCADERO.
06/08/1934	05-23--?	35.80	120.33	C	3.5		F	ATASCADERO AND SAN MIGUEL.
06/08/1934	05-36--?	35.80	120.33	C	3.0			
06/08/1934	05-42--?	35.80	120.33	B	4.5		F	ATASCADERO, BIG SUR, COALINGA, KING CITY, PASO ROBLES, AND WESTHAVEN.
06/08/1934	05-50--?	35.80	120.33	D			F	IV AT ATASCADERO; ALSO FELT AT COALINGA AND SAN LUIS OBISPO.
06/08/1934	09-30--?	35.80	120.33	B	4.0		F	ATASCADERO AND PARKFIELD.
06/08/1934	15-30--?	35.80	120.33	C	3.5			
06/08/1934	16-30--?	35.80	120.33	D			F	PARKFIELD.
06/08/1934	23-23--?	35.80	120.33	B	4.0		F	NEAR PARKFIELD.
06/10/1934	06-47--?	35.80	120.33	C	3.0			
06/10/1934	08-03--?	35.80	120.33	B	4.5		F	NEAR PARKFIELD; IV AT SAN MIGUEL.
06/10/1934	20-02--?	35.80	120.33	D			F	IV AT SAN MIGUEL; ALSO PARKFIELD AND WOODY.
06/11/1934	03-25--?	35.80	120.33	C	3.0			
06/12/1934	10-47--?	35.80	120.33	C	3.5			
06/14/1934	14-55--?	35.80	120.33	C	4.0		F	IV AT ATASCADERO; ALSO FELT AT SAN MIGUEL AND TEMPLETON.
06/14/1934	15-54--?	35.80	120.33	C	4.0		F	III AT ATASCADERO AND SAN MIGUEL.
06/14/1934	19-26--?	35.80	120.33	C	4.5		F	ATASCADERO AND TEMPLETON.
06/14/1934	22-02--?	35.80	120.33	C	3.5		F	ATASCADERO.
06/15/1934	04-48--?	35.80	120.33	C	3.0			
06/16/1934	23-03--?	36.50	121.00	D	4.0		F	IV AT HOLLISTER AND MONTEREY, AND III AT GONZALES, PARKFIELD, AND SALINAS.
07/02/1934	18-44--?	35.80	120.33	B	3.0			
08/04/1934	-?-18--?	35.80	120.33	B	3.0			
08/21/1934	03-37--?	36.08	120.58	D			F	IV IN STONE CANYON.
08/25/1934	18-52--?	34.42	119.75	C	2.5			
08/26/1934	03-02--?	35.57	119.85	B	3.0			
09/06/1934	23-24--?	36.00	120.55	C	3.0			
09/16/1934	14-38--?	35.83	120.33	C	3.5			
10/07/1934	-?-18--?	34.55	120.78	C	3.5			

MM/DD/YY	HR/MN/SE	NORTH LAT	WEST LONG	QUALITY	MAG.	STA. REC.	FELT	MAXIMUM INTENSITY - COMMENTS
10/08/1934	04-57--?	34.50	119.58	C	2.0			
10/10/1934	10-52--?	34.55	120.78	C	3.0			
10/19/1934	15-39--?	35.80	120.33	C	3.0			
11/04/1934	22-17--?	34.53	119.67	B	3.0			
11/21/1934	01-02--?	34.58	119.62	B	2.5			
12/01/1934	13-05--?	36.00	121.50	D			F	15 MI. S OF PARAISO; V AT PIEDRAS BLANCAS LIGHT AND IV AT PARAISO.
12/02/1934	16-07--?	35.97	120.58	C	4.0		F	SAN MIGUEL.
12/03/1934	01-54--?	35.95	121.50	C	4.5		F	IV AT BRYSON, KING CITY, AND PARAISO; ALSO FELT AT PARKFIELD, PASO ROBLES, SAN LUCAS, AND SAN MIGUEL.
12/17/1934	11-10--?	34.58	120.33	B	4.5		F	VI AT LOS ALAMOS.
12/17/1934	13-51--?	34.58	120.33	C	2.5		F	LOS ALAMOS.
12/17/1934	15-16--?	34.55	119.67	C	2.5			
12/17/1934	15-35--?	34.58	120.33	C	2.5			
12/18/1934	03-09--?	34.58	120.33	C	4.0		F	LOS ALAMOS.
12/18/1934	04-34--?	34.58	120.33	C	3.0		F	LOS ALAMOS.
12/18/1934	05-28--?	34.58	120.33	C	3.0		F	LOS ALAMOS.
12/19/1934	20-39--?	34.28	119.50	B	2.5			
12/20/1934	12-37--?	34.58	120.33	C	2.5		F	LOS ALAMOS.
12/20/1934	12-39--?	34.58	120.33	C	3.0			
12/20/1934	22-21--?	34.58	120.33	C	3.0			
12/23/1934	16-08--?	34.58	120.33	C	2.5			
12/24/1934	10-22--?	34.58	120.33	B	3.0		F	LOS ALAMOS.
12/24/1934	16-26--?	35.93	120.48	B	5.0		F	IV AT LOS ALAMOS AND SHANDON; ALSO FELT AT KING CITY TEMPLETON.
12/25/1934	04-03--?	34.58	120.33	C	3.0			
01/06/1935	04-04--?	35.98	120.48	C	4.0		F	IV AT PARKFIELD; ALSO FELT AT SHANDON.
01/06/1935	04-25--?	35.90	120.45	D			F	IV AT PARKFIELD.
01/06/1935	04-40--?	35.98	120.48	C	4.0		F	IV AT PARKFIELD AND III AT SHANDON.
01/07/1935	-?-11--?	35.75	119.67	D	3.0			
01/23/1935	03-16--?	34.58	120.33	C	3.5		F	IV AT LOS ALAMOS.
01/27/1935	09-49--?	34.50	119.62	B	2.5			
02/18/1935	04-02--?	35.93	120.48	C	3.5			
02/19/1935	14-17--?	35.93	120.48	D	3.0			
02/28/1935	19-06--?	35.80	120.33	C	3.0			
03/03/1935	11-26--?	36.42	121.75	C	3.0			
03/06/1935	23-14--?	34.43	119.87	C	3.5		F	III AT SANTA BARBARA.
03/19/1935	03-59--?	34.55	120.78	B	4.0			OFF POINT ARGUELLO.
04/05/1935	10-13--?	35.93	120.48	C	3.5			
05/05/1935	12-58--?	34.58	119.68	C	2.5			
05/18/1935	04-36--?	34.58	120.33	B	3.5		F	IV AT LOS ALAMOS.
05/19/1935	03-44--?	34.58	120.33	C	3.0			
05/20/1935	23-44--?	34.58	120.33	C	3.0			
05/27/1935	16-08--?	35.37	120.97	C	3.0		F	III AT TEMPLETON.
06/10/1935	02-02--?	35.33	119.83	C	3.5			
06/18/1935	08-52--?	34.60	119.60	C	2.0			
06/23/1935	23-53--?	34.55	119.68	C	3.0			

TABLE 2.5-1

MM/DD/YY	HR/MN/SE	NORTH LAT	WEST LONG	QUALITY	MAG.	STA. REC.	FELT	MAXIMUM INTENSITY - COMMENTS
06/30/1935	23-28--?	36.00	121.00	D	4.0		F	SE OF SALINAS; III AT HOLLISTER.
07/25/1935	04-16--?	35.80	120.33	C	3.0		F	V AT PARKFIELD.
07/28/1935	06--?--?	35.70	121.12	B	4.0		F	SAN SIMEON.
08/06/1935	19-05--?	34.62	119.62	C	3.0		F	SANTA BARBARA.
08/07/1935	22-30--?	34.55	120.78	C	3.5			
08/09/1935	17-14--?	36.17	120.98	C	3.5		F	PRIEST VALLEY.
08/31/1935	09-28--?	34.50	119.70	C	2.5			
10/18/1935	09-24--?	35.80	120.70	D	3.5		F	IV AT PARKFIELD - AFTERSHOCK.
10/22/1935	18-37--?	35.93	120.48	C	4.0		F	PARKFIELD.
10/25/1935	19-43--?	36.40	121.55	D			F	13 MI. W OF SOLEDAD; IV AT SAN BENITO.
10/26/1935	10-46--?	35.85	121.40	D			F	AFTERSHOCK.
12/22/1935	06-54--?	34.55	120.78	C	3.0			
02/03/1936	09-12--?	34.75	119.75	C	2.5			
02/21/1936	23-06--?	34.42	119.67	C	3.0			
02/22/1936	-?-18--?	34.42	119.67	C	3.0			
02/22/1936	-?-21--?	34.42	119.67	C	2.5			
02/22/1936	-?-23--?	34.42	119.67	C	3.0			
02/22/1936	04-55--?	34.42	119.67	C	3.0			
03/06/1936	03-45--?	35.90	120.40	D	3.0			
03/17/1936	01-55--?	36.50	120.92	C	4.0		F	IV AT CHUALAR, HOLLISTER, AND TRES PINOS.
03/18/1936	09-07--?	35.93	120.48	C	2.5			
03/27/1936	-?-58--?	34.55	120.78	C	3.0			
03/29/1936	09-26--?	34.50	119.62	C	2.5			
05/20/1936	17-22--?	35.93	120.48	C	3.0			
05/23/1936	04-41--?	36.17	120.92	C	4.0		F	IV AT KING CITY.
05/27/1936	19-55--?	36.50	121.17	C	4.5			SAN BENITO COUNTY.
06/24/1936	12-23--?	35.12	120.08	C	3.0		F	SAN LUIS OBISPO CO.; IV AT LOS ALAMOS.
07/13/1936	18-09--?	34.50	119.60	D	2.5			
07/22/1936	04-03--?	34.50	119.80	C	2.5			
07/30/1936	09-36--?	34.57	119.63	C	3.0			
09/07/1936	16-47--?	34.37	120.38	C	3.0			
09/09/1936	04-54--?	34.37	120.38	C	4.0		F	LOS ALAMOS.
09/10/1936	21-21--?	34.40	120.40	D	3.0			
09/12/1936	13-56--?	34.75	120.33	C	3.5			
09/15/1936	-?-09--?	34.50	120.50	D	2.5			
10/16/1936	15-30--?	34.83	120.58	C	4.0			NEAR CASMALIA.
10/16/1936	15-36--?	34.83	120.58	C	3.0			
10/17/1936	01-17--?	34.83	120.58	C	3.0			
10/19/1936	14-01--?	34.83	120.58	C	3.0			
11/01/1936	15-10--?	34.55	120.78	B	4.0			OFF POINT ARGUELLO.
11/02/1936	01-29--?	34.55	120.78	C	3.0			
11/05/1936	14-30--?	35.85	121.40	D			F	HOLLISTER.
11/08/1936	16-51--?	34.55	120.78	C	3.0			
11/08/1936	22-43--?	34.55	120.78	C	3.0			
11/18/1936	17-15--?	35.35	120.60	D			F	POZO, SAN LUIS OBISPO, AND SANTA MARGARITA.
11/18/1936	18-02--?	34.70	120.25	C	4.5		F	IV AT ARROYO GRANDE, ATASCADERO, BETTERAVIA, LOS ALAMOS OCEANO, POZO, SAN LUIS OBISPO, AND SANTA MARGARITA.

MM/DD/YY	HR/MN/SE	NORTH LAT	WEST LONG	QUALITY	MAG.	STA. REC.	FELT	MAXIMUM INTENSITY - COMMENTS
11/22/1936	02-16--?	34.58	120.78	C	3.5			
11/25/1936	21-51--?	34.58	120.78	C	3.0			
12/23/1936	17-16--?	35.93	120.48	B	3.5			
12/26/1936	01-12--?	34.55	119.68	C	2.5			
01/12/1937	15-44--?	34.50	120.80	D	3.0			
01/28/1937	17-36--?	34.43	119.87	C	2.5			
02/16/1937	17-40--?	34.55	120.78	C	4.0			OFF POINT ARGUELLO.
02/17/1937	03-33--?	36.50	121.58	C	4.5		F	9 MI. SE OF PAICINE; FELT AT ANTELOPE, HOLLISTER, AND PANOCHE.
02/20/1937	09-58--?	35.93	120.48	C	4.0		F	PARKFIELD AND PASO ROBLES.
02/22/1937	18-10--?	36.17	121.53	C	4.0		F	KING CITY.
02/24/1937	13-37--?	34.50	119.70	C	2.0			
02/25/1937	03-20--?	34.50	119.70	C	2.0			
03/26/1937	21-35--?	34.60	119.70	C	3.5			
03/31/1937	17-43--?	34.50	119.70	C	3.0			
04/17/1937	08-30--?	34.60	119.70	C	2.5			
04/30/1937	08-16--?	34.50	119.70	D	2.5			
05/31/1937	15-33--?	36.50	120.70	C	3.0			
06/02/1937	09-32--?	34.40	119.70	C	2.5			
07/31/1937	14-18--?	34.22	119.55	C	3.0			
07/31/1937	15-14--?	34.22	119.55	C	2.5			
08/15/1937	19-01--?	36.50	120.70	D	3.0			
08/22/1937	01-56--?	35.00	121.00	D	3.5			
09/16/1937	02-48--?	35.93	120.48	B	3.5		F	NEAR PARKFIELD; FELT AT BRADLEY.
09/18/1937	13-29--?	36.50	121.50	D	4.0		F	9 MI. SE OF PAICINES; FELT AT CHUALAR, SALINAS, AND SPRECKLES.
09/22/1937	02-41--?	34.50	119.70	C	3.0			
09/29/1937	22-39--?	34.50	119.70	C	3.0			
10/13/1937	08-32--?	34.40	119.70	C	2.5			
11/01/1937	21-40--?	36.50	121.40	D			F	6 MI. N OF GONZALES.
11/03/1937	10--?--?	36.15	121.00	D			F	V AT SAN LUCAS; FELT ALSO AT KING CITY AND SAN ARDO.
11/22/1937	04-12--?	34.55	120.78	C	4.5		F	OFF POINT ARGUELLO; V AT BUELLTON, GOLETA, PISMO BEACH, POINT D SANTA MARIA, AND IV AT ARLIGHT, BETTERAVIA, BICKNELL, E, GAVIOTA, GUADALUPE, LOMPOC, LOS ALAMOS, LOS OLIVOS, SANTA URF.
11/22/1937	04-51--?	34.55	120.78	C	3.5			
11/28/1937	09-55--?	34.55	120.78	C	3.5			
12/03/1937	15-28--?	34.55	120.78	C	4.0		F	OFF POINT ARGUELLO; FELT AT GAVIOTA AND POINT CONCEPTION.
12/03/1937	21-13--?	34.55	120.78	C	3.5			
12/05/1937	01-36--?	36.00	121.00	D	3.5		F	19 MI. S OF LOS BANOS; V AT LOS BANOS.
12/05/1937	01-37--?	36.00	121.00	D	4.0			SAN BENITO COUNTY.
12/05/1937	02-05--?	36.00	121.00	D	3.0		F	19 MI. S OF LOS BANOS.
12/24/1937	11-57--?	34.50	120.80	D	4.0		F	OFF POINT ARGUELLO. FELT AT CASMALIA, LOS ALAMOS, POINT CONCEPTION.
12/25/1937	13-01--?	36.00	120.00	D	3.0			
01/01/1938	01-59--?	34.55	120.78	C	3.5			

MM/DD/YY	HR/MN/SE	NORTH LAT	WEST LONG	QUALITY	MAG.	STA. REC.	FELT	MAXIMUM INTENSITY - COMMENTS
01/18/1938	04-35--?	34.55	120.78	B	3.5			
01/24/1938	04-38--?	34.55	120.78	C	3.5			
01/25/1938	12-24--?	34.55	120.78	C	3.5			
02/01/1938	18-14--?	34.55	120.78	C	3.5			
02/20/1938	14--?--?	34.55	120.78	C	3.5			
02/21/1938	10-59--?	35.93	120.78	C	3.0			
03/04/1938	15-14--?	34.30	119.57	C	2.5			
03/04/1938	18-25--?	34.30	119.57	C	2.5			
04/12/1938	01-50--?	34.55	120.78	C	3.5			
05/10/1938	10-32--?	36.20	121.30	D	4.5		F	BIG SUR, HOLLISTER, KING CITY, PINNACLES, SALINAS, SOLEDAD, SOQUEL, AND TRES PINOS-6 SHOCKS FELT AT PINNACLES.
05/10/1938	10-41--?	36.20	121.30	D	4.0		F	SAN BENITO.
05/13/1938	19-34--?	36.20	121.30	D	4.0			MONTEREY COUNTY.
05/27/1938	22-03--?	36.20	120.00	D	3.5			
06/01/1938	05-17--?	34.55	119.68	D			F	SANTA BARBARA.
06/01/1938	06-17--?	34.55	119.68	D	3.0			
06/06/1938	02-55--?	34.50	119.67	C	3.0			
09/16/1938	06-11--?	36.40	121.20	D	4.0		F	PINNACLES.
09/27/1938	10-21--?	34.50	119.70	C	2.5			
09/27/1938	12-23--?	36.30	120.90	C	5.0		F	OVER AN AREA OF 9000 SQ. MI. OF WEST-CENTRAL CALIFORNIA, ALONG THE COAST AS FAR NORTH AS PESCADERO AND SOUTH TO SAN LUIS OBISPO. INLAND IT WAS FELT AT COALINGA, MENDOTA, AND STEVENSON, WITH A V AT BIG SUR, BRYSON, CHUALAR, GONZALES, GREENFIELD, HARMONY, HOLLISTER, JOLON, LOCKWOOD, PAICINES, PARAISO, PINNACLES, SAN ARDO, SAN BENITO, SAN LUCAS, SOLEDAD, AND SPRECKLES, AND IV AT BEN LOMOND, CAMBRIA, CARMEL, CASTROVILLE, DOS PALOS, GILROY, KING CITY, LOS BANOS, MENDOTA, MONTEREY, PASO ROBLES, PRIEST, SALINAS, SAN LUIS OBISPO, TRES PINOS, WATSONVILLE, ETC.
09/27/1938	16-20--?	36.45	121.25	D			F	PAICINES AND PINNACLES.
09/29/1938	12-12--?	34.55	120.78	C	4.0			OFF POINT ARGUELLO.
10/02/1938	18-45--?	34.33	119.58	C	4.0		F	SANTA BARBARA AND SUMMERLAND.
10/24/1938	13-40--?	36.45	121.25	D			F	HOLLISTER AND PINNACLES.
10/28/1938	10-07--?	35.80	120.33	C	3.5			
11/01/1938	22-46--?	35.12	120.08	C	3.0			
11/16/1938	13-39--?	35.80	120.33	C	3.0			
11/22/1938	15-30--?	35.93	120.48	B	4.5		F	NEAR PARKFIELD; FELT AT ATASCADERO, CAMBRIA, CRESTON, MORRO BAY, PARKFIELD, PASO ROBLES, SAN MIGUEL, AND SHANDON.
01/01/1939	-?-53--?	34.58	120.33	C	3.0			
01/21/1939	07-08--?	36.45	121.25	D			F	PINNACLES.
01/22/1939	15-52--?	34.40	119.70	C	2.5			
02/05/1939	03-30--?	35.65	120.65	D			F	PASO ROBLES.
02/09/1939	06-44--?	35.93	120.48	C	3.0		F	NEAR PARKFIELD.
02/12/1939	03-12--?	34.42	119.83	B	3.0		F	GOLETA AND SANTA BARBARA .
03/24/1939	02-49--?	34.55	120.78	C	3.5			

MM/DD/YY	HR/MN/SE	NORTH LAT	WEST LONG	QUALITY	MAG.	STA. REC.	FELT	MAXIMUM INTENSITY - COMMENTS
03/25/1939	03-45--?	36.45	121.25	D			F	PINNACLES.
03/30/1939	10-11--?	34.50	119.80	C	2.5			
05/02/1939	18-49--?	35.93	120.48	C	4.0		F	IV AT PARKFIELD.
05/03/1939	07-55--?	34.55	120.78	C	3.0			
05/03/1939	12-39--?	35.65	120.65	D			F	PASO ROBLES.
05/18/1939	23--?--?	35.80	120.33	C	3.0			
06/15/1939	21-12--?	34.50	119.70	C	2.5			
06/17/1939	04-30--?	34.75	120.25	D			F	LOS ALAMOS. REPORTS OF SEVERAL SHOCKS.
06/24/1939	12-55--?	35.85	120.85	D			F	BRADLEY.
06/24/1939	13-02--?	36.40	121.00	C	5.5		F	OVER AN AREA OF 10,000 SQ. MI. IN WEST-CENTRAL CALIFORNIA, ALONG THE COAST AS FAR NORTH AS HALF MOON BAY AND SOUTH TO ESTERO BAY. INLAND IT WAS FELT AT COALINGA, TRANQUILITY, AND VOLTA, WITH A VII AT HOLLISTER, VI AT KING CITY AND PAICINES, V AT CAYUCOS, SOLEDAD, AND SPRECKLES, AND IV AT PAICINES, V AT CAYUCOS, SOLEDAD, AND SPRECKLES, AND IV AT CAMBRIA, CARMEL, CASTROVILLE, CHUALAR, GILROY, GONZALES, LOCKWOOD, MILPITAS, MONTEREY, NIPOMO, PASO ROBLES, PINNACLES, SALINAS, SAN ARDO, SAN BENITO, SAN JUAN, SAN MIGUEL, SAN SIMEON, SANTA CRUZ, TRES PINOS, AND WATSONVILLE.
07/04/1939	10-49--?	36.40	121.00	C	4.0		F	HOLLISTER, PAICINES, AND SALINAS.
07/10/1939	18-33--?	36.40	121.25	D			F	PINNACLES.
07/24/1939	09-30--?	36.25	121.80	D			F	BIG SUR.
07/24/1939	13--?--?	36.00	121.15	D			F	JOLON.
09/06/1939	01-53-43	34.58	120.42	C	3.0			
09/07/1939	02-50-30	35.42	121.08	C	3.0		F	OFF SAN LUIS OBISPO CO.; FELT AT CAMBRIA.
09/08/1939	01-57--?	34.75	120.25	D			F	LOS ALAMOS.
09/08/1939	05--?--?	34.75	120.25	D			F	LOS ALAMOS.
09/12/1939	-?--?-47	34.25	119.75	C	3.0			
09/24/1939	11-57-40	36.40	121.00	D	3.5			
10/06/1939	04-39--?	35.80	121.50	D	3.5			
10/17/1939	19-21-41	34.55	120.78	C	3.5			
10/17/1939	20-42-43	34.55	120.78	C	4.0			OFF POINT ARGUELLO.
11/02/1939	14-02--?	34.40	120.50	D			F	POINT CONCEPTION LIGHT STATION.
11/04/1939	14-11-33	36.20	120.90	D	3.0		F	SALINAS AND SAN LUCAS.
12/14/1939	03-45-18	36.10	120.00	D	3.0			
12/25/1939	15-36-23	34.28	119.83	C	3.5			
12/28/1939	12-15-38	35.80	120.33	B	5.0		F	OVER AN AREA OF 15,000 SQ. MI. IN WEST-CENTRAL CALIFORNIA, ON THE COAST FROM SANTA CRUZ SOUTH TO POINT ARGUELLO, AND INLAND TO LOST HILLS AND FRESNO. V AT COALINGA, FRESNO, GREENFIELD, PRIEST, SAN ARDO, AND SAN LUCAS, AND IV AT APTOS, ATASCADERO, BIG SUR, CAMBRIA, CARMEL, CASTROVILLE, CAYUCOS, CHUALAR, GONZALES, HOLLISTER, KING CITY, MENDOTA, MONTEREY, MORRO BAY, PARKFIELD, PASO ROBLES, PINNACLES, SALINAS, SAN JUAN BAUTISTA, SAN LUIS OBISPO, SANTA CRUZ, SOLEDAD, TAFT, ETC.

MM/DD/YY	HR/MN/SE	NORTH LAT	WEST LONG	QUALITY	MAG.	STA. REC.	FELT	MAXIMUM INTENSITY - COMMENTS
12/29/1939	04--?--?	36.40	121.25	D			F	PINNACLES.
12/30/1939	15-24-37	35.80	120.33	D	3.5		F	NEAR PARKFIELD. FELT AT SAN LUCAS.
02/27/1940	11-40-25	34.25	119.50	B	3.0			
05/21/1940	10-05-34	35.28	120.48	B	4.0		F	ATASCADERO, CAMBRIA, CAYUCOS, MORRO BAY, PASO ROBLES, PISMO BEACH, AND SAN LUIS OBISPO.
06/16/1940	09-25-04	34.55	120.78	C	4.0		F	OFF POINT ARGUELLO; FELT AT GUADALUPE AND LOS ALAMOS.
06/26/1940	08-56--?	36.08	120.32	C	3.5			
06/28/1940	04-06-42	34.55	120.78	C	3.0			
08/13/1940	22-07-29	36.23	120.32	B	4.0			(DEPT. OF WATER RESOURCES DATA.)
08/31/1940	08-52-46	34.55	120.78	B	3.5			
09/07/1940	10-36-30	36.50	121.50	D	3.5			
09/07/1940	10-38-36	36.50	121.50	D	3.5			
09/07/1940	13-02-06	36.50	121.50	D	4.5		F	CARMEL AND SALINAS.
10/20/1940	22-18-45	34.55	120.78	C	3.0			
11/10/1940	10-25-10	34.35	119.77	C	4.0		F	SANTA BARBARA CHANNEL; FELT AT GOLETA, PARADISE CAMP, AND SANTA BARBARA.
11/17/1940	21-23-43	35.00	119.50	C	3.0			
01/29/1941	08-54-01	34.48	119.53	B	3.0			
02/04/1941	03-19-12	34.55	119.68	C	3.0			
02/04/1941	03-42-09	34.55	119.68	C	3.0			
02/08/1941	15-58-50	34.55	119.68	C	3.5		F	SANTA BARBARA.
02/09/1941	23-49-18	34.50	119.70	C	2.0			
02/11/1941	06-43-30	34.27	119.57	B	3.5		F	SANTA BARBARA.
02/12/1941	20-10-24	34.40	119.70	C	3.0			
02/14/1941	22-19-06	34.40	119.70	C	2.5			
05/07/1941	16-17-34	34.55	120.78	C	3.5			
05/15/1941	03-29--?	36.15	120.35	D			F	COALINGA.
05/15/1941	06--?--?	36.15	120.35	D			F	COALINGA.
07/01/1941	07-50-57	34.33	119.58	A	6.0		F	SANTA BARBARA; FELT OVER AN AREA OF 20,000 SQ. MI. VIII AT CARPINTERIA AND SANTA BARBARA, VII AT GOLETA AND VENTURA, VI AT FILLMORE, KEYSTONE, LOS ALAMOS, OJAI, OXNARD, PORT HUENEME, SANTA PAULA, SUMMERLAND, AND WHEELER SPRINGS, AND V AT ACTON, ALTADENA, ARLIGHT, ARTESIA, ARVIN, BETTERAVIA, BUELLTON, BURBANK, CAMARILLO, CANOGA PARK, CASMALIA, CAYUCOS, CHATSWORTH, COMPTON, EL SEGUNDO, GAVIOTA, GLENDALE, HERMOSA BEACH, INGLEWOOD, LA CRESCENTA, LAGUNA BEACH, LANCASTER, LOMITA, LOMPOC, LONG BEACH, LOS ANGELES, LOS OLIVOS, MAYWOOD, MCKITTRICK, MONTALVO, MOORPARK, NEWBURY PARK, NEWPORT, NIPOMO, NORTH HOLLYWOOD, OCEANO, ORCUTT, PASADENA, PATTIWAY, IRU, POINT CONCEPTION, SANDBERG, SAN NICHOLAS ISLAND, SAN PEDRO, SANTA ANA, SANTA MARIA, SANTA MONICA, SANTA YNEZ, SIERRA MADRE, SIMI, STANTON, SUNLAND, SURF, TEHACHAPI, UPPER SESPE MOUNTAINS, VALYERMO, WHEELER RIDGE, AND WHITTIER.
07/01/1941	07-57--?	34.33	119.58	B	3.0			
07/01/1941	07-58--?	34.33	119.58	B	3.5			

MM/DD/YY	HR/MN/SE	NORTH LAT	WEST LONG	QUALITY	MAG.	STA. REC.	FELT	MAXIMUM INTENSITY - COMMENTS
07/01/1941	08-05--?	34.33	119.58	B	3.0			
07/01/1941	08-07--?	34.33	119.58	B	3.0			
07/01/1941	08-10--?	34.33	119.58	B	3.0			
07/01/1941	08-13--?	34.33	119.58	B	3.0			
07/01/1941	08-15--?	34.33	119.58	B	3.0			
07/01/1941	08-19--?	34.33	119.58	B	4.0		F	AFTERSHOCK OF 07-50-57 (THIS DATE).
07/01/1941	08-21--?	34.33	119.58	B	4.0		F	AFTERSHOCK OF 07-50-57.
07/01/1941	08-25--?	34.33	119.58	B	3.5			
07/01/1941	08-30--?	34.33	119.58	B	4.0		F	AFTERSHOCK OF 07-50-57.
MM/DD/YY	HR/MN/SE	NORTH LAT	WEST LONG	QUALITY	MAG.	STA. REC.	FELT	MAXIMUM INTENSITY - COMMENTS
07/01/1941	08-48--?	34.33	119.58	B	4.0		F	AFTERSHOCK OF 07-50-57.
07/01/1941	08-58--?	34.33	119.58	B	4.0		F	AFTERSHOCK OF 07-50-57.
07/01/1941	09-05--?	34.33	119.58	B	4.0		F	AFTERSHOCK OF 07-50-57.
07/01/1941	09-45--?	34.33	119.58	B	4.0		F	AFTERSHOCK OF 07-50-57.
07/01/1941	10-25--?	34.33	119.58	B	4.0		F	AFTERSHOCK OF 07-50-57.
07/01/1941	12-37--?	34.33	119.58	B	3.0			
07/01/1941	14-22--?	34.33	119.58	B	3.0			
07/01/1941	18-13--?	34.33	119.58	B	3.0			
07/01/1941	18-20--?	34.33	119.58	B	4.0		F	AFTERSHOCK OF 07-50-57.
07/01/1941	19-48--?	34.33	119.58	B	3.0			
07/01/1941	20-15--?	34.33	119.58	B	3.5			
07/01/1941	22-51--?	34.33	119.58	B	3.5			
07/01/1941	23-54--?	34.33	119.58	B	4.5		F	AFTERSHOCK OF 07-50-57; FELT AT FILLMORE, GAVIOTA, LOS ALAMOS, AND SANTA BARBARA.
07/02/1941	-?-17--?	34.33	119.58	B	3.0			
07/02/1941	04-33--?	34.33	119.58	B	3.5			
07/02/1941	08-45--?	34.33	119.58	B	3.5			
07/02/1941	11-41--?	34.33	119.58	B	3.0			
07/02/1941	22-19--?	34.33	119.58	B	4.0		F	AFTERSHOCK OF 07-50-57.
07/03/1941	-?-25--?	34.33	119.58	B	3.5			
07/03/1941	19-26--?	34.33	119.58	B	4.0		F	AFTERSHOCK OF 07-50-57.
07/07/1941	01-06--?	34.33	119.58	B	3.0			
07/07/1941	06-25--?	34.33	119.58	B	3.5			
07/08/1941	19-37--?	34.33	119.58	B	3.0			
07/12/1941	16-18--?	34.33	119.58	B	4.5		F	AFTERSHOCK OF 07-50-57; FELT AT FILLMORE, GLENDALE, MONTROSE, SATICOY, SAUGUS, AND WHEELER SPRINGS.
07/12/1941	16-41--?	34.33	119.58	B	3.0			
07/12/1941	21-07--?	34.33	119.58	B	3.0			
07/12/1941	21-12--?	34.33	119.58	B	3.0			
07/13/1941	06-11--?	34.33	119.58	B	3.5			
07/16/1941	23-10--?	34.33	119.58	B	3.0			
07/17/1941	18-31--?	34.33	119.58	B	3.0			
07/27/1941	12-44--?	34.33	119.58	B	3.0			
07/31/1941	13-23--?	34.33	119.58	B	3.0			
08/02/1941	12-31-19	34.33	119.58	C	3.0			
08/09/1941	05-05-24	34.33	119.58	C	3.5			

MM/DD/YY	HR/MN/SE	NORTH LAT	WEST LONG	QUALITY	MAG.	STA. REC.	FELT	MAXIMUM INTENSITY - COMMENTS
08/12/1941	22-35-24	34.33	119.58	C	3.5			
08/19/1941	10-20-25	34.33	119.58	C	3.0			
08/25/1941	06-58-22	34.33	119.58	C	3.0			
08/27/1941	17-11-02	34.33	119.58	C	3.0			
08/29/1941	08-43-24	34.60	120.30	C	3.0			
09/08/1941	03-12-45	34.33	119.58	B	4.5		F	AFTERSHOCK OF 07/01/41, 07-50-57. V AT GOLETA AND SANTA BARBARA; FELT STRONGLY AT LOS ALAMOS AND SUMMERLAND.
09/08/1941	03-14-23	34.33	119.58	B	4.0		F	TWIN SHOCK OF 03-12-45; SAME "FELT" REPORT.
09/08/1941	04-45-16	34.33	119.58	B	3.5		F	SANTA BARBARA.
09/09/1941	03-23-17	34.33	119.58	B	3.5		F	SANTA BARBARA.
09/09/1941	13-44-46	34.33	119.58	B	3.0			
09/14/1941	01-45-18	34.33	119.58	B	4.0		F	AFTERSHOCK OF 07/01/41, 07-50-57.
09/14/1941	02-20-42	34.33	119.58	B	3.0			
09/15/1941	01-37-02	34.33	119.58	B	4.0		F	GOLETA, SANTA BARBARA, AND SUMMERLAND.
09/15/1941	01-55-18	34.33	119.58	B	3.0			
09/15/1941	02-49-06	34.33	119.58	B	3.5			
09/16/1941	07-27--?	34.33	119.58	B	3.5			
09/25/1941	05-12-56	34.33	119.58	B	4.0		F	GOLETA AND SANTA BARBARA.
10/07/1941	12-05-42	34.33	119.58		3.0			
10/19/1941	23-22-19	34.33	119.58	B	3.0			
11/05/1941	16-36--?	35.00	121.00	D	3.5		F	OFF POINT CONCEPTION; FELT AT SAN SIMEON.
11/17/1941	17-30-27	34.33	119.58	C	3.0			
11/18/1941	18-08-10	34.33	119.58	C	4.0		F	CARPINTERIA AND SANTA BARBARA.
11/21/1941	16-56-03	34.33	119.58	C	4.0		F	GOLETA AND SANTA BARBARA.
11/25/1941	20-01-48	34.33	119.58	C	3.0			
11/28/1941	06-33--?	35.00	120.00	D	3.5			
12/08/1941	-?-29-42	36.00	121.00	D	3.5			
12/22/1941	-?-54-09	35.93	120.48	C	4.0		F	NEAR PARKFIELD-NOT RECORDED ON BERKELEY NETWORK.
01/06/1942	09-20--?	36.15	120.65	D			F	PRIEST VALLEY-RECORDED AT TINEMAHA.
01/06/1942	09-23--?	36.15	120.65	D			F	PRIEST VALLEY-RECORDED AT TINEMAHA.
01/08/1942	18-21-05	34.13	119.58	C	2.5			
01/18/1942	11-35--?	36.40	121.25	D			F	PINNACLES.
01/18/1942	16-50--?	36.40	121.25	D			F	PINNACLES.
02/19/1942	18-33--?	36.40	121.25	D			F	PINNACLES.
03/09/1942	05-57-42	34.30	119.60		3.0			
03/25/1942	-?--?--?	36.40	121.25	D			F	PINNACLES; LIGHT SHOCK.
04/19/1942	04-02-47	34.30	119.60	D	3.0			
04/22/1942	05-32-52	35.30	119.50	D	3.0			
05/08/1942	17-19-13	34.33	119.58	C	3.0			
06/06/1942	06-42-11	34.35	119.85	C	3.0		F	GOLETA.
06/29/1942	21-07-30	35.60	120.80	D	4.0		F	IV AT CAMBRIA AND SAN LUIS OBISPO.
07/19/1942	10-42-07	36.40	121.10	D	1.6			SW OF LLANADA.
09/15/1942	10-36-33	36.13	122.18	B	3.0			SW OF KING CITY.
10/04/1942	10--?--?	34.60	120.00	D			F	IV AT SANTA YNEZ PEAK.
10/11/1942	23-48-23	36.48	121.40	C	1.9			FORESHOCK OF QUAKE ON OCTOBER 15 AT 13-53-56.
10/15/1942	13-53-56	36.48	121.40	B	4.3		F	IV AT BIG SUR, GONZALES, GREENFIELD, HOLLISTER, SALINAS, AND SOLEDAD.

MM/DD/YY	HR/MN/SE	NORTH LAT	WEST LONG	QUALITY	MAG.	STA. REC.	FELT	MAXIMUM INTENSITY - COMMENTS
10/18/1942	08--?--?	36.00	121.00	D			F	CAMBRIA.
10/18/1942	12-01-42	36.00	121.00	D			F	V AT CAMBRIA.
10/19/1942	10-23--?	34.50	119.65	D			F	V AT SANTA BARBARA.
10/20/1942	10-25--?	36.00	121.00	D			F	V AT CAMBRIA.
10/26/1942	01-09-01	36.40	121.60	D	1.8			DEPTH ABOUT 12 KM.
12/02/1942	11-46--?	34.33	119.58	C	3.5		F	V AT SANTA BARBARA.
12/06/1942	16-57-49	35.93	120.48	C	3.5			
01/24/1943	06-55-57	34.33	119.58	C	3.0			
03/16/1943	09-27-47	34.28	119.60	C	3.0			
04/01/1943	13-39-66	34.68	121.75	B	3.1			OFF COAST, WEST OF POINT ARGUELLO.
06/29/1943	02-50-53	36.50	121.10	D	3.1			SW OF LLANADA.
07/05/1943	16-30-29	36.38	121.83	C	3.9			SOUTH OF SALINAS.
07/15/1943	-?-44-42	36.00	120.15	D			F	NEAR AVENAL.
08/07/1943	16-59-47	34.28	119.57	C	3.5			
08/12/1943	15-56-33	34.75	121.15	C	3.5			
08/27/1943	08-16-53	34.43	119.87	C	3.5		F	IV AT SANTA BARBARA.
09/13/1943	12-40--?	35.65	120.65	D			F	PASO ROBLES, POSSIBLY GUN FIRE.
09/18/1943	17-07-16	34.37	119.58	C	3.0			
10/22/1943	12--?--?	36.00	120.90	D			F	SAN ARDO; 2 SHOCKS.
10/26/1943	22-10--?	34.75	120.25	D			F	LOS ALAMOS.
10/31/1943	17-54-06	35.80	120.40	D	3.5			
10/31/1943	20--?--?	36.40	121.00	D			F	LONOAK.
11/08/1943	11-33-46	36.00	119.92	C	3.0		F	KETTLEMAN HILLS; FELT AT AVENAL.
11/30/1943	21-57-18	36.30	120.50	D	4.0			NEAR COALINGA.
12/01/1943	04-51--?	36.50	121.10	D			F	SAN BENITO.
01/04/1944	18-06-40	34.10	120.40	D	3.3			
02/18/1944	16-29-37	34.10	119.52	C	2.1			
02/21/1944	13--?-11	36.17	120.93	C	3.8			WEST OF PRIEST.
03/06/1944	21-32-16	36.40	121.25	C	3.4			NE OF PARAISO.
04/03/1944	02-33--?	34.50	121.40	D	4.0			OFF POINT ARGUELLO.
04/12/1944	15-33-10	34.27	119.52	C	4.0		F	OFF CARPINTERIA; FELT EAST OF SANTA BARBARA.
06/13/1944	08-27-32	34.67	120.50	C	4.6		F	NEAR LOMPOC; VI AT LOS ALAMOS AND IV AT SANTA MARIA.
06/13/1944	08-46-43	34.67	120.50	C	4.0		F	AFTERSHOCK OF 08-27-32.
06/13/1944	11-07-24	34.67	120.50	C	4.4		F	AFTERSHOCK OF 08-27-32.
07/11/1944	22-33--?	36.50	121.10	D			F	SAN BENITO.
07/15/1944	19-22-37	34.37	119.62	C	3.1			
09/04/1944	02-47-46	35.00	120.00	D	3.4		F	LOS ALAMOS.
09/04/1944	05--?--?	35.00	120.00	D			F	LOS ALAMOS.
09/15/1944	14-12-42	34.70	120.20	D	2.6		F	KETTLEMAN HILLS REGION; FELT AT PARKFIELD.
09/18/1944	01-30--?	35.00	120.00	D	3.5			
11/04/1944	08-12-01	36.33	120.08	C	3.4			
11/08/1944	16-12-36	34.33	119.72	C	3.1			
11/28/1944	10-36--?	35.80	120.00	D	3.3			
11/30/1944	18-53-15	34.72	120.42	C	4.1		F	NEAR LOS ALAMOS; FELT AT LOS ALAMOS AND LOS OLIVOS.
12/02/1944	15-09-12	35.80	120.00	D	3.2			
01/27/1945	17-50-31	34.75	120.67	C	3.9			
02/25/1945	20-18-38	36.00	120.48	C	3.6			

MM/DD/YY	HR/MN/SE	NORTH LAT	WEST LONG	QUALITY	MAG.	STA. REC.	FELT	MAXIMUM INTENSITY - COMMENTS
04/15/1945	22-59-57	34.13	119.83	C	3.1			
06/11/1945	03-54-52	34.50	120.80	D	3.2			
07/11/1945	16-13--?	35.67	121.25	D	4.0		F	NEAR SAN SIMEON; IV AT CAMBRIA.
07/28/1945	02-33-48	34.70	120.10	D	4.2		F	EAST OF SANTA MARIA; IV AT LOS ALAMOS.
09/04/1945	12-38-31	34.32	119.63	C	3.2			
09/07/1945	11-34-20	35.83	120.75	C	4.2		F	NEAR BRADLEY; IV AT CAMBRIA, PARKFIELD, PASO ROBLES, AND SAN MIGUEL.
11/04/1945	-?-46-34	36.38	121.28	C	3.3			NEAR SOLEDAD.
02/09/1946	02-55-28	34.33	119.92	C	2.5			
02/10/1946	11-01-19	36.50	121.00	D	4.2		F	OVER AN AREA OF 2000 SQ. MI. IN WEST CENTRAL CALIFORNIA. V AT SAN BENITO, AND IV AT BIG SUR, CHUALAR, GREENFIELD, HOLLISTER, LONOAK, SAN LUCAS, SAN MIGUEL, SANTA CRUZ, AND SOLEDAD.
02/15/1946	12-07-00	35.90	121.45	D			F	PARKFIELD; LIGHT SHOCK.
04/19/1946	12-50--?	34.00	120.40	D			F	SANTA MARIA.
07/08/1946	19-59-44	34.83	120.53	C	3.2			
08/06/1946	04-55-07	34.95	120.18	C	2.8		F	E OF SANTA MARIA; FELT AT LOS ALAMOS.
09/02/1946	10-09-47	34.18	119.62	C	3.0			
09/09/1946	11-20--?	34.90	120.40	D			F	SANTA MARIA.
09/19/1946	06-35-44	35.83	119.67	C	3.2			
10/24/1946	18-26-50	34.37	119.62	C	2.7			
11/22/1946	09-47-59	34.83	120.68	D	3.0			
11/27/1946	14-44-51	35.50	120.92	C	4.3		F	NEAR CAYUCOS; V AT MORRO BAY AND SANTA MARGARITA; ALSO FELT ATASCADERO, LOS ALAMOS, PISMO BEACH, AND SAN LUIS OBISPO.
12/13/1946	-?-40-01	34.17	119.53	C	3.5			
01/06/1947	21-05-47	35.85	120.47	C	3.6			
01/13/1947	19-38-31	34.32	119.65	C	2.2			
01/14/1947	20-49-27	34.23	119.65	C	2.7			
01/18/1947	12--?-42	34.20	121.50	D	3.3			
01/19/1947	19-32--?	35.60	120.30	D	3.1		F	PASO ROBLES.
02/05/1947	06-14--?	38.23	120.65	B	5.0		F	VI AT LONOAK, V AT COALINGA, IDRIA, AND KING CITY, AND IV AT BIG SUR, HURON, PARKFIELD, SAN ARDO, AND WESTHAVEN.NEAR COALINGA - AFTERSHOCK OF 2/5/47 OF 06-14--?.
02/25/1947	11-45-18	36.20	120.50	D	4.2			
03/23/1947	16-04-51	35.15	121.30	D	3.7			
03/27/1947	09-16-46	35.00	121.00	D	4.2		F	OFF COAST; V AT LOMPOC.
04/29/1947	07-44--?	34.33	119.55	C	3.2			
06/25/1947	18-39-53	34.25	119.50	C	3.1		F	NEAR CARPINTERIA.
06/25/1947	13-41-21	34.25	119.50	C	3.6		F	NEAR CARPINTERIA.
06/25/1947	18-48-26	34.25	119.50	C	2.5			
06/25/1947	20-55-16	34.25	119.50	C	3.2		F	NEAR CARPINTERIA.
06/25/1947	20-55-54	34.25	119.50	C	3.8			
07/13/1947	05-35--?	36.08	121.10	D	3.4			SOUTH OF KING CITY.
07/14/1947	05-40-06	35.92	119.92	C	4.0		F	KETTLEMAN HILLS; IV AT KETTLEMAN CITY.
10/6/1947	18-39--?	36.50	121.23	A	3.2			EAST OF GONZALES.
12/14/1947	05-42--?	36.45	121.08	B	3.4			SW OF LLANADA.

MM/DD/YY	HR/MN/SE	NORTH LAT	WEST LONG	QUALITY	MAG.	STA. REC.	FELT	MAXIMUM INTENSITY - COMMENTS
12/16/1947	09-21-03	36.25	120.77	C	3.6		F	IV AT SAN LUCAS.
12/18/1947	19-30-06	36.12	120.90	D			F	IV AT PARKFIELD.
12/25/1947	06-05--?	35.60	121.10	D			F	CAMBRIA.
12/25/1947	06-20--?	35.60	121.10	D			F	CAMBRIA.
01/11/1948	05-37-28	36.43	121.48	B	4.3		F	IV AT HOLLISTER.
02/01/1948	17--?-54	34.42	119.92	C	3.0			
02/15/1948	08-04-06	35.88	120.37	A	3.4			EAST OF PARKFIELD.
03/07/1948	07-46-22	36.10	120.40	D	3.0			NEAR COALINGA.
03/10/1948	23-24-34	34.43	119.73	C	2.6			
03/18/1948	09-35-05	34.40	119.60	C	2.8			
03/29/1948	02-40--?	35.85	121.40	D			F	IV AT HOLLISTER.
04/23/1948	15-23-43	34.10	120.93	C	3.7			
05/05/1948	06-47-06	34.45	119.72	B	2.7			
05/07/1948	12--?-32	36.20	121.90	D	3.0			WEST OF PRIEST.
05/09/1948	11-10--?	34.75	120.25	D			F	V AT LOS ALAMOS.
07/14/1948	11-05-37	34.67	120.92	C	3.2			
07/17/1948	05-26-31	34.55	120.05	C	3.4			
07/28/1948	01-30-57	36.05	120.53	C	3.1			SE OF PRIEST.
07/29/1948	13-16-23	35.12	120.47	C	3.4			
08/04/1948	10-22-57	35.92	120.33	C	3.6			
09/03/1948	23-42-26	34.33	119.53	C	3.9		F	SANTA BARBARA.
09/17/1948	15-41-01	34.40	119.62	C	3.1			
10/27/1948	03-05--?	34.75	120.25	D			F	IV AT LOS ALAMOS.
10/29/1948	03-04-59	34.10	120.40	D	3.4		F	V AT ARLIGHT AND POINT ARGUELLO LIGHT STATION.
11/02/1948	19-06-45	34.37	119.58	C	2.9			
12/04/1948	06-44-20	34.43	119.72	C	2.8			
12/04/1948	23-32-51	34.42	119.50	C	2.7			
12/20/1948	04-42-46	35.80	121.50	C	4.5		F	OFF COAST, NEAR PIEDRAS BLANCAS POINT; III AT SAN SIMEON.
12/31/1948	14-35-46	35.67	121.40	B	4.6		F	ALONG THE COAST FROM LOMPOC TO MOSS LANDING; VI AT SAN SIMEON AND V AT CAYUCOS, CRESTON, MOSS LANDING, AND PIEDRAS BLANCAS LIGHT STATION.
01/25/1949	04-29--?	34.90	120.40	D			F	V AT ORCUTT AND SANTA MARIA.
03/27/1949	06-31-16	34.25	119.62	C	2.6			
04/06/1949	14-07--?	35.00	120.00		2.6			
04/08/1949	13-17-07	34.60	120.35	C	3.2		F	IV AT LOS ALAMOS.
04/14/1949	01-46-12	34.28	119.52	C	2.6			
04/23/1949	09-18-09	36.38	121.37	C	3.7			NORTH OF PARAISO.
05/06/1949	04-23-46	34.50	121.00	C	3.4			
05/10/1949	06-20--?	35.90	120.40	D			F	SANTA MARIA - SLIGHT.
05/10/1949	11--?--?	35.90	120.40	D			F	SANTA MARIA - SLIGHT.
05/16/1949	03-01-03	34.72	120.02	C	3.2			
05/17/1949	23-57-55	35.63	121.15	D	4.1		F	IV AT SAN SIMEON.
06/27/1949	10-35-31	35.80	121.10	D	4.5		F	V AT SAN ARDO AND SAN MIGUEL; ALSO FELT AT PASO ROBLES, SAN LUIS OBISPO, AND SANTA MARGARITA.
07/21/1949	16-50--?	36.15	120.35	D			F	IV AT COALINGA.
07/21/1949	17-01--?	36.15	120.35	D			F	IV AT COALINGA.
07/24/1949	03-04-05	36.00	120.00	D	2.3			SE. KINGS C0. AFTER SHOCK AT 06-26--?, MAG. 2.0.

TABLE 2.5-1

MM/DD/YY	HR/MN/SE	NORTH LAT	WEST LONG	QUALITY	MAG.	STA. REC.	FELT	MAXIMUM INTENSITY - COMMENTS
07/27/1949	18-21-35	34.53	120.37	C	3.6			
08/01/1949	-?-07-24	36.90	121.20	D	3.0			SOUTH OF KING CITY.
08/07/1949	01-38-43	36.50	121.50	D	2.3			NO. MONTEREY CO.
08/10/1949	09-17-39	36.50	121.00	C	2.6			CENTRAL SAN BENITO CO.
08/22/1949	03--?--?	36.00	120.00	D			F	KETTLEMAN HILLS. FIFTH SHOCK IN 2 WEEKS.
08/26/1949	16-52-32	34.50	120.50	D	4.2		F	NEAR POINT CONCEPTION. VI AT ARLIGHT AND SURF. IV AT GUADALUPE, LOMPOC, AND LOS ALAMOS.
08/27/1949	14-15--?	34.50	120.50	D			F	ARLIGHT. SLIGHT SHOCK.
08/27/1949	14-51-46	34.50	120.50	D	4.9		F	NEAR POINT CONCEPTION. VI AT ARLIGHT, LOMPOC, AND SUDDEN. V AT COSMALIA, LOS ALAMOS, NIPOMO, SANTA BARBARA, AND SURF.
08/29/1949	12-07-20	36.00	120.10	D	3.0		F	IV IN AVENAL AND KETTLEMAN CITY.
10/28/1949	08-07-02	36.80	120.90	C	2.6			NW OF PRIEST.
11/17/1949	05-06-06	34.80	120.70	D	2.8		F	IV AT SANTA MARIA.
12/28/1949	09-17-12	36.20	120.70	D	2.6			NEAR PRIEST.
02/19/1950	08-29-44	34.50	120.70	D	3.5			
03/09/1950	23-43-19	36.35	121.22	C	3.2		F	NORTH OF KING CITY; V AT ROBLES DEL RIO.
03/22/1950	01-31-57	35.97	120.63	C	3.7			
03/29/1950	12-43-20	35.97	120.88	D	3.5			
04/15/1950	11-56-32	35.75	119.62	C	4.6		F	NE OF LOST HILLS; V AT ASH MOUNTAIN, (SEQUOIA NATIONAL PARK), KERNVILLE, AND SHAFTER, AND IV AT BUTTONWILLOW, JAWBONE AQUEDUCT STATION, LOST HILLS, THREE RIVERS, AND VISALIA.
04/21/1950	13-17-29	34.38	119.58	B	3.0		F	IV AT SANTA BARBARA.
04/26/1950	07-23-29	35.20	120.60	C	3.5		F	V AT SANTA MARIA; ALSO FELT AT ORCUTT.
04/26/1950	07-38--?	35.20	120.60	D			F	SANTA MARIA.
05/21/1950	18-59-03	34.57	119.63	C	2.6			
05/21/1950	19-26-48	35.88	119.73	C	3.4			
05/24/1950	01-46-57	36.43	120.77	C	2.9			SE OF LLANADA.
07/13/1950	15-01-47	34.33	119.50	C	2.8		F	OFF CARPINTERIA; V AT MONTECITO; ALSO FELT AT SANTA BARBARA AND NEARBY AREAS.
08/01/1950	21-08-43	36.20	122.23	B	2.0			OFF COAST, WEST OF BIG SUR.
08/02/1950	06-50-48	34.67	120.63	C	3.3			
08/23/1950	09-10--?	34.40	119.50	D			F	IV AT RINCON POINT; FELT AT CARPINTERIA.
09/24/1950	04-45--?	34.50	120.50	D			F	III AT ARLIGHT.
09/24/1950	12-23--?	34.22	119.58	C	3.3			
09/24/1950	21-51-44	36.20	120.50	D	2.9			EAST OF PRIEST.
10/20/1950	08-23-25	36.33	121.07	C	2.7			SOUTH OF KING CITY.
11/21/1950	04-30--?	30.90	120.40	D			F	SANTA MARIA.
03/02/1951	02-13-44	36.10	120.60	D	3.1			SE OF PRIEST
03/04/1951	13-32--?	34.90	120.40	D			F	IV AT SANTA MARIA; 2 SHOCKS.
03/05/1951	09-50--?	34.90	120.40	D			F	IV AT SANTA MARIA.
03/10/1951	05-35--?	34.50	120.50	D			F	IV AT ARLIGHT.
03/15/1951	13-50-43	35.02	120.48	C	3.8		F	IV AT LOS ALAMOS.
03/26/1951	06-07-34	34.62	119.50	C	3.5		F	IV AT OJAI AND SUMMERLAND; FELT AT VENTURA.
05/04/1951	03-28-36	36.20	120.20	D	3.1			FORESHOCK OF QUAKE AT 20-08-10.
05/04/1951	20-08-10	36.20	120.20	D	3.2			EAST OF COALINGA.

MM/DD/YY	HR/MN/SE	NORTH LAT	WEST LONG	QUALITY	MAG.	STA. REC.	FELT	MAXIMUM INTENSITY - COMMENTS
05/06/1951	03-18-03	36.40	120.40	D	2.8			NORTH OF COALINGA.
05/25/1951	05-11-18	36.30	120.30	D	3.1			NORTH OF COALINGA.
05/29/1951	05-08-24	35.08	119.65	C	3.2		F	ELKHORN HILLS; IV IN CUYAMA VALLEY.
05/31/1951	06-28-42	36.30	120.20	D	2.7			NE OF COALINGA.
06/16/1951	19-01-17	34.40	120.08	C	3.3			
06/19/1951	06-13-47	35.97	120.42	C	3.6			SOUTH OF COALINGA.
07/01/1951	-?-13-19	36.20	120.95	B	3.2			EAST OF KING CITY.
07/07/1951	05-53-33	34.75	120.75	C	3.5			
08/02/1951	05-09-25	36.35	121.27	B	3.9		F	NEAR GREENFIELD; IV AT BIG SUR, AT 7 MI. S OF HOLLISTER, AND ROBLES DEL RIO.
08/08/1951	19-42--?	34.80	120.40	D			F	IV AT ORCUTT.
08/09/1951	09-20-48	36.15	121.75	C	2.2			NEAR BIG SUR.
08/25/1951	01-04-10	36.47	121.15	B	3.1			SW OF LLANADA.
08/28/1951	22-12-27	34.60	121.00	D	3.5		F	OFF POINT ARGUELLO; III AT LOS ALAMOS.
09/18/1951	02-30--?	36.25	121.80	D			F	IV AT BIG SUR.
09/19/1951	22-50--?	36.25	121.80	D			F	IV AT BIG SUR.
10/03/1951	13-44-33	35.92	120.52	C	3.8			
10/26/1951	16-25-40	34.42	119.73	C	3.0			
11/17/1951	03-19-48	34.70	120.50	D	2.5		F	NEAR LOMPOC; III AT LOS ALAMOS.
11/25/1951	23-15-39	35.33	119.50	B	3.8			
12/20/1951	04-13-06	36.00	120.05	C	3.7			
01/24/1952	-?-32-38	34.18	119.88	C	2.7			
01/30/1952	11-05-33	36.30	121.13	C	2.7			NEAR KING CITY.
01/31/1952	20-09-02	34.18	119.53	C	2.6			
01/31/1952	21-33-12	36.40	121.40	C	3.6			SOUTHEAST CF SOLEDAD.
02/09/1952	22-26-39	34.07	120.75	C	3.6			
03/25/1952	09-18-50	34.18	120.95	C	3.6			
04/02/1952	05-21-10	36.45	121.25	B	3.1			NEAR SOLEDAD.
05/07/1952	05-45--?	34.40	119.60	D			F	IV AT MONTECITO AND SUMMERLAND.
06/18/1952	04--?--?	34.60	120.65	D			F	IV AT POINT ARGUELLO LIFEBOAT STATION.
07/01/1952	15-29-24	34.30	119.80	D	3.1			
07/15/1952	06-07-55	36.42	121.00	C	2.5			ABOUT 15 MI. NE OF KING CITY.
07/27/1952	18-15-14	34.18	119.70	C	3.1			
07/27/1952	20-20-35	34.22	119.67	C	3.2			
07/27/1952	20-30-05	34.20	119.67	B	3.5			
08/07/1952	19-l6-12	34.33	120.68	C	3.6		F	OFF POINT CONCEPTION; IV AT LOS ALAMOS.
08/11/1952	21-42-29	34.17	119.67	C	3.1			
08/23/1952	20-10--?	34.85	119.50	D			F	IV AT VENTUCOPA - SECOND SHOCK AT 21-20--?.
08/30/1952	14-58-11	34.35	119.62	B	3.3			
09/01/1952	12-03--?	34.30	119.60	D	3.0			
09/12/1952	21--?-15	34.25	119.70	C	3.0			
09/14/1952	11-46-06	35.90	120.30	D	3.3			
10/09/1952	14-46-02	34.20	122.20	D	4.6			(DEPT. OF WATER RESOURCES DATA)

MM/DD/YY	HR/MN/SE	NORTH LAT	WEST LONG	QUALITY	MAG.	STA. REC.	FELT	MAXIMUM INTENSITY - COMMENTS
11/22/1952	07-46-37	35.73	121.20	B	6.0		F	6 MI. NORTH OF SAN SIMEON, NEAR BRYSON; FELT OVER AN AREA OF 20,000 SQ. MI. VII AT BRADLEY AND BRYSON, VI AT ARROYO GRANDE, ATASCADERO, CAMBRIA, CAMP COOKE, CARMEL VALLEY, CAYUCOS, CHUALAR, CRESTON, GORDA STATION, GUADALUPE, HARMONY, HEARST RANCH, KING CITY, LOCKWOOD, LONOAK, MORRO BAY, OCEANO, PARKFIELD, PASO ROBLES, PISMO BEACH, SALINAS, SAN ARDO, SAN LUIS OBISPO, SAN SIMEON, SANTA MARGARITA, AND TEMPLETON, AND V AT AVENAL, BEN LOMOND, BIG SUR, BUELLTON, BUTTONWILLOW, CARUTHERS, CASMALIA, CHOLAME, COALINGA, CORCORAN, DOS PALOS, HOLLISTER, HUASNA, KETTLEMAN CITY, LOMPOC, LOST HILLS, LUCIA, MARICOPA, MONTEREY, MOSS LANDING, NIPOMO, ORCUTT, PAICINES, RIVERDALE, SAN MIGUEL, SANTA CRUZ, SANTA MARIA, SHAFTER, STRATFORD, SUDDEN, AND SURF.
11/22/1952	08-02-40	35.73	121.20	B	3.2			SAN SIMEON AFTERSHOCK.
11/22/1952	08-29-47	35.73	121.20	B	3.1			SAN SIMEON AFTERSHOCK.
11/22/1952	08-53-04	35.73	121.20	B	3.4		F	SAN SIMEON AFTERSHOCK; IV AT ARVIN, CALIENTE, JOLON, LOST HILLS, MALIBU, MARICOPA, MCFARLAND, MIRACLE HOT SPRINGS, MORGAN HILL, NIPOMO, PISMO BEACH, AND SHAFTER.
11/22/1952	11-08-44	35.73	121.20	B	3.1			SAN SIMEON AFTERSHOCK.
11/22/1952	11-45-31	35.73	121.20	B	3.1			SAN SIMEON AFTERSHOCK.
11/22/1952	12-34-44	35.73	121.20	B	3.0			SAN SIMEON AFTERSHOCK.
11/22/1952	13-37-31	35.73	121.20	B	4.0		F	SAN SIMEON AFTERSHOCK; V AT CALIENTE, MIRACLE HOT SPRINGS, AND WHEELER SPRINGS.
11/22/1952	19-25-21	35.73	121.20	B	3.9			SAN SIMEON AFTERSHOCK.
11/22/1952	19-36-27	35.70	121.20	D	3.1			SAN SIMEON AFTERSHOCK.
11/22/1952	23-39-20	35.70	121.20	D	3.1			SAN SIMEON AFTERSHOCK.
11/23/1952	09-22-35	36.00	120.90	D	3.2			20 MI. SE OF KING CITY.
11/23/1952	18-40-19	35.67	121.17	C	4.2			SAN SIMEON AFTERSHOCK.
11/25/1952	19-17-54	36.20	120.00	D	3.2			
11/25/1952	20-14-45	35.73	121.20	C	3.6			SAN SIMEON AFTERSHOCK.
11/25/1952	21-59-17	35.73	121.20	C	4.4			SAN SIMEON AFTERSHOCK.
11/26/1952	13-32-09	35.73	121.20	C	3.5			SAN SIMEON AFTERSHOCK.
11/27/1952	17-37-05	35.70	121.20	D	3.3			SAN SIMEON AFTERSHOCK.
11/28/1952	10-22-33	35.90	121.20	D	3.0			SAN SIMEON AFTERSHOCK.
11/29/1952	16--?--?	36.00	121.15	D			F	IV AT JOLON - TIME MAY BE 04--?--? ON 11/30/1952.
11/29/1952	23-15-58	35.70	121.20	D	3.5			SAN SIMEON AFTERSHOCK.
12/05/1952	01-05-57	36.50	120.70	D	3.0			14 MI. SE OF LLANADA.
12/06/1952	23-50--?	35.66	120.65	D			F	IV AT PASO ROBLES; FELT AT ADELAIDA.
12/12/1952	-?-27-07	36.40	120.97	B	3.0		F	17 MI. NE OF KING CITY; III AT LONOAK.
12/25/1952	16-44-10	34.40	121.40	D	3.6			
01/12/1953	13-05-18	35.80	121.10	D	3.2			14 MI. NE OF SAN SIMEON.
01/24/1953	-?--?--?	35.90	121.00	D			F	TEN SHOCKS REPORTED FELT FROM 1/24 TO 1/31 AT BRYSON (E. WEFERLING RANCH).
01/29/1953	20-31-19	35.80	121.10	D	3.1			14 MI. NE OF SAN SIMEON.

MM/DD/YY	HR/MN/SE	NORTH LAT	WEST LONG	QUALITY	MAG.	STA. REC.	FELT	MAXIMUM INTENSITY - COMMENTS
02/03/1953	14-50-18	35.47	120.75	C	4.1		F	12 MI. NNW OF SAN LUIS OBISPO; V AT ATASCADERO, BRYSON, CRESTON, MORRO BAY, SANTA MARGARITA, AND IV AT CAYUCOS, PASO ROBLES, SAN LUIS OBISPO, AND TEMPLETON.
02/05/1953	02-54-12	35.90	121.00	D	2.8		F	IV AT BRYSON (E. WEFERLING RANCH).
02/15/1953	15-30--?	35.90	121.00	D			F	BRYSON (E. WEFERLING RANCH).
02/17/1953	08-06--?	35.90	121.00	D			F	III AT BRYSON (PLEYTO SCHOOL) - SEVERAL MILD SHOCKS REPORTED FELT DAILY SINCE SHOCK OF 11/21/52, 23-46-38 (NOT LISTED).
02/18/1953	14-10--?	35.90	121.00	D			F	BRYSON (E. WEFERLING RANCH) - MILD.
03/01/1953	18-53--?	35.90	121.00	D			F	V AT BRYSON.
03/04/1953	03-40--?	35.90	121.00	D			F	BRYSON (PLEYTO SCHOOL) - LIGHT.
03/15/1953	21--?-32	34.87	121.53	C	3.7			
03/18/1953	05-03--?	35.90	121.00	D			F	III AT BRYSON (PLEYTO SCHOOL).
03/29/1953	17-19-48	35.90	120.20	D	3.7			
04/08/1953	-?-59-20	34.80	120.60	D	3.6		F	NEAR CASMALIA; IV AT LOS ALAMOS.
04/15/1953	-?-29-10	35.83	121.07	C	3.1		F	14 MI. NNE OF SAN SIMEON; IV AT BRYSON.
04/15/1953	05-30--?	35.90	121.00	D			F	BRYSON - LIGHT.
04/29/1953	05-26-53	36.00	121.15	C	3.5		F	14 MI. S OF KING CITY - USCGS GIVES TIME AS 05-26-52, LOCATION AS N35.8 121.2W, REPORT AS NEAR BRYSON; V AT PLEYTO SCHOOL. 22 MI. NE OF KING CITY.
05/01/1953	22-16-51	36.40	120.80	D	3.0			
05/08/1953	08-15--?	34.65	120.45	D			F	III AT LOMPOC.
05/14/1953	03-36--?	36.00	120.00	D	3.3			
05/14/1953	09-36-09	35.75	121.08	B	3.7		F	9 MI. NE OF SAN SIMEON - USCGS GIVES N35.52 121.28W, OFF CAMBRIA; V AT BRYSON.
05/15/1983	07-15--?	35.90	121.00	D			F	IV AT BRYSON (PLEYTO SCHOOL).
05/28/1953	03-51-13	35.88	120.50	B	4.3		F	20 MI. SW OF COALINGA; IV AT PASO ROBLES AND III AT SAN MIGUEL.
05/28/1953	07-58-33	35.88	120.50	C	3.5		F	AFTERSHOCK OF 03-51-13; FELT AT SAN MIGUEL.
05/29/1953	10-20-16	35.90	121.20	D	2.9			20 MI. SOUTH OF KING CITY.
05/31/1953	23-51-17	36.10	120.40	D	3.2			NEAR COALINGA.
06/04/1953	11-40--?	35.50	120.50	D			F	V AT CRESTON - PROBABLY A BLAST.
06/06/1953	20-26-33	36.00	120.30	D	2.9			10 MI. SOUTH OF COALINGA.
06/19/1953	11-24-50	36.30	120.70	D	2.8			20 MI. EAST OF KING CITY.
06/22/1953	15-22-35	35.93	120.38	C	4.3		F	15 MI. WSW OF COALINGA; FELT AT COALINGA AND PASO ROBLES.
07/01/1953	22-17-20	34.60	121.35	D	3.2		F	OFF POINT ARGUELLO; IV AT POINT ARGUELLO LIGHT STATION.
08/14/1953	01-40-06	36.30	120.30	D	2.9			8 MI. NORTH OF COALINGA.
08/14/1953	09-22-50	36.50	121.20	D	2.3			20 MI. NORTH OF KING CITY.
09/02/1953	09-41-20	35.90	120.80	D	3.0			30 MI. SE OF KING CITY.
09/03/1953	11--?--?	35.50	120.50	D			F	CRESTON.
09/04/1953	03-54-25	35.90	120.32	C	3.5		F	15 MI. SOUTH OF COALINGA; IV AT CRESTON AND PASO ROBLES.
09/22/1953	07-36-58	36.40	121.20	D	3.8			NORTH OF KING CITY.
09/23/1953	06-21-51	35.70	121.10	D	3.5		F	NEAR SAN SIMEON; V AT BRYSON.
10/01/1953	03-56-15	36.25	121.83	C	3.4		F	25 MI. S OF MONTEREY; IV AT BIG SUR.
10/16/1953	03-45-35	35.95	120.53	C	3.4			SOUTHWEST OF COALINGA.
10/21/1953	16-02-38	34.32	119.70	B	4.0		F	OFF SANTA BARBARA; V AT SANTA BARBARA AND VICINTIY, AND IV AT GOLETA AND LOS PRIETOS RANGER STATION.

MM/DD/YY	HR/MN/SE	NORTH LAT	WEST LONG	QUALITY	MAG.	STA. REC.	FELT	MAXIMUM INTENSITY - COMMENTS
10/24/1953	13-24-30	35.90	121.10	D	3.6			SOUTH OF KING CITY.
10/25/1953	08-43-25	36.50	121.50	D	3.2			NORTHWEST OF KING CITY.
11/02/1953	-?-52-06	36.40	121.30	D	3.4			NORTHWEST OF KING CITY.
01/04/1954	23-03-11	36.12	120.63	B	3.2			14 MI. WEST OF COALINGA.
01/05/1954	-?-23-23	35.93	120.00	C	3.0			SOUTHEAST OF COALINGA.
01/15/1954	22-02-18	36.50	121.23	C	2.6			NORTH OF KING CITY.
01/24/1954	19-06-45	35.78	121.08	C	3.1			30 MI. SOUTH OF KING CITY.
01/26/1954	09-43-22	34.50	120.33	C	3.8		F	W OF LAS CRUCES; III AT SANTA YNEZ.
03/09/1954	19-55-30	35.90	120.50	D	3.6		F	16 MI. SSE OF COALINGA; FELT NEAR PARKFIELD.
03/15/1954	22-43-50	35.00	120.70	D	3.4			
03/18/1954	12-07-53	35.40	120.90	D	3.0			NORTHWEST OF SAN LUIS OBISPO.
04/01/1954	12-04-38	36.05	120.20	C	3.3			6 MI. SOUTHEAST OF COALINGA.
04/09/1954	07-38-23	35.78	121.08	D	3.1			10 MI. NORTHEAST OF SAN SIMEON.
04/09/1954	14-58--?	35.90	121.00	D			F	IV AT BRYSON (PLEYTO SCHOOL); SECOND SHOCK REPORTED FELT AT 23-40--?.
04/20/1954	09-32-18	36.63	121.03	D	2.6			12 MI. NORTHEAST OF KING CITY.
05/10/1954	14-24-28	36.08	120.80	C	3.1		F	NE OF SAN ARDO - SLIGHT AT KING CITY.
06/04/1954	11-58-38	36.45	121.13	C	3.5			16 MI. SOUTHWEST OF LLANADA.
07/05/1954	07-25-39	36.20	121.80	D	3.2			30 MI. SOUTH OF MONTEREY.
08/13/1954	13-36-44	34.25	120.50	C	3.2			
08/13/1954	13-44-23	34.25	120.50	C	3.2			
08/19/1954	11-45-08	34.25	120.50	C	3.2			
08/21/1954	22-50-49	35.47	121.33	B	3.3			40 MI. SOUTH OF HOLLISTER.
08/22/1954	08-34-40	34.33	120.67	C	3.8			
08/22/1954	12-36-07	34.33	120.67	C	3.8			
12/22/1954	21-12-24	36.00	121.00	D	3.7		F	SE OF KING CITY; III AT KING CITY.
12/22/1954	21-12-28	36.00	120.60	D	3.8			
01/07/1955	14-50-22	34.40	119.60	D	3.0			
01/18/1955	13-30--?	36.20	121.85	D			F	IV REPORTED FELT AT BIG SUR.
02/05/1955	07-10-19	35.80	121.40	C	3.3			WEST OF SAN SIMEON.
02/27/1955	03-17-51	36.25	120.83	C	2.9		F	EAST OF KING CITY; IV IN PRIEST VALLEY.
03/02/1955	03-30--?	36.00	120.70	D			F	IV REPORTED FELT IN INDIAN VALLEY.
03/02/1955	15-59-01	36.00	120.93	B	4.8		F	18 MI. SE OF KING CITY; FELT OVER 7000 SQ. MI. OF W CENTRAL CALIF. USCGS MAG. 5.1. VI AT ADELAIDA, BRYSON, INDIAN VALLEY, SAN ARDO, SAN LUCAS, AND TEMPLETON.
03/02/1955	20-02-53	36.00	120.93	B	3.7			AFTERSHOCK OF QUAKE AT 15-59-01.
03/05/1955	08-46-36	36.10	121.10	D	2.0			SOUTH OF KING CITY.
03/06/1955	10-47-32	35.92	120.90	D	3.2			SOUTHEAST OF KING CITY.
04/04/1955	20-56-56	36.08	121.00	C	3.2			SOUTHEAST OF KING CITY.
04/27/1955	09-28-08	35.90	121.20	D	2.8			SOUTHWEST OF KING CITY.
05/14/1955	20--?--?	36.35	121.85	D			F	IV REPORTED FELT AT BIG SUR AND SANTA CRUZ.
05/16/1955	18-22-52	35.92	120.58	C	3.0			SOUTHWEST OF COALINGA.
05/30/1955	09-38-29	36.25	121.25	C	3.0			WEST OF KING CITY.
05/31/1955	01-45-53	36.40	121.25	B	3.0			NORTH OF KING CITY.
06/13/1955	14-55-12	36.30	121.30	C	2.5			NORTH OF KING CITY.
06/19/1955	05-36-33	35.62	121.10	C	2.5			SOUTHEAST OF SAN SIMEON.
07/06/1955	11-29-18	36.50	121.42	C	3.4			SOUTH OF HOLLISTER.

MM/DD/YY	HR/MN/SE	NORTH LAT	WEST LONG	QUALITY	MAG.	STA. REC.	FELT	MAXIMUM INTENSITY - COMMENTS
07/06/1955	13-18-53	36.50	121.50	D	2.7			SOUTH OF HOLLISTER.
07/28/1955	12-07-52	36.50	121.40	D	2.6			SOUTH OF HOLLISTER.
09/21/1955	18-06-52	36.50	121.00	D	3.3			NORTH OF KING CITY.
10/22/1955	07-04-18	36.22	120.33	C	4.2		F	V AT AND 14 MI. NW OF COALINGA.
11/02/1955	19-40-06	36.00	120.92	A	5.2		F	55 MI. NNW OF SAN LUIS OBISPO; FELT OVER 7000 SQ. MI. OF COASTAL W CENTRAL CALIF. VI AT ADELAIDA RD. (14 MI. W OF PASO ROBLES), BRYSON, KING CITY, PASO ROBLES, SAN ARDO, SAN LUCAS, AND SAN MIGUEL.
11/18/1955	09-03-30	35.90	120.50	D	2.9			SOUTHWEST OF COALINGA.
11/19/1955	07-20--?	34.50	119.65	D			F	REPORTED FELT AT SANTA BARBARA.
11/19/1955	10-59-41	36.03	120.90	C	3.3			SOUTHEAST OF KING CITY.
11/21/1955	21-14-18	36.10	119.90	D	3.5			
12/11/1955	20-10-38	36.27	120.72	C	3.5			NORTHWEST OF COALINGA.
12/16/1955	14-43-11	36.03	120.87	C	3.8		F	SOUTHWEST OF KING CITY; FELT AT ATASCADERO, PASO ROBLES, AND SAN MIGUEL.
12/29/1955	13-33-17	36.45	121.25	C	3.4			NORTH OF KING CITY.
02/14/1956	22-15-08	36.50	121.10	D	2.8			SOUTHWEST OF LLANADA.
03/15/1956	15-26-11	36.50	121.20	D	2.6			SOUTHEAST OF HOLLISTER.
04/03/1956	09-26-02	36.45	121.23	B	2.7			SOUTH OF HOLLISTER.
04/10/1956	11-24-21	36.43	121.48	C	2.9			SOUTHEAST OF MONTEREY.
04/10/1956	20-53-21	36.30	121.00	D	2.9			NORTHEAST OF KING CITY.
05/01/1956	15-06-33	36.50	121.00	D	2.5			SOUTH OF HOLLISTER.
05/04/1956	08-16-14	35.75	121.07	B	3.1			NORTHEAST OF SAN SIMEON.
05/04/1956	08-16-16	35.95	120.93	D	3.5			
05/15/1956	10-45--?	34.90	120.40	D			F	REPORTED FELT AT SANTA MARIA.
06/11/1956	-?-48-37	36.00	120.97	C	3.2			SOUTHEAST OF KING CITY.
06/15/1956	23-42-03	36.30	121.80	D	2.8			SOUTH OF MONTEREY.
07/09/1956	23-15--?	35.10	120.50	D			F	III REPORTED FELT NEAR HUASNA.
07/23/1956	08-03-48	36.30	121.30	D	4.7		F	NW OF KING CITY; FELT OVER 4000 SQ. MI. OF COASTAL CENTRAL CALIF. V AT BIG SUR, CHUALAR, GONZALES, GREENFIELD, 7.5 MI. S OF HOLLISTER, KING CITY, PASO ROBLES, SAN BENITO, AND SAN JUAN BAUTISTA.
07/23/1956	08-20-37	36.50	121.40	D	3.1			AFTERSHOCK OF QUAKE AT 08-03-48.
07/31/1956	-?-40-43	34.15	119.60	C	3.2			
07/31/1956	17-25--?	35.10	120.50	D			F	IV REPORTED FELT AT HUASNA.
08/09/1956	-?-08-49	34.37	119.80	B	4.0		F	OFF SANTA BARBARA; IV AT LOS PRIETOS RANGER STATION.
08/10/1956	23-24-03	35.90	121.30	D	3.0			SOUTHWEST OF KING CITY.
08/20/1956	05-10-33	36.48	121.48	B	3.2		F	NEAR GONZALES; IV AT PINNACLES NATIONAL MONUMENT.
09/15/1956	-?-34-37	36.30	120.30	D	2.7			NORTH OF COALINGA.
10/10/1956	20-02-24	34.70	121.00	D	3.8			
11/12/1956	10-13--?	36.30	120.10	C	3.3			
11/16/1956	03-23-09	35.95	120.47	B	5.0		F	SW OF COALINGA; FELT OVER 8000 SQ. MI. FROM HOLY CITY TO BETTERAVIA TO FIREBAUGH. VI AT KING CITY, MEE RANCH (LONOAK), AND SAN LUCAS.
11/19/1956	13-53-53	35.98	120.57	C	3.3		F	SOUTHWEST OF COALINGA; III AT ADELAIDA (15 MI. WEST OF PASO ROBLES).
11/20/1956	03-42-44	34.70	120.50	C	3.6		F	IV AT LOS ALAMOS; III FELT AT 07-42--?, 11/21/1956.

MM/DD/YY	HR/MN/SE	NORTH LAT	WEST LONG	QUALITY	MAG.	STA. REC.	FELT	MAXIMUM INTENSITY - COMMENTS
12/11/1956	10-56-53	35.88	120.47	C	4.1			NEAR PARKFIELD.
12/28/1956	13-39-37	35.90	121.10	D	2.6			NORTHEAST OF SAN SIMEON.
01/01/1957	09-25--?	35.50	120.65	D			F	REPORTED FELT AT ATASCADERO.
01/29/1957	21-19-53	35.87	122.12	C	4.9		F	OFF COAST NW OF SAN SIMEON; FELT OVER 5000 SQ. MI. OF COASTAL CENTRAL CALIF. V AT BIG SUR, CAMBRIA, CARMEL VALLEY, HARMONY, KING CITY, LUCIA, MARINA, AND SEASIDE, AND IV GENERALLY FROM MOSS LANDING TO 20 MI. W OF COALINGA TO SAN LUIS OBISPO.
02/03/1957	07-57-12	34.50	121.20	C	3.9			
02/08/1957	04-45-38	36.50	121.20	D	2.8			NORTH OF KING CITY.
02/08/1957	21-20--?	36.50	122.00	D			F	SHARP SHOCK FELT MONTEREY PEN. (BSSA).
02/09/1957	08-10--?	35.50	120.65	D			F	IV REPORTED FELT AT ATASCADERO.
02/14/1957	-?-31-30	35.10	119.80	D	2.4			
02/14/1957	10-30-27	36.00	120.60	C	3.6			
02/16/1957	11-43-50	34.30	119.53	C	3.5			
03/09/1957	14-38-28	34.70	119.60	C	2.9			
03/09/1957	14-59-21	34.70	119.60	C	2.4			
04/05/1957	-?-40--?	34.75	120.25	D			F	IV REPORTED FELT AT LOS ALAMOS.
06/21/1957	20-46-42	35.10	120.90	D	3.7		F	OFF COAST; FELT AT SAN LUIS OBISPO AND MORRO BAY.
07/02/1957	09-18-22	34.37	119.88	B	3.4		F	W OF SANTA BARBARA; FELT AT SANTA BARBARA.
07/02/1957	12-59-05	34.37	119.88	B	3.3			
07/02/1957	13-58-28	34.37	119.88	B	3.2			
07/21/1957	01-29-20	36.43	121.22	B	3.1			NORTH OF KING CITY.
08/03/1957	09-31-22	36.25	120.88	C	2.5			EAST OF KING CITY.
08/18/1957	03-05-25	34.47	120.13	C	3.4			
08/18/1957	11-08-23	34.47	120.13	C			F	N OF GAVIOTA; FELT AT CACHUMA RESERVOIR.
08/21/1957	07-36-54	36.47	121.52	C	3.6			NORTHWEST OF KING CITY.
08/28/1957	01-13-57	34.58	121.00	C	3.5			
09/12/1957	21-36--?	35.50	121.00	D			F	II FELT AT P G AND E PLANT, MORRO BAY.
09/21/1957	06-54-26	36.40	121.10	D	2.8			NORTH OF KING CITY.
09/21/1957	15-32--?	35.50	121.00	D			F	II FELT AT P G AND E PLANT, MORRO BAY.
09/25/1957	23-33-31	36.50	121.50	D	2.7			SOUTH OF HOLLISTER.
10/01/1957	12-55-57	36.47	121.23	C	3.3			SOUTHWEST OF LLANADA.
10/05/1957	14-42--?	34.75	120.25	D			F	IV REPORTED FELT AT LOS ALAMOS.
10/19/1957	-?-04-38	36.10	120.87	B	3.3			SOUTHEAST OF KING CITY.
10/28/1957	11-41-02	34.33	120.00	C	2.8			
11/05/1957	23-50-52	34.72	120.33	C	3.4			
11/18/1957	01-11-42	36.38	121.23	C	3.1			NORTHWEST OF KING CITY.
11/18/1957	07-26-32	36.50	121.70	D	3.3			SOUTHEAST OF MONTEREY.
12/31/1957	22-32-55	36.40	121.00	D	2.9			NORTHEAST OF KING CITY.
01/07/1958	17-13-16	35.70	120.80	D	3.0			NORTH OF SAN LUIS OBISPO.
01/18/1958	08-12--?	35.55	120.65	D			F	REPORTED FELT AT PASO ROBLES.
01/21/1958	21-22-08	36.40	120.50	D	2.9			NORTHWEST OF COALINGA.
01/23/1958	07-06-46	34.38	119.58	B	2.6		F	E OF SANTA BARBARA; IV AT SANTA BARBARA.
01/28/1958	07-12-54	36.50	121.10	D	2.2			SOUTHWEST OF LLANADA.
03/26/1958	13-12-30	36.20	120.30	D	2.4			NEAR COALINGA.
03/27/1958	20-26-14	35.90	121.50	D	2.8			NORTHWEST OF SAN SIMEON.

MM/DD/YY	HR/MN/SE	NORTH LAT	WEST LONG	QUALITY	MAG.	STA. REC.	FELT	MAXIMUM INTENSITY - COMMENTS
03/31/1958	17-38-23	36.50	121.10	D	2.7			SOUTHWEST OF LLANADA.
04/10/1958	08-32-33	36.45	121.12	C	2.9			SOUTHWEST OF LLANADA.
06/05/1958	17-12-50	36.40	121.10	D	3.1			NORTH OF KING CITY.
06/15/1958	07-02-33	36.50	121.38	C	2.9			FORESHOCK OF QUAKE AT 07-05-34.
06/18/1958	07-05-34	36.50	121.38	C	3.3			SOUTH OF HOLLISTER.
06/21/1958	01-03-31	36.40	120.40	D	2.1			SOUTHWEST OF FRESNO.
07/02/1958	17-56-26	36.50	121.30	D	2.8			SOUTHWEST OF LLANADA.
08/08/1958	18-43-01	36.30	121.20	D	2.7			FORESHOCK OF 13-43-15 - RECORDS MIXED.
08/08/1958	13-43-15	36.30	121.20	D	3.9		F	NORTHWEST OF KING CITY; IV AT BIG SUR.
08/18/1958	05-30-42	35.80	121.30	D	3.4			NEAR SAN SIMEON.
09/01/1958	11-31-42	36.10	120.80	D	3.2			SOUTHEAST OF KING CITY.
09/21/1958	07-24-55	36.35	121.12	C	4.0		F	NORTH OF KING CITY; VI AT SAN BENITO; ALSO FELT AT SOLEDAD.
09/21/1958	14-23-01	36.50	121.05	C	2.7			SOUTHWEST OF LLANADA.
10/03/1958	04-25-51	34.37	119.50	B	3.7		F	FROM CARPINTERIA TO GOLETA.
10/10/1958	13-05-16	35.93	120.50	B	4.5		F	SOUTHWEST OF COALINGA; FELT OVER AN AREA OF APPROXIMATELY 3500 SQ. MI. OF THE SOUTHWEST-CENTRAL REGION OF CALIFORNIA - APPEARS TO HAVE BEEN FELT MORE STRONGLY AT PARKFIELD THAN ELSEWHERE; V AT ADELAIDA, CAMP ROBERTS, COALINGA, HARMONY, LONE PINE INN, OILFIELD, PARKFIELD, PASO ROBLES, AND SAN ARDO.
10/15/1958	16-16-44	35.50	121.20	D	3.2			NEAR SAN SIMEON.
11/06/1958	20-11-57	36.08	120.88	C	3.1			SOUTHEAST OF KING CITY.
11/16/1958	09-34-04	34.50	119.83	C	4.0		F	NW OF SANTA BARBARA; FELT OVER 600 SQ. MI. FROM SANTA YNEZ TO VENTURA; V AT CARPINTERIA, GOLETA, AND SANTA BARBARA.
11/27/1958	06-04-26	36.37	121.15	C	3.9		F	WEST OF LLANADA; FELT SLIGHTLY AT CARMEL.
11/27/1958	13-39-01	36.20	120.80	D	3.1			EAST OF KING CITY.
12/15/1958	14-58-49	36.20	120.40	D	3.0			NEAR COALINGA.
12/15/1958	15-24-01	36.20	120.40	D	3.0		F	NEAR COALINGA; IV AT COALINGA.
12/30/1958	01-34-15	35.92	119.80	C	3.2			
01/11/1959	05-18-26	36.20	120.80	D	2.5			WEST OF COALINGA.
02/07/1959	05-51-02	36.10	120.00	D	3.0			SOUTHEAST OF KING CITY.
02/27/1959	21-35-01	36.25	120.75	C	3.1			SOUTHEAST OF LLANADA.
03/13/1959	02-44-27	35.80	120.30	D	2.5			SOUTH OF COALINGA.
03/14/1959	02-43-41	35.70	121.30	D	3.6			WEST OF SAN SIMEON.
03/20/1959	05-12-09	36.48	121.17	B	2.9			SOUTHWEST OF LLANADA.
03/25/1959	05-34-17	34.25	119.58	C	2.5		F	SANTA BARBARA CHANNEL; IV AT CARPINTERIA.
04/08/1959	07-41-57	36.37	121.20	B	3.4			NORTH OF KING CITY.
04/09/1959	14-03-11	36.38	121.15	C	2.5			NORTH OF KING CITY.
04/21/1959	09-36-23	36.40	120.40	D	3.0			NORTH OF COALINGA.
04/21/1959	12-31-10	36.10	121.10	D	2.2			NEAR KING CITY.
04/22/1959	19-04-25	36.20	120.90	D	2.6			NEAR KING CITY.
05/13/1959	14-28-10	36.48	121.03	C	2.6			SOUTHWEST OF LLANADA.
05/14/1959	01-34-09	36.50	121.20	D	2.4			SOUTHWEST OF LLANADA.
05/20/1959	10-15-55	36.30	120.40	D	2.6			NORTHWEST OF COALINGA.
06/01/1959	03-47-24	36.50	121.23	C	2.4			SOUTHWEST OF LLANADA.
06/20/1959	15-01-17	36.50	121.30	D	2.9			SOUTH OF VINEYARD.

TABLE 2.5-1

MM/DD/YY	HR/MN/SE	NORTH LAT	WEST LONG	QUALITY	MAG.	STA. REC.	FELT	MAXIMUM INTENSITY - COMMENTS
06/21/1959	09-24-07	34.32	119.67	B	3.3			
07/18/1959	01-11-47	36.50	121.30	D	2.5			SOUTH OF VINEYARD.
08/05/1959	03--?-34	35.95	120.48	C	3.5		F	SOUTHEAST OF COALINGA (NEAR PARKFIELD; FELT STRONGEST AT PARKFIELD; IV FELT AT PASO ROBLES).
09/05/1959	05-45-34	36.50	121.70	D	3.8			SOUTHWEST OF VINEYARD.
10/01/1959	04-35-35	34.43	120.57	B	4.5		F	OFF POINT CONCEPTION; VI AT GAVIOTA PASS AND V AT GAVIOTA, GOLETA, AND LOMPOC.
10/01/1959	05-52-55	34.20	119.50	C	3.2			
10/11/1959	02-03-09	36.45	121.12	C	4.1		F	SOUTHWEST OF LLANADA; FELT AT SALINAS.
10/24/1959	23-12-54	36.47	121.40	C	3.2			SOUTH OF HOLLISTER.
10/25/1959	03-33-13	36.50	121.20	D	2.4			SOUTHEAST OF VINEYARD.
10/25/1959	03-34-02	36.50	121.32	C	3.0			SOUTH OF VINEYARD.
10/26/1959	09-56-01	36.40	121.10	D	3.0			SOUTHEAST OF VINEYARD.
11/25/1959	09-28-22	35.20	121.20	D	3.5			SOUTH OF KING CITY.
11/26/1959	07-02-05	36.40	121.40	D	2.7			SOUTH OF VINEYARD.
12/11/1959	05-55-26	35.60	120.60	D	3.5			SOUTHEAST OF VINEYARD.
12/25/1959	20-38-28	36.00	120.60	D	3.1			SOUTHEAST OF VINEYARD.
12/29/1959	14-53-08	35.75	120.30	C	3.5		F	NEAR CHOLAME; FELT AT PASO ROBLES.
01/02/1960	22-51-48	35.40	121.20	D	4.0			NW OF SAN LUIS OBISPO.
01/04/1960	12-18-20	36.20	120.70	D	3.2			WEST OF COALINGA.
02/14/1960	08-34-30	35.80	121.70	D	2.8			WEST OF SAN SIMEON.
02/25/1960	06-34-31	36.50	121.20	D	2.7			SOUTHWEST OF LLANADA.
02/28/1960	02-55-32	34.33	119.95	C	3.1			
03/21/1960	20-46-39	36.50	120.73	C	2.5			SOUTHEAST OF LLANADA.
03/26/1960	21-39-21	36.22	121.00	C	2.7			EAST OF KING CITY.
03/29/1960	11-46-42	36.50	121.10	C	2.4			SOUTHEAST OF VINEYARD.
03/31/1960	08-35-09	36.40	121.20	D	2.6			SOUTHEAST OF VINEYARD.
04/02/1960	13-02-10	35.97	120.33	C	2.7			SOUTH OF COALINGA.
04/02/1960	19-01-12	36.20	120.60	D	3.4			WEST OF COALINGA.
04/09/1960	08-01-14	36.50	121.13	B	3.6			SOUTHEAST OF HOLLISTER.
05/04/1960	09-44-32	36.42	120.72	C	3.4			SOUTHEAST OF LLANADA.
05/15/1960	06-07-23	36.43	121.27	C	2.5			SOUTH OF VINEYARD.
06/11/1960	17-39-48	36.30	120.90	D	3.7			SOUTHEAST OF VINEYARD, DIABLO RANGE.
06/19/1960	19-51-20	36.20	121.90	D	2.6			SOUTHWEST OF BIG SUR.
06/24/1960	18-13-12	36.45	121.22	B	3.5			SOUTHEAST OF VINEYARD.
07/14/1960	03-22-23	35.60	120.40	D	3.0			NORTHEAST OF SAN LUIS OBISPO.
07/20/1960	-?-59-36	35.80	119.80	D	2.8			NORTHEAST OF SAN LUIS OBISPO.
07/30/1960	02-16-29	36.43	120.28	C	2.5			SOUTHWEST OF FRESNO.
08/09/1960	08-59-47	36.20	120.20	D	3.2			EAST OF COALINGA.
08/10/1960	03-03-50	36.47	121.40	D	3.2			SOUTH OF VINEYARD.
08/26/1960	08-57-24	38.33	121.13	C	3.0			SOUTHEAST OF VINEYARD.
09/10/1960	01-18-22	36.47	121.05	C	2.7			SOUTHEAST OF HOLLISTER.
09/10/1960	20-49-12	36.45	121.28	D	2.8			SOUTHWEST OF LLANADA.
10/08/1960	-?-02-29	36.50	121.67	C	3.0			SOUTHWEST OF VINEYARD.
11/03/1960	07-13-40	36.43	121.07	C	2.7			SOUTH-SOUTHWEST OF LLANADA.
11/18/1960	04-36-44	36.38	121.20	C	3.0			NORTH-NORTHWEST OF KING CITY.

MM/DD/YY	HR/MN/SE	NORTH LAT	WEST LONG	QUALITY	MAG.	STA. REC.	FELT	MAXIMUM INTENSITY - COMMENTS
12/01/1960	14-23-49	34.33	119.85	B	3.2			OFF SANTA BARBARA.
12/15/1960	08-28-08	36.40	121.30	D	3.0			SOUTH OF HOLLISTER.
12/27/1960	03-57-55	36.00	121.10	D	3.3			SOUTH OF KING CITY.
01/06/1961	20-46-36	35.80	120.20	D	3.4			SE OF PARKFIELD.
02/02/1961	12-31--?	36.35	121.20	D	2.2			NORTHWEST OF KING CITY.
02/21/1961	15-46-58	34.37	119.53	C	2.8			SE OF SANTA BARBARA.
03/14/1961	04-15--?	36.40	121.20	D	3.4			SOUTHEAST OF VINEYARD.
03/29/1961	16--?-11	36.50	121.50	D	2.5			SOUTH OF VINEYARD.
04/07/1961	12-21-19	36.20	120.40	D	2.9			NORTH OF COALINGA.
04/08/1961	04-55-26	36.00	121.20	D	2.7			SOUTH OF KING CITY.
04/08/1961	09-29-47	36.10	120.43	B	3.4			NEAR COALINGA.
04/08/1961	12-52-16	36.12	120.43	C	2.7			AFTERSHOCK OF QUAKE AT 09-29-47.
04/11/1961	09-08-11	36.00	120.10	D	2.7			SOUTHEAST OF KING CITY.
04/12/1961	04-59-08	35.92	120.50	C	2.6			SOUTHWEST OF COALINGA.
04/19/1961	18-16-35	36.40	121.58	C	3.3			SOUTHEAST OF MONTEREY.
05/25/1961	14-19-05	36.33	121.00	C	3.4			NORTHEAST OF KING CITY.
05/25/1961	14-19-35	36.33	121.00	B	3.4			NORTHEAST OF KING CITY.
06/01/1961	06-47-20	36.33	121.32	B	2.7			NORTHWEST OF KING CITY.
06/01/1961	14-11-30	36.45	121.20	C	2.6			NORTH OF KING CITY.
06/18/1961	12-50-59	36.18	120.83	C	2.1			EAST OF KING CITY.
06/25/1961	13-15-26	36.48	121.35	C	3.6		F	SOUTH OF HOLLISTER; FELT IN HOLLISTER AREA. INTENSITY IV 7.5 MI. SOUTH OF HOLLISTER AT HARRIS RANCH.
06/26/1961	11-30-22	35.77	122.00	C	2.5			OFF SAN SIMEON COAST.
07/22/1961	18-01-55	36.40	121.20	C	4.0		F	NORTHEAST OF PARAISO; FELT AT PINNACLES NATIONAL MONUMENT (ABOUT 25 MI. SOUTHEAST OF HOLLISTER).
07/31/1961	-?-07-09	35.82	120.37	C	4.7		F	SAN LUIS OBISPO; FELT OVER AN AREA OF 5000 SQ. MI. OF WEST CENTRAL CALIFORNIA. INTENSITY V AT ATASCADERO, CHOLAME, CRESTON, PARKFIELD, SAN LUIS OBISPO, AND TEMPLETON.
08/01/1961	06-12-54	36.43	120.85	C	3.1			SOUTH OF LLANADA.
08/17/1961	17-14-45	36.33	120.95	B	3.1			NORTHEAST OF KING CITY.
09/14/1961	15-12-20	34.32	119.63	C	2.7			
09/14/1961	15-14-38	34.32	119.63	C	2.8			
09/27/1961	02-02-06	36.33	121.25	C	2.7			EAST OF PARAISO.
09/29/1961	15-39-58	36.33	120.88	B	2.4			SOUTH OF LLANADA.
10/12/1961	06-31-11	35.80	121.30	D	2.3			NORTH OF SAN SIMEON.
10/29/1961	11-47-33	36.33	120.92	C	2.0			EAST OF PARAISO.
11/05/1961	10-43-57	36.03	120.10	D	2.0			EAST OF LLANADA.
11/29/1961	04-49-03	35.15	120.13	C	3.0			SOUTHEAST OF KING CITY.
12/06/1961	03-27-30	36.43	121.85	B	2.4			SOUTH OF MONTEREY.
12/14/1961	07-28-44	36.48	121.08	B	2.1			SOUTHWEST OF LLANADA.
01/04/1962	03-56-10	36.40	121.40	C	3.0	11		NORTHWEST OF KING CITY.
01/31/1962	08-33-15	34.88	120.68	C	3.6			
02/01/1962	06-37-57	34.88	120.68	C	4.5		F	WEST OF GUADALUPE; FELT OVER AN AREA OF 3000 SQ. MI. V AT ARROYO GRANDE, AVILA BEACH, CASMALIA, GROVER CITY, GUADALUPE, HALCYON, OCEANO, POINT ARGUELLO, AND SHELL
02/01/1962	07-58-12	34.38	120.68	C	3.7			
02/04/1962	11-43-34.1	36.42	121.27	C	3.2	12		

MM/DD/YY	HR/MN/SE	NORTH LAT	WEST LONG	QUALITY	MAG.	STA. REC.	FELT	MAXIMUM INTENSITY - COMMENTS
02/07/1962	13--?-70	34.30	122.10	D	3.9			
03/05/1962	07-44-01	34.60	121.60		4.5		F	OFF COAST NEAR LOMPOC; V AT MORRO BAY AND PISMO BEACH.
03/06/1962	03-40-22	34.60	121.60	D	3.6			
03/10/1962	08-07-21	34.60	121.60	D	4.2			OFF COAST NEAR LOMPOC.
03/10/1962	13-40-48	34.60	121.60	D	4.0			OFF COAST NEAR LOMPOC.
03/10/1962	15-24-21	34.60	121.60	D	3.5			
03/12/1962	21-32-09	34.60	121.60	D	3.9			
03/23/1962	22-10-18	34.28	120.20	C	2.9			
03/24/1962	03-38-41.8	36.20	119.78	B	3.4	19		SOUTH OF FRESNO.
04/02/1962	03-06-03.2	36.25	120.10	B	3.7	16	F	EAST OF COALINGA; V IN TEHACHAPI.
04/15/1962	08-41-02.3	36.42	120.62	B	4.7	23	F	SOUTHEAST OF LLANADA; V AT IDRIA.
05/04/1962	20-52-32	35.27	119.55	B	2.8			
05/05/1962	-?-55-20	34.20	121.50	D	3.3			
09/03/1962	17-53-33.1	36.47	121.07	C	2.6	8	F	SOUTHWEST OF LLANADA; FELT IN HOLLISTER.
09/11/1962	01-34-31	36.03	121.23	B	3.3	16		SOUTHWEST OF KING CITY.
09/16/1962	18-12-35	34.48	119.68	B	4.0		F	NEAR SANTA BARBARA; V AT LOS PRIETOS.
09/16/1962	18-17-09	34.48	119.68	C	2.2			
09/16/1962	18-31-17	34.52	119.77	B	2.9			
09/21/1962	05-07-18	34.47	119.58	B	3.0			
09/29/1962	19-47-32	34.47	119.70	B	2.9			
10/13/1962	17-49-39.5	36.35	120.42	B	3.7	17		NORTHEAST OF PRIEST.
12/15/1962	-?-40-20.9	36.47	120.63	B	2.9	13		NORTH OF PRIEST.
01/09/1963	06-04-25.7	35.98	120.35	B	3.2	14	F	SE OF PRIEST; III AT WHEELER RIDGE.
02/09/1963	02-52-14.5	35.98	121.69	C	2.8	8		OFF COAST S OF BIG SUR.
02/12/1963	03-44-30.9	36.50	121.32	B	2.6	10		S OF VINEYARD.
02/22/1963	15-56-21.9	35.11	121.44	C	3.3	15		OFF COAST, SW OF MORRO BAY.
02/22/1963	15-56-36.0	35.67	120.83	D	3.6			
04/04/1963	01--?-58	35.80	121.50		2.5	6		NW OF SAN SIMEON.
04/10/1963	01-38-56.8	36.42	121.05		2.9	11		SW OF LLANADA.
04/11/1963	14-02-31.8	36.20	120.87		2.9	13		NW OF PRIEST.
04/20/1963	16-37-33.0	36.38	120.96		3.0	14		SOUTH OF LLANADA.
05/10/1963	10-17-57.1	36.37	120.98		2.5	9		SOUTH OF LLANADA.
06/01/1963	05-19--0.2	34.33	119.54	B	2.0			
07/02/1963	12--?-24.9	34.86	119.80	C	2.0			
07/04/1963	03-20-41.0	34.77	120.02	C	3.2			
07/06/1963	23-32-30.4	34.78	120.63	B	3.3			
08/15/1963	21-02-32.2	35.97	121.02		3.6	15		NEAR JOLON; FORESHOCK OF FOLLOWING--
08/15/1963	21-21-32.1	35.91	121.06		3.9	18	F	NEAR JOLON; FELT AT HARRIS RANCH.
08/16/1963	08-12-13.6	36.06	121.01		3.2	10		NEAR JOLON; AFTERSHOCK OF PRECEDING.
09/06/1963	03-54-34	36.22	121.48		2.6	8		WEST OF PARAISO.
11/01/1963	14-05-56.0	35.56	120.23		3.4	9		EAST OF ATASCADERO.
11/01/1963	14-06--0.4	35.75	120.47	C	3.2			
11/18/1963	07-31-38.5	36.22	120.30	C	3.5		F	IV 15 MI. NE OF SAN MIGUEL.
11/18/1963	10-54-45.4	36.38	120.32		2.7	11		NE OF COALINGA.
11/19/1963	03-33-09.2	36.42	121.03		2.9	10		SW OF LLANADA.
12/12/1963	17-10-48.5	34.98	119.51	C	3.1			
02/10/1964	05-47-25.0	35.75	120.94		3.9	19		NE OF PASO ROBLES.

MM/DD/YY	HR/MN/SE	NORTH LAT	WEST LONG	QUALITY	MAG.	STA. REC.	FELT	MAXIMUM INTENSITY - COMMENTS
03/20/1964	13-15-51.0	36.40	121.03		2.6	7		SW OF LLANADA.
04/28/1964	15-01-48.3	36.23	121.08		2.8	7		NEAR KING CITY.
05/07/1964	17-53-58.3	36.43	120.54		2.5	5		N OF PRIEST.
06/06/1964	11-47-39.0	34.63	121.40	D	4.3			
06/20/1964	09-21-51.4	34.13	120.67	C	3.1			
07/24/1964	07-09-35.9	36.47	121.18		2.9	15		NE OF PARAISO.
08/30/1964	03-41-10.4	36.29	121.94		2.9	7		OFF COAST NW OF POINT SUR.
09/12/1964	01-45-53.5	36.08	120.49		3.1	10		SE OF PRIEST.
10/17/1964	23-43-22.6	36.21	120.92		3.3	14		NW OF PRIEST.
11/08/1964	01-19-19.0	36.00	120.00		4.0	15		E OF AVENAL.
11/08/1964	13-45-51.1	36.34	121.32		3.1	16		NEAR PARAISO.
11/18/1964	01-47-34.0	35.98	121.13		2.7	8		SW OF KING CITY.
11/25/1964	12-49-41.8	36.21	120.78		2.8	15		NW OF PRIEST.
12/05/1964	13-55-57.5	36.02	121.08		2.6	12		W OF SAN ARDO.
12/11/1964	03-35-38.8	34.24	119.76	B	3.5			
12/25/1964	11-21-13.2	35.97	121.18		2.6	5		N OF LAKE NACIMIENTO.
12/27/1964	18-58-59.4	36.46	121.06		2.6	7		SW OF LLANDA.
01/13/1965	04-20-48.2	36.45	120.58		2.6	9		NE OF PRIEST.
01/26/1965	08-34-30.7	35.72	120.54		3.0	12		SE OF PRIEST.
01/26/1965	08-36-36.6	35.92	120.27	C	3.1			
01/26/1965	08-38-16.4	36.04	120.26	C	3.1			
02/21/1965	18-39-18.3	35.67	120.43		3.1	12		E OF PASO ROBLES.
03/28/1965	02-32-21.0	36.20	120.40		3.5			(USCGS)
04/06/1965	20-49-24.4	35.95	121.46		2.5	7		N OF SAN SIMEON.
04/08/1965	01-05-40.6	36.03	121.40		3.0	10		N OF SAN SIMEON.
04/09/1965	12-50-19.3	36.03	120.64		3.0	10		S OF PRIEST.
04/18/1965	03-58-52.4	36.50	121.23		2.7	7		NEAR PINNACLES NATIONAL MONUMENT
04/24/1965	07-29-47.1	34.91	120.14	C	3.6			
05/12/1965	17-55-08.7	35.49	121.17		3.0	6		SW OF SAN SIMEON.
06/07/1965	15-06-47.6	36.50	121.13		2.5	10		NEAR PINNACLES NATIONAL MONUMENT.
06/20/1965	02-56-43.5	36.33	120.37		2.7	11		N OF COALINGA.
06/30/1965	15-21-27.7	36.35	120.71		2.5	9		N OF PRIEST.
07/23/1965	05-31-52.7	35.71	121.23		3.4	13		N OF SAN SIMEON.
07/24/1965	15-25-57.4	36.36	120.98		2.5	7		SW OF LLANADA.
08/01/1965	06-47-27.3	36.23	120.85		2.5	7		NW OF PRIEST.
08/01/1965	13-28-32.9	36.23	120.84		2.5	6		AFTERSHOCK OF 06-47-27.3.
08/13/1965	07-36-08.4	36.46	121.08		2.6	9		SW OF LLANADA.
08/13/1965	13-46-16.5	34.35	119.63	B	3.7		F	IV AT CARPINTERIA AND SANTA BARBARA.
08/13/1965	21-28-51.8	36.48	121.13		2.4	8		W OF LLANADA.
08/15/1965	23-06-52.5	36.00	120.20		4.0		F	AT PAICINES.
08/21/1965	20-09-35.4	36.46	121.07		2.5	8		SW OF LLANADA.
09/06/1965	18--?-57.8	35.96	120.36	C	3.4			
09/12/1965	08-50-05.5	36.49	121.12		2.5	7		W OF LLANADA.
09/19/1965	15-42-07.8	35.98	120.34	C	4.8		F	V AT ARMONA, AVENAL, CHOLAME, KETTLEMAN CITY, AND STRATFORD.
10/22/1965	02-29-22	36.00	121.70		2.7	6		OFF COAST, W OF KING CITY.
12/02/1965	22-29-13.0	36.20	121.68		2.8	9		W OF PARAISO.

MM/DD/YY	HR/MN/SE	NORTH LAT	WEST LONG	QUALITY	MAG.	STA. REC.	FELT	MAXIMUM INTENSITY - COMMENTS
01/28/1966	01-49-47.4	35.83	120.45		3.0		F	PARKFIELD SEQUENCE; MC EVILLY, ET AL, (1967) THE PARKFIELD, CALIFORNIA EARTHQUAKE OF 1966, BULL. SEISM. SOC. AM.
02/01/1966	-?-20-44.3	36.03	120.57		2.9			PARKFIELD SEQUENCE - SEE 01/28/1966 AT 01-49-47.4.
02/14/1966	-?-24-03.9	36.02	120.57		2.4			PARKFIELD SEQUENCE - SEE 01/28/1966 AT 01-49-47.4.
02/25/1966	01-34-38.0	36.05	120.63		2.4			PARKFIELD SEQUENCE - SEE 01/28/1966 AT 01-49-47.4.
03/31/1966	21-38-45.2	36.05	120.60		2.5			PARKFIELD SEQUENCE - SEE 01/28/1966 AT 01-49-47.4.
04/05/1966	20-44-58.7	36.24	120.85		2.7	9		10 KM NW OF PRIEST (UC BERKELEY SEISMOGRAPH STATION (SS)).
04/12/1966	15-31-39.8	36.07	120.70		2.3			PARKFIELD SEQUENCE.
05/11/1966	17-37-01.1	35.98	120.57		2.3			PARKFIELD SEQUENCE.
05/23/1966	08-07-37.6	36.02	120.57		2.5			PARKFIELD SEQUENCE.
05/23/1966	08-11-07.0	36.02	120.57		2.2			PARKFIELD SEQUENCE.
05/27/1966	15-36-03.7	35.98	120.49		2.7			PARKFIELD SEQUENCE.
06/18/1966	16-32-17.6	35.96	120.53		2.0			PARKFIELD SEQUENCE.
06/20/1966	23-19-18.8	36.33	120.96		2.8	9		NE OF KING CITY.
06/24/1966	21-42-50.4	36.50	120.85		3.1	10		SE OF LLANADA.
06/28/1966	01--?-31.5	35.95	120.52		3.1		F	PARKFIELD SEQUENCE; FELT AT CHOLAME, PARKFIELD, VALLETON, AND WORK RANCH.
06/28/1966	01-14-55	35.95	120.50		1.8			PARKFIELD SEQUENCE.
06/28/1966	04-08-55.2	35.97	120.50		5.1			PARKFIELD SEQUENCE FIRST MAIN SHOCK (FELT REPORTS FOR THE 2 MAIN SHOCKS ARE NOT SEPARATED.) FELT OVER 20,000 SQ. MI., MINOR SURFACE FAULTING ALONG SAN ANDREAS FAULT FROM PARKFIELD TO CHOLAME (20 MI.), MAXIMUM DISPLACEMENT 4 IN. VII AT CHOLAME AND PARKFIELD, VI AT ANNETTE, BITTERWATER VALLEY, COALINGA, HIDDEN VALLEY RANCH, PASO ROBLES, SAN LUIS OBISPO, SAN MIGUEL, SHAFTER, SHANDON, SLACK CANYON, VALLETON, WAITI RANCH, AND WORK RANCH, AND V AT ADELAIDA, ALPAUGH, ARROYO GRANDE, ATASCADERO, AVILA BEACH, BAKERSFIELD, BAYWOOD PARK, BRYSON, BURREL, BUTTONWILLOW, EARLIMART, FELLOWS, FRAZIER PARK, GREENFIELD, HARMONY, INDIAN VALLEY, KETTLEMAN CITY, KING CITY, LAPANZA, LOST MARICOPA, MEE RANCH, MORRO BAY, MOSS LANDING, MUSICK, NIPOMO, OCEANO, OLD RIVER, PANOCHE, PINE CANYON, PISMO BEACH, POZO, PRIEST VALLEY, SAN ARDO, SAN JOAQUIN, SAN LUCAS, SAN SIMEON, SIMMLER, STRATFORD, TEMPLETON, AND VANDENBURG A.F.B.
06/28/1966	04-09-53	35.95	120.50					PARKFIELD SEQUENCE.
06/28/1966	04-18-34.0	35.95	120.53		2.6		F	PARKFIELD SEQUENCE - FELT AT CANTUA CREEK AND SOQUEL.
06/28/1966	04-26-13.4	35.95	120.50		5.5		F	PARKFIELD SEQUENCE - SECOND MAIN SHOCK.
06/28/1966	04-26-28	35.95	120.50					PARKFIELD SEQUENCE.
06/28/1966	04-26-34	35.95	120.50					PARKFIELD SEQUENCE.
06/28/1966	04-27-37	35.95	120.50					PARKFIELD SEQUENCE.
06/28/1966	04-27-58	35.95	120.50					PARKFIELD SEQUENCE.
06/28/1966	04-28-19	35.95	120.50					PARKFIELD SEQUENCE.
06/28/1966	04-28-36	35.95	120.50		4.5			PARKFIELD SEQUENCE.
06/28/1966	04-28-46	35.95	120.50					PARKFIELD SEQUENCE.

MM/DD/YY	HR/MN/SE	NORTH LAT	WEST LONG	QUALITY	MAG.	STA. REC.	FELT	MAXIMUM INTENSITY - COMMENTS
06/28/1966	04-29-13	35.95	120.50					PARKFIELD SEQUENCE.
06/28/1966	04-31-55	35.95	120.50		3.0			PARKFIELD SEQUENCE.
06/28/1966	04-32-50	35.95	120.50		3.5		F	PARKFIELD SEQUENCE - FELT AT CANTUA CREEK, CHOLAME, AND HERNANDEZ.
06/28/1966	04-34-59.1	35.81	120.40		3.0			PARKFIELD SEQUENCE.
06/28/1966	04-39-08.1	35.95	120.50		3.0		F	PARKFIELD SEQUENCE - FELT AT PARKFIELD AND WORK RANCH.
06/28/1966	04-42-33.6	35.83	120.38		2.4			PARKFIELD SEQUENCE.
06/28/1966	04-43-54.8	35.95	120.57		2.7			PARKFIELD SEQUENCE.
06/28/1966	04-46-22	35.95	120.50		3.0			PARKFIELD SEQUENCE.
06/28/1966	04-51-43	35.95	120.50		2.4			PARKFIELD SEQUENCE.
06/28/1966	05--?-59.5	35.85	120.40		3.1			PARKFIELD SEQUENCE.
06/28/1966	05-03-44.7	35.88	120.45		2.4			PARKFIELD SEQUENCE.
06/28/1966	05-09-48.3	35.83	120.13		2.5			PARKFIELD SEQUENCE.
06/28/1966	05-12-42.5	35.92	120.47		2.9			PARKFIELD SEQUENCE.
06/28/1966	05-17-05	35.95	120.50		2.1			PARKFIELD SEQUENCE.
06/28/1966	05-21-05	35.95	120.50		2.0			PARKFIELD SEQUENCE.
06/28/1966	05-29-14.9	35.92	120.48		2.1			PARKFIELD SEQUENCE.
06/28/1966	05-37-04.6	35.88	120.44		2.5			PARKFIELD SEQUENCE.
06/28/1966	05-40-19.4	35.94	120.48		2.7			PARKFIELD SEQUENCE.
06/28/1966	05-45-59.1	35.75	120.33		3.2			PARKFIELD SEQUENCE.
06/28/1966	05-48-26	35.95	120.50		2.2			PARKFIELD SEQUENCE.
06/28/1966	05-51-34.0	35.86	120.44		2.1			PARKFIELD SEQUENCE.
06/28/1966	05-52-06	35.95	120.50		2.3			PARKFIELD SEQUENCE.
06/28/1966	05-52-58	35.95	120.50		2.4			PARKFIELD SEQUENCE.
06/28/1966	05-56--?	35.95	120.50		2.1			PARKFIELD SEQUENCE.
06/28/1966	06-11-03.5	35.81	120.35		2.6			PARKFIELD SEQUENCE.
06/28/1966	06-32-17.9	35.94	120.52		3.4		F	PARKFIELD SEQUENCE - FELT AT CHOLAME, COALINGA, AND PARKFIELD.
06/28/1966	06-35-11.4	35.80	120.38		3.0			PARKFIELD SEQUENCE.
06/28/1966	06-39-31.2	35.90	120.47		2.2			PARKFIELD SEQUENCE.
06/28/1966	07-01-03.8	35.92	120.48		2.2			PARKFIELD SEQUENCE.
06/28/1966	07-33-52.7	35.90	120.45		2.7			PARKFIELD SEQUENCE.
06/28/1966	07-41-43	35.95	120.50		2.3			PARKFIELD SEQUENCE.
06/28/1966	07-45-48.3	35.90	120.47		3.0		F	PARKFIELD SEQUENCE - FELT AT CHOLAME AND PARKFIELD.
06/28/1966	08-14-48.6	35.83	120.42		2.4			PARKFIELD SEQUENCE.
06/28/1966	08-47-52.4	35.85	120.42		2.0			PARKFIELD SEQUENCE.
06/28/1966	08-54-49.5	35.92	120.50		2.3			PARKFIELD SEQUENCE.
06/28/1966	08-59-52.3	35.85	120.42		2.5			PARKFIELD SEQUENCE.
06/28/1966	09-31-26.5	35.77	120.35		2.4			PARKFIELD SEQUENCE.
06/28/1966	09-35-54.3	35.77	120.36		2.2			PARKFIELD SEQUENCE.
06/28/1966	09-56-09.7	35.83	120.40		2.5			PARKFIELD SEQUENCE.
06/28/1966	10-15-53.3	35.92	120.53		2.1			PARKFIELD SEQUENCE.
06/28/1966	10-20-16.4	35.85	120.42		2.3			PARKFIELD SEQUENCE.
06/28/1966	10-23-22.8	35.55	120.42		2.0			PARKFIELD SEQUENCE.
06/28/1966	10-23-22.8	35.94	120.48		2.5			PARKFIELD SEQUENCE.
06/28/1966	10-46-22.9	35.94	120.50		2.0			PARKFIELD SEQUENCE.
06/28/1966	11-15-13.9	35.85	120.42		2.0			PARKFIELD SEQUENCE.

MM/DD/YY	HR/MN/SE	NORTH LAT	WEST LONG	QUALITY	MAG.	STA. REC.	FELT	MAXIMUM INTENSITY - COMMENTS
06/28/1966	11-28-41.4	35.85	120.38		2.0			PARKFIELD SEQUENCE.
06/28/1966	11-30-14.0	35.90	120.47		2.2			PARKFIELD SEQUENCE.
06/28/1966	12-31-52.1	35.94	120.48		2.5			PARKFIELD SEQUENCE.
06/28/1966	12-52-22.0	35.97	120.53		2.3			PARKFIELD SEQUENCE.
06/28/1966	13-48-22	35.97	120.53		2.7			PARKFIELD SEQUENCE.
06/28/1966	14-13-09.3	35.94	120.48		2.6			PARKFIELD SEQUENCE.
06/28/1966	14-21-36.3	35.94	120.48		2.2			PARKFIELD SEQUENCE.
06/28/1966	14-51-53.6	35.90	120.47		2.3			PARKFIELD SEQUENCE.
06/28/1966	18-12-19.4	35.92	120.50		2.3			PARKFIELD SEQUENCE.
06/28/1966	18-22-32.4	35.92	120.50		2.0			PARKFIELD SEQUENCE.
06/28/1966	18-54-55.3	35.88	120.45		2.5			PARKFIELD SEQUENCE.
06/28/1966	19-59-37.8	35.92	120.47		2.8			PARKFIELD SEQUENCE.
06/28/1966	20--?-38.7	35.92	120.48		2.5			PARKFIELD SEQUENCE.
06/28/1966	20-46-56.4	35.77	120.40		3.1		F	PARKFIELD SEQUENCE - FELT AT BAR B RANCH AND WORK RANCH.
06/28/1966	22-01-13.9	35.85	120.44		2.0			PARKFIELD SEQUENCE.
06/28/1966	22-37-56.7	35.88	120.42		2.0			PARKFIELD SEQUENCE.
06/28/1966	23-57-22.3	35.77	120.35		2.5			PARKFIELD SEQUENCE.
06/29/1966	-?-17-32.6	35.85	120.44		2.3			PARKFIELD SEQUENCE.
06/29/1966	02-19-39.9	35.92	120.52		3.6		F	PARKFIELD SEQUENCE - FELT AT CHOLAME, PARKFIELD, AND WORK RANCH.
06/29/1966	04-06-40.3	35.92	120.53		2.8			PARKFIELD SEQUENCE.
06/29/1966	07-28-59.4	35.92	120.48		2.3			PARKFIELD SEQUENCE.
06/29/1966	08-55-52.4	35.88	120.45		2.9			PARKFIELD SEQUENCE.
06/29/1966	09-20-50.1	35.78	120.36		2.5			PARKFIELD SEQUENCE.
06/29/1966	10-13-44.0	35.97	120.50		2.3			PARKFIELD SEQUENCE.
06/29/1966	10-56-58.8	35.75	120.33		3.0			PARKFIELD SEQUENCE.
06/29/1966	12-30-09.0	35.94	120.50		2.4			PARKFIELD SEQUENCE.
06/29/1966	13-11-59.7	35.82	120.38		3.1		F	PARKFIELD SEQUENCE - FELT AT CHOLAME AND PARKFIELD.
06/29/1966	15-18-38.9	35.95	120.33		2.0			PARKFIELD SEQUENCE.
06/29/1966	15-34-22.2	35.92	120.48		2.3			PARKFIELD SEQUENCE.
06/29/1966	16-03-30.1	35.86	120.45		2.1			PARKFIELD SEQUENCE.
06/29/1966	17-10-28.3	35.82	120.36		2.0			PARKFIELD SEQUENCE.
06/29/1966	19-53-25.9	35.95	120.53		5.0		F	PARKFIELD SEQUENCE - FELT AT ADELAIDA, BITTERWATER, CHOLAME, COALINGA, FRESNO, MEE RANCH, MORRO BAY, SAN LUIS OBISPO, SAN MIGUEL, SANTA MARGARITA, SHANDON, AND WORK RANCH.
06/29/1966	20-44-40.0	35.74	120.28		2.5			PARKFIELD SEQUENCE.
06/29/1966	23-48-12.0	35.74	120.28		2.3			PARKFIELD SEQUENCE.
06/30/1966	01-17-36.1	35.86	120.45		4.1			PARKFIELD SEQUENCE.
06/30/1966	03-36-16.8	35.92	120.47		2.6			PARKFIELD SEQUENCE.
06/30/1966	05-04-12.9	35.88	120.45		2.0			PARKFIELD SEQUENCE.
06/30/1966	06-07-21.5	35.94	120.48		2.4			PARKFIELD SEQUENCE.
06/30/1966	06-23-32.4	35.90	120.47		2.1			PARKFIELD SEQUENCE.
06/30/1966	07-37-12.1	35.90	120.47		2.0			PARKFIELD SEQUENCE.
06/30/1966	08-01-38.4	35.90	120.47		2.9			PARKFIELD SEQUENCE.
06/30/1966	11-07-55.1	35.78	120.33		2.8			PARKFIELD SEQUENCE.

MM/DD/YY	HR/MN/SE	NORTH LAT	WEST LONG	QUALITY	MAG.	STA. REC.	FELT	MAXIMUM INTENSITY - COMMENTS
06/30/1966	13-26-05.7	35.78	120.35		2.3			PARKFIELD SEQUENCE.
06/30/1966	13-29-56.6	35.86	120.40		2.0			PARKFIELD SEQUENCE.
06/30/1966	13-40-50.9	35.83	120.38		2.1			PARKFIELD SEQUENCE.
06/30/1966	16-05-02.7	35.97	120.50		2.3			PARKFIELD SEQUENCE.
06/30/1966	19-06-17.5	35.86	120.42		2.1			PARKFIELD SEQUENCE.
07/01/1966	09-41-21.9	35.94	120.52	3.2			F	PARKFIELD SEQUENCE - FELT AT WORK RANCH.
07/02/1966	12-08-34.8	35.79	120.33		3.7		F	PARKFIELD SEQUENCE - FELT AT PARKFIELD.
07/02/1966	12-16-15.8	35.81	120.35		3.4		F	PARKFIELD SEQUENCE - FELT AT PARKFIELD.
07/02/1966	12-25-06.8	35.80	120.35		3.1		F	PARKFIELD SEQUENCE - FELT AT PARKFIELD.
07/05/1966	18-54-54.5	35.92	120.48		3.0		F	PARKFIELD SEQUENCE - FELT AT PARKFIELD.
07/25/1966	22-49-39	36.40	120.30		2.5	4		NE OF COALINGA.
07/27/1966	08-12- 0.2	35.90	120.48		3.0			PARKFIELD SEQUENCE.
08/03/1966	12-39-05.8	35.80	120.38		3.4		F	PARKFIELD SEQUENCE; V AT CHOLAME, PARKFIELD, AND WORK RANCH.
08/04/1966	-?-54-24.5	35.74	121.35		3.0	8		NW OF SAN SIMEON.
08/07/1966	17-03-24.9	35.94	120.55		3.0			PARKFIELD SEQUENCE.
08/19/1966	22-51-20.1	35.90	120.45		3.3			PARKFIELD SEQUENCE.
09/07/1966	-?-20-50.5	35.83	119.94		3.2	9		SE OF COALINGA.
09/18/1966	15-09-55.7	35.74	120.35		3.1			PARKFIELD SEQUENCE.
10/27/1966	12-06-03.9	35.94	120.50		3.8		F	PARKFIELD SEQUENCE; V AT ATASCADERO, AVENAL, COALINGA, PARKFIELD, SAN MIGUEL, TEMPLETON, AND WORK RANCH.
11/05/1966	13-31-31.2	35.94	120.50		3.3			PARKFIELD SEQUENCE.
11/18/1966	23-39-42.3	35.75	120.33		3.3			PARKFIELD SEQUENCE.
12/30/1966	10-23-48	36.47	120.40		2.5	4		N OF COALINGA.
01/08/1967	23-03-50.9	35.90	120.40		2.8	8		35 KM SE OF PRIEST (UC BERKELEY SS).
01/09/1967	23-18-59.5	35.86	120.10		3.1	9		SE OF COALINGA.
02/01/1967	13-55-54.1	35.70	120.25		3.0	8		NE OF SAN LUIS OBISPO.
02/26/1967	15-17-53.9	36.40	121.06		2.5	9		SW OF LLANADA.
03/13/1967	21-59-48.4	36.00	120.61		3.1	8	F	15 KM S OF PRIEST (UC BERKELEY SS). IV AT SAN MIGUEL; FELT AT INDIAN VALLEY AND RANCHITO CANYON.
03/21/1967	02-24-28.3	36.21	120.85		2.8	8		17 KM NW OF PRIEST (UC BERKELEY SS).
03/23/1967	11-39-56.4	36.16	120.18		3.0	5		20 KM E OF COALINGA.
04/13/1967	09-06-42.5	36.15	120.80		2.7	8		13 KM W OF PRIEST (UC BERKELEY SS).
05/17/1967	14-16-52.2	35.95	120.73		3.0	6		30 KM S OF PRIEST (UC BERKELEY SS).
06/03/1967	20-10-53.0	35.71	121.48		2.6	7		OFF COAST NW OF SAN SIMEON.
06/06/1967	06-11-38.5	35.81	120.43		3.0	10	F	40 KM SE OF PRIEST (UC BERKELEY SS); IV AT WORK RANCH; FELT IN INDIAN VALLEY, SOUTHERN MONTEREY COUNTY, AND VINEYARD CANYON.
06/13/1967	12-54-10.7	35.81	121.50		3.3	10		OFF COAST, 35KM NW OF SAN SIMEON.
07/24/1967	07-08-52.9	35.96	120.50		3.7	9		PARKFIELD AREA.
07/28/1967	14-44-40.1	35.75	121.38		3.0	6		NEAR SAN SIMEON.
08/01/1967	22-14-13.0	35.75	121.40		2.7	6		NW OF SAN SIMEON.
08/08/1967	18-11-20.3	36.42	120.42		2.5	7		N OF COALINGA.
08/12/1967	18-57-40.4	35.80	120.45		4.1	18	F	PARKFIELD AREA; V AT ESTRELLA AREA, HOG CANYON ROAD TO PARKFIELD, AND SHANDON, AND IV AT CHOLAME.

MM/DD/YY	HR/MN/SE	NORTH LAT	WEST LONG	QUALITY	MAG.	STA. REC.	FELT	MAXIMUM INTENSITY - COMMENTS
08/12/1967	23-21-07.8	36.11	120.80		2.8	6		SE OF KING CITY.
08/12/1967	23-22-05.3	36.13	120.76		2.5	7		SE OF KING CITY.
08/17/1967	23-12-02.7	35.91	121.50		2.6	5		NW OF SAN SIMEON.
08/25/1967	02-28-14.4	35.81	121.27		2.7	6		NW OF SAN SIMEON.
08/25/1967	16-35-27.8	36.05	120.00		3.2	7		SE OF COALINGA.
08/25/1967	16-40-50.2	36.01	119.95		3.0	7		SE OF COALINGA.
08/31/1967	18-10-40.4	35.86	121.35		2.8	7		NW OF SAN SIMEON.
09/09/1967	21-35-05.6	35.81	121.63		2.4	3		OFF SHORE SAN SIMEON.
10/14/1967	12-02-43.6	36.50	120.61		2.7	5		NEAR MT. CIERVO.
10/21/1967	12-05-21.8	35.83	120.46		3.1	7		PARKFIELD AREA.
10/25/1967	23-05-30.5	35.73	121.45		2.6	4		NEAR SAN SIMEON.
11/11/1967	22-10-06.8	36.50	120.81		3.3	9		S OF PANOCHE VALLEY.
11/11/1967	22-33-47.5	36.48	120.78		2.8	6		S OF PANOCHE VALLEY.
11/12/1967	07-11-20.4	36.48	120.80		2.6	7		S OF PANOCHE VALLEY.
11/14/1967	-?--?-51.7	35.78	120.53		3.1	3		PARKFIELD.
11/25/1967	15-27-43.4	36.46	121.06		2.5	6		BEAR VALLEY.
12/21/1967	05-13-11.3	35.36	120.85		2.6	3		S OF SAN SIMEON.
12/21/1967	19-08-53.8	35.91	119.53		3.1	5		NW OF DELANO.
12/21/1967	23-58-60.2	35.93	120.56		3.0	3		PARKFIELD.
12/31/1967	23-48-13.5	35.75	120.45		4.3	3	F	PARKFIELD AREA; V AT CRESTON, PARKFIELD, SALINAS DAM, SAN MIGUEL, SHANDON, TEMPLETON, AND WORK RANCH.
02/03/1968	19-07-26.4	35.73	121.25		2.8	5		NEAR SAN SIMEON.
02/23/1968	20-20-57.9	35.86	121.31		2.5	7		EAST OF HOLLISTER.
03/25/1968	11-32-07.4	36.37	120.70		3.6	8	F	SE OF LLANADA; MAXIMUM INTENSITY V.
03/28/1968	04-53-26.5	36.36	120.19		3.1	5	F	SE OF COALINGA; FELT AT AVENAL - INTENSITY IV.
04/14/1968	06-20-54.6	36.18	121.65		2.5	6		SE OF MONTEREY.
04/23/1968	15-09-14.9	35.52	120.82		3.4	7		SE OF SAN SIMEON.
04/27/1968	14-32-37.4	36.22	120.83		2.7	7		NW OF PRIEST (UC BERKELEY SS).
04/28/1968	06-31-32.9	35.46	120.83		3.5	7		NW OF SAN LUIS OBISPO.
05/31/1968	07-07-37.9	35.80	120.60		3.0	5		S OF COALINGA.
06/11/1968	11-43-28.1	35.90	121.70		3.3	9		OFFSHORE, NW OF SAN SIMEON.
06/22/1968	12-50-50.1	36.43	121.04		2.9	9		S OF LLAN
07/03/1968	17-52-52	35.80	121.50		2.5	7		NW OF SAN SIMEON.
07/29/1968	04-27-51.9	36.38	120.69		2.7	9		N OF PRIEST (UC BERKELEY SS).
07/29/1968	05-29-19.9	36.37	120.70		2.8	9		N OF PRIEST (UC BERKELEY SS).
07/31/1968	-?-49-25.4	36.37	120.70		2.9	9		N OF PRIEST (UC BERKELEY SS).
08/19/1968	16-30-18.2	36.40	121.91		3.3	9		S OF CARMEL.
09/01/1968	21-56-24.4	36.45	121.02		2.7	8		E OF PINNACLES NATIONAL MONUMENT.
11/06/1968	08-58-23.2	35.88	120.45		2.8	10	F	NEAR PARKFIELD; FELT NEAR SAN MIGUEL.
11/10/1968	04-06-03.9	35.70	121.18		3.2	9		NEAR SAN SIMEON.
11/17/1968	01-03-47.0	36.29	120.94		3.0	6		NEAR KING CITY.
12/11/1968	12-19-52.4	35.81	120.48		3.0	10		NEAR PARKFIELD.
12/16/1968	01-14-10.9	36.17	120.85		2.7	7		W OF PRIEST (UC BERKELEY SS).
01/09/1969	09-42-47.2	35.94	120.57		3.8	7	F	CHOLAME VALLEY; FELT IN PARKFIELD AND SLACK CANYON - MAXIMUM INTENSITY V.
02/04/1969	-?-45-25	36.40	120.38		3.0	4		NORTH OF COALINGA.

MM/DD/YY	HR/MN/SE	NORTH LAT	WEST LONG	QUALITY	MAG.	STA. REC.	FELT	MAXIMUM INTENSITY - COMMENTS
06/19/1969	07-05-08	36.12	119.58		3.5	8	F	NEAR TULARE; FELT IN CORCORAN, DINUBA, HANFORD, IVANHOE, LEMON COVE, STRATHMORE, AND TIPTON. MAXIMUM INTENSITY IV.
06/24/1969	14-25-37	36.42	120.13		3.0	4		SOUTHWEST OF FRESNO.
07/16/1969	04-06-35	35.83	120.28		3.2	7		15 KM SOUTHEAST OF PARKFIELD.
09/06/1969	13-44-45	35.30	121.10		3.8	10	F	50 KM WEST OF SAN LUIS OBISPO.
09/16/1969	03-32-24	36.18	120.80		2.5	8		13 KM WEST OF PRIEST (UC BERKELEY SS).
10/02/1969	06--?-58.9	36.32	120.32		3.3	10		10 KM NORTH OF COALINGA.
11/17/1969	20-49-10.4	36.43	121.05		4.4	10	F	NNE OF KING CITY; FELT IN MONTEREY - SWAYED BUILDINGS IN SALINAS
11/19/1969	06-23-50	36.45	121.52		4.2	8	F	GONZALES AND SALINAS VALLEY; FELT IN SALINAS AND SANTA CRUZ - RATTLED WINDOWS IN MONTEREY.
11/26/1969	-?-06-59	36.48	120.60		2.5	6		50 KM NORTHEAST OF KING CITY.
11/30/1969	15-11-54	35.30	120.90		2.5	10		20 KM EAST OF KING CITY; 2 SMALL FORESHOCKS RECORDED.
12/10/1969	13-25-31	35.75	120.40		3.5	7		40 KM SOUTH OF COALINGA.
12/14/1969	19-07-57	35.92	120.68		3.2	9		20 KM NORTH OF PASO ROBLES.
01/29/1970	02-49-12.9	36.11	120.99		2.5	6		20 KM SOUTHWEST OF KING CITY.
02/01/1970	21-19-45.7	36.41	121.08		2.6	12		30 KM EAST OF PARAISO.
02/08/1970	-?-14-13.3	36.40	120.97		2.7	13		25 KM SOUTH OF LLANADA.
02/09/1970	16--?-46.1	35.77	120.35		3.1	16		60 KM SOUTH OF PRIEST (UC BERKELEY SS).
02/14/1970	15-44-58.0	36.09	120.64		2.8	14		5 KM SOUTH OF PRIEST (UC BERKELEY SS).
04/18/1970	13-16-53.4	36.49	120.01		3.0	15		35 KM SOUTHWEST OF FRESNO.
04/21/1970	22-29-25.9	35.66	120.43		3.0	8		65 KM SOUTH OF PRIEST (UC BERKELEY SS).
04/23/1970	03-25-18.9	35.97	121.45		2.5	10		25 KM SOUTHWEST OF KING CITY.
05/27/1970	10-42-19.3	35.99	120.91		3.4	8		40 KM SOUTHWEST OF PRIEST (UC BERKELEY SS).
07/20/1970	23-24-55	35.95	121.57		2.5	5		8 KM SOUTH OF LOPEZ POINT - OFFSHORE.
07/21/1970	05-24-16.1	35.99	121.57		2.5	5		5 KM SOUTHEAST OF LOPEZ POINT.
08/05/1970	06-47-36.4	35.82	119.94		2.9	8		KETTLEMAN HILLS.
08/05/1970	16-51-45.7	36.23	121.69		3.0	11		25 KM SOUTHWEST OF PARAISO.
08/13/1970	05-06-19.8	36.17	121.70		3.7	11		20 KM WEST OF LOPEZ POINT.
09/05/1970	11-29-11	36.20	120.10		3.1	4		EAST-NORTHEAST OF COALINGA.
09/10/1970	23-45-59	36.40	120.50		3.2	11		30 KM NORTHWEST OF COALINGA.
09/11/1970	15-20-08	35.98	120.05		3.3	9		8 KM EAST OF AVENAL.
09/16/1970	18-22-10.7	35.96	121.27		2.6	7		NEAR MILPITAS.
10/07/1970	17-57-06.3	36.30	121.40		2.5	9		30 KM NORTHWEST OF KING CITY.
12/01/1970	06-05-59	35.38	121.13		3.3	7	F	25 KM WEST OF MORRO BAY; INTENSITY V AT BRYSON - NO DAMAGE.
12/12/1970	22-29-20	35.65	121.55		2.5	6		30 KM WEST OF SAN SIMEON.
01/02/71	06-27-37.5	35°55.1'	120°32.2'		3.0			10 km NW of Parkfield
01/16/71	05-33-27.8	36°00'	120°12'		3.1			Kettleman Hills
01/26/71	21-53-53	35°12'	120°42'		3.0			Near San Luis Obispo.
01/31/71	12-22-49.5	35°55.6'	120°30.6'		3.0			NW of Parkfield; sharp, rapid jolting at Shandon.
04/05/71	01-40-34.2	36°24.8'	120°59.0'		3.0			20 km SE of Pinnacles National Monument.
04/19/71	09-35-58.8	36°13.7'	120°50.3'		3.0			25 km E of King City.
04/29/71	02-13-15.7	36°30.3'	120°32.5'		3.0			40 km NW of Coalinga.
06/20/71	12-41-39.8	35°3'	120°20'		3.4			Near Cholame.
07/06/71	09-24-35	35°34'	121°35'		3.0			SW of San Simeon.

MM/DD/YY	HR/MN/SE	NORTH LAT	WEST LONG	QUALITY	MAG.	STA. REC.	FELT	MAXIMUM INTENSITY - COMMENTS
07/21/71	09-14-26.2	36°13.7'	120°50.8'		3.2			Near Coalinga.
08/06/71	20-03-16.3	36°00.8'	120°02.2'		3.0			Near Coalinga.
10/06/71	14-43-30.6	35°51.3'	120°22.5'		3.5			S of Coalinga; intensity IV at Cholame, Parkfield, and Shandon.
10/21/71	22-09-45.4	35°58.8'	120°50.2'		3.7			SE of King City; intensity V at San Ardo (small objects shifted) and intensity IV at Jolon, King City, Lockwood, Pine Canyon, and San Lucas.
11/07/71	14-03-30.4	35°31.2'	119°50.2'		4.0			SE of Coalinga.
11/18/71	04-03-52.4	36°14.5'	120°50.6'		3.4			NE of King City.
11/30/71	09-45-42.8	36°03.6'	119°53.4'		3.0			SE of Coalinga.

END OF SELECTED EARTHQUAKES

END OF QUAKES PROGRAM FOR SELECTION OF EARTHQUAKES

TABLE 2.5-2

SUMMARY, REVISED EPICENTERS OF REPRESENTATIVE SAMPLES OF EARTHQUAKES OFF THE COAST OF CALIFORNIA NEAR SAN LUIS OBISPO

Date	Event Number	Original Hypocenter Revised Hypocenter Lat.	Long.	Distance Hypocenter Moved, km	Error Ellipse km	Mag., M_L
May 27, 1935	1	35.370 35.621	120.960 121.639	66NW	7 x 14	3.0
Sept. 7, 1939	6	35.420 35.459	121.070 121.495	40W	8 x 8	3.0
Oct. 6, 1939	7	35.800 36.232	121.500 121.763	54NW	16 x 31	3.5
July 11, 1945	8	35.670 35.809	121.250 121.408	21NW	7 x 24	4.0
Mar. 23, 1947	12	35.150 34.577	121.300 121.137	66S	12 x 24	3.7
Mar. 27, 1947	15	35.000 34.739	121.000 120.896	32SW	20 x 20	4.2
Dec. 20, 1948	9	35.800 35.683	121.500 121.364	16SE	9 x 38	4.5
Dec. 31, 1948	10	35.670 35.598	121.400 121.226	17SE	8 x 29	4.6
Nov. 22, 1952 Bryson Earthquake	17	35.730 35.830 35.836	121.190 121.170 121.204	U.C. Berkeley Richter (1969) 12N	7 x 24	6.0
Mar. 13, 1954	21	35.000 34.960	120.690 120.490	19E	9 x 18	3.4
Mar. 5, 1955	23	35.600 35.863	121.400 121.149	38NE	15 x 29	3.3
June 21, 1957	25A	35.100 35.255	120.900 120.951	15NW	10 x 19	3.7
Jan. 2, 1960	26	35.400 35.778	121.190 121.066	44NE	15 x 29	4.0
Feb. 1, 1962	52	34.880 35.031	120.670 120.846	22NW	6 x 16	4.5

TABLE 2.5-2

Date	Event Number	Original Hypocenter Revised Hypocenter Lat.	Long.	Distance Hypocenter Moved, km	Error Ellipse km	Mag., M_L
Mar. 5, 1962	54	34.600 34.622	121.590 121.416	17E	8 x 10	4.5
Mar. 10, 1962	54A	34.600 34.667	121.590 121.372	22NE	6 x 20	4.2
Feb. 22, 1963	28	35.110 34.730	121.440 121.400	42S	7 x 28	3.3
Sept. 6, 1969	31	35.300 35.355	121.090 121.033	9NE	5 x 10	3.6
Oct. 22, 1969	56	34.830 34.649	121.340 121.471	23SW	14 x 50	5.4

TABLE 2.5-3

DISPLACEMENT HISTORY OF FAULTS IN THE SOUTHERN COAST RANGES OF CALIFORNIA

Fault	Distance From Diablo Site, miles	Time of Principal Activity	Youngest Formation Cut By Fault	Oldest Formation Capping Fault
San Andreas	45	Mid-Tertiary - present		Currently active
Faults in ground between San Andreas and Sur-Nacimiento-Rinconada, La Panza, Cuyama, Red Hills, East Huasna	18-45	Tertiary	Pleistocene (possible Holocene) (Ref. 14)	Not Known
Sur-Nacimiento (zone)	18	Late Mesozoic, (Benioff-subduction zone)	Pleistocene (possible Holocene) (Ref. 14)	Late Quaternary terrace deposits (Ref. 11)
West Huasna-Suey	11	Late Tertiary	Post late-Miocene	Late Quaternary terrace deposits (Ref. 36)
Edna	4.5	Late Tertiary	Plio-Pleistocene (Paso Robles Fm)	Late Pleistocene (Ref. 20)
Miguelito	5	Late Tertiary	Early Pliocene (Miguelito Member of Careaga Fm) (Ref. 21)	Poss. capped by mid-Pliocene Squire Member of Careaga Fm; Plio-Pleistocene Paso Robles Fm

TABLE 2.5-3

Fault	Distance From Diablo Site, miles	Time of Principal Activity	Youngest Formation Cut By Fault	Oldest Formation Capping Fault
Faulting in the Mesozoic rocks near Pt. San Luis	4	Mesozoic	Mesozoic	Late Pleistocene (Ref. 20)
Unnamed faults near Pt. San Simeon	35	Probable Tertiary	Not known; possible Holocene	Not known
Offshore structural zone	4.5	Late Tertiary	Possible Holocene (Ref. 19) (northern part)	Holocene-upper Pliocene (Ref. 19) (southern part)
Faults in the Santa Maria Basin	40	Not known	Possible Pleistocene (orcutt Fm) (Ref. 23)	Pleistocene-Holocene

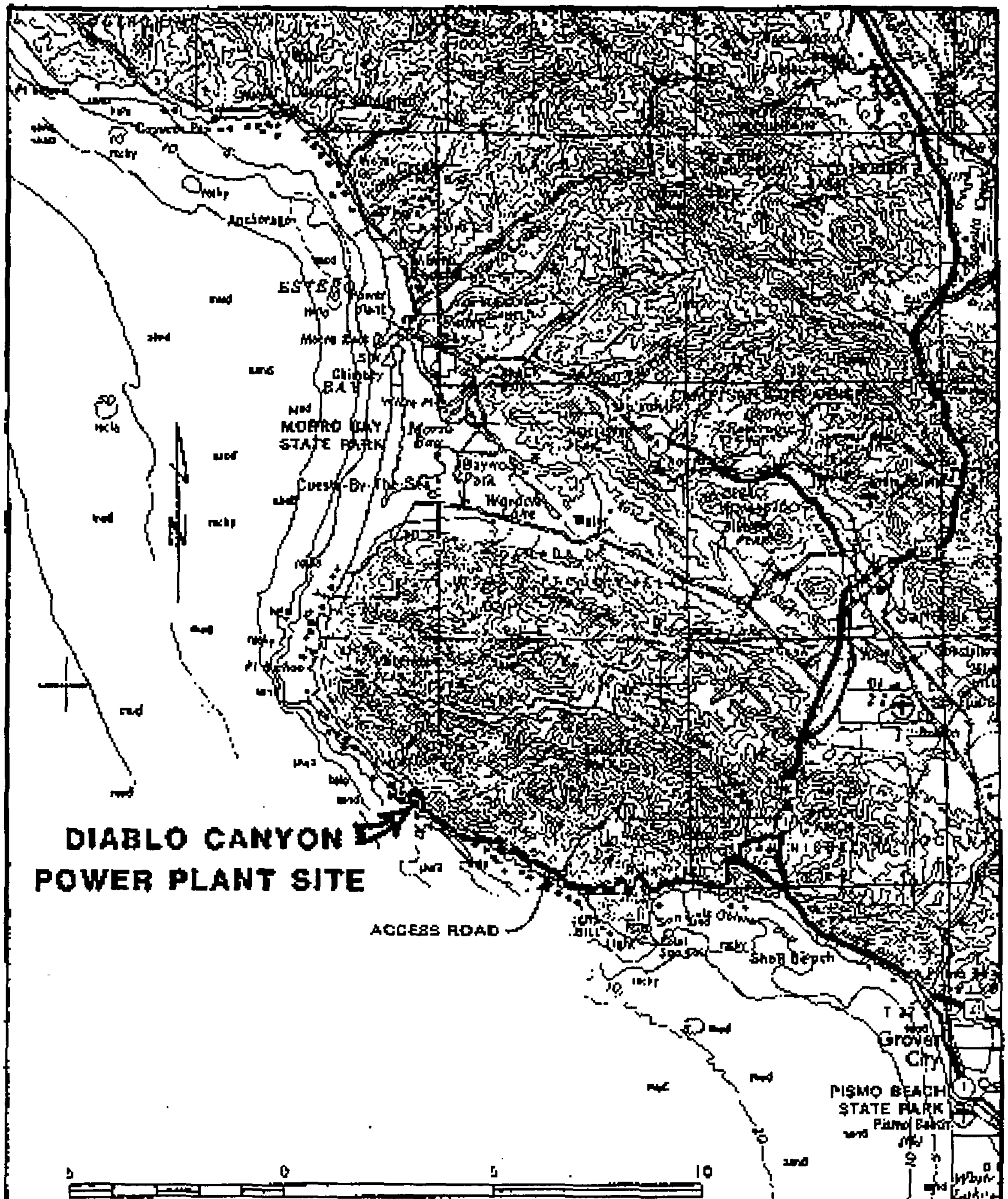

FSAR UPDATE
UNITS 1 AND 2 DIABLO CANYON SITE
FIGURE 2.5-1 PLANT SITE LOCATION AND TOPOGRAPHY

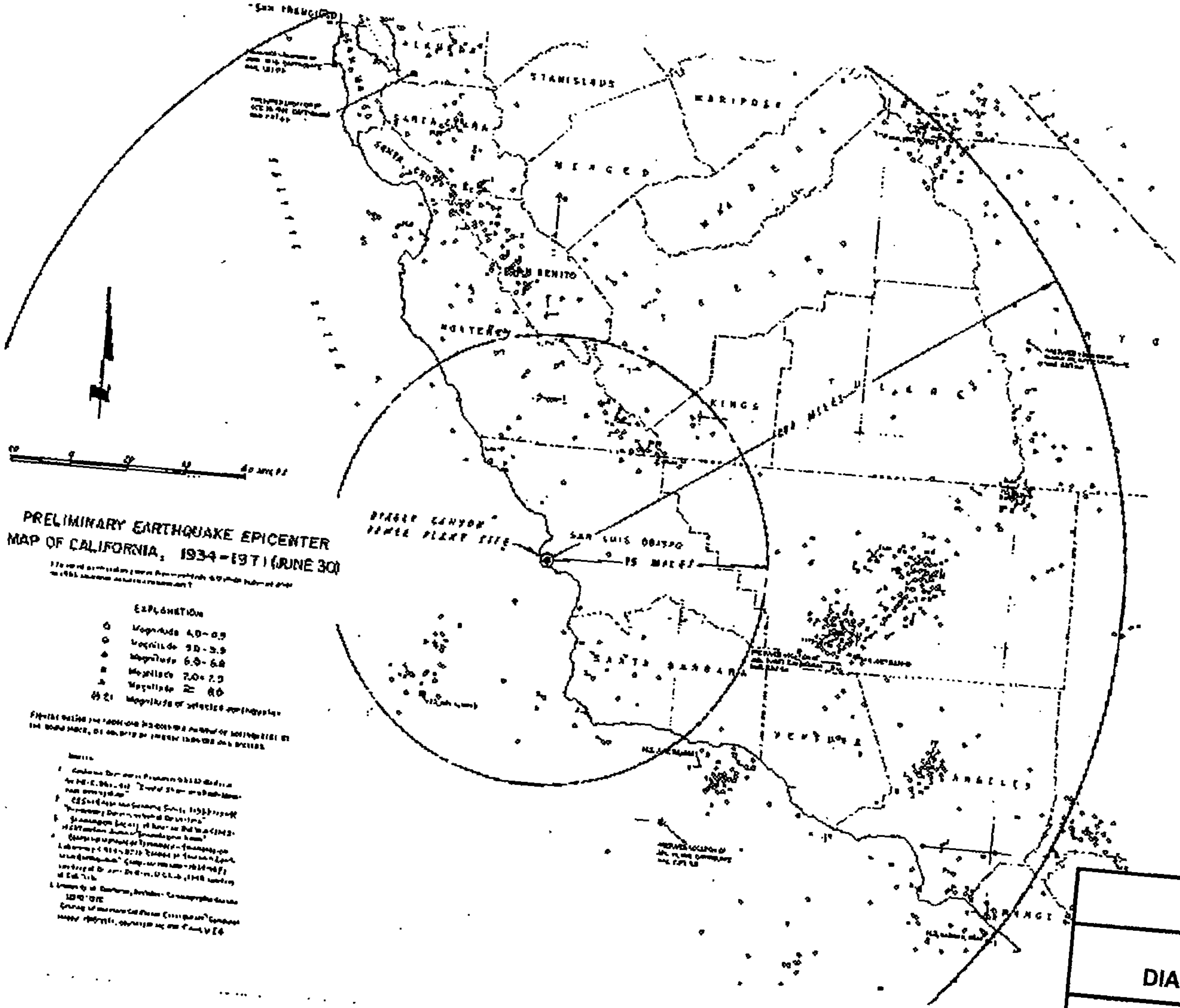

FSAR UPDATE

UNITS 1 AND 2
DIABLO CANYON SITE

FIGURE 2.5-2
EARTHQUAKE EPICENTERS
WITHIN 200 MILES OF PLANT SITE

Revision 11 November 1996

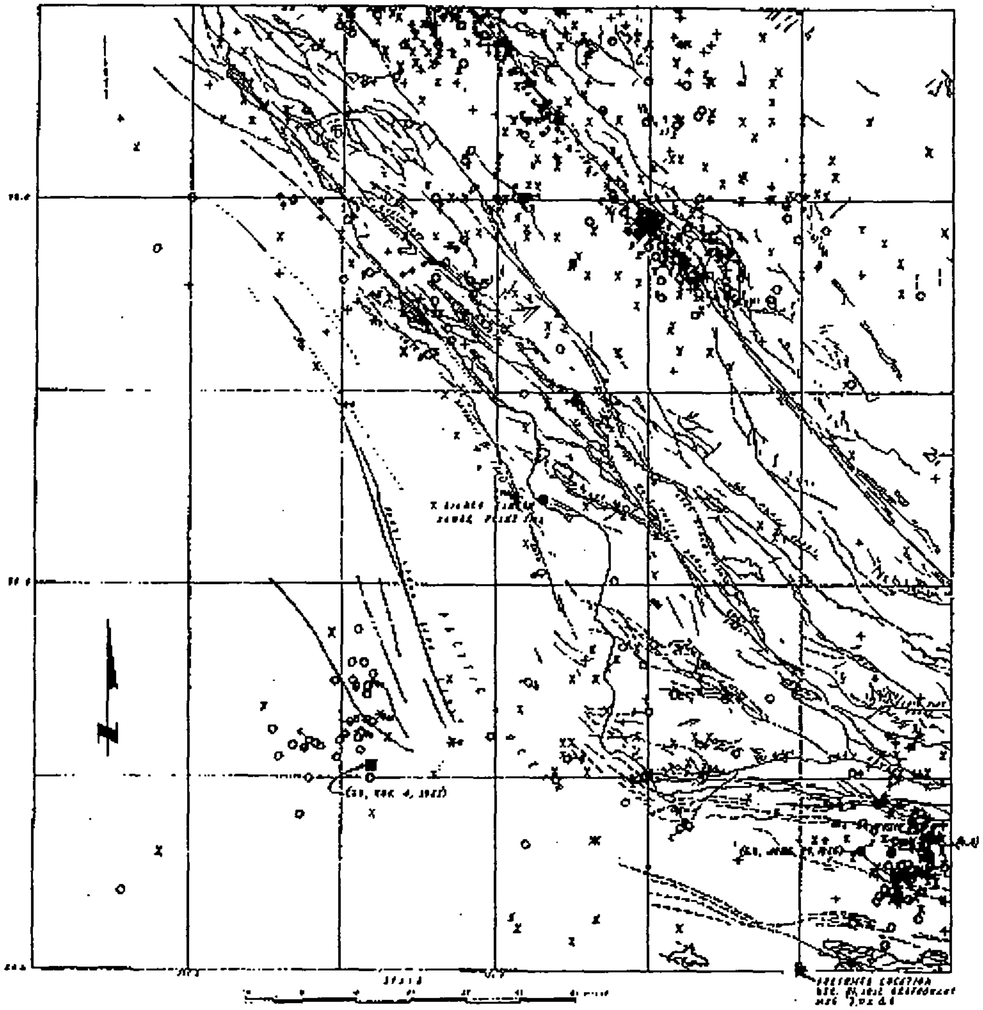

EXPLANATION

EARTHQUAKE EPICENTER DATA

FSAR UPDATE

UNITS 1 AND 2
DIABLO CANYON SITE

FIGURE 2.5-3
FAULTS AND EARTHQUAKE EPICENTERS WITHIN 75 MILES OF PLANT SITE (FOR EARTHQUAKES WITH ASSIGNED MAGNITUDES)

Revision 11 November 1996

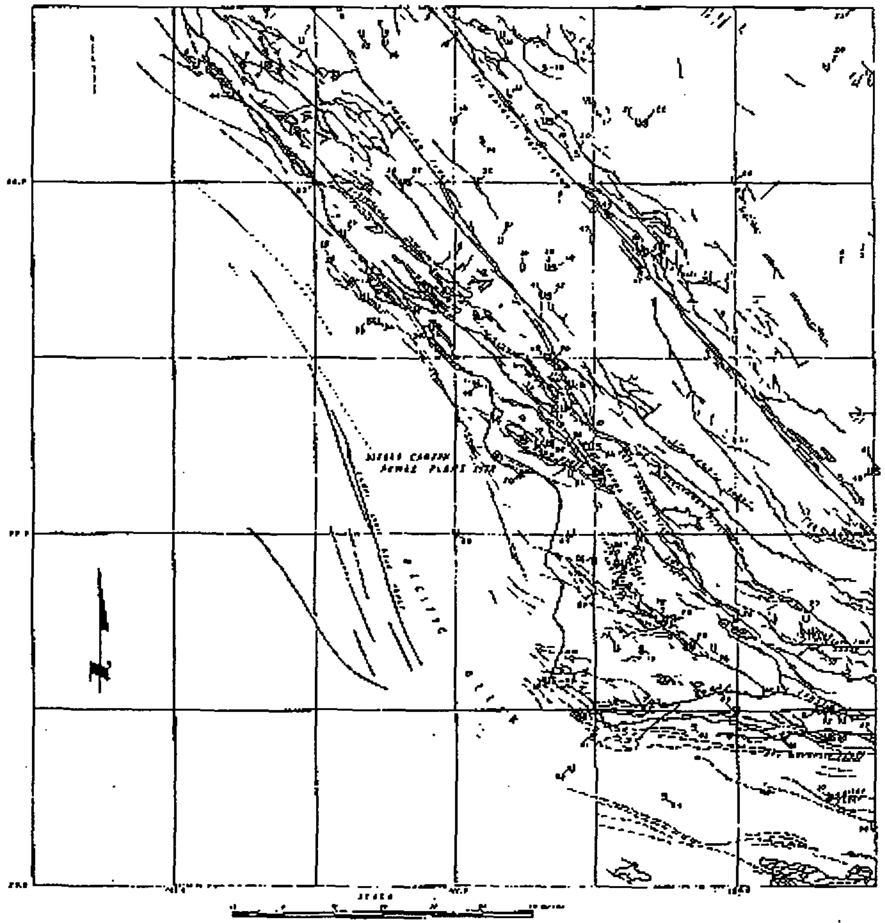

EXPLANATION

FSAR UPDATE

UNITS 1 AND 2
DIABLO CANYON SITE

FIGURE 2.5-4
FAULTS AND EARTHQUAKE EPICENTERS WITHIN 75 MILES OF PLANT SITE (FOR EARTHQUAKES WITH ASSIGNED INTENSITIES ONLY)

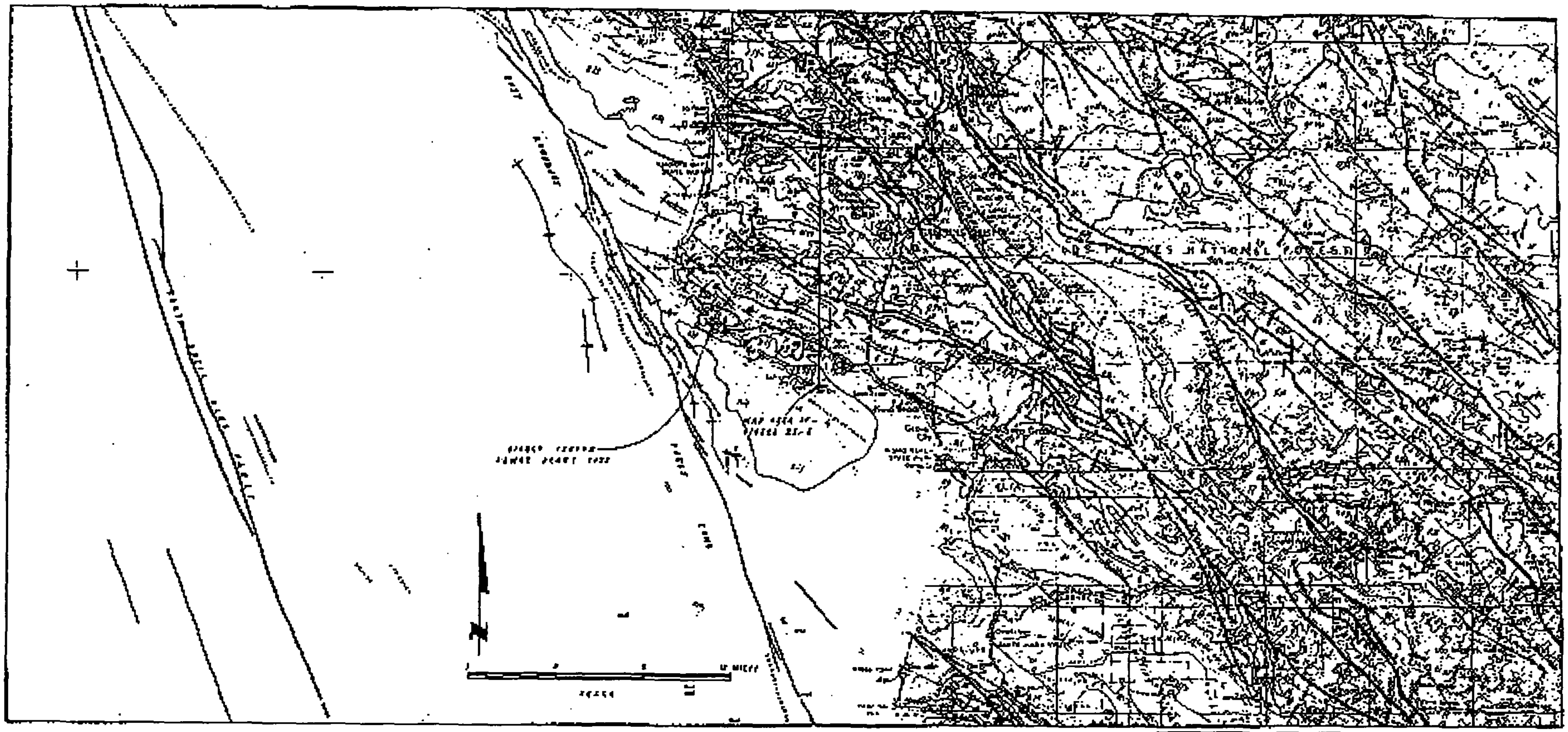

FSAR UPDATE

UNITS 1 AND 2
DIABLO CANYON SITE

FIGURE 2.5-5
GEOLOGIC AND TECTONIC MAP OF SOUTHERN COAST RANGES IN THE REGION OF PLANT SITE
(SHEET 1 OF 2)

Revision 11 November 1996

EXPLANATION

GEOLOGIC UNITS

CENOZOIC

SEDIMENTARY DEPOSITS AND ROCKS

Q	HOLOCENE AND PLEISTOCENE NONMARINE (INCLUDES ALLUVIAL AND MARINE DEPOSITS, UNDIVIDED.
Qls	LARGE LANDSLIDES, WHERE MAPPED SEPARATELY.
Qs	DUNE SAND DEPOSITS, WHERE MAPPED SEPARATELY.
QPc	PLIO-PLEISTOCENE AND PLIOCENE NONMARINE.
P	PLIOCENE MARINE
M	MIOCENE MARINE
Φc	OLIGOCENE NONMARINE
E	EOCENE MARINE
Ep	PALEOCENE MARINE

VOLCANIC ROCKS

Tv	TERTIARY VOLCANIC ROCKS
Tvp	TERTIARY PYROCLASTIC ROCKS, (INCLUDING VOLCANIC MUDFLOW DEPOSITS.
Ti	TERTIARY INTRUSIVE ROCKS.

MESOZOIC

SEDIMENTARY AND METAMORPHIC ROCKS

Ku	UPPER CRETACEOUS MARINE ROCKS
Kl	LOWER CRETACEOUS MARINE ROCKS
KJf	FRANCISCAN ASSEMBLAGE (PREDOMINANTLY SEDIMENTARY AND META-SEDIMENTARY ROCKS. INCLUDES FRANCISCAN MELANGE)
J	JURASSIC MARINE ROCKS (INCLUDES KNOXVILLE FORMATION)
m	METAMORPHIC ROCKS OF PRE-TERTIARY AGE, UNDIVIDED.

METAVOLCANIC ROCKS

Mzv	MESOZOIC METAVOLCANIC ROCKS (INCLUDING FRANCISCAN VOLCANIC ROCKS).

PLUTONIC ROCKS

grMz	MESOZOIC GRANITIC ROCKS
um	MESOZOIC ULTRAMAFIC ROCKS

UNITS [illegible] "CORE COMPLEXES"

SYMBOLS

GEOLOGIC CONTACT, DASHED WHERE APPROXIMATE OR WHERE QUATERNARY DEPOSITS ARE INVOLVED.

FAULT (SOLID LINE WHERE LOCATION IS WELL DEFINED; DASHED LINE WHERE APPROXIMATE OR INFERRED; DOTTED WHERE CONCEALED.

ANTICLINAL AXIS - WITH PLUNGE INDICATED. (SOLID LINE WHERE LOCATION IS WELL DEFINED; DASHED WHERE APPROXIMATE OR INFERRED; DOTTED WHERE CONCEALED.

SYNCLINAL AXIS - WITH PLUNGE INDICATED. (SOLID LINE WHERE LOCATION IS WELL DEFINED; DASHED WHERE APPROXIMATE OR INFERRED; DOTTED WHERE CONCEALED.

NOTES

1. MAP BASE FROM PARTS OF SAN LUIS OBISPO AND SANTA MARIA SHEETS, U.S. GEOLOGICAL SURVEY 1:250,000 SCALE TOPOGRAPHIC MAP SERIES

2. GEOLOGIC DATA FROM:

   "GEOLOGIC MAP OF CALIFORNIA" [illegible], SCALE 1:250,000; PRELIMINARY, UNPUBLISHED, CALIFORNIA DIVISION OF MINES AND GEOLOGY. (COMPILED BY C.W. JENNINGS)

   LOCALLY SUPPLEMENTED WITH DATA FROM:

   [illegible], [illegible], 1965, GEOLOGY OF THE COASTAL PORTION OF THE SAN LUIS RANGE, SAN LUIS OBISPO COUNTY CALIF., UNPUBLISHED M.S. THESIS, UNIV. SOUTHERN CALIF.

   JAHNS, R.H., 1966, GEOLOGY OF THE DIABLO CANYON POWER PLANT SITE, SAN LUIS OBISPO COUNTY, CALIFORNIA; 1967 SUPPLEMENTARY REPORTS I AND II; 1968 SUPPLEMENTARY REPORT III, UNPUBLISHED, REPORTS TO THE PACIFIC GAS AND ELECTRIC COMPANY.

   HALL, C.A., [illegible], U.S.G.S. MAP MF [illegible].

   EARTH SCIENCES ASSOCIATES, [illegible], OFFSHORE INVESTIGATION.

FSAR UPDATE
UNITS 1 AND 2 DIABLO CANYON SITE
FIGURE 2.5-5 GEOLOGIC AND TECTONIC MAP OF SOUTHERN COAST RANGES IN THE REGION OF PLANT SITE (SHEET 2 OF 2)

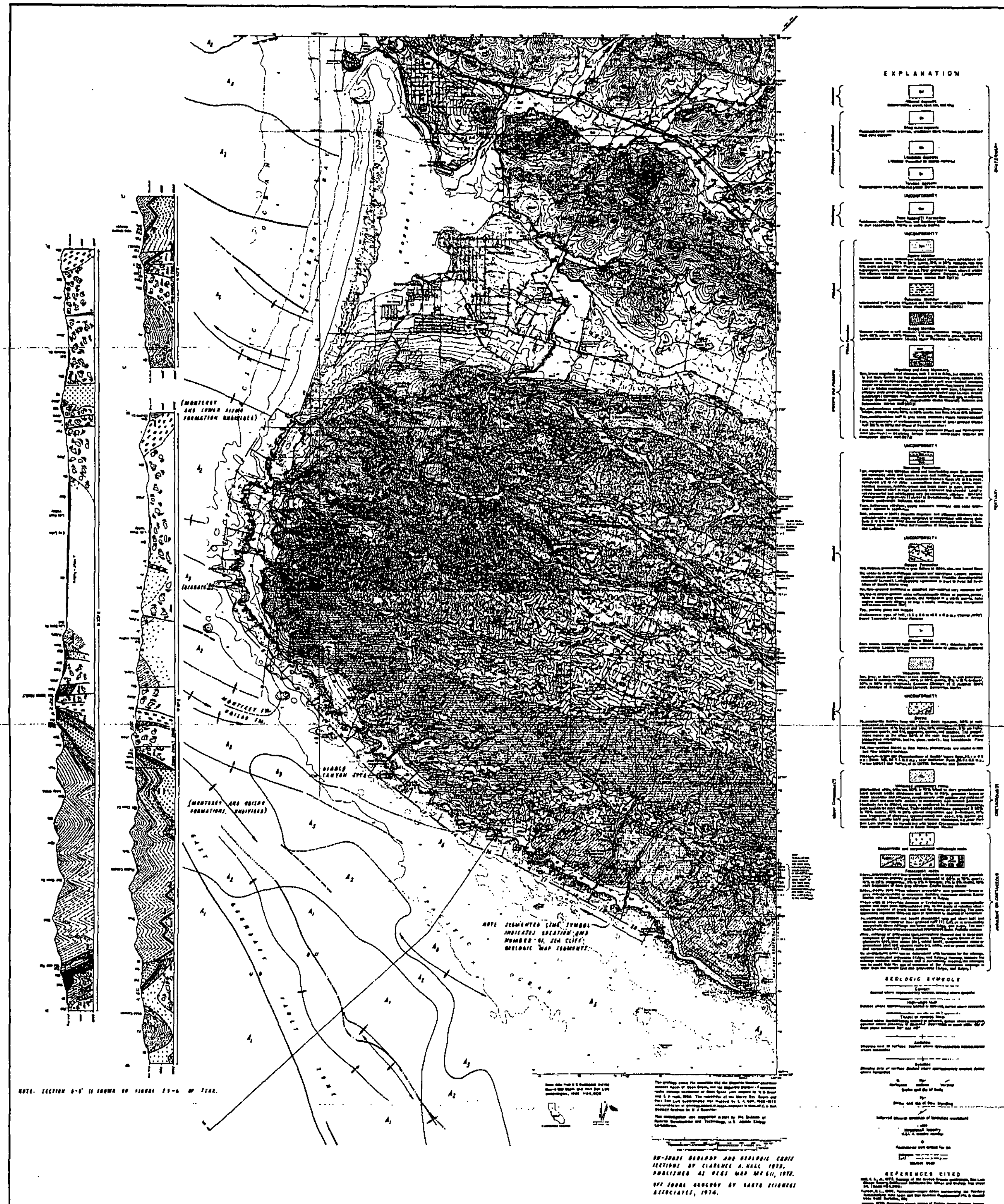

GEOLOGIC MAP OF THE MORRO BAY SOUTH AND PORT SAN LUIS QUADRANGLES, SAN LUIS OBISPO COUNTY, CALIFORNIA

EXPLANATION FOR GEOLOGIC MAP OF THE OFFSHORE AREA

MAP UNITS

MAP ACOUSTIC UNIT	STRATIGRAPHIC EQUIVALENT
A_1	UPPER PART OF PISMO FORMATION (ABOVE MIGUELITO AND EDNA MEMBERS).
A_2	MONTEREY FORMATION AND LOWER PART OF PISMO FORMATION (MIGUELITO AND EDNA MEMBERS). INCLUDES OBISPO FORMATION IN THE AREA OFFSHORE FROM DIABLO CANYON
A_3	FRANCISCAN AND GREAT VALLEY SEQUENCE BASEMENT ROCKS, UNDIVIDED. LOCALLY MAY INCLUDE SOME OBISPO FORMATION.

MAP SYMBOLS

CONTACT, DASHED WHERE POORLY CONTROLLED.

FAULT, DASHED WHERE POORLY CONTROLLED.

BURIED FAULT

ANTICLINE

SYNCLINE

FSAR UPDATE
UNITS 1 AND 2
DIABLO CANYON SITE
FIGURE 2.5 – 6
GEOLOGIC MAP OF THE MORRO BAY SOUTH AND PORT SAN LUIS QUADRANGLES, SAN LUIS OBISPO COUNTY, CALIFORNIA, AND ADJACENT OFFSHORE AREA.

Revision 11 November 1996

(ORIGINALLY: PLATE VIII APPENDIX 2.5D)

FSAR UPDATE
UNITS 1 AND 2
DIABLO CANYON SITE
FIGURE 2.5 – 6
GEOLOGIC MAP OF THE MORRO BAY SOUTH AND PORT SAN LUIS QUADRANGLES, SAN LUIS OBISPO *COUNTY, CALIFORNIA, AND ADJACENT OFFSHORE AREA.*

ESA 1119
SEPT 1974

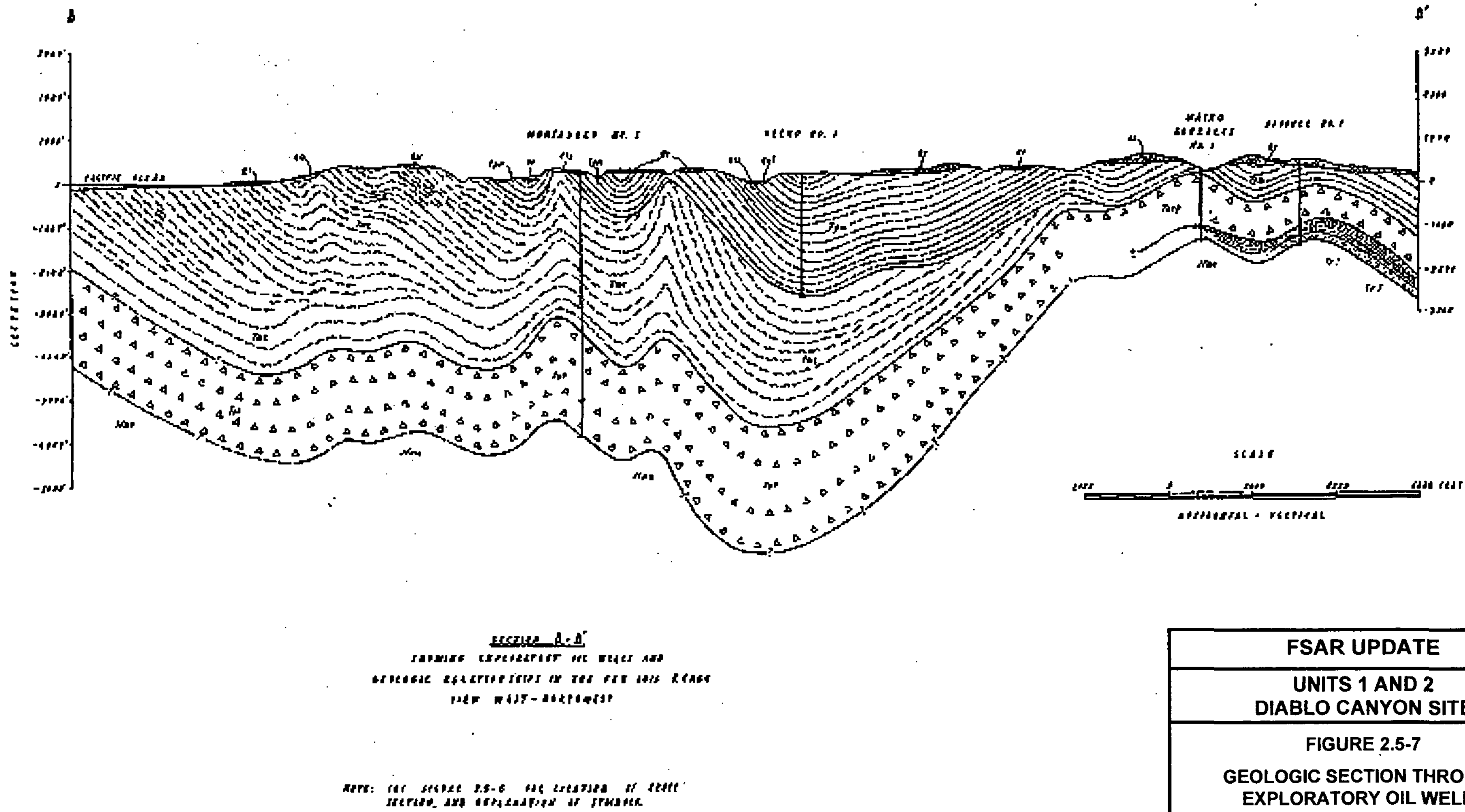

FSAR UPDATE

UNITS 1 AND 2
DIABLO CANYON SITE

FIGURE 2.5-7

GEOLOGIC SECTION THROUGH
EXPLORATORY OIL WELLS
IN THE SAN LUIS RANGE

Revision 11 November 1996

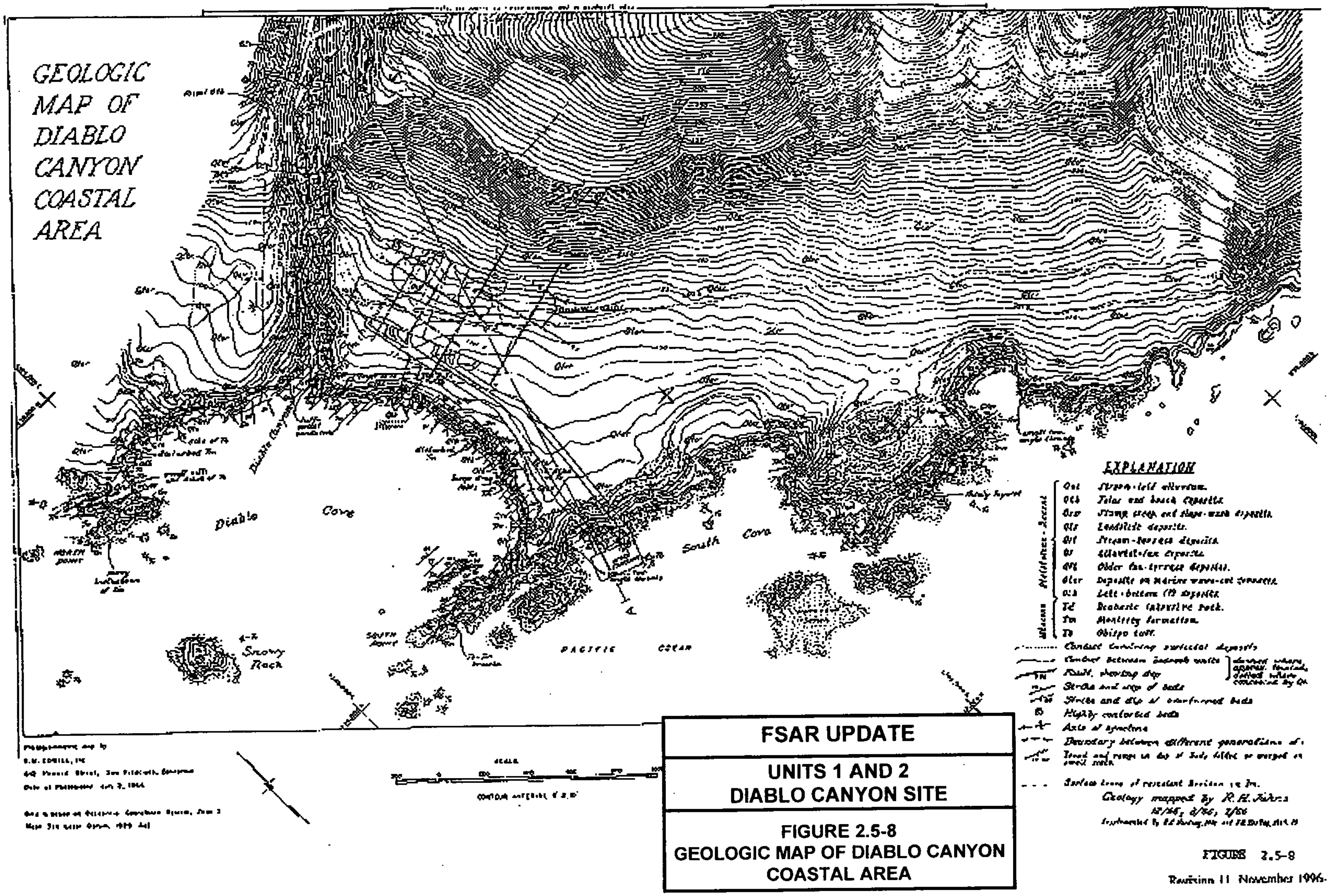

FSAR UPDATE

UNITS 1 AND 2
DIABLO CANYON SITE

FIGURE 2.5-8
GEOLOGIC MAP OF DIABLO CANYON
COASTAL AREA

Revision 11 November 1996

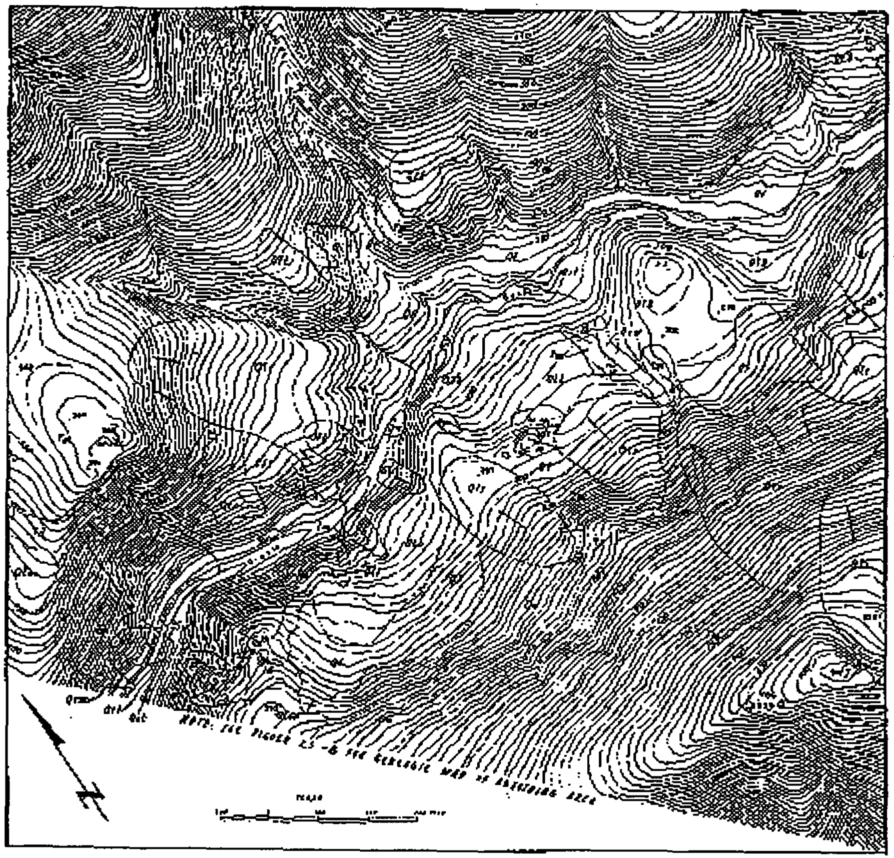

EXPLANATION

PLEISTOCENE – RECENT

Qal	STREAM-LAID ALLUVIUM
Qsw	SLUMP, CREEP, AND SLOPE-WASH DEPOSITS
Qls	LANDSLIDE DEPOSITS.
Qst	STREAM-TERRACE DEPOSITS
Qf	ALLUVIAL-FAN DEPOSITS
Qft	OLDER FAN-TERRACE DEPOSITS
Qtr	DEPOSITS ON MARINE WAVE-CUT TERRACES.
Qlb	LAKE-BOTTOM (?) DEPOSITS

MIOCENE

Td	DIABASIC INTRUSIVE ROCK
Tm	MONTEREY FORMATION.

CONTACT INVOLVING SURFICIAL DEPOSITS.

CONTACT BETWEEN BEDROCK UNITS. DASHED WHERE APPROX. LOCATED; DOTTED WHERE CONCEALED BY QUAT.

70 STRIKE AND DIP OF BEDS

40-70 TREND AND RANGE IN DIP OF BEDS FOLDED OR WARPED ON A SMALL SCALE.

GEOLOGY MAPPED BY [illegible] AND [illegible] JOHNSON, 1967, SUPPLEMENTED BY [illegible], 1969.

FSAR UPDATE
UNITS 1 AND 2 DIABLO CANYON SITE
FIGURE 2.5-9 GEOLOGIC MAP OF SWITCHYARD AREA

Revision 11 November 1996

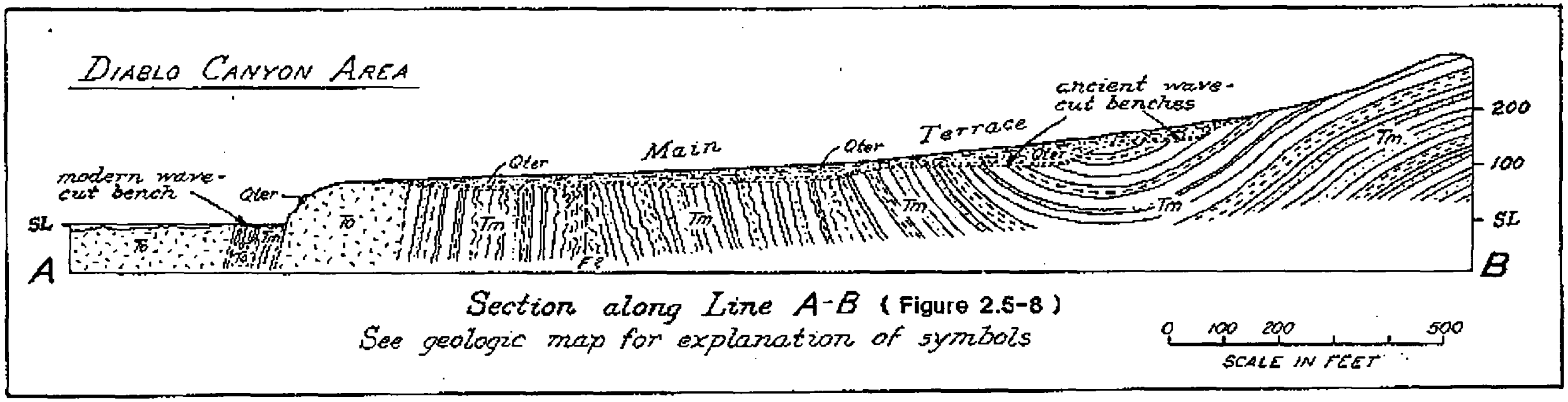

FSAR UPDATE

UNITS 1 AND 2
DIABLO CANYON SITE

FIGURE 2.5-10
GEOLOGIC SECTION THROUGH
THE PLANT SITE

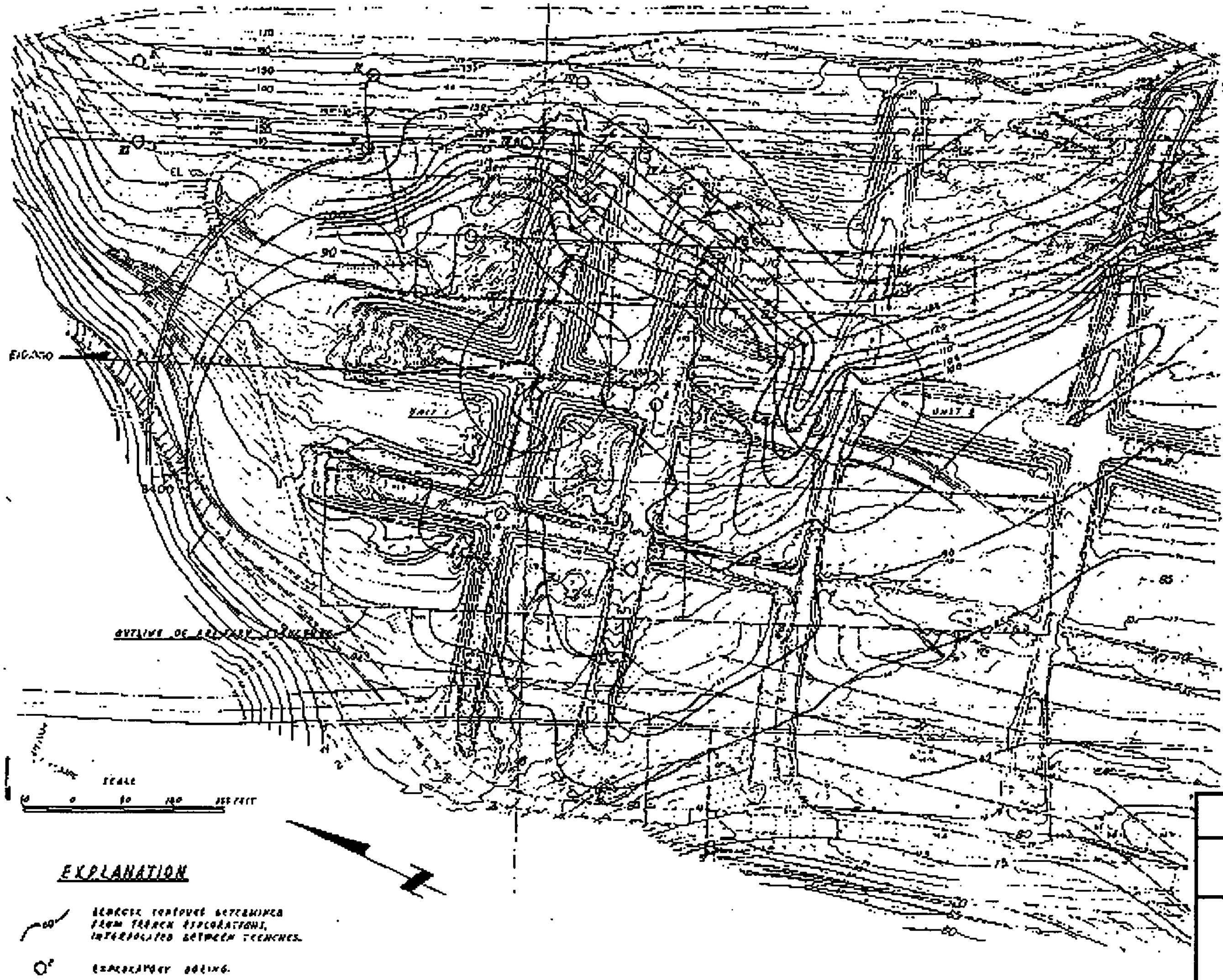

FSAR UPDATE

UNITS 1 AND 2
DIABLO CANYON SITE

FIGURE 2.5-11
SITE EXPLORATION FEATURES
AND BEDROCK CONTOURS

Revision 11 November 1996

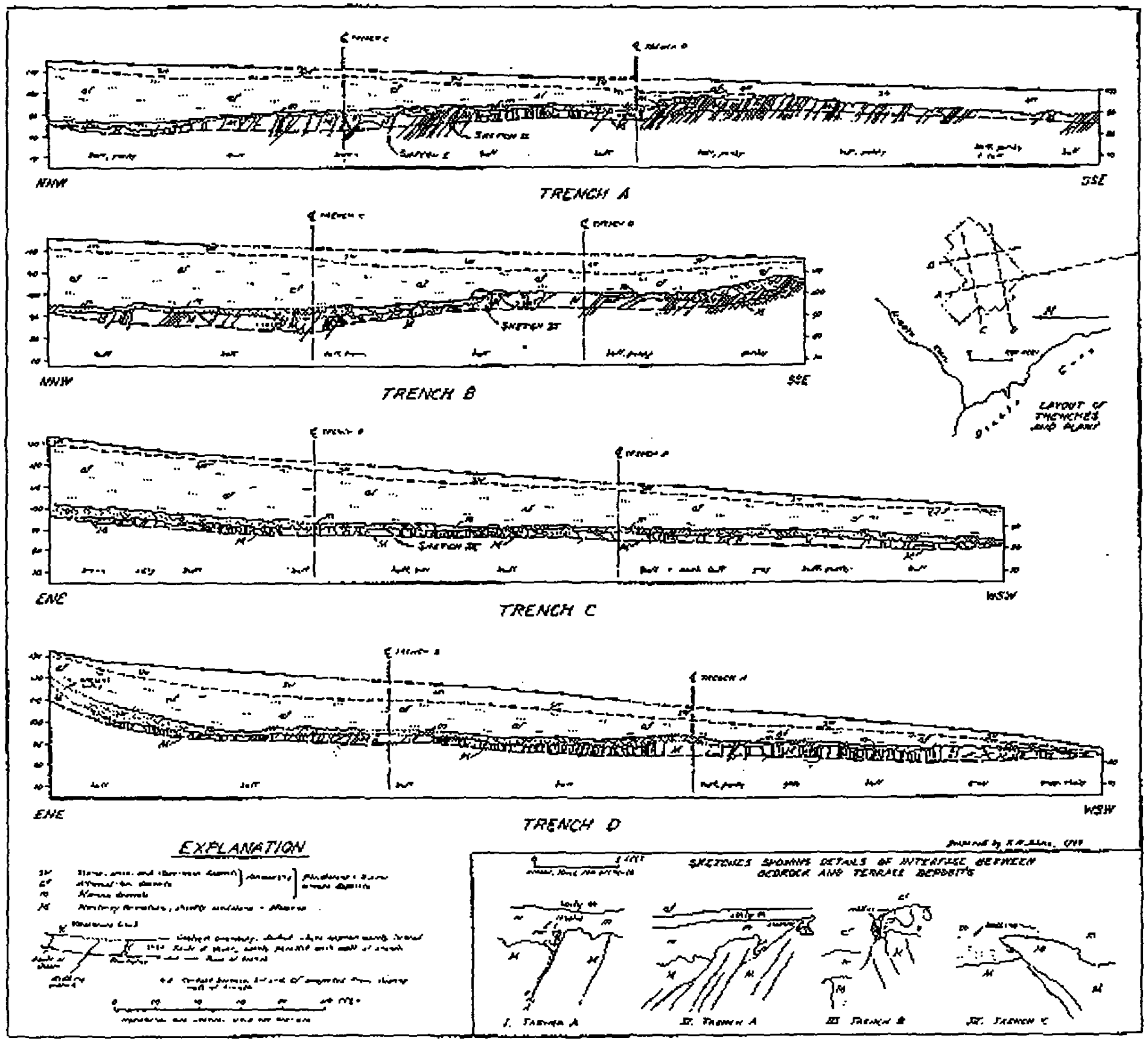

FSAR UPDATE

UNIT 1
DIABLO CANYON SITE

FIGURE 2.5-12
GEOLOGIC SECTIONS AND SKETCHES ALONG EXPLORATORY TRENCHES

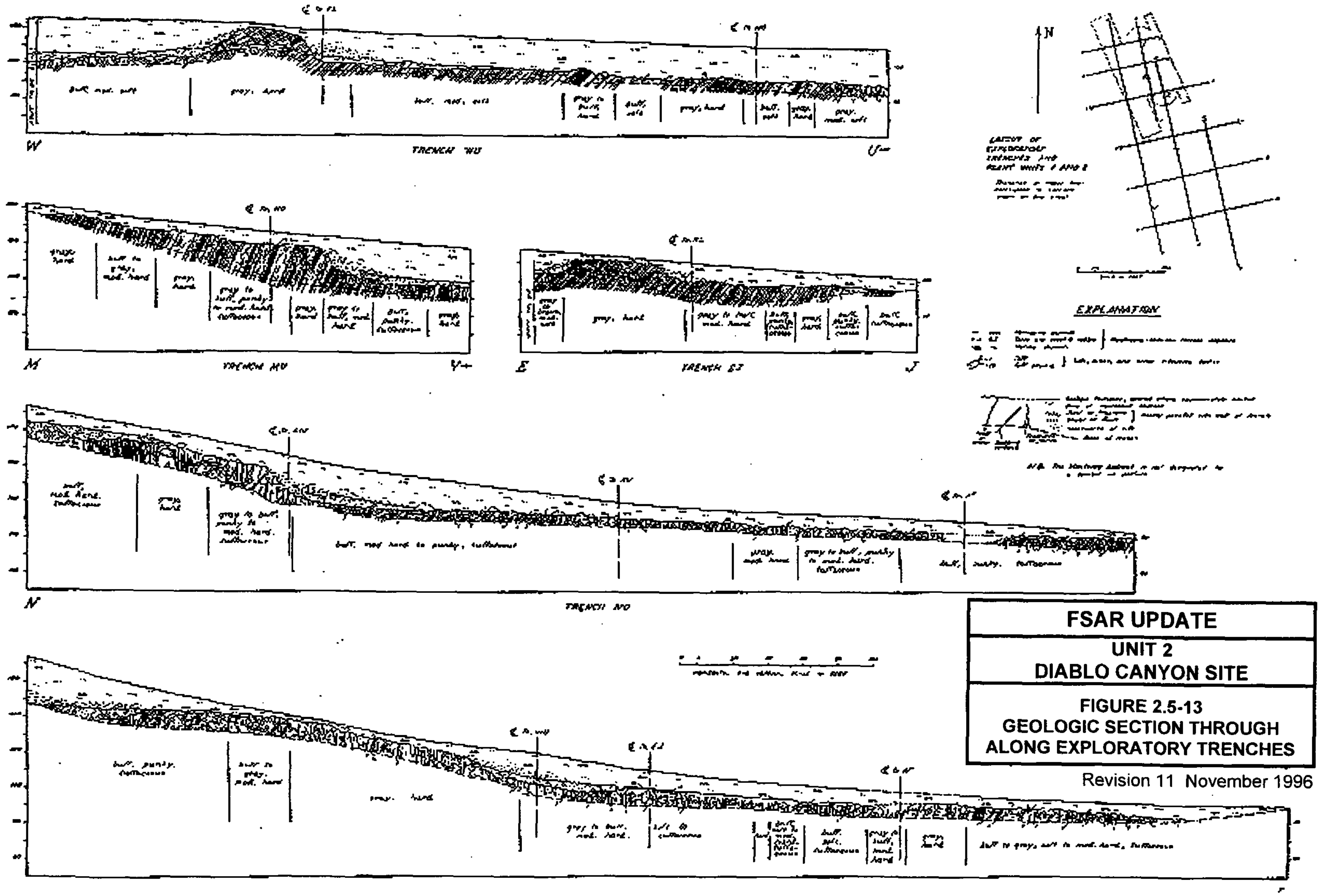

FSAR UPDATE

UNIT 2
DIABLO CANYON SITE

FIGURE 2.5-13
GEOLOGIC SECTION THROUGH
ALONG EXPLORATORY TRENCHES

Revision 11 November 1996

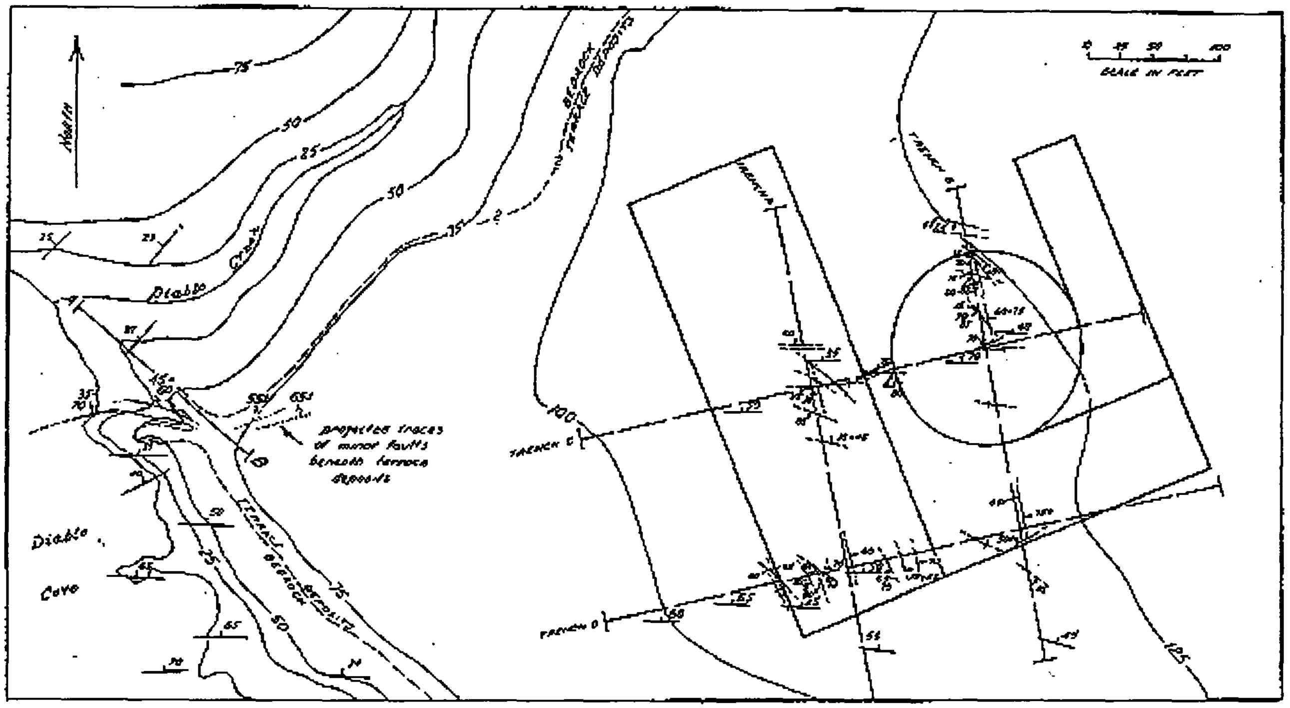

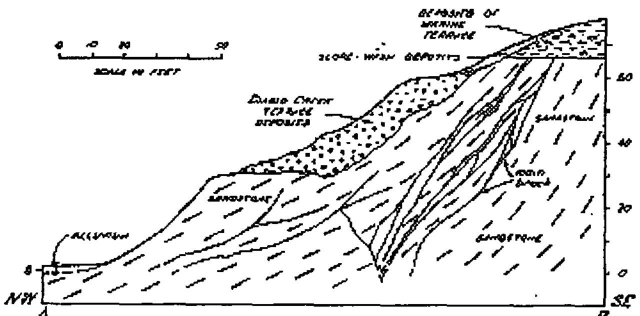

Section Along Line A-B

EXPLANATION

Strike and dip of beds

Generalized trace of bedding (in section only)

Fault or shear, showing dip and trend and plunge of slickensides

Vertical fault or shear

Center line of exploratory trench

Outline of power plant structure

FSAR UPDATE

UNITS 1 AND 2
DIABLO CANYON SITE

FIGURE 2.5-14
RELATIONSHIPS OF FAULTS AND SHEARS AT PLANT SITE

Revision 11 November 1996

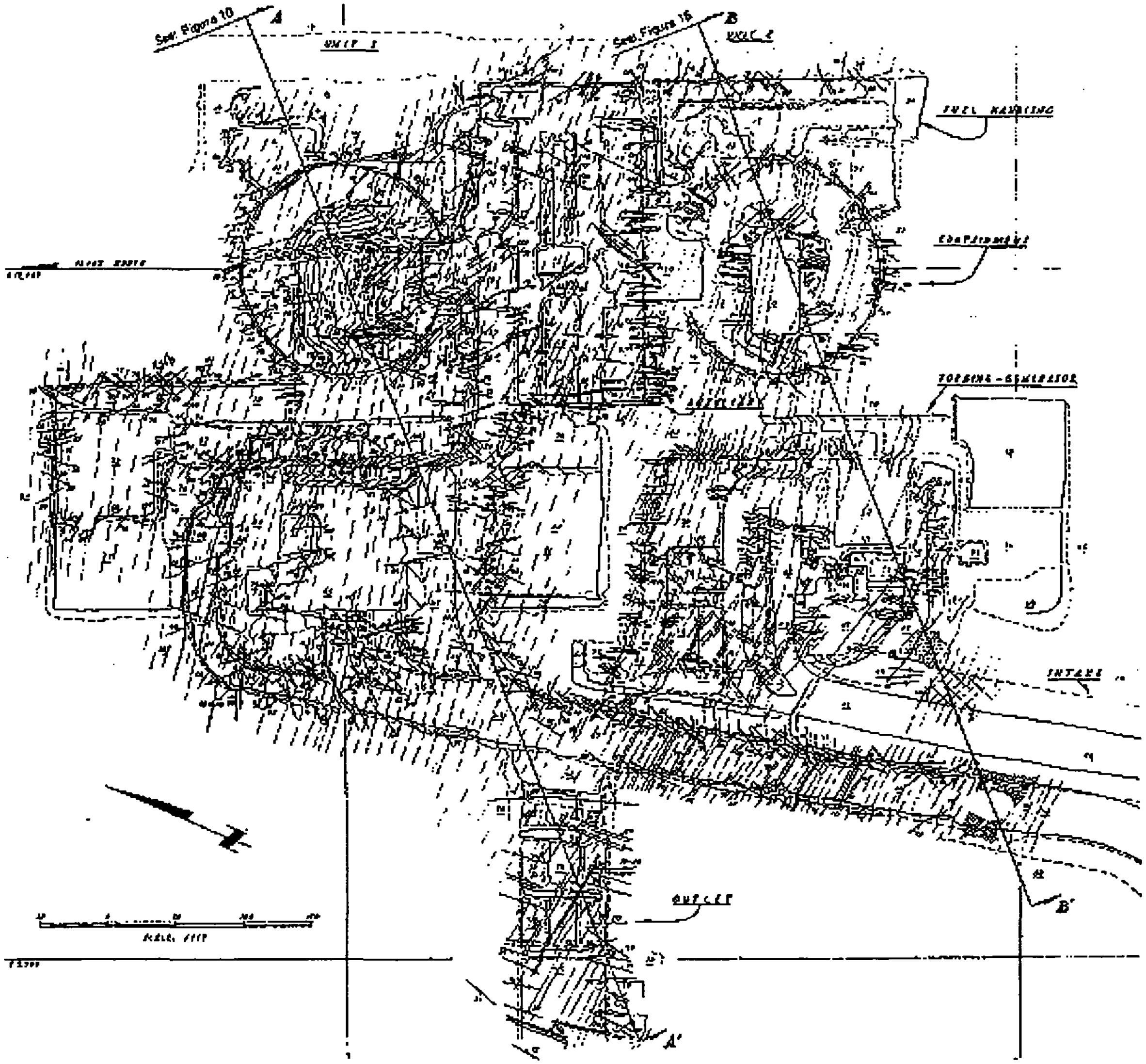

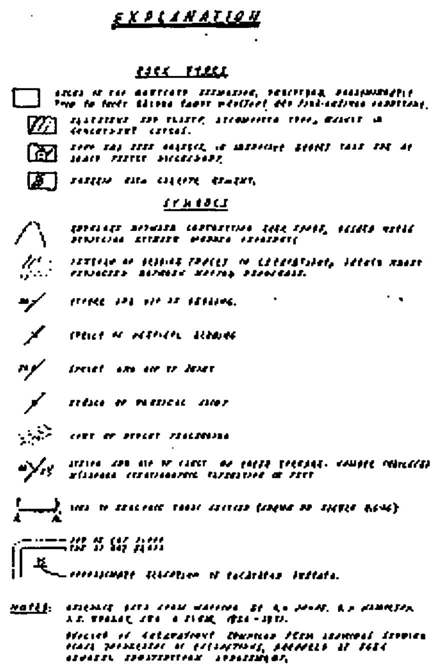

FSAR UPDATE

**UNITS 1 AND 2
DIABLO CANYON SITE**

**FIGURE 2.5-15
GEOLOGIC MAP OF EXCAVATIONS
FOR PLANT FACILITIES**

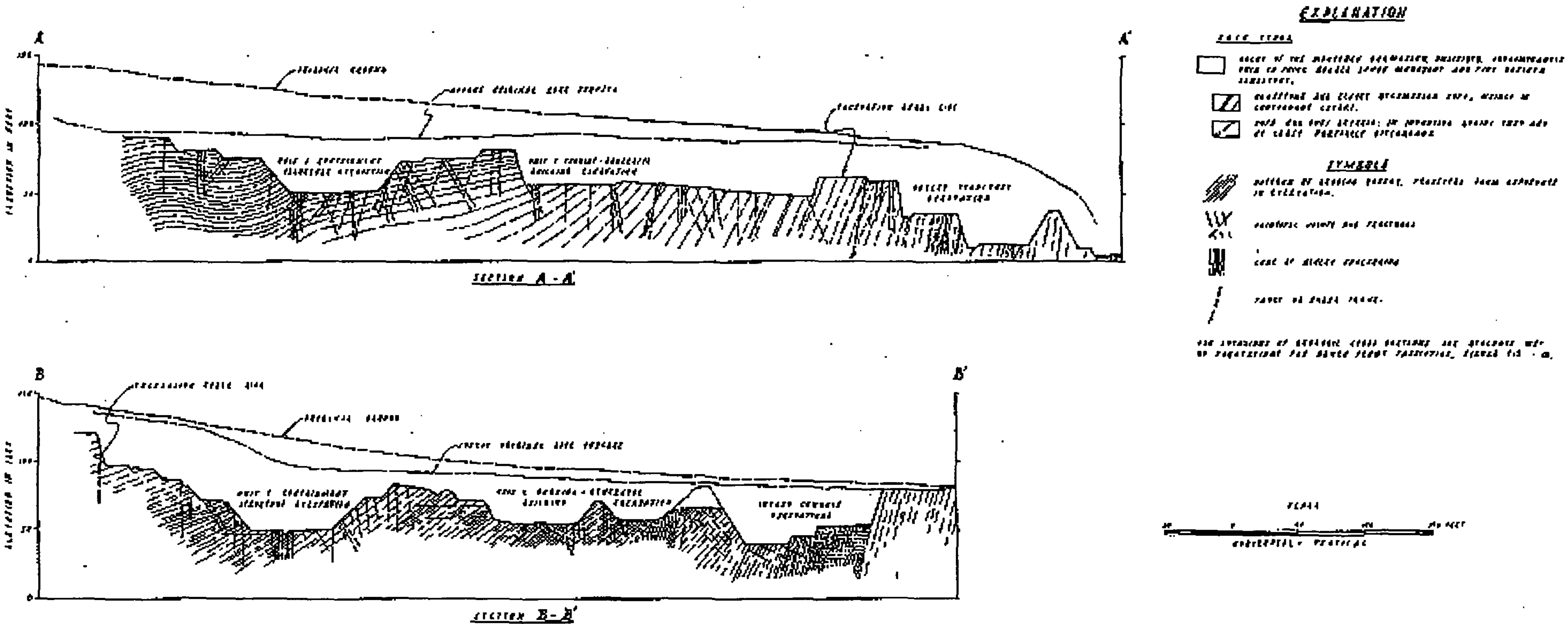

FSAR UPDATE

**UNITS 1 AND 2
DIABLO CANYON SITE**

**FIGURE 2.5-16
GEOLOGIC SECTIONS THROUGH
EXCAVATIONS FOR PLANT FACILITIES**

Revision 11 November 1996

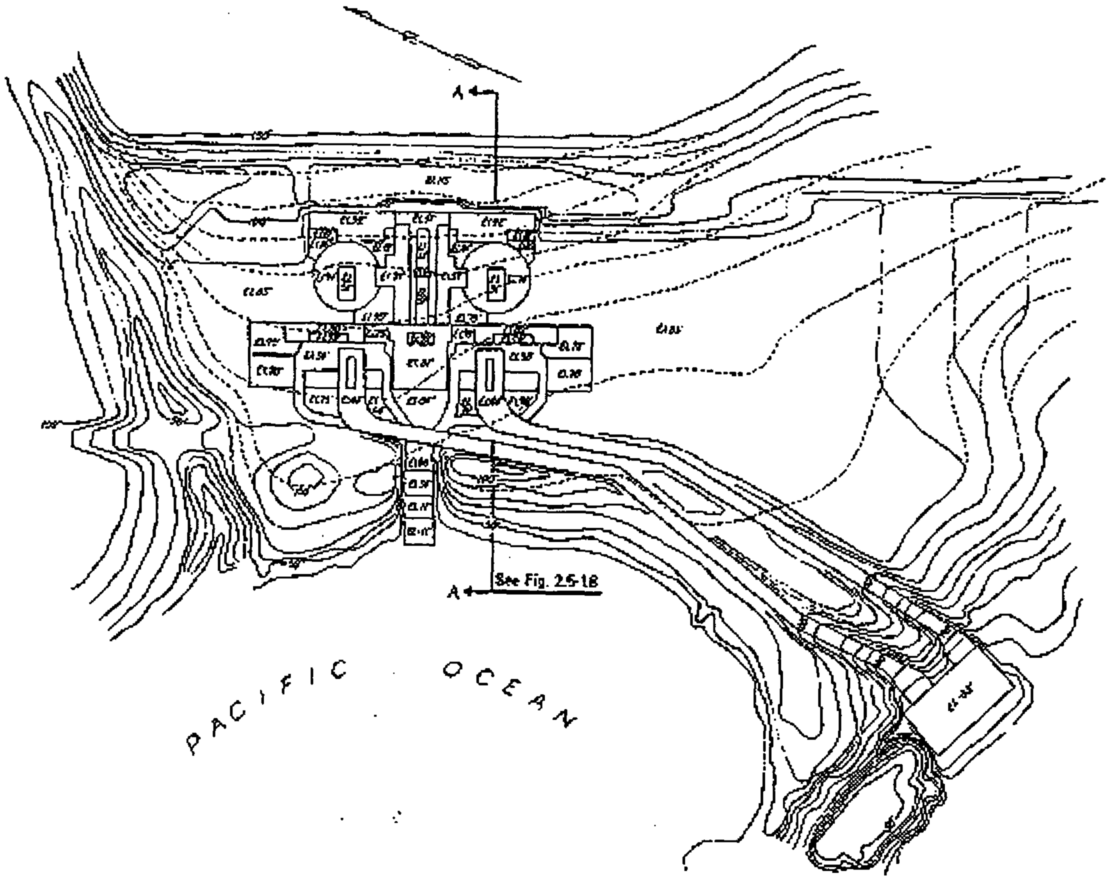

FSAR UPDATE

UNITS 1 AND 2
DIABLO CANYON SITE

FIGURE 2.5-17

PLAN OF EXCAVATION AND BACKFILL

Revision 11 November 1996

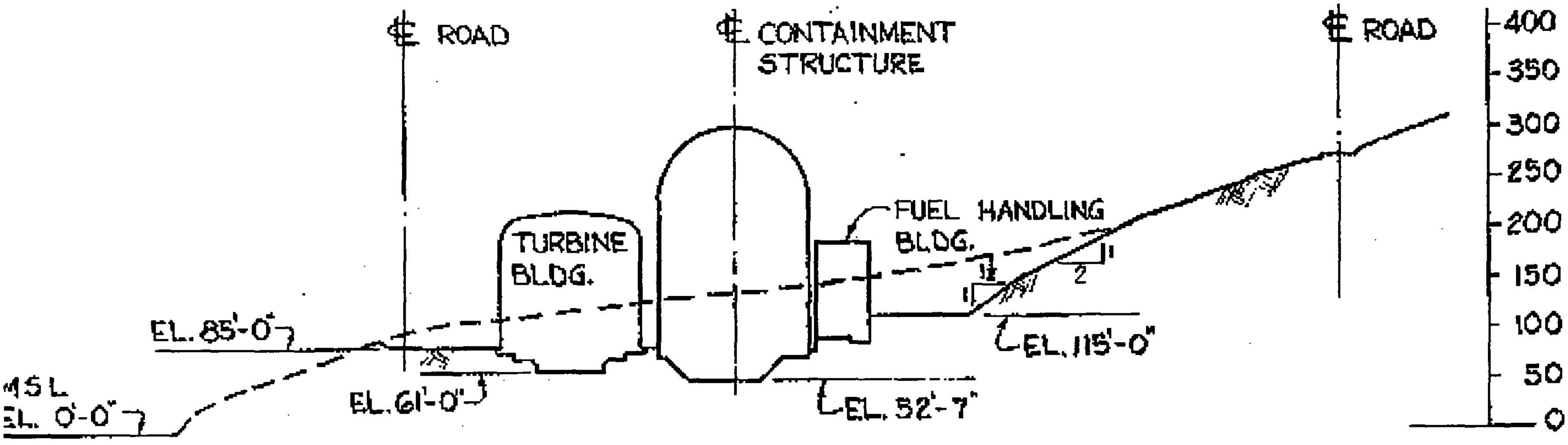

SECTION A-A

FROM FIGURE 2.5-17

FSAR UPDATE
UNITS 1 AND 2 DIABLO CANYON SITE
FIGURE 2.5-18 SECTION A-A EXCAVATION AND BACKFILL

Revision 11 November 1996

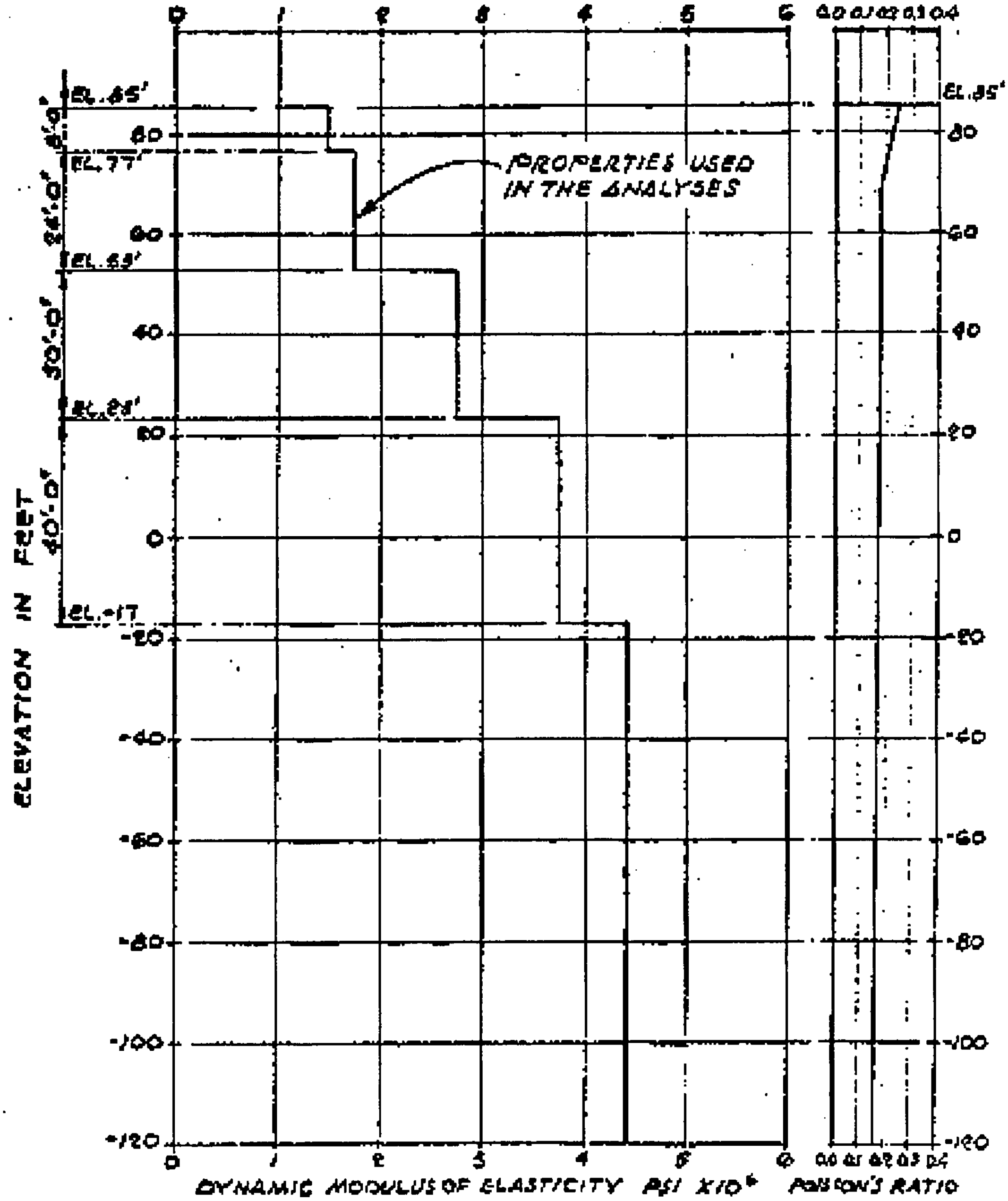

FSAR UPDATE
UNITS 1 AND 2 DIABLO CANYON SITE
FIGURE 2.5-19 SOIL MODULE OF ELASTICITY AND POISSON'S RATIO

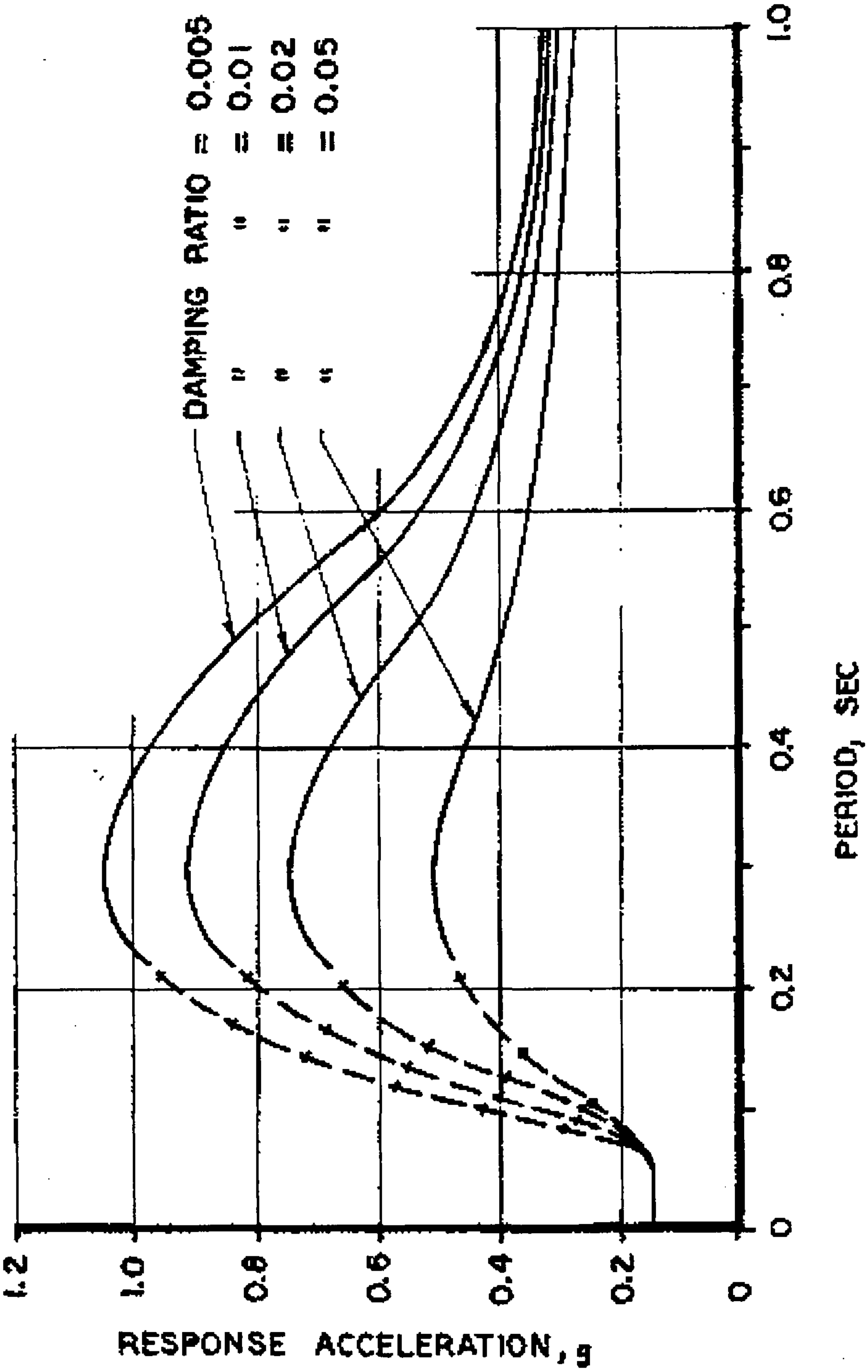

FSAR UPDATE
UNITS 1 AND 2 DIABLO CANYON SITE
FIGURE 2.5-20 SMOOTH RESPONSE ACCELERATION SPECTRA – EARTHQUAKE "B"

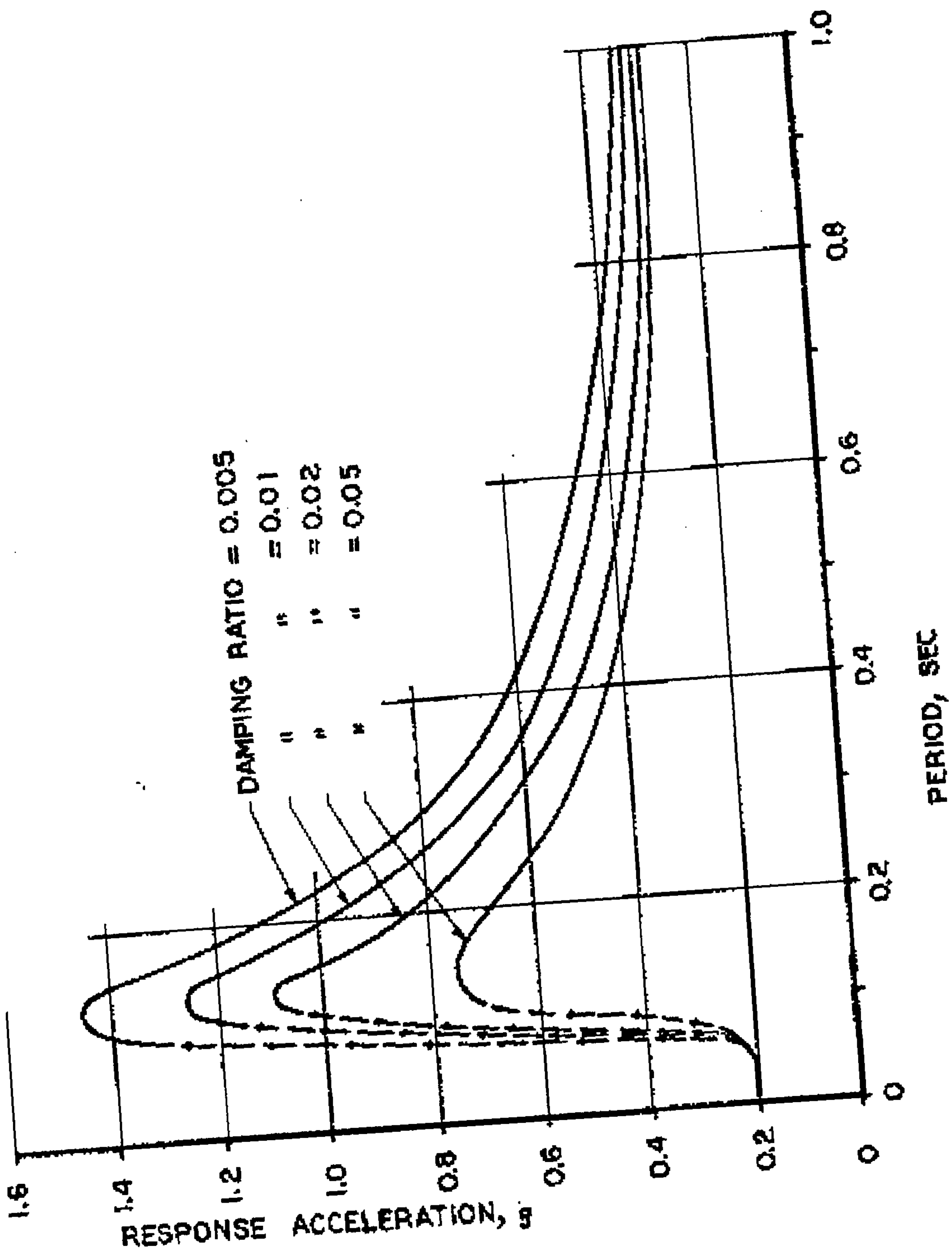

FSAR UPDATE
UNITS 1 AND 2 DIABLO CANYON SITE
FIGURE 2.5-21 SMOOTH RESPONSE ACCELERATION SPECTRA – EARTHQUAKE "D" MODIFIED

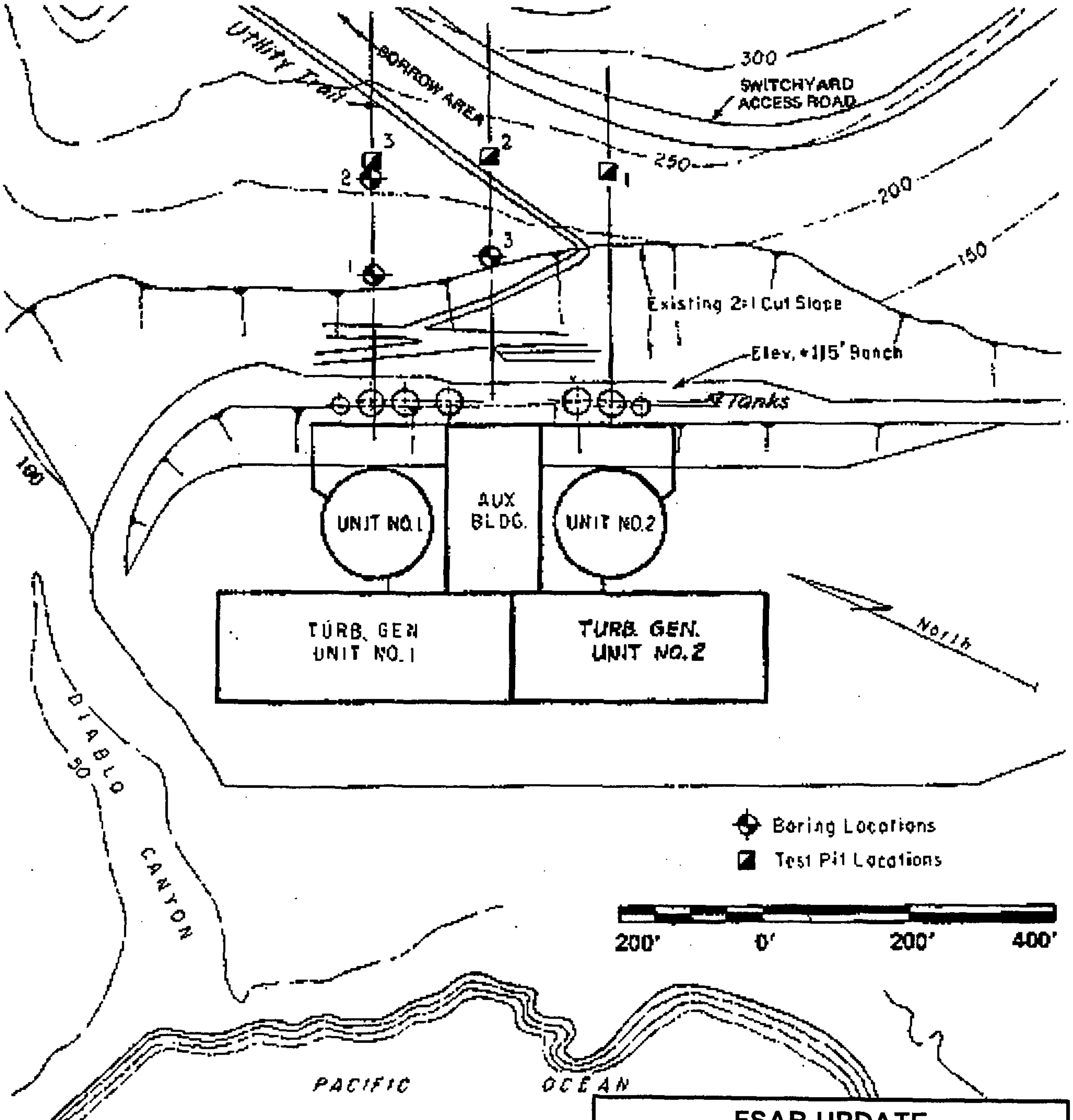

FSAR UPDATE

UNITS 1 AND 2
DIABLO CANYON SITE

FIGURE 2.5-22

POWER PLANT SLOPE PLAN

Revision 11 November 1996

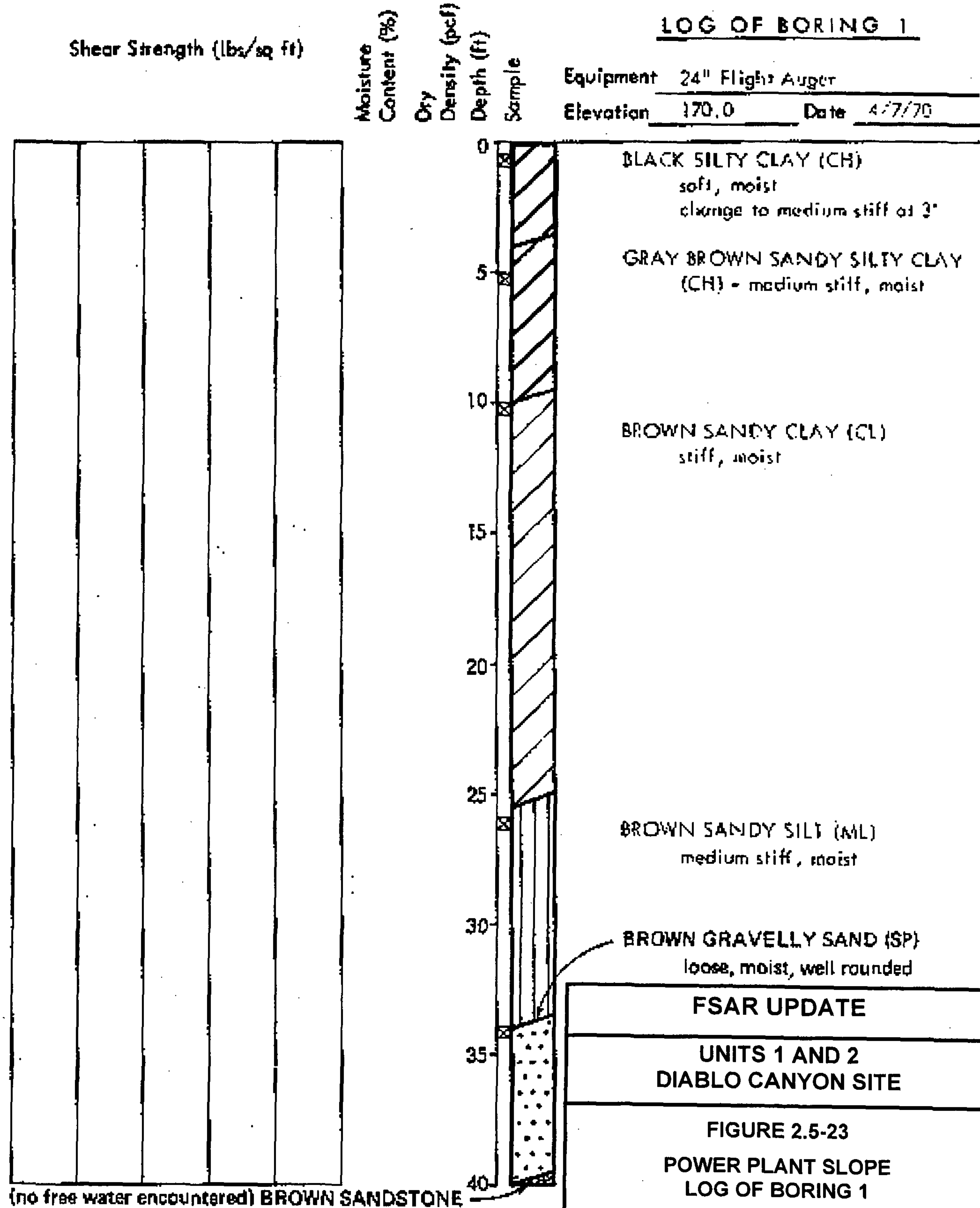

FSAR UPDATE

UNITS 1 AND 2
DIABLO CANYON SITE

FIGURE 2.5-23
POWER PLANT SLOPE
LOG OF BORING 1

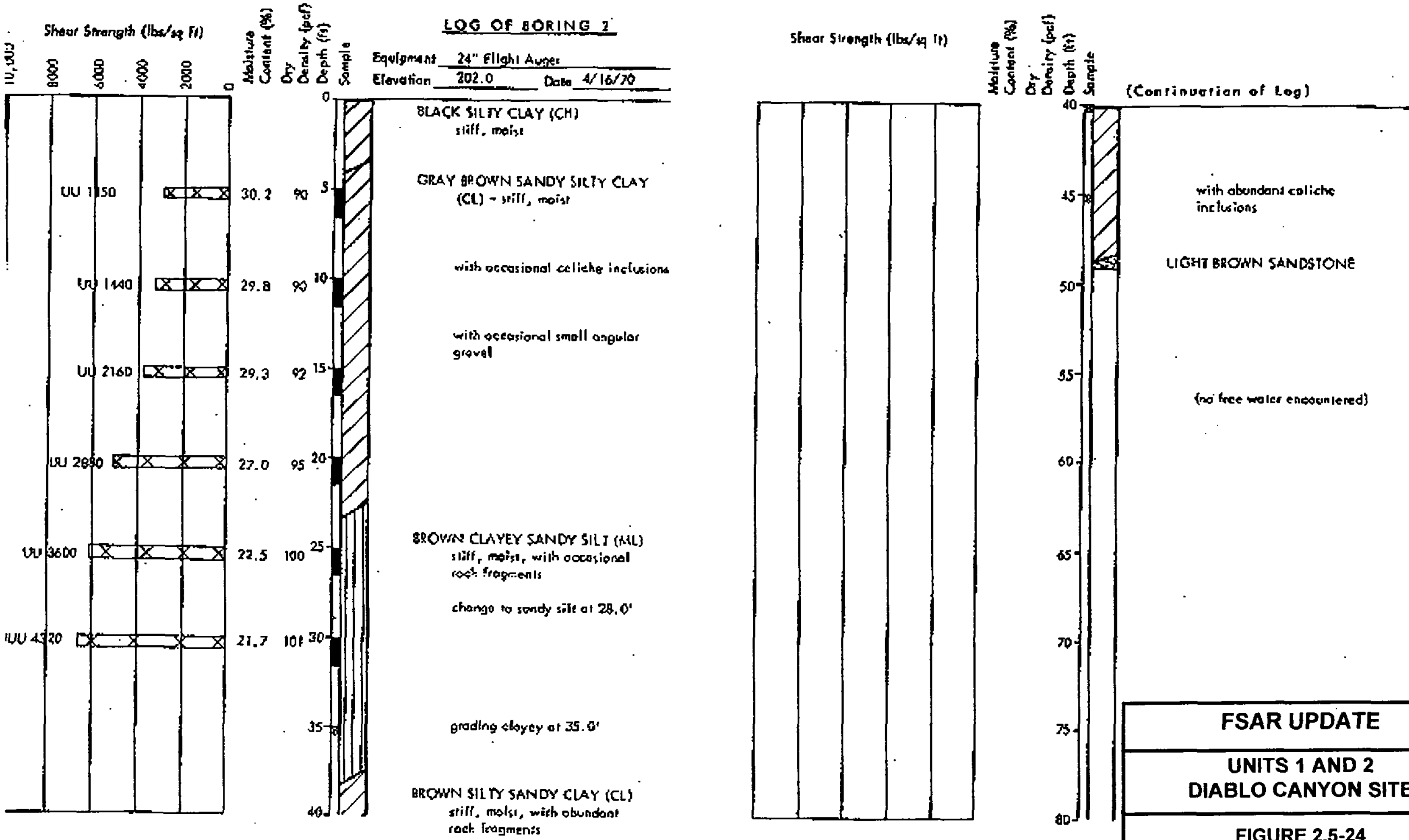

FSAR UPDATE

UNITS 1 AND 2
DIABLO CANYON SITE

FIGURE 2.5-24

POWER PLANT SLOPE
LOG OF BORING 2

Revision 11 November 1996

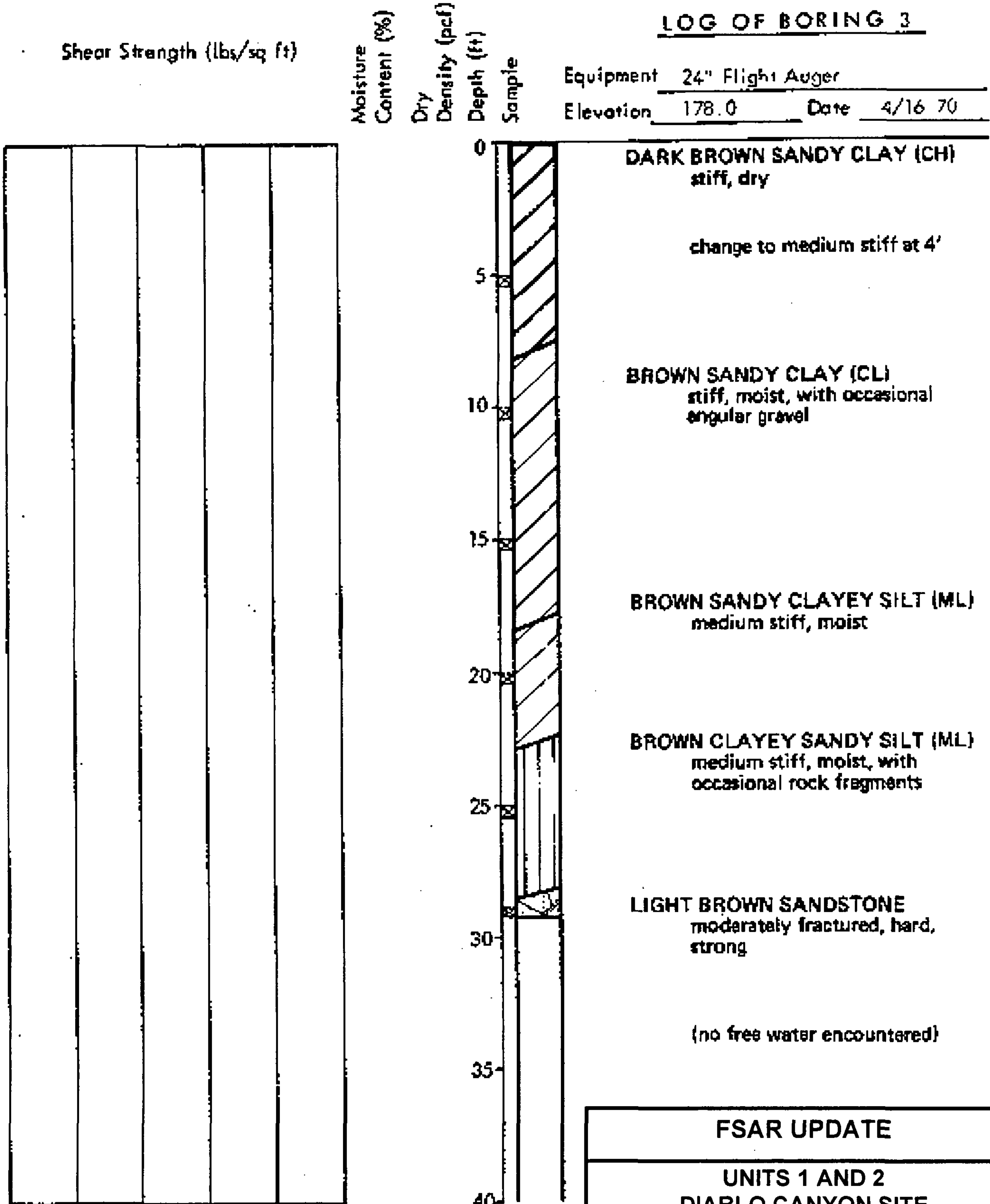

FSAR UPDATE

UNITS 1 AND 2
DIABLO CANYON SITE

FIGURE 2.5-25

POWER PLANT SLOPE
LOG OF BORING 3

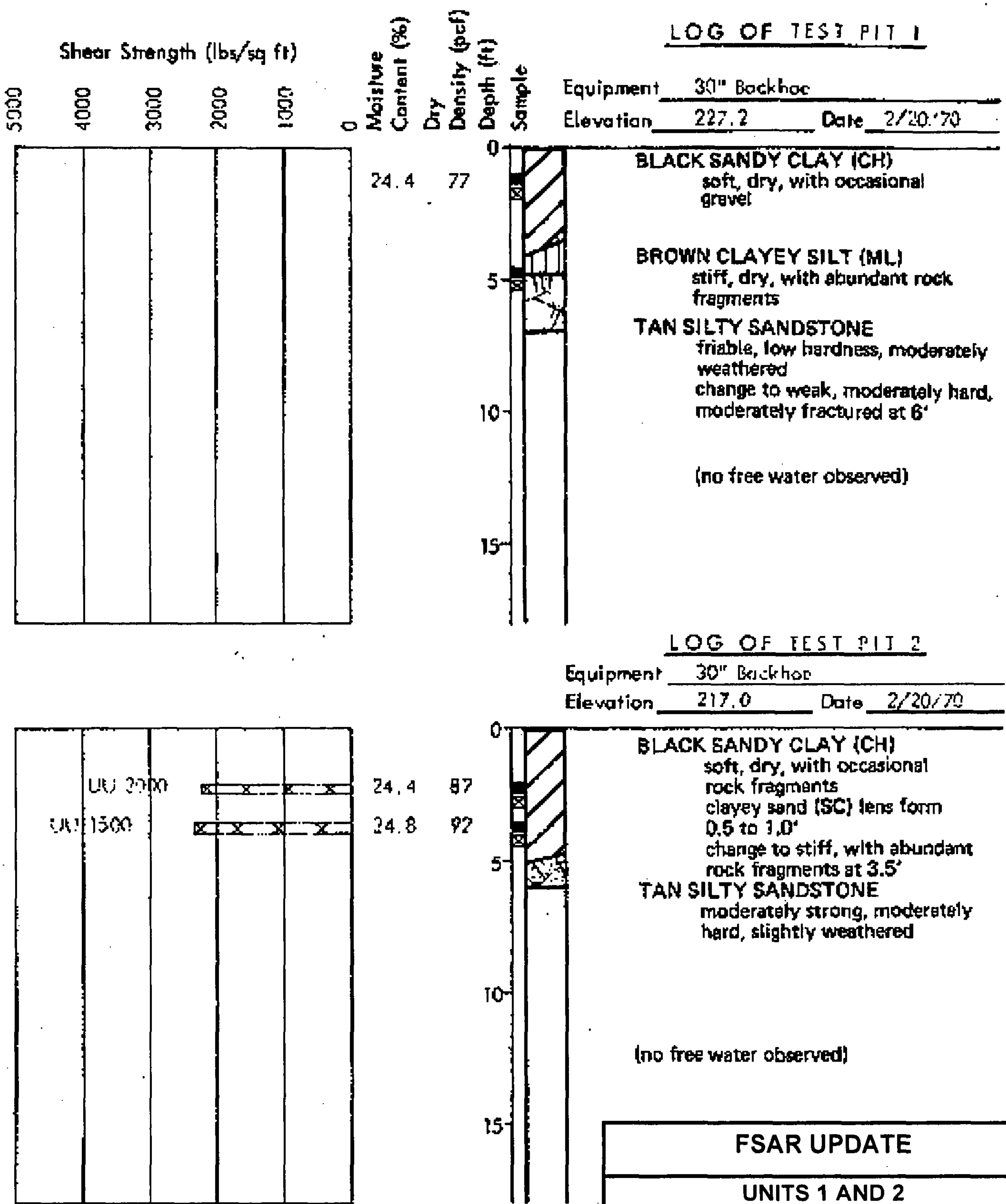

FSAR UPDATE

UNITS 1 AND 2
DIABLO CANYON SITE

FIGURE 2.5-26

POWER PLANT SLOPE
LOG OF TEST PITS 1 & 2

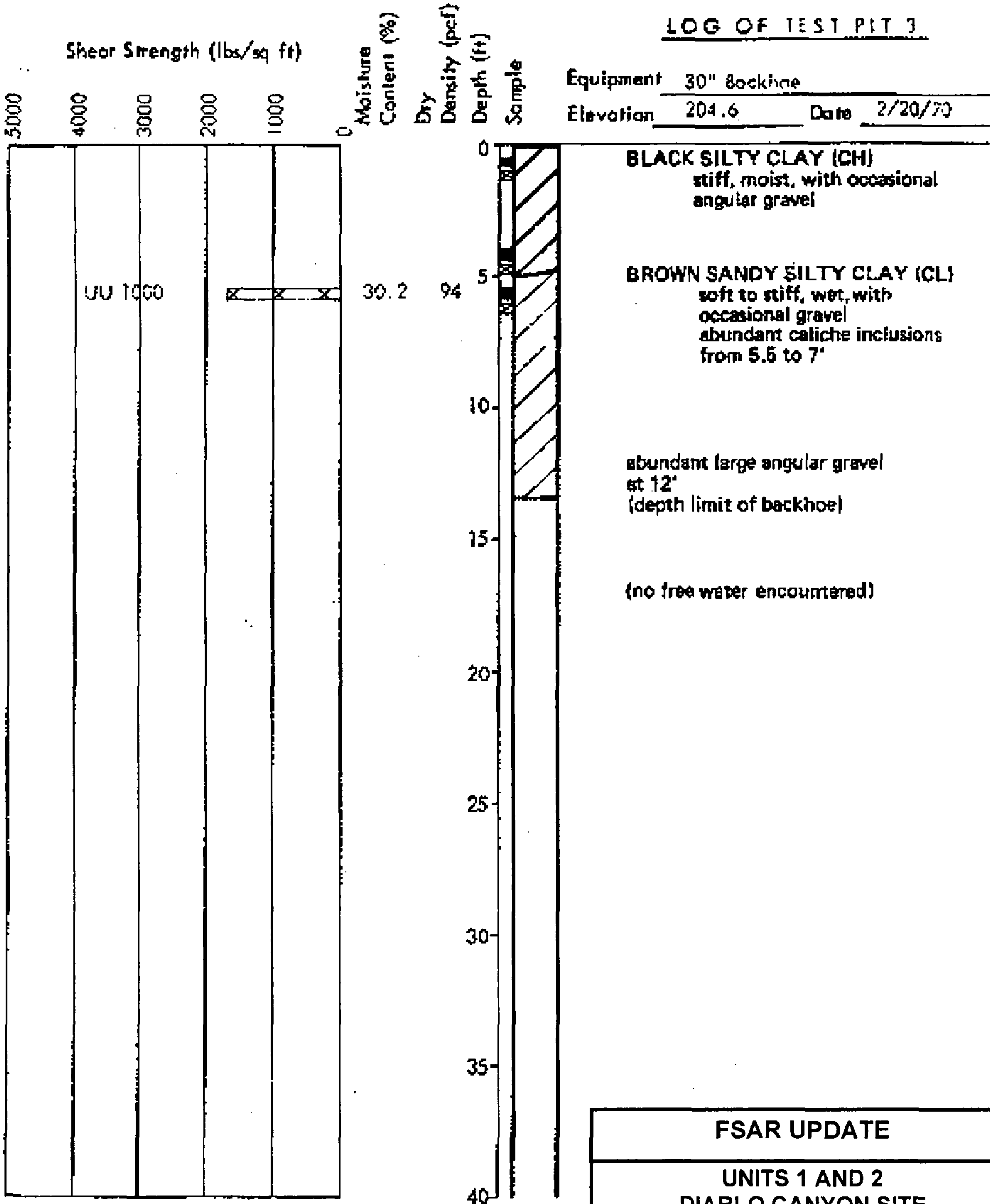

FSAR UPDATE

UNITS 1 AND 2
DIABLO CANYON SITE

FIGURE 2.5-27

POWER PLANT SLOPE
LOG OF TEST PIT 3

MAJOR DIVISIONS				TYPICAL NAMES
COARSE GRAINED SOILS (MORE THAN HALF IS LARGER THAN #200 SIEVE)	GRAVELS (MORE THAN HALF COARSE FRACTION IS LARGER THAN NO. 4 SIEVE SIZE)	CLEAN GRAVELS WITH LITTLE OR NO FINES	GW	WELL GRADED GRAVELS, GRAVEL – SAND MIXTURES
			GP	POORLY GRADED GRAVELS, GRAVEL – SAND MIXTURES
		GRAVELS WITH OVER 12% FINES	GM	SILTY GRAVELS, POORLY GRADED GRAVEL - SAND - SILT MIXTURES
			GC	CLAYEY GRAVELS, POORLY GRADED GRAVEL - SAND - CLAY MIXTURES
	SANDS (MORE THAN HALF COARSE FRACTION IS SMALLER THAN NO. 4 SIEVE SIZE)	CLEAN SANDS WITH LITTLE OR NO FINES	SW	WELL GRADED SANDS, GRAVELLY SANDS
			SP	POORLY GRADED SANDS, GRAVELLY SANDS
		SANDS WITH OVER 12% FINES	SM	SILTY SANDS, POORLY GRADED SAND - SILT MIXTURES
			SC	CLAYEY SANDS, POORLY GRADED SAND - CLAY MIXTURES
FINE GRAINED SOILS (MORE THAN HALF IS SMALLER THAN #200 SIEVE)	SILTS AND CLAYS (LIQUID LIMIT LESS THAN 50)		ML	INORGANIC SILTS AND VERY FINE SANDS, ROCK FLOUR, SILTY OR CLAYEY FINE SANDS, OR CLAYEY SILTS WITH SLIGHT PLASTICITY
			CL	INORGANIC CLAYS OF LOW TO MEDIUM PLASTICITY, GRAVELLY CLAYS, SANDY CLAYS, SILTY CLAYS, LEAN CLAYS
			OL	ORGANIC CLAYS AND ORGANIC SILTY CLAYS OF LOW PLASTICITY
	SILTS AND CLAYS (LIQUID LIMIT GREATER THAN 50)		MH	INORGANIC SILTS, MICACEOUS OR DIATOMACIOUS FINE SANDY OR SILTY SOILS, ELASTIC SILTS
			CH	INORGANIC CLAYS OF HIGH PLASTICITY, FAT CLAYS
			OH	ORGANIC CLAYS OF MEDIUM TO HIGH PLASTICITY, ORGANIC SILTS
HIGHLY ORGANIC SOILS			Pt	PEAT AND OTHER HIGHLY ORGANIC SOILS

UNIFIED SOIL CLASSIFICATION SYSTEM

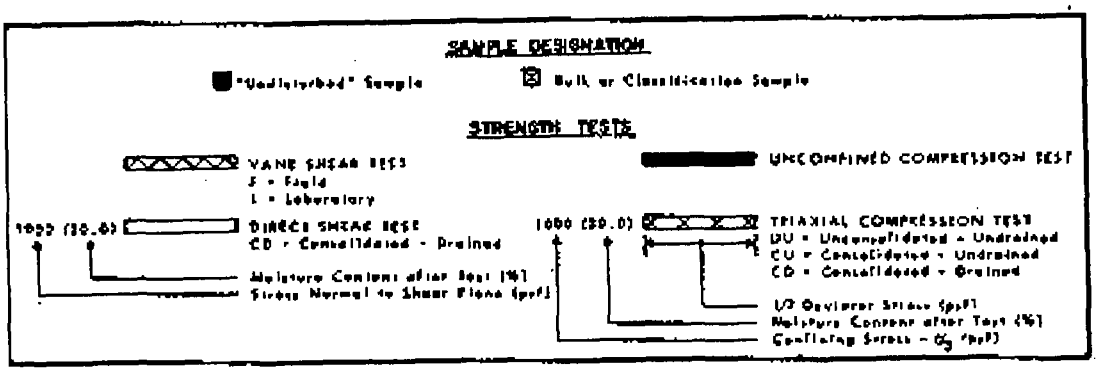

KEY TO TEST DATA

FSAR UPDATE
UNITS 1 AND 2 DIABLO CANYON SITE
FIGURE 2.5-28 POWER PLANT SLOPE SOIL CLASSIFICATION CHART AND KEY TO TEST AREA

Revision 11 November 1996

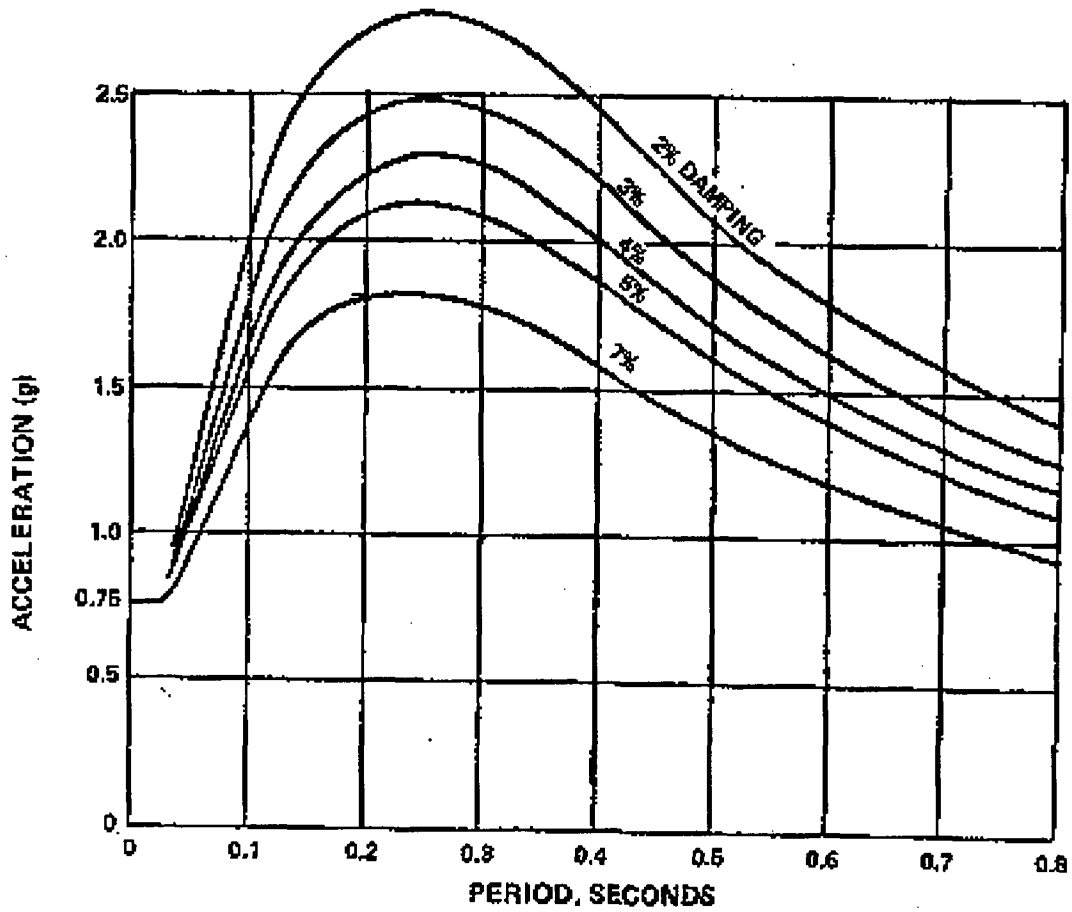

FSAR UPDATE
UNITS 1 AND 2 DIABLO CANYON SITE
FIGURE 2.5-29 FREE FIELD SPECTRA HORIZONTAL HOSGRI 7.5M/BLUME

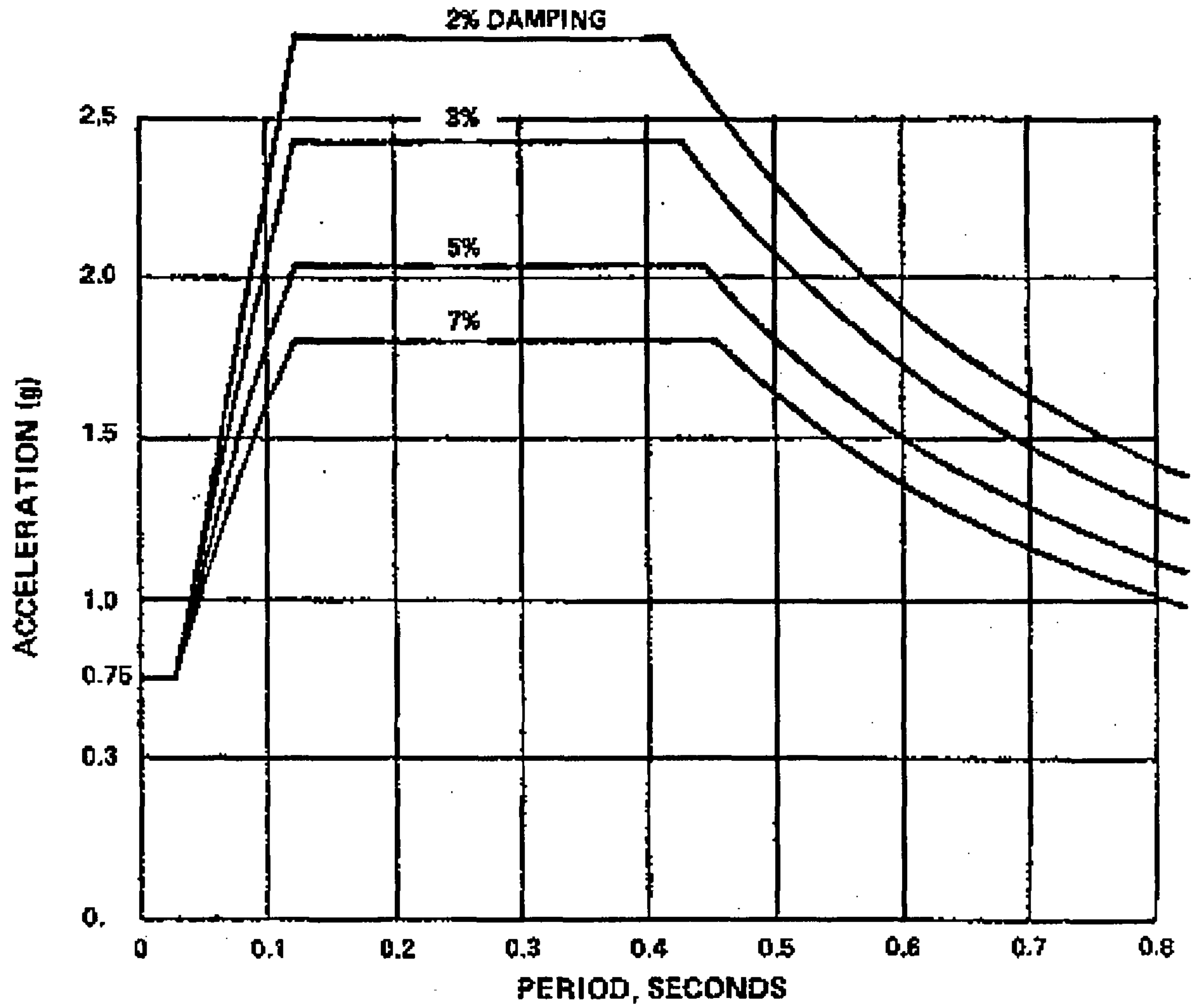

FSAR UPDATE
UNITS 1 AND 2 DIABLO CANYON SITE
FIGURE 2.5-30 FREE FIELD SPECTRA HORIZONTAL HOSGRI 7.5M/NEWMARK

Revision 11 November 1996

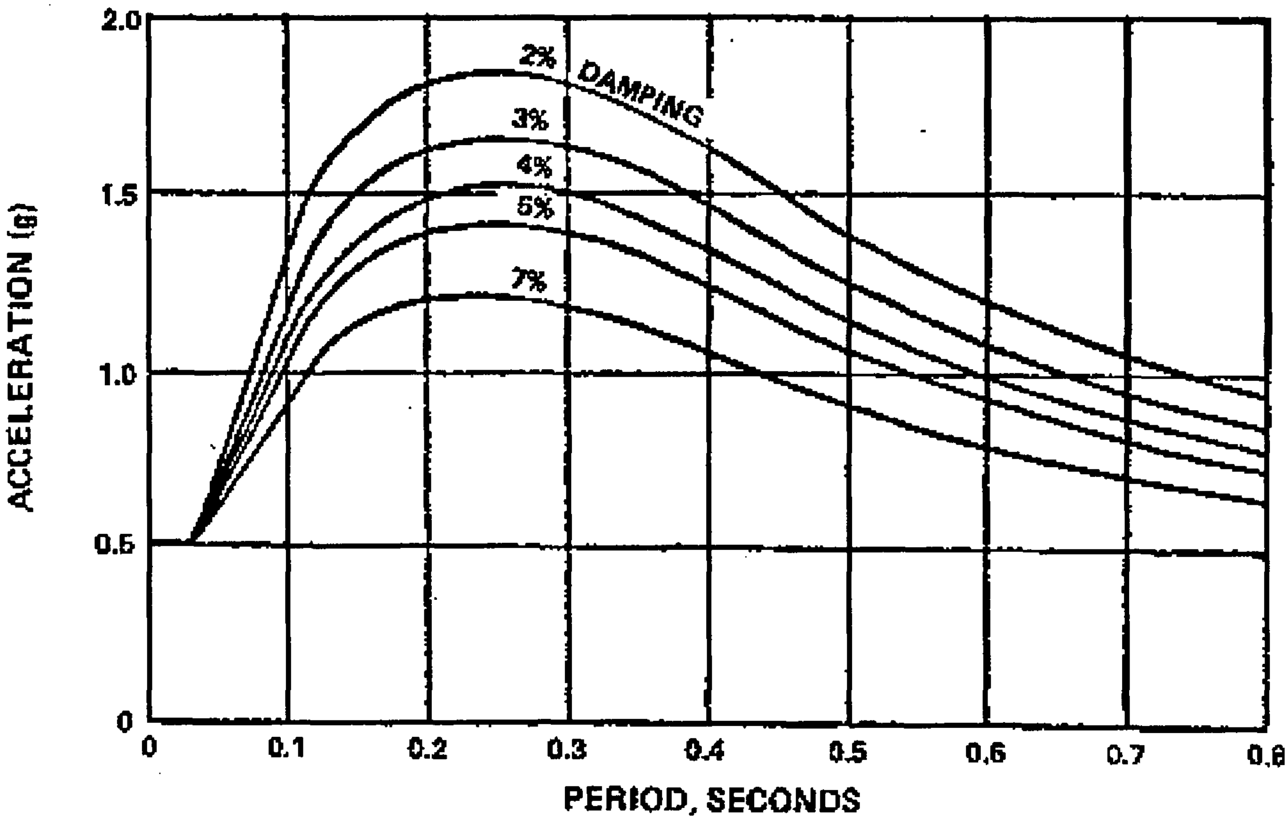

FSAR UPDATE

UNITS 1 AND 2
DIABLO CANYON SITE

FIGURE 2.5-31
FREE FIELD SPECTRA
VERTICAL
HOSGRI 7.5M/BLUME

Revision 11 November 1996

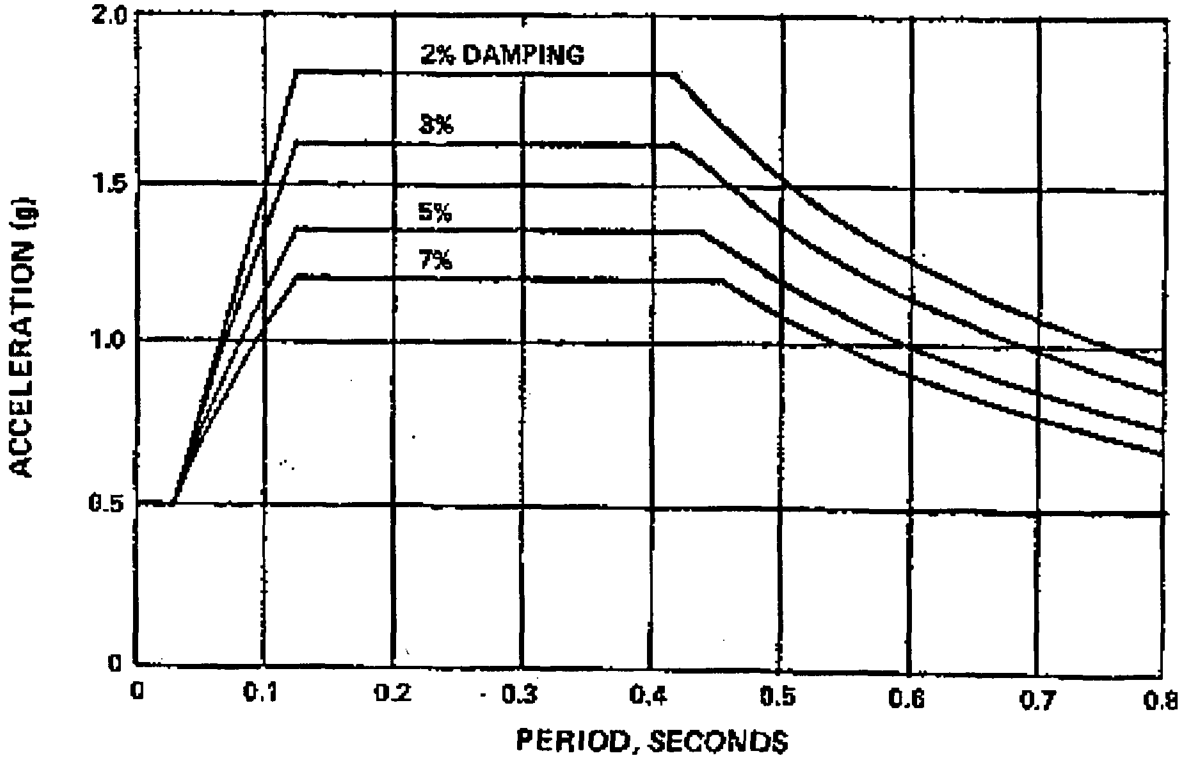

FSAR UPDATE
UNITS 1 AND 2 DIABLO CANYON SITE
FIGURE 2.5-32 FREE FIELD SPECTRA VERTICAL HOSGRI 7.5M/NEWMARK

Revision 11 November 1996

3.2 CLASSIFICATION OF STRUCTURES, SYSTEMS, AND COMPONENTS

This section provides a guide to the classification of the DCPP structures, systems, and components (SSCs).

Criterion 1 of the July 1967 GDC requires that systems and components essential to the prevention of accidents be designed, fabricated, erected, and tested to quality standards commensurate with the importance of the safety functions to be performed. This section describes how Criterion 1 has been implemented by relating the classifications of SSCs to the various criteria, codes, regulations, and standards that dictate specific quality requirements.

In this regard, it is recognized that during the design and construction of DCPP Units 1 and 2, significant industry and regulatory changes were made in establishing common methods of classification, e.g., ANSI N18.2(1), SG 26(2), SG 29(3), and NRC Regulatory Guide (RG) 1.143(6). These methods all differ slightly in detail from those used for the DCPP, but the form and intent of all are equivalent, as will be shown in the following discussion of: (a) the seismic classification of SSCs, and (b) the system quality group classification of pressure-containing components of fluid systems.

Classifications of instruments and controls and requirements for them are discussed in Section 7.1.

3.2.1 SEISMIC CLASSIFICATION

Criterion 2 of the July 1967 GDC, and Appendix A to 10 CFR 100, Seismic and Geologic Siting Criteria for Nuclear Power Plants, require that nuclear power plant SSCs important to safety be designed to withstand the effects of earthquakes. Specifically, Appendix A to 10 CFR 100 requires that all nuclear power plants be designed so that, if the safe shutdown earthquake (SSE) occurs, all structures and components important to safety remain functional. Plant features important to safety are those necessary to ensure (a) the integrity of the reactor coolant pressure boundary, (b) the capability to shut down the reactor and maintain it in a safe shutdown condition, or (c) the capability to prevent or mitigate the consequences of accidents that could result in potential offsite exposures comparable to the guideline exposures of 10 CFR 100.

The SSE of Appendix A to 10 CFR 100 is equivalent to the DCPP double design earthquake (DDE) (see References 9 and 10 for final resolution of issues raised in Supplemental Safety Evaluation Reports 7, 8, and 31 relative to the SSE). Similarly, the operating basis earthquake (OBE) of Appendix A to 10 CFR 100 is equivalent to the DCPP DE.

DCPP's capability to withstand a postulated Richter magnitude 7.5 earthquake centered along an offshore zone of geologic faulting known as the "Hosgri Fault" has been reviewed. Guidance for determining the SSCs designed to remain functional in the

B/5

event of an SSE is provided in SG 29. These plant features, including their foundations and supports, are designated as Seismic Category I in SG 29. DCPP SSCs, and their seismic design classifications comply with the intent of SG 29. However, since DCPP design and construction had progressed substantially prior to the issuance of SG 29, different terminology is often used.

Plant features that correspond to Seismic Category I, as identified in SG 29, are designed to remain functional during the design basis earthquakes that they are required to withstand: the DE (equivalent to the OBE of SG 29), the DDE (equivalent to the SSE of SG 29), and/or the postulated Hosgri earthquake (HE). Design Class I plant features are designed to maintain their structural integrity in the event of both the DE/DDE and HE. They may or may not be designed to remain operable for the DE/DDE or HE; the design basis function of the equipment determines whether it is qualified for active or passive function for a DE/DDE and/or an HE.

All plant features designated as Design Class I are also Seismic Category I. SSCs not identified as Seismic Category I in SG 29, are referred to by the guide as Nonseismic Category I features. Under the DCPP classification system, Design Class II features may or may not be Seismic Category I.

SSCs important to reactor operation but not essential to safe shutdown and isolation of the reactor, and failure of which would not result in the release of substantial amounts of radioactivity, are classified as Design Class II.

SSCs not related to reactor operation or safety are classified as Design Class III.

Power and auxiliary service piping systems (as defined in ANSI B31.1, Paragraph 100.1), which might otherwise be considered as Design Class III, are classified as Design Class II (i.e., Design Class III is not used for power and auxiliary service piping systems).

In addition, Appendix B to 10 CFR 50, Quality Assurance Criteria for Nuclear Power Plants and Fuel Reprocessing Plants, requires that SSCs important to safety be designed and constructed in accordance with the quality assurance requirements described in Appendix B. Therefore, as described in Chapter 17, the requirements of the DCPP Quality Assurance Program apply to all SSCs classified as Design Class I. This ensures that plant features important to safety have met the requirements of Appendix B. Specific quality assurance requirements may also be applied to selected Design Class II features.

The general applicability and requirements of the design class, quality/code class classification, and seismic category are provided in Tables 3.2-1 and 3.2-2.

The classifications of specific SSCs are provided in the DCPP Q-List (see Reference 8). The DCPP Q-List is controlled by a written PG&E procedure. The procedure requires that all non-editorial changes to the contents of the Q-List be reviewed pursuant to the

requirements of 10 CFR 50.59. Access to the Q-List is available through hard copy or electronically at PG&E. The piping schematic drawings are illustrated in Figures 3.2-1 through 3.2-27.

The piping symbol system that appears on all piping schematics and drawings to indicate piping fabrication, erection, and test criteria can be correlated to the design and quality code classes as follows:

Piping Schematic Correlation

Piping Symbol	Design Class	Quality Code Class
A	I	I
B	I	II
@[a]	I/II	II/None
C	I	III
D	I	III
E	II	None
F	II	None
G	II	None
G1	II	None
H	II	None
J	I	III
-[b]	I	Not Applicable
-[b]	II or III	None

Those SSCs, including their foundations and supports, that have been classified as Design Class I and designed to remain functional in the event a DDE or HE occurs, and to which the requirements of the Quality Assurance Program apply, are:

(1) The reactor coolant pressure boundary

(2) The reactor core and reactor vessel internals

(3) Systems [see Note (i)](c) or portions of systems that are required for emergency core cooling, postaccident containment heat removal, or postaccident containment atmosphere cleanup [see Note (v)]

[a] The symbol '@' is referred to in the FSAR Update and the Q-List. However, this symbol is not used on the piping schematics for Code Class designation; the line is bubbled (i.e., -0-0-) and the notes describe the applicable code(s).
[b] For HVAC system ductwork symbols, see Figures 3.2-1A and 3.2-2A.
[c] See Notes at the end of this subsection.
[a] The 1971 edition of the ASME Boiler and Pressure Vessel Code, Section III, Nuclear Power Plant Components, uses the term Class I in lieu of Class A.

(4) Systems or portions of systems that are required for reactor shutdown and residual heat removal

(5) Those portions of the main steam, feedwater, and steam generator blowdown systems extending from and including the secondary side of the steam generators up to and including the outermost containment isolation valves, and connected piping up to and including the first valve (including a safety or relief valve) that is either normally closed or capable of automatic closure during all modes of normal reactor operation [see Note (v)]

(6) Auxiliary saltwater, component cooling water, and auxiliary feedwater systems or portions of these systems that are required for emergency core cooling, postaccident containment heat removal, postaccident containment atmosphere cleanup, and residual heat removal

(7) Component cooling water system and seal water systems, or portions of these systems that are required for functioning of other systems or components important to safety

(8) Those portions of systems (other than the radioactive waste management systems) that contain or may contain radioactive material and whose postulated failure could result in conservatively calculated potential offsite exposures in excess of 0.5 rem whole body (or its equivalent to parts of the body) at the site boundary or beyond

(9) Systems or portions of systems that are required to supply fuel for emergency equipment

(10) Systems or portions of systems that are required for (a) post accident monitoring of RG 1.97 Category 1 variables and (b) actuation of systems important to safety

(11) The protection system [see Note (ii)]

(12) The spent fuel storage pool structure, including the spent fuel racks.

(13) The reactivity control systems, i.e., control rods, control rod drives, and boron injection system, that are required to achieve safe shutdown of the plant

(14) The control room, including its associated vital equipment and life support systems, and any structures or equipment inside or outside of the control room whose failure could result in incapacitating injury to the operators

(15) Reactor containment structure, including penetrations [see Note (iv)]

(16) Systems or portions of systems that are required to provide heating, ventilating, and/or air conditioning for safety-related equipment/areas

(17) Portions of the onsite electric power system, including the onsite electric power sources, that provide the emergency electric power needed for functioning of plant features included in Items (1) through (16) above

(18) Portions of the spent fuel pool cooling system used to remove spent fuel decay heat from the spent fuel pool, and portions of the refueling water purification system used to recirculate and cleanup the contents of the refueling water storage tank

Notes:

(i) A system boundary includes those portions of the system required to accomplish the specified safety function and connected piping up to and including the first valve (including a safety or relief valve) that is either normally closed or capable of automatic closure when the safety function is required.

(ii) For purposes of these criteria, the protection system encompasses all electrical and mechanical devices and circuitry (from sensors to actuation devices input terminals) involved in generating those signals associated with the protective function. These signals include those that actuate reactor trip and, in the event of a serious reactor accident, that actuate ESFs such as containment isolation, safety injection, pressure reduction, and air cleaning.

(iii) SSCs that form interfaces between Design Class I and Design Class II or III features are designed to Design Class I requirements.

(iv) Certain valves in these systems that are used for accident mitigation only, and do not support safe shutdown following an HE, were qualified for active function for an HE to provide increased conservatism in accordance with Reference 7.

3.2.2 SYSTEM QUALITY GROUP CLASSIFICATIONS

GDC 1 requires that systems and components essential to the prevention of accidents be designed, fabricated, erected, and tested to quality standards commensurate with the importance of the safety functions to be performed. This section describes the quality classification system that has been used to implement quality standards that satisfy Criterion 1 for DCPP fluid systems and fluid system components. The discussion also shows the relationship of this classification system to fluid system and fluid system components classification systems in ANSI N18.2, Nuclear Safety Criteria for the Design of Stationary Pressurized Water Reactor Plants[1], and SG 26.

DCPP SSCs are classified as Design Class I, II, or III. Design Class I is Seismic Category I and is further categorized as PG&E Quality/Code Class I, II, or III.

Design Classes II or III are usually Nonseismic Category I and have no PG&E quality/code class designation. Specific requirements as dictated by the quality standards applicable to the respective commercial (ASME, ANSI, or ASA) code classes are also applicable. However, some Design Class II components have been seismically designed, e.g., items in the Seismically Induced Systems Interaction Program, specific components required for post-HE shutdown, CCW header C components, and items that were designed for the DE pursuant to RG 1.143. For this reason, there is not a direct correlation between design class and seismic category (except that all Design Class I features are Seismic Category I). In addition, the classification of Seismic Category I does not indicate which of the three design basis earthquakes a feature has been qualified for, nor whether that qualification is for passive or active function (except that all electrical Class 1E and Instrument Class IA components are qualified to remain operable for all three design basis earthquakes). The design basis function of the equipment determines the type of seismic qualification required. These classifications and their relationships are illustrated in Table 3.2-2 and discussed below.

3.2.2.1 Design Class I, Quality/Code Class I Fluid Systems and Fluid System Components

10 CFR 50.55a requires that certain components of the reactor coolant pressure boundary be designed, fabricated, erected, and tested in accordance with the requirements for Class A[a] components of Section III of the ASME Boiler and Pressure Vessel Code, or the most recently available industry codes and standards. Code Class I has been applied to those components of the reactor coolant pressure boundary and implements the quality standards that satisfy the requirements of Section 50.55a, 10 CFR 50. DCPP Code Class I components of the reactor coolant pressure boundary are listed in the DCPP Q-List[8], along with the industry codes and standards used for their design, fabrication, erection, and test. The Code Class I classification includes the components of the reactor coolant pressure boundary identified as Safety Class I in ANSI N18.2 and Quality Group A in SG 26.

3.2.2.2 Design Class I, Quality/Code Class II Fluid Systems and Fluid System Components

Generally, Code Class II has been applied to include fluid systems and fluid system components that are either:

(1) Part of the reactor coolant boundary, but excluded from Code Class I requirements by Section 50.55a of 10 CFR 50

(2) Not part of the reactor coolant pressure boundary, but part of:

(a) Systems or portions of systems[(b)] that are required for emergency core cooling, postaccident containment heat removal, or postaccident containment atmosphere cleanup

(b) Systems or portions of systems that are required for reactor shutdown and residual heat removal

(c) Those portions of the main steam, feedwater, and steam generator blowdown systems extending from and including the secondary side of steam generators up to and including the outermost containment isolation valves, and connected piping up to and including the first valve (including a safety or relief valve) that are either normally closed or capable of automatic closure during all modes of normal reactor operation

(d) Systems or portions of systems that are connected to the reactor coolant pressure boundary and are not capable of being isolated from the boundary during all modes of normal reactor operation by two valves, each of which is either normally closed or capable of automatic closure

Code Class II fluid systems and fluid system components are listed in the DCPP Q-List (see Reference 8), along with the industry codes and standards used for their design, fabrication, erection, and testing.

3.2.2.3 Design Class I, Quality/Code Class III Fluid Systems and Fluid System Components

Generally, Code Class III has been applied to include fluid systems and fluid system components not part of the reactor coolant pressure boundary, nor included in Code Class II, but part of:

(1) Auxiliary saltwater, component cooling water, and auxiliary feedwater systems, or portions of these systems that are required for (a) emergency core cooling, (b) postaccident containment heat removal, (c) postaccident containment atmosphere cleanup, and (d) residual heat removal from the reactor

(2) Systems or portions of systems that are connected to the reactor coolant pressure boundary and are capable of being isolated from the boundary during all modes of normal reactor operation by two valves, each of which is either normally closed or capable of automatic closure

---

(b) The system boundary includes those portions of the system required to accomplish the specified safety function and connected piping up to and including the first valve (including a safety or relief valve) that is either normally closed or capable of automatic closure when the safety function is required.

(3) Those portions of systems other than radioactive waste management systems that contain or may contain radioactive material, and whose postulated failure could result in conservatively calculated potential offsite exposures in excess of 0.5 rem whole body (or its equivalent to parts of the body) at the site boundary or beyond

(4) Component cooling water system and seal water systems, or portions of these systems, that are required for functioning of other systems or components important to safety

(5) Portions of the spent fuel pool cooling system required for spent fuel cooling, and the refueling water purification system whose postulated failure could result in a loss of refueling water storage tank inventory

Code Class III fluid systems and fluid system components are listed in the DCPP Q-List (see Reference 8), along with the industry codes and standards used for their design, fabrication, erection, and testing.

3.2.2.4 Other Fluid Systems and Fluid System Components

Fluid systems and fluid system components that are not part of the reactor coolant pressure boundary, not essential to shut down the reactor and maintain it in a safe condition, and not essential to prevent or mitigate the consequences of accidents that could result in potential offsite exposures comparable to the guideline exposures of 10 CFR 100, are not included in the Design Class I classification.

These other systems and components are classified as Design Class II or III and are listed in the DCPP Q-List (see Reference 8), along with the industry codes and standards used for their design, fabrication, erection, and testing. They comprise a design class, but have not been assigned a code class. Design Class II includes the fluid systems and fluid system components identified as Quality Group D in SG 26 and as radioactive waste management system in RG 1.143, i.e., those fluid systems and fluid system components that contain or may contain radioactive material, but whose failure would not result in calculated potential exposures in excess of 0.5 rem whole body (or its equivalent to parts of the body) at the site boundary. These fluid systems and fluid system components are in conformance with the accepted industry codes and standards in effect during the design and construction of DCPP. If they were designed and constructed to codes and standards outside of the requirements of SG 26 or RG 1.143, additional quality standards have normally been applied so that the intent has been met.

3.2.2.5 Summary of System Quality Group Classifications

Table 3.2-2 summarizes the design and quality group classifications applied to the DCPP SSCs and their relationships to the other methods of classification.

Generally, codes and standards were applied prior to issuance of the latest codes and standards, such as the 1971 edition of the ASME Boiler and Pressure Vessel Code, Section III, Nuclear Power Plant Components. In some cases, fluid systems and components were designed and built to codes and standards outside the requirements of SG 26, ANSI N18.2, and RG 1.143 definitions. The classification for those fluid systems and fluid system components that do not fall within the strict definition of SG 26, ANSI N18.2, and RG 1.143 were established prior to ANSI N18.2, SG 26, RG 1.143, and the issuance of revised industry codes and standards. For these fluid systems and fluid system components, the design specifications specified the accepted industry codes and standards in effect during the design and construction of DCPP.

While some portions of the fire protection system components are designated Design Class I, the system is not required to ensure the integrity of the reactor coolant pressure boundary or to shut down the reactor and maintain it in a safe shutdown condition. Fire protection features meet the requirements defined in BTP APCSB 9.5-1 (Reference 5) after 1979 and, where designated Design Class I, are designed to withstand the effects of an HE.

3.2.3 REFERENCES

1. Nuclear Safety Criteria for the Design of Stationary Pressurized Water Reactor Plants. N18.2 American Nuclear Society, August 1970 Draft.

2. Quality Group Classifications and Standards for Water, Steam, and Radioactive Waste Containing Components of Nuclear Power Plants, SG 26, Atomic Energy Commission.

3. Seismic Design Classification, SG 29, US Atomic Energy Commission.

4. Spent Fuel Storage Facility Design Basis, RG 1.13, Nuclear Regulatory Commission.

5. Guidelines for Fire Protection for Nuclear Power Plants, BTP APCSP 9.5-1, Nuclear Regulatory Commission.

6. Design Guidance for Radioactive Waste Management Systems, Structures, and Components Installed in Light-Water-Cooled Nuclear Power Plants, RG 1.143, Nuclear Regulatory Commission.

7. PG&E Letter to the NRC, DCL-92-198 (LER 1-92-015).

8. Classification of Structures, Systems, and Components for Diablo Canyon Power Plant Units 1 and 2 (Q-List), PG&E.

9. Letter from NRC (L. F. Miller) to PG&E (G. M. Rueger), dated December 13, 1993, Subject: NRC Inspection of Diablo Canyon Units 1 and 2 (Report No. 50-275, 50-323/93-31) [pages 1 and 2].

10. Letter from NRC (A. W. Beach) to PG&E (G. M. Rueger), dated August 15, 1994, Subject: NRC Inspection Report 50-275/94-18; 50-323/94-18 (Notice of Violation) [pages 14 and 15].

3.2.4 REFERENCE DRAWINGS

Figures representing controlled engineering drawings are incorporated by reference and are identified in Table 1.6-1. The contents of the drawings are controlled by DCPP procedures.

TABLE 3.2-1

DESIGN CLASSIFICATION OF STRUCTURES, SYSTEMS, AND COMPONENTS

Design Class I	Design Class II	Design Class III
Applicability		
Plant features important to safety, including plant features required to assure (1) the integrity of the reactor coolant pressure boundary, (2) the capability to shut down the reactor and maintain it in a safe shutdown condition, or (3) the capability to prevent or mitigate the consequences of accidents which could result in potential offsite exposures comparable to the guideline exposures of 10 CFR 100.	Plant features important to reactor operation, but not essential to safety, including plant features not required to be Design Class I.	Plant features not related to reactor operation or safety.

Design Class I	Design Class II	Design Class III
Requirements		
1. Quality Standards - Plant features required to meet AEC GDC-1.	1. Quality Standards - Plant features not required to meet AEC GDC-1.	1. Quality Standards - Plant features not required to meet AEC GDC-1.
2. Quality Assurance - Plant features required to meet Appendix B to 10 CFR 50.	2. Quality Assurance - Plant features not required to meet Appendix B to 10 CFR 50. Specific QA requirements may be applied to selected features.	2. Quality Assurance – Plant features not required to meet Appendix B to 10 CFR 50.
3. Seismic Design – Plant features required to meet GDC-2 and Appendix A to 10 CFR 100. Plant features designed to withstand effects of double design earthquake (DDE). Features are also designed to maintain their structural integrity (and in some cases their operability) during a Hosgri earthquake.	3. Seismic Design - Plant features not required to meet GDC-2 and Appendix A to 10 CFR 100. Plant features not designed to withstand effects of design earthquakes except for items as required by RG. 1.143, and for selected features where specifically designated.	3. Seismic Design – Plant features not required to meet GDC-2 and Appendix A to 10 CFR 100. Plant features not designed to withstand effects of design Earthquakes, except where specifically designated.

TABLE 3.2-2

DESIGN AND QUALITY GROUP CLASSIFICATIONS

PG&E Engineering			Seismic Design Classification[a]	Quality Group Classification[f]		Remarks
Design Class	Quality/Code Class	Piping Symbol	NRC Reg. Guide 1.29	ANSI N18.2 Safety Group	NRC Reg. Guide 1.26 Quality Group	Other Codes and Standards
I	I	NONE[b]	Category I	1	A	ASA B31.1-1955; ASME B&PV Code, Section III-1971
I	I	A[h]	Category I	1	A	ANSI B31.1-1967; B31.7-1969 with 1970 Addenda, Class I
I	II	B	Category I	2	B	ANSI B31.7-1969 with 1970 Addenda, Class II
I	II	@[g]	Category I	2	B	ANSI B31.1-1967; ASME B&PV Code Section I-1968; Section III-1968
I	III	C	Category I	3	C	ANSI B31.7-1969 With 1970 Addenda, Class III
I	III	D[i]	Category I	3	C	ANSI B31.1-1967; ANSI B31.7-1969 with 1970 Addenda, Class III
II[d]	-	G	Category I[j]			ANSI B31.1-1967 and NFPA Standards
I	III	J[k]	Category I	-	-	ANSI B31.1-1967
II	-	E	Non-Category I	NNS	-	ANSI B31.1, 1967
II	-	F	Non-Category I[e]	NNS	D[c]	ANSI B31.1 1967; RG Guide 1.143

PG&E Engineering			Seismic Design Classification[a]	Quality Group Classification[f]		Remarks
Design Class	Quality/Code Class	Piping Symbol	NRC Reg. Guide 1.29	ANSI N18.2 Safety Group	NRC Reg. Guide 1.26 Quality Group	Other Codes and Standards
II[d]	-	G1	Non-Category I	-	-	NFPA Standards
II	-	H	Non-Category I	NNS	D[c]	ANSI B31.1-1967; RG Guide 1.143
II	-	-	Non-Category I	-	-	Applicable industry codes and standards
III	-	-	Non-Category I	-	-	Applicable industry codes and standards
II	-	@[m]	Non-Category I	NNS	-	ASME B&PV Code, Section I-1980

Notes:

(a) General Design Criterion 2 (1967), Appendix A to 10 CFR 50, and Appendix A to 10 CFR 100.

(b) Reactor coolant loop and pressurizer surge line piping. Design to ASA B31.1-1955 using Nuclear (N) Code Cases N-7, N-9, and N-10. Fabrication, erection, and inspection to ASME B&PV Code Section III-1971.

(c) Radioactive system (PG&E QA Class R). Future activities such as repair, replacement, maintenance, or testing shall be performed per RG. 1.143 for those portions of the systems designated as F or H in Figures 3.2-1 through 3.2-27.

(d) The fire protection system may not have been designed or constructed under a quality assurance program meeting all requirements of 10 CFR 50, Appendix B. However, activities such as repair, replacement, maintenance, or testing shall be performed in accordance with the QA recommendations described in Appendix A to NRC Branch Technical Position 9.5.1 and PD OM8 (PG&E QA Class G). Quality requirements administered shall be commensurate with the safety function of the SSC.

(e) Seismic qualification requires Design Earthquake analysis.

(f) Regulatory Guide 1.26 (formerly AEC Safety Guide 26) establishes quality group classifications for reactor coolant pressure boundary and remaining safety-related components containing radioactive material, water, or steam. Other systems not covered by this guide include instrument and service air, diesel engine and its generators and auxiliary support systems, diesel fuel, emergency and normal ventilation, fuel handling, and radioactive waste management systems.

The Code Class I classification generally includes the fluid systems and components identified as Safety Class I in ANSI N18.2 and Quality Group A in AEC Safety Guide 26. However, the classification and quality standards for Diablo Canyon fluid systems and components were established prior to the existence of these documents and, therefore, do not always fall within their strict definitions. All Code Class I fluid systems and components are in accordance with the accepted industry codes and standards that were in effect during the design and construction of Diablo Canyon. If fluid systems and components were designed and constructed to codes and standards outside of the requirements of the above-mentioned documents, additional quality standards have normally been applied, so that their intent has been met.

The Code Class II classification generally includes the fluid systems and components identified as Safety Class 2a in ANSI N18.2 and Quality Group B in AEC Safety Guide 26. However, the classification and quality standards for Diablo Canyon fluid systems and components were established prior to the existence of these documents and, therefore, do not always fall within their strict definitions. All Code Class II fluid systems and components are in accordance with the accepted industry codes and standards that were in effect during the design and construction of Diablo Canyon. If fluid systems and components were designed and constructed to codes and standards outside of the requirements of the above-mentioned documents, additional quality standards have normally been applied, so that their intent has been met.

The Code Class III classification generally includes the fluid systems and components identified as Safety Classes 2b and 3 in ANSI N18.2 and Quality Group C in AEC Safety Guide 26. However, the classification and quality standards for Diablo Canyon fluid systems and components were established prior to the existence of these documents and, therefore, do not always fall within their strict definitions. All Code Class III fluid systems and components are in accordance with the accepted industry codes and standards that were in effect during the design and construction of Diablo Canyon. If fluid systems and components were designed and constructed to codes and standards outside of the requirements of the above- mentioned documents, additional quality standards have normally been applied, so that their intent has been met.

An exception exists to the above for Quality Code Class III piping Code Class D piping. These are systems or portions of systems which were originally constructed as Design Class II and were subsequently upgraded to Design Class I because of later requirement. For such piping, the design analysis is in accordance with Design Class I criteria. All construction, repair, or replacement performed after the upgrade is in accordance with Design Class I requirements.

(g) Feedwater piping from the (final) main feedwater check valve to the steam generator; auxiliary feedwater from the main feedwater line back to the second check valve; main steam piping from the steam generator to the main steam isolation valve; steam generator blowdown piping from the steam generator to the first valve outside containment; design to ANSI B31.1-1967; fabrication, erection, and inspection to ASME B&PV Code Section I-1968. Requirements for the main steam safety valves are in accordance with ASME B&PV Code Section III-1968.

(h) Design to ANSI B31.1-1967. Fabrication, erection, and inspection to ANSI B31.7-1969 with 1970 Addenda, Class I.

(i) This piping code class applies to: (1) the spent fuel pool cooling loop; (2) the auxiliary feedwater pump suction piping from the fire water storage tank; and (3) the refueling water purification loop from and to the refueling water storage tank. This piping was upgraded from Design Class II Code Class E. B31.1 applies for work performed prior to the upgrade. B31.7 applies to work performed after the upgrade.

(j) Piping is seismically qualified for the Hosgri earthquake.

(k) Piping originally installed as Design Class II and has been qualified seismically for the Hosgri earthquake, but is Design Class I for repair, replacement, and new construction.

(l) Certain Design Class II and III SSCs have seismic qualification requirements and may be designated as Seismic Category I; these SSCs are designated as QA Class S.

(m) Auxiliary Boiler 0-2 and its external piping conforms to ASME B&PV Code Section I-1980 through summer 1980 Addenda.

3.7 SEISMIC DESIGN

3.7.1 SEISMIC INPUT

This section describes the DE, the DDE, and the postulated 7.5M HE.

In addition to the above three earthquakes, PG&E conducted, as described below, a program to reevaluate the seismic design for DCPP. On November 2, 1984, the NRC issued the DCPP Unit 1 Facility Operating License DPR-80. In License Condition 2.C(7) of DPR-80, the NRC stated, in part: "PG&E shall develop and implement a program to reevaluate the seismic design bases used for the Diablo Canyon Power Plant."

PG&E's reevaluation effort in response to the license condition was titled the "Long Term Seismic Program" (LTSP). PG&E prepared and submitted to the NRC the "Final Report of the Diablo Canyon Long Term Seismic Program" in July 1988 (Reference 19). The NRC reviewed the Final Report between 1988 and 1991, and PG&E prepared and submitted written responses to NRC questions resulting from that review. In February 1991, PG&E issued the "Addendum to the 1988 Final Report of the Diablo Canyon Long Term Seismic Program." (Reference 20) In June 1991, the NRC issued Supplement 34 to the Diablo Canyon Safety Evaluation Report (SSER) (Reference 21), in which the NRC concluded that PG&E had satisfied License Condition 2.C(7) of DPR-80. In the SSER the NRC requested certain confirmatory analyses from PG&E, and PG&E subsequently submitted the requested analyses. The NRC's final acceptance of the LTSP is documented in a letter to PG&E dated April 17, 1992 (Reference 22).

The LTSP contains extensive databases and analyses that update the basic geologic and seismic information in this FSAR Update. However, the LTSP material does not alter the design bases for DCPP. In SSER 34 (Reference 21), the NRC states, "The Staff notes that the seismic qualification basis for Diablo Canyon will continue to be the original design basis plus the Hosgri evaluation basis, along with associated analytical methods, initial conditions, etc."

PG&E committed to the NRC in a letter dated July 16, 1991 (Reference 23), that certain future plant additions and modifications, as identified in that letter, would be checked against insights and knowledge gained from the LTSP to verify that the plant margins remain acceptable.

A completed listing of bibliographic references to the LTSP reports and other documents are provided in References 19, 20, and 21.

3.7.1.1 Design Response Spectra

Section 2.5.2 provides a discussion of the earthquakes postulated for the DCPP site and the effects of these earthquakes in terms of maximum free-field ground motion accelerations and corresponding response spectra at the plant site. The maximum

B/6

vibratory accelerations at the plant site would result from either Earthquake B or Earthquake D-modified, depending on the natural period of the vibrating body. Response acceleration spectra curves for horizontal free-field ground motion at the plant site from Earthquake B, Earthquake D-modified, and HE are presented in Figures 2.5-20, 2.5-21, and 2.5-29 through 32, respectively.

For design purposes, the response spectra for each damping value from Earthquake B and Earthquake D-modified are combined to produce an envelope spectrum. The acceleration value for any period on the envelope spectrum is equal to the larger of the two values from the Earthquake B spectrum and the Earthquake D-modified spectrum. Vertical free field ground accelerations, and the vertical free-field ground motion response spectra are assumed to be two-thirds of the corresponding horizontal spectra.

The DE is the hypothetical earthquake that would produce these horizontal and vertical vibratory accelerations. The DE corresponds to the operating basis earthquake (OBE), as described in Appendix A to 10 CFR 100 (Reference 7).

To ensure adequate reserve energy capacity, Design Class I structures and equipment are reviewed for the DDE. The DDE is the hypothetical earthquake that would produce accelerations twice those of the DE. The DDE corresponds to the SSE, as described in Appendix A to 10 CFR 100 (Reference 7).

PG&E was requested by the NRC to evaluate the plant's capability to withstand a postulated Richter magnitude 7.5 earthquake centered along an offshore zone of geologic faulting, generally referred to as the Hosgri Fault. This evaluation is discussed in the various chapters when it is specifically referred to as the Hosgri evaluation or Hosgri event evaluation.

Acceleration response spectra curves for horizontal and vertical free field ground motion at the plant site from the HE are the Newmark and Blume spectra described in Section 2.5. The vertical free field response spectra are two-thirds of the corresponding horizontal spectra.

3.7.1.2 Design Response Spectra Derivation

The free-field ground motion acceleration time-histories used in the dynamic analyses of the containment structure, auxiliary building, turbine building, and intake structure are developed by the following procedure: The response spectra for 2 percent damping for Earthquake B and Earthquake D-modified are enveloped to produce a single response spectrum (DE intensity). A time-history is then developed that produces a spectrum with no significant deviation from the smooth DE-envelope spectrum. This procedure eliminates undesirable peaks and valleys that exist in the response spectrum calculated directly from Earthquake B and Earthquake D-modified records.

A similar procedure is used to obtain a free-field ground motion acceleration time-history for the DDE. The free-field ground motion acceleration time-histories for the DE and

DDE are shown in Figures 3.7-1 and 3.7-2, respectively. Comparison of the response spectrum computed from the time-history with the smoothed envelope spectrum is shown in Figure 3.7-3 (2 percent damping) and in Figure 3.7-4 (5 percent damping). These spectra are calculated at period intervals of 0.01 seconds, which adequately define the spectra.

For the HE evaluation of containment structure, auxiliary building, turbine building, and intake structure, the horizontal input motions are reduced from free-field motions to account for the presence of the structures that have large foundations. These reduced inputs have been derived by spatial averaging of acceleration across the foundations of each structure by the Tau filtering procedure (Reference 12). The resulting horizontal response spectra for these structures are shown in Figures 3.7-4A through 3.7-4F.

For HE evaluation of outdoor water storage tanks and smaller structures, the horizontal design response spectra are the free-field horizontal response spectra. HE vertical design response spectra are the free-field vertical response spectra. For design purposes, the Newmark spectra are used, or alternately the Blume spectra are used, with adjustment in certain frequency ranges as necessary so that they do not fall below the corresponding Newmark spectra.

Acceleration time-histories used in the analysis of the containment and intake structures, auxiliary building, and turbine building are shown in Figures 3.7-4G through 3.7-4M. Comparison of the response spectrum computed from each time-history with the corresponding design response spectrum for 7 percent damping is shown in Figures 3.7-4N through 3.7-4T.

3.7.1.3 Critical Damping Values

The specific percentages of critical damping used for Design Class I SSCs, and the Design Class II turbine building and intake structure are listed in the following table:

Type of Structure	% of Critical Damping		
	DE	DDE	HE
Containment structures and all internal concrete structures	2.0	5.0	7.0
Other conventionally reinforced concrete structures above ground, such as shear walls or rigid frames	5.0	5.0	7.0
Welded structural steel assemblies	1.0	1.0	4.0
Bolted or riveted steel assemblies	2.0	2.0	7.0
Mechanical components (PG&E purchased)	2.0	2.0	4.0
Vital piping systems (except reactor coolant loop)[(a)]	0.5	0.5	3.0[(b)]

Type of Structure	% of Critical Damping DE	DDE	HE
Reactor coolant loop[a][c]	1.0	1.0	4.0
Replacement Steam Generators[f]	2.0	4.0	4.0
Integrated Head Assembly[g]	4.9	6.85	6.85
CRDMs[h]	5.0	5.0	5.0
Foundation rocking (containment structure only)[d]	5.0	5.0	NA[e]

(a) ASME Code Case N-411 damping may be used provided it is applied to all earthquake cases and used in response spectrum modal superposition analysis. When used, pipe displacements are checked for adequacy of clearances and pipe mounted equipment accelerations are verified against project qualification criteria.
For equipment and components modeled inline, damping should be consistent with RG 1.61; a composite damping value may be used for the analysis of these piping systems. A log of calculations is kept that indicates which calculations have used Code Case N-411 damping.

Request for NRC approval for the use of ASME Code Case N-411 was made in letter DCL-86-009, dated January 22, 1986. NRC approval was granted by letter on April 7, 1986

(b) Two percent of critical damping is used for piping less than or equal to 12 inches in diameter.

(c) Although a damping value of 1 percent is used for the DE and DDE analyses of the reactor coolant loop (RCL), damping values of greater than 4 percent have been measured experimentally for the RCL in full-size power plants (Reference 8). These testing programs have been reviewed and approved by the NRC. The damping values recommended in RG 1.61 are acceptable for use in analysis of mechanical equipment and systems. (References 24-26)

(d) Five percent of critical damping is used for structures founded on rock for the purpose of computing the response in the rocking mode, and 7 percent of critical damping is used for the purpose of computing the response in the translation mode.

(e) Analysis utilizes fixed base.

(f) These values are valid for replacement steam generator (RSG) internals and shell components up to the RSG nozzle to pipe/tube connections in the RCS, MS, and FW systems and the interface between the RSG shell and upper and lower lateral and lower vertical supports. The restrictions imposed by WCAP 7921-AR (Reference 8) shall be observed when applying these values. (Reference 27)

(g) Damping values for the IHA are based on Regulatory Guide 1.61, Revision 1 (Reference 31), Tables 1 and 2, using a weighted average for "Welded Steel or Bolted Steel with Friction Connections" and "Bolted Steel with Bearing Connections". See PG&E Document 6023227-19 (Reference 30) for computation of weighted average value. Computation of weighted average value was approved in Reference 32.

(h) Damping values for the CRDMs are based on Regulatory Guide 1.61, Revision 1 (Reference 31), as approved in Reference 33.

3.7.1.4 Bases for Site-Dependent Analysis

Site conditions used to develop the shape of site seismic design response spectra are described in Section 2.5.2.

3.7.1.5 Soil-Supported Design Class I Structures

All Design Class I plant structures are founded on rock or on concrete fill.

3.7.1.6 Soil-Structure Interaction

Soil-structure interaction effects are considered as described in Section 3.7.2.1.7.

3.7.1.7 Hosgri Evaluation

The criteria and methods used to review the major structures for response to the postulated 7.5M HE are discussed in this chapter. A comparison of the DE and the DDE criteria with the HE evaluation criteria is given in Table 3.7-1 for the containment and auxiliary building, Tables 3.7-1A for the turbine building, 3.7-1B for the intake structure, and 3.7-1C for the outdoor water storage tanks, respectively.

3.7.2 SEISMIC SYSTEM ANALYSIS

In accordance with Revision 1 to RG 1.70, paragraphs under the headings below Seismic Analysis Methods and Description of Seismic Analyses, apply to all seismic analysis performed, i.e., both seismic system analysis and seismic subsystem analysis. Paragraphs under subsequent headings in this section provide discussion of specific topics applicable to seismic system analysis. Discussion of specific topics applicable to seismic subsystem analysis is provided in Section 3.7.3. The seismic analysis of Design Class I SSCs is based on input motions of the DE, DDE, and HE described in Section 3.7.1.

3.7.2.1 Seismic Analysis Methods

Four dynamic methods of seismic analysis are used for Design Class I SSCs: time-history modal superposition, response spectrum modal superposition, response spectrum single-degree-of-freedom, and the method for rigid equipment and piping.

The concept of modal analysis and each of the four methods of seismic analysis are discussed in subsequent paragraphs.

3.7.2.1.1 Modal Analysis

The structure, system, or component is represented as a mathematical model that is in the form of lumped masses interconnected by springs or finite elements. The mathematical model typically has one, two, or three degrees of freedom for each lumped mass or node point, but could have as many as six degrees of freedom for each lumped mass or node point.

Each multiple-degree-of-freedom (multidegree) system has the same number of normal modes as it has degrees of freedom. The characteristics of a normal mode of vibration is that, under certain conditions, the multidegree system could vibrate freely in that mode alone, and during such vibration the ratio of displacements of any two masses is constant with time. These ratios define the characteristic shape of the mode. For any vibration of the multidegree system, the motion in any of the individual normal modes can be treated as an independent single-degree-of-freedom system, and the complete motion of the multidegree system can be obtained by superimposing the independent motions of the individual modes.

The natural frequencies and characteristic shapes are determined by solution of the equations of motions for free vibrations.

3.7.2.1.2 Time-History Modal Superposition

The time-history of response in each mode is determined from the acceleration time-history input by integration of the equations of motion. The modal responses are combined by algebraic sum to produce an accurate summation at each step.

3.7.2.1.3 Response Spectrum Modal Superposition

The response spectrum is a plot, for all periods of vibration, of the maximum acceleration experienced by a single-degree-of-freedom vibrating body during a particular earthquake. The response spectrum modal superposition method of analysis applies to multidegree systems and is based on the concept of modal analysis. The modal equation of motion for a multidegree system is analogous to the equation of motion for a single degree of freedom. The maximum response in each mode is calculated, and modal responses (displacements, accelerations, shears, moments, etc.) are combined by the square root of the sum of the squares (SRSS) method.

3.7.2.1.4 Response Spectrum, Single-Degree-of-Freedom

Many components can be accurately represented by a single-degree-of-freedom mathematical model. The response spectrum method of analysis is applicable and the concept of modal analysis is not required.

3.7.2.1.5 Static Equivalent Method

When it can be shown that a sub-system is rigid, a static analysis may be performed. The zero period acceleration obtained from the applicable response spectra curve may be used in static calculations.

3.7.2.1.6 Application

All Design Class I structures, components, systems, and piping are designed by time-history modal superposition, response spectrum modal superposition, response spectrum single-degree-of-freedom, or the method for rigid equipment and piping, except the following:

(1) Mechanical equipment whose seismic adequacy is verified by testing as described in Section 3.9

(2) Electrical and instrumentation equipment whose seismic adequacy is verified as described in Section 3.10

(3) Certain Design Class I piping less than 2-1/2 inches in diameter that is restrained according to criteria described in Section 3.7.2.1.7.4

(4) Reactor internals, fuel elements, control rod drive assemblies, and control rod drives, as described in Section 3.7.3.15.

3.7.2.1.7 Description of Seismic Analyses

3.7.2.1.7.1 Design Class I Structures

Dynamic analyses by the time-history modal superposition method were performed for the containment structure and the auxiliary building. Acceleration time-histories were obtained at specific points in the structures, and response spectra were calculated from these. In order to provide for possible variations in the parameters used in the dynamic analyses, such as mass values, material properties, and material sections, the calculated spectra were modified. For DE and DDE analyses, it is estimated that the calculated period of the structure could vary by approximately 10 percent, and to account for this the peaks of the spectra were correspondingly widened. Similarly, for HE analyses, peaks of the spectra are widened 5 percent on the low period side and 15 percent on the high period side. The modified spectra, known as "smooth spectra," are used in the design of Design Class I equipment and piping located in the containment structure and auxiliary building.

A detailed analytical static model of the auxiliary building was used to distribute the seismic inertial forces and moments to various walls, diaphragms, and columns, as described in Section 3.8.2.4.

Allowable stresses for Design Class I structures are presented in Section 3.8.

Containment Structure Model

(1) DE and DDE events

The containment structure calculations relative to responses to DE and DDE events are performed with a computer program for analysis of axisymmetric structures by the finite element method. The foundation rock mass and the containment structure are modeled as one structure system to consider the effect of rock-structure interaction, as shown in Figure 3.7-5. The boundary dimensions of the model are selected such that they do not have a significant effect on the response of the structure. The exterior shell and internal structure are modeled using shell elements with four degrees of freedom at each nodal point. There are a total of 156 nodal points and 140 elements in the model. The weight of mechanical equipment in the structure is included in the calculation of equivalent mass density for the structure elements. Values of elastic constants for the rock mass and their variation with depth are based on field measurements made at the plant site (see Section 2.5).
To substantiate that the coupling effect is small at the reactor pressure vessel (RPV) elevation, two floor response spectra were generated for a decoupled interior concrete structure model and a coupled RPV and the interior concrete structure model, respectively. The RPV model is a simplified one-degree-of-freedom system, with its natural frequency matching the fundamental mode of the DCPP vessel. The RPV model is attached to Node 2 of the interior concrete structure model at the vessel support elevation by the spring of the vessel model.

Floor response spectra for the decoupled and the coupled models were very similar, indicating that the coupling effect at this low elevation is very small. More importantly, the response spectra magnitude of the decoupled model is consistently higher than the coupled model between 0.05 to 0.40 seconds, and is equal at all other natural periods. This shows that, indeed, the decoupled model is more conservative.

(2) Hosgri event

The dynamic analysis for HE is performed for exterior shell, interior concrete structures, and the annulus steel structure. The description of these structural components is given in Section 3.8.1.

The elements used in the analysis of exterior shell consist of annular rings of shell elements as shown in Figure 3.7-5A. The model consists of 27 nodal points and 26 elements. A typical shell element has four degrees-of-freedom as shown in Figure 3.7-7. The axisymmetric model is used to compute the translational response of the structure due to the horizontal and vertical ground motion. Since the center of mass and the center of rigidity coincide, the translational analysis does not yield any torsional response. The torsional responses are obtained from separate lumped mass models as shown in Figure 3.7-5B. These lumped mass models account for 5 percent and 7 percent accidental eccentricities. The responses from axisymmetric model and the lumped mass models are combined by absolute sum for 5 percent eccentricity and by SRSS for 7 percent eccentricity.

The dynamic analysis of containment internal structure is divided into two parts: concrete interior structure and annulus steel structure.

(a) Concrete interior structure mainly comprised of reactor cavity walls and crane wall is represented by an axisymmetric model as shown in Figure 3.7-5A. The model as shown in Figure 3.7-5A contains 22 nodal points and 22 elements. Because the center of mass and the center of rigidity coincide, the analysis does not yield torsional modes. Therefore, a separate lumped mass model, as shown in Figure 3.7-5C, is used to consider torsional response. Figure 3.7-5D is used to compute vertical responses of the concrete interior structures due to the HE. The lumped mass stick with model points 1, 7, 18, 29, and 40 represent the concrete walls. The annulus steel is modeled by five frames located along the circumference as shown. This model was developed at an early stage of the project to estimate vertical responses of both annulus steel and concrete structures from the HE. However, subsequently detailed models were developed for the annulus steel as described later and the model of Figure 3.7-5D is used for the vertical analysis of the concrete interior structures only.

The models of Figures 3.7-5A, 3.7-5C, and 3.7-5D represent concrete interiors up to elevation 140 feet which is the operating floor of the containment. The secondary shield walls housing the steam generators do extend above elevation 140 feet; however, the mass of these walls above elevation 140 feet is small compared to the total concrete mass and, therefore, lumping the mass at elevation 140 feet of the walls that extend above elevation 140 feet has little effect on the dynamic behavior of concrete internals below elevation 140 feet.

(b) Several models are developed for the vertical dynamic analysis of annulus steel. Each model represents a steel frame with a column at the outside perimeter, crane wall at the inside perimeter, and the radial beam. Figure 3.7-5E represents a typical model.

The horizontal responses of the annulus steel are considered to be the same as the concrete interior structures as computed from model of Figure 3.7-5A. This consideration is supported by:

- The study results showing that the amplification above 20 Hz for the annulus steel is negligible; and

- The modal analysis of steel frames shows that the first mode of vibration, which is the predominant mode, is approximately 20 Hz.

(3) Input boundary motions

In the seismic analysis of the finite element model, for DE and DDE, the motions at the boundary of the rock mass are required as input. These boundary motions are derived using procedures described in the following steps:

(a) The finite element model of the rock mass only (without the structure) is subjected to a unit impulse acceleration acting at the rock mass boundaries. As a result, the acceleration time-history (impulse response that reflects the rock mass properties) is obtained at the center nodal point on the surface of the rock mass.

(b) The impulse response function, together with the desired free-field ground motion, is used as input to a deconvolution program. The required boundary motion is obtained as the output. This boundary motion, when used as input to the nodes along the horizontal and vertical boundaries of the rock mass model, produces a time-history at the center nodal point on the surface of the model that is equivalent to the free-field motion. To check the accuracy of the derived boundary motion, the rock mass without the structure is analyzed using this motion as input, and the computed free-field ground motion at the center nodal point on the surface of the rock mass is obtained. The computed free-field spectrum is calculated for this surface motion and compared with the DE- or DDE-smoothed spectrum. Due to approximations involved in the analytical methods used to derive the boundary motions, the computer spectra show slight deviations from the desired smoothed spectra. To account for these deviations, the structural response

results are then conservatively scaled upward by appropriate correction factors.

The boundary motions derived from the procedure described above are used to complete the analysis of the containment structure.

For the HE, the analytical models are considered fixed as shown in Figures 3.7-5A, 3.7-5B, 3.7-5C, and 3.7-5D. The analysis is performed using the input motions as specified in Section 3.7.1.2.

Containment Polar Crane

The polar crane as described in Sections 9.1.4 and 3.8.1 is an overhead gantry crane, supported by the crane wall inside the containment.

A nonlinear time-history analysis is performed for the crane to consider the possibility of wheel uplift and/or slack in the hook cable. The crane structure model is shown in Figure 3.7-7A. Structural members are represented as beam elements; wheel assemblies as nonlinear gap elements with compression stiffness only, and a hook cable is represented as a truss element with no compression capability. A step-by-step integration procedure is employed to determine the response. The time-step for integration is 0.005 sec. Seismic input is provided by simultaneous, independent time-histories in three directions (two horizontal and one vertical). These time-histories are developed at the top of the crane wall from the dynamic analysis described in Section 3.7.2.1.7.1 above.

Pipeway Structure

To obtain seismic responses in the pipeway structure, a combined model is used consisting of containment exterior shell, pipeway-framing members, and the mainsteam and feedwater piping which are supported by the framing members. The three-dimensional pipeway structure model consists of steel platforms supported on structural steel columns, containment shell and auxiliary and turbine buildings. This structure is represented in the model by beam elements (approximately 900). Oversized holes are provided to support pipeway structure beams on the auxiliary and turbine buildings. Accordingly, the model is decoupled from auxiliary and turbine buildings in the horizontal direction. The horizontal coupling between pipeway framing model and containment model is achieved by rigid links. The main steam and feedwater lines are included in the model since they represent significant masses for the pipeway structure.

The combined containment-pipeway structure model was excited by acceleration time-history at the containment base.

(1) DE and DDE events

Equivalent static analyses of the pipeway structure are performed for the DE and DDE events as described in Section 3.8.6. The adequacy of these analyses is confirmed by a time-history dynamic analysis.

(2) Hosgri event

The response spectra are generated using the time-history dynamic analysis method. The effect of accidental torsion is included as discussed for the containment structure model in Section 3.7.2.1.7.1. These response spectra are used for qualification of equipment and components. The structural qualification is performed using the response spectrum dynamic modal superposition method for the Unit 1 pipeway structure and using the equivalent static method for the Unit 2 pipeway structure.

Auxiliary Building

The dynamic time-history analysis of the auxiliary building is performed with a computer program for analysis of a spring and lumped mass model. Two horizontal models and a vertical model, shown in Figure 3.7-13, are used. Each model is fixed at the base (elevation 85 feet). Each horizontal model consists of five lumped masses with two degrees of freedom at each mass point, one translational degree of freedom in the horizontal direction, and one rotational degree of freedom about the vertical axis. The vertical model for HE evaluation consists of five lumped masses with one translational degree of freedom in the vertical direction at each mass point.

The masses are represented as the mass of the slab plus one-half of the walls immediately above and below the slab, with an appropriate live load on each floor to account for the effect of small pieces of equipment, concrete pads for equipment, tanks, pumps, and incidental weight not otherwise considered. Weights of cranes, storage tanks, and other large pieces of equipment are included at the appropriate mass points. Location of the centers of masses and rigidities are calculated to consider torsional modes of vibration. Mass moments of inertia and torsional rigidities are calculated by conventional structural analysis methods.

The soil at elevation 100 feet is represented by soil springs as shown in Figure 3.7-13. The stiffnesses of these foundation springs are derived by considering the case of a rigid plate on a semi-infinite elastic half-space with a horizontal surface (References 2, 3, and 4). The auxiliary building is a broad-based and comparatively low-rise structure, and therefore rocking is insignificant.

For HE evaluation, dynamic time-history analysis of flexible floor slabs is performed using finite element models composed of plate elements. Columns supporting the slabs are represented by springs. In each model, masses of slab, equipment, piping, and other items are concentrated at appropriate nodal points. A typical flexible slab model is

shown in Figure 3.7-13A. Input excitation is the vertical acceleration time-history at the slab supports, obtained from the vertical analysis of the auxiliary building model.

Dynamic time-history analysis of the fuel handling area crane support structure is performed using one model to represent six end-bay frames and a second model to represent six middle bay frames. Each model is fixed at its base and uses beam and truss elements to represent all significant structural members. Structure masses are concentrated at appropriate nodal points. The model representing the middle bay frames is shown in Figure 3.7-13B. Input excitations are translational and rotational acceleration time-histories at elevation 140 feet obtained from analysis of the auxiliary building model.

Outdoor Water Storage Tanks

The axisymmetric and 3-D SAP IV mathematical models used in the HE finite element analysis are shown in Figures 3.7-14, 3.7-15, 3.7-15A, and 3.7-15B. The axisymmetric model using the AXIDYN computer program is used to analyze the effects of gravity loading, hydrostatic pressure, structure inertial forces, and hydrodynamic loads consisting of impulsive and convective pressures caused by the seismic event. The fluid impulsive effects are modeled as effective fluid inertia masses attached to appropriate concrete elements (see Reference 13). The 3-D SAP IV model is used to assess the effects of the nonaxisymmetric vault opening on the stresses in and around the opening area. The loads determined from dynamic analysis using axisymmetric model are input as static loads in the 3-D SAP IV model. All tanks except the firewater and transfer tank are analyzed as fixed base models.

The exterior tank of the firewater and transfer tank is analyzed as a fixed base, whereas the inner steel tank is pinned at the base in the finite-element analyses.

For horizontal direction, a response spectrum, modal superposition analysis is performed with an axisymmetric model to determine the combined dynamic effects of structure inertial forces and impulsive pressures due to the horizontal earthquake. Gravity, hydrostatic pressure, and convective pressure loads are analyzed statically. The tanks analyzed are refueling water storage tank and firewater and transfer tank. No additional analysis is done for condensate tank since it is similar to refueling water storage tank.

For the SAP IV nonaxisymmetric model, an equivalent, static, lateral load analysis based on accelerations computed from the axisymmetric model analysis is performed for the refueling water storage tank to determine the structure response maxima. The results of this analysis are applicable to other outdoor water storage tanks because they have similar vault openings and are of comparable size. The axisymmetric analyses have shown that responses of these tanks are generally similar to refueling tank.

Since the fundamental period is approximately 0.033 sec in the vertical direction, the empty tanks are determined to be rigid in that direction. Considering the possibility that

fluid may not act as a rigid mass during vertical motion, effects of the vertical earthquake are obtained by scaling the results of the analysis for gravity loading and hydrostatic pressure by a factor of 1.0 for the HE (2/3 x 0.75 x amplification factor of 2). For the DE and the DDE, HE finite-element analysis results are used as the basis for evaluation. The HE responses are adjusted by the ratio of peak spectral accelerations for the DE, or the DDE, and by appropriate damping ratios.

3.7.2.1.7.2 Turbine Building and Intake Structure

The turbine building and the intake structure are Design Class II. However, Design Class I equipment is located inside: component cooling water (CCW) heat exchangers, 4160V vital switchgear, emergency diesel generators, and other Class I systems in the turbine building, and auxiliary saltwater (ASW) pumps, piping, and instrumentation in the intake structure. In order to provide assurance that the function of Design Class I equipment will not be adversely affected, these structures are reviewed to ensure that they would not collapse in the unlikely event of an HE. The vulnerability of the main turbine steam valves to seismically induced falling debris is reviewed and is described in Section 3.5.

The structural evaluation of the turbine building and intake structure for the HE earthquake was performed using the response spectrum dynamic modal superposition method. In addition, a time-history dynamic analysis is performed to generate DE, DDE, and HE response spectra.

Turbine Building

Turbine building horizontal analyses use one model to represent the Unit 1 portion of the building, which extends from column line 1 to 19, and a second model to represent the Unit 2 portion of the building, which extends from column line 19 to 35. The models are fixed at the base and are composed of truss, beam, and plane stress elements. The Unit 1 horizontal model, shown in Figures 3.7-15C and 3.7-15D, has a total of approximately 500 nodal points and 1000 elements. The Unit 2 horizontal model is similar.

Four models representing different areas of the building are used to represent the building in the vertical direction. The models are fixed at the base and consist of plate, beam, and truss elements. Three of the models are three-dimensional extending the full building height and width, and together represent the building from column lines 1 to 17 and 19 to 35. The fourth model is two-dimensional extending to elevation 140 feet only and represents the building between column lines 17 and 19. The vertical model used to represent the building between lines 1 and 5 and between lines 31 and 35 is shown in Figures 3-7.15E and 3.7-15F. This model has over 500 nodes and over 1100 elements. Additional models are used to represent bridge crane effects. Analyses consider that both the Unit 1 and the Unit 2 bridge cranes may be located in the Unit 1 or the Unit 2 portion of the building with one of the cranes lifting 135 tons.

Structural evaluation of the turbine pedestal for the HE earthquake is performed using the response spectrum dynamic modal superposition method. The possibility of impingement between the turbine building structure and the turbine pedestal is considered in the response calculations, with the assumption that limited local structural damage, such as concrete chipping or spalling, is permissible provided the overall safety of the structures or the Class I equipment is not impaired. Three-dimensional fixed base models are used to evaluate loading of the pedestals in the horizontal and vertical directions. The model shown in Figure 3.7-15G represents the Unit 1 turbine pedestal. The Unit 2 model is similar. Pedestal members are modeled as beam elements with rigid joints to account for the stiff zones at beam-column intersections. Pedestal and turbine-generator masses are included at appropriate nodal points. The models each include approximately 270 nodes and 210 elements.

Intake Structure

The seismic analysis of the intake structure was carried out by initially separating the structure into two basic parts: (a) the pump-deck base, consisting of the massive land-side portion of the structure, from elevation -31.5 feet to the -2.1-foot pump-deck level; and (b) the remainder of the structural system. The analysis demonstrated that the massive pump-deck base below the 2.1-foot level would not amplify the ground motion. Hence, the pump-deck base need not be considered in the analysis of the remainder of the structure.

The three-dimensional mathematical model is used for the north-south and east-west/vertical analysis. Figures 3.7-15H and 3.7-15I show a typical finite element model. The model is fixed at the base and uses typical finite-element methods of discretization suitable for the structural system. Floor slabs and walls are modeled as flat-plate elements primarily to capture in-plane behavior. The slabs are shown to be rigid in the vertical direction by a separate simplified analysis. Some thick shear walls near the symmetry plane of the structure in the east-west direction are modeled as three-dimensional solid elements. There are six degrees of freedom for each node - three translational and three rotational degrees of freedom.

For the north-south analysis, the effect of the virtual mass of contained water has been considered by including the total mass of water tributary to the transverse flow straighteners (or piers). This method is considered reasonable because the relatively short distance between piers inhibits the tendency of the water to slosh and thereby reduce its virtual mass. A high-tide condition, with sea level at elevation +3.4 feet (MSL), is assumed for the analysis.

For the east-west/vertical analysis, the effect of water due to an earthquake is considered negligible because it is assumed that the water can flow in and out of the structure and will exert relatively little force on the structure.

Static and dynamic lateral earth pressures on the east wall of the intake structure are considered in the calculation of the in-place shear stress for the east-west walls and

roof slabs. The earth pressure influence is combined by SRSS method with the seismic forces.

3.7.2.1.7.3 Design Class I Mechanical Equipment

Reactor Coolant Loop

The RCLs and their support systems are analyzed for seismic loads based on a three-dimensional, multi-mass elastic dynamic model, as discussed in Section 5.2. Table 3.7-24 shows the fundamental mode frequency ranges for RCL primary equipment (steam generator, reactor coolant pump, and reactor pressure vessel). The stress analyses for faulted condition loadings of these components from a Hosgri earthquake are provided in Section 5.2.1.15. The analyses of the reactor internals, fuel elements, control rod drive assemblies, and control rod drives are described in Section 3.7.3.15.

Other Design Class I Mechanical Equipment

Design Class I mechanical equipment is grouped into: (a) equipment purchased directly by PG&E, and (b) equipment supplied by Westinghouse.

(1) Equipment purchased directly by PG&E

Equipment is considered rigid if all natural periods are equal to or less than 0.05 seconds for the DE and the DDE, and 0.03 seconds for the HE. Rigid equipment is designed for the maximum acceleration of the supporting structure at the equipment location. Flexible equipment is analyzed by response spectrum methods. Hydrodynamic analysis of rigid tanks is performed using the methods described in Reference 6. Flexible tanks were analyzed by the methods described in Reference 13.

Load combinations and allowable stresses for Design Class I equipment are given in Section 3.9.

(2) Equipment supplied by Westinghouse Electric Corporation

The seismic response of Design Class I piping and components is determined by response spectrum methods. The system is evaluated for the simultaneous occurrence of one horizontal and the vertical seismic input motions. For each mode, the results for the vertical excitation are added absolutely to the separate results for the north-south or east-west directions. The larger of the two values so determined at each point in the model is considered as the earthquake response. Details of the response spectrum analyses are as follows:

(a) If a component falls within one of the many categories that has been previously analyzed using a multi-degree-of-freedom model

and shown to be relatively rigid, the equipment specification for the component is checked to ensure that the equivalent static g-values specified are larger than the building floor response spectrum values and therefore are conservative. Equipment is considered to be rigid relative to the building if its natural frequencies are all greater than 20 cycles per second for the DE and DDE, and 33 cycles per second for HE.

(b) If the component cannot be categorized as similar to a previously analyzed component that has been shown to be relatively rigid, an analysis is performed as described below.

Design Class I mechanical equipment, including heat exchangers, pumps, tanks, and valves, are analyzed using a multi-degree-of-freedom modal analysis. Appendages, such as motors attached to motor-operated valves, are included in the models. The natural frequencies and normal modes are obtained using analytical techniques developed to solve eigenvalue-eigenvector problems. A response spectrum analysis is then performed using horizontal and vertical umbrella spectra that encompass the appropriate floor response spectra developed from the building time-history analyses.

The simultaneous occurrence of horizontal and vertical motions are included in the analyses. These response spectra are combined with the modal participation factors and the mode shapes to give the structural response for each mode from which the modal stresses are determined. The combined total seismic response is obtained by adding the individual modal responses utilizing the SRSS method.

Under certain conditions, the natural frequency of the equipment is not calculated. Under those conditions, using the appropriate damping value, the peak value of acceleration response curve is used to calculate the inertia forces. This method of calculation is termed the pseudo-dynamic method.

Components and supports of the RCS are designed for the loading combinations given in Section 5.2. Components are designed in complete accordance with the ASME Boiler and Pressure Vessel Code, Section III, Nuclear Vessels, and the USAS Code for Pressure Piping. The allowable stress limits for these components and supports are also given in Section 5.2. The loading combinations and stress limits for other components and supports are given in Section 3.9.

The Hosgri evaluation of the RCS is discussed in Section 5.2. All components and supports of the RCS satisfy criteria demonstrating qualification for the HE.

3.7.2.1.7.4 Design Class I Piping

Criteria

The following criteria determine the type of seismic analysis performed for Design Class I piping:

(1) 2-1/2 inches in diameter and larger

Seismic analysis is performed by the response spectrum, modal superposition method.

(2) Less than 2-1/2 inches in diameter

Seismic analysis is performed by the response spectrum modal superposition method for all Unit 2 piping. In Unit 1, piping less than 2-1/2 inches in diameter was analyzed by sampling criteria in which systems representing the worst case configurations or reflecting generic concerns were selected for analysis by the response spectrum modal superposition method. The remainder was qualified by criteria that limit the periods of free vibration to valves that assure only moderate amplification of piping responses.

Model

Three dimensional mathematical models are used in the response spectrum modal superposition analyses. A typical mathematical model is shown in Figure 3.7-26.

Valves and valve operators are included where appropriate in the piping models as eccentric masses. Pipe supports, restraints and equipment having a natural frequency of 20 Hz or greater are modeled as being rigid restraints. Where Design Class II piping connects to Design Class I piping, sufficient Design Class II piping is included in the model to assure qualification of the Design Class I piping and code boundary.

Allowable Stresses

Load combinations and allowable stresses for Design Class I piping are given in Section 3.9.

3.7.2.2 Natural Frequencies and Response Loads

The natural frequencies and seismic response results summarized in the following sections for the major plant structures are representative of the seismic analyses

performed for the operating license review (Reference 18), but may not reflect minor changes associated with subsequent plant modifications.

Containment Structure

(1) DE and DDE

The natural periods for all significant modes of the containment structure are listed in Table 3.7-2. The corresponding mode shapes are shown in Figure 3.7-6. The shell forces and moments in a typical element of the model are defined in Figure 3.7-7.

The containment structure seismic analysis provides acceleration time-histories, maximum absolute accelerations, displacements, shell forces and moments, total shears, and total overturning moments. These maximum response values are listed in Tables 3.7-3 through 3.7-8 for the nodal points indicated in Figure 3.7-5.

Acceleration response spectra for the containment are calculated from the acceleration time-histories, and corresponding smooth spectra are prepared. Typical smooth spectra are shown in Figures 3.7-8 through 3.7-12.

(2) HE

The natural periods and significant modes of vibration are listed in Table 3.7-8A. Modes having a period of vibration less than 0.03 sec (frequency greater than 33 Hz) are considered to be insignificant. As shown in Table 3.7-8A three sets of periods are given for the exterior shell:

(a) Translational mode determined from model of Figure 3.7-5A

(b) Torsional and translational mode determined from Figure 3.7-5B

(c) Vertical modes determined from Figure 3.7-5D

Table 3.7-8B gives the horizontal and vertical maximum absolute accelerations and Table 3.7-8C gives the maximum relative horizontal and vertical displacement. Table 3.7-8D gives the maximum shell forces and moments. Tables 3.7-8E and 3.7-8F give the maximum total shear forces, overturning moments, torsional moments, and axial forces for the containment shell.

The horizontal floor response spectra, including the effects of accidental torsion of the structure, at the inside face of the exterior

shell are shown in Figures 3.7-12A and 3.7-12B. To develop these spectra, the translational spectra are combined with the torsional spectra from the 5 percent and 7 percent accidental eccentricities. The combined translational and torsional spectra are then combined on an SRSS basis with the horizontal component due to the vertical input to yield the spectra shown in Figures 3.7-12A and 3.7-12B.

The vertical floor spectra are shown in Figures 3.7-12C and 3.7-12D. Tables 3.7-8G and 3.7-8H show the accelerations, displacements, stress, and moments for the containment interior structures as a result of the horizontal dynamic analysis.

For the interior structure, the Newmark input generally produces a higher structure response than does the Blume input. Figures 3.7-12E through 3.7-12G show the response spectra for the interior structure at elevation 140 feet, which is the operating floor for the containment. The spectra are for the horizontal, torsional, and vertical response.

For the annulus structural steel frames, a separate vertical dynamic analysis is carried out for each frame as shown in Figures 3.7-12H and 3.7-12I for Units 1 and 2, respectively. Tables 3.7-8I and 3.7-8J list the frequencies and participation factors for frame number 6 which is a typical annulus steel radial frame. After the response spectra are generated in the vertical direction for each radial frame, they are enveloped according to their locations. As shown in Figures 3.7-12H and 3.7-12I, the annulus is divided into the five major sectors (called sector frames) and the response spectra for any sector frame at given elevation are derived from enveloping the response spectra of radial frames located in that sector. Typical enveloped response spectra are shown in Figures 3.7-12J and 3.7-12K. As discussed earlier, the annulus structure does not amplify the horizontal motion of the interior concrete.

Therefore, the horizontal spectra for the concrete interior structures are used for the annulus steel. Table 3.7-8K lists the natural frequencies for horizontal seismic motion. As mentioned in Section 3.7.2.1.7, the first mode frequencies are approximately 20 Hz or higher and, therefore, for the rationale given earlier, the annulus is considered rigid in the horizontal direction.

Containment Polar Crane

Maximum displacements for various nodes for the polar crane are given in Table 3.7-8L. The member forces and bending moments are shown in Tables 3.7-8M and Table 3.7-8N. The typical response spectra are shown in Figures 3.7-12L and 3.7-12M.

Pipeway Structure

The modal analysis indicates that the minimum frequency of the model is 1.6 Hz and there are 100 modes below 33 cps indicating many closely spaced modes. The containment structure and the piping modes are included in the results since a composite model is analyzed as discussed in Section 3.7.2.1.7.1. The mode shapes indicate there are no global structural modes of the pipeway structure itself; instead, there are many local modes.

The input horizontal acceleration time-histories are scaled up by a factor of 1.06 to approximate the accidental eccentricity of masses. Five input cases are considered for the seismic analysis: The Blume horizontal time-history in E-W and N-S direction, the Newmark horizontal time-history in E-W and N-S direction, and the Newmark time-history in the vertical direction. Typical response spectra for pipeway structure are shown in Figures 3.7-12N through 3.7-12S.

Auxiliary Building

The natural periods for all significant modes of the auxiliary building are listed in Tables 3.7-9 through 3.7-11. Frequencies for significant modes of the fuel handling crane support structure are listed in Tables 3.7-11A and 3.7-11B.

Acceleration response spectra for the auxiliary building are calculated from the acceleration time-histories at the mass points and corresponding smooth spectra are developed. Typical spectra are shown in Figures 3.7-16 through 3.7-25 and 3.7-21A through 3.7-21I.

Maximum absolute accelerations, relative displacements, story shears, overturning moments, and torsional moments in the auxiliary building are listed in Tables 3.7-12 through 3.7-23. Maximum absolute accelerations and relative displacements in the fuel handling crane support structure are listed in Tables 3.7-8O and 3.7-8P; the displacements are obtained from static analysis of the detailed model described in Section 3.8.2.4.

Turbine Building

Natural frequencies of vibration in the horizontal direction in all significant modes of the Unit 1 portion of the building, for the condition where two bridge cranes are centered near column line 10.6, are listed on Table 3.7-23A. Corresponding

horizontal frequencies for the Unit 2 portion of the building are similar. Natural frequencies of vibration in the vertical direction for all significant modes of the building between column lines 1 and 5 are listed on Table 3.7-23B. Corresponding vertical frequencies for the Unit 2 portion of the building are similar.

Acceleration response spectra for the turbine building are calculated from acceleration time-histories at the mass points and corresponding smooth spectra are developed. Typical spectra are shown in Figures 3.7-25A through 3.7-25M.

Maximum absolute accelerations and relative displacements in the Unit 1 portion of the building are listed in Tables 3.7-23C and 3.7-23D. Corresponding accelerations and displacements in the Unit 2 end of the building are similar.

Natural periods for all significant modes of the turbine pedestal model are listed in Table 3.7-23E. Maximum relative displacements of the pedestal model are listed in Table 3.7-23F.

Intake Structure

The natural periods and participation factors for all significant modes of the intake structure are listed in Tables 3.7-23G. Acceleration response spectra for the intake structure are calculated from the acceleration time-histories at the selected mass points, and corresponding smooth spectra are developed as specified in Figure 3.7-4A. Typical spectra are shown in Figures 3.7-25N through 3.7-25T. Maximum absolute acceleration, relative maximum displacements are listed in Table 3.7-23H.

Outdoor Water Storage Tanks

The natural periods for significant modes of the refueling water storage tanks and fire water and transfer tank are listed in Tables 3.7-23I and 3.7-23J.

3.7.2.3 Procedures Used to Lump Masses

3.7.2.3.1 Structures

The mass of the structure is assumed to be concentrated at particular locations on the model. These locations coincide with either floor levels, significant points where dynamic response is required as input for piping and equipment, nodal points in the finite element model, or any other points required to accurately define the natural frequencies and mode shapes for the significant modes. The torsional effect for containment, auxiliary building, turbine building, and intake structure is considered as discussed in Section 3.7.2.10.

3.7.2.3.2 Equipment and Piping

The mass of the equipment and piping systems is assumed to be concentrated at particular locations on the model. These locations coincide with either actual masses such as pumps, motors, valve restraints and anchors, or any other points required to accurately define the natural frequencies and mode shapes of the significant modes.

3.7.2.4 Rocking and Translational Response Summary

Methods used to consider soil-structure interaction for Design Class I structures are described in Section 3.7.2.1.7.1.

3.7.2.5 Methods Used to Couple Soil with Seismic-System Structures

The procedures used to represent the containment structure and surrounding rock mass as a finite element model, and the procedures used to derive the stiffnesses of foundation springs for the auxiliary building are described in Section 3.7.2.1.7.1.

3.7.2.6 Development of Floor Response Spectra

Floor response spectra are developed using time-history modal superposition analyses as described in Section 3.7.2.1.7.1.

3.7.2.7 Differential Seismic Movement of Interconnected Components

Components and supports of the RCS are designed for the loading combinations and stress limits given in Section 5.2. The loading combinations and stress limits for other components and supports are given in Section 3.9.

3.7.2.8 Effects of Variations on Floor Response Spectra

Consideration of the effects on floor response spectra of possible variations in the parameters used for the structural analysis is discussed in connection with the development of smooth spectra in Section 3.7.2.1.7.1.

3.7.2.9 Use of Constant Vertical Load Factors

The Design Class I structures are heavy, massive, reinforced concrete, rigid-type structures and are founded on competent hard rock. For such structures, insignificant amplification of vertical motions can be expected, the critical factor in design being the response of the structures to horizontal earthquake motions. The containment structure and auxiliary building including Class I systems and components are designed for DE and DDE, using a vertical static coefficient equal to two-thirds of the peak horizontal ground motion, unless otherwise noted. For the HE, a dynamic analysis in the vertical direction is carried out as discussed in Section 3.7.2.1.7.1.

3.7.2.10 Method Used to Account for Torsional Effects

The containment structure is essentially axisymmetric and therefore has insignificant torsional response. The torsional response of the auxiliary building is calculated by use of a combined translational and torsional mathematical model in the seismic system time-history modal superposition analysis, as described in Section 3.7.2.1.7.1.

For the Hosgri evaluation of Design Class I structures, the effect of accidental torsion is included as an additional eccentricity in the mathematical models. The additional eccentricity is the greater of 5 percent of the building dimension in the direction perpendicular to the applied loads, when torsional and translational effects are

combined together, and the 7 percent of the building dimension in the direction perpendicular to the applied loads, when torsional and translational effects are computed independently and combined by the SRSS method.

For Hosgri evaluation of the Design Class II turbine building, including the turbine pedestal and the intake structure, a torsional response is calculated by the use of finite element models which include both translation and torsion. In addition, the effect of accidental eccentricity is accounted for by a 10 percent increase in the structural responses for the turbine building and intake structure. For the turbine pedestal, a static torsional moment corresponding to a 5 percent eccentricity is added to the dynamic analysis in each horizontal direction.

3.7.2.11 Comparison of Responses

Time-history analyses only are performed for Design Class I structures. Response spectrum analyses are not performed because the time-history produces spectra that represent reasonably the criteria response spectra.

3.7.2.12 Methods for Seismic Analysis of Dams

There are no dams associated with the DCPP.

3.7.2.13 Methods to Determine Design Class I Structure Overturning Moments

The maximum overturning moments for Design Class I structures are determined as part of the time-history modal superposition analyses. Vertical earthquake is considered to act concurrently with the maximum horizontal overturning moments.

3.7.2.14 Analysis Procedure for Damping

Structures are analyzed using modal superposition techniques, and element or material-associated damping ratios are given in Section 3.7.1.3. "Composite" or modal damping ratios in structural systems comprised of different element material types are selected based on an inspection of the significant mode shapes, and on the assumption that the

contribution of each material to the composite effective modal damping is proportional to the elastic energy induced in each material. The following criteria and procedures are applied on a-mode-by mode basis to evaluate and conservatively determine composite damping values:

(1) Where a particular mode primarily indicates response of a single element type, the damping ratio corresponding to that element type is assigned to that mode. Where all but a negligible amount of the elastic energy is induced in, for example, concrete or rock, the damping ratio appropriate to these materials is applied. Similarly, where a lightly damped material exhibits a major portion of the elastic energy of the mode, a conservative choice is made to use the damping ratio of that material for that mode. In most cases for this plant, the modes are well defined according to material types; composite damping values can be selected on the basis of a visual inspection of mode shapes and no additional numerical computations are required.

(2) In a few instances, the above criteria cannot be applied because a particular mode indicates response of several element types. The damping ratio for that mode is conservatively estimated based on the degree of participation of the different elements. Table 3.7-10 lists the participation factors for the auxiliary building. The elastic energy induced in the different elements is estimated and the composite damping values assigned in proportion to the elastic energy.

(3) Mass-weighted composite modal-damping is used for the DE and DDE analysis of the turbine building.

The approach described above is consistent with currently accepted techniques, and in all cases the damping values are selected conservatively. The use of this approach results in design that can conservatively resist the seismic motions postulated for the DCPP.

3.7.2.15 Combination of Components of Earthquake Motion For Structures

For DE and DDE analysis maximum structural response due to one horizontal and the vertical component of earthquake motion are combined by the absolute sum method. For HE analysis the maximum structural responses due to each of the three components of earthquake motion are combined by the SRSS method.

3.7.3 SEISMIC SUBSYSTEM ANALYSIS

3.7.3.1 Determination of Number of Earthquake Cycles

Where fatigue is a criterion, it is assumed that there are 20 occurrences of the DE, each producing 20 cycles of maximum response.

3.7.3.2 Basis for Selection of Forcing Frequencies

Design Class I equipment and piping is analyzed by the response spectrum method or the pseudo-dynamic method, using floor response spectra, unless it can be shown to be rigid, as discussed in Section 3.7.2.1. Accordingly, a special procedure to avoid certain frequencies is not needed.

3.7.3.3 Procedure for Combining Modal Responses

The method and procedure for combining modal responses are described in Sections 3.7.2.1 and 3.7.3.4.

3.7.3.4 Root Mean Square Basis

Closely spaced modes in Design Class I piping are analyzed by the response spectrum modal superposition method where all modal responses are combined by the SRSS method to obtain total response.

A study was conducted to evaluate the effects of combining modes with closely spaced modal frequencies by the absolute sum method. For closely spaced modes, the combined total response was obtained by taking the absolute sum of the closely spaced modes and then taking the SRSS with all other modes. Twenty-nine piping systems were studied, representing approximately 10 percent of the total number of piping systems analyzed. Of these 29 piping systems, 8 systems had no closely spaced frequencies and 8 systems had closely spaced frequencies which were in the rigid period range and therefore required no further study.

The remaining 13 systems had some modal frequencies in the flexible range that could be termed closely spaced. Of these, 5 systems had low seismic stresses with an adequate margin of safety, so that any possible increase in seismic stresses due to a combination of closely spaced frequencies by the absolute sum method would not affect the safety of the piping systems. In addition, 6 systems had closely spaced frequencies, but study of the mode shapes revealed that the seismic stresses would not be significantly affected by the absolute sum of these modal responses.

For the 2 remaining systems, it was not possible to positively conclude that the effects of combining the modes with closely spaced frequencies by absolute sum would be minimal by inspecting the stresses or mode shapes. Therefore, these 2 systems were reanalyzed by computer, and it was found that if the seismic responses of the modes with closely spaced frequencies were combined by the absolute sum method, the increase in stress would be less than 1 percent.

It was therefore concluded that the combination of modal responses of piping systems by the SRSS method is adequate and conservative.

3.7.3.5 Design Criteria and Analytical Procedures for Piping

Stresses induced in Design Class I piping from relative movement of anchor points (points where all degrees of freedom are fixed), whether due to building or equipment movement, are considered with stresses calculated in the piping response spectrum modal superposition analyses.

PG&E has developed specific guidelines for the design of Class I pipe supports that account for such items as allowable deflections, forces, gaps, and moments imposed on the supports. Allowable stresses and loads are described in more detail in Section 3.9.

A study (Reference 9) has also been performed to evaluate the stresses in piping systems, assuming failure of a single hydraulic or mechanical pipe snubber during a seismic event. Results of the study indicate that the probability of a snubber failing to snub and causing a pipe failure was sufficiently low that no additional design restraints had to be imposed.

As an additional control, hydraulic snubbers are visually inspected and functionally tested. These surveillance requirements are detailed in the DCPP Equipment Control Guidelines (see Chapter 16).

At the request of the NRC in April 18, 1984, in its order to modify Facility Operating License No. DPR-76, PG&E developed a program to review the small and large bore pipe supports for the specific concerns raised by that order.

The specific items requested by the NRC were as follows:

(1) PG&E shall complete the review of all small-bore piping supports which were reanalyzed and requalified by computer analysis. The review shall include consideration of the additional technical topics, as appropriate, contained in License Condition No. 7 below.

(2) PG&E shall identify all cases in which rigid supports are placed in close proximity to other rigid supports or anchors. For these cases PG&E shall conduct a program that assures loads shared between these adjacent supports and anchors result in acceptable piping and support stresses. Upon completion of this effort, PG&E shall submit a report to the NRC Staff documenting the results of the program.

Design procedures were revised to address this issue.

(3) PG&E shall identify all cases in which snubbers are placed in close proximity to rigid supports and anchors. For these cases, utilizing snubber lock-up motion criteria acceptable to the staff, PG&E shall demonstrate that acceptable piping and piping support stresses are met. Upon

completion of this effort, PG&E shall submit a report to the NRC Staff documenting the results.

Design procedures were revised to address this issue.

(4) PG&E shall identify all pipe supports for which thermal gaps have been specifically included in the piping thermal analyses. For these cases the licensee shall develop a program for periodic inservice inspection to assure that these thermal gaps are maintained throughout the operating life of the plant. PG&E shall submit to the NRC Staff a report containing the gap-monitoring program.

Rather than establishing a gap-monitoring program, the piping analysis and procedures were modified to eliminate the thermal gaps in the analyses.

(5) PG&E shall provide to the NRC the procedures and schedules for the hot walkdown of the main steam system piping. PG&E shall document the main steam hot walkdown results in a report to the NRC Staff.

(6) PG&E shall conduct a review of the "Pipe Support Design Tolerance Clarification" program (PSDTC) and "Diablo Problem" system (DP) activities. The review shall include specific identification of the following:

(a) Support changes, which deviated from the defined PSDTC program scope;

(b) Any significant deviations between as-built and design configurations stemming from the PSDTC or DP activities; and

(c) Any unresolved matters identified by the DP system.

The purpose of this review is to ensure that all design changes and modifications have been resolved and documented in an appropriate manner. Upon completion PG&E shall submit a report to the NRC Staff documenting the results of this review.

(7) PG&E shall conduct a program to demonstrate that the following technical topics have been adequately addressed in the design of small and large-bore piping supports:

(a) Inclusion of warping normal and shear stresses due to torsion in those open sections where warping effects are significant.

(b) Resolution of differences between the AISC Code and Bechtel criteria with regard to allowable lengths of unbraced angle sections in bending.

(c) Consideration of lateral/torsional buckling under axial loading of angle members.

(d) Inclusion of axial and torsional loads due to load eccentricity where appropriate.

(e) Correct calculation of pipe support fundamental frequency by Rayleigh's method.

(f) Consideration of flare bevel weld effective throat thickness as used on structural steel tubing with an outside radius of less than 2T.

The above considerations were incorporated in the applicable design procedures.

All of the above specific concerns were addressed and resolved to the satisfaction of the NRC.

3.7.3.6 Basis for Computing Combined Response

As a minimum, mechanical equipment is designed for a vertical static coefficient equal to 2/3 of the peak horizontal ground motion for DE and DDE analysis. For HE analysis, specific vertical floor response spectra are used. Horizontal and vertical responses are combined by absolute sum.

Equipment is reviewed for a vertical force determined from a response spectrum, as described in Section 3.7.2.1.7.3, 3.7.3.15, and 5.2.

The horizontal and vertical responses of Design Class I piping are determined from the two-dimensional response spectrum modal superposition analyses described in Section 3.7.2.1.7.4. Response spectra at the applicable piping support attachment elevations are enveloped to obtain the final design response spectra. The vertical and one horizontal response are combined by absolute sum on the modal level. Modal responses are combined by the SSRS method. The two two-dimensional results are then enveloped to obtain the total response. Figure 3.7-26 shows a typical piping mathematical model. Figure 3.7-29 illustrates the derivation of the design response spectra for a typical piping system.

In many cases, earthquake piping stresses due to DDE are not directly calculated. Instead, the results from the DE piping analysis are doubled to represent the DDE. This approach was chosen because review of the design spectra showed that the DDE

accelerations did not exceed twice the DE accelerations. Since pipe stress is linear with accelerations, this approach is conservative.

3.7.3.7 Amplified Seismic Responses

Components that can be adequately characterized as a single-degree-of-freedom system are considered to have a modal participation of one.

3.7.3.8 Use of Simplified Dynamic Analysis

All methods of seismic analysis used for Design Class I structures, components, systems, and piping are described in Section 3.7.2.

Two methods of dynamic seismic analysis are used for Design Class I components and piping that are different than multiple-degree-of-freedom, modal analysis methods. The first of these is the response spectrum, single-degree-of-freedom method used for components whose dynamic behavior can be accurately represented by a single-degree-of-freedom mathematical model. The second of these is the method for rigid components where the component is designed for the maximum acceleration experienced by the supporting structure at the location of support, if all natural periods of the component are less than, or equal to, 0.05 seconds (33 Hz for HE in piping analysis).

The pseudo-dynamic method of analysis is used for certain items of mechanical equipment as described in Section 3.7.2. The basis for this method is described in Section 3.7.2.1.7.3.

Certain Unit 1 Design Class I piping less than 2-1/2 inches in diameter is restrained according to criteria described in Section 3.7.2.1.7.4.

3.7.3.9 Modal Period Variation

Consideration of the effects on floor response spectra of possible variations in the parameters used for structural analysis is discussed in connection with the development of smooth spectra in Section 3.7.2.1.7.1.

3.7.3.10 Torsional Effects of Eccentric Masses

Where appropriate, valves and valve operators are included as eccentric masses in the mathematical models for piping seismic analysis, as described in Section 3.7.2.1.7.4.

3.7.3.11 Piping Outside Containment Structure

The procedures used to determine piping stresses resulting from relative movement between anchor points (points where all degrees-of-freedom are fixed) are discussed in Section 3.7.3.5. The forces exerted by piping on anchor points, including the

containment structure penetrations, are included in the evaluation of stresses for Design Class I structures.

Buried Design Class I piping is confined by sand backfill in rock trenches. The piping material is ASTM A-53 or A-106 carbon steel.

3.7.3.12 Interaction of Other Piping With Design Class I Piping

Mathematical models for Design Class I piping seismic analyses normally originate and terminate at anchor points. Where Design Class II piping connects to Design Class I piping sufficient Design Class II piping is included in the mathematical model to assure qualification of the Design Class I piping and code boundary.

3.7.3.13 System Interaction Program

PG&E developed a program to consider seismically-induced physical interactions between nonsafety-related SSCs and Design Class I SSCs. The methodology and results of this interaction study are presented in Reference 10 and are summarized as follows. The objective of the program was to establish confidence that when subjected to seismic events of severity up to and including the HE, SSCs important to safety shall not be prevented from performing their intended safety functions as a result of physical interactions caused by seismically induced failures of nonsafety-related SSCs. In addition, safety-related SSCs shall not lose the redundancy required to compensate for single failures as a result of such interactions.

To accomplish the program, PG&E defined as targets all SSCs required to safely shut down the plant and maintain it in a safe shutdown condition, and certain accident-mitigating systems. Initial plant operating modes of normal operation, shutdown, and refueling were considered in the selection of the target equipment. All nonsafety-related SSCs were defined as sources.

Interactions between source and target equipment were postulated by an interdisciplinary Interaction Team. The Interaction Team postulated interactions during walkdowns of the target equipment, using previously established guidelines and criteria. The Interaction Team also recommended resolutions to the postulated interactions. The findings of the Interaction Team were evaluated during a subsequent office-based technical evaluation. Any modifications deemed necessary were reviewed after completion by the Interaction Team to ensure that no new interactions were created by the modifications themselves.

The program was subjected to an independent audit by PG&E's Quality Assurance Department and a review by an Independent Review Board which reported its findings to a managing consultant who, in turn, reported his findings to PG&E management.

3.7.3.14 Field Location of Supports and Restraints

Seismic supports and restraining devices for Design Class I piping are located as follows:

3.7.3.14.1 Two Inches in Diameter and Less

Field-routed and vendor-furnished piping 2 inches and less in diameter is supported by the piping installation contractor's field personnel in accordance with criteria supplied by PG&E's engineering staff on Approved for Construction drawings. These criteria specify size, type, spacing, and permissible locations for seismic supports and restraining devices. Prior to initial fuel loading, the completed installation of this piping was reviewed by an experienced piping engineer from PG&E's engineering staff to ensure compliance with the criteria and the observance of good design practice.

3.7.3.14.2 Larger Than 2 Inches in Diameter

The size, type, and location of each support or restraining device on each line is shown on Approved for Construction drawings.

The procedures followed during development of the Approved for Construction drawings provide assurance that the field location and the seismic design of supports and restraining devices are consistent with the assumptions made in the seismic analysis. These procedures are:

(1) The locations of supports and restraining devices are established on preliminary drawings.

(2) The locations shown on the preliminary drawings are used to develop the mathematical model for the seismic analysis, and the seismic analysis is performed. If the results show piping stresses higher than allowable, adjustments are made in the location, and/or the type of support or restraining device, and the seismic analysis is repeated.

(3) The reactions calculated as part of the seismic analysis, combined with other loads, are used for final design of piping supports and restraining devices.

(4) When the design is complete, drawings are issued as Approved for Construction to the piping installation contractor. Installation of supports and restraining devices is in accordance with Approved for Construction drawings.

3.7.3.15 Seismic Analyses for Fuel Elements, Control Rod Assemblies, and Control Rod Drives

3.7.3.15.1 Reactor Vessel Internals Evaluation - DE, DDE, and HE

Nonlinear dynamic seismic analysis of the reactor pressure vessel (RPV) system includes the development of the system finite element model and the synthesized time history accelerations. Both of these developments for the seismic time history analysis are discussed below.

The basic mathematical model for seismic analysis is essentially similar to a LOCA model in that the seismic model includes the hydrodynamic mass matrices in the vessel/barrel downcomer annulus to account for the fluid-solid interactions. On the other hand, the fluid-solid interactions in the LOCA analysis are accounted through the hydraulic forcing functions generated by Multiflex Code (Reference 3). Another difference between the LOCA and seismic models is the difference in loop stiffness matrices. The seismic model uses the unbroken loop stiffness matrix, whereas the LOCA model uses the broken loop stiffness matrix. Except for these two differences, the RPV system seismic model is identical to that of LOCA model.

The RPV system finite element model for the nonlinear time history dynamic analysis consists of three concentric structural sub-models connected by nonlinear impact elements and linear stiffness matrices. The first sub-model, shown in Figure 3.7-27A, represents the reactor vessel shell and its associated components. The reactor vessel is restrained by four reactor vessel supports (situated beneath alternate nozzles) and by the attached primary coolant piping. Also shown in Figure 3.7-27A is a typical RPV support mechanism.

The second sub-model, shown in Figure 3.7-27B, represents the reactor core barrel, thermal shield, lower support plate, tie plates, and the secondary support components for Unit 1 (PGE); whereas, for Unit 2 (PEG) the second sub-model is shown in Figure 3.7-27C (core barrel with neutron pads instead of thermal shield).

These sub-models are physically located inside the first, and are connected to them by stiffness matrices at the vessel/internals interfaces. Core barrel to reactor vessel shell impact is represented by nonlinear elements at the core barrel flange, upper support plate flange, core barrel outlet nozzles, and the lower radial restraints.

The third and innermost sub-model, shown in Figure 3.7-27D, represents the upper support plate assembly consisting of guide tubes, upper support columns, upper and lower core plates, and the fuel. The fuel assembly simplified structural model incorporated into the RPV system model preserves the dynamic characteristics of the entire core. For each type of fuel design the corresponding simplified fuel assembly model is incorporated into the system model. The third sub-model is connected to the first and second by stiffness matrices and nonlinear elements.

As mentioned earlier, fluid-structure or hydroelastic interaction is included in the reactor pressure vessel model for seismic evaluations. The horizontal hydroelastic interaction is significant in the cylindrical fluid flow region between the core barrel and the reactor vessel annulus. Mass matrices with off-diagonal terms (horizontal degrees-of-freedom only) attach between nodes on the core barrel, thermal shield and the reactor vessel. The mass matrices for the hydroelastic interactions of two concentric cylinders are developed using the work of Reference 36. The diagonal terms of the mass matrix are similar to the lumping of water mass to the vessel shell, thermal shield, and core barrel. The off-diagonal terms reflect the fact that all the water mass does not participate when there is no relative motion of the vessel and core barrel. It should be pointed out that the hydrodynamic mass matrix has no artificial virtual mass effect and is derived in a straight-forward, quantitative manner.

The matrices are a function of the properties of two cylinders with the fluid in the cylindrical annulus, specifically, inside and outside radius of the annulus, density of the fluid, and length of the cylinders. Vertical segmentation of the reactor vessel and the core barrel allows inclusion of radii variations along their heights and approximates the effects beam mode deformation. These mass matrices were inserted between the selected nodes on the core barrel, thermal shield, and the reactor vessel as shown in Figure 3.7-27E.

The seismic evaluations are performed by including the effects of simultaneous application of time history accelerations in three orthogonal directions. For the DE, DDE and HE, the Westinghouse generated synthesized time history accelerations at the reactor vessel support were used. Whereas, for the long term seismic program (LTSP), response spectra at the reactor vessel supports, with five percent critical damping the synthesized time history accelerations at the reactor vessel supports, were supplied by Pacific Gas and Electric (PG&E) via Reference 35. The detailed seismic analyses results of the RPV system are documented in Reference 34.

The WECAN computer code, which is used to determine the response of the reactor vessel and its internals, is a general-purpose finite element code. In the finite element approach, the structure is divided into a finite number of discrete members or elements. The inertia and stiffness matrices, as well as the force array, are first calculated for each element in the local coordinates. Employing appropriate transformations, the element global matrices and arrays are assembled into global structural matrices and arrays, and used for dynamic solution of the system equations.

The results of the nonlinear seismic dynamic analyses include the transient displacements and impact loads for various elements of the mathematical model. These displacements, impact loads, and linear component loads (forces and moments) are then used by cognizant organizations for detailed component evaluations to assess the structure of the reactor vessel, reactor internals, and the fuel. Note that the linear component forces and moments are not the direct output from the modal superposition analysis but rather are obtained by post-processing the data saved from the nonlinear time history analysis.

From the modal analysis (free vibration analysis), the system eigenvalues and eigenvectors are stored on a magnetic tape to be used later in the modal superposition analysis. The validity of a complex system structural model is generally verified by comparing the calculated fundamental frequency of the system with the available test data frequency. The fundamental core barrel frequency of a four-loop thermal shield core barrel is known from test data to be approximately 6.6 to 7.0 Hz. The results of Diablo Canyon Unit 1 modal analysis show that the core barrel fundamental beam mode frequency is close to 7.0 Hz, thereby verifying the applicability of the system model for the desired analysis.

Note that the preceding paragraphs describe RPV and internals system dynamic analyses for which the WECAN computer code was used. Current analyses (such as the dynamic analyses performed in support of the replacement vessel head project) utilize the ANSYS computer code. The methodology used to develop the ANSYS system models is consistent with the methodology used to develop historic WECAN models. The direct time integration method is used in ANSYS to solve the dynamic equations of motion for the system; whereas the nonlinear mode superposition method is used in WECAN to solve the dynamic equations of motion for the system.

3.7.3.15.2 Fuel Assembly Evaluation

The fuel assembly design adequacy under DDE and HE conditions was assessed through a combination of mechanical tests and analyses. The information obtained from the fuel assembly and component structural tests provided the fundamental mechanical constants for the finite element model used in the fuel analysis.

The analysis of the fuel is performed in two steps. The first step involves analysis of the detailed reactor core model, which includes the reactor vessel, internals, and a simplified model of the fuel (Figures 3.7-27A thru 3.7-27E). This dynamic analysis uses seismic time history motion at the reactor vessel support elevation (Elevation 102 ft.). The second step of the fuel analysis involves running a detailed fuel assembly model using the WEGAP code. This detailed model (Figure 3.7-27F) conservatively represents an entire row of full-length fuel assemblies (15 total).

The fuel assembly model consists of a series of beam elements with torsional springs located at the various fuel assembly grid elevations to simulate the fuel assembly dynamic characteristics. The values of the mechanical constants such as the rigidity modulus and the torsional stiffness were selected to accurately represent the experimentally determined fuel assembly modal stiffness and natural frequencies.

The time history motion for the upper and lower core plates and core barrel are simultaneously applied to the simulated fuel assembly model as illustrated in Figure 3.7-27F. These input motions were obtained from the time history analysis of the reactor vessel and internals finite element model.

The maximum grid impact forces and the fuel assembly maximum deflection are determined with the reactor core model.

Because of the basic fuel assembly design configuration, the assembly impacting is restricted to the grid locations. The seismic and LOCA loads at each grid were combined using the SRSS method to obtain the design maximum loads. These loads are compared with the allowable grid load, which is determined based on the test data using 95 percent confidence level on the true mean criteria. The results of the Unit 1 and Unit 2 evaluations indicated the possibility of some deformation of fuel grids at a small number of specific locations. An analysis of the effects of this grid deformation has shown the core geometry will remain coolable (Reference 29). Note that with the acceptance of the DCPP leak-before-break analysis by the NRC, dynamic LOCA loads resulting from pipe rupture events in the main reactor coolant loop piping no longer have to be considered in the design basis structural analyses and included in the loading combinations (see Section 3.6.2.1.1.1). Only the much smaller LOCA loads from RCS branch line breaks have to be considered.

3.7.3.15.3 Control Rod Drive Mechanism Evaluation

The replacement CRDMs were evaluated using a combination of linear and nonlinear finite element models which included the CRDM housings, RPV head adapters, and the integrated head assembly. The following models and analysis methods were employed for the specified earthquakes:

(1) DE and DDE: The horizontal analyses for the DE and DDE were based on a nonlinear model. The horizontal DE and DDE acceleration time-histories at the seismic plate elevation and the reactor vessel support elevation were used as inputs to the model. The vertical analyses for the DE and DDE were based on a linear model. The vertical DE and DDE response spectra at the reactor vessel head elevation were used as input to the model.

(2) HE: The horizontal and vertical analyses for the HE were based on a linear model. The horizontal and vertical HE response spectra at the seismic plate elevation and the reactor vessel head elevation were used as input to the model.

3.7.3.15.4 CRDM Support System Evaluation

The integrated head assembly CRDM seismic support structure, tie rods, and head lifting legs were evaluated using linear elastic 3-D finite element models of the support system. Tension-only capability of the tie rods was modeled. The loading from the CRDMs was addressed through the inclusion of a simplified representation of the pressure housings, including the appropriate lumped masses.

In general, the qualification was based on the response spectrum superposition method using the envelope of the spectra at the 140 foot elevation of the containment interior

concrete (attachment point for the tie rods for the tie rods to the reactor cavity walls) and on the reactor vessel lifting lugs and pads (attachment point for the integrated head assembly ring beam to the head) for the DE, DDE, HE, and LOCA load cases. These analyses were supplemented with the time history modal superposition method for the determination of DDE loads for selected connections.

3.7.4 SEISMIC INSTRUMENTATION PROGRAM

3.7.4.1 Comparison With NRC Regulatory Guide 1.12, Revision 2

The seismic instrumentation consists of strong motion triaxial accelerometers that sense and record ground motions. This instrumentation meets the intent of RG 1.12, Revision 2. Enhancements to the seismic instrumentation have been made to improve the system effectiveness. The enhancements include supplemental accelerometers and rapid processing of the ground motion data. The enhancements exceed the intent of RG 1.12, Revision 2, and are not considered part of the licensing basis.

3.7.4.2 Location and Description of Instrumentation

Seismic instrumentation is provided in accordance with RG 1.12, Revision 2, paragraph 1.2. All instruments are rigidly mounted so their records can be related to movement of the structures and ground motion. All are accessible for periodic servicing and for obtaining readings.

3.7.4.2.1 Strong Motion Triaxial Accelerometers

Strong motion triaxial accelerometers provide time-histories of acceleration for each of three orthogonal directions. These histories are recorded in the accelerometer housings. The instruments start recording upon actuation of a seismic trigger which has an adjustable threshold. Six strong motion triaxial accelerometers are provided in accordance with RG 1.12. Revision 2, paragraph 1.2. Supplemental accelerometers provide ground motion data beyond the regulatory guidance and are not part of the licensing commitment,

3.7.4.3 Control Room Operator Notification

Operation of the strong motion triaxial accelerometers (ESTA01 or ESTA28) will activate an annunciator in the control room and provide indications on the earthquake force monitor (EFM) in the RSI panel. The EFM will display the acceleration levels for all areas of both the Unit 1 containment base sensor (ESTA01) and the free field sensor (ESTA28). For the Emergency Plan event classification, it also provides a status of level exceedance for any axis on both sensors within a few minutes. The setpoint thresholds are set in accordance with Emergency Plan Action Levels.

3.7.4.4 Comparison of Measured and Predicted Responses

In the event of an earthquake that produces significant ground motions, all seismic instruments are read and the readings compared to the corresponding design values. This comparison, together with information provided by other plant instrumentation and an inspection of safety-related systems, forms the basis for a judgment on severity, level, and the effects of the earthquake.

3.7.5 SEISMIC DESIGN CONTROL

3.7.5.1 Equipment Purchased Directly by PG&E

The position of PG&E's engineering staff in the corporate structure is shown in Figures 17.1-1 and 17.1-2. The procedures for specifying technical and quality assurance requirements in purchase orders and specifications are included in Sections 17.4, 17.5, and 17.8.

The seismic design requirements developed from the structure seismic system analysis are included in the purchase order or specification for Design Class I equipment. The purchase order or specification requires that the manufacturer submit seismic qualification data of the equipment to be furnished, for review by the responsible PG&E engineer. The procurement is approved only when all seismic design criteria are met.

3.7.5.2 Equipment Supplied by Westinghouse

The following procedure is implemented for Design Class I mechanical equipment that falls within one of the many categories analyzed as described in Section 3.7.2 and shown to be rigid (frequency > 33 Hz).

(1) Equivalent static acceleration factors for the horizontal and vertical directions must be checked against those in the Design Criteria Memoranda (DCM). Westinghouse must certify the adequacy of the equipment to meet the seismic requirements as described in Section 3.7.2 for DE, DDE, and HE.

(2) Westinghouse must check to ensure that the given equivalent static acceleration factors are less than or equivalent to those given in the equipment analysis.

(3) Westinghouse must perform the necessary reanalysis to the procedures and criteria presented herein for those cases, where required, due to revised DE, DDE, and HE seismic response spectra.

All other Design Class I equipment must be analyzed or tested as described in Sections 3.7.2 and 3.10.

Design control measures and design documentation for all Design Class I SSCs are in accordance with formalized quality assurance procedures. These procedures are presented in Chapter 17, Quality Assurance.

3.7.6 SEISMIC EVALUATION TO DEMONSTRATE COMPLIANCE WITH THE HOSGRI EARTHQUAKE REQUIREMENTS UTILIZING A DEDICATED SHUTDOWN FLOWPATH

3.7.6.1 Post-Hosgri Shutdown Requirements and Assumed Conditions

In response to a request from the NRC, PG&E evaluated the ability of DCPP to shut down following the occurrence of a 7.5M earthquake due to a seismic event on the Hosgri fault. This evaluation is presented in Reference 15, which was amended several times after it was first issued in order to respond to questions by the NRC and reflect agreements made at meetings with the NRC. The final document describes the method proposed by PG&E to shut down the plant after the earthquake, assuming a loss of all offsite power, but no concurrent accident, using only equipment qualified to remain operable following such an earthquake.

For this purpose, valves that are required to operate to achieve shutdown following the earthquake were qualified for active function to the Hosgri parameters, whereas other valves, which might have an active function for postaccident mitigation, but were not required to operate to achieve shutdown following the earthquake, were qualified for passive function (pressure boundary integrity) to the Hosgri parameters. This is consistent with the DCPP design basis stated in FSAR Section 3.7.1.1 that the DDE is the SSE for DCPP, and that the guidelines presented in RG 1.29 apply to the DDE.

In addition, pursuant to the NRC request, it was necessary to demonstrate that DCPP could be shut down following an HE in order to protect the health and safety of the public. The Hosgri evaluation presented in Reference 15 demonstrated this. To provide increased conservatism, PG&E has subsequently qualified all active valves for active function for an HE pursuant to a commitment made in Reference 17.

3.7.6.2 Post-Hosgri Safe Shutdown Flowpath

The flowpath qualified to enable shutdown of the plant following an HE is defined in Chapter 5 of Reference 15. For this purpose, safe shutdown was defined as cold shutdown. It assumes concurrent loss of offsite power, a single active failure, but no concurrent accident or fire. Local manual operation of equipment from outside the control room is acceptable for taking the plant from hot standby to cold shutdown.

3.7.6.2.1 Hot Standby

Hot standby is achieved by feeding the steam generators using the auxiliary feedwater system and by release of steam to the atmosphere through the 10 percent steam dump valves. Although other long term cooling water sources may be available, only the

seismically qualified condensate storage tank and firewater storage tank are assumed to be available.

3.7.6.2.2 Cold Shutdown

Cold shutdown is achieved by use of the normal charging system flow path. Depressurization is performed using auxiliary spray (alternatively, the PORVs may be used). Boration to cold shutdown concentration is accomplished using boric acid from the boric acid storage tanks via the emergency borate valve 8104 and using a centrifugal charging pump (CCP1 or CCP2) charging through valves FCV-128, HCV-142, 8108, 8107, and 8146 or 8147. Sampling capability to verify boron concentration is available. While reactor coolant pump seal injection flow would be available, the seal water return flow path and the normal letdown flow path are assumed not to be available. Calculations have shown that even with letdown unavailable, by taking credit for shrinkage of the reactor coolant during cooldown, sufficient volume is available in the reactor coolant system to borate to cold shutdown using 4 percent boric acid.

Once the RCS is less than or equal to 390 psig and 350°F, the normal RHR system is placed into service, along with the portions of the component cooling water and auxiliary salt water systems which support RHR operation.

3.7.6.2.3 Single Active Failure

Systems and components used to perform the post-Hosgri shutdown described above have redundant counterparts except for components along the normal charging flowpath, which lacks redundancy since its redundant flow path for emergency boration is the high pressure safety injection flow path. Use of that redundant flow path is not postulated for post-Hosgri shutdown, however, so adequate redundancy had to be incorporated into the normal charging flowpath to enable cold shutdown following the HE. For this purpose, the Hosgri evaluation assumed that manual bypass valves 8387B or 8387C would be used in the event that fail-open valve FCV-128 was to fail closed. Manual bypass valve 8403 would be used in the event that fail-closed valve HCV-142 was to fail closed. Fail-open valve FCV-110A and manual bypass valve 8471 would be used in the event that motor-operated valve 8104 was to fail closed. Valves 8146 and 8147 were assumed redundant for normal charging, and valves 8145 and 8148 were assumed redundant for pressurizer auxiliary spray. Valves with pneumatic operators, which are required to operate to achieve shutdown, were fitted with seismically qualified air or nitrogen accumulators to enable their operation in spite of the loss of their instrument air or nitrogen supply. Although some of these valves do not have safety-related operators since they are not required for accident mitigation, they are seismically qualified to ensure their operability for post-Hosgri shutdown.

3.7.6.2.4 Equipment Required for Post-Hosgri Shutdown

The equipment determined to be required to achieve post-Hosgri cold shutdown in the manner described above is presented in Sections 7.3 and 9.2 of Reference 15. Some minor revisions to the list of valves required have been made, and are reflected in the latest revision of the active valve list, FSAR Table 3.9-9. Instrument Class IA, Instrument Class IB, Category 1, and on a case-by-case basis, Instrument Class ID instrumentation are qualified to the Hosgri parameters, and assumed to be operable following an HE. Additional instrumentation determined to be required is presented in Section 7.3 of Reference 15. Some revisions have been made to that list; the revised list of required instrumentation is presented in Reference 16. The electrical Class 1E system is also qualified to the Hosgri parameters, and is assumed to be operable following an HE.

3.7.7 REFERENCES

1. Deleted in Revision 4.

2. Lawrence Livermore Laboratory, Soil-Structure Interaction: The Status of Current Analysis Methods and Research, NUREG/CR-1780, January 1981. (Section by J. M. Roesset.)

3. J. E. Luco, Independence Functions for a Rigid Foundation on a Layered Medium, Nuclear Engineering and Design, Vol. 31, 1974.

4. R. V. Whitman and F. E. Richardt, Design Procedures for Dynamically Loaded Foundations, Journal of Soil Mechanics and Foundations Division, SM6, Nov. 1967.

5. G. Bohm, Seismic Analysis of Reactor Internals for Pressurized Water Reactors, First National Congress of Pressure Vessel and Piping Technology, ASME Panel on Seismic Analysis & Design of Pressure Vessel and Piping Components, San Francisco, May 10-12, 1971.

6. U.S. Atomic Energy Commission (Division of Reactor Development) Publication TID - 7024, Nuclear Reactors and Earthquakes.

7. Appendix A to 10 CFR 100, Seismic and Geologic Siting Criteria for Nuclear Power Plants.

8. Damping Values of Nuclear Power Plant Components, WCAP-7921-AR, May 1974.

9. Stress Evaluation of Piping Systems Assuming Single Snubber Failures, Letter dated January 24, 1978, from P.A. Crane (PG&E) to J.F. Stolz (NRC).

10. Description of the Systems Interaction Program for Seismically Induced Events, Revision 4, August 29, 1980.

11. Answer to the NRC Staff Questions on the Westinghouse Evaluation of the Effect of Grid Deformation on ECCS Performance, transmitted via letter May 11, 1978, P.A. Crane to J.F. Stolz.

12. Supplement No. 5 to the Safety Evaluation of the Diablo Canyon Nuclear Power Station, Units 1 and 2, Nuclear Regulatory Commission, Division of Reactor Licensing, Washington, DC, September 1976.

13. "Dynamics of Fixed-Base Liquid Storage Tanks," Velestsos, A.S. and T.Y. Yang; Proceedings of U.S.-Japan Seminar on Earthquake Engineering Research with Emphasis on Lifeline Systems, Tokyo, November 1976.

14. Westinghouse 1981 ECCS Evaluation Model Using the BASH Code, WCAP-10266-P-A, Rev. 2, March 1987.

15. Seismic Evaluation for Postulated 7.5M Hosgri Earthquake, DCPP Units 1&2, PG&E.

16. PG&E Design Change Package N-47546.

17. PG&E Letter to the NRC, DCL-92-198 (LER 1-92-015).

18. Phase I Final Report - Design Verification Program, Diablo Canyon Power Plant, Revision 14, transmitted via letter dated October 14, 1983, J. O. Schuyler (PG&E) to D. G. Eisenhut (NRC).

19. Final Report of the Diablo Canyon Long Term Seismic Program, July 1988, PG&E.

20. Addendum to the 1988 Final Report of the Diablo Canyon Long Term Seismic Program, February 1991, PG&E.

21. NUREG-0675, Supplement Number 34, Safety Evaluation Report Related to the Operation of Diablo Canyon Nuclear Power Plant, Units 1 and 2, NRC, June 1991.

22. NRC letter to PG&E, "Transmittal of Safety Evaluation Closing Out Diablo Canyon Long-Term Seismic Program," April 17, 1992.

23. PG&E letter to the NRC, "Long Term Seismic Program - Future Plant Modifications," DCL-91-178, July 16, 1991.

24. Supplement No. 7 to the Safety Evaluation of the Diablo Canyon Nuclear Power Station, Units 1 and 2, Nuclear Regulatory Commission, Division of Reactor Licensing, Washington, DC, May 1978.

25. Supplement No. 8 to the Safety Evaluation of the Diablo Canyon Nuclear Power Station, Units 1 and 2, Nuclear Regulatory Commission, Division of Reactor Licensing, Washington, DC, November 1978.

26. Damping Values for Seismic Design of Nuclear Power Plants, Regulatory Guide 1.61, USAEC, October 1973.

27. PG&E Licensing Basis Impact Evaluation 2005-03, "Replacement Steam Generator Seismic Damping Values," May 25, 2005.

28. Deleted in Revision 20.

29. WCAP-16946-P, Revision 2, Diablo Canyon Vessel Closure Head and Integrated Head Assembly Project - Impact of IHA on Reactor Vessel, Internals, Fuel, and Loop Piping, September 2010.

30. PG&E Document 6023227-19, "Damping Values for Use in the Integrated Head Assembly Seismic Response Analysis at Diablo Canyon Power Plant (DCPP) Units 1 and 2."

31. Damping Values for Seismic Design of Nuclear Power Plants, Regulatory Guide 1.61, Revision 1, USNRC.

32. License Amendment Nos. 208 (DPR-80) and 210 (DPR-82), "Damping Values for the Seismic Design and Analysis of the Reactor Vessel Integrated Head Assembly," USNRC, September 29, 2010.

33. License Amendment Nos. 207 (DPR-80) and 209 (DPR-82), "Critical Damping Values for Control Rod Drive Mechanism Pressure Housings," USNRC, July 30, 2010

34. Bhandari, D. R., et al., System Dynamic Seismic and LOCA Analyses of Reactor Pressure Vessel System for the Pacific Gas and Electric Company Diablo Canyon Power Plants (DCPP) Units 1 & 2, WCAP-14693, Revision 1, February 11, 1997 (Westinghouse Proprietary Class 2).

35. Pacific Gas and Electric Company Transmittal Letter 229643 dated March 28, 1996 from M. J. Angus to John Hoebel

36. Fritz, R. J., The Effects of Liquids on the Dynamic Motions of Immersed Solids, Trans. ASME, Journal of Engineering for Industry, 1972, pp. 167-173.

TABLE 3.7-1

CONTAINMENT AND AUXILIARY BUILDING
CRITERIA COMPARISON

Parameters	HE	DE	DDE
Seismic input, horizontal	0.75g	0.2g	0.4g
Seismic input, vertical	2/3 of horizontal dynamic amplification considered	Static - 2/3 of horizontal ground spectra	Static-2/3 of horizontal ground spectra
Accidental torsion	5% and 7% eccentricity	Not considered	Not considered
Foundation filtering	Tau = 0.040[a]	Not applicable	Not applicable
Response combination	3-D SRSS	2-D ABSUM	2-D ABSUM
Damping values	7%	2% concrete[b] 2% steel	5% concrete 2% steel
Ductility	Allowed in some areas	Not considered	Not considered
Material properties	Based on test values	Min specified values	Min specified values
Response spectra broadening (based on frequency)	+5%, -15%	±10%	±10%
Response spectra peaks clip		10% (for containment only)	10% (for containment only)

(a) 0.052 for auxiliary building.

(b) 5% for auxiliary building.

TABLE 3.7-1A

TURBINE BUILDING
CRITERIA COMPARISON

Parameters	HE	DE and DDE[a]
Seismic input, horizontal	0.75g	0.2g (DE) 0.4g (DDE)
Seismic input, vertical	2/3 of horizontal dynamic amplification Considered	Static - 2/3 of horizontal ground spectra
Accidental torsion	5% and 7% eccentricity, or equivalent Note (b)	Not considered
Foundation filtering	Tau = 0.080 (Blume input) Tau = 0.067 (Newmark input)	Not applicable
Response combination	3-D SRSS	2-D ABSUM
Damping values	7%	5% concrete 2% steel
Ductility	Concrete 1.3 Steel 3 (6 locally)	Not considered
Material properties	Based on test values	Min specified values
Response spectra broadening (based on frequency)	+5%, -15%	±10%
Response spectra peaks clip		10%

(a) DE and DDE analysis is performed only to generate response spectra for systems qualification.

(b) Equivalent method is used as described in Section 3.7.2.10.

TABLE 3.7-1B

INTAKE STRUCTURE
CRITERIA COMPARISON

Parameters	Hosgri	DE and DDE for Systems Qualifications Only
Seismic input, horizontal	Hosgri 7.5M	DE (0.20g) DDE (0.40g)
Seismic input, vertical	2/3 of horizontal spectra with Tau = 0.0 Dynamic amplification Considered	Static 2/3 of ground horizontal spectra
Accidental torsion	Horizontal floor response spectra increased by 10%	Not considered
Foundation filtering	Tau - 0.04	Not applicable
Response combination	3-D-SRSS	Not applicable
Damping values % critical	7%	5%
Ductility	Concrete 1.3; Steel 3, with up to 6 locally[a]	Not considered
Material properties	Based on test values	Minimum specified values
Floor response spectra broadening (based on frequency)	+5%, -15%	Structural peaks clipped 10% and widened by ± 10%

(a) Or as may be required to demonstrate that function of Design Class I equipment will not be adversely affected.

TABLE 3.7-1C

OUTDOOR STORAGE TANKS
CRITERIA COMPARISON

Parameters	Hosgri	DE and DDE
Seismic input, horizontal	Hosgri 7.5M	DE (0.20g) DDE (0.40g)
Seismic input, vertical	2/3 ZPA (0.75g) of horizontal spectra with Amplification considered Tau = 0.0	Static 2/3 ZPA of horizontal ground spectra
Accidental torsion	Not applicable	Not applicable
Response combination	3-D SRSS	2-D ABSUM
Damping	7%-All tanks with concrete cover	5%-All tanks with concrete cover
	4%-Firewater tank without concrete cover	1%-Firewater tank without concrete cover
Material properties	Based on test values	Minimum specified values

TABLE 3.7-2

CONTAINMENT STRUCTURE
PERIODS OF VIBRATION

Mode No.	Period, T, in sec
1	0.255
2	0.093
3	0.088
4	0.073
5	0.060
6	0.058
7	0.057
8	0.051
9	0.051

Table 3.7-3

CONTAINMENT STRUCTURE
MAXIMUM ABSOLUTE ACCELERATIONS

Structure	Nodal Point[(a)]	Elevation, ft	Maximum Absolute Acceleration, g DE Analysis	Maximum Absolute Acceleration, g DDE Analysis
Exterior structure	2	301.64	1.275	2.083
	8	274.37	1.032	1.736
	10	258.27	0.907	1.567
	14	231.00	0.743	1.177
	17	205.58	0.837	1.358
	23	181.08	0.911	1.369
	26	155.83	0.866	1.292
	34	130.58	0.713	1.080
	37	109.67	0.492	0.793
Interior structure	19-22	140.00	0.735	1.195
	24	127.00	0.597	0.982
	27-30	114.00	0.478	0.773
	32	110.00	0.455	0.726
	38	102.00	0.384	0.601
Base slab	47-58	88.58	0.291	0.483

(a) See Figure 3.7-5.

Table 3.7-4

CONTAINMENT STRUCTURE
MAXIMUM DISPLACEMENTS

Structure	Nodal Point[a]	Elevation, ft	Maximum Displacement Inches	
			DE Analysis	DDE Analysis
Exterior structure	2	301.64	0.666	1.063
	8	274.37	0.602	0.967
	10	258.27	0.562	0.911
	14	231.00	0.480	0.807
	17	205.58	0.389	0.695
	23	181.08	0.314	0.587
	26	155.83	0.248	0.459
	34	130.58	0.180	0.327
	37	109.67	0.115	0.212
Interior structure	19-22	140.00	0.083	0.139
	24	127.00	0.069	0.114
	27-30	114.00	0.056	0.090
	32	110.00	0.053	0.084
	38	102.00	0.043	0.068
Base slab	47-58	88.58	0.030	0.050

(a) See Figure 3.7-5.

Table 3.7-5

CONTAINMENT STRUCTURE
MAXIMUM SHELL FORCES AND MOMENTS[a] - DE ANALYSIS

Nodal[b] Point	Elevation, ft	Shell Moments, kip-ft/ft			Shell Forces, kips/ft		
		M_{SS}	M_{TT}	M_{ST}	F_{SS}	F_{TT}	F_{ST}
2	301.64	0.21	0.21	28.99	2.74	3.84	3.75
8	274.37	0.33	0.44	2.96	14.47	32.07	23.85
10	258.27	1.76	0.91	1.63	21.04	40.91	32.80
14	231.00	9.17	2.94	0.36	37.68	42.73	48.97
17	205.58	5.74	1.26	0.27	63.59	33.27	66.44
23	181.08	7.58	2.54	0.31	91.25	37.79	79.59
26	155.83	5.69	1.49	0.50	110.72	36.31	91.43
34	130.58	4.31	1.01	0.27	151.69	31.20	108.65
37	109.67	8.26	2.75	0.19	174.13	18.99	122.66
57	88.58	1.01	0.14	2.23	209.79	63.73	127.22

(a) See Figure 3.7-7.

(b) See Figure 3.7-5.

Table 3.7-6

CONTAINMENT STRUCTURE
MAXIMUM SHELL FORCES AND MOMENTS[a] - DDE ANALYSIS

Nodal[b] Point	Elevation, ft	Shell Moments, kip-ft/ft			Shell Forces, kips/ft		
		M_{SS}	M_{TT}	M_{ST}	F_{SS}	F_{TT}	F_{ST}
2	301.64	0.36	0.37	47.17	4.30	6.33	6.04
8	274.37	0.62	0.76	4.77	22.00	53.37	39.37
10	258.27	2.71	1.46	2.63	32.58	67.71	54.58
14	231.00	15.29	4.92	0.50	60.01	71.93	83.06
17	205.58	8.14	1.64	0.37	103.39	53.31	110.30
23	181.08	11.39	3.96	0.45	154.79	56.72	132.95
26	155.83	8.27	2.21	0.77	190.50	54.24	162.53
34	130.58	6.07	1.36	9.42	251.35	46.24	195.36
37	109.67	15.95	5.31	0.34	282.88	30.75	217.34
57	88.58	1.74	0.23	4.18	338.73	110.90	220.62

(a) See Figure 3.7-7.

(b) See Figure 3.7-5.

Table 3.7-7

CONTAINMENT STRUCTURE
MAXIMUM TOTAL SHEARS

Structure	Associated[a] Nodel Point	Elevation, ft	Maximum Shears, kips x 10^3 DE Analysis	DDE Analysis
Exterior structure	2	301.64	0.19	0.66
	8	274.37	5.81	9.38
	10	258.27	8.49	13.91
	14	231.00	11.39	19.55
	17	205.58	15.00	25.02
	23	181.08	17.95	29.98
	26	155.83	20.63	36.66
	34	130.58	24.53	44.18
	37	109.67	27.83	49.42
	57	88.58	29.55	51.39
Interior structure	19 & 22	140.00	8.06	13.23
	27 & 30	114.00	10.27	16.87
	49 & 54	88.58	18.85	30.96
Total base shear	49, 54, & 57	88.58	35.05	59.99

(a) See Figure 3.7-5.

Table 3.7-8

CONTAINMENT STRUCTURE
MAXIMUM TOTAL OVERTURNING MOMENTS

Structure	Associated[a] Nodel Point	Elevation, ft	Maximum Overturning Moment kips-ft x 10^6 DE Analysis	DDE Analysis
Exterior structure	2	301.64	0.00	0.00
	8	274.37	0.12	0.18
	10	258.27	0.27	0.41
	14	231.00	0.61	0.97
	17	205.58	1.03	1.67
	23	181.08	1.48	2.50
	26	155.83	1.79	3.08
	34	130.58	2.45	4.07
	37	109.67	2.82	4.58
	57	88.58	3.39	5.48
Interior structure	19 & 22	140.00	0.06	0.10
	27 & 30	114.00	0.20	0.33
	49 & 54	88.58	0.76	1.24
Total O.T.M. at base	49, 54 & 57	88.58	3.48	5.62

(a) See Figure 3.7-5.

TABLE 3.7-8A

PERIODS OF VIBRATION AND PERCENT PARTICIPATION FACTORS

	Containment Exterior Structure					
	Translational[a] Horizontal Model		Coupled Translation[b] Plus Torsion Model		Vertical Model	
Mode No	Period (sec)	Percent Participation Factor	Period (sec)	Percent Participation Factor	Period (sec)	Participation Factor
1	0.225	44.97	0.217	58.85	0.081	51.72
2	0.081	22.75	0.109	0.32	0.051	16.72
3	0.053	3.73	0.074	25.86	0.046	2.62
4	0.053	7.88	0.041	12.35	0.046	3.81
5	0.047	1.96	0.039	5.63	0.044	11.84
6	0.045	0.043			0.043	0.05
7	0.043	9.91			0.040	7.96
8	0.041	1.66			0.038	3.15
9	0.037	1.70			0.035	1.25
10	0.036	1.71			0.035	0.88
11	0.033	1.18				
12	0.032	2.12				

(a) Axisymmetric model (see Figure 3.7-5A).
(b) Lumped-mass model with 5% accidental eccentricity (see Figure 3.7-5B).

TABLE 3.7-8B

CONTAINMENT EXTERIOR STRUCTURE
MAXIMUM ABSOLUTE HORIZONTAL AND VERTICAL ACCELERATIONS

		Absolute Horizontal Acceleration (g)		Absolute Vertical Acceleration (g)	
Nodal[b] Point	Elevation (ft)	Blume-Hosgri[a] Horizontal Input	Vertical Input	Blume-Hosgri Horizontal Input	Vertical Input
2	301.64	2.21	0.02	0.075	1.600
8	274.37	2.07	0.15	0.450	1.020
10	258.27	1.95	0.28	0.511	0.882
14	231.00	1.70	0.28	0.532	0.810
17	205.58	1.44	0.11	0.475	0.759
19	181.08	1.23	0.14	0.416	0.703
20	155.83	1.00	0.17	0.334	0.633
22	130.58	0.80	0.18	0.228	0.575
23	109.67	0.75	0.16	0.122	0.538

(a) Effective horizontal acceleration at containment shell due to absolute sum of horizontal response and torsional response from 5% eccentricity.

(b) See Figure 3.7-5A.

TABLE 3.7-8C

CONTAINMENT EXTERIOR STRUCTURE
MAXIMUM HORIZONTAL AND VERTICAL DISPLACEMENTS

		Horizontal Displacement (in.)		Vertical Displacement (in.)	
Nodal[(a)] Point	Elevation (ft)	Blume-Hosgri Horizontal Input	Vertical Input	Blume-Hosgri Horizontal Input	Vertical Input
2	301.64	1.120	0.002	0.032	0.108
8	274.37	1.012	0.009	0.198	0.076
10	258.27	0.943	0.020	0.228	0.066
14	231.00	0.802	0.020	0.240	0.056
17	205.58	0.642	0.008	0.221	0.049
19	181.08	0.515	0.009	0.195	0.041
20	155.83	0.379	0.011	0.158	0.031
22	130.58	0.253	0.012	0.109	0.020
23	109.67	0.151	0.012	0.058	0.010

(a) See Figure 3.7-5A.

TABLE 3.7-8D

CONTAINMENT EXTERIOR STRUCTURE
MAXIMUM SHELL FORCES AND MOMENTS

		Shell Forces (kip/ft)[a]						Shell Moments (kip-ft/ft)[a]					
		Blume-Hosgri Horizontal Input			Vertical Input			Blume-Hosgri Horizontal Input			Vertical Input		
Nodal[b] Point	Elevation (ft)	F_{SS}	F_{TT}	F_{ST}	F_{SS}	F_{TT}	F_{ST}	M_{SS}	M_{TT}	M_{ST}	M_{SS}	M_{TT}	M_{ST}
2	301.64	4.48	7.35	6.85	26.04	10.32	0	0.80	0.39	57.55	3.68	2.94	0
8	274.37	23.05	59.90	44.80	27.97	28.90	0	0.72	0.86	5.87	2.66	1.09	0
10	258.27	34.80	77.10	53.15	31.00	28.24	0	2.85	1.59	3.24	3.12	1.36	0
14	231.00	65.60	86.55	101.00	42.95	9.45	0	17.40	5.42	0.64	11.24	1.24	0
17	205.58	118.00	51.40	143.00	57.41	13.38	0	7.80	1.27	0.23	5.86	1.12	0
19	181.08	185.50	47.00	73.50	63.95	11.60	0	11.75	3.86	0.32	3.14	1.40	0
20	155.83	235.00	40.15	200.00	65.85	7.89	0	12.40	2.96	0.69	3.51	1.37	0
22	130.58	325.50	37.80	219.50	66.95	10.76	0	5.99	1.13	0.27	2.08	2.32	0
23	109.67	376.00	36.25	240.50	67.06	0	0	19.05	6.26	0.26	6.99	2.78	0

(a) See Figure 3.7-7.

(b) See Figure 3.7-5A.

TABLE 3.7-8E

CONTAINMENT EXTERIOR STRUCTURE
MAXIMUM TOTAL SHEARS AND MAXIMUM OVERTURNING MOMENTS

Nodal[b] Point	Elevation (ft)	Maximum Shear Force (kips x 10^3)[a] Blume-Hosgri Horizontal Input	Maximum Overturning Moment (kip-ft x 10^6)[a] Blume-Hosgri Horizontal Input
2	301.64	0.34	--
8	274.37	10.50	0.18
10	258.27	15.94	0.44
14	231.00	23.67	1.06
17	205.58	32.49	1.91
19	181.08	39.44	3.00
20	155.83	45.39	3.80
22	130.58	49.70	5.26
23	109.67	55.05	6.08
27	88.58	55.81	7.31

(a) Vertical Input does not produce a net shear force.

(b) See Figure 3.7-5A.

TABLE 3.7-8F

CONTAINMENT EXTERIOR STRUCTURE
MAXIMUM TOTAL TORSIONAL MOMENTS AND AXIAL FORCES

Nodal[b] Point	Elevation (ft)	Blume-Hosgri Total Torsional Moment (kip-ft x 10^3)[a] Horizontal Input	Axial Force(kips x 10^3)[c]
2	301.64	5.49	1.52
8	274.37	67.61	9.93
10	258.27	136.94	12.82
14	231.00	216.36	19.36
17	205.58	293.17	25.88
19	181.08	353.32	28.83
20	155.83	400.00	29.69
22	130.58	427.78	30.18
23	109.67	439.99	30.23

(a) Vertical input does not produce a net torque.

(b) See Figure 3.7-5A.

(c) Due to vertical input.

TABLE 3.7-8G

CONTAINMENT INTERIOR STRUCTURE
MAXIMUM ABSOLUTE HORIZONTAL ACCELERATIONS AND DISPLACEMENTS

		Newmark-Hosgri			
Nodal[a] Point	Elevation (ft)	Horizontal Acceleration (g)	Torsional Acceleration (rad/sec^2)	Displacement (in.)	Rotation (rad x 10^{-5})
28	140.00	0.92	0.07	0.06	1.21
34	114.00	0.70	0.05	0.03	0.82

(a) See Figure 3.7-5A.

TABLE 3.7-8H

CONTAINMENT INTERIOR STRUCTURE
MAXIMUM TOTAL SHEARS, OVERTURNING MOMENTS,
AND TORSIONAL MOMENTS[a]

Nodal[b] Point	Elevation (ft)	Shear (kips x 10^3) Blume-Hosgri	Shear (kips x 10^3) Newmark-Hosgri	Overturning Moment (kip-ft x 10^3) Blume-Hosgri	Overturning Moment (kip-ft x 10^3) Newmark-Hosgri	Torsional Moment[c] (kip-ft x 10^3) Blume-Hosgri	Torsional Moment[c] (kip-ft x 10^3) Newmark-Hosgri
34	114.00	6.52	6.64	74.55	78.82	136.68	146.48
37	114.00	10.80	11.23	227.89	239.55		
48	88.58	10.08	10.40	219.60	229.31	266.06	283.99
49	88.58	13.26	13.73	544.10	560.76		

(a) Due to horizontal input only.

(b) See Figure 3.7-5A.

(c) Values obtained from lumped-mass model shown in Figure 3.7-5C.

TABLE 3.7-8I

UNIT 1
VERTICAL DYNAMIC ANALYSIS - FRAME NO. 6
SUMMARY OF MODAL PARTICIPATION FACTORS AND FREQUENCIES

Mode	Frequency	X-Direction	Y-Direction	Z-Direction	X-Rotation	Y-Rotation	Z-Rotation
1	11.4	0.00	0.00	0.71	0.0	-541.0	0.0
2	16.8	0.00	0.00	0.09	0.0	-63.0	0.0
3	20.6	0.00	0.00	-0.08	0.0	54.0	0.0
4	21.9	0.00	0.00	0.09	0.0	-65.0	0.0
5	24.1	0.00	0.00	0.03	0.0	-31.0	0.0
6	24.4	0.00	0.00	-0.01	0.0	13.0	0.0
7	24.9	0.00	0.00	-0.03	0.0	22.0	0.0
8	26.2	0.00	0.00	-0.01	0.0	-5.0	0.0
9	28.4	0.00	0.00	-0.50	0.0	304.0	0.0
10	29.3	0.00	0.00	0.20	0.0	-124.0	0.0
11	33.2	0.00	0.00	-0.04	0.0	30.0	0.0

NOTE: X is in the Radial direction.
Y is in the Longitudinal direction.
Z is in the Vertical direction.

TABLE 3.7-8J

UNIT 2
VERTICAL DYNAMIC ANALYSIS - ANNULUS FRAME 6
SUMMARY OF MODAL PARTICIPATION FACTORS AND FREQUENCIES

Mode	Frequency	X-Direction	Y-Direction	Z-Direction	X-Rotation	Y-Rotation	Z-Rotation
1	11.6	.00	0.70	.00	.00	.00	82.0
2	16.0	.00	-0.09	.00	.00	.00	-7.7
3	16.46	.00	0.07	.00	.00	.00	6.6
4	22.9	.00	-0.07	.00	.00	.00	-13.0
5	23.87	.00	0.02	.00	.00	.00	-2.0
6	24.0	.00	0.00	.00	.00	.00	7.0
7	27.8	.00	0.00	.00	.00	.00	-8.1
8	32.28	.00	0.08	.00	.00	.00	-15.0

NOTE: X is in the Radial direction.
Y is in the Longitudinal direction.
Z is in the Vertical direction.

TABLE 3.7-8K

CONTAINMENT ANNULUS STRUCTURES UNITS 1 AND 2
NATURAL FREQUENCIES FOR HORIZONTAL
SEISMIC GROUND MOTION

Unit	Elevation	Mode	Frequency (cps)
1	101	1	20.95
		2	21.69
	106	1	20.16
		2	21.47
	117	1	20.24
		2	22.78
2	101	1	22.46
		2	22.79
	106	1	19.98
		2	22.20
	117	1	19.98
		2	25.79

TABLE 3.7-8L

POLAR GANTRY CRANE
MAXIMUM DISPLACEMENTS, HOSGRI

Condition	Node	Longitudinal Direction (in.)	Transverse Direction (in.)	Vertical Direction (in.)
Unloaded	75	-	-	1.54
	7	0.94	0.52	1.54
	17	5.40	3.91	1.53
	25	6.00	5.36	1.53
	31	6.00	5.59	1.74
	39	5.96	5.07	1.41
	47	5.96	4.82	1.66
	77	-	-	1.66
	72	9.85	15.74	0.94
Loaded, 200 tons	75	-	-	1.33
	7	1.05	0.44	1.33
	17		3.34	1.45
	25	6.18	4.52	1.32
	31	6.18	4.75	1.47
	39	6.18	4.09	-1.96
	47	6.18	4.46	0.89
	77	-	-	0.90
	72	9.41	13.85	-3.60

Notes:

1. All displacements are measured relative to base of crane.

2. For node numbers, refer to Figure 3.7-7A.

TABLE 3.7-8M

POLAR GANTRY CRANE
MAXIMUM FORCES,
HOSGRI - UNLOADED CONDITION

Element	Node	Axial Force Compression (kips)	Bending Moment About Axis 2 (kip-in.)	Bending Moment About Axis 3 (kip-in.)
11	9	27	20,000	2,110
2	11	594	17,700	14,700
3	15	545	9,000	78,400
10	19	9	22,100	6,580
4	21	474	6,730	84,700
4	23	474	5,030	102,000
12	27	70	11,500	10,900
9	33	4	6,960	9,400
13	35	147	97,900	15,000
22		44	0	3,890
16	45	161	100,000	13,600
24	49	4	10,500	10,700
30	51	367	9,710	102,000
30	53	367	2,530	84,500
25	57	4	21,400	4,140
29	59	501	21,900	78,200
28	63	520	20,500	13,700
26	67	29	23,600	2,200

Note:

1. For node and element numbers, refer to Figure 3.7-7A.

TABLE 3.7-8N

POLAR GANTRY CRANE
MAXIMUM FORCES,
HOSGRI - LOADED CONDITION

Element	Node	Axial Force Compression (kips)	Bending Moment About Axis 2 (kip-in.)	Bending Moment About Axis 3 (kip-in.)
11	9	40	30,900	2,430
2	11	830	24,400	9,780
3	15	812	25,600	94,000
10	19	11	28,900	7,310
4	21	652	8,390	102,000
4	23	652	7,620	126,000
12	27	109	12,700	13,300
9	33	5	9,050	12,900
13	35	199	120,000	18,300
22	41	58	-	3,390
16	45	210	120,000	18,200
24	49	4	13,700	13,800
30	51	571	10,300	125,000
30	53	571	3,430	103,000
25	57	5	22,300	5,310
29	59	723	22,200	95,000
28	63	739	20,300	17,000
26	67	39	23,100	2,500

Note:

1. For node and element numbers, refer to Figure 3.7-7A.

TABLE 3.7-8O

FUEL HANDLING CRANE SUPPORT STRUCTURE
MAXIMUM ABSOLUTE ACCELERATIONS

Load Case	Location	Acceleration,[(a)] g		
		NS	EW	Vertical
HE	El 188 ft	1.7	1.6	1.1
	Columns, El 166 ft	1.6	1.3	0.6
DE	El 188 ft	0.8	0.5	(b)
	Columns, El 166 ft	0.7	0.4	(b)

(a) Accelerations are average of accelerations from models 2.1 and 2.2.

(b) DE vertical equivalent static analysis coefficient is 0.13 g.

TABLE 3.7-8P

FUEL HANDLING CRANE SUPPORT STRUCTURE
MAXIMUM RELATIVE DISPLACEMENTS

Load Case	Location	Displacements[(a)], in. NS	EW
HE	El 188 ft	2.0	8.8
	Columns, El 166 ft	1.8	7.1
DE	El 188 ft	0.9	2.8
	Columns, El 166 ft	0.9	2.3

(a) Displacements are from static analysis of detailed fuel handling crane support structure model described in Section 3.8.2.4. Displacements are relative to elevation 140 ft.

TABLE 3.7-9

AUXILIARY BUILDING
PERIODS OF VIBRATION - DE ANALYSIS

	N-S Direction		W Direction	
Mode No.	Period, T, (sec)	Translational Participation Factor	Period, T, (sec)	Translational Participation Factor
1[a]	0.641	0.0	0.688	8.6
2[a]	0.327	8.9	0.641	0.0
3	0.073	48.1	0.072	68.7
4	0.059	48.7	0.065	0.0
5	0.037	20.0	0.040	20.6
6	0.031	1.5	0.031	0.0

(a) Steel superstructure modes (one translational and the other torsional).

TABLE 3.7-10

AUXILIARY BUILDING HORIZONTAL MODEL
PERIODS AND PARTICIPATION FACTORS - HE ANALYSIS

COUPLED - TRANSLATIONAL PLUS TORSION

	North-South Model with 5% Eccentricity to East		North-South Model with 5% Eccentricity to West		East-West Model with 5% Eccentricity	
Mode No.	Period (sec)	Translation Participation Factor	Period (sec)	Translation Participation Factor	Period (sec)	Translation Participation Factor
1[a]	.641	-0.0	.641	0.0	.688	8.6
2[a]	.327	8.9	.327	8.9	.641	0.0
3	.070	-41.2	.075	-47.6	.074	60.2
4	.061	54.7	.056	49.4	.062	33.2
5	.036	-19.7	.037	-19.4	.039	-20.8
6	.030	-3.8	.030	7.0	.030	3.1
7	.025	-15.3	.026	14.6	.028	-17.9
8	.024	19.6	.023	-19.2	.023	14.8
9	.015	2.8	.016	7.8	.017	11.3
10	.014	13.9	.014	-11.7	.014	9.0

(a) Steel superstructure modes (one translational and the other torsional).

TABLE 3.7-11

AUXILIARY BUILDING VERTICAL MODEL
PERIODS AND PARTICIPATION FACTORS - HE ANALYSIS

Mode Number[(a)]	Period (sec)	Participation Factor
1[(b)]	0.085	-6.0
2	0.033	67.9

(a) Only modes below 33 Hz are listed.

(b) Steel superstructure roof mode.

TABLE 3.7-11A

FUEL HANDLING CRANE SUPPORT STRUCTURE HORIZONTAL MODELS FREQUENCIES OF VIBRATION[(a)]

DE, DDE, AND HE ANALYSES

	Model 2.1		Model 2.2	
First[(b)] Fundamental Modal Direction	Frequency (cps)	Modal Effective Mass %	Frequency (cps)	Modal Effective Mass (%)
E-W	1.6	85.0	1.6	86.0
N-S	3.1	88.0	2.7[(a)]	92.0

(a) For Model 2.2 see Figure 3.7-13B. Model 2.1 represents six end bay frames and is similar.

(b) Other modes have insignificant contributions, and are not included.

TABLE 3.7-11B

FUEL HANDLING CRANE SUPPORT STRUCTURE
VERTICAL MODEL FREQUENCIES OF VIBRATION[(a)(b)]

DE, DDE, AND HE ANALYSES

Model 2.1		Model 2.2	
Frequency (hz)	Modal Effective Mass (% of roof)	Frequency (hz)	Modal Effective Mass (% of roof)
10.6	19	10.1	23
16.9	23	16.6	26
20.7	2	22.8	1

(a) Only significant modes with frequencies less than 33 hz are shown. For models 2.1 and 2.2, 99 modes and 105 modes were extracted, respectively, with frequencies up to 105 hz.

(b) For model 2.2, see Figure 3.7-13B. Model 2.1 represents six end bay frames and is similar.

TABLE 3.7-12

AUXILIARY BUILDING
MAXIMUM ABSOLUTE ACCELERATIONS-DE ANALYSIS

		Maximum Absolute Accelerations		
		N-S Direction		E-W Direction
Mass[a] Point	Elevation, ft	Horizontal Acceleration, g	Rotational Acceleration rad/sec^2	Horizontal Acceleration, g
6	188.0	0.554	0.0004	0.313
1	163.0	0.375	0.0217	0.435
2	140.0	0.300	0.0187	0.324
3	115.0	0.259	0.0115	0.291
4	100.0	0.230	0.0055	0.257

(a) See Figure 3.7-13.

TABLE 3.7-13

AUXILIARY BUILDING
MAXIMUM RELATIVE DISPLACEMENTS-DE ANALYSIS

		Maximum Relative Displacement		
		N-S Direction		E-W Direction
Mass[a] Point	Elevation, ft	Horizontal Translation, in.	Rotation radians x 10^{-6}	Horizontal Translation, in.
6	188.0	0.575	1.624	1.447
1	163.0	0.022	4.087	0.025
2	140.0	0.015	3.308	0.018
3	115.0	0.009	2.014	0.012
4	100.0	0.004	0.975	0.006

(a) See Figure 3.7-13.

TABLE 3.7-14

AUXILIARY BUILDING
MAXIMUM STORY SHEARS-DE ANALYSIS

Element[(a)]	Maximum Story Shears, kips x 10^3 N-S Direction	Maximum Story Shears, kips x 10^3 E-W Direction
5	1.3	0.7
1	3.8	4.8
2	26.3	24.6
3	40.0	42.7
4	28.5	28.4

(a) See Figure 3.7-13.

TABLE 3.7-15

AUXILIARY BUILDING
MAXIMUM OVERTURNING MOMENTS-DE ANALYSIS

Element[a]	Maximum O.T. Moments, kips - ft x 10^6 N-S Direction	Maximum O.T. Moments, kips - ft x 10^6 E-W Direction
5	0.06	0.04
1	0.08	0.10
2	0.74	0.68
3	1.32	1.30
4	1.76	1.74

(a) See Figure 3.7-13.

TABLE 3.7-16

AUXILIARY BUILDING
MAXIMUM TORSIONAL MOMENTS DUE TO
EARTHQUAKE IN N-S DIRECTION-DE ANALYSIS

Element[(a)]	Maximum Torsional Moments, kip - ft x 10^5
5	0.004
1	0.265
2	14.080
3	19.810
4	9.139

(a) See Figure 3.7-13.

TABLE 3.7-17

AUXILIARY BUILDING
MAXIMUM ABSOLUTE ACCELERATIONS - HE ANALYSIS
EARTHQUAKE IN N-S DIRECTION

Mass[a] Point	Elevation, ft	Blume-Hosgri Horizontal Acceleration, g		Newmark-Hosgri Horizontal Acceleration, g		Blume-Hosgri Rotational Acceleration, rad/sec^2		Newmark-Hosgri Rotational Acceleration, rad/sec^2	
		5% E	5% W	5% E	5% W	5% E	5% W	5% E	5% W
6	188.0	1.57	1.56	1.37	1.36	-	-	-	-
1	163.0	1.13	1.10	1.25	1.21	.0981	.1477	.1102	.1646
2	140.0	0.84	0.77	0.90	0.84	.0604	.0895	.0710	.1018
3	115.0	0.71	0.70	0.72	0.66	.0370	.0516	.0431	.0590
4	100.0	0.67	0.66	0.58	0.61	.0175	.0239	.0206	.0275

(a) See Figure 3.7-13.

TABLE 3.7-18

AUXILIARY BUILDING
MAXIMUM ABSOLUTE ACCELERATIONS - HE ANALYSIS
EARTHQUAKE IN E-W DIRECTION

Mass[a] Point	Elevation, ft	Blume-Hosgri Horizontal Acceleration, g	Newmark-Hosgri Horizontal Acceleration, g	Blume-Hosgri Rotational Acceleration, rad/sec^2	Newmark-Hosgri Rotational Acceleration, rad/sec^2
6	188.0	1.11	1.24	.0015	.0017
1	163.0	1.11	1.22	.1162	.1292
2	140.0	0.94	1.00	.0769	.0881
3	115.0	0.72	0.75	.0452	.0527
4	100.0	0.66	0.62	.0213	.0246

(a) See Figure 3.7-13.

TABLE 3.7-19

AUXILIARY BUILDING
MAXIMUM RELATIVE DISPLACEMENTS - HE ANALYSIS
EARTHQUAKE IN N-S DIRECTION

Mass[a] Point	Elevation, ft	Blume-Hosgri Horizontal Translation, in.		Newmark-Hosgri Horizontal Translation, in.		Blume-Hosgri Rotation radians x 10^{-6}		Newmark-Hosgri Rotation radians x 10^{6}	
		5% E	5% W	5% E	5% W	5% E	5% W	5% E	5% W
6	188.0	1.63	1.62	1.42	1.42	-	-	-	-
1	163.0	0.06	0.06	0.06	0.07	9.589	18.901	10.961	21.001
2	140.0	0.04	0.04	0.04	0.04	8.034	14.091	9.135	15.472
3	115.0	0.02	0.02	0.02	0.02	4.785	8.530	5.468	9.361
4	100.0	0.01	0.01	0.01	0.01	2.256	4.044	2.576	4.444

(a) See Figure 3.7-13.

TABLE 3.7-20

AUXILIARY BUILDING
MAXIMUM RELATIVE DISPLACEMENTS - HE ANALYSIS
EARTHQUAKE IN E-W DIRECTION

Mass[a] Point	Elevation, ft	Blume-Hosgri Horizontal Translation, in.	Newmark-Hosgri Horizontal Translation in.	Blume-Hosgri Rotation radians x 10^{-6}	Newmark-Hosgri Rotation radians x 10^{6}
6	188.0	5.08	5.63	6.153	6.897
1	163.0	0.07	0.07	14.616	16.354
2	140.0	0.05	0.05	11.219	12.484
3	115.0	0.03	0.03	7.078	7.873
4	100.0	0.02	0.02	3.471	3.854

(a) See Figure 3.7-13.

TABLE 3.7-21

AUXILIARY BUILDING
MAXIMUM STORY SHEARS - HE ANALYSIS

	Earthquake in N-S Direction				Earthquake in E-W Direction	
	Blume-Hosgri Shear kips x 10^3		Newmark-Hosgri Shear kips x 10^3		Blume-Hosgri Shear kips x 10^3	Newmark-Hosgri Shear kips x 10^3
Element[a]	5% E	5% W	5% E	5% W	±5%	±5%
5	3.6	3.6	3.2	3.2	2.6	2.9
1	12.4	12.4	13.7	13.6	12.3	13.6
2	65.6	58.4	71.9	63.3	71.0	76.2
3	106.2	100.0	115.2	101.5	115.0	122.5
4	84.5	86.7	90.2	85.8	75.8	80.2

(a) See Figure 3.7-13.

TABLE 3.7-22

AUXILIARY BUILDING
MAXIMUM OVERTURNING MOMENTS - HE ANALYSIS

	Earthquake in N-S Direction				Earthquake in E-W Direction	
	Blume-Hosgri Moment kips x 10^6		Newmark-Hosgri Moment kips x 10^6		Blume-Hosgri Moment kips x 10^6	Newmark-Hosgri Moment kips x 10^6
Element[(a)]	5% E	5% W	5% E	5% W	±5%	±5%
5	0.18	0.17	0.15	0.15	0.12	0.14
1	0.27	0.27	0.30	0.29	0.27	0.29
2	1.85	1.66	2.05	1.74	1.96	2.11
3	3.41	3.12	3.73	3.21	3.65	3.90
4	4.68	4.42	5.11	4.46	4.80	5.15

(a) See Figure 3.7-13.

TABLE 3.7-23

AUXILIARY BUILDING
MAXIMUM TORSIONAL MOMENTS - HE ANALYSIS

	Earthquake in N-S Direction				Earthquake in E-W Direction	
	Blume-Hosgri Torsional Moment kips x 105		Newmark-Hosgri Torsional Moment kips x 10^5		Blume-Hosgri Torsional Moment kips x 10^5	Newmark-Hosgri Torsional Moment kips x 10^5
Element[(a)]	5% E	5% W	5% E	5% W	±5%	±5%
5	0.01	0.02	0.01	0.02	0.01	0.02
1	0.82	1.71	0.89	1.88	1.30	1.45
2	35.36	60.41	39.93	66.53	44.98	50.14
3	48.24	85.27	55.16	93.73	68.81	76.67
4	21.14	38.00	24.14	41.73	32.59	36.19

(a) See Figure 3.7-13.

TABLE 3.7-23A

TURBINE BUILDING HORIZONTAL MODEL (LOADED CRANE CASE 2)[(a)]
FREQUENCIES OF VIBRATION[(b)] - HE ANALYSIS[(d)]

Mode No.	Frequency Hz	Participation Factor	
		North-South	East-West
1[(c)]	1.39	0.00	3.01
4[(c)]	3.32	2.59	0.00
18	5.81	-4.75	0.77
19	5.86	-0.02	-3.32
21	6.03	-0.32	-2.29
22	6.19	0.76	-2.60
23	6.37	-1.16	0.81
24	6.43	-2.66	-0.66
26	6.78	0.24	-1.74
27	7.10	-2.02	0.50
28	7.18	1.08	-1.32
29	7.32	-2.13	0.62
30	7.36	1.02	-0.03
31	7.43	-1.51	-0.61
32	7.57	0.44	-2.59
33	7.62	1.83	1.42
36	7.99	-2.04	-0.95
38	8.32	-1.70	-0.94
39	8.38	-3.16	-0.70
40	8.47	2.47	1.17
44	9.09	0.30	-1.78
56	10.71	0.28	-1.54
65	11.52	1.54	-0.14
82	13.10	-0.39	2.02
83	13.15	0.29	-1.43
89	14.02	0.01	1.79
92	14.32	-0.11	1.87
93	14.78	0.33	1.04
100	16.60	-0.31	1.54
101	16.74	0.13	2.00
102	16.81	0.52	-1.78
103	17.03	1.65	-0.22
104	17.26	-1.46	-0.54
111	18.16	0.12	1.11
115	18.93	-1.68	-0.10
147	22.29	1.00	-0.41
165	23.89	-0.89	0.49

TABLE 3.7-23A

(a) For Case 2, the Unit 1 crane has a 15-ton load and is located at column line 9, and the Unit 2 crane has a 50-ton load and is located at column line 12.2.

(b) 210 modes were extracted with frequencies ranging from 1.39 Hz to 33.01 Hz. Shown above are the modes with the twenty highest participation factors in each direction. The cumulative modal masses of the 210 modes represent 95% of the total weight of the building.

(c) Modes 1 and 4 are the principal modes of the superstructure.

(d) Note that the results in this table correspond with the seismic analysis performed for the operating license review (Reference 18) and may not reflect the latest as-built configuration of the turbine building.

TABLE 3.7-23B

TURBINE BUILDING VERTICAL MODEL NO. 1
FREQUENCIES OF VIBRATION[(a)] - HE ANALYSIS[(c)]

Mode No.	Frequency Hz	Participation Factor
1[(b)]	2.80	0.65
2[(b)]	2.80	0.38
5[(b)]	5.07	-0.48
15	7.48	2.00
17	7.75	-1.55
21	8.71	1.04
23	9.16	-0.55
33	10.70	-0.40
35	10.87	0.52
40	11.38	0.53
54	13.34	-0.36
59	14.02	0.43
61	14.23	0.57
62	14.40	0.31
63	14.46	-0.87
64	14.56	0.28
78	16.68	0.30
83	17.36	-0.65
89	18.29	0.48
115	22.03	-0.29

(a) 187 modes were extracted, ranging from 2.80 Hz to 33.01 Hz. Shown above are the modes with the 20 highest participation factors. The cumulative modal mass of the 187 modes represents 94% of the total weight of the building.

(b) Modes 1, 2, and 5 represent significant modes for the superstructure and overhead crane.

(c) Note that the results in this table correspond to the seismic analysis performed for the operating license review (Reference 18) and may not reflect the latest as-built configuration of the turbine building.

TABLE 3.7-23C

TURBINE BUILDING MODEL
LOADED CRANE CASES
MAXIMUM ABSOLUTE ACCELERATIONS - HE ANALYSIS[b]

Elevation, ft	Location Bent	Line	Acceleration[a], g N-S	E-W	Vertical
104 & 107	1 to 5	A-G	--	1.16	1.54
	5 to 15	A-G	--	1.18	1.99
	15 to 17	A-G	--	1.06	2.49
	17 to 19	A-G	--	1.11	--
	1 to 19	A-G	1.22	--	--
119 & 123	1 to 5	A-G	--	1.84	2.16
	5 to 15	A-G	--	2.08	2.35
	15 to 17	A-G	--	1.83	2.43
	17 to 19	A-G	--	1.68	1.30
	1 to 19	A-G	2.20	--	--
140	1 to 5	A-G	--	1.37	1.68
	5 to 15	A-G	--	2.19	1.91
	15 to 17	A-G	--	1.24	1.29
	17 to 19	A-G	--	1.11	1.32
	1 to 19	A-G	1.91	--	--
159	1.9 to 4.8	G	--	1.29	0.73
	5.7 to 15	G	--	2.51	0.70
	16 to 19	G	--	1.51	0.59
	1.9 to 19	G	1.57	--	--
193	1.9 to 4.8	A, G	--	--	0.91
	5.7 to 15	A, G	--	--	0.70
	16 to 19	A, G	--	--	0.59
Roof	1 to 1.9	A-D	3.97	1.60	

TABLE 3.7-23C

(a) Acceleration values are zero period accelerations of floor response spectra. At and below elevation 140 feet, values are for the case of a single unloaded crane; values for the case of two cranes with one crane loaded are similar.

(b) Note that the results in this table correspond to the seismic analysis performed for the operating license review (Reference 18) and may not reflect the latest as-built configuration of the turbine building.

TABLE 3.7-23D

TURBINE BUILDING MODELS
LOADED CRANE CASES
MAXIMUM RELATIVE DISPLACEMENTS - HE ANALYSIS[b]

Elevation, ft	Location: Bent	Location: Line	Displacement[a], in.: N-S	Displacement[a], in.: E-W	Displacement[a], in.: Vertical
104 & 107	1 to 5	A-G	0.08	0.07	0.25
	5 to 15	A-G	0.07	0.16	0.75
	15 to 17	A-G	0.04	0.13	1.31
	17 to 19	A-G	0.06	0.68	--
119, 123, & 125	1 to 5	A-G	0.25	0.23	0.52
	5 to 15	A-G	0.60	0.42	0.82
	15 to 17	A-G	0.80	0.35	0.62
	17 to 19	A-G	0.90	1.02	0.45
140	1 to 5	A-G	0.22	0.18	0.37
	5 to 15	A-G	0.20	0.58	0.03
	15 to 17	A-G	0.20	0.28	0.13
	17 to 19	A-G	0.20	0.83	0.42
159	1 to 5	G	0.42	2.06	0.39
	5 to 15	G	0.42	3.22	0.31
	15 to 17	G	0.41	2.97	0.06
	17 to 19	G	0.42	3.98	--
193	1 to 5	A-G	1.92	5.89	0.13
	5 to 15	A-G	1.09	8.76	0.05
	15 to 17	A-G	1.21	9.64	0.08
	17 to 19	A-G	1.32	11.46	--
Roof	1 to 1.9	A-D	2.60	3.64	--

(a) Displacement values are based on response spectrum analysis.

(b) Note that the results in this table correspond to the seismic analysis performed for the operating license review (Reference 18) and may not reflect the latest as-built configuration of the turbine building.

TABLE 3.7-23E

TURBINE PEDESTAL MODEL
FREQUENCIES OF VIBRATION[(a)] - HE ANALYSIS

Mode No.	Frequency (Hz)	Participation Factor N-S	Participation Factor E-W	Participation Factor Vertical
1	3.09	--	27.2	--
2	3.54	--	3.6	--
3	4.23	27.6	--	0.4
11	15.14	0.3	--	-14.1
12	15.96	-0.3	--	8.0
23	20.94	-0.5	--	12.1
25	21.69	--	--	-9.1
27	22.06	--	4.0	--
30	23.36	-0.2	--	-8.0
36	26.11	--	-3.4	--
45	30.34	2.1	--	2.2
46	30.54	2.4	--	-5.2
47	30.94	-2.7	--	4.0
49	31.89	-3.5	--	3.0
50	32.14	--	2.7	--

(a) 50 modes were extracted, ranging in frequency from 3.09 Hz to 32.14 Hz. Shown above are the modes with the five highest participation factors for each direction.

TABLE 3.7-23F

TURBINE PEDESTAL MODEL
MAXIMUM RELATIVE DISPLACEMENTS - HE ANALYSIS

Nodal Point[(a)]	North-South Direction (in.)	East-West Direction (in.)	Vertical Direction (in.)
9	.71	1.30	0.006
35	.73	1.22	0.006
58	.74	1.40	0.006
81	.75	1.63	0.006
102	.76	1.59	0.005
123	.76	1.67[(c)]	0.005

(a) Nodal points are identified in Figure 3.7-15G.

(b) Vertical displacement includes dead load displacement.

(c) Effects of load redistribution are included.

TABLE 3.7-23G

SIGNIFICANT PERIODS OF VIBRATION AND PERCENT PARTICIPATION FACTORS
INTAKE STRUCTURE

	North-South Model		East-West Vertical Model		
Mode Number	Period (sec)	Percent Participation Factor	Period (sec)	East-West Percent Participation Factor	Vertical Percent Participation Factor
2	0.081	0.5	0.081	0.0	0.1
3	0.081	0.1	0.081	0.0	0.0
4	0.081	0.2	0.081	0.0	0.0
5	0.080	1.1	0.080	0.0	0.0
6	0.079	2.5	0.079	0.0	0.3
7	0.078	0.8	0.078	0.0	0.1
9	0.069	0.1	0.065	0.1	0.1
10	0.066	2.1	0.065	0.4	0.0
11	0.065	3.5	0.064	0.2	0.0
12	0.064	0.2	0.064	0.0	0.0
13	0.064	0.4	0.064	0.0	0.0
14	0.064	0.0	0.064	0.0	0.0
15	0.064	0.2	0.063	0.4	0.1
17	0.063	0.0	0.063	0.1	0.1
18	0.063	0.3	0.062	0.4	0.0
19	0.060	0.7	0.060	0.1	0.9
21	0.049	0.8	0.049	1.7	0.7
22	0.049	1.4	0.048	2.1	0.6
23	0.048	1.1	0.048	0.3	0.0
24	0.047	2.7	0.047	2.4	0.6
25	0.047	2.1	0.046	3.4	1.4
33	0.034	1.4	0.033		7.4
35	0.032	1.6	0.032	3.0	5.4
36	0.031	3.4	0.031	1.3	4.7

TABLE 3.7-23H

MAXIMUM RELATIVE DISPLACEMENTS AND
MAXIMUM ABSOLUTE ACCELERATIONS (HOSGRI)
INTAKE STRUCTURE

Nodal Point[a]	Elevation (ft)	North-South Displacement (in.)	East-West Displacement (in.)	Vertical Displacement (in.)	North-South Acceleration (g)	East-West Acceleration (g)	Vertical Acceleration (g)
330	+32.0	0.025	0.044	0.010	2.36	2.15	0.65
312	+24.4	0.016	0.029	0.008	1.50	1.55	0.65
71	+17.5	0.120	0.011	0.010	1.58	0.66	0.61
73	+17.5	0.065	0.011	0.007	0.94	0.66	0.54
74	+17.5	0.058	0.011	0.005	0.85	0.66	0.51
284	+17.5	0.009	0.019	0.007	0.64	1.00	0.62
363	+11.0	0.008	0.012	0.003	0.64	0.87	0.54
80	-2.1	0.133	0.007	0.010	1.71	0.70	0.59
83	-2.1	0.066	0.005	0.006	0.98	0.71	0.52
87	-16.8	0.251	0.003	0.005	3.14	0.72	0.52
89	-16.8	0.050	0.002	0.003	1.12	0.73	0.50

(a) See Figure 3.7-15F.

TABLE 3.7-23I

OUTDOOR WATER STORAGE TANKS
SUMMARY OF SIGNIFICANT PERIODS AND PERCENT PARTICIPATION FACTORS
REFUELING WATER STORAGE TANK

Mode No.	Period (sec)	Modal Participation Factor %
1	0.132	50.7
2	0.052	22.6

TABLE 3.7-23J

OUTDOOR WATER STORAGE TANKS
SUMMARY OF SIGNIFICANT PERIODS AND PERCENT PARTICIPATION FACTORS
FIREWATER AND TRANSFER TANK

	Load Case 1[(a)]		Load Case 2[(b)]	
Mode No.	Period (sec.)	Modal Participation Factor %	Period (sec.)	Modal Participation Factor %
1	0.12124	54.91	0.1234	48.4
2	0.04985	21.26	0.06318	6.21

(a) Load Case 1: Inner and outer tanks are filled with water up to design level
(b) Load Case 2: Inner tank is filled to design level, outer tank is empty

Table 3.7-24

FUNDAMENTAL MODE FREQUENCY RANGES
FOR RCL PRIMARY EQUIPMENT

	Frequency, Hz
Steam Generator	6.7 – 9.0
Reactor coolant pump	6.7 - 7.2
Reactor pressure vessel	16.8 - 17.0

TABLE 3.8-1

TESTING OF REINFORCING BARS FOR DESIGN CLASS I CONCRETE STRUCTURES
COMPARISON OF PROGRAM USED ON DIABLO CANYON POWER PLANT WITH REGULATORY GUIDE 1.15

Diablo Canyon Power Plan	Regulatory Guide 1.15
The number of test specimens required for acceptance is in accordance with ASTM A 615, Deformed Billet-Steel Bars for Concrete-Reinforcement, American Society for Testing and Materials. Additional samples were tested as part of the splice testing program. The requirements for acceptance testing are more stringent than ASTM A 615 in that all tests must be conducted using the full section of the bar.	At least one full-diameter specimen from each bar size should be tested for each 50 tons or fraction thereof of reinforcing bars that are produced from each heat and used in Category I structures.
Test procedures are in accordance with ASTM A 615-68.	The test procedures should be in accordance with ASTM A 370-68, Standard Methods and Definitions for Mechanical Testing of Steel Products, American Society for Testing and Materials.
Acceptance standards are in accordance with ASTM A 615-68 using full sections of the bars as rolled. Bend test requirements described in Item 3, Sheet 2 of 2, are more stringent than those in Supplemental Requirements (S-1) of ASTM A 615-72.	The acceptance standards should be in accordance with ASTM A 615-72, Standard Specification for Deformed Billet-Steel Bars for Concrete Reinforcement, American Society for Testing and Materials, including Supplemental Requirement (S-1)[a] using full sections of the bars as rolled.

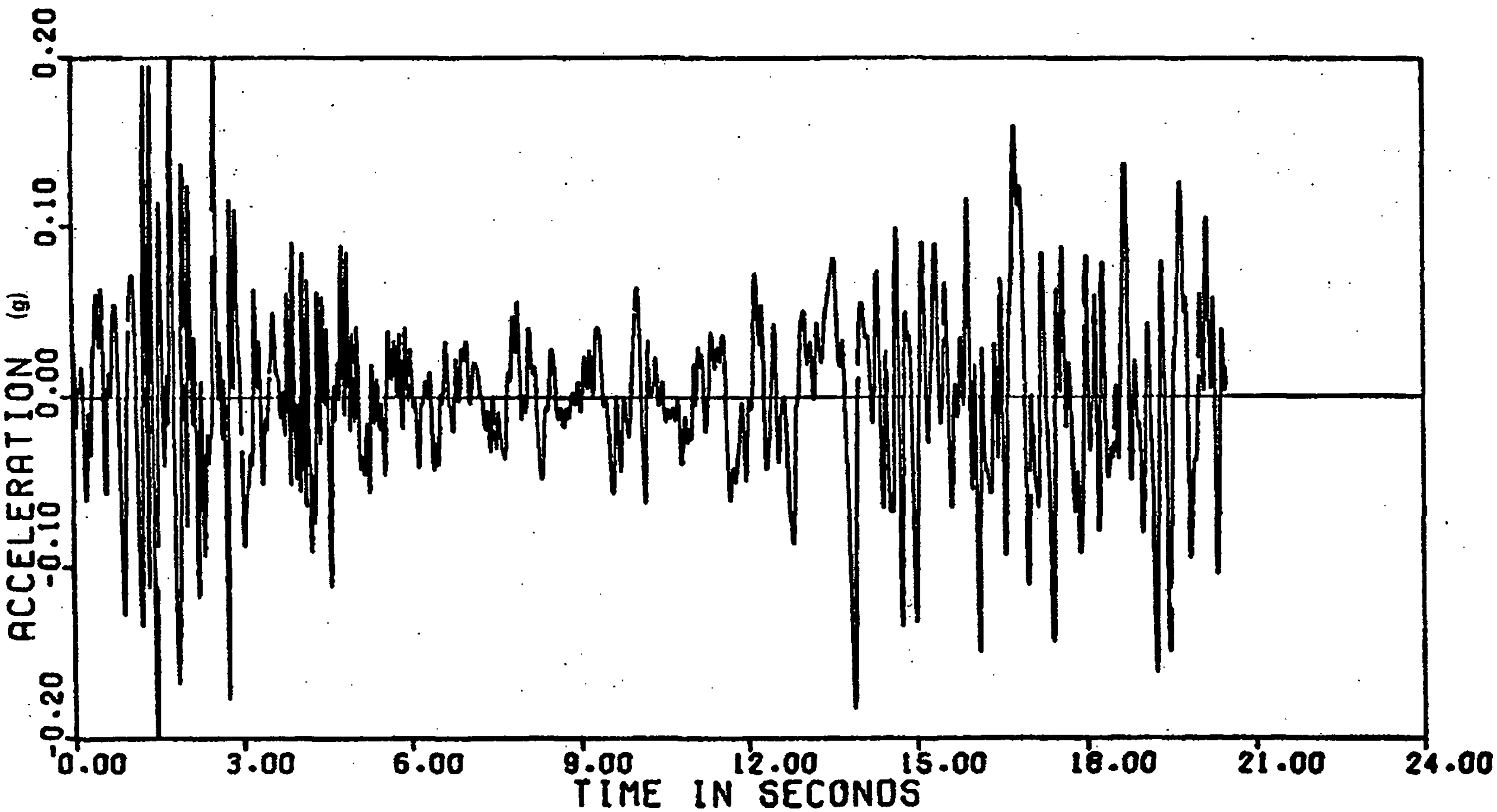

FSAR UPDATE

UNITS 1 AND 2
DIABLO CANYON SITE

FIGURE 3.7-1

FREE FIELD GROUND MOTION

DE ANALYSIS

Revision 11 November 1996

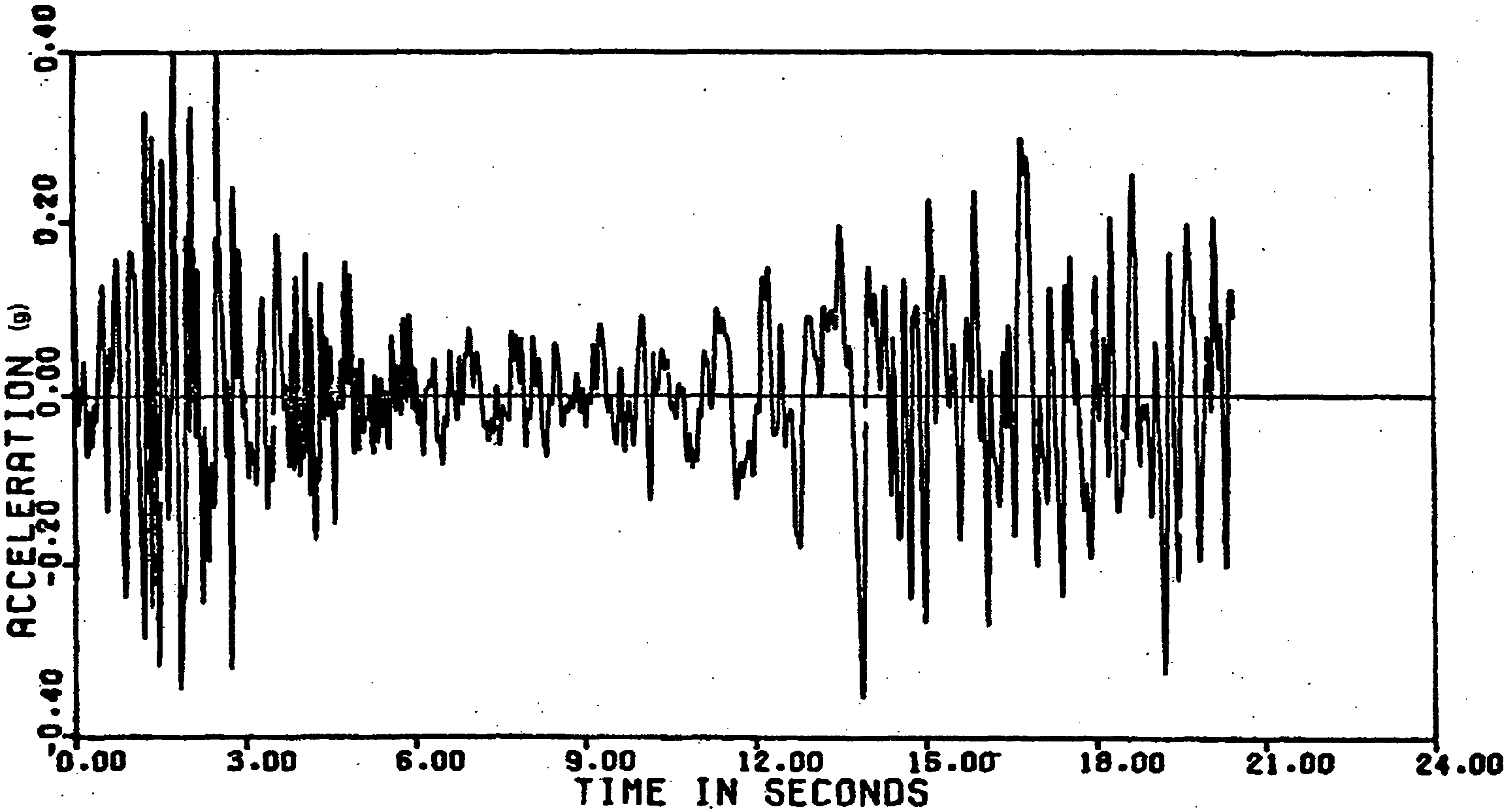

FSAR UPDATE

UNITS 1 AND 2
DIABLO CANYON SITE

FIGURE 3.7-2

FREE FIELD GROUND MOTION

DDE ANALYSIS

Revision 11 November 1996

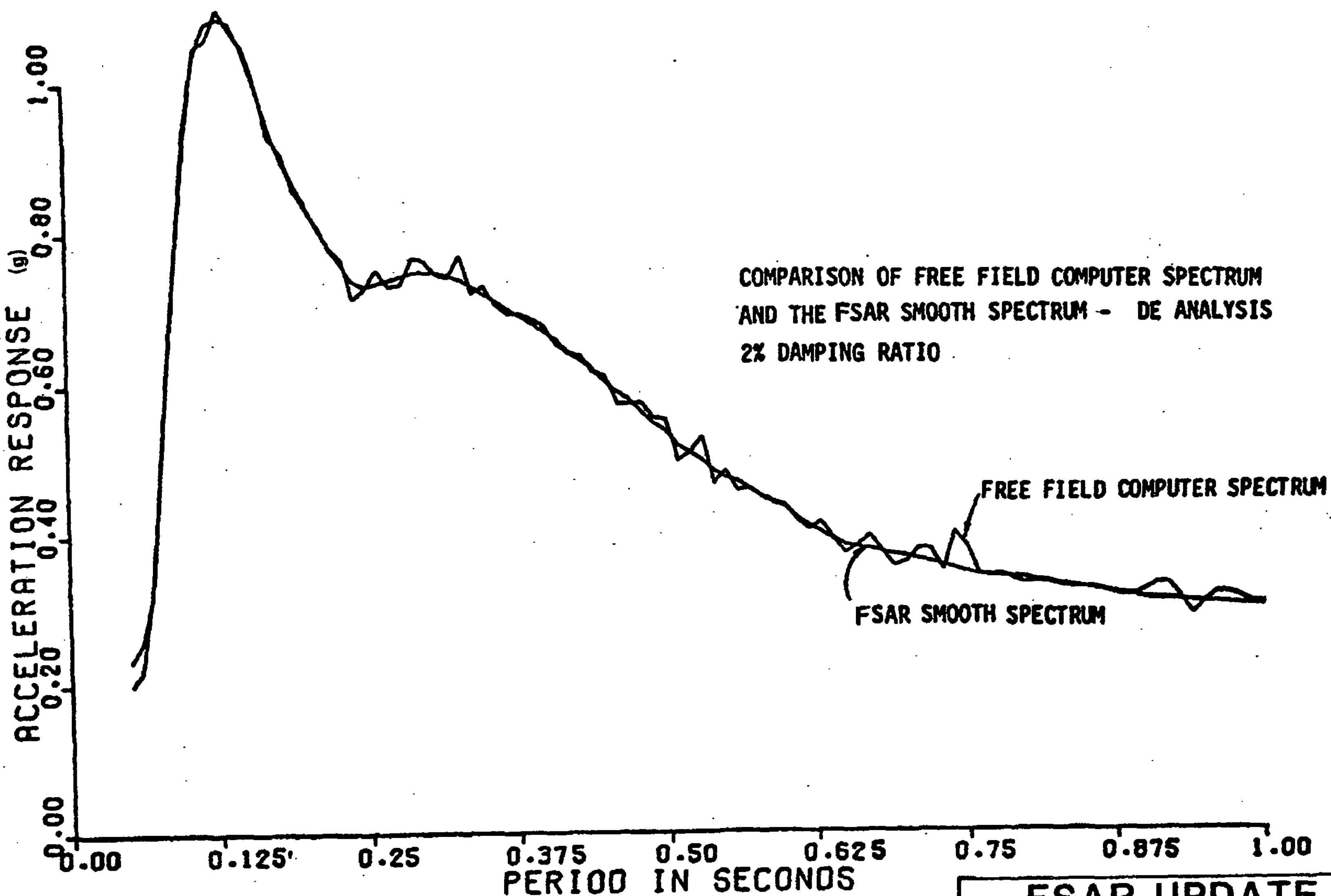

FSAR UPDATE

UNITS 1 AND 2
DIABLO CANYON SITE

FIGURE 3.7-3
COMPARISON OF SPECTRA
2% DAMPING RATIO

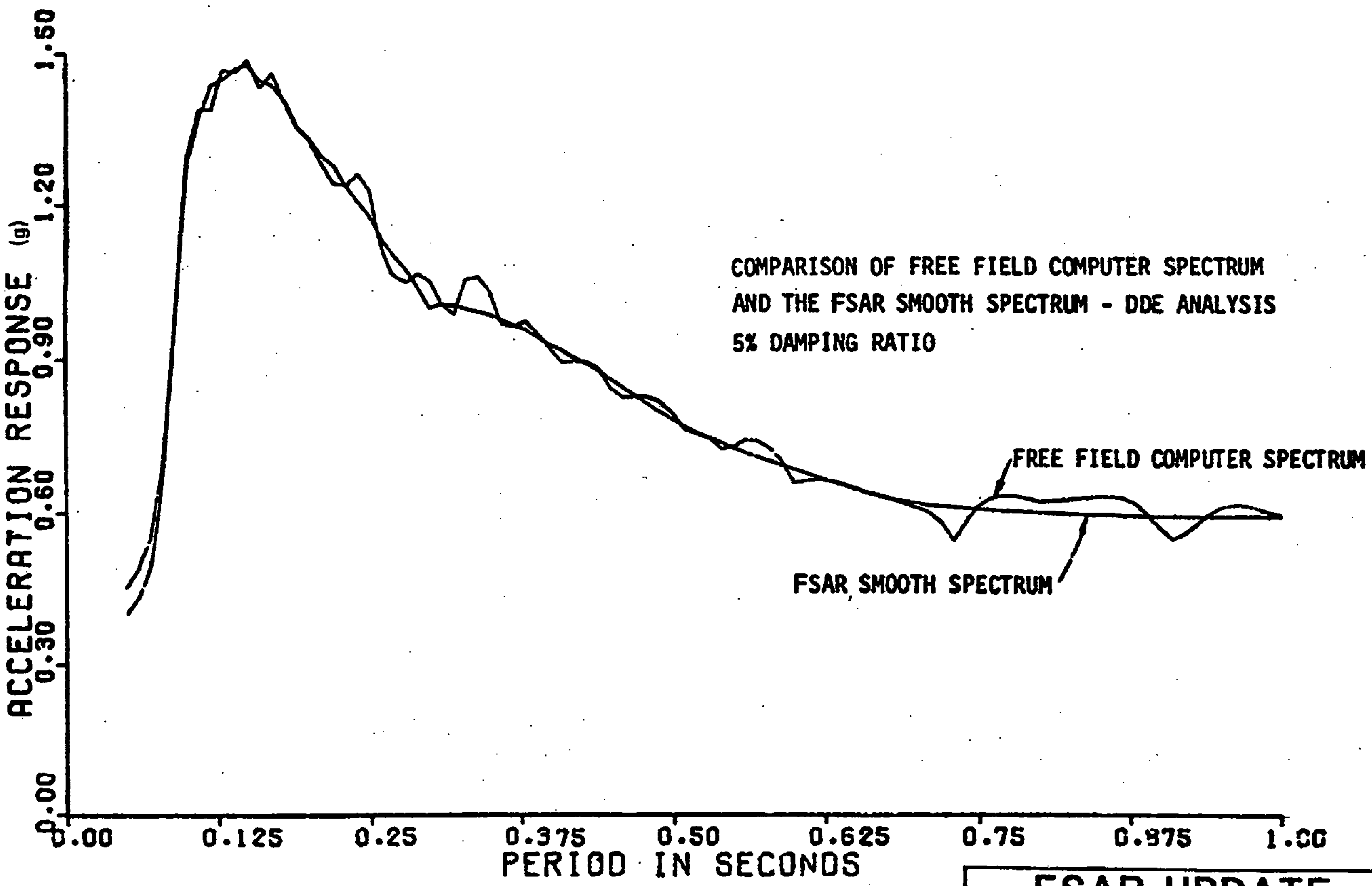

FSAR UPDATE
UNITS 1 AND 2 DIABLO CANYON SITE
FIGURE 3.7-4 COMPARISON OF SPECTRA 5% DAMPING RATIO

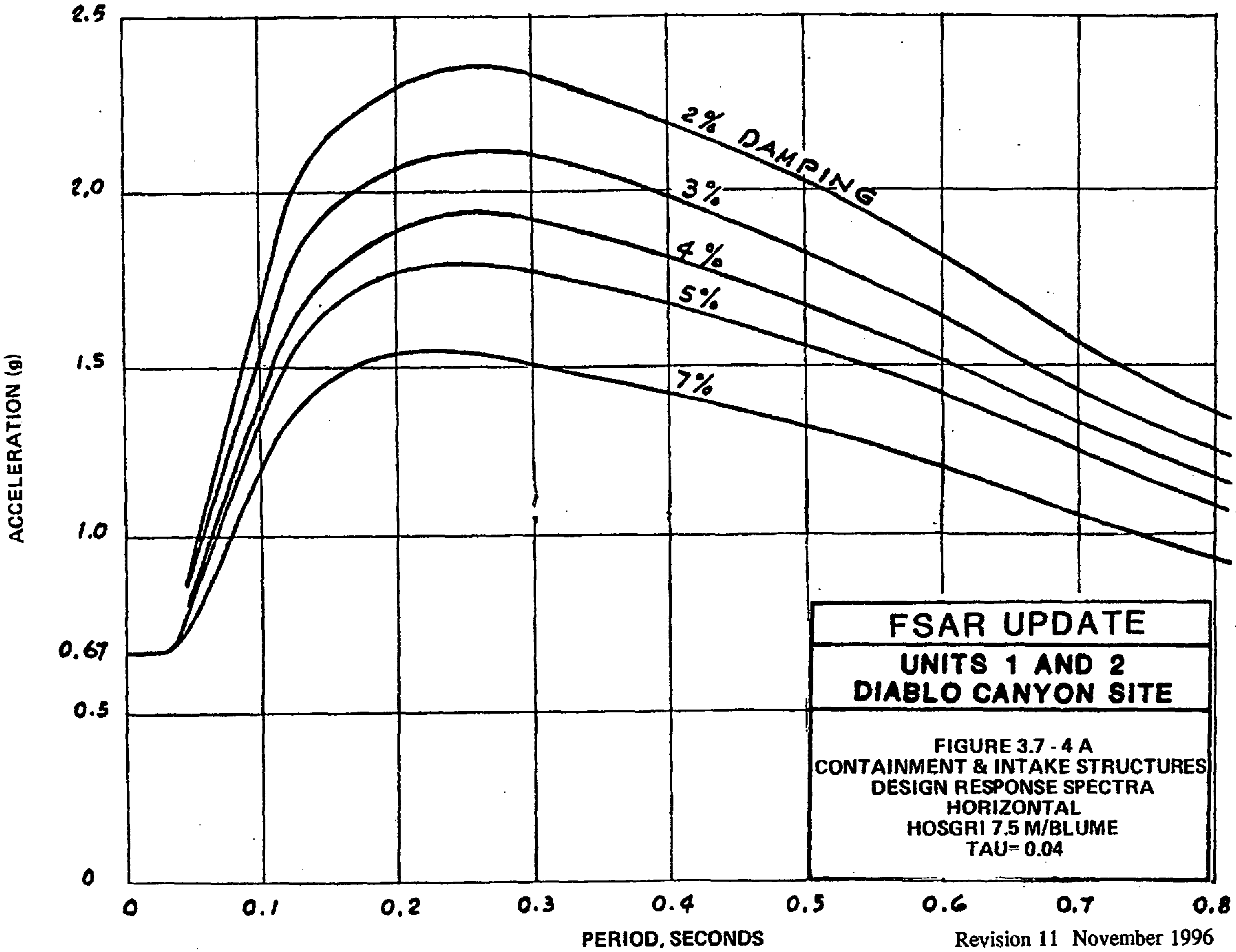

FSAR UPDATE

UNITS 1 AND 2
DIABLO CANYON SITE

FIGURE 3.7 - 4 A
CONTAINMENT & INTAKE STRUCTURES
DESIGN RESPONSE SPECTRA
HORIZONTAL
HOSGRI 7.5 M/BLUME
TAU= 0.04

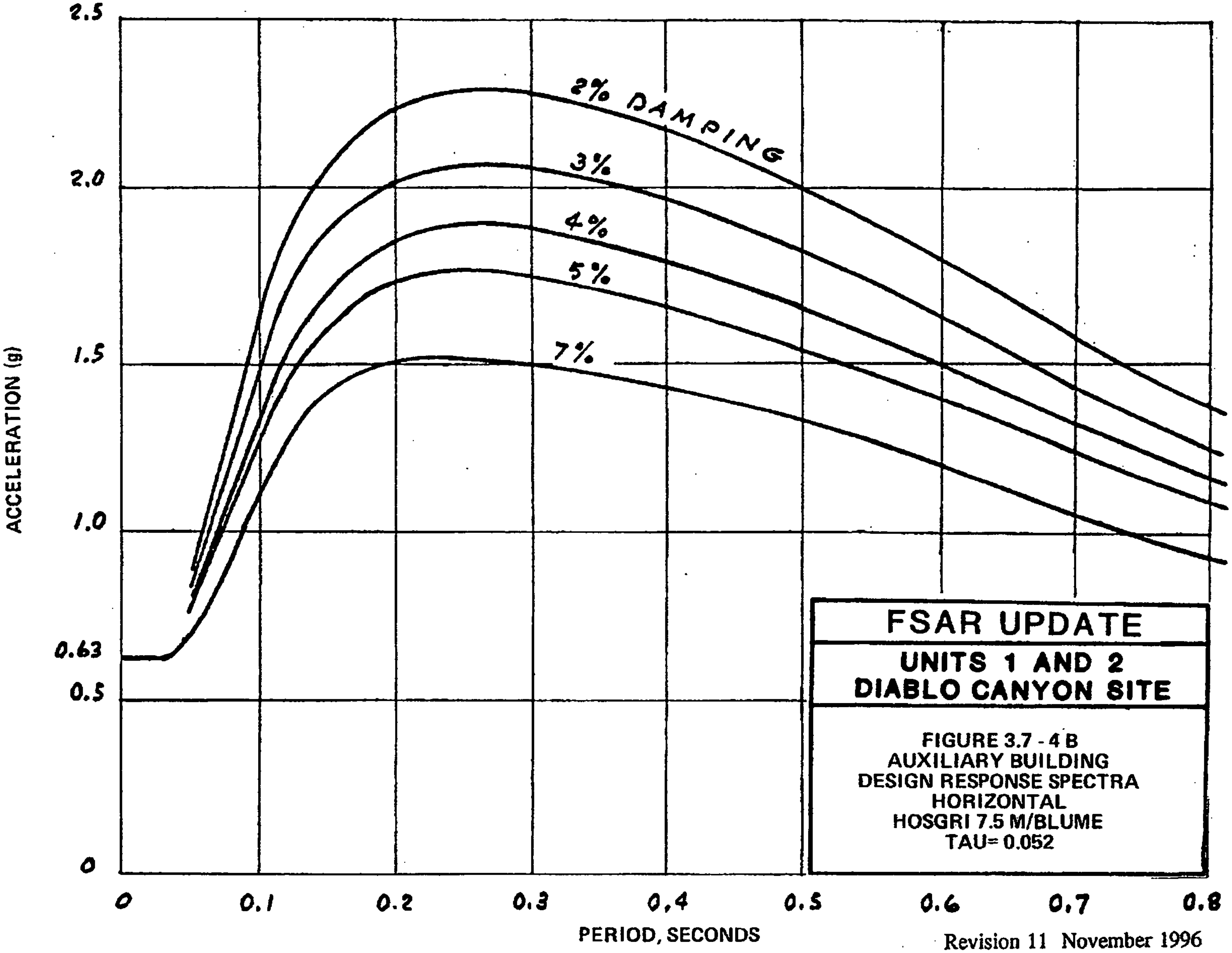

FSAR UPDATE

UNITS 1 AND 2
DIABLO CANYON SITE

FIGURE 3.7 - 4 B
AUXILIARY BUILDING
DESIGN RESPONSE SPECTRA
HORIZONTAL
HOSGRI 7.5 M/BLUME
TAU= 0.052

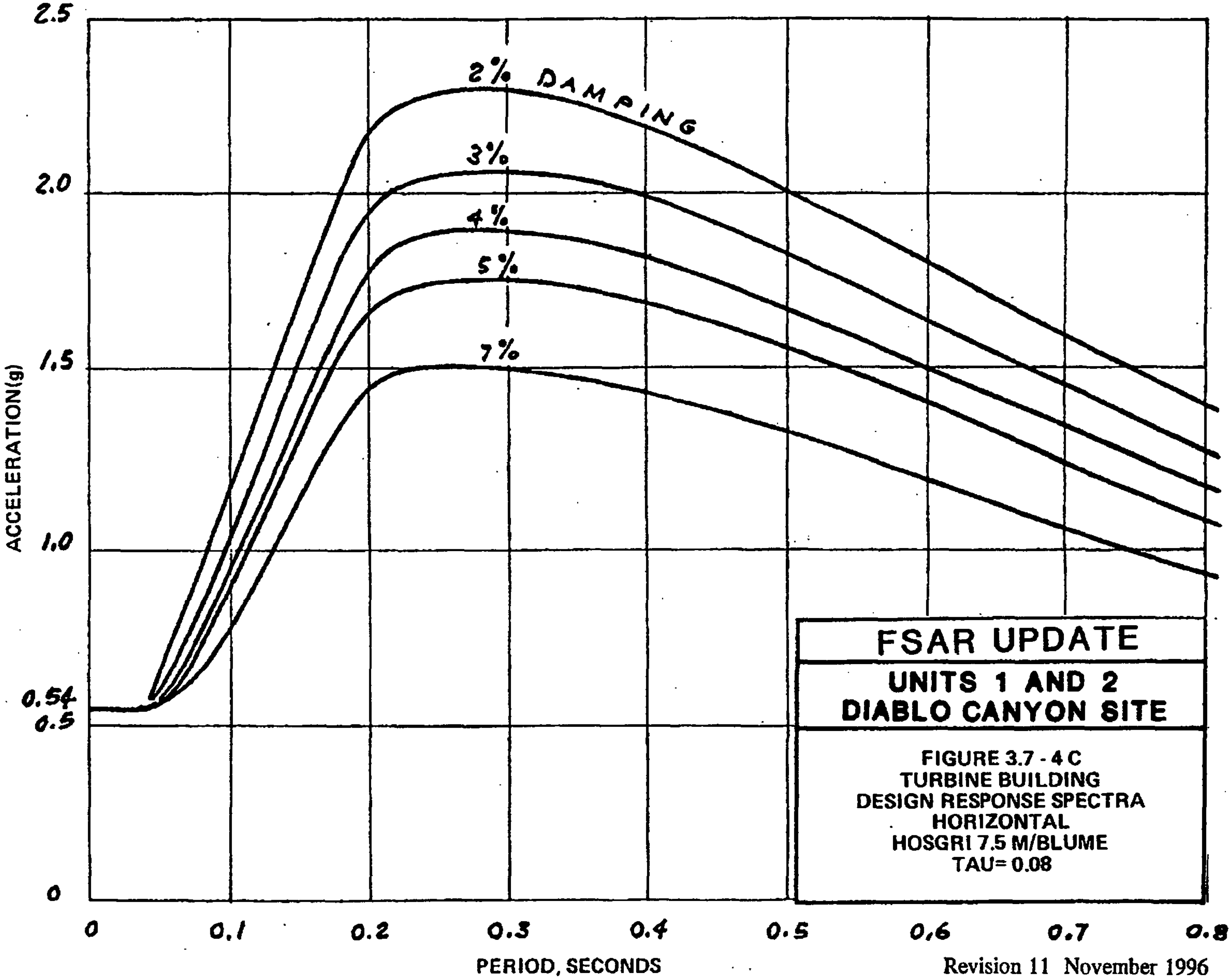

FSAR UPDATE

UNITS 1 AND 2
DIABLO CANYON SITE

FIGURE 3.7 - 4 C
TURBINE BUILDING
DESIGN RESPONSE SPECTRA
HORIZONTAL
HOSGRI 7.5 M/BLUME
TAU= 0.08

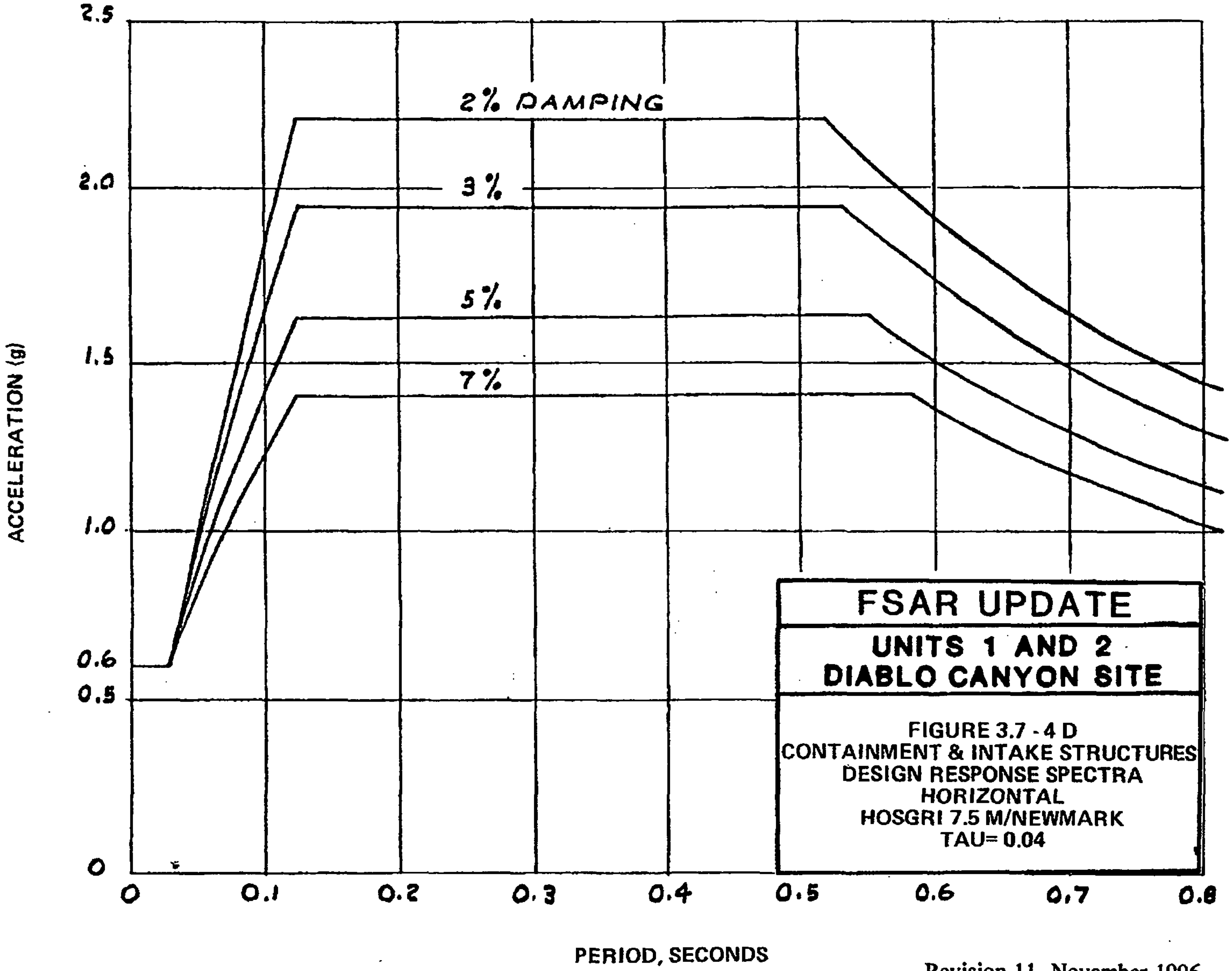

FSAR UPDATE

UNITS 1 AND 2
DIABLO CANYON SITE

FIGURE 3.7 - 4 D
CONTAINMENT & INTAKE STRUCTURES
DESIGN RESPONSE SPECTRA
HORIZONTAL
HOSGRI 7.5 M/NEWMARK
TAU= 0.04

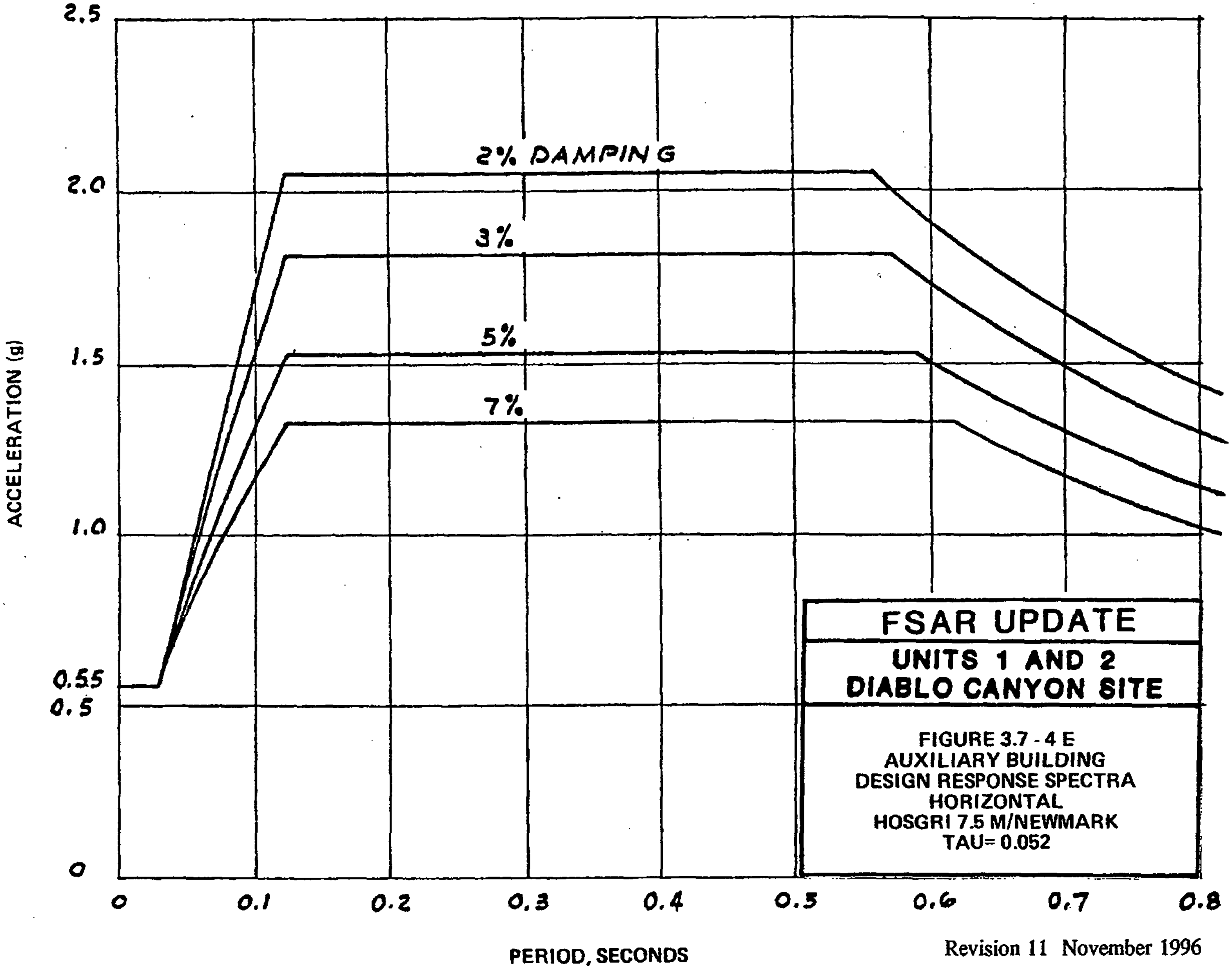

FSAR UPDATE

UNITS 1 AND 2
DIABLO CANYON SITE

FIGURE 3.7 - 4 E
AUXILIARY BUILDING
DESIGN RESPONSE SPECTRA
HORIZONTAL
HOSGRI 7.5 M/NEWMARK
TAU= 0.052

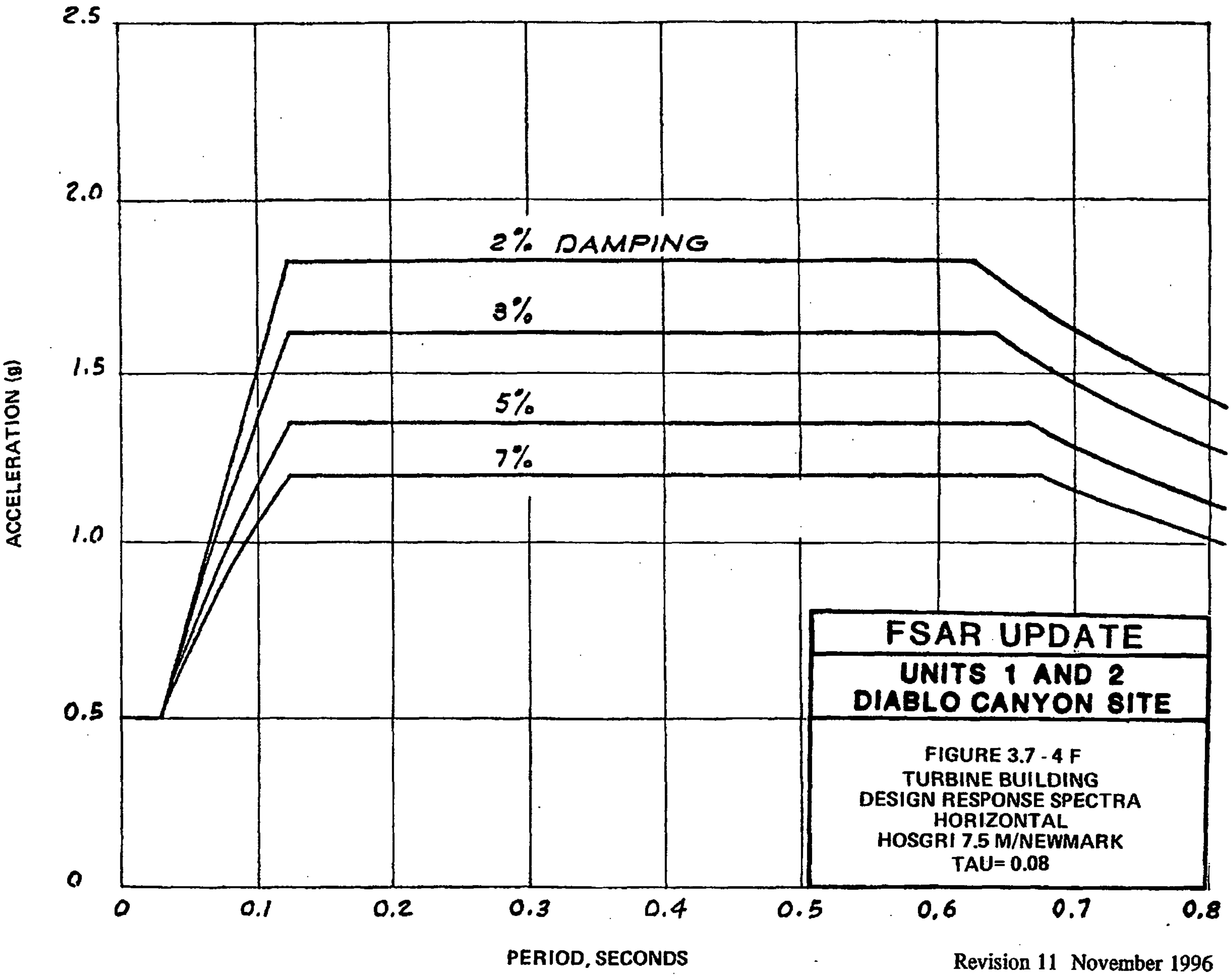

FSAR UPDATE

UNITS 1 AND 2
DIABLO CANYON SITE

FIGURE 3.7 - 4 F
TURBINE BUILDING
DESIGN RESPONSE SPECTRA
HORIZONTAL
HOSGRI 7.5 M/NEWMARK
TAU= 0.08

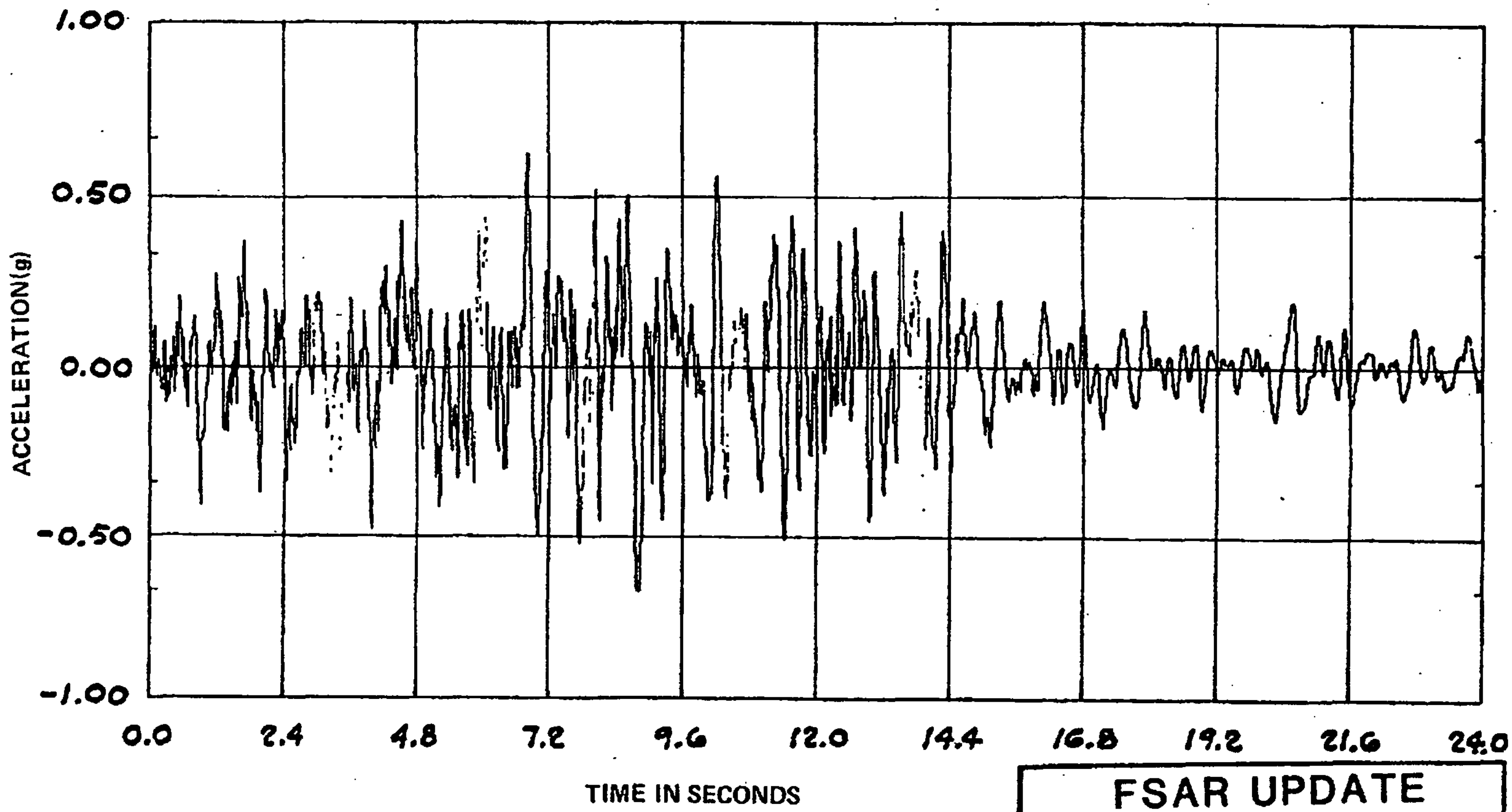

FSAR UPDATE

UNITS 1 AND 2
DIABLO CANYON SITE

FIGURE 3.7 - 4 G
CONTAINMENT & INTAKE STRUCTURES
HORIZONTAL TIME - HISTORY
HOSGRI 7.5M/BLUME
TAU = 0.04

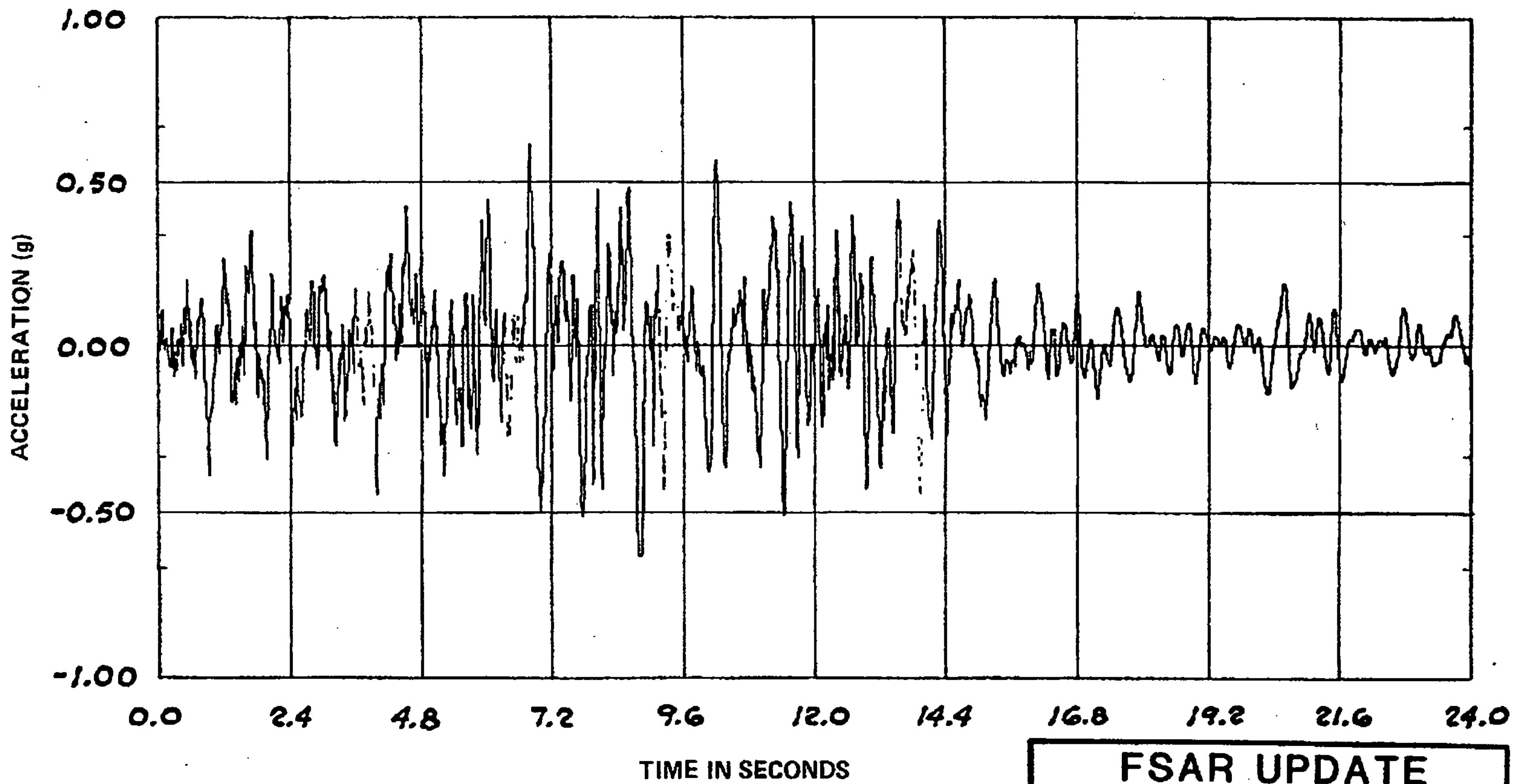

FSAR UPDATE

UNITS 1 AND 2
DIABLO CANYON SITE

FIGURE 3.7 - 4 H
AUXILIARY BUILDING
HORIZONTAL TIME - HISTORY
HOSGRI 7.5 M/BLUME
TAU= 0.052

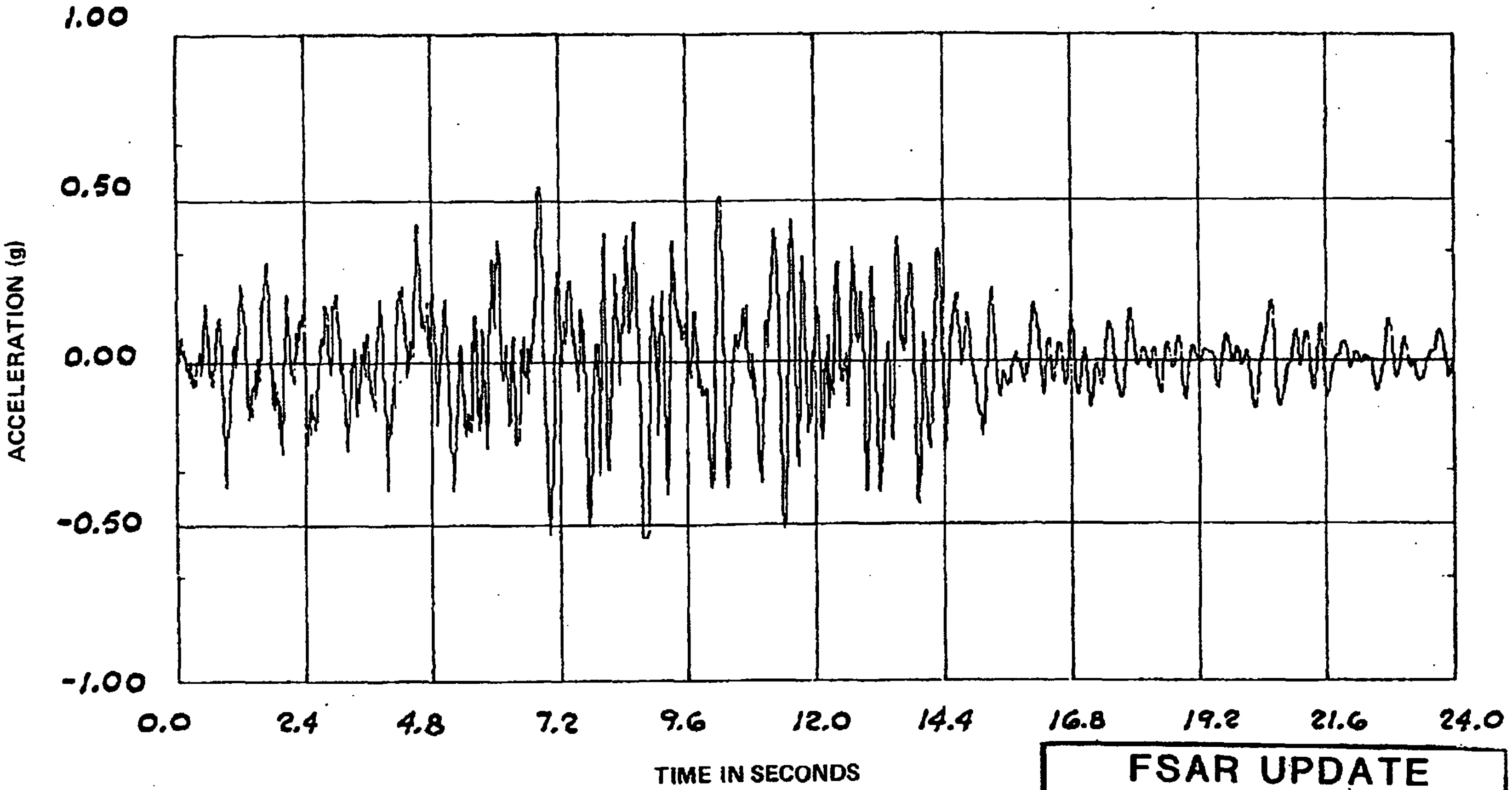

FSAR UPDATE

UNITS 1 AND 2
DIABLO CANYON SITE

FIGURE 3.7 - 4 I
TURBINE BUILDING
HORIZONTAL TIME - HISTORY
HOSGRI 7.5 M/BLUME
TAU= 0.080

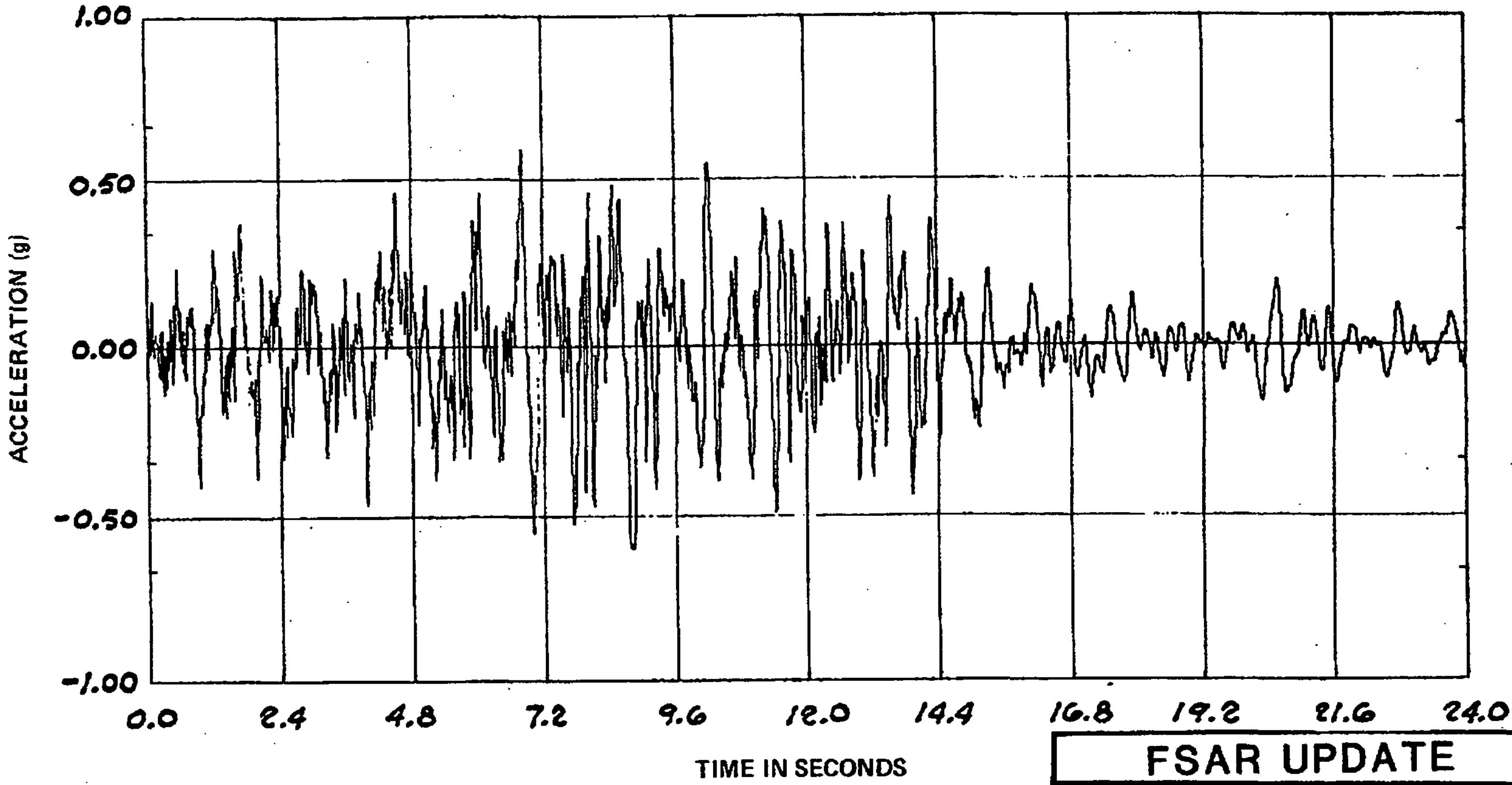

FSAR UPDATE

UNITS 1 AND 2
DIABLO CANYON SITE

FIGURE 3.7 - 4 J
CONTAINMENT & INTAKE STRUCTURES
HORIZONTAL TIME - HISTORY
HOSGRI 7.5M/NEWMARK
TAU = 0.04

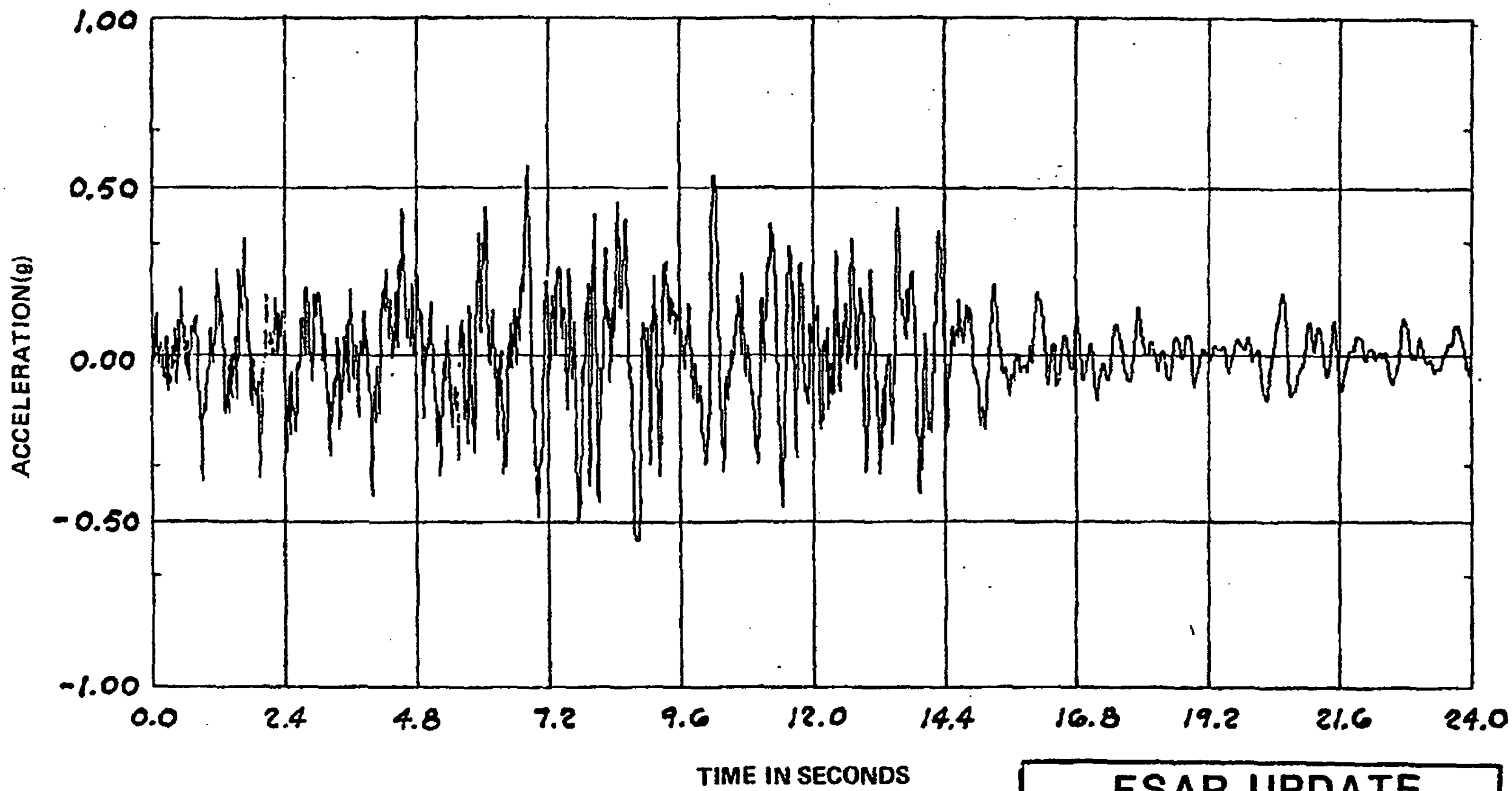

FSAR UPDATE

UNITS 1 AND 2
DIABLO CANYON SITE

FIGURE 3.7 - 4 K
AUXILIARY BUILDING
HORIZONTAL TIME - HISTORY
HOSGRI 7.5M/NEWMARK
TAU= 0.052

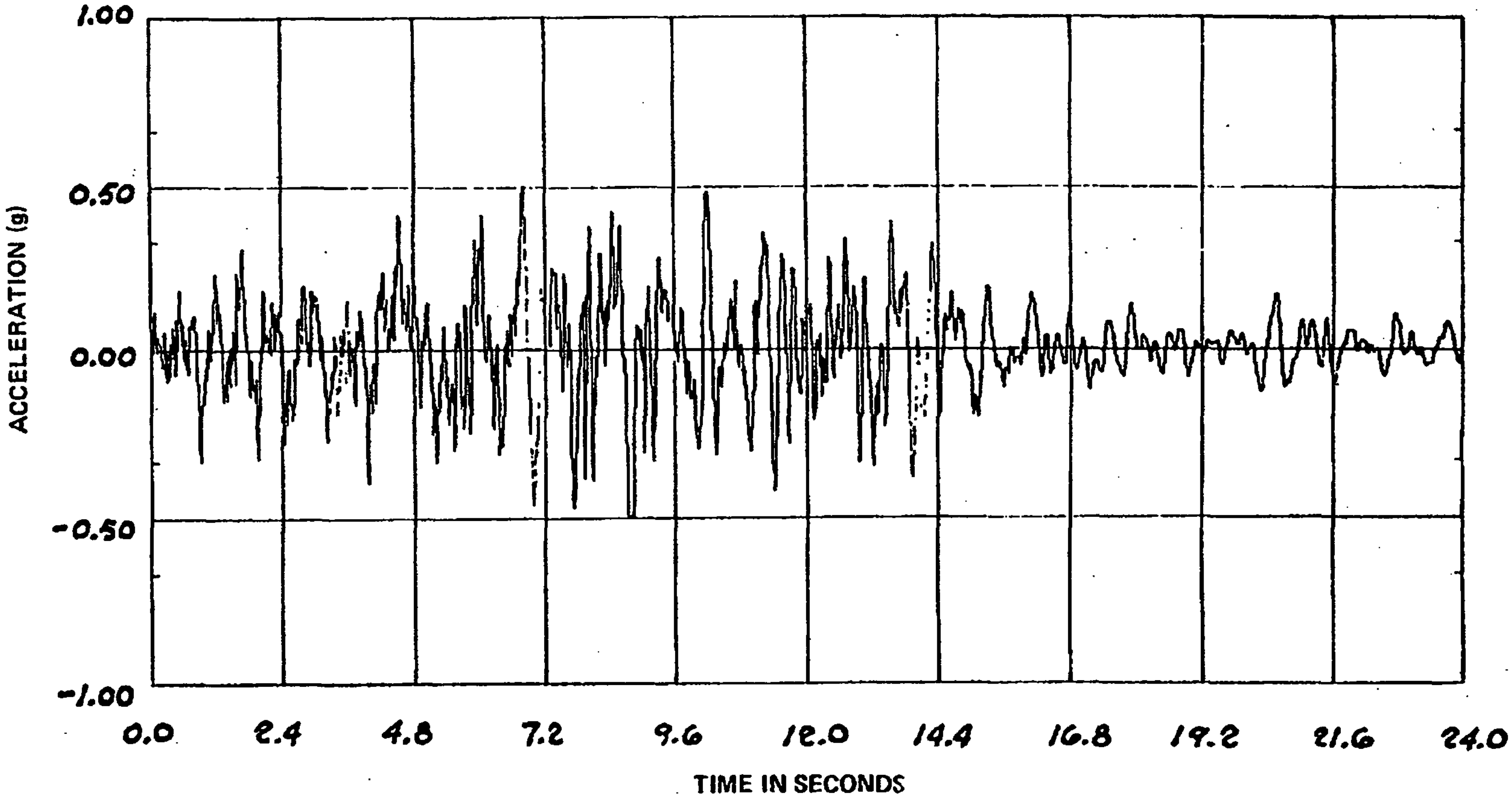

FSAR UPDATE

UNITS 1 AND 2
DIABLO CANYON SITE

FIGURE 3.7 - 4 L
TURBINE BUILDING
HORIZONTAL TIME - HISTORY
HOSGRI 7.5M/NEWMARK
TAU = 0.067

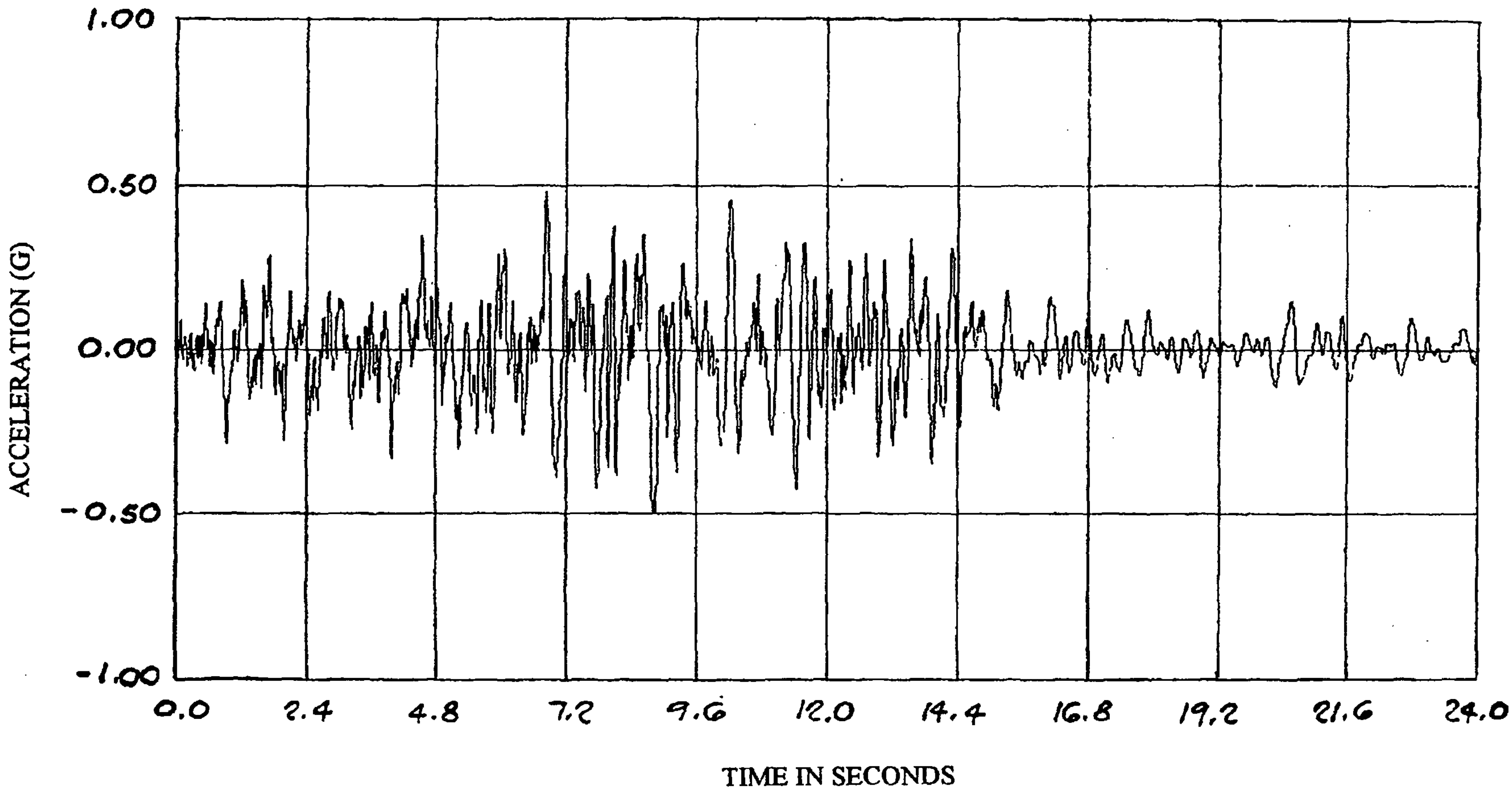

FSAR UPDATE

UNITS 1 AND 2
DIABLO CANYON SITE

FIGURE 3.7 - 4 M
VERTICAL TIME HISTORY
HOSGRI 7.5M/NEWMARK
TAU = 0.0

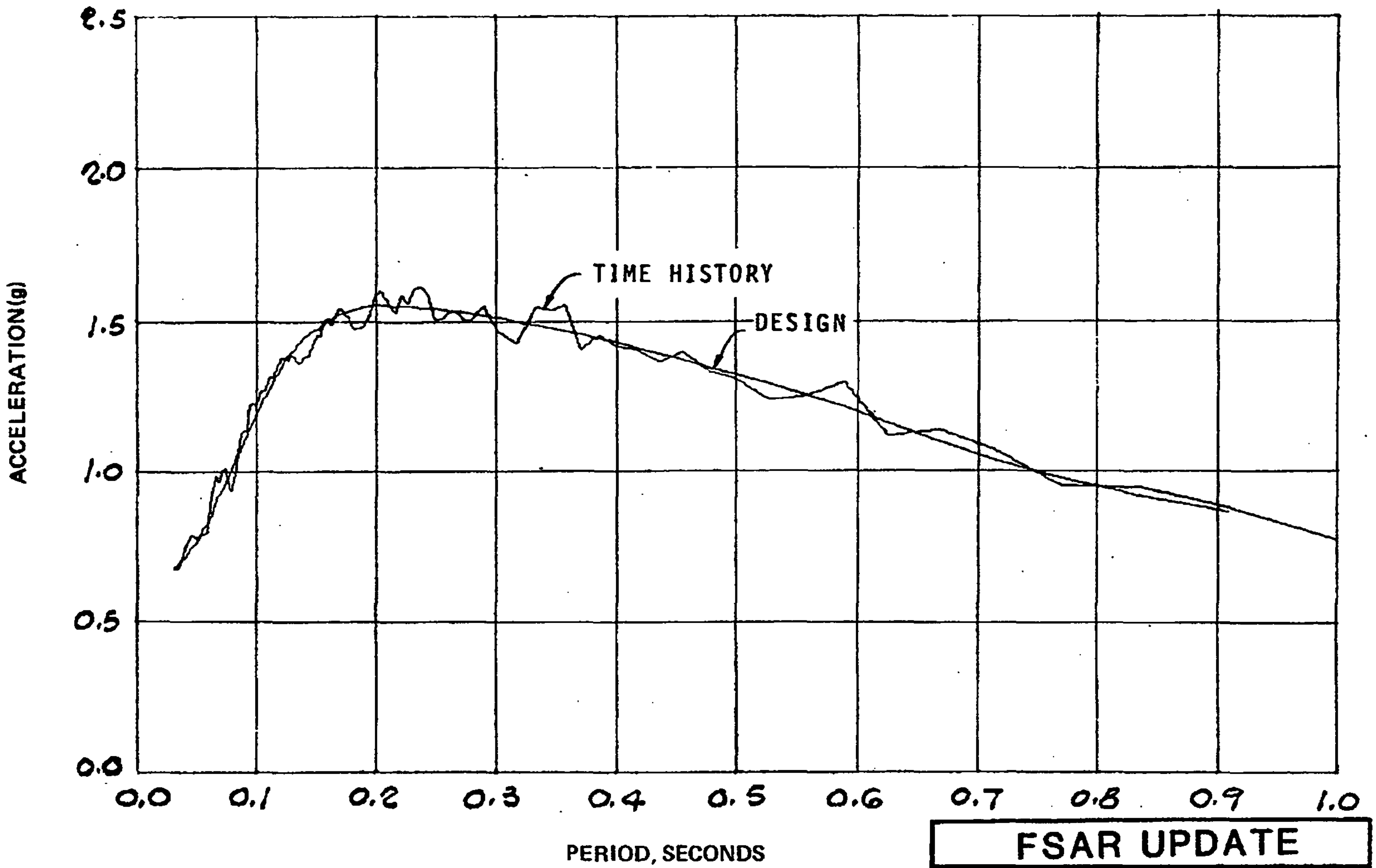

FSAR UPDATE

UNITS 1 AND 2
DIABLO CANYON SITE

FIGURE 3.7 - 4 N
CONTAINMENT & INTAKE STRUCTURES
COMPARISON OF SPECTRA
HORIZONTAL
HOSGRI 7.5 M/BLUME
TAU= 0.04, 7% DAMPING

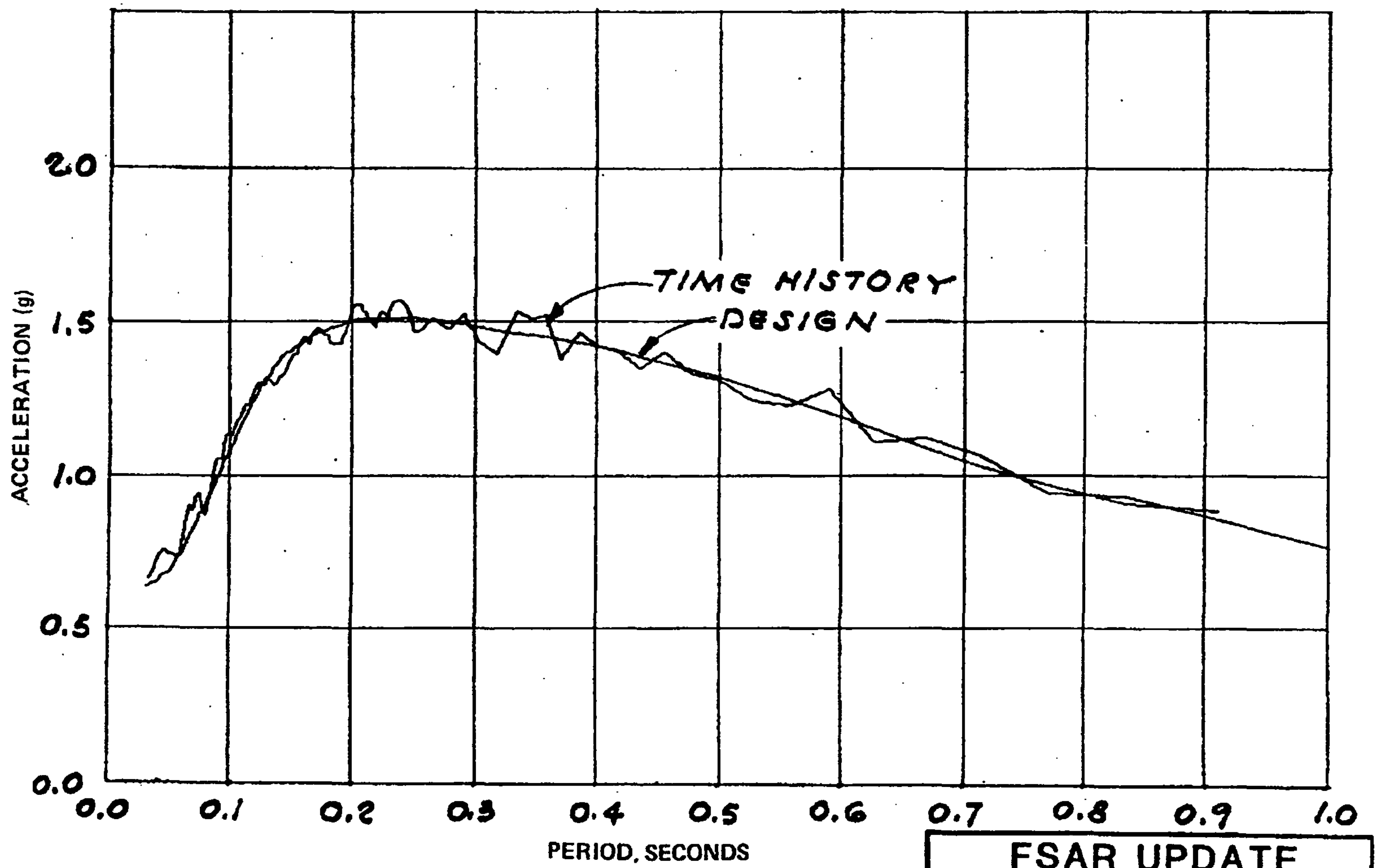

FSAR UPDATE

UNITS 1 AND 2
DIABLO CANYON SITE

FIGURE 3.7 - 4 O
AUXILIARY BUILDING
COMPARISON OF SPECTRA
HORIZONTAL
HOSGRI 7.5M/BLUME
TAU= 0.052, 7% DAMPING

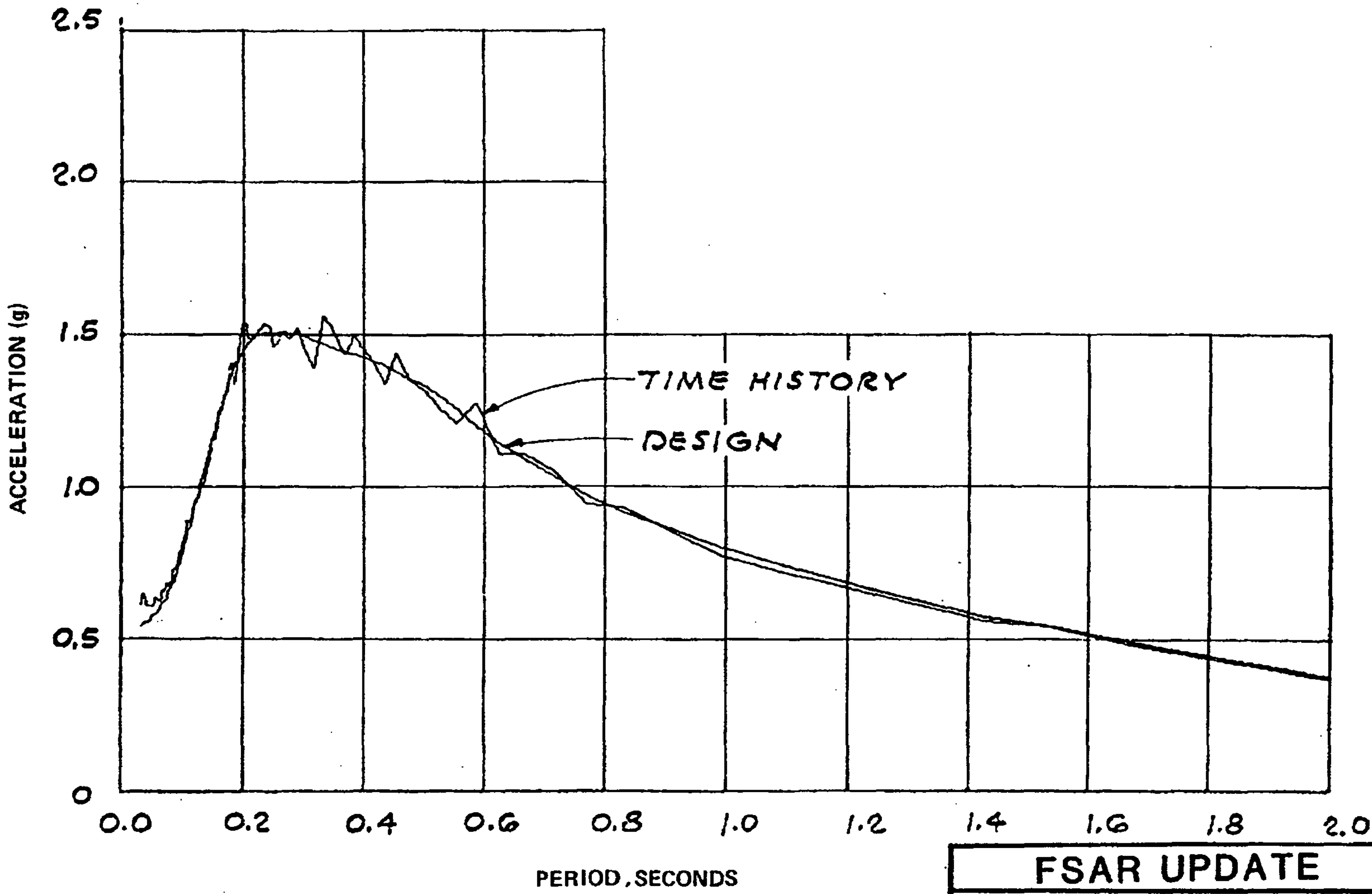

FSAR UPDATE

UNITS 1 AND 2
DIABLO CANYON SITE

FIGURE 3.7 - 4 P
TURBINE BUILDING
COMPARISON OF SPECTRA
HORIZONTAL
HOSGRI 7.5 M/BLUME
TAU = 0.080, 7% DAMPING

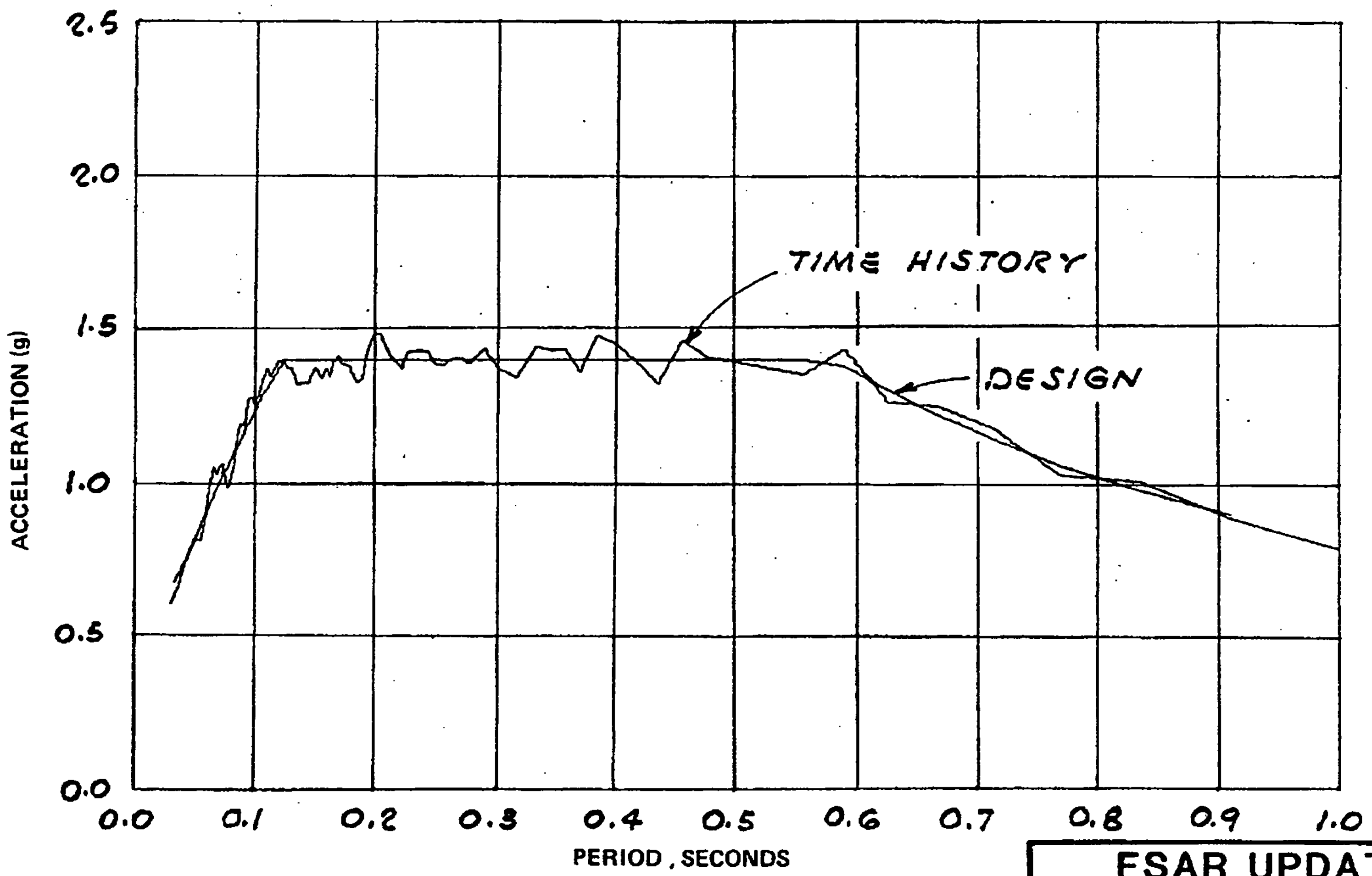

FSAR UPDATE

UNITS 1 AND 2
DIABLO CANYON SITE

FIGURE 3.7 - 4 Q
CONTAINMENT AND INTAKE
STRUCURES
COMPARISON OF SPECTRA
HORIZONTAL
HOSGRI 7.5 M/NEWMARK
TAU = 0.04, 7% DAMPING

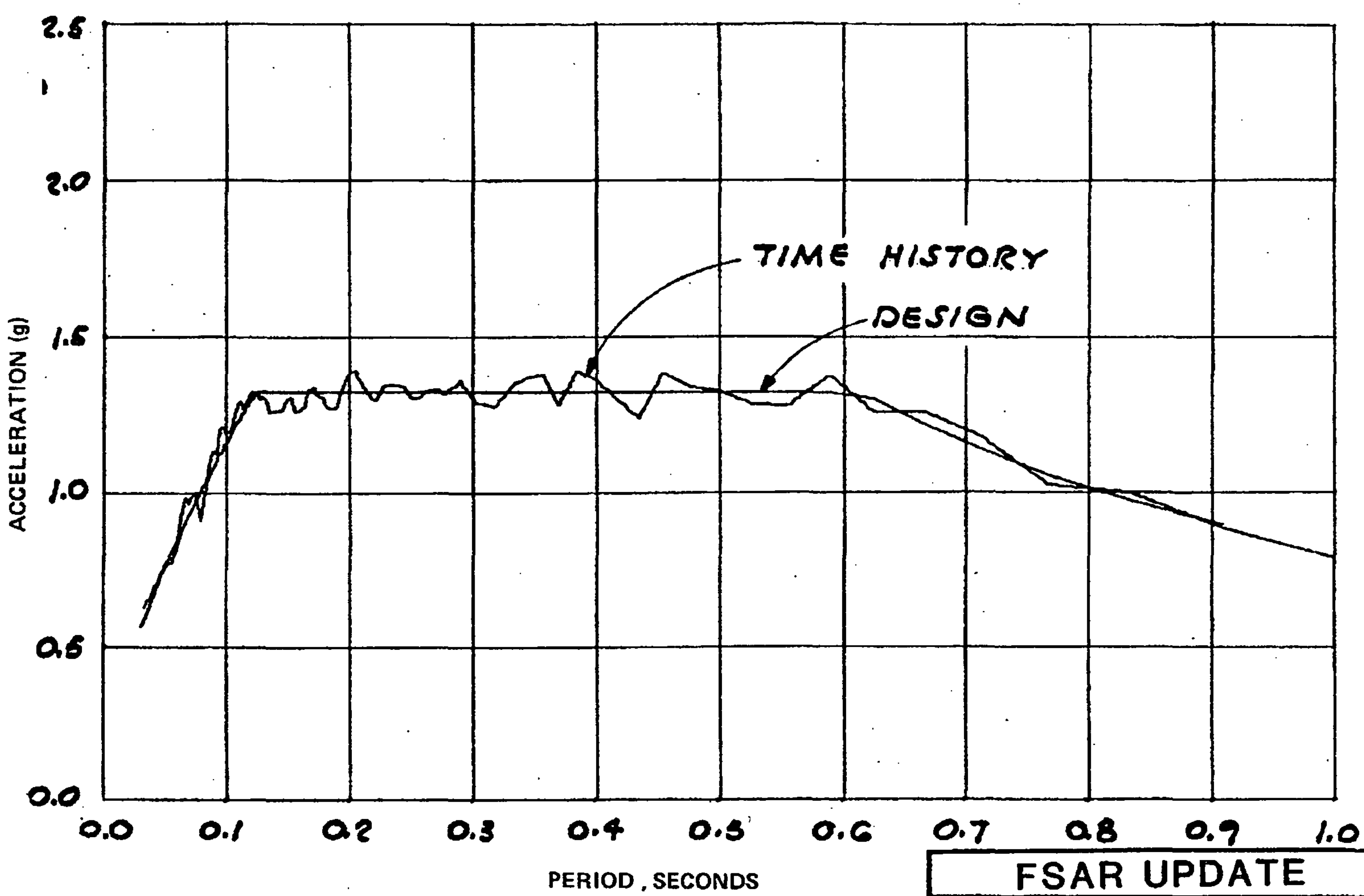

FSAR UPDATE

UNITS 1 AND 2
DIABLO CANYON SITE

FIGURE 3.7 - 4 R
AUXILIARY BUILDING
COMPARISON OF SPECTRA
HORIZONTAL
HOSGRI 7.5 M/NEWMARK
TAU= 0.052, 7% DAMPING

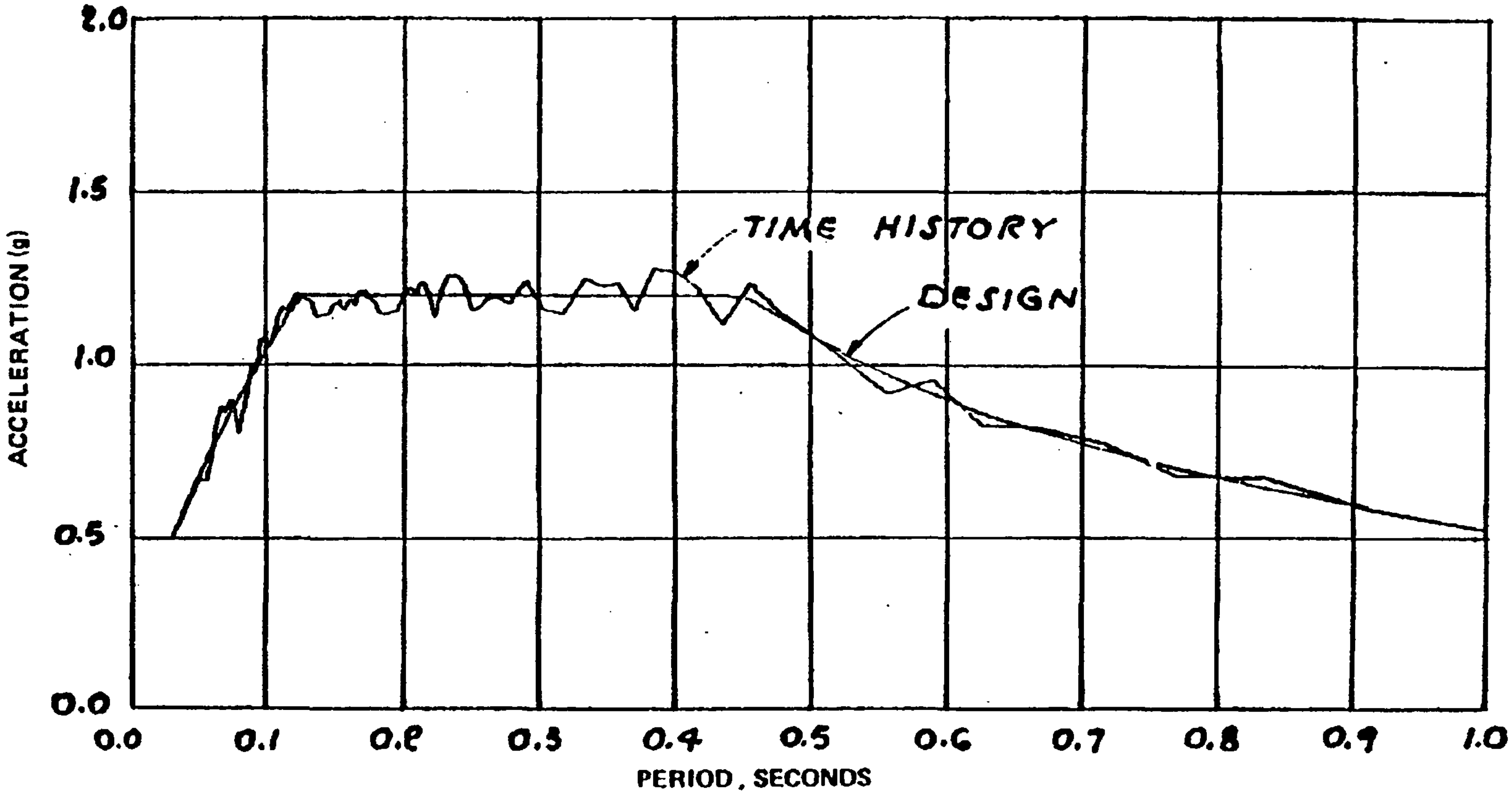

FSAR UPDATE
UNITS 1 AND 2 DIABLO CANYON SITE
FIGURE 3.7 - 4S COMPARISON OF SPECTRA VERTICAL HOSGRI 7.5 M/NEWMARK TAU = 0.0, 7% DAMPING

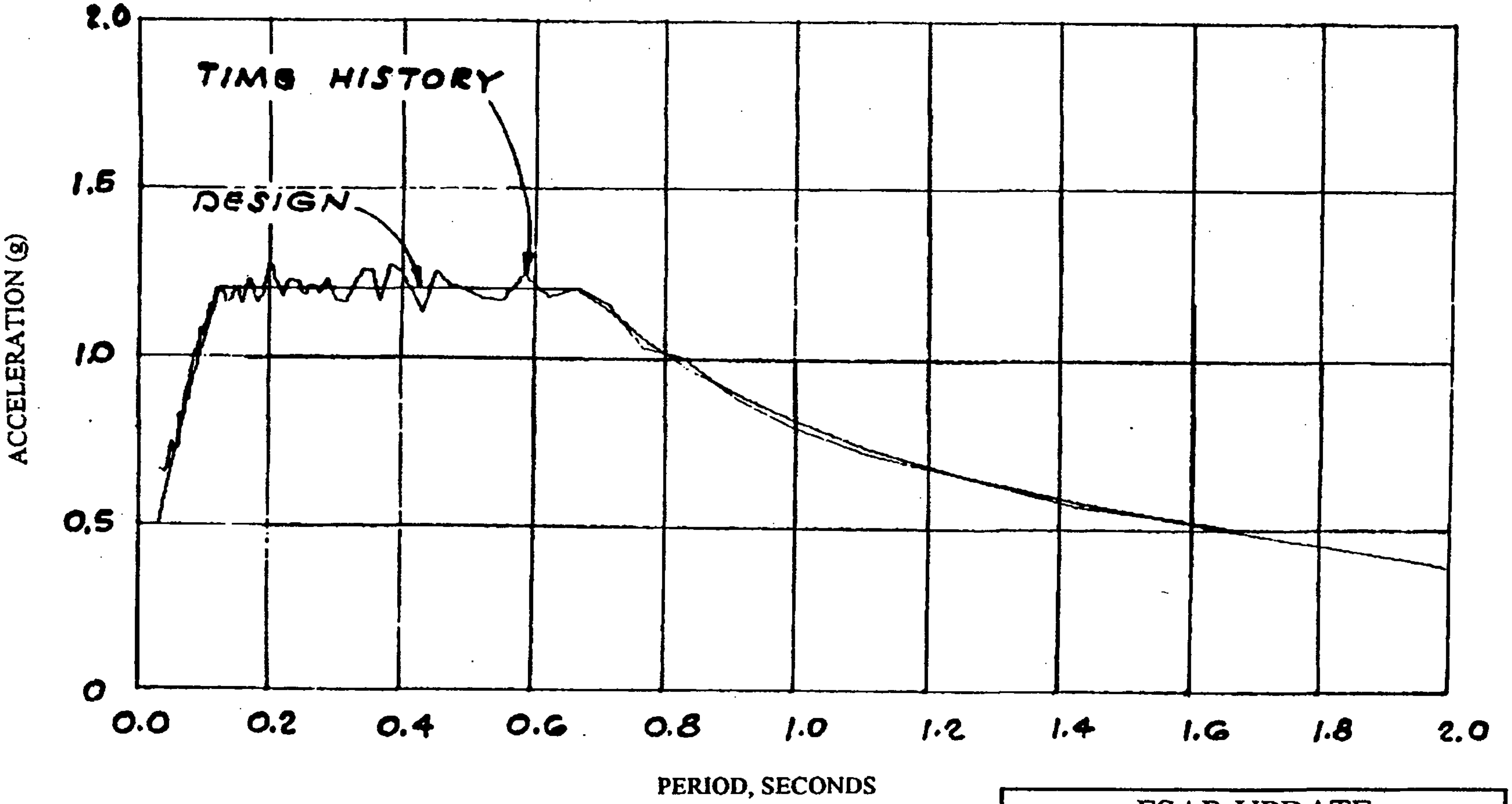

FSAR UPDATE

UNIT 1
DIABLO CANYON SITE

FIGURE 3.7 - 4 T
TURBINE BUILDING
COMPARISON OF SPECTRA
HORIZONTAL
HOSGRI 7.5M/NEWMARK
TAU = 0.067, 7% DAMPING

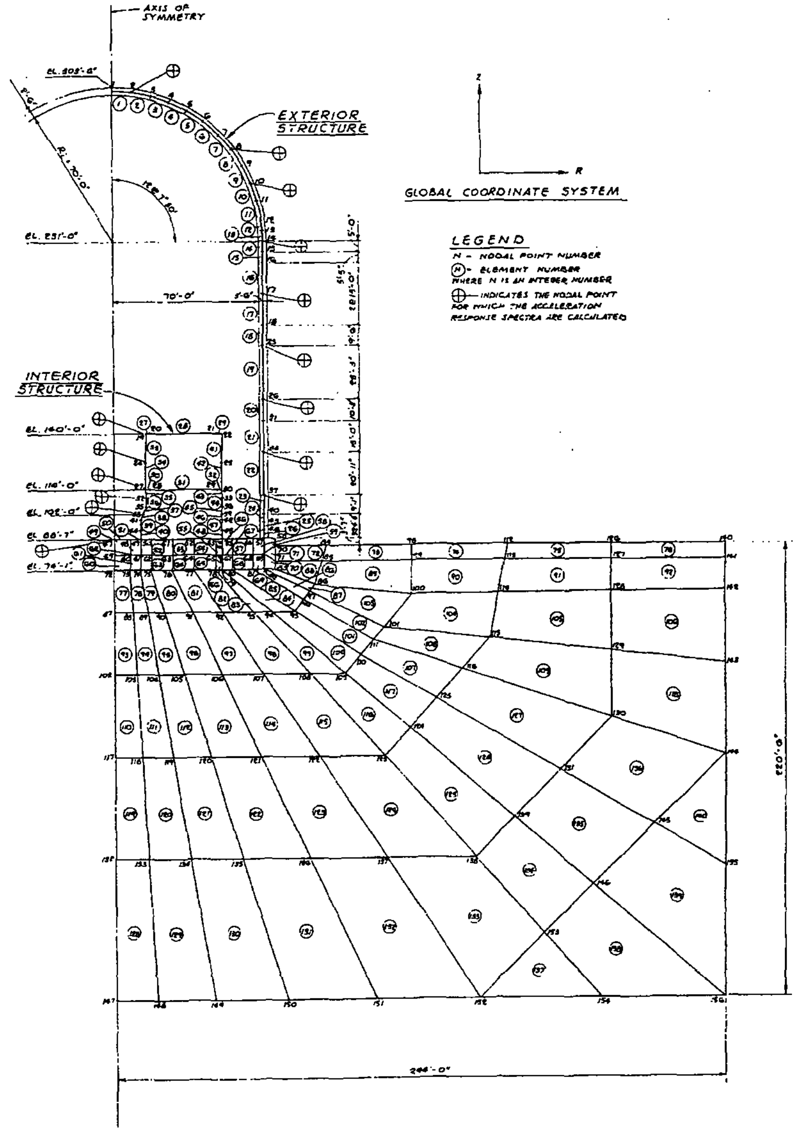

FSAR UPDATE

UNITS 1 AND 2
DIABLO CANYON SITE

FIGURE 3.7-5
CONTAINMENT STRUCTURE
FINITE ELEMENT MODEL

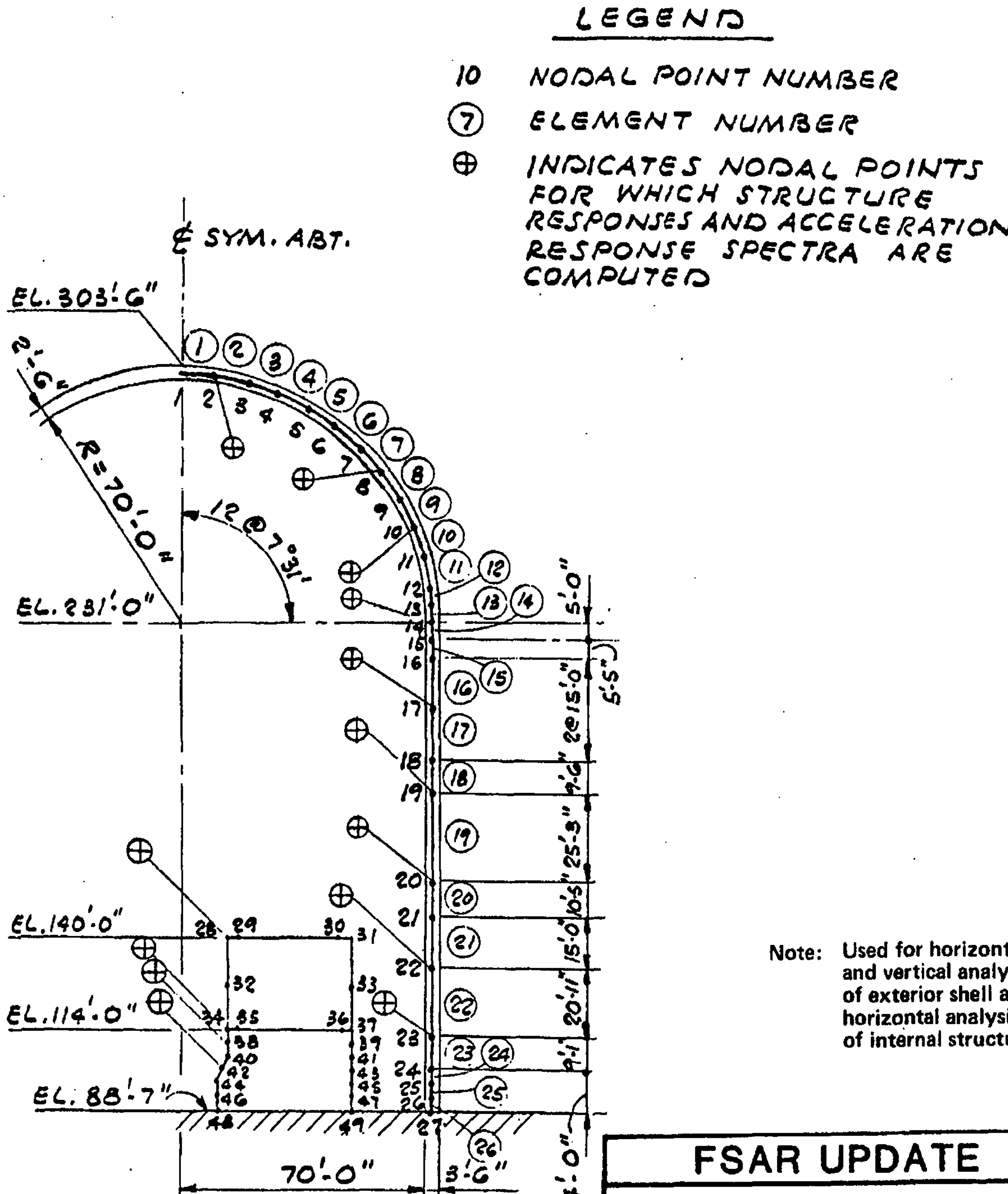

Note: Used for horizontal and vertical analysis of exterior shell and horizontal analysis of internal structure

FSAR UPDATE

UNIT 1
DIABLO CANYON SITE

FIGURE 3.7 - 5 A
CONTAINMENT STRUCTURE
FINITE ELEMENT MODEL

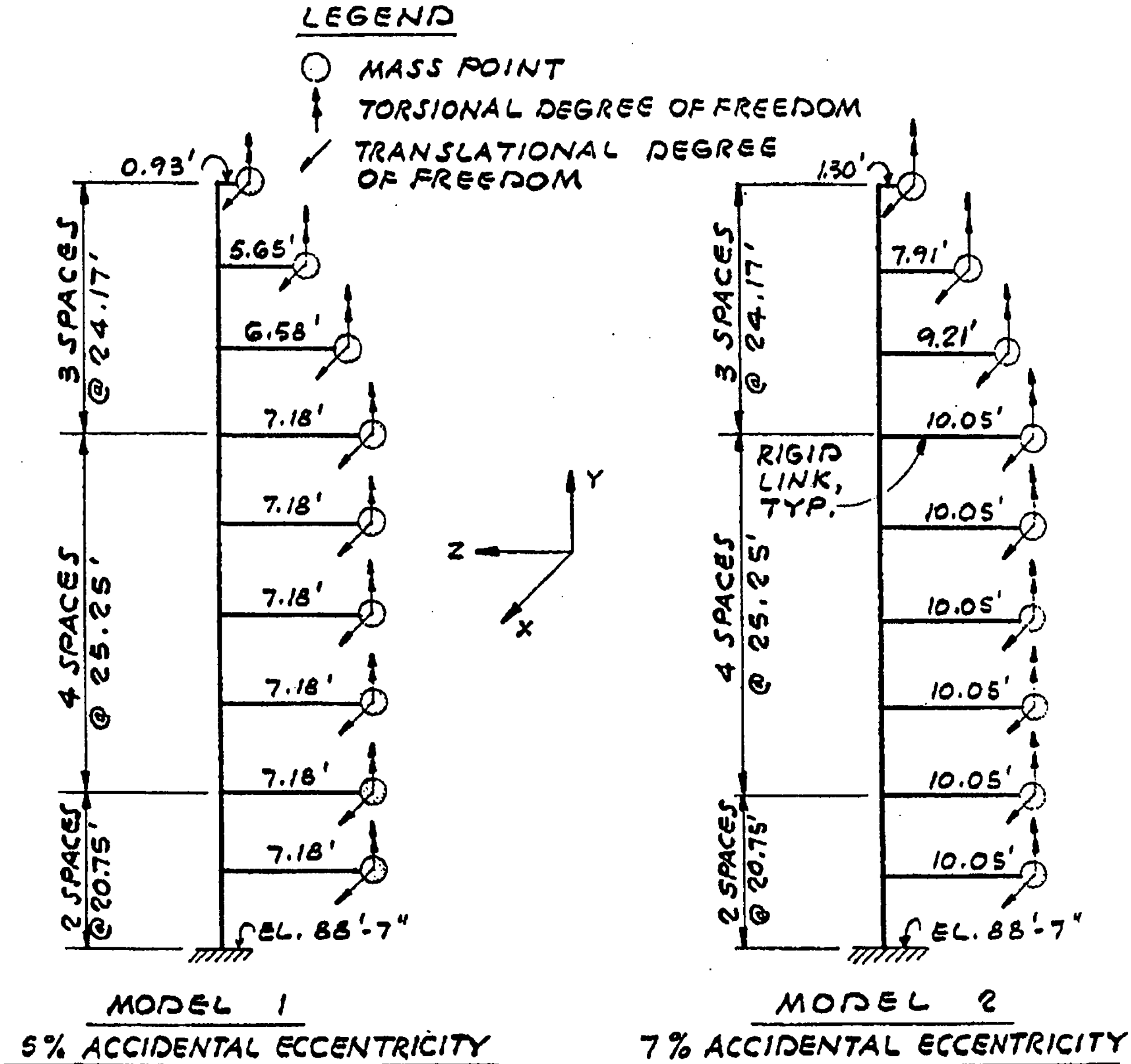

FSAR UPDATE

UNIT 1
DIABLO CANYON SITE

FIGURE 3.7-5 B
CONTAINMENT STRUCTURE EXTERIOR
SHELL MATHEMATICAL MODELS
FOR TORSIONAL ANALYSIS

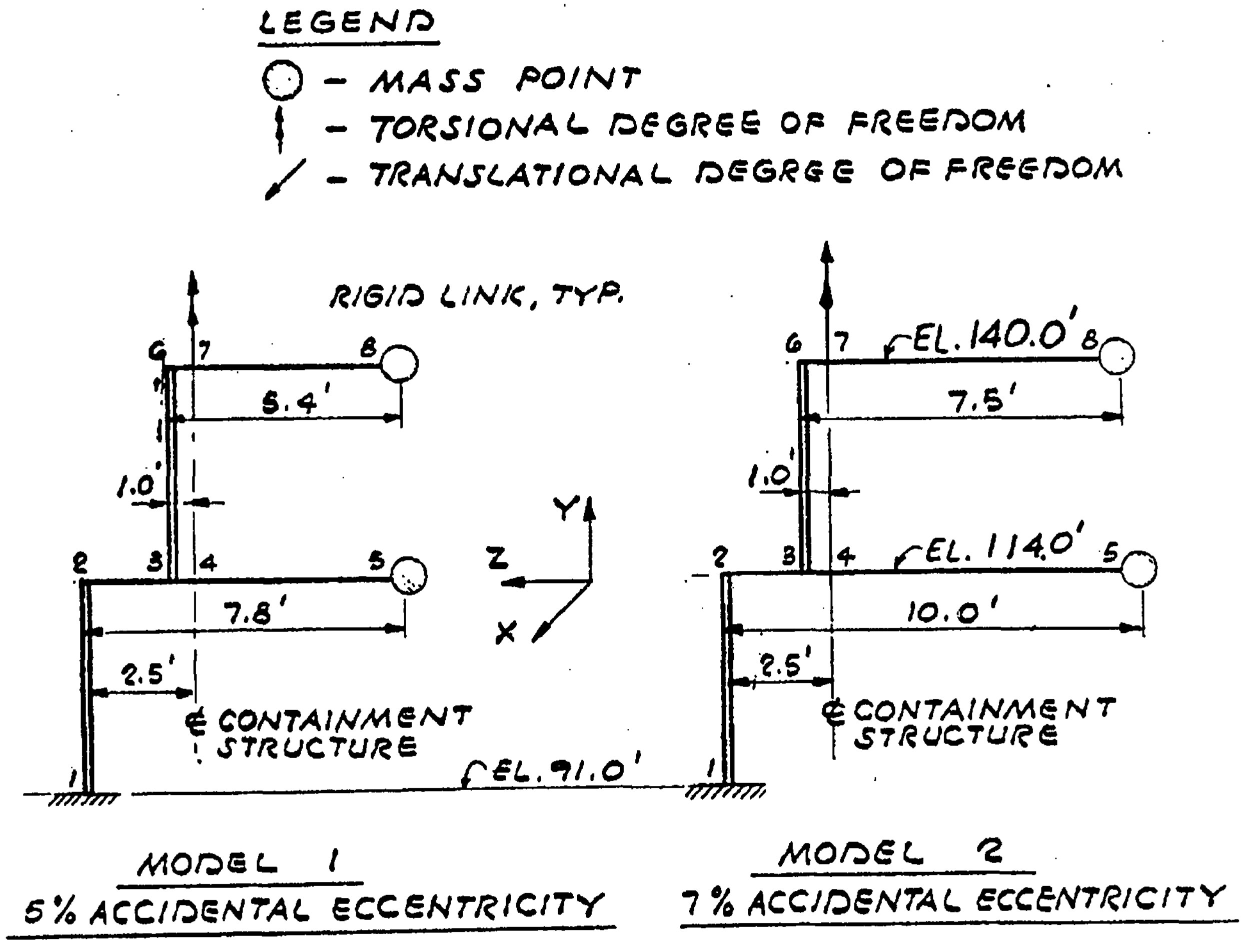

FSAR UPDATE

UNIT 1
DIABLO CANYON SITE

FIGURE 3.7-5 C
CONTAINMENT INTERIOR STRUCTURE
MATHEMATICAL MODEL FOR
HORIZONTAL AND TORSIONAL
ANALYSIS

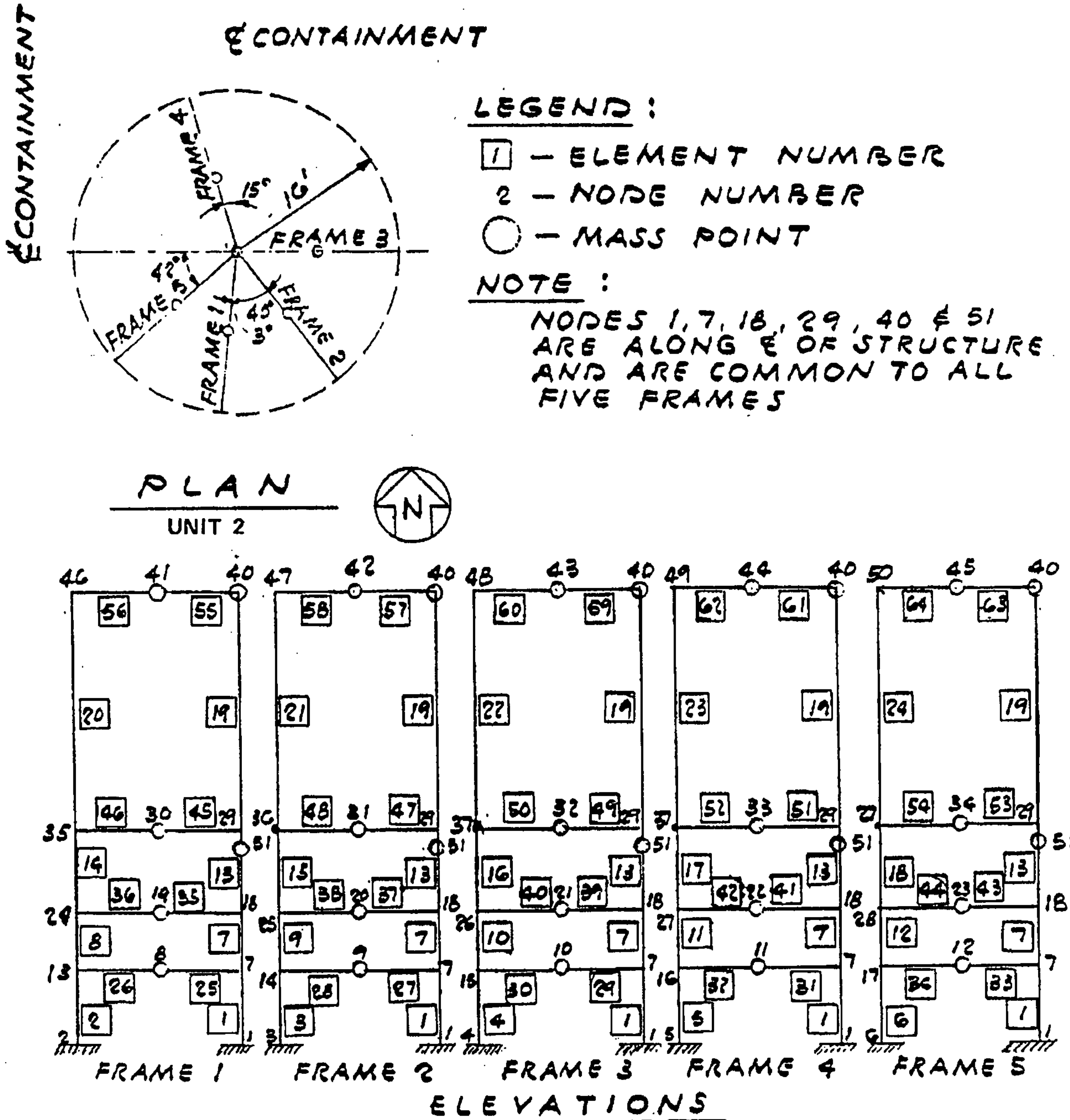

FSAR UPDATE

UNIT 2
DIABLO CANYON SITE

FIGURE 3.7-5 D
MATHEMATICAL MODEL FOR VERTICAL ANALYSIS OF CONTAINMENT INTERIOR STRUCTURE

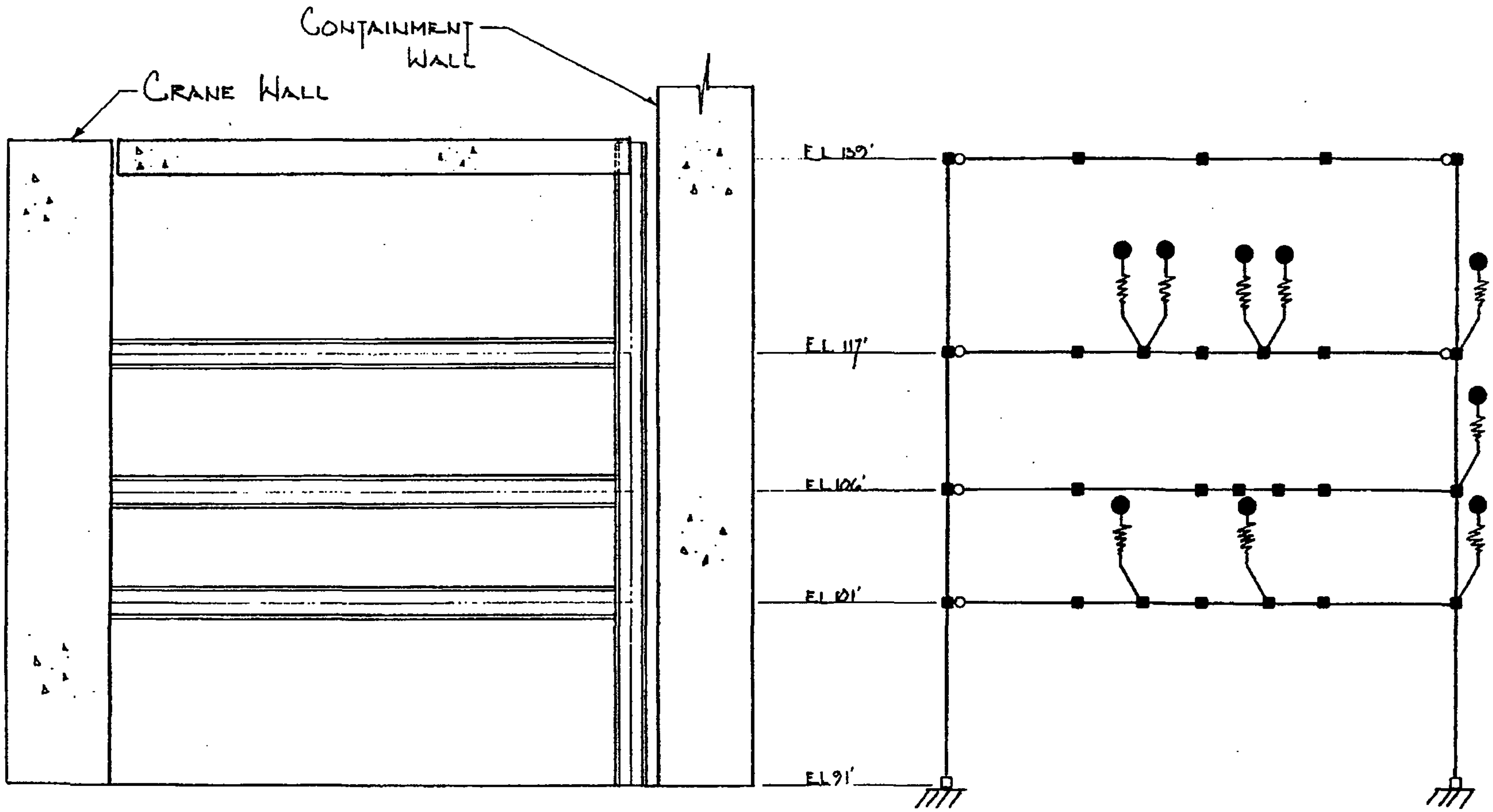

FSAR UPDATE

UNIT 1
DIABLO CANYON SITE

FIGURE 3.7 - 5 E
FRAME ANALYSIS FOR
VERTICAL RESPONSE
COLUMN LINE 6
(FRAME 6)

Revision 11 November 1996

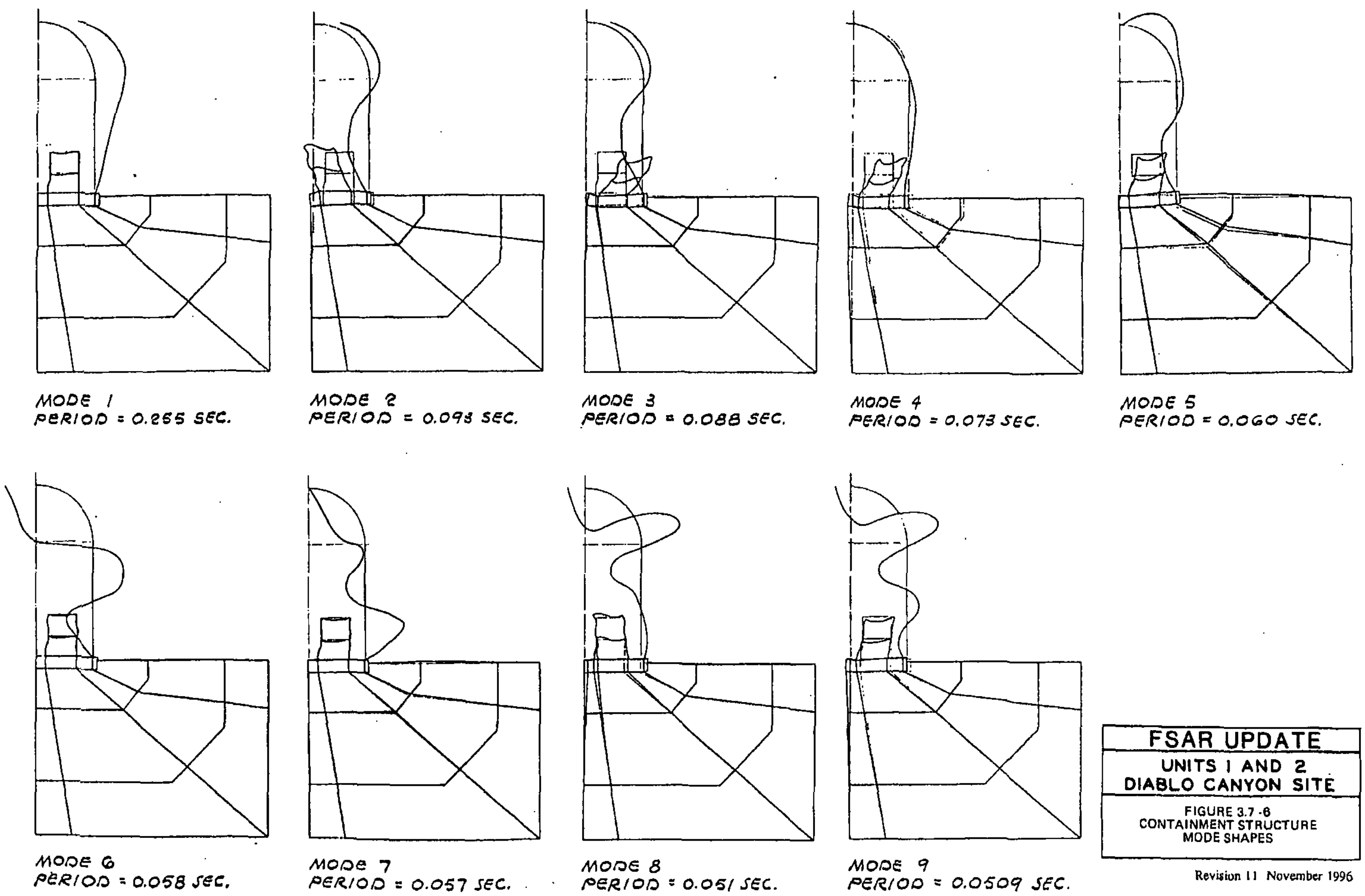

FSAR UPDATE

UNITS 1 AND 2
DIABLO CANYON SITE

FIGURE 3.7-6
CONTAINMENT STRUCTURE
MODE SHAPES

Revision 11 November 1996

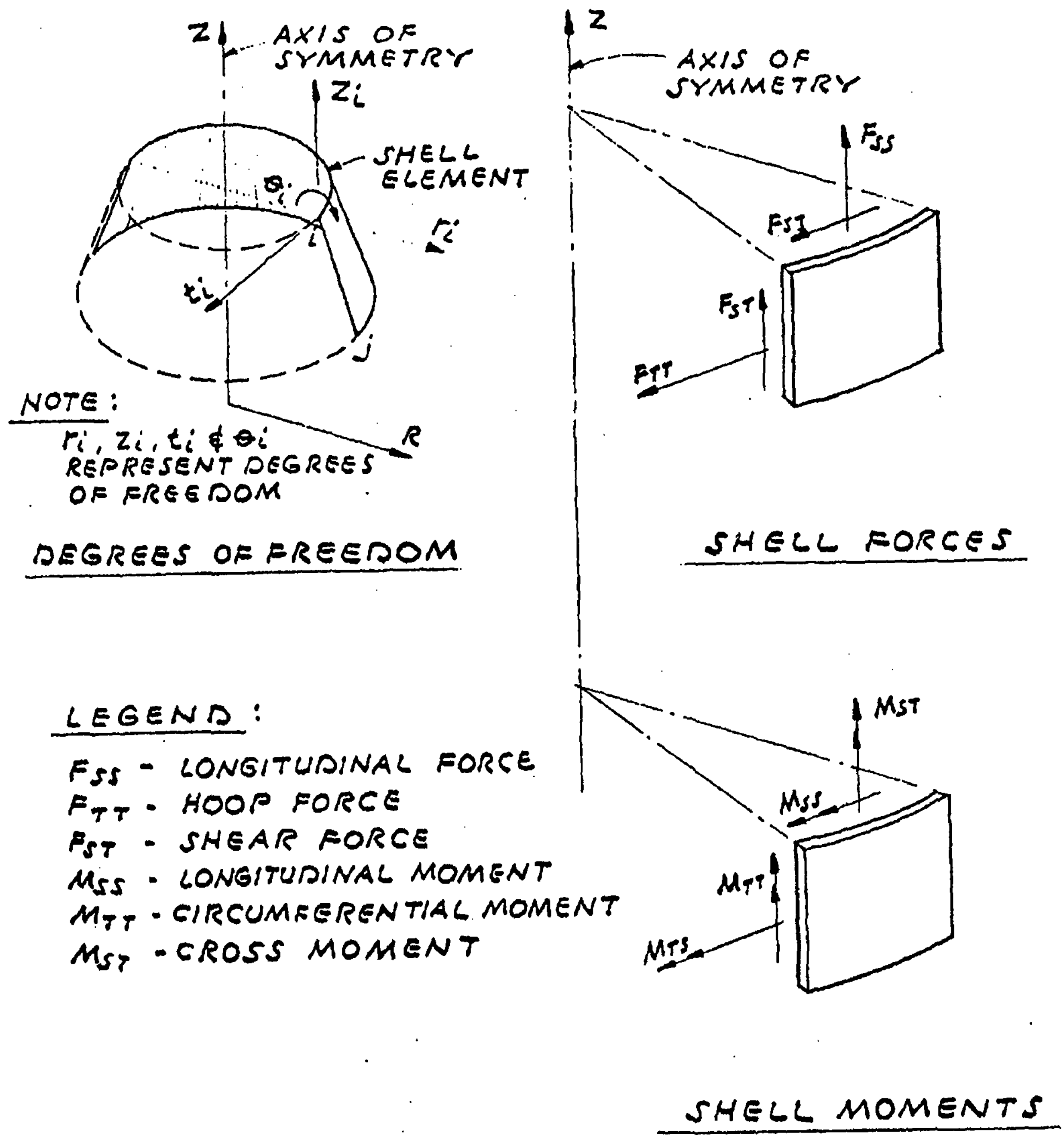

FSAR UPDATE

UNITS 1 AND 2
DIABLO CANYON SITE

FIGURE 3.7-7
CONTAINMENT STRUCTURE
SHELL FORCES AND MOMENTS
AND ELEMENT DEGREES OF FREEDOM

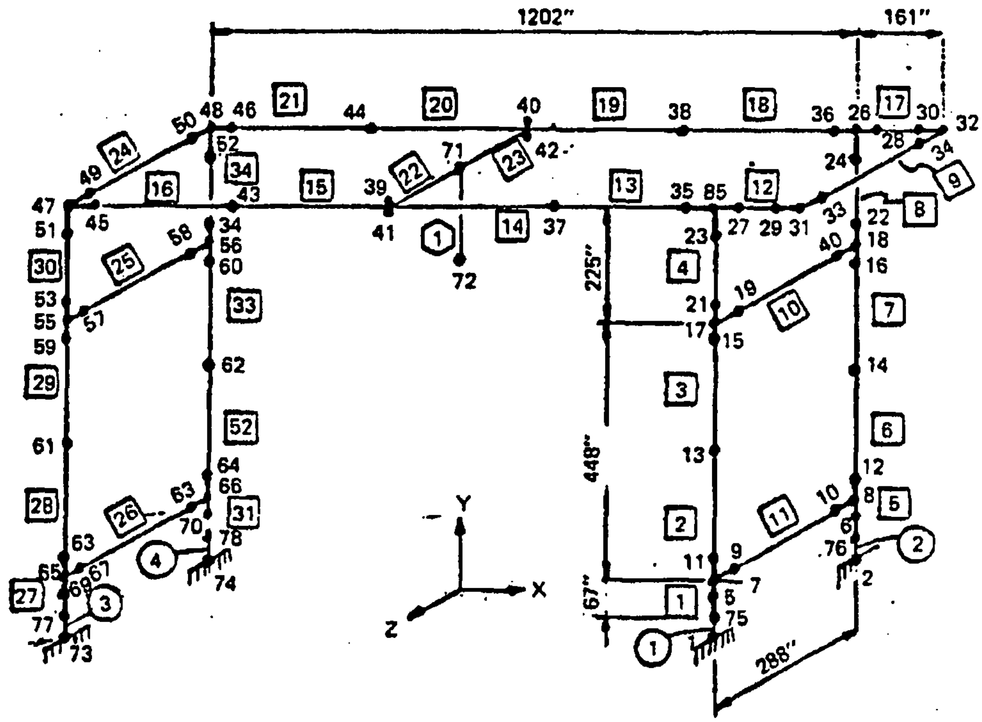

3-D NONLINEAR MODEL (ANSR)

KEY

1 NODE NUMBER

[1] BEAM-COLUMN ELEMENT

SEMI-RIGID BEAM-COLUMN ELEMENT

(1) TRUSS ELEMENT

(1) BOUNDARY-GAP ELEMENT

FSAR UPDATE
UNITS 1 AND 2 DIABLO CANYON SITE
FIGURE 3.7 - 7 A POLAR CRANE THREE-DIMENSIONAL NONLINEAR MODEL

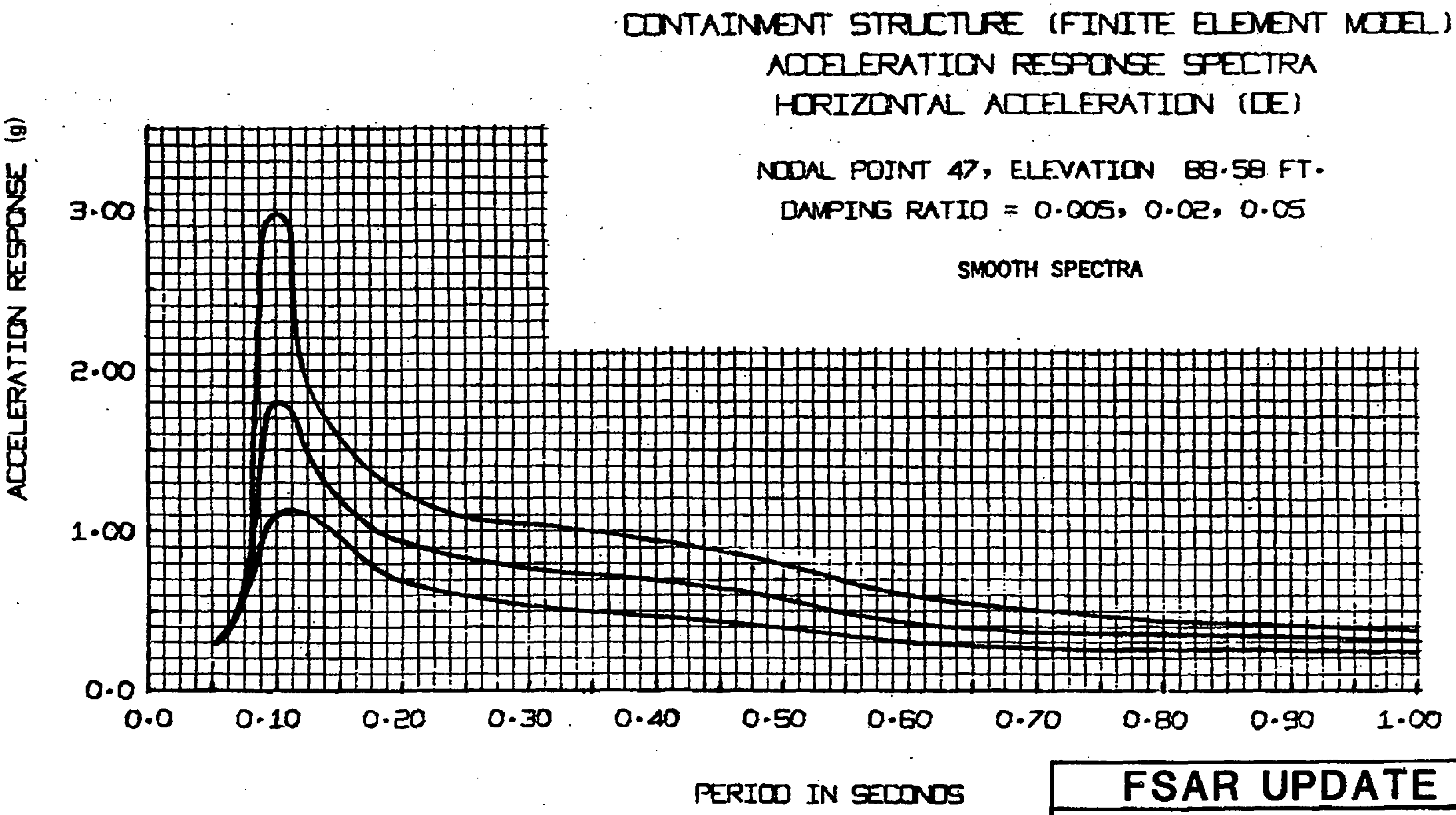

FSAR UPDATE

UNITS 1 AND 2 DIABLO CANYON SITE

FIGURE 3.7-8
CONTAINMENT STRUCTURE
TYPICAL SPECTRA

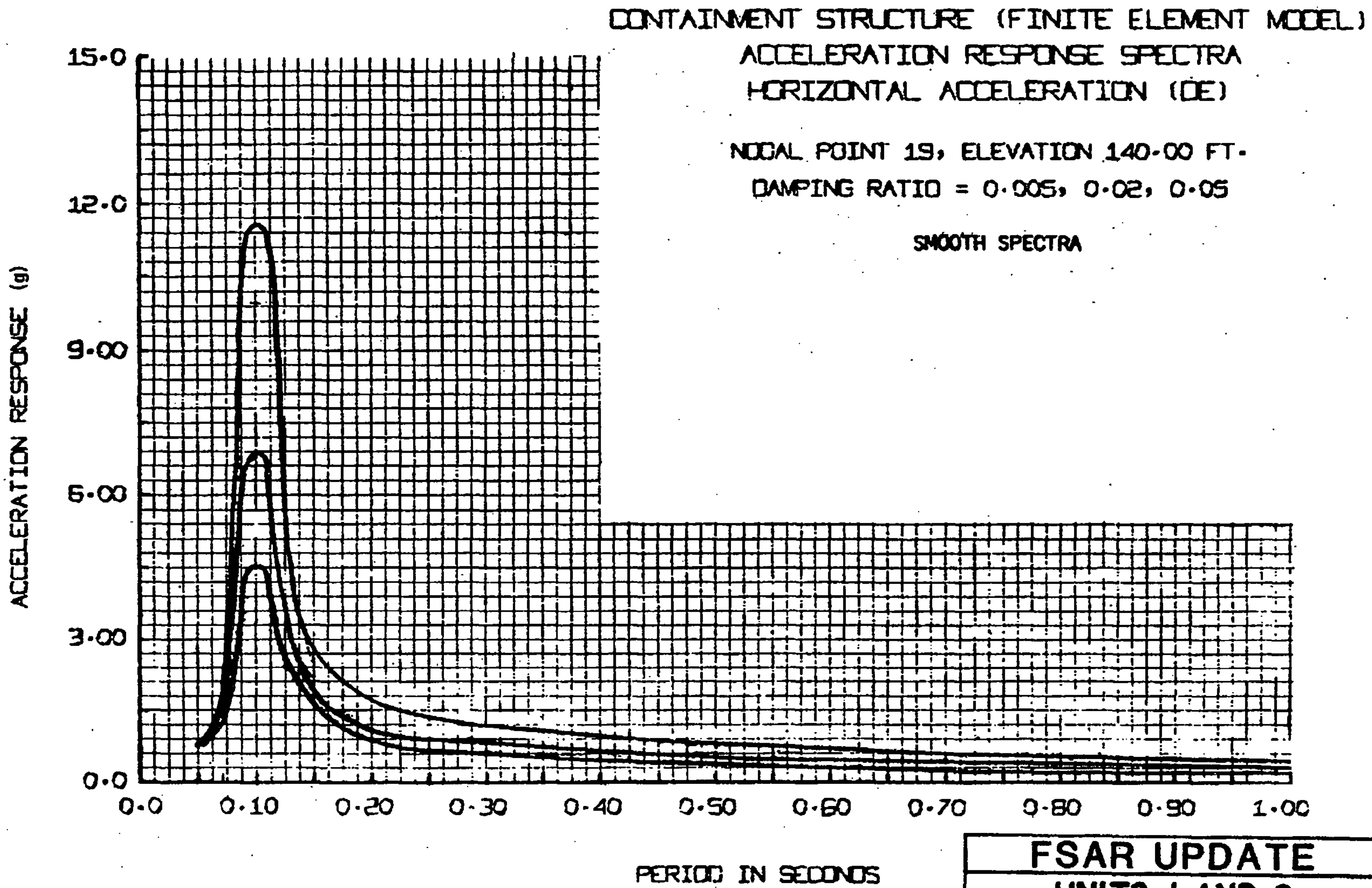

FSAR UPDATE

UNITS 1 AND 2
DIABLO CANYON SITE

FIGURE 3.7 - 9
CONTAINMENT STRUCTURE
TYPICAL SPECTRA

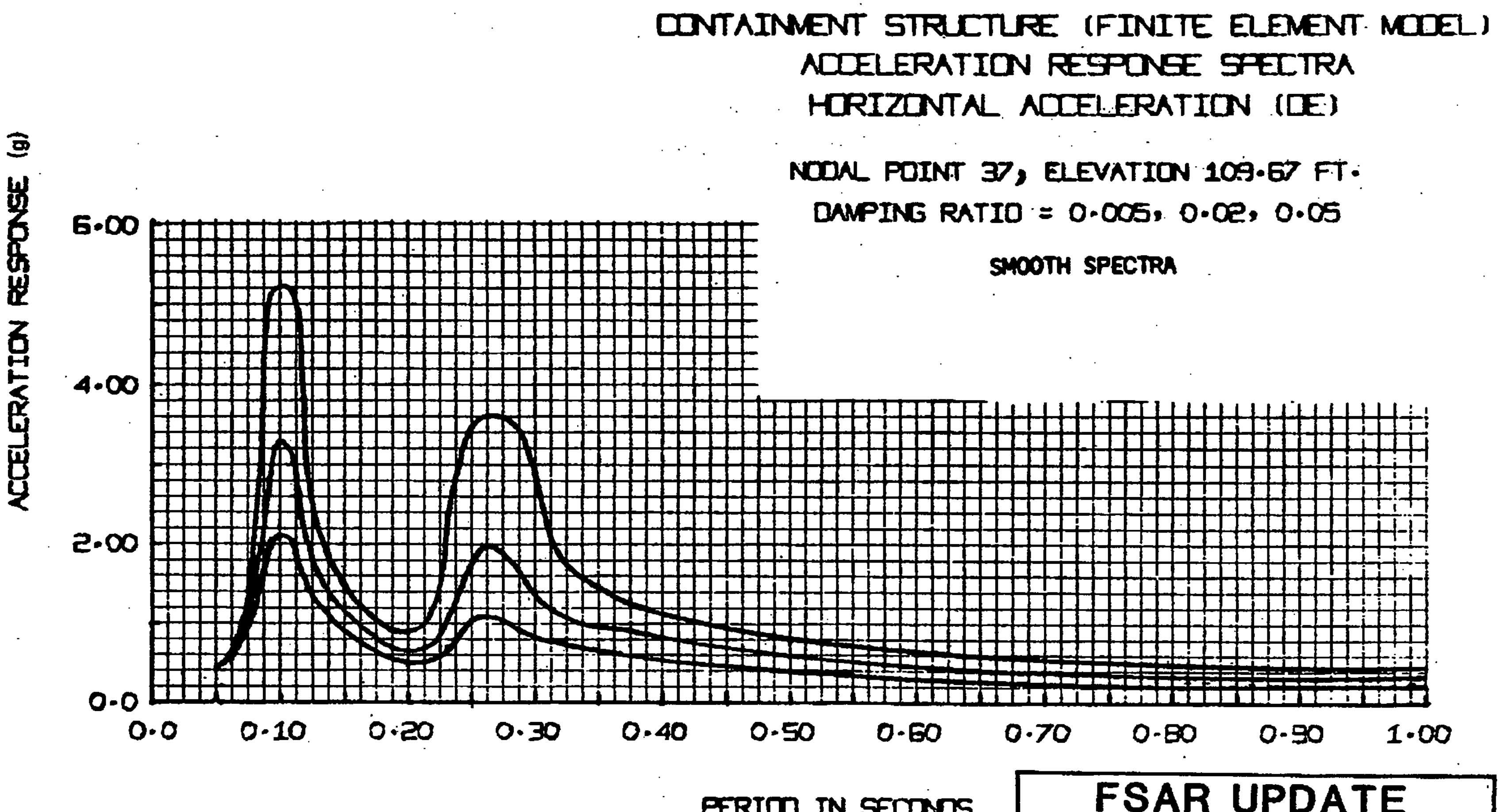

FSAR UPDATE

**UNITS 1 AND 2
DIABLO CANYON SITE**

FIGURE 3.7 - 10
CONTAINMENT STRUCTURE
TYPICAL SPECTRA

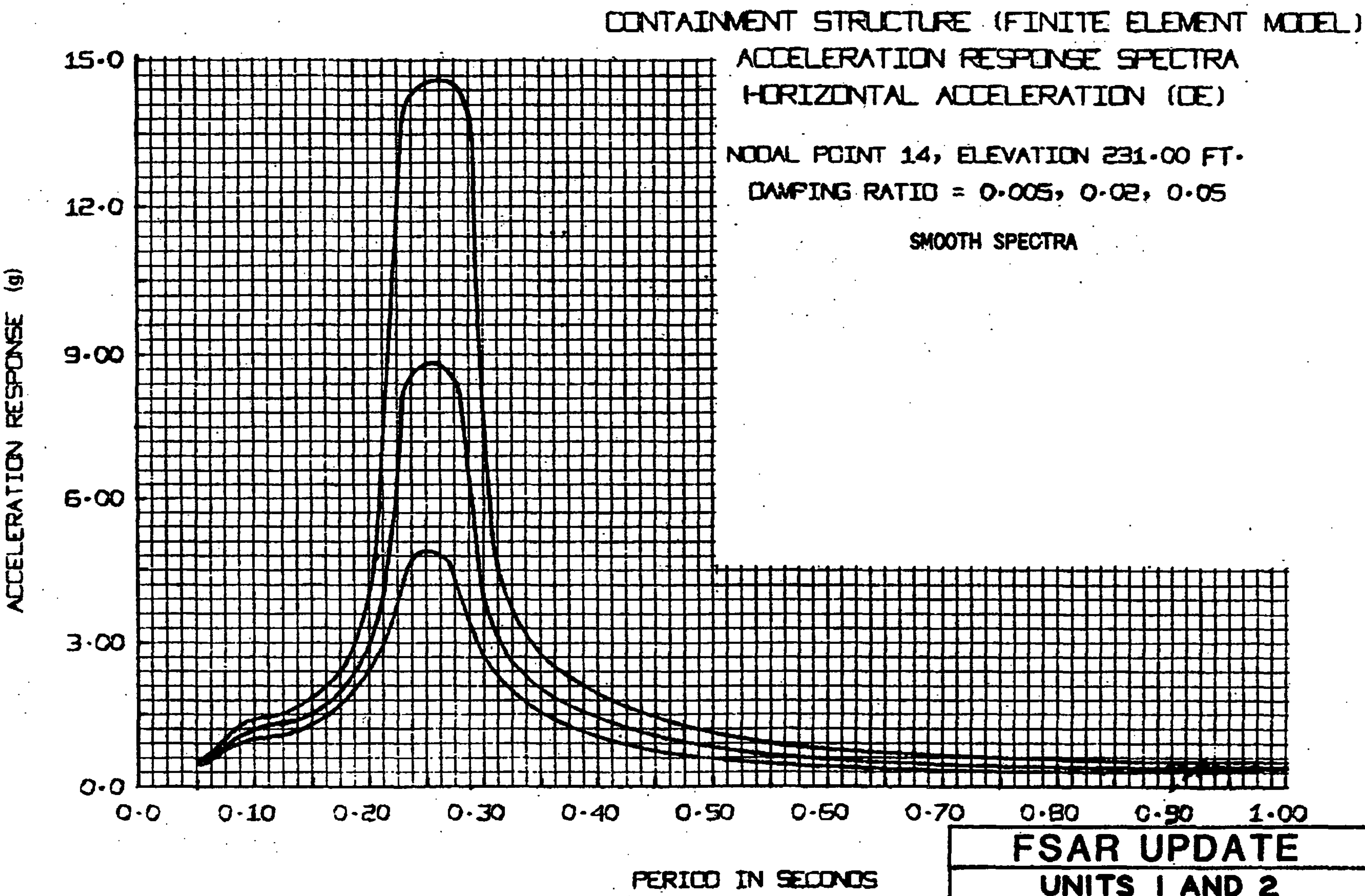

FSAR UPDATE

UNITS 1 AND 2
DIABLO CANYON SITE

FIGURE 3.7 - 11
CONTAINMENT STRUCTURE
TYPICAL SPECTRA

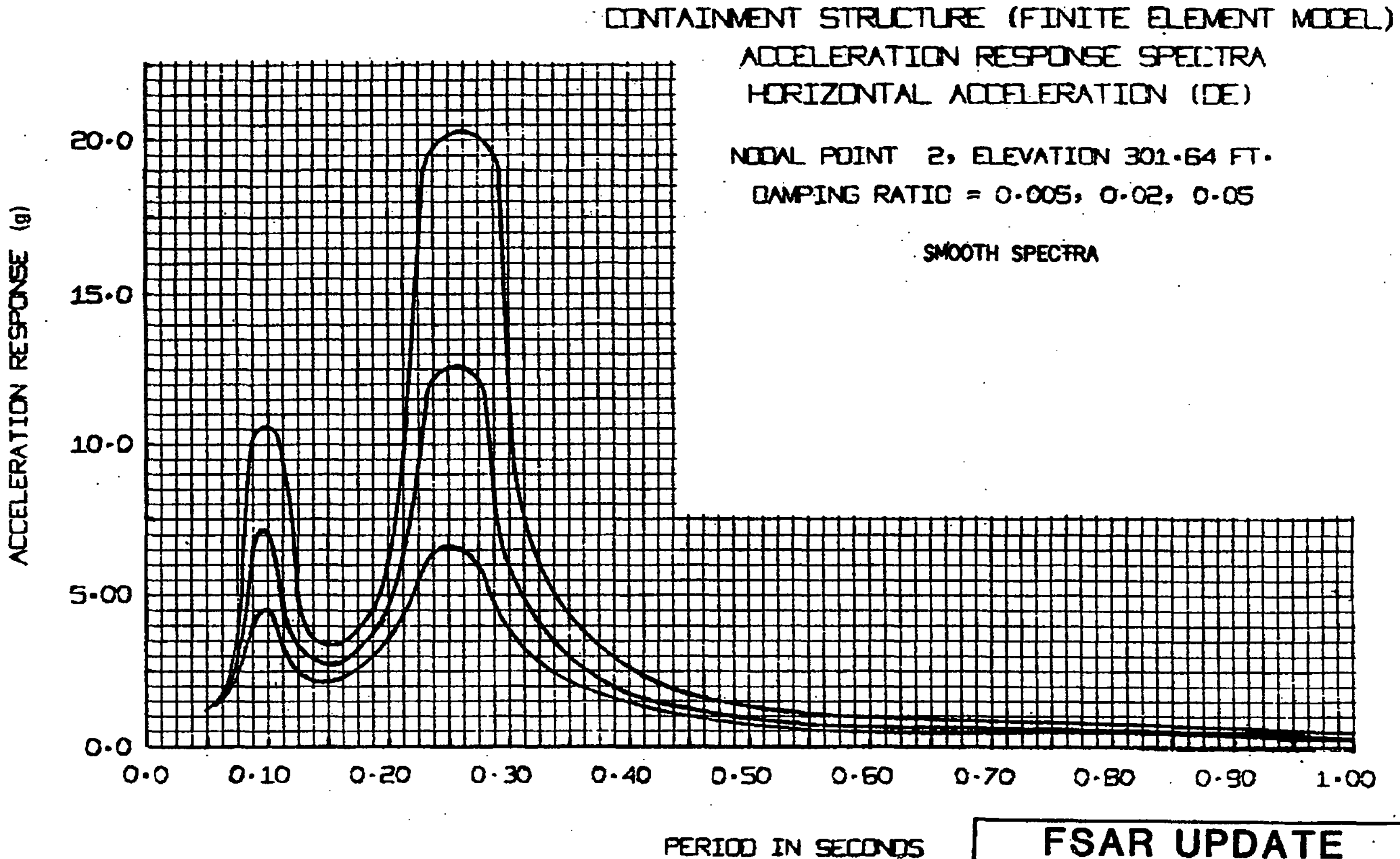

FSAR UPDATE

**UNITS 1 AND 2
DIABLO CANYON SITE**

FIGURE 3.7 - 12
CONTAINMENT STRUCTURE
TYPICAL SPECTRA

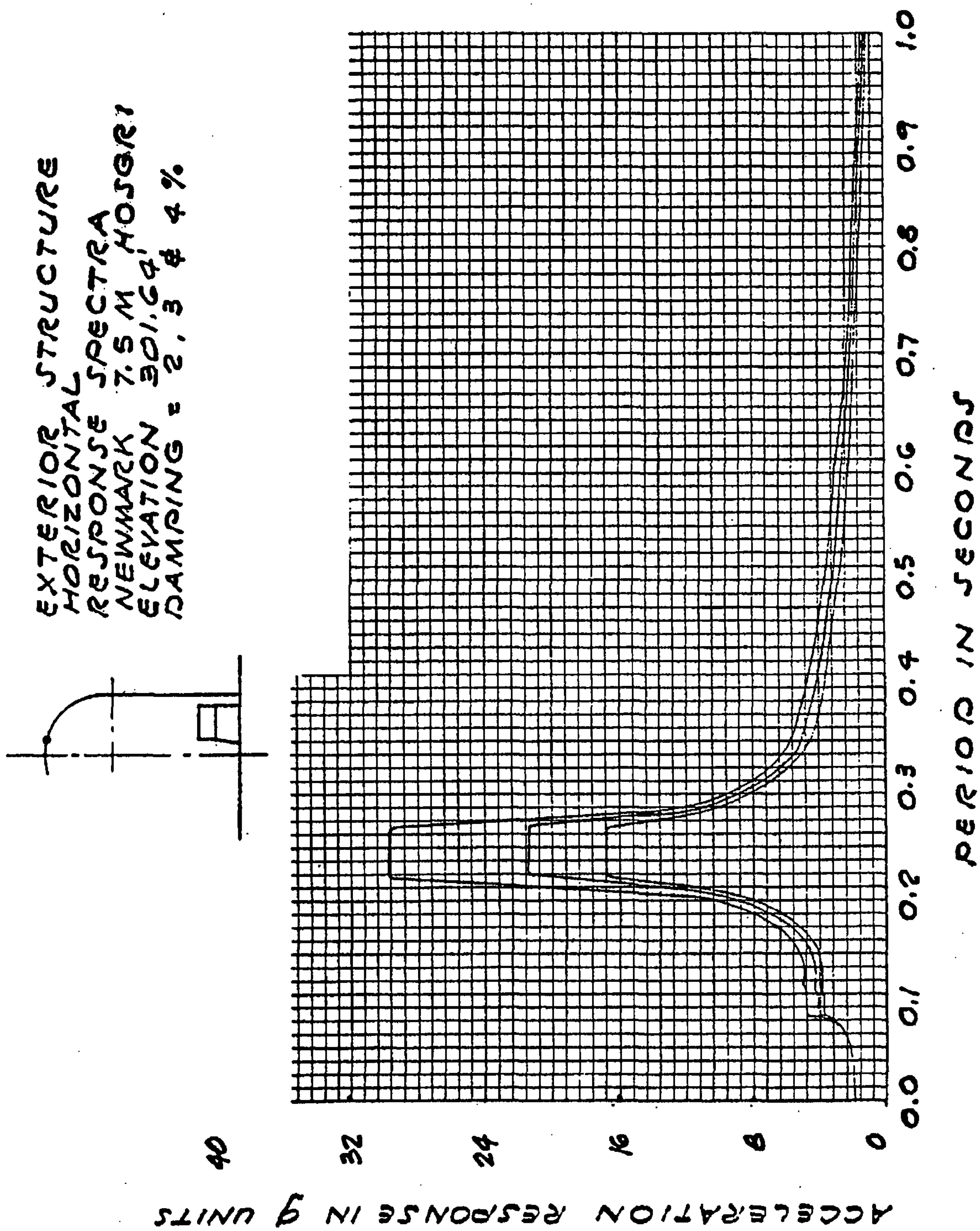

FSAR UPDATE

UNITS 1 AND 2
DIABLO CANYON SITE

FIGURE 3.7 - 12 A
CONTAINMENT STRUCTURE

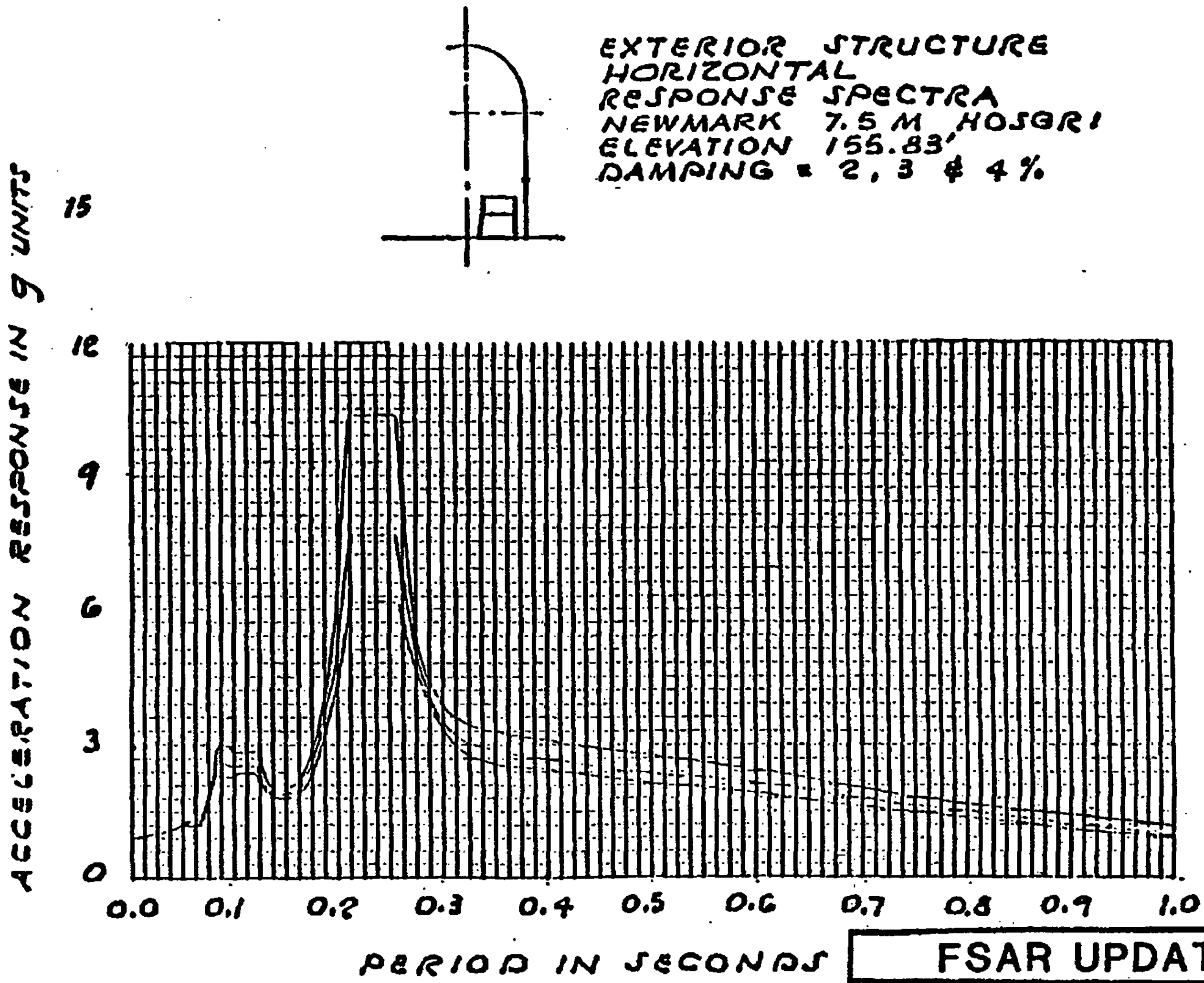

FSAR UPDATE

UNITS 1 AND 2
DIABLO CANYON SITE

FIGURE 3.7 - 12B
CONTAINMENT STRUCTURE

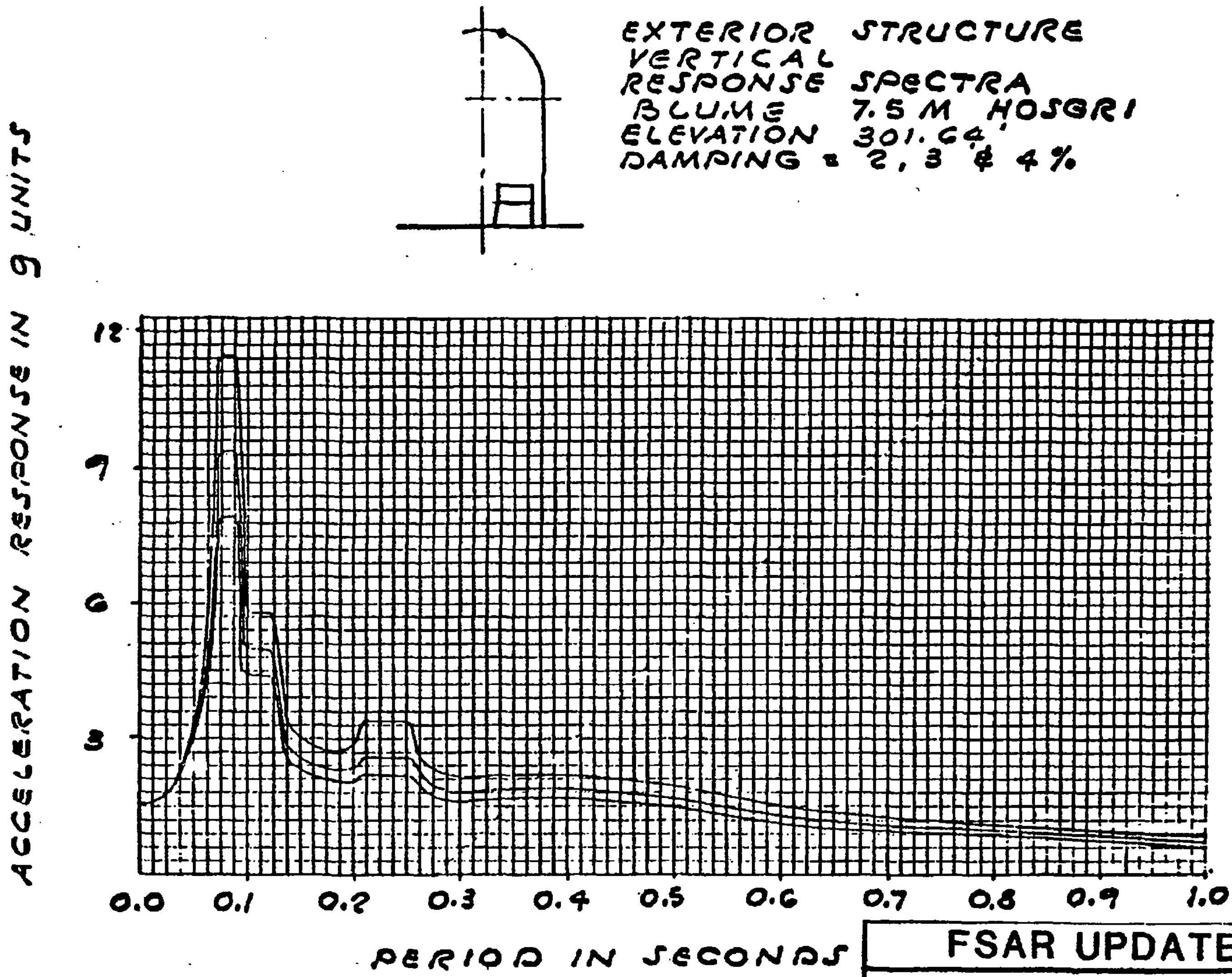

FSAR UPDATE

UNITS 1 AND 2
DIABLO CANYON SITE

FIGURE 3.7 - 12C
CONTAINMENT STRUCTURE

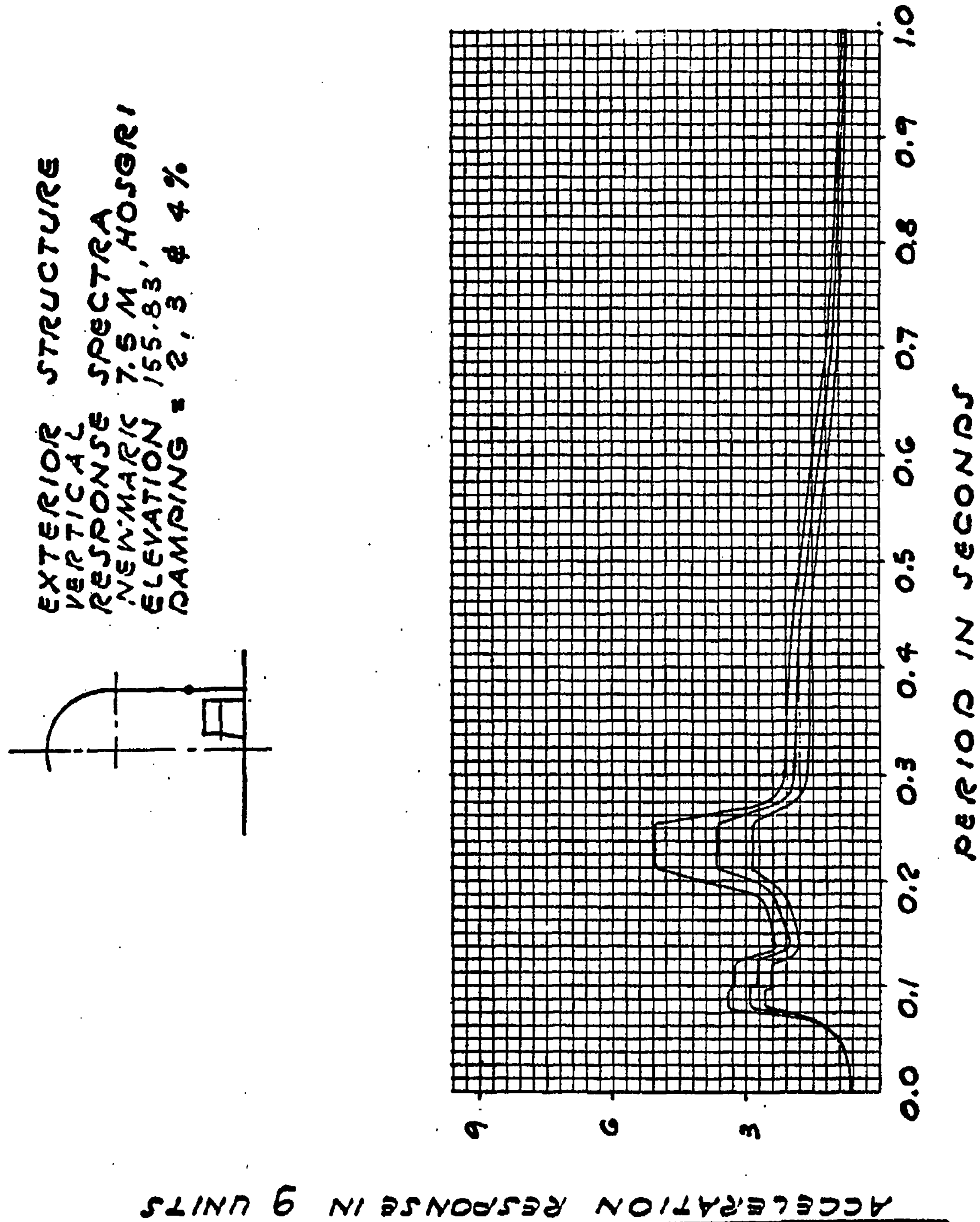

FSAR UPDATE

UNITS 1 AND 2
DIABLO CANYON SITE

FIGURE 3.7 - 12D
CONTAINMENT STRUCTURE

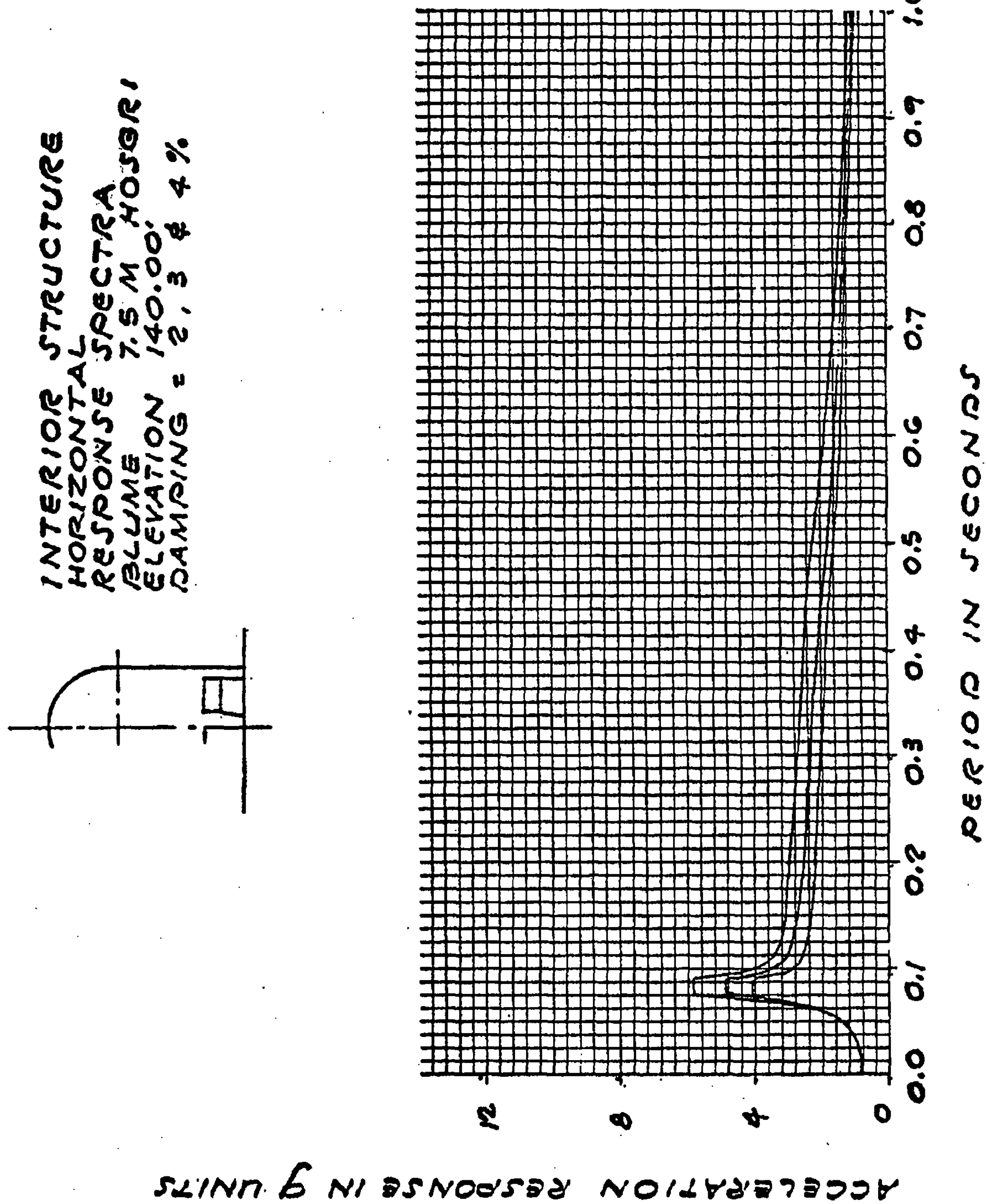

FSAR UPDATE

UNITS 1 AND 2
DIABLO CANYON SITE

FIGURE 3.7 - 12E
CONTAINMENT STRUCTURE

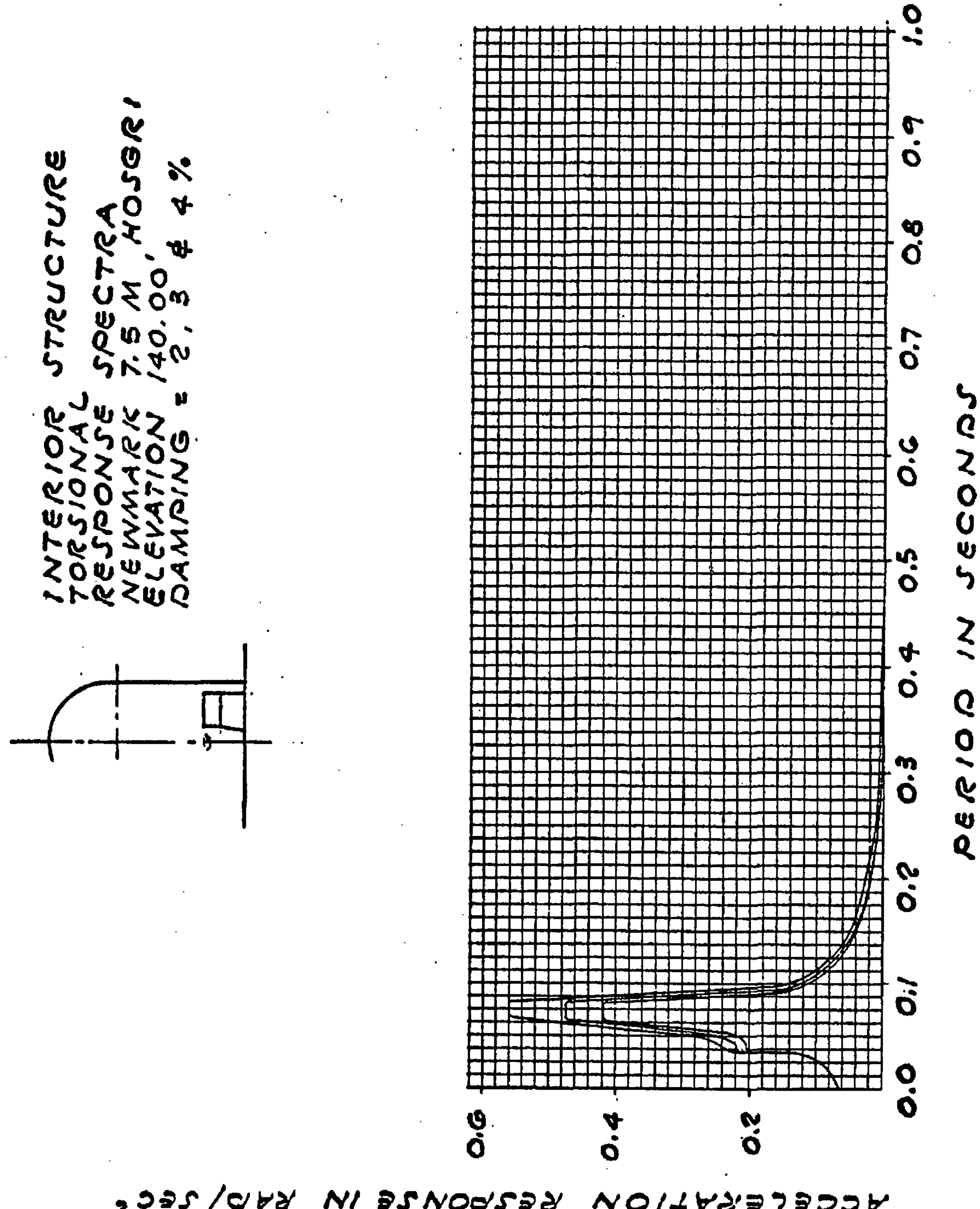

FSAR UPDATE

UNITS 1 AND 2
DIABLO CANYON SITE

FIGURE 3.7 - 12 F
CONTAINMENT STRUCTURE

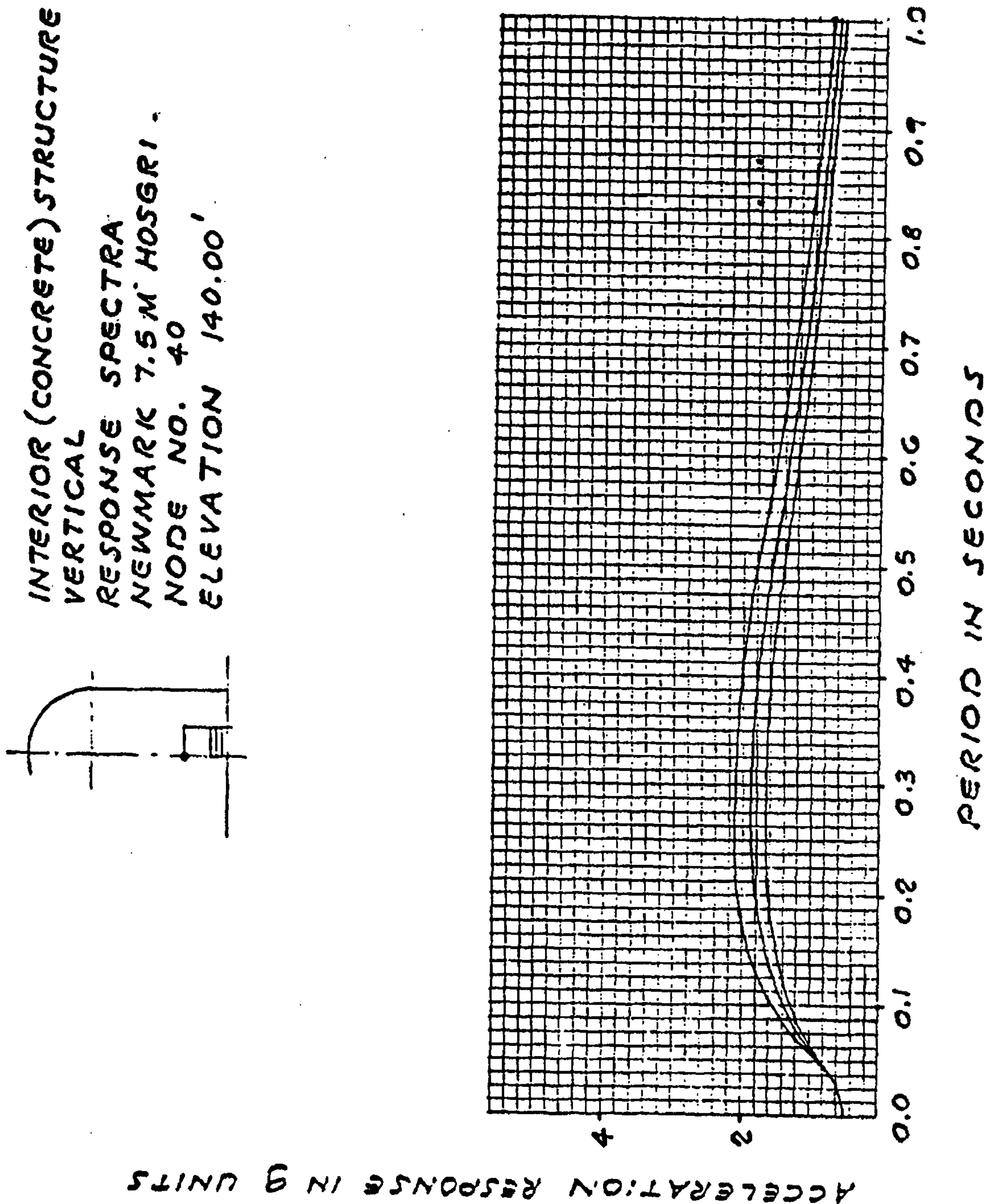

FSAR UPDATE

UNITS 1 AND 2
DIABLO CANYON SITE

FIGURE 3.7 - 12G
CONTAINMENT STRUCTURE

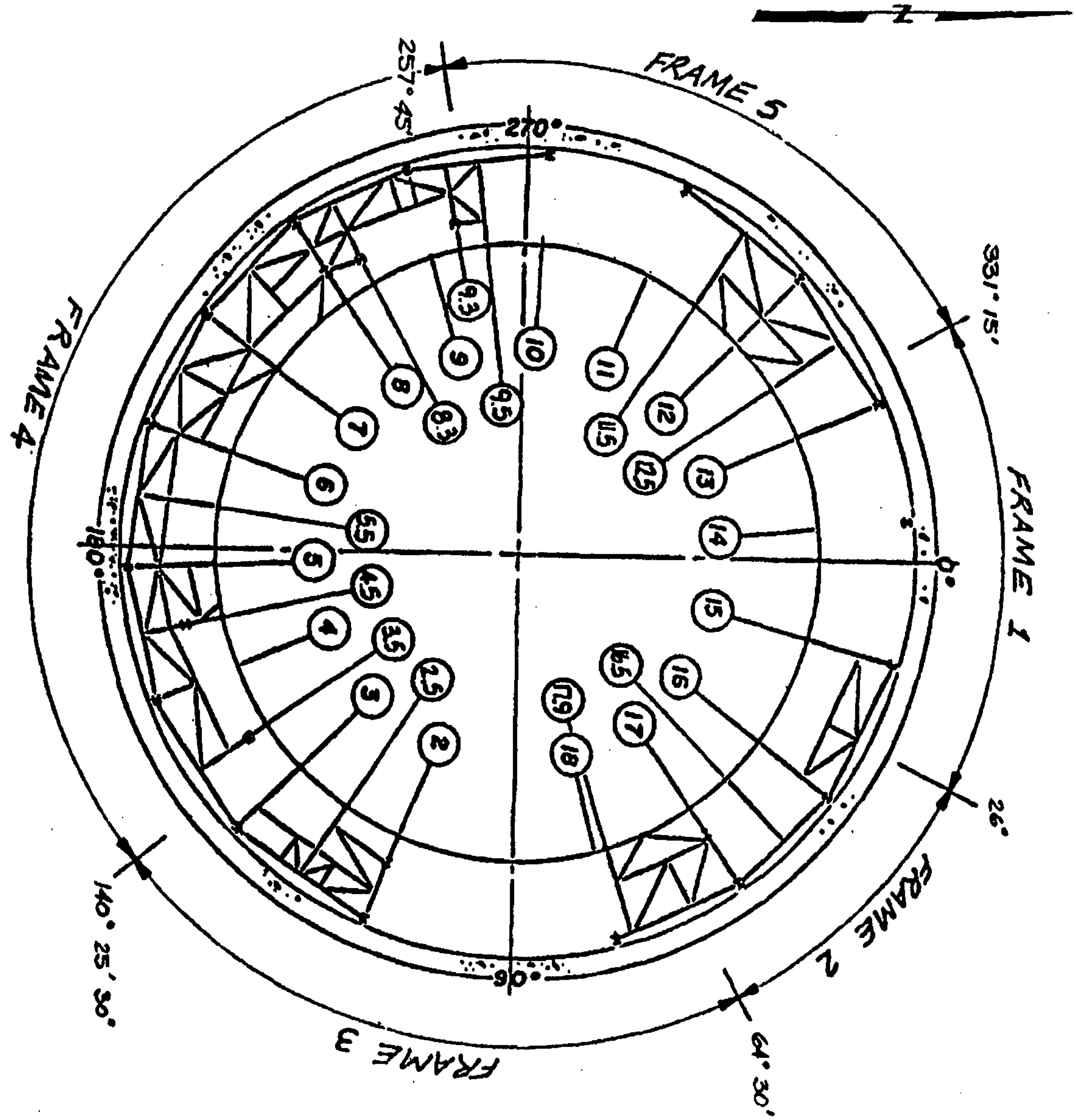

FSAR UPDATE
UNIT 1   **DIABLO CANYON SITE**
FIGURE 3.7 - 12 H   CONTAINMENT – ANNULUS STRUCTURE

Revision 11 November 1996

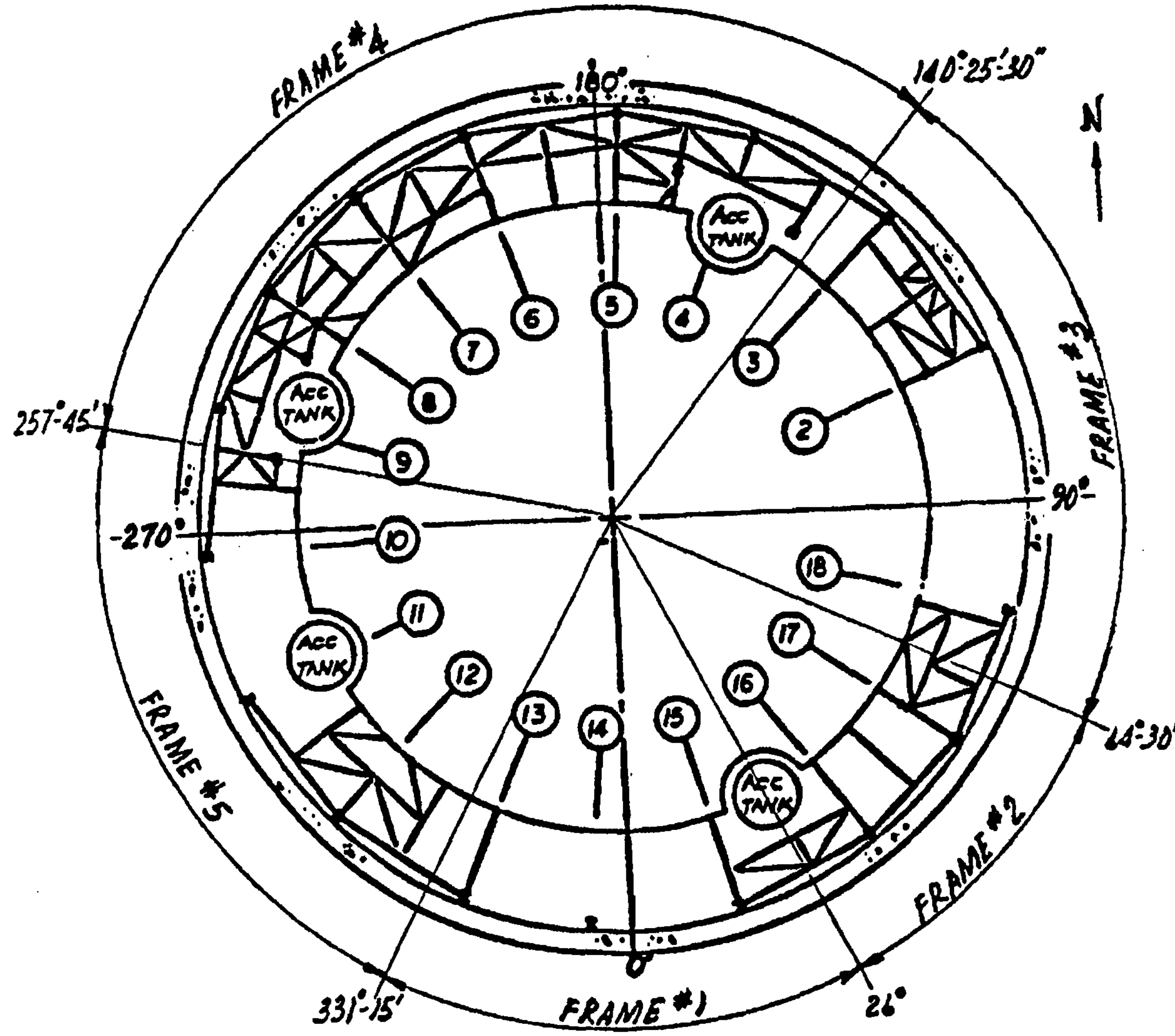

FSAR UPDATE

UNIT 2
DIABLO CANYON SITE

FIGURE 3.7 - 12 I
CONTAINMENT – ANNULUS STRUCTURE

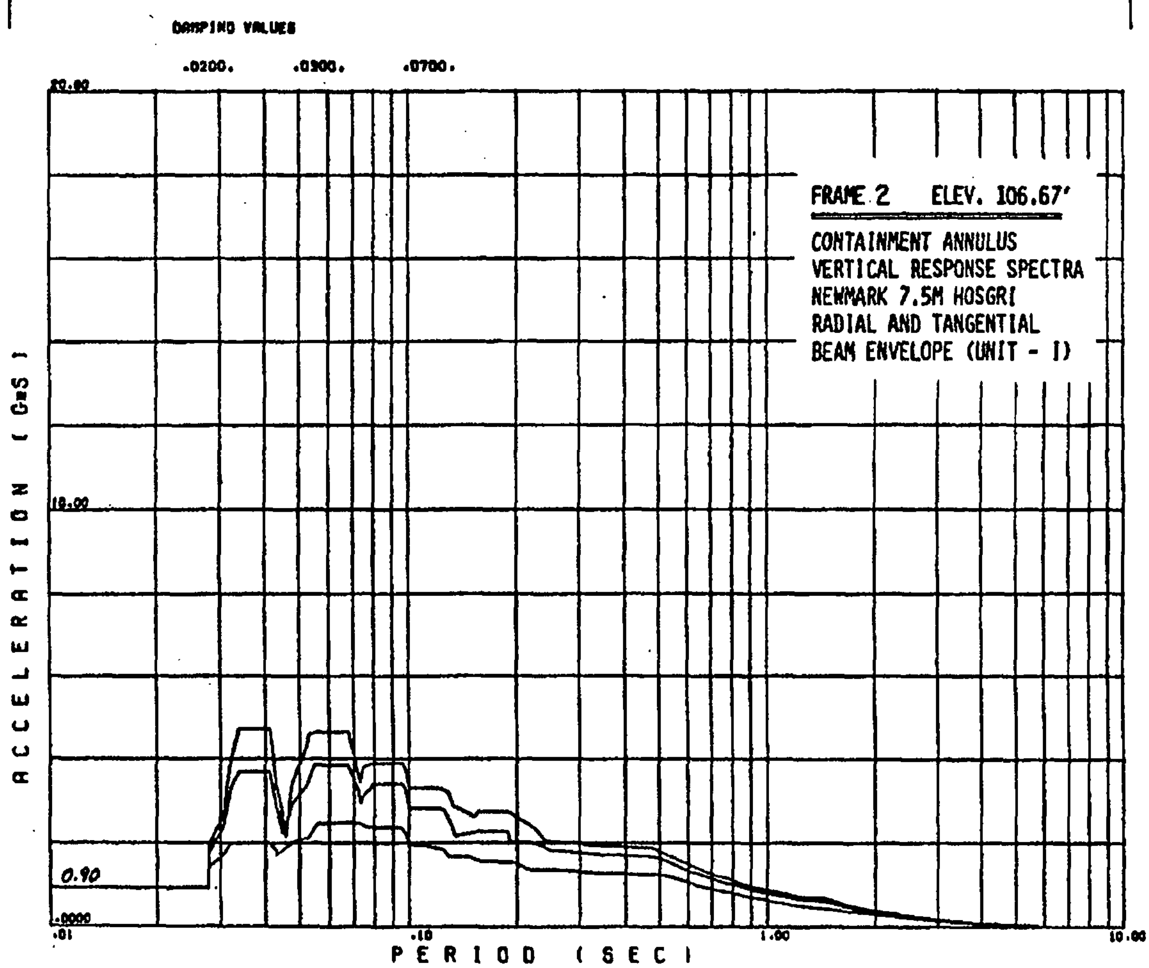

FSAR UPDATE

UNIT 1
DIABLO CANYON SITE

FIGURE 3.7 - 12 J
CONTAINMENT ANNULUS SPECTRA

Revision 11 November 1996

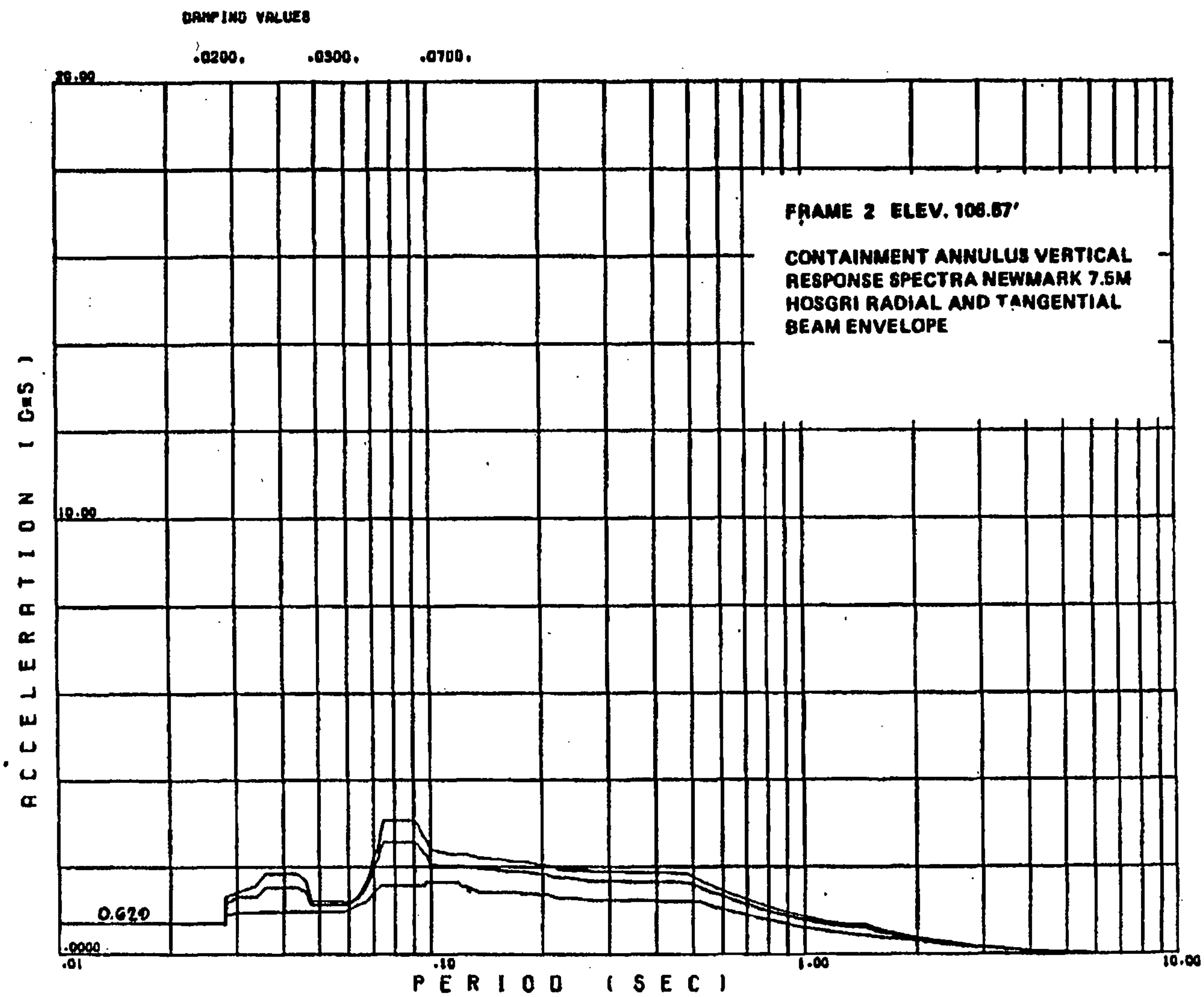

FSAR UPDATE

UNIT 2
DIABLO CANYON SITE

FIGURE 3.7 - 12 K
CONTAINMENT ANNULUS SPECTRA

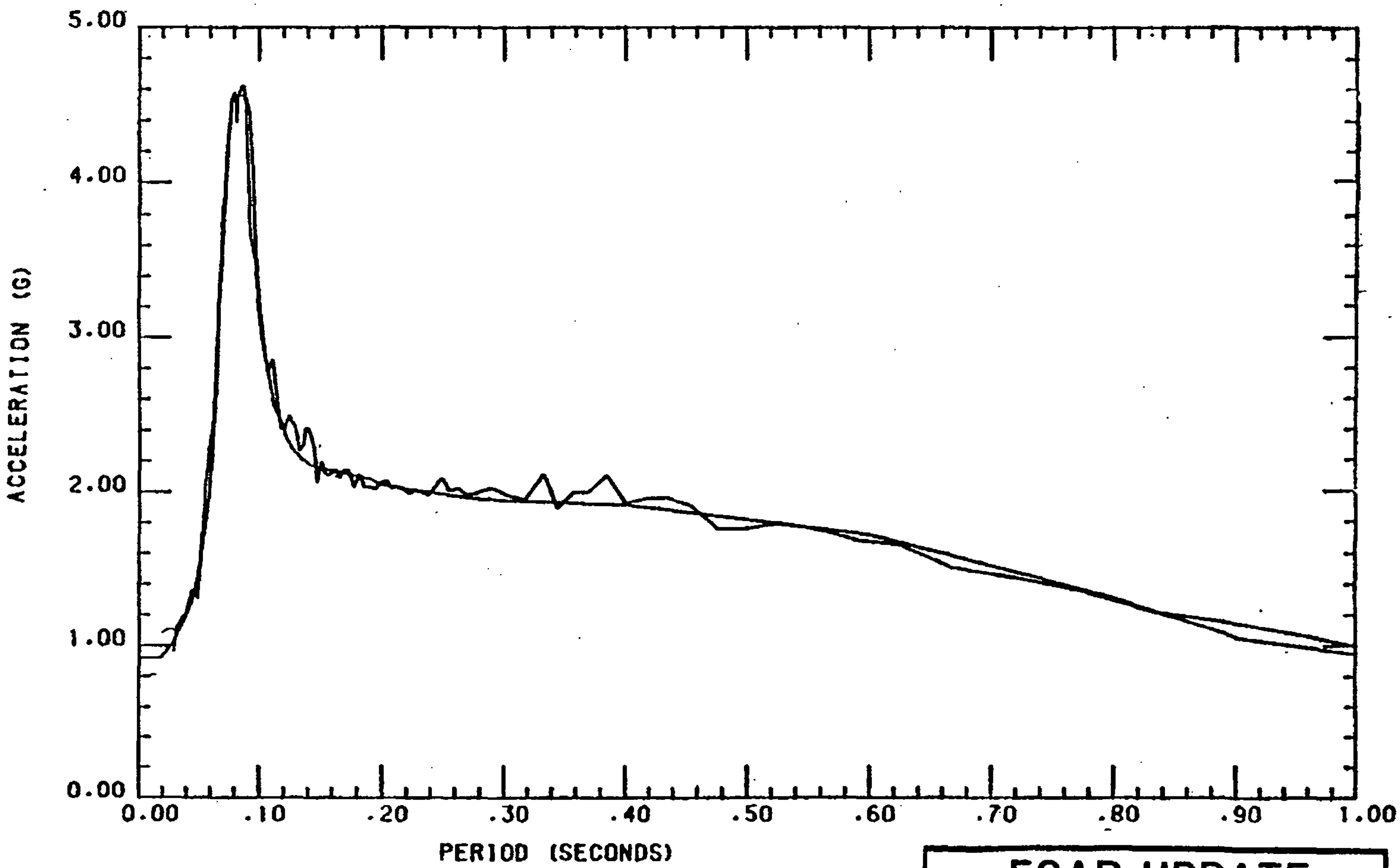

FSAR UPDATE

UNITS 1 AND 2
DIABLO CANYON SITE

FIGURE 3.7 - 12 L
POLAR CRANE HOSGRI HORIZONTAL SPECTRUM IN X DIRECTION WITH 4% DAMPING AT EL. 140'

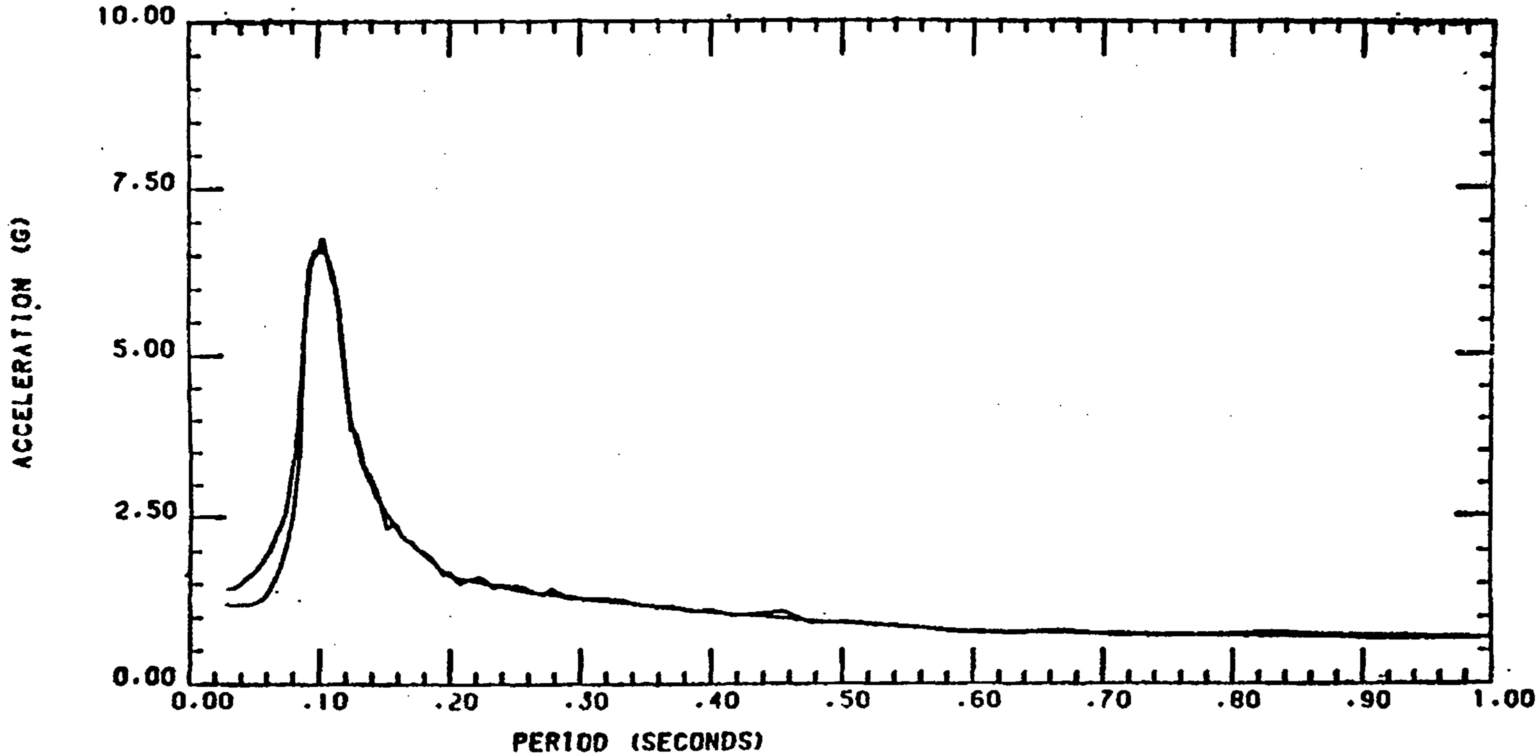

FSAR UPDATE

UNITS 1 AND 2
DIABLO CANYON SITE

FIGURE 3.7 - 12 M
POLAR CRANE DDE HORIZONTAL
SPECTRUM IN Z DIRECTION
WITH 5% DAMPING AT EL. 140'

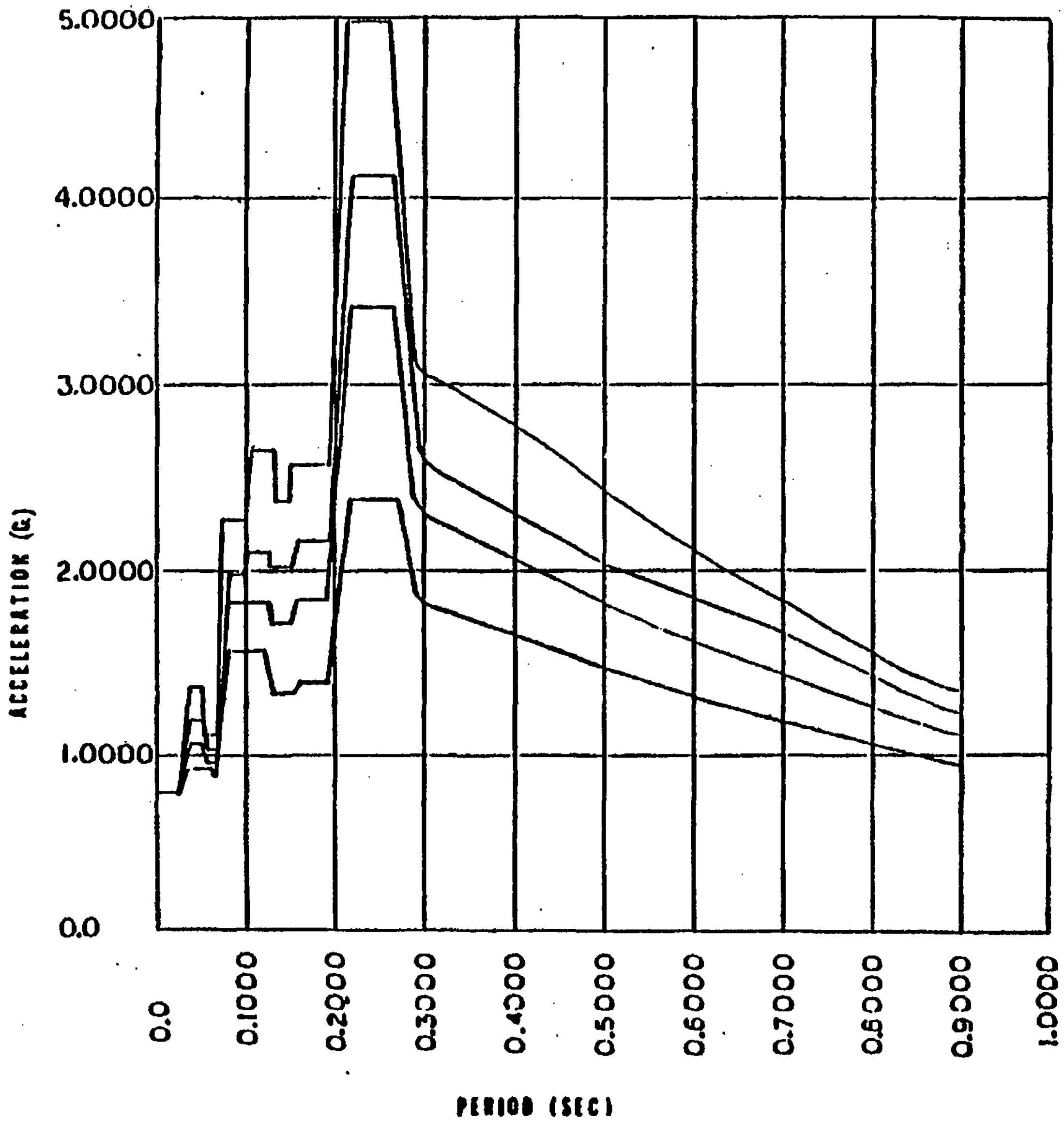

FSAR UPDATE

UNIT 1
DIABLO CANYON SITE

FIGURE 3.7 - 12 N
PIPEWAY STRUCTURE
HOSGRI BLUME N-S
RESPONSE SPECTRA
% DAMPING 2,3,4,7
ELEVATION 109'4"
NODE 893

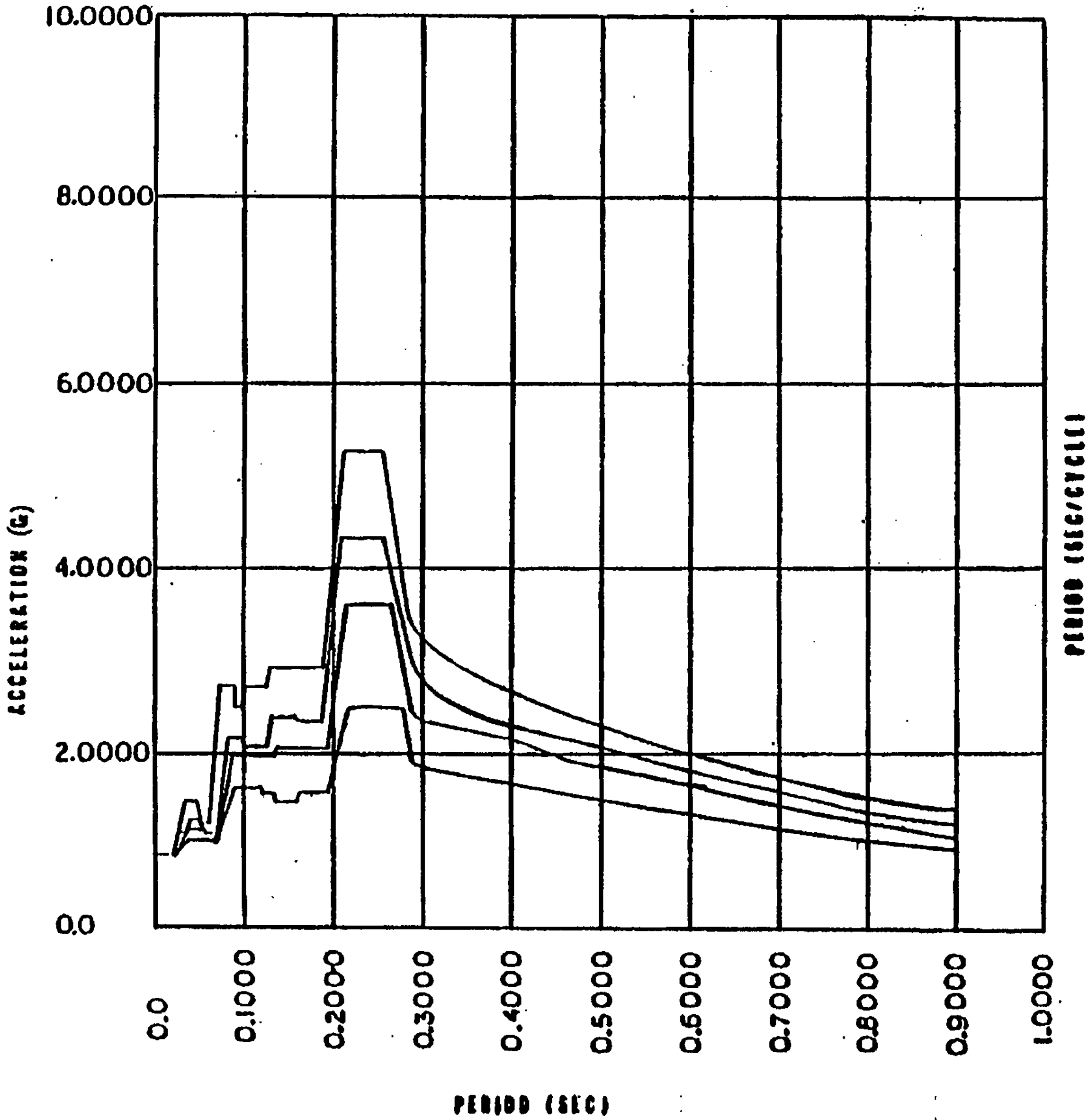

FSAR UPDATE
UNIT 1 **DIABLO CANYON SITE**
FIGURE 3.7 - 12 O PIPEWAY STRUCTURE HOSGRI BLUME E-W RESPONSE SPECTRA % DAMPING 2, 3 , 4, 7 ELEVATION 109'- 4" NODE 893

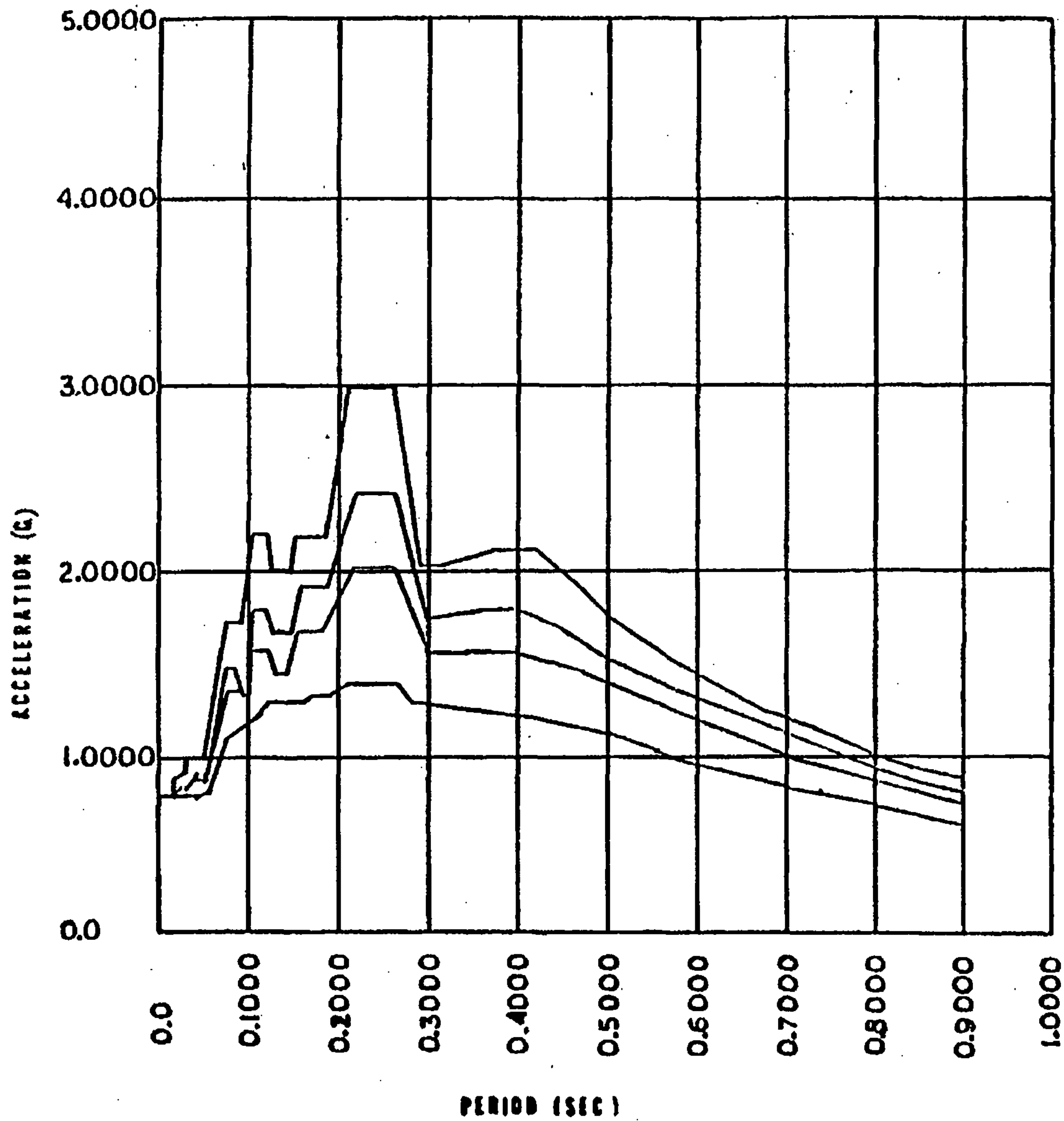

FSAR UPDATE

UNIT 1
DIABLO CANYON SITE

FIGURE 3.7 - 12P
PIPEWAY STRUCTURE
HOSGRI BLUME VERTICAL
RESPONSE SPECTRA
% DAMPING 2,3,4,7
ELEVATION 109'-4"
NODE 893

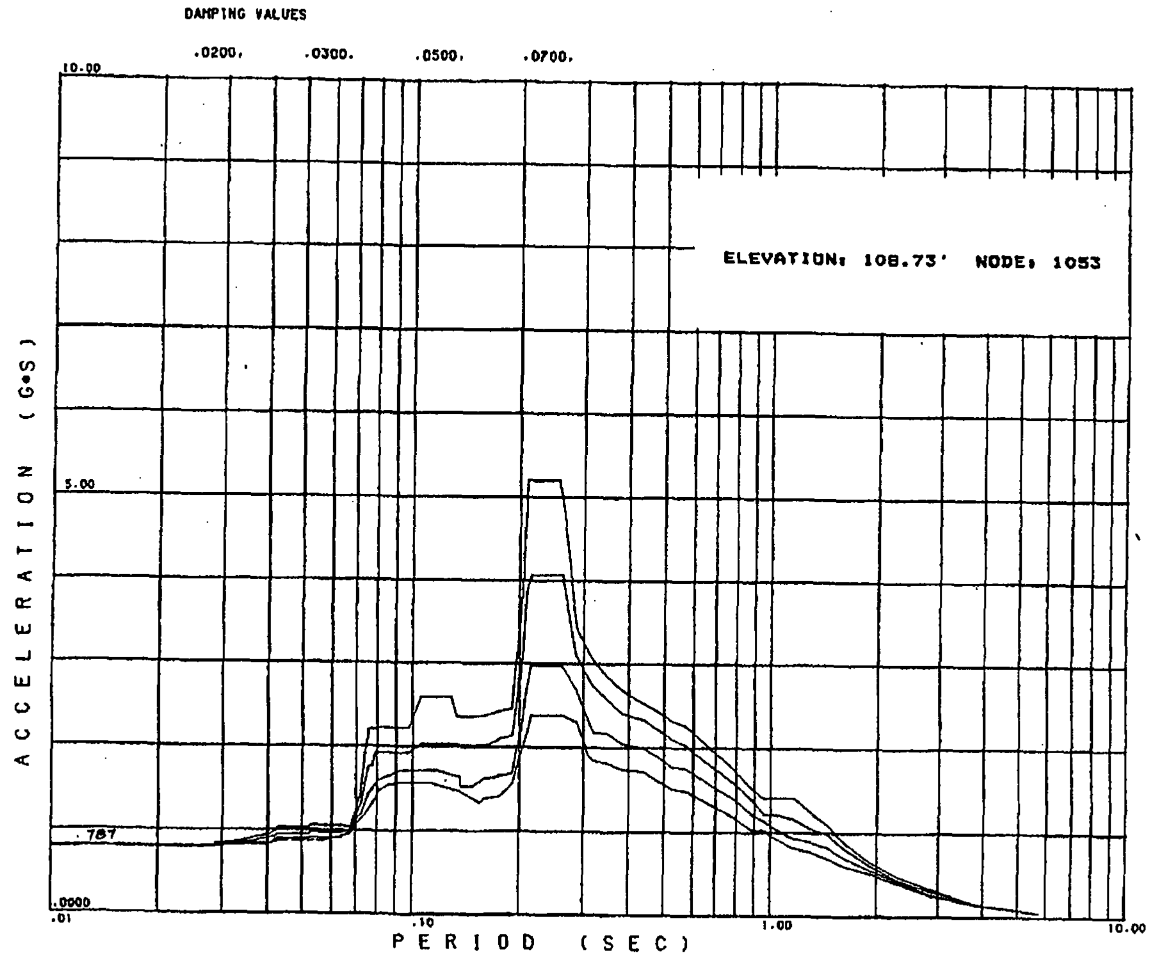

FSAR UPDATE

UNIT 2
DIABLO CANYON SITE

FIGURE 3.7 - 12Q
PIPEWAY STRUCTURE
HOSGRI BLUME N-S
RESPONSE SPECTRA

Revision 11 November 1996

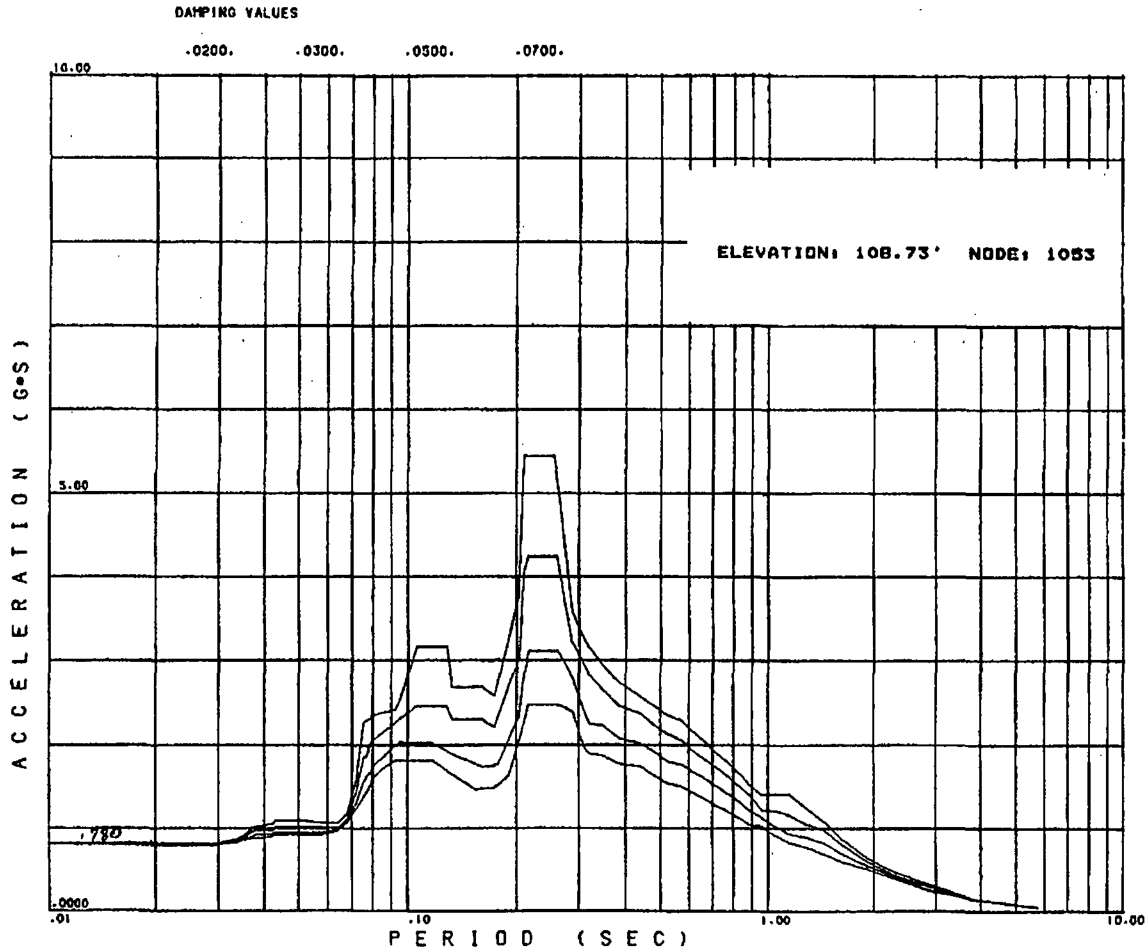

FSAR UPDATE

UNIT 2
DIABLO CANYON SITE

FIGURE 3.7 - 12R
PIPEWAY STRUCTURE
HOSGRI BLUME E-W
RESPONSE SPECTRA

Revision 11 November 1996

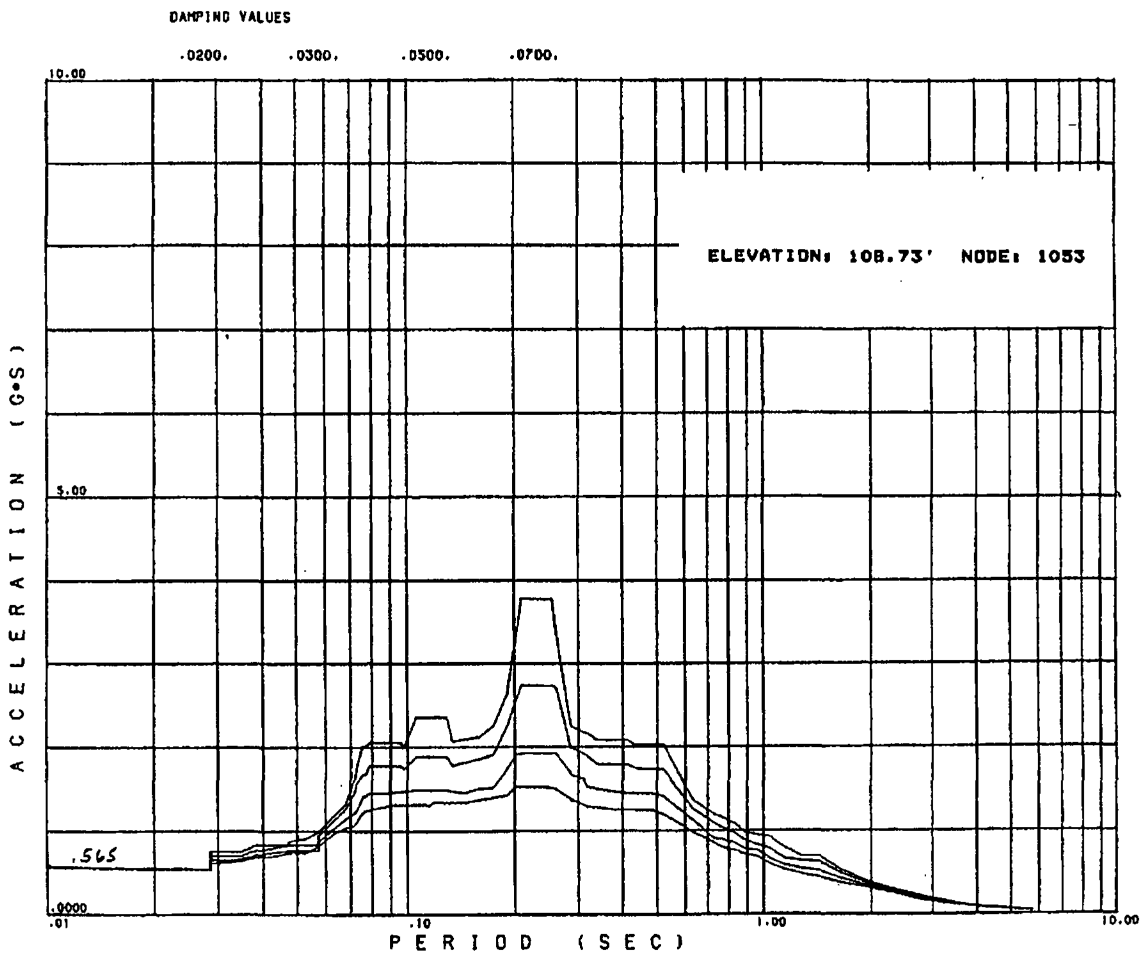

FSAR UPDATE

UNIT 2
DIABLO CANYON SITE

FIGURE 3.7 - 12 S
PIPEWAY STRUCTURE
HOSGRI BLUME VERTICAL
RESPONSE SPECTRA

Revision 11 November 1996

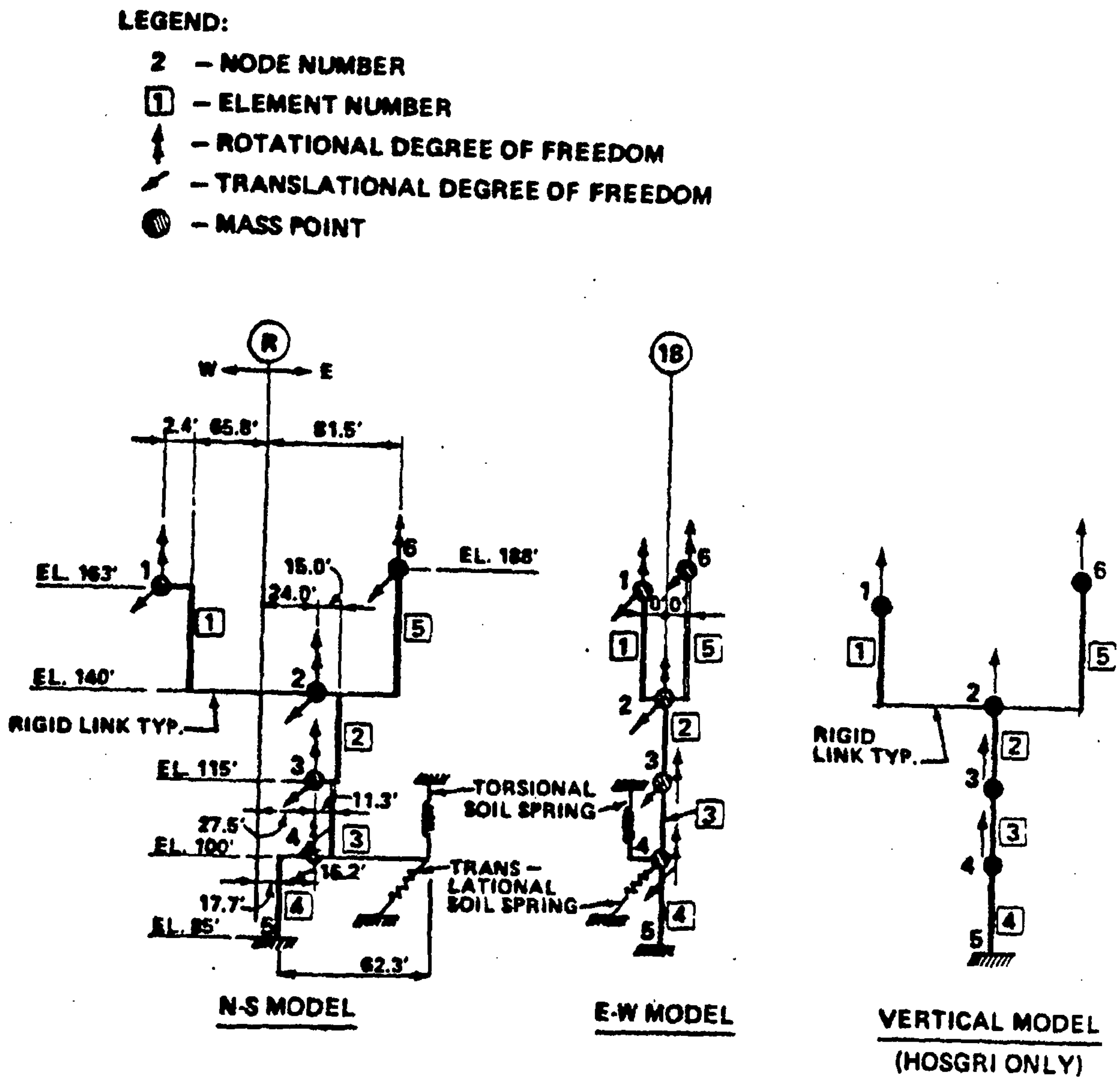

FSAR UPDATE

UNITS 1 AND 2
DIABLO CANYON SITE

FIGURE 3.7-13
AUXILIARY BUILDING
MATHEMATICAL MODEL

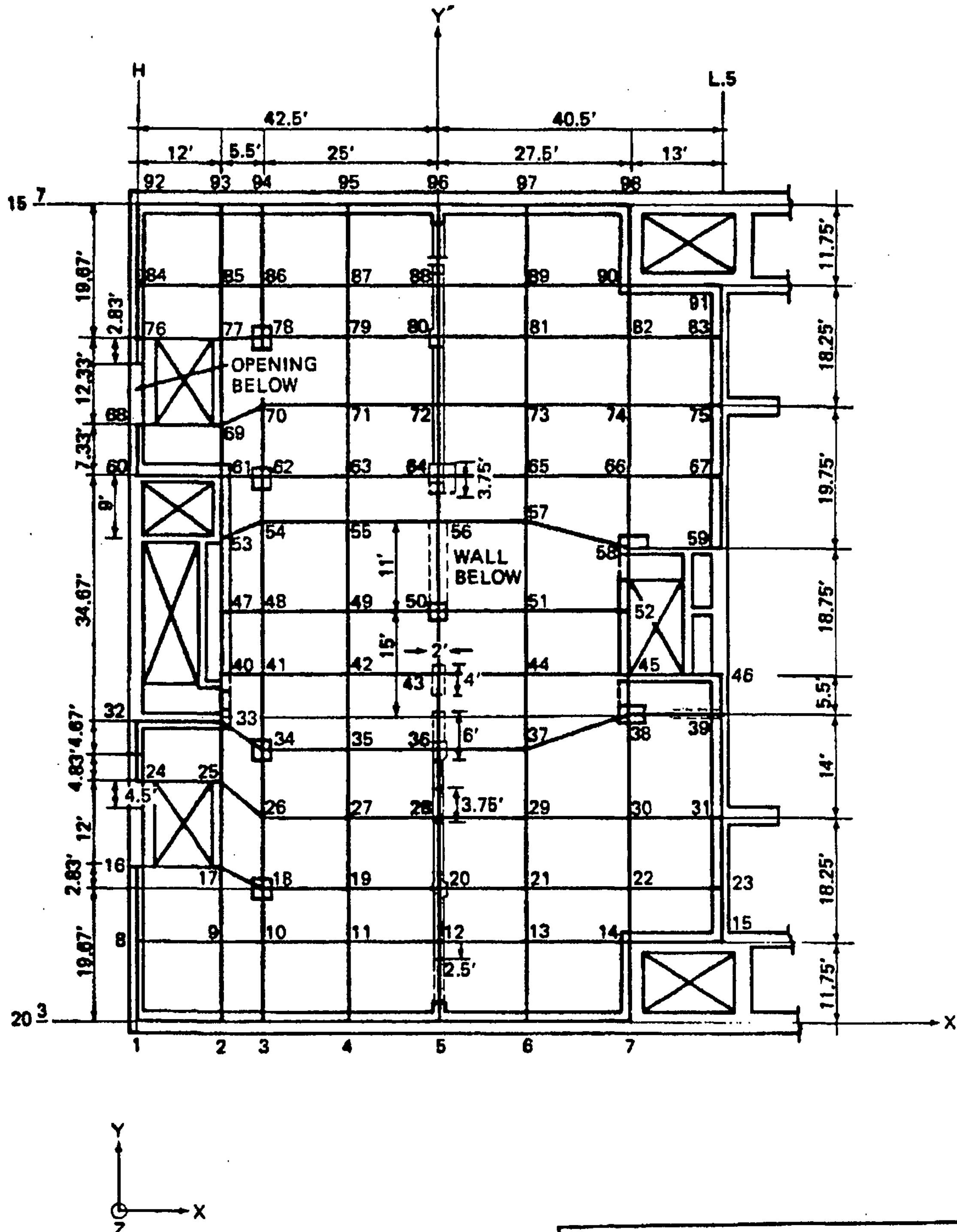

FSAR UPDATE

UNITS 1 AND 2
DIABLO CANYON SITE

FIGURE 3.7–13A

AUXILIARY BUILDING
FLEXIBLE SLAB MODEL

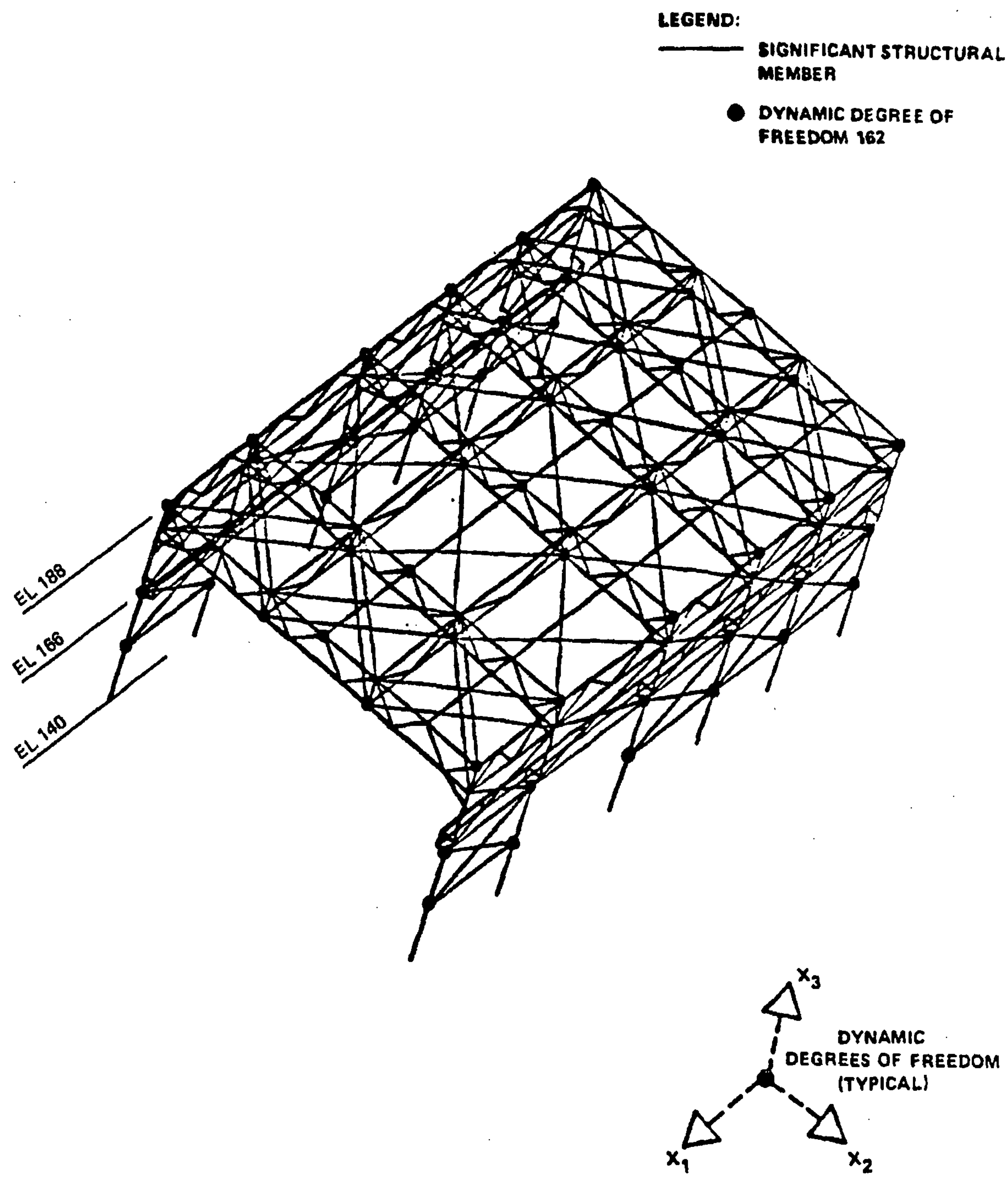

FSAR UPDATE

UNITS 1 AND 2
DIABLO CANYON SITE

FIGURE 3.7–13B

AUXILIARY BUILDING
FUEL HANDLING
CRANE SUPPORT STRUCTURE
MODEL NO. 2.2

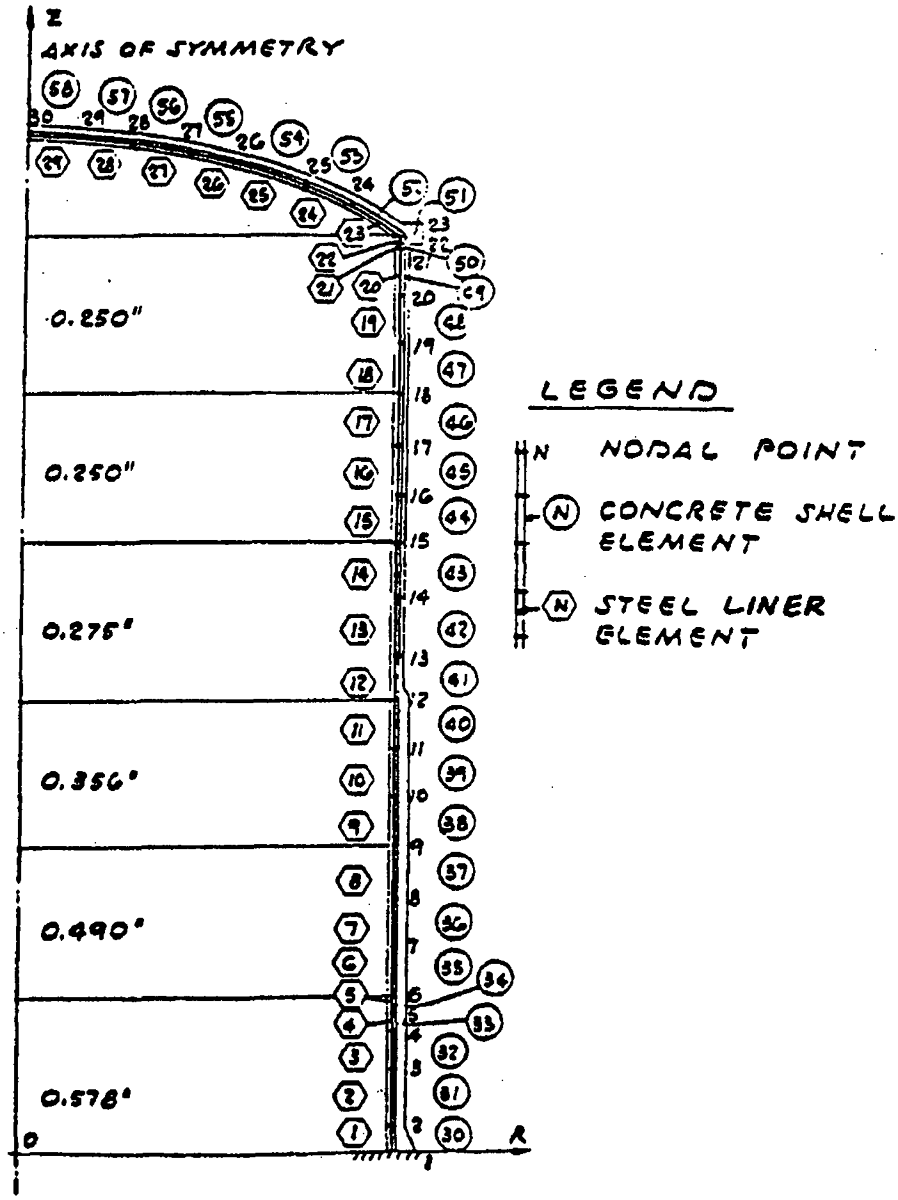

FSAR UPDATE
UNITS 1 AND 2 DIABLO CANYON SITE
FIGURE 3.7-14 OUTDOOR WATER STORAGE TANKS: REFUELING WATER TANK, AXISYMMETRIC MODEL

Revision 11 November 1996

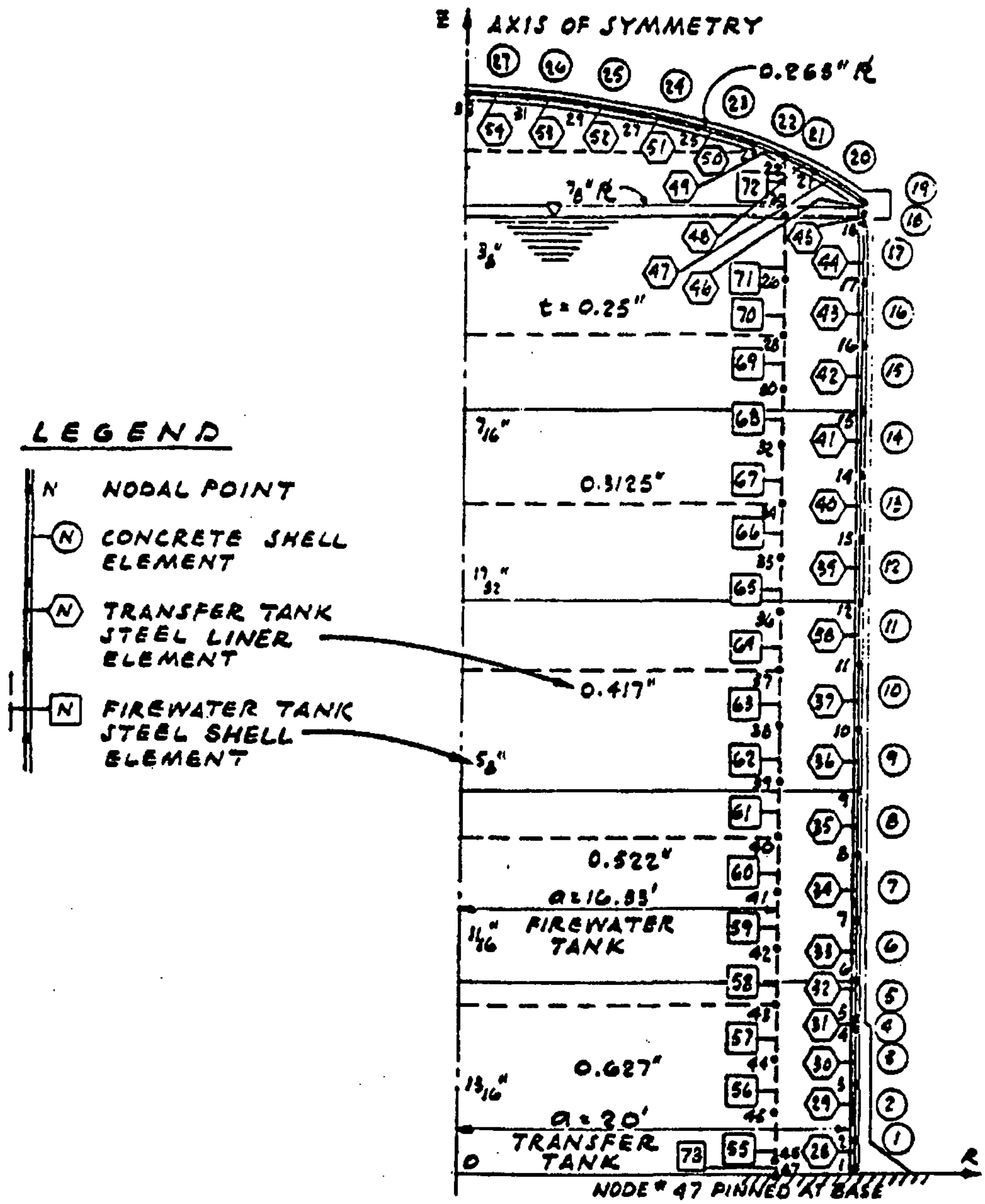

FSAR UPDATE

UNITS 1 AND 2
DIABLO CANYON SITE

FIGURE 3.7-15

OUTDOOR WATER STORAGE TANKS: FIREWATER AND TRANSFER TANK, AXISYMMETRIC MODEL

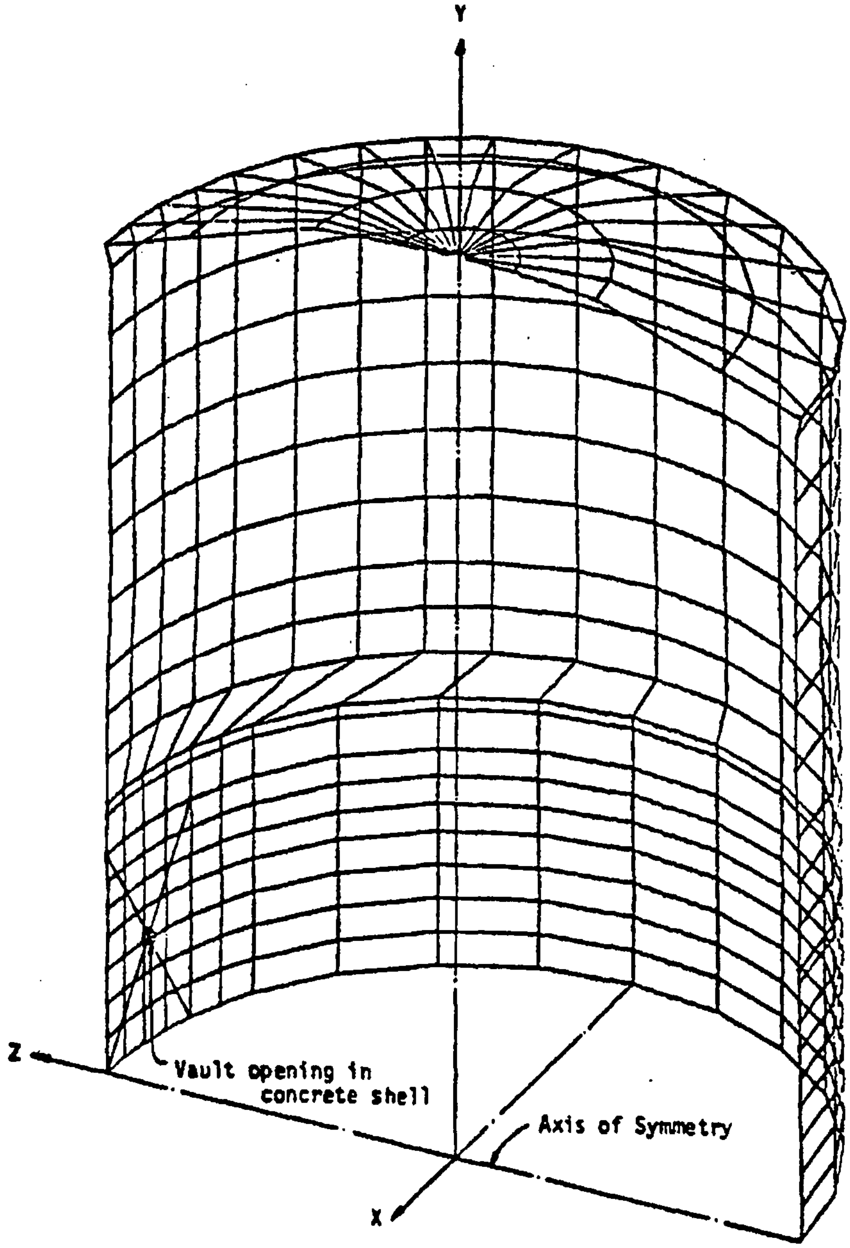

FSAR UPDATE

UNIT 1
DIABLO CANYON SITE

FIGURE 3.7 - 15 A
OUTDOOR WATER STORAGE TANKS:
REFUELING WATER TANK,
PERSPECTIVE VIEW OF
HALF-TANK MODEL

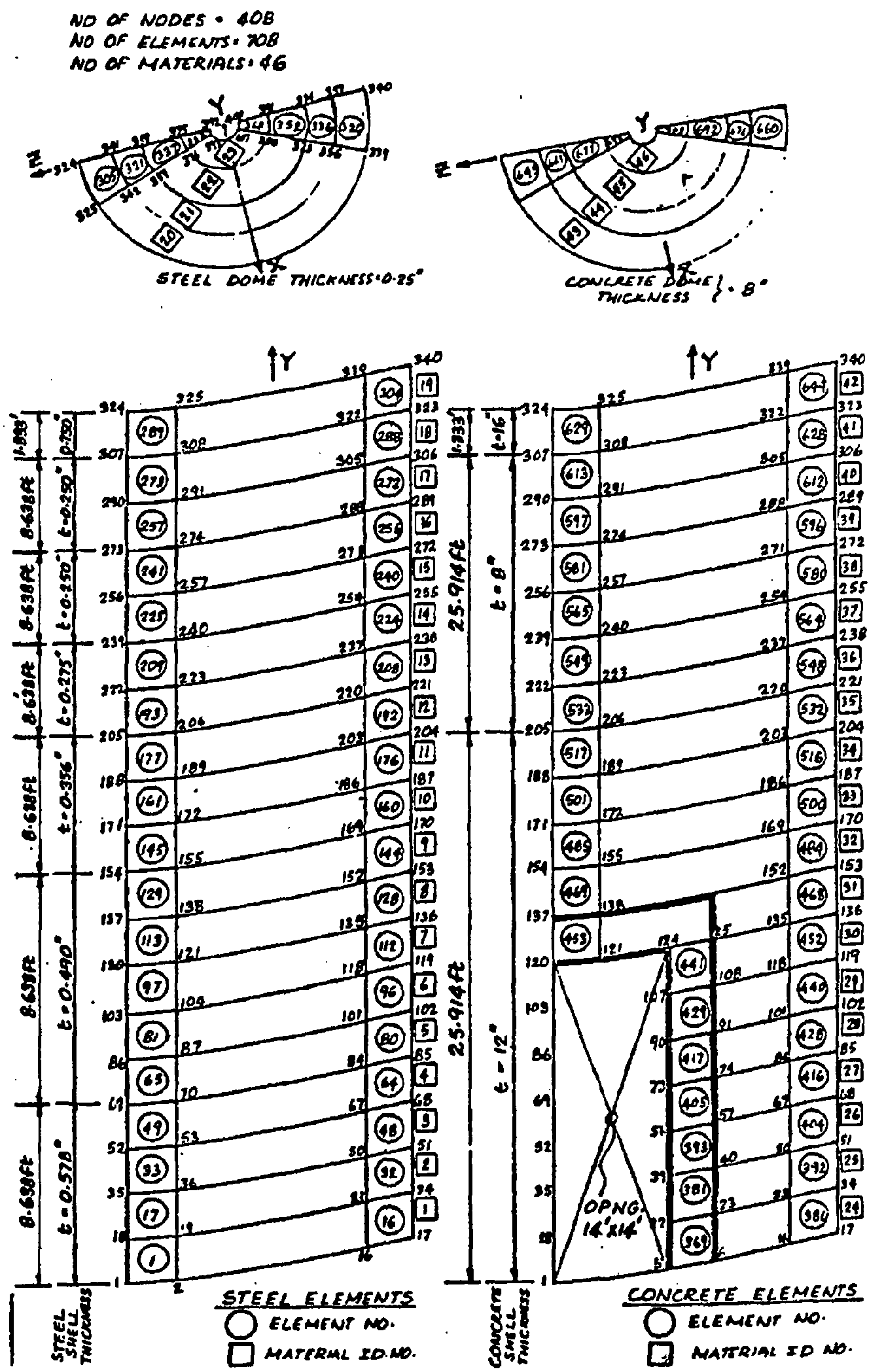

FSAR UPDATE

UNITS 1 AND 2 DIABLO CANYON SITE

FIGURE 3.7 - 15 B
HALF-TANK COMPUTER MODEL

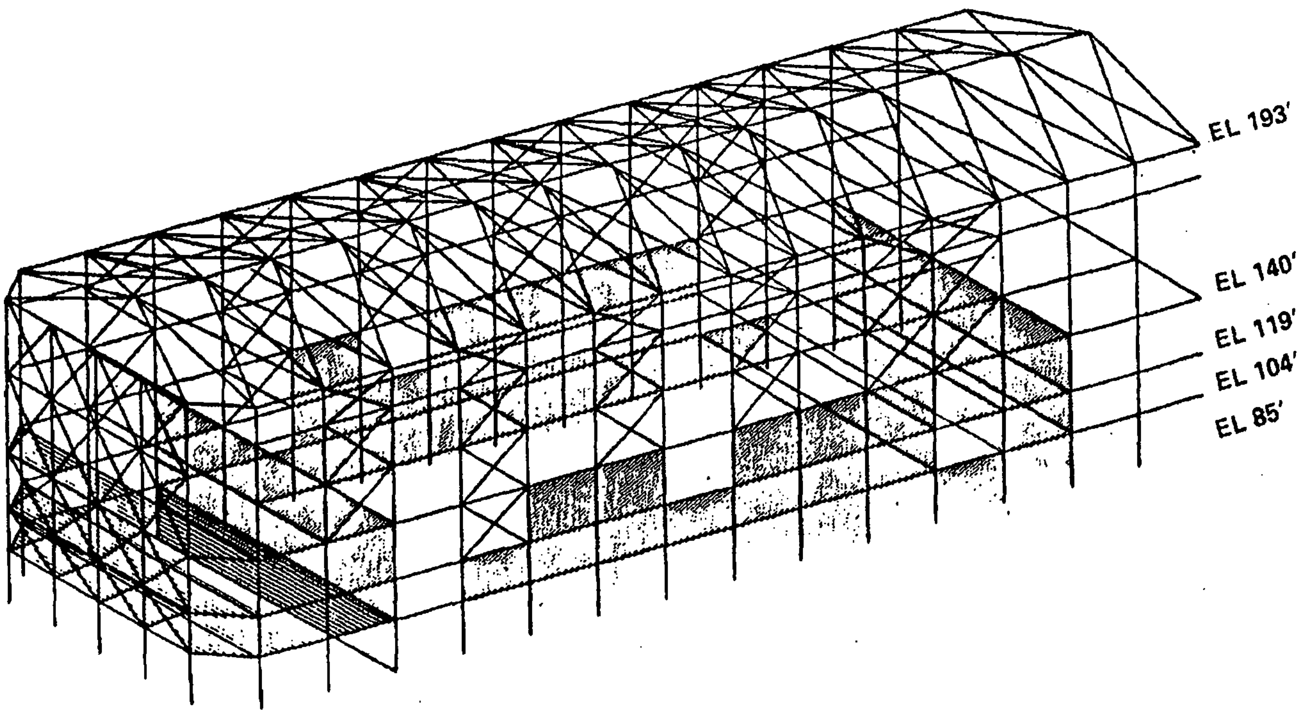

FSAR UPDATE

UNITS 1 AND 2
DIABLO CANYON SITE

FIGURE 3.7 - 15C
TURBINE BUILDING
UNIT 1 PORTION
HORIZONTAL MODEL
ISOMETRIC

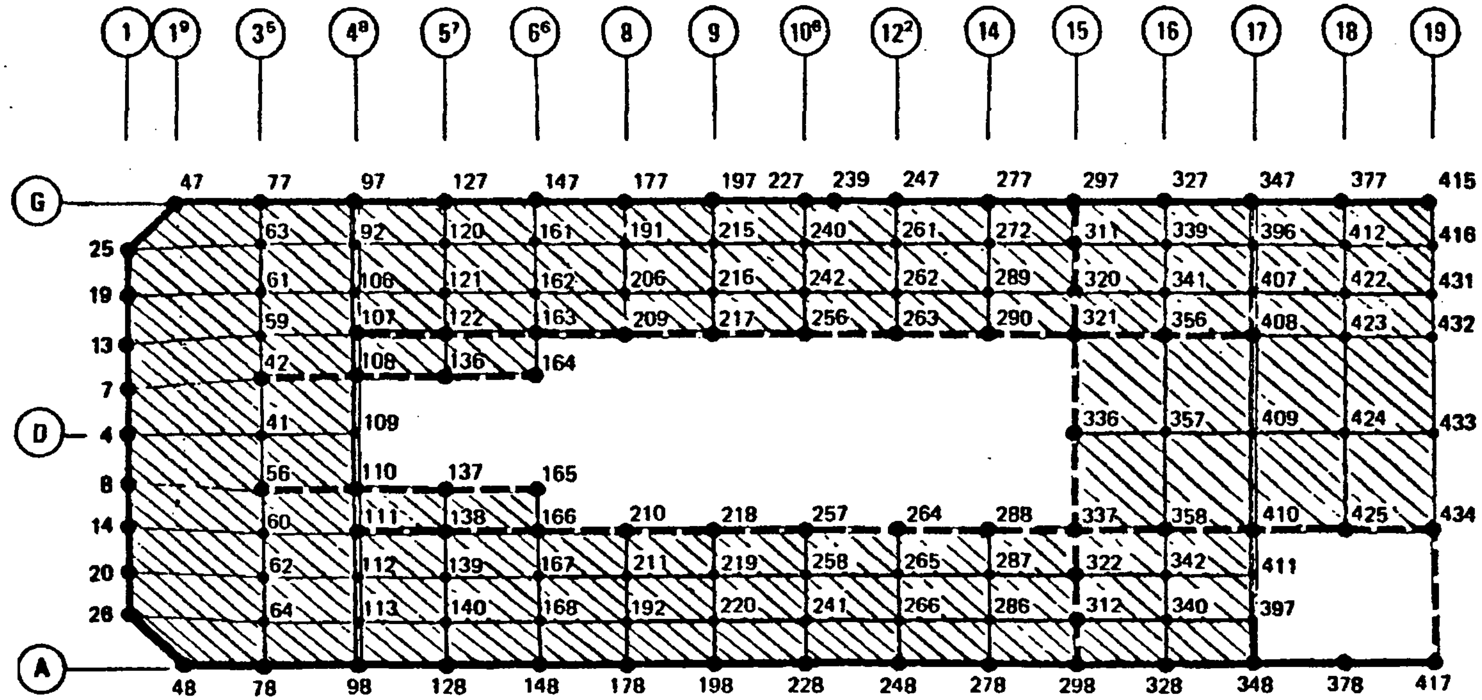

— — — — TRUSS ELEMENTS

——— BEAM ELEMENTS

PLANE STRESS ELEMENTS

FSAR UPDATE

UNITS 1 AND 2 DIABLO CANYON SITE

FIGURE 3.7 - 15 D
TURBINE BUILDING UNIT 1
PORTION HORIZONTAL
MODEL PLAN AT ELEV. 140′

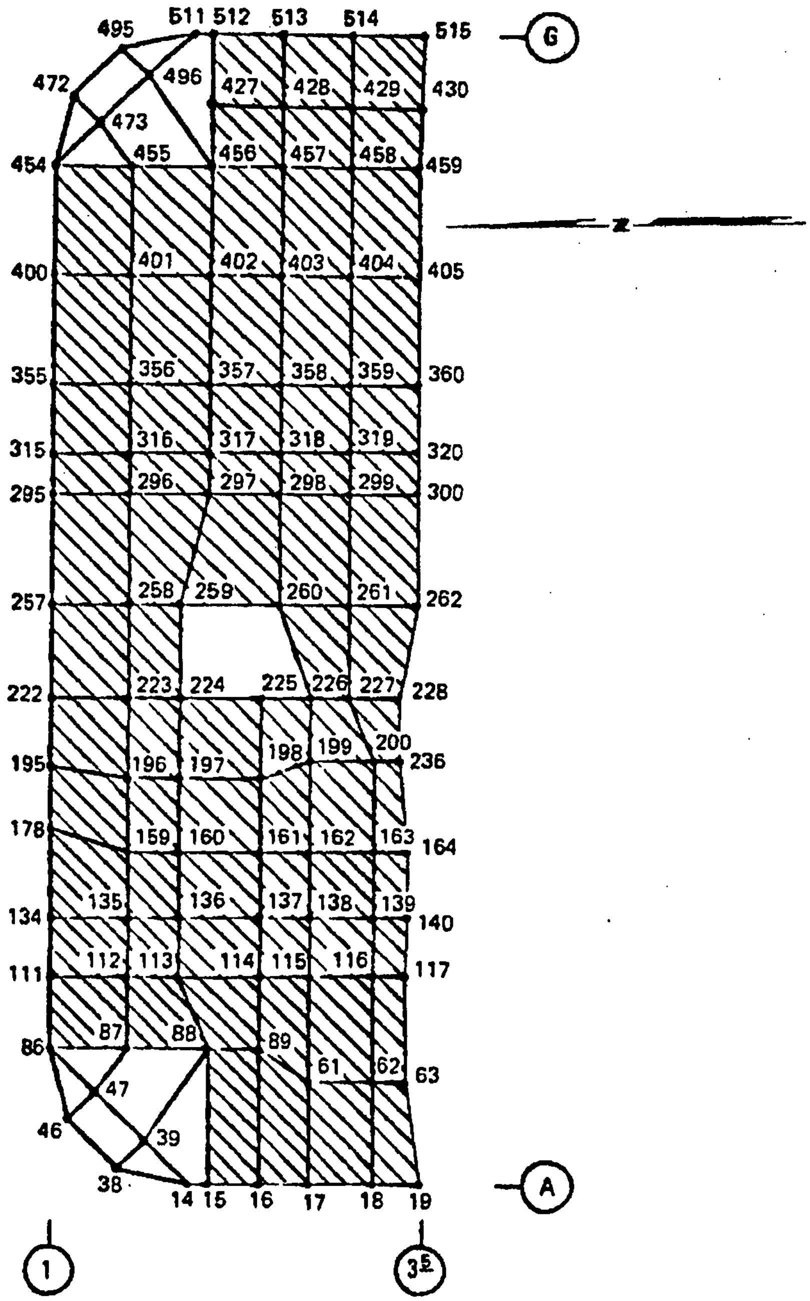

℄ ELEMENT

FSAR UPDATE

UNITS 1 AND 2
DIABLO CANYON SITE

FIGURE 3.7-15E
TURBINE BUILDING
VERTICAL MODEL NO. 1
PLAN AT ELEVATION 140′

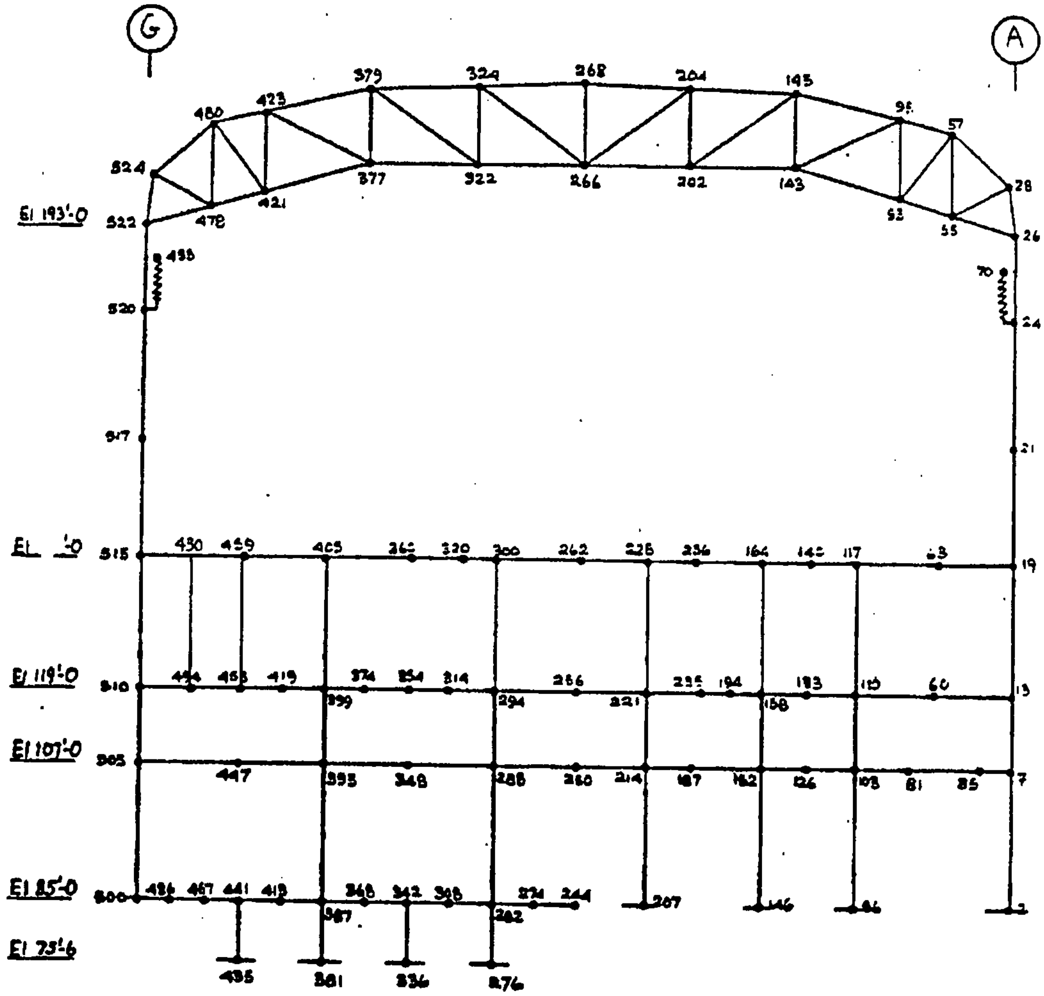

FSAR UPDATE

UNIT 1
DIABLO CANYON SITE

FIGURE 3.7 - 15 F
TURBINE BUILDING
VERTICAL MODEL NO.1
ELEVATION AT LINE 3.5

Revision 11 November 1996

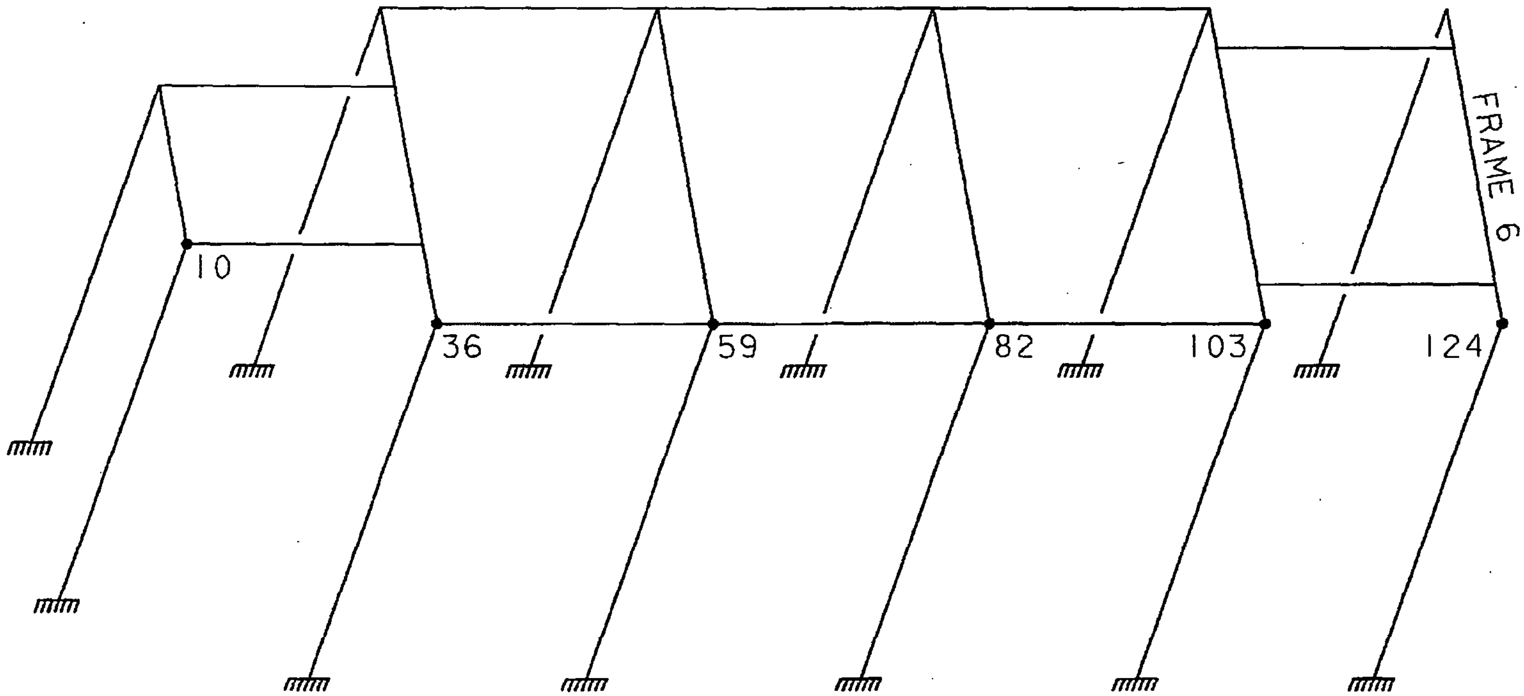

TOTAL NUMBER OF ELEMENTS = 208

FSAR UPDATE

UNIT 1
DIABLO CANYON SITE

FIGURE 3.7-15G
TURBINE PEDESTAL
SEISMIC ANALYSIS MODEL

Revision 17 November 2006

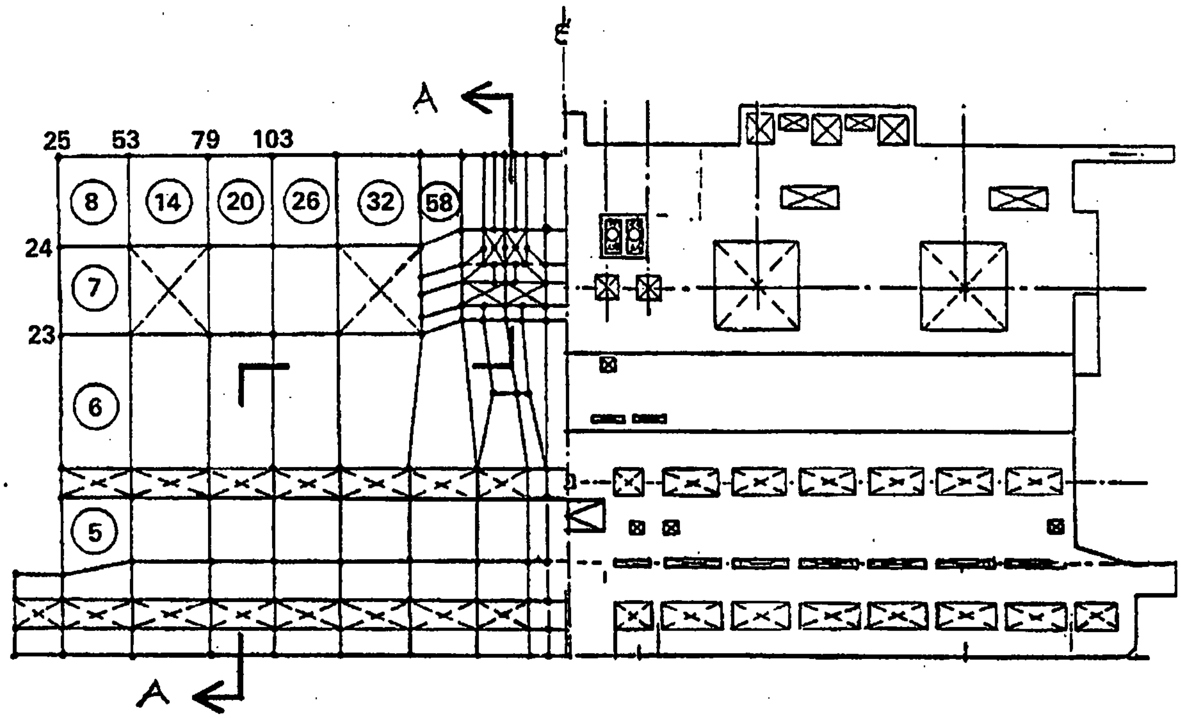

FSAR UPDATE

UNITS 1 AND 2
DIABLO CANYON SITE

FIGURE 3.7 - 15 H
INTAKE STRUCTURE
TOP DECK MATHEMATICAL MODEL,
ELEVATION + 17.5 FT.

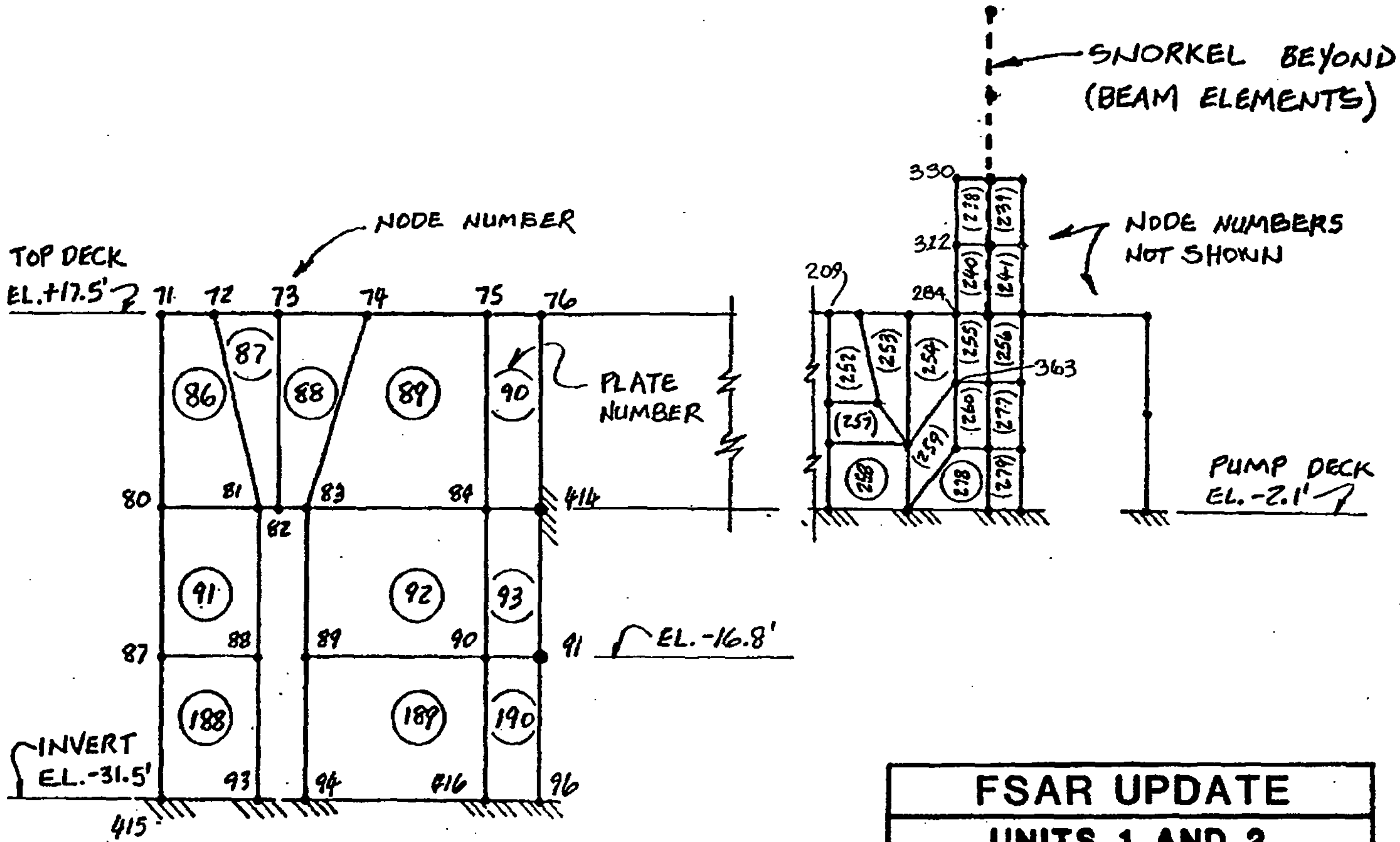

SEE FIG. 3.7-15 H FOR
LOCATION OF
SECTION A–A

FSAR UPDATE

UNITS 1 AND 2
DIABLO CANYON SITE

FIGURE 3.7-15I
INTAKE STRUCTURE
TRANSVERSE SECTION A-A
MATHEMATICAL MODEL

Revision 11 November 1996

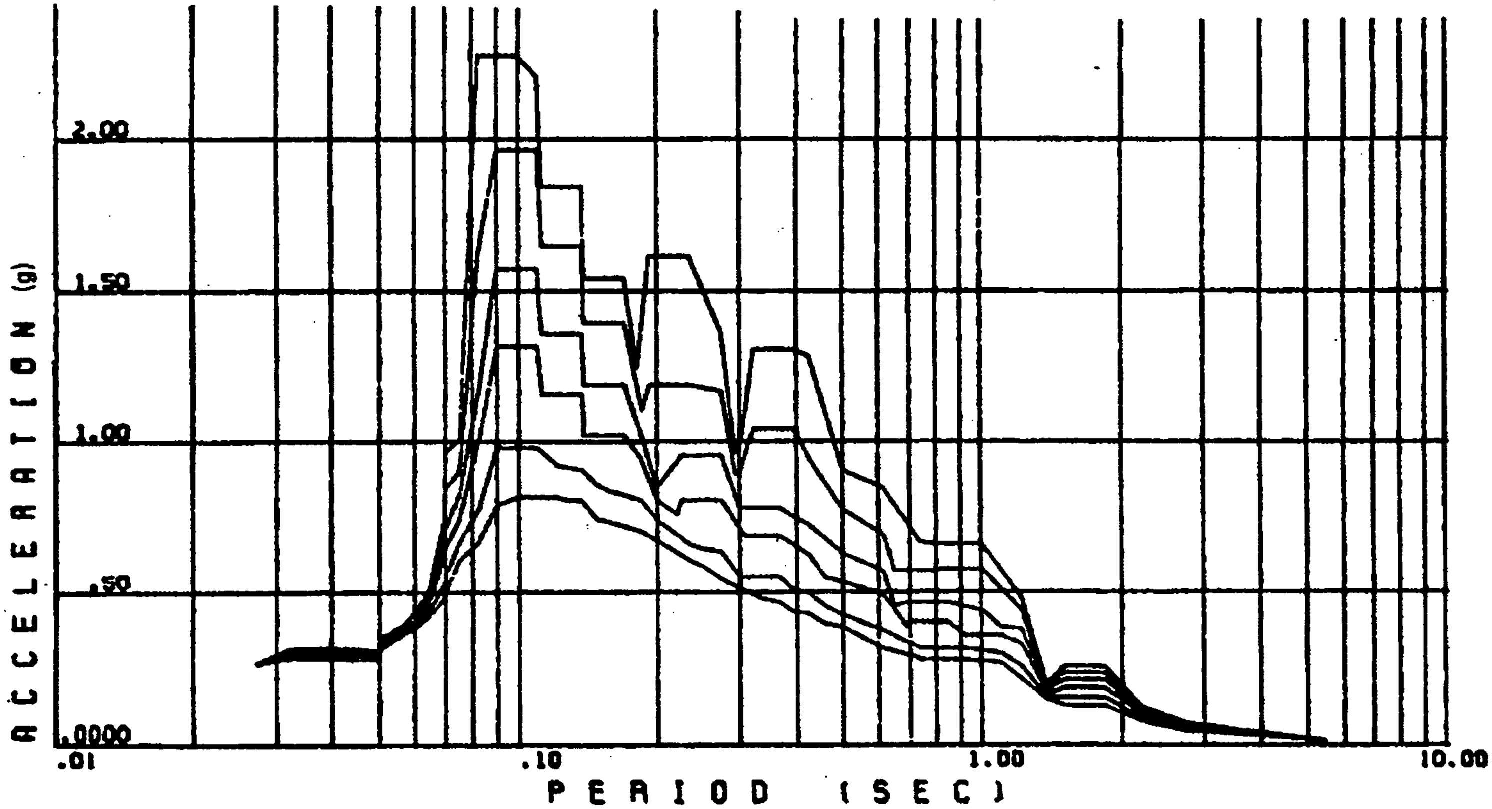

FSAR UPDATE

UNITS 1 AND 2
DIABLO CANYON SITE

FIGURE 3.7-16
AUXILIARY BUILDING
FLOOR ELEV. 100'–0" N–S
HORIZONTAL SPECTRA
DESIGN EARTHQUAKE
½, 1, 2, 3, 5, 7% DAMPING

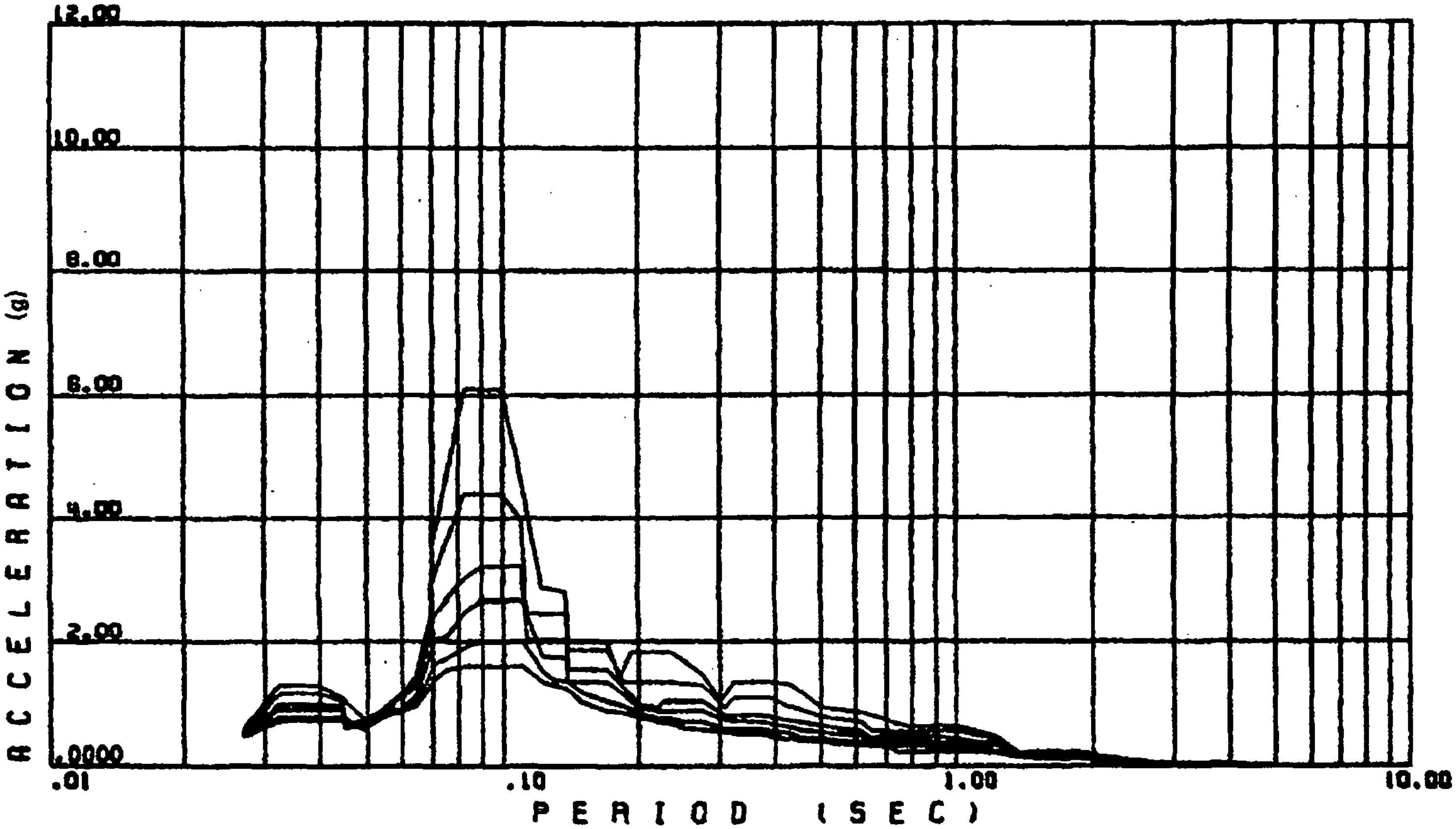

FSAR UPDATE

UNITS 1 AND 2
DIABLO CANYON SITE

FIGURE 3.7-17
AUXILIARY BUILDING
FLOOR ELEV. 163'–0" N–S
HORIZONTAL SPECTRA
DESIGN EARTHQUAKE
½, 1, 2, 3, 5, 7% DAMPING

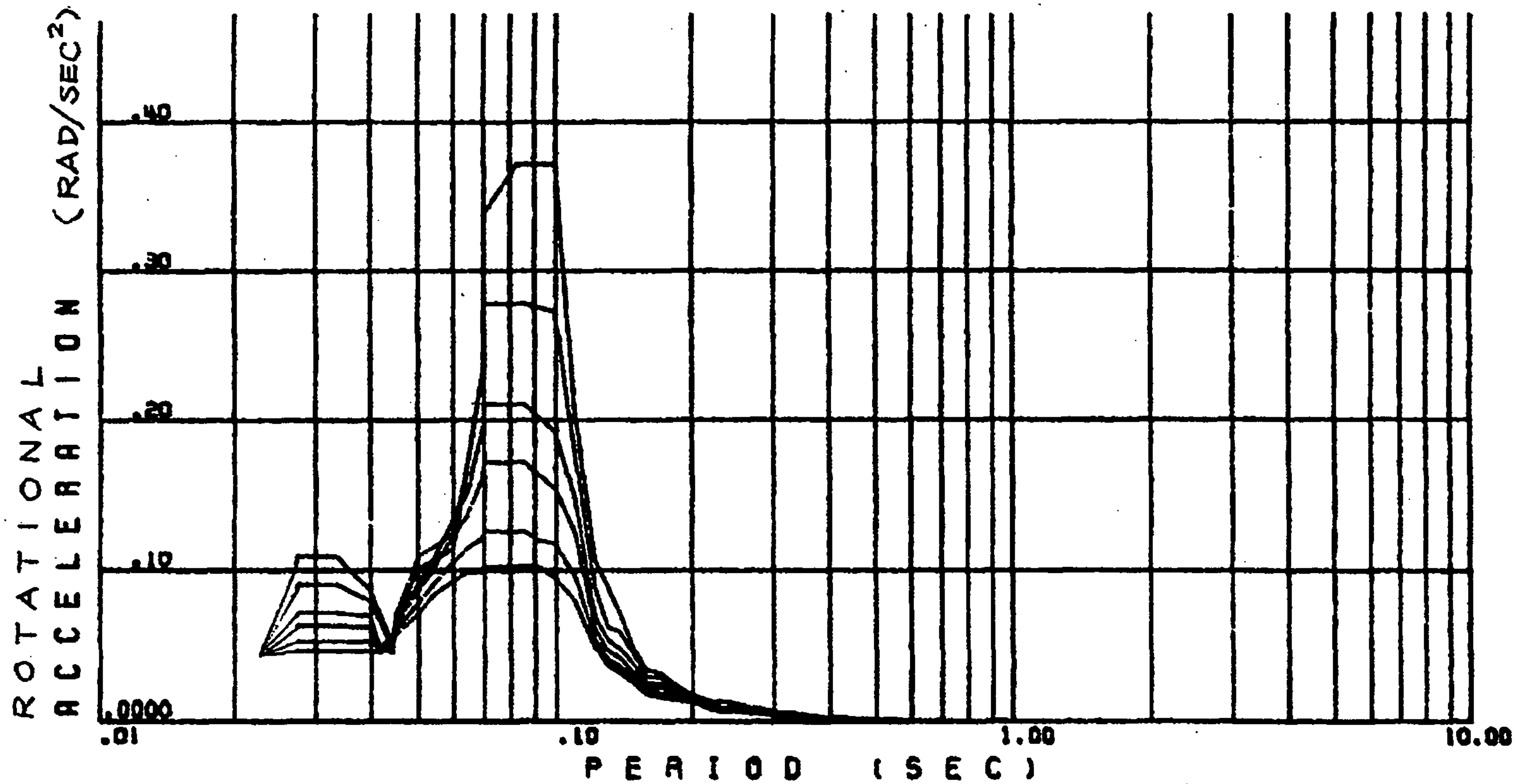

FSAR UPDATE

UNITS 1 AND 2 DIABLO CANYON SITE

FIGURE 3.7-18
AUXILIARY BUILDING
FLOOR ELEV. 163'–0"
N–S TORSIONAL SPECTRA
DESIGN EARTHQUAKE
½, 1, 2, 3, 5, 7% DAMPING

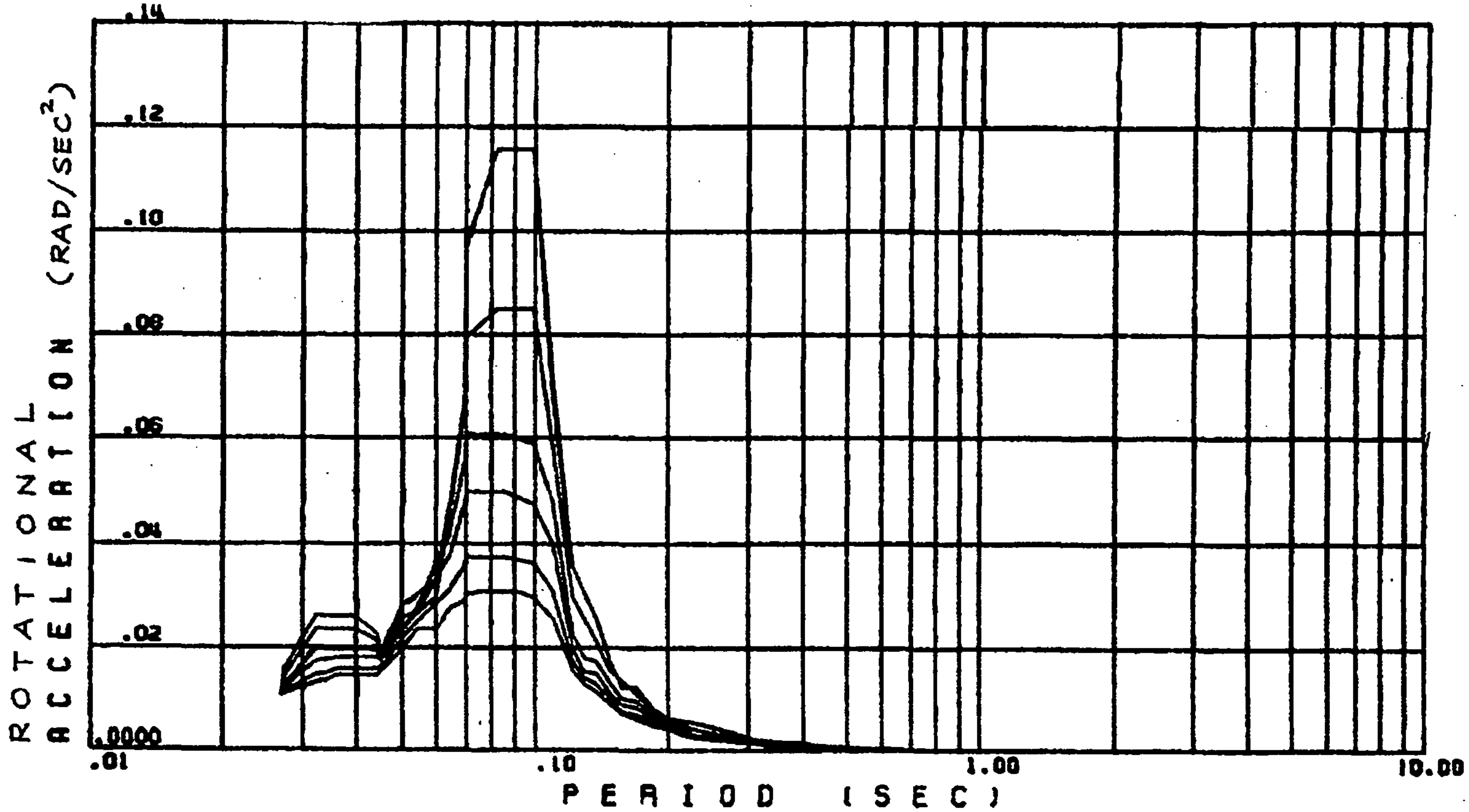

FSAR UPDATE

UNITS 1 AND 2
DIABLO CANYON SITE

FIGURE 3.7-19
AUXILIARY BUILDING
FLOOR ELEV. 100'–0"
N–S TORSIONAL SPECTRA
DESIGN EARTHQUAKE
½, 1, 2, 3, 5, 7% DAMPING

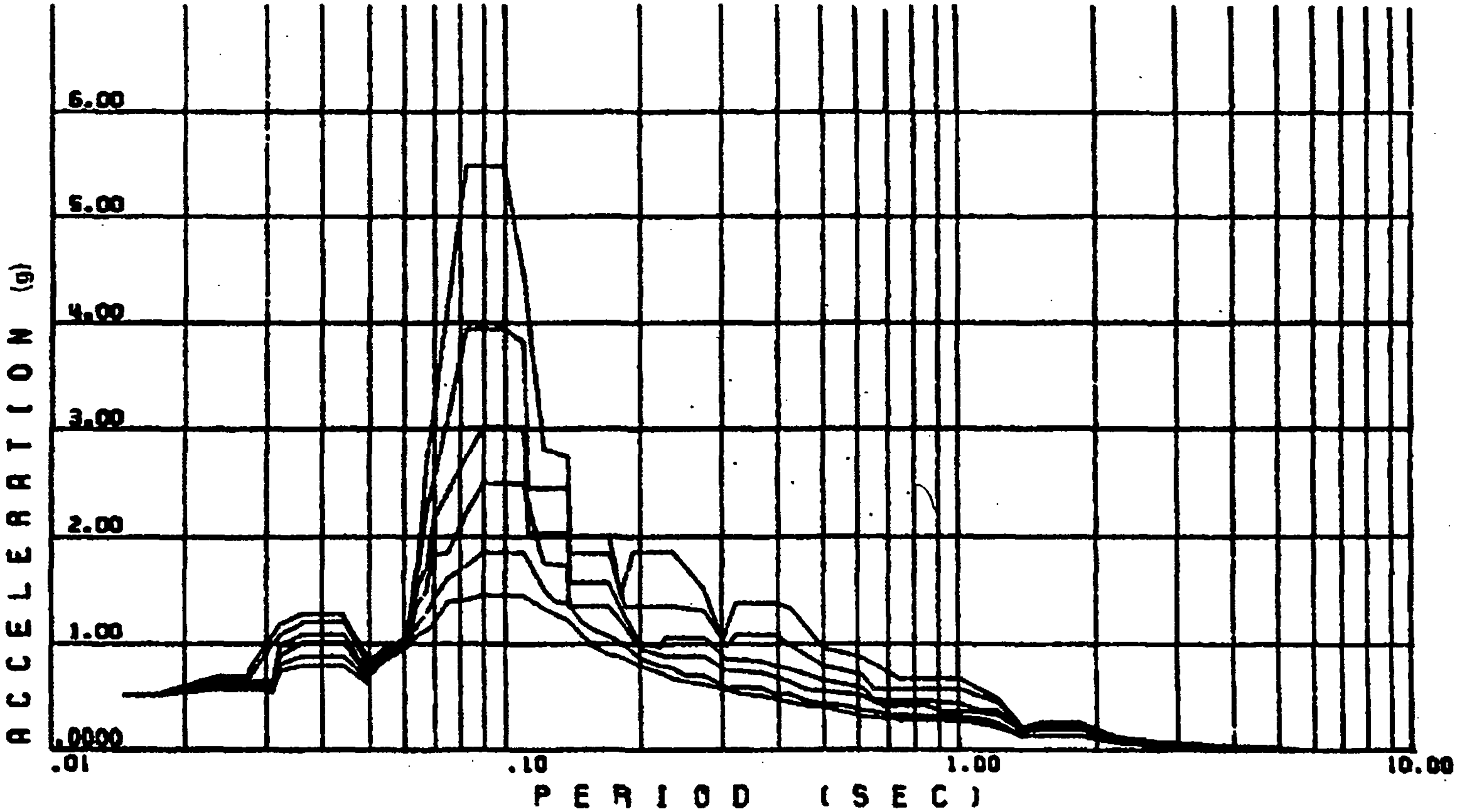

FSAR UPDATE

UNITS 1 AND 2
DIABLO CANYON SITE

FIGURE 3.7-20
AUXILIARY BUILDING
FLOOR ELEV. 163'–0" E–W
HORIZONTAL SPECTRA
DESIGN EARTHQUAKE
½, 1, 2, 3, 5, 7% DAMPING

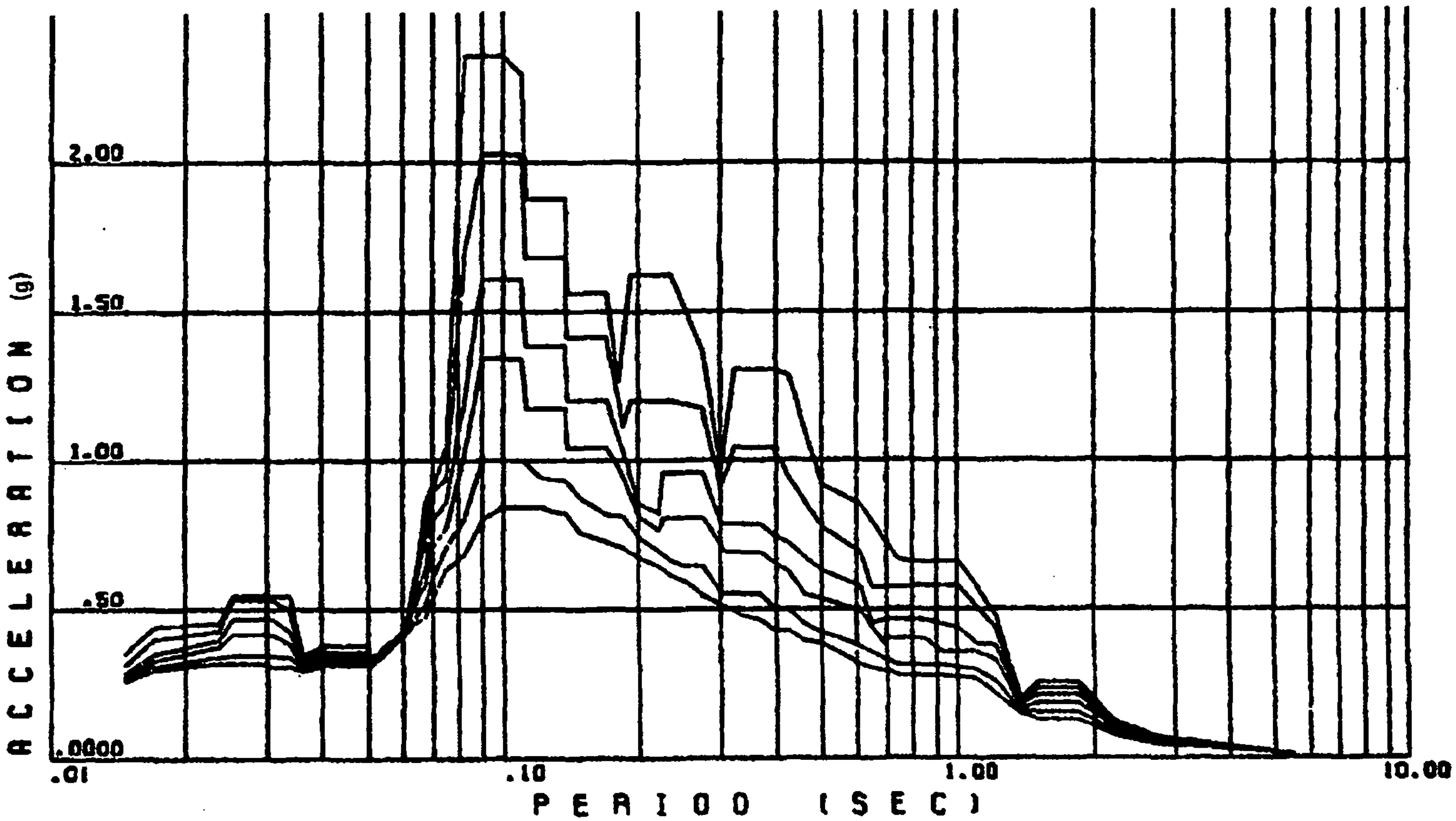

FSAR UPDATE

UNITS 1 AND 2
DIABLO CANYON SITE

FIGURE 3.7-21
AUXILIARY BUILDING
FLOOR ELEV. 100'–0"
E–W HORIZONTAL SPECTRA
DESIGN EARTHQUAKE
½, 1, 2, 3, 5, 7% DAMPING

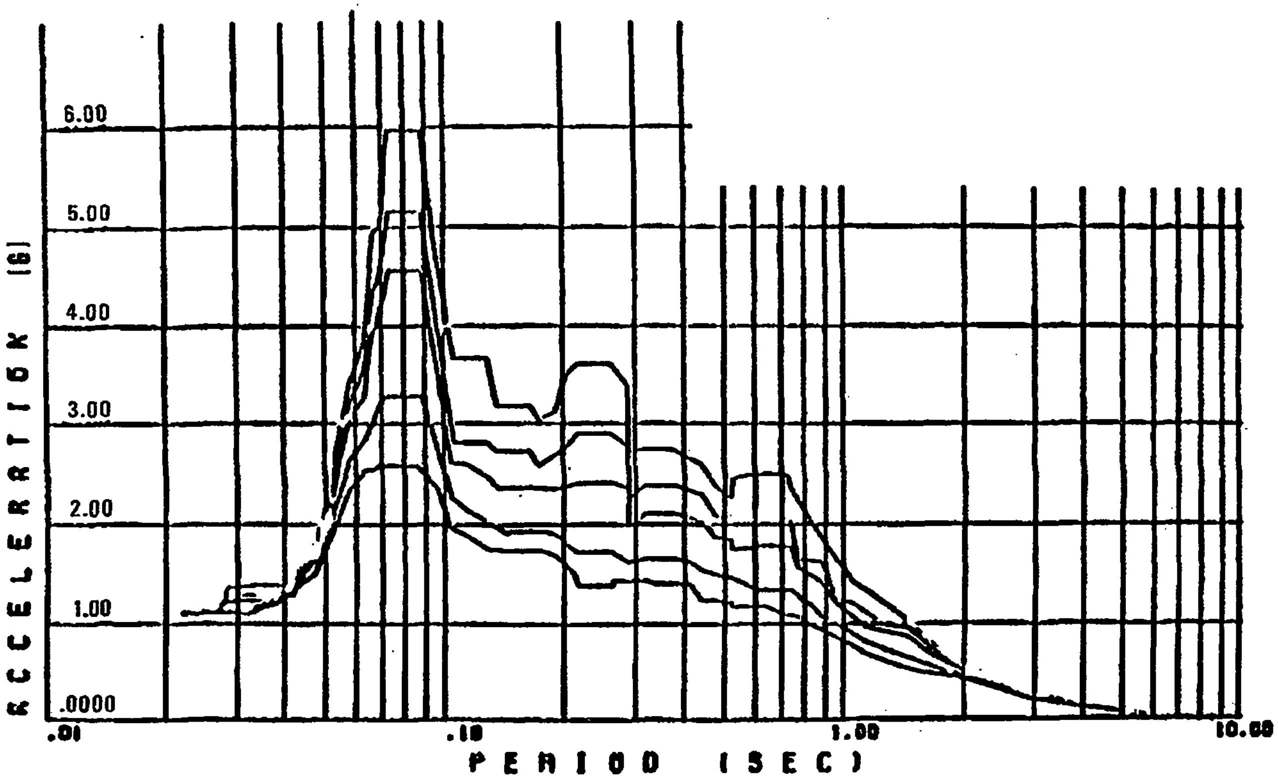

FSAR UPDATE

**UNITS 1 AND 2
DIABLO CANYON SITE**

FIGURE 3.7–21A

**AUXILIARY BUILDING
E–W HOSGRI
HORIZONTAL FLOOR SPECTRA
AT EL 140′–0″
2,3,4,7, AND 10% DAMPING**

Revision 11 November 1996

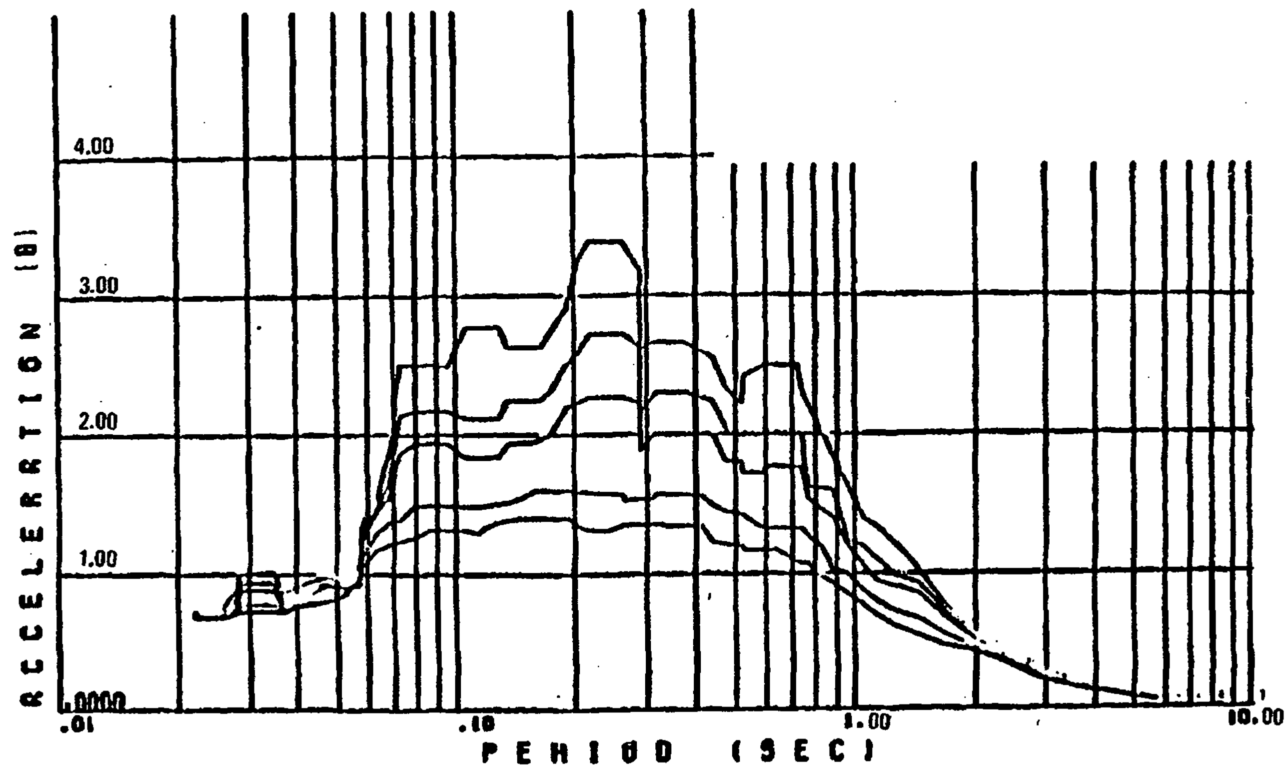

FSAR UPDATE

UNITS 1 AND 2
DIABLO CANYON SITE

FIGURE 3.7–21B

AUXILIARY BUILDING
E–W HOSGRI
HORIZONTAL FLOOR SPECTRA
AT EL 100'–0"
2,3,4,7, AND 10% DAMPING

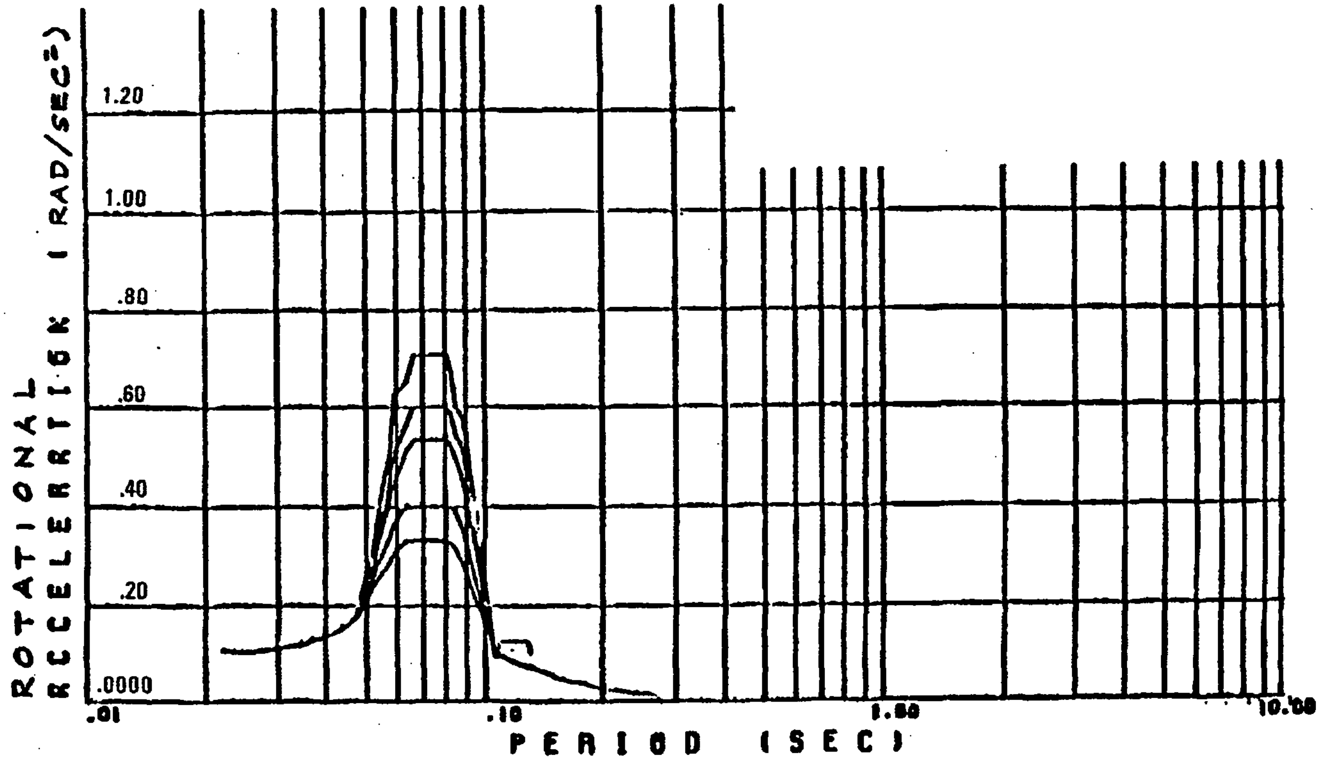

FSAR UPDATE

UNITS 1 AND 2
DIABLO CANYON SITE

FIGURE 3.7–21C
AUXILIARY BUILDING
E–W HOSGRI
TORSIONAL FLOOR SPECTRA
AT EL 140'–0"
2,3,4,7 and 10% DAMPING

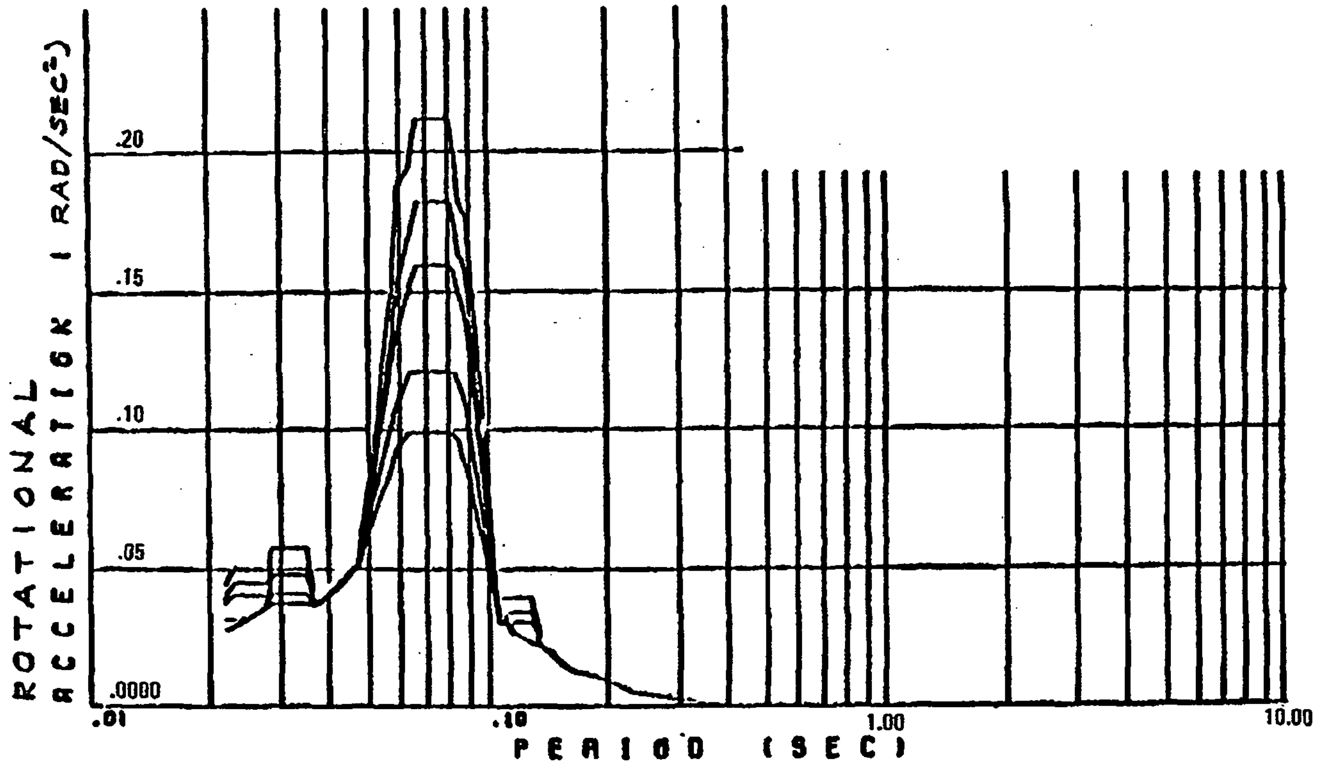

FSAR UPDATE

UNITS 1 AND 2
DIABLO CANYON SITE

FIGURE 3.7–21D

AUXILIARY BUILDING
E–W HOSGRI
TORSIONAL FLOOR SPECTRA
AT EL 100′–0″
2,3,4,7, AND 10% DAMPING

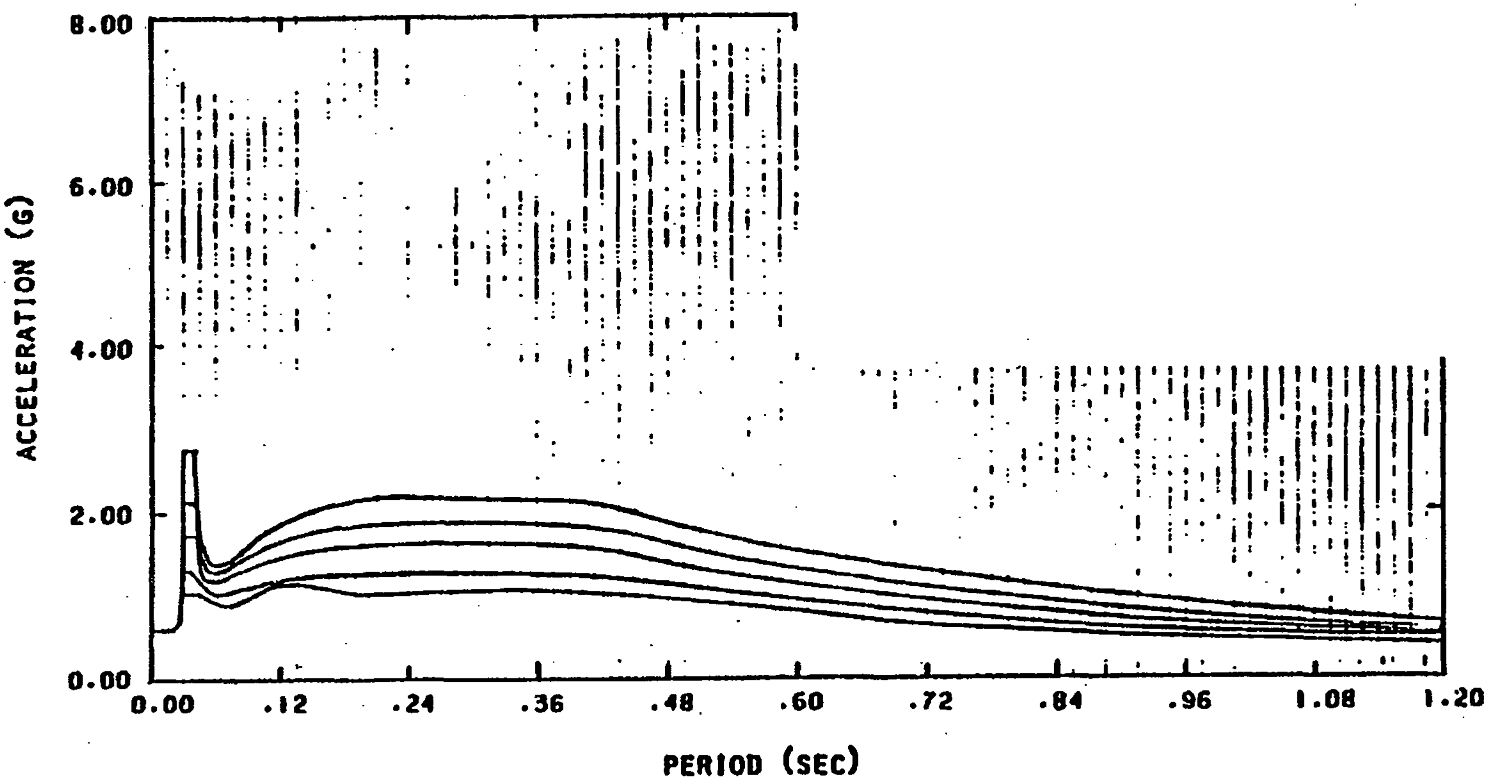

FSAR UPDATE

UNITS 1 AND 2
DIABLO CANYON SITE

FIGURE 3.7–21E

AUXILIARY BUILDING
HOSGRI VERTICAL SPECTRA
AT EL 140′–0″
2,3,4,7, AND 10% DAMPING

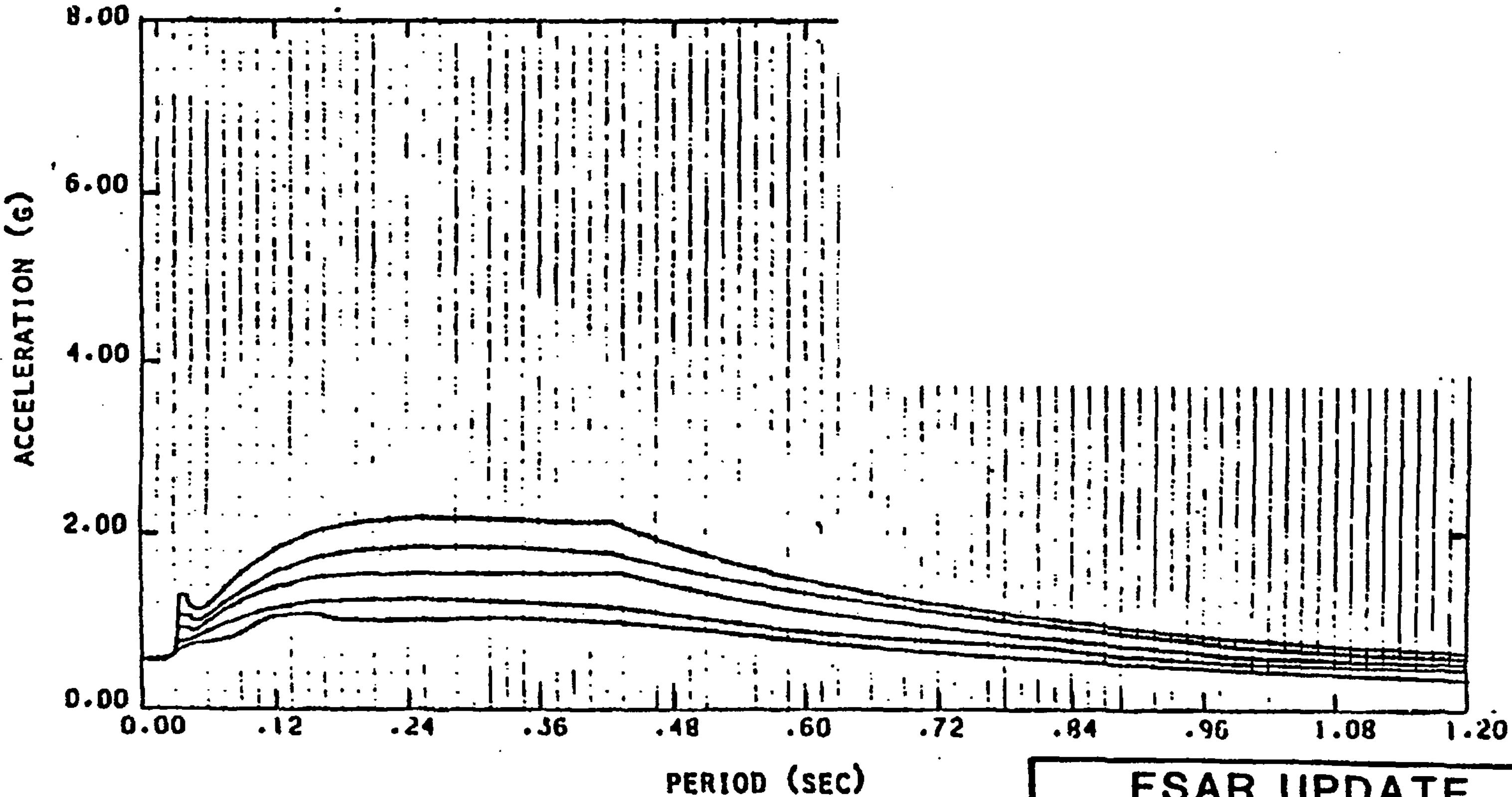

FSAR UPDATE

UNITS 1 AND 2
DIABLO CANYON SITE

FIGURE 3.7–21F

AUXILIARY BUILDING
HOSGRI VERTICAL SPECTRA
AT EL 100'–0"
2,3,4,7, AND 10% DAMPING

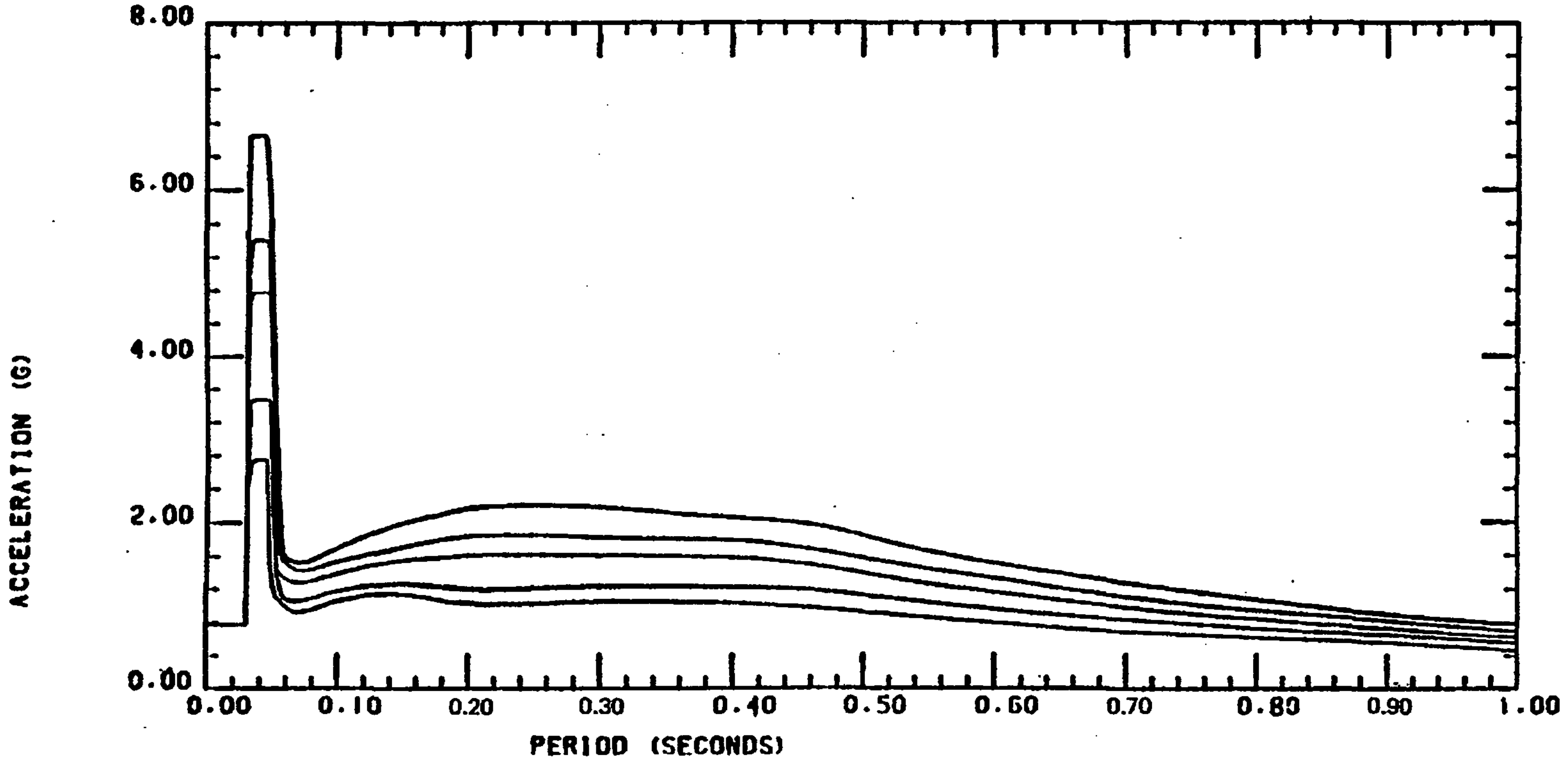

FSAR UPDATE

UNITS 1 AND 2
DIABLO CANYON SITE

FIGURE 3.7–21G

AUXILIARY BUILDING
HOSGRI VERTICAL SPECTRA
EL 100'–0" SLAB 2 NODE 51
2,3,4,7, AND 10%

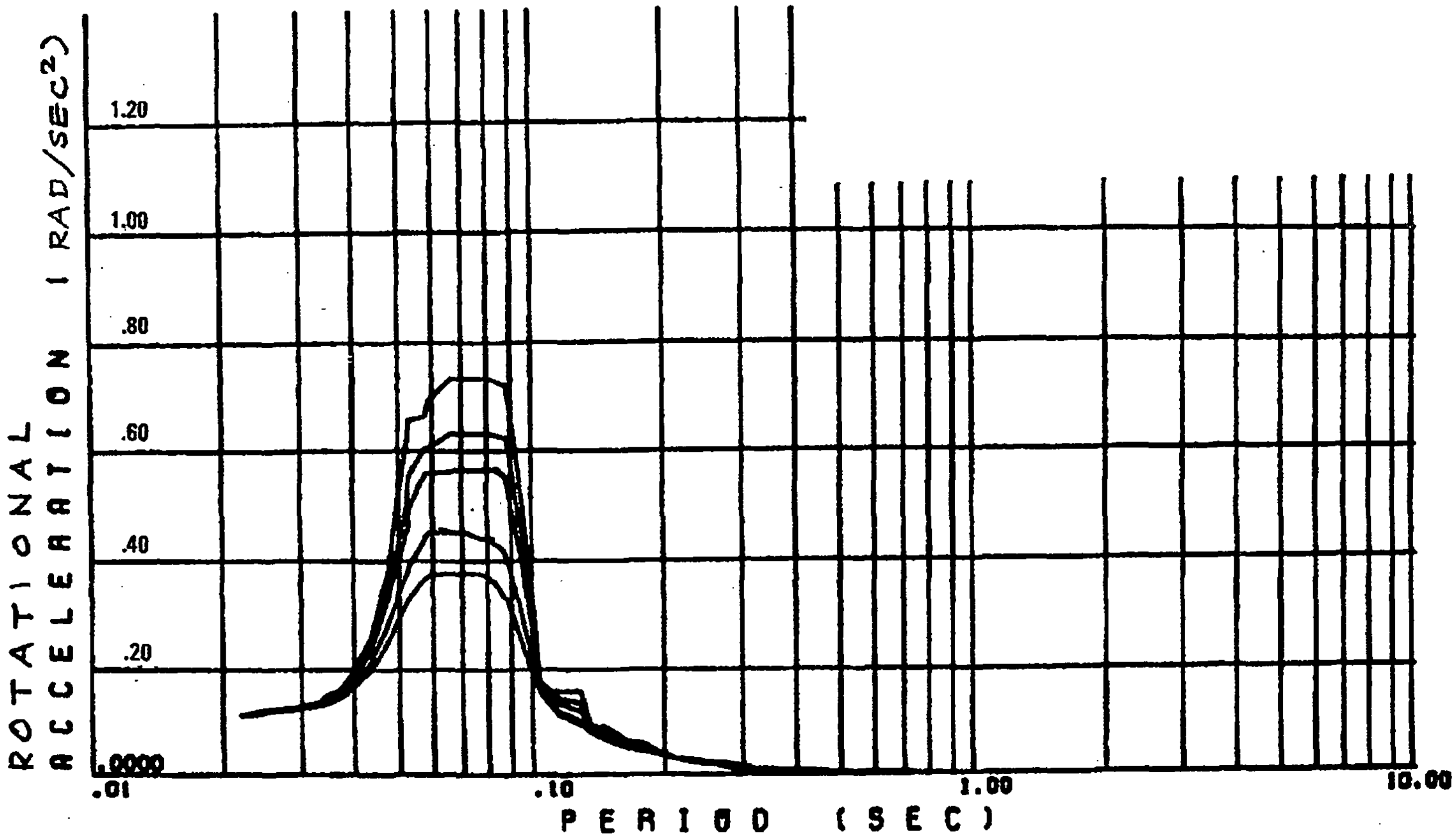

FSAR UPDATE

UNITS 1 AND 2
DIABLO CANYON SITE

FIGURE 3.7–21H

AUXILIARY BUILDING
N–S HOSGRI
TORSIONAL FLOOR SPECTRA
AT EL 140'–0"
2,3,4,7, AND 10% DAMPING

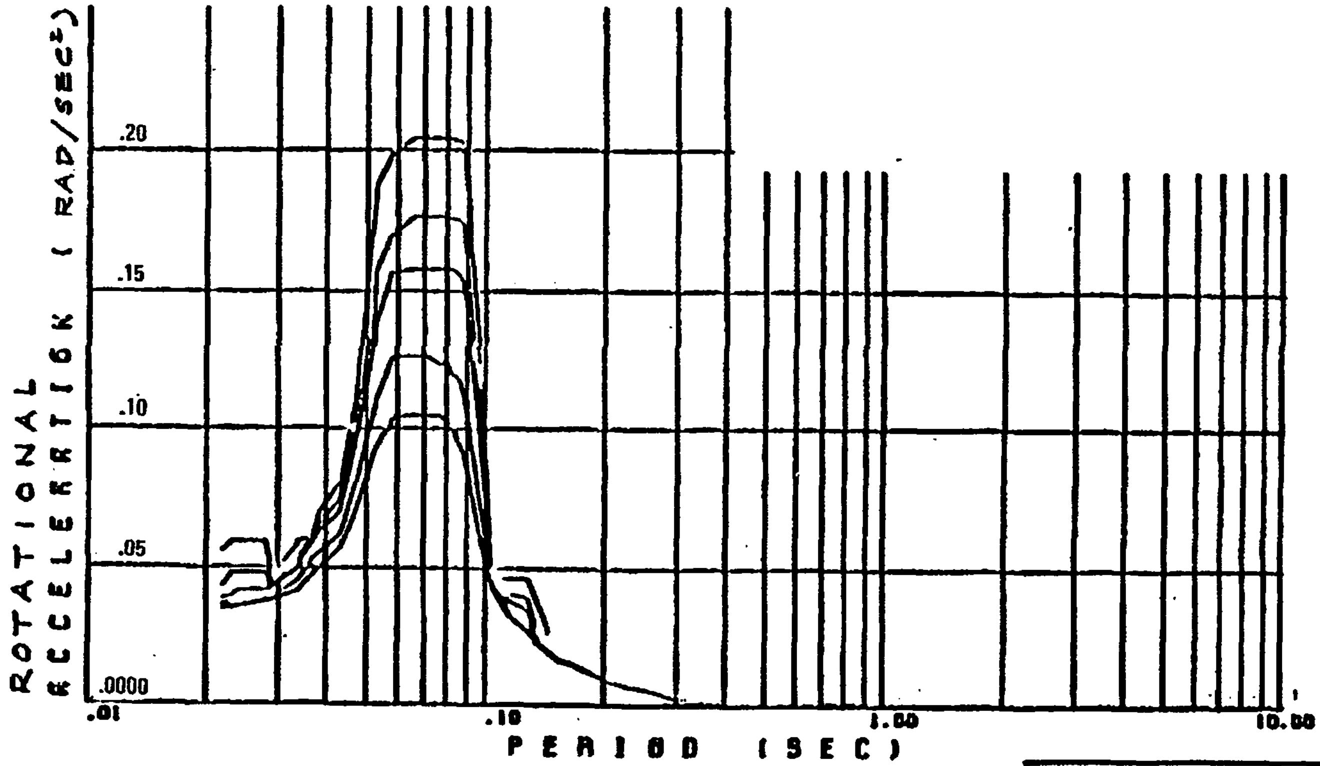

FSAR UPDATE

UNITS 1 AND 2
DIABLO CANYON SITE

FIGURE 3.7–21I

AUXILIARY BUILDING
N–S HOSGRI
TORSIONAL FLOOR SPECTRA
AT EL 100'–0"
2,3,4,7,AND 10% DAMPING

Revision 11 November 1996

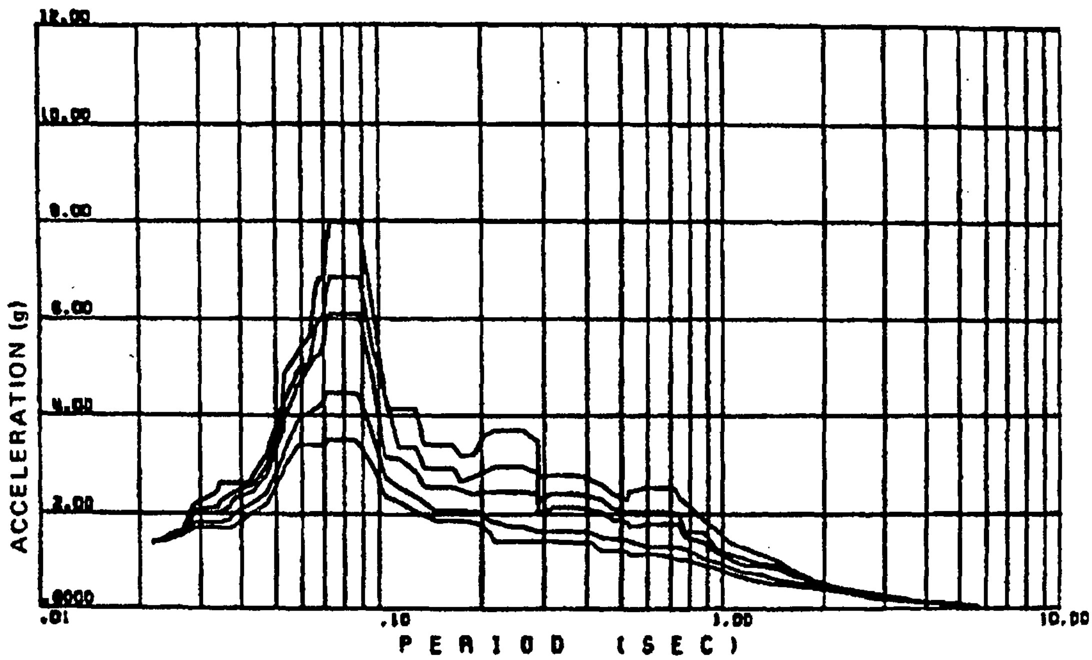

FSAR UPDATE

UNITS 1 AND 2
DIABLO CANYON SITE

FIGURE 3.7-22
AUXILIARY BUILDING
N–S HOSGRI
HORIZONTAL FLOOR SPECTRA
AT EL 163'-0"
NODE 1
2, 3, 4, 7, AND 10% DAMPING

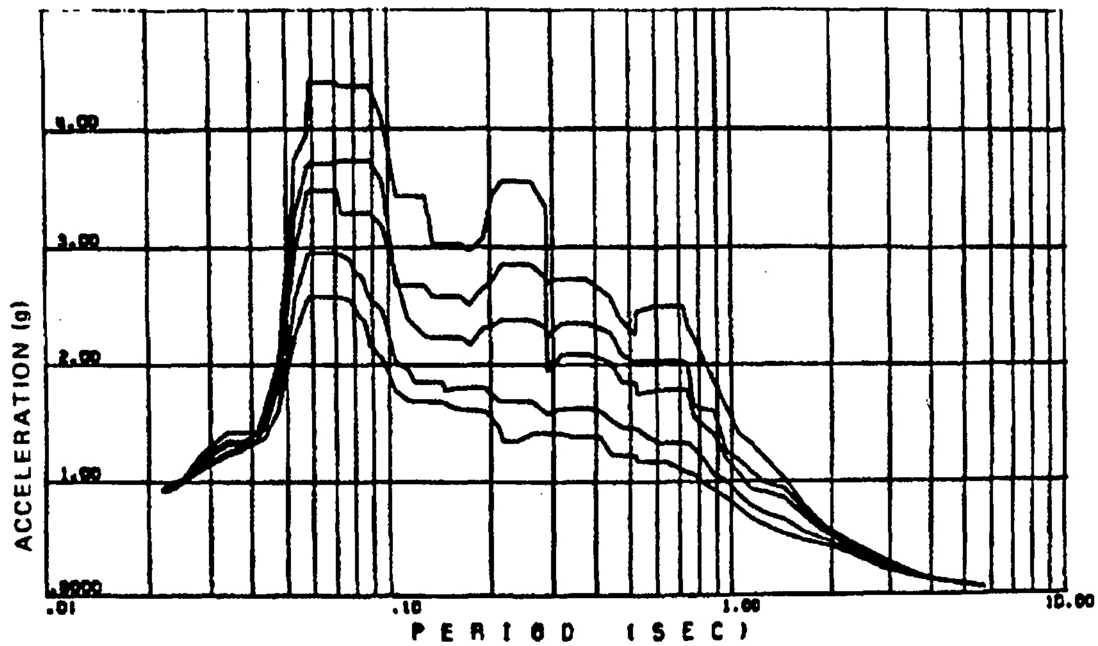

FSAR UPDATE

UNITS 1 AND 2
DIABLO CANYON SITE

FIGURE 3.7-23
AUXILIARY BUILDING
N–S HOSGRI
HORIZONTAL FLOOR SPECTRA
AT EL 140'-0"
NODE 2
2, 3, 4, 7, AND 10% DAMPING

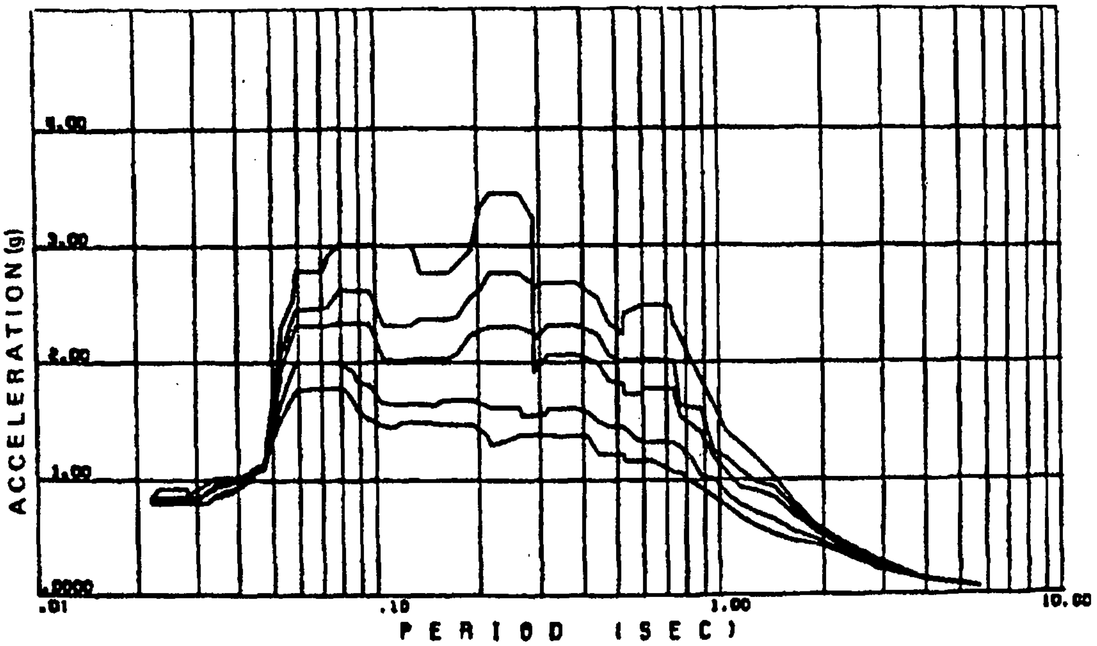

FSAR UPDATE
UNITS 1 AND 2 DIABLO CANYON SITE
FIGURE 3.7-24 AUXILIARY BUILDING N–S HOSGRI HORIZONTAL FLOOR SPECTRA AT EL 115'-0" NODE 3 2, 3, 4, 7, AND 10% DAMPING

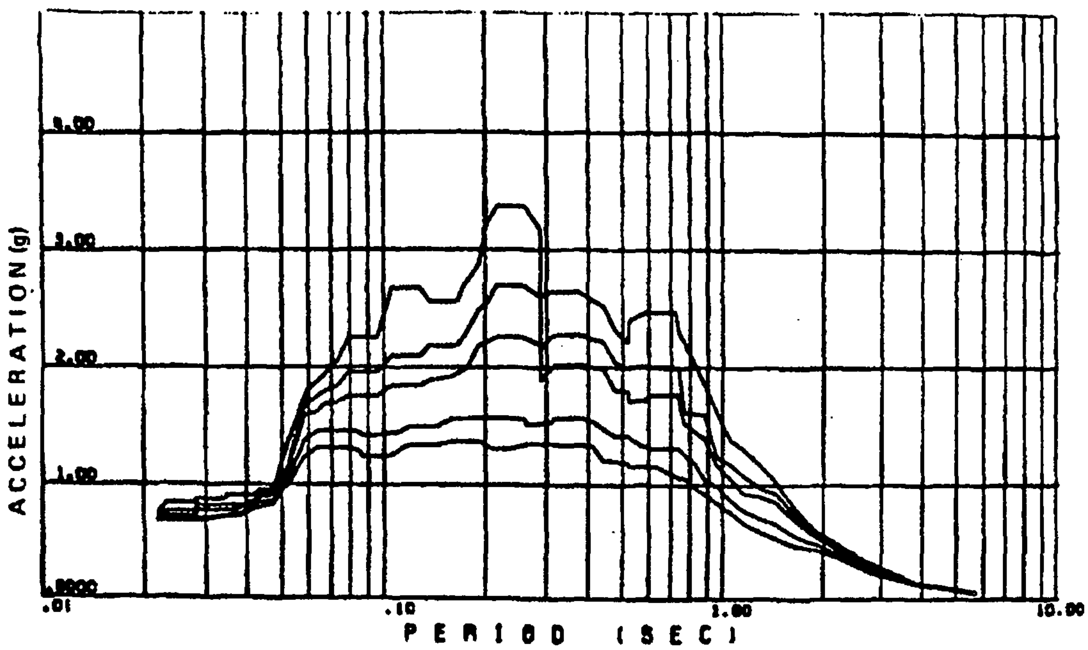

FSAR UPDATE

UNITS 1 AND 2
DIABLO CANYON SITE

FIGURE 3.7-25
AUXILIARY BUILDING
N-S HOSGRI
HORIZONTAL FLOOR SPECTRA
AT EL 100'-0"
NODE 4
2, 3, 4, 7, AND 10% DAMPING

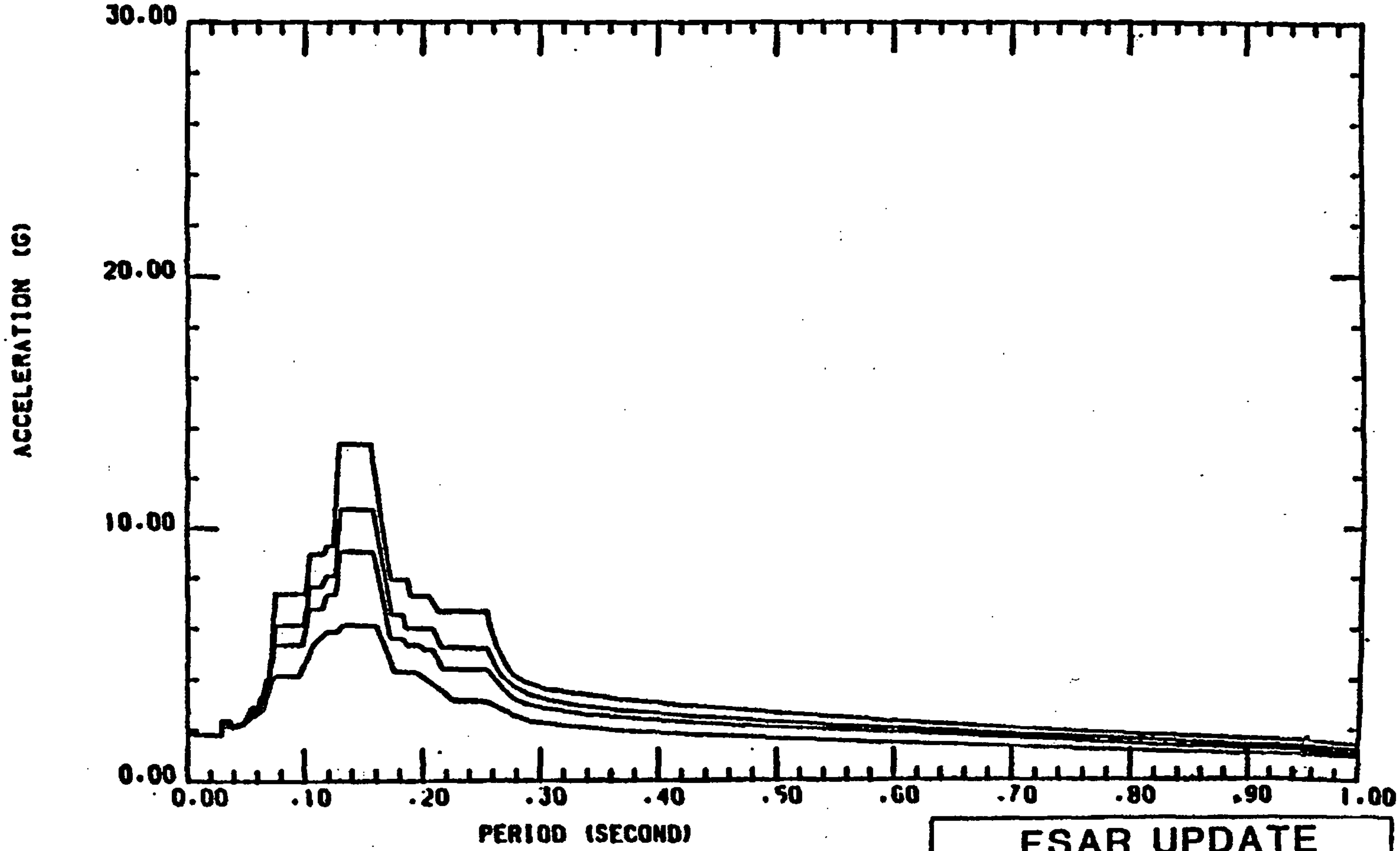

FSAR UPDATE

UNITS 1 AND 2
DIABLO CANYON SITE

FIGURE 3.7 - 25 A
TURBINE BUILDING
EL. 119'
4 KV SWITCHGEAR AREA
COLUMN LINES 1-4, D-G
HOSGRI E-W SPECTRA
2,3,4,7% DAMPING

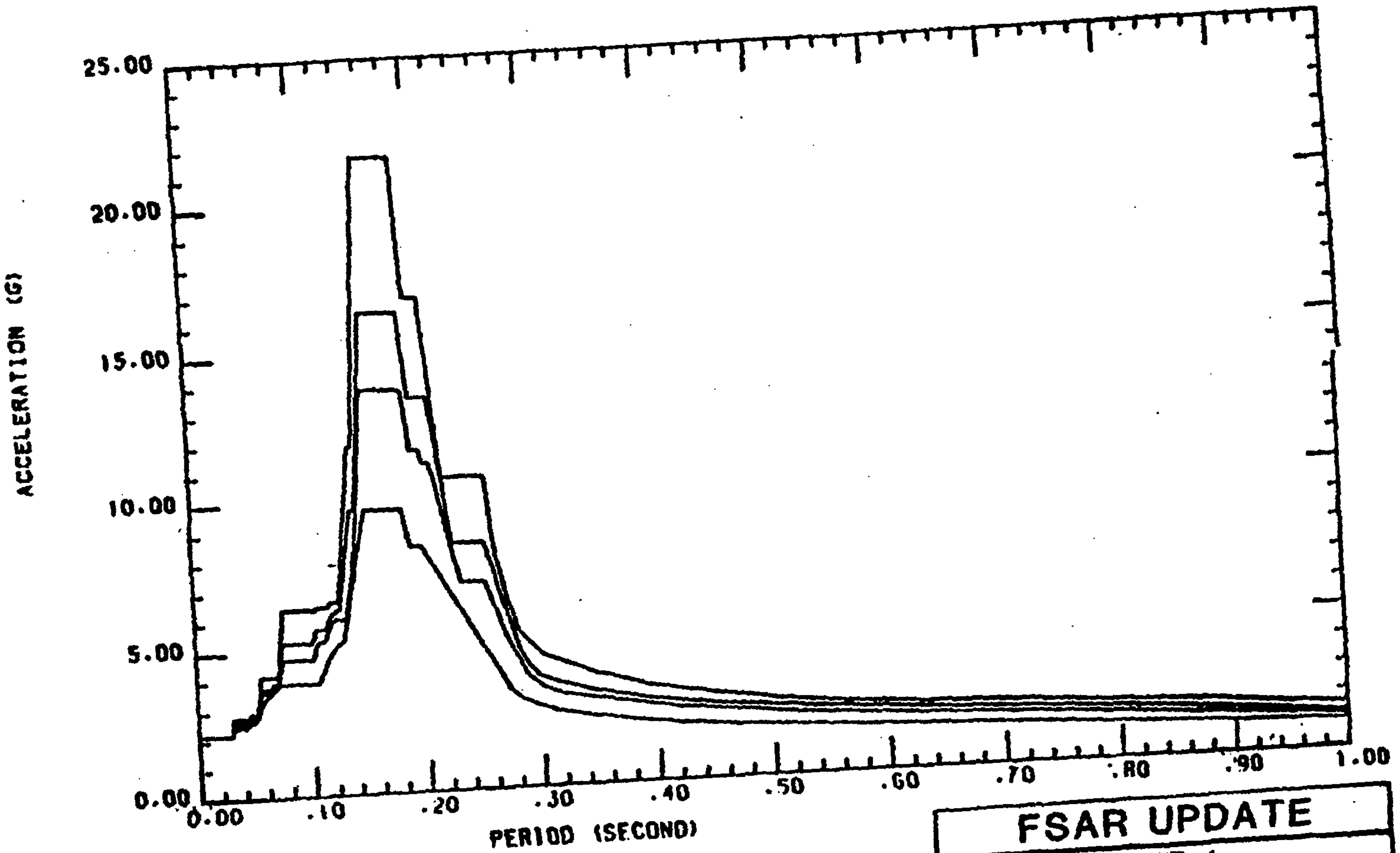

FSAR UPDATE

UNIT 1
DIABLO CANYON SITE

FIGURE 3.7 - 25B
TURBINE BUILDING EL. 140'
COLUMN LINES 5-15
HOSGRI E-W SPECTRA
2, 3, 4, 7% DAMPING

Revision 11 November 1996

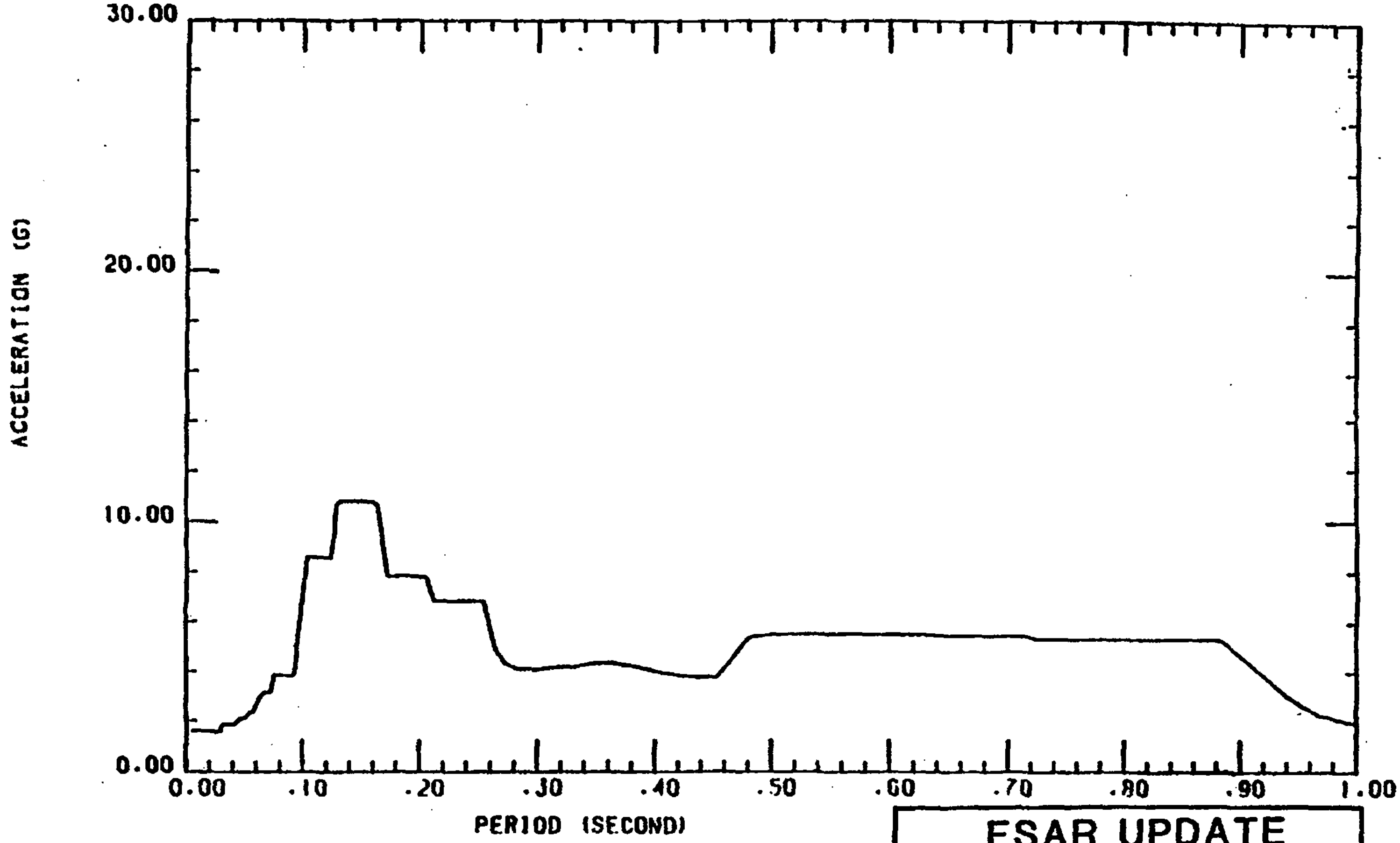

FSAR UPDATE

UNIT 1
DIABLO CANYON SITE

FIGURE 3.7 - 25 C
TURBINE BUILDING
ROOF LEVEL
COLUMN LINES 1 to 1.9, A-D
HOSGRI E - W SPECTRA
3% DAMPING

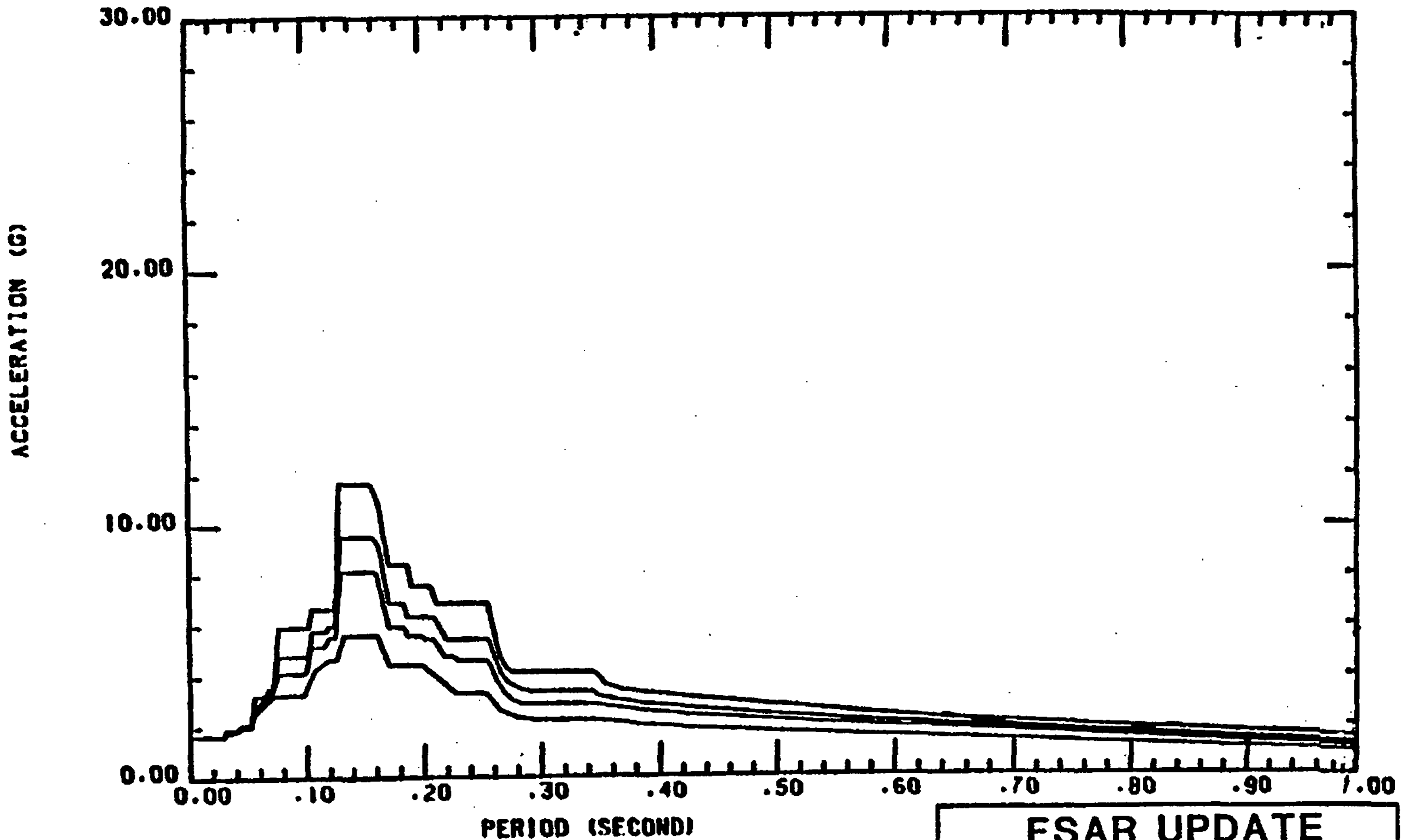

FSAR UPDATE

UNITS 1 AND 2
DIABLO CANYON SITE

FIGURE 3.7 - 25 D
TURBINE BUILDING
EL. 119'
4 KV SWITCHGEAR AREA
COLUMN LINES 1-4. D-G
HOSGRI N-S SPECTRA
2, 3, 4, 7% DAMPING

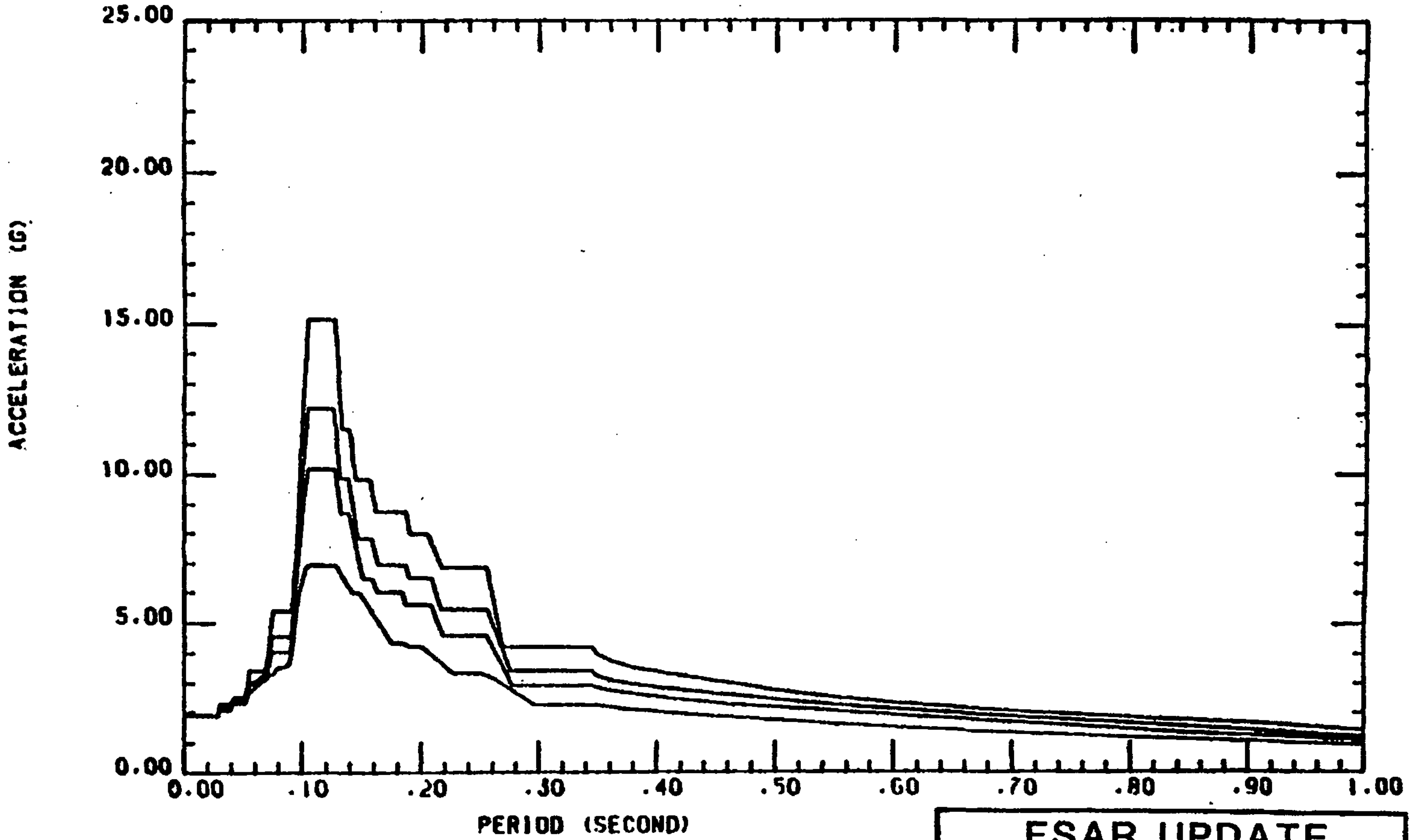

FSAR UPDATE

UNIT 1
DIABLO CANYON SITE

FIGURE 3.7 - 25 E
TURBINE BUILDING
EL. 140'
COLUMN LINES 1-19
HOSGRI N-S SPECTRA
2, 3, 4, 7% DAMPING

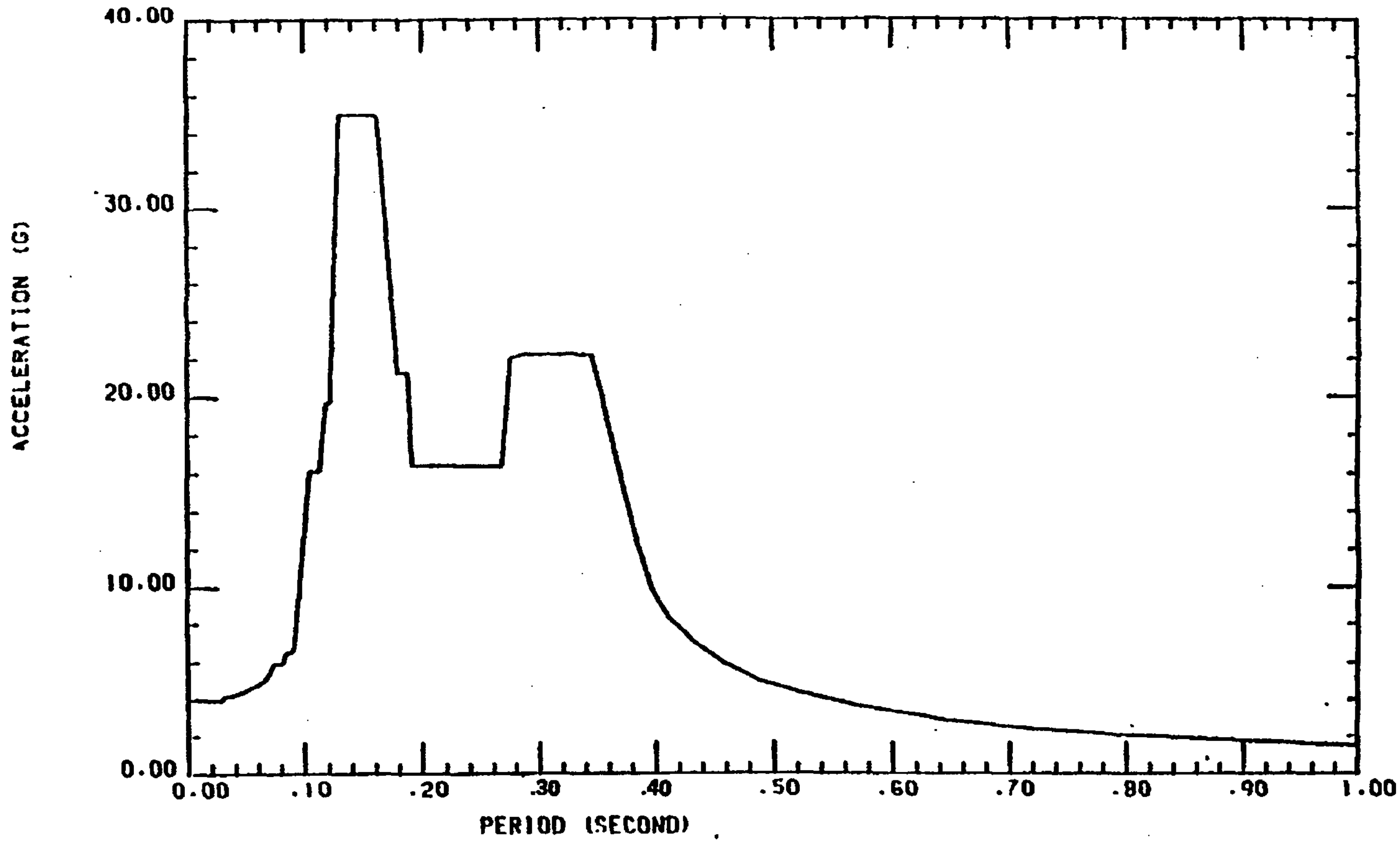

*Spectrum Enveloping the Spectra at Four Locations: Column Lines 1 & D, El. 193'
Column Lines 1 & A', El. 193'
Column Lines 1.9 & A, El. 193'
Column Lines 1.9 & D, El. 210.69'

FSAR UPDATE

UNITS 1 AND 2
DIABLO CANYON SITE

FIGURE 3.7 - 25 F
TURBINE BUILDING ROOF LEVEL
COLUMN LINES 1 to 1.9, A-D
HOSGRI N-S SPECTRA 3% DAMPING

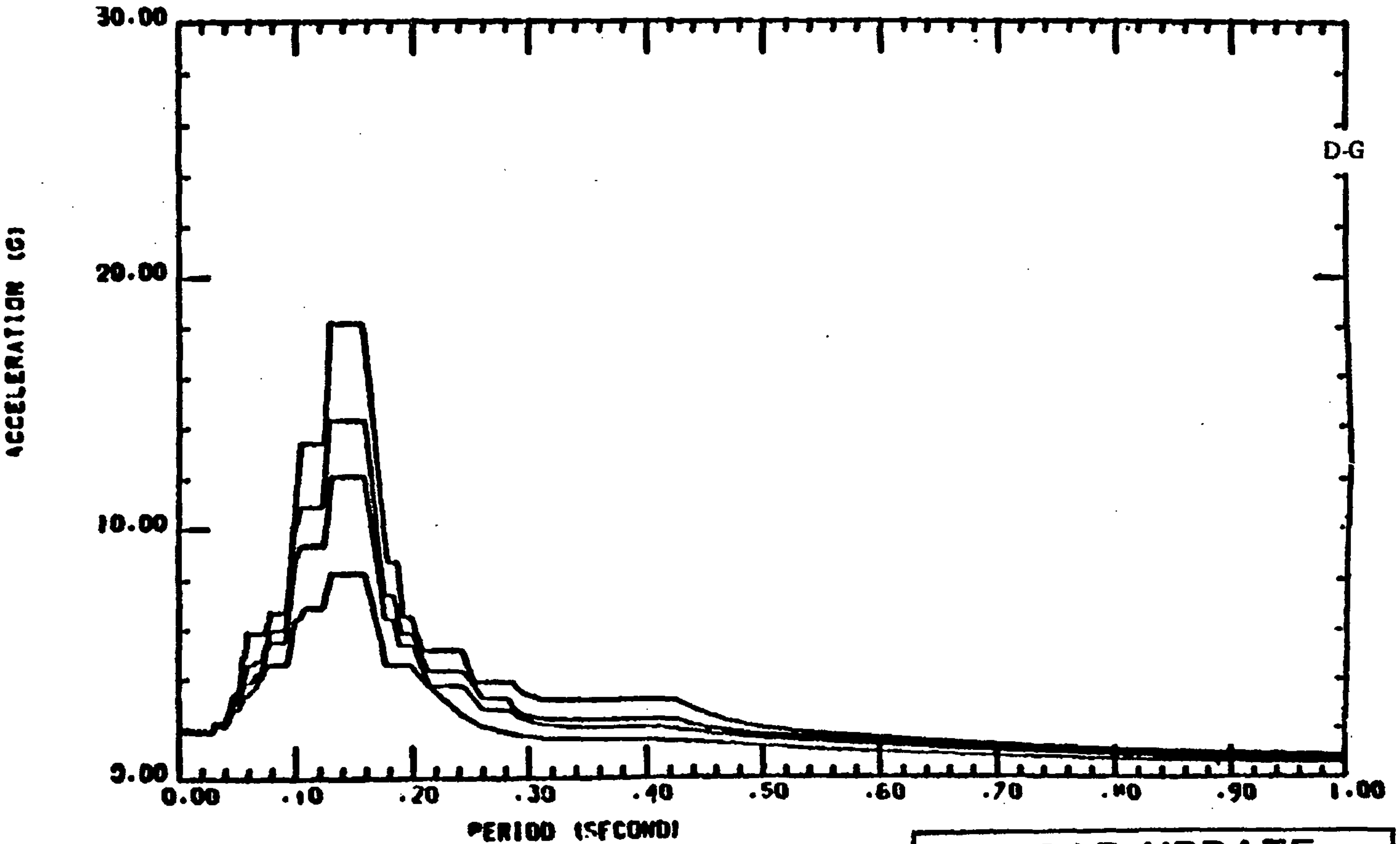

FSAR UPDATE

UNITS 1 AND 2
DIABLO CANYON SITE

FIGURE 3.7 - 25 G
TURBINE BUILDING
EL.119'
COLUMN LINES 1-4 & 32-35
D G 4 KV SWITCHGEAR AREA
HOSGRI VERTICAL SPECTRA
2, 3. 4, 7% DAMPING

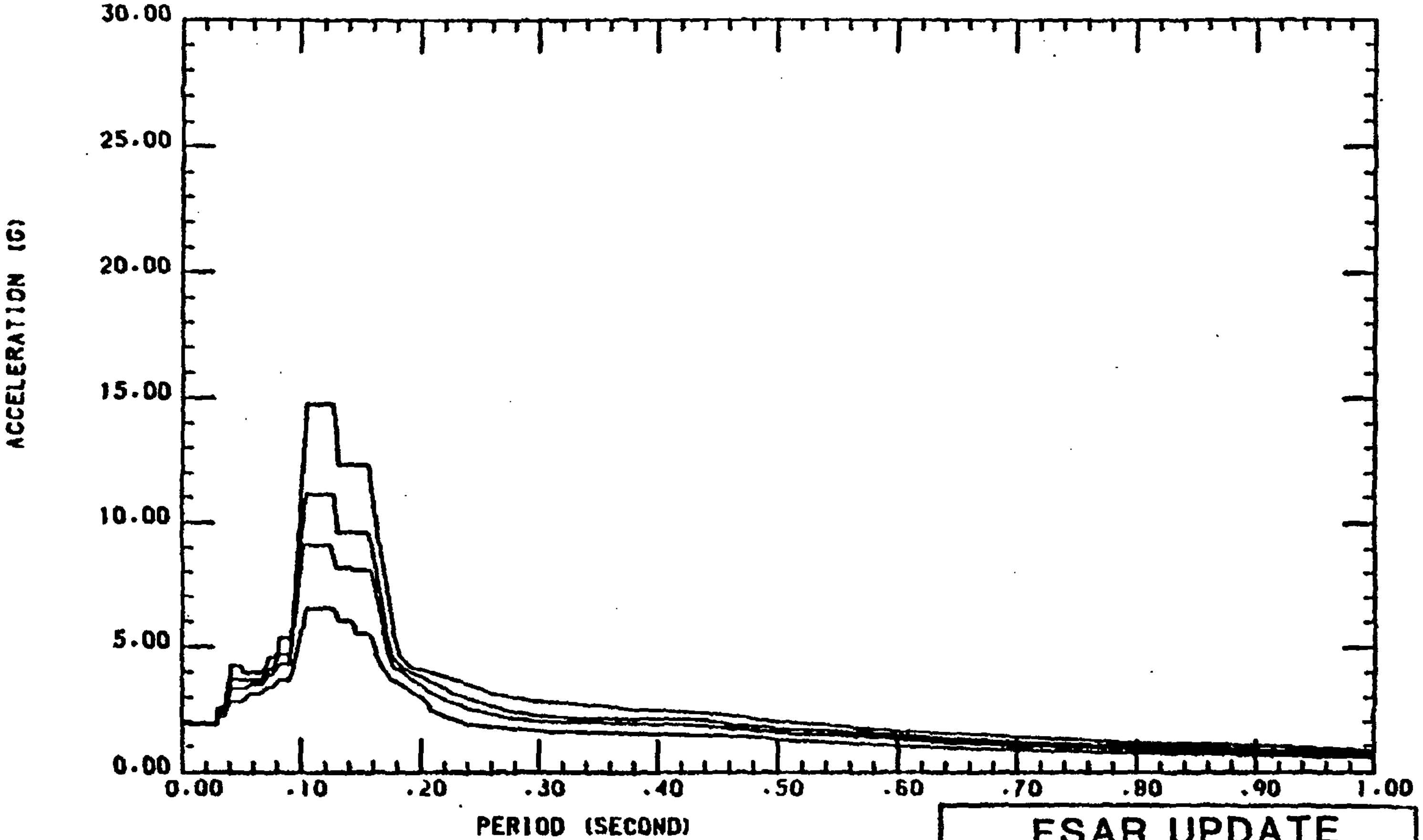

FSAR UPDATE

UNITS 1 AND 2
DIABLO CANYON SITE

FIGURE 3.7 - 25 H
TURBINE BUILDING
EL. 140'
COLUMN LINES
5- 15, 21 -31
HOSGRI VERTICAL SPECTRA
2, 3, 4, 7% DAMPING

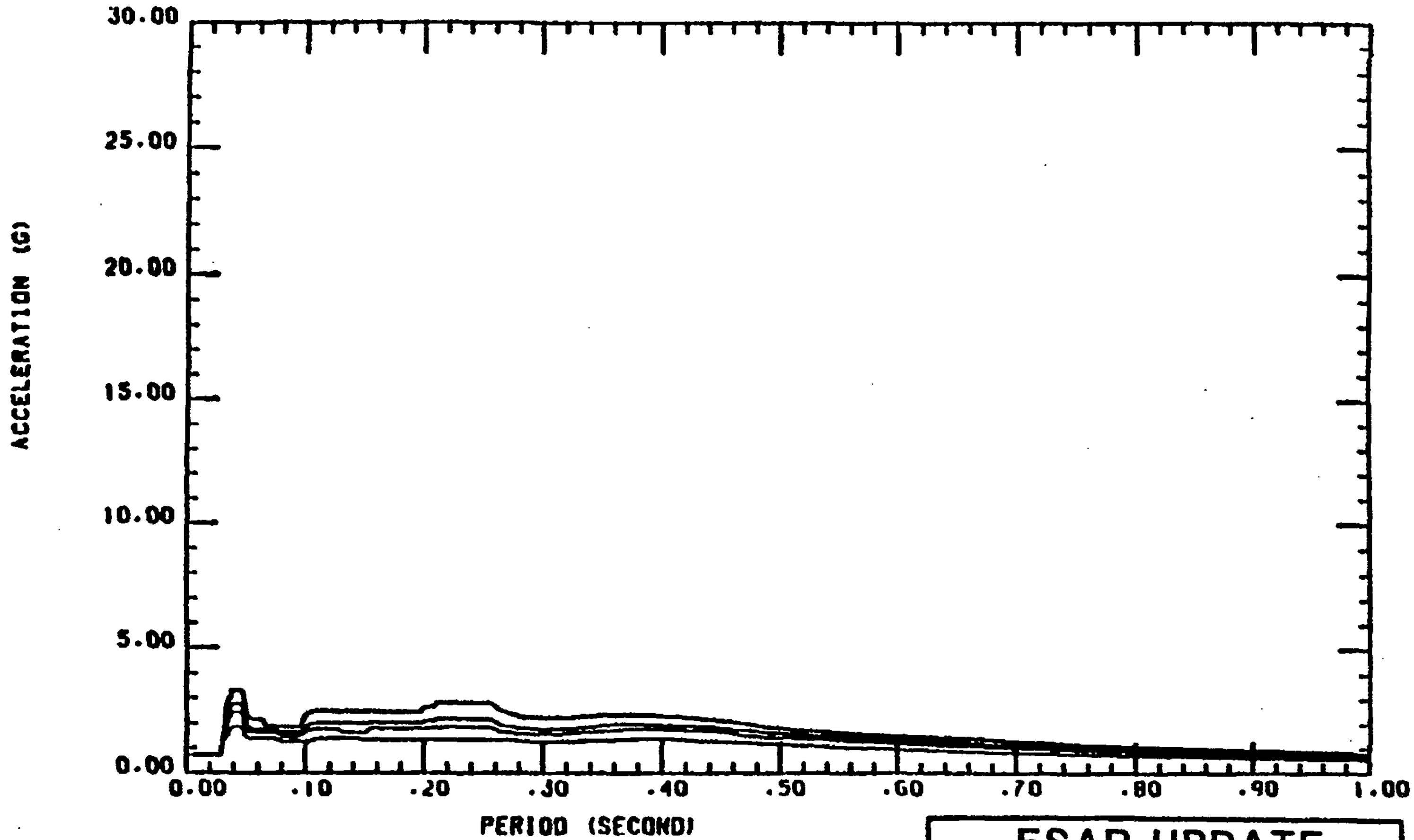

FSAR UPDATE
UNITS 1 AND 2 **DIABLO CANYON SITE**
FIGURE 3.7-25I TURBINE BUILDING EL. 193' BUILT UP COLUMNS ON LINE A&G FROM 5.7 TO 15 & 21 TO 30.3 HOSGRI VERTICAL SPECTRA 2, 3, 4, 7% DAMPING

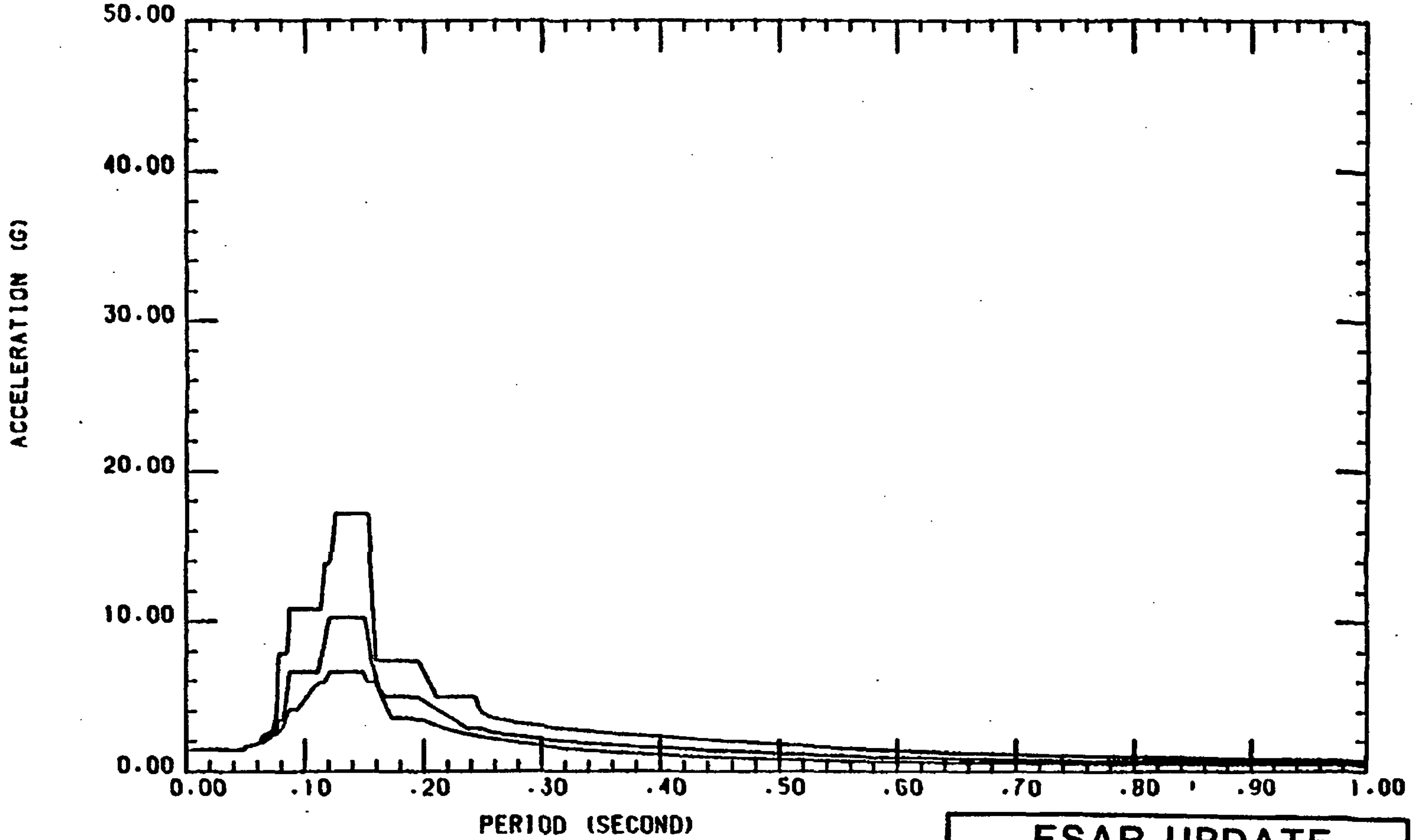

FSAR UPDATE

UNITS 1 AND 2
DIABLO CANYON SITE

FIGURE 3.7 - 25 J
TURBINE BUILDING
ELEV. 104'
COLUMN LINES 5 to 15
DDE E-W SPECTRA
1/2, 2, 5% DAMPING

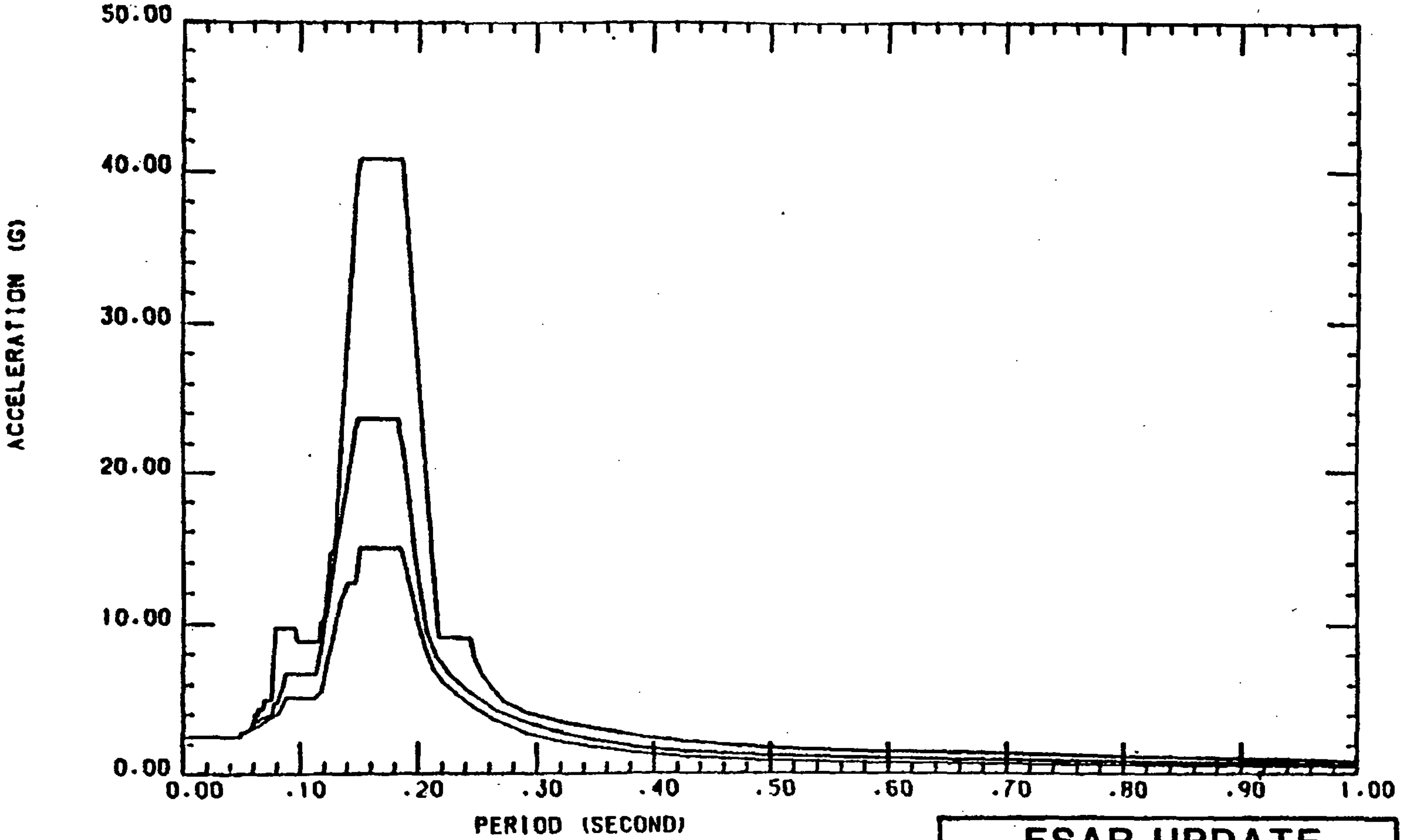

FSAR UPDATE

UNITS 1 AND 2
DIABLO CANYON SITE

FIGURE 3.7 - 25 K
TURBINE BUILDING
ELEV. 140'
COLUMN LINES 5-15
DDE E-W SPECTRA
1/2,2,5% DAMPING

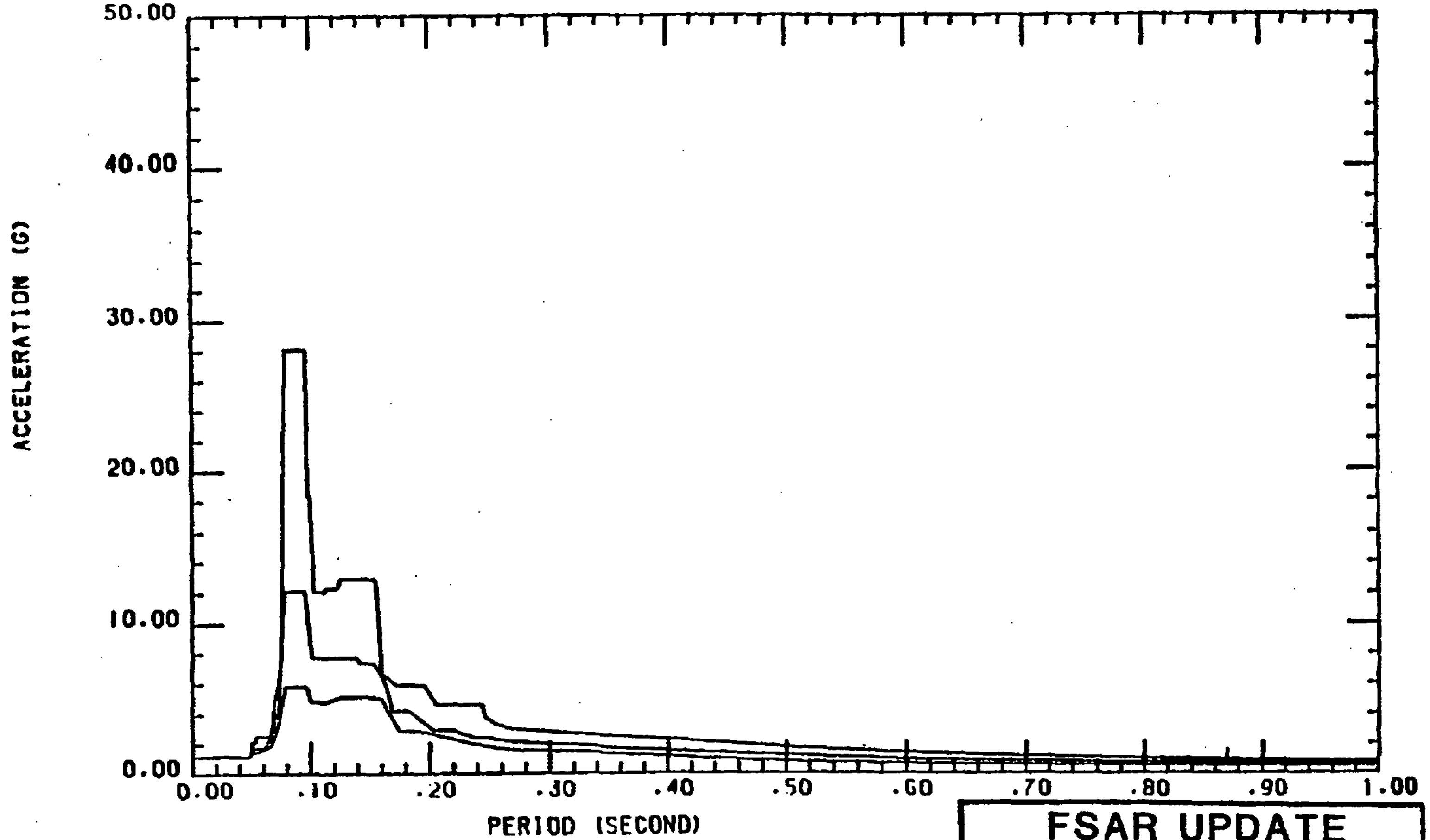

FSAR UPDATE

UNITS 1 AND 2
DIABLO CANYON SITE

FIGURE 3.7 - 25 L
TURBINE BUILDING
ELEV 104' & 107'
COLUMN LINES 1-19
DDE N-S SPECTRA
1/2, 2, 5% DAMPING

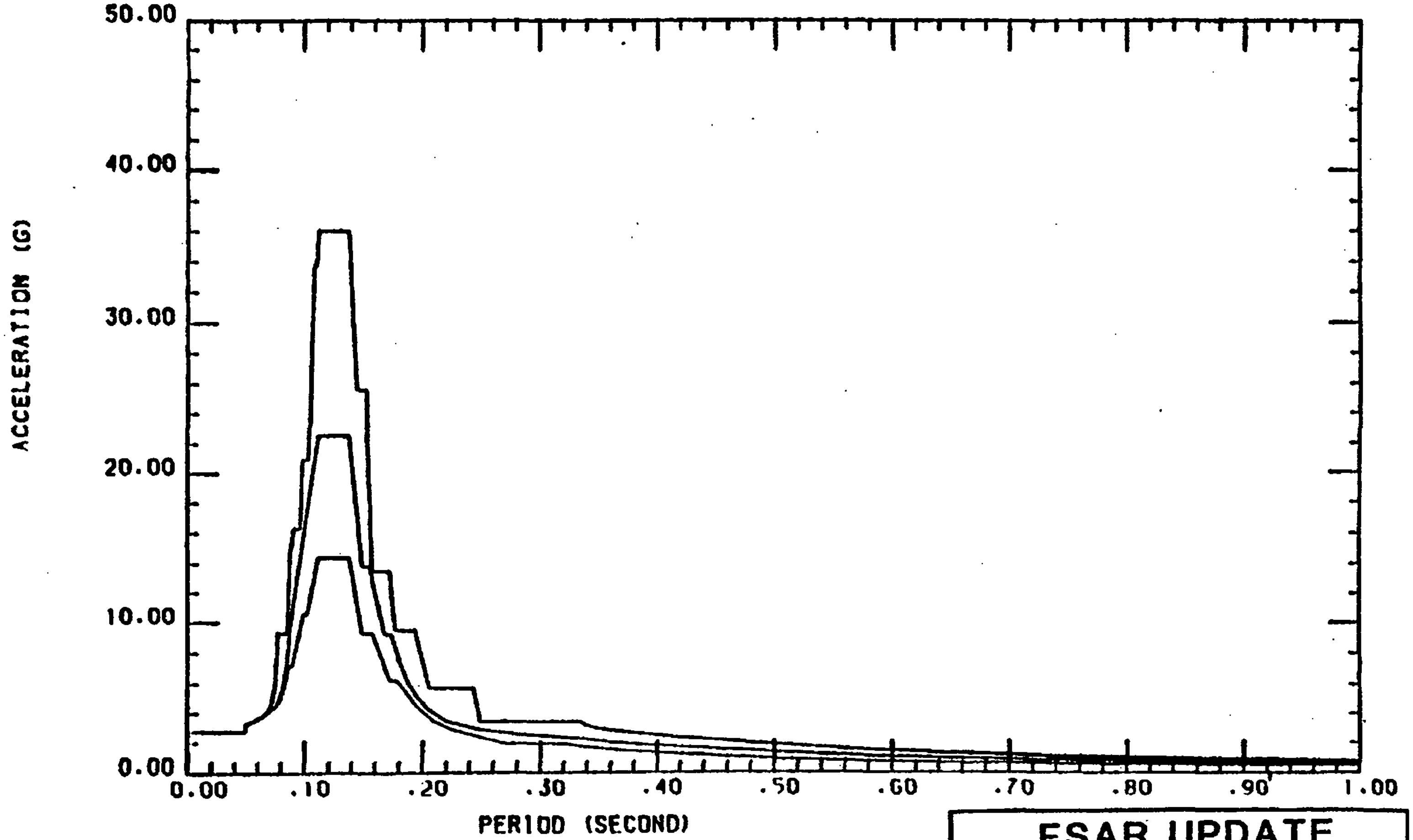

FSAR UPDATE

UNITS 1 AND 2
DIABLO CANYON SITE

FIGURE 3.7 - 25 M
TURBINE BUILDING
ELEV 140'
COLUMN LINES 1-19
DDE N-S SPECTRA
1/2, 2, 5% DAMPING

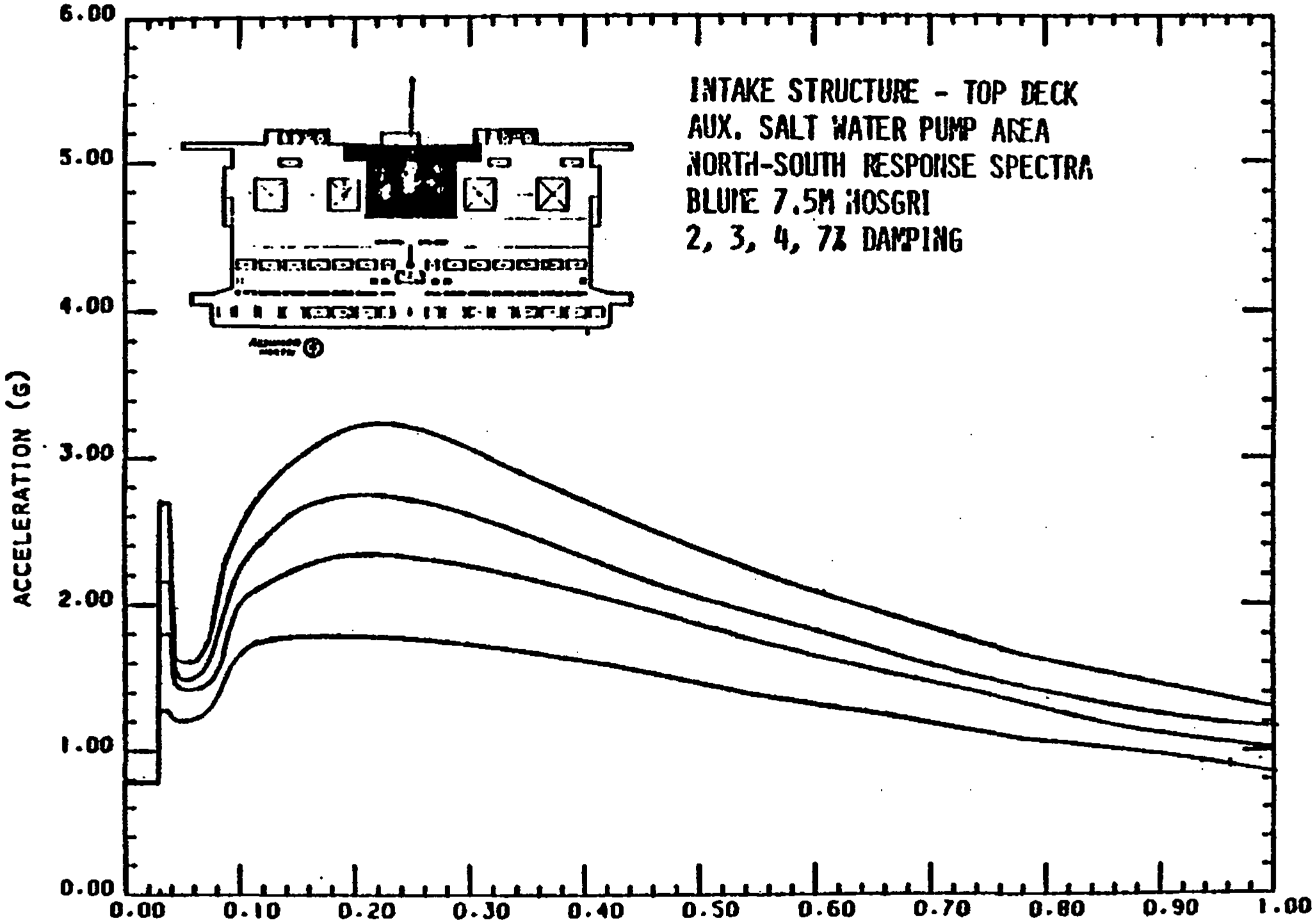

FSAR UPDATE

UNITS 1 AND 2
DIABLO CANYON SITE

FIGURE 3.7 - 25 N
INTAKE STRUCTURE
RESPONSE SPECTRA
BLUME 7.5 M HOSGRI

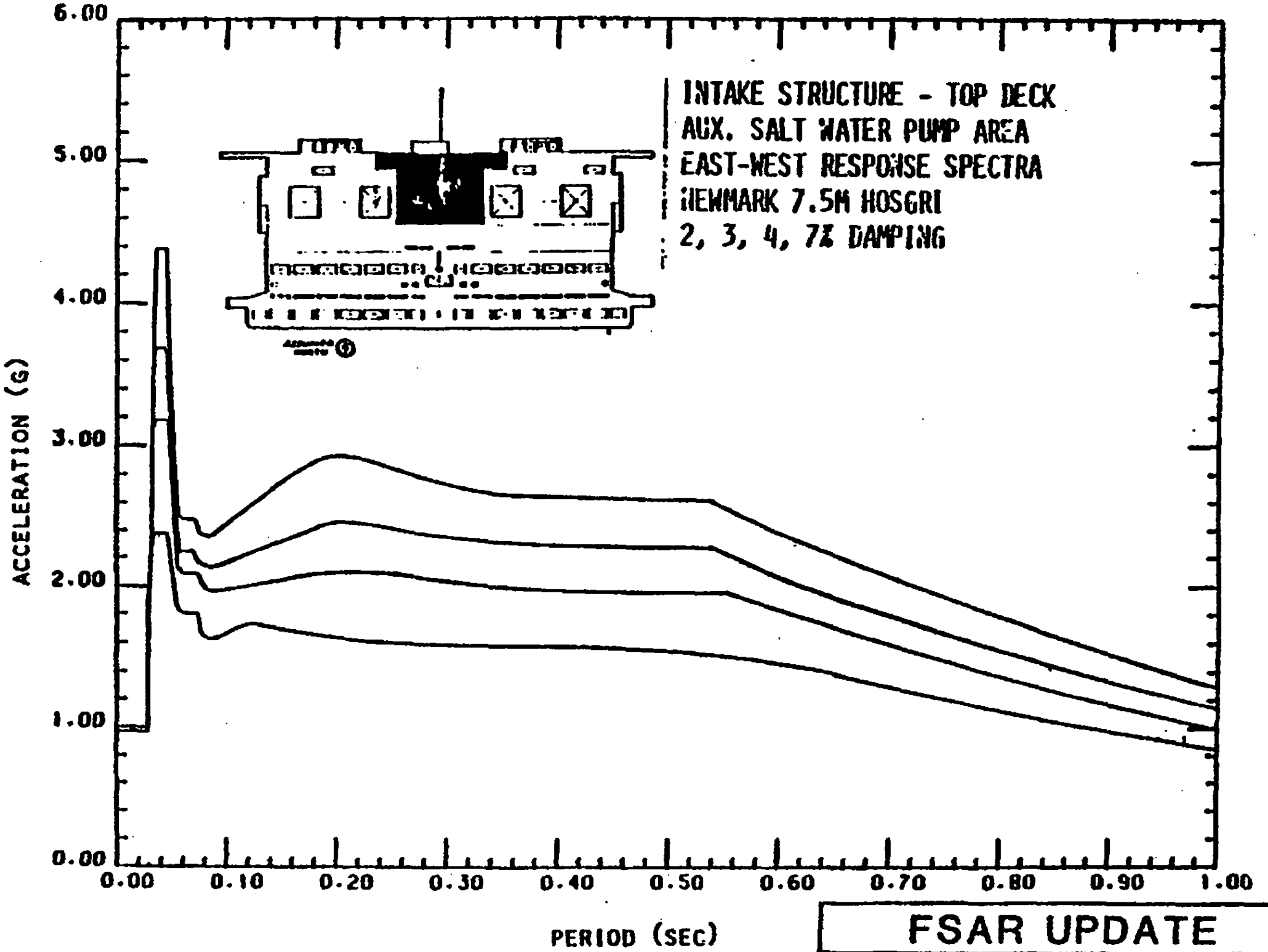

FSAR UPDATE
UNITS 1 AND 2 DIABLO CANYON SITE
FIGURE 3.7 - 25 O INTAKE STRUCTURE RESPONSE SPECTRA NEWMARK 7.5 M HOSGRI

Revision 11 November 1996

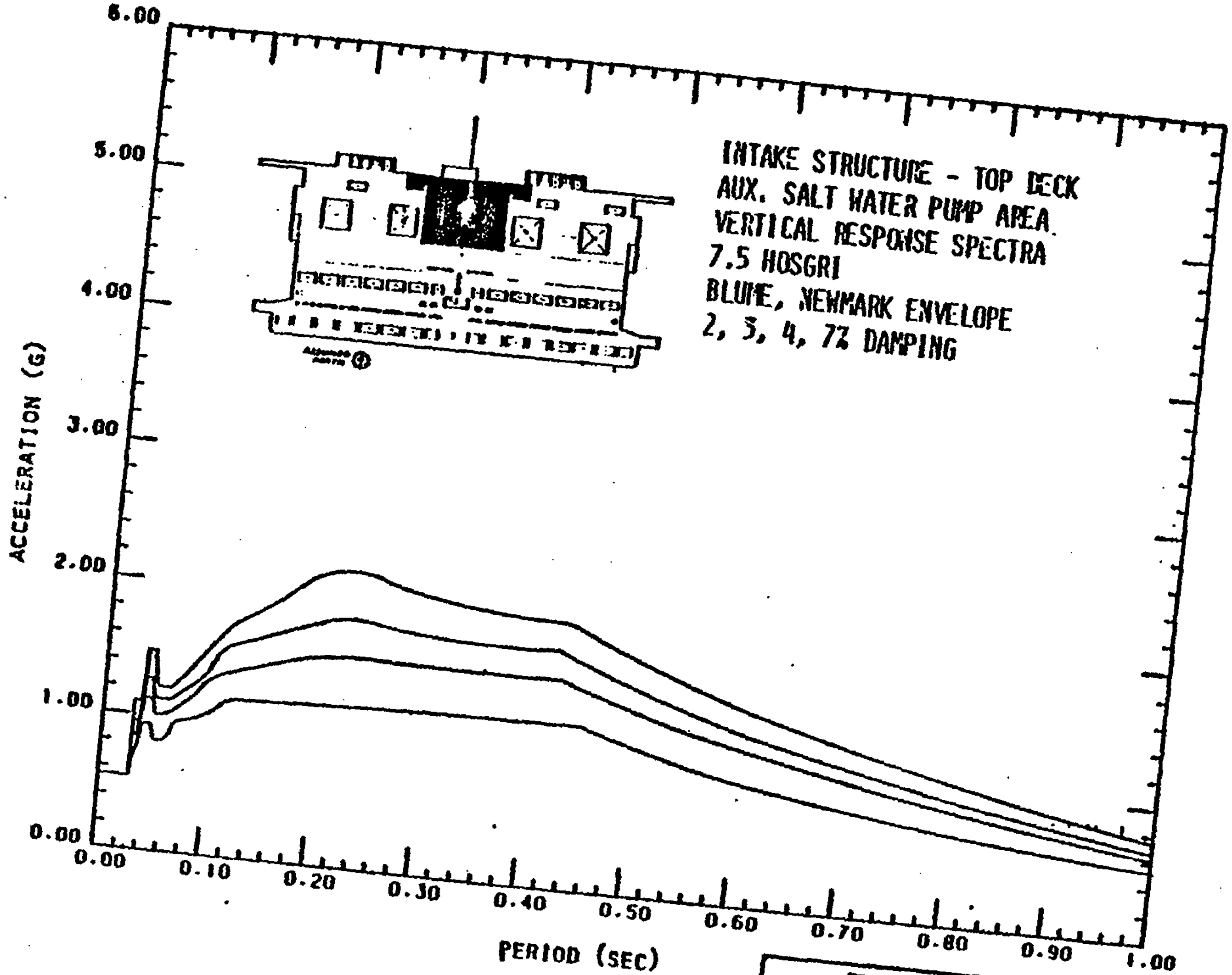

FSAR UPDATE

UNITS 1 AND 2
DIABLO CANYON SITE

FIGURE 3.7 - 25 P
INTAKE STRUCTURE VERTICAL
RESPONSE SPECTRA 7.5M/HOSGRI
BLUME, NEWMARK ENVELOPE

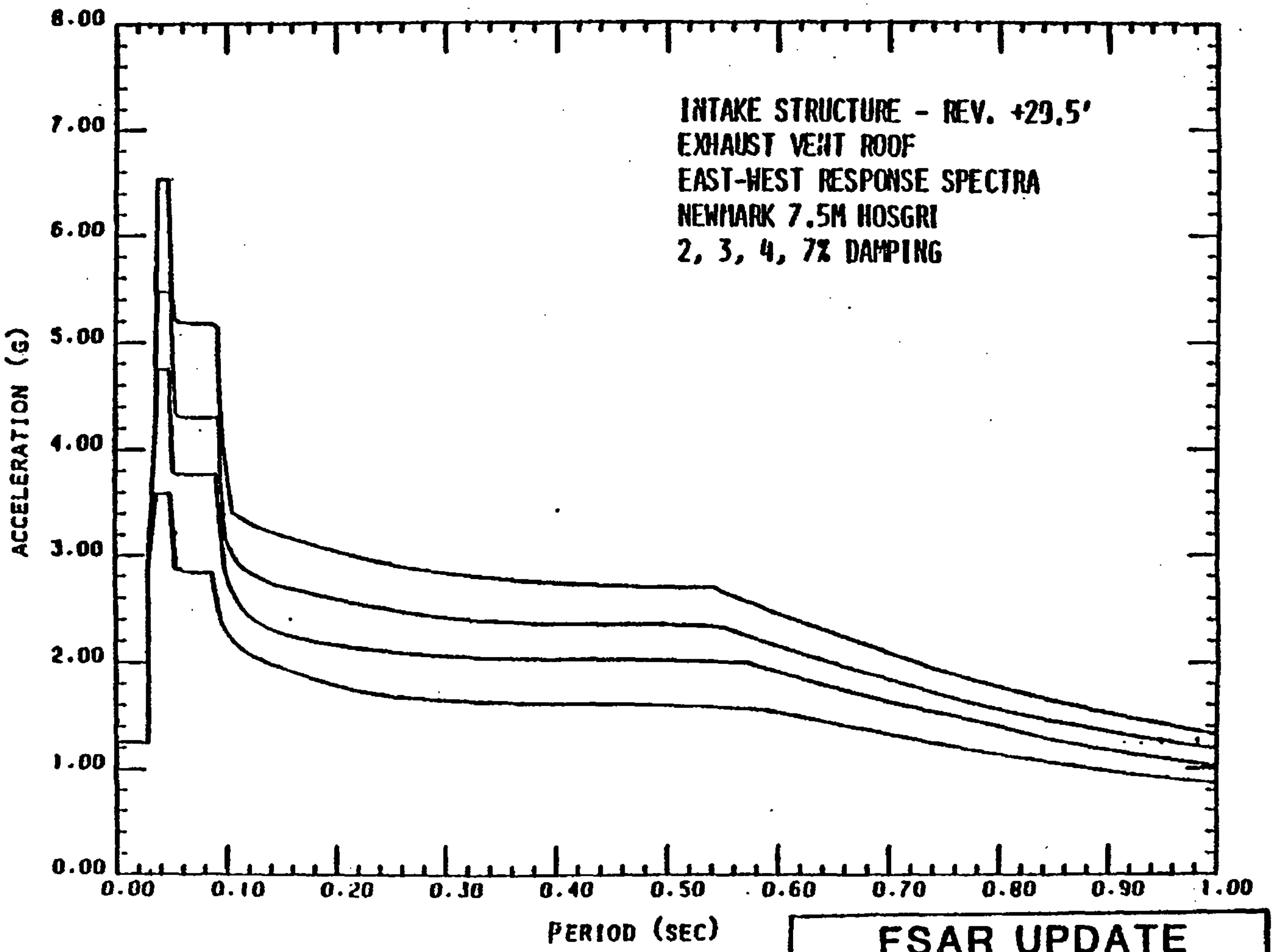

FSAR UPDATE
UNITS 1 AND 2 DIABLO CANYON SITE
FIGURE 3.7 - 25 Q INTAKE STRUCTURE RESPONSE SPECTRA NEWMARK 7.5 M HOSGRI

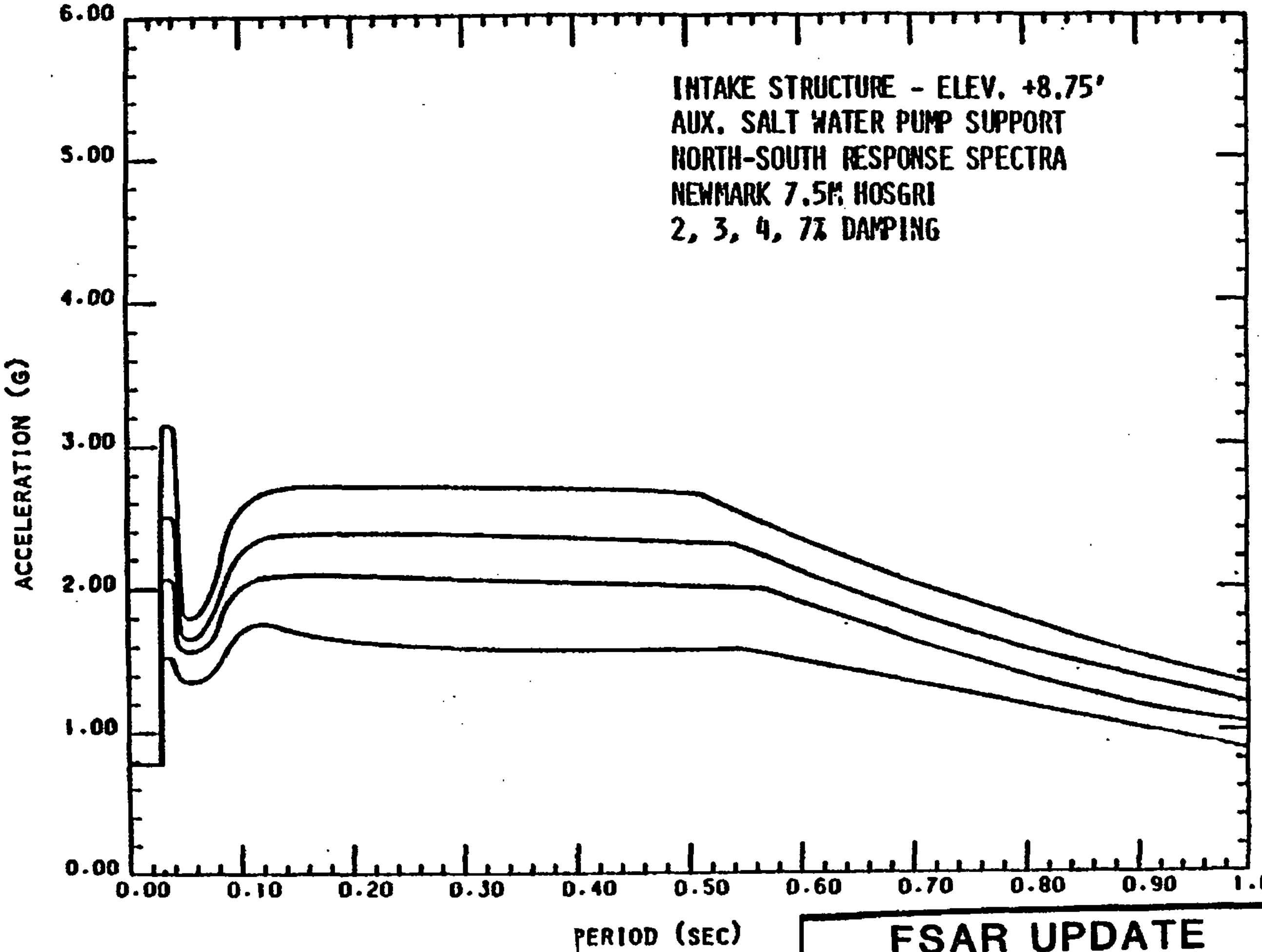

FSAR UPDATE

UNITS 1 AND 2
DIABLO CANYON SITE

FIGURE 3.7 - 25 R
INTAKE STRUCTURE
RESPONSE SPECTRA
NEWMARK 7.5 M HOSGRI

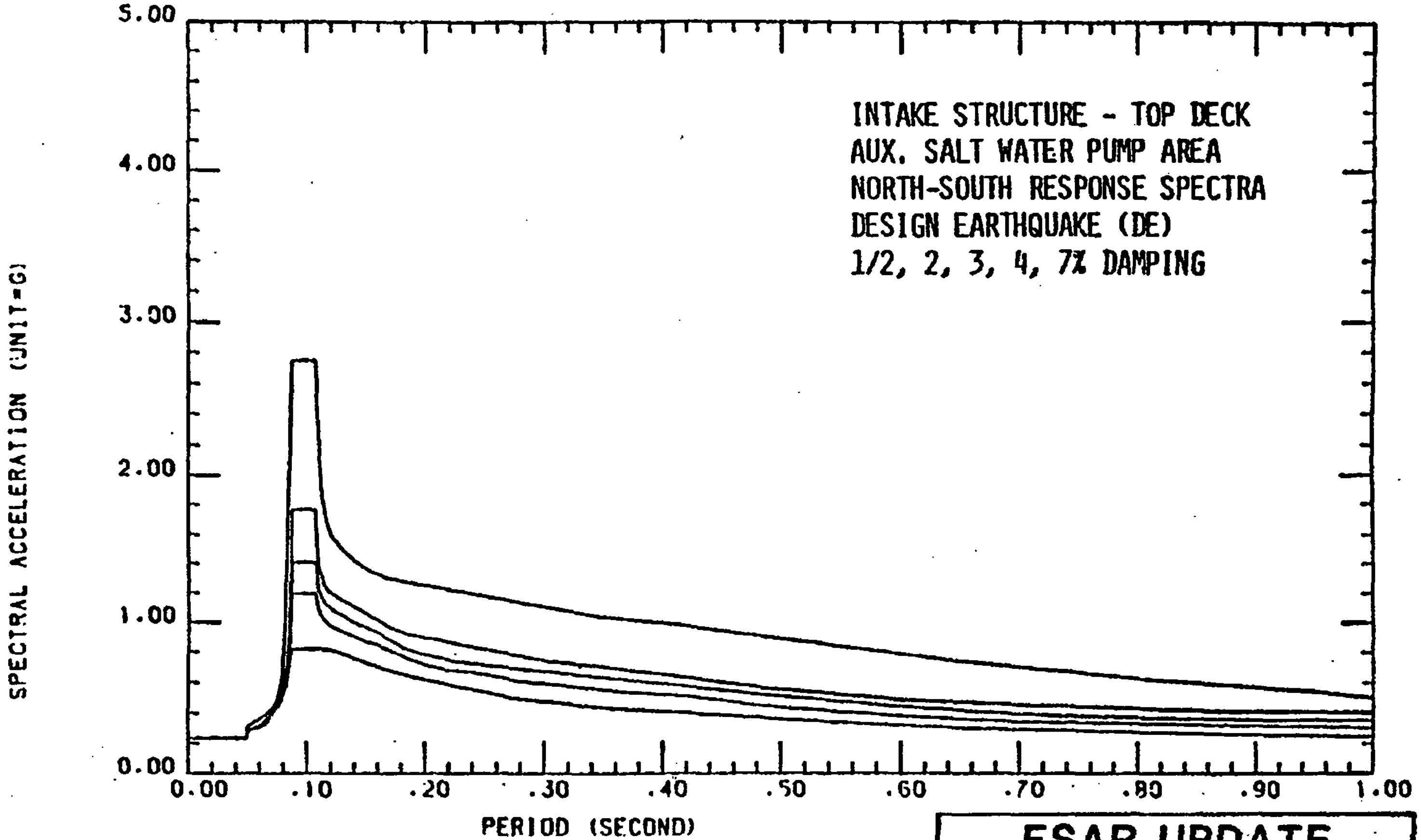

FSAR UPDATE

UNITS 1 AND 2
DIABLO CANYON SITE

FIGURE 3.7-25 S
INTAKE STRUCTURE
RESPONSE SPECTRA
DESIGN EARTHQUAKE (DE)

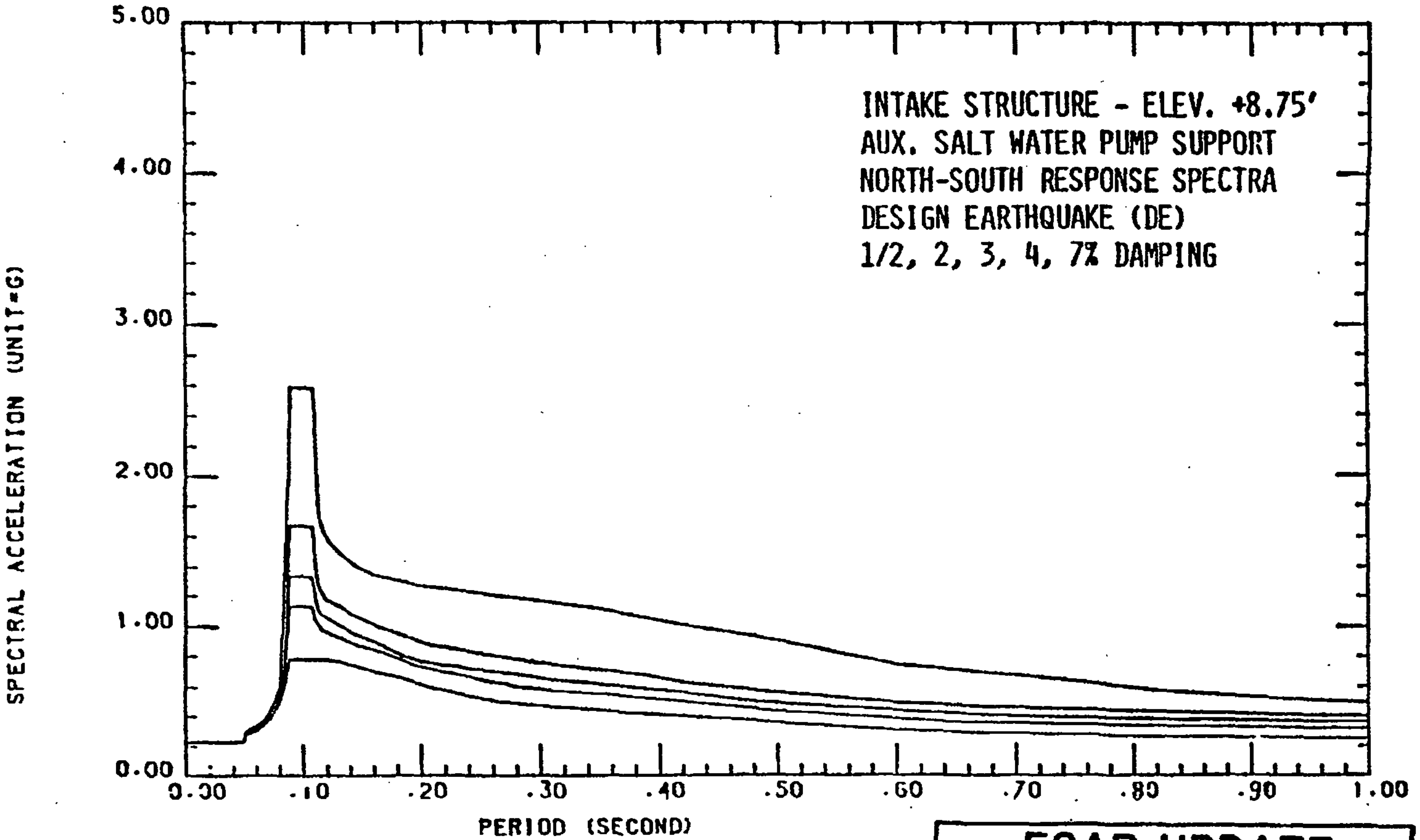

FSAR UPDATE

UNITS 1 AND 2
DIABLO CANYON SITE

FIGURE 3.7 - 25 T
INTAKE STRUCTURE
RESPONSE SPECTRA
DESIGN EARTHQUAKE (DE)

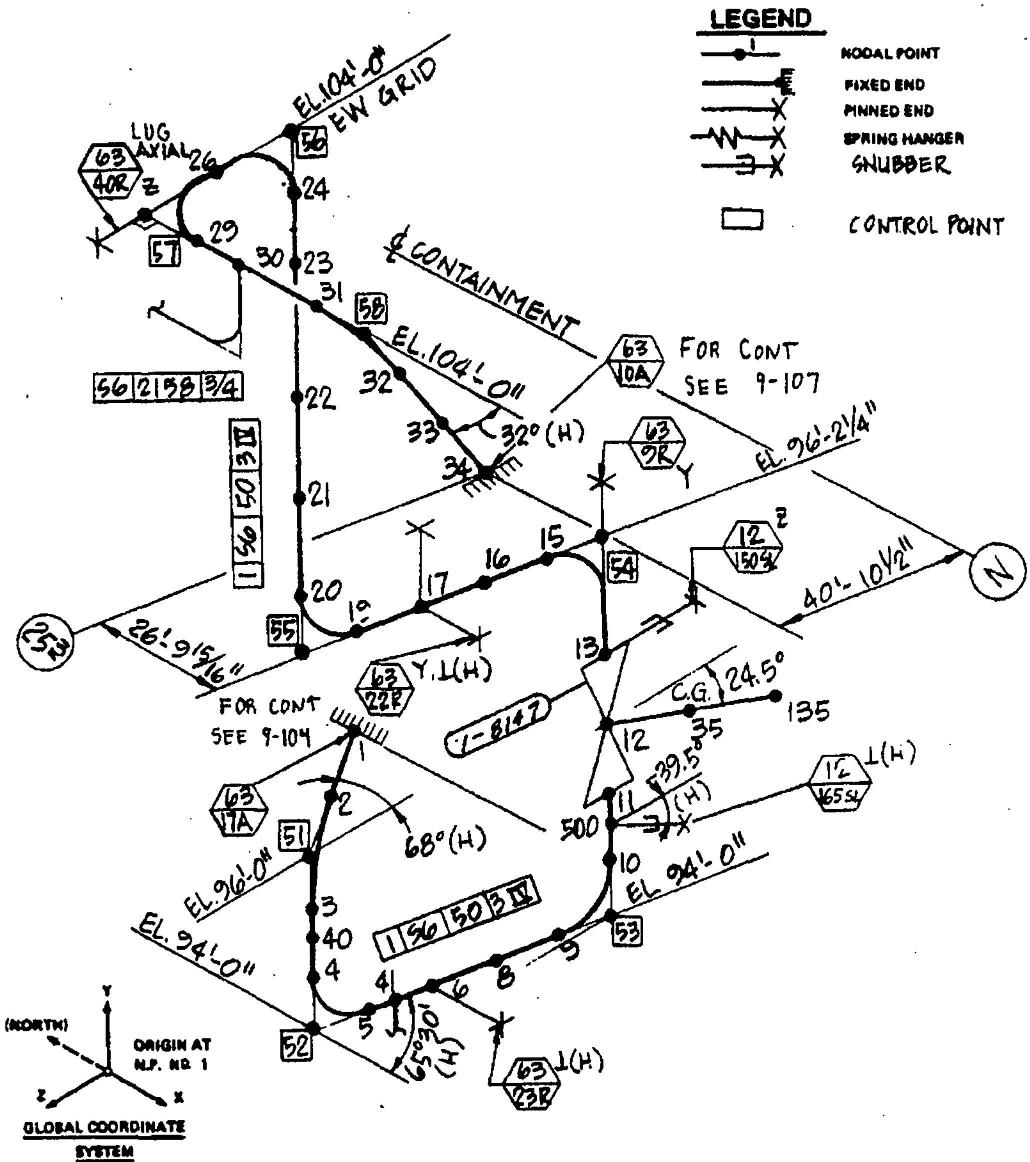

FSAR UPDATE

UNIT 1
DIABLO CANYON SITE

FIGURE 3.7-26
TYPICAL PIPING
MATHEMATICAL MODEL

Revision 11 November 1996

K_{rs} = RADIAL SUPPORT SPRING CONSTANT

K_{rot} = ROTATIONAL GROUND SPRING CONSTANT

K_t = TRANSLATIONAL GROUND SPRING CONSTANT

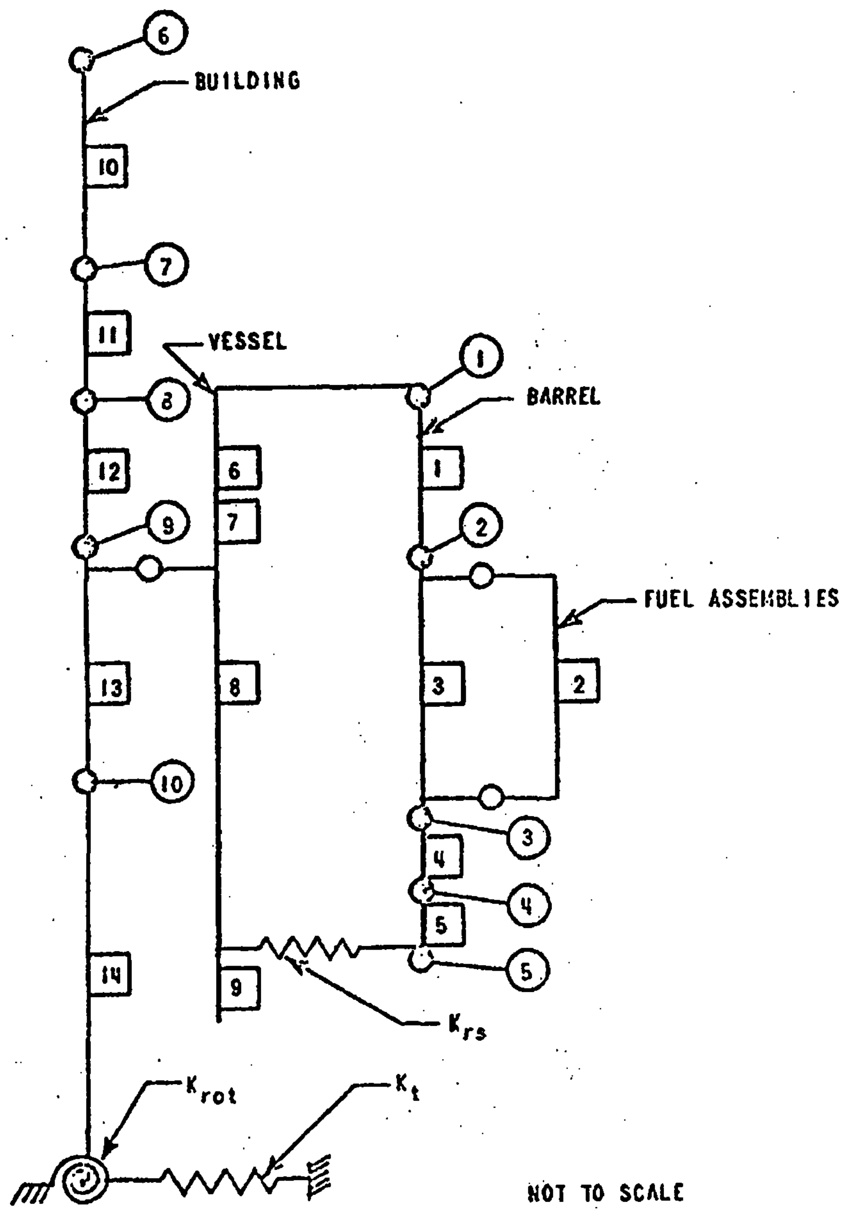

NOT TO SCALE

FSAR UPDATE

UNITS 1 AND 2
DIABLO CANYON SITE

FIGURE 3.7-27
REACTOR INTERNALS
MATHEMATICAL MODELS

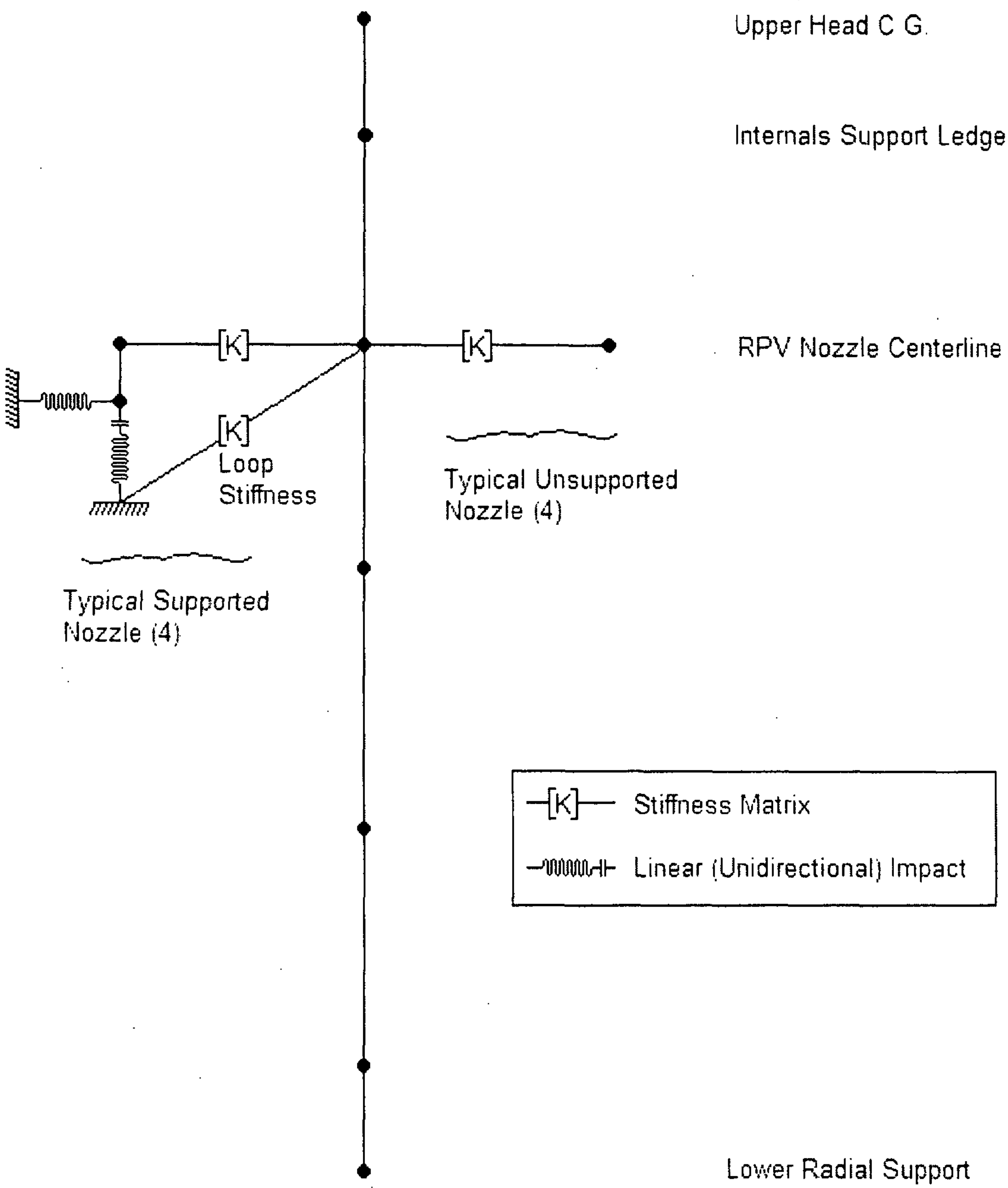

FSAR UPDATE

UNITS 1 AND 2
DIABLO CANYON SITE

FIGURE 3.7-27A

REACTOR PRESSURE VESSEL
SHELL SUBMODEL

Revision 20 November 2011

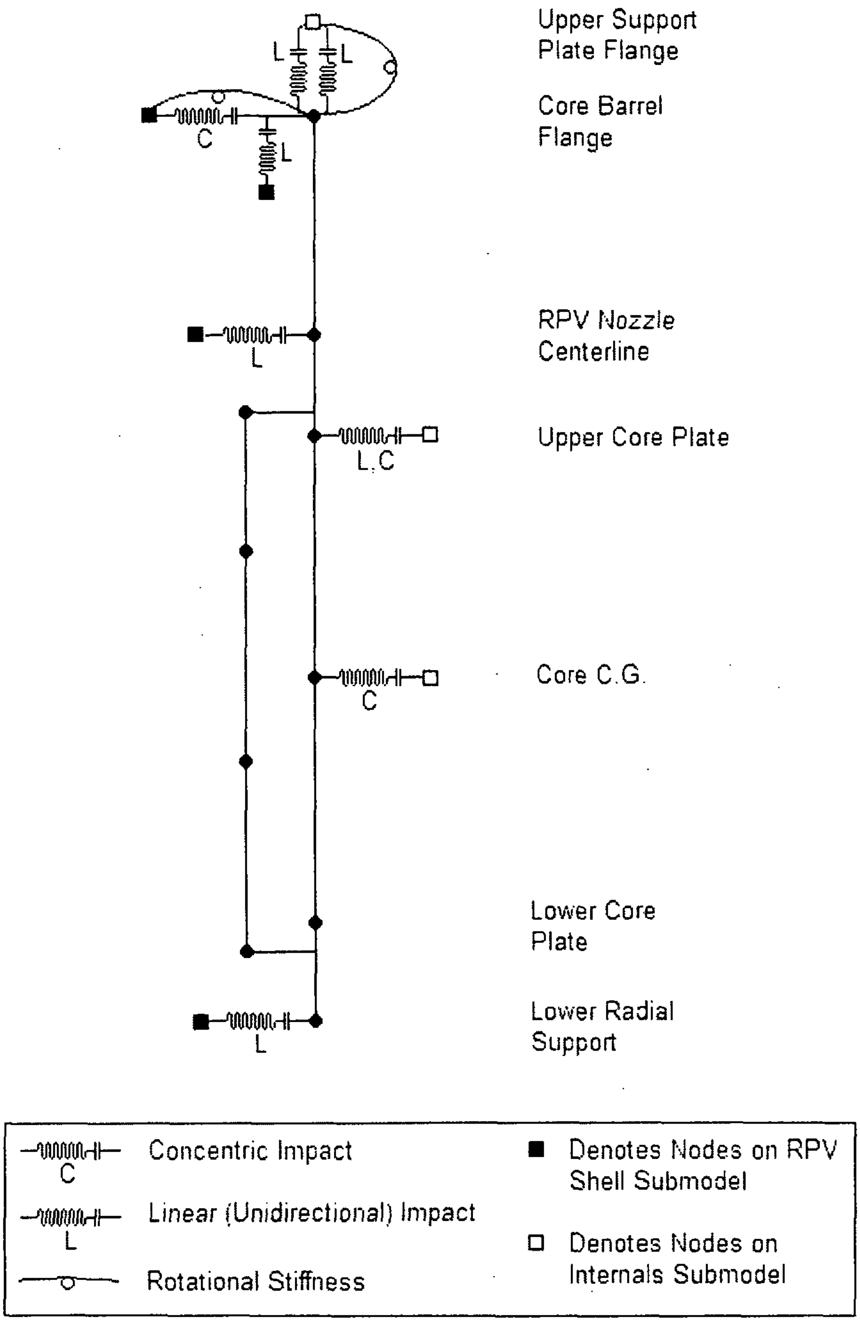

FSAR UPDATE
UNIT 1 DIABLO CANYON SITE
FIGURE 3.7-27B CORE BARREL SUBMODEL

Revision 20 November 2011

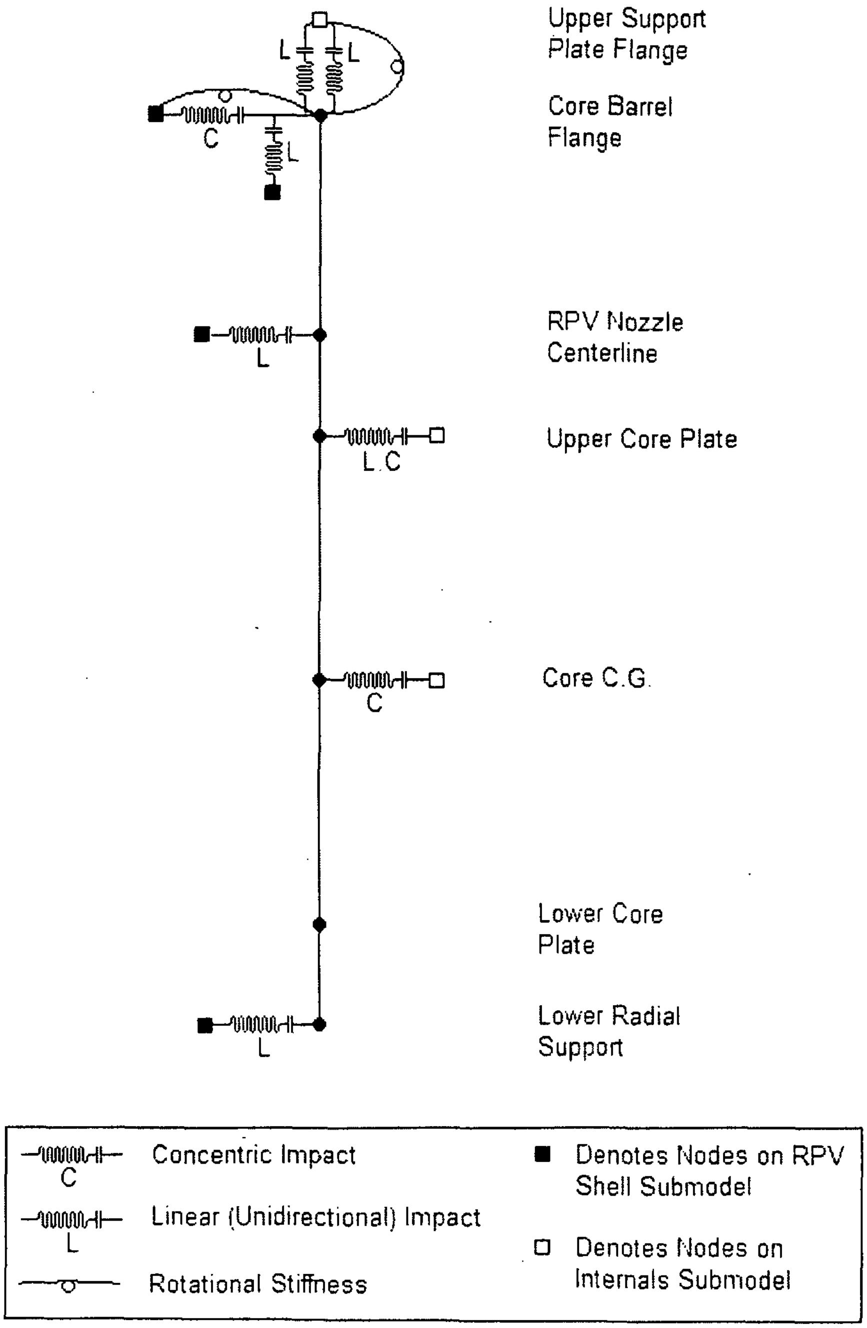

FSAR UPDATE
UNIT 2 DIABLO CANYON SITE
FIGURE 3.7-27C CORE BARREL SUBMODEL

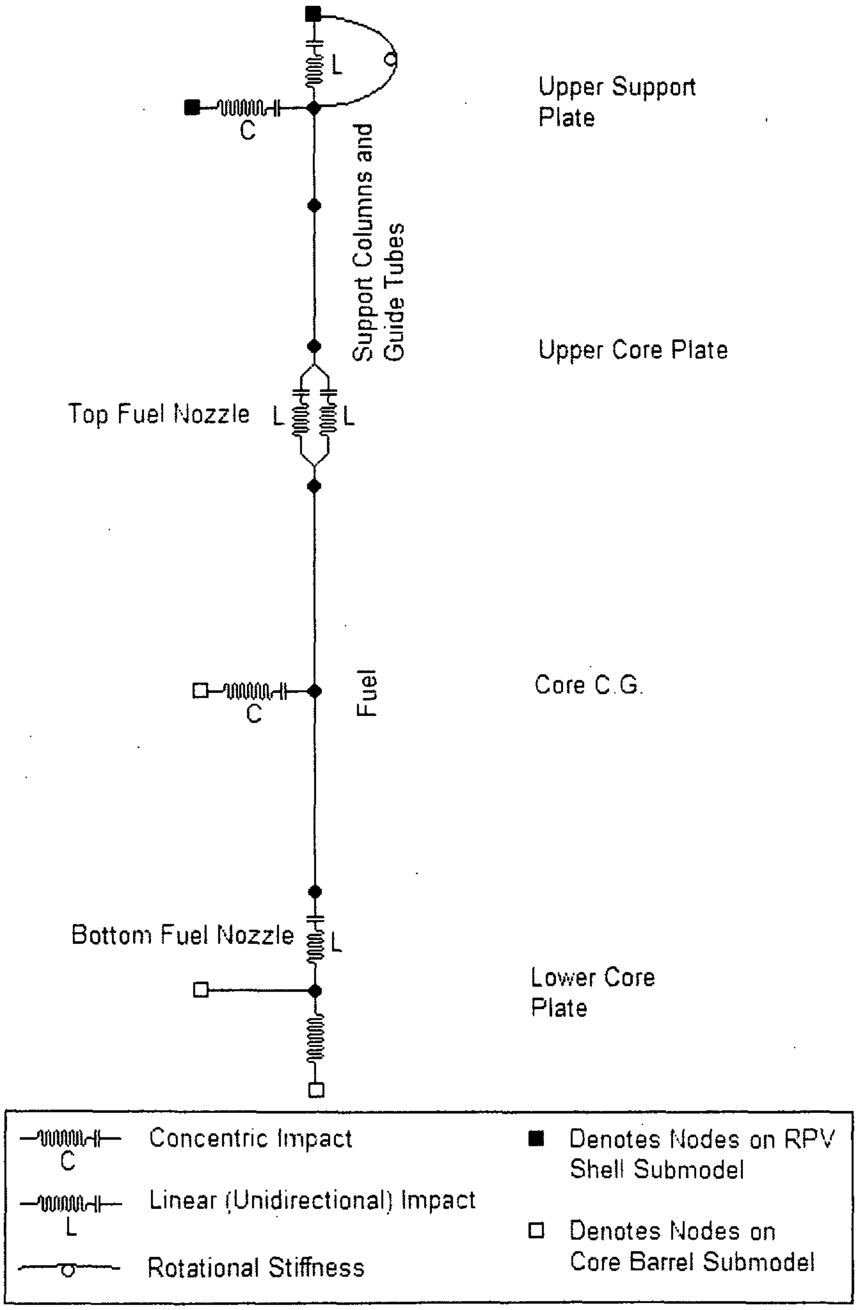

FSAR UPDATE

UNITS 1 AND 2
DIABLO CANYON SITE

FIGURE 3.7-27D

INTERNALS (INNERMOST) SUBMODEL

Revision 20 November 2011

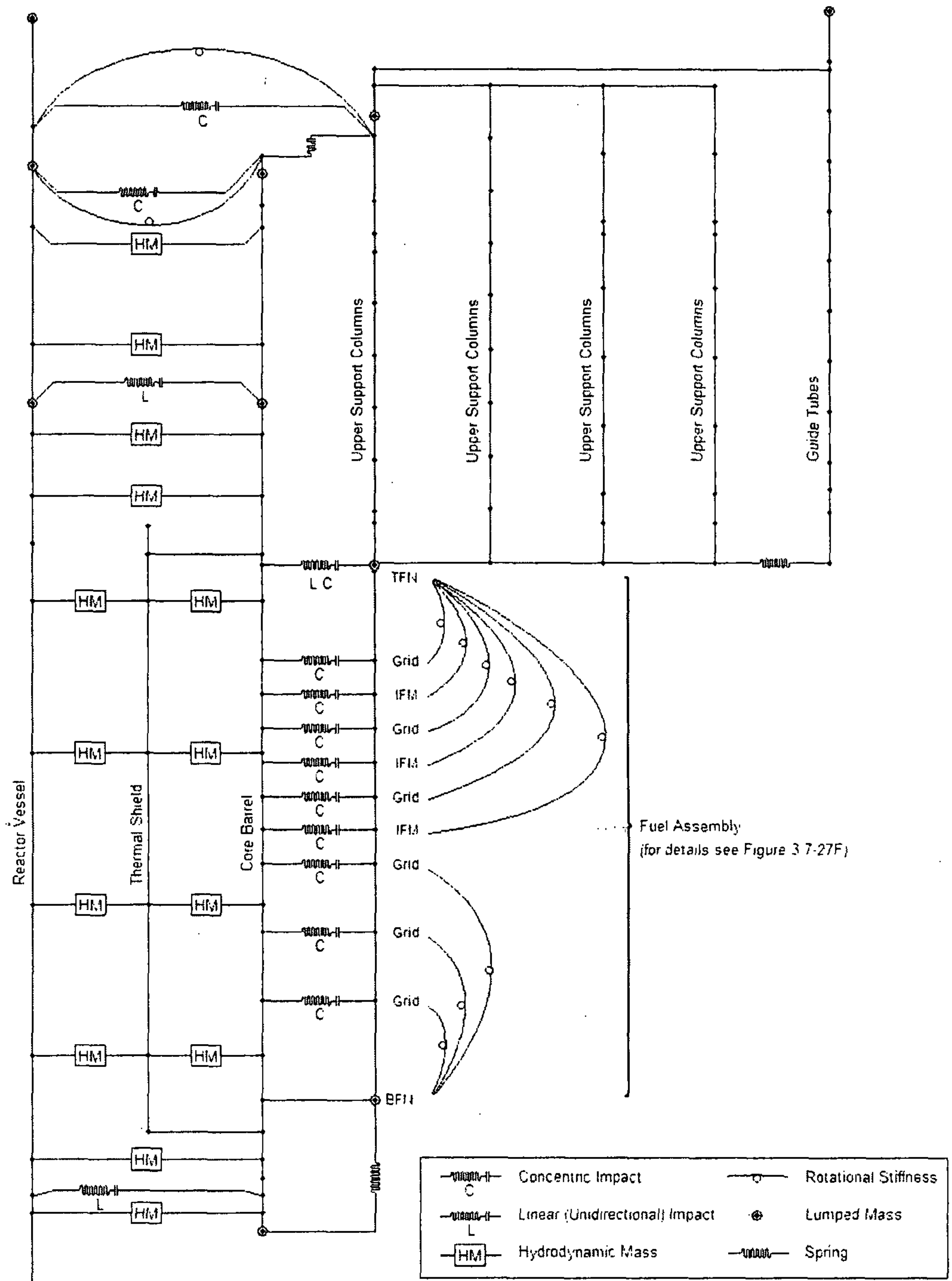

FSAR UPDATE

UNITS 1 AND 2
DIABLO CANYON SITE

FIGURE 3.7-27E

ASSEMBLED FINITE ELEMENT SYSTEM MODEL

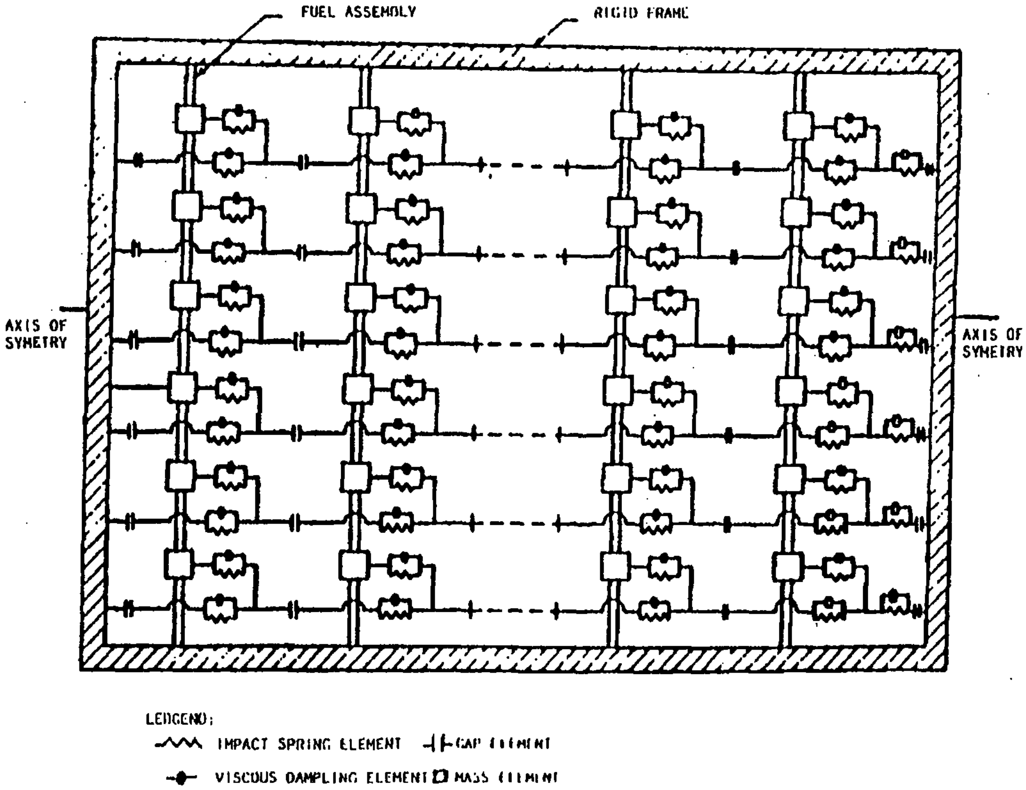

FSAR UPDATE
UNITS 1 AND 2 DIABLO CANYON SITE
FIGURE 3.7-27F SCHEMATIC REPRESENTATION OF COMPUTER MODEL USED TO ANALYZE CORE DYNAMIC RESPONSE

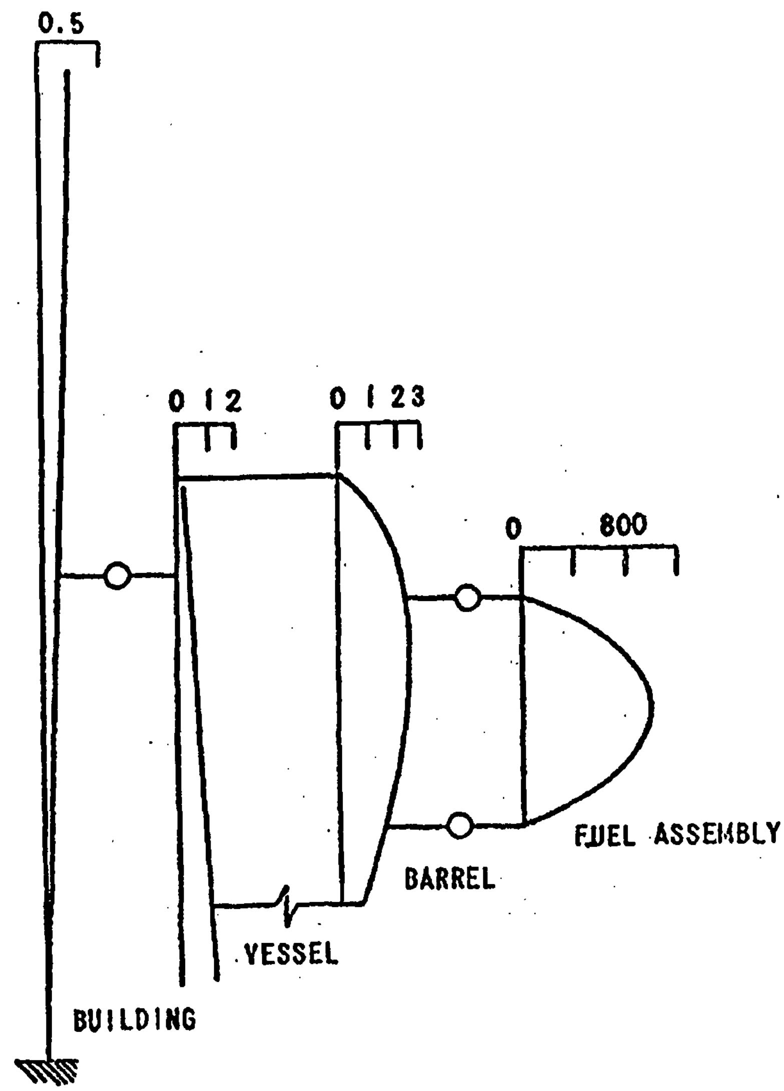

FSAR UPDATE
UNITS 1 AND 2
DIABLO CANYON SITE

FIGURE 3.7-28
REACTOR INTERNALS
FIRST MODE OF VIBRATION

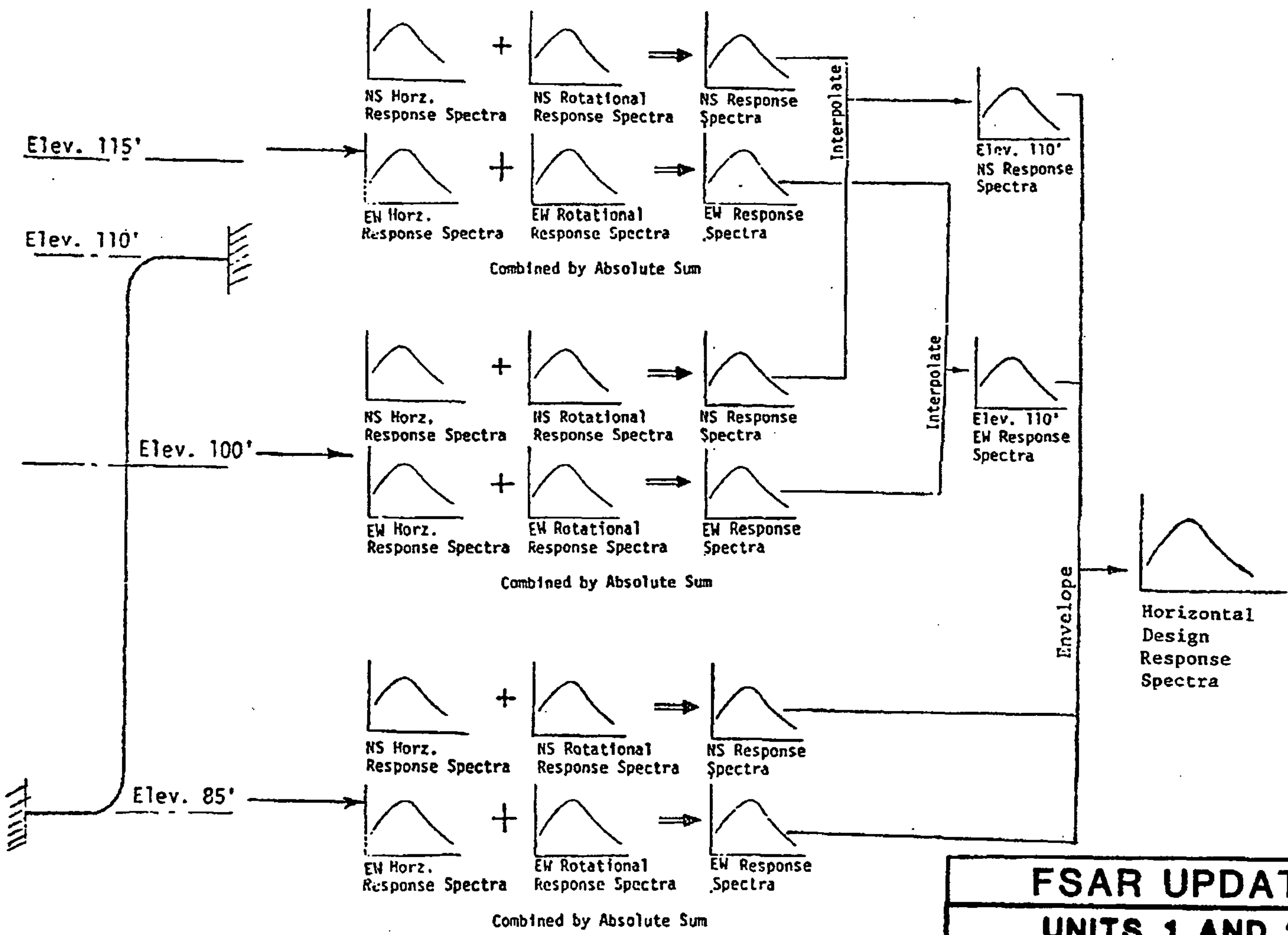

FSAR UPDATE

UNITS 1 AND 2 DIABLO CANYON SITE

FIGURE 3.7–29
DERIVATION OF
DESIGN RESPONSE SPECTRA
FOR A TYPICAL PIPING SYSTEM

3.8 DESIGN OF DESIGN CLASS I STRUCTURES

Figure 1.2-2 shows the location of all structures for DCPP Units 1 and 2. The design classification of plant structures is given in the DCPP Q-List (see Reference 8 of Section 3.2). In the Q-List, the following Design Class I structures are shown:

(1) Containment structure

(2) Auxiliary building

See Section 3.1 for discussion of the design of DCPP structures in conjunction with AEC General Design Criteria. The design of the containment structure is discussed in Section 3.8.1; the auxiliary building design is discussed in Section 3.8.2; and the Class I outdoor storage tanks, including the condensate storage, refueling water storage, and fire water tanks, are discussed in Section 3.8.3. The foundations and concrete supports of Class I structures are discussed in Section 3.8.4. Section 3.8.5 discusses the Design Class II turbine building and intake structure, both of which contain Design Class I equipment and components.

Note that the analytical results summarized in the following sections for the major plant structures are representative of the evaluations performed for the operating license review (Reference 31), but may not reflect minor changes associated with subsequent plant modifications.

3.8.1 CONTAINMENT STRUCTURE

3.8.1.1 Description of the Containment

The reactor containment for each unit is a steel-lined, reinforced concrete building of cylindrical shape with a dome roof that completely encloses the reactor and RCS. It ensures that essentially no leakage of radioactive materials to the environment would result even if gross failure of the RCS were to occur simultaneously with an earthquake of intensity twice the maximum postulated.

The containment structures for Units 1 and 2 are essentially identical, as mirror images. The following discussion applies to either unit:

The concrete outline and equipment locations are shown in Chapter 1. The exterior shell consists of a 142-foot-high cylinder, topped with a hemispherical dome. The minimum thickness of the concrete walls is 3.6 feet, and the minimum thickness of the concrete roof is 2.5 feet. Both have a nominal inside diameter of 140 feet and a nominal inside height of 212 feet. The concrete floor pad is 153 feet in diameter with a minimum thickness of 14.5 feet, with the reactor cavity near the center. The inside of the dome, cylinder, and base slab is lined with welded steel plate, which forms a leaktight membrane. The nominal thickness of the steel liner is 3/8-inch on the wall and dome and the nominal thickness of the steel liner on the base slab is 1/4-inch.

8/7

The containment is designed and will be maintained for a maximum internal pressure of 47 psig and a temperature of 271°F, coincident with a Double Design Earthquake.

The internal concrete structure approximates a 106-foot-diameter, 51-foot-high cylinder, with a slab on top. However, there are multiple openings and walls, such as the reactor support and the stainless steel lined refueling canal, which complicate the shape. The walls and top slab are generally 3 feet thick. This structure provides support for the reactor and components of the RCS, provides radiation shielding, and provides protection for the liner from postulated missiles originating from the RCS.

A polar crane is mounted on top of the internal concrete cylinder wall. The support of the polar crane, its connection to the concrete, and provisions to resist seismic forces are shown in Figure 3.8-23 and described in Section 9.1.4. Seismic analysis for the polar crane is discussed in Section 3.7.

The piping and electrical connections between equipment inside the containment structure and other parts of the plant are made through specially designed, leaktight penetrations. In addition to the piping and electrical penetrations, other penetrations are the 18-foot 6-inch diameter equipment hatch, the 9-foot 7-inch diameter personnel hatch, the 5-foot 6-inch diameter personnel emergency hatch, and the fuel transfer tube.

The 6-foot 7-inch by 13-foot ventilation duct is attached to the outside of the structure, extending from an elevation 25 feet above the base slab to the top of the dome. The duct is fabricated from steel plate with stiffeners.

A system of lightning rods is installed on the dome to protect against lightning damage.

The following paragraphs describe the various parts of the structure:

3.8.1.1.1 Exterior Shell

(1) *Reinforcing Steel*

The reinforcing steel arrangement is designed to provide continuous reinforcement for tensile and shear membrane forces in the cylinder and dome. The reinforcing in the cylinder wall consists of horizontal hoop bars, and inclined bars, oriented 60° from the horizontal. In Figure 3.8-1, layers (4) and (6) are the Number 18 hoop bars, spaced at 8-1/2 inches center-to-center vertically, and layers (3) and (5) are the inclined Number 18 bars spaced at 8-1/2 inches center-to-center, all spacing measured normal to the bars.

The dome reinforcing is accomplished by extending the inclined bars past the springline and over the dome. After crossing the dome, the same bar once again becomes an inclined bar in the cylinder. A layer (3) bar becomes a layer (5) bar after crossing the dome, as shown in

Figure 3.8-2. No inclined bars are terminated at the springline or in the dome.

The dome steel layout is based on the division of a sphere into 20 equilateral spherical triangles, as shown in Figure 3.8-3. At the springline, two sides of the triangles make an angle of 30° with the vertical. Thus, an inclined cylinder bar is parallel to the sides of the triangles at the springline. The inclined cylinder bars are extended into the dome so that they are always parallel to one side of a spherical triangle.

Figure 3.8-4 shows the five types of bars in the dome. When these five types are superimposed, there are three layers of reinforcing steel at every point above the pentagon ABCDE in Figure 3.8-3. Below pentagon ABCDE, the inclined bars make up two layers at every point, and bars similar to the cylinder hoop bars are used to provide reinforcing in the third direction.

Layers (1) and (2) (Figure 3.8-1) are inclined at 30° to the vertical and extend from the base slab to elevation 172 feet. These bars, spaced at 17 inches center-to-center, provide additional capacity to resist earthquake forces. Above elevation 170 feet, Number 4 bars are spaced at 12 inches center-to-center horizontally and vertically.

(2) *Splices*

All Number 18 bars are spliced by Cadwelding using "T-Series" sleeves, designed to develop the full tensile strength of the bar. As a general rule, splices are staggered a minimum of 3 feet.

For all penetrations except the equipment and personnel hatches, the Number 18 reinforcing bars are bent around openings. For the equipment and personnel hatch openings, a 2.5-inch-thick hexagonal collar, widened to 4 inches thick at the edges, is provided to transfer the reinforcing bar forces around the opening as shown in Figures 3.8-12 and 3.8-13. The reinforcing bars are Cadwelded to special studs threaded into the 4-inch edge of the hexagonal collar.

3.8.1.1.2 Liner

All liner seams are full penetration butt-welded, and are covered with steel channels welded to the inside of the structure. These "leak chase" channels provide a sensitive and accurate means of detecting leakage. They are arranged in zones so that one zone at a time may be pressurized to test the integrity of the liner plate welds.

The liner in the dome and cylinder wall is anchored by welded studs that extend into the concrete wall past the innermost layers of reinforcing steel. Three types of studs are used: a 3/8-inch diameter with an 8-1/2-inch shaft and a plain 4-inch "L" shaped arm, a

3/8-inch diameter with an 8-1/2-inch shaft and a threaded end, and a 1/2-inch diameter with an 11-inch shaft and a threaded end. All threaded studs are provided with an anchorage at the threaded end, and provide resistance to pullout that is equal to or greater than the 3/8-inch stud with a 4-inch arm. The studs are spaced a maximum of 19.6 inches on center (plus a placement tolerance of 1/2 inch) in a pattern that is compatible with the reinforcing steel, as shown in Figure 3.8-5.

For all penetrations in the exterior shell, a thickened plate is welded into the liner.

3.8.1.1.3 Penetrations

In general, a penetration consists of a sleeve embedded in the concrete wall and welded to the containment structure liner. The pipe, electrical conductor cartridge, duct, or access hatch passes through the embedded sleeve and one or both ends of the resulting annulus are closed off by welded end plates, bolted flanges, or flued heads. Typical electrical and piping penetrations are shown in Figures 3.8-6 through 3.8-10, and the fuel transfer tube penetration is shown in Figure 3.8-11. The penetrations are designed to maintain the same high degree of leaktight integrity afforded by the containment structure itself.

3.8.1.1.3.1 Electrical Penetrations

Electrical penetrations are either canister types or feed-through modules that allow electrical conductors to pass through the containment boundary. Penetrations are qualified for a single seal pressure boundary. The canister and feed-through modules are connected to the header plate, which is welded to the containment penetration sleeve. All penetrations are provided with a connection to allow periodic leak testing. The weld connecting the sleeve to the liner plate is provided with a leak chase channel for leak testing.

3.8.1.1.3.2 Piping Penetrations

Piping penetrations are provided for all piping passing through the containment boundary. Typical piping penetrations are shown in Figures 3.8-6 and 3.8-7. Several small pipes may pass through a single embedded sleeve to minimize the number of penetrations required. Welded end plates or flued heads are used to provide end closure. The welded joints are covered with a leak chase channel to allow periodic testing. The weld connecting the sleeve to the liner plate also has a leak chase channel.

Pipes carrying hot fluids through penetrations are designed to maintain the temperature of the concrete adjacent to the sleeve below 200°F under normal operating conditions.

Pipes and penetrations are anchored, as required, to resist the forces and movements incident at the penetration under normal and accident conditions, and to limit the loads imposed on the containment structure liner. Piping loads are transferred to the penetration sleeve and thence to anchors in the concrete wall rather than to the containment structure liner.

3.8.1.1.3.3 Equipment and Personnel Access Hatches

The equipment hatch is furnished with a double-gasketed flange and bolted dished door. Equipment up to a diameter of approximately 18 feet can be transferred into and out of the containment structure through this hatch. The hatch barrel is embedded in the containment structure wall and welded to the liner. Provision is made for pressurizing the space between the double gaskets of the door flanges and the weld seam leak chase channels at the sleeve-to-liner joint.

The two personnel hatches are double door, mechanically-latched, welded steel assemblies.

A quick-acting type equalizing valve connects each personnel hatch with the interior of the containment vessel for the purpose of equalizing pressure in the two systems when entering or leaving. The personnel hatch doors are interlocked to prevent simultaneous opening. Remote indicating lights and annunciators situated in the control room indicate the door operational status. Provision is made to permit bypassing the door interlocking system to allow doors to be left open during a plant cold shutdown. Each door hinge is capable of independent three-dimensional adjustment to assist proper seating. A lighting and communication system operating from an external supply is provided in the lock interior. Emergency access, to either the inner door from the containment interior, or to the outer door from outside, is possible by the use of special door unlatching tools. All doors on the personnel hatches are double gasketed and provided with fittings to allow pressurization of the space between the double gaskets.

3.8.1.1.3.4 Special Penetrations

(1) *Fuel Transfer Tube Penetration*

A fuel transfer tube penetration is provided for fuel movement between the refueling canal in the containment structure and the spent fuel pool. The penetration consists of a 20-inch-diameter stainless steel pipe installed inside a 24-inch-diameter pipe sleeve as shown in Figure 3.8-11. The inner pipe acts as the transfer tube and is fitted with a quick-opening hatch in the refueling canal and a standard gate valve in the spent fuel pool. This arrangement prevents leakage through the transfer tube in the event of an accident. The outer pipe is welded to the containment liner and provision is made, by use of a special seal ring to permit pressure testing all welds essential to the integrity of the penetration. Bellows expansion

joints are provided on the pipes to compensate for any differential movement between the two pipes or other structures.

(2) *Containment Supply and Exhaust Purge Ducts*

The ventilation system purge duct is equipped with two quick-acting tight-sealing valves (one inside and one outside the containment) to be used for isolation purposes. These valves are normally closed during reactor operation. They are manually opened for containment purging but are automatically closed upon a signal of high containment pressure or high containment radiation level. The space between the valves can be pressurized to check the integrity of the penetration. In addition, the shaft seals of the purge valves are equipped with double seals with provision for testing the space between.

(3) *Spare Penetrations*

Capped spare penetrations are provided. The welds between the sleeve and the liner and between the sleeve and the cap are covered with leak chase channels.

All spaces that are equipped for pressurization of penetrations and penetration sleeves are included in the same system of pressurization zones as the liner seam leak chase channels.

Several spare penetrations are also provided with capped, blind flanged or valved and capped end connections. These are 10 CFR 50 Appendix J Type B penetrations and are leak rate tested in accordance with Appendix J, Option B, as modified by approved exemptions.

(4) *Mini-Equipment Hatches (Penetrations 58 and 60)*

The mini-equipment hatch penetrations are provided to facilitate the passage of electrical cables and compressed air/water hoses into containment during refueling outages to support maintenance activities. Each of the two penetrations are comprised of flange connections on both sides of containment. The in-containment flanges are equipped with double O-Rings, which form a double containment isolation boundary. The in-containment blind flanges are provided with pressure test connections to permit pressure testing between the O-Rings. During plant outages, a temporary configuration is used to provide a containment pressure seal while the penetration blind flange is removed from service. Both the O-Rings and temporary blind flange assemblies prevent leakage through the penetrations in the event of an accident.

3.8.1.1.4 Base Slab and Shell-Base Slab Connection

The seams on the base slab and reactor cavity liner are full penetration butt-welded and are covered with leak chase channels. The leak chase channels are arranged in zones in the same manner as those on the exterior shell liner.

There are two penetrations through the base slab for recirculation lines. These are similar to penetrations used in the exterior shell. Weld seams between the liner and the penetration sleeve and between the penetration sleeve and internal, are covered with leak chase channels. The volume in the end of the penetration internal has a fitting for pressurization. These leak chase channels and the volume in the end of the penetration internal are connected in the zones of pressurization used for liner leak chase channels.

The detail of the shell-base slab connection is shown in Figure 3.8-14. The vertical wide flange steel beams provide a gradual transition of load carrying elements between the base slab and the cylinder, and resist the radial bending moments and shears. The beams are keyed and grouted in a groove at the base slab and extend approximately 20 feet up the wall. They do not participate in resisting either uplift due to pressure, or shear and tension forces due to earthquake.

The 3-foot 8-inch thick cylinder wall is designed to offer minimum bending resistance at the junction with the base slab. To achieve this the wall is divided into three layers, with the contact surface between the layers designed as a slip surface. The 12-inch inner layer, next to the liner plate, provides stiffness to the liner plate. The L-shaped stud anchors, welded to the liner plate, and layers (1) and (2) of the wall reinforcing bars are in this layer. The middle layer is the wide flange steel beams. The voids between the beam webs are filled with concrete. The outer layer is 20 inches thick. Layers (3) through (6) of the wall reinforcing bars are in this layer. The slip surface between layers is provided by covering both flanges of the steel beams with two sheets of Johns-Manville #60 asbestos sheet packing. This packing is graphite coated on one side, and the two sheets are placed with the graphite-coated sides in contact. PG&E has successfully used this means of providing sliding supports on penstock piers for several years. The inert nature of the material, and the fact that it is completely isolated from the atmosphere by a minimum of 20 inches of concrete, combine to ensure that it will be fully effective throughout the lifetime of the plant.

The detail at the bottom of each of these three layers is shown in Figure 3.8-14. The innermost and outermost layers have a 1-inch neoprene pad to allow slight rotation without crushing of the concrete. The center layers, consisting of the beams, have a 5-inch-deep pocket in which the beams are placed and grouted.

The diagonal wall reinforcing extends to the bottom of the base slab for anchorage, as shown in Figure 3.8-15. The base slab bars are bent up at 45° and passed through the diagonal bars. The ends of the base slab bars are provided with a mechanical anchorage consisting of a Cadweld sleeve and a steel plate.

The shell liner is anchored to the base slab by Number 14 rebar welded to the bottom course liner plate, which is 3/4-inch-thick. These rebars are embedded 8-1/2 feet in the base slab concrete.

3.8.1.1.5 Internal Structure

The internal structure that is shown in Figures 3.8-16 through 3.8-22 consists of the following parts:

(1) The lower operating floor at elevation 91 feet is a 2-foot-thick concrete slab placed over the containment structure base slab liner.

(2) The circular crane wall is a 3-foot-thick, 106-foot-OD reinforced concrete wall, concentric with the exterior shell, and extending vertically from the containment structure base slab liner at elevation 89 feet to the main operating floor at elevation 140 feet. The runway for the 200-ton polar gantry crane is located on top of the circular crane wall. This wall is anchored to the containment structure base slab by Number 18 reinforcing bars. This anchorage is developed through the containment structure base slab liner by means of Cadweld sleeves welded to each side of the liner at the same locations. The polar crane is shown in Figure 3.8-23.

(3) The reactor shield wall is a 34-foot-OD, 17-foot-ID reinforced concrete wall. This wall is anchored to the containment structure base slab in the same manner as the circular crane wall.

(4) The fuel transfer canal is a stainless steel lined cavity that can be filled with water during refueling. The vertical walls of the fuel transfer canal are 4 feet thick.

(5) The main operating floor at elevation 140 feet is a 3-foot-thick concrete slab supported by the circular crane wall and the fuel transfer canal walls. This slab is thickened locally up to 7 feet near openings.

(6) Main steam line restraint towers are reinforced concrete buttresses extending from the main operating floor at elevations 140 to 184 feet.

(7) Annulus platforms are structural steel platforms at elevations 117 and 140 feet, located between the circular crane wall and the exterior shell. Steel framing is also provided at elevations 106 feet 8 inches and 101 feet 5 inches for support of piping. Figures 3.8-21 and 3.8-22 provide the structural steel framing details for these platforms.

3.8.1.1.6 Polar Crane

The polar crane structural steel frame consists of:

(1) Two main box girders 120 feet long, 10 feet deep and 4 feet wide, spaced 24 feet apart

(2) Four gantry legs, 52 feet long and made of tapered box sections supporting the girders

(3) Two sill beams, 28 feet long with box sections to connect the gantry legs

(4) Four tie beams connecting main girders and gantry legs

The arrangement as described above is shown in Figure 3.8-23.

The sill beams are supported by two wheel assemblies each and are restrained by guide struts. These struts allow the wheels to uplift during a seismic event but guide the wheels back on to the rail.

3.8.1.2 Applicable Codes, Standards, and Specifications

3.8.1.2.1 Codes and Standards

The following codes and standards were used, insofar as they are applicable, in the design and/or construction of the containment structure:

(1) ACI Standard Building Code Requirements for Reinforced Concrete (ACI 318-63)

(2) Manual of Standard Practice for Detailing Reinforced Concrete Structures (ACI 315-65)

(3) Recommended Practice for Evaluation of Compression Test Results of Field Concrete (ACI 214-65)

(4) Inspection of the Cadweld Rebar Splice (Erico Products, Inc., RB-5M 768)

(5) Recommended Practices for Welding Reinforcing Steel, Metal Inserts, and Connections in Reinforced Concrete Construction, American Welding Society, AWS D 12.1-61

(6) AISC Specification for the Design, Fabrication, and Erection of Structural Steel for Buildings, February 12, 1969

(7) Construction of the containment structure liner conforms to the applicable parts of Part UW, "Requirements for Unfired Pressure Vessels Fabricated by Welding," Section VIII, ASME Boiler and Pressure Vessel Code, 1968 Edition, including Addenda through Summer 1968

(8) Those parts of penetration insert plates, penetration sleeves, airlocks, and access hatches, which form part of the pressure boundary, conform to Class B requirements of Section III, ASME Boiler and Pressure Vessel Code, 1968 Edition, including Addenda through Summer 1968

(9) Code for Welding in Building Construction, AWS D 1.0-69. Work performed prior to December 12, 1969 is in accordance with the earlier edition, AWS D 1.0-66. For inspection of non-ASME structural welds or new non-ASME work performed after January 1, 1988, the guidelines of Nuclear Construction Issues Group (Visual Weld Acceptance Criteria, Vol. 1-3, EPRI Report No. NP-5380, September 1987) (Reference 27) may be used except for those cases where:

   (a) Fatigue is a governing design condition

   (b) The weld allowables are permitted to be higher than those allowed by AWS D1.1 (such as the full penetration welds evaluation for the HE)

   (c) The weld is part of work performed in the ASME Section XI Inservice Inspection Program.

(10) Stud welding is in accordance with the Supplement to American Welding Society Specifications AWS D 1.0-66 and AWS D 2.0-66 on Requirements for Stud Welding

(11) Materials, and the quality control tests for materials conform to ASTM standards

(12) Pressure tests of the containment structure, leak chase channels, double penetration volumes, volumes between double seals, and volumes between double isolation valves are in accordance with the requirements of ANSI N45.4-1972, Leakage Rate Testing of Containment Structures for Nuclear Reactors, dated March 16, 1972

(13) SG 12, Instrumentation for Earthquake, dated March 10, 1971

(14) SG 18, Structural Acceptance Test for Concrete Primary Reactor containments, dated October 27, 1971

(15) ASME Section III, Division 2, 1980

(16) ASME Section III, Division 1, Subsection NE, 1974

(17) American Petroleum Institute (API) Code 650, Welded Steel Tanks for Oil Storage

(18) United States of America Standards Institute (USASI) - N6.2 Safety Standard for the Design, Fabrication and Maintenance of Steel Containment Structures, for Stationary Nuclear Power Reactors

3.8.1.2.2 Regulatory Guides

The following guidance documents were issued after construction at the DCPP was partially completed:

(1) SG 10, Mechanical (Cadweld) Splices in Reinforcing Bars of Concrete Containments, dated March 10, 1971

(2) RG 1.15, Testing of Reinforcing Bars for Category I Concrete Structures, dated December 28, 1972

(3) SG 19, Nondestructive Examination of Primary Containment Liner Welds, dated August 11, 1972

(4) RG 1.55, Concrete Placement in Category I Structures, dated June 1973

Because the corresponding programs for the DCPP were conservatively formulated, the inspection provided essentially equals, and in many cases exceeds, that provided by the regulatory position in the guides. Detailed comparisons of the program used for the DCPP with the regulatory position of RG 1.15, SG 10, and SG 19 are presented in Tables 3.8-1 through 3.8-3, respectively. The quality assurance program for the DCPP meets the requirements of RG 1.55. In regard to RG 1.55, the references used for guidance are those listed in Appendix A of the RG, as they existed at the time of the Preliminary Safety Analysis Report (PSAR).

3.8.1.2.3 ACI-ASME for Containments

The technical requirements of the code (Reference 3) were derived from the Building Code Requirements for Reinforced Concrete (ACI 318-71), from Section III, Division 1, of the ASME Boiler and Pressure Vessel Code, and from other codes and standards commonly applied to containment structure design, fabrication, and examination. The requirements for the DCPP containment structures are based on those same codes and standards, except that in many cases an earlier edition was applied to DCPP.

Tables 3.8-1, 3.8-2, and 3.8-3 compare the DCPP programs for reinforcing steel, Cadweld splices, and nondestructive examination of the liner with the regulatory position in RG 1.15, SG 10, and SG 19, respectively.

The general requirements of the code require third party inspection for all containment structure fabrication and construction. For DCPP, third party inspection was provided for fabrication and installation of all containment structure penetrations in accordance with the Class B requirements of Section III, ASME Boiler and Pressure Vessel Code.

3.8.1.3 Loads and Loading Combinations

3.8.1.3.1 Design Loads

The following loads were considered in the design of the containment structure:

3.8.1.3.1.1 Dead Loads

Dead loads consist of the weight of concrete, reinforcing steel, steel liner, structural steel, and permanent equipment loads. Equipment loads are supplied by the manufacturers.

3.8.1.3.1.2 Live Loads

Live loads consist of temporary equipment loads and a uniform load to account for the miscellaneous temporary loadings that may be placed on the structure.

3.8.1.3.1.3 Internal Pressure Due to Loss-of-Coolant Accident

The design peak internal pressure used for design purposes is 47 psig, which is greater than any of the peak pressures calculated in the detailed analysis reported in Chapter 6.

For design purposes, a maximum pressure differential of 15 psi due to the hypothetical LOCA was assumed to exist between the volume within the circular crane wall and the surrounding containment structure volume. The pressurizer enclosure maximum pressure differential was assumed to be 4 psi due to the vent openings provided. These values are greater than the values calculated in the detailed analysis reported in Chapter 6.

3.8.1.3.1.4 Loads Due to Thermal Expansion

These are loads resulting from the internal temperatures associated with normal operation and the hypothetical LOCA. The maximum internal atmospheric temperature during normal operation is 120°F. The temperature transients associated with the LOCA pressure and temperature are shown in Appendix 6.2C of this FSAR Update. The analyses of Appendix 6.2C correspond to a design load factor of 1.0. To determine the temperature transients for load factors equal to 1.25 and 1.5, steam tables are used.

3.8.1.3.1.5 Loads Due to Postulated Pipe Ruptures and Missile Impact

Design of the internal structure includes calculation of the effects of forces from postulated pipe ruptures transmitted through pipe restraints and equipment supports, jet forces for postulated pipe ruptures, and forces resulting from postulated missile impact. The forces from postulated pipe ruptures are calculated as described in Section 3.6. The forces from postulated missile impact are calculated as described in Section 3.5.

3.8.1.3.1.6 Earthquake Loads

Earthquake loads are based on a time-history modal superposition analysis of the containment structure and surrounding rock mass, as appropriate, as described in Section 3.7.2.

3.8.1.3.1.7 Wind Loads

Wind loads are determined in accordance with the criteria presented in Section 3.3.

3.8.1.3.1.8 Test Pressure

Internal pressure is applied to test the structural integrity of the containment vessel up to 115 percent of the design pressure. For this structure, the test pressure is 54 psig.

3.8.1.3.1.9 Negative Pressure

Negative pressure consists of loading from an internal negative pressure of 3.5 psig. This negative pressure has taken into account the Technical Specification limit on lower bound containment pressure and on inadvertent containment spray actuations, which would result in a 70°F temperature decrease.

3.8.1.3.1.10 Crane Operating Loads

Crane-operating loads include:

(1) Live load impact = (LI) = 0.2L

(2) Lateral operating load = (LAT) = 0.1 (L+TD)

(3) Longitudinal operating load = (LONG) = 0.1 (L+TD)

where:

L = Crane rated live load
TD = Trolley dead weight

3.8.1.3.2 Loading Combinations

The following loading combinations are used in design of the containment structure elements.

3.8.1.3.2.1 Operating Conditions

(1) Exterior Structure and Base Slab

Dead load, thermal load, DE, and negative pressure are considered as follows:

$$C = D + T_O + DE + NP \tag{3.8-1}$$

where:

C	=	required capacity of section based on the methods described in Section 3.8.1.5.1
D	=	dead load of structure and equipment loads
T_O	=	thermal loads during normal operating conditions
DE	=	loads resulting from the DE
NP	=	load due to negative pressure

(2) Internal Structure

For concrete structures, dead load, live load, thermal load, and DE load are considered as follows:

$$C = D + L + T_O + DE \tag{3.8-2}$$

For annulus steel structures, the load combinations are:

$$C = D + T_O + TH + FL \tag{3.8-3}$$

$$C = D + T_O + TH + FV + RVOT + DE \tag{3.8-4}$$

where:

FL	=	friction loads applied in the direction of thermal movements
FV	=	fast valve closure load
L	=	live load
RVOT	=	relief valve opening thrust load
TH	=	restrained thermal loads of the supported piping

(3) Polar Crane

C = D + TD + L + LI

C = D + TD + L + LAT

C = D + TD + L + LONG

C = D + TD + DE

3.8.1.3.2.2 Accident Conditions

(1) Exterior Shell and Base Slab

$$U = 1.0D \pm 0.05D + 1.5P_A + 1.0T'' \quad (3.8\text{-}5)$$

$$U = 1.0D \pm 0.05D + 1.25P_A + 1.0T' + 1.25DE \quad (3.8\text{-}6)$$

$$U = 1.0D \pm 0.05D + 1.0P_A + 1.0T + 1.0DDE \quad (3.8\text{-}7)$$

$$U = 1.0D \pm 0.05D + 1.0P_A + 1.0T + 1.0HE \quad (3.8\text{-}8)$$

where:

U	=	required load capacity of section based on the methods described in Section 3.8.1.5.2
P_A	=	load due to accident pressure
T	=	load due to maximum temperature associated with $1.0P_A$
T'	=	load due to maximum temperature associated with $1.25P_A$
T"	=	load due to maximum temperature associated with $1.5P_A$
DDE	=	loads resulting from the DDE
HE	=	loads resulting from the HE

(2) Internal Structure

For concrete structures, dead load, live load, earthquake load, compartment pressurization, pipe reactions associated with a postulated pipe rupture, jet forces, and missile loads are considered wherever occurring as follows:

$$U = D + L + DDE + CP + R + J + M \quad (3.8\text{-}9)$$

$$U = D + L + HE + CP + R + J + M \quad (3.8\text{-}10)$$

For annulus steel structures, the load combinations are:

U = D + DDE + THA + FV + RVOT (3.8-11)

U = D + HE (3.8-12)

where:

CP	=	compartment pressurization associated with a pipe break
R	=	pipe reactions associated with a postulated pipe rupture
J	=	jet impingement load
M	=	missile impact load
THA	=	restrained thermal expansion loads of the supported piping

(3) Polar Crane

U = D + TD + DDE + T_O

U = D + TD + L + HE

where:

T_O	=	thermal load induced by the temperature differential between the crane structure and supporting concrete structure, during operating condition
U	=	capacity of the section as determined from an increase of allowable stresses by a factor of 1.7

3.8.1.4 Design and Analysis Procedures

3.8.1.4.1 Analysis of Containment Cylinder and Dome

For the loading conditions described in Section 3.8.1.3.2, the exterior wall is subjected to membrane forces and moments. These forces and moments are shown in Figures 3.8-27 through 3.8-34, and have been calculated based on the overall elastic behavior of containment exterior wall and dome in accordance with the conventional close form solution. An exception is that at the juncture of cylinder wall and base slab, the meridional moment and shear forces are computed as described in Section 3.8.1.3.1.4.

The stresses in the reinforcing steel and concrete subject to the above membrane forces and moments are computed by assuming that the concrete cracks under tension. This involved resolving compatibility and equilibrium equations by an iterative method. The stress analysis is performed with two sets of assumptions: (a) the effect of the liner plate is neglected, and (b) the liner plate is included as a stress-carrying element. Since

the thicknesses of the cylinder and dome are small in comparison with the radii of curvature, they are analyzed as a thin walled shell structure.

(1) *Internal pressure and dead load*

The calculated membrane forces due to axisymmetric loads, such as internal pressure and dead load, are shown in Figure 3.8-27.

(2) *Earthquake*

Membrane forces are from the finite element, time-history modal superposition analysis described in Section 3.7.2. The plots of these membrane forces in the cylinder and dome due to the DE, DDE, and HE are shown in Figures 3.8-28 and 3.8-29, respectively. Shear forces in the dome due to the vertical input were calculated. Vertical input produces only radial shear, but no membrane shear. Radial shears were negligible when compared to membrane shears.

(3) *Wind*

Membrane forces from wind are shown in Figure 3.8-34. These are less than the membrane forces due to an earthquake.

(4) *Temperature*

Temperature loads are considered thermal gradients in the reinforced section, including the liner plate. The analysis procedure for thermal load is described in Section 3.8.1.4.4.

The combined membrane forces for the four accident loading conditions are shown in Figures 3.8-30, 3.8-31, 3.8-32, and 3.8-33.

3.8.1.4.2 Liner Anchors

The liner anchors are designed so that they have sufficient strength and flexibility to withstand any combination of liner stress and deformation that can be reasonably assumed to occur under accident loading conditions. The liner plate system is evaluated by developing allowable loads for attached threaded studs to support the mechanical or piping system. The load transfer mechanism from the external mechanical loads through the liner plate to the concrete stud system is developed to ensure the transfer of all loads into the concrete shell with all elements remaining elastic, while maintaining the leaktight boundary.

The concrete anchors are capable of accommodating the displacement of the liner plate under the operating and accident loading conditions.

3.8.1.4.3 Equipment and Personnel Hatch Openings

Membrane forces are transferred around the equipment hatch and personnel hatch openings by means of hexagonal-shaped steel collars to which the reinforcing steel is attached.

The analysis of the equipment hatch and personnel hatch openings takes into account the following:

(1) Direct membrane forces in the shell

(2) Force concentrations in the shell

(3) Bending effect in the shell

The area of the containment shell adjacent to the opening is extended beyond the opening far enough to make the effects of the opening negligible. This area is represented by a finite element mesh consisting of three parallel layers of plate elements which are interconnected by transverse beam elements representing the transverse normal and shear stiffness of concrete wall. The outer surface represents the hexagonal plate and outside reinforcement, the inner surface represents the sleeve, the liner plate and the inner reinforcement, and the intermediate layer represents the additional reinforcement around the opening. The hexagonal plate, sleeve, and liner plate are modeled by isotropic plate elements, and the reinforcement by orthotropic elements, in which the principal directions coincide with the directions of the reinforcement. The stiffness of concrete in the membrane directions is not included, because under tension the concrete is assumed to be cracked. The finite element model is shown in Figure 3.8-35. The analysis is performed by using BSAP/CE 800 computer program.

For axisymmetric loading, the vertical boundaries are restrained in the hoop direction. For the application of tangential shear force, the lower horizontal boundaries are restrained in the vertical and tangential directions. The vertical movement of the lower horizontal boundary is always restrained.

The internal pressure is applied to a large area of the shell wall adjacent to the opening and on the hatch. Since the hatch is not a part of the model, this pressure is transferred to the nodal point around the opening as nodal loads. The pressure on the containment shell and the nodal loads around the opening are applied in the radial direction. By examining the equilibrium of the sector of the wall isolated for modeling, having boundary conditions as described above, hoop membrane forces are induced to the model at the boundary conditions in which the following equation of equilibrium is met:

$$N\Theta = pR \qquad (3.8\text{-}13)$$

where:

$N\Theta$	=	hoop force
p	=	internal pressure
R	=	radius of cylinder

The isostress plots are shown in Figures 3.8-40 through 3.8-42. These stresses are the results of the load combination shown by Equation 3.8-5, which controls the stress evaluation.

3.8.1.4.4 Juncture of Cylinder and Base Slab

At the base of the cylinder, radial expansion from internal pressure is considered compatible with the stiffness of the base slab. In this region, the cylinder undergoes a transition from a very small radial displacement at the base slab to full membrane displacement a short distance up from the base slab. This displacement results in longitudinal curvature in the cylinder.

A system consisting of structural steel wide flange beams, embedded in the bottom 20 feet of the concrete cylinder wall and keyed into the base slab, as shown in Figure 3.8-14, provides radial shear strength. These structural steel beams are located continuously around the circumference of the cylinder and provide bending and shear strength adequate to ensure the integrity of the wall in the transition region.

3.8.1.4.5 Base Slab

The containment base slab is evaluated by performing static analysis of the model shown in Figure 3.8-43. The model is divided into discrete segments represented by beam elements in the two horizontal directions, which simulate the two way action of the base slab. The interconnecting nodal points are supported by horizontal and vertical springs which represent the properties of the underlying foundation rock. The horizontal and vertical stiffness of the containment shell, crane wall, and the reactor cavity are also represented by beams in the respective directions. The base slab model is analyzed for load combinations pertaining to the containment exterior structure as described in Sections 3.8.1.3.2.1 and 3.8.1.3.2.2.

The seismic loads resulting from the containment and the interior structures are applied at the appropriate nodal points. When these loads cause tension at the supports, the springs are released and an iterative analysis is performed until equilibrium is achieved. The results of the analyses are shown in Table 3.8-4, along with the corresponding allowable values.

3.8.1.4.6 Internal Structure

3.8.1.4.6.1 Concrete Structure

The principal structural features and design methods of the containment internal concrete structure are as follows:

The operating deck at elevation 140 feet is supported by the 3-foot-thick, 106-foot-OD circular crane wall, 4-foot-thick fuel transfer canal walls, and structural steel columns placed on the periphery next to the containment wall. The slab within the circular crane wall is, in general, 3 feet thick. Because of irregular shape, it is represented by approximate models with negative moments based on clamped edges and positive moments based on hinged edges. Because of large openings, it was necessary to thicken parts of the slab to 7 feet, and these parts are treated as beams spanning between the circular crane wall and fuel transfer canal walls. Outside the circular crane wall the operating deck consists of a 1-foot 6-inch-thick concrete slab supported on the circular crane wall and on steel beams on the periphery; steel grating is placed over steel beams. Lateral forces are transmitted to the circular crane wall through diaphragm action of concrete slabs. The circular crane wall provides support for the operating floor at elevation 140 feet and also acts as a primary system transmitting lateral loads into the base.

3.8.1.4.6.2 Annulus Structure

The principal structural features and design methods of the annulus structure are:

The structure consists of four main framing levels at elevations 140, 117, 106, and 101 feet. This framing system is located between the circular crane wall and the containment exterior shell. The operating deck at elevation 140 feet consists mainly of a 1-foot 6-inch-thick concrete slab supported on the circular crane wall and on steel beams by columns on the periphery near the exterior containment shell. Portions of the floor consist of steel grating supported on steel beams.

The framing system is anchored to the crane wall which provides all lateral support; lateral forces are transmitted to the circular crane wall through diaphragm action of the concrete slab at elevation 140 feet, and by structural framing system at other floor elevations. Vertical support is provided by the crane wall around the inner perimeter and by the concrete base slab at elevation 90.5 feet around the outer perimeter of the annulus. The annulus framing system is not attached to the exterior shell of the containment.

The annulus structure is modeled into a three-dimensional computer model and is analyzed by the BSAP and GT STRUDL computer programs for Units 1 and 2, respectively, using a method of equivalent static loads to represent seismic forces. Stresses in internal structure of containment building, including selected structural steel elements in the annulus framing system, are listed in Table 3.8-5.

3.8.1.4.7 Polar Crane

The polar crane is analyzed using a conventional frame analysis technique. The seismic analysis is described under Section 3.7.

3.8.1.4.8 Computer Programs

The main computer programs used for static and dynamic analyses of containment structure are listed in Table 3.8-6. The table also describes the general function of the programs and their respective verification measures.

3.8.1.5 Structural Acceptance Criteria

The structural acceptance criteria for the containment structure exterior shell and internal structure are as follows:

3.8.1.5.1 Operating Conditions

For operating conditions, the containment structure is designed for the allowable stresses of the applicable code such as ACI 318-63, AISC Specification for the Design, Fabrication, and Erection of Structural Steel for Buildings, and ASME Boiler and Pressure Vessel Code, except that the increase in allowable stress or decrease in load factor usually allowed for load combinations involving earthquake or wind forces is not used.

3.8.1.5.2 Accident Conditions

For accident conditions, the containment structure is designed for overall elastic behavior under all load combinations, except at the juncture of containment exterior wall and base slab where inelastic analysis was performed by taking into consideration cracking of concrete under tension.

For structural elements designed by strength method, the yield stress of the material is reduced by ϕ factors, which are determined as follows:

Exterior shell reinforcing, structural steel embedded in exterior shell, and liner plate	$\phi = 0.95$
Other structural steel	$\phi = 0.90$[a]
Reinforced concrete in base slab and internal structure	ϕ factor in accordance with ACI 318-63

[a] See footnote in discussion of loading combinations in Section 3.8.2.

The yield strength values of material under a non-Hosgri event are governed by the following codes:

Reinforced concrete	ACI 318-63
Structural steel	AISC
Hexagonal collars of equipment and personnel hatches	ASME Sect. III, Div. 2, and ASME Sect. III, Div. 1
Penetration sleeves	ASME Sect. III, Div. 1
Liner plate	Table CC-3720-1[b] ASME Sect. III, Div. 2

The yield strength of steel and the ultimate strength of concrete for the HE are taken as the average values of properly substantiated test results. However, in no case are the yield values used in strength computations of structural steel greater than 70 percent of the corresponding average ultimate strength values determined by the tests. The ϕ factors described above are still applicable in the HE. The average strength values for concrete are shown in Table 3.8-6A. The minimum and average yield and ultimate strength values for reinforcing and structural steel are shown in Table 3.8-6B.

For structural steel and concrete elements designed by normal working strength method, the allowable stresses determined by AISC and ACI 318-63 codes, respectively, are increased by 1.6 for the DDE and 1.7 for the HE, except for shear in structural steel which is determined by the Von Mises criterion as outlined in the commentary of AISC.

3.8.1.5.3 Factors of Safety

The factors of safety for the exterior shell and internal structure of the containment structure are at least as great as indicated by the load factors given in Section 3.8.1.3.2. The calculated stresses for the exterior shell are given in Figures 3.8-37 through 3.8-39, and the calculated stresses for the internal structure are given in Table 3.8-5.

Separations between the containment structure and the auxiliary building are adequate to ensure these structures will not impact each other when subject to design load combinations. Calculated displacements, separations, and factors of safety against impact are shown in Table 3.8-5B.

The relative seismic displacements between the containment structure exterior shell and the internal structure have been calculated as the sum of the maximum seismic displacement of each structure. Except for a few localized areas, the minimum cold gap

[b] Table CC-3720-1 is referred to establish acceptable design strain levels for the liner plate. The construction of the liner plate is pursuant to the specifications of Section 3.8.1.2.1(7).

between the internal structure and the exterior shell is 2 inches. The factors of safety against contact for all areas, including the localized areas, are greater than 2.33 for the governing seismic event, the DDE, after thermal effects on the gap are considered. The calculated factors of safety for the HE are greater than those for the DDE.

3.8.1.6 Materials, Quality Control, and Special Construction Techniques

During the first 16 months of construction, a PG&E civil engineer was assigned to the construction site on a full-time basis. This engineer was familiar with, and had participated in, the design of the containment structure. For the period he was on site, he was part of the Quality Assurance Department (described in Chapter 17) and his responsibilities included performing audits on the various construction quality assurance programs. This engineer was qualified as ANSI Level II for radiographic, magnetic particle, ultrasonic, and dye penetrant methods of nondestructive testing. In addition, other engineers from PG&E who were involved in the design of the containment structure maintained daily contact with the site by telephone calls, and made periodic visits to the site during construction.

Inspectors from PG&E's engineering staff performed regularly scheduled shop inspections on materials and components for the containment structure.

PG&E's construction staff provided a complete staff of resident engineers, field engineers, quality control engineers, and inspectors for supervision and inspection of construction operations at the site. Their responsibilities for quality control of the containment structure were as follows:

(1) To inspect materials delivered to the jobsite and examine supplier's certified test reports of physical and chemical properties

(2) To inspect handling and placing of concrete, reinforcing bars, embedded items, and forms

(3) To maintain an adequate force of qualified supervisory personnel at all times

(4) To maintain qualified personnel, as a part of its field engineering force, to perform a thorough inspection of each significant construction operation

(5) To supervise and be fully responsible for the quality of work performed by contractors

(6) To maintain records of inspections that were performed

Many of PG&E's construction personnel at the site attended a formal course of instruction in radiographic, magnetic particle, ultrasonic, and dye penetrant methods of

nondestructive testing. PG&E technicians staffed the onsite materials laboratory where tests on cement, aggregate, concrete, and reinforcing steel were performed.

3.8.1.6.1 Concrete

Concrete is a dense, durable mixture of sound aggregate, cement, water, and such admixtures as may be found advantageous. The concrete design strengths used in the containment structure are:

Exemption 4

Exterior Shell	3,000 psi
Base Slab	5,000 psi
Internal Structures	5,000 psi

The concrete compressive strength and the modulus of elasticity values used in the analysis for load combinations, including the HE, are given in Table 3.8-6A.

Concrete construction meets, as a minimum, the requirements of ACI 318-63, Building Code Requirements for Reinforced Concrete.

(1) *Cement*

Cement is clean, fresh, Type II, low alkali, moderate heat, Portland cement conforming to the specifications of ASTM C 150, except that the PG&E specification is more stringent in requiring that the compressive strengths for any mill-run or bin be not less than 1,700 psi at 3 days, 2,700 psi at 7 days, and 4,000 psi at 28 days, and that the loss on ignition be less than 2 percent. In addition, the following Optional Chemical Requirements of ASTM C 150 are required by PG&E specification:

(a) Total alkalis of the cement, calculated as the percent of Na_2O + 0.658 times the percent of K_2O, is limited to 0.60 percent.

(b) The sum of tricalcium silicate and tricalcium aluminate is limited to 58 percent. During manufacture, samples of cement were taken once each shift, or at the rate of one sample for every 2,000 barrels. After the quality history was established, in accordance with Section 5 of the Federal Test Method Standard Number 158a, testing was performed at the reduced testing rate specified in that standard. A report of the tests made on each sample was sent to PG&E engineering research staff. In addition, each shipment of cement was accompanied by a mill certificate, and a report of the average of all the individual tests was sent with the initial delivery from each new lot or grind.

Cement shipped to the batch plant was not placed in a plant bin unless it had been accepted by PG&E. In addition to the tests the cement

manufacturer performed, PG&E made the following tests on each new lot to ensure conformance with ASTM C 150:

- ASTM C 109:	Compressive Strength of Hydraulic Cement Mortars (using 2-inch cube specimens)
- ASTM C 114:	Chemical Analysis of Hydraulic Cement
- ASTM C 151:	Autoclave Expansion of Portland Cement
- ASTM C 191:	Time of Setting of Hydraulic Cement by Vicat Needle
- ASTM C 204:	Fineness of Portland Cement by Air Permeability Apparatus

The tests prescribed in ASTM C 114 were also performed periodically during storage to check for any effect on cement characteristics. These tests supplemented visual inspection during storage.

(2) *Aggregates*

Aggregates consist of inert materials that are clean, hard, durable, free from organic matter, not coated with clay or dirt, and conforming to ASTM Designation C 33, Standard Specification for Concrete Aggregates. In addition to the requirements of ASTM C 33, the PG&E specification requires that:

(a) Sodium Sulfate Test for Soundness (ASTM C 88). For fine aggregate, the portion retained on a Number 50 screen, be limited to a weighted average loss of no more than 8 percent after 5 cycles. For coarse aggregate, the weighted average loss after 5 cycles be no more than 10 percent

(b) Sand Equivalent Test (California Division of Highways Test Method Number California 217). Sand equivalent value be at least 75

(c) The fineness modulus be within the limits of 2.6 to 2.9

(d) Los Angeles Rattler Test (ASTM C 131) for coarse aggregate. Loss by weight using Grading A, be a maximum of 10 percent by weight at 100 revolutions and 40 percent by weight at 500 revolutions

(e) Cleanness Value (California Division of Highways Test Method Number California 227-B) for coarse aggregate. Cleanness value be at least 75

(f) Specific Gravity (ASTM C 127) for coarse aggregate. Specific gravity on a saturated surface dry basis be at least 2.60

(g) The chloride content of aggregate be no more than 440 ppm

The following tests were performed by the aggregate supplier at the frequency indicated:

Test	ASTM Destination	Frequency
Screen Analysis and Fineness Modulus	C 136	B
Clay Lumps and Friable Particles	C 142	D
Minus 200 Mesh	C 117	D
Organic Impurities	C 40	D
Soft Particles	C 235	D
Lightweight Particles	C 123	D
Specific Gravity	C 127 & 128	C
Absorption	C 127 & 128	C
Unit Weight	C 29	C
Los Angeles Abrasion (coarse)	C 131	E
Soundness	C 88	E
Effect of Organic Impurities on Fine Aggregate	C 87	F
Petrographic	C 295	F
Sand Equivalent Test	California Test Method 217	A
Cleanness Value	California Test Method 227-B	C

Frequency:

(a) Once each 100 tons, but not more than 10, nor less than one per day of production

(b) Once each 2,000 tons, but not less than one test per week during production

(c) Every 10,000 tons, or once every 10 days of production

(d) Every 20,000 tons, or once every 20 days of production

(e) Once for initial source approval, then once per 30,000 tons

(f) One per deposit

All tests except the Soundness Test (ASTM C 88) and Soft Particles (ASTM C 235) were also performed by PG&E on a periodic basis. Samples were taken at the place where the aggregate entered the batch bin.

(3) *Admixtures*

Admixtures conformed to the following ASTM standards:

(a)	Pozzolan	ASTM C 618	
(b)	Air Entraining Agent	ASTM C 260	
(c)	Water Reducing Agent	ASTM C 494	1.1.1, Type A

A certificate of compliance accompanied each load of admixture delivered to the construction site.

(4) *Water*

Water is clean and free from deleterious amounts of silt, oil, acids, alkali, salts, and organic substances. Chlorides, calculated as Cl, are limited to 1,000 ppm, and sulfates, calculated as SO_4, are limited to 1,000 ppm.

(5) *Concrete Mixing, Placing, and Testing*

The contractor was required to submit concrete mix designs meeting PG&E specification requirements. The mixes were designed in accordance with Method 2, Section 308, of ACI 301. PG&E's material

testing laboratory made sample batches of the proposed mixes and tested them according to:

(a) ASTM C 192, Making and Curing Concrete Test Specimens in the Laboratory

(b) ASTM C 39, Compressive Strength of Molded Concrete Cylinders

(c) ASTM C 143, Slump of Portland Cement Concrete by the Pressure Method

For each design mix, 7-day and 28-day compressive strength tests were made on 6 x 12 inch cylindrical samples in the laboratory.

The contractor was required to submit lift drawings, which showed the location of all construction joints and embedded items, for approval by PG&E. The lift drawings were approved prior to concrete placement. At construction joints in all structural concrete, the surface of the hardened concrete was roughened to expose the coarse aggregate by either bush hammering, wet sandblasting, or cutting with an air-water jet. Prior to placing the next lift of concrete, the surface of the hardened, cleaned concrete was wetted and given a 1/2-inch coat of bonding mortar on all horizontal joints. The bonding mortar had the same sand-cement ratio as the concrete mix, and had a water-cement ratio such as to make a thick slurry but, at most, no greater than that for the concrete. Vertical joints in walls were provided with shear keys. Vertical joints were staggered by at least 6 inches.

The concrete was batched and mixed in an automatic batching and mixing plant located at the construction site. Approved concrete mixes were punched on cards, and the appropriate card was inserted into the control console to initiate batching. The console automatically printed out the quantities of each material in the batch, and the time, date, batch number, and mix identification for each batch. Prior to plant startup, all weighing equipment was certified. This equipment was periodically checked to ensure continuing accuracy.

A full-time PG&E inspector checked the batching and mixing operation. The maximum temperature of concrete at placement was as follows:

(1) 55°F, base slab

(2) 70°F, internal structure and exterior shell

The concrete was placed within 45 minutes after introduction of water to the mix.

Concrete placement was inspected by PG&E inspectors. The concrete was either maintained in a moist condition for 7 days by approved methods, or coated with an approved curing compound.

Concrete was sampled at the frequency required by ACI 301-66. Sampling concrete and making, curing, and testing specimens was in accordance with:

(1)	ACTM C 172	Sampling Fresh Concrete
(2)	ASTM C 31	Making and Curing Concrete Compressive and Flexural Strength Test Specimens in the Field
(3)	ASTM C 39	Compressive Strength of Molded Concrete Cylinders
(4)	ASTM C 143	Slump of Portland Cement Concrete
(5)	ASTM C 231	Air Content of Freshly Mixed Concrete by the Pressure Method

All taking and testing of concrete samples was done by qualified PG&E personnel.

Compressive strength tests were evaluated in accordance with ACI 214. PG&E specifications required that 95 percent of all cylinders tested meet or exceed the specified strength for 5000 psi concrete, and 90 percent meet or exceed the specified strength for 3000 psi concrete. The correlation between field specimens and design strengths was evaluated continuously during construction.

The average strengths and coefficients of variations of concrete tested were:

Exemption 4

Mix	Design, psi	Cement[a], sacks/yd	Average Strength, psi	Coefficient of Variation	Number of Tests
Unit 1					
7AP	5000	7.5	6500	4.3%	11
8	5000	7.5	6400	6.5%	134
8A	5000	7.0	6220	8.3%	18
8AP	5000	6.6	6120	6.4%	43
9BP	3000	6.0	3800	7.0%	87
Unit 2					
8A	5000	7.0	6680	6.7%	40
8AP	5000	6.6	6200	7.1%	101

These coefficients of variation represent "excellent control" as defined in Table 2 of ACI 214-65.

Concrete in Unit 1 and 2 containments is Class AP for base slab and interior concrete and Class BP for cylinder and dome. Mixes designated 7AP, 8, 8A, and 8AP are Class AP. Mix 9BP is Class BP.

[a] Cement and pozzolan

3.8.1.6.2 Reinforcing Steel

Reinforcing steel is deformed billet-steel bar conforming to ASTM Designation A 615. All reinforcing bars in the containment structure are Grade 60, except for the following, which are Grade 40:

(1) Liner anchorages in the base slab

(2) Anchorages on the structural steel beams embedded at the base of the containment structure wall

Table 3.8-1 compares the program for testing of reinforcing bars at the DCPP to the requirements of RG 1.15, which was issued after construction at DCPP was partially complete. Table 3.8-1 also indicates those areas where the PG&E specification is more stringent than ASTM A 615.

Heat number identification was maintained on reinforcing steel from the start of manufacture through placement in the structure.

Physical and chemical test results were sent to the construction site with the first load of steel from each heat. Test values were checked by PG&E inspectors or quality control engineers.

Detailing was in accordance with ACI Standard 315-65, Manual of Standard Practice for Detailing Reinforced Concrete Structures. Bars to be bent were cold bent around pins of the following minimum diameters:

(1) Stirrups and ties - four times the bar diameter

(2) Number 8 bars or smaller - six times the bar diameter

(3) Numbers 9, 10, and 11 - eight times the bar diameter

(4) Numbers 14 and 18 - ten times the bar diameter

Fabrication tolerances were as follows:

(1) Cut length:

Number 14 and 18 bars	0 inch, -3/8 inch
All other bars	±1 inch

(2) Depth of truss bars:

Number 18 bars	±2 inch
All other bars	0 inch, -1/2 inch

(3)	Stirrups, ties, and spirals:	±1/2 inch
(4)	All other bends:	
	Number 14 and 18 bars	±1/2 inch
	All other bars	±1 inch

Placement tolerances were as follows:

(1)	Concrete cover to formed surfaces:	
	Number 14 and 18 bars	−1/2 inch, +2 inch
	All other bars	±1/2 inch
(2)	Longitudinal location of bends:	
	Number 14 and 18 bars	±2 inch
	All other bars	±1 inch
(3)	Depth of bars in slabs:	
	8 inches or less in thickness	±1/4 inch
	Over 8 inches in thickness	±1/2 inch
(4)	Lateral location in the plane of reinforcing:	±2 inch

Occasionally, reinforcing steel bars had to be moved to avoid interferences. In this situation, a bar could be moved, within the plane of the reinforcing layer or curtain, up to one-half the specified spacing. If this was not sufficient, the resulting arrangement was submitted to PG&E for approval. Also, if the bar had to be moved out of the reinforcing layer or curtain to avoid an interference by more than one bar diameter or the above tolerances, whichever was greater, the resulting arrangement was submitted to PG&E for approval.

Tack welding to reinforcing bars was not permitted.

Reinforcing steel placement was inspected by contractor quality control inspectors and by PG&E inspectors.

The average and minimum properties of the tested Number 18 bars in the containment structure were as follows (these values are also shown in Table 3.8-6B):

(1)	Yield	- minimum	61,750 psi
		- average	66,854 psi

(2)	Tensile	- minimum - average	93,750 psi 105,992 psi
(3)	Elongation	- minimum - average	7.0% 9.4%

3.8.1.6.3 Splices

(1) Cadweld Splices

Cadweld splices were used at all locations for primary reinforcing in the exterior shell and base slab. Cadweld splices were used in a few locations in the internal structure.

Quality control procedures for Cadweld splices are described in Table 3.8-2 that compares the program used at the DCPP to that required by SG 10. SG 10 was issued after construction at DCPP was partially complete.

The average and minimum strengths of tested Cadweld tensile samples were:

(a)	Minimum tensile strength	85,000 psi
(b)	Average tensile strength	97,725 psi
(c)	Number of tests	641
(d)	Number of Cadwelds placed	19,068

(2) Butt-welded Splices

Butt-welded splices were used in a few locations where there was insufficient room to properly mount the Cadweld crucible. The quality control measures applied are the same as those described in Section 3.8.2.6.3 for butt-welded splices.

(3) Lap Splices

Lap splices are in accordance with ACI 318-63.

3.8.1.6.4 Liner, Penetration Sleeves, and Penetration Internals

The containment structure liner is carbon steel, conforming to ASTM A 516, Carbon Steel Plates for Pressure Vessels for Moderate and Lower Temperature Service, Grade 70. This steel has a minimum yield strength of 38,000 psi, a minimum tensile

strength of 70,000 psi, and a minimum elongation of 17 percent in an 8-gage length at failure. Charpy V-notch impact tests were performed at +20°F, in accordance with ASTM A 370.

Penetration sleeves conform to one of the following three material specifications:

(1) ASTM A 106, Seamless Carbon Steel Pipe for High Temperature Service, Grade B, with the additional requirement that Charpy V-notch impact tests be performed at 0°F

(2) ASTM A 333, Seamless and Welded Steel Pipe for Low Temperature Service, Grade 1, except that Charpy V-notch impact tests are performed at 0°F

(3) ASTM A 516, Carbon Steel Plates for Pressure Vessels for Moderate and Lower Temperature Service, Grade 70, to ASTM A 300, except that Charpy V-notch impact tests were performed at 0°F

For all three material specifications, the Charpy impact tests were in accordance with the requirements of Paragraph N-330 of ASME Section III, 1968 edition.

Penetration internals conform to the following material specifications:

(1) Equipment and personnel hatches are ASME SA 516, Grade 70, to SA 300 with Charpy impact values at 0°F, in accordance with paragraph N-330 of ASME Section III, 1968 edition

(2) Carbon steel flued heads are ASME SA 105, Grade II, with Charpy impact tests at 0°F, in accordance with paragraph NB-2300 of Section III, ASME B&PV Code, 1971 edition. Ultrasonic and magnetic particle inspections are performed in accordance with Paragraphs NB 2542 and NB 2545, respectively

(3) Stainless steel flued heads are ASME SA 182, Grade F 304. Ultrasonic and liquid penetrant inspections are performed in accordance with Paragraphs NB 2542 and NB 2546, respectively

Welded studs attached to the liner meet the requirements of ASTM A 108, Grade 1015-1018.

The Charpy impact test temperatures stated in the paragraphs above were selected to be at least 30°F below the lowest service temperature in accordance with the ASME B&PV Code, Section III, 1968 Edition for Class B (containment) vessels. For future repair, replacement, or alteration of ferritic containment pressure boundary material, the notch toughness test requirements of Section III, NE-2300 will be used in lieu of the original requirements. Charpy impact tests will be performed at or below the

lowest service temperature and material 5/8 inch or less in thickness will be exempt from notch toughness testing. Further information on notch toughness testing of containment materials appears in Section 3.1.8.14.

Mill test reports certifying the physical and chemical properties of the liner plate delivered to the jobsite were required from the steel supplier. The average and minimum properties of liner plate are as follows:

The Charpy impact test temperature for the hexagonal collars was selected to be at least 30°F below the lowest service temperature in accordance with the ASME B&PV Code, Section III, 1968 Edition for Class B (containment) vessels. For future repair, replacement, or alteration of the hexagonal collars, the notch toughness test requirements of Section III, NE-2300 will be used in lieu of the original requirements. Charpy impact tests will be performed at or below the lowest service temperature and material 5/8 inch or less in thickness will be exempt from notch toughness testing. Further information on notch toughness testing of containment testing materials appears in Section 3.1.8.14.

Reactor Pit and Floor Plates		Unit 1	Unit 2
Yield Strength	- minimum	43,800 psi	39,800 psi
	- average	51,400 psi	55,100 psi
Tensile Strength	- minimum	71,000 psi	74,000 psi
	- average	76,500 psi	78,900 psi
Elongation	- minimum	19%	17%
	- average	25%	24%
Total number of heats		16	11
Total number of slabs		58	62
Total number of tests		58	62

Cylinder and Dome		Unit 1	Unit 2
Yield Strength	- minimum	41,900 psi	38,100 psi
	- average	48,800 psi	46,100 psi
Tensile Strength	- minimum	70,200 psi	70,100 psi
	- average	74,900 psi	73,681 psi
Elongation	- minimum	19%	18%
	- average	26.5%	25.4%

Cylinder and Dome	Unit 1	Unit 2
Total number of heats	23	22
Total number of slabs	251	255
Total number of tests	251	255

Fabrication of the containment structure liner conforms to the applicable parts of Part UW, Requirements for Unfired Pressure Vessels Fabricated by Welding, Section VIII, ASME Boiler and Pressure Vessel Code.

All of the welds were visually examined by contractor quality control inspectors. All field welds were also visually examined by PG&E inspectors.

Table 3.8-3 compares the program for nondestructive testing of containment structure liner welds, including penetration sleeves and inserts, used on the DCPP to that required by SG 19, which was issued after construction at DCPP was partially complete.

Erection tolerances for the liner were as follows:

The liner of the completed structure shall be substantially round. At points not more than 4 inches above the base, the radius of the 3/4-inch liner shall be 69 feet 11-13/16 inches plus or minus 1/2-inch. The maximum diameter of the 3/8-inch liner shall not exceed 140 feet 4 inches and the minimum diameter shall not be less than 139 feet 8 inches.

The liner shall be erected true and plumb. At any point the out-of-plumb shall not exceed 1/240 of the height of the point above the base. For any plate (10 feet ± in height), the out-of-plumpness shall not exceed 1/120.

Flat spots or local out-of-roundness shall not exceed 2 inches in 15 feet of arc.

The base liner shall not deviate from a plane surface between anchorages by more than 1/240.

Stud welding was in accordance with the Supplement to AWS Specification D1.0-66. The tolerance of the location of each stud was ± 1/2-inch. At the beginning of each work day, each welder attached at least two test studs that were then tested by bending the stud approximately 45 percent toward the plate to demonstrate the integrity of the stud-to-plate weld. If failure occurred in the weld, the welding procedure or technique was corrected and two successive studs successfully welded and tested before further studs were attached to the liner plate. These test studs were allowed to remain in place but are not considered as a part of the regular stud pattern required by the design. A 100 percent visual inspection of liner and stud anchors was made prior to pouring concrete.

3.8.1.6.5 Structural Steel

Hexagonal collars at the equipment hatch and personnel hatch meet the requirements of ASTM A 516, Grade 70, and ASTM A 300, except that Charpy V-notch impact tests were performed at 20°F.

The following quality control procedures were followed in the fabrication of the hexagonal steel collars at the equipment hatch and personnel hatch openings:

(1) The 4-inch-thick plate for the edge pieces was ultrasonically examined in accordance with ASTM A 435, except that scanning covered 100 percent of the surface.

(2) Fabrication conformed to the applicable parts of Part UW, Requirements for Unfired Pressure Vessels Fabricated by Welding, of Section VIII of the ASME Boiler and Pressure Vessel Code. All welds are full penetration butt welds and were 100 percent radiographed in accordance with Paragraph UW-51.

(3) The reinforcement plates were heat treated after fabrication in accordance with Paragraph UCS-56, Requirements for Postweld Heat Treatment, of Section VIII of the ASME Boiler and Pressure Vessel Code.

3.8.1.7 Testing and Inservice Surveillance Requirements

After each containment structure was complete, with liner, concrete, and all electrical and piping penetrations, equipment hatch and personnel locks in place, tests were performed as discussed in the following sections.

3.8.1.7.1 Structural Integrity Test

The structural integrity test was performed by pressurizing the containment structure with air up to 115 percent of design pressure, or 54 psig. During this test, structural deflections were measured, crack patterns in the concrete were measured and photographed, and strains in the liner and reinforcing steel measured electrically and recorded. The deflections, crack patterns, and strains were compared to the theoretical predictions to verify the structural integrity of the containment structure. The structural integrity test of each containment structure meets the requirements of RG 1.18, Structural Acceptance Test for Concrete Primary Reactor Containments.

The Unit 1 containment structure is a prototype concrete primary reactor containment, as defined in RG 1.18.

For the structural integrity test, the pressure was increased in increments to the maximum of 54 psig. Measurements were made at 0, 15, 25, 35, 47, and 54 psig during pressurization and again during depressurization. At each pressure level, the

deflection and strain gage readings were made after a 1-hour wait to allow adjustment of strains. The crack patterns were recorded both before and immediately after the test and at the maximum pressure level achieved during the test.

The instrumentation for Unit 1 was as follows:

The radial and vertical growth was measured by means of calibrated targets attached to the exterior shell and sighted by means of high magnification theodolites. Radial deflections were measured at three points on each of six equally spaced meridians: at the springline, at mid-height of the cylinder, and at the top of the base slab. Vertical deflections were measured at the springline and at the top of the dome.

The radial and tangential deflections of the containment structure wall were measured at twelve locations adjacent to the equipment hatch, which is the largest opening.

The pattern of cracks that exceed 0.01-inch in width were mapped or photographed near the base-wall intersection, at mid-height of the wall, at the springline of the dome, and around the equipment hatch. At each location, an area of at least 40 square feet was mapped or photographed.

Strain measurements were made at the following locations, in accordance with the requirements for prototype containment structures:

(1) In the wall at the top of the base mat

(2) In the wall at the equipment hatch, with one gauge located approximately 0.5 times the wall thickness from the edge of the opening

(3) In the wall at the level of the springline

(4) In the wall where pure membrane stress is anticipated, i.e., where there are no discontinuities

Inasmuch as the concrete is assumed cracked, and the strength of the concrete is neglected, strain measurements were made on the reinforcing steel and liner, rather than in the concrete. At the equipment hatch, additional strain measurements were made on the structural steel hexagonal collar. In the wall at the top of the base slab, additional strain measurements were made on the structural steel wide flange beams.

The method used for attaching strain gauges to Number 18 reinforcing bars is shown in Figure 3.8-44.

In evaluating the results of the structural integrity test, the deflection measurements were considered the most reliable result.

Strains, deflections, and crack patterns were compared to the theoretical predictions. The acceptance criterion was that actual readings had to be within 20 percent of the predicted values. This criterion was based on an evaluation of:

(1) Residual stress due to concrete shrinkage

(2) Measurement errors

(3) Temperature variations

(4) As-built deviations of the containment shell from a circular shape

(5) Actual results of other structural integrity tests (primarily at the R. E. Ginna plant)

The deflection measurement and crack mapping program for Unit 2 was identical to that for Unit 1.

3.8.1.7.2 Overall Integrated Leakage Rate Tests

During the depressurization phase of the structural integrity test, the sequence was stopped at 47 psig to conduct an overall integrated leakage rate test at design pressure.

During the overall integrated leakage rate tests, the double penetration and weld seam leak chase channel zones were open to the atmosphere inside the containment structure.

All leakage rate tests are conducted and evaluated in accordance with Appendix J of 10 CFR 50, Option B, as modified by approved exemptions.

3.8.1.7.3 Sensitive Leakage Rate Tests

A sensitive leakage rate test can be performed at some future date with only the volume of the weld seam leak chase channels and double penetrations included in the test. A sensitive leakage rate test would be performed with penetrations and leak chase channels at not less than the peak calculated containment internal pressure (Pa), and with the containment structure at atmospheric pressure.

3.8.1.7.4 Inservice Surveillance Requirements

Periodic leakage rate testing is performed in accordance with the requirements of Appendix J of 10 CFR 50. Inservice surveillance to ensure continued containment integrity is discussed in Section 6.2.1.4. Instrumentation employed to monitor containment status is described in Section 6.2.1.5.

3.8.2 OTHER DESIGN CLASS I STRUCTURES (AUXILIARY BUILDING)

3.8.2.1 Description of the Auxiliary Building

The auxiliary building is located between the Unit 1 and Unit 2 containment structures. It contains the control room that includes consoles and a fuel handling area for each unit. In addition, the auxiliary building contains equipment for the chemical and volume control systems, the safety injection systems, the residual heat removal systems, the component cooling water systems, the liquid radwaste systems, the gaseous radwaste system, and others.

The main floor levels in the auxiliary building are at elevations 85, 100, 115, and 140 feet. Elevations 60 and 73 feet are below ground level, which is at elevation 85 feet, except for the east side of the building where ground level is at elevation 115 feet. Floor plans at elevations 100, 115, and 140 feet are shown in Figures 3.8-60, 61, and 62.

The foundation of the auxiliary building is divided between 3 elevations. The structure is supported at elevations 85 feet (areas GE, GW, and L) 100 feet (area J), and elevation 60 feet (areas H and K).

Figure 1.2-2, Plant Layout, shows relative locations of the plant buildings. The general arrangement of equipment in the auxiliary building, including the fuel handling areas, is shown in Figures 1.2-4 through 1.2-11, Figures 1.2-21 through 1.2-26, and Figures 1.2-29 and 1.2-30. Generally, one-half of the auxiliary building is a mirror image of the other, with each half of the structure containing equipment for one unit. The control room is located at elevation 140 feet. The two fuel handling areas that contain the spent fuel pools, the fuel handling cranes, fuel racks, and related equipment are located on each side of the east end of the auxiliary building with the top of the spent fuel pools at elevation 140 feet.

The auxiliary building is a reinforced concrete shear wall structure, except for the fuel handling area crane support structure which is a structural steel moment resisting and braced frame structure supported on elevation 140 feet and extending up to elevation 188 feet. The shear walls and slabs of the auxiliary building are generally 2 feet thick. The walls of the spent fuel pools are 6 feet thick except for local areas around the fuel transfer tubes. The foundation slabs under the spent fuel pools have a minimum thickness of 5 feet. The spent fuel pool sides and bottoms are lined with stainless steel, 1/4-inch-thick on the bottoms and 1/8-inch nominal thickness on the sides. Representative concrete outlines, reinforcing steel arrangements, and structural steel details for the auxiliary building are shown in Figures 3.8-45 through 3.8-59.

The 125-ton overhead crane in the fuel handling area, shown in Figure 3.8-59, is equipped with restraints that prevent derailing from motions associated with an earthquake.

The only connections between the auxiliary building and other structures are the fuel transfer tube and miscellaneous piping. The fuel transfer tube is fitted with expansion bellows that allow relative movement between the auxiliary building, the containment structure exterior shell, and the internal structure of the containment structure. The design of the expansion bellows considers the maximum axial and lateral relative deflection. Piping systems are analyzed for the maximum relative displacements of the auxiliary building and other structures, and the piping anchor points in the structures are designed to withstand the resulting forces.

3.8.2.2 Applicable Codes, Standards, and Specifications

The following codes and standards are used in the design, construction, inspection, and testing of the auxiliary building:

(1) ACI Standard Building Code Requirements for Reinforced Concrete (ACI 318-63), except that design loading combinations are as described in Section 3.8.2.3.2

(2) Manual of Standard Practice for Detailing Reinforced Concrete Structures (ACI 315-65)

(3) Recommended Practice for Evaluation of Compression Test Results of Field Concrete (ACI 214-65)

(4) Inspection of the Cadweld Rebar Splice (Erico Products, Inc., RB-5M768)

(5) Recommended Practices for Welding Reinforcing Steel, Metal Inserts, and Connections in Reinforced Concrete Construction, American Welding Society AWS D12.1-61

(6) AISC Specification for the Design, Fabrication, and Erection of Structural Steel for Buildings, February 12, 1969

(7) Code for Welding in Building Construction, AWS D1.0-69. Work performed prior to December 12, 1969 is in accordance with the earlier edition, AWS D1.0-66. For inspection of non-ASME structural welds or new non-ASME work performed after January 1, 1988, the guidelines of Nuclear Construction Issues Group (Visual Weld Acceptance Criteria, Vol. 1-3, EPRI Report No. NP-5380, September 1987) may be used except for those cases where:

    (a) Fatigue is a governing design condition.

    (b) The weld allowables are permitted to be higher than those allowed by AWS D1.1 (such as the full penetration welds evaluation for HE).

(c) The weld is part of work performed in the ASME Section XI Inservice Inspection Program.

(8) Stud welding is in accordance with the Supplement to American Welding Society Specifications AWS D1.0-66 and AWS D2.0-66 on Requirements for Stud Welding

(9) Materials and the quality control tests for materials conform to ASTM standards

RG 1.15, Testing of Reinforcing Bars for Category I Concrete Structures (dated December 28, 1972), and RG 1.55, Concrete Placement in Category I Structures (dated June 1973), were issued after construction of the DCPP was nearly complete. A comparison of the program used for the DCPP with the regulatory position of RG 1.15 is presented in Table 3.8-1. The quality assurance program for the DCPP meets the requirements of RG 1.55. In regard to RG 1.55, the references used for guidance are those listed in Appendix A of the RG, as they existed at the time of the PSAR.

3.8.2.3 Loads and Loading Combinations

3.8.2.3.1 Design Loads

The following loads are considered in the design of the auxiliary building.

3.8.2.3.1.1 Dead Loads

Dead loads consist of the weight of the structure, and permanent equipment loads.

3.8.2.3.1.2 Live Loads

Live loads consist of temporary equipment loads and a uniform load to account for the miscellaneous temporary loadings that may be placed on the structure.

3.8.2.3.1.3 Earthquake Loads

Earthquake loads are based on a time-history modal superposition analysis. This analysis is described in Section 3.7.2.

3.8.2.3.1.4 Wind Loads

Wind loads are determined in accordance with the criteria presented in Section 3.3. However, considering the UBC and ASCE Paper 3269 pressures, the forces due to wind are much less than those due to earthquake; consequently, seismic loads, rather than wind, are entered into the load combination equations.

3.8.2.3.1.5 Thermal Loads

Thermal loads are loads induced by local increases in temperature. Thermal loads result from normal operating conditions and from postulated accident conditions.

3.8.2.3.1.6 Pipe Reaction Loads

Pipe reactions that result from hydraulic forces, thermal expansion, and seismic events, are transferred to the structure through pipe supports. Pipe reaction loads result from normal operating conditions and postulated accident conditions.

3.8.2.3.1.7 Jet and Missile Loads

Jet and missile loads are localized forces on structures in the immediate vicinity of a postulated pipe break. Jet forces result from the impingement of high energy fluid on an object. Missile forces result when a part possessing kinetic energy strikes an object.

Missile forces are calculated by the methods described in Section 3.5. Jet forces and pipe reactions from a postulated broken pipe are calculated as described in Section 3.6.

3.8.2.3.1.8 Pressure Loads

Pressure loads are forces generated by a postulated pipe break. Pressures from a postulated broken pipe are calculated as described in Section 3.6.

3.8.2.3.2 Loading Combinations

3.8.2.3.2.1 Normal Conditions

Dead load, live load, loads from the DE, thermal loads, and pipe reactions are considered in all possible combinations. Inasmuch as working stress design is used for normal operating loads, the factored load approach is not used. For each structural member, the combination of these loads that produces the maximum stress is used for design. Stated in equation form:

$$C = D + L + DE + T_o + R_o \qquad (3.8\text{-}14)$$

where:

C	=	required capacity of member based on the methods described in Section 3.8.2.5.1
D	=	dead load of structure and equipment loads
L	=	live load
DE	=	loads resulting from the DE
T_o	=	thermal loads during normal operating conditions
R_o	=	pipe reactions during normal operating conditions

3.8.2.3.2.2 Abnormal Conditions

Dead load, live load, earthquake loads, and loads associated with accidental pipe rupture are considered in the following combinations; for each structural member, the combination that produces the maximum stress is used for design:

Concrete Structural Elements

$$U = D + L + T_A + R_A + 1.5\ P_A \qquad (3.8\text{-}15)$$

$$U = D + L + T_A + R_A + 1.25\ P_A + 1.0\ (Y_j + Y_m + Y_r) + 1.25\ DE \qquad (3.8\text{-}16)$$

$$U = D + L + T_A + R_A + 1.0\ P_A + 1.0\ (Y_j + Y_m + Y_r) + DDE \qquad (3.8\text{-}17)$$

$$U = D + L + T_A + R_A + 1.0\ P_A + 1.0\ (Y_j + Y_m + Y_r) + HE \qquad (3.8\text{-}18)$$

where:

T_A = thermal loads on structure generated by a postulated pipe break, including T_O

R_A = pipe reactions on structure from unbroken pipe generated by postulated pipe break conditions, including R_O

PA = pressure load within or across a compartment and/or building generated by a postulated pipe break, and including an appropriate dynamic factor (DLF) to account for the dynamic nature of the load

Y_j = jet load on structure generated by a postulated pipe break, including an appropriate DLF

Y_m = missile impact load on a structure generated by, or during, a postulated pipe break, such as a whipping pipe, including an appropriate DLF

Y_r = reaction on structure from broken pipe generated by a postulated pipe break, including an appropriate DLF

U = ultimate strength required to resist design loads based on the methods described in ACI 318-63. See Section 3.8.2.5.2 for equation 3.8-16 through 3.8-18

DDE = loads resulting from the DDE

HE = loads resulting from an HE

Steel Structural Elements

Where elastic working stress design methods are used[(a)(b)]:

$$1.6S^{(a)} = D+L+T_A^{(b)}+R_A+P_A \qquad (3.8\text{-}19)$$

$$1.6S^{(a)} = D+L+T_A^{(b)}+R_A+P_A+1.0(Y_j+Y_m+Y_r)+DE \qquad (3.8\text{-}20)$$

$$1.6S^{(a)} = D+L+T_A^{(b)}+R_A+P_A+1.0(Y_j+Y_m+Y_r)+DDE \qquad (3.8\text{-}21)$$

$$1.7S = D+L+T_A^{(b)}+R_A+1.0P_A+1.0(Y_j+Y_m+Y_r)+HE \qquad (3.8\text{-}22)$$

Where plastic design methods are used:

$$0.90Y^{(a)} = D+L+T_A^{(b)}+R_A+1.5P_A \qquad (3.8\text{-}23)$$

$$0.90Y^{(a)} = D+L+T_A^{(b)}+R_A+1.25P_A+1.0(Y_a+Y_m+Y_r)+1.25DE \qquad (3.8\text{-}24)$$

$$0.90Y^{(a)} = D+L+T_A^{(b)}+R_A+1.0P_A+1.0(Y_j+Y_m+Y_r)+DDE \qquad (3.8\text{-}25)$$

$$1.0Y = D+L+T_A^{(b)}+R_A+1.0P_A+1.0(Y_j+Y_m+Y_r)+HE \qquad (3.8\text{-}26)$$

where:

S = required section strength based on elastic design methods and the allowable stresses[(c)] defined in Part 1 of the AISC "Specifications for the Fabrication and Erection of Structural Steel for Buildings," February 12, 1969

Y = required section strength based on plastic design methods[(c)] described in Part 2 of AISC Specifications for the Design, Fabrication and Erection of Structural Steel for Buildings, February 12, 1969

(a) For existing structures, the 1.6 factor applied to the required section strength, S, and the 0.90 reduction factor applied to the required section strength, Y, are increased to 1.7 and 1, respectively. In such situations, however, it is verified that deflections will not result in the loss of function of any safety-related system.

(b) Thermal loads are neglected when it can be shown that they are secondary and self-limiting in nature and where the material is ductile.

(c) See Section 3.8.2.5 regarding material properties used in conjunction with load combinations including HE.

For both concrete and steel structural elements, both cases of L having its full value present during the postulated pipe rupture, or being completely absent, are checked.

3.8.2.4 Design and Analysis Procedures

Structural analysis of the auxiliary building is performed by the traditional methods of engineering analysis for structural steel and reinforced concrete structures. These methods are based on the principles of equilibrium, compatibility of deformations, and predictions of material strength by the methods of the AISC Specifications for the Design, Fabrication, and Erection of Structural Steel for Buildings (AISC Code), and the ACI Standard Building Code Requirements for Reinforced Concrete (ACI Code).

The use of these codes is discussed in Section 3.8.2.5. The following sections discuss the specific design methods used for the structural steel and concrete parts of the auxiliary building.

3.8.2.4.1 Structural Steel

The fuel handling area crane support structure is a 370 x 60 x 50-foot high steel framed structure clad with metal siding and covered by metal decking and built-up roofing. The structure is supported on concrete walls at elevation 140 feet on the eastern side of the auxiliary building. Lateral forces are resisted by steel cross-braced frames in the north-south direction, moment resisting frames in the east-west direction, and by the roof, which is a trussed and cross-braced diaphragm covered with metal decking.

Acceleration profiles and forces from the analyses described in Section 3.7.2.1.7.1 are applied to a detailed static model of the entire fuel handling area crane support structure to obtain forces for the stress evaluation of the structural members and connections and to obtain structural displacements. Various crane and lifted load positions are considered. The stress evaluation is carried out for the load combinations described in Section 3.8.2.3. Stresses are evaluated against the criteria in Section 3.8.2.5. The calculated stress ratios for the most critical members are given in Table 3.8-7.

3.8.2.4.2 Concrete

The vertical and the lateral load-resisting system of the auxiliary building consists of reinforced concrete columns and walls tied together with reinforced concrete slabs. The evaluation of these elements is carried out for the loading combinations given in Section 3.8.2.3, according to the criteria in Section 3.8.2.5.

The seismic forces and moments are based on the response of the auxiliary building seismic models described in Section 3.7. A detailed analytical model of the auxiliary building is then developed to distribute forces and moments to the various walls, diaphragms, and columns.

Slabs

Slabs are evaluated separately for out-of-plane loads and in-plane loads.

For out-of-plane loads, shear stresses and moments are calculated assuming one-way or two-way slab action as appropriate. Out-of-plane capacity-to-demand ratios for selected slabs are shown in Tables 3.8-8 through 3.8-10. The slab in-plane capacities are investigated at critical sections. The selection of these sections is based on the location of numerous openings across the entire section of the diaphragm and the magnitudes of shear, moment, and axial forces on the entire section. The in-plane capacity-to-demand ratios for the concrete slabs are shown in Tables 3.8-11 through 3.8-13.

Walls

The critical wall elements are selected based on the magnitude of demand loads and presence of openings. The forces and moments for the governing load combination in those elements are compared to their respective capacities, and the capacity-to-demand ratios are shown in Tables 3.8-14 through 3.8-16.

Concrete Columns

The concrete columns are evaluated for axial and flexural loads. Flexural loads on columns due to the vertical loads are determined by considering frame action with the slabs. Flexural loads include the effect of minimum eccentricity specified by ACI 318-63. Column moments due to interstory drift are found to be negligible. Capacity-to-demand ratios for selected columns are shown in Table 3.8-17.

3.8.2.4.3 Load Dissipation to the Foundation

The adequacy of the structural system, at and below elevation 85 feet, to dissipate lateral loads to the rock foundation is evaluated for the load combinations given in Section 3.8.2.3.2. The results, given in Tables 3.8-18 through 3.8-23, and illustrated for HE loads in Figures 3.8-63 and 3.8-64, indicate the adequacy of the system to dissipate the loads.

3.8.2.4.4 Computer Programs

Computer programs used in the structural analysis, and the verification measures used, are listed in Table 3.8-6.

3.8.2.5 Structural Acceptance Criteria

For DE and DDE load combinations, the nominal design strength for concrete and specified yield strength for reinforcing and structural steel are considered. For load combinations including HE, however, the actual material properties are used. See

Sections 3.8.2.6.1, 3.8.2.6.2, and 3.8.2.6.4 for material properties associated with concrete, reinforcing steel, and structural steel, respectively. See Section 3.8.2.6.5 for allowable stresses for bolted connections. Ductility, when applied for HE load combinations, is in accordance with Table 3.8-24.

3.8.2.5.1 Normal Loads

For normal loads, the auxiliary building is designed for the allowable working stresses of ACI 318-63, as supplemented by Section 3.8.2.5.3, and Part 1 of the AISC Code, except that the increase in allowable stress usually allowed for load combinations involving earthquake forces is not used.

3.8.2.5.2 Abnormal Loads

For abnormal loads, the auxiliary building is designed for overall elastic behavior. For concrete elements, the strength design method of ACI 318-63 applies, as supplemented by Section 3.8.2.5.3. For the evaluation of steel elements using elastic design methods, the allowable stresses are defined in Part 1 of AISC Code. For the evaluation of steel elements using "plastic design," Part 2 of the same AISC specifications applies.

The capacity for the various concrete structural elements is based on the yield strength of the material, reduced by a factor, f, which provides for the possibility that small, adverse variations in material strengths, workmanship, dimensions, and control, while individually within required tolerances and the limits of good practice, occasionally may be additive. The f-factors used are in accordance with ACI 318-63.

For load combinations involving Y_j, Y_m, and Y_r, local stresses due to these concentrated loads may exceed the allowable provided there is no loss of function. See Reference 6, Enclosure Number 3, Document (B), for more detailed information concerning the acceptance criteria for these load combinations.

3.8.2.5.3 In-Plane Loads on Concrete Elements

The design of slab diaphragms and shear walls for in-plane forces is not explicitly covered by ACI 318-63. Section 104 of ACI 318-63 allows criteria based on test data to be used for the design of elements not covered by its provisions. Consequently, the document entitled "Recommended Evaluation Criteria for Diablo Canyon Nuclear Power Plant Auxiliary Building Walls and Diaphragms" (Reference 7) is developed to provide criteria for evaluation of auxiliary building shear walls and floor diaphragms for in-plane seismic forces, including the simultaneous effects of out-of-plane forces.

Accordingly, the structural elements are evaluated as follows:

(1) The columns are evaluated by the provisions of ACI 318-63 for all loading conditions.

(2) The slabs and walls are evaluated for out-of-plane loads according to ACI 318-63, and for in-plane loads according to Reference 7.

3.8.2.5.4 Factors of Safety

The calculated capacity-to-demand ratio for selected structural elements of the auxiliary building are given in Tables 3.8-7 through 3.8-17. In all cases, these ratios are greater than the minimum allowable value of 1. Therefore, all structural elements satisfy the criteria.

The gap between the auxiliary building and the containment structure, as well as the factor of safety against the structure impacting during a seismic event, is discussed in Section 3.8.1.5.3. Separations between the auxiliary building and the turbine building are adequate to ensure these structures will not impact each other when subject to design load combinations. Calculated displacements, separations, and factors of safety against impact are shown in Table 3.8-23A.

3.8.2.6 Materials, Quality Control, and Special Construction Techniques

Sections 3.8.1.6.1 and 3.8.1.6.2 for the containment structure also apply to the auxiliary building, except as superseded by information in the following paragraphs.

3.8.2.6.1 Concrete

Concrete strengths are shown below.

Walls and slabs below elevation 85 feet; slabs 4 feet and thicker at elevation 85 feet; slab at elevation 85 feet bounded by column lines 16.8 - 19.2 - L - H:

Design f'c = 3000 psi (DE and DDE combinations)

All other concrete:

Design f'c = 5000 psi (DE and DDE combinations)

Average 28-day strengths are used with HE load combinations. The average strengths of representative mixes are as follows:

Design Strength	Average 28-day Strength	Number of Tests
3000 psi	3920 psi	167
5000 psi	5650 psi	368

3.8.2.6.2 Reinforcing Steel

Reinforcing steel is ASTM A 615, Grade 40, except in some locations where Grade 60 is used. ASTM minimum values are used with DE and DDE load combinations. Average test values are used with HE load combinations. The average and minimum properties of representative bar sizes, are as follows:

	#8		#11	
	Grade 40	Grade 60	Grade 40	Grade 60
Design Yield Strength, psi	40,000	60,000	40,000	60,000
Average Yield Strength, psi	49,655	66,189	48,302	68,582
Minimum Yield Strength, psi	41,200	60,250	42,950	61,710
Average Tensile Strength, psi	82,236	102,403	81,074	105,822
Minimum Tensile Strength, psi	74,392	96,500	72,940	94,390
Average Elongation, %	18.9	13.94	14.82	14.41
Minimum Elongation, %	13.0	11.0	8.5	9.4
Total Number of Heats	67	18	91	56

3.8.2.6.3 Splices

The majority of splices in the auxiliary building are lap splices, made in accordance with ACI 318-63. Cadweld splices are used in some locations in the auxiliary building. The quality control procedures described for Cadweld splices in the containment structure also apply to Cadweld splices in the auxiliary building.

Butt-welded splices are used where a section of wall has to be temporarily left open for access, and in certain other locations. Butt-welded splices are made in accordance with ACI 318-63, and the American Welding Society's Recommended Practices for Welding Reinforcing Steel, Metal Inserts, and Connections in Reinforced Concrete Construction, using the "short-arc" process or low hydrogen stick electrodes by the shielded arc process. Both processes have minimum preheat and interpass temperatures of 400°F. Completed welds are wrapped with a protective blanket of insulating material to avoid rapid cooling.

Procedure qualification and welder qualification are as follows:

(1) A welding procedure qualification test is made for each position and for each grade and size of bar. The test consists of two tension tests and one nick break test. Bars may not be rolled during welding.

(2) Welder qualification tests are made for each position, type of electrode, grade and size of bar, and joint design. Qualification for one size of bar is considered qualification for all smaller sizes. Each test consists of one tension and one nick break test. Bars may not be rolled during welding.

(3) Tension specimens are tested to failure and must comply with the minimum tensile requirements for the grade of reinforcing steel.

(4) The nick break specimen is broken and visually examined for soundness. The specimen must exhibit the following: the sum of the longest dimension of all inclusions visible in any one joint must not exceed ½-inch; no inclusion may be closer to the weld surface than a distance equal to the largest dimension of the inclusion; there must be no incomplete fusion or lack of penetration or cracks in the weld or base metal.

Testing percentages applicable to butt-welded splices for each welder, position, and grade of bar are as follows:

(1) Two out of the first ten splices

(2) Six out of the next 90 splices

(3) Four out of second and subsequent 100 splice units

Qualification for one size of bar is considered as qualification for all smaller sizes.

3.8.2.6.4 Structural Steel

Structural steel is ASTM A 36 and ASTM A 441; ASTM minimum values are used with DE and DDE load combinations, and average test values are used with HE load combinations. Minimum and average values are as follows:

	ASTM A36	ASTM A441
Design Yield (ksi)	36	42

Testing of structural steel installed through 1977 gave the following:

	ASTM A36	ASTM A441
Average Test Yield (ksi)	43.95	51.62
Average Test Ultimate (ksi)	68.04	75.91

Charpy impact tests were performed on all structural steel at the following temperature:

Framing for pipe rupture restraints	40°F
Structural steel	20°F

3.8.2.6.5 Structural Bolts

Structural bolts are ASTM A307, A325, and A490, allowable stresses per Table 1.5.2.1 of the AISC "Specifications for the Design, Fabrication and Erection of Structural Steel for Buildings," February 12, 1969, are used with the DE, DDE, and HE load

combinations. However, it is acceptable to increase the allowable stresses for the Hosgri load combinations, based on the results of properly substantiated testing (References 34 through 38).

3.8.3 OUTDOOR WATER STORAGE TANKS

3.8.3.1 Description of the Outdoor Water Storage Tanks

The Design Class I outdoor storage tanks, located adjacent to east of auxiliary building, are steel studded tanks with concrete shielding, as shown in Figure 3.8-65, sheets 1 and 2.

There are two refueling water storage tanks and two condensate water storage tanks, one to service each unit of the plant. The firewater and transfer tank, which serves both Units 1 and 2, is made up of two concentric cylindrical steel tanks connected by a common dome roof. The inner cylindrical tank is the firewater tank and the outer tank is the transfer tank. The structural configuration of the condensate tanks is similar to that of the refueling water storage tanks.

The Design Class I tanks are supported on concrete fill down to bed rock and are anchored to bed rock with rock anchors as shown in Figure 3.8-65, Sheet 2.

3.8.3.2 Applicable Codes, Standards, and Specifications

The following codes and standards are used in the design, construction, inspection, and testing of the outdoor water storage tanks.

(1) ACI Standard Building Code Requirements for Reinforced Concrete (ACI 318-63, and ACI 318-71)

(2) Manual of Standard Practice for Detailing Reinforced Concrete Structures (ACI 315-65)

(3) Recommended Practices for Welding Reinforcing Steel, Metal Inserts, and Connections in Reinforced Concrete Construction, American Welding Society AWS D12.1-75

(4) AISC Specification for the Design, Fabrication, and Erection of Structural Steel for Buildings, 6th and 7th Editions

(5) Code for Welding in Building Construction, AWS D1.1-77, Rev. 2. Work performed prior to (December 12, 1969) is in accordance with the earlier edition, AWS D1.0-66. For inspection of non-ASME structural welds or new non-ASME work performed after January 1, 1988, the guidelines of Nuclear Construction Issues Group (Visual Weld Acceptance Criteria,

Vol. 1-3, EPRI Report No. NP-5380, September 1987) may be used except for those cases where:

(a) Fatigue is a governing design condition.

(b) The weld allowables are permitted to be higher than those allowed by AWS D1.1 (such as full penetration weld evaluation for the HE).

(c) The weld is part of work performed in the ASME Section XI Inservice Inspection Program.

(6) Stud loading is in accordance with the Supplement to American Welding Society Specifications AWS D1.0-66 and AWS D2.0-66 on Requirements for Stud Welding

(7) Materials and quality control tests for materials conform to ASTM standards

(8) ASME Section VIII, Division 2, 1974

(9) AWWA D100, American Waterworks Association, Standard to Steel Tanks, Standpipes Reservoirs and Elevated Tanks for Water Storage

3.8.3.3 Loads and Loading Combinations

3.8.3.3.1 Normal Conditions

$$C = D + HS + 1.0\ DE + 1.0\ R_O \qquad (3.8\text{-}27)$$

where:

C = required load capacity of section as described in Section 3.8.3.5.1
D = dead load of tank
HS = hydrostatic load
DE = loads resulting from DE
R_O = pipe reactions during normal operating conditions, including dead, thermal, and DE loads.

3.8.3.3.2 Abnormal Conditions

$$U = D + HS + 1.0\ DDE + 1.0\ R_A \qquad (3.8\text{-}28)$$

$$U = D + HS + 1.0\ HE + 1.0\ R_A \qquad (3.8\text{-}29)$$

where:

D and HS are defined in Section 3.8.3.3.1, and

U	=	strength required to resist abnormal loads as described in Section 3.8.2.5.2
DDE	=	loads resulting from the DDE
HE	=	loads resulting from the HE
R_A	=	pipe reactions during abnormal conditions, including dead, thermal, and DDE or HE loads

3.8.3.4 Design and Analysis Procedures

Condensate storage tanks, the refueling water storage tanks, the primary water storage tanks, and the fire water and transfer water tanks were originally designed to meet the criteria based on the DE, DDE, and HE. The code used in designing the tanks was AWWA D100, 1967, with stress allowables restricted to those permitted by ASME Section VIII, Division 2. Revised security criteria called for additional resistance to bullet penetration and explosives and required all the above steel tanks, except the primary water storage tanks, to be modified with minimum reinforced concrete protection as determined by Argonne National Laboratory. The Design Class I tanks with concrete protection were reevaluated for DE, DDE, and HE using finite-element computer models as described in Section 3.7.

The stresses in the stiffeners and the steel liner plate around the vault openings were determined by hand calculation and compared with the stress allowables. The forces, moments, and stresses in the refueling water storage tank resulting from dead load, hydrostatic pressure, hydrodynamic loads, and seismic loads are listed in Table 3.8-25. These values are within the allowable limits as described in Section 3.8.3.5.

3.8.3.5 Structural Acceptance Criteria

3.8.3.5.1 Normal Loads

For normal loads, the outdoor water storage tanks are designed for the allowable working stresses of the ACI 318-63 for concrete, Part 1 of the AISC Specification, 6^{th} Edition for structural steel components, and ASME Section VIII, Division 2, 1974, for steel liner plates.

3.8.3.5.2 Abnormal Loads

For abnormal loads, the outdoor water storage tanks are designed for overall elastic behavior. For concrete elements the strength design method of ACI 318-63 applies for DDE loads and of ACI 318-71 for HE loads. For the evaluation of structural steel elements using elastic design methods, for the loading condition including DDE loads, 1.6 times AISC 6th Edition, Part 1 allowables are used; whereas, for the HE load combination, Part 2 of AISC 7th Edition, the Plastic Design method applies.

The steel liner plates are evaluated by using stress intensities as defined in ASME Section VIII, Division 2, 1974, and applying a factor of 0.9 to the minimum specified yield strength for DDE, and 1.0 to the yield strength based on test results for HE load conditions. For local stress intensities around nozzles in the vault opening area for DDE loads, a factor of 1.0 to the minimum specified yield strength applies, whereas for HE loads, a factor of 2.4 to the ASME Section VIII, Division 2, 1974, allowable values applies.

3.8.3.5.3 Factors of Safety

The calculated capacity-to-demand ratios for critical structural elements of the outdoor water storage tanks are greater than the minimum allowable value of 1. Therefore, all structural elements satisfy the criteria.

3.8.3.6 Materials, Quality Control, and Special Construction Techniques

The quality control measures discussed in Sections 3.8.1.6.1 and 3.8.1.6.2 for the containment structure also apply to Design Class I tanks.

3.8.3.6.1 Materials Tank Walls and Roof Dome

Condensate and Inner and Outer Tank Walls of Firewater and Transfer Tank	-	Carbon steel liner plates and stiffeners conform to ASTM A-516 GR 60. The Condensate Storage Tanks are coated with an epoxy coating and the Fire Water and Transfer Tank is coated with Vinyl Paint. Carbon steel studs conform to ASTM A108 GR 1015- 1018.
Refueling Water Tank	-	Stainless steel liner plates and stiffeners conform to ASTM A-240 Type 304L. Stainless steel studs conform to ASTM A276 type 304 annealed.

All Tanks, Except Inner Tank of Firewater and Transfer Tank:

- Concrete strength (minimum specified) f_C = 4 ksi
- Rebar conforms to ASTM A615, GR 60, fy = 60 ksi (minimum specified)

3.8.4 FOUNDATIONS AND CONCRETE SUPPORTS

The foundation structures for the containment and the auxiliary building are included in Sections 3.8.1 and 3.8.2, respectively. The foundations of the Class I outdoor water storage tanks are described in this section.

3.8.4.1 Foundations for Design Class I Tanks

The following Design Class I concrete-protected steel tanks are located adjacent to the east side of the auxiliary building on reinforced concrete foundation slabs:

(1) Condensate water storage tank (one for each unit)

(2) Refueling water storage tank (one for each unit)

(3) Fire water and transfer tank (common to both units)

3.8.4.1.1 Description of the Foundation Slabs

Each of the condensate water storage tanks and refueling water storage tanks has a separate, circular foundation slab. The fire water tank and the transfer tank, which serves both units, are concentric tanks on a common circular foundation slab. Each of the foundation slabs is shown in Figure 3.8-65 and consists of a 1-foot-thick reinforced concrete slab with an integral edge beam tied to a reinforced concrete wall. Each of the tanks, except for the fire water tank, is anchored to its foundation slab with ASTM A 193, Grade B7 anchor bolts. The bolt diameters are 1-1/4 inches for the condensate water storage tanks and the transfer tank, and 1-3/8 inches for the refueling water storage tanks. The wall of the fire water tank is welded to an insert plate in the foundation.

The tank foundation slabs are resting on concrete fill anchored to bedrock with rock anchors. The reinforced concrete protective walls of the steel tanks are anchored to bedrock as shown in Figure 3.8-65, Sheet 2.

3.8.4.1.2 Applicable Codes, Standards, and Specifications

The foundation slabs for the Design Class I outdoor storage tanks listed are designed and constructed in accordance with the ACI 318-63.

3.8.4.1.3 Loads and Loading Combinations

The foundation slabs for the Design Class I outdoor storage tanks are designed for dead loads, hydrostatic load, and seismic load:

$$C = DL + HS + EQ + R \qquad (3.8\text{-}30)$$

where:

C = total load on foundation
DL = dead load of tank
HS = hydrostatic load

EQ	=	maximum seismic loads including inertial, impulsive, and convective loads
R	=	pipe reaction load including dead, thermal, and seismic loads

3.8.4.1.4 Design and Analysis Procedures

The foundation slabs with concrete fill are designed to prevent overturning and sliding of the tank and limit bearing pressure to 80 ksf. The rock anchors attaching the tank to the foundation are designed so that the maximum uplift force is within the allowable capacity provided in Figure 3.8-65, Sheet 2.

3.8.4.1.5 Structural Acceptance Criteria

Stresses in the reinforced concrete foundation slabs are limited to the allowable values in ACI 318-63.

3.8.4.1.6 Materials, Quality Control, and Special Construction Techniques

The quality control measures discussed in Sections 3.8.1.6.1 and 3.8.1.6.2 for the containment structure also apply to the Design Class I tank foundations.

Material strengths for the Design Class I tank foundation slabs are as follows:

(1) Concrete strength of foundation slab and concrete fill is 3000 psi.

(2) Reinforcing steel in foundation slab is ASTM A 615, Grade 40.

(3) Rock anchors conform to VSL 28, strand #ER5-28, with double corrosion protection and are fully grouted with concrete strength of 4000 psi.

3.8.4.2 Concrete and Structural Steel Supports

Concrete and structural steel supports for RCS components are described and evaluated in Section 5.5.14. Loading combinations for these supports are discussed in Section 5.2.

3.8.5 DESIGN CLASS II STRUCTURES CONTAINING DESIGN CLASS I EQUIPMENT

The turbine building and the intake structure are Design Class II structures that contain Design Class I equipment. The turbine building contains the component cooling heat exchangers, emergency diesel generators, 4.16-kV vital switchgear, control room pressurization system, and other Class I systems. The intake structure contains the auxiliary saltwater (ASW) pumps and associated equipment.

To ensure that the Design Class I equipment would not be affected by failure of the Design Class II structures, both the turbine building and the intake structure are evaluated for the HE, using responses from the dynamic analyses discussed in Section 3.7.

The capability of the intake structure to protect the ASW system during design flood events is evaluated to ensure this capability, as described in Sections 2.4 and 3.4.

The OTSC is located in the turbine building buttresses and is designed to meet seismic loading criteria.

3.8.5.1 Turbine Building

3.8.5.1.1 Description

The turbine building was originally designed as a Design Class II structure using static equivalent seismic loads. Subsequently, the building was dynamically analyzed and designed to assure that it would not collapse and impair the function of Class I equipment during a DDE. Later, during the Hosgri evaluation, the building was reevaluated again and upgraded to withstand the Hosgri seismic loads. As a result of the Hosgri evaluation, buttresses and concrete walls were added to the turbine building, and internal modifications, such as reinforcing main columns, strengthening floor diaphragms, and roof and wall bracing, were made.

The turbine pedestal was originally designed as a Design Class II structure, using static equivalent seismic loads. During the Hosgri evaluation, the pedestal was reevaluated and upgraded to withstand the Hosgri seismic loads. As a result of the Hosgri evaluation, six piers were posttensioned and the pedestal-to-building separations were increased along the east and west sides of the pedestal.

The turbine building is located adjacent to the west side of the auxiliary building as shown in Figure 1.2-2, Plant Layout. The general layout of equipment in the turbine building, including the turbine generators, is shown in Figures 1.2-13 through 1.2-20, Figures 1.2-24 through 1.2-27, and Figures 1.2-30 through 1.2-32. Generally, the Unit 1 and Unit 2 portions of the turbine building are opposite hand and similar to the other, with each portion of the structure containing equipment for one unit. Exceptions are the presence of a machine shop and material storage area common to both units in the Unit 1 portion, and the OTSC in the Unit 2 portion of the structure.

Main floor levels in the turbine building are at elevations 85, 104, 119, and 140 feet. The foundation of the building is at elevation 85 feet. Representative plans at the main floor levels roof truss lower chord level, and a typical section are shown in Figures 3.8-66 through 3.8-71.

The turbine building is a reinforced concrete shear wall structure except for the superstructure, which is a structural steel moment resisting and braced frame structure

extending from elevation 140 feet to elevation 217 feet. Shear walls generally range from 16 to 29 inches thick. Floors are 10- to 12-inch-thick reinforced concrete slabs or 1/2-inch-thick steel plate, supported on steel framing and steel columns. The reinforced concrete foundation mat is generally 3 feet thick except under the turbine pedestal, where the thickness is 10 feet. Reinforced concrete turbine pedestals, one for each unit, are located in the building; six piers of each pedestal are posttensioned. The pedestals are structurally isolated from the building floors and extend from the common foundation slab, elevation 85 feet, to elevation 140 feet. Two 135-ton overhead cranes are located in the building.

3.8.5.1.2 Applicable Codes, Standards, and Specifications

The following codes and standards are used in the HE evaluation, and in the design, construction, inspection, and testing of HE modifications to the turbine building:

(1) ACI Standard Building Code Requirements for Reinforced Concrete (ACI 318-71) except that, for the HE evaluation and design, the 1973 Supplement to ACI 318 is used and design load combinations are as described in Section 3.8.5.1.3

(2) Manual of Standard Practice for Detailing Reinforced Concrete Structures (ACI 315-74)

(3) Recommended Practice for Evaluation of Compression Test Results of Field Concrete (ACI 214-65)

(4) Recommended Lateral Force Requirements, 1974 Seismology Committee Structural Engineers Association of California (SEAOC)

(5) Recommended Practices for Welding Reinforcing Steel, Metal Inserts, and Connections in Reinforced Concrete Construction, American Welding Society (AWS D12.1-75)

(6) AISC Specification for the Design, Fabrication, and Erection of Structural Steel for Buildings, February 12, 1969, is generally used for steel structures. AISC Specification, dated November 1, 1978, is also used for evaluating selected connections.

(7) Code for Welding in Building Construction (AWS D1.1 Rev. 2-77). For inspection of non-ASME structural welds or new non-ASME work performed after January 1, 1988, the guidelines of Nuclear Construction Issues Group (Visual Weld Acceptance Criteria, Vol. 1-3, EPRI Report No. NP-5380, September 1987) may be used except for those cases where:

    (a) Fatigue is a governing design condition

(b) The weld allowables are permitted to be higher than those allowed by AWS D1.1 (such as full penetration weld evaluation for the HE)

(c) The weld is part of work performed in the ASME Section XI Inservice Inspection Program

(8) Materials and the quality control tests for materials conform to ASTM standards

3.8.5.1.3 Loads and Loading Combinations

3.8.5.1.3.1 Design Loads

The following loads are considered in the HE evaluation of the turbine building.

3.8.5.1.3.1.1 Dead Loads

Dead loads consist of the weight of the structure, permanent attachments and permanent equipment.

3.8.5.1.3.1.2 Live Loads

Live loads consist of any actual live loads acting on the element considered.

3.8.5.1.3.1.3 Seismic Loads

Seismic loads are based on a response spectrum modal superposition analysis. This analysis is described in Section 3.7.2.

3.8.5.1.3.2 Loading Combination

Concrete Structural Elements

$$U = D + L + HE \quad (3.8\text{-}31)$$

where:

U	=	Strength determined in accordance with the methods described in ACI 318-71 and 1973 Supplement, except strength of shear walls is based on method described in Section 3(c) of the 1974 SEAOC. (See also Section 3.8.5.1.5.)
D	=	dead load
L	=	live load
HE	=	loads resulting from an HE

Steel Structural Elements

Where plastic design methods are used:

$$Y = D + L + HE \qquad (3.8\text{-}32a)$$

Where elastic working stress design methods are used:

$$1.7S = D + L + HE \qquad (3.8\text{-}32b)$$

where:

S = required section strength based on elastic design methods and the allowable stresses defined in Part 1 of the AISC Specification for the Design, Fabrication, and Erection of Structural Steel for Buildings, February 12, 1969

Y = required section strength based on plastic design methods described in Part 2 of AISC Specification for the Design, Fabrication, and Erection of Structural Steel for Buildings, February 12, 1969 (See also Section 3.8.5.1.5.)

3.8.5.1.4 Design and Analysis Procedures

Structural analysis of the turbine building is based on the traditional methods of engineering analysis for structural steel and reinforced concrete structures. These methods are based on the principles of equilibrium, compatibility of deformations, and predictions of material strength by the methods of the AISC Code and the ACI Code. The use of these codes is discussed in Section 3.8.5.1.5.

The lateral force resisting system of the turbine building above elevation 140 feet consists of moment resisting bents, formed by steel roof trusses and steel plate columns, steel cross-brace frames at exterior walls, and a steel bracing system in the plane of the roof truss lower chords. At and below elevation 140 feet, lateral resistance is provided by concrete and steel plate floors acting as diaphragms; by concrete shear walls; by concrete buttresses along the east and west sides of the building; and by steel cross-braced frames above elevation 104 feet at the north and south ends of the building. Vertical forces are transmitted to the foundation by the steel plate columns, concrete walls, and interior steel columns which support the steel floor framing system.

HE forces on the lateral force resisting system of the turbine building and the turbine pedestal are based on the response of the turbine building and pedestal seismic models described in Section 3.7. In some cases detailed analytical models are developed to calculate building member forces. Structural evaluation of members is performed for the load combinations described in Section 3.8.5.1.3. The evaluation considers bridge crane location and lifted load as described in Section 3.7. Members are evaluated

against the acceptance criteria in Section 3.8.5.1.5. Results of the evaluation are shown in Tables 3.8-26 and 3.8-27.

Computer programs used in the structural analysis and the verification measures are listed in Table 3.8-6.

3.8.5.1.5 Structural Acceptance Criteria

For HE load combinations actual material properties are used. Lateral force resisting elements are allowed inelastic deformation subject to the ductility limits shown in Table 3.8-24. The strength of concrete elements is determined in accordance with the methods of ACI 318-71 and the 1973 Supplement. Strength of concrete shear walls is determined in accordance with Section 3(c) of 1974 SEAOC. Strength of steel elements is determined in accordance with the AISC Code, February 12, 1969.

Calculated forces and capacities for selected structural elements of the turbine building and turbine pedestals are compared in Tables 3.8-26 and 3.8-27. Generally, the predicted forces in combination with earthquake effect do not exceed member strengths. A limited number of members are found to exhibit inelastic behavior which does not exceed the allowable ductility limits of Table 3.8-24. Therefore, all structural elements satisfy the criteria.

Separations between the turbine building's primary structure and the turbine pedestal are adequate to ensure these structures will not impact each other when subject to the HE load combination. The relative displacements between these structures are summarized in Table 3.8-27A.

3.8.5.1.6 Materials, Quality Control, and Special Construction Techniques

The turbine building, including the turbine pedestals, was originally constructed prior to 1978. Following the HE evaluation of the plant, modifications to the turbine building and the turbine pedestals were made during the period 1978 to 1979. Materials installed during these two periods are described in the following paragraphs.

3.8.5.1.6.1 Concrete

Design strengths of concrete are as follows:

	Age, days	Compressive Strength, psi
Original construction:		
East-west walls	28	5000
Elevation 140 feet floor	60	5000
All other concrete	28	3000

Hosgri Modifications:		
Concrete above elevation 85 feet	28	5000
All other concrete	28	3000
Modifications for sixth diesel generator addition, all associated concrete	28	4000

Average strengths are used with the HE load combination. The average strengths are as follows:

	Age, days (except as noted)	Compressive Strength, psi
Original Construction:		
Turbine pedestal	6 years[a]	6000
East-west walls	28	5500
Elevation 140 feet floor	60	6590
All other concrete	28	3870
Hosgri Modifications:		
Concrete above elevation 85 feet	28	5680
All other concrete	28	4260

3.8.5.1.6.2 Reinforcing Steel

Reinforcing steel is ASTM A615, Grade 40, except in some locations where grade 60 is used. Average test values are used with HE load combinations. Properties of the reinforcing steel are as follows:

	Grade 40	Grade 60
Design yield strength, psi	40,000	60,000
Original construction		
Average yield strength, psi	51,400	65,900
Average tensile strength, psi	80,600	101,400
Hosgri Modifications		
Average yield strength, psi	51,900	67,000
Average tensile strength, psi	81,300	106,500

[a] Turbine pedestal concrete strength is based on cylinder tests of 6-year-old stored specimens. The strength is verified by rebound hammer tests and by tests of concrete core samples.

3.8.5.1.6.3 Structural Steel

Structural steel is ASTM A36 except for reinforcing bars installed at flanges of some columns along column lines A and G where ASTM A572 Grade 50, is used. Properties of the structural steel are as follows:

	ASTM A36	ASTM A572, Gr 50
Design yield strength, psi	36,000	50,000
Original construction		
Average yield strength, psi	44,000	
Average tensile strength, psi	68,000	
Hosgri Modifications		
Elevation 140 and 119 feet floor plate		
Average yield strength, psi	40,800	
Average tensile strength, psi	69,300	
Other structural steel		
Average yield strength, psi	44,500	55,200
Average tensile strength, psi	68,200	87,400

3.8.5.2 Intake Structure

3.8.5.2.1 Description of Intake Structure

The seismic Design Class II intake structure is a reinforced concrete building constructed with 3,000 psi minimum-specified-strength concrete. The structure has plan dimensions of approximately 240 x 100 feet. The long dimension corresponds to the north-south direction, and is parallel to the seaward face of the structure. The intake structure is backfilled by rock on three sides, and has water on the fourth (western) side. The top deck of the structure has a maximum elevation of +17.5 feet. A concrete ventilation tower with steel coaxial ventilation pipe extends to an elevation of +49.4 feet. The structure is supported by a concrete mat foundation at elevation -31.5 feet. Figures 3.8-72 through 3.8-74 illustrate plans at elevations +17.5, -2.1, and -31.5 feet; Figures 3.8-75 through 3.8-77 illustrate representative sections through the structure.

The top level of the structure consists of an 18-inch-thick concrete slab, except for the roadway area where it is 24 inches thick. Openings, as shown in Figure 3.8-72, are provided to allow removal of pumps, screens, and gates. The pump deck floor at elevation -2.1 feet supports the four main circulating water pumps and the four seismic Design Class I ASW pumps. Design Class I ASW equipment is located in ventilated watertight compartments. The structure is symmetric about a vertical plane in the east-west direction through its centerline.

3.8.5.2.2 Applicable Codes, Standards, and Specifications

The following codes and standards were used in the Hosgri evaluation and the design, construction, inspection, and testing of the intake structure.

(1) ACI Standard Building Code Requirements for Reinforced Concrete (ACI 318-63, ACI 318-71, ACI 318-77)

(2) Manual of Standard Practice for Detailing Reinforced Concrete Structures (ACI 315-65)

(3) Recommended Practices for Welding Reinforcing Steel, Metal Inserts and Connections in Reinforced Concrete Construction, American Welding Society AWS D12.1-75

(4) AISC Specification for the Design, Fabrication and Erection of Structural Steel for Buildings, February 12, 1969, and November 1, 1978

(5) Code for Welding in Building Construction, AWS D1.1-77, Rev. 2. For inspection of non-ASME structural welds or new non-ASME work performed after January 1, 1988, the guidelines of Nuclear Construction Issues Group (Visual Weld Acceptance Criteria, Vol. 1-3, EPRI Report No. NP-5380, September 1987) may be used except for those cases where:

    (a) Fatigue is a governing design condition

    (b) The weld allowables are permitted to be higher that those allowed by AWS D1.1 (such as the full penetration welds evaluation for the HE)

    (c) The weld is part of work performed in the ASME Section XI Inservice Inspection Program

(6) Recommended Lateral Force Requirements 1974 Seismology Committee, Structural Engineers Association of California (SEAOC)

(7) Materials and quality control tests for materials conform to ASTM standards

3.8.5.2.3 Loads and Loading Combination

Seismic Load Combination

$$U = D + L + HE \qquad (3.8\text{-}33)$$

where:

D	=	dead load of the structure and equipment loads
L	=	live load
HE	=	loads resulting from HE
U	=	strength required to resist design loads as described in Section 3.8.5.2.5

Wave Load Combination

$$U = D + L + W_f \qquad (3.8\text{-}34)$$

where:

U, D, and L are as defined in (1) above
W_f = wave force associated with breakwater degraded to MLLW

3.8.5.2.4 Design and Analysis Procedures

3.8.5.2.4.1 General

Structural analysis of the intake structure is performed by the traditional methods of engineering analysis for structural steel and reinforced concrete structures. These methods are based on the principles of equilibrium, compatibility of deformations, and predictions of material strength by the methods of the AISC Code, and the ACI Code. The use of these codes is discussed in Section 3.8.5.2.5.

3.8.5.2.4.2 Seismic Forces

A time-history dynamic analysis is performed with a computer program to determine the structure response spectra. A response spectrum dynamic modal superposition analysis is performed to determine structure response maxima. The analytical procedure using modal superposition methods is described in Section 3.7.2.

The demands resulting from the combination of north-south, east-west, and vertical components of the HE, in conjunction with dead loads, actual live loads, and soil pressures, are less than the yield capacity of the major portion of the structure, including the area housing the Class I ASW. The only exceptions are some of the flow straighteners (or piers) that exhibit stresses beyond code values. However, these piers demonstrate ductility properties that would preclude structural failure. The ductilities are within allowables as stated in Section 3.8.5.2.5. Table 3.8-28 presents the results of the analysis.

The intake structure is reviewed to verify that there is an adequate factor of safety against sliding and overturning, and the foundation pressure is within the allowable value of 50 ksf as described in Reference 13.

3.8.5.2.4.3 Wave Forces

As shown in Figures 3.8-78 and 3.8-79, a scaled, three-dimensional physical model of the cooling water intake basin, the intake structure, and a hypothetically damaged breakwater was constructed to examine the wave effects on the intake structure as described in References 8 and 9.

Based on the test results, the intake structure was modified to mitigate wave slam (high magnitude, high frequency) pressure behind the curtain wall and to withstand the measured pressures on the bottom of the slab.

The ASW pump compartments were modified to provide the required ventilation on the Design Class I equipment and to prevent flooding due to combined tsunami and storm wave runup conditions as described in Chapter 2. As discussed in Section 3.3.2.3.2.10, the ASW pump compartment modifications were reviewed for a tornado with missiles.

A risk analysis, as described in Reference 14, was performed to determine the frequency of vessel impact with the intake structure which houses the ASW pumps. In the analysis, the breakwater was assumed to be degraded to the MLLW level. The analysis considered only large vessels (greater than 250 tons displacement), since impact on the intake structure by smaller vessels was concluded, on the basis of a deterministic analysis, to be inconsequential to the safety-related function of the ASW pumps.

The results of risk analysis for frequency of impact indicate a frequency of 6.7×10^{-6} breakwater boundary crossings per year for storm-independent analysis and 1.9×10^{-5} breakwater boundary crossings per year for storm-dependent analysis. The probability of large vessels, therefore, crossing the degraded breakwater and impacting the intake structure is quite low.

3.8.5.2.5 Structural Acceptance Criteria

For the load combinations given in Section 3.8.5.2.3, the intake structure is designed so that it does not sustain damage that would adversely affect the function of the Class I ASW system and prevent it receiving an adequate supply of water.

For load combinations with seismic force, strength is based on SEAOC 1974 concrete shear walls; ACI 318-63 and ACI 318-71 for other concrete members; and AISC, Seventh Edition, Part II for steel members. Lateral force resisting elements are allowed inelastic deformation consistent with ductility factors indicated in Table 3.8-24. For these elements, the allowable stress limitations given in the codes above need not apply.

For load combinations with wave forces, strength is based on ACI 318-71 and AISC, Seventh Edition, Part II for all structural members except for ASW pump compartment

modifications. For the latter, strength is based on ACI 318-77 and 1.6 times AISC Eighth Edition, Part I allowable values.

3.8.5.2.6 Materials, Quality Control, and Special Construction Techniques

The intake structure was originally constructed prior to 1981. As a result of January 1981 storm damage to the west-breakwater, hydraulic model studies of wave effects on the intake structure were conducted in 1982 (References 8 through 12), and the intake structure was modified to withstand these wave effects.

The material strengths for these periods are provided below:

Concrete

Prior to 1981	Minimum specified fc'	=	3000 psi @ 28 days
	Average test values fc'	=	3630 psi
1981 modifications	Minimum specified fc'	=	5000 psi @ 28 days

Reinforcing Steel

Prior to 1981	ASTM A615, Grade 40;	Minimum specified fy	= 40 ksi
		Average test values fy	= 49.6 ksi
1981 Modifications	ASTM A615, Grade 60;	Minimum specified fy	= 60 ksi

Structural Steel

Prior to and after1981	ASTM A36;	Minimum specified fy	= 36 ksi

3.8.6 PIPEWAY STRUCTURES

3.8.6.1 Description of Pipeway Structures

The pipeway structure for each unit is a steel frame structure attached to the outside of the containment shell, the auxiliary building, and the turbine building as shown in Figure 3.8-80. The pipeway structure in one unit is essentially a mirror image of the other. The primary function of the pipeway structure is to support main steam and feedwater piping. The pipeway structure has five major platforms located at elevations 109, 114, 118, 127, and 138 feet. Connections between the pipeway structure and the auxiliary and turbine buildings are provided with slotted holes oriented such that horizontal motions cannot be transmitted between the structures.

3.8.6.2 Applicable Codes, Standards, and Specifications

3.8.6.2.1 Codes

The following codes and standards are used, insofar as they are applicable, in the design and/or construction of the pipeway structure.

(1) AISC Specification for Design, Fabrication, and Erection of Structural Steel for Buildings, February 12, 1969

(2) ACI Standard Building Code Requirements for Reinforced Concrete (ACI-318-63)

(3) Standard code for welding in building construction (AWS D1.0-69). For inspection of non-ASME structural welds or new non-ASME work performed after January 1, 1988, the guidelines of Nuclear Construction Issues Group (*Visual Weld Acceptance Criteria*, Vol. 1-3, EPRI Report No. NP-5380, September 1987) may be used except for those cases where:

   a) Fatigue is a governing design condition.

   b) The weld allowables are permitted to be higher than those allowed by AWS D1.1 (such as the full penetration weld evaluation for the HE).

   c) The weld is part of work performed in the ASME Section XI Inservice Inspection Program.

(4) Materials, and the quality control tests for materials, conform primarily to ASTM and ASME standards. Additional materials and supplemental quality assurance requirements conform to ANSI standards

3.8.6.3 Loads and Loading Combinations

3.8.6.3.1 Design Loads

The following loads are considered in the design of the pipeway structure.

3.8.6.3.1.1 Dead Loads

Dead loads consist of the weight of the structure, piping, pipe rupture restraints, electrical raceways, and equipment.

3.8.6.3.1.2 Live Loads

Live loads are temporary loads that may be placed on the structure. These are considered small in relative magnitude and, therefore, are considered negligible.

3.8.6.3.1.3 Earthquake Loads

Earthquake loads are as described in Section 3.7.2.1.7.1.

3.8.6.3.1.4 Wind Loads

Wind loads are determined in accordance with the criteria presented in Section 3.3. However, the forces due to wind are much less than those due to earthquake; consequently, seismic loads, rather than wind, are entered into the load combination equations.

3.8.6.3.1.5 Thermal Loads

Thermal loads are those induced by the main steam and feedwater pipes through the support system. These loads are considered negligible.

3.8.6.3.2 Loading Combinations

The following loading combinations are used in the design of the pipeway structure.

3.8.6.3.2.1 Normal Conditions

Dead loads and design earthquake (DE) are considered as follows:

$$S = D + DE \qquad (3.8\text{-}35)$$

where:

S	=	required capacity of structural members based on the method described in Section 3.8.6.5.1
D	=	dead load
DE	=	loads resulting from the DE

3.8.6.3.2.2 Abnormal Conditions

Where elastic working stress design methods are used:

$$1.6S = D + DDE \qquad (3.8\text{-}36)$$

$$1.7S = D + DDE + Yr \qquad (3.8\text{-}37)$$

1.7S = D + 1.25DE + Yr (3.8-38)

1.7S = D + HE (3.8-39)

Where plastic design methods are used:

1.0Y = D + DDE + Yr (3.8-40)

1.0Y = D + 1.25DE + Yr (3.8-41)

where:

DDE	=	loads resulting from the DDE
HE	=	loads resulting from the HE
Yr	=	reaction on structure from a broken pipe, generated by a postulated pipe break, including an appropriate dynamic load factor (DLF)
Y	=	required section strength based on plastic design methods described in Part 2 of the AISC specification referenced in Section 3.8.6.2.1

3.8.6.4 Design and Analysis Procedures

3.8.6.4.1 Hosgri Event

Seismic forces from the response spectrum dynamic analysis described in Section 3.7.2.1.7.1 are used in the stress evaluation of the Unit 1 pipeway structure. The Unit 2 pipeway structure is evaluated using a detailed three-dimensional model and the static equivalent method of seismic analysis described in Section 3.7.2.1.7.1. The calculated stress ratios for the most critical members are given in Table 3.8-5A.

3.8.6.4.2 Design Earthquake and Double Design Earthquake

Member forces are calculated using corresponding Hosgri forces adjusted in proportion to ratios of DE or DDE to HE spectral accelerations. These forces are used in the stress evaluation of the Unit 1 and 2 pipeway structures. Stresses obtained by this method are confirmed by time-history dynamic analysis described in Section 3.7.2.1.7.1. Calculated stress ratios for the most critical members are given in Table 3.8-5A.

3.8.6.4.3 Computer Programs

Computer programs used in the structural analysis and the verification measures are listed in Table 3.8-6.

3.8.6.5 Structural Acceptance Criteria

For DE and DDE load combinations in the absence of pipe break loads (Yr), the minimum specified yield strength for structural steel is considered. For load

combinations including HE or Yr, the actual material properties are used. In addition, the following conditions apply.

3.8.6.5.1 Normal Conditions

For normal conditions, the pipeway structure is designed to the allowable working stresses in Part 1 of the AISC Code, February 12, 1969; however, the increase in allowable stress usually allowed for load combinations involving earthquake forces is not used.

3.8.6.5.2 Abnormal Conditions

For abnormal conditions, the pipeway structure, in general, is designed for overall elastic behavior. For load combinations (3.8-37), (3.8-38), (3.8-40), and (3.8-41) of Section 3.8.6.3.2.2, the acceptance criteria described therein should be satisfied first without considering the effect of Yr. When considering the effect of Yr, local section strength capacities may be exceeded provided there is no loss of function of any safety-related system.

3.8.6.5.3 Factors of Safety

The calculated capacity-to-demand ratio for the most critical members of the pipeway structure are given in Table 3.8-5A. In all cases these ratios are greater than the minimum allowable value of 1.0. Therefore, all structural elements satisfy the criteria.

3.8.6.6 Materials, Quality Control, and Construction Techniques

Structural steel is ASTM A441 and ASTM A516 Grade 70. ASTM minimum specified values are used with DE and DDE load combinations in the absence of Yr. Average test values are used with load combinations that include HE or Yr. Minimum and average values are as follows:

	ASTM A441	ASTM A516
Minimum yield strength, psi	45,000	38,000
Average yield strength, psi	51,600	51,040

High strength bolts, nuts, and washers used for connections are predominantly ASTM A490. Some ASTM A325 bolts are also used when found acceptable. Impact tests for structural steel and high strength bolts were performed in accordance with ASTM Standard Method A370 at 0°F.

Welding electrodes conform to ASTM A233, E70 series low hydrogen.

Where indicated on drawings, nondestructive testing was performed as required utilizing ultrasonic or magnetic particle techniques.

Approved substitute for ASTM A441 structural steel is ASTM A572 Grade 42. For any new construction after May 2004, the structural steel used may be A572 Grade 42. The impact test is required for this new steel.

3.8.7 SAFETY-RELATED MASONRY WALLS

In accordance with Reference 28, safety-related masonry walls (see Section 3.8.7.1) have been reevaluated and modified as necessary using conservative design and analysis procedures, and structural acceptance criteria as specified in Section 3.8.7.5. Design and analysis methods and structural acceptance criteria are in accordance with Reference 29. NRC Staff acceptance of the wall reevaluation design and analysis methods is documented in Reference 30.

3.8.7.1 Description of Safety-Related Masonry Walls

Safety-related masonry walls are those walls which support safety-related piping or equipment, or whose failure could prevent a safety-related system from performing its intended safety function. Safety-related walls are located in the auxiliary and turbine buildings at locations identified in Figures 3.8-83, -84, and -85, and are evaluated in accordance with Reference 29. These walls are fire walls or nonbearing partitions serving various functions and are not required to resist tornado or missile loads and are not part of the buildings lateral force resisting system. Some of the walls support small piping, conduits, or instrumentation tubing. A few walls support concrete or metal deck ceilings.

All walls are single width, 8 or 12 inches thick, fully grouted, and reinforced in the horizontal and vertical directions with steel reinforcing bars. The bottoms of all walls are tied to the building structure.

In general, walls extend to the underside of the floor structure, where lateral support is provided by a structural supporting system. A separation joint filled with compressible material is provided at the top and side boundaries of all walls where they abut the building structure floors or columns. Walls are braced with steel members. The bottoms of some walls are connected to the floor with bolted steel angles. Some walls are strengthened by steel plates bolted to each face of the wall.

3.8.7.2 Applicable Codes, Standards, and Specifications

The following codes and standards are used in the design, construction, inspection, and testing of safety-related masonry walls:

(1) Building Code Requirements for Concrete Masonry Structures (ACI 531-79) and Commentary (ACI 531R-79)

(2) AISC Specification for the Design, Fabrication, and Erection of Structural Steel for Buildings, February 12, 1969

(3) Materials and quality control tests for materials conform to the applicable ASTM standards

3.8.7.3 Loads and Loading Combinations

3.8.7.3.1 Design Loads

The following loads are considered in the evaluation of safety-related masonry walls:

3.8.7.3.1.1 Dead Loads

Dead loads consist of the weight of the wall and supported items.

3.8.7.3.1.2 Live Loads

Live loads consist of occupancy loads, if any, acting on the wall.

3.8.7.3.1.3 Earthquake Loads

Earthquake loads are those resulting from the HE. The loads are based on the response spectrum, single-degree-of-freedom method described in Section 3.7.2.1. The percentage of critical damping used is 7 percent.

3.8.7.3.1.4 Thermal Loads

Thermal loads are loads induced by local increases in temperature resulting from normal operating and from postulated accident conditions.

3.8.7.3.1.5 Pipe Reaction Loads

Pipe reactions result from hydraulic forces, thermal expansion, and seismic events. These loads are transferred to the structure through pipe supports and result from normal operating conditions and postulated accident conditions.

3.8.7.3.1.6 Pressure Loads

Pressure loads are forces generated by a postulated pipe break. Pressures from a postulated broken pipe are calculated as described in Section 3.6.

3.8.7.3.1.7 Loads and Loading Combinations

The following load combinations are used in evaluation of safety-related masonry walls:

$$U = D + L + To + Ro + HE$$

U = D + L + Ta + Ra + 1.5Pa

U = D + L + Ta + Ra + 1.0Pa + HE

where:

U	=	strength determined using acceptance criteria described in Section 3.8.7.5
D	=	dead load
L	=	live load
To	=	thermal loads during normal operating conditions
Ro	=	pipe reactions during normal operating conditions
HE	=	loads resulting from an HE
Ta	=	thermal loads generated by a postulated pipe break, including To
Pa	=	pressure load generated by a postulated pipe break
Ra	=	pipe reactions from unbroken pipes generated by postulated pipe break conditions, including Ro

3.8.7.4 Design and Analysis Procedures

Evaluation of safety-related masonry walls is performed using traditional methods of engineering analysis. Proper consideration is given to boundary conditions, cracking of sections, and the dynamic behavior of the walls. Both in-plane and out-of-plane loads and interstory drift effects are considered.

HE forces on the walls are based on applicable building floor response spectra generated by the analysis described in Section 3.7.2.1. In some cases, detailed models of the walls and supporting steel members are used to calculate forces and stresses in the walls.

HE forces on the walls including wall reactions are calculated by linear elastic analysis. Applied forces on the walls include the combined effects of vertical loads and horizontal out-of-plane wall deflections (P-Δ effect). Masonry wall stiffnesses are based on best estimate (median) properties, which are:

E_m = 750 f'm
F'_m = 1950 psi
f_r = $4(f'_m)^{0.5}$

The stiffness and strength of walls strengthened with steel plates at each face are based on wall panel tests. Drypack grout at the top of the walls is treated as unreinforced and is not relied upon to withstand earthquake loads. An additional evaluation of the walls is performed to address the variability of material properties, workmanship, and construction tolerances.

Computer programs used in the structural analysis and the verification measures are listed in Table 3.8-6.

3.8.7.5 Structural Acceptance Criteria

In the evaluation of safety related masonry walls for load combinations, including HE or pipe break loads, actual material properties may be used.

The moment capacity of a masonry wall is not less than the moment produced by the applied loads. Moment capacity of the masonry wall is determined using the strength design method, with a strength reduction factor, ϕ, equal to 1.0. Allowable masonry shear stress is 1.3 x 1.1 $(f'_m)^{0.5}$, where f'_m is as defined in Section 3.8.7.4. Allowable masonry bearing stress is 2.5 x 0.25 (f'_m). Analysis of the behavior of masonry walls strengthened with steel plates is substantiated by tests. Allowable forces on steel members are based on 1.6 times allowable stresses defined in the AISC Code, Part 1, or 0.9 times member strengths defined in the AISC Code, Part 2.

3.8.7.6 Materials, Quality Control, and Special Construction Techniques

3.8.7.6.1 Masonry Units

Masonry units are hollow, load-bearing, open-ended lightweight units of ASTM Designation C90, Grade A. The average compressive test strength of masonry units is 3400 psi on the net area.

3.8.7.6.2 Reinforcing Steel

In general reinforcing steel is ASTM A615, Grade 40. The average yield strength by test is 51,400 psi.

In limited areas, reinforcing steel is ASTM A615, Grade 60. The average yield strength by test is 64,200 psi.

3.8.7.6.3 Core Fill

Grout having a minimum specified compressive strength of 2000 psi is placed in all masonry unit cells. The average tested compressive strength is 3285 psi.

3.8.7.6.4 Mortar

Mortar is ASTM Designation C270, Type S.

3.8.7.6.5 Construction Inspection

Inspection procedures meet the intent of Section 4.5 of Building Code Requirements for Concrete Masonry Structures (ACI 531-79).

3.8.8 PERMANENT SPENT FUEL STORAGE RACKS

3.8.8.1 Description of the Spent Fuel Pool and Racks

The description of the SFP is provided in Sections 3.8.2.1 and 9.1.2.2. Each fuel pool has 16 high density fuel rack modules as shown in Figure 9.1-2. They are free-standing and consist of individual cells with an 8.85 by 8.85-inch square cross-section, each of which stores a single Westinghouse PWR fuel assembly. The number of cells varies from 34 to 110 per module. The cells are fabricated by welding two formed stainless steel channels, which are welded together by stainless steel gap channels to provide the required predetermined distance between the cells. Typically, each module is provided with four support legs, three of which are adjustable and one fixed. The adjustable support legs are used to achieve a leveled free-standing position on the pool floor. For ease of installation and to reduce potential interferences with liner seam welds, each rack support leg is supported on a bridge plate. Typically, each rack module is equipped with girdle bars located near the top, which are designed to accommodate seismically induced impact loads.

3.8.8.2 Applicable Codes, Standards, and Specifications

The following codes and standards are used in the design and construction of the racks.

(1) AISC Specification for the Design, Fabrication, and Erection of Structural Steel for Buildings, 1969 Edition

(2) ASME Boiler and Pressure Vessel Code, Section III and Subsection NF, 1983 Edition

(3) AEC "Spent Fuel Storage Facility Design Basis," SG 13, March 1971

(4) Westinghouse Fuel Assembly, Storage and Refueling Equipment Design Interface Specification No. F-8, Rev. 8

(5) NRC "OT Position for Review and Acceptance of Spent Fuel Storage and Handling Applications," April 14, 1978, and "Modifications to the OT Position," January 18, 1979, letters from B. K. Grimes to All Power Reactor Licensees

(6) Appendix D to Standard Review Plan, Section 3.8.4, "Technical Position on Spent Fuel Pool Racks," Revision 0, July 1981, NRC

3.8.8.3 Loads and Loading Combinations

The loads and loading combinations and the corresponding acceptance criteria are as follows (Reference 20):

Loading Combination		Stress Limit
(a)	D $D + T_o$ $D + T_o + E$	Level A service limits
(b)	$D + T_a + E$ $D + T_o + P_f$	Level B service limits
(c)	$D + T_f + E'$ $D + F_d$	Level D service limits (The functional capability of the fuel racks should be demonstrated)

where:

D	=	Dead weight-induced stresses (including fuel assembly weight)
F_d	=	Force caused by the accidental drop of the heaviest load from the maximum possible height
P_f	=	Upward force on the racks caused by postulated stuck fuel assembly
E	=	DE
E'	=	HE
T_o	=	Differential temperature induced loads (normal or upset condition)
T_a	=	Differential temperature induced loads (abnormal design conditions)

3.8.8.4 Design and Analysis of Racks

3.8.8.4.1 Design Basis Rack Model

The racks are analyzed using a nonlinear dynamic model as shown in Figure 3.8-81. The model simulates the rack as a single stick supported on a rigid base with supports. Impact springs are provided at the girdle bar and the baseplate locations to account for rack-to-rack and/or rack-to-wall impact. The legs are represented by 4 impact springs to account for the impact as well as frictional sliding. The rattling of the fuel assemblies in cells is considered by the use of additional impact springs. The model includes 2 mass points comprising 8 degrees of freedom. Mass 1 is located in the rack module and has 6 degrees of freedom, (i.e., 3-dimensional space with 3 linear translations and 3 rotations). Mass 2 is located at the top of the fuel and moves with 2 translational degrees of freedom. The lower mass point of the fuel assembly is lumped with the rack module mass (Reference 20).

3.8.8.4.2 Design Basis Rack Analysis and Results

Due to the complexity of the nonlinear time-history analysis, the racks, in general, are analyzed using a single rack model (Figure 3.8-81) that uses conservative model parameters. The seismic input motions are provided in the form of three orthogonal time histories at the fuel pool liner location. A minimum value of 0.2 and a maximum value of 0.8 are used for the range of friction coefficients between the rack supports and the pool liner (Reference 23). The effects of fluid are considered in accordance with the method advanced by Fritz (Reference 24). The impact springs are set at values to produce conservative impact forces. Parametric studies have been performed to evaluate the effects of various design variables such as friction coefficients, size of rack, fuel loading (partially loaded, fully loaded, or empty) on rack, spacing between racks (corner rack vs. non-corner rack), fabrication tolerance, etc. The bounding loads are obtained from those parametric analyses, which are then used for the design of rack components.

The racks have been analyzed to store LOPAR, VANTAGE 5, and ZIRLO fuel assemblies. The impact loads between the cell wall and the fuel assemblies are less than those provided by Westinghouse.

3.8.8.4.3 Multi-Rack Confirmatory Model

The design basis analysis includes several conservative assumptions applied to a single rack model to obtain conservative impact loads. To confirm the adequacy of this methodology, additional multi-rack analyses have been performed (References 21 and 22).

Figure 3.8-82 shows the two-dimensional dynamic model used in this analysis. Each rack is represented by four degrees of freedom simulating fuel rattling, translation, and rocking of the racks. The parameters for the model are developed in a manner similar to those used for the design basis model, except more realistic assumptions are made to compute the fluid coupling coefficients and spring constants.

3.8.8.4.4 Multi-Rack Confirmatory Analysis and Results

The analyses are performed using the nonlinear time history method. The governing horizontal (east-west) and vertical ground motions are applied simultaneously to the model. Parametric studies have been performed to evaluate the effects of various friction coefficients, fuel loading on racks, sizes of racks, lateral gaps, and fabrication tolerances. The results of the analysis demonstrate that the use of conservative model parameters in the design basis analysis (Reference 20) yields conservative rack and fuel assembly impact loads.

3.8.8.5 Materials, Quality Control, and Special Construction Techniques

The materials for both Region 1 and Region 2 rack modules are:

Stainless steel sheet and plate	ASTM A-240-304L
Weld filler material	ASME SFA-5-9 Type 308L and 308LSI
Top part of support	ASTM 479-S21800
Bottom part of support	ASTM SA564-630

3.8.8.6 Design and Analysis of Pool Structure

The existing pool structure was evaluated for postulated interactions of the rack modules with the structure as a result of the seismic event. The effect of the change in fuel rack mass on global dynamic response of the pool structure was considered. The change in global mass was determined to be on the order of 1 percent to 2 percent, therefore, the change in dynamic response is insignificant.

The pool walls were evaluated for the out-of-plane effects due to hydrostatic, hydrodynamic, thermal, and seismic loads. They adequately meet the loading combinations and acceptance criteria in Sections 3.8.2.3.2 and 3.8.2.5, respectively. The walls were also checked for additional impact loads that may result from the rack-to-wall impact and they meet the acceptance criteria of Section 3.8.2.5.

The liner was evaluated for the maximum vertical impact load and maximum horizontal sliding load and was determined to be adequate for leak tightness. The concrete slab that supports the liner was evaluated for the floor impact load using the allowable values specified in ACI 349-80 (Reference 25). The liner in-plane loadings that result from the sliding of the rack and thermal effects were evaluated in accordance with the allowable strains and anchor displacements as specified in ASME Section III, Division II, 1983 (Reference 26).

3.8.9 REFERENCES

1. Timoshenko and Woinowsky-Krieger, Theory of Plates and Shells, McGraw-Hill, Inc., New York, 1959, Second Edition.

2. Deleted.

3. Code for Concrete Reactor Vessels and Containments, ACI Standard 359-75.

4. PG&E's response to Governor George Deukmejian's and Joint Intervenors' first set of interrogatories (Docket Nos. 50-275 and 50-323): Interrogatory Number 2 – Unit 1; Interrogatory Number 3 - Unit 2.

5. PG&E's first supplemental response to Governor Deukmejian's and Joint Intervenors' first set of interrogatories. (Docket Nos. 50-275 and 50-323.)

6. Letter dated August 13, 1973, with enclosures, (Docket Nos. 50-275 and 50-323) from A. Giambusso of the AEC to F. T. Searls of PG&E.

7. Recommended Evaluation Criteria for Diablo Canyon Nuclear Power Plant Auxiliary Building Walls and Diaphragms, by Jack R. Benjamin and Associates, Inc., dated February 11, 1983, prepared for Bechtel Power Corporation, San Francisco, California.

8. The Height Limiting Effects of Sea Floor Terrain Features and of Hypothetically Extensively Reduced Breakwaters on Wave Action at Diablo Canyon Sea Water Intake, by Omar J. Lillevang, Fredric Raichlen, Jack C. Cox, March 15, 1982.

9. The Investigation of Wave-Structure Interactions for the Cooling Water Intake Structure of the Diablo Canyon Nuclear Power Plant, by Fredric Raichlen, December 1982.

10. Criteria for Selection of Critical Wave Directions, Omar J. Lillevang, November 2, 1982.

11. Wave Effects on Intake Structure at Diablo Canyon Units 1 and 2, E. N. Matsuda, January 1983.

12. Investigation of Seawater Injection into the Auxiliary Saltwater Pump Room Due to the Splash Runup During the Design Flood Events at Diablo Canyon, P. J. Ryan, January 1983.

13. Geotechnical Studies on Intake Structure, Water Storage Tanks, Diesel Fuel Oil Storage Tanks, for Diablo Canyon Power Plant, San Luis Obispo County, California, by Harding-Lawson Associates, April 12, 1978.

14. Frequency of Vessel Impact with the Diablo Canyon Intake Structure, by Jack R. Benjamin and Associates, December 10, 1982.

15. Deleted in Revision 10.

16. Deleted in Revision 10.

17. Deleted in Revision 10.

18. Deleted in Revision 10.

19. Deleted in Revision 4.

20. Seismic Analysis Report, Seismic Analysis of High Density Fuel Racks for PG&E for Diablo Canyon Nuclear Power Station, Rev. 3, September 3, 1986, A. Soler, TM #779.

21. "Additional Information on Rack to Rack Interaction," Enclosure 1 to PG&E Letter No. DCL-87-070, dated April 7, 1987.

22. "Three-Dimensional Studies (ACORN 10 and ACORN 12)," Enclosure to PG&E Letter No. DCL-87-082, dated April 23, 1987.

23. Rabinowicz, E., Friction Coefficient Value for a High Density Fuel Storage System, Report to General Electric Nuclear Energy Program Division, November 23, 1977.

24. Fritz, R.J., The Effect of Liquids on the Dynamic Motions of Immersed Solids, Journal of Engineering for Industry, pp. 167-173, February 1972.

25. ACI Standard 349-80, Code Requirements for Nuclear Safety Related Concrete Structures, American Concrete Institute, Detroit, Michigan.

26. ASME Boiler and Pressure Vessel Code, American Society of Mechanical Engineers, Section III, Division II, 1983.

27. EPRI NP-5380 Final Report, Visual Weld Acceptance Criteria, Volumes 1-3 (Nuclear Construction Issues Group (NCIG) NCIG-01, Revision 2, NCIG-02 Revision 2, and NCIG-03 Revision 1), September 1987.

28. PG&E Letter DCL-90-289, with enclosure, from J.D. Shiffer to NRC, December 14, 1990.

29. PG&E Letter DCL-91-026, with enclosure, from J.D. Shiffer to NRC, February 12, 1991.

30. Letter dated September 18, 1991, with enclosure, (Docket Nos. 50-275 and 50-323) from R.P. Zimmerman of NRC to J.D. Shiffer of PG&E.

31. Letter from PG&E (J. O. Schuyler) to the NRC (D. G. Eisenhut), Design Verification Program Phase I Final Report, Diablo Canyon Unit 1, October 14, 1983.

32. Deleted in Revision 20

33. Deleted in Revision 20

34. Enova Engineering Services, "Position Paper on Shear Strength of A325 Bolts as Specified by the 7th Edition of AISC," dated July 3, 2008.

35. J. W. Fisher and Associates, "Review Comments on Position Paper on Shear Strength of A325 Bolts as Specified by the 7th Edition of the AISC Manual," dated July 10, 2008.

36. NRC (D.P. Allison) Letter to PG&E, "Summary of Meeting Held on February 4, 1977 to Discuss the Diablo Canyon Seismic Design Reevaluation," with enclosures (Docket Nos. 50-275 and 50-323), dated May 18, 1977.

37. NRC, Safety Evaluation Report Related to the Operation of of the Diablo Canyon Nuclear Power Station, Units 1 and 2, NUREG-0675, Supplement No. 7, dated May 1978.

38. Robert P. Kennedy Structural Mechanics Consulting, "Comments on Position Paper on Shear Strength of A325 Bolts as Specified by the 7th Edition of AISC," Report No. RPK-80704, dated July 4, 2008.

39. PG&E Calculation 52.15.9.11, Revision 2, "Evaluation of Fuel Handling Building Crane and Fuel Handling Building Steel Superstructure of Added Loads Due to Attachment of Redundant Tension Links for Spent Fuel Transfer Cask Handling", Page 133.

3.8.10 REFERENCE DRAWINGS

Figures representing controlled engineering drawings are incorporated by reference and are identified in Table 1.6-1. The contents of the drawings are controlled by DCPP procedures.

Diablo Canyon Power Plan	Regulatory Guide 1.15
In addition to the requirements of ASTM A 615, the Company specification requires the following: 1. Grade 60 bars be limited in carbon and manganese content to a maximum of 0.45% and 1.3% respectively. 2. Performance of a check analysis, which is listed as an option in ASTM A 615. 3. No. 14 and No. 18 bars be subjected to a 90° bend test using a pin having a diameter eight times the diameter of the bar.	Where any material property such as yield strength to tensile strength ratio, ductility, weldability or other similar property is relied upon by the designer or constructor, then the reinforcing bar chemistry should be controlled to the extent required to achieve the desired material property, and confirmatory testing should be performed.
Deformations were inspected during production to ensure conformance with ASTM A 615.	Deformations of the reinforcing bars should be inspected to assure their compliance with ASTM A 615-72 and with the licensee's specifications pertinent to bonding and other purposes which are dependent on the deformation characteristics.
Adequacy of deformations for splicing was demonstrated by the tensile tests of the Cadweld splices. See Table 3.8-2.	Adequacy of deformations for splicing will be demonstrated by the tensile tests of the splices. mechanical splice. See Safety Guide 10, "Mechanical (Cadweld) Splices in Reinforcing Bars of Category I Concrete Structures."

(a) Supplemental Requirement (S-1) is for a 90° bend test, using a pin diameter 10 times the bar diameter, on No. 14 and No. 18 bars.

TABLE 3.8-2

MECHANICAL (CADWELD) SPLICES IN REINFORCING BARS OF CONCRETE CONTAINMENTS
COMPARISON OF PROGRAM USED ON DIABLO CANYON POWER PLANT WITH SAFETY GUIDE 10

Diablo Canyon Power Plant	Safety Guide 10
Prior to production splicing, each operator was instructed by a representative of the manufacturer. Each operator (a crew consisted of an operator and a helper) prepared one qualification splice for each of the splice positions for which he was qualified. The qualification splice was made using the same materials as those used in the structures. The completed qualification splices had to pass visual inspection and develop the minimum tensile strength of the reinforcing steel. A manufacturer's representative was present for at least the first 20 production splices for each crew to verify that proper procedures were being used and quality splices obtained.	1. <u>Crew Qualification</u> - Each member of splicing crew (or each crew if the members work as a crew) should prepare two qualification splices for each of the splice positions (e.g., horizontal, vertical, diagonal) to be used. The qualification splices should be made using the same materials (e.g., bar, sleeve, powder) as those to be used in the structure. The completed qualification splices should meet the requirements specified by the designer of the containment structure and approved by the licensee, pass visual inspection as provided by Paragraph 2 below, and meet the tensile tests as provided by Paragraph 3 below.
All completed splices were visually inspected in accordance with the recommendations of the Erico Co. inspection manual RB-5M 768, Inspection of the Cadweld Rebar Splice. This visual inspection included both ends of the sleeve, the tap hole, and measurement of void area.	2. <u>Visual Inspection</u> - All completed mechanical splices should be inspected at both ends of the splice sleeve and at the tap hole in the center of the splice sleeve in accordance with the requirements specified by the designer of the containment structure and approved by the licensee.
In addition, at least twice daily for each Cadweld crew, an inspector observed the entire splicing operation including cleaning of rebar ends, spacing of rebar, centering of rebar ends, loading the crucible,	Among the items should be included in these specifications are longitudinal centering of sleeve on the spliced ends, allowable voids in filler metal, extent of leaking of filler metal,

Diablo Canyon Power Plant	Safety Guide 10
and firing the charge. The Cadweld procedure specified for the DCPP includes placing a mark 12 inches ± 1/4-inch back from the end of the bar. This line was used as a reference to determine if the bar ends are centered in the sleeve. Acceptance criteria for splice tensile tests is as follows: No splice in the test series may have a tensile value below 125% of the specified yield point stress, and no more than 5 % of the splices tested may have an ultimate tensile strength less than 85% of that specified. The average tensile strength of all splices in the test series must equal or exceed the ASTM specified minimum ultimate strength.	permissible gap between rebar ends, cartridge size, gas blowout, amount of packing and slag at the tap hole. Splices that fail to pass visual inspection should be discarded and replaced, and should not be used as tensile test samples. 3. Tensile Testing - Splice samples may be production splices (i.e., those cut directly from in place reinforcing) or sister splices (i.e., those removable splices made in-place next to production splices and under the same conditions). Splice samples should be subjected to tensile tests in accordance with the sampling frequency specified in Paragraph 4a or Paragraph 4b below, to determine conformance with the following acceptance standards: a. The tensile strength of each sample tested should be equal or exceed 125 percent of the minimum yield strength specified in the ASTM standard appropriate for the grade of reinforcing bar using loading rates set forth in ASTM Specification A 370 dated August 15, 1968. b. The average tensile strength of each group of 15 consecutive samples should equal or exceed the guaranteed ultimate tensile strength specified for the reinforcing bar.

Diablo Canyon Power Plant	Safety Guide 10
	If any sample tested fails to meet the provisions of Paragraph 3a above, the procedure of Paragraph 5a below should be followed.
	If the average tensile strength of the 15 samples tested fails to meet the provisions of Paragraph 3b above, the procedure of Paragraph 5b below should be followed.
Testing frequency for each crew, position, and grade of bar was as follows:	4. Tensile Test Frequency - Separate test cycles should be established for mechanical splices in horizontal, vertical, and diagonal bars, for each bar size, and for each splicing crew as follows:
One out of the first 10 splices. This splice must be a production splice for No. 18, Grade 60 bars and a sister splice for other sizes and grades of bar.	a. Test Frequency for Production Splice Test Samples. If only production splices are tested, the sample frequency should be:
Three out of the next 90 splices for No. 18, Grade 60 bars and one out of the next 90 splices for all other sizes and grades of bar.	1 of the first 10 splices 1 of the next 90 splices 2 of the next and subsequent units of 100 splices
Three out of second and subsequent 100 splice units for No. 18, Grade 60 bars and one out of second and subsequent 100 splice units for all other sizes and grades of bar.	b. Test Frequency for Combinations of Production and Sister Splices. If production and sister splices are tested, the sample frequency should be:
At least 25% of the total number of No. 18, Grade 60 test splices must be made by cutting out	

TABLE 3.8-2

Diablo Canyon Power Plant	Safety Guide 10
production splices on a random basis. The remaining test splices may be made by having test bars tie wired alongside the production bars and spliced in sequence with those bars. The minimum length of the spliced bars is 3 feet.	1 production splice of the first 10 production splices 1 production and 3 sister splices, for the next 90 production splices 3 splices, either production or sister splices, for the next and subsequent units of 100 splices. At least 1/4 of the total number of splices tested should be production splices.
In the event a splice should fail the tensile test criteria, the specimen was to be examined by a testing laboratory. Based on the results of this investigation, additional splices by the crew responsible, as directed by the Engineer, were to be taken from the structure to ensure that there are no other defective splices. The procedures of the crew responsible for making the failed splice were to be reviewed, and if necessary, the crew retrained and requalified.	5. Procedure for Substandard Tensile Test Results a. If any production or sister splice tested fails to meet the tensile test specification of Paragraph 3a and the observed rate of splices that fail the tensile test at that time does not exceed 1 for each 15 consecutive test samples, the sampling procedure should be started anew. If any production or sister splice used for testing fails to meet the tensile test specification in Paragraph 3a, and the observed rate of splices that fail the tensile test exceeds 1 for each 15 consecutive test samples, mechanical splicing should be stopped. In addition, the adjacent production splices on each side of the last failed splice and 4 other splices distributed uniformly throughout the balance of the 100 production splices under investigation should be tested,

TABLE 3.8-2

Diablo Canyon Power Plant	Safety Guide 10
	and an independent laboratory analysis should be made to identify the cause of all failures. The results of these tests should be evaluated by the designer of the containment structure and the licensee to determine the required corrective action. The designer and the licensee should specify the extent of repairs necessary and the actions required to prevent further failures from the identified causes.
	b. If two or more splices from any of these 6 additional splice samples fail to meet the tensile test specification of Paragraph 3a, the balance of the 100 production splices under investigation should be rejected and replaced.
	When mechanical splicing is resumed, the sampling procedure should be started anew.
	If the average tensile strength of the 15 consecutive samples fails to meet the provisions of paragraph 3b above, the designer of the containment structure and the licensee should evaluate and assess the acceptability of the reduced average tensile strength with respect to the required strength at the location from which the samples were taken.

TABLE 3.8-3

NONDESTRUCTIVE EXAMINATION OF PRIMARY CONTAINMENT LINER WELDS
COMPARISON OF PROGRAM USED ON DIABLO CANYON POWER PLANT WITH SAFETY GUIDE 19

Diablo Canyon Power Plant	Safety Guide 19
	1. Nondestructive Examination of Liner Seam Welds
For each welder and welding position, the first 10 feet of weld was examined radiographically. Thereafter, a minimum of 10% of the welding (to at least include all intersections of joints) was progressively examined radiographically as welding was performed. This was done on a random basis with the location specified in such a manner that an approximately equal number of radiographs were taken from the work of each welder. The techniques of radiographic examination of welds were in accordance with Paragraph UW-51 of Section VIII, ASME Boiler and Pressure Vessel Code (ASME B&PV Code). See Notes 1 and 2.	a. For each welder and welding position (flat, horizontal, and overhead), the first 10 feet of weld, and one spot (not less than 12 inches in length) in each additional 50 foot increment of weld (weld test unit) or fraction thereof should be examined radiographically in accordance with the techniques prescribed in Section V, "Nondestructive Examination," of the ASME Boiler and Pressure Vessel Code (ASME B&PV Code). In any case, a minimum of 2 percent of all liner seam welds should be examined by radiography.
Where radiographic examination of liner seal welds was not feasible, a minimum 10% of the welding (to at least include all locations where there are welded backing strip splices and intersections) was examined by magnetic particle or liquid penetrant testing. Magnetic particle testing was in accordance with Appendix VI of Section VIII, ASME B&PV Code. Liquid penetrant testing was in accordance with Appendix VIII of Section VIII, ASME B&PV Code. See Notes 1 and 2.	b. Where radiographic examination of liner seam welds is not feasible or where the weld is located in areas which will not be accessible after construction, the entire length of weld should be examined by the magnetic particle method or by the ultrasonic method in accordance with the techniques prescribed in Section V of the ASME BP&V Code for such examination methods.

Diablo Canyon Power Plant	Safety Guide 19
All liner seam welds were tested for leaktightness in accordance with the following method:	c. All liner seam welds should be tested for leaktightness in accordance with the following method (or other methods of equivalent sensitivity):
Immediately preceding the test, a soap solution is applied to the weld. The application of the soap solution must not precede the vacuum box by more than 3 minutes. The vacuum box, which contains a viewing window, is placed over the area to be tested and evacuated to a 5 psi differential with the atmospheric pressure.	Immediately preceding the test, a soap solution (or other appropriate solution) should be applied to the weld. A vacuum box containing a viewing window should be placed over the area to be tested and evacuated to produce at least 5 psi differential with the atmospheric pressure. Leaks in welds, if present, should be detected by formation of bubbles. The solution used for the test should have bubble formation properties adequate for identification of leaks. The test solution should be checked every hour, with a suitable test leak to verify the bubble formation property of the solution used.
Leak chase channels are installed over the liner welds. Upon completion of one zone of leak chase channels, the zone was tested at the containment structure design pressure of 47 psi. The acceptance criteria is that there be no loss of pressure within 2 hours as indicated by a pressure gauge.	d. Where leak chase system channels are installed over liner welds, channel-to-liner plate welds should be tested for leak- tightness by pressurizing the channels to containment design pressure. If any indicated loss of channel test pressure occurs within 2 hours, as evidenced by a test gauge, the channel-to-liner welds should be soap bubble tested in accordance with the above procedure.

Diablo Canyon Power Plant	Safety Guide 19
	2. Nondestructive Examination of Penetration, Airlock, and Access Opening Welds
All welds in penetration, airlocks, and access openings that are not backed by concrete were fully examined in accordance with Class B requirements of Section III, ASME B&PV Code. See Notes 1, 2, 3, and 4. All welds between flued heads and pipelines were fully examined in accordance with the Class II requirements of ANSI B 31.7, Nuclear Power Piping.	a. All welds in penetration, airlocks, and access openings that are not backed by concrete, such as welds between penetrations and flued fittings and pipelines, should be fully examined in accordance with examination methods of NE-5120 of Section III of the ASME B&PV Code employing the techniques prescribed in Section V of that code.
Welds backed by concrete in the vicinity of penetrations were examined as follows: 1. Welds between the penetration sleeve and insert plate were fully examined in accordance with the Class B requirements of Section III, ASME B&PV Code. See Notes 1, 2, and 4. 2. Welds between the insert plate and the liner were examined under the same criteria as liner seam welds. All welds backed by concrete in the containment structure are carbon steel.	b. All welds in the vicinity of penetrations and access openings that are backed by concrete, such as welds between penetration and reinforcing plate,[a] penetration and liner, reinforcing plate and liner, liner insert and liner, reinforcing plate and frames for airlocks and access openings, and liners and frames for airlocks and access openings, should be fully examined (1) in accordance with Paragraph 2a above or (2) by magnetic particle, or liquid penetrant when a nonmagnetic weld is used, in accordance with the techniques prescribed in Section V of the ASME B&PV Code.

(a) Thickened liner insert which provides local reinforcement.

Diablo Canyon Power Plant	Safety Guide 19
Examination of welds in penetrant assemblies and in the vicinity of penetrations is described in the preceding paragraphs.	c. All welds in bellow type expansion joints provided in penetration assemblies or appurtenances to the containment vessel should be magnetic-particle or liquid-penetrant tested when a nonmagnetic weld is used, in accordance with the techniques prescribed in Section V of ASME B&PV Code for such examination methods.
	3. Qualification of Welders and Welding Procedures
The qualification of welders, welding machine operators, and welding procedures was in accordance with Section IX, "Welding Qualifications," of the ASME B&PV Code. See Note 2.	The qualification of welders, welding machine operators, and welding procedures should be in accordance with Section IX, "Welding Qualifications," of the ASME B&PV Code.
	4. Qualification of Nondestructive Examination Personnel
Nondestructive examinations were performed by personnel qualified in accordance with the appropriate parts of the ASME B&PV Code. See Notes 1 and 2.	Nondestructive examination should be performed by personnel designated by the licensee or his agent and qualified in accordance with the provisions of Section V of the ASME B&PV Code.
	5. Selection of Spots for Radiographic Examination
The spots of liner seam welds to be radiographically examined were selected on a random basis with the locations selected such that all intersections	The spots of liner seam welds to be radiographically examined should be randomly selected, but no two spots in adjacent weld test units

Diablo Canyon Power Plant	Safety Guide 19
of joints were examined, and an approximately equal number of radiographs were taken from the work of each welder. The location covered by each radiograph was recorded.	should be closer than 10 feet and their locations should be recorded.
	6. Time of Examination
Nondestructive examinations were done progressively as welding was performed.	All examinations should be performed as soon as practicable after the linear increment of weld to be examined is completed.
	7. Acceptance Standards
	a. Containment Liner Seam Welds Examined by Radiography
Where a spot in the seam weld is judged acceptable in accordance with Paragraph UW-51 of Section VIII, ASME B&PV Code, the entire weld test unit represented by this spot radiograph is considered acceptable. See Notes 2 and 3.	Where a spot in the seam weld is judged acceptable in accordance with the referenced standards of NE-5120 of Section III of the ASME B&PV Code, the entire weld test unit represented by this spot radiograph is considered acceptable.
	b. Containment Liner Seam Welds Examined by Ultrasonic or Magnetic Particle
Where a spot in the seam weld examined by magnetic particle or liquid penetrant method is judged	Seam welds examined by ultrasonic or magnetic particle methods are considered acceptable

Diablo Canyon Power Plant	Safety Guide 19
acceptable, in accordance with the acceptance criteria referenced in Section VIII, ASME B&PV Code, the entire weld seam represented by the examination is considered acceptable. See Notes 2 and 3.	provided the examinations meet the acceptance standards referenced for such examination methods in NE-5120 of Section III of the ASME B&PV Code.
The acceptance criterion for the vacuum box test is that no leaks be detected.	c. <u>Soap Bubble Leak Tests of Containment Liner Welds</u> Liner welds are considered acceptable provided no leakage is detected by soap bubble tests (or by other methods of equivalent sensitivity).
	d. <u>Penetration, Airlock, and Access Opening Welds</u>
Penetration, airlock, and access opening welds that are not backed by concrete are considered acceptable provided the examinations meet the acceptance standards referenced for Class B vessels in Section III, ASME B&PV Code. See Notes 2, 3, and 4. Welds between flued heads and pipelines are considered acceptable provided the examinations meet the acceptance standards referenced for Class II piping in ANSI B31.7, Nuclear Power Piping.	Penetration, airlock, and access opening welds are considered acceptable provided the examinations meet the acceptance standards referenced in NE-5120 of Section III of the ASME B&PV Code. Welds in bellows type expansion joints are considered acceptable if the examinations meet the acceptance standards referenced in magnetic particle and liquid penetrant methods in NE-5120 of Section III.

Diablo Canyon Power Plant	Safety Guide 19
Welds between the penetration sleeve and insert plate are considered acceptable provided the examinations meet the acceptance standards referenced for Class B vessels in Section III, ASME B&PV Code. See Note 2.	
	8. Repair and Reexamination a. Containment Liner Seam Welds Examined by Radiography
If a radiographed spot failed to meet the specified acceptance standards, two additional spots of the same length were radiographically examined in the same weld seam at locations away from the original spot, but in welds performed by the same welder or welder operator. The locations of these additional spots were determined as provided for the original spot examination.	When a radiographed spot fails to meet the specified acceptance standards, two additional spots should be radiographically examined in the same weld test unit at locations at least one foot removed (on each side) from the original spot. The locations of these additional spots should be determined by the examiner using the same procedure followed in the selection of the original spot for examination and the examination results should determine the following corrective actions:
If the two additional spots examined showed welding that meets the specified acceptance standards, the entire weld represented by the three radiographs is judged acceptable. The defective welding disclosed by the first of the three radiographs was removed and repaired.	(1) If the two additional spots examined meet the specified acceptance standards, the entire weld unit represented by the three spot radiographs is considered acceptable. However, the defective welding disclosed by the first of the three radiographs should be repaired by welding.

Diablo Canyon Power Plant	Safety Guide 19
If either of the two additional spots examined showed welding that does not comply with the specified acceptance standards, the entire portion of the seam represented was considered unacceptable or, optionally, the entire weld represented was completely radiographed and defective welding corrected to meet the specific acceptance standards.	(2)If either of the two additional spots examined fails to meet the specified acceptance standards, the entire weld test unit is considered unacceptable. The entire weld should be removed and the joint should be rewelded or, optionally, the entire weld unit may be completely radiographed and defective welding only need be repaired.
Repair welding was performed using a qualified procedure. The rewelded joints or weld repaired areas were completely reradiographed and meet the specified acceptance standards.	(3)Repair welding should be performed using a procedure as specified under regulatory position 3. above. The weld repaired areas in each weld test unit should be spot radiographed at one selected location to meet the acceptance criteria specified in regulatory position 7.a. or 8.a. (1). above.
	b.<u>Containment Liner Seam Welds Examined by Ultrasonic or Magnetic Particle</u>
If a weld that had been examined did not comply with the specified acceptance standards, additional examination was performed to the same extent as required for radiography. The weld was repaired and reexamined in accordance with the provisions of Section VIII of the ASME B&PV Code. See Notes 2 and 3.	When a weld which has been examined does not comply with the specified acceptance standards, the weld should be repaired and reexamined in accordance with the provisions of Section III of the ASME B&PV Code.

Diablo Canyon Power Plant	Safety Guide 19
	c. Soap Bubble Tests of Containment Liner Welds
If a weld was judged unacceptable because leakage is repaired. Repair welding was performed using a procedure qualified as specified for production welds. The weld repaired areas were reexamined by soap bubble leakage retesting.	Welds judged unacceptable because leakage is detected by the soap bubble test (see regulatory position 7.c. above) should be repaired. Repair welding should be performed using a qualified procedure as specified under regulatory position 3. above. The weld repaired areas should be reexamined by soap bubble leakage retesting.
	d. Penetration, Airlock and Access Opening Welds
If a weld was judged unacceptable on a penetration sleeve airlock, or access opening, the weld was repaired and reexamined in accordance with the provisions for Class B vessels of Section III of the ASME B&PV Code. See Notes 2 and 3.	Welds judged acceptable in accordance with regulatory position 7.d. should be repaired and reexamined in accordance with the provisions of Section III of the ASME B&PV Code.
	9. Records
Retention of records is discussed in Chapter 17.	Records of radiographs and other nondestructive examinations including those for repaired defective welds should be retained by the licensee in compliance with the provisions of Section XVII, "Quality Assurance Records," of Appendix B to 10 CFR Part 50, "Quality Assurance Criteria for Nuclear Power Plants and Fuel Reprocessing Plants."

Notes:

1. Section V, ASME B&PV Code, which provides techniques for nondestructive examination applicable to all sections of the ASME B&PV Code, was first published in July 1971. Although it may eventually replace the corresponding parts of other sections of the ASME B&PV Code, the individual sections still contain techniques for nondestructive examinations.

2. References in the table to ASME B&PV Code for the Diablo Canyon plant refer to 1968 Edition, including addenda through Summer 1968.

3. NE-5120, Section III, ASME B&PV Code, requires examination technique and acceptance criteria in accordance with Section VIII, ASME B&PV Code (Paragraph UW-51 for radiography).

4. Class B requirements of Section III, ASME B&PV Code, specify radiographic examination and acceptance criteria in accordance with Paragraph UW-51, Section VIII, ASME B&PV Code.

TABLE 3.8-4

CONTAINMENT BUILDING
BASE SLAB STRESS RATIOS[a]

Beam No.[b]	Operating Moment Demand (ft-k)	Operating Moment Capacity (ft-k)	Accident Moment Demand (ft-k)	Accident Moment Capacity (ft-k)	Accident With Hosgri Moment Demand (ft-k)	Accident With Hosgri Moment Capacity (ft-k)	Stress Ratio
62	15,293 --	37,640 -50,600	12,827 -37,772	36,925 -156,900	20,134 -44,967	41,250 -175,875	2.05
225	59,630 --	88,835 -18,275	75,492 --	279,275 -54,375	109,844 --	314,000 -61,083	1.49
43	12,126 --	51,880 -18,275	56,623 --	167,925 -54,375	69,444 --	188,124 -61,083	2.71
24	14,483 --	25,940 -9,138	64,157 --	83,963 -27,188	68,263 --	94,062 -30,541	1.31
129	23,425 --	88,835 -18,275	76,480 --	279,275 -54,375	93,238 --	314,000 -61,083	3.65
216	23,013 --	37,640 -50,600	19,780 -21,785	36,925 -156,900	26,007 -67,471	41,250 -175,875	1.59
171	1,898 -6,884	6,675 -30,360	-- -37,497	22,155 -94,140	5,831 -55,206	24,750 -105,525	1.91

(a) Stress Ratio = $\frac{\text{Capacity}}{\text{Demand}}$

(b) See Figure 3.8-38: + = Tension on bottom - = Tension on top

TABLE 3.8-5

CONTAINMENT BUILDING INTERNAL STRUCTURE
STRESS RATIOS IN SELECTED ELEMENTS

Description of Member	Location of Member	Load Combination[(a)]	Demand	Capacity	Stress Ratio[(b)]
Rebar in 3-ft concrete wall	Crane wall: 1. Vertical bar 2. Hoop bar	D + L + DDE + CP + R + J + M	58 ksi 54 ksi	60 ksi 60 ksi	1.03 1.11
4-ft concrete wall	Fuel transfer canal: 1. Wall @ N & S from el 113 ft-1 1/2 in. to el 140 ft	D + L + DDE + CP + R + J + M	343 k-ft	381 k-ft	1.11
	2. Wall @ W from el 113 ft-1 1/2 in. to el 140 ft	D + L + DDE + CP + R + J + M	162 k-ft	216 k-ft	1.33
Rebar in 2-ft concrete wall	Fuel transfer canal wall @ W from el 88 ft to el 113 ft-1 1/2 in.	D + L + DDE + CP + R + J + M	22 ksi	60 ksi	2.72
3-ft concrete slab	Fuel transfer canal floor @ el 113 ft-1 1/2 in.	D + L + DDE + CP + R + J + M	258 k-ft	269 k-ft	1.04
4-ft Concrete Slab	Fuel transfer canal floor @ el 104 ft	D + L + DDE + CP + R + J + M	306 k-ft	381 k-ft	1.24
Rebar in 6-ft concrete wall	Reactor cavity wall: 1. Vertical bar	D+L+DDE+CP+R+J+M	15 ksi	60 ksi	4.0
	2. Hoop bar	D + L + DDE + CP + R + J + M	26 ksi	60 ksi	2.3
3-ft concrete slab	Floor @ el 140 ft	D + L + DE + T	46 k-ft	93 k-ft	2.02

(a) Load combinations with Hosgri do not govern.
(b) Stress Ratio $= \frac{\text{Capacity}}{\text{Demand}}$

Description of Member	Location of Member	Load Combination[(a)]	Demand	Capacity	Stress Ratio[(b)]
4 ft 6 in. concrete slab	Floor @ el 140 ft	D + L + DE + T	156 k-ft	229 k-ft	1.46
5 ft concrete slab	Floor @ el 140 ft	D + L + DDE + CP + R + J + M	328 k-ft	500 k-ft	1.52
10 in. concrete slab	Annulus platform @ el 130 ft	D + L + DE + T	10 k-ft	39 k-ft	3.90
1 ft 6 in. concrete slab	Annulus platform @ el 140 ft	D + L + DE + T	35 k-ft	57 k-ft	1.62
W21x73	Annulus platform @ el 130 ft	D + L + DE + T + TH + FV + RVOT	22 ksi	24 ksi	1.09
W21x62	"	"	8 ksi	22 ksi	2.75
W12x40	"	"	9 ksi	22 ksi	2.44
W12x65	Annulus platform column	"	124 k (Unit 1)	268 ksi	2.16
W12x65	"	"	205 k (Unit 2)	268 ksi	1.31
W12x99	"	"	212 k (Unit 1)	366 k	1.73
W21x55	Annulus platform @ el 140 ft	"	24 ksi (Unit 1)	27 ksi	1.12
W21x82	"	"	11 ksi (Unit 1)	22 ksi	2.00
W21x68	"	"	17 ksi (Unit 1)	22 ksi	1.29
W21x96	"	"	23 ksi (Unit 1)	27 ksi	1.17

Description of Member	Location of Member	Load Combination[(a)]	Demand	Capacity	Stress Ratio[(b)]
W24x100	Annulus platform @ el 140 ft	D + DDE + THA + FV + RVOT	28 (Unit 2)	37.4	1.34
W21x96	"	"	18 (Unit 2)	37.4	2.08
W21x68	"	"	21 (Unit 2)	37.4	1.78
W21x55	"	"	16 (Unit 2)	37.4	2.33
W24x100	"	D + HE	21 (Unit 2)	44.8	2.13
W21x96	"	"	20 (Unit 2)	44.8	2.21
W21x68	"	"	17 (Unit 2)	44.8	2.64
W21x55	"	"	13 (Unit 2)	44.8	3.45
W12x65	Annulus platform column	D + DDE + THA + FV + RVOT	260 (Unit 2)	45.6	1.75
W12x99	"	"	270 (Unit 2)	45.6	1.69
W12x65	"	D + HE	357 (Unit 2)	55.7	1.56
W12x99	"	D + HE	365 (Unit 2)	55.7	1.53

TABLE 3.8-5A

CONTAINMENT BUILDING PIPEWAY STRUCTURE STRESS RATIOS IN SELECTED MEMBERS

Description of Member	Location of Member Unit	Elevation	Load Combination	Stress Ratio[(a)]
W8 x 40	1	114	D + DE	1.10
W8 x 40	1	114	D + DE	1.07
W8 x 40	1	114	D + DE	1.07
W14 x 111	2	109	D + DE	1.72
W14 x 111	2	109	D + DE	1.79
W14 x 111	2	109	D + DE	1.59
W8 x 40	1	114	D + DDE	1.11
W8 x 40	1	114	D + DDE	1.20
W8 x 40	1	114	D + DDE	1.20
W14 x 111	2	109	D + DDE	2.78
W14 x 111	2	109	D + DDE	1.89
W14 x 111	2	109	D + DDE	1.92
W8 x 40	1	114	D + DDE + Yr	1.06
W14 x 111	1	119	D + DDE + Yr	1.27
W14 x 202	1	119	D + DDE + Yr	1.32
W14 x 202	2	114	D + DDE + Yr	1.52
W8 X 17	2	109	D + DDE + Yr	1.11
W14 x 111	2	109	D + DDE + Yr	1.25
W8 x 40	1	114	D + HE	1.05
W8 x 40	1	114	D + HE	1.09
W8 x 40	1	114	D + HE	1.05
W14 x 111	2	109	D + HE	1.03
W10 x 31	2	109	D + HE	1.06
W12 x 106	2	138	D + HE	1.11

(a) Stress ratio = $\frac{\text{Capacity}}{\text{Demand}}$

TABLE 3.8-5B

CONTAINMENT AND AUXILIARY BUILDINGS COMPARISON OF DISPLACEMENTS AND SEPARATIONS

Elevation (ft)	Maximum Relative Seismic Displacement[a] DDE	HE	Minimum Separation (in.)[c]	Minimum Factor of Safety Against Contact[e]
188	6.76	9.59	22	2.06
140	0.44	0.37	8	5.29
115	0.27	0.23	2[d]	3.05
100	0.17	0.11	1.25[d]	4.12

(a) Maximum relative seismic displacements are calculated as sum of maximum containment and auxiliary building displacements.

(b) Not Used.

(c) Minimum separation is measured at normal ambient temperature and pressure.

(d) Except for a few localized areas, the minimum separation is 4 inches at elevations 100 ft and 115 ft.

(e) The factor of safety is determined from the relative seismic displacements after the thermal and pressure effects are conservatively accounted for.

TABLE 3.8-6

VERIFICATION OF COMPUTER PROGRAMS

Program Name	General Function	Verification Measure
AISCBM/CE401	Analysis, design, and investigation of structural steel framing system in accordance with AISC specification	Bechtel Verification Manual
ANSR	Linear/nonlinear static and dynamic analysis finite-element program	URS/Blume QA Manual
AXIDYN	Static and dynamic analysis of axisymmetric structures	URS/Blume QA Manual
BLUME SAP IV	General-purpose linear elastic finite-element static and dynamic analysis	URS/Blume QA Manual
BSAP/CE800	General-purpose linear elastic finite-element static and dynamic analysis	Bechtel Verification Manual
BSAP-POST/ CE201&CE217	Postprocessing for BSAP computer program	Bechtel Verification Manual
CECAP/CE987	Computes stress in rebars and liner plate by considering cracking in concrete	Bechtel Verification Manual
Drain-2D	Nonlinear 2-D static and dynamic analysis	URS/Blume QA Manual
FINEL/CE801	Performs finite element static analysis by considering cracking and yielding	Bechtel Verification Manual
LOCAL STRESS/ME210	Calculates local stress in cylindrical shells due to external loading	Bechtel Verification Manual
SMIS	Matrix manipulation program	URS/Blume QA Manual
SPECTRA/CE802	Computes response spectra from acceleration time-histories	Bechtel Verification Manual
STAND/ME425	Design and evaluation of pipe support base plate with concrete anchor bolt assemblies	Bechtel Verification Manual

TABLE 3.8-6

Program Name	General Function	Verification Measure
THERMAL STRESS/ ME643	Performs thermal and stress analysis for 2-D plane or axisymmetric structures	Bechtel Verification Manual
BECHTEL ANSYS/ CE798	Large general-purpose linear/nonlinear static and dynamic analysis	Bechtel Verification Manual
BECHTEL STRUDL/ CE901	Finite element static/dynamic analysis, and design of structures	Bechtel Verification Manual
EASE2/E2SPEC	Linear elastic finite-element static and dynamic analysis computer program	Verification by Control Data Corporation
PG&E STRUDL	General purpose static and dynamic structural analysis	Partial verification of program as originally received. Complete verification performed on a case-by-case basis for each application.
GTSTRUDL/CE701	General-purpose static and dynamic finite element code	Verification by Control Data Corporation
PIPERUP	Performs nonlinear elastic/plastic analysis of 3-D piping system subject to static/dynamic time-history forcing functions	Nuclear Services Corporation Verification Manual
STARDYNE/CE991	General-purpose finite-element static and dynamic analysis	Bechtel Verification Verification
RAP	Pipe whip restraint design program	Nuclear Services Corporation Verification Manual
WECAN	Modal superposition time history analysis and static analysis of structure	Westinghouse Verification Manual
ADDA	Postprocessor to sum the time history responses for two different sets of modes	Westinghouse Verification Manual

TABLE 3.8-6

Program Name	General Function	Verification Measure
TAPES	To reformat the time history response tapes from ADDA for input to GENSPC	Westinghouse Verification Manual
GENSPC2	To calculate the modal response spectra	Westinghouse Verification Manual
COMBSPC	To combine the response spectra by SRSS	Westinghouse Verification Manual
SPREAD	To transform the scale of the spectra from frequency to period and plot the combined response spectra	Westinghouse Verification Manual
MARG3	Qualification analysis of structure	Westinghouse Verification Manual
SAP90	General-purpose linear elastic finite-element static and dynamic analysis	Computers and Structures, Inc. Verification Manual
SAP2000	General-purpose linear and non-linear finite-element program for static and dynamic analysis	Computers and Structures, Inc. Verification Manual
PC-SPECTRA	Pre- and post-processor for response spectra data	PG&E Nuclear Computer Program Acceptance Report

TABLE 3.8-6A

AVERAGE CONCRETE STRENGTH

CONTAINMENT AND INTERIOR STRUCTURE

Component	Average f' (test value) (psi)	E_c [(a)] (psi)
Base slab to elevation 87 ft	6330	4.53×10^6
Skin pour at elevation 89 ft	6330	4.53×10^6
Interior	6330	4.53×10^6
Skin pour	3850	4.54×10^6
Soldier beams	3850	4.54×10^6
Exterior walls	3850	4.54×10^6
Dome	3850	4.54×10^6

(a) $E_c = 57,000 (f_c)^{1/2}$ per AC1 318-71, in psi

TABLE 3.8-6B

STEEL STRENGTH DATA

CONTAINMENT AND INTERIOR STRUCTURE

Structure	Designation of Steel	Yield (psi) Minimum	Yield (psi) Average	Ultimate (psi) Minimum	Ultimate (psi) Average
		Reinforcing Steel			
Containment (1 and 2) Exterior #18s	ASTM 615, Grade 60	61,750	66,854	93,750	105,992
Containment (1 and 2) Interior #11s	Grade 60	62,820	68,079	96,795	105,556
		Structural Steel			
ASTM	A36	36,100	43,950	58,200	68,040
ASTM	A441	42,100	51,620	67,200	75,910
ASTM	A516	45,800	51,040	72,200	79,170

TABLE 3.8-7

AUXILIARY BUILDING
FUEL HANDLING CRANE SUPPORT STRUCTURE
STRUCTURAL MEMBERS AND ANCHORAGES STRESS RATIOS

	Description Of Members And Their Functions	Stress Ratios[a] [b] Hosgri	DDE	DE
BRACES	Top Chord Roof	1.7	1.5	1.9
	Bottom Chord Roof	1.1	1.2	1.3
	East-West Elevation Diagonals	1.1	1.1	1.4
	N-S Truss Diagonals, West and East Exterior/Interior	1.9	≥ 1.6	≥ 2.0
	East-West Truss Diagonals	1.1	≥ 1.3	≥ 1.1
	East-West Truss Knee	1.1	≥ 1.3	≥ 1.5
CHORDS	North South Trusses, Top	3.4	4.0	4.2
	North South Trusses, Bottom	3.2	4.0	4.3
	East-West Trusses, Top	1.1	1.6	1.9
	East-West Trusses, Bottom	1.1	1.4	1.8
LATERAL & VERTICAL	Frame Horizontals, West and East Sides	4.5	4.8	5.9
	Vertical Columns	1.0	1.1	1.0
	East-West Truss Struts	1.2	1.4	1.6
BASE ANCHORAGE	Axial Tensions	1.0	1.1	1.6
	Axial Compressions	1.3	1.4	1.7
	Lateral Shears	1.9	2.2	2.3

(a) Stress Ratio = $\frac{\text{Capacity}}{\text{Demand}}$

(b) Refer to Calculation 52.15.7.1.1.15 for stress ratios.

TABLE 3.8-8

AUXILIARY BUILDING SLABS STRESS RATIOS[(a)(b)]
OUT-OF-PLANE LOADS (DE)

Slab Location	Member	Shear, psi Demand	Shear, psi Capacity	Moment, kips-ft Demand	Moment, kips-ft Capacity	Stress Ratio
El 73 ft						
Area bounded by column[(c)]	Slab	49	60	24	30	1.2
lines H, U, 15.7, 16.8	Beam	48	60	100	140	1.2
El 85 ft						
Area bounded by column lines H, U, 16.8, 19.2	Slab	64	78	82	120	1.2
El 100 ft & 115 ft						
Area bounded by column[(c)]	Slab	48	78	75	88	1.2
lines H, T, 10.7, 15.7	Beam	70	120	340	470	1.4
El 115 ft						
Area bounded by column lines U, V, 15.7, 20.3	Slab	45.0	78.0	27.0	32.00	1.2
El 115 ft						
Area bounded by column	Slab	59	78	56	67	1.2
lines H, L.5, 15.7, 20.3	Beam	170	210	2,000	2,400	1.2
El 140 ft						
Area bounded by column[(c)]	Slab	120	130	2,050	2,390	1.1
lines H, T, 10.7, 15.7	Beam	130	140	1450	1640	1.1
El 140 ft						
Area bounded by column[(c)]	Slab	55	78	59	77	1.3
lines R, V, 15.7, 17.4	Beam	89	97	2,010	2,240	1.1
El 140 ft						
Area bounded by column lines H, L, 15.7, 20.3	Slab	57.0	78.0	382.0	455.00	1.2
El 154-1/2 ft						
Area bounded by column	Slab	30	78	14	17	1.2
lines L, R, 15.7, 17.4	Beam	60	78	76	100	1.3
El 163-1/3 ft						
Area bounded by column lines H, L, 15.7, 20.3	Composite[(d)] Beam	9,300	14,000	2,260	2,300	1.02

(a) Stress ratio = $\frac{\text{Capacity}}{\text{Demand}}$ for shear or moment, whichever is smaller.
(b) This does not include the effects of pipe break loads which are evaluated locally in accordance with provisions of Reference 6.
(c) Counterpart in Unit 2 is similar.
(d) These values are for structural steel beams embedded in the slab.

TABLE 3.8-9

AUXILIARY BUILDING SLABS STRESS RATIOS[(a)b)]
OUT-OF-PLANE LOADS (DDE)

Slab Location	Member	Shear, psi Demand	Shear, psi Capacity	Moment, kips-ft Demand	Moment, kips-ft Capacity	Stress Ratio
El 73 ft						
Area bounded by column[(c)] lines H, U, 15.7, 16.8	Slab	53	91	27	56	1.7
	Beam	53	93	110	260	1.8
El 85 ft						
Area bounded by column lines H, U, 16.7, 19.2	Slab	72	120	93	220	1.7
El 100 ft & 115 ft						
Area bounded by column[(c)] lines H, T, 10.7, 15.7	Slab	51	120	81	167	2.1
	Beam	130	200	360	900	1.5
El 115 ft						
Area bounded by column lines U, V, 15.7, 20.3	Slab	49	120	30	62	2.1
El 115 ft						
Area bounded by column lines H, L.5, 15.7, 20.3	Slab	66	120	63	130	1.8
	Beam	190	330	2,200	4,600	1.7
El 140 ft						
Area bounded by column[(c)] lines H, T, 10.7, 15.7	Slab	120	190	2,110	4,310	1.6
	Beam	130	200	1,500	3,140	1.5
El 140 ft						
Area bounded by column[(c)] lines R, V, 15.7, 17.4	Slab	56	120	60	150	2.1
	Beam	93	150	2,110	4,030	1.9
El 140 ft						
Area bounded by column lines H, L, 15.7, 20.3	Slab	61	120	411	858	2.0
El 154-1/2 ft						
Area bounded by column lines L, R, 15.7, 17.4	Slab	32	120	15	33	2.2
	Beam	64	120	81	190	1.9
El 163-1/3 ft						
Area bounded by column lines H, L, 15.7, 20.3	Composite[(d)] Beam	11,000	20,000	2,200	3,100	1.4

(a) Stress ratio = $\frac{\text{Capacity}}{\text{Demand}}$ for shear or moment, whichever is smaller.
(b) This does not include the effects of pipe break loads which are evaluated locally in accordance with provisions of Reference 6.
(c) Counterpart in Unit 2 is similar.
(d) These values are for structural steel beams embedded in the slab.

TABLE 3.8-10

AUXILIARY BUILDING SLABS STRESS RATIOS[(a)(b)]
OUT-OF-PLANE LOADS (HE)

Slab Location	Member	Shear, psi Demand	Shear, psi Capacity	Moment, kips-ft Demand	Moment, kips-ft Capacity	Stress Ratio
El 73 ft						
Area bounded by column[(c)]	Slab	65	110	32	56	1.7
lines H, U, 15.7, 16.8	Beam	63	110	130	260	1.7
El 85 ft						
Area bounded by column lines H, U, 16.8, 19.2	Slab	91	130	120	270	1.4
El 100 ft & 115 ft						
Area bounded by column[(c)]	Slab	68	130	110	200	1.8
lines H, T, 10.7, 15.7	Beam	170	220	480	1,100	1.3
El 115 ft						
Area bounded by column lines U, V, 15.7, 20.3	Slab	60.0	130.00	36.0	74.00	2.0
El 115 ft						
Area bounded by column	Slab	100	130	120	150	1.2
lines H, L.5, 15.7, 20.3	Beam	300	360	4,300	5,500	1.2
El 140 ft						
Area bounded by column[(c)]	Slab	160	200	2,720	5,220	1.3
lines H, T, 10.7, 15.7	Beam	170	200	2,140	3,770	1.2
El 140 ft						
Area bounded by column[(c)]	Slab	72	130	79	180	1.8
lines R, V, 15.7, 17.4	Beam	145	160	3,280	4,870	1.1
El 140 ft						
Area bounded by column lines H, L, 15.7, 20.3	Slab	105.0	130.00	710.0	1,062.00	1.2
El 154-1/2 ft						
Area bounded by column[(c)]	Slab	65	130	29	41	1.4
lines L, R, 15.7, 17.4	Beam	92	130	150	230	1.4
El 163-1/3 ft						
Area bounded by column lines H, L, 15.7, 20.3	Composite[(d)] Beam	16,000	24,000	3,900	4,200	1.1

(a) Stress ratio = $\frac{\text{Capacity}}{\text{Demand}}$ for shear or moment, whichever is smaller.

(b) This does not include the effects of pipe break loads which are evaluated locally in accordance with provisions of Reference 6.

(c) Counterpart in Unit 2 is similar.

(d) These values are for structural steel beams embedded in the slab.

TABLE 3.8-11

AUXILIARY BUILDING SLABS STRESS RATIOS[f]
IN-PLANE LOADS (DE)

Elevation, ft	Section[e][g] Number	Shear[c], kip		Moment[d], k-ft		Stress Ratio
		Demand	Capacity[a]	Demand	Capacity[b]	
100	1-a	60	2,200	2,650	25,300	9.5
100	1-b	170	2,300	5,700	21,600	3.8
100	2-a	320	2,880	9,500	91,900	9.0
100	2-b	110	1,060	700	6,350	9.1
100	2-c	10	220	50	600	>10.0
115	1	300	2,240	7,350	23,200	3.2
115	2-a	240	4,350	200	50,900	>10.0
115	2-b	120	490	2,100	4,100	2.0
115	3-a	260	1,260	2,650	7,700	2.9
115	3-b	280	1,280	2,150	18,100	4.6
115	4	1,460	8,100	29,700	289,000	5.5
140	1	380	2,240	2,500	4,800	1.9
140	2-a	320	4,130	5,100	64,000	>10.0
140	2-b	270	2,100	3,050	13,800	4.5
140	3-a	160	430	1,950	4,950	2.5
140	3-b	390	1,530	5,900	16,300	2.8
140	4	1,840	8,580	39,500	443,000	4.7

(a) Shear capacity is calculated for the section subjected to demand moment and axial force.
(b) Moment capacity is calculated for the section subjected to demand axial force.
(c) Shear capacities and demands are rounded to the nearest 10 kips or 3 significant digits.
(d) Moment capacities and demands are rounded to the nearest 50 ft-kips or 3 significant digits.
(e) Section location is shown on Figures 3.8-60 through 3.8-62.
(f) Stress ratio = $\frac{\text{Capacity}}{\text{Demand}}$ for shear or moment, whichever is smaller
(g) Component in Unit 2 is similar.

TABLE 3.8-12

AUXILIARY BUILDING SLABS STRESS RATIOS[f]
IN-PLANE LOADS (DDE)

Elevation, ft	Section[e][g] Number	Shear[c], Kip		Moment[d], k-ft		Stress Ratio
		Demand	Capacity[a]	Demand	Capacity[b]	
100	1-a	110	3,710	3,400	73,300	>10.0
100	1-b	310	3,770	9,850	63,100	6.4
100	2-a	610	4,800	14,900	303,000	7.9
100	2-b	200	1,770	1,250	17,000	8.9
100	2-c	10	370	50	1,100	>10.0
115	1	500	3,730	15,400	88,700	5.8
115	2-a	430	7,240	3,550	167,000	>10.0
115	2-b	240	1,130	4,500	16,500	3.7
115	3-a	330	2,090	2,900	12,000	4.1
115	3-b	450	2,140	2,350	42,600	4.8
115	4	2,920	13,500	60,000	1,000,000	4.6
140	1	750	3,730	4,250	43,300	5.0
140	2-a	840	6,890	6,150	200,000	8.2
140	2-b	510	3,500	5,550	36,200	6.5
140	3-a	240	720	2,550	10,300	3.0
140	3-b	590	2,550	8,900	46,400	4.3
140	4	3,700	14,300	79,000	1,110,000	3.9

(a) Shear capacity is calculated for the section subjected to demand moment and axial force.
(b) Moment capacity is calculated for the section subjected to demand axial force.
(c) Shear capacities and demands are rounded to the nearest 10 kips or 3 significant digits.
(d) Moment capacities and demands are rounded to the nearest 50 ft-kips or 3 significant digits.
(e) Section location is shown on Figures 3.8-60 through 3.8-62.
(f) Stress ratio = $\frac{\text{Capacity}}{\text{Demand}}$ for shear or moment, whichever is smaller
(g) Component in Unit 2 is similar.

TABLE 3.8-13

AUXILIARY BUILDING SLABS STRESS RATIOS[f]
IN-PLANE LOADS (HE)

Elevation, ft	Section[e][g] Number	Shear[c], Kip		Moment[d], k-ft		Stress Ratio
		Demand	Capacity[a]	Demand	Capacity[b]	
100	1-a	170	4,350	3,650	86,100	>10.0
100	1-b	510	4,500	13,000	65,000	5.0
100	2-a	930	5,580	18,500	180,000	6.0
100	2-b	290	1,830	1,500	13,300	6.3
100	2-c	20	360	100	1,250	>10.0
115	1	770	3,730	25,000	88,500	3.5
115	2-a	710	7,700	11,300	231,000	>10.0
115	2-b	400	1,120	8,050	16,400	2.0
115	3-a	480	2,330	3,100	14,500	4.7
115	3-b	820	2,500	3,200	48,900	3.0
115	4	3,940	15,500	117,000	1,170,000	3.9
140	1	1,120	3,870	9,200	38,000	3.5
140	2-a	1,170	8,010	7,300	240,000	6.8
140	2-b	900	4,150	7,750	43,100	4.6
140	3-a	450	830	3,250	13,800	1.8
140	3-b	970	3,010	11,300	50,700	3.1
140	4	5,210	14,500	157,000	1,160,000	2.8

(a) Shear capacity is calculated for the section subjected to demand moment and axial force
(b) Moment capacity is calculated for the section subjected to demand axial force
(c) Shear capacities and demands are rounded to the nearest 10 kips or 3 significant digits
(d) Moment capacities and demands are rounded to the nearest 50 ft-kips or 3 significant digits
(e) Section location is shown on Figures 3.8-60 through 3.8-62
(f) Stress ratio = $\frac{\text{Capacity}}{\text{Demand}}$ for shear or moment, whichever is smaller
(g) Component in Unit 2 is similar

TABLE 3.8-14

AUXILIARY BUILDING CONCRETE WALLS
STRESS RATIOS (DE)[a]

Wall Location	Elev., ft	Shear, psi Demand	Shear, psi Capacity[b]	Moment 10^3, k-ft Demand	Moment 10^3, k-ft Capacity[b]	Stress Ratio
On line H (15.7-20.3)	100	120	230	57	188	1.9
	85	160	330	9	173	1.9
On line J (11.7-15.7)[c]	100	130	270	35	126	2.0
	85	150	280	47	126	1.8
On line T(6.4-15.7)[c]	100	75	200	141	343	2.4
	85	85	220	164	664	2.6
On line T (16.8-19.2)	100[d]	55	210	15	65	3.8
On line U.5 (10.3-12.9)[c]	100[d]	45	155	20	113	3.4
On line V (15.7-20.3)	100	50	100	32	250	2.0
	85	50	90	67	245	1.8
On line V (6.4-15.7)[c]	100[d]	70	360	82	200	2.4
On line 6.4 (V-S)[c]	100	80	250	85	158	1.9
	85	100	340	20	31	1.6
On line 10.3 (T-V)[c]	100[d]	80	250	54	146	2.7
On line 12.9 (T-V)[c]	100[d]	80	240	54	145	2.7
On line 15.7 (H-T.6)[c]	100	110	250	382	782	2.1
	85	110	220	481	818	1.7
On line 15.7 (H-T.6)[c]	100	110	260	7	19	2.3
	85	60	170	12	19	1.6

(a) Stress ratio = $\frac{\text{Capacity}}{\text{Demand}}$ for shear or moment, whichever is smaller

(b) Axial demand effect is included in the capacities

(c) Counterpart in Unit 2 is similar

(d) Wall does not extend below elevation 100 ft

TABLE 3.8-15

AUXILIARY BUILDING CONCRETE WALLS
STRESS RATIOS (DDE)[a]

		Shear, psi		Moment 10^3, k-ft		
Wall Location	Elev., ft	Demand	Capacity[b]	Demand	Capacity[b]	Stress Ratio
On line H (15.7-20.3)	100	240	390	114	407	1.6
	85	310	550	178	556	1.8
On line J (11.7-15.7)[c]	100	250	450	62	253	1.8
	85	290	460	90	253	1.6
On line T (6.4-15.7)[c]	100	140	340	273	987	2.4
	85	170	370	316	1086	2.2
On line T (16.8-19.2)	100[d]	110	350	31	147	3.2
On line U.5(10.3-12.9)[c]	100[d]	85	260	40	244	3.0
On line V (15.7-20.3)	100	90	170	63	394	1.9
	85	100	150	133	327	1.5
On line V (6.4-15.7)[c]	100[d]	140	600	133	400	3.0
On line 6.4 (V-S)[c]	100	160	420	141	333	2.4
	85	190	570	34	92	2.7
On line 10.3 (T-V)[c]	100[d]	160	420	105	280	2.6
On line 12.9 (T-V)[c]	100[d]	160	410	106	268	2.5
On line 15.7 (H-T.6)[c]	100	220	420	553	1205	1.9
	85	220	370	740	1155	1.6
On line 15.7 (U-V)[c]	100	220	430	13	32	1.9
	85	115	290	23	30	1.3

(a) Stress ratio = $\frac{\text{Capacity}}{\text{Demand}}$ for shear or moment, whichever is smaller
(b) Axial demand effect is included in the capacities
(c) Counterpart in Unit 2 is similar
(d) Wall does not extend below elevation 100 ft

TABLE 3.8-16

AUXILIARY BUILDING CONCRETE WALLS
STRESS RATIOS (HE)[a]

Wall Location	Elev., ft	Shear, psi Demand	Shear, psi Capacity[b]	Moment 10^3, k-ft Demand	Moment 10^3, k-ft Capacity[b]	Stress Ratio
On line H (15.7-20.3)	100	400	480	176	504	1.2
	85	510	630	270	682	1.2
On line J (11.7-15.7)[c]	100	390	500	107	313	1.3
	85	440	580	145	313	1.3
On line T (6.4-15.7)[c]	100	190	310	438	860	1.6
	85	230	320	493	979	1.4
On line T (16.8-19.2)	100[d]	150	350	42	168	2.3
On line U.5 (10.3-12.9)[c]	100[d]	130	190	60	197	1.5
On line V (15.7-20.3)	100	140	200	90	489	1.4
	85	150	170	182	405	1.15
On line V (6.4-15.7)[c]	100[d]	220	640	291	500	1.7
On line 6.4 (V-S)[c]	100	380	460	301	434	1.2
	85	390	450	63	84	1.15
On line 10.3 (T-V)[c]	100[d]	330	480	220	339	1.4
On line 12.9 (T-V)[c]	100[d]	270	460	199	324	1.6
On line 15.7 (H-T.6)[c]	100	330	520	666	1494	1.6
	85	320	450	859	1425	1.4
On line 15.7 (U-V)[c]	100	340	480	19	36	1.4
	85	160	300	30.5	32.6	1.07

(a) Stress ratio = $\frac{\text{Capacity}}{\text{Demand}}$ for shear or moment, whichever is smaller
(b) Axial demand effect is included in the capacities
(c) Counterpart in Unit 2 is similar
(d) Wall does not extend below elevation 100 ft

TABLE 3.8-17

AUXILIARY BUILDING COLUMNS STRESS RATIOS[a]

Column Location[b]	Stress Ratio		
	DE	DDE	HE
14 - J.7	2.9	3.7	2.6
15 – N	5.3	7.7	4.8
15 - R.8	3.6	3.3	2.5
15 - J.7	1.04	1.8	1.3
15 – S	1.9	2.9	2.3

(a) Stress ratio = $\frac{\text{Capacity}}{\text{Demand}}$

(b) Counterpart in Unit 2 is similar

TABLE 3.8-18

AUXILIARY BUILDING SHEAR DISSIPATION TO FOUNDATION (DE NORTH-SOUTH)

Building Portion Location[a]	Shear Demand at Elevation 85 ft.					
	Shear from Upper Level					
	Direct Shear, kips	Torsional Shear, kips[b]	Torsional + Direct Shear, kips	Inertial Load at El 85 ft, kips	Total, kips	Remarks
Central Portion	23,600	1,800	25,400	4,400	29,800	Capacity is 57,900 kips
North Wing	2,300 900 200 4,700 600	500 100	2,800 1,000 200 4,700 600	600 600 400	10,900	Load is directly dissipated to the foundation
South Wing	2,300 900 200 4,700 600	500 100	2,800 1,000 200 4,700 600	600 600 400	10,900	Load is directly dissipated to the foundation

Shear Capacity at Elevation 85 ft (Central Portion)

Capacity of diaphragm to dissipate shear force to the foundation at elevation 85 ft (kips)	by bearing by rebar tension	4,700 + 18,000 = 22,700 1,100 + 1,100 = 2,200
Shear capacity of walls below elevation 85 ft (kips)		33,000
Total shear capacity at and below elevation 85 ft (kips)		57,900

(a) For building portion location only, see Figures 3.8-63 and 3.8-64
(b) Torsional shears on only one side of the center of rigidity are considered

TABLE 3.8-19

AUXILIARY BUILDING SHEAR DISSIPATION TO FOUNDATION (DE EAST-WEST)

Building Portion Location[a]	Shear Demand at Elevation 85 ft. — Shear from Upper Level: Direct Shear, kips	Torsional Shear, kips	Torsional + Direct Shear, kips	Inertial Load at El 85 ft, kips	Total, kips	Remarks
Central Portion	35,500	-0-	35,500	4,400	39,900	Capacity is 76,200 kips
North Wing	900 1,100 400 400	-0-	900 1,100 400 400	600 600 400	4,400	Load is directly dissipated to the foundation
South Wing	900 1,100 400 400	-0-	900 1,100 400 400	600 600 400	4,400	Load is directly dissipated to the foundation

Shear Capacity at Elevation 85 ft (Central Portion)

Capacity of diaphragm to dissipate shear force to the foundation at elevation 85 ft (kips)	4,100 4,100
Shear capacity of walls below elevation 85 ft (kips)	68,000
Total shear capacity at and below elevation 85 ft (kips)	76,200

(a) For building portion location only, see Figures 3.8-63 and 3.8-64

TABLE 3.8-20

AUXILIARY BUILDING SHEAR DISSIPATION TO FOUNDATION (DDE NORTH-SOUTH)

Building Portion Location[(a)]	Shear Demand at Elevation 85 ft.					Remarks
	Shear from Upper Level			Inertial Load at El 85 ft, kips	Total, kips	
	Direct Shear, kips	Torsional Shear, kips[(b)]	Torsional + Direct Shear, kips			
Central Portion	46,500	3,700	50,200	9,200	59,400	Capacity is 115,700 kips
North Wing	4,300 1,600 400 9,100 1,200	1,000 300 100	5,300 1,900 500 9,100 1,200	1,100 1,100 800	21,000	Load is directly dissipated to the foundation
South Wing	4,300 1,600 400 9,100 1,200	1,000 300 100	5,300 1,900 500 9,100 1,200	1,100 1,100 800	21,000	Load is directly dissipated to the foundation

<u>Shear Capacity at Elevation 85 ft (Central Portion)</u>

Capacity of diaphragm to dissipate shear force to the foundation at elevation 85 ft (kips)	by bearing by rebar tension	11,000 + 42,000 = 53,000 1,000 + 1,900 = 3,800
Shear capacity of walls below elevation 85 ft (kips)		58,000
Total shear capacity at and below elevation 85 ft (kips)		115,700

(a) For building portion location only see Figures 3.8-63 and 3.8-64
(b) Torsional shears on only one side of the center of rigidity are considered

TABLE 3.8-21

AUXILIARY BUILDING SHEAR DISSIPATION TO FOUNDATION (DDE EAST-WEST)

Building Portion Location[a]	Shear Demand at Elevation 85 ft.: Shear from Upper Level: Direct Shear, kips	Torsional Shear, kips	Torsional + Direct Shear, kips	Inertial Load at El 85 ft, kips	Total, kips	Remarks
Central Portion	68,700	-0-	68,700	9,200	77,900	Capacity is 128,000 kips
North Wing	1,600 2,100 900 700	-0-	1,600 2,100 900 700	1,100 1,100 800	8,300	Load is directly dissipated to the foundation
South Wing	1,600 2,100 900 700	-0-	1,600 2,100 900 700	1,100 1,100 800	8,300	Load is directly dissipated to the foundation

<u>Shear Capacity at Elevation 85 ft (Central Portion)</u>

Capacity of diaphragm to dissipate shear force to the foundation at elevation 85 ft (kips)	7,000 7,000
Shear capacity of walls below elevation 85 ft (kips)	114,000
Total shear capacity at and below elevation 85 ft (kips)	128,000

(a) For building portion location only see Figures 3.8-63 and 3.8-64

TABLE 3.8-22

AUXILIARY BUILDING SHEAR DISSIPATION TO FOUNDATION (HE NORTH-SOUTH)[(a)]

Building Portion Location[(a)]	Shear Demand at Elevation 85 ft. Shear from Upper Level: Direct Shear, kips	Torsional Shear, kips[(b)]	Torsional + Direct Shear, kips	Inertial Load at El 85 ft, kips	Total, kips	Remarks
Central Portion	63,000	9,000	72,000	12,500	84,500	Capacity is 136,800 kips
North Wing	5,700 2,100 500 12,200 1,700	2,300 500 300	8,000 2,600 800 12,200 1,700	1,600 1,600 1,000	29,500	Load is directly dissipated to the foundation
South Wing	5,700 2,100 500 12,200 1,700	2,300 500 300	8,000 3,600 800 12,200 1,700	1,600 1,600 1,000	29,500	Load is directly dissipated to the foundation

<u>Shear Capacity at Elevation 85 ft (Central Portion)</u>

Capacity of diaphragm to dissipate shear force to the foundation at elevation 85 ft (kips)	by bearing by rebar tension	14,600 + 48,400 = 63,000 2,940 + 2,400 = 4,800
Shear capacity of walls below elevation 85 ft (kips)		69,000
Total shear capacity at and below elevation 85 ft (kips)		136,800

(a) For illustration, see Figures 3.8-63 and 3.8-64.
(b) Torsional shears on only one side of the center of rigidity are considered.

TABLE 3.8-23

AUXILIARY BUILDING SHEAR DISSIPATION TO FOUNDATION (HE EAST-WEST)[(a)]

Building Portion Location[(a)]	Shear Demand at Elevation 85 ft.					Remarks
	Shear from Upper Level					
	Direct Shear, kips	Torsional Shear, kips[(b)]	Torsional + Direct Shear, kips	Inertial Load at El 85 ft, kips	Total, kips	
Central Portion	84,700	5,300	90,000	12,500	102,500	Capacity is 154,200 kips
North Wing	2,000 2,500 1,100 900	1,600 1,900 600 100	3,600 4,400 1,700 1,000	1,600 1,600 1,000	14,900	Load is directly dissipated to the foundation
South Wing	2,000 2,500 1,100 900		2,000 2,500 1,100 900	1,600 1,600 1,000	10,700	Load is directly dissipated to the foundation

Shear Capacity at Elevation 85 ft (Central Portion)

Capacity of Diaphragm to Dissipate Shear Force to the Foundation at Elevation 85 ft (kips)	8,600 8,600
Shear Capacity of Walls Below Elevation 85 ft (kips)	137,000
Total Shear Capacity at and Below Elevation 85 ft (kips)	154,200

(a) For illustration, see Figures 3.8-63 and 3.8-64.
(b) Torsional shears on only one side of the center of rigidity are considered.

TABLE 3.8-23A

AUXILIARY BUILDING AND TURBINE BUILDING
COMPARISON OF DISPLACEMENTS AND SEPARATIONS

Elevation (ft)	Maximum Total Displacement (in.)[a] DDE	HE	Separation (in.)	Minimum Factor of Safety Against Contact
163	2.7	4.5	8.0	1.78
140	0.9	0.9	8.0	8.89
115	0.7	1.1	8.0	7.27
100	0.5	0.7	3.0	4.29

(a) Displacements are calculated as sum of maximum auxiliary and turbine building displacements.

TABLE 3.8-24

DUCTILITY[a]

Structure	Blume Ductility	Newmark Ductility	
Containment	1.3[b]	1.0[b]	
Auxiliary Building	1.3[b]	1.0[b]	
		Class I	Class II
Turbine Building	[c]	1.0[b]	[c]
Intake	[c]	1.0[b]	[c, d]

(a) Ductilities are on story basis; however, floor response spectra were, in general, computed on an elastic analysis basis.

(b) Under normal conditions Newmark ductility is 1.0 maximum; higher ductility may be considered for special cases where supporting evidence justifies its use. Blume ductility for Class I structures is 1.3, and may be used only in specific situations.

(c) Concrete 1.3; steel 3, with up to 6 locally.

(d) Or as may be required to demonstrate that function of Design Class I equipment will not be adversely affected.

TABLE 3.8-25

REFUELING WATER STORAGE TANK
STRESS RATIO[a]

		$DL + HS + DE + R_A$			$DL + HS + DDE + R_A$			$DL + HS + HE + R_A$		
Force Component	Material	Demand	Capacity	Stress Ratio	Demand	Capacity	Stress Ratio	Demand	Capacity	Stress Ratio
Longitudinal force, Kips/ft	Concrete	63.5	96.0	1.51	121.2	216.0	1.78	133.3	216.0	1.62
Circumferential force, kips/ft	Concrete	54.4	96.0	1.76	71.5	216.0	3.02	79.6	216.0	2.71
In plane shear force, kips/ft	Concrete	26.1	45.5	1.74	52.1	77.4	1.49	58.9	77.4	1.31
Longitudinal moment, Kips-ft/ft	Concrete	40.4	78.2	1.94	56.3	179.7	3.19	58.6	179.7	3.07
Stress intensity outside vault opening area, $Kips/in^2$	Steel	6.4	16.7	2.61	11.2	22.5	2.01	15.4	40.6	2.64
Stress intensity within vault opening area, $Kips/in^2$	Steel	12.1	16.7	1.38	20.5	22.5	1.10	34.0	40.6	1.19

(a) Stress Ratio = $\frac{\text{Capacity}}{\text{Demand}}$

TABLE 3.8-26

TURBINE BUILDING
STRUCTURAL STEEL MEMBERS
STRESS RATIOS (HE)

Member Description	Stress Ratios[a]
Exterior columns, lines A and G	[b]
East-west roof trusses – chords	1.2[c]
East-west roof trusses – diagonals	1.0[c]
North-south walls diagonal tension bracing	1.1[c]
North-south walls diagonal compression bracing	1.0[c]
Crane runway girder	[b]
Floor beams	[b]

(a) Stress Ratio = $\frac{\text{Capacity}}{\text{Demand}}$

(b) Inelastic deformation occurs, ductility meets limits of Table 3.8-24.

(c) Effects of force redistribution are included.

TABLE 3.8-27

TURBINE BUILDING
CONCRETE MEMBERS
STRESS RATIOS (HE)[a]

Member	Location	Stress Ratios[b]
Wall, line A	Elev. 85 ft (20-30.3)	1.9
Wall, line G	Elev. 85 ft (20-30.3)	1.3
Wall, line 19	Elev. 123 ft (A-G)	1.1
Buttress, line 27	Elev. 85 ft	1.5
Floor slab	Elev. 140 ft line 21 (A-C), line C (19-21)	1.2 1.5[c]
Turbine Pedestal	Frame 6 (See Figure 3.7-15G)	1.0[d]

(a) Stress Ratio = $\frac{\text{Capacity}}{\text{Demand}}$ for shear or moment, whichever is smaller.

(b) Axial demand effect is included in the capacity.

(c) Effects of concrete cracking are considered.

(d) Effects of force distribution are included.

TABLE 3.8-27A

TURBINE BUILDING AND TURBINE PEDESTAL (UNITS 1 & 2)[a]
COMPARISON OF DISPLACEMENTS AND SEPARATIONS AT EL 140 FT
HE ANALYSIS

Side of Pedestal Location	Maximum Calculated Displacement, in.[b]			Minimum Separation, in.[c]	Factor of Safety Against Contact
	Building	Pedestal	Total		
East	0.53	1.67	2.20	2.88	1.31
West	0.58	1.67	2.25	3.00	1.33
North	0.20	0.73	0.93	1.25	1.34
South	0.21	0.76	0.97	1.31	1.35

(a) Values shown are for Unit 1 or Unit 2, whichever has the lowest factor of safety.

(b) Displacements are an envelope of maximum displacements calculated using Newmark-Hosgri design response spectra.

(c) Separations are an envelope of minimum as-built separations.

TABLE 3.8-28

INTAKE STRUCTURE
CAPACITIES AND DUCTILITIES OF FLOW STRAIGHTENERS (OR PIERS)[1]

Pier	P (Tension)	M	M_{allow}	U (Ductility)
1	129.0	10,600	15,600	N/A
2	81.5	14,300	15,900	N/A
3	44.6	15,700	16,100	N/A
4	24.1	16,400	16,200	1.24
5	39.1	17,300	16,100	1.33
6	141.0	17,700	15,500	1.44
7	146.0	16,300	15,400	1.32

Notes:

(1) These values are due to the Newmark earthquake, which governs for all piers:

P = Axial tension, kips

M = Moment, in.-kips (value of M based on linear analysis)

M_{allow} = Factored (0=0.90) ultimate moment capacity including tension effects

u = Ductility of tensile steel (ratio between calculated strain to yield strain)

TABLE 3.9-1

LOAD COMBINATIONS AND ACCEPTANCE CRITERIA FOR PRESSURIZER SAFETY AND RELIEF VALVE PIPING

Combination	Plant/System Operation Condition	Load Combination	Piping Allowable Stress Intensity
Upstream of Valves			
1	Normal	N	1.0 S_h
2	Upset	N + DE + SOT_U	1.2 S_h
3	Emergency	N + SOT_E	1.8 S_h
4	Faulted	N + MAX(DDE, HOSGRI) + SOT_F	2.4 S_h
5	Faulted(Note 5)	N + LOCA + MAX(DDE, HOSGRI) + SOT_F	2.4 S_h
Downstream of Valves			
1	Normal	N	1.0 S_h
2	Upset	N + SOT_U	1.2 S_h
3	Upset	N + DE + SOT_U	1.8 S_h
4	Emergency	N + SOTE	1.8 S_h
5	Faulted	N + MAX(DDE, HOSGRI) + SOT_F	2.4 S_h
6	Faulted(Note 5)	N + LOCA + MAX(DDE, HOSGRI) + SOT_F	2.4 S_h

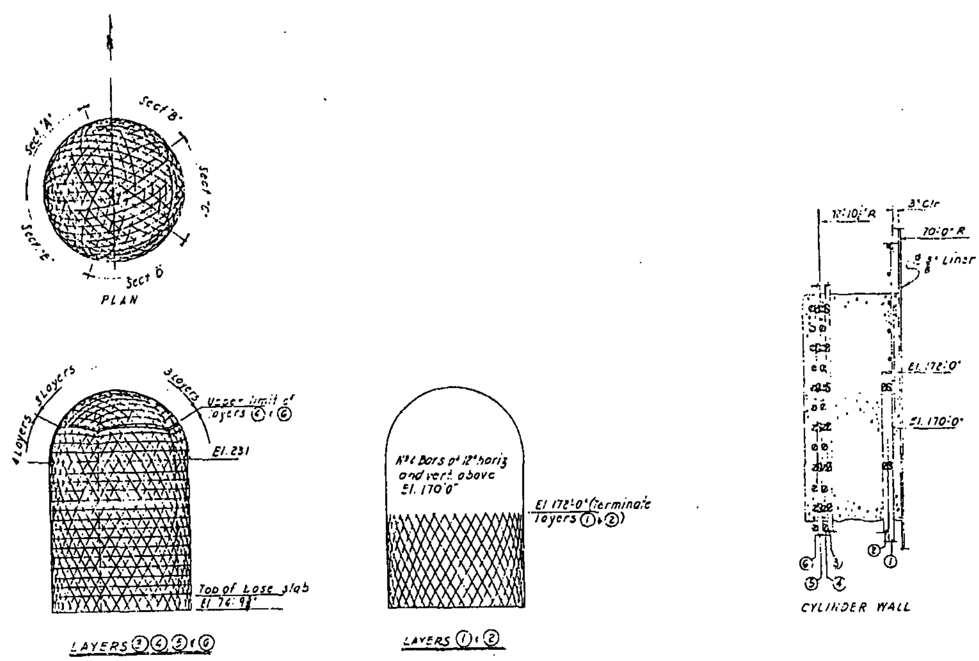

FSAR UPDATE

UNITS 1 AND 2
DIABLO CANYON SITE

FIGURE 3.8-1

CONTAINMENT STRUCTURE
REINFORCING STEEL ARRANGEMENT

Revision 11 November 1996

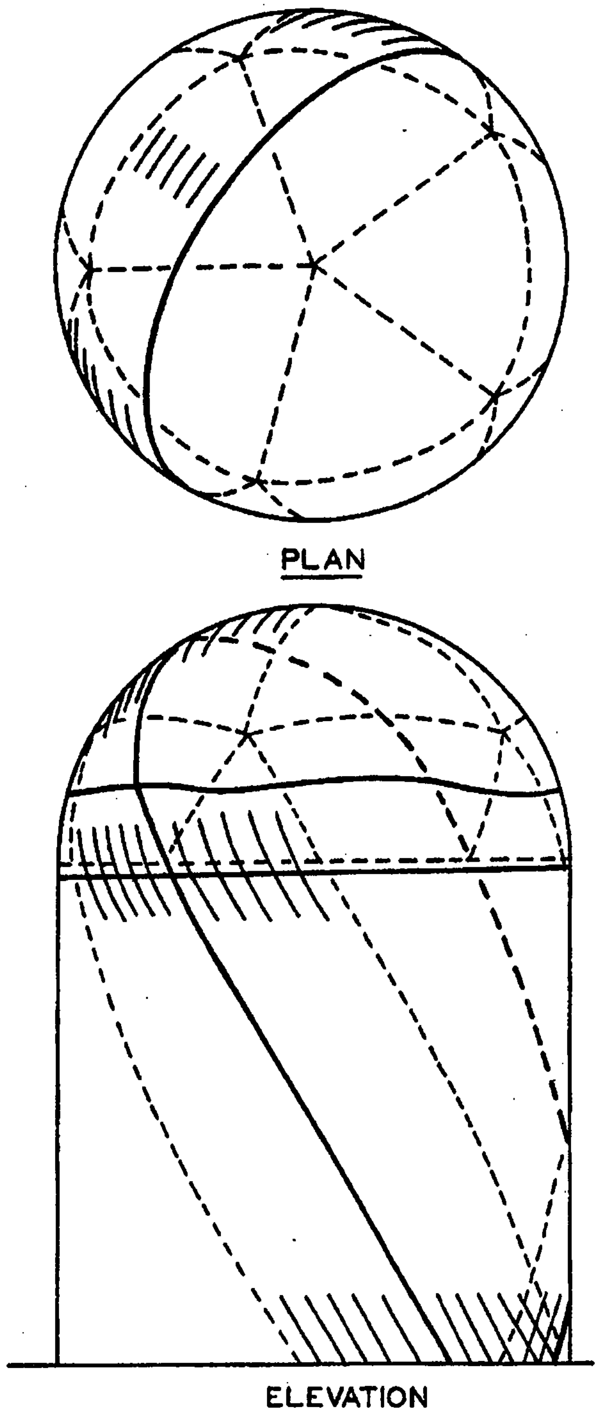

FSAR UPDATE

UNITS 1 AND 2
DIABLO CANYON SITE

FIGURE 3.8-2

CONTAINMENT STRUCTURE

TYPICAL REINFORCING LOOP

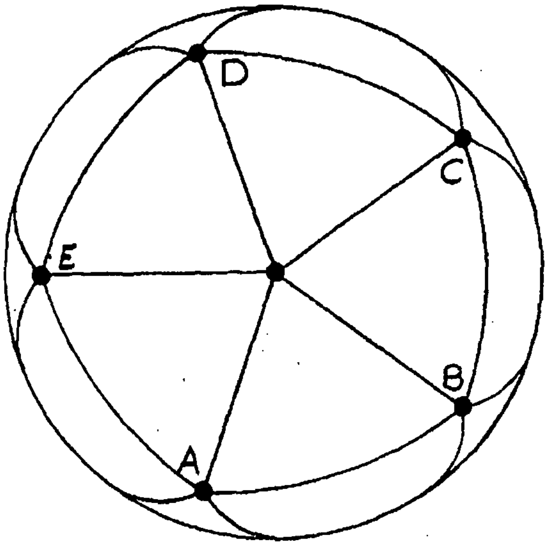

SKETCH 1

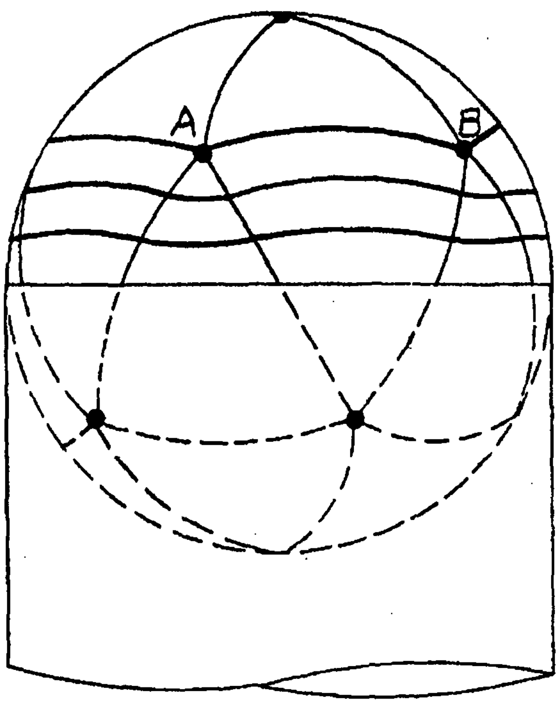

SKETCH 2

FSAR UPDATE

UNITS 1 AND 2
DIABLO CANYON SITE

FIGURE 3.8-3

CONTAINMENT STRUCTURE

DOME SPHERICAL TRIANGLES

Revision 11 November 1996

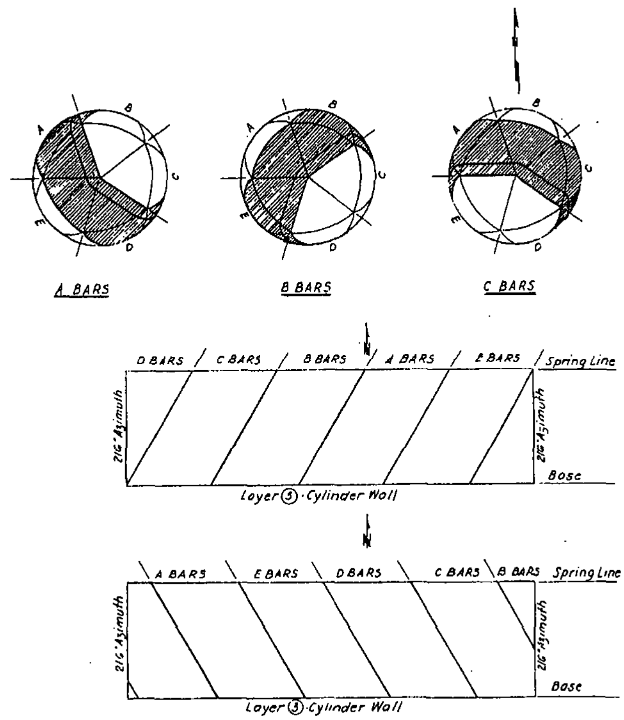

FSAR UPDATE

UNITS 1 AND 2
DIABLO CANYON SITE

FIGURE 3.8-4

CONTAINMENT STRUCTURE
DOME AND CYLINDER BARS

Revision 11 November 1996

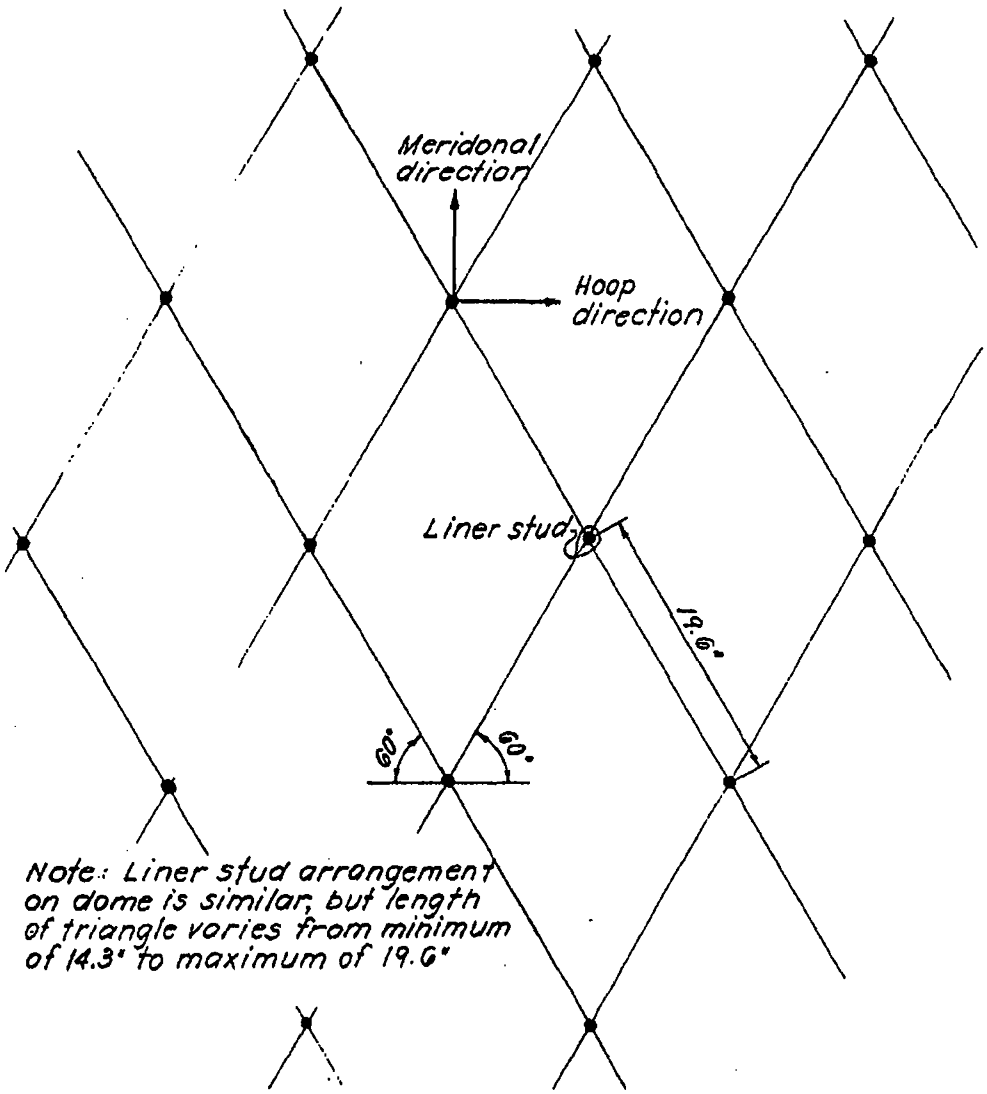

Note: Liner stud arrangement on dome is similar, but length of triangle varies from minimum of 14.3" to maximum of 19.6"

FSAR UPDATE

UNITS 1 AND 2
DIABLO CANYON SITE

FIGURE 3.8-5

CONTAINMENT STRUCTURE
LINER STUD ARRANGEMENT

Revision 11 November 1996

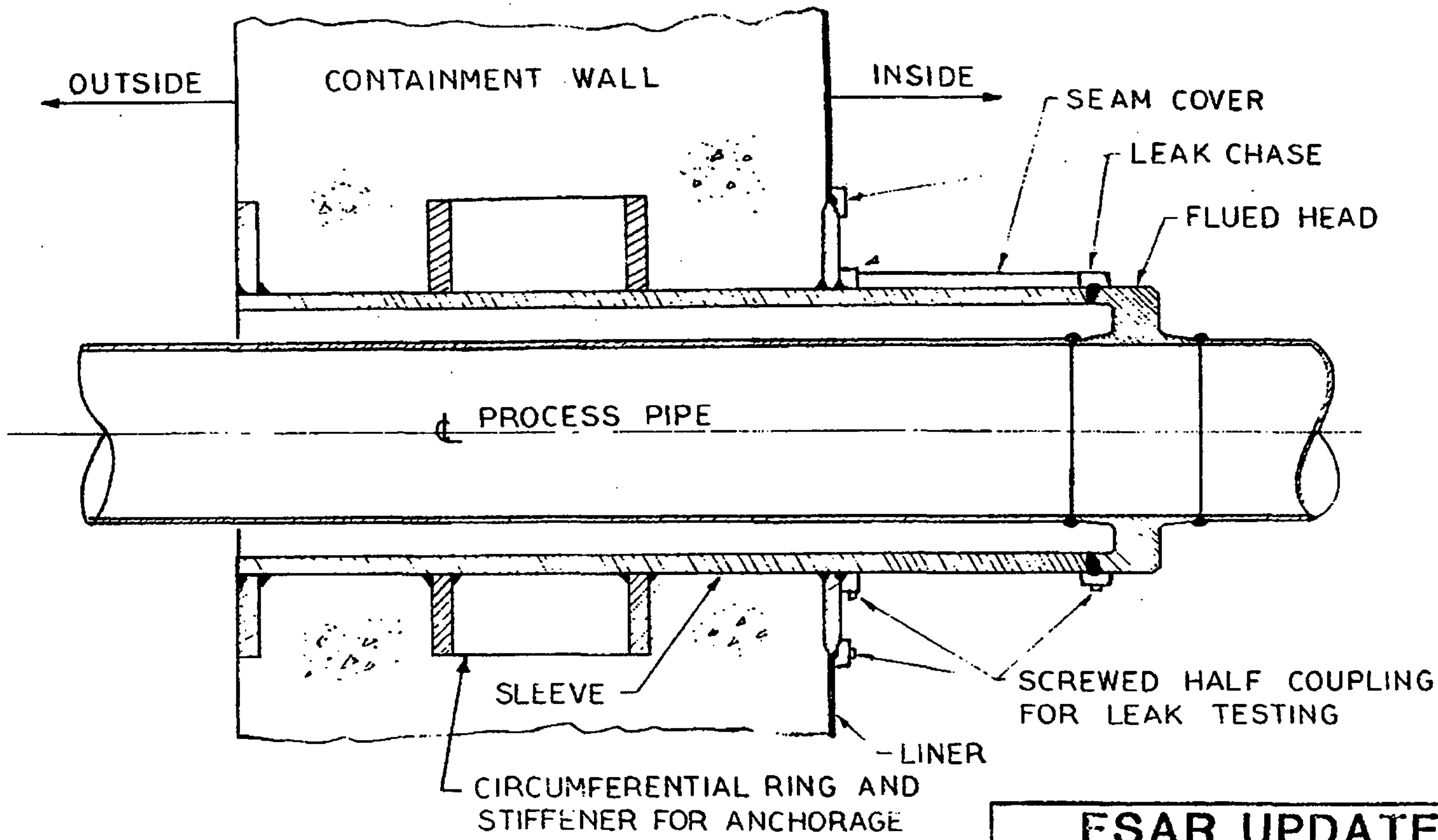

FSAR UPDATE

UNITS 1 AND 2
DIABLO CANYON SITE

FIGURE 3.8-6

CONTAINMENT STRUCTURE

TYPICAL PIPING PENETRATION

Revision 11 November 1996

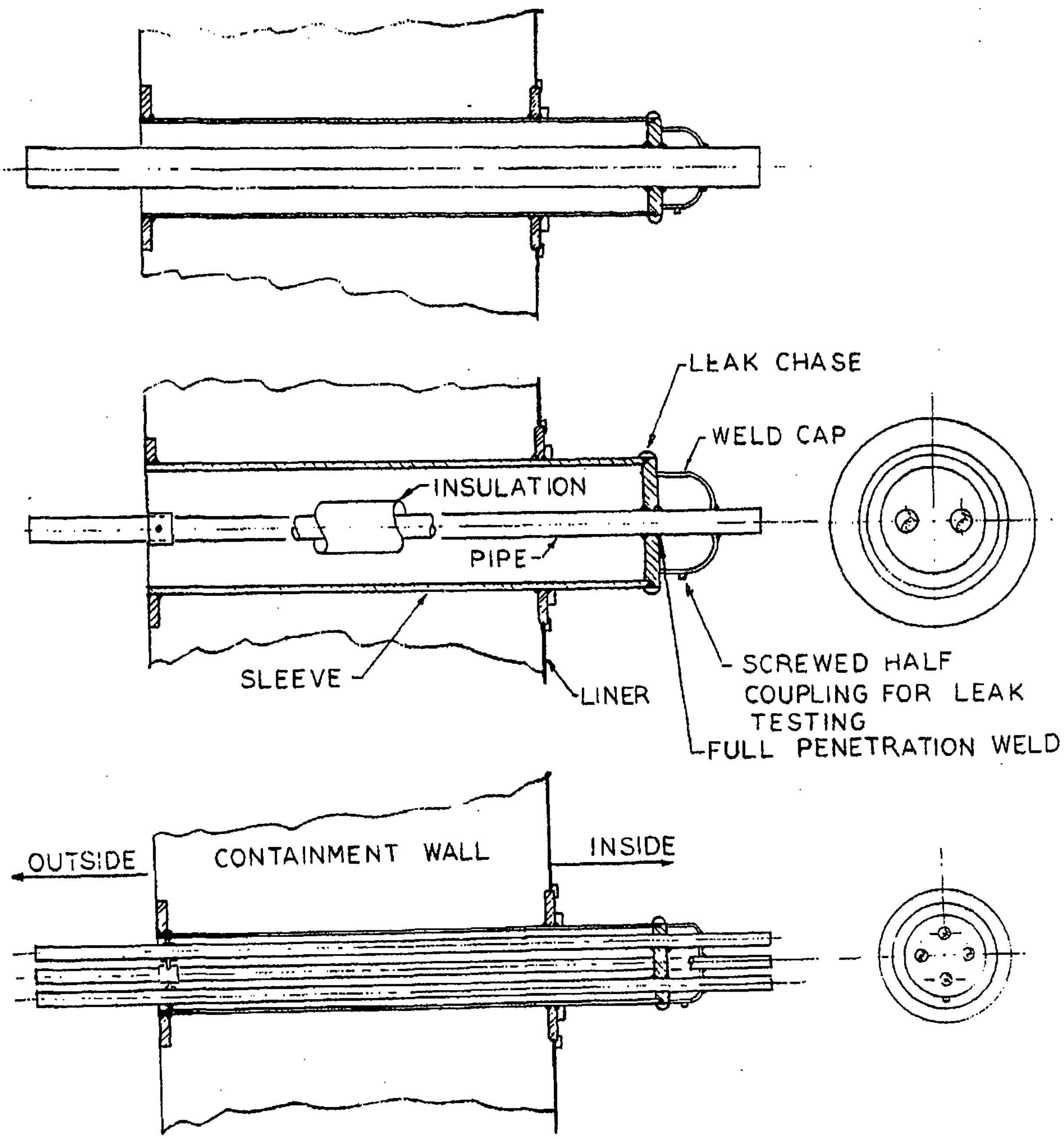

FSAR UPDATE

UNITS 1 AND 2
DIABLO CANYON SITE

FIGURE 3.8-7

CONTAINMENT STRUCTURE

TYPICAL PIPING PENETRATION

Revision 11 November 1996

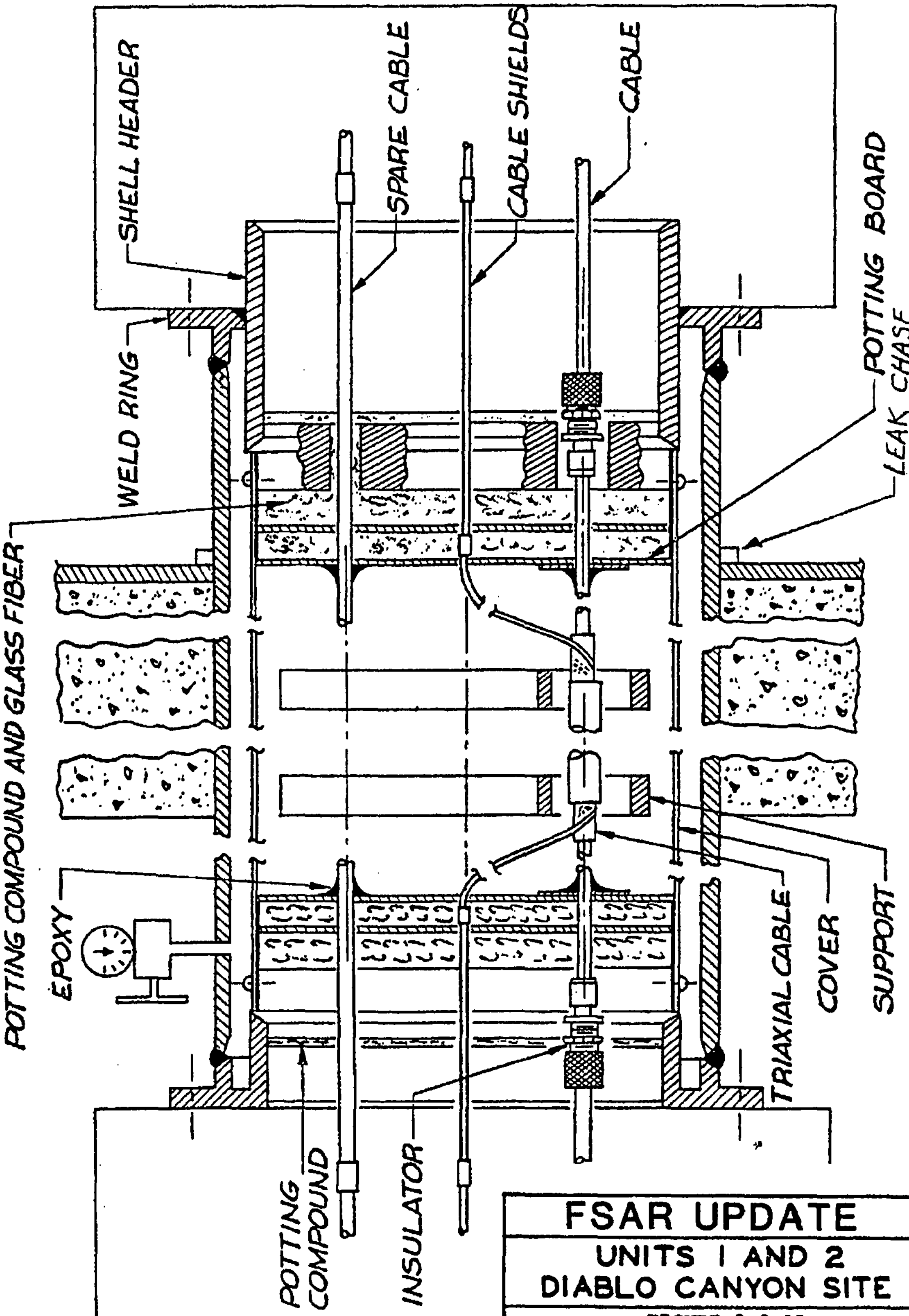

FSAR UPDATE
UNITS 1 AND 2
DIABLO CANYON SITE

FIGURE 3.8-10

CONTAINMENT STRUCTURE
TYPICAL INSTRUMENTATION PENETRATION

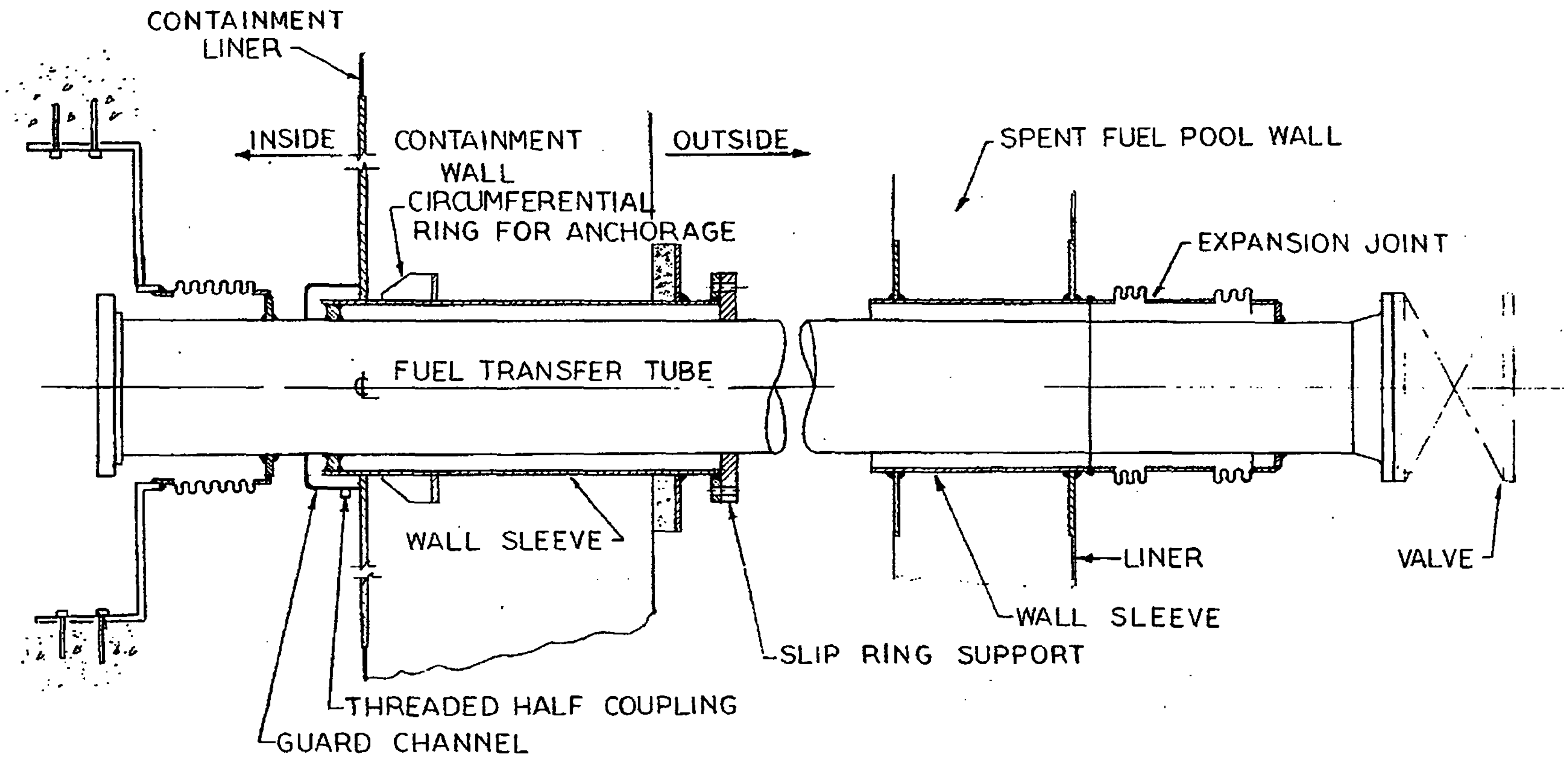

FSAR UPDATE

UNITS 1 AND 2
DIABLO CANYON SITE

FIGURE 3.8-11

CONTAINMENT STRUCTURE

FUEL TRANSFER TUBE PENETRATION

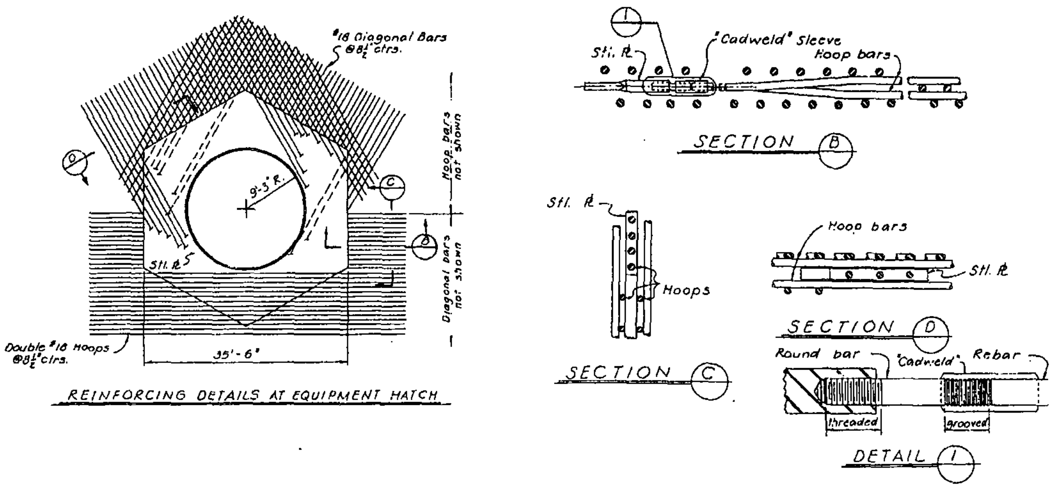

FSAR UPDATE
UNITS 1 AND 2 DIABLO CANYON SITE
FIGURE 3.8-12 CONTAINMENT STRUCTURE HEXAGONAL COLLARS

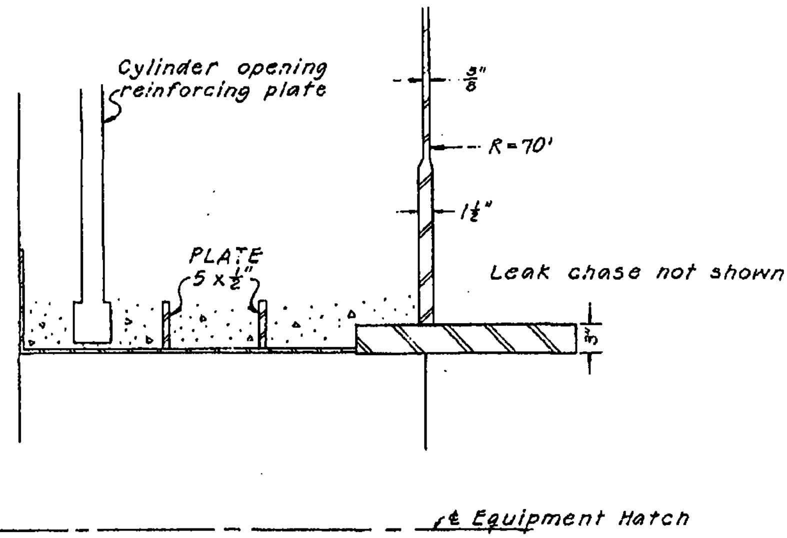

EQUIPMENT HATCH

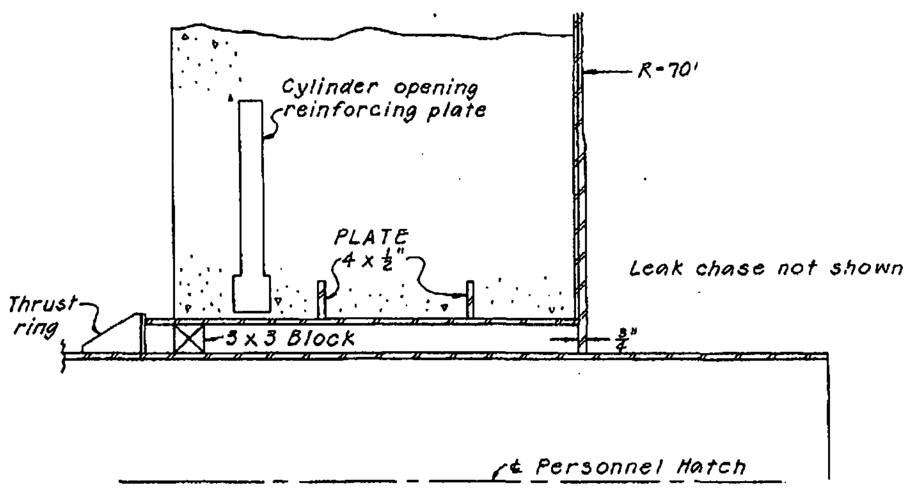

Unit 1 PERSONNEL HATCH

FSAR UPDATE
UNITS 1 AND 2 DIABLO CANYON SITE
FIGURE 3.8-13 CONTAINMENT STRUCTURE ACCESS HATCH SLEEVES

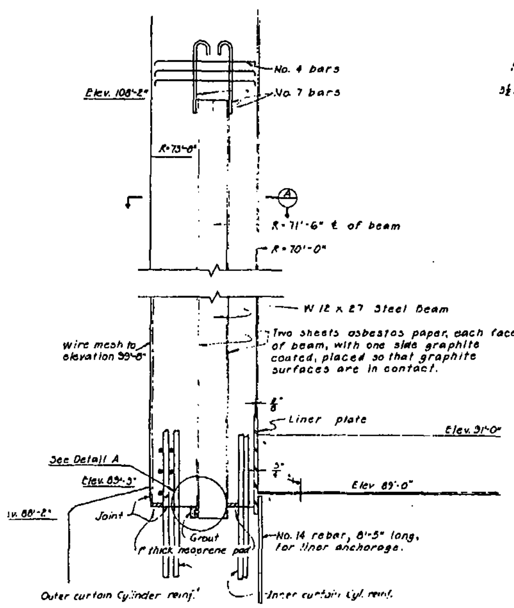

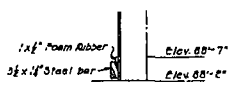

DETAIL A

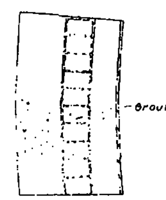

SECTION A

NOTES:

SEE FIGURE 3.8-15 FOR REINFORCING STEEL IN THIS REGION.

FSAR UPDATE

UNITS 1 AND 2
DIABLO CANYON SITE

FIGURE 3.8-14
CONTAINMENT STRUCTURE
EMBEDDED BEAMS
CYLINDER-BASE SLAB JUNCTURE

Revision 11 November 1996

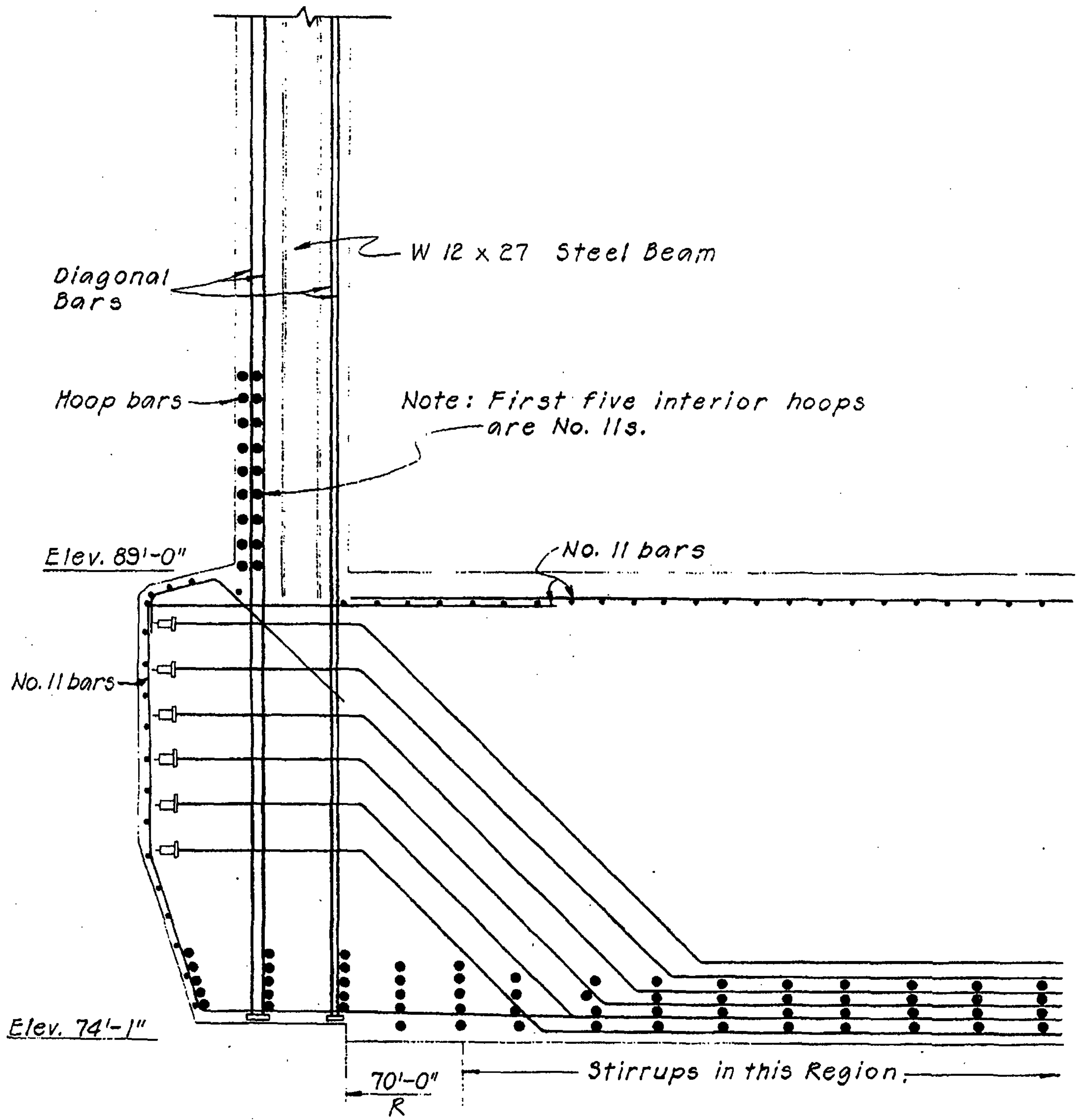

Bars are No. 18 unless noted.

FSAR UPDATE

UNITS 1 AND 2 DIABLO CANYON SITE

FIGURE 3.8-15
CONTAINMENT STRUCTURE
REINFORCING STEEL
BASE SLAB AND WALL

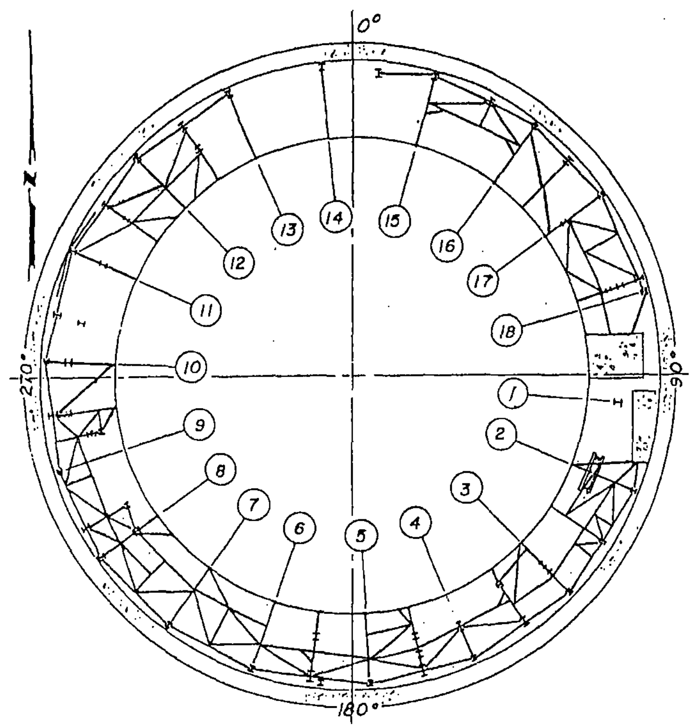

FRAMING PLAN T.O.S. EL 101'-4 1/2"

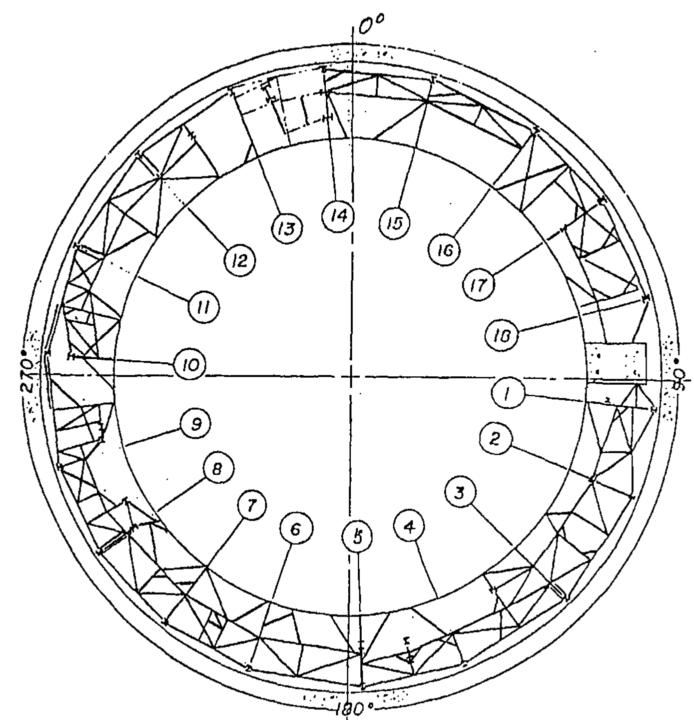

FRAMING PLAN T.O.S. EL 106'-8"

FSAR UPDATE
UNIT 1
DIABLO CANYON SITE
FIGURE 3.8-21, (Sheet 1 of 2)
INTERNAL STRUCTURE
ANNULUS PLATFORM
ELEVATIONS 101 AND 106'

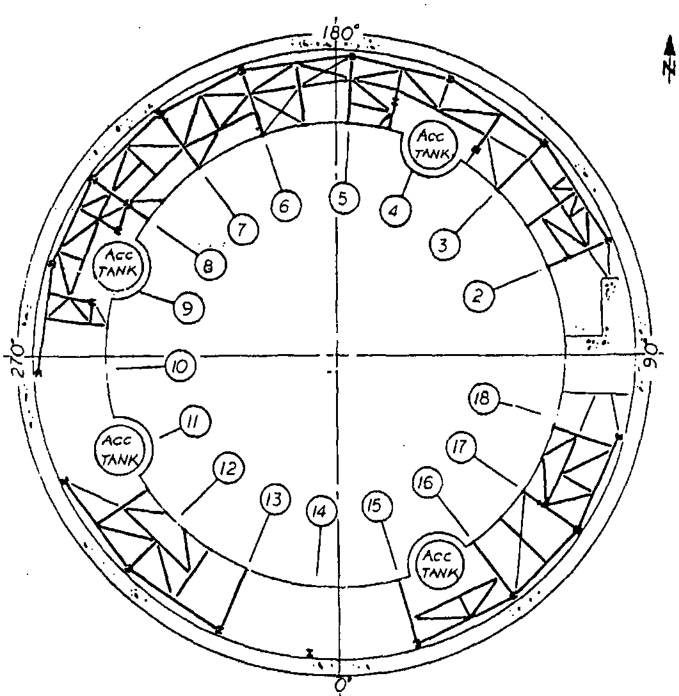

FRAMING PLAN T.O.S. EL. 101'-4½"

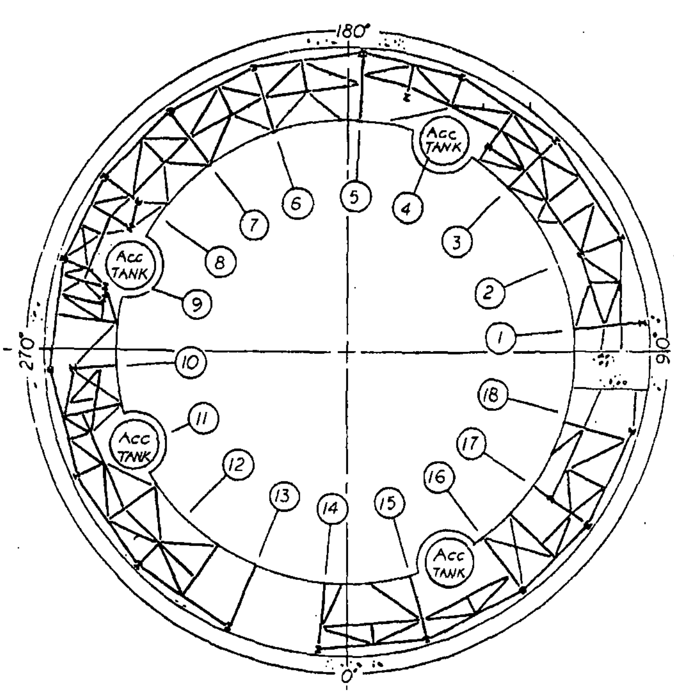

FRAMING PLAN T.O.S. EL. 106'-8"

FSAR UPDATE
UNIT 2
DIABLO CANYON SITE
FIGURE 3.8-21, (Sheet 2 of 2)
INTERNAL STRUCTURE
ANNULUS PLATFORM
ELEVATIONS 101 AND 106'

Revision 11 November 1996

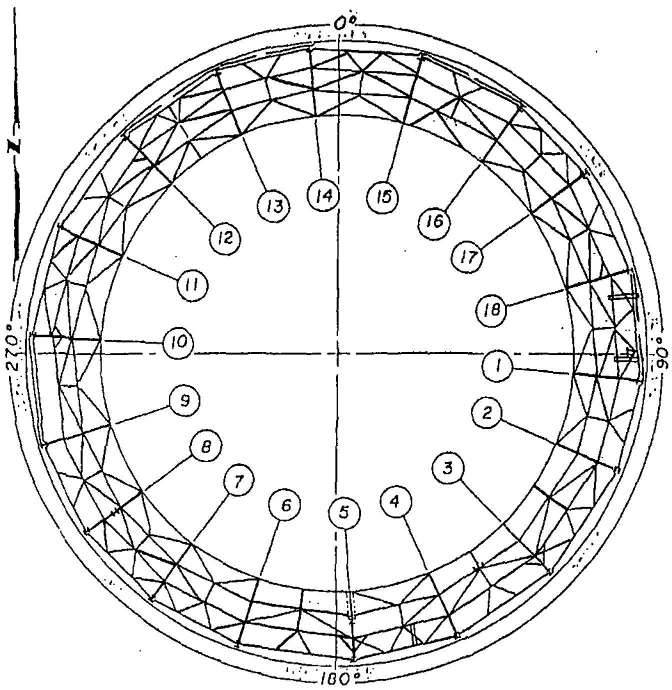

FRAMING PLAN T.O.S. EL 116'-10 3/4"

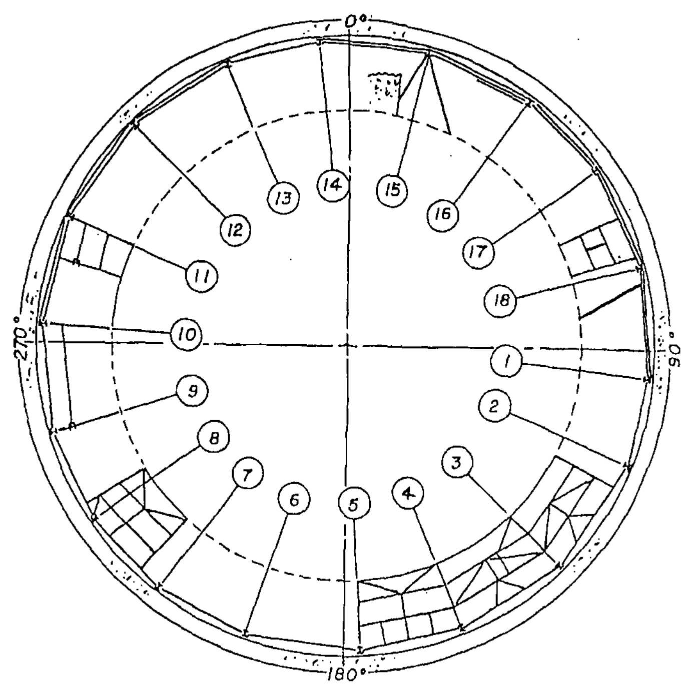

FRAMING PLAN T.O.S. EL 139'-10 3/4"

FSAR UPDATE
UNIT 1 **DIABLO CANYON SITE**
FIGURE 3.8-22 (Sheet 1 of 2) INTERNAL STRUCTURE ANNULUS PLATFORM ELEVATIONS 117 AND 140'

Revision 11 November 1996

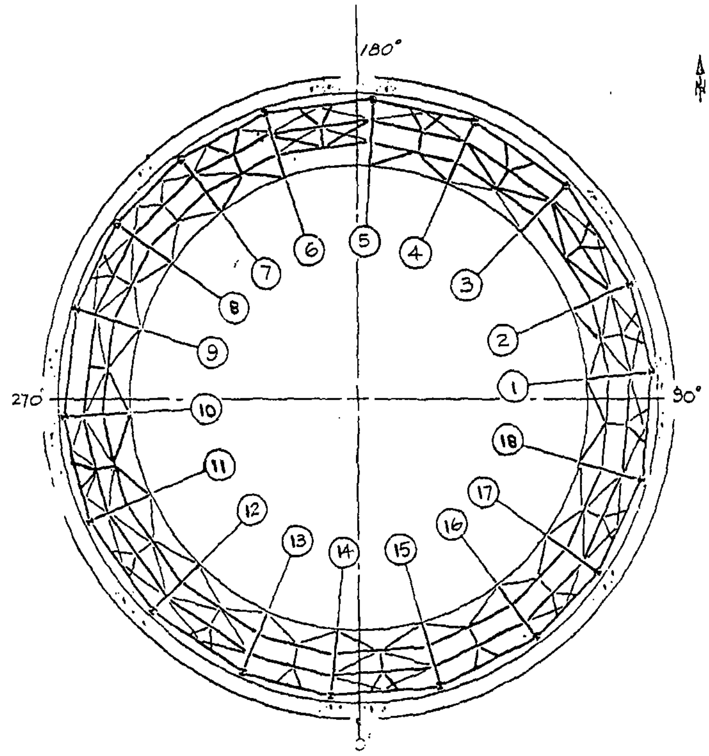

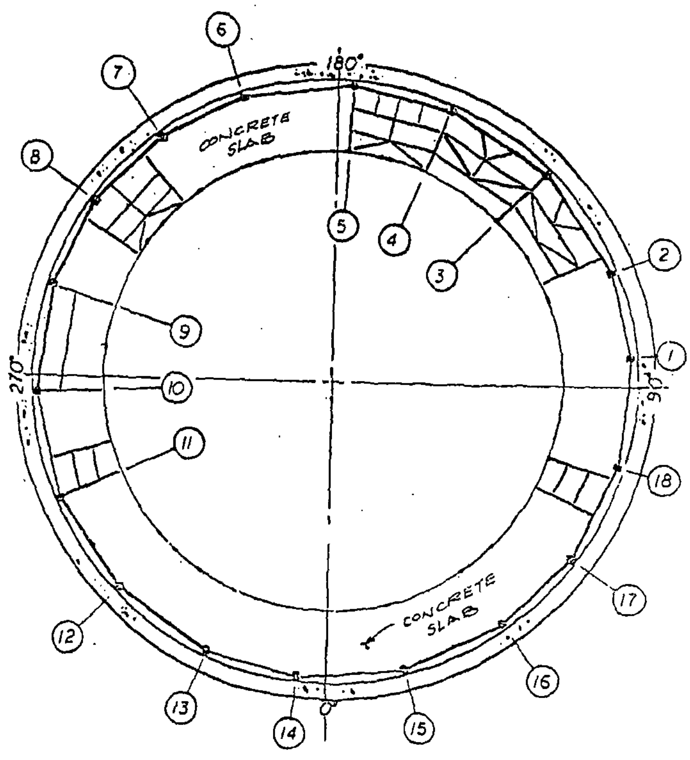

FSAR UPDATE

UNIT 2
DIABLO CANYON SITE

FIGURE 3.8-22 (Sheet 2 of 2)
INTERNAL STRUCTURE
ANNULUS PLATFORM
ELEVATIONS 117 AND 140'

Revision 11 November 1996

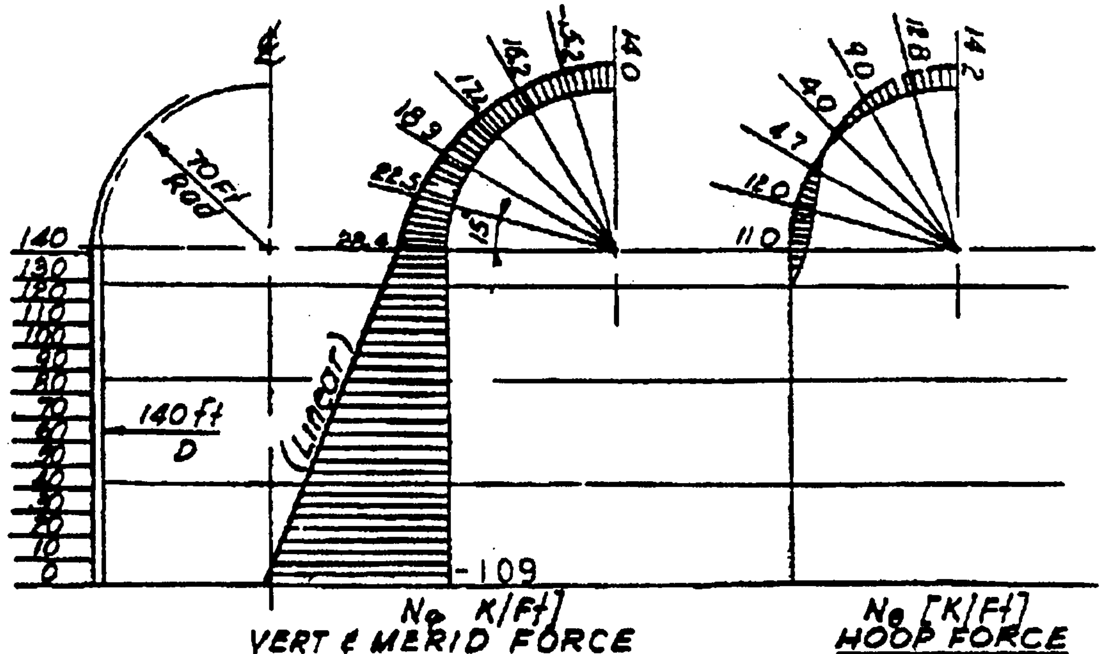

MEMBRANE FORCES DUE TO DEAD LOAD (1.00 D)

SCHEMATIC, NOT TO SCALE

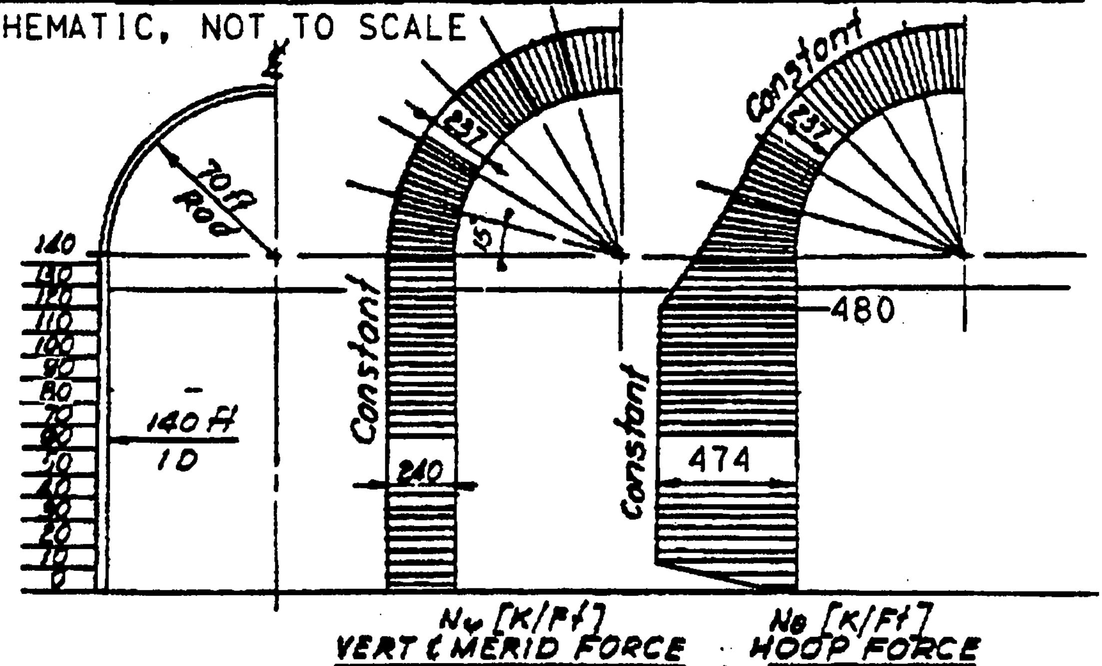

MEMBRANE FORCES DUE TO DESIGN PRESSURE (1.0 P)

SCHEMATIC, NOT TO SCALE

FSAR UPDATE

UNITS 1 AND 2
DIABLO CANYON SITE

FIGURE 3.8-27
CONTAINMENT STRUCTURE
MEMBRANE FORCES
DEAD LOAD AND PRESSURE

Revision 11 November 1996

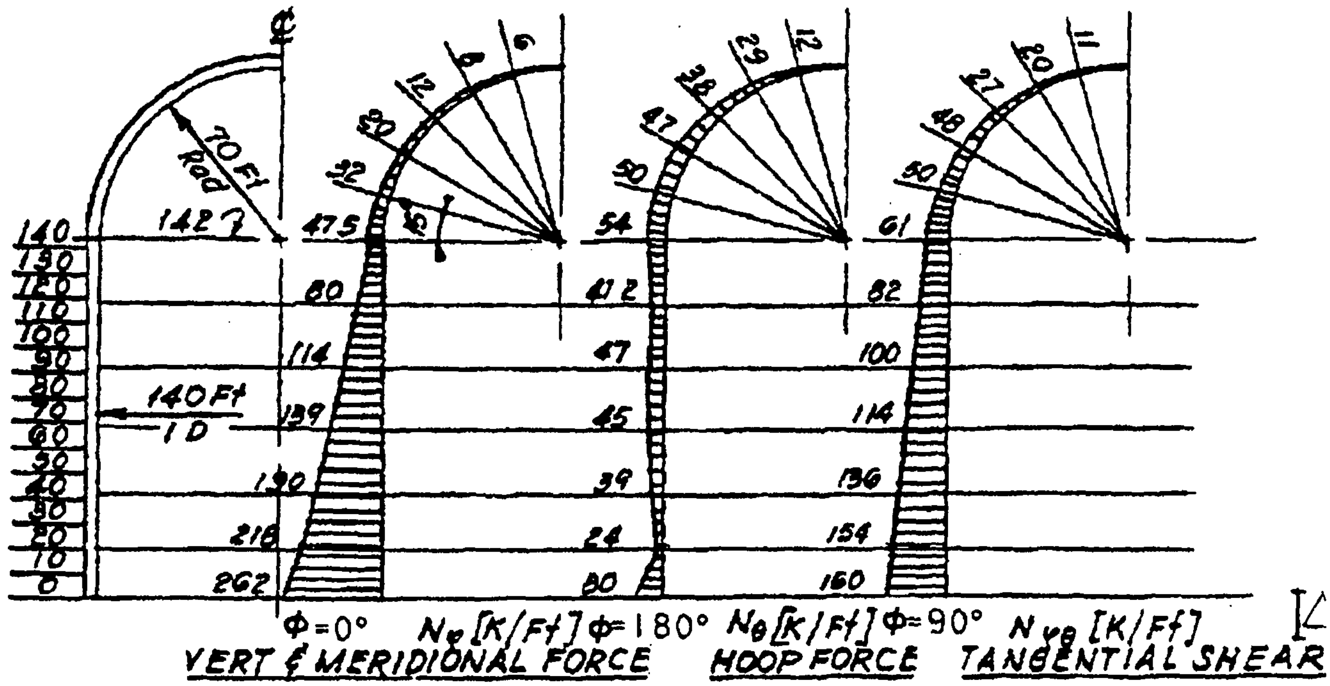

MEMBRANE FORCES DUE TO 1.25x DESIGN EARTHQUAKE (1.25DE)

SCHEMATIC, NOT TO SCALE

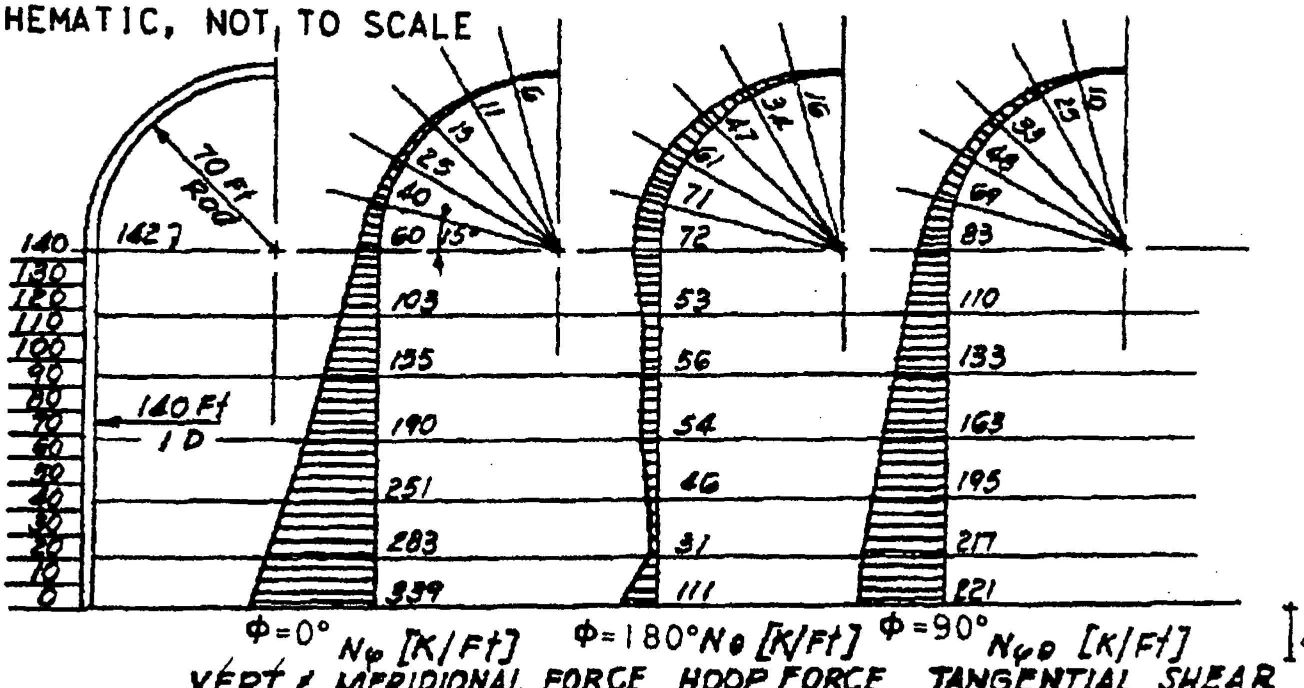

MEMBRANE FORCES DUE TO DOUBLE DESIGN EARTHQUAKE (DDE)

SCHEMATIC, NOT TO SCALE

FSAR UPDATE
UNITS 1 AND 2 DIABLO CANYON SITE
FIGURE 3.8-28 CONTAINMENT STRUCTURE MEMBRANE FORCES DE and DDE EARTHQUAKES

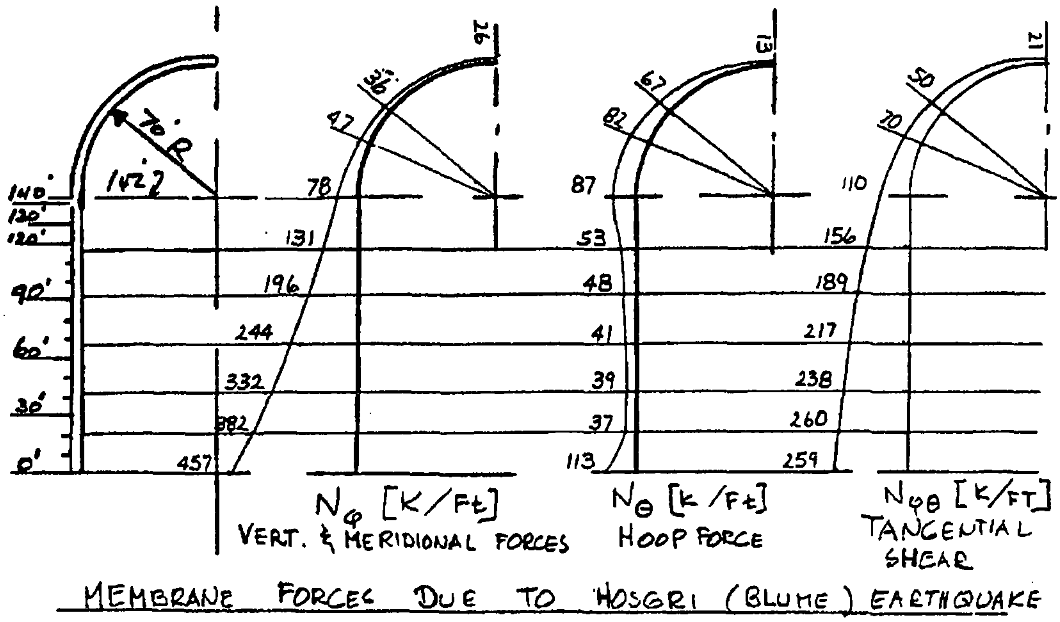

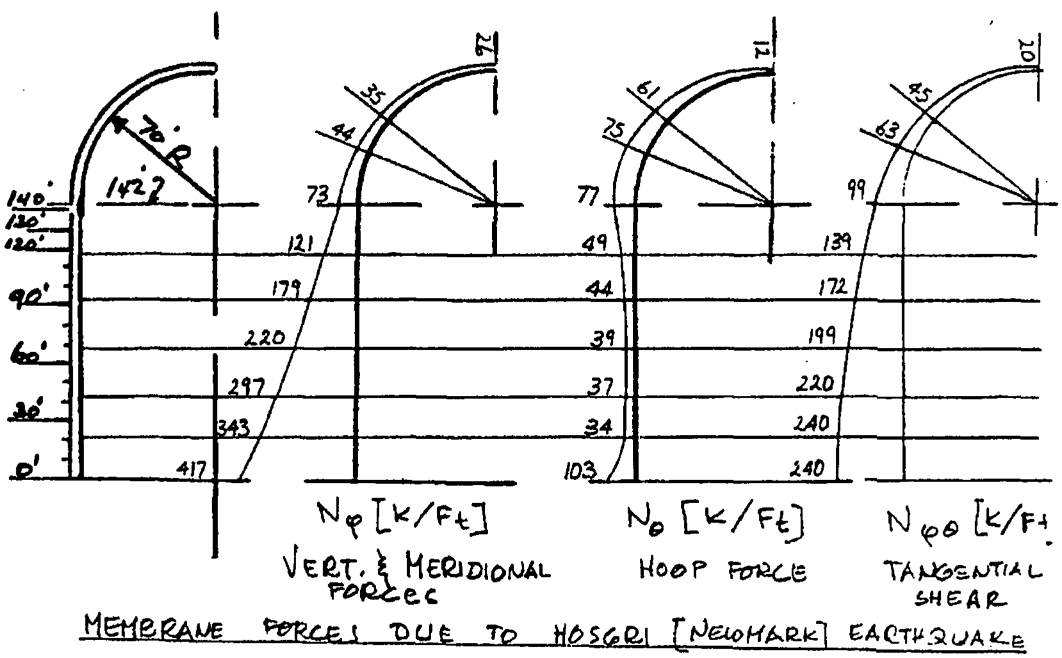

FSAR UPDATE

UNITS 1 AND 2
DIABLO CANYON SITE

FIGURE 3.8-29
CONTAINMENT STRUCTURE
MEMBRANE FORCES
HOSGRI EARTHQUAKE

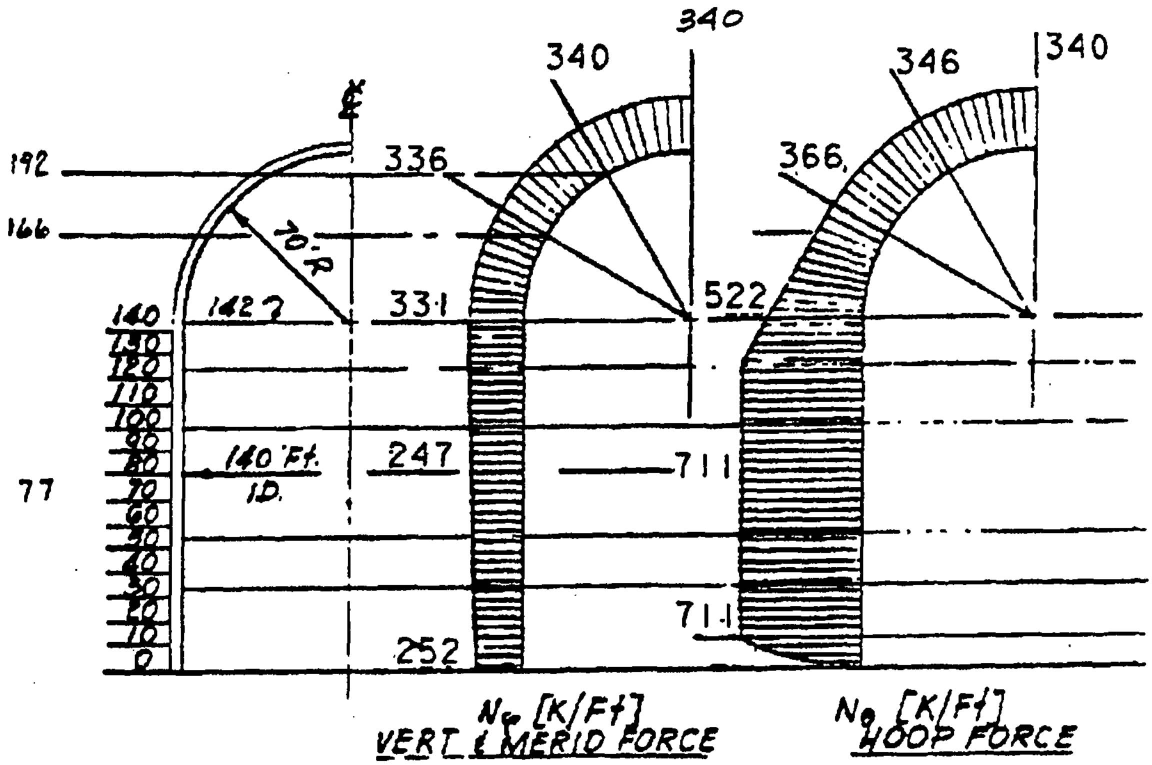

MAMBRANE FORCES

DUE TO LOAD CONDITION (I) U = 1.0D ± .05D + 1.5P +1.0T°

SCHEMATIC NOT TO SCALE

FSAR UPDATE

UNITS 1 AND 2
DIABLO CANYON SITE

FIGURE 3.8-30
CONTAINMENT STRUCTURE
MEMBRANE FORCES
ACCIDENT CONDITION 1

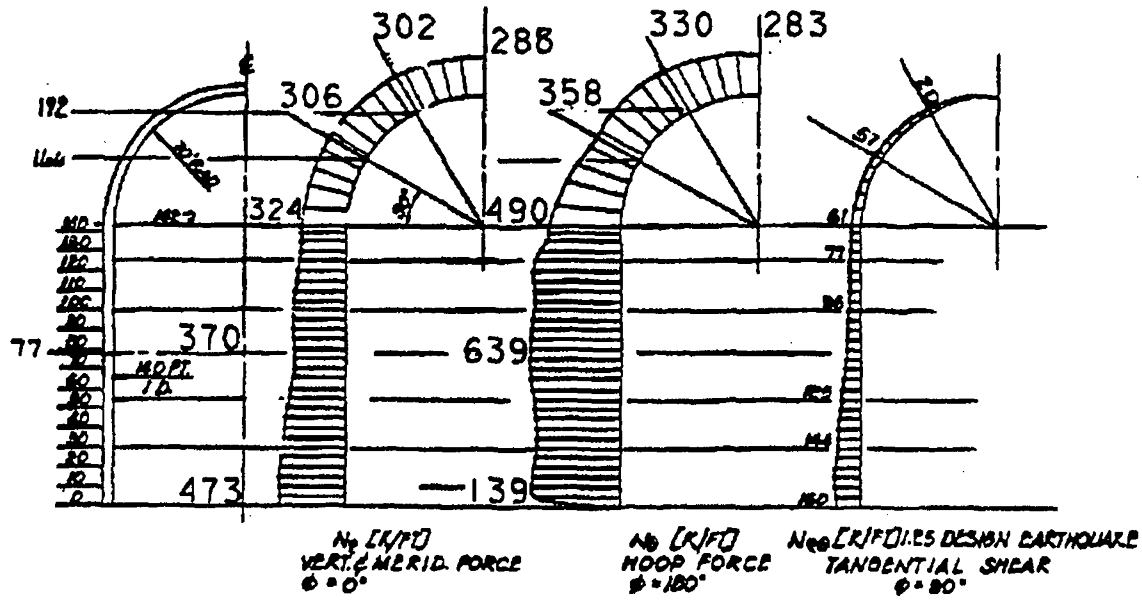

MAMBRANE FORCES

DUE TO LOAD CONDITION (2) U = 1.0D ± .05D + 1.25P + 1.25DE

SCHEMATIC NOT TO SCALE

FSAR UPDATE

UNITS 1 AND 2
DIABLO CANYON SITE

FIGURE 3.8-31
CONTAINMENT STRUCTURE
MEMBRANE FORCES
ACCIDENT CONDITION 2

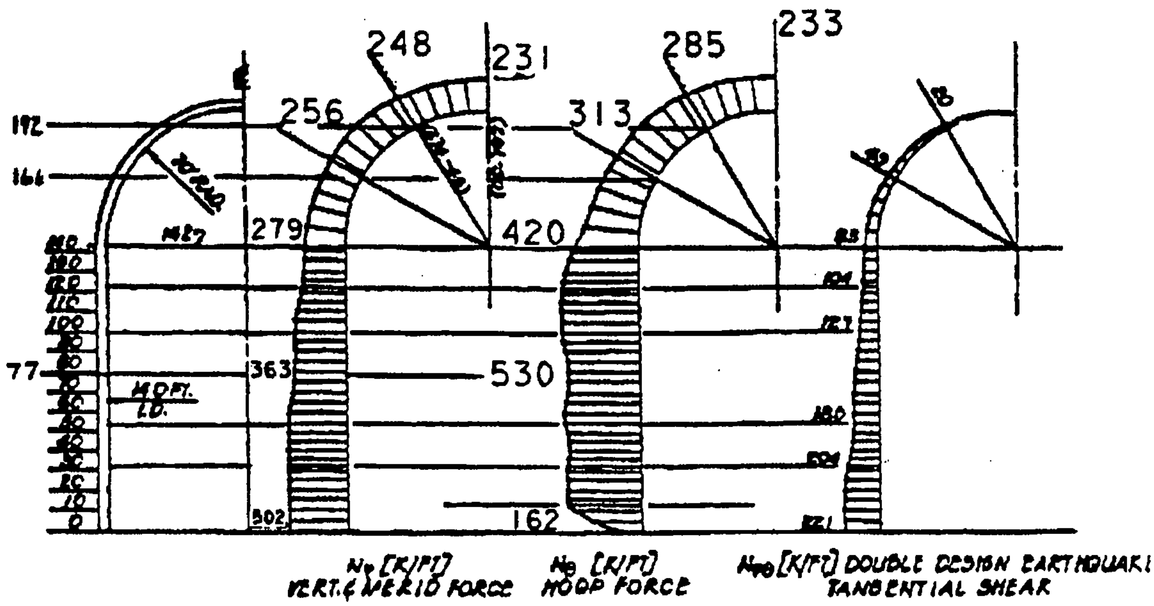

MAMBRANE FORCES

NOTE VALUES ARE FORCES IN REBAR

FORCES DUE TO LOAD CONDITION (3) U = 1.0D ± .05D + 1.0P + 1.0T + 1.0DDE

SCHEMATIC NOT TO SCALE

FSAR UPDATE

UNITS 1 AND 2 DIABLO CANYON SITE

FIGURE 3.8-32 CONTAINMENT STRUCTURE MEMBRANE FORCES ACCIDENT CONDITION 3

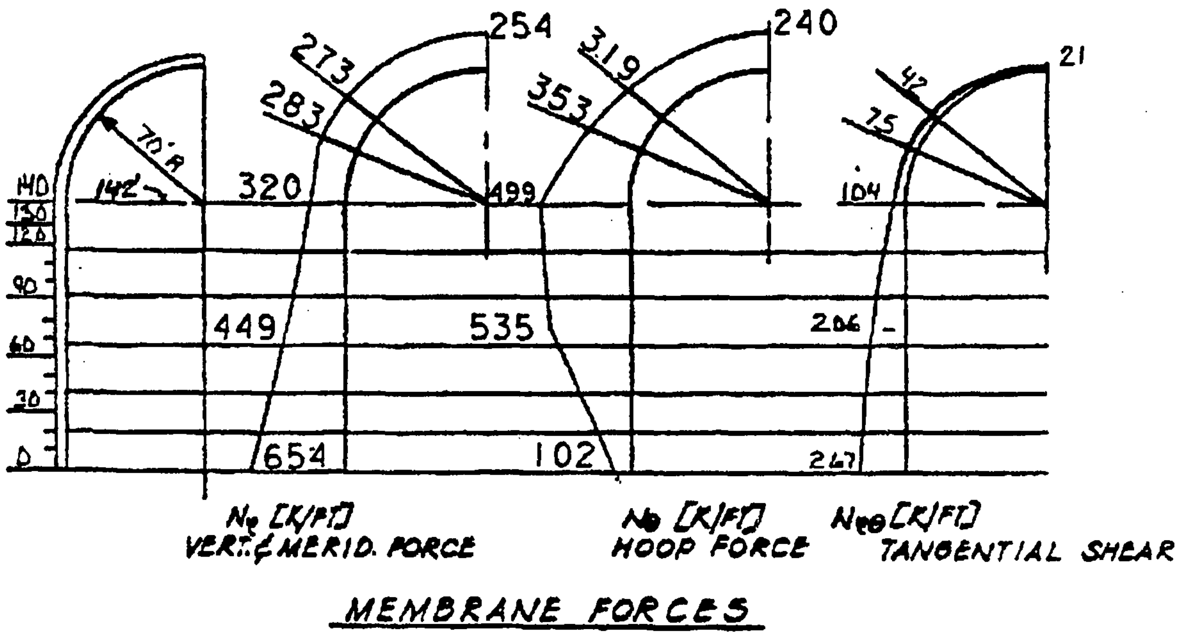

FORCES DUE TO LOAD CONDITION (4): U= (1 ± .05) D + P_A + T +HE

SCHEMATIC NOT TO SCALE

FSAR UPDATE

UNITS 1 AND 2
DIABLO CANYON SITE

FIGURE 3.8-33
CONTAINMENT STRUCTURE
MEMBRANE FORCES
ACCIDENT CONDITION 4

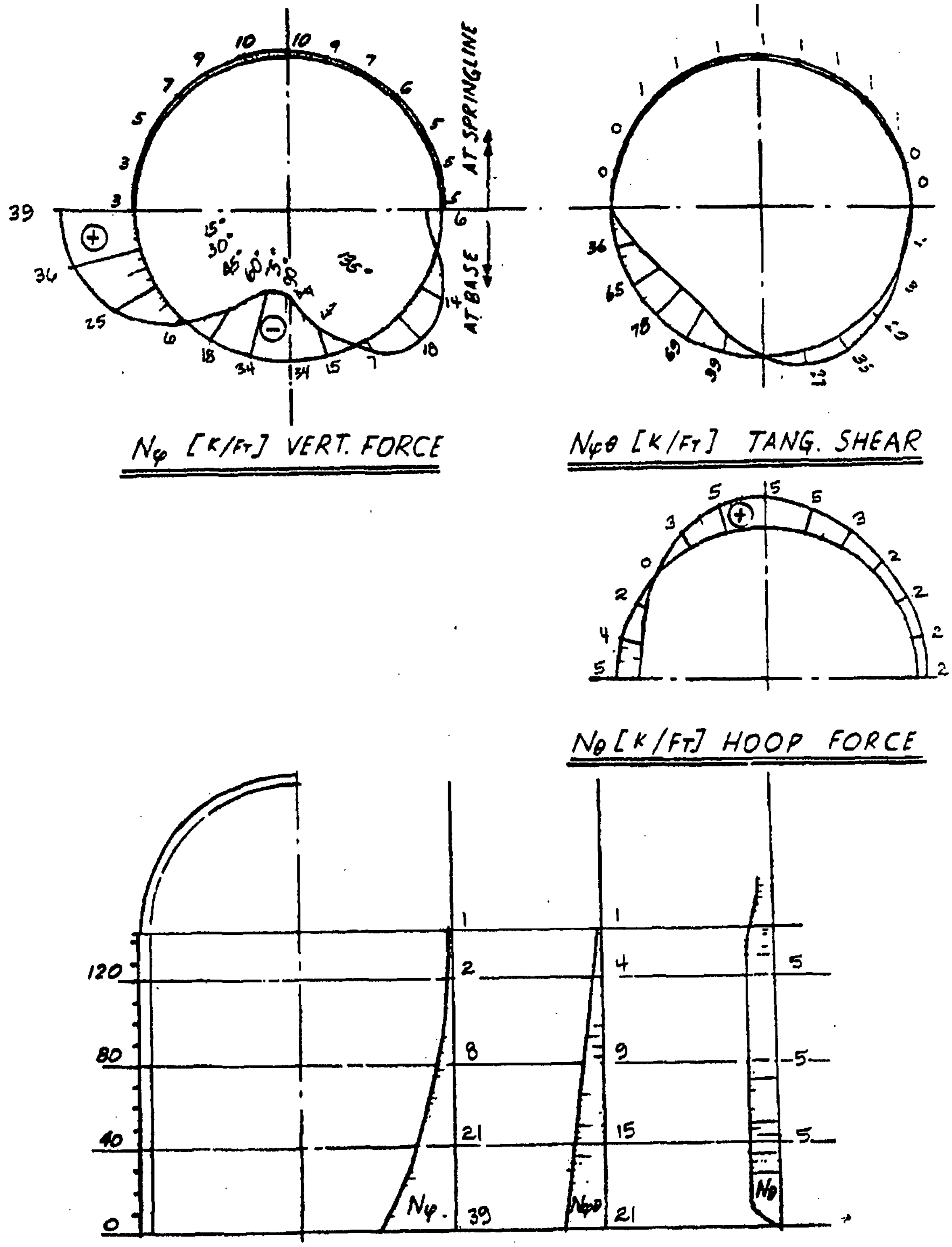

MEMBRANE FORCES DUE TO 80 MPH WIND

FSAR UPDATE
UNITS 1 AND 2
DIABLO CANYON SITE

FIGURE 3.8-34
CONTAINMENT STRUCTURE
MEMBRANE FORCES
WIND LOAD

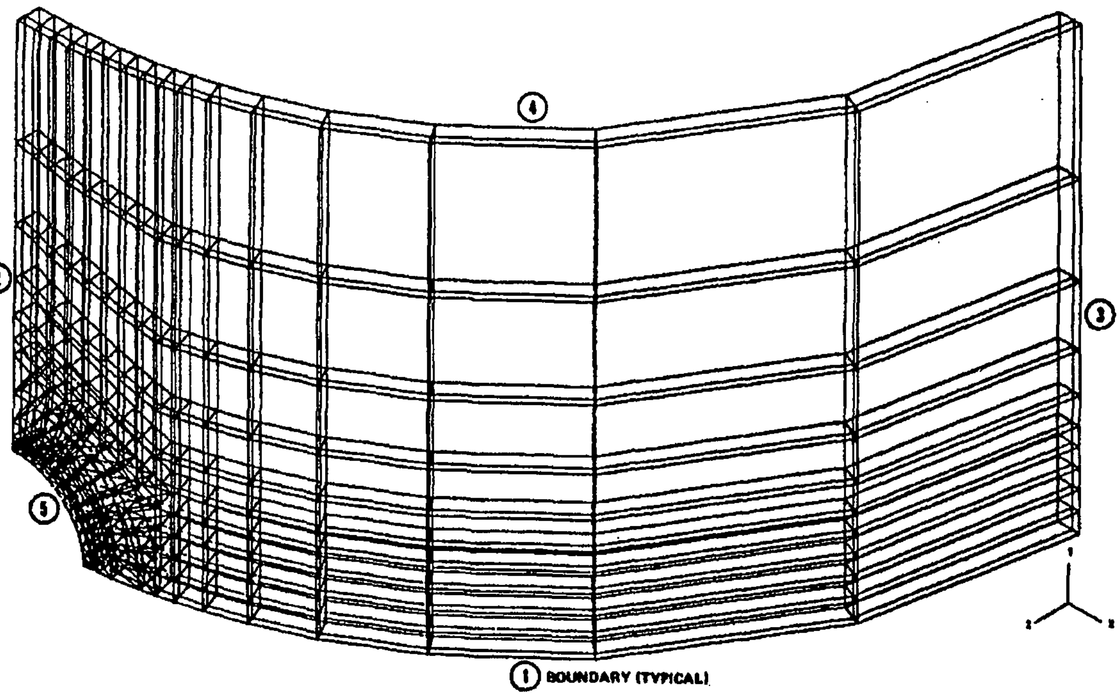

FSAR UPDATE
UNITS 1 AND 2 DIABLO CANYON SITE
FIGURE 3.8-35 CONTAINMENT STRUCTURE EQUIPMENT HATCH ANALYTICAL MODEL ISOMETRIC VIEW

Revision 11 November 1996

CRACKED SECTION

CONDITION (a) $C = 1.0D + 0.05D + 1.5P + 1.0T''$

ELEVATION (ABOVE BASE SLAB)		LINER NOT CONSIDERED – REBAR STRESSES 1	2	3	LINER CONSIDERED – REBAR STRESSES 1	2	3	LINER STRESS σ_{MAX}	σ_{MIN}
ALLOWABLE STRESS		57.0	57.0	57.0	57.0	57.0	57.0		
DOME	212				42.8	42.8	42.8	-5.1	-5.1
DOME	185				42.8	44.5	42.8	-3.4	-5.2
DOME	169				42.3	41.0	42.3	-5.6	-7.0
	142	38.7	52.6	38.7	42.2	50.3	42.2	2.1	-6.5
CYLINDER	83	34.3	54.4	34.3	39.7	51.9	39.7	2.7	-10.2
CYLINDER	0	19.0	0	19.0	31.6	0	31.6	-23.8 (*)	-52.7 (*)

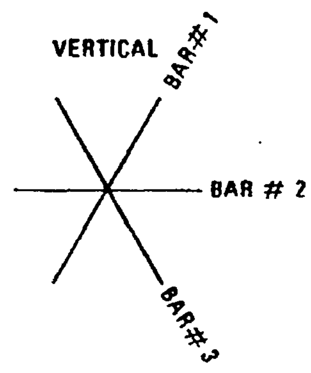

ALL STRESSES IN KIPS/SQUARE INCH

MINUS SIGN INDICATES COMPRESSION

(*) Maximum strain levels for the liner plate are within acceptable limits.

FSAR UPDATE

UNITS 1 AND 2 DIABLO CANYON SITE

FIGURE 3.8-37

CONTAINMENT STRUCTURE EXTERIOR SHELL STRESSES ACCIDENT CONDITION 1

Revision 11 November 1996

CRACKED SECTION – LINER CONSIDERED

CONDITION		$U = 1.0D \pm 0.05D + 1.25P + 1.0T' + 1.25DE$					$U = 1.0D \pm 0.05D + 1.0P + 1.0T' + 1.0\ DDE$				
		REBAR STRESSES			LINER STRESS		REBAR STRESSES			LINER STRESS	
ELEVATION (ABOVE BASE SLAB)		1	2	3	σ_{MAX}	σ_{MIN}	1	2	3	σ_{MAX}	σ_{MIN}
ALLOWABLE STRESS		57.0	57.0	57.0			57.0	57.0	57.0		
212	DOME	38.7	38.3	37.7	-8.4	-8.5	32.1	31.6	30.9	-8.6	-8.6
185	DOME	41.7	40.7	35.5	-5.9	-8.1	36.0	34.1	27.9	-6.0	-8.2
169	DOME	42.7	37.6	34.2	-9.0	-8.0	37.6	31.7	26.2	-8.1	-8.3
142		45.2	44.9	32.9	-1.6	-7.8	41.0	37.5	24.2	-2.4	-7.4
83	CYLINDER	50.1	45.1	31.0	-.9	-5.7	48.9	36.7	22.7	-2.0	-2.9
0	CYLINDER	43.8	0	29.3	-10.4 (*)	-47.2 (*)	46.6	0	22.9	-4.8 (*)	-39.1 (*)

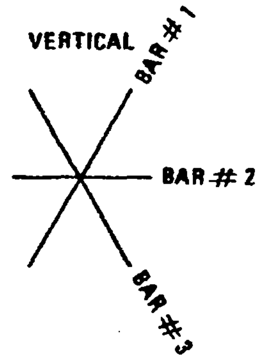

ALL STRESSES IN KIPS/SQUARE INCH

MINUS SIGN INDICATES COMPRESSION

NOTE:
REBAR STRESSES FOR REBAR IN OUTER LAYER ONLY.

(*) Maximum strain levels for the liner plate are within acceptable limits.

FSAR UPDATE

UNITS 1 AND 2 DIABLO CANYON SITE

FIGURE 3.8-38

CONTAINMENT STRUCTURE EXTERIOR SHELL STRESSES ACCIDENT CONDITIONS 2 AND 3

CRACKED SECTION

CONDITION (c) C = 1.00 ± 0.05D + 1.0P + 1.0T + 1.0 HE

	ALLOWABLE STRESS ELEVATION (FT) (ABOVE BASE SLAB)	REBAR STRESSES * 1	REBAR STRESSES * 2	REBAR STRESSES * 3		LINER PLATE * STRESS MAX	LINER PLATE * STRESS MIN	
		63.5	63.5	63.5				
DOME	213	33.6	31.4	32.2		-6.4	-8.6	WITH LINER PLATE
DOME	185	37.7	34.7	28.4		-4.9	-6.7	WITH LINER PLATE
DOME	169	39.6	31.9	26.1		-6.7	-7.7	WITH LINER PLATE
CYLINDER	142	44.2	36.8	23.0		-2.6	-6.0	WITH LINER PLATE
CYLINDER	83	53.4	37.5	18.4		-1.2	-2.8	WITH LINER PLATE
CYLINDER	83	61.2	38.1	11.0				WITHOUT LINER PLATE
CYLINDER	0	49.5	0	24.8		-1.0 (*)	-38.1 (*)	WITH LINER PLATE

(*) Maximum strain levels for the liner plate are within acceptable limits.

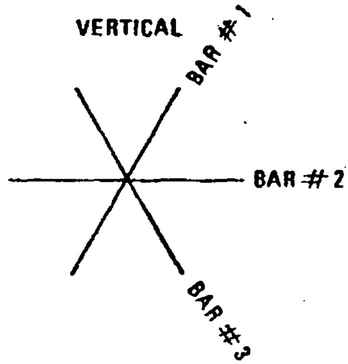

ALL STRESSES IN KIPS/SQUARE INCH

MINUS SIGN INDICATES COMPRESSION

* STRESSES ARE MAXIMUM OR MINIMUM AT ANY SECTION:

FSAR UPDATE

UNITS 1 AND 2 DIABLO CANYON SITE

FIGURE 3.8-39

CONTAINMENT STRUCTURE, EXTERIOR SHELL STRESSES – ACCIDENT CONDITION 4

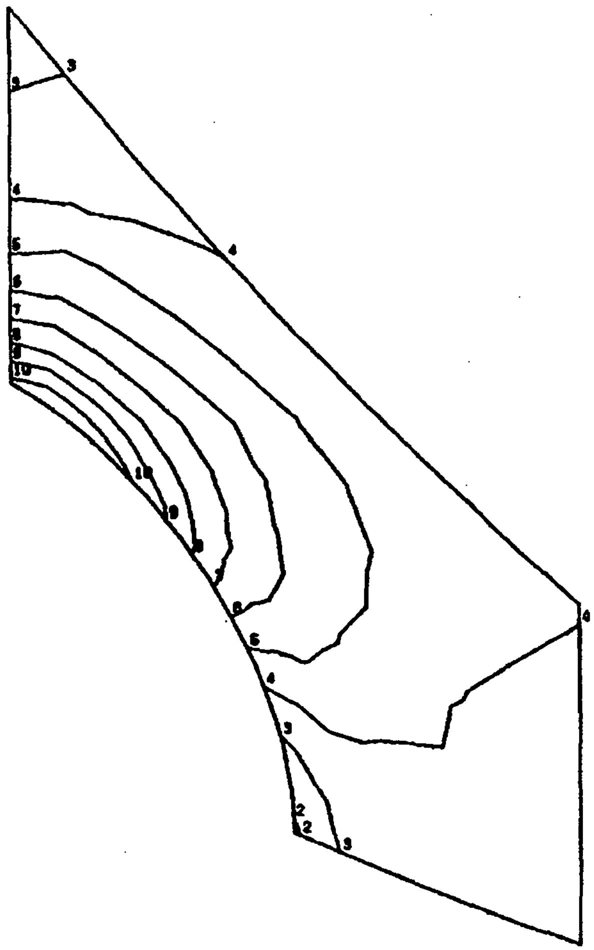

CONTOURING INFORMATION

LEVEL	VALUE
1	.13600+05
2	.17000+05
3	.20400+05
4	.23800+05
5	.27200+05
6	.30600+05
7	.34000+05
8	.37400+05
9	.40800+05
10	.44200+05

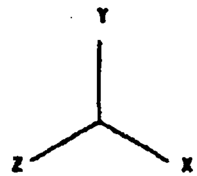

FSAR UPDATE

UNITS 1 AND 2
DIABLO CANYON SITE

FIGURE 3.8-40

EQUIPMENT HATCH HEXAGONAL PLATE MAXIMUM STRESSES (1.05D + 1.5P + T")

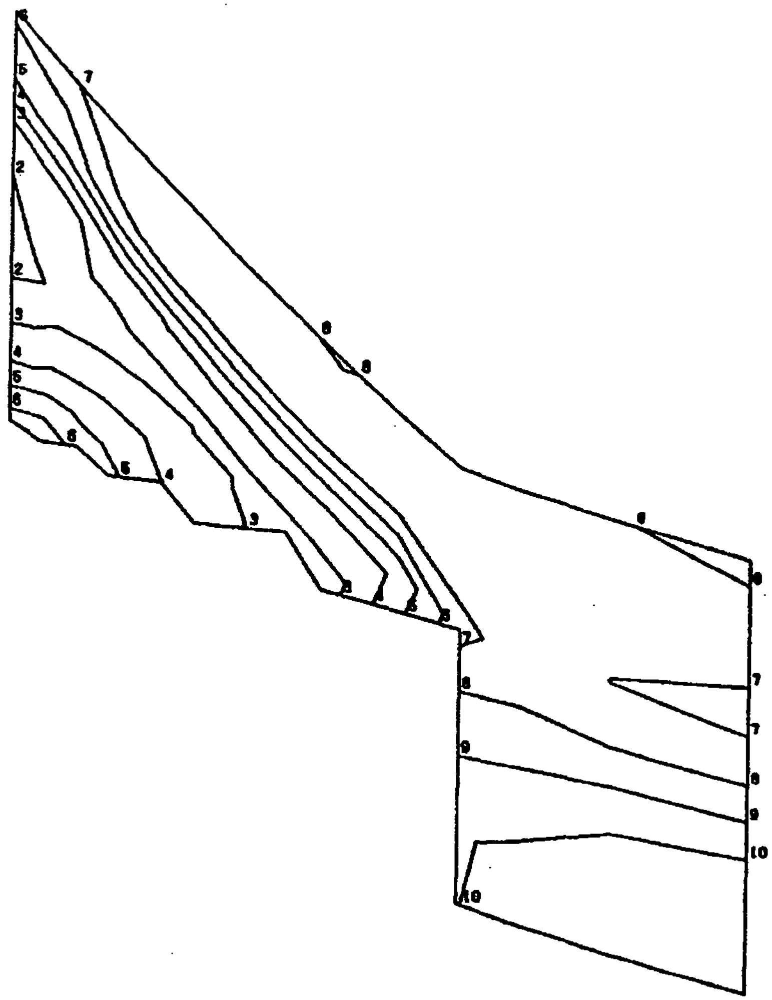

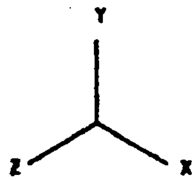

FSAR UPDATE

**UNITS 1 AND 2
DIABLO CANYON SITE**

FIGURE 3.8-41

EQUIPMENT HATCH HOOP
REINFORCEMENT STRESSES
(1.05D + 1.5P + T'')

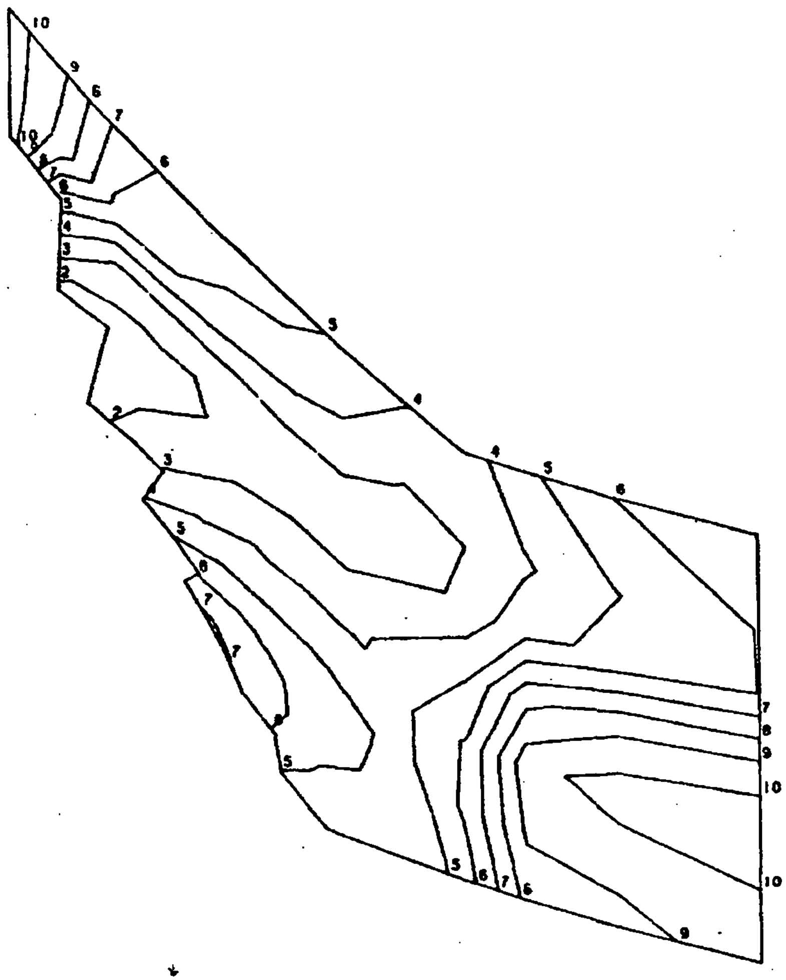

CONTOURING INFORMATION

LEVEL	VALUE
1	.96000+04
2	.12000+05
3	.14400+05
4	.16800+05
5	.19200+05
6	.21600+05
7	.24000+05
8	.26400+05
9	.28800+05
10	.31200+05

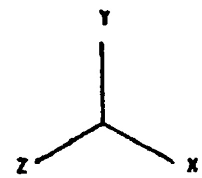

FSAR UPDATE

UNITS 1 AND 2
DIABLO CANYON SITE

FIGURE 3.8-42
EQUIPMENT HATCH DIAGONAL
REINFORCEMENT STRESSES
(1.05D + 1.5P + T")

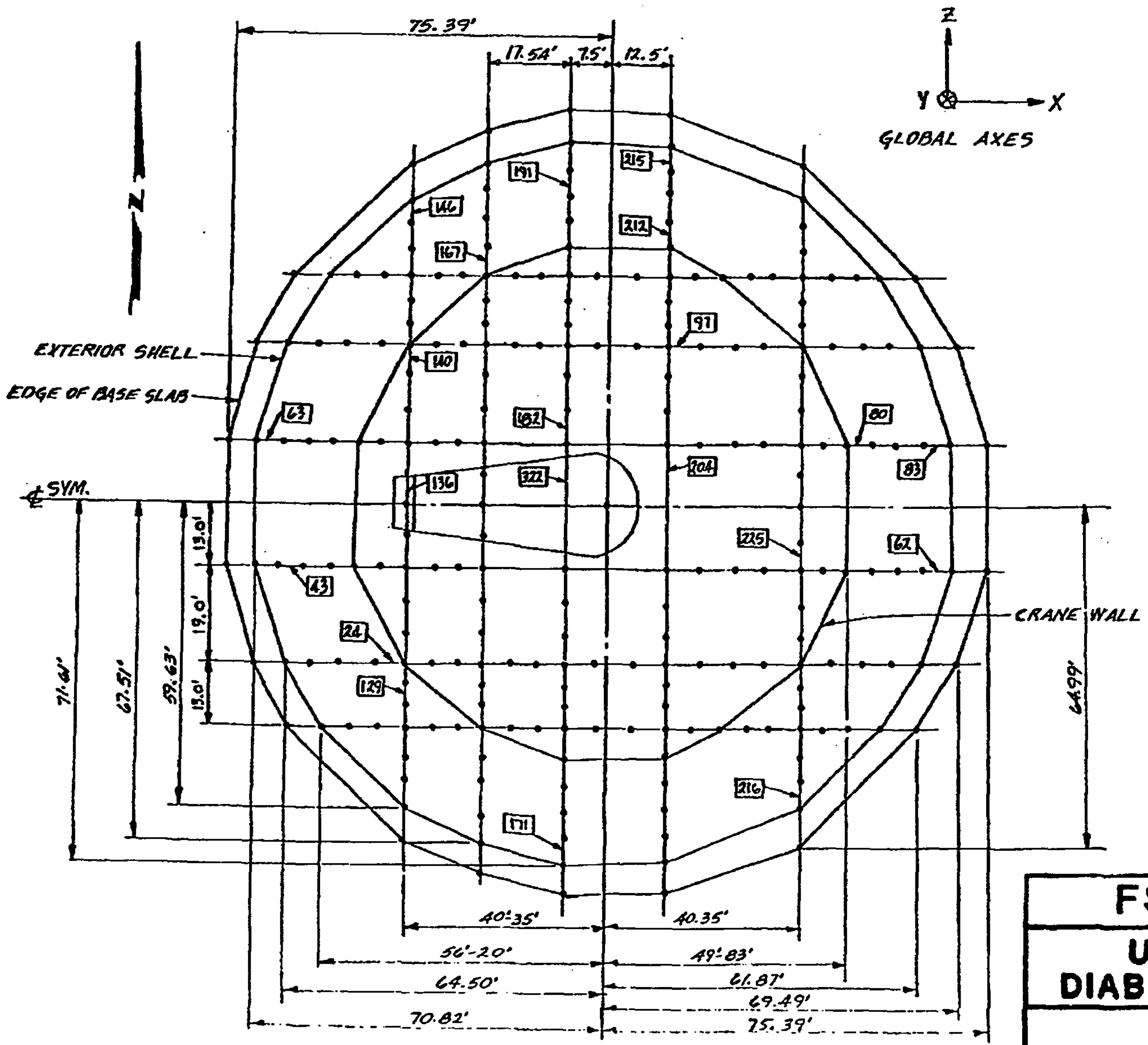

FSAR UPDATE

UNITS 1 AND 2 DIABLO CANYON SITE

FIGURE 3.8-43

CONTAINMENT BASE SLAB MODEL

NOTES FOR FIELD INSTALLATION

1. REMOVE MILL SCALE AND POLISH REBAR SURFACE INSIDE OF DIAMOND AREA
2. BOND SHIM ASSEMBLY TO POLISHED REBAR
3. PLACE SEALANT AND PROTECTIVE COVER OVER SHIM ASSEMBLY.

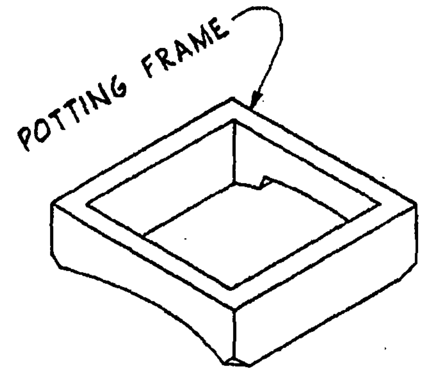

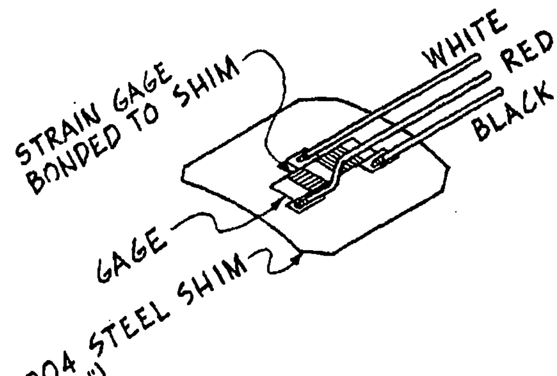

SHIM ASSEMBLY

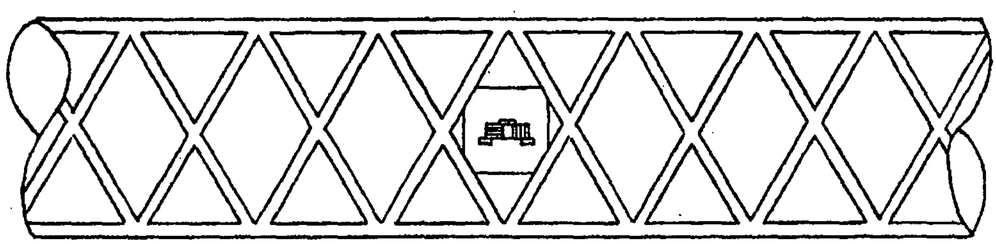

FSAR UPDATE
UNITS 1 AND 2 DIABLO CANYON SITE
FIGURE 3.8-44 CONTAINMENT STRUCTURE TYPICAL REBAR STRAIN GAUGE

Revision 11 November 1996

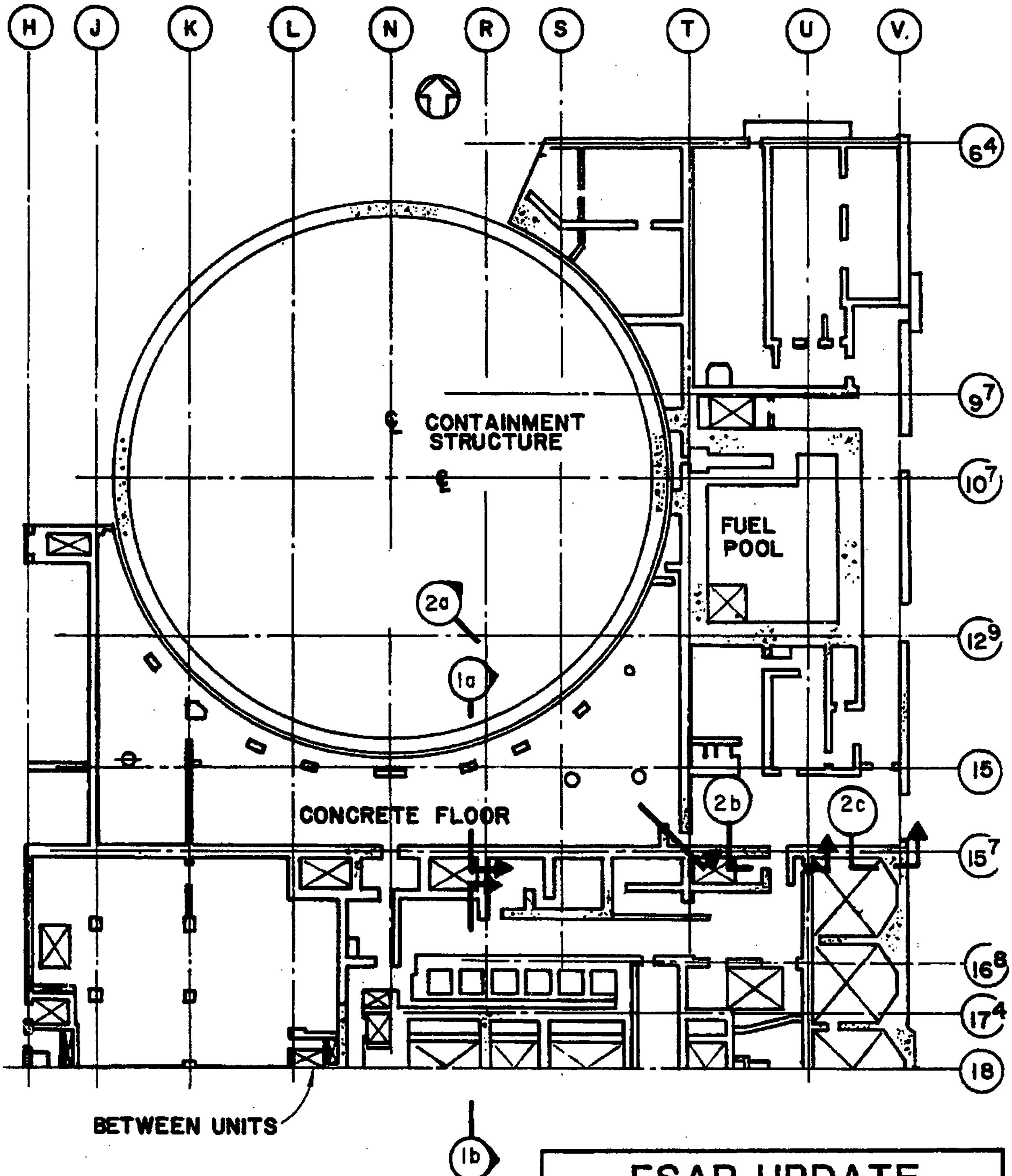

FSAR UPDATE

UNIT 1
DIABLO CANYON SITE

FIGURE 3.8-60

AUXILIARY BUILDING
FLOOR PLAN AT EL 100'-0"

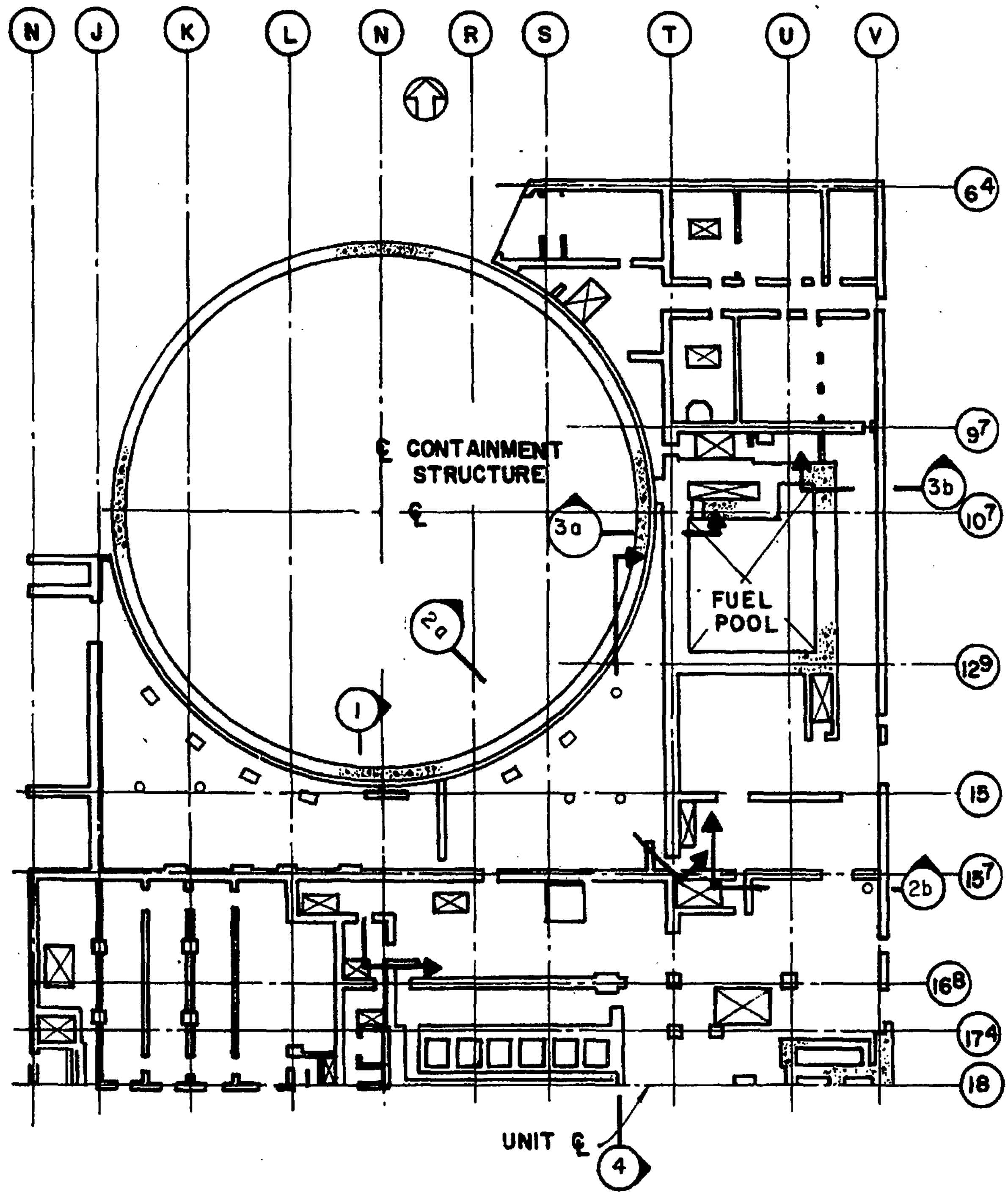

FSAR UPDATE

UNIT 1
DIABLO CANYON SITE

FIGURE 3.8-61

AUXILIARY BUILDING
FLOOR PLAN AT EL 115'-0"

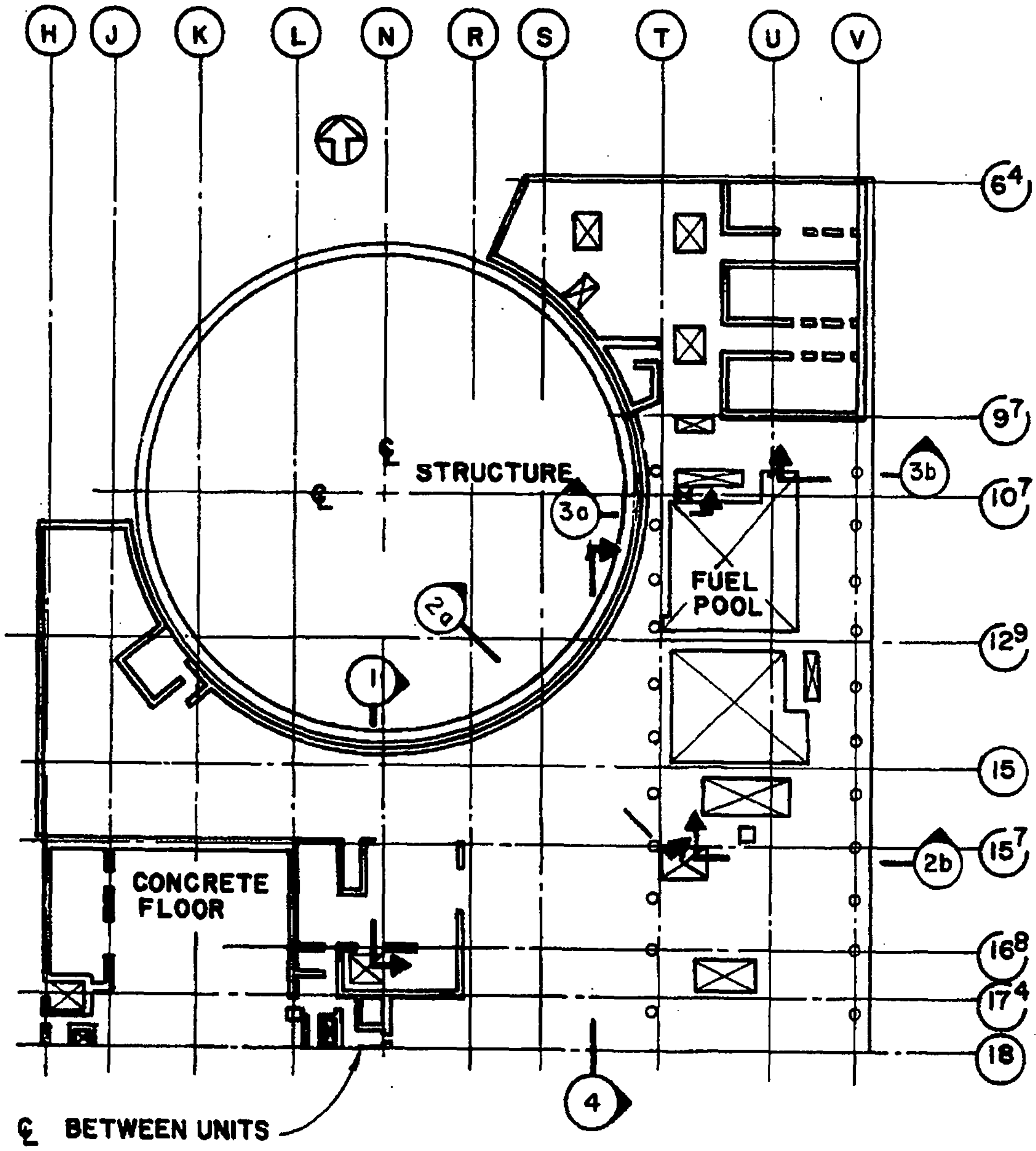

FSAR UPDATE

UNIT 1
DIABLO CANYON SITE

FIGURE 3.8-62
AUXILIARY BUILDING
FLOOR PLAN AT EL 140'-0"

Revision 11 November 1996

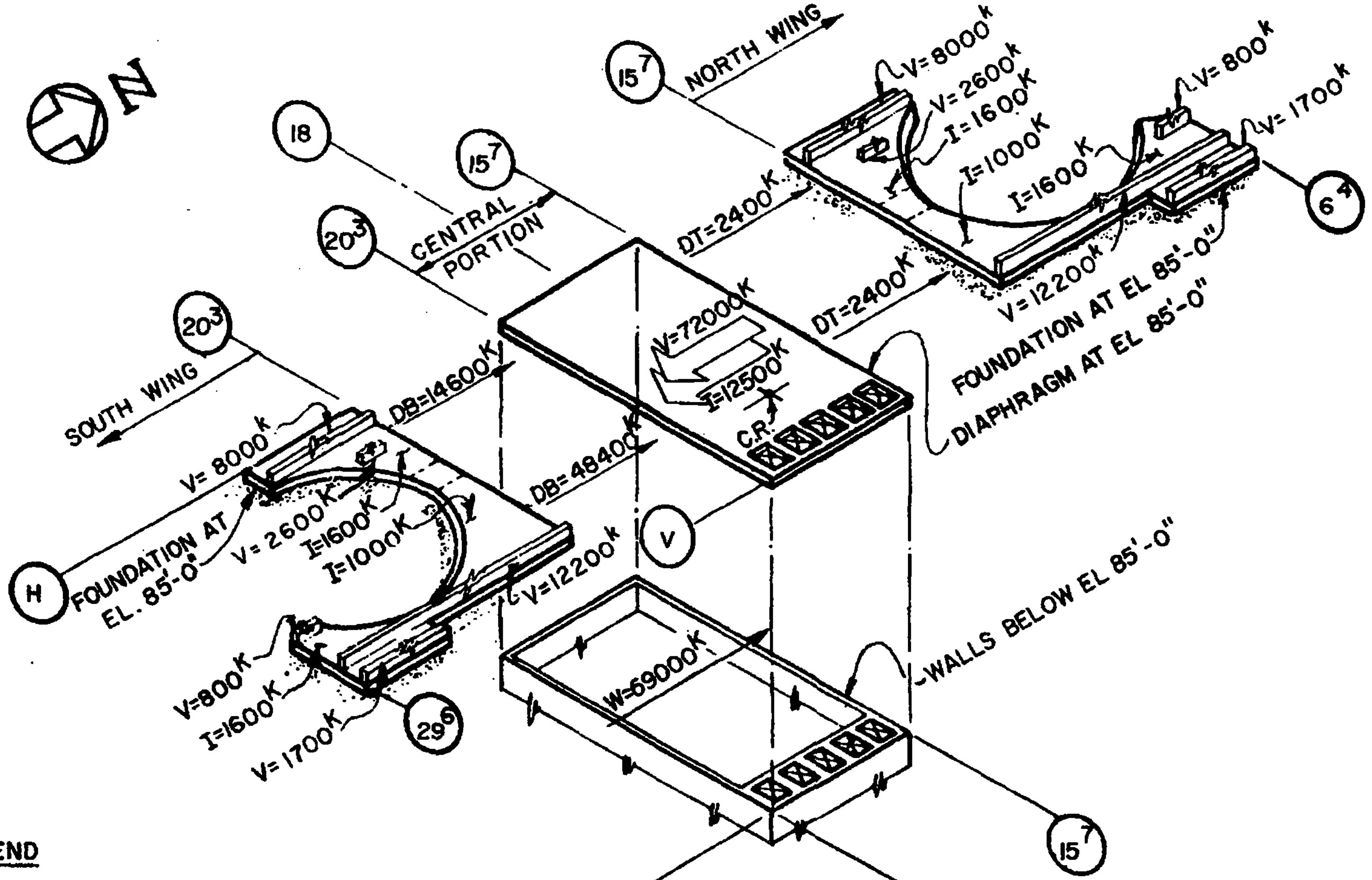

LEGEND

V= DEMAND SHEAR FORCE IN THE WALLS (KIPS)
I= DEMAND INERTIA LOAD AT EL. 85'-0" (KIPS)
W= SHEAR CAPACITY OF WALLS BELOW EL. 85'-0" (KIPS)
DT= CAPACITY THROUGH DIAPHRAGM REBAR TENSION (KIPS)
DB= CAPACITY THROUGH DIAPHRAGM BEARING (KIPS)

NOTE: DEMAND SHEARS IN WALLS WEST OF CENTER OF RIGIDITY CONSIDER DIRECT PLUS POSITIVE TORSIONAL SHEARS. THOSE IN WALLS EAST OF CENTER OF RIGIDITY CONSIDER ONLY DIRECT SHEARS.

FSAR UPDATE

UNITS 1 AND 2
DIABLO CANYON SITE

FIGURE 3.8-63
AUXILIARY BUILDING
LOAD DISSIPATION TO FOUNDATION
HOSGRI N – S

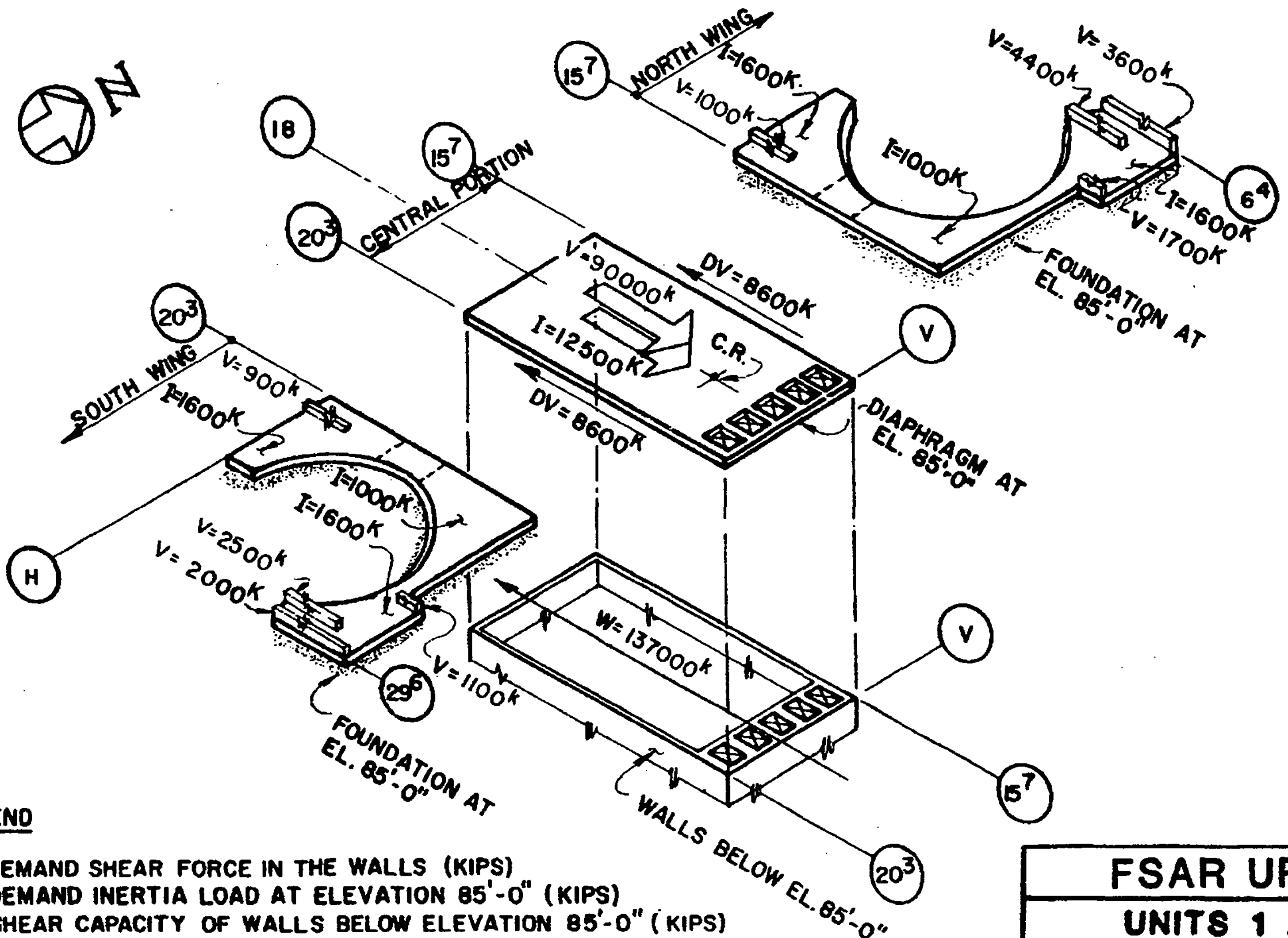

LEGEND

V= DEMAND SHEAR FORCE IN THE WALLS (KIPS)
I= DEMAND INERTIA LOAD AT ELEVATION 85'-0" (KIPS)
W= SHEAR CAPACITY OF WALLS BELOW ELEVATION 85'-0" (KIPS)
DV= SHEAR CAPACITY OF DIAPHRAGM (KIPS)

NOTE: WALLS NORTH OF LINE 18 CONSIDER DIRECT PLUS POSITIVE TORSIONAL EFFECT AND THOSE SOUTH OF LINE 18 CONSIDER ONLY DIRECT SHEARS.

FSAR UPDATE

UNITS 1 AND 2 DIABLO CANYON SITE

FIGURE 3.8-64
AUXILIARY BUILDING
LOAD DISSIPATION TO FOUNDATION
HOSGRI E – W

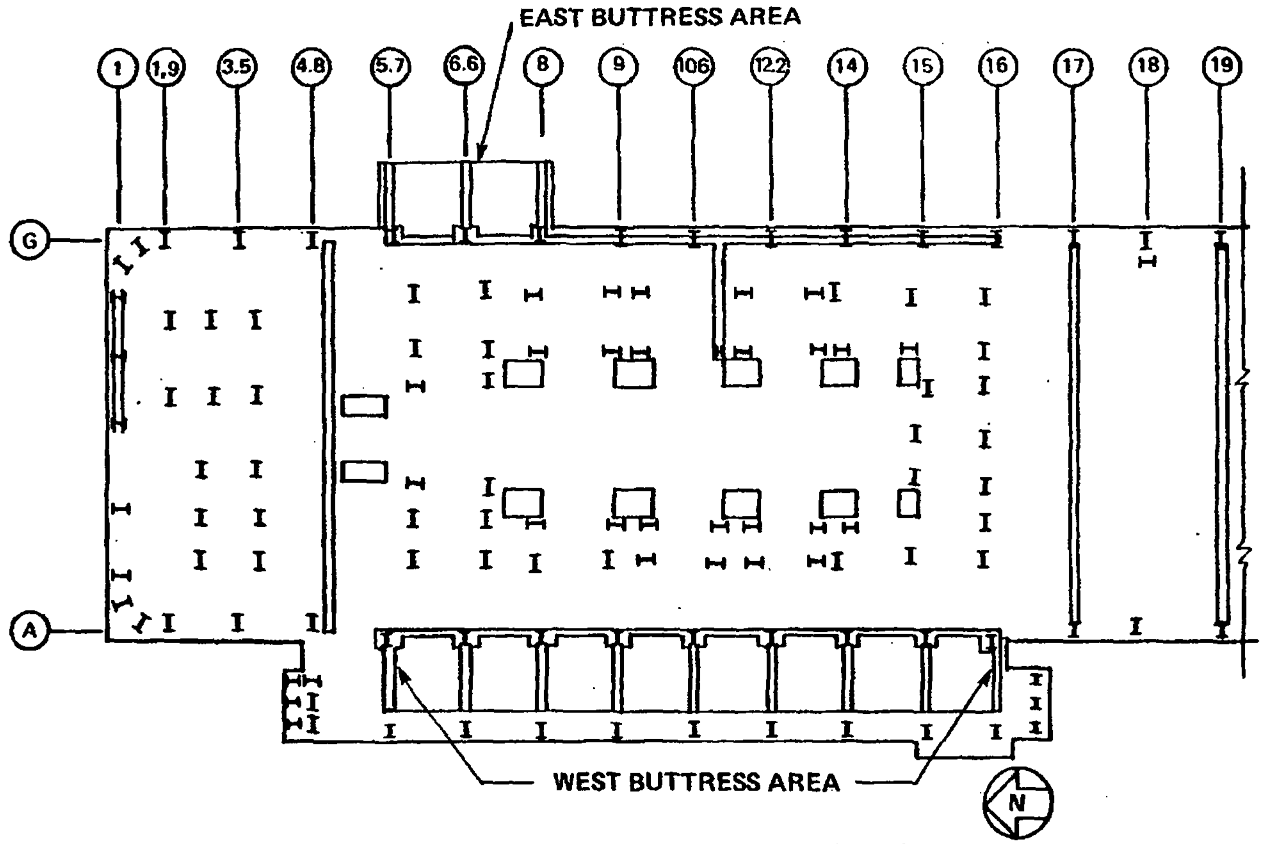

FSAR UPDATE

UNITS 1 AND 2
DIABLO CANYON SITE

FIGURE 3.8-66

TURBINE BUILDING
PLAN AT EL. 85'

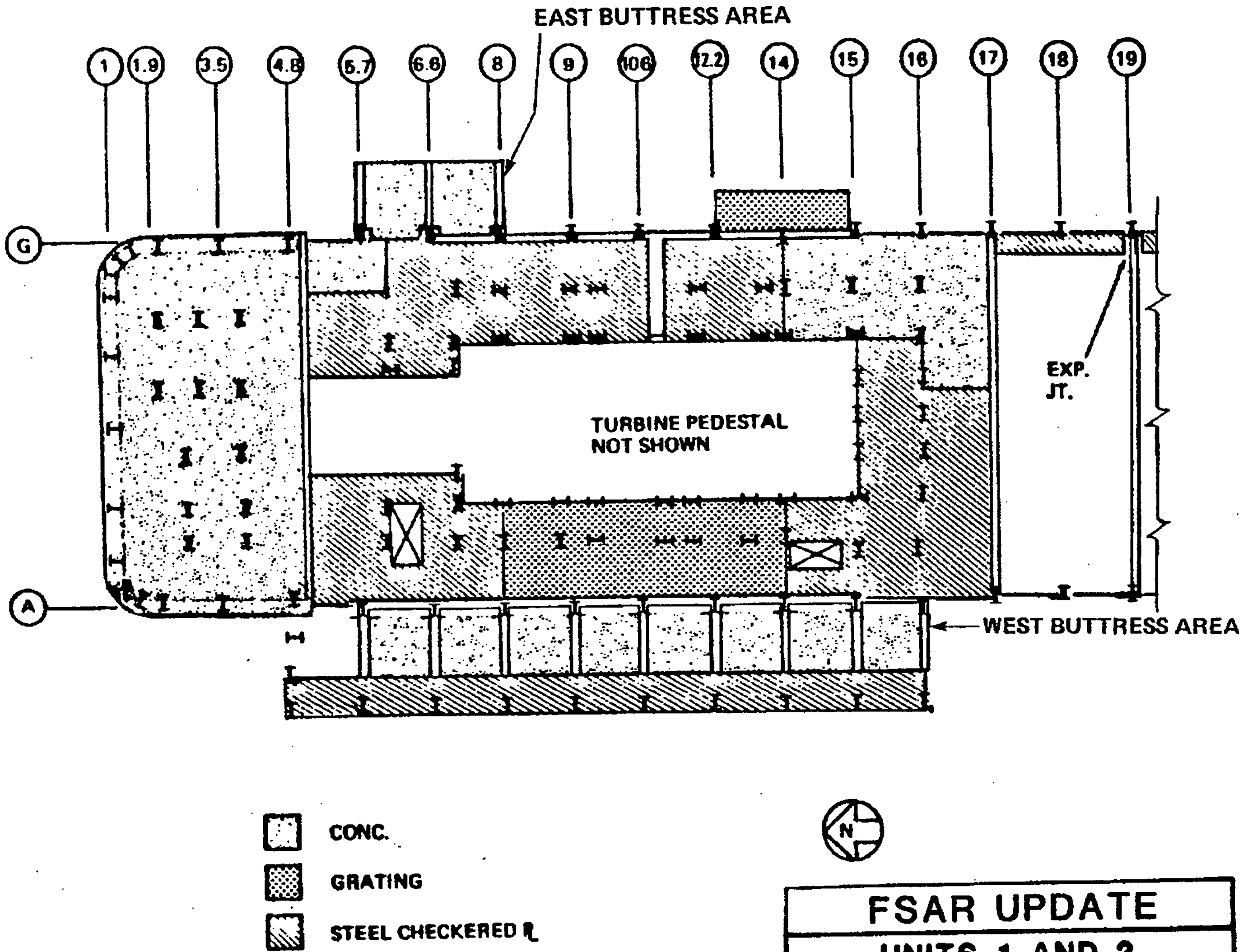

FSAR UPDATE

UNITS 1 AND 2
DIABLO CANYON SITE

FIGURE 3.8–67

TURBINE BUILDING
PLAN AT EL. 104'

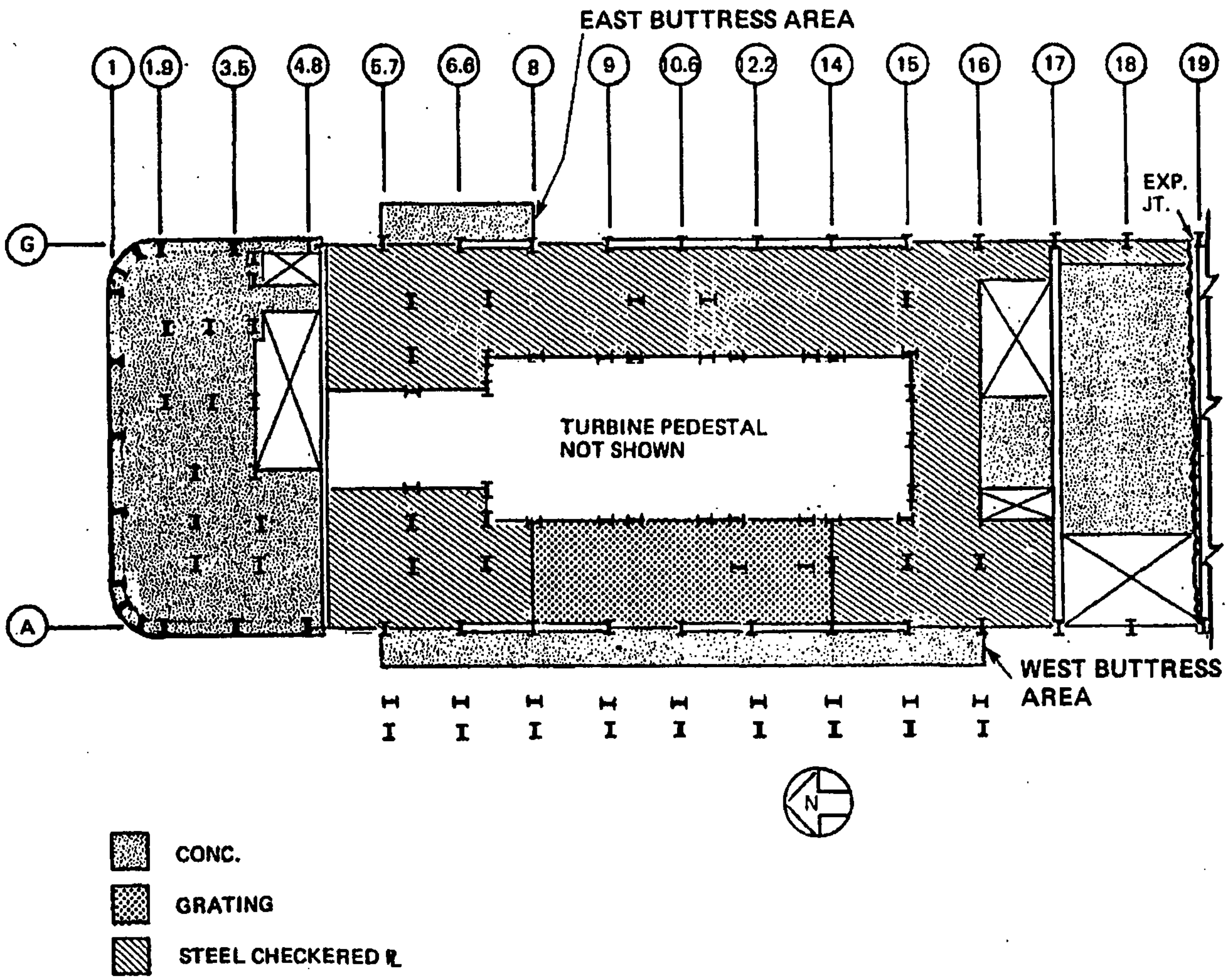

FSAR UPDATE
UNITS 1 AND 2 DIABLO CANYON SITE
FIGURE 3.8–68 TURBINE BUILDING PLAN AT EL. 119'

Revision 11 November 1996

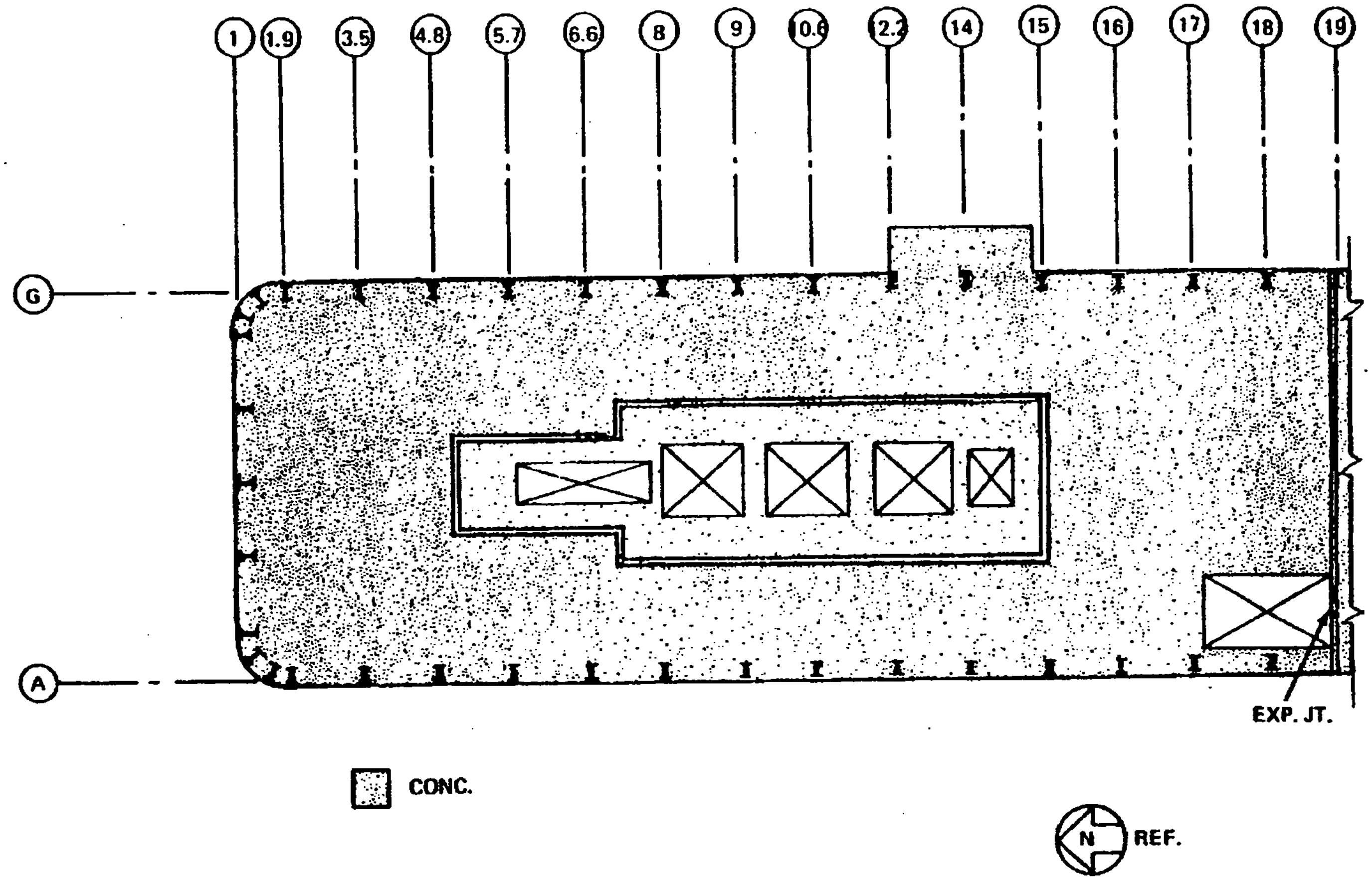

FSAR UPDATE

UNITS 1 AND 2
DIABLO CANYON SITE

FIGURE 3.8–69

TURBINE BUILDING
PLAN AT EL. 140'

Revision 11 November 1996

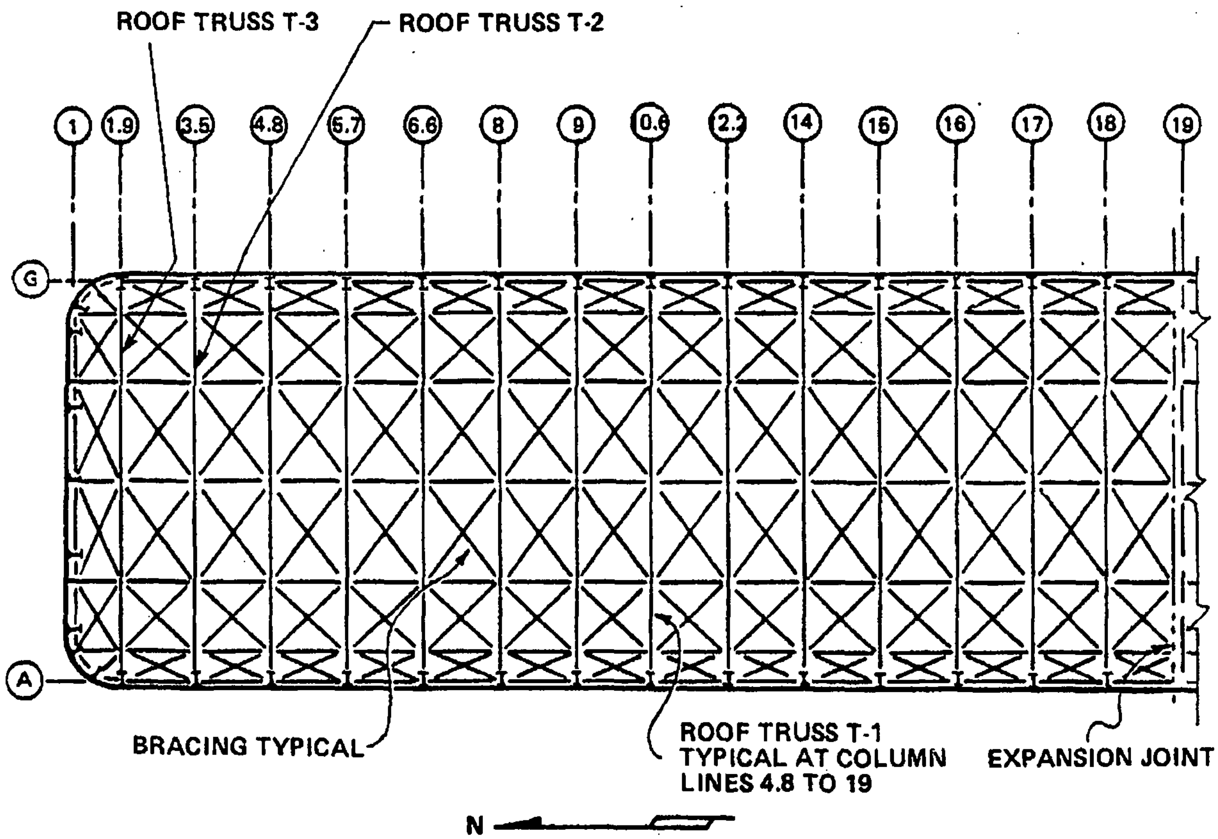

FSAR UPDATE

UNITS 1 AND 2
DIABLO CANYON SITE

FIGURE 3.8–70

TURBINE BUILDING
PLAN AT LOWER CHORD OF
ROOF TRUSS

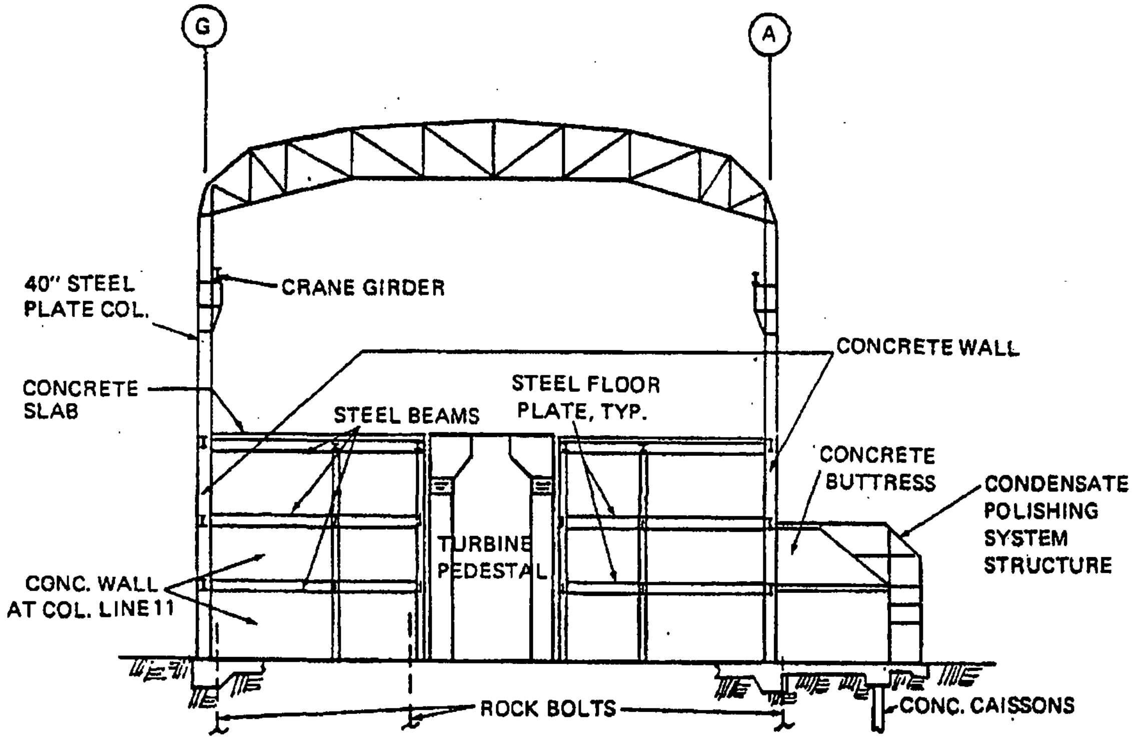

FSAR UPDATE

UNITS 1 AND 2
DIABLO CANYON SITE

FIGURE 3.8–71

TURBINE BUILDING
TYPICAL SECTION

Revision 11 November 1996

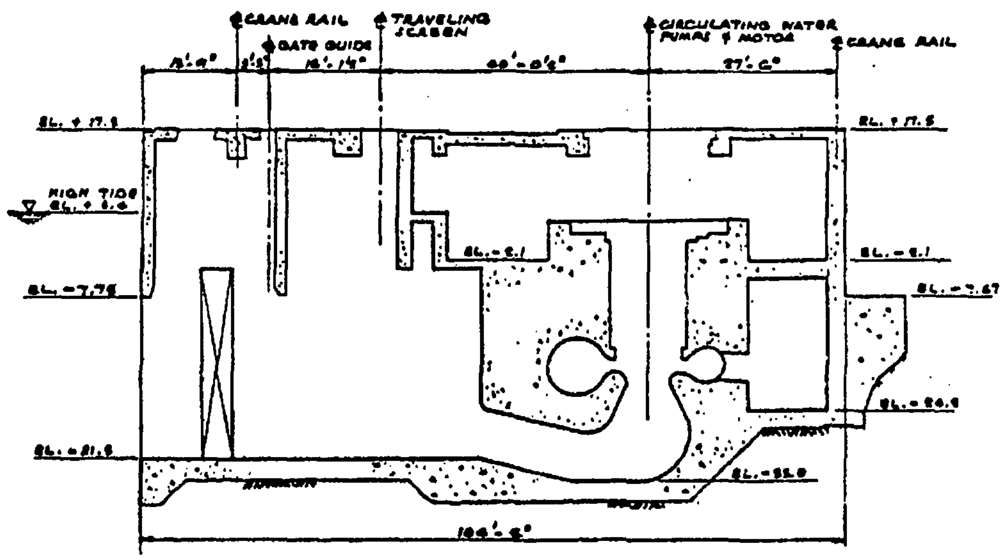

FSAR UPDATE

UNITS 1 AND 2 DIABLO CANYON SITE

FIGURE 3.8–75

INTAKE STRUCTURE TRANSVERSE SECTION A

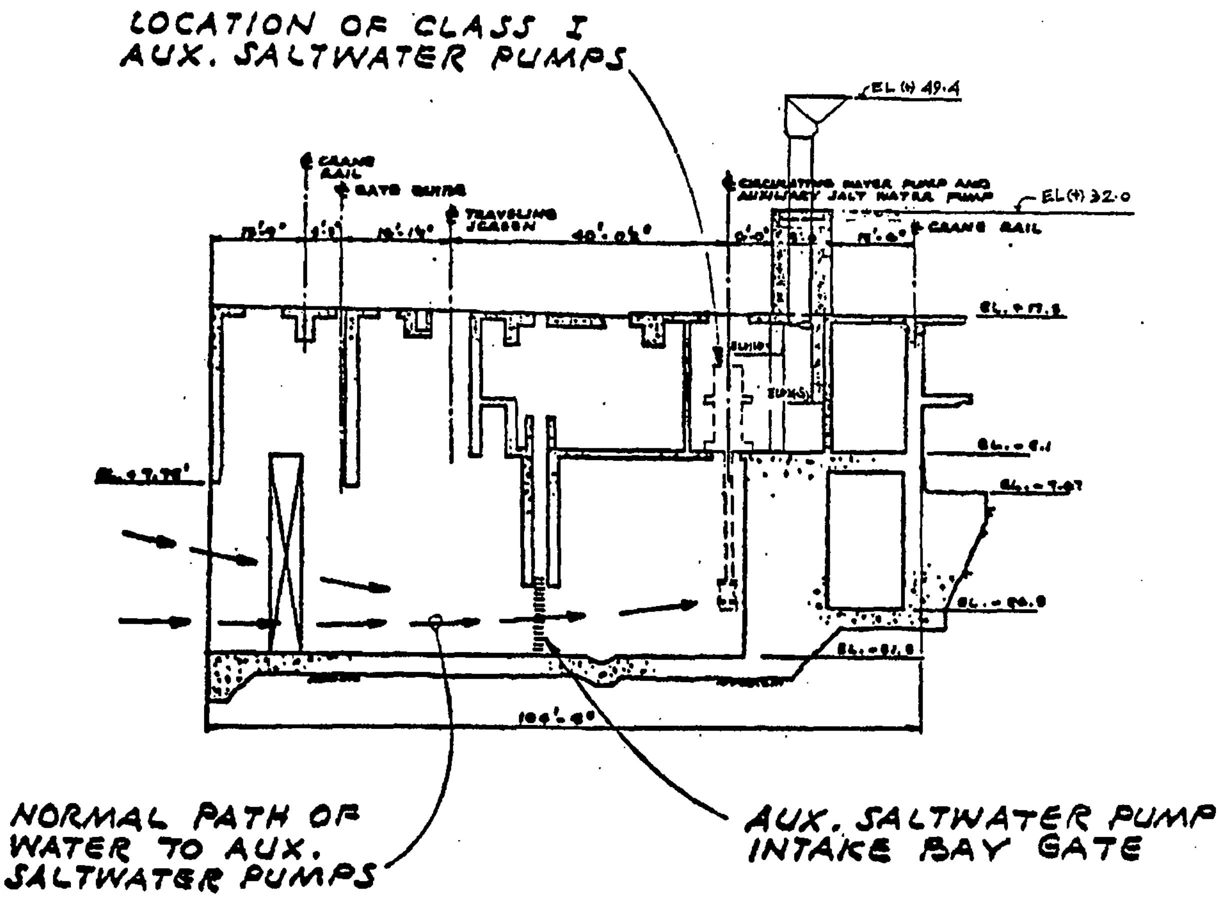

FSAR UPDATE

UNITS 1 AND 2
DIABLO CANYON SITE

FIGURE 3.8-76
INTAKE STRUCTURE
TRANSVERSE SECTION B

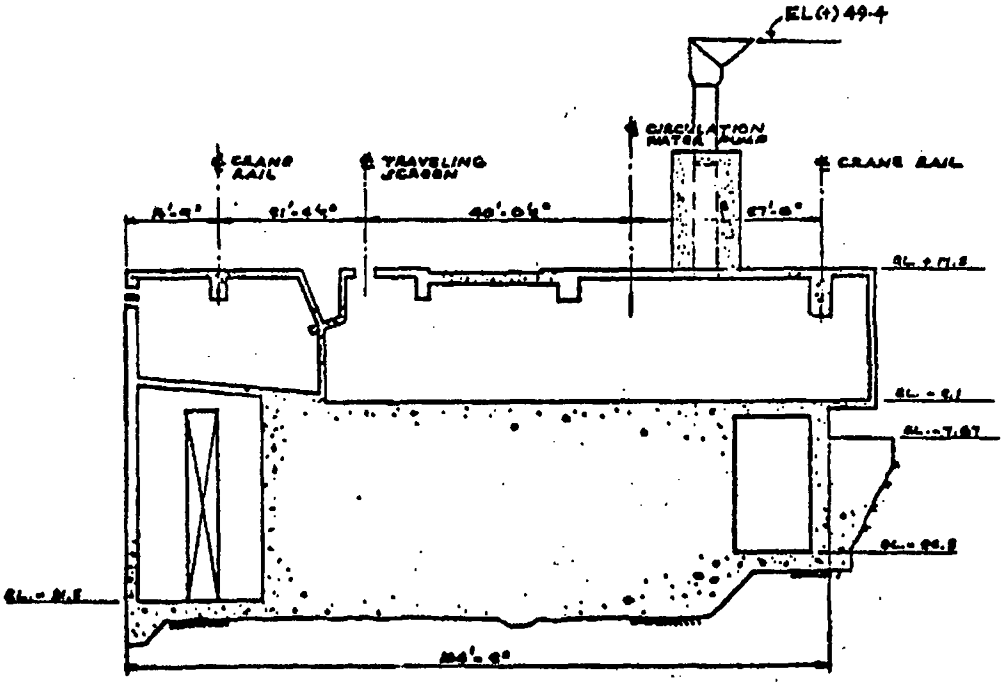

FSAR UPDATE

UNITS 1 AND 2
DIABLO CANYON SITE

FIGURE 3.8–77

INTAKE STRUCTURE
TRANSVERSE SECTION C

Revision 11 November 1996

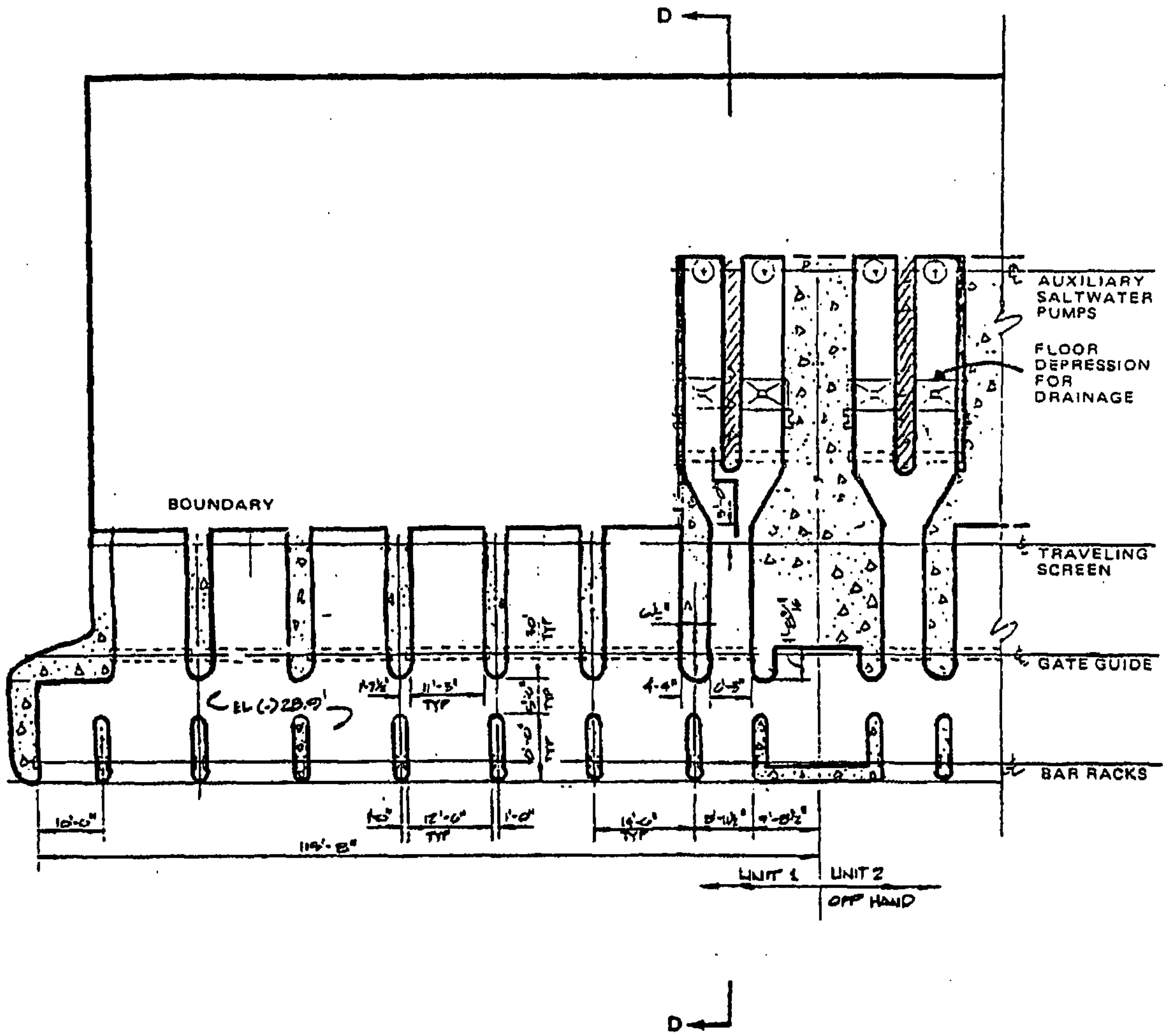

FSAR UPDATE

UNITS 1 AND 2
DIABLO CANYON SITE

FIGURE 3.8–78

INTAKE STRUCTURE
WAVE SCALE MODEL
PLAN-INVERT (UNIT 1)
NTS

Revision 11 November 1996

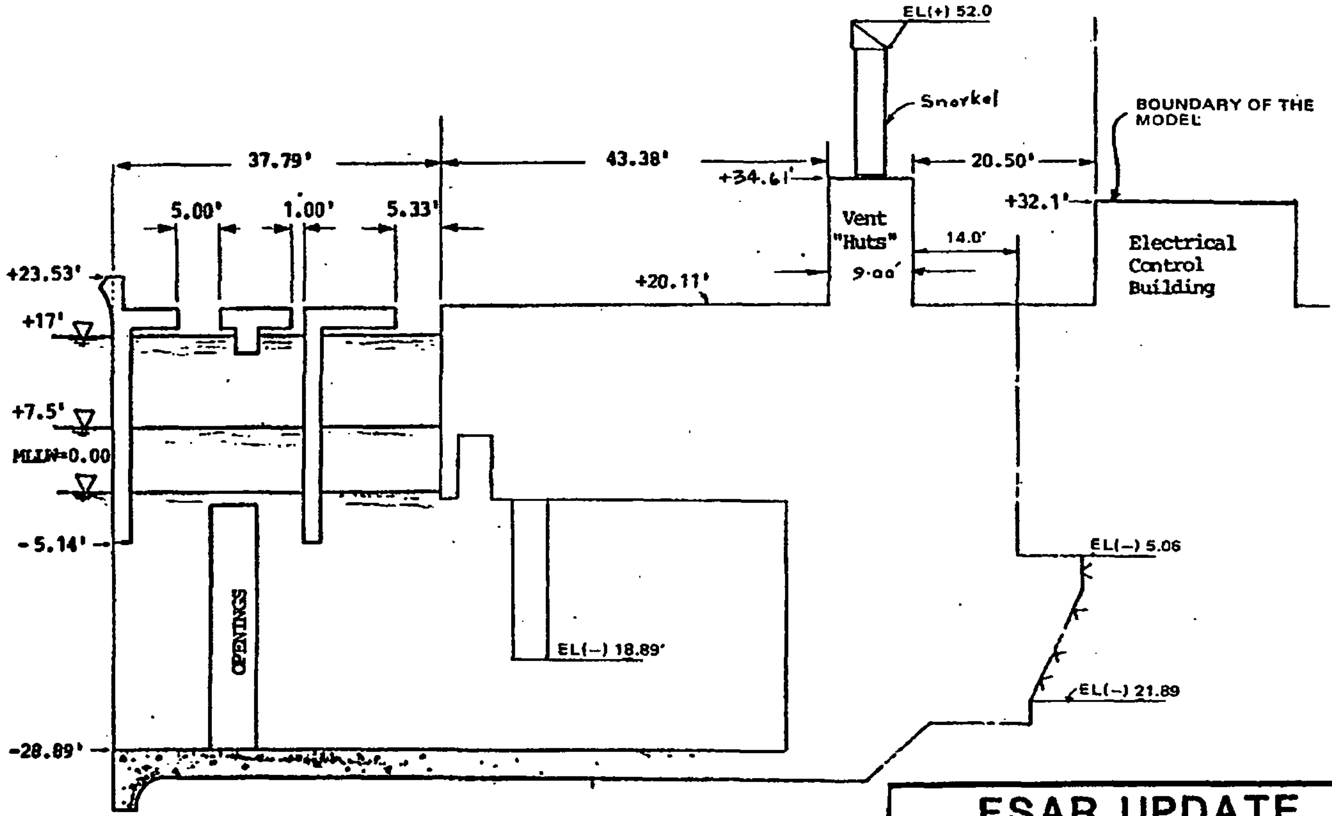

NOTE: (All Elevations Refer to Mean Lower Low Water Datum)

FSAR UPDATE

UNITS 1 AND 2
DIABLO CANYON SITE

FIGURE 3.8–79

INTAKE STRUCTURE
WAVE SCALE MODEL
TRANSVERSE SECTION D

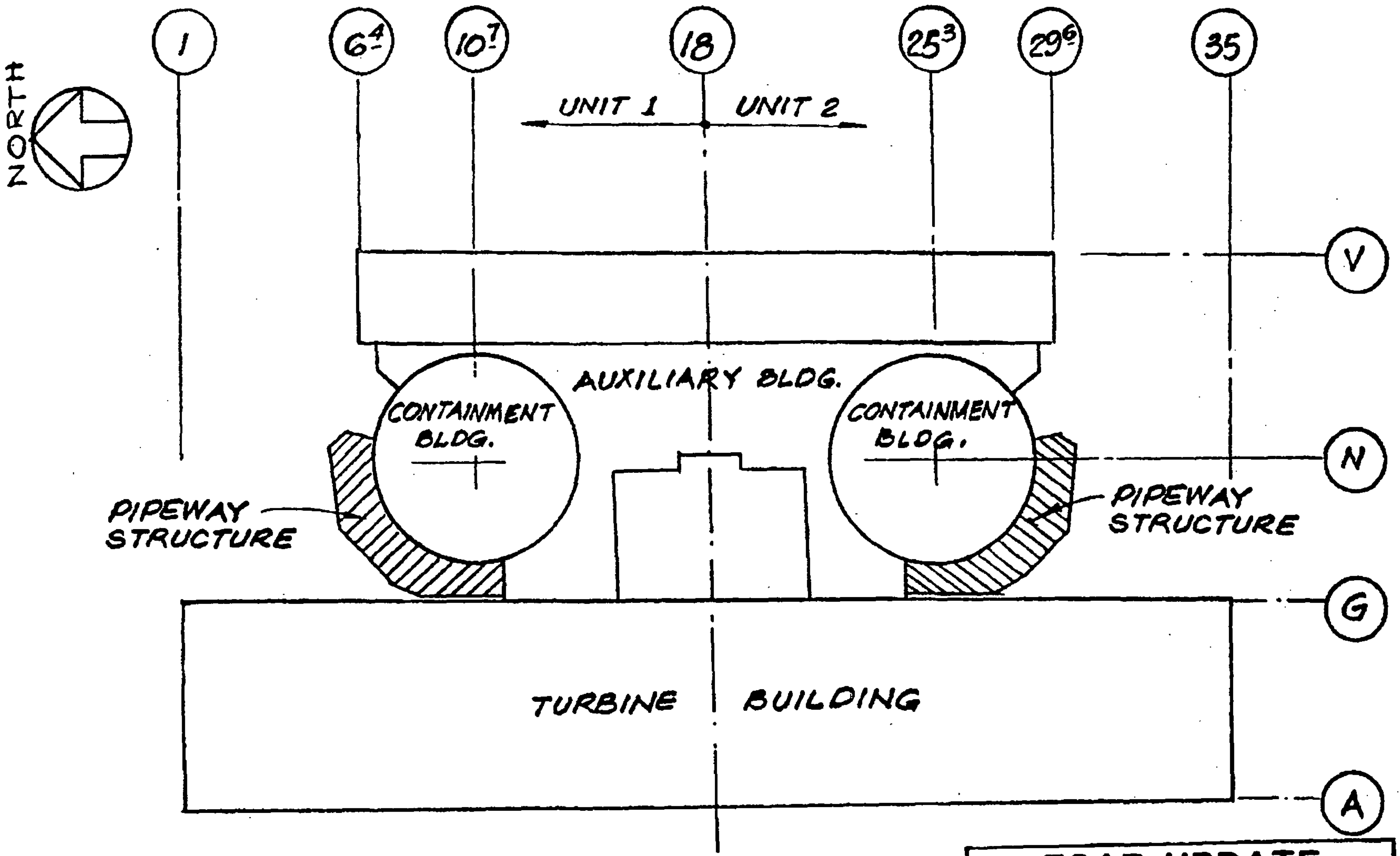

FSAR UPDATE

UNITS 1 AND 2 DIABLO CANYON SITE

FIGURE 3.8–80
PIPEWAY STRUCTURE LAYOUT

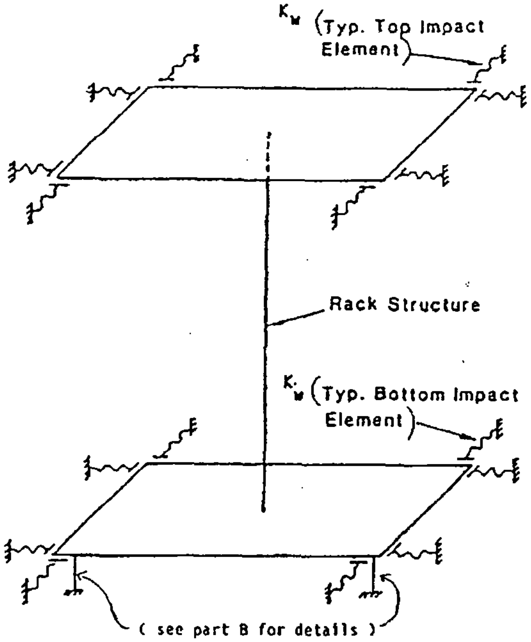

Part A. Three-Dimensional Representation of Rack Dynamic Model

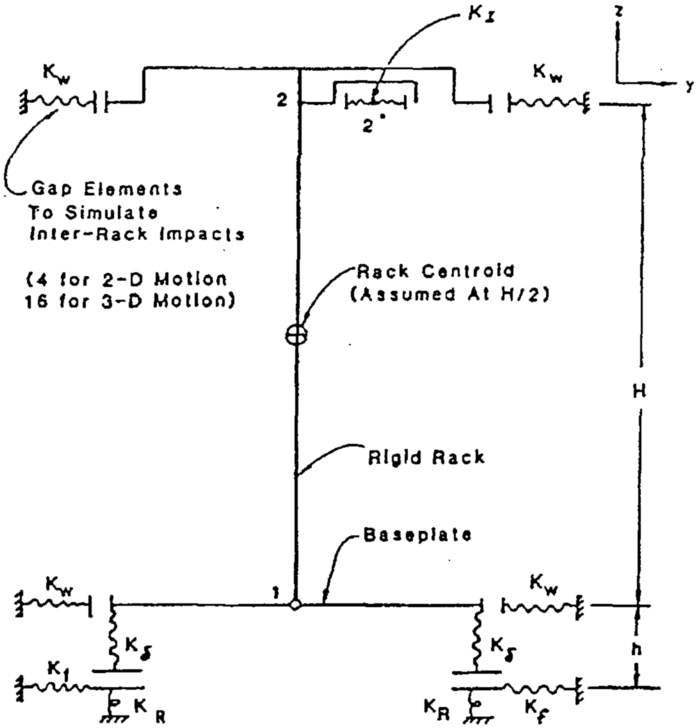

Part B. Two-Dimensional Representation of Rack Dynamic Model

FSAR UPDATE
UNITS 1 AND 2 DIABLO CANYON SITE
Figure 3.8-81. Rack Dynamic Model

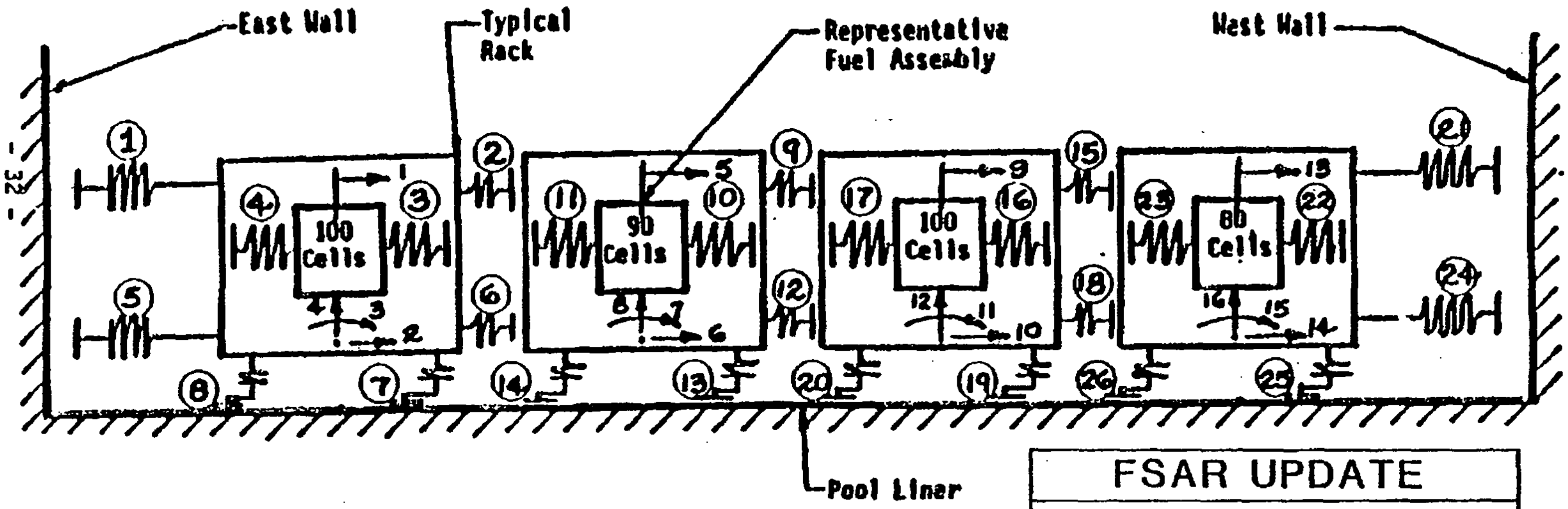

- 32 -

FSAR UPDATE

UNITS 1 AND 2
DIABLO CANYON SITE

Figure 3.8-82.

MULTI-RACK MODEL

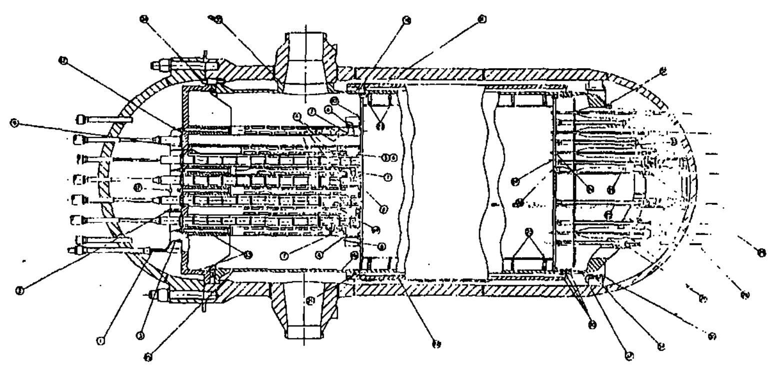

	FEATURES TO BE EXAMINED	COMMENTS AND OBSERVATIONS BEFORE FUNCTIONAL TEST
1	THERMOCOUPLE CONDUIT CLAMPS INSIDE THE THERMOCOUPLE COLUMN	
2	CLAMP ARRANGEMENTS AT THE MOUNTING BRACKET LOCATIONS.	
3	[illegible]	
4	ACCESSIBLE [illegible] CONDUIT CLAMPS INSIDE THE UPPER SUPPORT COLUMNS.	
5	ACCESSIBLE WELD JOINTS AT THE THERMOCOUPLE [illegible] INSTRUMENTED COLUMNS	
6	WELD JOINTS ON ACCESSIBLE SUPPORT COLUMN [illegible] (THERMOCOUPLE SUPPORT HARDWARE)	
7	[illegible] AT ACCESSIBLE LOCATIONS [illegible] SUPPORT COLUMNS [illegible]	
8	[illegible] OF THE ACCESSIBLE PROTRUDING THERMOCOUPLE TIPS	
9	THERMOCOUPLE COLUMN AND GUIDE TUBE SCREW LOCKING DEVICES.	
10	ACCESSIBLE SUPPORT COLUMN [illegible] PLATE, AND CORE PLATE [illegible] DEVICES.	
11	UPPER CORE PLATE INSERTS.	
12	CONDUIT CONNECTOR FITTINGS AND CROSS RUN CLAMP ARRANGEMENTS.	
13	[illegible] OUTER HOLLOW ROUNDS	
14	ACCESSIBLE GUIDE TUBE WELDS.	
15	UPPER BARREL TO FLANGE GIRTH WELD	
16	UPPER BARREL TO LOWER BARREL GIRTH WELD	
17	LOWER BARREL TO CORE SUPPORT GIRTH WELD	
18	UPPER CORE PLATE ALIGNING PIN WELDS AND BEARING SURFACES	
19	OUTLET NOZZLE INTERFACE SURFACE CONDITION.	
20	THERMAL SHIELD [illegible] TO BARREL, AND WELD TO THE THERMAL SHIELD [illegible]	
21	THERMAL SHIELD INTERFACE AT THE [illegible]	
22	IRRADIATION SPECIMEN BASKET WELDS.	
23	BAFFLE ASSEMBLY SCREW LOCKING ARRANGEMENTS AT THE TOP AND THE BOTTOM FORMER ELEVATIONS.	
24	CORE SUPPORT COLUMN TO LOWER CORE PLATE SCREW LOCKING DEVICES, ON RANDOMLY CHOSEN [illegible]	
25	CORE SUPPORT COLUMN [illegible] ACCESS.	
26	ACCESSIBLE (?) INSTRUMENTATION GUIDE COLUMN LOCKING COLLARS NEAREST THE [illegible]	
27	LOCKING DEVICES OF THE BOTTOM INSTRUMENTATION GUIDE COLUMNS.	
28	LOCKING DEVICES ON THE SECONDARY CORE SUPPORT.	
29	ACCESSIBLE LOCKING DEVICES OF THE [illegible] INSTRUMENTATION COLUMN [illegible]	
30	RADIAL SUPPORT KEY LOCKING ARRANGEMENTS AND BEARING SURFACES.	
31	HEAD AND VESSEL ALIGNING PIN SCREW LOCKING DEVICES AND BEARING SURFACES	
32	CONTACT AT INTERFACE OF THE ACCESSIBLE INSTRUMENTATION GUIDE COLUMNS.	
33	CONTACT AT INTERFACE OF THE ACCESSIBLE CORE SUPPORT COLUMN [illegible]	
34	VESSEL CLEVIS LOCKING ARRANGEMENTS AND BEARING SURFACES	
35	VESSEL NOZZLE INTERFACE SURFACE CONDITION	

FSAR UPDATE

UNIT 1
DIABLO CANYON SITE

FIGURE 3.9-1
VIBRATION CHECKOUT - FUNCTIONAL
TEST INSPECTION DATA

Revision 11 November 1996

3.9 MECHANICAL SYSTEMS AND COMPONENTS

3.9.1 DYNAMIC SYSTEM ANALYSIS AND TESTING

A mechanical design description of the internals and core components showing the differences and similarities between the two DCPP units is presented in Section 4.2.2. The dynamic analysis techniques and methods used to determine and confirm the dynamic response of the reactor internals are presented in the following section. Detailed information of the dynamic system analysis and testing is presented in the reports listed in Section 3.9.6. Chapter 14 describes the plant initial tests and operation.

A description of the analyses used in the design of safety-related mechanical equipment, such as pumps and heat exchangers, to withstand the DE, DDE, and HE seismic loadings is provided in Section 3.7.

3.9.1.1 Vibration Operational Test Programs

This section describes the nature of flow-induced vibrations in the reactor coolant loops and the analyses performed to ensure such vibrations are at an acceptable level.

3.9.1.1.1 Main Piping System, Flow-Induced Vibration

Pressure pulses, from the reactor coolant pump impeller are prevented from resulting in flow-induced vibrations in the main piping systems of the RCL. The reactor coolant pump perturbing frequency is quite high when compared to the piping natural frequency. Frequency separation, therefore, ensures a very small probability of self-excited or sympathetic vibration.

3.9.1.1.2 Reactor Internals Flow-Induced Vibration

The dynamic behavior of reactor components has been studied using experimental data obtained from operating reactors along with results of model tests and static and dynamic tests. The following procedures have been performed in the study of thermal shield vibration:

(1) During a test program performed with a 1/7th-scale model, the natural frequencies of the thermal shield in water and the maximum vibration amplitude were measured.

(2) Shaker test programs performed on a prototype thermal shield with the actual boundary conditions provided full-scale natural frequencies and mode shapes in air. These modes were established by measuring accelerations at the center, top (support elevation), and bottom of the shield. In Figure 3.9-3, the results obtained are plotted for n = 4 and correspond to a thermal shield with eight supports which are indicated on

8/8

the same figure. The amplitudes of vibration are fitted with a curve y = A sin 4*q*.

(3) Maximum displacements were measured during the preoperational reactor test and were correlated with the information obtained in the 1/7th-scale model and shaker test.

(4) In Figure 3.9-4, the maximum amplitudes of vibration are plotted as measured on a thermal shield with six supports. The experimental points have been least-square fitted with a curve y = A sin 3*q*.

In general, the study follows two parallel procedures. Frequencies and spring constants are derived analytically, and these values are confirmed from the results of the tests. Damping coefficients are established experimentally, and forcing functions are estimated from pressure fluctuations measured during operation and in models. In parallel, the responses of important reactor structures were measured during preoperational reactor tests and the frequencies and mode shapes of the structures obtained. Once all the dynamic parameters were obtained as explained above, the forcing functions could be estimated. Internals behavior during reactor operation is measured using mechanical devices and nuclear noise methods.

Some components, such as control rod guide tubes, fuel rods, and incore instrumentation tubes are subjected to cross flow and parallel flow with respect to the axis of the structure. For both cases, cross and parallel, the response is obtained after the forcing function and the damping of the system are determined.

3.9.1.1.3 Vibration Monitoring

Since internals of four loop reactors are designed and manufactured to essentially the same procedures, processes, and similar drawings, the response of these structures is similar. Performance data from the instrumentation of actual reactors, as well as mechanical and flow scale models, are available (References 2, 4, and 5). The pre- and post-operational flow test examinations of the Indian Point II Plant internals, the four loop prototype plant, have been completed indicating that all the components performed as predicted. No evidence or sign of damage or incipient failure was found.

The testing programs consisted of measurements of the stresses, deflections, and responses of selected key points in the internals structures during hot functional and low power physics tests. The main purpose of this testing program was to ensure that no unexpected large amplitudes of vibration existed in the internals structure during operation. The tests were extended to provide data and results on what were assumed to be indicators of overall core support structure performance and to verify particular stress and deflection quantities.

3.9.1.1.4 Loose-Parts Monitoring

A loose-parts monitoring system is provided for early detection of possible loose parts in the RCS, in order to reduce the probability of loose parts causing damage to RCS components. This system is described in Section 4.4.5.

3.9.1.2 Dynamic Testing Procedure

During startup functional testing, piping, including supports and restraints, of certain systems was observed carefully by experienced startup personnel. At selected points of calculated maximum movement, visual inspection and/or measurements were taken and compared with those calculated to establish that stress limits are not exceeded.

If vibration was noted to cause piping or supports movements beyond those allowed, corrective action in the form of additional or redesigned supports, snubbers, etc. was taken and the system was retested to determine that vibrations have been reduced to an acceptable level. Stress analysis on the system was rerun if deemed necessary by the designer. The systems and transients included in this program are listed below:

(1) Reactor coolant pumps start

(2) Reactor coolant pumps trip

(3) Main steam turbine stop valves trip

(4) Steam dump to condenser valves open

(5) Main steam safety and relief valves lift and blowdown

(6) Pressurizer relief valves lift and blow down (Unit 1 only)

(7) Auxiliary feedwater pump turbine stop valve trip

(8) Charging pumps start and trip

(9) Safety injection pumps start and trip

(10) Residual heat removal (RHR) pumps start and trip

(11) Containment spray pumps start and trip

(12) Accumulators discharge to loops

(13) Pressurizer spray valves open and trip closed

(14) Pressurizer power relief valves open

Locations of observation points for piping movements for preoperational piping vibration tests for the above systems were determined from dynamic analysis performed on the piping systems, with system stiffness and restraint locations taken into account. Observed deflections were compared with code allowable values.

3.9.1.3 Dynamic System Analysis Methods for Reactor Internals

To verify structural adequacy of reactor internal components and the reactor core for Diablo Canyon Units, nonlinear LOCA and seismic dynamic analyses are performed. These dynamic analyses are performed for both LOCA cold and hot leg breaks, as well as for seismic excitations of DDE, Hosgri (HE), and Long Term Seismic Program (LTSP).

For faulted conditions, the response of reactor internals due to DDE and LOCA conditions are additive by the SRSS (Square Root of the Sum of Squares) method. An HE or LTSP and LOCA are also considered to occur simultaneously and, therefore, the combined response is considered by SRSS. The methods and techniques for these dynamic analyses are described below.

3.9.1.3.1 LOCA (Loss-Of-Coolant-Accident) Analysis

Details of the RPV system finite element model which is used in these analyses are described. Results of these analyses consist of the nodal time history displacements and the interface impact loads on the reactor vessel, reactor internals and the core. The time history displacements of all major components such as reactor vessel head, vessel bottom and the vessel/barrel nozzles are also generated for their later use in the component stress analyses.

The RPV system finite element model consists of three concentric structural submodels connected by nonlinear impact elements and linear stiffness matrices. The first sub-model represents the reactor vessel shell and its associated components. The reactor vessel is restrained by four reactor vessel supports (situated beneath alternate nozzles) and the attached primary coolant piping.

The second sub-model represents the reactor core barrel, thermal shield, lower support plate, tie plates, and the secondary support components for Unit 1, whereas, for Unit 2 the second sub-model is identical to that of unit 1 except that it has core barrel with neutron pads instead of thermal shield.

These sub-models are physically located inside the first, and are connected to them by stiffness matrices at the internals support ledges. The core barrel to the reactor vessel shell impact is represented by nonlinear elements at the core barrel flange, upper support plate flange, core barrel outlet nozzles, and the lower radial restraints. In addition, vertical impact loads on the fuel assembly top and bottom nozzles.

The third and innermost sub-model represents the upper support plate assembly consisting of guide tubes, upper support columns, upper and lower core plates, and fuel. The third sub-model is connected to the first and second by stiffness matrices and nonlinear elements. The fluid-solid interactions in the LOCA analysis are accounted for through the hydraulic forcing functions generated by Multiflex Code (Reference 3).

The WECAN computer code, which is used to determine the response of the reactor vessel and its internals, is a general purpose finite element code. In the finite element approach, the structure is divided into a finite number of discrete members or elements. The inertia and stiffness matrices, as well as the force array, are first calculated for each element in the local coordinates. Employing appropriate transformations, the element global matrices and arrays are assembled into global structural matrices and arrays, and used for dynamic solution of the differential equation of motion for the structure.

The WECAN Code solves equations of motion using the nonlinear modal superposition theory. Initial computer runs such as dead weight analysis and the vibration (modal) analyses are made to set the initial vertical interface gaps and to calculate eigen values and eigenvectors. The modal analysis information is stored on magnetic tapes, and is used in a subsequent computer run which solves equations of motion. The first time step performs the static solution of equations to determine steady state solution under normal operating hydraulic forces. After the initial time step, WECAN calculates the dynamic solution of equations of motion, nodal displacements, and impact forces, which are stored on tape for post-processing.

Reactor internals response to both cold and hot leg pipe ruptures was analyzed. The LOCA hydraulic forcing functions used in the RPV system analyses were obtained for hypothetical breaks considered in the main loop line. However, with the acceptance of DCPP Leak-Before-Break (LBB) by USNRC (Reference 14), the dynamic effects of breaks in the main reactor coolant loop no longer have to be considered in the design basis of analyses. Only the next most limiting breaks in auxiliary lines have to be considered.

Note that the preceding paragraphs describe the RPV and internals system dynamic analyses for which the WECAN computer code was used. Current analyses (such as the dynamic analyses performed in support of the replacement reactor vessel head project) utilize the ANSYS computer code. The methodology used to develop the ANSYS system models is consistent with the methodology used to develop historic WECAN models. The direct time integration method is used in ANSYS to solve the dynamic equations of motion for the system; whereas the nonlinear mode superposition method is used in WECAN to solve the dynamic equations of motion for the system.

The breaks considered for the replacement vessel head project included: (1) the accumulator line; (2) the pressurizer surge line; and (3) the residual heat removal line.

3.9.1.3.2 Reactor Internals Components Subjected to Horizontal Excitations

The analysis methodology is summarized below for components that are subject to horizontal excitations during LOCA conditions. The components include the core barrel, guide tubes, and upper support columns. It should be noted that with the acceptance of DCPP Leak-Before-Break (Reference 14), the dynamic effects of the main reactor coolant loop piping no longer have to be considered in the design basis analysis. Only the dynamic effects of the next most limiting breaks of auxiliary lines need to be considered; and consequently the components will experience considerably less load than those from the main loop line breaks.

3.9.1.3.2.1 Core Barrel

For the hydraulic analysis of the pressure transients during hot leg blowdown, the maximum pressure drop across the barrel is a uniform radial compressive impulse. The barrel was analyzed for dynamic buckling using the following conservative assumptions:

(1) The effect of the fluid environment is neglected (water stiffening is not considered).

(2) The shell is treated as simply supported.

During cold leg blowdown, the upper barrel is subjected to a nonaxisymmetric expansion radial impulse that changes as the rarefaction wave propagates both around the barrel and down the outer flow annulus between vessel and barrel. The analysis of transverse barrel response to cold leg blowdown was performed as follows:

(1) The upper core barrel was treated as a simply supported cylindrical shell of constant thickness between the upper flange weldment and the lower core barrel weldment. No credit was taken for the supports at the barrel midspan offered by the outlet nozzles. This assumption leads to conservative deflection estimates of the upper core barrel.

(2) The upper core barrel was analyzed as a shell with four variable sections to model the support flange, upper core barrel, reduced girth weld section, and a portion of the lower core barrel.

(3) The barrel with the core and neutron shield panels[a] was analyzed as a beam elastically supported at the lower radial support, and the dynamic response obtained.

While the above described blowdown analyses were performed in the original analysis, with the acceptance of the DCPP leak-before-break analysis by the NRC (Reference 14), dynamic loads resulting from pipe rupture events in the main reactor coolant loop piping

[a] Neutron shield panels on Unit 2 only.

no longer have to be considered in the design basis structural analyses. Only the much smaller loads from RCS branch line breaks have to be considered.

3.9.1.3.2.2 Guide Tubes

The dynamic loads on rod cluster control guide tubes are more severe for a LOCA caused by hot leg rupture than for an accident by cold leg over the rod cluster control guide tubes. Thus, the analysis was performed only for a hot leg blowdown.

The guide tubes in closest proximity to the ruptured outlet nozzle are the most severely loaded. The transverse guide tube forces during the hot leg blowdown decrease with increasing distance from the ruptured nozzle location.
A detailed structural analysis of the rod cluster control guide tubes was performed to establish the equivalent cross section properties and elastic end support conditions. An analytical model was verified both dynamically and statically by subjecting the control rod cluster tube to a concentrated force applied at the transition plate. In addition, the guide tube was loaded experimentally using a load distribution to conservatively approximate the hydraulic loading. The experimental results consist of a load deflection curve for the rod cluster control guide tube, plus verification of the deflection criteria to ensure rod cluster control insertion.

While the above described blowdown analyses were performed in the original analysis, with the acceptance of the DCPP leak-before-break analysis by the NRC (Reference 14), dynamic loads resulting from pipe rupture events in the main reactor coolant loop piping no longer have to be considered in the design basis structural analyses. Only the much smaller loads from RCS branch line breaks have to be considered.

3.9.1.3.2.3 Upper Support Column

Upper support columns located close to the broken nozzle during the hot leg break will be subjected to transverse loads due to cross flow. The loads applied to the columns were computed with a method similar to the one used for the guide tubes, i.e., by taking into consideration the increase in flow across the column during the accident. The columns were studied as beams with variable sections and the resulting stresses were obtained using the reduced section modulus at the slotted portions. The models used for static (or steady-state dynamic) analysis are:

- The upper support, deep beam, and upper core plate were modeled with flat shell elements, the support columns with three-dimensional beam elements, and the fuel assemblies and holddown springs with three-dimensional spring elements. Because of symmetry, a one-eighth slice of the upper package was modeled. The core plate is perforated and was modeled as a geometrically equivalent solid plate that has elastic constants modified according to the theory of perforated plates.

- Columns of two different lengths were modeled: the long columns connecting the plates and the short columns connecting the beam grid with the upper core plate.

- The lower support structure was modeled using a finite-element structural analysis computer program. The lower core plate and upper core support, as well as the lower part of the core barrel, was represented by flat triangular shell elements. Reduced plate strength, due to the perforations, was accounted for by using an equivalent elastic modulus and Poisson ratio in the calculations. This structure was loaded with various vertical forces, due to normal and abnormal operation, and the deflections and stresses are obtained for each case. The experimental values were converted according to basic scaling laws and applied to the prototype structure. The test values are larger, as expected, since they are obtained in the absence of the core plate and support columns structures, making the lower core support more flexible. Using the same model, this code was also used to compute stresses and deformation due to nonuniform temperature distributions. With temperature at the component surfaces and the gradient generated by the γ-heat generation as input for the system code, the deflected shape of the structure was obtained.

Stresses in components, such as the perforated upper and lower core plates, core support plate, and top support plate, were then computed using the stress intensification factor provided by the standard theory of perforated plates.

3.9.1.4 Correlation of Test and Analytical Results

The program used to establish the integrity of reactor internals has involved extensive design analysis, model testing, and post-hot functional inspection. Additionally, a full-size reactor has been instrumented to measure the dynamic behavior of a plant the size and type of DCPP. Measured values have been compared to predicted values.

The Indian Point II reactor has been established as the prototype for the DCPP Unit 1 internals verification program. The Trojan plant (Portland General Electric Company) provides additional internals verification for Unit 2. (Unit 1 has a thermal shield similar to Indian Point II; Unit 2 has neutron panels similar to Trojan.)

The only significant differences between the DCPP units' internals and Indian Point II are the modifications resulting from the use of a 17 x 17 fuel array in place of 15 x 15, and the replacement of the annular thermal shield with neutron shield panels. The change to neutron shield panels applies only to Unit 2. The change to 17 x 17 applies to both Units 1 and 2.

The only structural changes in the internals resulting from the design change from the 15 x 15 to the 17 x 17 fuel assembly are in the support columns and assembly guide tubes. The new 17 x 17 guide tubes are stronger and more rigid, hence they are less susceptible to flow-induced vibration problems. The fuel assembly itself is relatively unchanged in mass and spring rate, and thus no significant deviation is expected from the 15 x 15 fuel assembly vibration characteristics.

The remainder of the core structure design is identical to the prototypes that have been tested and proven to be well within design expectations and limits.

The Trojan plant is the lead plant featuring neutron panels and 17 x 17 fuel assemblies.

The Trojan plant internals were instrumented for strain measurements on the core barrel and on the guide tube subject to highest cross flow. The data obtained provided verification of Westinghouse analysis and scale model predictions of neutron panels and 17 x 17 internals behavior in a full-size plant.

The Four Loop Internals Assurance Program conducted on Indian Point II, supplemented by the Trojan data on neutron shield panels and 17 x 17 fuel assemblies, jointly satisfy the intent of RG 1.20 (Reference 12) with respect to adequate plant testing of internals similar to those employed at DCPP. The core support structures received, in addition, the normal pre- and post-hot functional testing examination for integrity in accordance with Paragraph D, "Regulations for Reactor Internals Similar to the Prototype Design," of RG 1.20. This examination included the points shown in Figure 3.9-1 for Unit 1 and Figure 3.9-2 for Unit 2, and also:

(1) All major load bearing elements of the reactor internals relied on to retain the core structure in place

(2) The lateral, vertical, and torsional restraints provided within the vessel

(3) Those locking and bolting devices whose failure could adversely affect the structural integrity of the internals

(4) Those other locations on the reactor internal components that are similar to those which were examined on the prototype Indian Point II and Trojan designs

The interior of the reactor vessel was also examined for evidence of loose parts or foreign material. Specifically, the inside of the vessel was inspected before and after the hot functional tests, with all the internals removed, to verify that no loose parts or foreign materials were in evidence.

Lower Internals

A particularly close inspection was made on the following items or areas, using a 5x or 10x magnifying glass or penetrant test where applicable. The locations of these areas are shown in Figures 3.9-1 and 3.9-2 for Units 1 and 2, respectively:

(1) Upper barrel flange and girthweld

(2) Upper barrel to lower barrel girthweld

(3) Upper core plate aligning pin (examine for any shadow marks, burnishing, buffing, or scoring; check for the soundness of lockwelds)

(4) Irradiation specimen basket welds

(5) Baffle assembly locking devices (check for lockweld integrity)

(6) Lower barrel to core support girthweld

(7) For Unit 1, the flexible tie connections (flexures) at the lower end of the thermal shield

(8) For Unit 2, the neutron shield panel locking devices and dowel pin cover plate welds (examine the connections for evidence of change in tightness of lockweld integrity)

(9) Radial support key welds to barrel

(10) Insert locking devices (examine soundness of lockwelds)

(11) Core support columns and instrumentation guide tubes (check all the joints for tightness and soundness of the locking devices)

(12) Secondary core support assembly welds

(13) Lower radial support lugs and inserts (Examine for any shadow marks, burnishing, buffing, or scoring. Checking the integrity of the lockwelds: these members supply the radial and torsional constraint of the internals at the bottom relative to the reactor vessel while permitting axial growth between the two. One would expect to see, on the bearing surfaces of the key and keyway, burnishings, buffing, or shadowing marks that would indicate pressure loading and relative motion between the two parts. Some scoring of engaging surfaces is also possible and acceptable.)

(14) For Unit 1, mounting blocks thermal shield to core barrel (examine the connections for evidence of change in tightness or lockweld integrity)

(15) For Units 1 and 2, gaps at baffle joints (check for gaps between baffle and top former and at baffle-to-baffle joints)

Upper Internals

A particularly close inspection was made on the following items or areas, using a magnifying glass of 5x or 10x magnification where necessary:

The locations of these areas are shown in Figures 3.9-1 and 3.9-2 for Units 1 and 2, respectively.

(1) Thermocouple conduits, clamps, and couplings

(2) Guide tube, support column, and thermocouple column assembly locking devices

(3) Support column and conduit assembly clamp welds

(4) Upper core plate alignment inserts (Examine for any shadow marks, burnishing, buffing or scoring. Check for tightness and lock device integrity)

(5) Connections of the support columns, mixing devices, and orifice plates to the upper core plate (check for tightness and lock device integrity)

(6) Thermocouple conduit gusset and clamp welds

(7) Thermocouple end-plugs (check for tightness)

(8) Guide tube closure welds, tube-transition plate welds, and card welds

Acceptance standards are the same as required in the shop by the original design drawings and specifications.

During the hot functional test, the internals were subjected to a total operating time at greater than normal full flow conditions (four pumps operating) of at least 10 days. This provides a cyclic loading of approximately 10^7 cycles on the main structural elements of the internals. In addition, there was some operating time with only one, two, and three pumps operating. No signs of abnormal wear were found, no harmful vibrations were detected, and no apparent structural changes took place; therefore, the four loop core support structures are considered to be structurally adequate and sound for operation.

3.9.1.5 Analysis Methods Under LOCA Loadings

The analysis methods used to confirm the structural design adequacy of the RCS under LOCA loadings are described in Section 5.2.1. With the acceptance of the DCPP leak-before-break analysis by the NRC (Reference 14), dynamic LOCA loads resulting from pipe rupture events in the main reactor coolant loop piping no longer have to be considered in the design basis structural analyses; only the much smaller LOCA loads from RCS branch line breaks have to be considered (see Section 3.6.2.1.1.1). Since the breaks postulated for the original analyses are more severe than those that are now required to be considered, the original analyses are conservative.

3.9.1.6 Analytical Methods for ASME Code Class I Components

Plastic instability allowable limits given in ASME Section III are not used when dynamic analysis is performed, except as noted in Section 5.2.1.11. The analysis methods have the limits established by the ASME Section III for Normal, Upset, and Emergency conditions. For these cases, the limits are sufficiently low to ensure that the analysis is not invalidated. For ASME Code Class I components, the stress limits for faulted loading conditions are specified in Section 5.2. For ASME components other than Class I and components not covered by the ASME Code, the stress limits for faulted loading conditions are specified in Sections 3.9.2 and 3.9.3, respectively. These faulted condition limits are established in such a manner that there is an equivalence with the adopted elastic limits and consequently will not invalidate the elastic system analysis.

3.9.1.7 Design and Analysis Details for the Pressurizer Safety and Relief System

The method of analysis for safety valves and relief valves suitably accounts for the time-history of loads acting during and subsequent to valve opening (i.e., less than one second). The fluid-induced forcing functions are calculated for pertinent safety valve and relief valve discharge cases using one-dimensional equations for the conservation of mass, momentum, and energy.

The calculated forcing functions are applied at locations along the associated piping. Application of these forcing functions to the associated piping model constitutes the dynamic time-history analysis.

The dynamic response of the piping system is determined for the input forcing functions. Therefore, a dynamic amplification factor is inherently accounted for in the analyses.

Snubbers or strut-type restraints are used as required. The stresses resulting from the loads produced by the sudden opening of a relief or safety valve are combined with stresses due to other pertinent loads and are shown to be allowable limits of the ANSI B31.1/B31.7 Codes. Also, the analyses show that the loads applied to the nozzles of the safety and relief valves do not exceed the maximum loads specified by the manufacturer.

The pressurizer safety and relief valve discharge piping systems provide overpressure protection for the RCS. The three spring-loaded safety valves, located on top of the pressurizer, are designed to prevent system pressure from exceeding design pressure by more than 10 percent. The three power-operated relief valves, also located on top of the pressurizer, are designed to prevent system pressure from exceeding the normal operating pressure by more than 100 psi. The valve outlet side is sloped to prevent the formation of water pockets. The safety valves have been converted from water-seated to steam-seated, and the water loop seal was eliminated by providing a continuous drain.

The pressurizer safety valves, manufactured by Crosby, are self-actuated, spring-loaded valves with backpressure compensation. The power-operated relief valves, manufactured by Masoneilan, are air-operated globe valves, capable of automatic operation via high pressure signal or remote manual operation. The safety valves and relief valves are located in the pressurizer cubicle and are supported by the attached piping which, in turn, is supported by a system of beams, struts, and snubbers. If the pressure exceeds the setpoints, the valves open. With a pressurizer safety valve water loop seal (now eliminated), the water slug from the loop seal discharges and the water slug, driven by high system pressure, generates transient thrust forces at each location where a change in flow direction occurs. The valve discharge conditions are considered in the analysis of the PSARV piping systems as follows: (a) the three safety valves remain closed, and (b) the three relief valves open simultaneously while the safety valves are closed. In addition to these two cases, which consider water seal discharge (water slug followed by steam), solid water from the pressurizer (cold overpressure) is also investigated. Even though the water loop seal has been eliminated, the analysis has not been revised to reflect any added margins because the valve discharge conditions without the water slug are less severe than those originally considered with the water slug.

For each pressurizer safety and relief piping system, an analytical hydraulic model is developed. The piping from the pressurizer nozzle to the relief tank nozzle is modeled as a series of single pipes. The pressurizer is modeled as a reservoir which contains stream at constant pressure (approximately 2500 psia for safety system and approximately 2350 psia for relief system) and at constant temperature of approximately 680°F. The pressurizer relief tank is modeled as a sink which contains steam and water mixture.

Fluid acceleration inside the pipe generates reaction forces on all segments of the line which are bounded at either end by an elbow or bend. Reaction forces resulting from fluid pressure and momentum variations are calculated. These forces are defined in terms of the fluid properties for the transient hydraulic analysis. Unbalanced forces are calculated for each straight segment of pipe from the pressurizer to the relief tank. The time histories of these forces are used for the subsequent structural analysis of the pressurizer safety and relief lines.

The structural model used in the seismic analysis of the safety and relief lines is modified for the valves thrust analysis to represent the safety and relief valve discharge. The time-history hydraulic forces are applied to the piping system lump mass points. The dynamic solution for the valve thrust is obtained by using a modified predictor-corrector-integration technique and normal mode theory.

The time-history solution is performed in subprogram FIXFM3. The input to this subprogram consists of the natural frequencies and normal modes, applied forces, and nonlinear elements. The natural frequencies and normal modes for the modified pressurizer safety and relief line dynamic model are determined with the WESTDYN program. The support loads are computed by multiplying the support stiffness matrix and the displacement vector at each support point. The time-history displacements of the FIXFM3 subprogram are used as input to the WESDYN2 subprogram to determine the internal forces, deflections, and stresses at each end of the piping elements.

The loading combinations considered in the analysis of the pressurizer safety and relief valve (PSARV) piping are given in Table 3.9-1. These load combinations are consistent with the final recommendations of the piping subcommittee of the EPRI PWR PSARV performance test program.

3.9.2 ASME CODE CLASS II AND III COMPONENTS

This section discusses the design criteria for DCPP Code Class II and III components. The design of these components is based on the requirements of various codes and standards that were in effect when the items were purchased. These codes and standards have been widely used by the nuclear industry and were, to a large extent, incorporated or referenced in the 1971 edition of the ASME Boiler and Pressure Vessel Code, Section III. If the 1971 edition of the ASME Boiler and Pressure Vessel Code, Section III, had been available during the design of DCPP, all these Code Class II and III components would have been in accordance with the requirements for ASME Code Class II and III components.

The DCPP Q-List (see Reference 8 of Section 3.2) lists the codes and standards to which Code Class II and III components were designed. The quality group classifications for DCPP fluid systems and fluid systems components are described in Section 3.2.2.

3.9.2.1 Plant Conditions and Design Loading Combinations

Design pressure, temperature, and other loading conditions that provide the bases for design of fluid systems or components are presented in the corresponding sections that describe the components and systems; see Chapters 6, 7, 9, and 11. Design codes, standards, and their applicability to systems and components are presented in Section 3.2.2.

3.9.2.2 Design Loading Combinations

Design Criteria for Westinghouse Code Class II and III components, are provided in Tables 3.9-2 through 3.9-7. Table 3.9-8 provides design information for selected tanks.

3.9.2.3 Design Stress Limits

Stress limits for Westinghouse ASME Code Class II and III components are provided in Table 3.9-2 through 3.9-7. Stress limits were selected to comply with the intent of ASME Code Section III and are sufficiently low to provide assurance that no gross deformation will occur in active components and that the active components[a] will operate as required following the event. The limits established for passive (inactive) components[b] are intended to ensure that violation of the pressure retaining boundary will not occur.

The designs of the condensate storage tanks, refueling water storage tanks, and the fire water and transfer tank are based on the AWWA D100, 1967 Code, with stress allowables restricted to those permitted by ASME Code Section VIII, Division 1. The design basis of these tanks is discussed in Section 3.8.3. Piping stresses resulting from the seismic analyses are combined with deadload stresses, pressure stresses, and other stresses caused by other sustained loads, as suggested in ANSI B31.1 by the following equations:

$$\frac{PDo}{4t_n} + \frac{0.75iM_A}{Z} \leq 1.0S_h \qquad (3.9\text{-}1)$$

$$\frac{PDo}{4t_n} + \frac{0.75iM_A}{Z} + \frac{0.75iM_B}{Z} \leq 1.2S_h \qquad (3.9\text{-}2)$$

$$\frac{PDo}{4t_n} + \frac{0.75iM_A}{Z} + \frac{0.75iM_B'}{Z} \leq 1.8S_h \qquad (3.9\text{-}3)$$

$$\frac{PDo}{4t_n} + \frac{0.75iM_A}{Z} + \frac{0.75iM_B''}{Z} \leq 2.4S_h \qquad (3.9\text{-}4)$$

$$\frac{iMc}{Z} \leq S_A \qquad (3.9\text{-}5)$$

where:

S_h = basic material allowable stress at operating temperature, psi

---

(a) Active components are those whose operability is relied upon to perform a safety function such as safe shutdown of the reactor or mitigation of the consequences of a postulated pipe break in the reactor coolant pressure boundary.

(b) Passive components are those whose operability (e.g., valve opening or closing, pump operation, or trip) are not relied upon to perform a safety function.

P	=	internal pressure, psig
Do	=	outside diameter of pipe, in
t_n	=	nominal wall thickness of pipe, in
Z	=	section modulus, in^3
i	=	stress intensification factor. The product of 0.75 x i shall never be taken as less than 1
M_A	=	resultant moment loading on cross section due to deadload and other sustained loads, in-lb
M_B	=	one-half of the resultant moment due to DE loads plus one-half of the full range of the resultant moment due to DE seismic anchor movements (SAM) if not included in Equations 3.9-5 or 3.9-6
M_B'	=	same as M_B except that moments from DDE are used instead of DE and anchor movements due to DDE are excluded
M_B''	=	same as M except the moments from HE are used instead of DE and anchor movements due to HE are excluded
M_C	=	the larger of (a) the full range of resultant moment due to seismic anchor movements (SAM), or (b) the range of resultant moment due to normal thermal expansion and anchor movements plus one-half of the full range of resultant moment due to SAM, in-lb
S_A	=	$f\,(1.25\ S_c + 0.25\ S_h)$
S_c	=	basic allowable stress at cold (ambient) temperature, psi
f	=	stress range reduction factor for cyclic loading = 1 (There are no events causing more than 7000 loading cycles for DCPP)

If Equation 3.9-5 is not satisfied, then the following equation must be satisfied:

$$\frac{PDo}{4t_n} + \frac{0.75iM_A}{Z} + \frac{iM_C}{Z} \le (S_h + S_A) \qquad (3.9\text{-}6)$$

For hydrodynamic loadings the following stress equations must be satisfied:

$$\frac{PDo}{4t_n} + \frac{0.75iM_A}{Z} + \frac{0.75iM_D}{Z} \le 1.2S_h \qquad (3.9\text{-}7)$$

$$\frac{PDo}{4t_n} + \frac{0.75iM_A}{Z} + \frac{0.75i}{Z}(M_B{}^2 + M_D{}^2)^{1/2} \le 1.8S_h \qquad (3.9\text{-}8)$$

where:

M_D	=	one half of the resultant moment due to hydrodynamic loads

All Design Class I pipe stresses were found to be within allowable limits specified in Equations 3.9-1 to 3.9-8.

3.9.2.4 Analytical and Empirical Methods for the Design of Pumps and Valves

The Quality Code Class II and III pumps and valves were designed and constructed to Design Class I standards and manufactured under approved quality assurance programs. PG&E inspectors routinely performed audits, inspections, and witnessed testing of Quality Code Class II and III components as they were manufactured.

Quality Code Class II and III pumps and valves were designed in accordance with the codes and standards listed in the DCPP Q-List (see Reference 8 of Section 3.2) and Table 3.2-2. These were the codes and standards that were in effect when the items were purchased. The stress limits selected are sufficiently low to provide assurance that no gross deformations will occur in active components; therefore, the active components will perform as required.

The pumps purchased by Westinghouse were analyzed for the forces resulting from seismic accelerations in the horizontal and vertical directions applied simultaneously. The pumps were designed to have a natural frequency in excess of 30 cps to eliminate any amplification of the seismic floor accelerations in the pump support structures.

The Westinghouse pumps were subjected to a series of tests prior to installation in the plant. The in-shop tests included (a) hydrostatic tests to 150 percent of the design pressure, (b) seal leakage tests, (c) net positive suction head (NPSH) tests to develop the minimum suction head necessary to allow operation, and (d) functional performance tests.

The pumps purchased by PG&E were designed in accordance with ASME standards or PG&E power plant pump standards. The design standards required were determined for each pump by reviewing the pump service conditions. Seismic calculations provided by the manufacturers were reviewed by PG&E to ensure that the loads developed from the combination of the design seismic horizontal and vertical acceleration did not exceed those allowed by applicable codes or standard engineering practices. Seismic calculations were not requested when the seismic adequacy could be ensured by testing or a comparative review of pump design. Hydrostatic tests to 150 percent of design pressure were performed on the pumps purchased by PG&E. The pumps also were subjected to performance tests consistent with the requirements of the Hydraulic Institute Standards or PG&E's power plant pump standards.

In addition to the above described tests, which were performed prior to installation in the plant, numerous tests were performed on the pumps during the preoperational test period. Cold hydrostatic pressure tests, hot functional qualification tests, periodic inservice inspections, and periodic inservice operational tests are performed on Quality Code Class II and III pumps after installation in the plant. These tests verify the functional ability of the pumps and ensure the operability of active safety-related pumps for the design life of the plant.

The supports of all Quality Code Class II and III pumps were designed to withstand the effects of the DE and reviewed for the DDE and HE. These considerations prevent supports of active safety-related pumps from deflecting and impairing the operability of the pump.

The Quality Code Class II and III valves purchased by Westinghouse were designed to the pressure and temperature requirements of the American Standard Association (ASA) B16.5 or the Manufacturers Standardization Society Standard Practice No. 66 (MSS SP66). The valves were tested to the requirements of MSS SP61. These tests included hydrostatic shell and seat leakage tests.

The Quality Code Class II and III valves purchased by the Company were designed, manufactured, and tested in accordance with the Draft ASME Code for Pumps and Valves for Nuclear Power, November 1968 or later editions, the ASME Code, Section III, 1974 edition, ANSI B16.5, and/or the MSS SP66.

In situ seismic testing of five representative valves was performed at the DCPP site. The purpose of this testing was to demonstrate that valves would indeed function when subjected to simulated seismic loads. Each valve was subjected to a static load applied at the center of gravity of the extended structure. The load was applied in the direction that would yield the largest deflection for the given load. While the valve was held in the deflected position, the valve was stroked. Any differences in deflected valve stroking time, line voltage, and motor current (as compared to the undeflected readings) would indicate the effect of a seismic event on valve operability. The valve was again stroked open and closed after removal of the static load to demonstrate that the valve had returned to its initial condition.

The five selected valves tested by this method performed satisfactorily while subjected to the simulated load. The operability indicators of motor current, voltage, and valve stroke time were essentially the same for both the deflected and undeflected tests. During the preoperational piping dynamics effects test program described in Section 3.9.1.2, any excessive piping deflections and vibrations were noted and corrected. Since all valves are supported as part of adjoining piping, this program ensures that the deflections by the pipe (and valve) supports will not impair the operability of active safety-related valves. The attention given to the design, manufacture, and testing of the Quality Code Class II and III pumps and valves ensures that the components will operate as required during or following any expected plant transient.

An evaluation and tabulation of all active valves is presented in Tables 3.9-9 and 6.2-39. An active valve is a valve that must perform a mechanical motion in order to shut down the plant or mitigate the consequences of a postulated event. The position each valve assumes on power failure is listed in these tables.

The design approach and criteria used to ensure the protection of all critical systems and containment from the effects of pipe whip, are presented in Section 3.6. Section 3.6 also presents the criteria for postulated pipe breaks. Section 3.6 also discusses that with the

acceptance of the DCPP leak-before-break analyses by the NRC (Reference 14), the dynamic effects of breaks in the main reactor coolant loop piping no longer have to be considered in the design basis analyses (see Section 3.6.2.1.1.1). Only the dynamic effects of postulated breaks in the RCS branch lines and other high energy lines have to be considered.

3.9.2.5 Design and Installation Criteria, Pressure-Relieving Devices

The main steam safety valves are located outside the primary containment directly on main steam leads 1 and 2, and on external headers on main steam leads 3 and 4. Five safety valves are provided for each steam generator, for a total of 20 safety valves. The safety valve headers and main steam lead connections were designed to ANSI B31.1-1967. Fabrication and erection were in accordance with the ASME Boiler and Pressure Vessel Code, Section I, 1968.

The safety valves are of the single discharge type and were built in accordance with ASME Boiler and Pressure Vessel Code, Section III. The valve discharge consists of an elbow attached to the safety valve outlet. The elbow discharges into a stack that is structurally independent of the valve and is oriented at approximately 36° to the vertical centerline of the safety valve. The stacks are supported to restrain the discharge reactions. Provisions are made to ensure that the safety valve discharge elbow and stack have adequate clearances during all phases of operation.

With the above safety valve discharge arrangement, the sustained blow force developed during valve operation intersects the vertical centerline of the safety valve header nozzle and the base of the header nozzle extrusion. The safety valve nozzles on the headers and on the main steam leads have been analyzed to ensure that the sustained forces developed during valve operation will not develop stresses in excess of those allowed by ANSI B31.1.

The main steam leads are anchored by the main steam flued heads which are structurally located in the reactor containment wall and are supported for the deadweight, thermal, seismic, and safety valve forces that may develop within the Design Class I portion. The two external safety valve headers on main steam leads 3 and 4 are independently supported in a similar fashion.

3.9.2.6 Stress Levels for Design Class I Components and Supports

The loading combinations and acceptance criteria used for piping (except for PSARV piping) primary equipment, and primary equipment supports in the Westinghouse scope of analysis are provided in Table 5.2-5, 5.2-6, 5.2-7, and 5.2-8, and also in Table 3.9-2 through 3.9-7. The load combinations and acceptance criteria used by Westinghouse for the PSARV analysis are provided in Table 3.9-1 and are consistent with the final recommendations of the piping subcommittee of the EPRI PWR PSARV performance test program.

Maximum allowable stresses for various loading combinations on hangers within B31.1 Code jurisdiction are as follows:

	DE	DDE	HE
Tension	0.417 Fy	0.9 Fy	Least of 1.2 Fy or 0.7 Fu
Shear	0.694 Fv	1.44 Fv	1.44 Fv
Compression	0.694 Fa	1.33 Fa	1.33 Fa
Bending	0.694 Fb	1.5 Fb	1.88 Fb
Bearing	0.625 Fy	Not Applicable	Not Applicable

where Fy, Fu, Fv, Fa, and Fb are from Part 5 of the AISC Steel Construction Manual, 7th Edition.

Supporting structures (supplemental steel) are in accordance with the 7th Edition of the AISC Steel Construction Manual. The stress limits and load combinations used by PG&E for equipment and equipment supports for their scope of analysis are:

DE Seismic Event

Component	Stress Limits[(a)(b)(c)(d)]
(Except cast iron) (active or inactive)	$Q_m \leq 1.1$ S $(Q_m$ or $Q_L) + Q_b \leq 1.65$ S
Inactive cast iron, pressure-retaining components	$Q_p \leq 0.1\ S_u$ $(Q_m$ or $Q_L) + Q_b \leq 1.5 \times 0.1\ S_u$
Inactive cast iron, nonpressure-retaining components	$(Q_m$ or $Q_L) + Q_b \leq 1.0 \times 0.2\ S_u$

(a) Q_m = general membrane stress, ksi. This stress is equal to the average stress across the solid section under consideration. It excludes discontinuities and concentrations and is produced only by pressure and other mechanical loads.

(b) Q_L = local membrane stress, ksi. This stress is the same as Q_m except that it includes the effect of discontinuities.

(c) Q_b = bending stress, ksi. This stress is equal to the linear varying portion of the stress across the solid section under consideration, excludes discontinuities and concentration, and is produced only by mechanical loads.

(d) S = material allowable stress listed in either 1971 or 1974 ASME Code, Section III, or the code the component was purchased and manufactured under, allowable stress values. The allowable stress shall correspond to the highest metal temperature at the section under consideration during the condition under consideration.

Support Element	
Plate and shell[(e)]	$Q_m \leq 1.0$ S $Q_m + Q_b \leq 1.5$ S
Linear[(f)]	1974 ASME Code, Section III, Appendix XVII and Subsection NF
Bolts	1974 ASME Code, Section III, Appendix XVII and/or Code Case 1644, and/or AISC Manual, 7th Edition

DDE/HE Seismic Event

Component	Stress Limits (see notes a, b, c)
Inactive (Except cast iron)	$Q_m \leq 2.0$ S $(Q_m$ or $Q_L) + Q_b \leq 2.4$ S
Active (Except cast iron)	$Q_m \leq 1.2$ S $(Q_m$ or $Q_L) + Q_b \leq 1.8$ S
Inactive cast iron, pressure-retaining components	$Q_p \leq 0.1\ S_u$ $(Q_m$ or $Q_L) + Q_b \leq 2.4 \times 0.1\ S_u$
Inactive cast iron, nonpressure-retaining components	$(Q_m$ or $Q_L) + Q_b \leq 2.0 \times 0.2\ S_u$
Support Elements	
Plate and shell (see note e) (active components)	$Q_m \leq 1.2$ S $(Q_m + Q_b) \leq 1.8$ S

(e) Plate and shell type supports: Plate and shell type component supports are supports such as vessel skirts and saddles that are fabricated from plate and shell elements and are normally subjected to a biaxial stress field.

(f) S = material allowable stress listed in either 1971 or 1974 ASME Code, Section III, or the code the component was purchased and manufactured under, allowable stress values. The allowable stress shall correspond to the highest metal temperature at the section under consideration during the condition under consideration.

Plate and shell (inactive components)	$Q_m \leq 2.0$ S $(Q_m + Q_b) \leq 2.4$ S Linear 1974 ASME Code, Section III, Appendix XVII, (see note f) Subsection NF and Appendix F (stresses not to exceed S_y[(g)] for active components)
Bolts	1974 ASME Code, Section III, Appendix XVII and/or Code Case 1644 plus Appendix F and/or ASIC Manual, 7th Edition

Load Combinations

(3.1.1)	$DE + P_n + T_n + D + N + O$
(3.1.2)	$DDE + P_a + T_a + D + N + O$
(3.1.3)	$HE + P_n + D + N + O$

where the following loads apply, as applicable:

HE	=	loads from Hosgri earthquake
P_n	=	Pressure, normal
P_a	=	Pressure, accident
T_n	=	Temperature, normal
T_a	=	Temperature, accident
DE	=	DE
DDE	=	DDE
D	=	Deadweight
N	=	Nozzle
O	=	Operating

Table 3.9-12 lists PG&E Class I equipment that has been seismically qualified.

3.9.2.7 Field Run Piping Systems

All Category I piping and pipe supports designed in the field are either analyzed or designed to a conservative standard, provided by PG&E engineering staff, for seismic and thermal loads.

(g) S_y = material allowable stress listed in either 1971 or 1974 ASME Code, Section III, or the code the component was purchased and manufactured under, minimum yield stress. The yield stress shall correspond to the highest metal temperature at the section under consideration during the condition under consideration.

3.9.3 CORE AND REACTOR INTERNALS

3.9.3.1 Core and Internals Integrity Analysis (Mechanical Analysis)

Stainless steel clad silver-indium-cadmium alloy absorber rods are resistant to radiation and thermal damage, thereby ensuring their effectiveness under all operating conditions. Rods of similar design have been successfully used in the original and reload cores of San Onofre, Connecticut Yankee, and others.

Two burnable poison rods (Reference 6) of smaller length but similar in design to those used in DCPP were exposed to in-pile test conditions in the Saxton Test Reactor in October 1967. A visual examination of the rods was made in early June 1968 and a visual and profilometer examination was made on July 30, 1968, after an exposure of 1900 effective full power hours (approximately 25 percent B^{10} depletion). The rods were found to be in excellent condition and profilometry results showed no dimensional variation from the initial condition.

An experimental verification of the reactivity worth calculations for borosilicate glass tubing has been accomplished. Similar rods have been successfully operated in the Ginna Reactor (Reference 7) with no evidence of deficiency.

Manufacturing defects did not appear during the hot functional tests because any manufacturing defects were detected in the shop or during the assembly period. The basic program that is currently being used to ensure adequacy of manufacturing practices consists of:

(1) Extremely thorough nil ductility temperature and quality assurance programs at the internals vendors

(2) Extensive visual examination at the plant site prior to hot functional testing of the primary system

(3) Running the hot functional test with full flow for 240 hours that accumulates approximately 10^7 cycles on the majority of the core structure components

(4) Reexamining all areas of the internals after the 240-hour hot functional test

The response of the reactor core and vessel internals under excitation produced by a simultaneous complete severance of a reactor coolant pipe and seismic excitation for a typical Westinghouse pressurized water reactor plant internals was determined. The following mechanical functional performance requirements applied:

(1) Following the DBA, the basic operational or functional requirement to be met for the reactor internals is that the plant shall be shut down and cooled in an orderly fashion so that fuel cladding temperature is kept within

specified limits. This implies that the deformation of certain critical reactor internals must be kept sufficiently small to allow core cooling.

(2) For large breaks, the reduction in water density greatly reduces the reactivity of the core, thereby shutting down the core whether the rods are tripped or not. The subsequent reflooding of the core by the ECCS with borated water maintains the core in a subcritical state. Therefore, the main requirement is to ensure effectiveness of the ECCS. Insertion of the control rods, although not needed, gives further assurance of the ability to shut the plant down and keep it in a safe shutdown condition.

(3) The functional requirements for the core structures during the DBA are shown in Table 3.9-10. The inward upper barrel deflections are controlled to ensure no contacting of the nearest rod cluster control guide tube. The outward upper barrel deflections are controlled in order to maintain an adequate annulus for the coolant between the vessel inner diameter and core barrel outer diameter.

(4) The rod cluster control guide tube deflections are limited to ensure operability of the control rods.

(5) To ensure no column loading of rod cluster control guide tubes, the upper core plate deflection is limited to the value shown in Table 3.9-10.

(6) The reactor has mechanical provisions that are sufficient to maintain the design core and internals and to ensure that the core is intact with acceptable heat transfer geometry following transients arising from the DBA operating conditions (References 2, 8, and 13).

(7) The core internals are designed to withstand mechanical loads arising from DE, DDE, and pipe ruptures (References 2, 4, 8, and 13).

While these performance requirements originally had to be met for load combinations that included the contribution from a main RCS loop line break, with the acceptance of the DCPP leak-before-break analysis by the NRC (Reference 14), dynamic loads resulting from pipe rupture events in the main reactor coolant loop piping no longer have to be considered in the design basis structural analyses and included in the loading combinations; only the much smaller loads from RCS branch line breaks have to be considered (see Section 3.6.2.1.1.1).

3.9.3.2 Faulted Conditions

The following events were considered in the faulted conditions category:

(1) Loads produced by a double-ended pipe rupture of the main coolant loop DBA for both the cold and hot leg breaks. The methods of analysis adopted were related to the type of accident assumed (cold leg break or hot leg break).

(2) Response due to a DDE or HE, as described previously in the seismic analysis

(3) Most unfavorable combination of DDE and DBA. Maximum stresses obtained in each case were added in the most conservative manner.

Maximum stress intensities are compared with allowables for each condition. When fatigue is of concern, the applicable stress concentrations factors are utilized and peak stresses are used to establish the usage factor. Elastic analysis is used to obtain the response of the structure and the stress analysis for each component is performed on an elastic basis. For faulted conditions, stresses are above yield in a few locations. For these cases only, when deformation requirements exist, a plastic analysis is independently performed to ensure that functional requirements are maintained (guide tubes deflections and core barrel expansions). The elastic limit allowable stresses are used to compare with the results of the analysis. No inelastic stress limits are used.

These analyses showed that the stresses and deflections that would result following a faulted condition are less than those that would adversely affect the integrity of the structures. Also, the natural and applied frequencies were such that resonance problems should not occur.

While these events and event combinations were considered in the original analysis for faulted conditions, with the acceptance of the DCPP leak-before-break analysis by the NRC (Reference 14), dynamic loads resulting from pipe rupture events in the main reactor coolant loop piping no longer have to be considered in the design basis structural analyses and included in the loading combinations; only the much smaller loads from RCS branch line breaks have to be considered (see Section 3.6.2.1.1.1).

3.9.3.3 Reactor Internals Response Under LOCA and Seismic Excitations

The reactor vessel/internals/fuel system dynamic analyses for Diablo Canyon Units 1 & 2 were performed in the 1987-1988 timeframe to verify structural adequacy of the core during transition from 17x17 standard fuel to 17x17 VANTAGE 5 fuel. These dynamic analyses were performed for the LOCA and seismic design conditions of DE, DDE, and Hosgri; and details of these analyses are given in Reference 15. At that time, the impact of new Long Term Seismic Program (LTSP) spectra on the reactor internals and the core was not evaluated. Since the LTSP spectra at the dominant structural

frequencies of the reactor core are not bounded by the spectra used in 1987-1988, a new reactor vessel/internals/fuel system (i.e., RPV system) seismic analysis was performed in 1996 using the LTSP spectra. The results of LTSP seismic analysis together with results of DE, DDE, Hosgri, and LOCA from 1987-1988 analyses for the VANTAGE 5 Zircaloy fuel and the ZIRLO fuel are also documented in Reference 15.

The system mathematical models for Diablo Canyon Units 1 & 2 used in the LOCA and seismic analyses are three-dimensional nonlinear finite element models, which are described in detail in Reference 15. The major difference between the LOCA and seismic models is that the seismic model includes the hydrodynamic mass matrices in the vessel/barrel downcomer annulus to account for the fluid-solid interactions. The fluid-solid interactions in the LOCA analysis are accounted through the hydraulic forcing functions generated by Multiflex Code (Reference 3). Another difference between the LOCA and seismic models is the difference in loop stiffness matrices. The seismic model uses the unbroken loop stiffness matrix, whereas the LOCA model uses the broken loop stiffness matrix. Except for these two differences, the RPV system seismic model is identical to that of the LOCA model.

It is important to note that the LOCA analyses described below are the analyses originally performed for the RCS faulted conditions. With the acceptance of the DCPP Leak-Before-Break (LBB) by the USNRC (Reference 14), the dynamic LOCA loads resulting from the pipe rupture events in the main reactor coolant loop piping no longer have to be considered in the design basis structural analyses and including the loading combinations. With LBB acceptance, the next most limiting breaks which need to be considered are the auxiliary line breaks consisting of accumulator line, pressurizer surge line and RHR line. The LOCA loads imposed on the RPV system from these auxiliary line breaks are generally significantly lower than those obtained from the main loop line breaks discussed below. This reduction in LOCA loads for the auxiliary line breaks is due to the fact that the auxiliary lines have a smaller break size, location of the breaks are farther away from the vessel nozzles, and the absence of cavity pressurization loads.

It should also be noted that, in general, for faulted conditions the imposed loading on the reactor vessel and its internals due to seismic (DDE) and LOCA conditions are additive by the square root of the sum of squares (SRSS) method. A Hosgri Earthquake (HE) and LOCA are also considered to occur simultaneously and, therefore, the combined loading is considered by SRSS. Therefore, with LBB invoked, the combination of LOCA and seismic loads on the RPV system will be considerably lower than those obtained from main loop piping breaks.

3.9.3.3.1 Reactor Internals Response Under Seismic Excitations.

The seismic analysis included the effects of simultaneous application of time history accelerations in three orthogonal directions. The LTSP response spectra at the reactor vessel supports with five percent critical damping was used by Pacific Gas and Electric (PG&E) to synthesize time history accelerations, and these time history accelerations

were supplied to Westinghouse by PG&E via Reference 16. The Westinghouse generated synthesized time history accelerations for DE, DDE, and Hosgri response spectra were used in a 1987-1988 analyses. The references of these Westinghouse generated synthesized time histories are also given in Reference 15.

As mentioned earlier, fluid-structure or hydroelastic interaction is included in the reactor pressure vessel model for seismic evaluations. The horizontal hydroelastic interaction is significant in the cylindrical fluid flow region between the core barrel and the reactor vessel annulus. Mass matrices with off-diagonal terms (horizontal degrees-of-freedom only) attach between nodes on the core barrel, thermal shield and the reactor vessel shell (see, e.g., Figure 2-5 of Reference 15, assembled finite element model for Unit 1). The mass matrices for the hydro-elastic interactions of two concentric cylinders are developed using the work of Reference 17. For the case of an incompressible, frictionless fluid displaced in the annulus due to motion of the cylinders, the expression for the hydrodynamic mass matrix connecting the inner and outer cylinders is derived. The diagonal terms of the mass matrix are similar to the lumping of water mass to the vessel shell, thermal shield, and core barrel. The off-diagonal terms reflect the fact that all the water mass does not participate when there is no relative motion of the vessel and core barrel. It should be pointed out that the hydrodynamic mass matrix has no artificial virtual mass effect and is derived in a straight-forward, quantitative manner.

The matrices are a function of the properties of two cylinders with the fluid in the cylindrical annulus, specifically, inside and outside radius of the annulus, density of the fluid and length of the cylinders. Vertical segmentation of the reactor vessel and the core barrel allows inclusion of radii variations along their heights and approximates the effects of beam mode deformation. These mass matrices were inserted between the selected nodes on the core barrel, thermal shield, and the reactor vessel (see Figure 2-5 of Reference 15).

The WECAN computer code, which is used to determine the response of the reactor vessel and its internals, is a general purpose finite element code. In the finite element approach, the structure is divided into a finite number of discrete members or elements. The inertia and stiffness matrices, as well as the force array, are first calculated for each element in the local coordinates. Employing appropriate transformations, the element global matrices and arrays are assembled into global structural matrices and arrays, and used for dynamic solution of the differential equation of motion for the structure.

Note that the preceding paragraphs describe the RPV and internals system dynamic analyses for which the WECAN computer code was used. Current analyses (such as the dynamic analyses performed in support of the replacement vessel head project) utilize the ANSYS computer code. The methodology used to develop the ANSYS system models is consistent with the methodology used to develop historic WECAN models. The direct time integration method is used in ANSYS to solve the dynamic equations of motion for the system; whereas the nonlinear mode superposition method is used in WECAN to solve the dynamic equations of motion for the system.

3.9.3.3.2 Reactor Internals Response During Loss-Of-Coolant-Accident (LOCA) Conditions

The mechanical response of the reactor coolant system subjected to a LOCA transient is performed in three steps. First, the reactor coolant system is analyzed for the effects of loads induced by normal operation which include thermal, pressure and dead weight effects. From this analysis, the loop mechanical forces acting on the RPV that would result from the release of equilibrium forces at the break locations are obtained. In the second step, the loop mechanical loads, reactor internal hydraulic forces, jet impingement forces, and reactor cavity pressurization forces are simultaneously applied; and the RPV displacements due to the LOCA are calculated. Finally, the structural integrity of the reactor coolant loop and component supports to deal with the LOCA are evaluated by applying the reactor vessel displacements to a mathematical model of the reactor coolant loop.

In 1987-1988, the RPV system LOCA analyses for the Diablo Canyon units were performed for the most limiting breaks consisting of: (a) RPV inlet nozzle break, (b) RPV outlet nozzle break, and (c) RCP outlet nozzle break. These break locations have been determined by detailed stress and fatigue analyses of the reactor coolant loop piping system (Reference 18). As mentioned earlier, the RPV system finite element model for LOCA analysis is identical to that of the seismic model except that it does not have hydrodynamic mass matrices in the downcomer region.

In 2005, the RPV system LOCA analysis was performed for the Unit 2 barrel/baffle region conversion from downflow to the upflow configuration. For DCPP Unit 2, considering LBB acceptance, the next most limiting auxiliary line breaks are the pressurizer surge line break (98.31 in^2) on the hot leg and the accumulator line break (60.13 in^2) on the cold leg. Postulated residual heat removal (RHR) auxiliary line breaks are bounded by the pressurizer surge line break for Unit 2.

In order to study LOCA hydraulic forces for the DCPP Unit 2 Upflow Conversion Program, the following vessel/internal break cases were analyzed:

1. Pressurizer Surge Line Break
2. Accumulator Line Break

A 1 millisecond break-opening-time (BOT) was employed in the vessel forces analyses for DCPP Unit 2, consistent with the MULTIFLEX licensing requirements. All break cases used flexible beam modeling for the core barrel. The analysis conservatively assumed a limiting full power RCS cold leg temperature of 526°F (including uncertainty) which bounds the minimum cold leg temperature of 531.9°F (excluding uncertainty) for DCPP Unit 2. These conditions bound the most severe operating conditions, which encompasses Tavg coastdown conditions. Thus, the effects of a Tavg coastdown are accounted for in the vessel forces analysis. In addition, the Delta-54 replacement steam generator (RSG) was accounted for in the analyses. Previous studies have shown that the steam generator design has a relatively insignificant effect on the vessel

forces analyses, so operation of Unit 2 with either the original Model 51 steam generators or the Delta-54 stream generators is acceptable with respect to the vessel forces analyses.

Following a postulated LOCA pipe rupture, forces are imposed on the reactor vessel and its internals. These forces result from the release of the pressurized primary system coolant, and for guillotine pipe breaks from the disturbance of the mechanical equilibrium in the piping system prior to the rupture. The release of pressurized coolant results in traveling depressurization waves in the primary system. These depressurization waves are characterized by a wave-front with low pressure on one side and high pressure on the other. The wave-front translates and reflects throughout the primary system until the system is completely depressurized. The rapid depressurization results in transient hydraulic loads on the mechanical equipment of the system. The release of coolant resulting from a postulated RPV nozzle break also results in a pressure increase in the region surrounding the postulated break. Pressurization occurs rapidly in the cavity around the reactor vessel, which can exert an asymmetric force on the outside of the vessel.

The loads on the RPV and internals that result from the depressurization of the system and from the pressurization of the area around the break may be categorized as: (a) reactor internal hydraulic loads (vertical and horizontal), (b) reactor coolant loop mechanical loads, (c) reactor cavity pressurization loads (only for breaks at the RPV safe end locations), and (d) jet impingement loads. Description of such loads acting for a typical reactor vessel inlet or outlet nozzle is given below (for more details, see Reference 6), and these loads are combined into a single time history forcing function which are then applied to the RPV system finite element model.

3.9.3.3.2.1 Reactor Pressure Vessel Internal Hydraulic Loads

Depressurization waves propagate from the postulated break location into the reactor vessel through either a hot leg or a cold leg nozzle. After a postulated cold leg break, the depressurization path for waves entering the reactor vessel is through the nozzle that contains the broken pipe and into the region between the core barrel and the reactor vessel (that is, the downcomer region). The initial wave propagates up, around, and down the downcomer annulus, then up through the region circumferentially enclosed by the core barrel, that is, the fuel region. In the case of a cold leg break, the region of the downcomer annulus close to the break depressurizes rapidly but, because of the restricted flow areas and finite wave speed (approximately 3000 feet per second), the opposite side of the core barrel remains at a high pressure. This results in a net horizontal force on the core barrel and the reactor vessel. As the depressurization wave propagates around the downcomer annulus and up through the core, the core barrel differential pressure reduces and, similarly, the resulting hydraulic forces drop.

In the case of a postulated break in the hot leg, the wave follows a similar depressurization path, passing through the outlet nozzle and directly into the upper internals region depressurizing the core and entering the downcomer annulus from the

bottom exit of the core barrel. Thus, after a hot leg break, the downcomer annulus would be depressurized with very little difference in pressure forces across the outside diameter of the core barrel. A hot leg break produces less horizontal force because the depressurization wave travels directly to the inside of the core barrel (so that the downcomer annulus is not directly involved), and internal differential pressures are not as large as for a cold leg break of the same size. Since the differential pressure is less for a hot leg break, the horizontal force applied to the core barrel is less for hot leg break than for a cold leg break. For breaks in both the hot leg and cold leg, the depressurization waves continue to propagate by reflection and translation through the reactor vessel and loops.

The MULTIFLEX computer code (Reference 3) calculates the hydraulic transients within the entire primary coolant system. It considers subcooled, transition, and two-phase (saturated) blowdown regimes. The MULTIFLEX code employs the method of characteristics to solve the conservation laws, and assumes one-dimensionality of flow and homogeneity of the liquid-vapor mixture. The MULTIFLEX code considers a coupled fluid-structure interaction by accounting for the deflection of constraining boundaries, which are represented by separate spring-mass oscillator system. A beam model of the core support barrel has been developed from the structural properties of the core barrel; in this model, the pressure as well as the wall motions are projected onto the plane parallel to the broken nozzle. The spatial pressure variation at each time step is transformed into ten horizontal forces, which act on the ten mass points of the beam model. Each flexible wall is bounded on either side by a hydraulic flow path. The motion of the flexible wall is determined by solving the global equations of motions for the masses representing the forced vibration of an undamped beam.

The reanalysis performed in support of the conversion of the barrel/baffle region for Unit 2 has made use of the MULTIFLEX 3.0 (Reference 9) computer code. The MULTIFLEX versions are an extension of the BLODWN-2 computer code and includes mechanical structure models and their interactions with the thermal-hydraulic system. Both versions of the MULTIFLEX code share a common hydraulic modeling scheme, with differences being confined to a more realistic downcomer hydraulic network and a more realistic core barrel structural model that accounts for non-linear boundary conditions and vessel motion. Generally, this improved modeling results in lower, more realistic, but still conservative hydraulic forces on the core barrel. The NRC staff has accepted (Reference 10) the use of MULTIFLEX 3.0 for calculating the hydraulic forces on reactor vessel internals (Reference 11).

3.9.3.3.2.2 Reactor Coolant Loop Mechanical Loads

The loop mechanical loads result from the release of normal operating forces present in the pipe prior to the separation as well as transient hydraulic forces in the reactor coolant system. The magnitudes of the loop release forces are determined by performing a reactor coolant loop analysis for normal operating loads (that is, pressure, thermal, and deadweight). The loads existing in the pipe at the postulated break location are calculated and are "released" at the initiation of the LOCA transient by

application of the loads to the broken piping ends. These forces are applied with a ramp time of one millisecond because of the assumed instantaneous break opening time.

3.9.3.3.2.3 Reactor Cavity Pressurization Loads

Reactor cavity forces arise from the steam and water that are released into the reactor cavity through the annulus around the broken pipe. These forces occur only for postulated breaks at the RPV nozzle safe end locations. The reactor cavity is pressurized asymmetrically, with high pressures on the side adjacent to the break. The horizontal differences in pressure across the reactor cavity result in horizontal forces on the reactor vessel. Vertical forces on the reactor vessel arise from similar variations in pressures on the upper and lower head and the tapered parts of the vessel.

3.9.3.3.2.4 Jet Impingement Loads

The jet impingement load is an axial force along the broken pipe centerline that is caused by the pressure of the escaping jet of coolant acting on the exposed pipe cross section at the break location. The jet force is calculated by multiplying the saturation pressure corresponding to the temperature of the coolant at break location times the cross-sectional area of the pipe. This force is applied with a ramp time of one millisecond.

3.9.3.4 Acceptance Criteria

3.9.3.4.1 Structural Adequacy of Reactor Internal Components

The reactor internal components of Diablo Canyon Units 1 and 2 are not ASME Code components because Sub-section NG of the ASME Boiler and Pressure Code edition applicable to DCPP Units reactor internals did not include design criteria for the reactor internals. However, these components were originally designed to meet the intent of the 1971 Edition of Section III of the ASME Boiler and Pressure Vessel Code with addenda through the Winter 1971. The allowable stress limits for the design basis accident (DBA) for core support structures are based on limits specified in Section 5.2.1.

3.9.3.4.2 Allowable Deflection and Stability Criteria.

The criterion for acceptability in regard to mechanical integrity analyses is that adequate core cooling and core shutdown must be ensured. This implies that the deformation of reactor internals must be sufficiently small so that the geometry remains substantially intact. Consequently, the limitations established on the reactor internals are concerned principally with the maximum allowable deflections and stability of the components.

For faulted conditions, deflections of critical internal structures are limited to values given in Table 3.9-10. In a hypothesized vertical displacement of internals, energy

absorbing devices limit the displacement to 1.25 inches by contacting the vessel bottom head.

Upper Core Barrel

The upper core barrel has the following deformation limits:

(1) To ensure shutdown and cooldown of the core during cold leg blowdown, the basic requirement is a limitation on the outward deflection of the barrel at the locations of the inlet nozzles connected to unbroken lines. A large outward deflection of the upper barrel in front of the inlet nozzles, accompanied with permanent strains, could close the inlet area and restrict the cooling water coming from the accumulators. Consequently, a permanent barrel deflection in front of the unbroken inlet nozzles larger than a certain limit, called "no loss of function" limit, could impair the efficiency of the ECCS.

(2) During the hot leg break, the rarefaction wave enters through the outlet nozzle into the upper internals region and thus depressurizes the core and then enters the downcomer annulus from the bottom exit of the core barrel. This depressurization of the annulus region subjects the core barrel to external pressures and this condition requires a stability check of the core barrel during hot leg break. Therefore, to ensure rod insertion and to avoid disturbing the control rod cluster guide structure, the barrel should not interfere with the guide tubes.

Control Rod Cluster Guide Tubes

The deflection limits of the guide tubes were established from test data (see Table 3.9-10).

Upper Package

The local vertical deformation of the upper core plate, where a guide tube is located, shall be less than 0.100 inch. This deformation will cause the plate to contact the guide tube, since the clearance between the plate and the guide tube is 0.100 inch. This limit will prevent the guide tubes from undergoing compression. For a plate local deformation of 0.150 inch, the guide tube will be compressed and deformed transversely to the upper limit previously established. Consequently, the value of 0.150 inch is adopted as the no loss function local deformation with an allowable limit of 0.100 inch. These limits are given in Table 3.9-10.

3.9.3.5 Methods of Analysis

Faulted condition LOCA analyses were originally performed for limiting breaks of the reactor vessel inlet nozzle and reactor vessel outlet nozzle with a limited displacement

allowing a break area of 115 in^2. Subsequent calculations of the loop displacements found the maximum displacement at the reactor vessel inlet and outlet nozzles was 81in^2, confirming the 115 in^2 break area was a conservative assumption. These original 115 in^2 break area forces were later confirmed to be bounding relative to LOCA forces generated for 81 in^2 limited displacement breaks calculated at reduced operating temperatures consistent with temperature coastdown. Although the leak-before-break analysis (Reference 14) now allows for exclusion of main loop piping breaks from the design basis, no credit has yet been taken for the smaller branch line areas (60 in^2 for the largest cold leg branch line - the accumulator line) in the current reactor vessel LOCA forces analyses for Unit 1. When credit for this break area reduction is taken, it is expected to provide substantial margin relative to the existing design basis accident loads.

For the Unit 2 conversion to the upflow configuration, as previously mentioned, the pressurizer surge line break (98.31 in^2) on the hot leg and the accumulator line break (60.13 in^2) on the cold leg were analyzed with the MULTIFLEX 3.0 code. The analysis used a 1 millisecond BOT, consistent with the MULTIFLEX licensing requirements. All break cases used flexible beam modeling for the core barrel. The analysis conservatively assumed limiting full power RCS temperatures for DCPP Unit 2. These conditions bound the most severe operating conditions, which encompasses Tavg coastdown conditions. The effects of a Tavg coastdown are thus accounted for in the vessel forces analyses. Additionally, the Delta-54 RSG was included in the analyses. Previous studies have shown that the steam generator design has a relatively insignificant effect on the vessel forces analyses, so operation of either Unit 1 or Unit 2 with either the original Model 51 steam generator or the Delta-54 steam generator configuration is acceptable with respect to the vessel forces analyses.

3.9.3.5.1 Blowdown Forces Due to Cold and Hot Leg Break

A USNRC approved FORTRAN-IV computer program called MULTIFLEX (Reference 3) is used to calculate the local fluid pressure, flow, and density transients that occur during a LOCA. MULTIFLEX is an extension of the BLODOWN-2 computer code and includes mechanical structure models and their interaction with the thermal-hydraulic system.

The analysis is performed for the subcooled decompression period of the transient, where the hydraulic loads are the greatest. These loads are used for the structural evaluation of the reactor pressure vessel support system, in conjunction with other loads associated with a LOCA and with a safe shutdown earthquake (SSE).

3.9.3.5.2 FORCE2 and LATFORC Models for Blowdown

The MULTIFLEX code evaluates the pressure and velocity transients throughout the RCS. These pressure and velocity transients are made available to the programs FORCE2 and LATFORC, which utilize detailed geometric descriptions in evaluating the loadings on the reactor internals.

LATFORC (Reference 3) is used to calculate the horizontal force components on the vessel, core barrel, and thermal shield as a function of elevation and time using the MULTIFLEX hydraulic data. The force components significant to the horizontal forces are primarily a function of the pressure times area.

FORCE2 (Reference 3) is used to calculate the vertical force components acting on the reactor vessel and internals. Each reactor component for which FORCE2 calculations are required is designated as an element and assigned an element number. Forces acting on each of the elements are calculated summing the effects of:

(1) The pressure differential across the element.

(2) Flow stagnation on, and unrecovered orifice losses across, the element.

(3) Friction losses along the element.

The most significant assumption made for the analysis is that the thermal-hydraulic analysis has been performed to include mechanical structural models of the core barrel, which allows for fluid structure interaction in the downcomer region of the vessel to decrease the peak pressures calculated on the core barrel and vessel. No other fluid structure interaction has been modeled in the vessel LOCA forces calculation.

3.9.3.5.3 Reactor Vessel/Internals/Fuel Analysis Under LOCA Conditions

The three dimensional LOCA analysis of the RPV system (i.e., reactor vessel/internals/fuel) is discussed in Section 3.9.1.3.1, and Section 3.9.1.3.2 provides insight into the description of major core support components during LOCA transients.

3.9.3.5.4 Reactor Vessel/Internals/Fuel Analysis Under Seismic Conditions

The three dimensional Seismic analysis of the RPV system (i.e., reactor vessel/internals/fuel) is discussed in Section 3.7.2, and the methods of analyses for seismic loads of major subsystems are discussed in Section 3.7.3.

3.9.3.5.5 Methods and Results (Mechanical)

To verify structural adequacy of the reactor internal components and the core under LOCA and seismic loading, nonlinear time history dynamic analyses of the RPV system were performed to generate component interface loads as well as the time history displacements of the lower core plate, upper core plate, and the core barrel. These time history displacements of the core plates and the barrel were then used by Nuclear Fuel Division (NFD) to determine the fuel grid impact loads and the structural adequacy of the core components.

Reference 15 documents in detail the results of RPV system LOCA and seismic analyses. From these analyses it is seen that the reactor internals component interface

loads for the Diablo Canyon units during LOCA, seismic and combined (SRSS LOCA + seismic) are bounded by those of the Generic 4-Loop Stress Report (Reference 19). In the generic stress report, the four-loop reactor internals components are analyzed to meet the ASME Code stress requirements.

The results also indicate that the maximum deflections in the critical structures are below the established allowable limits (see e.g., Table 3.9-10). During the hot leg break, the core barrel does not buckle, and during the cold leg break has stresses that are within allowable limits. The design evaluation of the internals structure is presented in Section 4.2.2.

It should be reiterated that LOCA analyses described above are for the main loops line breaks; and with the LBB acceptance, the next most limiting breaks which need to be considered are the auxiliary line breaks consisting of the accumulator line, the pressurizer surge line, and the RHR line. The LOCA loads imposed on the RPV system from these auxiliary line breaks are generally significantly lower than those obtained from the main loop line breaks. Therefore, with LBB the combination of LOCA and seismic loads on the RPV system will yield higher margins of safety.

For DCPP Unit 2, an upflow conversion in conjunction with the upper head temperature reduction program has been implemented. The impacts due to these modifications were evaluated and documented in Reference 20.

3.9.3.6 Control Rod Drive Mechanisms

The control rod drive mechanisms are Class A components designed to meet the stresses of the ASME Boiler and Pressure Vessel Code and therefore are presented in Section 4.2.

3.9.4 NON-DESIGN CLASS I COMPONENTS

Several non-Design Class I components were also seismically qualified to preclude seismic interaction with Design Class I equipment and/or to ensure structural integrity of the component cooling water system.

3.9.5 MISCELLANEOUS PRESSURIZED GAS CONTAINERS

Table 3.9-11 provides a summary of all storage tanks containing significant quantities (over 100 lbs) of gas under pressure in excess of 100 psig. These tanks are of both Design Class I and II.

3.9.6 REFERENCES

1. Deleted.

2. Bohm, Indian Point Unit No. 2 Internals Mechanical Analysis for Blowdown Excitation, WCAP-7822, December 1971.

3. Takeuchi, K. et al., MULTIFLEX, A FORTRAN IV Computer Program for Analyzing Thermal-Hydraulic Structure System Dynamics," WCAP-8708-P-A (Westinghouse Proprietary Class 2), WCAP-8709-A, NES Class 3 (Non-Proprietary), September 1977.

4. Moore, Westinghouse PWR Core Behavior Following a Loss-of-Coolant Accident, WCAP-7422, September 1971.

5. Bohm, and J. P. Lafaille, Reactor Internals Response under a Blowdown Accident, First Intl. Conf. on Structural Mech. in Reactor Tech., Berlin, September 20-24, 1971.

6. Wood et al., Use of Burnable Poison Rods in Westinghouse Pressurized Water Reactors, WCAP-7113, October 1967.

7. Barry et al., Topical Report - Power Distribution Monitoring in the R.E. Ginna PWR, WCAP-7756, September 1971.

8. Gesinski, Fuel Assembly Safety Analysis for Combined Seismic and Loss-of-Coolant Accident, WCAP-7950, July 1972.

9. Takeuchi, K. et al., MULTIFLEX 3.0, A FORTRAN IV Computer Program for Analyzing Thermal-Hydraulic-Structural System Dynamics Advanced Beam Model," WCAP-9735, Revision 2, Westinghouse Proprietary Class 2/WCAP-9736, Revision 1, Non-Proprietary, February 1998.

10. Letter, T. H. Essig (USNRC) to Lou Liberatori (WOG), Safety Evaluation of Topical Report WCAP-15029, "Westinghouse Methodology for Evaluating the Acceptability of Baffle-Former-Barrel Bolting Distributions Under Faulted Load Conditions", (TAC No. MA1152)," November 10, 1998 (Enclosure 1 – Safety Evaluation Report.

11. Schwirian, R. E., et al., Westinghouse Methodology for Evaluating the Acceptability of Baffle-Former-Barrel Bolting Distributions Under Faulted Load Conditions, WCAP-15029-P-A, Westinghouse Proprietary Class 2 / WCAP-15030-NP-A, Revision 0, Non-Proprietary, January 1999.

NOTES:

(1) This table is applicable to the seismically designed portion of downstream non-Category I piping necessary to isolate the response, and to assure acceptable valve loading on the discharge nozzle.

(2) See SOT definitions and other load abbreviations.

(3) The bounding number of valves (and discharge sequence if setpoints are significantly different) for the applicable system operating transient defined on this page should be used.

(4) Use SRSS for combining dynamic load responses.

(5) The LOCA loads used in this load combination in the original analyses were the loads resulting from breaks in the main reactor coolant loop. With the acceptance of the DCPP leak-before-break analyses by the NRC, LOCA loads resulting from breaks in the main RCS loop piping no longer have to be considered in the design basis structural analyses and included in the load combinations. Only the LOCA loads from RCS branch line breaks have to be considered.

Abbreviations

N	=	Sustained loads during normal plant operation
SOT	=	System Operating Transient
SOT_U	=	Relief Valve Discharge Transient
SOT_E	=	Safety Valve Discharge Transient
SOT_F	=	Max (SOT_U; SOT_E)
DE	=	Design Earthquake
DDE	=	Double Design Earthquake
HOSGRI	=	Hosgri earthquake
LOCA	=	Loss-of-coolant accident
S_h	=	Basic material allowable stress at maximum (hot) temperature

TABLE 3.9-2

HOSGRI AND DDE SEISMIC LOADING COMBINATIONS AND STRUCTURAL CRITERIA MECHANICAL EQUIPMENT[1]

COMPONENT (2, 3)	LOADING COMBINATIONS (4)	CRITERIA (7, 8, 9, 10, 11, 12, 13, 14)	
Tanks, Heat Exchangers, Filters, Demineralizers	Deadweight + Pressure + HOSGRI/DDE + Nozzle/Piping Loads	σ_m $(\sigma_m$ or $\sigma_L) + \sigma_b$	$\leq 2.0S$ $\leq 2.4S$
Active Pumps	Deadweight + Pressure + HOSGRI/DDE + Nozzle/Piping Loads + Operating Loads	σ_m $(\sigma_m$ or $\sigma_L) + \sigma_b$	$\leq 1.2S$ $\leq 1.8S$
Inactive Pumps	Deadweight + Pressure + HOSGRI/DDE + Nozzle/Piping Loads + Operating Loads	σ_m $(\sigma_m$ or $\sigma_L) + \sigma_m$	$\leq 2.0S$ $\leq 2.4S$
Active Valves	Deadweight + Pressure + HOSGRI/DDE + Nozzle/Piping Loads + Operating Loads[12]	Extended Structure: Pressure Boundary: Valve Nozzles: Bolting:	$\sigma_m \leq 1.2S$ $(\sigma_m$ or $\sigma_L)$ $+ \sigma_b \leq 1.8S$ or S_y (higher of) ANSI B16.5 or MSS-SP-66 (5) $\sigma_m \leq 2.0S$
Inactive Valves	Deadweight + Pressure + HOSGRI/DDE + Nozzle/Piping Loads + Operating Loads[12]	Extended Structure: Pressure Boundary: Valve Nozzles: Bolting:	$\sigma_m \leq 2.0S$ $(\sigma_m$ or $\sigma_L)$ $+ \sigma_b \leq 2.4S$ ANSI B16.5 or MSS-SP-66 (6) $\sigma_m \leq 2.0S$

TABLE 3.9-2

COMPONENT (2, 3)	LOADING COMBINATIONS (4)	CRITERIA (7, 8, 9, 10, 11, 12, 13, 14)	
Inactive Cast Iron Pressure Retaining Components	Deadweight + Pressure + HOSGRI/DDE + Nozzle/Piping Loads + Operating Loads(12)	σ_p $(\sigma_m \text{ or } \sigma_L) + \sigma_b$	$0.1\ S_u$ $\leq 2.4 \times 0.1\ S_u$
Inactive Cast Iron Non-pressure Retaining Components	Deadweight + Pressure + HOSGRI/DDE + Nozzle/Piping Loads + Operating Loads(12)	$(\sigma_m \text{ or } \sigma_L) + \sigma_b$	$\leq 2.0 \times 0.2\ S_u$

Notes:

(1) See Chapter 5 Table 5.2-8 for structural components.

(2) Active: Mechanical equipment which is needed to go from normal full power operation to safe shutdown following the earthquake and which must perform mechanical motions during the course of accomplishing its design function.

(3) Inactive: Mechanical Equipment which is not required to perform mechanical motions in taking the plant from normal full power operation to safe shutdown following the earthquake.

(4) Nozzle loads shall include piping loads transmitted to the component during the HOSGRI/DDE earthquake.

(5) Piping loads at piping/active-valve interfaces shall be limited such that maximum fiber stresses in the piping at the interface are less than the piping yield strength at temperature (S_y).

(6) Valves, being stronger than the attached piping and having a proven history without any gross failures of pressure boundaries, can safely transmit piping loads without compromising their pressure retaining integrity. Therefore piping integrity assures valve integrity.

(7) σ_m = *General membrane stress. This stress is equal to the average stress across the solid section under consideration,* excludes discontinuities and concentrations and is produced only by mechanical loads.

Notes: (Cont'd)

(8) σ_L = Local membrane stress. This stress is equal to the same as σ_m except that it includes the effect of discontinuities.

(9) σ_b = Bending stress. This stress is equal to the linear varying portion of the stress across the solid section under consideration, excludes discontinuities and concentrations, and is produced only by mechanical loads.

(10) S = 1971 or 1974 ASME Code allowable stress. The allowable stress shall correspond to the highest metal temperature at the section under consideration during the condition consideration.

(11) S_y = 1971 or 1974 ASME Code minimum yield stress. The yield stress shall correspond to the highest metal temperature at the section under consideration during the condition consideration.

(12) Except racked-out valves.

(13) σ_p = Local membrane stress. This stress is equal to the average stress across the solid section under consideration. It excludes discontinuities and concentrations and is produced only by pressure.

(14) S_u = Material minimum tensile strength listed in either the code the component was purchased and manufactured under, or ASME Code Section III.

TABLE 3.9-3

HOSGRI AND DDE SEISMIC LOADING COMBINATIONS AND STRUCTURAL CRITERIA MECHANICAL EQUIPMENT SUPPORTS AND STRUCTURAL COMPONENT[1]

ELEMENT	LOADING COMBINATIONS (4, 5)	CRITERIA (6, 7, 8, 9, 10, 11, 12, 13)	
Linear[3]	Deadweight + HOSGRI/DDE + Nozzle/Piping Loads	1974 ASME Code Appendix XVII, Subsection NF, and Appendix F or AISC Manual, 7th Edition[11] (Stresses not to exceed S_y for active components supports)	
Plate and shell[2] (active components)	Deadweight + HOSGRI/DDE + Nozzle/Piping Loads	σ_m $(\sigma_m + \sigma_b)$	$\leq 1.2S$ $\leq 1.8S$ or S_y
Plate and shell (inactive components)	Deadweight + HOSGRI/DDE + Nozzle/Piping Loads	σ_m $(\sigma_m + \sigma_b)$	$\leq 2.0S$ $\leq 2.4S$
Bolts	Deadweight + HOSGRI/DDE + Nozzle/Piping Loads	1974 ASME Code Section III, Appendix XVII, Code Case 1644-6 and Appendix F, or AISC Manual, 7th Edition	

Notes:

(1) Includes reactor cavity manipulator crane, spent fuel pit bridge crane, flux mapping transfer devices and rcs seal table and parts. qualification of reactor cavity manipulator crane, spent fuel pit bridge crane, and flux mapping transfer device, not required for DDE (required for HOSGRI only in order to insure structural integrity and preclude seismic interaction).

(2) Plate and shell type supports: Plate and shell type components supports are supports such as vessel skirts and saddles which are fabricated from plate and shell elements and are normally subjected to a biaxial stress field.

Notes (Continued):

(3) Linear type support: A linear type component support is defined as acting under essentially as single components of direct stress. Such elements may also be subjected to shear stresses. Examples of such structural elements are: tension and compression struts, beams and columns subjected to bending, trusses, frames, rings, arches, and cables.

(4) Nozzle loads shall be those nozzle loads acting on the supported components during the HOSGRI/DDE earthquake.

(5) Plus operating loads, as applicable.

(6) σ_m = General membrane stress. This stress is equal to the average stress across the solid section under consideration, excludes discontinuities and concentrations and is produced only by mechanical loads.

(7) σ_b = Bending stress. This stress is equal to the linear varying portion of the stress across the solid section under consideration, excludes discontinuities and concentrations, and is produced only by mechanical loads.

(8) S = 1971 or 1974 ASME Code allowable stress value. The allowable stress shall correspond to the highest metal temperature at the section under consideration during the condition under consideration.

(9) S_y = 1971 or 1974 ASME Code minimum yield stress. The yield stress shall correspond to the highest metal temperature at the section under consideration during the condition under consideration.

(10) For the reactor cavity manipulator crane, the spent fuel pit bridge crane, and the flux mapping transfer device, the stress limits for the above loading combinations are obtained by increasing the normal condition allowable stresses by a factor of 1.7.

(11) The reference, "AISC Manual, 7th Edition," where used in this section, refers to the AISC Code, Part 5, "Specification for the Design, Fabrication and Erection of Structural Steel for Buildings," 1969 version.

(12) σ_p = Local membrane stress. This is equal to the average stress across the solid section under consideration. It excludes discontinuities and concentrations and is produced only by pressure.

(13) S_u = Material minimum tensile strength listed in either the code the component was purchased and manufactured under, or ASME Code Section III.

TABLE 3.9-4

DE SEISMIC LOADING COMBINATIONS AND STRUCTURAL CRITERIA MECHANICAL EQUIPMENT[1]

COMPONENT (2, 3)	LOADING COMBINATIONS (4)	CRITERIA (7, 8, 9, 10, 11, 12, 13, 14)	
Tanks, heat-exchangers filters, demineralizers	Deadweight + Pressure + DE + Nozzle/Piping Loads.	σ_m $(\sigma_m$ or $\sigma_L) + \sigma_b$	$\leq 1.0S$[13] $\leq 1.65S$
Active pumps	Deadweight + Pressure + DE + Nozzle/Piping Loads + Operating Loads.	σ_m $(\sigma_m$ or $\sigma_L) + \sigma_b$	$\leq 1.1S$ $\leq 1.65S$
Inactive pumps	Deadweight + Pressure + DE + Nozzle/Piping Loads + Operating Loads.	σ_m $(\sigma_m$ or $\sigma_m) + \sigma_b$	$\leq 1.1S$ $\leq 1.65S$
Active valves	Deadweight + Pressure + DE + Nozzle/Piping Loads + Operating Loads.[12]	Extended structure:	$\sigma_m \leq 1.1S$ $(\sigma_m$ or $\sigma_L)$ $+ \sigma_b \leq 1.0S_y$
		Pressure boundary: valve nozzles: bolting:	ANSI B16.5 or MSS-SP-66 (6) $\sigma_b \leq 2.0S$
Inactive valves	Deadweight + Pressure + DE + Nozzle/Piping Loads + Operating Loads.[12]	Extended structure:	$\sigma_b \leq 1.1S$ $(\sigma_m$ or $\sigma_L)$ $+ \sigma_b \leq 1.0S_y$
		Pressure boundary: valve nozzles: bolting:	ANSI B16.5 or MSS-SP-66 (6) $\sigma_m \leq 2.0S$

TABLE 3.9-4

COMPONENT (2, 3)	LOADING COMBINATIONS (4)	CRITERIA (7, 8, 9, 10, 11, 12, 13, 14)	
Inactive cast iron, pressure retaining components	Deadweight + Pressure + DE + Nozzle/Piping Loads + Operating Loads(12)	σ_p $(\sigma_m \text{ or } \sigma_L) + \sigma_b$	$\leq 0.1\ S_u$ $\leq 1.5 \times 0.1\ S_u$
Inactive cast iron non-pressure retaining Components	Deadweight + Pressure + DE + Nozzle/Piping Loads + Operating Loads(12)	$(\sigma_m \text{ or } \sigma_L) + \sigma_b$	$\leq 1.0 \times 0.2\ S_u$

Notes:

(1) See Chapter 5, Table 5.2.8 for sructural components.

(2) Active: Mechanical equipment which is needed to go from normal full power operation to safe shutdown following the earthquake and which must perform mechanical motions during the course of accomplishing its design function.

(3) Inactive: Mechanical equipment which is not required to perform mechanical motions in taking the plant from normal full power operations to safe shutdown following the earthquake.

(4) Nozzle loads shall include piping loads transmitted to the component during the DE earthquake.

(5) Deleted.

(6) Valves, being stronger than the attached piping and having a proven history without any gross failures of pressure boundaries, can safely transmit piping loads without compromising their pressure retaining integrity. Therefore, piping integrity assures valve integrity.

(7) σ_m = General membrane stress. This stress is equal to the average stress across the solid section under consideration, excludes discontinuities and concentrations and is produced only by mechanical loads.

(8) σ_L = Local membrane stress. This stress is the same as σ_m except that it includes the effect of discontinuities.

Notes (Continued):

(9) σ_b = Bending stress. The stress is equal to the linear varying portion of the stress across the solid section under consideration, excludes discontinuities and concentrations, and is produced only by mechanical loads.

(10) S_y = 1971 or 1974 ASME code allowable stress value. The allowable stress shall correspond to the highest metal temperature at the section under consideration during the condition under consideration.

(11) Except racked-out valves.

(12) The primary membrane stress limit for pressure vessels under DE loading is conservatively selected to be lower than the level permitted by the present ASME Code, in order to insure that it is also conservative with respect to earlier editions of the code of which these components were designed.

(13) σ_p = Local membrane stress. This is equal to the average stress across the solid section under consideration. It excludes discontinuities and concentrations and is produced only by pressure.

(14) S_u = Material minimum tensile strength listed in either the code the component was purchased and manufactured under, or ASME Code Section III.

TABLE 3.9-5

DE SEISMIC LOADING COMBINATION
STRUCTURAL CRITERIA MECHANICAL EQUIPMENT SUPPORTS
AND STRUCTURAL COMPONENTS[1]

ELEMENT (2, 3)	LOADING COMBINATIONS (4,5)	CRITERIA (6,7, 8)	
Linear[3]	Deadweight + DE + Pressure + Nozzle/Piping Loads	1974 ASME Code *Section* III Appendix XVII, Subsection NF or AISC Manual, 7th Edition.	
Plate and shell[2] (active components)	Deadweight + DE + Pressure + Nozzle/Piping Loads	σ_m $(\sigma_m + \sigma_b)$	$\leq$ 1.0S $\leq$ 1.5S
Plate and shell (inactive components)	Deadweight + DE + Pressure + Nozzle/Piping Loads	σ_m $(\sigma_m + \sigma_b)$	$\leq$ 1.0S $\leq$ 1.5S
Bolts	Deadweight + DE + Pressure + Nozzle/Piping Loads	1974 ASME Code Section III Appendix XVII, Code Case 1644-6 or AISC Manual, 7th Edition.	

Notes:

(1) Includes RCS seal table and parts. Qualification of reactor cavity manipulator crane and spent fuel pit bridge crane and flux mapping transfer *device not required for DE. Structural integrity insured by HOSGRI qualification.*

(2) Plate and shell type supports: Plate and shell type component supports are supports such as vessel skirts and saddles which are fabricated from plate and shell elements and are normally subjected to a biaxial stress field.

(3) Linear type support: A linear type component support is defined as acting under essentially a single component of direct stress. Such elements may also be subjected to shear stresses. Examples of such structural elements are: tension and compression struts, beams and columns subjected to bending, trusses, frames, rings, arches, and cables.

(4) Nozzle loads shall be those nozzle loads acting on the supported component during the DE earthquake.

(5) Plus Operating Loads, as applicable.

(6) σ_m = General membrane stress. This stress is equal to the average stress across the solid section under consideration, excludes discontinuities and concentrations and is produced only by mechanical loads.

(7) σ_b = Bending stress. This stress is equal to the linear varying portion of the stress across the solid section under consideration, excludes discontinuities and concentrations, and is produced only by mechanical loads.

(8) S_y = 1971 or 1974 code allowable stress value. The allowable stress shall correspond to the highest metal temperature at the section under consideration during the condition under consideration.

TABLE 3.9-6

NORMAL CONDITIONS LOADING COMBINATIONS AND STRUCTURAL CRITERIA MECHANICAL EQUIPMENT[1]

COMPONENT (2, 3)	LOADING COMBINATIONS (4)	CRITERIA (7, 8, 9, 10, 11, 12, 13)	
Tanks, heat-exchangers filters, demineralizers	Deadweight + Pressure + Nozzle/ Piping Loads.	σ_m $(\sigma_m$ or $\sigma_L) + \sigma_b$	$\leq 1.0S$ $\leq 1.5S$
Active pumps	Deadweight + Pressure + Nozzle/ Piping Loads + Operating Loads.	σ_m $(\sigma_m$ or $\sigma_L) + \sigma_b$	$\leq 1.0S$ $\leq 1.5S$
Inactive pumps	Deadweight + Pressure + Nozzle/ Piping Loads + Operating Loads.	σ_m $(\sigma_m$ or $\sigma_L) + \sigma_b$	$\leq 1.0S$ $\leq 1.5S$
Active valves	Deadweight + Pressure + Nozzle/ Piping Loads + Operating Loads.	Extended Structure:	$\sigma_m \leq 1.0S$ $(\sigma_m$ or $\sigma_L) +$ $\sigma_b \leq 1.5S$
		Pressure Boundary: Valve Nozzles: Bolting:	ANSI B16.5 or MSS-SP-66 (6) $\sigma_m \leq 2.0S$
Inactive valves	Deadweight + Pressure + Nozzle/ Piping Loads + Operating Loads.	Extended Structure:	$\sigma_m \leq 1.1S$ $(\sigma_m$ or $\sigma_L)$ $+ \sigma_b \leq 1.5S$
		Pressure Boundary: Valve Nozzles: Bolting:	ANSI B16.5 or MSS-SP-66 (6) $\sigma_m \leq 2.0S$

TABLE 3.9-6

COMPONENT (2, 3)	LOADING COMBINATIONS (4)	CRITERIA (7, 8, 9, 10, 11, 12, 13)	
Inactive cast iron, pressure retaining Components	Deadweight + Pressure + Nozzle/Piping Loads + Operating Loads(12)	σ_p $(\sigma_m$ or $\sigma_L) + \sigma_b$	$\leq 0.1\ S_u$ $\leq 1.5 \times 0.1\ S_u$
Inactive cost iron non-pressure retaining Components	Deadweight + Pressure + Nozzle/Piping Loads + Operating Loads(12)	$(\sigma_m$ or $\sigma_L) + \sigma_b$	$\leq 1.0 \times 0.2\ S_u$

Notes:

(1) See Chapter 5, Table 5.2.8 for structural components.

(2) Active: Mechanical equipment which is needed to go from normal full power operation to safe shutdown following the earthquake and which must perform mechanical motions during the course of accomplishing its design function.

(3) Inactive: Mechanical equipment which is not required to perform mechanical motions in taking the plant from normal full power operations to safe shutdown following the earthquake.

(4) Nozzle loads shall include piping loads transmitted to the component during the normal conditions.

(5) Deleted.

(6) Valves, being stronger than the attached piping and having a proven history without any gross failures of pressure boundaries, can safely transmit piping loads without compromising their pressure retaining integrity. Therefore, piping integrity assures valve integrity.

TABLE 3.9-6

Notes (Continued):

(7) σ_m = General membrane stress. This stress is equal to the average stress across the solid section under consideration, excludes discontinuities and concentrations and is produced only by mechanical loads.

(8) σ_L = Local membrane stress. This stress is the same as σ_m except that it includes the effect of discontinuities.

(9) σ_b = Bending stress. The stress is equal to the linear varying portion of the stress across the solid section under consideration, excludes discontinuities and concentrations, and is produced only by mechanical loads.

(10) S = 1971 or 1974 ASME code allowable stress value. The allowable stress shall correspond to the highest metal temperature at the section under consideration during the condition under consideration.

(11) S_y = 1971 or 1974 ASME code yield stress value. The yield stress shall correspond to the highest metal temperature at the section under consideration during the condition under consideration.

(12) S_p = Local membrane stress. This is equal to the average stress across the solid section under consideration. It excludes discontinuities and concentrations and is produced only by pressure.

(13) S_u = Material minimum tensile strength listed in either the code the component was purchased and manufactured under, or ASME Code Section III.

TABLE 3.9-7

NORMAL CONDITIONS LOADING COMBINATIONS AND STRUCTURAL CRITERIA MECHANICAL EQUIPMENT SUPPORTS AND STRUCTURAL COMPONENTS[1]

ELEMENT	LOADING COMBINATIONS [4, 5]	CRITERIA [6, 7, 8]	
Linear[3]	Deadweight + Nozzle/Piping Loads	1974 ASME Code Appendix XVII, Subsection NF or AISC Manual, 7th Edition	
Plate and shell[2] (active components)	Deadweight + Nozzle/Piping Loads	σ_m $(\sigma_m + \sigma_b)$	$\leq$ 1.0S (and/or 1974 ASME Code, $\leq$ 1.5S Subsection NF)
Plate and shell (inactive components)	Deadweight + Nozzle/Piping Loads	σ_m $(\sigma_m + \sigma_b)$	$\leq$ 1.0S (and/or 1974 ASME Codes, $\leq$ 1.5S Subsection NF)
Bolts	Deadweight + Nozzle/Piping Loads	1974 ASME Code Appendix XVII, Code Case 1644-6 or AISC Manual, 7th Edition	

TABLE 3.9-7

Notes:

(1) Includes RCS seal table and parts. Qualification of reactor cavity manipulator crane and spent fuel pit bridge crane and flux mapping transfer device not required for DE. Structural integrity insured by HOSGRI qualification.

(2) Plate and shell type supports: Plate and shell type component supports are supports such as vessel skirts and saddles which are fabricated from plate and shell elements and are normally subjected to a biaxial stress field.

(3) Linear type support: A linear type component support is defined as acting under essentially a single component of direct stress. Such elements may also be subjected to shear stresses. Examples of such structural elements are: tension and compression struts, beams and columns subjected to bending, trusses, frames, rings, arches, and cables.

(4) Nozzle loads shall be those nozzle loads acting on the supported component during the normal conditions.

(5) Plus Operating Loads, as applicable.

(6) σ_m = General membrane stress. This stress is equal to the average stress across the solid section under consideration, excludes discontinuities and concentrations and is produced only by mechanical loads.

(7) σ_b = B ending stress. This stress is equal to the linear varying portion of the stress across the solid section under consideration, excludes discontinuities and concentrations, and is produced only by mechanical loads.

(8) S = 1971 or 1974 code allowable stress value. The allowable stress shall correspond to the highest metal temperature at the section under consideration during the condition under consideration.

TABLE 3.9-8

TANK DESIGN

Storage Function	Design Code	Tank Plate Material	ASME Code Allowable Design Stress, (psi)	Code
Boric acid	ASME Sec. VIII, Div. 1 (no code stamp)	ASTM A240 T304	16,000	ASME Sec. VIII, Div. 1
Liquid holdup	ASME Sec. III, Class C	ASTM A240 T304	16,000	ASME Sec. VIII, Div. 1
Component cooling water surge	ASME Sec. VIII,	ASTM A285 Gr. C	13,750	ASME Sec. VIII, Div. 1
Waste gas decay	ASME Sec. III, Class C	ASTM A285 Gr. C	13,750	ASME Sec. VIII, Div. 1
Diesel fuel oil storage (underground)	UL 58	ASTM A36	12,650	ASME Sec. VIII, Div. 1
Volume control	ASME Sec. III, Class C	ASTM A240 T304	16,000	ASME Sec. VIII, Div. 1

TABLE 3.9-8

Storage Function	Design Code	Tank Plate Material	ASME Code Allowable Design Stress, (psi)	Code
Accumulator	ASME Sec. III, Class C	ASTM A516 Gr. 70 W/ A240 T304 Cladding	17,500	ASME Sec. VIII, Div. 1
Boron injection	ASME Sec. III, Class C	ASTM A516 Gr. 70 W/ A240 T304L Cladding	17,500	ASME Sec. VIII, Div. 1
Spray additive	ASME Sec. VIII, Div. 1 (no code stamp)	ASTM A240 T304	16,000	ASME Sec. VIII, Div. 1
Transfer storage & firewater	AWWA D100	ASTM A516 Gr. 60	19,500	ASME Sec. VIII, Div. 2
Reactor coolant drain tank	ASME Sec. III, Class C	ASTM A240 T304	16,000	ASME Sec. VIII, Div. 1
Waste concentrates holding	ASME Sec. III, Class C	ASTM A240 T304	16,000	ASME Sec. VIII, Div. 1

TABLE 3.9-8

Storage Function	Design Code	Tank Plate Material	ASME Code Allowable Design Stress, (psi)	Code
Spent Resin Storage	ASME Sec. III, Class C	ASTM A240 T304	16,000	ASME Sec. VIII, Div. 1
Equipment Drain Receiver	ASME Sec. VIII, Div. 1 (no code stamp)	ASTM A240 T304	16,000	ASME Sec. VIII, Div. 1

1. ASME Section III - American Society of Mechanical Engineers, Boiler and Pressure Vessel, Section III (1968, 1971).
2. ASME Section VIII - American Society of Mechanical Engineers, Boiler and Pressure Vessel Code, Section VIII (1968, 1971) Div. 1.
3. UL-58 - Underwriters Standards, Steel Underground Tanks for Flammable and Combustible Liquids.
4. AWWAD100 - American Waterworks Association, Standard for Steel Tanks, Standpipes Reservoirs and Elevated Tanks for Water Storage.

LIST OF ACTIVE VALVES

System or Service Description	Valve Identification	FSAR Fig. No.	Body Type	Size in.	Actuator Type	Valve Position On Failure	Position for Safe Shutdown[a]	Failure Analysis Comments
AUX FW PUMP 1 TURBINE GOV	FCV-15	3.2-4	Globe	-	Speed Governor	NA	Open	11
MSIV BYPASS – LEAD 4	FCV-22	3.2-4	Globe	3	Air	Closed	Closed	
MSIV BYPASS – LEAD 3	FCV-23	3.2-4	Globe	3	Air	Closed	Closed	
MSIV BYPASS – LEAD 2	FCV-24	3.2-4	Globe	3	Air	Closed	Closed	
MSIV BYPASS – LEAD 1	FCV-25	3.2-4	Globe	3	Air	Closed	Closed	
MAIN STM LEAD 2 TO AUX FW PUMP 1 TURBINE	FCV-37	3.2-4	Gate	4	Motor	FA	Operable	10, 25
MAIN STM LEAD 3 TO AUX FW PUMP 1 TURBINE	FCV-38	3.2-4	Gate	4	Motor	FA	Operable	10, 25
MAIN STEAM ISOL LEAD 1	FCV-41	3.2-4	Swing Check	28	Air	See Note 7	Closed	7
MAIN STEAM ISOL LEAD 2	FCV-42	3.2-4	Swing Check	28	Air	See Note 7	Closed	7
MAIN STEAM ISOL LEAD 3	FCV-43	3.2-4	Swing Check	28	Air	See Note 7	Closed	7

System or Service Description	Valve Identification	FSAR Fig. No.	Body Type	Size in.	Actuator Type	Valve Position On Failure	Position for Safe Shutdown[(a)]	Failure Analysis Comments
MAIN STEAM ISOL LEAD 4	FCV-44	3.2-4	Swing Check	28	Air	See Note 7	Closed	7
MN STM TO AUX FW PUMP 1 TURBINE	FCV-95	3.2-4	Gate	4	Motor	FA	Open	11
BORIC ACID BLENDER INLET	FCV-110A	3.2-8	Globe	2	Air	Open	Open	23
STEAM GEN NO. 1 TO BLOWDN TANK	FCV-151	3.2-8	Globe	3	Air	Closed	Closed	
AUX FP TURB 1 STM INLET	FCV-152	3.2-4	Globe	4	Manual	NA	Open	11
STEAM GEN NO. 2 TO BLOWDN TANK	FCV-154	3.2-4	Globe	3	Air	Closed	Closed	
STEAM GEN NO. 3 TO BLOWDN TANK	FCV-157	3.2-4	Globe	3	Air	Closed	Closed	
STEAM GEN NO. 4 TO BLOWDN TANK	FCV-160	3.2-4	Globe	3	Air	Closed	Closed	
CTMT H_2 SAMPLE SUPPLY IN CTMT	FCV-235	3.2-23	Globe	3/8	Solenoid	Closed	Operable	
CTMT H_2 SAMPLE SUPPLY OUT CTMT	FCV-236	3.2-23	Globe	3/8	Solenoid	Closed	Operable	

System or Service Description	Valve Identification	FSAR Fig. No.	Body Type	Size in.	Actuator Type	Valve Position On Failure	Position for Safe Shutdown[(a)]	Failure Analysis Comments
CTMT H_2 SAMPLE RETURN OUT CTMT	FCV-237	3.2-23	Globe	3/8	Solenoid	Closed	Operable	
CTMT H_2 SAMPLE SUPPLY IN CTMT	FCV-238	3.2-23	Globe	3/8	Solenoid	Closed	Operable	
CTMT H_2 SAMPLE SUPPLY OUT CTMT	FCV-239	3.2-23	Globe	3/8	Solenoid	Closed	Operable	
CTMT H_2 SAMPLE RETURN OUT CTMT	FCV-240	3.2-23	Globe	3/8	Solenoid	Closed	Operable	
STM GEN 4 BD SAMPLE OS CNTMT	FCV-244	3.2-4	Globe	¾	Air	Closed	Closed	
STM GEN 3 BD SAMPLE OS CNTMT	FCV-246	3.2-4	Globe	¾	Air	Closed	Closed	
STM GEN 2 BD SAMPLE OS CNTMT	FCV-248	3.2-4	Globe	¾	Air	Closed	Closed	
STM GEN 1 BD SAMPLE OS CNTMT	FCV-250	3.2-4	Globe	¾	Air	Closed	Closed	
RC DRN PPS DISCH IN CNTMT	FCV-253	3.2-19	Ball	2-1/2	Air	Closed	Closed	
RC DRN PPS DISCH OUT CNTMT	FCV-254	3.2-19	Ball	2-1/2	Air	Closed	Closed	

System or Service Description	Valve Identification	FSAR Fig. No.	Body Type	Size in.	Actuator Type	Valve Position On Failure	Position for Safe Shutdown[a]	Failure Analysis Comments
RC DRN TANK VENT HEADER IN CONTAINMENT	FCV-255	3.2-19	Ball	3/4	Air	Closed	Closed	
RC DRN TANK VENT HEADER OUT CONTAINMENT	FCV-256	3.2-19	Ball	3/4	Air	Closed	Closed	
RC DRN TANK GAS ANALYZER OUT CONTAINMENT	FCV-257	3.2-19	Ball	1/2	Air	Closed	Closed	
RC DRN TANK GAS ANALYZER IN CONTAINMENT	FCV-258	3.2-19	Ball	1/2	Air	Closed	Closed	
RC DRN TANK N2 SUPPLY OUT CONTAINMENT	FCV-260	3.2-19	Ball	3/4	Air	Closed	Closed	
CCW SUPPLY HEADER C	FCV-355	3.2-14	B'fly	20	Motor	FAI	Closed	
CCW TO RC PUMPS	FCV-356	3.2-14	B'fly	10	Motor	FAI	Closed	
RCP THERMAL BARRIER CCW RETURN	FCV-357	3.2-14	Globe	6	Motor	FAI	Closed	
EXCESS LETDOWN HT EXCH CCW RETURN	FCV-361	3.2-14	B'fly	4	Air	Closed	Closed	
RCP OIL COOLER CCW RETURN	FCV-363	3.2-14	B'fly	6	Motor	FAI	Closed	
RHR HT EXCHANGER 2 CCW RETURN	FCV-364	3.2-14	B'fly	12	Air	21	Functional	10

System or Service Description	Valve Identification	FSAR Fig. No.	Body Type	Size in.	Actuator Type	Valve Position On Failure	Position for Safe Shutdown[(a)]	Failure Analysis Comments
RHR HT EXCHANGER 3 CCW RETURN	FCV-365	3.2-14	B'fly	12	Air	21	Functional	10
CCW SUPPLY HEADER A	FCV-430	3.2-14	B'fly	30	Motor	FAI	Open	
CCW SUPPLY HEADER B	FCV-431	3.2-14	B'fly	30	Motor	FAI	Open	
RAW WATER STG RES AUX FEED PUMP 1	FCV-436	3.2-3	B'fly	8	Manual	FAI	Open	
RAW WATER STG RES AUX FEED PUMPS 2 & 3	FCV-437	3.2-3	B'fly	8	Manual	FAI	Open	
MAIN FEEDWATER ISOLATION LEAD 1	FCV-438	3.2-3	Gate	16	Motor	FAI	Closed	5
MAIN FEEDWATER ISOLATION LEAD 2	FCV-439	3.2-3	Gate	16	Motor	FAI	Closed	5
MAIN FEEDWATER ISOLATION LEAD 3	FCV-440	3.2-3	Gate	16	Motor	FAI	Closed	5
MAIN FEEDWATER ISOLATION LEAD 4	FCV-441	3.2-3	Gate	16	Motor	FAI	Closed	5
AUX SALTWATER PUMPS CROSS	FCV-495	3.2-17	B'fly	24	Motor	FAI	Operable	
AUX. SALTWATER PUMPS CROSS	FCV-496	3.2-17	B'fly	24	Motor	FAI	Operable	

System or Service Description	Valve Identification	FSAR Fig. No.	Body Type	Size in.	Actuator Type	Valve Position On Failure	Position for Safe Shutdown[a]	Failure Analysis Comments
CNT BLDG SUMP PP DISCHARGE IN CNTMT	FCV-500	3.2-19	Ball	2	Air	Closed	Closed	
CNT BLDG SUMP PP DISCHARGE OUT CNTMT	FCV-501	3.2-19	Ball	2	Air	Closed	Closed	
STEAM GEN 1 MAIN FW SUPPLY	FCV-510	3.2-3	Globe	16	Air	Closed	Closed	
STEAM GEN 2 MAIN FW SUPPLY	FCV-520	3.2-3	Globe	16	Air	Closed	Closed	
STEAM GEN 3 MAIN FW SUPPLY	FCV-530	3.2-3	Globe	16	Air	Closed	Closed	
STEAM GEN 4 MAIN FW SUPPLY	FCV-540	3.2-3	Globe	16	Air	Closed	Closed	
CNT WEST INSTRUMENT AIR	FCV-584	3.2-25	Ball	2	Air	Closed	Closed	
AUX SW TO CCW HT EXCH NO. 1	FCV-602	3.2-17	B'fly	24	Air	Open	21, 22	
AUX SW TO CCW HT EXCH NO. 2	FCV-603	3.2-17	B'fly	24	Air	Open	21, 22	
CNTMT FIRE WATER ISOLATION	FCV-633	3.2-18	Globe	3	Air	Closed	21, 22	

System or Service Description	Valve Identification	FSAR Fig. No.	Body Type	Size in.	Actuator Type	Valve Position On Failure	Position for Safe Shutdown[a]	Failure Analysis Comments
RHR PUMP 1 RECIRC	FCV-641A	3.2-10	Globe	2	Motor	FAI	Functional	
RHR PUMP 2 RECIRC	FCV-641B	3.2-10	Globe	2	Motor	FAI	Functional	
CNTMT ISO CHPS EXHAUST	FCV-658	3.2-23	Gate	4	Motor	FAI	Functional	
CNTMT ISO CHPS EXHAUST	FCV-659	3.2-23	Gate	4	Motor	FAI	Functional	
CONT PURGE SUPPLY IC	FCV-660	3.2-23	B'fly	48	Air	Closed	Closed	
CONT PURGE SUPPLY OC	FCV-661	3.2-23	B'fly	48	Air	Closed	Closed	
CONT VAC/PRESS RELIEF 1C	FCV-662	3.2-23	B'fly	12	Air	Closed	Closed	
CONT PRESSURE RELIEF OC	FCV-663	3.2-23	B'fly	12	Air	Closed	Closed	
CONT VACUUM RELIEF OC	FCV-664	3.2-23	B'fly	12	Air	Closed	Closed	
CNTMT ISO CHPS EXHAUST	FCV-668	3.2-23	Gate	4	Motor	FAI	Functional	
CNTMT ISO CHPS EXHAUST	FCV-669	3.2-23	Gate	4	Motor	FAI	Functional	
CNT AIR SAMPLE (INSIDE CNT)	FCV-678	3.2-23	Ball	1	Air	Closed	Closed	5
CNT AIR SAMPLE (OUTSIDE CNT)	FCV-679	3.2-23	Ball	1	Air	Closed	Closed	5

System or Service Description	Valve Identification	FSAR Fig. No.	Body Type	Size in.	Actuator Type	Valve Position On Failure	Position for Safe Shutdown[a]	Failure Analysis Comments
CNT AIR SAMPLE (OUTSIDE CNT)	FCV-681	3.2-23	Ball	1	Air	Closed	Closed	5
POST-LOCA SAMPLING SYST	FCV-696	3.2-19	Globe	3/8	Solenoid	Closed	Closed	5
POST-LOCA SAMPLING SYST	FCV-697	3.2-19	Globe	3/8	Solenoid	Closed	Closed	5
POST-LOCA SAMPLING SYST	FCV-698	3.2-23	Globe	3/8	Solenoid	Closed	Closed	5
POST-LOCA SAMPLING SYST	FCV-699	3.2-23	Globe	3/8	Solenoid	Closed	Closed	5
POST-LOCA SAMPLING SYST	FCV-700	3.2-23	Globe	3/8	Solenoid	Closed	Closed	5
RCP OIL COOLER CCW RETURN	FCV-749	3.2-14	B'fly	6	Motor	FAI	Closed	
RCP THERMAL BARRIER CCW RETURN	FCV-750	3.2-14	Globe	6	Motor	FAI	Closed	
STEAM GEN NO. 1 BLOWDOWN AND SAMPLE	FCV-760	3.2-4	Globe	3	Air	Closed	Closed	
STEAM GEN NO. 2 BLOWDOWN AND SAMPLE	FCV-761	3.2-4	Globe	3	Air	Closed	Closed	
STEAM GEN NO. 3 BLOWDOWN AND SAMPLE	FCV-762	3.2-4	Globe	3	Air	Closed	Closed	

System or Service Description	Valve Identification	FSAR Fig. No.	Body Type	Size in.	Actuator Type	Valve Position On Failure	Position for Safe Shutdown[(a)]	Failure Analysis Comments
STEAM GEN NO. 4 BLOWDOWN AND SAMPLE	FCV-763	3.2-4	Globe	3	Air	Closed	Closed	
STEAM GEN NO. 1 MAIN FW SUPPLY BY-PASS	FCV-1510	3.2-3	Globe	6	Air	Closed	Closed	
STEAM GEN NO. 2 MAIN FW SUPPLY BY-PASS	FCV-1520	3.2-3	Globe	6	Air	Closed	Closed	
STEAM GEN NO. 3 MAIN FW SUPPLY BY-PASS	FCV-1530	3.2-3	Globe	6	Air	Closed	Closed	
STEAM GEN NO. 4 MAIN FW SUPPLY BY-PASS	FCV-1540	3.2-3	Globe	6	Air	Closed	Closed	
CHG PUMPS DISCH TO REGEN HT EXCH	HCV-142	3.2-4	Globe	3	Air	Closed	21	23
RHR TO COLD LEGS 3 & 4	HCV-637	3.2-10	Ball	8	Air	Open	Open	
RHR TO COLD LEGS 1 & 2	HCV-638	3.2-10	Ball	8	Air	Open	Open	
DSL FO DAY TK 1-2 HEADER B	LCV-85	3.2-21	Ball	1-1/2	Air	Closed	Functional	
DSL FO DAY TK 2-1 HEADER B	LCV-86	3.2-21	Ball	1-1/2	Air	Closed	Functional	
DSL FO DAY TK 1-3 HEADER B	LCV-87	3.2-21	Ball	1-1/2	Air	Closed	Functional	
DSL FO DAY TK 1-2 HEADER A	LCV-88	3.2-21	Ball	1-1/2	Air	Closed	Functional	

System or Service Description	Valve Identification	FSAR Fig. No.	Body Type	Size in.	Actuator Type	Valve Position On Failure	Position for Safe Shutdown[a]	Failure Analysis Comments
DSL FO DAY TK 2-1 HEADER A	LCV-89	3.2-21	Ball	1-1/2	Air	Closed	Functional	
DSL FO DAY TK 1-3 HEADER A	LCV-90	3.2-21	Ball	1-1/2	Air	Closed	Functional	
AUX FEEDWATER FROM TURB AFW PP TO SG 1	LCV-106	3.2-3	Globe	2	Motor	FAI	Operable	4
AUX FEEDWATER FROM TURB AFW PP TO SG 2	LCV-107	3.2-3	Globe	2	Motor	FAI	Operable	4
AUX FEEDWATER FROM TURB AFW PP TO SG 3	LCV-108	3.2-3	Globe	2	Motor	FAI	Operable	4
AUX FEEDWATER FROM TURB AFW PP TO SG 4	LCV-109	3.2-3	Globe	2	Motor	FAI	Operable	4
AUX FEEDWATER FROM MOTOR AFW PP TO SG 1	LCV-110	3.2-3	Globe	2	Electro Hydraulic	Open	Operable	4
AUX FEEDWATER FROM MOTOR AFW PP TO SG 2	LCV-111	3.2-3	Globe	2	Electro Hydraulic	Open	Operable	4
VOLUME CONTROL TANK TO CHARG PUMPS	LCV-112B	3.2-8	Gate	4	Motor	FAI	Closed	5
VOLUME CONTROL TANK TO CHARG PUMPS	LCV-112C	3.2-8	Gate	4	Motor	FAI	Closed	5
AUX FEEDWATER FROM MOTOR AFW PP TO SG 4	LCV-113	3.2-3	Globe	2	Electro Hydraulic	Open	Operable	4

System or Service Description	Valve Identification	FSAR Fig. No.	Body Type	Size in.	Actuator Type	Valve Position On Failure	Position for Safe Shutdown[(a)]	Failure Analysis Comments
AUX FEEDWATER FROM MOTOR AFW PP TO SG 3	LCV-115	3.2-3	Globe	2	Electro Hydraulic	Open	Operable	4
STEAM GEN 1 10% ATM STM DUMP	PCV-19	3.2-4	Globe	8	Air	Closed	Functional 21	
STEAM GEN 2 10% ATM STM DUMP	PCV-20	3.2-4	Globe	8	Air	Closed	Functional 21	
STEAM GEN 3 10% ATM STM DUMP	PCV-21	3.2-4	Globe	8	Air	Closed	Functional 21	
STEAM GEN 4 10% ATM STM DUMP	PCV-22	3.2-4	Globe	8	Air	Closed	Functional 21	
PRESSURIZER POWER-OPERATED RELIEF	PCV-455C	3.2-7	Globe	3	Air	Closed	Functional 21	8,12
PRESSURIZER POWER-OPERATED RELIEF	PCV-456	3.2-7	Globe	3	Air	Closed	Functional 21	8,12
CONT PURGE EXHAUST 1C	RCV-11	3.2-23	B'fly	48	Air	Closed	Closed	
CONT PURGE EXHAUST OC	RCV-12	3.2-23	B'fly	48	Air	Closed	Closed	
MAIN STM SAFETY LEAD 1	RV-3	3.2-4	Relief	6	Spring	NA	Operable	9
MAIN STM SAFETY LEAD 1	RV-4	3.2-4	Relief	6	Spring	NA	Operable	9

System or Service Description	Valve Identification	FSAR Fig. No.	Body Type	Size in.	Actuator Type	Valve Position On Failure	Position for Safe Shutdown[(a)]	Failure Analysis Comments
MAIN STM SAFETY LEAD 1	RV-5	3.2-4	Relief	6	Spring	NA	Operable	9
MAIN STM SAFETY LEAD 1	RV-6	3.2-4	Relief	6	Spring	NA	Operable	9
MAIN STM SAFETY LEAD 2	RV-7	3.2-4	Relief	6	Spring	NA	Operable	9
MAIN STM SAFETY LEAD 2	RV-8	3.2-4	Relief	6	Spring	NA	Operable	9
MAIN STM SAFETY LEAD 2	RV-9	3.2-4	Relief	6	Spring	NA	Operable	9
MAIN STM SAFETY LEAD 2	RV-10	3.2-4	Relief	6	Spring	NA	Operable	9
MAIN STM SAFETY LEAD 3	RV-11	3.2-4	Relief	6	Spring	NA	Operable	9
MAIN STM SAFETY LEAD 3	RV-12	3.2-4	Relief	6	Spring	NA	Operable	9
MAIN STM SAFETY LEAD 3	RV-13	3.2-4	Relief	6	Spring	NA	Operable	9
MAIN STM SAFETY LEAD 3	RV-14	3.2-4	Relief	6	Spring	NA	Operable	9
CCW SURGE TK RV	RV-45	3.2-14	Relief	3	Spring	NA	Operable	
MAIN STM SAFETY LEAD 4	RV-58	3.2-4	Relief	6	Spring	NA	Operable	9
MAIN STM SAFETY LEAD 4	RV-59	3.2-4	Relief	6	Spring	NA	Operable	9
MAIN STM SAFETY LEAD 4	RV-60	3.2-4	Relief	6	Spring	NA	Operable	9

System or Service Description	Valve Identification	FSAR Fig. No.	Body Type	Size in.	Actuator Type	Valve Position On Failure	Position for Safe Shutdown[a]	Failure Analysis Comments
MAIN STM SAFETY LEAD 4	RV-61	3.2-4	Relief	6	Spring	NA	Operable	9
MAIN STM SAFETY LEAD 1	RV-222	3.2-4	Relief	6	Spring	NA	Operable	9
MAIN STM SAFETY LEAD 2	RV-223	3.2-4	Relief	6	Spring	NA	Operable	9
MAIN STM SAFETY LEAD 3	RV-224	3.2-4	Relief	6	Spring	NA	Operable	9
MAIN STM SAFETY LEAD 4	RV-225	3.2-4	Relief	6	Spring	NA	Operable	9
FIRE WATER TANK CROSSTIE	8X42B (FP-0-306)	3.2-18	Gate	8	Manual	NA	Open	
FIRE WATER TANK CROSSTIE BYPASS	8X42B (FP-0-307)	3.2-18	Gate	8	Manual	NA	Open	
PRESSURIZER POWER RELIEF ISO	8000A	3.2-7	Gate	3	Motor	FAI	Operable	
PRESSURIZER POWER RELIEF ISO	8000B	3.2-7	Gate	3	Motor	FAI	Operable	
PRESSURIZER POWER RELIEF ISO	8000C	3.2-7	Gate	3	Motor	FAI	Operable	
PRESSURIZER SAFETY	8010A	3.2-7	R.V.	6	Spring	NA	Functional	9
PRESSURIZER SAFETY	8010B	3.2-7	R.V.	6	Spring	NA	Functional	9

System or Service Description	Valve Identification	FSAR Fig. No.	Body Type	Size in.	Actuator Type	Valve Position On Failure	Position for Safe Shutdown[a]	Failure Analysis Comments
PRESSURIZER SAFETY	8010C	3.2-7	R.V.	6	Spring	NA	Functional	9
PRESSURIZER RELIEF TK PRIMARY WTR	8029	3.2-7	Ball	3	Air	Closed	Closed	
PRESSURIZER RELIEF TK GAS ANALYZER IC	8034A	3.2-7	Globe	3/8	Air	Closed	Closed	
PRESSURIZER RELIEF TK GAS ANALYZER OC	8034B	3.2-7	Globe	3/8	Air	Closed	Closed	
PRESSURIZER RELIEF TK N2 SUPPLY	8045	3.2-7	Dia-phragm	3/4	Air	Closed	Closed	
REACTOR VESSEL HEAD VENT SYS	8078A	3.2-7	Globe	1	Solenoid	Closed	Operable	
REACTOR VESSEL HEAD VENT SYS	8078B	3.2-7	Globe	1	Solenoid	Closed	Operable	
REACTOR VESSEL HEAD VENT SYS	8078C	3.2-7	Globe	1	Solenoid	Closed	Operable	
REACTOR VESSEL HEAD VENT SYS	8078D	3.2-7	Globe	1	Solenoid	Closed	Operable	
REACTOR COOL PPS SEAL WTR RET	8100	3.2-7	Gate	4	Motor	FAI	Closed	

System or Service Description	Valve Identification	FSAR Fig. No.	Body Type	Size in.	Actuator Type	Valve Position On Failure	Position for Safe Shutdown[(a)]	Failure Analysis Comments
BORIC ACID TO CHARGING PPS	8104	3.2-8	Globe	2	Motor	FAI	Operable	
CENTRIFUGAL I CHG PPS RECRC	8105	3.2-8	Globe	2	Motor	FAI	Functional	5
CENTRIFUGAL CHG PPS RECRC	8106	3.2-8	Globe	2	Motor	FAI	Functional	5
CHG PPS DISCH TO LETDOWN HX	8107	3.2-8	Gate	3	Motor	FAI	Functional	
CHG PPS DISCH TO LETDOWN HX	8108	3.2-8	Gate	3	Motor	FAI	Functional	
REACT COOL PPS SEAL WTR RET	8112	3.2-8	Gate	4	Motor	FAI	Closed	
LETDOWN LINE RV	8117	3.2-8	Relief	2	Spring	Open	Closed	
RCP SEAL WTR RTN RV	8121	3.2-8	Relief	2	Spring	Open	Closed	
SEAL WTR HX INLET RV	8123	3.2-8	Relief	2	Spring	Open	Closed	
CHARGING PUMP SUCTION HEADER	8125	3.2-8	Relief	3/4	Spring	Open	Closed	
PRESSURIZER AUX SPRAY	8145	3.2-8	Globe	2	Air	Closed	Operable 21	

System or Service Description	Valve Identification	FSAR Fig. No.	Body Type	Size in.	Actuator Type	Valve Position On Failure	Position for Safe Shutdown[a]	Failure Analysis Comments
CHG PUMP TO LOOP 4 COLD LEG	8146	3.2-8	Globe	3	Air	Open	Operable 21	
CHG PUMP TO LOOP 3 COLD LEG	8147	3.2-8	Globe	3	Air	Open	Operable 21	
RCS PRESSURIZER AUX SPRAY	8148	3.2-8	Globe	2	Air	Closed	Operable 21	
LETDOWN LINE ISOL	8149A	3.2-8	Globe	2	Air	Closed	Closed	
LETDOWN LINE ISOL	8149B	3.2-8	Globe	2	Air	Closed	Closed	
LETDOWN LINE ISOL	8149C	3.2-8	Globe	2	Air	Closed	Closed	
LETDOWN LINE ISOL	8152	3.2-8	Globe	2	Air	Closed	Closed	
CCP 1 FCV-128 MANUAL BYPASS	8387B	3.2-8	Globe	3	Manual	NA	Functional	23
CCP 2 FCV-128 MANUAL BYPASS	8387C	3.2-8	Globe	3	Manual	NA	Functional	23
HCV-142 MANUAL BYPASS	8403	3.2-8	Globe	3	Manual	NA	Functional	23
MANUAL EMERGENCY BORATE VALVE	8471	3.2-08	Diaphragm	2	Manual	NA	Functional	23

System or Service Description	Valve Identification	FSAR Fig. No.	Body Type	Size in.	Actuator Type	Valve Position On Failure	Position for Safe Shutdown[a]	Failure Analysis Comments
BA TRANSFER PUMP SUCTION CROSSTIE	8476	3.2-8	Diaphragm	2	Manual	NA	Open	23
RHR PP 1 SUCT	8700A	3.2-10	Gate	14	Motor	FAI	Operable	
RHR PP 2 SUCT	8700B	3.2-10	Gate	14	Motor	FAI	Operable	
RHR SUCTION FROM LOOP 4 HOT LEG	8701	3.2-10	Gate	14	Motor	FAI	Operable	
RHR SUCTION FROM LOOP 4 HOT LEG	8702	3.2-10	Gate	14	Motor	FAI	Operable	
RHR DISCHARGE TO HOT LEGS 1 & 2	8703	3.2-10	Gate	12	Motor	FAI	Functional	10, 19
RHR SUCTION PIPING RV	8707	3.2-10	Relief	3	Spring	Open	Closed	
RHR COOLDOWN LINE RV	8708	3.2-10	Relief	3/4	Spring	Open	Closed	
RHR HT EXCH 1 TO RCS HOT LEGS 1 & 2	8716A	3.2-10	Gate	8	Motor	FAI	Operable	
RHR HT EXCH 2 TO RCS HOT LEGS 1 & 2	8716B	3.2-10	Gate	8	Motor	FAI	Operable	
CHARGING INJECT LINE DISCHARGE	8801A	3.2-9	Gate	4	Motor	FAI	Open	

System or Service Description	Valve Identification	FSAR Fig. No.	Body Type	Size in.	Actuator Type	Valve Position On Failure	Position for Safe Shutdown[a]	Failure Analysis Comments
CHARGING INJECT LINE DISCHARGE	8801B	3.2-9	Gate	4	Motor	FAI	Open	
SAFETY INJECT PUMP 1 DISCH TO HOT LEGS 1 & 2	8802A	3.2-9	Gate	4	Motor	FAI	Operable	19
SAFETY INJECT PUMP 2 DISCH TO HOT LEGS 3 & 4	8802B	3.2-9	Gate	4	Motor	FAI	Operable	19
CHARG PUMPS TO CHARGING INJECT LINE	8803A	3.2-9	Gate	4	Motor	FAI	Open	10
CHARG PUMPS TO CHARGING INJECT LINE	8803B	3.2-9	Gate	4	Motor	FAI	Open	10
RHR HT EXCH 1 TO CHG PPS SUCT	8804A	3.2-9	Gate	8	Motor	FAI	Functional	13
RHR HT EXCH 2 TO CHG PPS SUCT	8804B	3.2-9	Gate	8	Motor	FAI	Functional	13
RWST TO CHARG PUMP SUCT	8805A	3.2-9	Gate	8	Motor	FAI	Open	10
RWST TO CHARG PUMP SUCT	8805B	3.2-9	Gate	8	Motor	FAI	Open	10
CHARGING PPS SIS PPS SUC CROSSTIE	8807A	3.2-9	Gate	4	Motor	FAI	Functional	10, 13

System or Service Description	Valve Identification	FSAR Fig. No.	Body Type	Size in.	Actuator Type	Valve Position On Failure	Position for Safe Shutdown[a]	Failure Analysis Comments
CHARGING PPS SIS PPS SUC CROSSTIE	8807B	3.2-9	Gate	4	Motor	FAI	Functional	10, 13
RHR HT EXCH 1 TO COLD LEGS 1 & 2	8809A	3.2-9	Gate	8	Motor	FAI	Functional	20
RHR HT EXCH 2 TO COLD LEGS 3 & 4	8809B	3.2-9	Gate	8	Motor	FAI	Functional	20
SIS PUMP 1 DISCH TO COLD LEGS	8821A	3.2-9	Gate	4	Motor	FAI	Functional	
SIS PUMP 2 DISCH TO COLD LEGS	8821B	3.2-9	Gate	4	Motor	FAI	Functional	
SIS PUMP DISCH TO COLD LEGS	8835	3.2-9	Gate	4	Motor	FAI	Open	14
SI PUMP DISCHARGE RV	8851	3.2-9	Relief	¾	Spring	Open	Closed	
SI PUMP DISCHARGE RV	8853A	3.2-9	Relief	¾	Spring	Open	Closed	
SI PUMP DISCHARGE RV	8853B	3.2-9	Relief	¾	Spring	Open	Closed	
ACCUM RV	8855A	3.2-9	Relief	1	Spring	Open	Closed	
ACCUM RV	8855B	3.2-9	Relief	1	Spring	Open	Closed	
ACCUM RV	8855C	3.2-9	Relief	1	Spring	Open	Closed	

System or Service Description	Valve Identification	FSAR Fig. No.	Body Type	Size in.	Actuator Type	Valve Position On Failure	Position for Safe Shutdown[(a)]	Failure Analysis Comments
ACCUM RV	8855D	3.2-9	Relief	1	Spring	Open	Closed	
RHR HT EXCH OUTLET RELIEF RV	8856A	3.2-10	Relief	2	Spring	Open	Closed	
RHR HT EXCH OUTLET RELIEF	8856B	3.2-10	Relief	2	Spring	Open	Closed	
SI PUMP SUCT HEADER RV	8858	3.2-9	Relief	3/4	Spring	Open	Closed	
ACCUM TEST IN CTMT	8871	3.2-9	Globe	3/4	Air	Closed	Closed	
ACCUM N2 SUPPLY HEADER	8880	3.2-9	Globe	1	Air	Closed	Closed	
SAFETY INJECTION TEST LINE	8883	3.2-9	Globe	3/4	Air	Closed	Closed	5
SAFETY INJECT PUMP NO. 1 SUCT	8923A	3.2-9	Gate	6	Motor	FAI	Operable	
SAFETY INJECT PUMP NO. 2 SUCT	8923B	3.2-9	Gate	6	Motor	FAI	Operable	
ACCUM TEST OUTSIDE CONTAINMENT	8961	3.2-9	Globe	3/4	Air	Closed	Closed	
SAFETY INJECT PUMP MIN. RECIRC. VALVES	8974A	3.2-9	Globe	2	Motor	FAI	Operable	
SAFETY INJECT PUMP MIN. RECIRC. VALVES	8974B	3.2-9	Globe	2	Motor	FAI	Operable	

System or Service Description	Valve Identification	FSAR Fig. No.	Body Type	Size in.	Actuator Type	Valve Position On Failure	Position for Safe Shutdown[(a)]	Failure Analysis Comments
RWST TO SAFETY INJECTION PUMP SUCT	8976	3.2-9	Gate	8	Motor	FAI	Open	14
RWST TO RHR PUMP SUCTION	8980	3.2-9	Gate	12	Motor	FAI	Operable	14
CNTMT SUMP TO RHR PP1 SUCT	8982A	3.2-10	Gate	14	Motor	FAI	Operable	
CNTMT SUMP TO RHR PP2 SUCT	8982B	3.2-10	Gate	14	Motor	FAI	Operable	
SPRAY ADDITIVE SYSTEM	8987	3.2-12	Relief	3/4	Spring	Open	Close	
SPRAY ADD TK OUT ISOL	8994A	3.2-12	Gate	3	Motor	FAI	Open	10
SPRAY ADD TK OUT ISOL	8994B	3.2-12	Gate	3	Motor	FAI	Open	10
CNTMT SPRAY PP 1 DISCHG	9001A	3.2-12	Gate	8	Motor	FAI	Open	10
CNTMT SPRAY PP 2 DISCHG	9001B	3.2-12	Gate	8	Motor	FAI	Open	10
RHR HT EXCH 1 TO CONT SPRAY	9003A	3.2-12	Gate	8	Motor	FAI	Open	10
RHR HT EXCH 2 TO CONT SPRAY	9003B	3.2-12	Gate	8	Motor	FAI	Open	10

System or Service Description	Valve Identification	FSAR Fig. No.	Body Type	Size in.	Actuator Type	Valve Position On Failure	Position for Safe Shutdown[a]	Failure Analysis Comments
RCS SAMPLE	9351A	3.2-11	Globe	3/8	N_2	Closed	Operable (21)	23
RCS SAMPLE	9351B	3.2-11	Globe	3/8	N_2	Closed	Operable (21)	23
PRESS STEAM SPACE IN CONTMT	9354A	3.2-7	Globe	3/8	Air	Closed	Closed	
PRESS STEAM SPACE OUT CONTMT	9354B	3.2-7	Globe	3/8	Air	Closed	Closed	
PRESS LIQUID SPACE IN CONTMT	9355A	3.2-7	Globe	3/8	Air	Closed	Closed	
PRESS LIQUID SPACE OUT CONTMT	9355B	3.2-7	Globe	3/8	Air	Closed	Closed	
HOT LEGS 1 & 4 IN CONTMT SAMPLE	9356A	3.2-7	Globe	3/8	N_2	Closed	Operable 21	
HOT LEGS 1 & 4 IN CONTMT SAMPLE	9356B	3.2-7	Globe	3/8	N_2	Closed	Operable 21	
ACCUM SAMPLE HDR IN CONTAINMENT	9357A	3.2-9	Globe	3/8	Air	Closed	Closed	
ACCUM SAMPLE HDR OUT CONTAINMENT	9357B	3.2-9	Globe	3/8	Air	Closed	Closed	

System or Service Description	Valve Identification	FSAR Fig. No.	Body Type	Size in.	Actuator Type	Valve Position On Failure	Position for Safe Shutdown[a]	Failure Analysis Comments
CCW PUMP SUCT CROSSTIE VALVE (2 VALVES ON LINES 97 & 2285)	CCW-4 & -5	3.2-14	B'fly	20	Manual	NA	Closed	
CCW PUMP 1-2 DISCH ISOLATION (TO HDR B)	CCW-16	3.2-14	B'fly	20	Manual	NA	Closed	
CCW PUMP 1-3 DISCH ISOLATION (TO HDR B)	CCW-17	3.2-14	B'fly	20	Manual	NA	Closed	
CCW PUMP 1-1 DISCH ISOLATION (TO HDR A)	CCW-18	3.2-14	B'fly	20	Manual	NA	Closed	
CCW PUMP 1-2 DISCH ISOLATION (TO HDR A)	CCW-19	3.2-14	B'fly	20	Manual	NA	Closed	
CCW HDR C SUPPLY FROM HDR A	CCW-23	3.2-14	B'fly	24	Manual	NA	Closed	
CCW HDR C SUPPLY FROM HDR B	CCW-24	3.2-14	B'fly	24	Manual	NA	Closed	
MAIN STEAM LEAD ONE 10% STEAM DUMP ISOLATION	MS-1015	3.2-4	Gate	8	Manual	NA	Closed Note 24	
MAIN STEAM LEAD TWO 10% STEAM DUMP ISOLATION	MS-2015	3.2-4	Gate	8	Manual	NA	Closed Note 24	
MAIN STEAM LEAD THREE 10% STEAM DUMP ISOLATION	MS-3015	3.2-4	Gate	8	Manual	NA	Closed Note 24	

System or Service Description	Valve Identification	FSAR Fig. No.	Body Type	Size in.	Actuator Type	Valve Position On Failure	Position for Safe Shutdown[a]	Failure Analysis Comments
MAIN STEAM LEAD FOUR 10% STEAM DUMP ISOLATION	MS-4015	3.2-4	Gate	8	Manual	NA	Closed Note 24	

(a) The valves whose positions are listed in this column are those valves whose operability is relied on to perform an active function such as safe shutdown of the reactor or mitigation of the consequences of a Design Basis Accident coincidental with loss of offsite power. An entry of "functional" or equivalently "operable" means that the valve must be capable of being opened and/or closed to perform its active function. For DCPP, safe shutdown is defined as Mode 3 following an accident (SSER 7 and SSER 22), Mode 5 following a Hosgri earthquake (Section 3.7.6.2), and Mode 3, followed by Mode 5 within 72 hours, following an Appendix R fire (10 CFR 50, Appendix R).

Failure Analysis Comment Notes:

1. Deleted in Revision 9.
2. Deleted in Revision 9.
3. Deleted in Revision 9.
4. Valve is provided for control. Failure, open or close, is remedied by redundant train and EOP RNO actions.
5. Valve provides isolation. Failure to close is remedied by valve in series.
6. Deleted in Revision 9.
7. Locally mounted air accumulators protected against compressed air system failure by check valves can hold open the main steam isolation valves for a short duration of time after the compressed air system is lost. In the event of loss of all air to the main steam isolation valves, the valves will fail closed.
8. These valves are provided for controlled steam release. Failure to open is remedied by redundant valves. Failure to close is remedied by closure of series valve or system shutdown.
9. These valves provide vessel protection. Failure to open is remedied by redundant valves in parallel. Valve size limits flow on failure to close.
10. Valve provides isolation. Failure to close (or stay closed) is remedied by a redundant valve in series. Failure to open (or stay open) is remedied by a redundant line (or system).
11. Valve opens to start device. Failure to open is remedied by use of redundant system.
12. Air-operated valve operation is not required for safe shutdown.
13. Used during recirculation mode.

Failure Analysis Comment Notes (continued)

14. Valve provides isolation. Failure to stay open could defeat system function. "Hot" short could close valve, but is not considered credible.
15. Deleted in Revision 9.
16. Deleted in Revision 9.
17. Deleted in Revision 9.
18. Deleted in Revision 9.
19. Valves operated (opened) during changeover from cold leg recirculation to hot leg injection. Failure to stay closed during cold leg injection or cold leg recirculation could defeat system function. "Hot" short could open valve but is not considered credible.
20. Valve 8809A operated (closed) during the changeover from cold leg injection to cold leg recirculation. Valve 8809B operated (closed) during the changeover from cold leg recirculation to hot leg recirculation. Failure of one valve to stay open during cold leg injection remedied by redundant system.
21. Air operated valves required to operate or maintain position after a loss of the compressed air system are supplied with compressed gas from the backup air/nitrogen supply system. See Section 9.3.1.6 for details.
22. If one of the CCW heat exchangers is valved out-of-service, then backup air is supplied to the respective CCW heat exchanger saltwater inlet valve to maintain the valve closed. This ensures all ASW flow is directed to in-service CCW heat exchangers.
23. Valve does not have an active safety function to support accident mitigation or Mode 3 safe shutdown. Valve is active to support achieving post-Hosgri cold shutdown in the manner defined in the Hosgri Report. Valve needs to be seismically qualified for active function for Hosgri only.
24. Valve has an active safety function to support accident mitigation or Mode 3 safe shutdown. Valve is passive to support achieving post-Hosgri cold shutdown in the manner defined in the Hosgri Report.
25. Normal position for Safe Shutdown is Open. For Containment Isolation and the condition described in section 6.5.3.4, valve must be Operable.

Abbreviations:

FCV	=	Flow control valve	RCP	=	Reactor coolant pump	B'fly	=	Butterfly
LCV	=	Level control valve	FAI	=	Fail as is	RC	=	Reactor coolant
PCV	=	Pressure control valve	PP & PPS	=	Pump(s)	CCW	=	Component cooling water
HCV	=	Hand control valve	CNT	=	Containment	RHR	=	Residual heat removal
RV	=	Relief valve	CHG	=	Charging	AWF	=	Auxiliary feedwater
TCV	=	Temperature control valve	DSL FO	=	Diesel fuel oil	NA	=	Not applicable

TABLE 3.9-10

MAXIMUM DEFLECTIONS ALLOWED FOR REACTOR INTERNAL SUPPORT STRUCTURES FOR FAULTED CONDITIONS

Component	Allowable Deflection, Inches	No Loss of Function Deflection, Inches
Upper Barrel		
Radial inward	4.1	8.2
Radial outward	1.0	1.0
Upper Core Plate	0.100[a]	0.150
Rod Cluster Control Guide Tubes	1.0	1.75

(a) Only to ensure that the plate will not touch a guide tube.

PRESSURIZED GAS CONTAINERS (Above 100 psig)

Vessel	Design Class	Design Code	Design Pressure	Vessel Operating Pressure	Vessel Volume[c]	Type Relief Device[a]	Relief Set-point	Stored Energy ft-lb(ea)	Attached Piping Vessel Location	Attached Piping Design Class	Attached Piping Largest Size	Deviations from OSHA 29 CFR Section 1910
CO_2 storage tanks (Cardox)	I	ASME B&PV Code Sec. VIII	363 psig	300 psig	7.5 ton	Relief valve Pop safety	341 psig 357 psig	N.A.[b]	Turbine building	II	6 in.	None
Diesel generator starting air receivers	I	ASME B&PV Code Sec. VIII	342 psig	250 psig	53 cu ft	Relief valve	260 psig	3×10^6	Turbine building	I	2 in.	None
Diesel generator turbocharger booster air receivers	I	ASME B&PV Code Sec. VIII	342 psig	250 psig	106 cu ft	Relief valve	260 psig	5.9×10^6	Turbine building	I	2 in.	None
Air plant receiver	II	ASME B&PV Code Sec. VIII-Div. I	120 psig	110 psig	650 cu ft	Relief valve	115 psig	12.6×10^6	Turbine building	III	4 in.	None
N_2 storage vessels	II	ASME B&PV Code Sec. VIII Case 1205	2450 psig	2200 psig	51 cu ft per vessel	Relief valve rupture disk	2450 psig 3500 psig ± 5%	34.5×10^6	Yard vault	III	3/4 in.	None
Instrument air receivers	II	ASME B&PV Code Sec. VIII	120 psig	105 psig per receiver 2 receivers	152 cu ft	Relief valve	110 psig	3×10^6	Auxiliary building & intake Structure	III	2 in.	None
H_2 storage vessels	II	ASME B&PV Code Sec VIII Case1205	2450 psig	2200 psig	51 cu. ft. per vessel 6 vessels	Relief Valve Rupture Disc	2450 psig 3500 psig ± 5%	34.5×10^6	Yard Vault	III	3/4 in.	None

TABLE 3.9-11

Vessel	Design Class	Design Code	Design Pressure	Vessel Operating Pressure	Vessel Volume(c)	Type Relief Device[a]	Relief Set-point	Stored Energy ft-lb(ea)	Attached Piping: Vessel Location	Attached Piping: Design Class	Attached Piping: Largest Size	Deviations from OSHA 29 CFR Section 1910
H_2 bottles standard commercial bottles (rental)	II	ICC Std. 3A	3225 psig	2000 psig	6.7 cu. ft. bottle 4 bottles	Relief Valve	3200 psig	6,000	Turbine Building	II	3/4 in.	None
CO_2 bottles standard commer-cial bottles (rental)	II	ICC Std. 3A	3225 psig	2000 psig	75 lb CO_2 per vessel 11 vessels	Relief Valve	3200 psig	2.245×10^6 (Calc. M-634)	Intake Structure	III	1/2 in.	None
Compressed breath air storage vessels	II	ASME B&PV Code Sec. VIII	3873 psig	3500 psig	21 cu. ft. per vessel 9 vessels	Relief Valve	3870 psig	23.4×10^6	Unit 2 Turbine Building	III	3/4 in.	None
Carbon dioxide Storage bottles	II	ICC Std. 3AA-2265	2265 psig	2000 psig	1.5 cu. ft. per bottle 16 bottles	Relief Valve	2200 psig		Turbine Building Elev. 85'	II	2 in.	None
N_2 storage bottles	II	ICC Std. 3AA-3500	3500 psig	2800 psig	1.5 cu. ft. per bottle 4 bottles	Relief Valve	3000 psig		Aux Bldg	II	1 in.	None
Argon storage bottles	II	ICC Std. 3AA-2015	2015 psig	2000 psig	1.5 cu. ft. per bottle 5 bottles	Relief Valve	2015 psig		Penetration Area	II	1 in.	None

(a) Relief setpoint and capacity based on the applicable design code.

(b) Filled with liquid, which requires heat input to flash.

(c) Table lists significant gas quantities greater than 100 lbs net weight

TABLE 3.9-12

MECHANICAL EQUIPMENT SEISMIC
QUALIFICATION RESULTS
UNIT 1

Equipment	Location Building/ Elevation, ft	Qualification Method	Qualifying Spectra HE, DDE, DE	Damping Value Used
Feedwater System				
AFW Pump (Motor Driven)	Aux/100	A	DE DDE HE	R R R
AFW Pump Motor	Aux/100	A	DE DDE HE	R R R
AFW Pump (Turbine-driven)	Aux/100	A	DE DDE HE	R R R
AFW Pump Turbine	Aux/100	A	DE DDE HE	R R R
CVC System				
Boric Acid Tank and Heater	Aux/115	A	DE DDE HE	2 2 4
Safety Injection System				
SI Pump Lube Oil Filter Stand	Aux/85	A	DE DDE HE	R R R

TABLE 3.9-12

Equipment	Location Building/ Elevation, ft	Qualification Method	Qualifying Spectra HE, DDE, DE	Damping Value Used
Component Cooling System				
CCW Pump	Aux/73	A	DE DDE HE	R R R
CCW Pump Motor	Aux/73	A	DE DDE HE	R R R
CCW Heat Exchanger	Turb/85	A	DE DDE HE	2 2 4
CCW Surge Tank	Aux/163	A	DE DDE HE	R R R
CCW Pump Lube Oil Cooler	Aux/73	A	DE DDE HE	R R R
Makeup Water System				
Makeup Water Transfer Pump and Motor	Aux/100	A	DE DDE HE	R R R

Equipment	Location Building/ Elevation, ft	Qualification Method	Qualifying Spectra HE, DDE, DE	Damping Value Used
Saltwater System				
ASW Pump and Motor	Intake/-2	A	DE DDE HE	R R 4
Fire Protection System				
Fire Pump	Aux/115	A	DE DDE HE	R R R
Fire Pump Motor	Aux/115	A	DE DDE HE	R R R
Portable Fire Pump (diesel)	MSS/85	T	DE DDE HE	R R R
Diesel Generator System				
Diesel Generator	Turb/85	A, T	DE DDE HE	2 2 4

Equipment	Location Building/ Elevation, ft	Qualification Method	Qualifying Spectra HE, DDE, DE	Damping Value Used
Diesel Transfer Pump	MSS/77	A	DE	R
			DDE	R
			HE	R
Diesel Transfer Pump Motor	MSS/77	A	DE	R
			DDE	R
			HE	R
Diesel Transfer Filter	MSS/77	A	DE	R
			DDE	R
			HE	R
Diesel Transfer Strainer	MSS/77	A	DE	R
			DDE	R
			HE	R
Priming Tank	Turb/85	A	DE	R
			DDE	R
			HE	R
Starting Air Receiver	Turb/85	A	DE	2
			DDE	2
			HE	4
Turbocharger Air Receiver	Turb/85	A	DE	R
			DDE	R
			HE	R

TABLE 3.9-12

Equipment	Location Building/ Elevation, ft	Qualification Method	Qualifying Spectra HE, DDE, DE	Damping Value Used
Ventilation System				
Containment H_2 Purge Supply Filters	Aux/100	A	DE DDE HE	R R R
Containment H_2 Purge Exhaust Filters	Aux/115	A	DE DDE HE	R R R
Containment Fan Cooler Box	Cont/140	A	DE DDE HE	R R R
Gaseous Radwaste System				
Waste Gas Compressor	Aux/60	A	DE[(a)]	R
Waste Gas Moisture Separator	Aux/60	A	DE[(a)]	R
Waste Gas Decay Tank	Aux/60	A	DE[(a)]	R

(a) Qualified for DE only per Regulatory Guide 1.143.

(b) Legend:

A = Qualification by analysis (Qualification Method Column)
T = Qualification by testing
R = Rigid

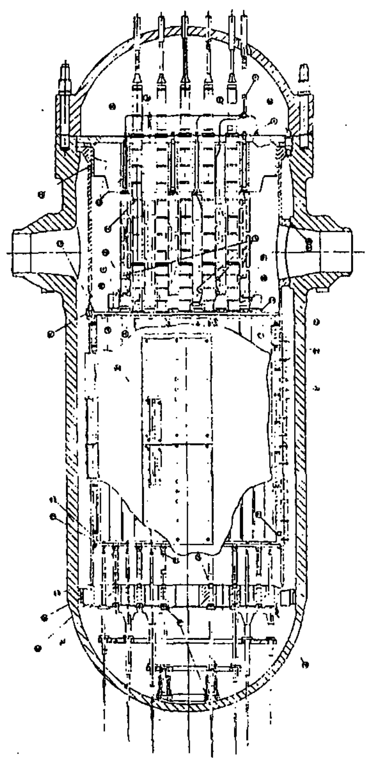

	FEATURES TO BE EXAMINED	COMMENTS AND OBSERVATIONS BEFORE FUNCTIONAL TEST	COMMENTS AND OBSERVATIONS AFTER FUNCTIONAL TEST
[illegible]	[illegible]		
[illegible]	[illegible]		
[illegible]	[illegible]		
[illegible]	[illegible]		
[illegible]	[illegible]		
[illegible]	[illegible]		
[illegible]	[illegible]		
[illegible]	[illegible]		
[illegible]	[illegible]		
[illegible]	[illegible]		
[illegible]	[illegible]		
[illegible]	[illegible]		
[illegible]	[illegible]		
[illegible]	[illegible]		
[illegible]	[illegible]		
[illegible]	[illegible]		
[illegible]	[illegible]		
[illegible]	[illegible]		
[illegible]	[illegible]		
[illegible]	[illegible]		
[illegible]	[illegible]		
[illegible]	[illegible]		
[illegible]	[illegible]		
[illegible]	[illegible]		
[illegible]	[illegible]		
[illegible]	[illegible]		
[illegible]	[illegible]		
[illegible]	[illegible]		
[illegible]	[illegible]		
[illegible]	[illegible]		
[illegible]	[illegible]		
[illegible]	[illegible]		
[illegible]	[illegible]		
[illegible]	[illegible]		
[illegible]	[illegible]		

FSAR UPDATE

UNIT 2

DIABLO CANYON SITE

FIGURE 3.9-2

VIBRATION CHECKOUT - FUNCTIONAL TEST INSPECTION DATA

SHOP TEST ACCELEROMETER DATA

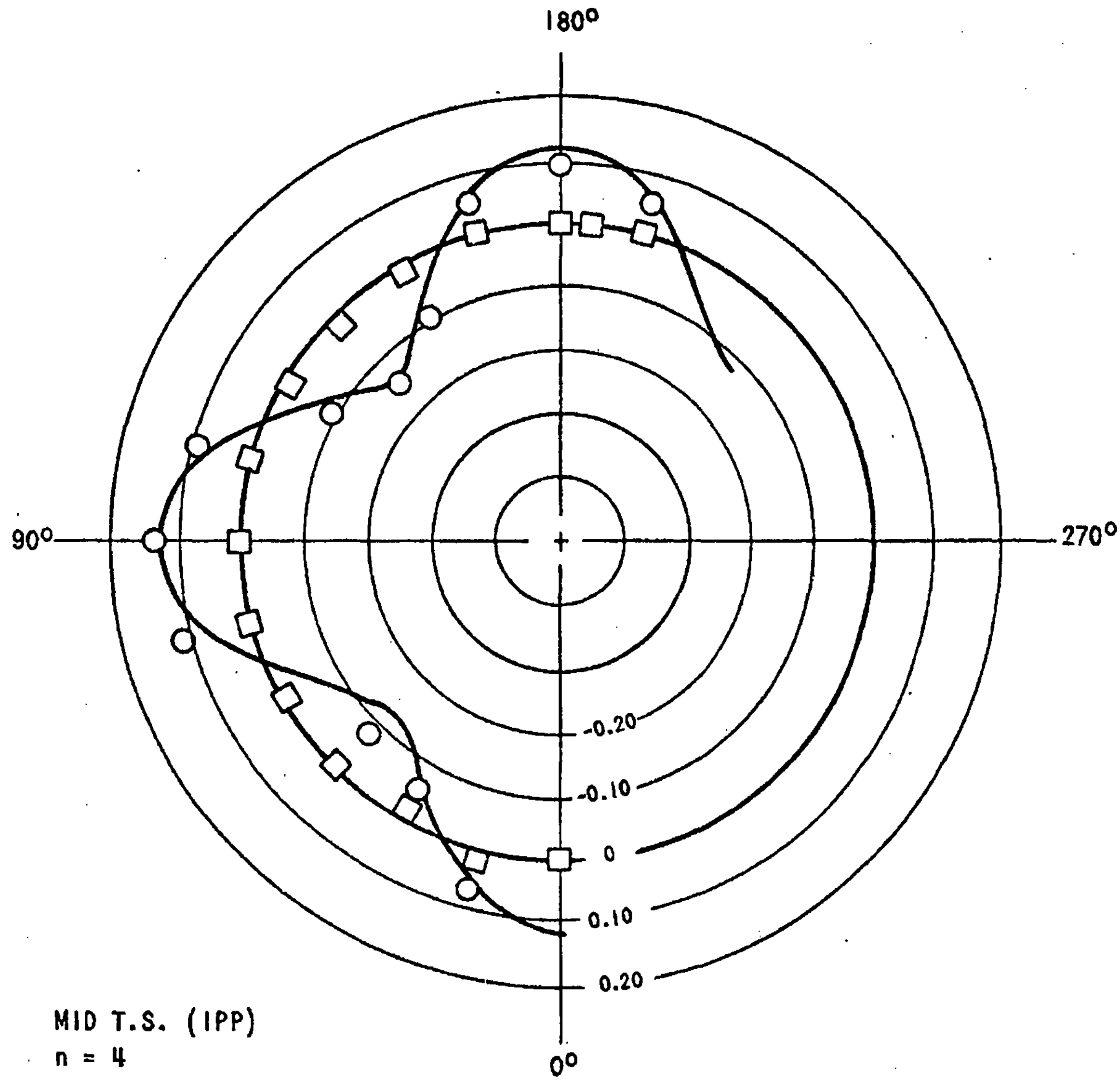

MID T.S. (IPP)
n = 4
f = 72 H_z FORCE = 6 LB
CURVE = 0.12 COS 4θ (LEAST SQUARE)
○ MIDDLE ☐ BOTTOM

FSAR UPDATE

UNIT 1
DIABLO CANYON SITE

FIGURE 3.9-3
THERMAL SHIELD, MODEL SHAPE n=4
OBTAINED FROM SHAKER TEST

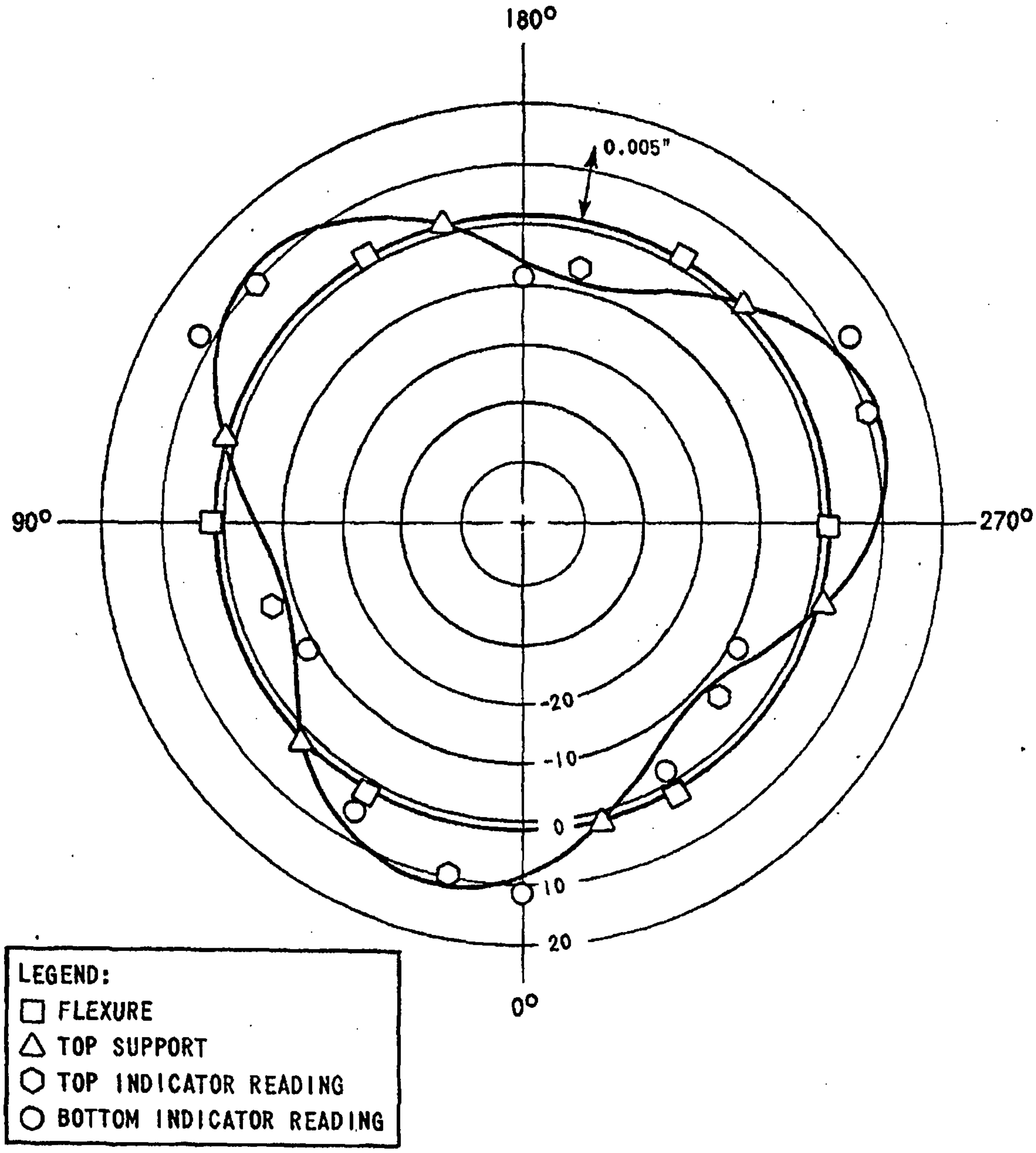

FSAR UPDATE

UNIT 1
DIABLO CANYON SITE

FIGURE 3.9-4
THERMAL SHIELD, MAXIMUM AMPLITUDE OF VIBRATION DURING PREOPERATIONAL TEST

3.10 SEISMIC DESIGN OF DESIGN CLASS I INSTRUMENTATION, HVAC, AND ELECTRICAL EQUIPMENT

3.10.1 SEISMIC DESIGN CRITERIA

The Design Class I instrumentation, HVAC, and electrical equipment are capable of performing their nuclear safety functions during and after a DDE or the postulated 7.5M HE. The seismic levels for DDE and HE are given in Section 3.7. Instrument Class IA instrumentation is capable of performing its active nuclear safety functions during and after a DDE or HE. Instrument Class IB Category 1 instrumentation is capable of performing its active nuclear safety functions after a DDE or HE. Other Design Class I instrumentation is capable of performing the passive function of maintaining Class I pressure boundary integrity during and after a DDE or HE. In addition, some of the Design Class I instrumentation may have active seismic qualification; these instruments are identified on a case-by-case basis.

Performance criteria for Design Class I instrumentation, HVAC, and electrical equipment are as follows: (a) The reactor protection system shall be able to shut down the unit and maintain it in safe shutdown condition. (b) The electrical equipment is able to perform its required functions of providing electrical power, control, instrumentation, and protection for the ESF. (c) No device shall fail to initiate and maintain its safety function, nor shall it prevent other safety devices from performing their safety function.

The original seismic qualification of most equipment was done in accordance with IEEE 344-1971 (Reference 1) for DDE levels. As a result of changes in spectra the Design Class I equipment has been reevaluated, based on response spectra derived from the HE as well as the DDE levels discussed in Section 3.7. In the process of reevaluation, some equipment had to be requalified because: (a) its previous qualification was not adequate to envelop the HE input, or (b) concerns had been raised about the adequacy of the justification for the previous qualification methods. Requalification of the equipment, according to the guidance contained in IEEE Standard 344-1975 (Reference 2) and NRC RG 1.100 (Reference 3) was performed where necessary.

Tables 3.10-1 and 3.10-2 list instrumentation and electrical equipment that have been seismically qualified. The tables provide references to appropriate sections where qualification is described. Table 3.10-3 lists HVAC equipment that has been seismically qualified.

The seismic qualification of the equipment is based on the free-field ground motions described in Section 3.7.1. Effects of amplification of ground accelerations due to the response of the building at the location of the equipment were derived from the time-history modal superposition analyses made for the structures, as described in Section 3.7.

B/9

12. Comprehensive Vibration Assessment Program for Reactor Internals During Preoperational and Initial Startup Testing, NRC, RG 1.20.

13. PG&E Letter DCL-88-288, LAR 88-08, Request to Use VANTAGE 5 Fuel Assemblies, November 29, 1989.

14. Letter dated March 2, 1993, Leak-Before-Break Evaluation of Reactor Coolant System Piping for DCPP Units 1 and 2, (Docket Nos. 50-275 and 50-323), from Sheri R. Peterson of the NRC to Gregory M. Rueger of PG&E.

15. Bhandari, D. R. ,et. Al, System Dynamic Seismic and LOCA Analyses of Reactor Pressure Vessel System for the Pacific Gas and Electric Company Diablo Canyon Power Plants (DCPP) Units 1 & 2, WCAP-14693, Revision 1, February 11, 1997 (Westinghouse Proprietary Class 2).

16. Pacific Gas and Electric Company Transmittal Letter 229643 dated March 28, 1996 from M. J. Angus to John Hoebel.

17. Fritz, R. J., The Effects of Liquids on the Dynamic Motions of Immersed Solids, Trans. ASME, Journal of Engineering for Industry, 1972, pp. 167-173.

18. WCAP-8172-A, Pipe Breaks for the LOCA Analysis of the Westinghouse Primary Coolant Loop, January 1975.

19. WNEP-7904, 4 Loop Standard Generic Stress Report - Structural and Fatigue Analyses.

20. WCAP-16487-P, Revision 1, Diablo Canyon Nuclear Power Plant Unit 2 Upflow Conversion and Upper Head Temperature Reduction Engineering Report, March 2006.

In addition to direct seismic effects on Design Class I equipment, PG&E has also given consideration to possible seismically induced physical interactions between nonsafety-related SSCs and Design Class I SSCs. The methodology and results of this interaction study are presented in Reference 4, and are provided in summary form in Section 3.7.3.13. Appropriate design modifications were performed where the study indicated safety functions of Design Class I equipment might be affected due to seismic interaction.

3.10.2 SEISMIC ANALYSES, TESTING PROCEDURES, AND RESTRAINT MEASURES

The effects of seismic accelerations were determined either by physical tests, mathematical analyses, or engineering judgment. Mathematical analyses of structural elements were made for Design Class I exposed electrical raceways, for equipment supports, and also for some equipment. Physical tests of equipment were made either on one of the units being supplied or on one of a similar type. Choice of method used to determine seismic capability of the equipment and devices was based on the supplier's judgment of what would be adequate and appropriate.

3.10.2.1 Nuclear Reactor Instrumentation and Protection Systems

The seismic testing of Westinghouse-supplied electrical and control equipment is documented in WCAP-8021 (Reference 5). The testing conforms to the procedures of IEEE-344-1971. The radiation monitoring cabinet and the Tracerlab scintillation detector and liquid sampler equipment are not safety-related, and these portions of WCAP-8021 are not applicable. The radiation monitoring system cabinet at DCPP has been upgraded to Design Class I (see Section 3.10.2.26). Details of the original seismic analysis and testing procedures for Design Class I instruments and electrical equipment are summarized in Table 3.10-1 and the following sections.

Typical items of equipment have been type tested under simulated seismic motion in the form of sine beats. This testing was done with conservatively large accelerations over a range of applicable frequencies and conformed to the procedures given in IEEE 344-1971. The peak test input accelerations used in those tests were checked to verify that they are larger than the requirements derived by structural analyses of DDE and HE levels. Westinghouse Electric Company, the supplier, made dynamic tests of typical samples of this equipment to confirm its seismic adequacy. Included in this test program were the racks for the nuclear instrumentation system; the process control and protection sets; the solid-state protection system cabinets and its safeguards test cabinets and auxiliary safeguards cabinets; the inverters for the power supply; pressure and differential pressure transmitters; the reactor trip switchgear; and main coolant loop resistance temperature detectors. Details of these tests are given in Table 3.10-1 and in Sections 3.10.2.1.1 to 3.10.2.1.9.

3.10.2.1.1 Nuclear Instrumentation

As described in Reference 5, a typical two-cabinet unit of the Westinghouse nuclear instrumentation system (NIS) and radiation monitoring system (RMS) has been seismically tested. The NIS equipment was contained in one cabinet and the RMS equipment was mounted in the other cabinet. The two cabinets were attached and mounted on a two-cabinet base to simulate the support or adjoining cabinets. A typical NIS installation consists of four cabinets.

The NIS cabinet contained one source range channel, one intermediate range channel, and one power range channel located and mounted in the same configuration as the plant installation. Since any DBA described in this FSAR Update can be terminated within acceptable limits by the power range channels, only the power range channel was energized and monitored. The other NIS channels mounted in the cabinet served to simulate the mass distribution and weight in an actual installation.

Shutdown procedures contain the following provisions in the event that the source range channels are rendered inoperative due to a seismic event:

(1) The operator will take appropriate action to preclude boron dilution

(2) Prior to cooldown, boric acid will be added to the reactor coolant to ensure that the concentration is sufficient to maintain the reactor in a subcritical state

During seismic testing an external test signal was applied to the equipment so that the power range output signal was 100 percent full power. The test input signals, analog output signals, and bistable output signals were monitored during test. The tripping action of the bistable amplifier circuitry was checked after each series of tests to insure that the simulated earthquake had not impaired this function.

Only one instance of mechanical malfunction occurred as a result of this level of testing. Drawer latch damage occurred during side-to-side testing at higher g levels. A new fastening mechanism has been designed and the design submitted to the NRC (Reference 6). This modification was implemented at DCPP. A demonstration test for seismic operability of the NIS equipment was performed with multiple frequency, multiple axis inputs. The test, reported in Reference 7, indicated that the equipment will operate during a seismic event as required.

The neutron detector for the NIS power range channel has been tested using sinusoidal inputs in both the horizontal and vertical directions at accelerations at least equal to those calculated for the DCPP. Neutron current measurements were made during the tests, and current, resistance and capacitance checks were made after the tests. No significant changes were found and there was no mechanical damage to the detector.

In addition, a two-section power range excore neutron detector was tested using multiple frequency, multiple axis inputs in a support assembly which simulated a detector holder. The multiple frequency inputs were developed in accordance with the guidelines set forth in Reference 8. The test response spectra envelope the DDE and HE inputs.

During the multiple frequency test, the detector was energized from a high voltage power supply, and an AC signal was imposed in each of the two signal electrodes to determine proper electrical operability.

At the completion of the tests, there was no observable mechanical damage and the electrical recordings revealed only a transient type electrical disturbance of one of the two signals. The signal perturbations were small in amplitude and would not cause any loss of protection capability of the NIS during normal operation. Subsequent detector acceptance tests performed by the detector manufacturer did not disclose any abnormal permanent change in the electrical or neutron sensitivity characteristics. Thus the NIS Power Range Detector will operate as required during and after the DCPP postulated seismic events.

3.10.2.1.1.1 Radiation Monitoring

Qualification of the radiation monitoring panels in the control room is based on shake table tests performed on the panels for Victoreen. The racks were shaketable tested with the monitoring equipment in place. See Section 3.10.2.26

3.10.2.1.2 Solid-State Protection System

The three-bay, two-train SSPS was seismically tested as described in Section 2.5 of Reference 5. During the seismic test, a typical reactor trip matrix and typical safeguards actuation matrix were energized and monitored. Before each test, the circuitry was placed in a pre-trip condition. During the actual shaking, the circuitry was deliberately tripped and changed to a post-trip condition. The functional integrity of the system was thus demonstrated by observing a satisfactory change of state on demand. Relay contact positions necessary to show the operability were recorded during the tests.

No mechanical problems occurred during the vertical axis tests. In the side-to-side axis test at lower "g" levels, the two lefthand cabinet-to-base bolts repeatedly loosened and were deformed until it became necessary to replace these with more hardened bolts. During subsequent testing at these levels in the side-to-side axis, these bolts failed completely on the last sine-beat test. Before performing the front-to-back test, twelve additional cabinet-to-base bolts were installed making a total of 24 bolts fastening the cabinet to its base. This change has been incorporated into the SSPS cabinets at DCPP.

The functions monitored by recorders were: undervoltage trip, train trouble, and SI signal. Test switches were operated during the third sine beat simulating a reactor trip

and safeguards actuation, causing a change in amplitude of the recorded signals for under voltage trip and SI.

During the front-to-back axis test, the signal indicated several momentary trips (contact closures) before the test switches were operated. Also, at 7 Hz and 9.5 Hz, this signal indicated a momentary trip and then a permanent change of state (latch up) on the first bounce on the output (slave) relays. The permanent change of state was caused by the armature of the same relays bouncing closed. This closing allowed their mechanical latch mechanism to operate. These maloperations could have initiated safeguards actuation. However, they would not have negated a valid safeguard actuation or reactor trip. Although SI was prematurely actuated, the under voltage coil tripped when called upon to do so.

The duration of the momentary contact closure was probably short enough not to cause a false safety injection signal. The probability of spurious initiation of safety injection due to any earthquake is therefore very small. The seismic tests performed have demonstrated that the postulated seismic event will not prevent a legitimate safety injection signal from being actuated, either during or after the event. Reference 9 presents an analysis of the consequences of seismic-induced actuation of protection system relays by considering the possible actuation of each contact of the relays studied and describing the resulting effect of inadvertent equipment actuation.

The relays which exhibited contact bounce and mechanical latching were replaced by a new type of relay which was seismically qualified by single-axis sine-beat and multiple frequency sine-beat testing. Input levels for the tests were determined from the measured acceleration response at the cabinet during the cabinet tests described in Section 2.5 of Reference 5. Seismic qualification of these replacement relays is documented in Reference 10.

Due to obsolescence issues, the original SSPS printed circuit boards (PCBs) can be replaced with newer vintage boards supplied by Westinghouse. The replacement PCBs have been seismically qualified by Westinghouse. The seismic qualification is documented in Reference 49.

3.10.2.1.3 Process Control and Protection Equipment

Originally, seismic testing was performed using a three-cabinet unit mounted on a common base as defined in Section 2.4 of Reference 5. The three-cabinet test assembly included at least one of each type of module used in all of the various process protection and safeguards actuation channels. Both analog and bistable output signals were recorded. All reactor trips and safeguards actuation signals were continuously recorded and some bistable signals of less importance (e.g., alarms circuits) were monitored with lights. The basis for determining the functional integrity of the reactor trip and safeguards actuation signals was that these signals should remain unchanged during the test and should be capable of changing state after the test if called upon to do so.

The tripping action of the bistable amplifier circuitry was checked after each series of tests to insure that the seismic test input had not impaired this function.

During front-to-back testing of the circuit board, an internal power supply circuit board disengaged from its connector causing complete failure of the module. Restraining clamps were installed on the circuit board and the test was repeated successfully. These clamps have since been installed on all similar modules. All recorded electrical signals performed properly during and after the tests.

In addition, as part of the overall program to demonstrate the adequacy of the seismic test previously conducted, multiple frequency, multiple axis test (Reference 11) were performed on an entire typical channel, including signal conditioning circuits and the bistables, of the process instrumentation system. The results of the bistable tests show that the electrical functions of each bistable module maintained electrical operability both during and after each seismic event. In addition, no spurious bistable actions were observed.

Subsequently, the Eagle 21 system replaced the Hagan protection system within the existing racks. The Eagle 21 system has been seismically qualified on a generic basis by Westinghouse (see References 40 through 42) in accordance with requirements from References 43 and 44. A site-specific seismic analysis was also performed to ensure that the Eagle 21 generic testing performed by Westinghouse encompasses the DCPP installed condition (see Reference 45), which included the effects of the top entry conduit stiffness.

3.10.2.1.4 Instrument AC Inverters

A prototype UPS and regulating transformer of the DCPP UPS system was tested as described in PG&E engineering seismic file No. ES-68-1.

The UPS and regulating transformer were tested while loaded at 20 kVA; and the ac output voltage, current and frequency were monitored during the seismic test. The presence of a continuous ac output voltage both during and after the test formed the basis for determining the functional integrity of the UPS system.

During seismic testing the static inverter maintained structural integrity and functional operability. No variation or loss of 120 Vac output voltage was observed during or after the test. Therefore, the static inverter will perform its safety related functions during and after the postulated DCPP seismic events.

3.10.2.1.5 Pressure and Differential Pressure Transmitters (Westinghouse)

Originally the safety related pressure transmitters provided by Westinghouse for DCPP were installed to sense the following conditions:

- Containment Pressure (CP)
- Reactor Coolant Level using the Reactor vessel Level Instrumentation System (RVLIS)

The transmitters were mounted during seismic qualification to a rigid fixture. The pressure and differential pressure transmitters tested are the following:

Equipment	Function Group	Manufacturer	Model No.
Differential Pressure Transmitter	CP	ITT/Barton	332/351
Differential Pressure Transmitter	RVLIS	ITT/Barton	752

As described in Section 2.8 of Reference 13, the Barton Model 332 transmitter was seismically tested. Subsequently, the containment pressure transmitters were replaced with Rosemount differential pressure transmitter Model 1154 (refer to Section 3.10.2.11 for qualification of this model transmitter). The Barton Model 351 pressure sensors are used in conjunction with the Rosemount transmitter Model 1154 to measure containment pressure.

Seismic testing of the Barton Model 752 differential pressure transmitters is detailed in WCAP-8687, Supplement 2-E04A (Reference 15). Seismic testing was performed using multiple frequency, multiple axis tests. During seismic tests, the transmitters were pressurized to approximately mid-scale with a 2,000-psig static pressure. The output of the transmitters was monitored continuously. The Barton 752 differential pressure transmitters maintain their integrity and performed their safety-related functions as required during and after seismic testing. Subsequently, the RVLIS level transmitters manufactured by Barton were replaced with Rosemount differential pressure-transmitter Model 1153 (refer to Section 3.10.2.11 for qualification of this model transmitter). The RVLIS Rosemount transmitters retain the use of the Barton Model 353 pressure sensors.

3.10.2.1.6 Reactor Trip Switchgear

Seismic testing of a typical reactor trip switchgear was performed as described in Reference 16. The basis for determining the functional integrity of the equipment was the following: (a) the breakers should trip open on loss of voltage to the undervoltage trip device during the testing sequence, and (b) all breaker outputs, including secondary contact outputs to the various protection system, should maintain proper contact condition of open or closed position.

The electrical functions of the equipment were monitored both during and after the seismic test (Reference 16) to ensure that the equipment was operating properly and performing the required safety related functions. This monitoring consisted of recording output signal voltages, and the input signal voltage to the undervoltage trip. The tripping action of each breaker through the undervoltage trip circuitry was checked

during the after each series of test to verify that the simulated earthquake had not impaired this function.

The recordings of all electrical signals indicated proper and complete functioning of the equipment both during and after all testing. No secondary contact chattering, no false breaker closing and no false breaker opening was observed.

The test results show that the functions of this equipment were maintained within the established criteria, both during and after each simulated seismic condition. During seismic testing a modification kit was installed within the reactor trip switchgear to enhance its seismic capabilities. This modification kit has been installed in the DCPP reactor trip switchgear.

3.10.2.1.7 Resistance Temperature Detectors

Resistance temperature detectors (RTDs) are ruggedly built devices designed to withstand the high temperature and pressure of the fluid in the reactor coolant system. They are also designed to withstand severe seismically induced vibration, and the reactor coolant RTDs are designed to withstand the flow-induced vibration from the reactor coolant flow.

The RTDs are mounted in the reactor coolant piping, on the containment sump wall, and on rigid support structures. The reactor coolant RTDs are installed in thermowells mounted into the main coolant piping.

The seismic testing described in Reference 35 was performed on the Weed reactor coolant RTDs. The test inputs were random frequency, biaxial sine wave vibrations for a range of 1 through 1000 Hz. During the test, the RTDs were operated and their input/output signals were monitored. No mechanical damage was observed, and the input/output signals remained within acceptable limits.

The seismic testing described in Reference 36 was performed on the Conax RTDs. The test inputs were random frequency, biaxial sine wave vibrations for a range of 1 through 200 Hz. During the test, the RTDs were operated and their input/output signals were monitored. No mechanical damage was observed, and the input/output signals remained within acceptable limits.

3.10.2.1.8 Safeguards Test Cabinet

As described in Reference 19, sine-beat testing was performed on a typical engineered safeguard test cabinet. The engineered safeguards test cabinet completed seismic testing without sustaining physical damage. The only functional anomaly observed during testing was the momentary opening of the normally closed contacts of certain test selection switches at particular frequencies.

These switches are used to set up and initiate individual tests. The normally closed contacts are used exclusively to reset the blocking relays of the engineered safeguards test cabinet upon completion of a test. When the blocking circuit is not in the test mode, the blocking relay is in the reset state. A momentary opening of the normally closed contacts, therefore, will have no effect on the state of the blocking relay.

Therefore, based on the seismic testing performed, the engineered safeguard test cabinet will perform its safety related function during and after the postulated DCPP seismic events.

3.10.2.1.9 Auxiliary Safeguards Cabinet

The auxiliary safeguards cabinet is structurally identical to the safeguards test cabinet (Section 3.10.2.1.8) and the component layout of the two cabinets is essentially the same. Therefore the results obtained from the test of the safeguards test cabinet were applied to the auxiliary safeguards cabinet.

The auxiliary safeguards cabinet was later analyzed by time history analysis to qualify the use of the rotary relay in the cabinet. This analysis is described in Reference 20.

The rotary relays have been tested separately using single axis, multiple frequency inputs. These tests are described in Reference 10.

The analysis response spectra of the auxiliary safeguards cabinet, at relay mount locations, was found to be enveloped by the relay test response spectra. Therefore both the auxiliary safeguards cabinet and relays will function properly during and after the DCPP postulated seismic event.

3.10.2.2 Main Control Board and Console

The main control board is located within the control room at elevation 140 ft in the auxiliary building. It has two major structures: main control board (MCB) section and control console.

Seismic qualification of the MCB and central console is demonstrated by analysis as described in Reference 21. The analysis consisted of the following tasks:

(1) Modeling of the MCB so that its analytical frequencies correlate to those obtained from the field test

(2) Response spectrum analysis of the model using the given spectra to evaluate structural adequacy

(3) Modification of MCB to address overstress condition

(4) Response spectrum analysis of the modified MCB model to compute loads for structural evaluation

(5) Transient dynamic analysis of the modified model to generate in-equipment response spectra (IERS) for device qualification

The MCB section and central console are modeled using the general purpose finite element computer code, WECAN (Reference 22). The MCB is modeled as a linearly elastic system of beam, plate and lumped mass elements.

In addition, In-situ testing of the unmodified structure was performed to identify local panel modes. This consisted of tap tests of the vertical and bench panels as described in Reference 23.

Response spectrum analyses were performed to compute structural loads using DDE and HE required response spectra. Two dimensional shocks were considered in the evaluation. Maximum elemental stresses were obtained from the two sets of response spectrum analyses.

The structural analyses of the unmodified design indicated some overstress which is a result of the changes in spectra from the original HE loadings. To reconcile the overstressed conditions and simultaneously provide the additional advantage of increasing the overall structural frequencies to above the peak of the floor response spectra, modifications have been done on top of the main control board. These modifications lead to a much lower stress condition and increase the board's overall structural frequencies to values exceeding the peak of the input spectra.

The results of stress analyses for the modified design show that the maximum member stress is about 85 percent of allowable. A comparison of the required and as-built weldments demonstrates that the existing weldments exceed the required weldments. Buckling stability of all MCB structural members has also been evaluated. There exists, at least a factor of safety of three against buckling.

Transient dynamic analyses of the modified structural model and performed to obtain the IERS for use in qualifying board mounted devices. Two sets of transient analyses are performed using two directional seismic excitation with one horizontal and one vertical direction. The synthesized floor excitation is employed in a transient dynamic analysis using the modal superposition integration procedure. Five percent of critical damping is assumed in the analyses.

The central console is a U-shaped electrical cabinet consisting of three bolted sections, welded to the main control room floor. The structure is modeled using WECAN, similar to the main control board. Results of modal analyses of the console structural model show the lowest overall fundamental frequency to be 70 Hz.

Since the console model has no frequencies below 33 Hz, it is classified as a rigid structure, and stress evaluations are performed using the static method. Uniform static acceleration equal to the floor response spectra ZPA are applied to the console structural model. Stresses computed by the SRSS method are observed to be well below the allowables. No weldments and buckling evaluations are performed due to the obvious integrity apparent from the low stress conduit.

As all console frequencies are in the rigid range, the IERS for console mounted devices are the floor response spectra.

The IERS obtained from MCB and console analysis were used for seismically qualifying the MCB mounted devices as described in Reference 24. Qualification tests were performed to determine if the structural integrity and functional operability of the devices are maintained for the seismic level.

Devices tested were supplied by PG&E and are representative of all the Design Class I devices used in the MCB. Indicators, recorders, switches, power supply, and light box were tested. The seismic qualification was achieved by subjecting the devices to multiple frequency, multiple axis seismic testing such that the response spectrum envelops the IERS obtained from analysis. It was concluded from the tests that all of the Design Class I devices will maintain their structural integrity and functional operability during and after the postulated seismic event. In addition, three cathode ray tube (CRT) displays have been located in the central console. Seismic tests were performed to insure that these CRTs will not become missile sources.

3.10.2.3 Hot Shutdown Panel

This panel is a backup panel used if the control room must be evacuated and the plant brought to a hot shutdown condition. It contains indicators, control switches, and hand-auto stations for proportional control. These give indication and control over various pumps and valves in the auxiliary feedwater, component cooling water, boration control, and containment fan cooler systems. Additionally, the 10 percent steam dump valves are controlled from the hot shutdown panel, but the control loops for that function are not Design Class I.

3.10.2.3.1 Qualification of the Panel

The panel consists of an enclosure 5 feet 10 inches wide, 6 feet 6 inches high, and 3 feet deep, with two panels inside, one on a vertical plane, the other tilted up 30° from the horizontal. The enclosure is mounted on four channels which are welded to a box comprised of 10-inch WF beams. This box is welded to steel plates embedded in the concrete floor of the auxiliary building at elevation 100 feet.

A three-dimensional response spectra analysis has been performed on a finite element model developed for the hot shutdown control panel. This analysis has shown the subject panel is qualified for DE, DDE, and HE seismic events.

3.10.2.3.2 Qualification of Individual Instruments

The types of components in the panel that are Class 1E are indicators (Westinghouse Model VX252), control switches (Cutler-Hammer Type 10250T), and hand-auto control stations (Fisher Model TL-123 in Model MC-707 instrument power supply/cases). Other devices (e.g., Hagan Pneumatic Loading Stations and Westinghouse Type KA-241 indicators) are not Class 1E and have no need to meet seismic qualifications. These devices are separated from Class 1E devices by a barrier.

All required devices (VX252 indicators, W-2 switches, 10250T switches, TL-123 hand-auto stations) were qualified by test using multifrequency biaxial shake tests. The devices were mounted to closely simulate their mounting conditions on the panel. The indicator and the hand-auto station were calibrated before and after the tests to ensure that the tests had not affected the calibration. During the tests, an input was applied that produced a midscale output. The outputs were monitored for fluctuation, and no fluctuation or calibration shift greater than required accuracy was noted.

The control switches were tested in both the neutral and the "switched" positions. The contacts were monitored for chatter during the event, and were tested for proper operation afterwards. (It should be pointed out that since the safety function of these devices is to give the operator manual control of various devices, and the operator will not be expected to change switch position during the seismic event, no requirement exists to change inputs during the event.) No malfunctions of the switches were noted.

3.10.2.4 Local Instrument Panels

Local instrument panels are used as enclosures for Design Class I and non-Design Class I instrumentation throughout the plant. The panels perform no Design Class I function except to provide support for the Design Class I devices. The panels are supported at the top by fastening them to a wall or other suitable structure. The bottom is fastened to the floor or to the same structure as the top.

The panels were originally qualified by analysis performed by the panel vendor. The criteria for the panels were that they have a resonant frequency greater than 20 Hz, and that all stresses be below allowables.

Due to the large number of panels requiring qualification, a worst case analytical method was used. It was based on determination of the panel having the highest calculated stresses resulting from simultaneous horizontal and vertical seismic accelerations. Subsequent to their installation in the plant, several of the panels were modified to increase their stiffness.

The qualification of the panels is based on finite element models of several representative panels which include the effect of equipment mounted in the panel. The analysis took into account the various sizes, configurations, and locations, using an envelope of 2 percent DDE and 4 percent HE spectra.

The results of the analyses show that all panel stresses are below allowables. In addition, the panel response at Design Class I transmitter locations was derived for comparison with the test response spectra for Design Class I transmitters in the panels (see Section 3.10.2.11).

3.10.2.5 Instrument Panels PIA, PIB, and PIC

These instrument panels house various devices used to power plant transmitters and perform the necessary signal conditioning to provide alarm functions and send linear signals to indicators on the main control board. The typical parameters involved are CCW flows and heat exchanger DP, and refueling water storage tank (RWST) level, etc. Most of the components in them were originally in the power generation instrument rack (PGIR). The panels are mounted on reinforced concrete columns at about the 132-foot elevation in the cable spreading room.

The panels were originally qualified by analysis. A review of the original stress calculations indicates that nowhere would the stresses (bending or shear) due to postulated seismic loading exceed 50 percent of the yield point of the material.

The devices within the panels are Moore direct current alarms (DCAs), a thermocouple transmitter (TCT), square root transmitters (SRTs), signal conditioners (SCTs), power supplies, and relays. The DCA, TCT, and SRT devices were qualified as part of the original PGIR qualifications. The SCT unit is physically identical to the SRT unit, the only difference being minor electronic changes which are not of any seismic significance. These devices were tested using frequency sweep and dwell techniques that conform to IEEE 344-1971. The dwell inputs were 3 g horizontal and 2 g vertical over a range of 5 to 60 Hz. The devices were mounted in exactly the same configuration and used mounts similar to those used in the actual installation. The calibrations for the TCT and SRT devices were checked before and after the test. The maximum output errors were 0.1 percent for these devices. No lamp malfunctions or output (calibration) errors were found in the DCA device either during or after the tests.

The relays were qualified by comparison with the same relays installed in the ventilating control panel, physically installed nearby.

The panels were reanalyzed for the current seismic criteria for both the DDE and the HE. In addition, the seismic qualifications of the devices within the panels have been reviewed to the same seismic criteria. The analysis and the review have demonstrated that the instrument panels PIA, PIB, and PIC are seismically qualified to perform their safety function after the postulated seismic conditions.

Subsequent to the original qualification testing, replacement or additional devices to the panels have been installed. These devices are qualified by testing, analyses, or a combination of the two. Their qualification is documented in the engineering seismic files associated with the panels and/or devices.

3.10.2.6 Diesel Generator Excitation Cubicle and Control Cabinet

The diesel generator (DG) excitation cubicle and the control cabinet for DGs 1-1, 1-2, 1-3, 2-1, and 2-2, were originally seismically qualified for the DDE by the manufacturer. Subsequently, one excitation cubicle and one control cabinet were shake-table tested and qualified to the 1977 HE requirements.

The seismic qualification has been reviewed to the latest DDE and HE levels described in Section 3.7. Based on this review, it has been demonstrated that both the excitation cubicle and the control cabinet will perform their safety function during and after the specified seismic conditions.

The sixth excitation cubicle and control cabinet for DG 2-3 have been seismically qualified by shake-table testing.

3.10.2.7 Design Class I AC Electrical Distribution Equipment

The following sections describe the seismic qualification of Class 1E ac electrical distribution equipment.

3.10.2.7.1 4160 V Metal-Clad Switchgear

The original 4160 V metal-clad switchgear with General Electric (GE) 250 mVA 4.16 kV magneblast circuit breakers was seismically qualified by a combination of testing and analyses.

Later, it was discovered that 350 mVA circuit breakers should be used in place of the GE 250 mVA 4.16 kV magneblast circuit breakers. GE could not supply such breakers to the same switchgear. Consequently, PG&E decided to procure 350 mVA 4.16 kV breakers from NTS/PDS, which converted Japanese-made Yaskawa SF6 circuit breakers to fit the existing 4 kV switchgear. The new circuit breakers were installed during refueling outages 1R8 and 2R7.

New circuit breakers were seismically qualified by shake table testing (NTS report No. TR60431-95N-FR). The shake table testing was intended to achieve the following objectives.

(1) Demonstrate the structural integrity and functionality of the Yaskawa breakers.

(2) Demonstrate the structural integrity of as-installed 4 kV switchgear cubicles at DCPP with the Yaskawa breakers.

(3) Demonstrate the functional performance of the existing components (i.e., various relays and switches) installed in the existing 4 kV switchgear cubicles with replacement Yaskawa breakers.

(4) Instrument the test 4 kV switchgear cubicles with sufficient number of accelerometers to obtain accurate information on the dynamic response (response frequencies, test response spectra) at various cubicle locations. This information is to be used for further/future testing and analyses.

(5) Take immediate corrective actions to address significant anomalies observed during the test.

The initial seismic testing was performed at Wyle Laboratories in Huntsville, Alabama. Three seismic mock-up 4 kV switchgear cubicles were built to duplicate the design, material, and construction of cubicles G-5, G-12, and G-13 of Unit 1. A total of 18 OBE and SSE test runs were performed, including three runs of resonance search. Test results showed that the new breakers and mock-up cubicles successfully passed the minimum required 5 OBE tests.

For the SSE tests performed at Wyle Laboratories, excessive relay chatter at certain frequencies were noted. The excessive chatter was due to over-testing the equipment, which in turn was a result of Wyle Laboratories being unable to accurately control the test table response at 10 Hz and above due to resonance of the table. The over-test produced a significant amount of relay chatter, which caused the tripping and closing of breakers. The post test functional check showed that the breakers were functioning properly and had no structural damage.

To properly test the relays, supplemental SSE testing was performed at Farwell and Hendricks (F&H) Laboratories. The upper front doors of the G-12 and G-13 cubicles, where a majority of relays are mounted, were mounted on the F&H rigid test fixture. One 1200A breaker and one 2000A breaker, located adjacent to the test table, were fed by the relays. The SSE RRS obtained at relay locations on the G-12 and G-13 cubicles from the previous Wyle testing were reduced with the appropriate scaling factor to eliminate unnecessary over-testing. The supplemental SSE testing was successful. However, certain modifications (such as adding chokes to the breakers and removing the seal-ins from certain relays) were made when the new breakers were installed in the 4-kV switchgear.

Based on the above, the switchgear and its contents are qualified for the DE, DDE, Hosgri, and LTSP postulated seismic events at DCPP.

3.10.2.7.2 Potential Transformers 4160/120 V

There are a total of four potential transformers associated with each 4 kV vital switchgear. There is a potential transformer for each feeder; auxiliary, startup and the diesel generator and one for the bus itself. Potential transformers are normally an integral mechanical and electrical part of metal clad switchgear. However, the auxiliary and startup potential transformers were removed from the top of the 4160 V metal clad switchgear during the initial qualification testing performed in 1978.

In 1978, a potential transformer representing the auxiliary and startup potential transformer was separately shake-table tested and qualified for the Hosgri earthquake. A potential transformer representing the diesel generator and bus potential transformer was shake-table tested using a mock-up of cubicle H-7.

In 1995, a potential transformer was mounted above a mock-up of cubicle G-12 and a dummy weight, representing the weight of a potential transformer, was mounted above a mock-up of cubicle G-5. These two cubicles were included in the shake-table testing at Wyle Laboratories during the seismic qualification of the new SF6 breakers described in section 3.10.2.7.1.

The auxiliary and startup potential transformers that were originally at the 90-inch level of the vital switchgear have been relocated to rigid stands adjacent to the respective switchgear lineups. Electrically, they are still an integral part of the switchgear. The diesel generator and bus potential transformers located below the 90-inch level are still physically attached to the switchgear, with the exception of the diesel generator potential transformer on Unit 1 Bus F that was also moved to a rigid stand adjacent to the switchgear.

The seismic qualification has been reviewed for the latest DDE and HE levels. The comparison of the earlier test data with current seismic requirements and additional analysis demonstrate that the potential transformers are qualified to perform their safety function during and after the specified seismic conditions.

3.10.2.7.3 Safeguard Relay Boards

Originally, one safeguard relay board from Unit 1 was shake-table tested to qualify the relay boards for the seismic requirements of the DDE. New qualified relays were introduced to replace the ones that exhibited chatter. Relays whose chatter did not impair any safety function were not replaced. As a result of the 1978 HE reevaluation, one relay board of the six installed was shake-table tested to higher levels than the original test.

The qualification of the relay boards has been reviewed to the latest DDE and HE levels. Based on this review, it is concluded that the safeguard relay boards are seismically qualified to perform their safety function.

3.10.2.7.4 Vital 480 V Load Centers

The vital 480 V load centers were originally qualified for the DDE based on seismic tests on similar equipment conducted by the manufacturer. As a result of the 1978 HE reevaluation, the equipment was further qualified by shake-table testing. During the testing, the draw-out modules of the load center were equipped with hold-down brackets to prevent slamming of the modules and subsequent chatter of contacts. Chatter was detected also on the deenergized high-speed contactors of the Unit 2 fan cooler controllers while the low-speed contactor was energized.

As a result, all draw-out modules of the 480 V vital load centers have been equipped with hold-down brackets. The containment fan cooler motor controllers have been equipped with mechanical interlocks that prevent inadvertent closure of the deenergized high-speed contactor when the low-speed contactor is energized, and likewise prevent closure of the low-speed contactor when the high-speed is energized.

The load centers were qualified using a certain type of kickout spring. Subsequently, all load center contactors in question were checked in the field and the proper kickout springs (the one used in the qualification testing) were installed where necessary.

The qualification of the load centers has been reviewed to new 1983 seismic criteria for both the DDE and the postulated HE event described in Section 3.7. The comparison of the earlier test data with current seismic requirements and additional analysis demonstrates that the vital 480 V load centers are seismically qualified to perform their safety function during and after the specified seismic conditions. The qualification meets the requirements of IEEE 344-1975 and RG 1.100.

3.10.2.7.5 Vital Load Center Transformer

The vital load center transformers were originally seismically qualified for the DDE based on shake-table testing of a similar, but larger power transformer. Comparison was made which demonstrated that the test of the 1500-kVA transformers is applicable to qualify the 1000-kVA vital load center transformers installed.

The test results were further reviewed with regard to the 1977 requirements of the HE. It was found then that the earlier testing still qualified the transformer for the HE levels.

A further review of the original test with regard to current seismic requirements for both the DDE and HE concluded that the vital load center transformers are qualified for the above seismic criteria.

3.10.2.7.6 480 V Vital Load Center Auxiliary Relay Panels

The vital load center auxiliary relay panels were originally designed and constructed to meet DDE seismic requirements.

To qualify the panels and electrical components for the 1978 HE requirements, two typical panels were shake-table tested. This requalified all relay panels.

The qualification of the relay panels has been reviewed to current seismic criteria for both the DDE and the HE. The comparison of the earlier test data with the current seismic requirements and additional analysis demonstrates that the vital load center auxiliary relay panels are qualified to perform their safety function.

3.10.2.7.7 Instrument Power AC Panelboards

The instrument power ac panelboards were originally qualified for the DDE by seismic testing which includes multifrequency sine beat test and resonant frequency test. Subsequently, the equipment was requalified to the 1978 HE requirements based on comparison test data from the DDE tests above and shake-table testing for circuit breakers/panelboards of various manufacturers.

The qualification has been reevaluated to the current seismic requirements for both the DDE and the HE. The reevaluation includes the panelboard/component qualification by calculation and by comparison of 1978 shake-table test results to the current seismic criteria. The calculation verifies the equipment structure integrity, and the test results demonstrate that the current seismic criteria are met.

The reevaluation concludes that the instrument power ac panelboards remain seismically qualified.

3.10.2.8 Design Class I DC Electrical Equipment

The following subsections describe the seismic qualification of Class 1E dc electrical equipment.

3.10.2.8.1 Batteries

There are six vital "batteries" at DCPP, three in each unit. Each "battery" consists of 60 battery cells (see Section 8.3.2.2.1.3 for 59-cell configuration). The original Class 1E station batteries were C&D Model LCU-27. They were replaced in 1983 with C&D Model LC-25 battery cells. Currently, all vital batteries are C&D Model LCUN-33 cells.

Each vital battery (60 cells) is located in its own room in the auxiliary building at elevation 115 feet. In each battery room there are currently four battery racks; three are single-tier racks that hold 12 LCUN-33 battery cells each, and the fourth is a two-step rack that holds 24 of the cells.

The new battery cells (Model LCUN-33) were tested at Wyle Labs in Huntsville, Alabama. A rigid test rack was utilized. The test rack held four LCUN-33 cells. The new battery cells have been qualified by shake table testing for DE, DDE, and Hosgri design basis seismic events. They have also been evaluated for the LTSP requirements and were found to satisfy the LTSP acceptance criteria.

Two separate LCUN-33 tests were performed. First, unaged cells were tested to qualify the cells for installation in outage 1R5 and for a 5-year life. Next, another group of LCUN-33 cells were artificially aged and tested. The second test qualified the LCUN-33 cells for a 15-year life. The service life of LCUN-33 battery has been extended to 20 years per IEEE 535-1986 in 2006.

The new battery cells (Model LCUN-33) have been installed in Units 1 and 2 during the following refueling outages:

Unit 1		Unit 2	
Vital Battery	Outage/Year	Vital Battery	Outage Year
11	1R7/1995	21	2R5/1993
12	1R5/1992	22	2R7/1996
13	1R8/1997	23	2R8/1998

It is concluded that the station batteries C and D Model LCUN-33 will perform their safety function during and after DCPP design basis seismic events.

3.10.2.8.2 Station Battery Racks

Each vital battery (60 cells – see Section 8.3.2.2.1.3 for 59-cell configuration) is located in its own room in the auxiliary building at elevation 115 feet. In each battery room, there are currently four battery racks. Originally, all battery racks were single-tier racks. Each rack held 15 Model LC-25 cells. Since the new LCUN-33 battery cells are wider than the old cells, the existing single-tier rack would hold only 12 of the new cells. Accordingly, one of the existing single-tier racks was replaced with a new two-step rack that will hold 24 of the new battery cells. Currently, three of the existing racks are single-tier racks that hold 12 LCUN-33 battery cells each. The fourth is a two-step rack that holds 24 of the cells.

The original single-tier racks were supplied by C&D along with the original LCU-27 battery cells. The racks have since been modified by PG&E due to the 1978 Hosgri reevaluation, new stress analysis for the current DDE and Hosgri levels, and finally as a result of replacing the battery cells with the new Model LCUN-33.

Both the single-tier and the two-step racks have been seismically qualified by analysis and are qualified for DCPP design basis seismic events.

3.10.2.8.3 Battery Chargers

Originally, the battery chargers were seismically qualified for the DDE by dynamic testing. As a result of the 1978 HE reevaluation, one of the battery chargers was shake-table tested to qualify all chargers for the HE requirements.

Further shake table testing has been done on one of the battery chargers to current seismic requirement. The testing demonstrated that the battery charger will perform its safety function during and after the postulated seismic events. The testing qualifies all Class 1E battery chargers for both DDE and HE.

3.10.2.8.4 125 V DC Switchgear

The 125 Vdc switchgear was originally qualified for the DDE based on seismic tests performed on similar equipment conducted by the manufacturer.

As part of the 1978 HE reevaluation, a 125 Vdc switchgear from DCPP was shake-table tested. This switchgear is identical to the other five 125 Vdc vital switchgears installed in the plant. This test demonstrated the adequacy of the equipment's safety function during and after the postulated seismic condition.

The qualification of the dc switchgears has been re-reviewed to current seismic requirements for both the DDE and HE. The review confirms the adequacy of the qualification by comparison of the 1978 equipment test data to the current criteria. Based on the review, it is concluded that the 125 Vdc switchgears are qualified to perform their function during and after the DDE and the HE.

3.10.2.8.5 Motor Controller, 125 Vdc, for Valve FCV 95

The 125 Vdc motor controllers were installed at Units 1 and 2 in 1982. They have been seismically qualified to the seismic requirements of both the DDE and HE described in Section 3.7 by shake-table testing of one unit. The controller met all the test requirements; therefore, it is concluded that the motor controllers will perform their safety function during and after the specified seismic events.

3.10.2.9 Main Annunciator

Originally, the main annunciator cabinets were seismically qualified for the DDE by dynamic analysis. Visual annunciator components similar to those mounted in the cabinets were tested in operation by the supplier. The cabinets were reanalyzed again for the 1978 HE reevaluation. As a result, some bracing was added inside the cabinets. Components of the visual annunciator were shake-table tested and qualified for the HE requirements.

The seismic qualification of the annunciator cabinets and the visual annunciator components have been reviewed to the current requirements of both the DDE and HE. As a result of this review, the annunciator cabinets were further stiffened, particularly in the longitudinal axis. The components were found to meet the new seismic requirements.

The Sequence of Events Recorder (SER) components including the printer have been qualified by shake-table testing. The SER Cathode Ray Tube display and its microprocessor were shake-table tested to ensure they would not become a missile hazard but are not required to operate during and after a seismic event.

Subsequently, due to problems obtaining parts for the seismically-qualified printer, PG&E replaced the printer. The printer was replaced with a seismically qualified touch

screen and a computer (PC) interfacing with a nonseismically qualified desktop printer. The PC and touch screen were qualified by testing. After a seismic event, the operators will be able to view the alarms on the touch screen. Any compatible desktop printer can be obtained and used to print the data.

The main annunciator communicates via data link to remote multiplexers and visual annunciator drivers associated with the main generator, which are not seismically qualified. There is no failure mechanism of the data link, remote multiplexer, or remote visual annunciator drivers that can adversely impact the function of the main annunciator system following an earthquake. The main generator alarms provided by the multiplexers are Design Class II and are not needed to maintain the plant in a safe shutdown condition or to mitigate the consequences of seismic events (Reference 46).

The main annunciator system is considered to be important to plant operation. However, the main annunciator system is not required for safe shutdown of the reactor. To achieve high reliability, the main annunciator system is designed to remain functional during and after a Hosgri earthquake, and to operate during a momentary or extended loss of offsite power. To meet these performance goals, the main annunciator system was originally classified as a Class I system. However, since the main annunciator system is not designed to meet the single failure criterion, the system was reclassified to Class II.

3.10.2.10 Electrical Penetrations

Electrical penetrations of the containment structure must withstand the forces caused by a LOCA. The header plates are made of forged steel welded to the containment steel liner and therefore have considerably more strength than is needed to meet seismic conditions. The penetrations are approximately 5 feet long and contain insulated electrical conductors of stranded copper. These conductors are supported within the penetration and at the terminal boxes attached to each end of the penetration.

The electrical penetrations were originally seismically qualified for the DDE by static analysis, meeting the requirements of paragraph 3.1.3 of IEEE 344-1971. A further seismic analysis was made for penetration of similar configurations for the Pilgrim 1 and Fitzpatrick 1 units. This analysis was used to qualify the penetration for the 1978 HE reevaluation.

Seismic testing performed by the manufacturer and a new analysis was used to qualify the penetrations to current requirements of the DDE and HE. The analysis demonstrates that the electrical penetrations will perform their safety function during and after the specified seismic conditions.

3.10.2.11 Pressure and Differential Pressure Transmitters

Seismic tests were performed on Barton Model 763 and 764 transmitters and Rosemount Model 1151, 1152, 1153, and 1154 transmitters as part of an environmental

test programs conducted by their respective manufacturers. The transmitters were subjected to simultaneous independent biaxial excitation using a random test input. The test included a resonant search, 5-DEs, and 1-DDE, in each of two test positions.

The transmitters were pressurized and operational throughout the test. The output of each transmitter was monitored during the test to verify proper operation. The results of the test verified that the transmitters will operate properly for both DDE and HE excitation.

The seismic qualification of Rosemount Model 1154 transmitters is based on similarity between Model 1154 and Model 1153 Series D transmitters (Reference 37, paragraph 7.2). As documented in References 38 and 39, the Model 1153 Series D transmitters were shake table tested per IEEE 344-1975 to DCPP seismic requirements.

During the seismic testing leak test, calibration check and voltage variation tests were performed.

All tested transmitters successfully met the acceptance criteria. Anomalies observed were determined not to have an impact on the transmitters' qualification (Reference page v in Wyle Test Report No. 45592-3 -- Appendix A of Reference 38). The test response spectra curves enveloped the applicable DCPP-required response spectra curves (Reference 39).

Seismic testing and analysis (Reference 50) was performed to qualify Rosemount 'Smart' transmitter model 3051C for use in Instrument Class IC Systems as defined in Section 7.1 (3). The seismic testing and analysis in Reference 50 also qualifies the use of Rosemount 'Smart' transmitter model 3051N for use in Instrument Class IA Systems as defined in Section 7.1 (1).

Seismic tests were also performed on two typical models of Barton transmitters, Models 368 and 369, pressurized to mid-range operation. The tests were performed at Wyle Laboratories on a biaxial shaking table. Results show that the requirements were met. The transmitters operated throughout the tests without malfunctioning. A helium leak test was made on the pressure boundary of the transmitter after the seismic tests. No leakage was detected. The instruments were qualified in conformance to the requirements of IEEE 344-1971, Paragraph 3, Method 2, simulated seismic test.

Additional seismic qualification tests have been performed on the Barton Model 332 pressure transmitter. These were part of a series of tests, documented in WCAP-8021, where selected types of safety-related essential equipment were subjected to vibration tests in the range of 1 to 35 Hz.

A preliminary search of the 1 to 35 Hz frequency range, using a sinusoidal input, was performed to identify any resonant condition. Any resonant frequencies found would be included with the test frequencies of the sine beat seismic input. The amplitude of the

sine beat was chosen such that it would be at least as great as the maximum acceleration that the equipment would experience during a DE horizontal ground acceleration of 0.4 g, augmented by building structural amplification. Tests were done independently for each of the two horizontal and the one vertical directions of motion. Throughout the duration of the testing, both the test and reference transmitters were energized, measuring a 50 psi input pressure on a 300 psi span. The 4 to 20 mA electric output of the transmitter was monitored during and after the test to check for any loss of function.

Based on the results of these tests, it is concluded that this transmitter will perform its required design function during, as well as following, a seismic event.

3.10.2.12 Raceway Supports

The Class 1E raceway systems (safety-related) consist of conduits, cable trays, and pull boxes supported by approximately 27,000 supports in each unit. The raceway supports are constructed primarily of bolted assemblies of cold-formed channel sections either of "Superstrut" (more than 90 percent) or "Unistrut" (approximately 10 percent) brand, which are spaced at 8-1/2 feet or less, unless otherwise approved by an engineering evaluation. The supports are attached to concrete or structure steel by bolted connections or welding. Based on the similarity of structural configuration, the raceway supports are grouped into more than 400 generic types.

3.10.2.12.1 Design and Acceptance Criteria

The raceway supports are required to withstand loads from DDE or HE. The supports, in their as-built conditions, are evaluated to ensure that they meet the following criteria.

Loading Combination

The horizontal component of seismic load (DDE or HE) either transverse or longitudinal to the raceways that results in the highest stress on the member under consideration is combined, by absolute sum, with the stresses or forces due to dead load and vertical seismic load.

Response Acceleration of Support System

Unless otherwise justified the floor response spectra where supports are located are used for evaluation. The horizontal response is taken as the greater of the building responses due to either the east-west or the north-south ground motion combined by absolute sum, with the corresponding torsional response, as appropriate.

Acceptance Criteria

The specifications used to review the design of the steel members are the AISI "Specification for Design of Cold Formed Steel Structural Members" (Reference 32,

Section 3.10.3) and Part 1 of the AISC "Specification for the Design, Fabrication and Erection of Structural Steel for Buildings" (Reference 33, Section 3.10.3) applicable to hot-rolled members. The allowable stress given in the AISC specification is increased by 60 percent as recommended by Standard Review Plan Section 3.8.4 (Reference 34, Section 3.10.2.12.3). The allowable stress for AISI is increased so that the margin against yielding is 1.0 or greater with the allowance for local yielding at connections. The allowable slip-shear capacity of bolted connections on strut members are established by statically testing support connections with various combination of nuts and bolt torque values. The design allowable is based on the support connection containing the type of nut (98 percent of the nuts actually used in the plant exhibit superior behavior) and the bolt torque value (more than 90 percent of the connections have significantly higher values) which very conservatively represent the as-built condition. In addition, a qualification criterion was established by performing dynamic tests on specimens having representative support configuration in determining acceptable shear capacity of the in-situ bolts. In some cases, the slip-shear capacities are based on manufacturer's recommended values. These shear capacities are for appropriate combination of nut types, bolt torque, and strut which have been verified by additional tests.

Permissible loads on conduit clamps are kept below 90 percent of the ultimate values. Clamps are also checked for interaction of pull-out and slip (either in transverse or longitudinal direction). The acceptance limit on fillet welds on cold-formed steel members is 60 percent greater than the allowable given in Section 4.2.1 of the AISI Specification. Spot-welds in composite superstrut channels are checked against allowable shear values developed from a testing program.

3.10.2.12.2 Evaluation

The electrical raceway systems are evaluated for seismic loading in the transverse, longitudinal, and vertical directions by following the methodology stated below.

Transverse Seismic Analysis

Each of the support types are evaluated against the acceptance criteria. The seismic loads used in the evaluation of the supports are based on system frequency of the support and adjacent span of the raceway. The damping value used for conduit supports is 7 percent. For cable tray supports, two separate frequency analyses are made to determine the spectral response. In the first analysis, the system frequency is obtained based on support frequency alone and 7 percent damping is used. In the second analysis, the system frequency is generated by combining the support frequency and the tray frequency. The seismic response is obtained based on 15 percent damped floor spectra. The second analysis is confirmatory and not a basis for the license. The larger of the two spectral values is used for evaluation.

Each support type is first evaluated for the generic case based on design, which results in maximum support response.

Any support that cannot be qualified for its generic case is investigated for its as-built condition.

Longitudinal Seismic Analysis

All Class 1E raceway systems are walked down and documented. The longitudinal seismic load is generated based on raceway system frequency and 7 percent damping. The peak response acceleration is used if the system frequency is less than 33 Hz; otherwise, the zero period acceleration is used. The seismic load is distributed among the supports in proportion to their longitudinal stiffness. The individual supports are evaluated for structural adequacy.

Vertical Seismic Analysis

The vertical seismic analysis uses the same methodology as the transverse seismic analysis.

3.10.2.13 Fire Pump Controller

The fire pump controllers for the plant interior system were upgraded to Class 1E when the fire protection system was upgraded. One controller was shake-table tested and qualified to 1978 HE seismic requirements.

The qualification has been reviewed to the current seismic criteria for both the DDE and HE. The comparison of earlier test data with the current seismic requirements demonstrates that the fire pump controllers are seismically qualified to perform their safety function during and after the specified seismic conditions.

3.10.2.14 Local Starters

Local starters were originally seismically qualified for the DDE based on shake-table testing by the manufacturer. As a result of the 1978 HE reevaluation, three representative starters were shake-table tested. The testing qualified all local starters for their respective locations. Other starters of different manufacture used for the HVAC systems were qualified by comparison to the starters tested. The qualification of the local starters has been reviewed to current seismic criteria for both the DDE and HE.

For the review of the qualification to current seismic requirements, the local starters were broken down into four groups:

(1) Starters located in the auxiliary and fuel handling buildings were qualified by comparison of the 1978 test data to the current seismic criteria. This includes contactors installed since the 1978 shake-table testing.

(2) Starters located at the turbine building 119-foot elevation were qualified by comparison of the 1978 test data to the current seismic criteria and by

comparison to identical starters shake-table tested for the turbine building 140-foot elevation.

(3) Starters located at the turbine building 140-foot elevation were installed after the 1978 electrical equipment testing program. One of these starters was shake-table tested to qualify the starters for the current seismic criteria.

(4) Starters located at the auxiliary building 154-foot elevation, some of which are of different manufacture, have been qualified by comparison to the starters tested. The starters tested were qualified to spectra with much higher accelerations than are required for the 154-foot elevation of the auxiliary building.

The aforementioned review of the earlier seismic testing to current criteria for both the DDE and HE and additional testing demonstrates that all local starters are qualified to perform their safety function during and after the specified seismic conditions.

3.10.2.15 Ventilation Control Logic and Relay Cabinet

The ventilation control logic and relay cabinets were originally vibration-tested in July 1973, and seismically qualified for the DDE. The cabinets were found to be rigid. As part of the 1978 HE reevaluation, components of the cabinets were shake-table tested again and qualified for the HE.

The seismic qualification of the ventilating control logic and relay cabinet and their components has been reviewed to the current seismic requirements of both the DDE and the HE. Based on the review, it has been concluded that the ventilation control logic and relay cabinets are seismically qualified to perform their safety function during and after the DDE and the HE.

As part of the Unit 1 and 2 AFHBVS control system replacement, a new programmable logic controller (PLC) system was installed. The seismic qualification of the Plant Operating Vent panels, POV1 and POV2, and their components were reviewed to the current seismic requirements of both the DDE and the HE. The POV panels were evaluated using analytical evaluation and the PLC was shake table tested by the supplier. Based on the review, it was concluded that the POV1 and POV2 cabinets are seismically qualified to perform their intended safety function during and after the DCPP design basis seismic events.

3.10.2.16 Fan Cooler Motors

The fan cooler units were qualified for seismic adequacy by a combination of analysis and testing. A seismic analysis of the fan cooler unit, including the motor, was made to verify that the units will not exceed the allowable stresses or deflections. The response spectrum method of analysis was used.

The fan motor assembly natural frequencies were calculated using a lumped mass model. Because of high natural frequencies (after adding stiffeners to the fan cooler assemblies), this system was analyzed as a rigid structure and equivalent static loads were applied. An additional unbalanced load of 1 g was assumed to occur in all rotating assemblies.

Limit values were in accordance with the elastic provisions of the AISC-69 specification. Bearing limits were taken as failure by brinelling under dynamic load (basic rating) from the manufacturer's catalog.

An analysis and an impact test were also made on an end bell of the motor. Based on these results, Westinghouse concluded that the containment fan-motor-cooler assembly structure could withstand the combination of required loads.

3.10.2.17 Pump Motors

Electric motors for Design Class I pumps were procured with the pumps to equipment specifications that covered the pump/motor assembly as a unit. These equipment specifications required that the equipment be adequately designed to accommodate seismic accelerations appropriate for the DE and DDE.

At the time of procurement of this equipment, there were no industry standards for seismic qualification of electric motors. However, methods and criteria employed in the design of large, integral horsepower electric motors lead to motor designs that are inherently capable of tolerating high seismic loadings without loss of function. Design considerations for motors of this type include maximum torque, critical shaft speed, bearing life, vibration, and cyclical loading. These considerations lead to motor designs that would not be governed by the application of seismic loads in the range of those appropriate for DCPP. Experience with such motors in applications subject to severe vibration and shock provides additional confirmation of seismic adequacy. Based on these considerations, it is the consensus of competent engineering practice that these motors are adequately designed to perform their safety function before, during, and after the DDE or HE.

In the case of the auxiliary saltwater pumps, which are vertically mounted, calculations indicated that seismic bracing in the horizontal direction was necessary to ensure that the first vibrational mode of the pump-and-motor assembly would be in the rigid range of the design spectra. Other pump-and-motor assemblies have natural frequencies well within the rigid range.

Analyses of pump-and-motor assemblies representative of those considered here have been performed and have shown substantial margin in stresses, deflections, and bearing loads for seismic loadings in the range of those appropriate for DCPP. Selected pump-and-motor assemblies for DCPP have also been analyzed using the

appropriate floor response spectra and both static and dynamic analysis methods. For all cases analyzed, seismic adequacy has been verified.

3.10.2.18 Electric Cables

Electric cables interconnecting pieces of equipment depend on raceways for support during seismic activity. Seismic criteria for raceway supports are described in Section 3.10.2.12. These cables are flexible and are fully supported along their entire length in conduit or tray. Adequate slack is provided to impose little or no tension on the wires. Where relative shifts between structures can occur, raceways are provided with flexible joints or are routed with adequate flexibility to ensure that the conductors remain undamaged and their associated supports meet their acceptance criteria. (Note that use of trays for Class 1E circuits is very limited, see Chapter 8.)

3.10.2.19 Motor-Operated Valves

PG&E-purchased motor-operated valves (MOVs) whose only safety function is to maintain a pressure boundary and which are not required to change position during or after an accident (passive valves), and those whose safety function includes both maintaining a pressure boundary and changing position during or after an accident (active valves), were qualified to acceleration levels less than or equal to allowable acceleration levels provided by the vendor or established by analysis. All Westinghouse-purchased MOVs were qualified to acceleration levels less than or equal to allowable acceleration levels provided by Westinghouse.

Limitorque MOV operators of the type installed on active Design Class I valves in DCPP Units 1 and 2 have been seismically qualified by test. Tests were conducted on various sized operators at g-levels from 3 to 10 g.

Operators were tested both while operating and while energized and not operating. The testing was single axis, performed along each of three mutually perpendicular major axes. Sine sweep testing was utilized over a range from 5 to 35 Hz, and was followed by 1- to 2-minute sinusoidal vibration at 34 Hz or at any resonant frequency below 35 Hz.

The test results for the MOV operators have been considered in the analysis of piping systems. The mass and resonant frequency of the operator is used as input in the piping analysis. The resulting acceleration levels are compared to the allowable levels to verify that the operator will function as required.

3.10.2.20 Control Room Ventilation System

The control relay and power panels are seismically qualified to the current seismic requirements for both the DDE and the HE. The qualification of the power panels is based on: shake-table testing on the similar equipment performed by the manufacturer, onsite resonance frequency test on the similar panelboard, extensive shake-table testing of electro-mechanical equipment containing circuit breakers or circuit breaker panelboards and testing of circuit breakers to the extent of the shake-table limit.

The qualification of the control relay panels is based on the actual shake-table testing of similar ventilation control relay cabinet installed in DCPP, containing the same control relays. Timing relays not found in this shake-test are seismically qualified based on the qualification of 4-kV switchgear equipment in which the identical timing relays were installed.

Test specimens similar to the installed equipment were evaluated for their adequacy of qualification. By comparison of the test data from those shake-table tests to the current seismic requirements, the test results of these equipment demonstrate that the specified seismic criteria are met for both the DDE and HE. It should be noted that the equipment is only needed for the control room ventilation and pressurization (CRVP) after an earthquake and not during the earthquake. Therefore it is concluded that the CRVP control relay and power panels are qualified to perform their safety function after the postulated seismic events such as the DDE and the HE.

The radiation and chlorine monitoring panel has been qualified by seismic simulation testing of a test specimen similar to the panel installed at the DCPP. The panel test specimen was welded to the test table and bolted to an adjacent structure in order to simulate the actual plant mounting conditions. The panel test specimen contained the following instruments: one radiation rate readout (Nuclear Measurements Corporation Model GA-2TMO), one radiation rate readout (Technical Associates Model FML-554), one chlorine analyzer (Capital Controls Model 1030), and one switch reset module. Dummy weights were used to simulate random biaxial seismic simulation tests in accordance with IEEE std. 344-1975. The function of the instruments was verified before and after the testing. The test response spectra have been verified to envelop the DDE and HE required response spectra. The chlorine detection function has been eliminated and the detectors are abandoned in place.

The radiation detector associated with the Nuclear Measurements radiation rate readout described above was also subjected to random biaxial seismic simulation tests. The test specimen was bolted to a rigid steel plate in order to simulate the mounting arrangement used at DCPP. The function of the device was verified before and after the test. The test table response spectra have been verified to envelop the DDE and HE required response spectra.

The radiation detector associated with the Technical Associates radiation readout and the chlorine detector associated with the Capitol Controls chlorine analyzer have also

been submitted to random biaxial seismic simulation tests. These two detectors were mounted into a 14-inch steel duct in order to simulate the mounting arrangement used at the DCPP. The function of the detectors was verified before and after the tests. The test response spectra envelops the required response spectra for both the DDE and HE cases. The chlorine detection function has been eliminated and the detectors are abandoned in place.

3.10.2.21 Subcooled Margin Monitors

The subcooled margin monitors (SCMMs) are located in PAM Panels 3 and 4. Subcooled margin is calculated and displayed by the reactor vessel level instrumentation system (RVLIS); therefore, seismic qualification of each SCMM is covered by the seismic qualification of the RVLIS cabinets (see Section 3.10.2.32.1).

Train A of the SCCM provides output to a recorder on PAM1. PAM1 seismic qualification is addressed in Section 3.10.2.22.

Train B of the SCCM provides output to a display on VB2. This display was qualified by testing.

3.10.2.22 Postaccident Monitoring Panels PAM1 and PAM2

These panels are located in the main control room and house various indicators and recorders used for postaccident monitoring. Typical parameters involved are reactor vessel level, containment hydrogen gas concentration, containment gross activity, etc. The panels were manufactured for PG&E by Trayer Engineering, Inc. Design Class I indicators and recorders were manufactured by Westinghouse, Leeds and Northrup, and other qualified suppliers.

Panel PAM1, with its associated instruments, was qualified by random biaxial seismic simulation tests. The tests were performed at Wyle Laboratories. The function of the devices was verified before and after seismic testing. The test response spectra have been verified to envelop the DDE and HE required response spectra.

Panel PAM2 has been qualified by an analysis that showed that the panel is rigid, with no resonant frequencies below 33 Hz. In addition, a static analysis was performed that showed that the combined seismic stresses do not exceed the allowable limits. The Design Class I instruments mounted in PAM2 have been qualified by seismic simulation tests. The test response spectra obtained from these random biaxial tests have been verified to envelop the DDE and HE spectra.

3.10.2.23 Pilot Solenoid Valves

Pilot solenoid valves are used to control the air supply to air-operated control valves. The pilot valves can be mounted either on or off the control valve actuator. The

required acceleration level for the pilot valves is 9 g's, which is based on the maximum allowable response for control valve actuators having Design Class I pilot valves.

The pilot solenoid valves have been qualified by tests performed on a variety of valve models by both the vendor, ASCO, and PG&E. The tests consisted typically of sine beat tests performed over the frequency range of 1 to 33 Hz. The minimum acceleration value met or exceeded the required level for the valves except at low frequencies, where the level was limited by testing machine capabilities. The function of the valves was verified before and after the testing.

3.10.2.24 Process Solenoid Valves

Design Class I process solenoid valves are used as containment isolation valves in the post-LOCA sampling system and containment hydrogen monitoring system. The valves were manufactured by Valcor Engineering.

The valves are located both inside and outside of containment. The valves inside containment are mounted to the annulus steel structure. The valves outside of containment are mounted to the exterior of the containment structure. The required acceleration level for the valves is an envelope of the DDE- and HE-required response spectra for both these locations.

The valves were qualified by a test performed by the vendor as part of an environmental qualification program. The test used a random biaxial input, with the devices mounted to the test table simulating an actual installation. The test procedure conformed with IEEE 344-1975. The test levels were sufficient to qualify the valves to their required acceleration level. The function of the valves was verified before and after the testing.

3.10.2.25 Containment Hydrogen Monitoring System

The containment hydrogen monitoring system (CHMS) consists of two redundant systems each consisting of an analyzer panel and a remote control panel. The analyzer panels are anchored to the floor in plant area GE at elevation 100 ft. The remote control panels for both systems are mounted in a panel (RCHMC) located in the post-LOCA sampling room in plant area GE at elevation 85 ft.

The Containment hydrogen monitoring system is Class II, Type C, Category 3, non safety related. The analyzer panels are Class II and anchorage of the analyzer panel has been seismically evaluated. Although the panel inserts for the Containment hydrogen monitor are non-safety related, the remote control panel (RCHMC) is Class I for the Class I circuits powering the related containment isolation valves.

The RCHMC panel has been structurally analyzed which includes the seismic mounting of non-safety related panel inserts. A detailed stress analysis was conducted that showed that the rack assembly is structurally adequate to withstand the DDE and HE loads.

3.10.2.26 Containment Purge Exhaust

Each monitor consists of a detector assembly and a Local Radiation Processor (LRP) located in Area L on the 100 ft elevation. The remote readout is located in the Radiation Monitoring System panel (RNRMS) in the Control Room. The detectors and LRPs are qualified by analysis based on a test simulation performed on similar equipment. The Control Room mounted equipment is qualified based on shaketable tests on the RNRMS panels performed for Victoreen. See Section 3.10.2.1.1.1.

3.10.2.27 Limit Switches

Limit switches are used to detect the position of control valves. Limit switches for motor-operated valves that are an integral part of the actuator are qualified as part of the assembly (see Section 3.10.2.19). Limit switches for air-operated valves and for motor-operated valves that are mounted on the valve actuator are qualified separately. The required acceleration level for these limit switches is 9 g, which is based on the maximum response allowable for valves having Class 1E limit switches.

Class 1E limit switches have been qualified by testing performed on several different styles. Tests have been performed by both the vendor and PG&E. These tests typically consisted of sine beats or sine dwells at 9 g peak acceleration over the frequency range of 1 to 33 Hz. Test acceleration levels met or exceeded the required level except at low frequency ranges where the level was limited to test machine capabilities. The test specimens were functionally tested before and after the vibration testing.

3.10.2.28 Containment High-Range Radiation Monitoring System

The containment high-range radiation monitoring system is used to monitor ambient gamma radiation in the containment following a LOCA. The system consists of two redundant detectors located in the containment at elevation 145 ft and a remote readout located in the postaccident monitoring panel PAM2 in the main control room. The system was supplied and qualified by Victoreen.

The radiation detectors and readouts have been qualified by random biaxial seismic simulation tests that were conducted as part of an environmental qualification test program. The test response spectra have been verified to envelop the required DDE and HE response spectra. There were no malfunctions experienced throughout the seismic tests. The test conformed to IEEE 344-1975.

3.10.2.29 Pressurizer Safety Relief Valve Position Indication

The pressurizer safety relief valve position indication system is an acoustic flow detection system that verifies valve position by sensing flow through the pressurizer relief lines. There are three channels, one for each relief valve. The system consists of

four components: detector, charge converter, signal conditioner, and remote readout. The detector is an accelerometer attached to the pressurizer relief line by a metal strap. The charge converters for all three channels are housed in a stainless steel enclosure, which is mounted to the wall adjacent to the pressurizer at elevation 145 ft in the containment. The signal conditioner is located in panel RCRM in the main control room. The remote readout is mounted in the main control board. All components of the system were supplied and qualified by Technology for Energy Corporation.

The equipment comprising the system was qualified as part of an environmental qualification program conducted by the vendor. The seismic portion of the testing was conducted in accordance with IEEE 344-1975. All of the system components were qualified by tests consisting of random input, independent triaxial excitation. Tests were conducted at Structural Dynamics Research Corporation. The test response spectra from these tests have been verified to envelop the applicable DDE and HE spectra. The function of the devices was verified before and after the testing.

3.10.2.30 Heating, Ventilating, and Air Conditioning Equipment

The qualification of safety-related heating, ventilating, and air conditioning (HVAC) equipment is reviewed according to DE, DDE, and HE criteria. This HVAC equipment is associated with the following safety-related systems:

(1) Forced draft shutter

(2) Diesel generator compartment ductwork

(3) Auxiliary saltwater compartment ventilation

(4) 4-kV switchgear ventilation

(5) 480 Vac switchgear ventilation

(6) Auxiliary building-fuel handling building ventilation

(7) Control room ventilation and pressurization system

The equipment and components of Class 1 HVAC systems are listed in Table 3.10-3. They have been reviewed for seismic qualification in accordance with the spectra, defined in Section 3.7.

The equipment listed in the table is organized into qualifying groups consisting of similar types of equipment. The component subject to the worst-case qualifying condition in each group has been reviewed for compliance with acceptance criteria. This worst-case analysis in turn envelops the other components in the respective groups.

All the items in the table were reviewed for identification of the qualifying spectra. Where the most current spectra exceed the conditions under which the component was previously analyzed, a new analysis was initiated. The results of the analysis confirmed the qualification of the component or identified a physical modification. Where analysis is not appropriate, equipment testing was used to demonstrate the design performed under the qualifying seismic conditions.

3.10.2.30.1 HVAC Duct and Duct Supports

The Class I HVAC duct system consists of ducts and approximately 2,000 supports in both units. HVAC ducts are made of cold-formed steel conforming to ASTM A525, A526, and A527 with the thickness varying depending upon the duct size. The duct supports are mostly structural steel angles. Supports are attached to concrete or structural steel by bolted connections or by welding. The ducts are fastened to the supports by means of screws, rivets, or stitch welds.

3.10.2.30.1.1 Design and Acceptance Criteria

The duct and duct supports are evaluated in their as-built condition to meet the following criteria:

Loading Combination

The ducts are evaluated for the concurrent dead weight, seismic load, and pressure load. The duct supports are evaluated for dead weight and seismic load. The pressure load is the negative operating pressure of the HVAC system and is not included in the evaluation of the duct supports. The seismic loads evaluated are DDE and HE loads. The horizontal component of seismic load (DDE or HE), either transverse or longitudinal to the ducts, that results in the highest stress in the member under consideration is combined, by absolute sum, with the stresses due to vertical seismic load. As an alternative, the seismic loads from each of the three directions are combined by SRSS method.

Response Acceleration of Support System

The applicable floor response spectra where the supports are located are used for evaluation of HVAC duct and duct supports. The corresponding horizontal spectra are combined, by absolute sum, with the corresponding torsional response, as appropriate.

Acceptance Criteria

The AISI "Specification for Design of Cold-formed Steel Structural Members" is used to evaluate the design of cold-formed steel members, and part 1 of the AISC "Specification for the Design, Fabrication, and Erection of Structural Steel for Buildings" is used for the design of hot-rolled members. The allowable stresses given in AISI and AISC Specification are increased by 60 percent.

3.10.2.30.1.2 Evaluation

For duct supports, the seismic loading is evaluated for vertical plus transverse horizontal loads and vertical plus longitudinal horizontal loads. The frequency of the coupled duct and duct support system is used in determining the spectral response. The damping values used are 2 percent for DDE and 7 percent for HE.

3.10.2.31 Electric Hydrogen Recombiner System

The model B electric hydrogen recombiner system (EHRS) is designed to control and reduce post-LOCA containment hydrogen levels. The system consists of three components; control panel, power supply, and recombiner. Two model B EHRSs are provided for the DCPP site.

The recombiner was subjected to multiple frequency multiple axis testing in accordance with IEEE 344-1975. The results of the seismic testing are provided in Reference 25. The recombiner was energized and at operating temperature before, during, and after each seismic test. Following the entire testing, the recombiner was inspected for damage. No disabling damage was found. An air flow test was conducted after testing and the results show no loss of air flow. The test response spectra were checked to envelope the DDE and HE response spectra, to confirm its seismic adequacy.

The power supply and control panel were tested at the same time as documented in Reference 26. Testing was done with conservatively large accelerations over a range of applicable frequencies and conformed to the procedures given in IEEE 344-1971. The peak test input accelerations used in the power supply and control panel tests were checked to verify that they are larger than the requirements derived by DDE and HE loadings.

After each seismic test the power supply was visually inspected for structural integrity and functional operability. Both units were found to operate satisfactorily.

3.10.2.32 Reactor Vessel Level Instrumentation System

The RVLIS consists of the following instrumentation:

- RVLIS/incore thermocouple cabinets (including remote display)
- Reactor coolant level differential pressure transmitters (see Section 3.10.1.5)
- Surface mounted RTDs
- High volume sensors
- Differential pressure indicating switches (hydraulic isolators)

Typical items of the above instrumentation and electronic equipment have been type tested using multiple frequency, multiple axis seismic testing. Testing was performed in accordance with the procedures given in IEEE 344-1975. The test response spectra

obtained from those tests were checked to envelope the DDE and HE response spectra.

3.10.2.32.1 RVLIS/Incore Thermocouple Cabinets

Two RVLIS/incore thermocouple cabinets (PAMs 3 and 4) are provided for DCPP application. Located within each cabinet are the microprocessor electronics, reactor coolant pump (RCP) status panel, and a remote display. The above RVLIS instrumentation is only required to operate normally before and after seismic excitation. The RCP status panel assembly is shown to be operational by the signals recorded during testing and the functional checks made after each simulated SSE. The remote display electronics must function normally by providing microprocessor output display formatted information.

The results of seismic testing of the original RVLIS/incore thermocouple cabinets are provided in Reference 27. The original remote display was not included in the cabinet tested. The original remote display was tested later to worst-case (maximum) in-cabinet response for the RVLIS/incore thermocouple cabinets. The seismic testing of the original remote display is documented in Reference 28.

Because the original Westinghouse-supplied system is obsolete and due to the lack of availability of replacement components, the obsolete RVLIS/incore thermocouple systems were replaced. The replacement processors, signal conditioners, and displays are seismically qualified by testing and analysis as documented in References 47 and 48 and PG&E Calculation IS-66.

3.10.2.32.2 Surface Mounted RTDs

There are 14 surface mounted RTDs used in RVLIS to measure the temperature of the reference leg impulse lines. As described in Reference 29, the surface mounted RTDs were subjected to single frequency, multiple axis sinusoidal tests and multiple frequency, multiple axis seismic tests. The RTDs tested were operational throughout all phases of the test sequence. Measurement of performance was by a evaluation of the recorded RTD output, periodic static calibrations, and numerous insulation surface mounted RTDs maintain their structural integrity and functional accuracy required.

3.10.2.32.3 High Volume Sensors

The high volume sensors are bellows designed for large volumetric displacement to accommodate thermal expansion postulated postaccident environment. The safety related performance requirement is that the sensor must maintain this pressure boundary and sensing interface between the process and filled pressure/differential pressure system without introducing any sensing errors.

The results of seismic testing are provided in Reference 30. Based upon the information provided therein, the high volume pressure sensor can successfully fulfill its safety related requirements during and after seismic testing.

3.10.2.32.4 Differential Pressure Indication Switches

The differential pressure indicating switches (hydraulic isolators) are used to seal off full process pressure in either direction and will actuate switches to indicate a unbalanced condition. The safety-related performance requirement for RVLIS is that the switch provide the isolation function without contributing a sensing error to the accuracy of a downstream pressure of differential pressure transmitter.

During the seismic test, adherence to this requirement is verified by monitoring the output of two reference transmitters receiving the pressure signal. While no safety related use is made of the switch contacts in the reactor vessel level indicating system, testing was designed to demonstrate the suitability of indicating switch use for other applications.

Seismic testing of the hydraulic isolators is provided in Reference 31. The hydraulic isolators sustained no physical damage during the seismic testing and performed their process sensing line isolation function successfully, with no leakage of the water fill.

3.10.2.33 Incore Flux Mapping Cabinets and Transfer Device

The incore flux mapping cabinets and flux mapping transfer device are non-safety related but have been seismically qualified for structural integrity for HE loadings.

The incore flux mapping cabinet is structurally identical to the NIS cabinets (see Section 3.10.2.1.1). The weight distribution of equipment within the cabinet would produce essentially the same dynamic results. Therefore the results obtained from the test of the NIS cabinets are applicable for the incore flux mapping cabinet structure.

The flux mapping transfer device is an assembly used to support control equipment to drive detectors into and out of thimbles in the reactor core. The flux mapping transfer device has been evaluated to maintain its structural integrity to withstand the HE for DCPP.

3.10.3 REFERENCES

1. The Institute of Electrical and Electronic Engineers, Inc., IEEE Standard 344-1971, Trial Use Guide For Seismic Qualification of Class I Electric Equipment for Nuclear Power Generating Stations.

2. IEEE Standard 344-1975, Recommended Practices for Seismic Qualification of Class IE Equipment for Nuclear Power Generating Stations.

3. USNRC RG 1.100, Revision 1, Seismic Qualification of Electrical Equipment for Nuclear Power Plants, August 1977.

4. Description of the Systems Interactions Program for Seismically Induced Events, Revision 4, August 1980.

5. Seismic Testing of Electrical and Control Equipment (PG&E Plants), WCAP-8021, May 1973.

6. Letter No. NS-CE-1609, Eicheldinger (Westinghouse) to Stolz (NRC), Subject: "Drawer Securing Method for NIS Rack," November 1977.

7. Seismic Operability Demonstration Testing of the Nuclear Instrumentation System Bistable Amplifier, WCAP-8830, October 1976.

8. General Method of Developing Multifrequency Biaxial Test Inputs for Bistables, WCAP-8624, September 1975.

9. Consequences of Seismic-Induced Actuation of Protection Systems Relays on the Diablo Canyon Nuclear Plant, Westinghouse Electric Corporation, July 1975.

10. Seismic Qualification of the Rotary Relay for Use in the Solid State Protection System, WCAP-8694, January 1976.

11. Seismic Operability Demonstrating Testing of the Westinghouse CID 7100 Series Process Instrumentation System Bistables, WCAP-8832, November 1976.

12. Deleted.

13. Seismic Testing of Electrical and Control Equipment, High Seismic Plants, WCAP-8921, December 1971.

14. Equipment Qualification Test Report Pressure Sensor, WCAP-8687, Supplement 2-E21A, Revision 1, March 1982.

15. Equipment Qualification Test Report Barton Differential Pressure Transmitter - Qualification Group B, WCAP-8687, Supplement 2-E04A, Revision 2, March 1983.

16. Seismic Testing of Electrical and Control Equipment, Type DB Reactor Trip Switchgear, WCAP-8821, Supplement 4, August 1974.

17. Deleted.

18. Deleted.

19. Seismic Testing of Electrical and Control Equipment Engineering Safeguards Test Cabinet for PG&E Plants, WCAP-8021, Supplement 1, May 1977.

20. Seismic Qualification of the Rotary Relay for Use in the Trojan and Diablo Canyon Auxiliary Safeguard Cabinets, WCAP-8941, February 1977.

21. Seismic Qualification of the Diablo Canyon Main Control Board, Central Console, WCAP-10358, August 1983.

22. Benchmark Problem Solutions Employed for Verification of the WECAN Code, WCAP-8929, June 1977.

23. Forced Vibration Testing of the Diablo Canyon Unit 1 Main Control Board, ANCO Engineers Inc., Document No. A-000047, May 1983.

24. Seismic Qualification Test Report for Diablo Canyon Main Control Board and Central Console Mounted Class 1E Devices, WCAP-8941, February 1977.

25. Qualification Testing for Model B Electric Hydrogen Recombiner, WCAP-9346, July 1978.

26. Electric Hydrogen Recombiner for PWR Containments Equipment Qualification Report, WCAP-7709-L, Supplement 2, September 1973.

27. Equipment Qualification Test Report, Reactor Vessel Level Instrumentation System/Incore Thermocouple Cabinet With 8080 Microprocessor Electronics and Reactor Cabinet Pump Station Panel, WCAP-8687, Supplement 2-E51A, July 1984.

28. Equipment Qualification Test Report, Remote Digital Display for the 8080 Microprocessor Electronics, WCAP-8687, Supplement 2-E46A, July 1984.

29. Equipment Qualification Test Report, Surface Mounted RTDs, WCAP-8687, Supplement 2-E48A, January 1983.

30. Equipment Qualification Test Report, High Volume Sensor-Group A, WCAP-8687, Supplement 2-E48A, January 1983.

31. Equipment Qualification Test Report, Differential Pressure Indicating Switch-Group, WCAP-8687, Supplement 2-E49A, January 1983.

32. American Iron and Steel Institute, Specification for the Design of Cold-Rolled Steel Structural Members, AISI, Washington, D.C., 1968.

33. American Institute of Steel Construction, Specification for the Design, Fabrication and Erection of Structural Steel for Buildings, AISC, Chicago, IL, Seventh Edition.

34. Office of Nuclear Reactor Regulation, Standard Review Plan, Section 3.8.4, NRC, Washington, D.C. (November 1975).

35. Seismic Confirmation of Weed Resistance Temperature Detectors For Diablo Canyon Unit 1 and Unit 2 Bypass Elimination System, WCAP-12714, Revision 2, February 1993.

36. Seismic Qualification Test Report of Class IE RTD and Thermocouple Temperature Sensors for Conax Corp., Report No. IPS-1165, Rev. A, June 18, 1984.

37. Rosemount Report D8400102, Qualification Report for Pressure Transmitter Model 1154, (PG&E DC 6000784-117).

38. Rosemount Report D8300040, Qualification Report for Pressure Transmitters Rosemount Model 1153 Series D, (PG&E DC 6000784-7-1).

39. PG&E Seismic Calculation No. IS-35, "Seismic Qualification of Rosemount Transmitters."

40. Equipment Qualification Test Report, Eagle 21 Process Protection System (Environmental and Seismic Testing), WCAP-8687, Supplement 2-E69A, Revision 0, May 1988.

41. Equipment Qualification Test Report, Eagle 21 Process Protection System (Environmental and Seismic Testing), WCAP-8687, Supplement 2-E69B, Revision 0, February 1990.

42. Equipment Qualification Test Report, Eagle 21 Process Protection System (Environmental and Seismic Testing), WCAP-8687, Supplement 2-E69C, Revision 0, February 1991.

43. Seismic Qualification of Electrical Equipment for Nuclear Power Plants, NRC Regulatory Guide 1.100, Revision 2, June 1988.

44. Recommended Practices for Seismic Qualification of Class 1E Equipment for Nuclear Power Generating Stations, IEEE 344-1987.

45. Seismic Conformation of Eagle 21 Digital Process Protection System Upgrade for Pacific Gas and Electric Company Diablo Canyon Power Plant Units 1 and 2, WCAP-13384, Revision 0, PG&E, September 1992.

46. PG&E Specification 1021-J-NPG, "Specification for Furnishing and Delivering Remote Multiplexer and Visual Annunciator Equipment Associated with the Main Annunciator Systems for Diablo Canyon Power Plant, Units 1 and 2."

47. Trentec Test Report No. 8Q017.0, dated 11/98.

48. Altran Calculation No. 98250-C-001, Revision 0, dated May 1999.

49. PG&E Seismic Calculation No. ES-66, "Seismic Qualification of Westinghouse Supplied SSPS Cabinets."

50. PG&E Seismic Calculation No. IS-88, "Seismic Qualification of Model 3015C/3015N Rosemount Transmitters."

TABLE 3.10-1

WESTINGHOUSE SUPPLIED CLASS IE INSTRUMENTATION AND ELECTRICAL EQUIPMENT SEISMIC CAPABILITIES

Equipment	Elev./Bldg.	Qualification Method	Qualifying Spectra HE, DDE, DE	FSAR Reference
Nuclear Instrumentation System Cabinet	140'/Aux.	T / A	HE, DDE, DE	3.10.2.1.1
Radiation Monitoring System Cabinets	140'/Aux.	T	HE, DDE, DE	3.10.2.1.1.1
Two-section Power Range Excore Neutron Detector	102'/Cont.	T	HE, DDE, DE	3.10.2.1.1
Solid State Protection System	140'/Aux.	T	HE, DDE, DE	3.10.2.1.2
Process Control and Protection System	128'/Aux.	T / A	HE, DDE, DE	3.10.2.1.3
Cont. Pressure Transmitter				
- Transmitter	109.67'/Cont. Exterior	T	HE, DDE, DE	3.10.2.1.5
- Sensor	109.67'/Cont.	T	HE, DDE, DE	3.10.2.1.5
Reactor Coolant Level Differential Pressure Transmitter	100'/Aux.	T	HE, DDE, DE	3.10.2.1.5
Reactor Trip Switchgear	115'/Aux.	T	HE, DDE, DE	3.10.2.1.6
Main Coolant Loop Resistance Temperature Detectors	117'/Cont.	T	HE, DDE, DE	3.10.2.1.7
Safeguards Test Cabinet	140'/Aux.	T	HE, DDE, DE	3.10.2.1.8
Aux. Safeguards Cabinet	128'/Aux.	T / A	HE, DDE, DE	3.10.2.1.9
Main Control Board	140'/Aux.	T / A	HE, DDE, DE	3.10.2.2
Electric Hydrogen Recombiner	140'/Cont.	T	HE, DDE, DE	3.10.2.31

TABLE 3.10-1

Equipment	Elev./Bldg.	Qualification Method	Qualifying Spectra HE, DDE, DE	FSAR Reference
Hydrogen Recombiner Control Panel and Power Supply	100'/Aux.	T	HE, DDE, DE	3.10.2.31
Reactor Vessel Level Instrumentation System/Incore Thermocouple Cabinets (PAMS 3 & 4)	140'/Aux.	T	HE, DDE, DE	3.10.2.32
Surface Mounted Resistance Temperature Detectors	140'/Cont.	T	HE, DDE, DE	3.10.2.32.2
High Volume Sensors	127'/Cont.	T	HE, DDE, DE	3.10.2.32.3
Hydraulic Isolators	89'/GW	T	HE, DDE, DE	3.10.2.32.4
Flux Mapping Transfer Device	127'/Cont.	A	HE	3.10.2.33
Incore Flux Mapping Cabinets	140'/Cont.	A	HE	3.10.2.33

A = Qualification by analysis (Qualification Method Column)
T = Qualification by testing
DE = Design Earthquake
DDE = Double Design Earthquake
HE = Hosgri Earthquake

TABLE 3.10-2

EQUIPMENT SEISMIC QUALIFICATION RESULTS:
ELECTRICAL, INSTRUMENTATION, AND CONTROLS

Equipment	Bldg./Elev.	Qualification Method	Qualifying Spectra HE, DDE, DE	FSAR Reference
Main annunciator	Aux/128	T / A	HE, DDE, DE	3.10.2.9
Battery chargers	Aux/115	T	HE, DDE, DE	3.10.2.8.3
Station battery	Aux/115	T / A	HE, DDE, DE	3.10.2.8.1
DC switchgear	Aux/115	T / A	HE, DDE, DE	3.10.2.8.4
Diesel generators				
a) Excitation cabinet	Turb/85	T / A	HE, DDE, DE	3.10.2.6
b) Engine control cabinet	Turb/85	T / A		
Electrical penetrations	Cont/Various	A	HE, DDE, DE	3.10.2.10
Emergency light packs	Various	T	HE, DDE, DE	–
Fire pump controller	Aux/115	T	HE, DDE, DE	3.10.2.13
Hot shutdown panel	Aux/100	T / A	HE, DDE, DE	3.10.2.3
Heat trace distribution panel	Aux/Various	A	HE, DDE, DE	N/A
Instrument power ac panelboards	Aux/115	T / A	HE, DDE, DE	3.10.2.7.7

TABLE 3.10-2

Equipment	Bldg./Elev.	Qualification Method	Qualifying Spectra HE, DDE, DE	FSAR Reference
Instrument panels PIA, PIB & PIC	Aux/128	A	HE, DDE, DE	3.10.2.5
Instrument (Panels A & B)	Aux/128	T / A		
Local instrument panels	Various	A	HE, DDE, DE	3.10.2.4
Local starters (LPF 36)	Turb/119	T	HE, DDE, DE	3.10.2.14
Local starters (LPS 96)	Turb/140	T	HE, DDE, DE	3.10.2.14
Local starters (LPG 66) E1 100/J	Aux/ Various	T / A	HE, DDE, DE	3.10.2.14
Local starter 125 Vdc (FCV 95)	Aux/100	T	HE, DDE, DE	3.10.2.8.5
Limit switches	Various	T	HE, DDE, DE	3.10.2.27
P&ΔP transmitters	Various	T	HE, DDE, DE	3.10.2.11
Safeguards relay board	Turb/119	T / A	HE, DDE, DE	3.10.2.7.3
Ventilation control				
a) Logic cabinet (POV1, POV2)	Aux/140	T / A	HE, DDE, DE	3.10.2.15
b) Relay cabinet (RCV1, RCV2)	Aux/128	T / A	HE, DDE, DE	3.10.2.15
c) Electro-mechanical devices	Aux/Various	T / A	HE, DDE, DE	3.10.2.15
Vital load center (480 Vac MCC)	Aux/100	T / A	HE, DDE, DE	3.10.2.7.4

TABLE 3.10-2

Equipment	Bldg./Elev.	Qualification Method	Qualifying Spectra HE, DDE, DE	FSAR Reference
Vital load center transformer (480 V)	Aux/100	T / A	HE, DDE, DE	3.10.2.7.5
Auxiliary relay panels (SPF, SPG, SPH)	Aux/100	T / A	HE, DDE, DE	3.10.2.7.6
Fan cooler starter	Aux/100	T / A		
Vital switchgear (4.16 kV)	Turb/119	T / A	HE, DDE, DE	3.10.2.7.1
Potential transformers	Turb/119	T / A	HE, DDE, DE	3.10.2.7.2
Air circuit breaker (pressurizer heaters)	Aux/100	A	HE, DDE, DE	–
Solenoid valves	Various	T	HE, DDE, DE	3.10.2.23
Postaccident monitor panels and instrument (PAMs 1 & 2)	Aux/140	T / A	HE, DDE, DE	3.10.2.22
Containment H2 monitors	GW/85 GE/100	T / A	HE, DDE, DE	3.10.2.25
Containment high-range radiation detector	F/145	T	HE, DDE, DE	3.10.2.28
Containment purge exhaust detectors and LRP	L/100	T / A	HE, DDE, DE	3.10.2.26
Instrument AC UPS	Aux/115	T	HE, DDE, DE	3.10.2.1.4

TABLE 3.10-2

Equipment	Bldg./Elev.	Qualification Method	Qualifying Spectra HE, DDE, DE	FSAR Reference
Control room air supply radiation monitors	H/158	T	HE, DDE, DE	3.10.2.20
Control room pressurization	Turb/145	T	HE, DDE, DE	3.10.2.20
Radiation monitors	H/140	T	HE, DDE, DE	3.10.2.20
Control room vent & press. control & power panels	Various	T / A	HE, DDE, DE	3.10.2.20
Pressurizer SRV	F/146	T	HE, DDE, DE	3.10.2.29
Position margin monitor	H/140			
Sub-cooled margin monitor (calculators)	H/140	T	HE, DDE, DE	3.10.2.21
Process solenoid valves	G/110 GW/110	T	HE, DDE, DE	3.10.2.24

A = Qualification by analysis (Qualification Method Column)
T = Qualification by testing
DE = Design Earthquake
DDE = Double Design Earthquake
HE = Hosgri Earthquake

TABLE 3.10-3

HVAC EQUIPMENT SEISMIC QUALIFICATION SPECTRA RESULTS

Equipment	Location[c] Building/ Elevation, ft	Qualification Method[c]	Qualifying Spectra[c]	Notes
Supply Fan 1 (S-1)	L/85	A	HE, DDE, DE	(b)
Supply Fan 1 (2S-1)	L/85	C	HE, DDE, DE	(b)
Supply Fan 2 (S-2)	L/85	A	HE, DDE, DE	(b)
Supply Fan 2 (2S-2)	L/85	C	HE, DDE, DE	(b)
Supply Fan 31 (S-31)	K/140	A	HE, DDE, DE	(b)
Supply Fan 32 (S-32)	K/140	A	HE, DDE, DE	(b)
Supply Fan 33 (S-33)	K/140	C	HE, DDE, DE	(b)
Supply Fan 34 (S-34)	K/140	C	HE, DDE, DE	(b)
Supply Fan 39 (S-39)	K/156	A	HE, DDE, DE	(b)
Supply Fan 40 (S-40)	K/156	A	HE, DDE, DE	(b)
Supply Fan 41 (S-41)	K/156	C	HE, DDE, DE	(b)
Supply Fan 42 (S-42)	K/156	C	HE, DDE, DE	(b)
Exhaust Fan 1 (E-1)	L/128	A	HE, DDE, DE	(b)
Exhaust Fan 1 (2E-1)	L/128	C	HE, DDE, DE	(b)
Exhaust Fan 2 (E-2)	L/128	A	HE, DDE, DE	(b)
Exhaust Fan 2 (2E-2)	L/128	C	HE, DDE, DE	(b)
Exhaust Fan 4 (E-4)	L/140	A	HE, DDE, DE	(b)
Exhaust Fan 4 (2E-4)	L/140	C	HE, DDE, DE	(b)
Exhaust Fan 5 (E-5)	L/140	A	HE, DDE, DE	(b)
Exhaust Fan 5 (2E-5)	L/140	C	HE, DDE, DE	(b)
Exhaust Fan 6 (E-6)	L/140	A	HE, DDE, DE	(b)
Exhaust Fan 6 (2E-6)	L/140	C	HE, DDE, DE	(b)
Exhaust Fan 101 (E-101)	ISA/15	A	HE, DDE, DE	(b)
Exhaust Fan 102 (E-102)	ISA/15	A	HE, DDE, DE	(b)

Equipment	Location[c] Building/ Elevation, ft	Qualification Method[c]	Qualifying Spectra[c]	Notes
Exhaust Fan 103 (E-103)	ISA/15	A	HE, DDE, DE	(b)
Exhaust Fan 104 (E-104)	ISA/15	A	HE, DDE, DE	(b)
Supply Fan 43 (S-43)	H/163	A	HE, DDE, DE	(b)
Supply Fan 44 (S-44)	H/163	A	HE, DDE, DE	(b)
Supply Fan 45 (S-45)	H/163	C	HE, DDE, DE	(b)
Supply Fan 46 (S-46)	H/163	C	HE, DDE, DE	(b)
Exhaust Fan 43 (E-43)	H/163	A	HE, DDE, DE	(b)
Exhaust Fan 44 (E-44)	H/163	A	HE, DDE, DE	(b)
Exhaust Fan 45 (E-45)	H/163	C	HE, DDE, DE	(b)
Exhaust Fan 46 (E-46)	H/163	C	HE, DDE, DE	(b)
Supply Fan 35 (S-35)	K/157	A	HE, DDE, DE	(b)
Supply Fan 36 (S-36)	K/157	A	HE, DDE, DE	(b)
Supply Fan 37 (S-37)	K/157	C	HE, DDE, DE	(b)
Supply Fan 38 (S-38)	K/157	C	HE, DDE, DE	(b)
Supply Fan 67 (S-67)	A/119	A	HE, DDE, DE	(b)
Supply Fan 67 (2S-67)	A/119	C	HE, DDE, DE	(b)
Supply Fan 68 (S-68)	A/119	A	HE, DDE, DE	(b)
Supply Fan 68 (2S-68)	A/119	C	HE, DDE, DE	(b)
Supply Fan 69 (S-69)	A/119	A	HE, DDE, DE	(b)
Supply Fan 69 (2S-69)	A/119	C	HE, DDE, DE	(b)
Compressor Unit 35 (CP-35)	K/156	A	HE, DDE, DE	(b)
Compressor Unit 36 (CP-36)	K/156	A	HE, DDE, DE	(b)
Compressor Unit 37 (CP-37)	K/156	C	HE, DDE, DE	(b)
Compressor Unit 38 (CP-38)	K/156	C	HE, DDE, DE	(b)
Condenser Unit 35 (CR-35)	K/157	A	HE, DDE, DE	(b)
Condenser Unit 36 (CR-36)	K/157	A	HE, DDE, DE	(b)

Equipment	Location(c) Building/ Elevation, ft	Qualification Method(c)	Qualifying Spectra(c)	Notes
Condenser Unit 37 (CR-37)	K/157	C	HE, DDE, DE	(b)
Condenser Unit 38 (CR-38)	K/157	C	HE, DDE, DE	(b)
Mode Damper 78 in. (1A)	L/128	A	HE, DDE, DE	(b)
Mode Damper 78 in. (2-1A)	L/128	C	HE, DDE, DE	(b)
Mode Damper 78 in. (1B)	L/128	A	HE, DDE, DE	(b)
Mode Damper 78 in. (2-1B)	L/128	C	HE, DDE, DE	(b)
Mode Damper 132x144 (3)	L/122	A	HE, DDE, DE	(b)
Mode Damper 132x144 (2-3)	L/122	C	HE, DDE, DE	(b)
Mode Damper 96x144 (5A)	L/107	A	HE, DDE, DE	(b)
Mode Damper 96x144 (2-5A)	L/107	C	HE, DDE, DE	(b)
Mode Damper 96x144 (5B)	L/107	A	HE, DDE, DE	(b)
Mode Damper 96x144 (2-5B)	L/107	C	HE, DDE, DE	(b)
Mode Damper 108x144 (6)	L/122	A	HE, DDE, DE	(b)
Mode Damper 108x144 (2-6)	L/122	C	HE, DDE, DE	(b)
Mode Damper 108x144 (9)	L/122	A	HE, DDE, DE	(b)
Mode Damper 108x144 (2-9)	L/122	C	HE, DDE, DE	(b)
Backdraft Damper for Supply Fan S-31 96x72	K/146	A	HE, DDE, DE	(b)
Backdraft Damper for Supply Fan S-32 96x72	K/146	A	HE, DDE, DE	(b)
Backdraft Damper for Supply Fan S-33 96x72	K/146	C	HE, DDE, DE	(b)
Backdraft Damper for Supply Fan S-34 96x72	K/146	C	HE, DDE, DE	(b)
Backdraft Damper for Exhaust Fan E-1 90x66	L/121	A	HE, DDE, DE	(b)
Backdraft Damper for Exhaust Fan 2E-1 90x66	L/121	C	HE, DDE, DE	(b)

TABLE 3.10-3

Equipment	Location[c] Building/ Elevation, ft	Qualification Method[c]	Qualifying Spectra[c]	Notes
Backdraft Damper for Exhaust Fan E-2 90x66	L/121	A	HE, DDE, DE	(b)
Backdraft Damper for Exhaust Fan 2E-2 90x66	L/121	C	HE, DDE, DE	(b)
Backdraft Damper for Exhaust Fan E-4 56x44	L/143	A	HE, DDE, DE	(b)
Backdraft Damper for Exhaust Fan 2E-4 56x44	L/143	A	HE, DDE, DE	(b)
Backdraft Damper for Exhaust Fan E-5 56x44	L/154	A	HE, DDE, DE	(b)
Backdraft Damper for Exhaust Fan 2E-5 56x44	L/154	A	HE, DDE, DE	(b)
Backdraft Damper for Exhaust Fan E-6 56x44	L/154	A	HE, DDE, DE	(b)
Backdraft Damper for Exhaust Fan 2E-6 56x44	L/154	A	HE, DDE, DE	(b)
Forced Draft Shutter Damper 30x48	G/96	A	HE, DDE, DE	(b)
Forced Draft Shutter Damper 30x48	G/96	C	HE, DDE, DE	(b)
Fire Damper 46x14 (FD-4)	H/125	A	HE, DDE, DE	(b)
Fire Damper 46x14 (2FD-4)	H/125	C	HE, DDE, DE	(b)
Fire Damper 46x14 (FD-5)	H/125	A	HE, DDE, DE	(b)
Fire Damper 46x14 (2FD-5)	H/125	C	HE, DDE, DE	(b)
Fire Damper 46x14 (FD-6)	H/125	A	HE, DDE, DE	(b)
Fire Damper 46x14 (2FD-6)	H/125	C	HE, DDE, DE	(b)
Carbon Tray Filters (EFC-1)	L/115	A	HE, DDE, DE	(b)
Carbon Tray Filters (2EFC-1)	L/115	C	HE, DDE, DE	(b)

TABLE 3.10-3

Equipment	Location[c] Building/ Elevation, ft	Qualification Method[c]	Qualifying Spectra[c]	Notes
Carbon Tray Filters (EFC-5)	L/148	A	HE, DDE, DE	(b)
Carbon Tray Filters (2EFC-5)	L/148	C	HE, DDE, DE	(b)
Carbon Tray Filters (EFC-6)	L/148	A	HE, DDE, DE	(b)
Carbon Tray Filters (2EFC-6)	L/148	C	HE, DDE, DE	(b)
Astrocel-Hepa Filters (EFH-1)	L/126	A	HE, DDE, DE	(b)
Astrocel-Hepa Filters (2EFH-1)	L/126	C	HE, DDE, DE	(b)
Astrocel-Hepa Filters (EFH-2a)	L/126	A	HE, DDE, DE	(b)
Astrocel-Hepa Filters (2EFH-2a)	L/126	C	HE, DDE, DE	(b)
Astrocel-Hepa Filters (EFH-2b)	L/105	A	HE, DDE, DE	(b)
Astrocel-Hepa Filters (2EFH-2b)	L/105	C	HE, DDE, DE	(b)
Astrocel-Hepa Filters (EFH-4)	L/150	A	HE, DDE, DE	(b)
Astrocel-Hepa Filters (2EFH-4)	L/150	C	HE, DDE, DE	(b)
Astrocel-Hepa Filters (EFH-5)	L/148	A	HE, DDE, DE	(b)
Astrocel-Hepa Filters (2EFH-5)	L/148	C	HE, DDE, DE	(b)
Astrocel-Hepa Filters (EFH-6)	L/148	A	HE, DDE, DE	(b)
Astrocel-Hepa Filters (2EFH-6)	L/148	C	HE, DDE, DE	(b)
Varicel-Roughing Filter (EFR-4)	L/154	A	HE, DDE, DE	(b)
Varicel-Roughing Filter (2EFR-4)	L/154	C	HE, DDE, DE	(b)
Varicel-Roughing Filter (EFR-5)	L/154	A	HE, DDE, DE	(b)
Varicel-Roughing Filter (2EFR-5)	L/154	C	HE, DDE, DE	(b)
Varicel-Roughing Filter (EFR-6)	L/154	A	HE, DDE, DE	(b)
Varicel-Roughing Filter (2EFR-6)	L/154	C	HE, DDE, DE	(b)
Filter Housing With Filters (FU-39)	K/155	A	HE, DDE, DE	(b)
Filter Housing With Filters (FU-41)	K/155	C	HE, DDE, DE	(b)

Equipment	Location[c] Building/ Elevation, ft	Qualification Method[c]	Qualifying Spectra[c]	Notes
Filter Box (FB-29)	H/163	A	HE, DDE, DE	(b)
Filter Box (2FB-29)	H/163	C	HE, DDE, DE	(b)
Electric Duct Heater (EH-30)	L/137	A	HE, DDE, DE	(b)
Chromalox Model TDH-54C (2EH-30)	J/138	C	HE, DDE, DE	(b)
Supply Fan 96 for CRPS (OS-96)	A/140	C	HE, DDE, DE	(b)
Supply Fan 97 for CRPS (OS-97)	A/140	C	HE, DDE, DE	(b)
Supply Fan 98 for CRPS (OS-98)	A/140	A	HE, DDE, DE	(b)
Supply Fan 99 for CRPS (OS-99)	A/140	A	HE, DDE, DE	(b)
Mode Damper 72 in. ϕ and Actuator (2A)	L/132	A	HE, DDE, DE	(b)
Mode Damper 72 in. ϕ and Actuator (2-2A)	L/132	C	HE, DDE, DE	(b)
Mode Damper 72 in. ϕ and Actuator (2B)	L/132	A	HE, DDE, DE	(b)
Mode Damper 72 in. ϕ and Actuator (2-2B)	L/132	C	HE, DDE, DE	(b)
Mode Damper 90x66 and Actuator (7)	L/102	A	HE, DDE, DE	(b)
Mode Damper 90x66 and Actuator (2-7)	L/102	C	HE, DDE, DE	(b)
Mode Damper 10 in. ϕ (13A)	K/97	A	HE, DDE, DE	(b)
Mode Damper 10 in. ϕ (2-13A)	K/97	C	HE, DDE, DE	(b)
Mode Damper 10 in. ϕ (13B)	K/97	A	HE, DDE, DE	(b)
Mode Damper 10 in. ϕ (2-13B)	K/97	C	HE, DDE, DE	(b)
Mode Damper 10 in. ϕ (14A)	GE/81	A	HE, DDE, DE	(b)
Mode Damper 10 in. ϕ (2-14A)	GE/81	C	HE, DDE, DE	(b)
Mode Damper 10 in. ϕ (14B)	GE/81	A	HE, DDE, DE	(b)
Mode Damper 10 in. ϕ (2-14B)	GE/81	C	HE, DDE, DE	(b)
Mode Damper 14 in. ϕ (15A)	GE/70	A	HE, DDE, DE	(b)

TABLE 3.10-3

Equipment	Location[c] Building/ Elevation, ft	Qualification Method[c]	Qualifying Spectra[c]	Notes
Mode Damper 14 in. ϕ (2-15A)	GE/70	C	HE, DDE, DE	(b)
Mode Damper 14 in. ϕ (15B)	GE/70	A	HE, DDE, DE	(b)
Mode Damper 14 in. ϕ (2-15B)	GE/70	C	HE, DDE, DE	(b)
Mode Damper 48 in. ϕ (35)	L/107	A	HE, DDE, DE	(b)
Mode Damper 48 in. ϕ (2-35)	L/107	C	HE, DDE, DE	(b)
Mode Damper 54 in. ϕ and Actuator (29)	L/150	A	HE, DDE, DE	(b)
Mode Damper 54 in. ϕ and Actuator (2-29)	L/150	C	HE, DDE, DE	(b)
Mode Damper 54 in. ϕ and Actuator (30)	L/150	A	HE, DDE, DE	(b)
Mode Damper 54 in. ϕ and Actuator (2-30)	L/150	C	HE, DDE, DE	(b)
Mode Damper 54 in. ϕ and Actuator (31)	L/150	A	HE, DDE, DE	(b)
Mode Damper 54 in. ϕ and Actuator (2-31)	L/150	C	HE, DDE, DE	(b)
Mode Damper 72x100 (4A)	L/107	A	HE, DDE, DE	(b)
Mode Damper 72x100 (2-4A)	L/107	C	HE, DDE, DE	(b)
Mode Damper 72x100 (4B)	L/107	A	HE, DDE, DE	(b)
Mode Damper 72x100 (2-4B)	L/107	C	HE, DDE, DE	(b)
Mode Damper 72x75 (8A)	L/133	A	HE, DDE, DE	(b)
Mode Damper 72x75 (2-8A)	L/133	C	HE, DDE, DE	(b)
Mode Damper 72x75 (8B)	L/115	A	HE, DDE, DE	(b)
Mode Damper 72x75 (2-8B)	L/115	C	HE, DDE, DE	(b)
Mode Damper 90x66 (10)	L/110	A	HE, DDE, DE	(b)
Mode Damper 90x66 (2-10)	L/110	C	HE, DDE, DE	(b)
Mode Damper 40x84 (12)	K/90	A	HE, DDE, DE	(b)
Mode Damper 40x84 (2-12)	K/90	C	HE, DDE, DE	(b)
Mode Damper 46x40 (16A)	K/95	A	HE, DDE, DE	(b)

TABLE 3.10-3

Equipment	Location[c] Building/ Elevation, ft	Qualification Method[c]	Qualifying Spectra[c]	Notes
Mode Damper 46x40 (2-16A)	K/95	C	HE, DDE, DE	(b)
Mode Damper 46x40 (16B)	K/95	A	HE, DDE, DE	(b)
Mode Damper 46x40 (2-16B)	K/95	C	HE, DDE, DE	(b)
Mode Damper 26x54 (17A)	K/94	A	HE, DDE, DE	(b)
Mode Damper 26x54 (2-17A)	K/94	C	HE, DDE, DE	(b)
Mode Damper 26x54 (17B)	K/94	A	HE, DDE, DE	(b)
Mode Damper 26x54 (2-17B)	K/94	C	HE, DDE, DE	(b)
Mode Damper 96x72 (20)	K/146	A	HE, DDE, DE	(b)
Mode Damper 96x72 (2-24)	K/146	C	HE, DDE, DE	(b)
Mode Damper 96x72 (21)	K/146	A	HE, DDE, DE	(b)
Mode Damper 96x72 (2-21)	K/146	C	HE, DDE, DE	(b)
Mode Damper 54x100 (22A)	K/141	A	HE, DDE, DE	(b)
Mode Damper 54x100 (2-22A)	K/141	C	HE, DDE, DE	(b)
Mode Damper 54x100 (22B)	K/132	A	HE, DDE, DE	(b)
Mode Damper 54x100 (2-22B)	K/132	C	HE, DDE, DE	(b)
Mode Damper 40x40 (23)	K/135	A	HE, DDE, DE	(b)
Mode Damper 40x40 (2-23)	K/135	C	HE, DDE, DE	(b)
Mode Damper 40x40 (23B)	K/135	A	HE, DDE, DE	(b)
Mode Damper 40x40 (2-23B)	K/135	C	HE, DDE, DE	(b)
Mode Damper 14x44 (24)	K/111	A	HE, DDE, DE	(b)
Mode Damper 14x44 (2-24)	K/111	C	HE, DDE, DE	(b)
Mode Damper 14x44 (24B)	K/111	A	HE, DDE, DE	(b)
Mode Damper 14x44 (2-24B)	K/111	C	HE, DDE, DE	(b)
Mode Damper 48x40 (26A)	K/87	A	HE, DDE, DE	(b)
Mode Damper 48x40 (2-26A)	K/87	C	HE, DDE, DE	(b)
Mode Damper 48x40 (26B)	K/87	A	HE, DDE, DE	(b)
Mode Damper 48x40 (2-26B)	K/87	C	HE, DDE, DE	(b)
Mode Damper 30x48 (25)	K/95	A	HE, DDE, DE	(b)
Mode Damper 30x48 (2-25)	K/95	C	HE, DDE, DE	(b)
Mode Damper 30x48 (25B)	K/95	A	HE, DDE, DE	(b)

TABLE 3.10-3

Equipment	Location[c] Building/ Elevation, ft	Qualification Method[c]	Qualifying Spectra[c]	Notes
Mode Damper 30x48 (2-25B)	K/95	C	HE, DDE, DE	(b)
Mode Damper 42x64 (33)	L/108	A	HE, DDE, DE	(b)
Mode Damper 42x64 (2-33)	L/108	C	HE, DDE, DE	(b)
Mode Damper 42x64 (34)	L/105	A	HE, DDE, DE	(b)
Mode Damper 42x64 (2-34)	L/105	C	HE, DDE, DE	(b)
Backdraft Damper for Supply Fan S-1 64x42	L/95	A	HE, DDE, DE	(b)
Backdraft Damper for Supply Fan 2S-1 64x42	L/95	C	HE, DDE, DE	(b)
Backdraft Damper for Supply Fan S-2 64x42	L/95	A	HE, DDE, DE	(b)
Backdraft Damper for Supply Fan 2S-2 64x42	L/95	C	HE, DDE, DE	(b)
Backdraft Damper 14 in. ϕ (OBD-1)	A/149	A	HE, DDE, DE	(b)
Backdraft Damper 14 in. ϕ (OBD-2)	A/149	A	HE, DDE, DE	(b)
Backdraft Damper 14 in. ϕ (OBD-3)	A/149	C	HE, DDE, DE	(b)
Backdraft Damper 14 in. ϕ (OBD-4) A/149	A/149	C	HE, DDE, DE	(b)
Quadrant Damper (QD 10 in. ϕ)	K/110	A	HE, DDE, DE	(b)
Quadrant Damper (QD 20 in. ϕ)	K/82	A	HE, DDE, DE	(b)
Quadrant Damper (QD 14 in. ϕ)	K/82	A	HE, DDE, DE	(b)
Quadrant Damper (QD 14 in. ϕ)	K/111	A	HE, DDE, DE	(b)
Quadrant Damper (QD 16 in. ϕ)	K/111	A	HE, DDE, DE	(b)
Quadrant Damper (QD 12 in. ϕ)	K/112	A	HE, DDE, DE	(b)
Quadrant Damper (QD 12 in. ϕ)	K/130	A	HE, DDE, DE	(b) (e)
Quadrant Damper (QD 10 in. ϕ)	K/132	A	HE, DDE, DE	(b) (e)

TABLE 3.10-3

Equipment	Location(c) Building/ Elevation, ft	Qualification Method(c)	Qualifying Spectra(c)	Notes
Quadrant Damper (QD 14 in. ϕ)	K/132	A	HE, DDE, DE	(b) (e)
Quadrant Damper (QD 12 in. ϕ)	K/134	A	HE, DDE, DE	(b) (e)
Quadrant Damper (QD 16 in. ϕ)	K/134	A	HE, DDE, DE	(b) (e)
Quadrant Damper (QD 16 in. ϕ)	K/131	A	HE, DDE, DE	(b) (e)
Quadrant Damper (QD 20 in. ϕ)	K/134	A	HE, DDE, DE	(b) (e)
Quadrant Damper (QD 14 in. ϕ)	K/134	A	HE, DDE, DE	(b) (e)
Quadrant Damper (QD 14 in. ϕ)	K/70	A	HE, DDE, DE	(b)
Quadrant Damper (QD 14 in. ϕ)	GE/70	A	HE, DDE, DE	(b)
Quadrant Damper (QD 14 in. ϕ)	H/79	A	HE, DDE, DE	(b)
Quadrant Damper (QD 20 in. ϕ)	H/65	A	HE, DDE, DE	(b)
Quadrant Damper (QD 28 in. ϕ)	J/132	A	HE, DDE, DE	(b)
Quadrant Damper (QD 16 in. ϕ)	L/141	A	HE, DDE, DE	(b)
Quadrant Damper (QD 14 in. ϕ)	GE/70	A	HE, DDE, DE	(b)
Quadrant Damper (QD 18 in. ϕ)	K/132	C	HE, DDE, DE	(b)
Quadrant Damper #52 (QD 48x24)	J/111	A	HE, DDE, DE	(b)
Quadrant Damper #2-52 (QD 48x24)	J/111	A	HE, DDE, DE	(b)
Quadrant Damper #54 (QD 42x42)	J/134	A	HE, DDE, DE	(b)
Quadrant Damper #2-54 (QD 42x42)	J/134	A	HE, DDE, DE	(b)
Quadrant Damper #46 (QD 38x14)	J/123	A	HE, DDE, DE	(b)
Quadrant Damper #2-46 (QD 38x14)	J/123	A	HE, DDE, DE	(b)
Quadrant Damper #33 (QD 40x40)	K/135	A	HE, DDE, DE	(b)
Quadrant Damper #2-33 (QD 40x40)	K/135	A	HE, DDE, DE	(b)
Quadrant Damper #34 (QD 14x10)	K/136	A	HE, DDE, DE	(b)
Quadrant Damper #2-34 (QD 14x10)	K/136	A	HE, DDE, DE	(b)
Quadrant Damper #35 (QD 46x14)	K/134	A	HE, DDE, DE	(b)
Quadrant Damper #2-35 (QD 46x14)	K/134	A	HE, DDE, DE	(b)
Quadrant Damper #24 (QD 14x14)	K/109	A	HE, DDE, DE	(b)
Quadrant Damper #2-24 (QD 14x14)	K/109	A	HE, DDE, DE	(b)
Quadrant Damper #31 (QD 54x100)	K/132	A	HE, DDE, DE	(b)
Quadrant Damper #2-31 (QD 54x100)	K/132	C	HE, DDE, DE	(b)

Equipment	Location(c) Building/ Elevation, ft	Qualification Method(c)	Qualifying Spectra(c)	Notes
Quadrant Damper #25 (QD 14x30)	K/111	A	HE, DDE, DE	(b)
Quadrant Damper #2-25 (QD 14x30)	K/111	A	HE, DDE, DE	(b)
Quadrant Damper #66 (QD 24x44)	K/92	A	HE, DDE, DE	(b)
Quadrant Damper #2-67 (QD 24x44)	K/92	A	HE, DDE, DE	(b)
Quadrant Damper #5 (QD 58x32)	K/81	A	HE, DDE, DE	(b)
Quadrant Damper #2-5 (QD 58x32)	K/81	C	HE, DDE, DE	(b)
Quadrant Damper #64 (QD 44x32)	K/81	A	HE, DDE, DE	(b)
Quadrant Damper #2-64 (QD 44x32)	K/81	A	HE, DDE, DE	(b)
Quadrant Damper #6 (QD 24x32)	K/81	A	HE, DDE, DE	(b)
Quadrant Damper #2-6 (QD 24x32)	K/81	A	HE, DDE, DE	(b)
Quadrant Damper #4 (QD 44x26)	K/82	A	HE, DDE, DE	(b)
Quadrant Damper #2-4 (QD 44x26)	K/82	A	HE, DDE, DE	(b)
Quadrant Damper #53 (QD 72x100)	L/100	A	HE, DDE, DE	(b)
Quadrant Damper #2-53 (QD 72x100)	L/100	C	HE, DDE, DE	(b)
Volume Damper (VD 24x24)	H/123	A	HE, DDE, DE	(b)
Volume Damper (VD 24x24)	H/124	A	HE, DDE, DE	(b)
Volume Damper (VD 27x21)	H/124	A	HE, DDE, DE	(b)
Quadrant Damper #19 (QD 38x44)	K/96	A	HE, DDE, DE	(b)
Quadrant Damper #2-19 (QD 38x44)	K/96	A	HE, DDE, DE	(b)
Quadrant Damper #15 (QD 20x12)	K/97	A	HE, DDE, DE	(b)
Quadrant Damper #2-15 (QD 20x12)	K/97	A	HE, DDE, DE	(b)
Quadrant Damper #20 (QD 20x44)	K/97	A	HE, DDE, DE	(b)
Quadrant Damper #2-20 (QD 20x44)	K/97	A	HE, DDE, DE	(b)
Quadrant Damper #14 (QD 72x24)	K/96	A	HE, DDE, DE	(b)
Quadrant Damper #2-14 (QD 72x24)	K/96	A	HE, DDE, DE	(b)
Quadrant Damper #28 (QD 18x16)	K/113	A	HE, DDE, DE	(b)
Quadrant Damper #2-28 (QD 18x16)	K/113	A	HE, DDE, DE	(b)
Quadrant Damper #29 (QD 16x18)	K/112	A	HE, DDE, DE	(b)
Quadrant Damper #2-29 (QD 16x18)	K/112	A	HE, DDE, DE	(b)

Equipment	Location(c) Building/ Elevation, ft	Qualification Method(c)	Qualifying Spectra(c)	Notes
Quadrant Damper #37 (QD 32x30)	K/132	A	HE, DDE, DE	(b)
Quadrant Damper #2-37 (QD 32x30)	K/132	A	HE, DDE, DE	(b)
Quadrant Damper #45 (QD 38x38)	J/120	A	HE, DDE, DE	(b)
Quadrant Damper #2-45 (QD 38x38)	J/120	A	HE, DDE, DE	(b)
Quadrant Damper (QD 24x24)	H/130	C	HE, DDE, DE	(b) (f)
Quadrant Damper (QD 18x24)	H/130	C	HE, DDE, DE	(b) (f)
Quadrant Damper #36 (QD 22x30)	K/131	A	HE, DDE, DE	(b)
Quadrant Damper #2-36 (QD 22x30)	K/131	A	HE, DDE, DE	(b)
Quadrant Damper #10 (QD 46x30)	K/78	A	HE, DDE, DE	(b)
Quadrant Damper #2-10 (QD 46x30)	K/78	A	HE, DDE, DE	(b)
Quadrant Damper #11 (QD 18x30)	K/79	A	HE, DDE, DE	(b)
Quadrant Damper #2-11 (QD 18x30)	K/79	A	HE, DDE, DE	(b)
Quadrant Damper #12 (QD 6x30)	K/79	A	HE, DDE, DE	(b)
Quadrant Damper #2-12 (QD 6x30)	K/79	A	HE, DDE, DE	(b)
Quadrant Damper #3 (QD 20x32)	K/69	A	HE, DDE, DE	(b)
Quadrant Damper #2-3 (QD 20x32)	K/69	A	HE, DDE, DE	(b)
Quadrant Damper #55 (QD 30x12)	H/61	A	HE, DDE, DE	(b)
Quadrant Damper #2-55 (QD 30x12)	H/61	A	HE, DDE, DE	(b)
Quadrant Damper #40 (QD 16x40)	J/152	A	HE, DDE, DE	(b)
Quadrant Damper #2-40 (QD 16x40)	J/152	A	HE, DDE, DE	(b)
Quadrant Damper #27 (QD 40x42)	K/110	A	HE, DDE, DE	(b)
Quadrant Damper #2-27 (QD 40x42)	K/110	A	HE, DDE, DE	(b)

Equipment	Location[c] Building/ Elevation, ft	Qualification Method[c]	Qualifying Spectra[c]	Notes
Quadrant Damper #26 (QD 36x42)	K/110	A	HE, DDE, DE	(b)
Quadrant Damper #2-26 (QD 36x42)	K/110	A	HE, DDE, DE	(b)
Quadrant Damper #18 (QD 40x26)	K/97			
Quadrant Damper #2-18 (QD 40x26)	K/97			
Quadrant Damper #2 (QD 30x66)	H/69	A	HE, DDE, DE	(b)
Quadrant Damper #2-2 (QD 30x66)	H/69	A	HE, DDE, DE	(b)
Quadrant Damper #1 (QD 24x72)	K/69	A	HE, DDE, DE	(b)
Quadrant Damper #2-1 (QD 24x72)	K/69	A	HE, DDE, DE	(b)
Quadrant Damper #43 (QD 86x48)	K/132	A	HE, DDE, DE	(b)
Quadrant Damper #2-43 (QD 86x48)	K/132	C	HE, DDE, DE	(b)
Quadrant Damper #42 (QD 36x18)	K/132	A	HE, DDE, DE	(b)
Quadrant Damper #2-42 (QD 36x18)	K/132	A	HE, DDE, DE	(b)
Quadrant Damper #8 (QD 36x18)	K/81	A	HE, DDE, DE	(b)
Quadrant Damper #2-8 (QD 36x18)	K/81	A	HE, DDE, DE	(b)
Quadrant Damper #9 (QD 36x18)	K/81	A	HE, DDE, DE	(b)
Quadrant Damper #2-9 (QD 36x18)	K/81	A	HE, DDE, DE	(b)
Quadrant Damper #41 (QD 56x50)	L/143	A	HE, DDE, DE	(b)
Quadrant Damper #2-41 (QD 56x50)	L/143	C	HE, DDE, DE	(b)
Quadrant Damper #65 (QD 60x30)	J/152	A	HE, DDE, DE	(b)
Quadrant Damper #2-65 (QD 60x30)	J/152	C	HE, DDE, DE	(b)
Quadrant Damper #49 (QD 38x30)	J/156	A	HE, DDE, DE	(b)
Quadrant Damper #2-49 (QD 38x30)	J/156	C	HE, DDE, DE	(b)
Quadrant Damper #7 (QD 84x72)	K/85	A	HE, DDE, DE	(b)
Quadrant Damper #2-7 (QD 84x72)	K/85	C	HE, DDE, DE	(b)
Quadrant Damper #13 (QD 54x48)	K/86	A	HE, DDE, DE	(b)
Quadrant Damper #2-13 (QD 54x48)	K/86	C	HE, DDE, DE	(b)

TABLE 3.10-3

Equipment	Location(c) Building/ Elevation, ft	Qualification Method(c)	Qualifying Spectra(c)	Notes
Quadrant Damper #32 (QD 37x78)	K/131	A	HE, DDE, DE	(b)
Quadrant Damper #2-32 (QD 37x78)	K/131	A	HE, DDE, DE	(b)
Motorized Damper 24 in. ϕ (2)	H/156	A	HE, DDE, DE	(b)
Motorized Damper 24 in. ϕ (2-2)	H/156	A	HE, DDE, DE	(b)
Motorized Damper 24 in. ϕ (2A)	H/160	A	HE, DDE, DE	(b)
Motorized Damper 24 in. ϕ (2-2A)	H/160	A	HE, DDE, DE	(b)
Motorized Damper 18 in. ϕ (3)	H/156	A	HE, DDE, DE	(b)
Motorized Damper 18 in. ϕ (2-3)	H/156	A	HE, DDE, DE	(b)
Motorized Damper 18 in. ϕ (3A)	H/160	A	HE, DDE, DE	(b)
Motorized Damper 18 in. ϕ (2-3A)	H/160	A	HE, DDE, DE	(b)
Motorized Damper 24 in. ϕ (7)	H/161	A	HE, DDE, DE	(b)
Motorized Damper 24 in. ϕ (2-7)	H/161	A	HE, DDE, DE	(b)
Motorized Damper 24 in. ϕ (7A)	H/159	A	HE, DDE, DE	(b)
Motorized Damper 24 in. ϕ (2-7A)	H/159	A	HE, DDE, DE	(b)
Motorized Damper 18 in. ϕ (8)	H/163	A	HE, DDE, DE	(b)
Motorized Damper 18 in. ϕ (2-8)	H/163	A	HE, DDE, DE	(b)
Motorized Damper 18 in. ϕ (8A)	H/163	A	HE, DDE, DE	(b)
Motorized Damper 18 in. ϕ (2-8A)	H/163	A	HE, DDE, DE	(b)
Motorized Damper 14 in. ϕ for CRPS (1)	A/143	A	HE, DDE, DE	(b)
Motorized Damper 14 in. ϕ for CRPS (2-1)	A/143	C	HE, DDE, DE	(b)
Motorized Damper 14 in. ϕ for CRPS (1A)	A/149	A	HE, DDE, DE	(b)
Motorized Damper 14 in. ϕ for CRPS (2-1A)	A/149	C	HE, DDE, DE	(b)
Motorized Damper 14 in. ϕ for CRPS (1B)	A/143	A	HE, DDE, DE	(b)
Motorized Damper 14 in. ϕ for CRPS (2-1B)	A/143	C	HE, DDE, DE	(b)
Motorized Damper 14 in. ϕ for CRPS (1C)	A/149	A	HE, DDE, DE	(b)
Motorized Damper 14 in. ϕ for CRPS (2-1C)	A/149	C	HE, DDE, DE	(b)
Limitorque Actuator for Motorized Damper (2)	H/156	T	HE, DDE, DE	(b)

Equipment	Location(c) Building/ Elevation, ft	Qualification Method(c)	Qualifying Spectra(c)	Notes
Limitorque Actuator for Motorized Damper (2-2)	H/156	T	HE, DDE, DE	(b)
Limitorque Actuator for Motorized Damper (2A)	H/160	T	HE, DDE, DE	(b)
Limitorque Actuator for Motorized Damper (2-2A)	H/160	T	HE, DDE, DE	(b)
Limitorque Actuator for Motorized Damper (3)	H/156	T	HE, DDE, DE	(b)
Limitorque Actuator for Motorized Damper (2-3)	H/156	T	HE, DDE, DE	(b)
Limitorque Actuator for Motorized Damper (3A)	H/160	T	HE, DDE, DE	(b)
Limitorque Actuator for Motorized Damper (2-3A)	H/161	T	HE, DDE, DE	(b)
Limitorque Actuator for Motorized Damper (7)	H/160	T	HE, DDE, DE	(b)
Limitorque Actuator for Motorized Damper (2-7)	H/161	T	HE, DDE, DE	(b)
Limitorque Actuator for Motorized Damper (7A)	H/159	T	HE, DDE, DE	(b)
Limitorque Actuator for Motorized Damper (2-7A)	H/159	T	HE, DDE, DE	(b)
Limitorque Actuator for Motorized Damper (8)	H/163	T	HE, DDE, DE	(b)
Limitorque Actuator for Motorized Damper (2-8)	H/163	T	HE, DDE, DE	(b)
Limitorque Actuator for Motorized Damper (8A)	H/163	T	HE, DDE, DE	(b)
Limitorque Actuator for Motorized Damper (2-8A)	H/163	T	HE, DDE, DE	(b)
Motorized Damper 18x16 (4)	H/163	A	HE, DDE, DE	(b)
Motorized Damper 18x16 (2-4)	H/163	C	HE, DDE, DE	(b)
Motorized Damper 36x24 (5)	H/163	A	HE, DDE, DE	(b)
Motorized Damper 36x24 (2-5)	H/163	C	HE, DDE, DE	(b)

Equipment	Location[c] Building/ Elevation, ft	Qualification Method[c]	Qualifying Spectra[c]	Notes
Motorized Damper 36x24 (6)	H/159	A	HE, DDE, DE	(b)
Motorized Damper 36x24 (2-6)	H/159	C	HE, DDE, DE	(b)
Motorized Damper 70x16 (9)	H/159	A	HE, DDE, DE	(b)
Motorized Damper 70x16 (2-9)	H/159	C	HE, DDE, DE	(b)
Motorized Damper 70x16 (9A)	H/159	A	HE, DDE, DE	(b)
Motorized Damper 70x16 (2-9A)	H/159	C	HE, DDE, DE	(b)
Motorized Damper 70x20 (10)	H/157	A	HE, DDE, DE	(b)
Motorized Damper 70x20 (2-10)	H/157	C	HE, DDE, DE	(b)
Motorized Damper 70x20 (10A)	H/157	A	HE, DDE, DE	(b)
Motorized Damper 70x20 (2-10A)	H/157	C	HE, DDE, DE	(b)
Motorized Damper 70x16 (11)	H/159	A	HE, DDE, DE	(b)
Motorized Damper 70x16 (2-11)	H/159	C	HE, DDE, DE	(b)
Motorized Damper 70x16 (11A)	H/159	A	HE, DDE, DE	(b)
Motorized Damper 70x16 (2-11A)	H/159	C	HE, DDE, DE	(b)
Motorized Damper 70x20 (12)	H/157	A	HE, DDE, DE	(b)
Motorized Damper 70x20 (2-12)	H/157	C	HE, DDE, DE	(b)
Motorized Damper 70x20 (12A)	H/157	A	HE, DDE, DE	(b)
Motorized Damper 70x20 (2-12A)	H/157	C	HE, DDE, DE	(b)
Motorized Damper 22x12 (13)	H/159	A	HE, DDE, DE	(b)
Motorized Damper 22x12 (2-13)	H/159	C	HE, DDE, DE	(b)
Motorized Damper 22x12 (14)	H/159	A	HE, DDE, DE	(b)
Motorized Damper 22x12 (2-14)	H/159	C	HE, DDE, DE	(b)
Balancing Damper 14 in. ϕ (1-15)	H/163	A	HE, DDE, DE	(b)
Balancing Damper 14 in. ϕ(2-15)	H/163	C	HE, DDE, DE	(b)
Balancing Damper 14 in. ϕ (1-16)	A/141	A	HE, DDE, DE	(b)
Balancing Damper 14 in. ϕ (2-16)	A/141	C	HE, DDE, DE	(b)
Shut-off Damper (48X48) (HD-43)	H/168	A	HE, DDE, DE	(b)
Shut-off Damper (48X48) (HD-44)	H/168	A	HE, DDE, DE	(b)
Shut-off Damper (48X48) (HD-45)	H/168	C	HE, DDE, DE	(b)
Shut-off Damper (48X48) (HD-46)	H/168	C	HE, DDE, DE	(b)

TABLE 3.10-3

Equipment	Location[c] Building/ Elevation, ft	Qualification Method[c]	Qualifying Spectra[c]	Notes
Back Draft Damper (E-21)	GW/96	A	HE, DDE, DE	(b)
Back Draft Damper (48X48) (BDD-43)	H/168	A	HE, DDE, DE	(b)
Back Draft Damper (48X48) (BDD-44)	H/168	A	HE, DDE, DE	(b)
Back Draft Damper (48X48) (BDD-45)	H/168	C	HE, DDE, DE	(b)
Back Draft Damper (48X48) (BDD-46)	H/168	C	HE, DDE, DE	(b)
Barber Colman Actuator for Motorized Damper 4	K/166	T	HE, DDE, DE	(b)
Barber Colman Actuator for Motorized Damper 2-4	K/166	C	HE, DDE, DE	(b)
Barber Colman Actuator for Motorized Damper 5	K/166	T	HE, DDE, DE	(b)
Barber Colman Actuator for Motorized Damper 2-5	K/166	C	HE, DDE, DE	(b)
Barber Colman Actuator for Motorized Damper 6	K/166	T	HE, DDE, DE	(b)
Barber Colman Actuator for Motorized Damper 2-6	K/166	C	HE, DDE, DE	(b)
Barber Colman Actuator for Motorized Damper (9)	K/159	T	HE, DDE, DE	(b)
Barber Colman Actuator for Motorized Damper (2-9)	K/159	T	HE, DDE, DE	(b)
Barber Colman Actuator for Motorized Damper (9A)	K/159	T	HE, DDE, DE	(b)
Barber Colman Actuator for Motorized Damper (2-9A)	K/159	T	HE, DDE, DE	(b)
Barber Colman Actuator for Motorized Damper (10)	H/157	T	HE, DDE, DE	(b)
Barber Colman Actuator for Motorized Damper (2-10)	H/157	T	HE, DDE, DE	(b)
Barber Colman Actuator for Motorized Damper (10A)	H/157	T	HE, DDE, DE	(b)
Barber Colman Actuator for	H/157	T	HE, DDE, DE	(b)

Equipment	Location[c] Building/ Elevation, ft	Qualification Method[c]	Qualifying Spectra[c]	Notes
Motorized Damper (2-10A)				
Barber Colman Actuator for Motorized Damper (11)	K/159	T	HE, DDE, DE	(b)
Barber Colman Actuator for Motorized Damper (2-11)	K/159	T	HE, DDE, DE	(b)
Barber Colman Actuator for Motorized Damper (11A)	K/159	T	HE, DDE, DE	(b)
Barber Colman Actuator for Motorized Damper (2-11A)	K/159	T	HE, DDE, DE	(b)
Barber Colman Actuator for Motorized Damper (12)	H/157	T	HE, DDE, DE	(b)
Barber Colman Actuator for Motorized Damper (2-12)	H/157	T	HE, DDE, DE	(b)
Barber Colman Actuator for Motorized Damper (12A)	H/157	T	HE, DDE, DE	(b)
Barber Colman Actuator for Motorized Damper (2-12A)	H/157	T	HE, DDE, DE	(b)
Barber Colman Actuator for Motorized Damper (13)	K/159	T	HE, DDE, DE	(b)
Barber Colman Actuator for Motorized Damper (2-13)	K/159	T	HE, DDE, DE	(b)
Barber Colman Actuator for Motorized Damper (14)	K/159	T	HE, DDE, DE	(b)
Barber Colman Actuator for Motorized Damper (2-14)	K/159	T	HE, DDE, DE	(b)
Limitorque Actuator for Motorized Damper (1)	A/143	T	HE, DDE, DE	(b)
Limitorque Actuator for Motorized Damper (2-1)	A/143	C	HE, DDE, DE	(b)
Limitorque Actuator for Motorized Damper (1A)	A/149	T	HE, DDE, DE	(b)
Limitorque Actuator for Motorized Damper (2-1A)	A/149	C	HE, DDE, DE	(b)
Limitorque Actuator for Motorized Damper (1B)	A/143	T	HE, DDE, DE	(b)
Limitorque Actuator for Motorized Damper (2-1B)	A/143	C	HE, DDE, DE	(b)

Equipment	Location[c] Building/ Elevation, ft	Qualification Method[c]	Qualifying Spectra[c]	Notes
Limitorque Actuator for Motorized Damper (1C)	A/149	T	HE, DDE, DE	(b)
Limitorque Actuator for Motorized Damper (2-1C)	A/149	C	HE, DDE, DE	(b)
Pneumatic Contromatics Operator for Fan S-1	L/91	T	HE, DDE, DE	(b)
Pneumatic Contromatics Operator for Fan 2S-1	L/91	C	HE, DDE, DE	(b)
Pneumatic Contromatics Operator for Fan S-2	L/91	T	HE, DDE, DE	(b)
Pneumatic Contromatics Operator for Fan 2S-2	L/91	C	HE, DDE, DE	(b)
Pneumatic Contromatics Operator for Fan S-31	K/150	T	HE, DDE, DE	(b)
Pneumatic Contromatics Operator for Fan S-33	K/150	C	HE, DDE, DE	(b)
Pneumatic Contromatics Operator for Fan S-32	K/150	T	HE, DDE, DE	(b)
Pneumatic Contromatics Operator for Fan S-34	K/150	C	HE, DDE, DE	(b)
Pneumatic Contromatics Operator for Fan E-1	L/135	T	HE, DDE, DE	(b)
Pneumatic Contromatics Operator for Fan 2E-1	L/135	C	HE, DDE, DE	(b)
Pneumatic Contromatics Operator for Fan E-2	L/135	T	HE, DDE, DE	(b)
Pneumatic Contromatics Operator for Fan 2E-2	L/135	C	HE, DDE, DE	(b)
Pneumatic Contromatics Operator for Fan E-4	L/146	T	HE, DDE, DE	(b)
Pneumatic Contromatics Operator for Fan 2E-4	L/146	C	HE, DDE, DE	(b)
Pneumatic Contromatics Operator	L/146	T	HE, DDE, DE	(b)

Equipment	Location(c) Building/ Elevation, ft	Qualification Method(c)	Qualifying Spectra(c)	Notes
for Fan E-5				
Pneumatic Contromatics Operator for Fan 2E-5	L/146	C	HE, DDE, DE	(b)
Pneumatic Contromatics Operator for Fan E-6	L/146	T	HE, DDE, DE	(b)
Pneumatic Contromatics Operator for Fan 2E-6	L/146	C	HE, DDE, DE	(b)
Motor for Supply Fan OS-96 (CRPS)	A/140'	A	HE, DDE, DE	(b)
Motor for Supply Fan OS-97 (CRPS)	A/140'	A	HE, DDE, DE	(b)
Motor for Supply Fan OS-98 (CRPS)	A/140'	A	HE, DDE, DE	(b)
Motor for Supply Fan OS-99 (CRPS)	A/140'	A	HE, DDE, DE	(b)
Fire Damper 46x14 (FD-1)	H/111	A	HE, DDE, DE	(b)
Fire Damper 46x14 (2FD-1)	H/111	C	HE, DDE, DE	(b)
Fire Damper 46x14 (FD-2)	H/111	A	HE, DDE, DE	(b)
Fire Damper 46x14 (2FD-2)	H/111	C	HE, DDE, DE	(b)
Fire Damper 46x14 (FD-3)	H/110	A	HE, DDE, DE	(b)
Fire Damper 46x14 (2FD-3)	H/110	C	HE, DDE, DE	(b)
Fire Damper 32x68 (FD-24)	J/100	A	HE, DDE, DE	(b)
Fire Damper 32x68 (2FD-24)	J/100	C	HE, DDE, DE	(b)
Motors for Fans E-43, E-44, S-43 and S-44	H/163	A	HE, DDE, DE	(b)
Motors for Fans E-45, E-46, S-45 and S-46	H/163	C	HE, DDE, DE	(b)
Fire Damper 42x24 (FD-25)	A/135	A	HE, DDE, DE	(b)
Fire Damper 42x24 (2FD-25)	A/135	C	HE, DDE, DE	(b)
Fire Damper 42x24 (FD-26)	A/135	A	HE, DDE, DE	(b)
Fire Damper 42x24 (2FD-26)	A/135	C	HE, DDE, DE	(b)
Fire Damper 42x24 (FD-27)	A/135	A	HE, DDE, DE	(b)

Equipment	Location(c) Building/ Elevation, ft	Qualification Method(c)	Qualifying Spectra(c)	Notes
Fire Damper 42x24 (2FD-27)	A/135	C	HE, DDE, DE	(b)
Fire Damper 36x39 (FD-19)	A/140	A	HE, DDE, DE	(b)
Fire Damper 36x39 (2FD-19)	A/140	C	HE, DDE, DE	(b)
Fire Damper 36x39 (FD-20)	A/140	A	HE, DDE, DE	(b)
Fire Damper 36x39 (2FD-20)	A/140	C	HE, DDE, DE	(b)
Fire Damper 36x39 (FD-21)	A/140	A	HE, DDE, DE	(b)
Fire Damper 36x39 (2FD-21)	A/140	C	HE, DDE, DE	(b)
Fire Damper 14x10 (FD-26)	H/151	T	HE, DDE, DE	(b)
Fire Damper 14x10 (2FD-26)	H/151	T	HE, DDE, DE	(b)
Fire Damper 20x10 (FD-27)	H/153	T	HE, DDE, DE	(b)
Fire Damper 20x10 (2FD-27)	H/153	T	HE, DDE, DE	(b)
Fire Damper 12x12 (FD-28)	H/158	T	HE, DDE, DE	(b)
Fire Damper 12x12 (2FD-28)	H/158	T	HE, DDE, DE	(b)
Varicel-Roughing Filter (EFR-1)	L/120	A	HE, DDE, DE	(b)
Varicel-Roughing Filter (2EFR-1)	L/120	C	HE, DDE, DE	(b)
Varicel-Roughing Filter (EFR-2a)	L/122	A	HE, DDE, DE	(b)
Varicel-Roughing Filter (2EFR-2a)	L/122	C	HE, DDE, DE	(b)
Varicel-Roughing Filter (EFR-2b)	L/104	A	HE, DDE, DE	(b)
Varicel-Roughing Filter (2EFR-2b)	L/104	C	HE, DDE, DE	(b)
Electric Duct Heater (EH-27)	H/163	A	HE, DDE, DE	(b)
Electric Duct Heater (2EH-27)	H/163	A	HE, DDE, DE	(b)
Electric Duct Heaters (OEH-28A & 28B)	Tech. Support Center/109	A	HE, DDE, DE	(a) (b)
Mode Damper 8 in. dia (0-17)	Tech. Support Center/109	A	HE, DDE, DE	(a) (b)

Equipment	Location[c] Building/ Elevation, ft	Qualification Method[c]	Qualifying Spectra[c]	Notes
Ceiling Registers & Diffusers Wall Registers & Diffusers(Unit 1)	Aux./Varies	A	HE, DDE, DE	(b)
Ceiling Registers & Diffusers Wall Registers & Diffusers (Unit 2)	Aux./Varies	A, C	HE, DDE, DE	(b)
Aluminum Air Outlets (26" wide or less) "Metalaire"	Aux./Varies	A	HE, DDE, DE	(b)
Aluminum Air Outlets (26" wide or less) "Metalaire" for Unit 2	Aux./Varies	C	HE, DDE, DE	(b)
Air Monitors (AM FE-5001, 5013, 5015, 5016, 5018A, 5018B, 5019 and 5020) and Flow Evaluators (FE-5014, 5017A and 5017B).	Aux./Varies	A	HE, DDE, DE	(b)
Air Monitors (AM 2-FE-5001, 5002, 5003, 5004, 5005, 5006, 5007, 5008, 5009, 5010, 5011, 5012, 5013, 5015, 5019 and 5020) and Flow Evaluators (2-FE-5014, 5017A, 5017B, 5018A, 5018B).	Aux./Varies	C	HE, DDE, DE	(b)
Air Flow Controllers Johnson Service R-317-1 for Fans	Aux./Varies	T	HE, DDE, DE	(b)
Pressure Reducing Valve Johnson Service R-130-A for Fan & Dampers	Aux./Varies	T	HE, DDE, DE	(b)
Restrictors Johnson Service T-5210-100 for Fans	Aux./Varies	T	HE, DDE, DE	(b)

Equipment	Location(c) Building/ Elevation, ft	Qualification Method(c)	Qualifying Spectra(c)	Notes
Solenoid Valves ASCO HT-8316-B15, C15 and D45; HT-8320-A20, A24 and A185; and HT-8331-A45 for Fans & Dampers	Aux./Varies	T	HE, DDE, DE	(b)
Speed Controllers ASCO VO221	Aux./Varies	T	HE, DDE, DE	(b)
Speed Controllers ASCO V0222 and VO223	Aux./Varies	C	HE, DDE, DE	(b)
Position Switches NAMCO D-2400-X-R2-WS for Dampers	Aux./Varies	T, C	HE, DDE, DE	(b)
Brandt Air Flow Controller (Pi-DPT-2000)	Aux./Varies	T, A	HE, DDE, DE	(b)
Portion of Refrigerant Piping with Solenoid Valve Exp. Valve with Sight Glass	H/158	T	HE, DDE, DE	(b)
Position Switches Allen-Bradley 802T-HW1 for Dampers	Aux./Varies	T	HE, DDE, DE	(b)
Position Switches Allen-Bradley 802T-HW1 for Dampers	Aux./Varies	C	HE, DDE, DE	(b)
Air Flow Switches Dwyer 1638 & 1640 for Fans	Aux./Varies, Turbine bldg., Technical Support Center/Varies	T, A	HE, DDE, DE	(a) (b)
Air Flow Switches McDonald-Miller AF1-S for Fans	Aux./Varies	T, A	HE, DDE, DE	(a) (b)
Thermostats Barber Colman TC-1191	H/145	T	HE, DDE, DE	(b)
Thermostats Penn T25A-13	H/120	T	HE, DDE, DE	(b)
Thermostats Penn T25A-B	H/120	C	HE, DDE, DE	(b)

TABLE 3.10-3

Equipment	Location[c] Building/ Elevation, ft	Qualification Method[c]	Qualifying Spectra[c]	Notes
Thermostats Penn A28AA	K/145	T	HE, DDE, DE	(b)
Thermostats Penn T26J-2	A/124	T	HE, DDE, DE	(b)
Thermostats Penn T26S-18	A/124	C	HE, DDE, DE	(b)
Control Relay Cabinets for CRC-1 and CRC-3	H/157	T, A	HE, DDE, DE	(b)
Control Relay Cabinets for CRC-6 and CRC-8	H/157	T, A	HE, DDE, DE	(b)
Common Control Relay Cabinets for CCRC-2	H/157	T, A	HE, DDE, DE	(b)
Common Control Relay Cabinets for CCRC-7	H/157	T, A	HE, DDE, DE	(b)
Control Panels for Compressors CP-35 & CP-36	H/156	T	HE, DDE, DE	(b)
Control Panels for Compressors CP-37 & CP-38	H/156	T	HE, DDE, DE	(b)
Heating Relay in Cabinet 3	H/157	T	HE, DDE, DE	(b)
Thermostat Honeywell Model T675A1565 & T6031A1029	H/154	T	HE, DDE, DE	(b)
Motors by Westinghouse for Fans S-1, S-2, S-31, S-32, S-39, S-40, E-1, E-2, E-4, E-5, E-6, E-101, E-102, E-103 and E-104	Aux./Varies Intake Structure/Varies	T	HE, DDE, DE	(b)
Motors by Westinghouse for Fans 2S-1, 2S-2, S-33, S-34, S-41, S-42,	Aux./Varies Intake Structure/Varies	C	HE, DDE, DE	(b)

Equipment	Location(c) Building/ Elevation, ft	Qualification Method(c)	Qualifying Spectra(c)	Notes
2E-1, 2E-2, 2E-4, 2E-5 and 2E-6				
Motors by GE, US Electric & Century for Fans CR-35, CR-36, S-35, S-36, S-67, S-68, S-69,	Aux./Varies & Turbine /Varies	T	HE, DDE, DE	(b)
Motors by GE, US Electric & Century for Fans CR-37, CR-38, S-37, S-38, 2S-67, 2S-68, 2S-69	Aux./Varies & Turbine/Varies	C	HE, DDE, DE	(b)
Flex connection in 48-in. ϕ Purge Air Supply Duct FC-1 & FC-2	L/Varies	A	HE, DDE, DE (Bldg. Displ. Per DCM C-28)	(b)
Flex connection in 48-in. ϕ Purge Air Supply Duct 2FC-1 & 2FC-2	L/Varies	C	HE, DDE, DE (Bldg. Displ. per DCM C-28)	(b)
Flex connection in 12-in. ϕ Excess Pressure Relief Duct FC-3 & FC-4	L/Varies	A	HE, DDE, DE (Bldg. Displ. per	(b)
Flex connection in 12-in. ϕ Excess Pressure Relief Duct 2FC-3 & 2FC-4	L/Varies	C	HE, DDE, DE (Bldg. Displ. per	(b)
Flex Connections in 14-in. Pipes OFC-11, through OFC-16, OFC-18 through OFC-21	Turbine bldg. /varies	A	HE, DDE, DE (Bldg. Displ. per DCM C-28)	(b)
Flex Connection in 14-in. Pipe OFC-17	Between Aux. bldg. & Turbine bldg./ 167	A	HE, DDE, DE (Bldg. Displ. per DCM C-28)	(b)
Flex Connection in 14-in. Pipe OFC-22	Aux. bldg./163	A	HE, DDE, DE (Bldg. Displ. Per DCM C-28)	(b) (d)
Flex Connection in 14-in. Pipe OFC-22 Unit 2	Aux. bldg./163	A	HE, DDE, DE (Bldg. Displ. Per DCM C-28)	(b) (d)

Equipment	Location[c] Building/ Elevation, ft	Qualification Method[c]	Qualifying Spectra[c]	Notes
Nutherm/Cleveland Airflow Switches Model AFS-951-1 for over heater in CRPS	H/169	T, A	HE, DDE, DE	(a) (b)
Motors for Compressors CP-35 and CP-36	H/154	A	HE, DDE, DE	(b)
Motors for Compressors CP-37 and CP-38	H/154	C	HE, DDE, DE	(b)
Fire Damper 24x12 (FD-7)	H/110	A	HE, DDE, DE	(b)
Fire Damper 24x12 (2FD-7)	H/110	C	HE, DDE, DE	(b)
Fire Damper 24x12 (FD-8)	H/110	A	HE, DDE, DE	(b)
Fire Damper 24x12 (2FD-8)	H/110	C	HE, DDE, DE	(b)
Fire Damper 24x12 (FD-9)	H/110	A	HE, DDE, DE	(b)
Fire Damper 24x12 (2FD-9)	H/110	C	HE, DDE, DE	(b)
Fire Damper (FD-34)	H/127	T	HE, DDE, DE	(b)
Fire Damper (2FD-34)	H/127	C	HE, DDE, DE	(b)
Fire Damper (FD-36)	H/127	T	HE, DDE, DE	(b)
Fire Damper (2FD-36)	H/127	C	HE, DDE, DE	(b)
Fire Damper (FD-38)	H/126	T	HE, DDE, DE	(b)
Fire Damper (FD-39)	H/126	T	HE, DDE, DE	(b)
Fire Damper (FD-40)	H/123	T	HE, DDE, DE	(b)
Fire Damper (FD-43)	A/119	T	HE, DDE, DE	(b)
Fire Damper (2FD-43)	A/119	C	HE, DDE, DE	(b)
Fire Damper (FD-44)	A/119	T	HE, DDE, DE	(b)
Fire Damper (2FD-44)	A/119	C	HE, DDE, DE	(b)
Fire Damper (FD-45)	A/119	T	HE, DDE, DE	(b)
Fire Damper (2FD-45)	A/119	C	HE, DDE, DE	(b)
Fire Damper (FD-10)	H/121	A	HE, DDE, DE	(b)
Fire Damper (2FD-10)	H/121	C	HE, DDE, DE	(b)

Equipment	Location(c) Building/ Elevation, ft	Qualification Method(c)	Qualifying Spectra(c)	Notes
Fire Damper (FD-11)	H/121	A	HE, DDE, DE	(b)
Fire Damper (2FD-11)	H/121	C	HE, DDE, DE	(b)
Fire Damper (FD-12)	H/121	A	HE, DDE, DE	(b)
Fire Damper (2FD-12)	H/121	C	HE, DDE, DE	(b)
Smoke Damper (SD-26)	H/151	A	HE, DDE, DE	(b)
Smoke Damper (2SD-26)	H/151	C	HE, DDE, DE	(b)
Smoke Damper (SD-27)	H/151	A	HE, DDE, DE	(b)
Smoke Damper (2SD-27)	H/151	C	HE, DDE, DE	(b)
Smoke Damper (SD-35)	H/127	A	HE, DDE, DE	(b)
Smoke Damper (2SD-35)	H/127	C	HE, DDE, DE	(b)
Smoke Damper (SD-37)	H/127	A	HE, DDE, DE	(b)
Smoke Damper (2SD-37)	H/127	C	HE, DDE, DE	(b)
Pneumatic Bettis Actuator for Damper (4A)	Aux/Varies	T	HE, DDE, DE	(b)
Pneumatic Bettis Actuator for Damper (2-4A)	Aux/Varies	T	HE, DDE, DE	(b)
Pneumatic Bettis Actuator for Damper (4B)		T	HE, DDE, DE	(b)
Pneumatic Bettis Actuator for Damper (2-4B)	Aux/Varies	T	HE, DDE, DE	(b)
Pneumatic Bettis Actuator for Damper (8A)		T	HE, DDE, DE	(b)
Pneumatic Bettis Actuator for Damper (2-8A)	Aux/Varies	T	HE, DDE, DE	(b)
Pneumatic Bettis Actuator for Damper (8B)		T	HE, DDE, DE	(b)
Pneumatic Bettis Actuator for Damper (2-8B)	Aux/Varies	T	HE, DDE, DE	(b)
Pneumatic Bettis Actuator for Damper (10)		T	HE, DDE, DE	(b)
Pneumatic Bettis Actuator for Damper (2-10)	Aux/Varies	T	HE, DDE, DE	(b)

Equipment	Location(c) Building/ Elevation, ft	Qualification Method(c)	Qualifying Spectra(c)	Notes
Power Regulator Co. Actuator for Damper (12)	Aux/Varies	T	HE, DDE, DE	(b)
Power Regulator Co. Actuator for Damper (16A)		T	HE, DDE, DE	(b)
Power Regulator Co. Actuator for Damper (2-16A)	Aux/Varies	C	HE, DDE, DE	(b)
Power Regulator Co. Actuator for Damper (16B)		T	HE, DDE, DE	(b)
Power Regulator Co. Actuator for Damper (2-16B)	Aux/Varies	C	HE, DDE, DE	(b)
Power Regulator Co. Actuator for Damper (17A)		T	HE, DDE, DE	(b)
Power Regulator Co. Actuator for Damper (2-17A)	Aux/Varies	C	HE, DDE, DE	(b)
Power Regulator Co. Actuator for Damper (17B)		T	HE, DDE, DE	(b)
Power Regulator Co. Actuator for Damper (2-17B)	Aux/Varies	C	HE, DDE, DE	(b)
Power Regulator Co. Actuator for Damper (20)		T	HE, DDE, DE	(b)
Power Regulator Co. Actuator for Damper (2-20)	Aux/Varies	C	HE, DDE, DE	(b)
Power Regulator Co. Actuator for Damper (21)	Aux/Varies	T	HE, DDE, DE	(b)
Power Regulator Co. Actuator for Damper (2-21)	Aux/Varies	C	HE, DDE, DE	(b)
Power Regulator Co. Actuator for Damper (22A)		T	HE, DDE, DE	(b)
Power Regulator Co. Actuator for Damper (2-22A)	Aux/Varies	C	HE, DDE, DE	(b)
Power Regulator Co. Actuator for Damper (22B)		T	HE, DDE, DE	(b)
Power Regulator Co. Actuator for Damper (2-22B)	Aux/Varies	C	HE, DDE, DE	(b)
Power Regulator Co. Actuator		T	HE, DDE, DE	(b)

Equipment	Location(c) Building/ Elevation, ft	Qualification Method(c)	Qualifying Spectra(c)	Notes
for Damper (23A)				
Power Regulator Co. Actuator for Damper (2-23)	Aux/Varies	C	HE, DDE, DE	(b)
Power Regulator Co. Actuator for Damper (23B)		T	HE, DDE, DE	(b)
Power Regulator Co. Actuator for Damper (2-23B)	Aux/Varies	C	HE, DDE, DE	(b)
Power Regulator Co. Actuator for Damper (24A)		T	HE, DDE, DE	(b)
Power Regulator Co. Actuator for Damper (2-24)	Aux/Varies	C	HE, DDE, DE	(b)
Power Regulator Co. Actuator for Damper (24B)		T	HE, DDE, DE	(b)
Power Regulator Co. Actuator for Damper (2-24B)	Aux/Varies	C	HE, DDE, DE	(b)
Power Regulator Co. Actuator for Damper (25A)		T	HE, DDE, DE	(b)
Power Regulator Co. Actuator for Damper (2-25)	Aux/Varies	C	HE, DDE, DE	(b)
Power Regulator Co. Actuator for Damper (25B)		T	HE, DDE, DE	(b)
Power Regulator Co. Actuator for Damper (2-25B)	Aux/Varies	C	HE, DDE, DE	(b)
Power Regulator Co. Actuator for Damper (26A)		T	HE, DDE, DE	(b)
Power Regulator Co. Actuator for Damper (2-26A)	Aux/Varies	C	HE, DDE, DE	(b)
Power Regulator Co. Actuator for Damper (26B)		T	HE, DDE, DE	(b)
Power Regulator Co. Actuator for Damper (2-26B)	Aux/Varies	C	HE, DDE, DE	(b)
Power Regulator Co. Actuator for Damper (33)		T	HE, DDE, DE	(b)
Power Regulator Co. Actuator for Damper (2-33)	Aux/Varies	C	HE, DDE, DE	(b)
Power Regulator Co. Actuator for Damper (34)		T	HE, DDE, DE	(b)

Equipment	Location[c] Building/ Elevation, ft	Qualification Method[c]	Qualifying Spectra[c]	Notes
Power Regulator Co. Actuator for Damper (2-34)	Aux/Varies	C	HE, DDE, DE	(b)
Pneumatic Parker-Hannifin Actuator for Mode Damper (1A)	L/127	A	HE, DDE, DE	(b)
Pneumatic Parker-Hannifin Actuator for Mode Damper (2-1A)	L/127	A	HE, DDE, DE	(b)
Pneumatic Parker-Hannifin Actuator for Mode Damper (1B)	L/131	C	HE, DDE, DE	(b)
Pneumatic Parker-Hannifin Actuator for Mode Damper (2-1B)	L/131	C	HE, DDE, DE	(b)
Pneumatic Parker-Hannifin Actuator for Damper (13A)	K/97	A	HE, DDE, DE	(b)
Pneumatic Parker-Hannifin Actuator for Damper (2-13A)	K/97	C	HE, DDE, DE	(b)
Pneumatic Parker-Hannifin Actuator for Damper (13B)	K/97	A	HE, DDE, DE	(b)
Pneumatic Parker-Hannifin Actuator for Damper (2-13B)	K/97	C	HE, DDE, DE	(b)
Pneumatic Parker-Hannifin Actuator for Damper (14A)	K/81	A	HE, DDE, DE	(b)
Pneumatic Parker-Hannifin Actuator for Damper (2-14A)	K/81	C	HE, DDE, DE	(b)
Pneumatic Parker-Hannifin Actuator for Damper (14B)	K/81	A	HE, DDE, DE	(b)
Pneumatic Parker-Hannifin Actuator for Damper (2-14B)	K/81	C	HE, DDE, DE	(b)
Pneumatic Parker-Hannifin Actuator for Damper (15A)	Aux/70	A	HE, DDE, DE	(b)
Pneumatic Parker-Hannifin Actuator for Damper (2-15A)	Aux/70	C	HE, DDE, DE	(b)
Pneumatic Parker-Hannifin Actuator for Damper (15B)	Aux/70	A	HE, DDE, DE	(b)
Pneumatic Parker-Hannifin Actuator for Damper (2-15B)	Aux/70	C	HE, DDE, DE	(b)

TABLE 3.10-3

Equipment	Location[(c)] Building/ Elevation, ft	Qualification Method[(c)]	Qualifying Spectra[(c)]	Notes
Position Switches NAMCO SL-3B1W & SL-170D for Dampers	L/115	T	HE, DDE, DE	(b)

(a) Turbine building, Unit 2, response spectra applicable for Qualification Spectra of equipment in the Technical Support Center.

(b) Envelope of 4% HE and 2% DDE Acceleration used in Qualification Spectra. Per DCM T-10 acceptance criteria, DE stresses shall not exceed the maximum allowable stress values specified in building codes (Uniform Building Code, 1973 and AISC, 1969). Increase in allowable stresses, permitted by code for seismic loads, shall not be used. In lieu of these, DDE and Hosgri stresses shall not exceed 90% of the yield strength and 150% of the AISC allowable stress, respectively.

(c) Legend:

ISA = Intake structure area
A = Qualification Spectra by analysis (Qualification Method column)
T = Qualification Spectra by testing
C = Comparison with similarly qualified equipment
DE = Design Earthquake
DDE = Double Design Earthquake
HE = Hosgri Earthquake

The letters in the Location column refer to standard area designations as defined in Figure 1.2-3, Piping and Mechanical Area Location Plan.

(d) Tag number of flexible connection OFC-22 has been duplicated.

(e) Quadrant dampers supported on flexible slab.

(f) Applicable to Units 1 and 2.